RECORD COPY
C.1
MICROFICHE

SANDIA REPORT

SAND92–0700/3 • UC–721
Unlimited Release
Printed December 1992

Preliminary Performance Assessment for the Waste Isolation Pilot Plant, December 1992

Volume 3: Model Parameters

8563634

SANDIA NATIONAL LABORATORIES
TECHNICAL LIBRARY

Sandia WIPP Project

Prepared by
Sandia National Laboratories
Albuquerque, New Mexico 87185 and Livermore, California 94550
for the United States Department of Energy
under Contract DE-AC04-76DP00789



654p.

Issued by Sandia National Laboratories, operated for the United States Department of Energy by Sandia Corporation.

NOTICE: This report was prepared as an account of work sponsored by an agency of the United States Government. Neither the United States Government nor any agency thereof, nor any of their employees, nor any of their contractors, subcontractors, or their employees, makes any warranty, express or implied, or assumes any legal liability or responsibility for the accuracy, completeness, or usefulness of any information, apparatus, product, or process disclosed, or represents that its use would not infringe privately owned rights. Reference herein to any specific commercial product, process, or service by trade name, trademark, manufacturer, or otherwise, does not necessarily constitute or imply its endorsement, recommendation, or favoring by the United States Government, any agency thereof or any of their contractors or subcontractors. The views and opinions expressed herein do not necessarily state or reflect those of the United States Government, any agency thereof or any of their contractors.

Printed in the United States of America. This report has been reproduced directly from the best available copy.

Available to DOE and DOE contractors from
Office of Scientific and Technical Information
PO Box 62
Oak Ridge, TN 37831

Prices available from (615) 576-8401, FTS 626-8401

Available to the public from
National Technical Information Service
US Department of Commerce
5285 Port Royal Rd
Springfield, VA 22161

NTIS price codes
Printed copy: A99
Microfiche copy: A01

SAND92-0700/3
Unlimited Release
Printed December 1992

Distribution
Category UC-721

Preliminary Performance Assessment for the Waste Isolation Pilot Plant, December 1992

Volume 3: Model Parameters

Sandia WIPP Project
Sandia National Laboratories
Albuquerque, New Mexico 87185

ABSTRACT

This volume documents model parameters chosen as of July 1992 that were used by the Performance Assessment Department of Sandia National Laboratories in its 1992 preliminary performance assessment of the Waste Isolation Pilot Plant (WIPP). Ranges and distributions for about 300 modeling parameters in the current secondary data base are presented in tables for the geologic and engineered barriers, global materials (e.g., fluid properties), and agents that act upon the WIPP disposal system such as climate variability and human-intrusion boreholes. The 49 parameters sampled in the 1992 Preliminary Performance Assessment are given special emphasis with tables and graphics that provide insight and sources of data for each parameter.

This volume of the report should be referenced as:

Sandia WIPP Project. 1992. *Preliminary Performance Assessment for the Waste Isolation Pilot Plant, December 1992. Volume 3: Model Parameters.* SAND92-0700/3. Albuquerque, NM: Sandia National Laboratories.

ACKNOWLEDGMENTS

The Waste Isolation Pilot Plant (WIPP) Performance Assessment (PA) Department is comprised of both Sandia National Laboratories (SNL) and contractor employees working as a team to produce these annual preliminary comparisons with Environmental Protection Agency (EPA) regulations, assessments of overall long-term safety of the repository, and interim technical guidance to the program. The on-site team, affiliations, and contributions to the 1992 performance assessment are listed in alphabetical order:

Performance Assessment Department

Name	Affil.*	Primary Author of Major Code	Area of Responsibility
R. Anderson	SNL		Department Manager
B. Baker	TEC		SEC02D, Hydrology, Office Manager
J. Bean	UNM		BRAGFLO, 2-Phase Flow
J. Berglund	UNM	CUTTINGS	Task Ldr., Cuttings/Cavings/Spallings, Engr. Mech.
S. Bertram-Howery	SNL		PA Liaison with DOE, Criteria Document, Test Phase Plan
W. Beyeler	SAI	PANEL, GARFIELD	Geostatistics, Analytical Models, CAMCON Systems Codes
K. Brinster	SAI		Geohydrology, Conceptual Models
R. Blaine	ECO		SEC02D, SECOTP, & CAMCON Systems Codes
T. Blaine	GC		Drilling Technology, Exposure Pathways Data
K. Byle	UNM		Software and Analysis QA
J. Chapman	TRI		Documentation V.3
D. Duncan	MAC		Data QA
K. Economy	ECO		SEC02D, SECOTP, Hydrology & Transport
D. Gallegos	SNL		Task Ldr., Hydrology, Geostatistics, NEA, PSAG
D. Galson	GS		NEA Working Groups, PSAG, PAAG, Human Intrusion
J. Garner	API	PANEL	Source Term, Sens. Anal.
A. Gilkey	UNM		CAMCON Systems Codes
L. Gomez	SNL		Task Ldr., Safety Assessments
M. Gruebel	TRI		EPA Regulations, Documentation V.1, Editor V.1
R. Guzowski	SAI		Geology, Scenario Construction
J. Helton	ASU	CCDFPERM	Task Ldr., Uncert./Scns. Anal., Probability Models, Editor V.4
S. Hora	UHH		Expert Elicitation, Probability Models
H. Iuzzolino	GC	CCDFCALC, CCDFPERM	LHS, CAMCON System Codes, Probability Models
R. Klett	SNL		EPA Regulations
P. Knupp	ECO	SECOTP	Comp. Fluid Dyn.
M. LaVenue	INT	GRASP-INV	Hydrology/Geostatistics

C. Leigh	SNL	GENII-S	Exposure Pathways
M. Marietta	SNL		Dep. Dept. Manager, Tech. Coord.
G. de Marsily	UP		Geostatistics Expert Group Chair
R. McCurley	UNM		CAMCON System Codes
B. Napier	PNL	GENII	Safety Assessments
A. Peterson	SNL		Task Ldr, Inventory
B. RamaRao	INT	GRASP-INV	Geostatistics
J. Rath	UNM		CAMCON System Codes
R. Rechard	SNL		Task Ldr. CAMCON, QA
P. Roache	ECO	SECO	Task Ldr., Comp. Fluid Dyn.
D. Rudeen	UNM		STAFF2D, SECOTP, Transport
J. Ruge	ECO		Multigrid Methods/BRAGFLO
T. Russell	ECO		Upscaling
K. Salari	ECO	SECOTP	Transport, Computational Fluid Dynamics
J. Sandha	SAI		INGRES, PA Data Base
J. Schreiber	SAI		BRAGFLO, 2-Phase Flow
D. Scott	TRI		Documentation V.2
P. Swift	TRI		Task Ldr., Geology, Climate Var., Documentation V.1 & 2, Editor V.1, 2, 4, & 5
M. Tierney	SNL		Task Ldr., CDF Constr., Probability Models, Ref. Data, Editor V.2 & 3
K. Trauth	SNL		Task Ldr., Expert Panels
P. Vaughn	API	BRAGFLO	Task Ldr., 2-Phase Flow & Waste Panel Chemistry, Editor V.4 & 5
T. Zimmerman	GRA		Geostatistics Test Problem

The foundation of the annual WIPP performance assessment is the underlying data set and understanding of the important processes in the engineered and natural barrier systems. Other SNL Departments are the primary source of these data and understanding. Assistance with the waste inventory comes from WEC and its contractors. We gratefully acknowledge the support of our departmental and project colleagues. Some individuals have worked closely with the performance assessment team, and we wish to acknowledge their contributions individually:

H. Batchelder	WEC	CH & RH Inventories
R. Beauheim	SNL	Natural Barrier System, Hydrologic Parameters
D. Borns	SNL	Geology, Geophysics
B. Butcher	SNL	Engineered Barrier System, Unmodified Waste-Form Parameters, Disposal Room Systems Parameters
L. Brush	SNL	Engineered Barrier System, Source Term (Solubility) and Gas Generation Parameters
L. Clements	ReS	Computer System Support
T. Corbet	SNL	Natural Barrier System, Geologic & Hydrologic Parameters, Conceptual Models
P. Davies	SNL	Natural Barrier System, Hydrologic & Transport Parameters, & 2-Phase Flow Mechanistic Modeling
P. Drez	DE	CH & RH Inventories
R. Finley	SNL	Repository Isolation Systems Parameters
F. Gelbard	SNL	Natural Barrier System, Retardation
E. Gorham	SNL	Natural Barrier System, Fluid Flow & Transport Parameters

R. Holt	CON	Geology
S. Howarth	SNL	Natural Barrier System, Hydrologic Parameters
R. Kehrman	WEC	Ch & RH Waste Characterization
K. Lickliter	BEC	EPA Regulations
R. Lincoln	SNL	Room Modeling
F. Mendenhall	SNL	Engineered Barrier System, Unmodified Waste Form Parameters, Waste Panel Closure (Expansion)
D. Munson	SNL	Reference Stratigraphy, Constitutive Models, Physical & Mechanical Parameters
C. Novak	SNL	Natural Barrier Systems, Chemistry
E. Nowak	SNL	Room Modeling, Source Term
J. Orona	ReS	Computer System Support
A. Stevens	SNL	DOE Liaison
J. Tillerson	SNL	Repository Isolation Systems Parameters
W. Wawersik	SNL	Fracturing
S. Webb	SNL	2-Phase Flow Sensitivity Analysis & Benchmarking

---

* Affiliation

API = Applied Physics Incorporated
ASU = Arizona State University
BEC = Benchmark Environmental Corp.
CON = Consultant
DE = Drez Environmental
ECO = Ecodynamics Research Associates
GC = Geo-Centers Incorporated
GRA = GRAM, Inc.
GS = Galson Sciences
INT = Intera
IT = International Technology
MAC = MACTEC
PNL = Pacific Northwest Laboratory
ReS = ReSpec
SAI = Scientific Applications International Corporation
SNL = Sandia National Laboratories
TEC = Technadyne Engineering Consultants
TRI = Tech Reps, Inc.
UHH = University of Hawaii at Hilo
UNM = University of New Mexico/New Mexico Engineering Research Institute
UP = University of Paris
WEC = Westinghouse Electric Corporation

Peer Review

Internal/Sandia
L. Gomez
D. Schafer

Management/Sandia
W. Weart

PA Peer Review Panel

R. Heath, Chair	University of Washington
R. Budnitz	Future Resources Associates, Inc.
T. Cotton	JK Research Associates, Inc.
J. Mann	University of Illinois
T. Pigford	University of California, Berkeley
F. Schwartz	Ohio State University

Department of Energy
R. Becker

Expert Panels

Futures

M. Baram	Boston University
W. Bell	Yale University
G. Benford	University of California, Irvine
D. Chapman	The World Bank, Cornell University
B. Cohen	University of Pittsburgh
V. Ferkiss	Georgetown University
T. Glickman	Resources for the Future
T. Gordon	Futures Group
C. Kirkwood	Arizona State University
H. Otway	Joint Research Center (Ispra), Los Alamos National Laboratory
M. Pasqualetti	Arizona State University
D. Reicher	Natural Resources Defense Council
N. Rosenberg	Resources for the Future
M. Singer	The Potomac Organization
T. Taylor	Consultant
M. Vinovskis	University of Michigan

Markers

D. Ast	Cornell University
V. Baker	University of Arizona
M. Brill	Buffalo Organization for Social and Technological Innovation
F. Drake	University of California at Santa Cruz
B. Finney	University of Hawaii at Manoa
D. Givens	American Anthropological Association
W. Goodenough	University of Pennsylvania
M. Kaplan	Eastern Research Group
J. Lomberg	Consultant
L. Narens	University of California at Irvine
F. Newmeyer	University of Washington
W. Sullivan	University of Washington
W. Williams	Case Western Reserve University

Source Term

C. Bruton	Lawrence Livermore National Laboratory
I-Ming Chou	U.S. Geological Survey
D. Hobart	Los Alamos National Laboratory
F. Millero	University of Miami

Retardation

R. Dosch	Sandia National Laboratories
C. Novak	Sandia National Laboratories
M. Siegel	Sandia National Laboratories

Geostatistics Expert Group

G. de Marsily, Chair	U. of Paris
R. Bras	Massachusetts Inst. of Tech.
J. Carrera	U. Politécnica de Cataluña
G. Dagan	Tel Aviv U.
A. Galli	Ecole des Mines de Paris
S. Gorlick	Stanford U.
P. Grindrod	Intera Sciences
A. Gutjahr	New Mexico Tech
D. McLaughlin	Massachusetts Inst. of Tech.
S. Neuman	U. of Arizona
C. Ravenne	Institut Français du Pétrole
Y. Rubin	U. of California, Berkeley

Report Preparation (TRI)

Illustration Editors

Volume 1: D. Marchand
Volume 2: D. Marchand
Volume 3: D. Pulliam

Dolores Miera and Leona Tartaglia of the Word Processing Department
R. Rohac, R. Andree, and the Illustration and Computer Graphics Departments
S. Tullar and the Production Department

PREFACE

This volume documents model parameters that were used in sensitivity and uncertainty studies by the Performance Assessment (PA) Department of Sandia National Laboratories in its 1992 preliminary comparison of the Waste Isolation Pilot Plant (WIPP) with the Environmental Protection Agency's (EPA's) *Environmental Standards for the Management and Disposal of Spent Nuclear Fuel, High-Level, and Transuranic Radioactive Wastes (40 CFR 191).*

Besides the DOE Project Integration and Site Offices in New Mexico, which oversee the project, the WIPP currently has two major participants: Sandia National Laboratories in Albuquerque, New Mexico, which functions as scientific investigator; and Westinghouse Electric Company, which is responsible for the management of WIPP operations. The specific tasks of Sandia are (1) characterizing the disposal system and surrounding region and responding to specific concerns of the State of New Mexico, (2) assessing the performance of the WIPP (e.g., assessing regulatory compliance with *40 CFR 191, Subpart B*, except the Assurance Requirements), (3) performing analytic, laboratory, field experiments, and applied research to nuclear waste disposal in salt, relevant to support tasks 1 and 2 (disposal system characterization and performance assessment), and (4) providing ad hoc scientific and engineering support (e.g., supporting environmental assessments such as Resource Conservation and Recovery Act (RCRA, 1976) and the National Environmental Policy Act (NEPA, 1969). This volume helps fulfill the performance assessment task.

For the performance assessment, the PA Department at Sandia maintains a data base, the secondary data base (SDB), which contains interpreted data from many primary sources. The data are used to form a conceptual model of the WIPP disposal system. The SDB provides a set of parameter values (median, range, and distribution type where appropriate) and the source of these values. As better information becomes available, the parameter values reported herein will be updated. Thus, this volume is only a snapshot of the data that supports parameters in the SDB compiled as of April 1992. Updated parameter reports will be issued annually as a separate volume of the *Preliminary Performance Assessment for the Waste Isolation Pilot Plant.* A previous data report was published in December 1991 (WIPP PA Division, 1991).

The 1992 comparison and background information on the comparison are reported in Volumes 1, 2, and 4 of this report:

> SNL (Sandia National Laboratories) WIPP PA Department. 1992. *Preliminary Performance Assessment for the Waste Isolation Pilot Plant, December 1992—Volume 1: Third Comparison with 40 CFR 191, Subpart B.* SAND92-0700/1. Albuquerque, NM: Sandia National Laboratories.
>
> SNL (Sandia National Laboratories) WIPP PA Department. 1992. *Preliminary Performance Assessment for the Waste Isolation Pilot Plant, December 1992—Volume 2: Technical Basis.* SAND92-0700/2. Albuquerque, NM: Sandia National Laboratories.
>
> SNL (Sandia National Laboratories) WIPP PA Department. 1993. *Preliminary Performance Assessment for the Waste Isolation Pilot Plant, December 1992—Volume 4: Sensitivity Analyses for 40 CFR 191, Subpart B.* SAND92-0700/4. Albuquerque, NM: Sandia National Laboratories.

The present volume documents parameter values used in models described in Volume 2; in turn, sensitivity and uncertainty analyses employing the models of Volume 2 are reported in Volumes 1 and 4.

Transforming data into distributions of model parameters is a major PA Department task. Although the PA Department is responsible for comparing the WIPP with *40 CFR 191, Subpart B*, the majority of data used for these comparisons is supplied by experimenters and analysts characterizing the disposal system and surrounding regional geology as noted in the acknowledgments.

In addition to individual contributors who established current data, earlier contributors are also acknowledged. Much of the data provided prior to 1991 is summarized in *Systems Analysis, Long-Term Radionuclide Transport, and Dose*

Assessments, Waste Isolation Pilot Plant (WIPP), Southeastern New Mexico; March 1989, edited by Lappin et al. (1989). Because of this report's wide circulation, we found it convenient to refer to this report as a data source, although in many cases it only summarizes others' work. Its selection as a source is not meant to diminish the contributions of the original authors. However, Lappin et al. (1989) is the first report in which ranges were assigned for many parameters, so it does provide a primary reference for these ranges. Furthermore, some of the data has not yet been published and thus Lappin et al. (1989) may be the only source until documentation is complete.

We appreciate the time and suggestions supplied by the final peer reviewers: D. R. Anderson (6342), E. D. Gorham (6119), R. C. Lincoln (6345), and J. R. Tillerson (6121). In addition, the editorial help on the text and over 100 illustrations provided respectively by J. Chapman and D. Pulliam of Tech Reps, Inc., Albuquerque, New Mexico, greatly improved the report.

CONTENTS

1 INTRODUCTION 1-1
1.1 Purpose and Organization of Report 1-1
1.2 Conventions 1-2
1.2.1 Probability Distribution Functions 1-2
1.2.2 Empirical Distribution Functions 1-6
1.2.3 Range 1-6
1.2.4 Mean and Sample Mean 1-6
1.2.5 Median and Sample Median 1-6
1.2.6 Variance and Coefficient of Variation 1-6
1.2.7 Categories of Distributions 1-7
Continuous Distributions 1-7
Discrete Distributions 1-10
Constructed Distributions (Data) 1-10
Constructed Distributions (Subjective) 1-10
Miscellaneous Categories 1-11
1.2.8 Key to Parameter Sheets 1-11
1.3 Background on Selecting Parameter Distributions 1-14
1.3.1 Requests for Data from Sandia Investigators and Analysts 1-14
Identify Necessary Data 1-15
Request Median Value and Distribution 1-15
Update Secondary Data Base 1-15
Perform Consequence Simulations and Sensitivity Analyses 1-15
Determine Whether Parameter Is Important in Analysis 1-15
1.3.2 Construction of Distributions 1-15
Step 1 1-16
Step 2 1-16
Step 3 1-16
Step 4 1-17
Step 5 1-17
1.3.3 Some Limitations on Distributions 1-17
No Scaling of Variability for Material-Property Parameters 1-17
General Absence of Correlations Among Parameters 1-21
1.3.4 Selection of Parameters for Sampling 1-21
1.4 Background on 1992 Probability Consequence Models 1-21
1.4.1 Two-Phase Flow: BRAGFLO 1-21
Notes on Relative Permeability and Capillary Pressure 1-23
Notes on Gas-Generation Terms 1-24
Note on Reservoir Porosity 1-27
1.4.2 Human Intrusion: CCDFPERM 1-27
Inhomogeneous Poisson Process 1-29
Application to Computational-Scenario Probabilities 1-29
1.4.3 Cuttings Removal: CUTTINGS 1-30
Flow Regime 1-32
Shear Stress 1-32
1.4.4 Repository Discharge: PANEL 1-34
Waste Mobilization 1-35
Approximations in Panel 1-36
1.4.5 Fluid Flow in Culebra: SECO2D 1-37
Groundwater Flow 1-37
Effects of Climate Change 1-38

1.4.6 Solute Transport in Culebra: SECO/TP 1-38
Mass Transport in Fracture System 1-39
Mass Storage in Clay Coatings and Matrix 1-41
The Mass Transfer Term 1-42
Initial and Boundary Conditions 1-42
1.4.7 Waste-Filled Room Deformation: SANCHO 1-42
Elastic/Secondary Creep Model for Intact Salt 1-43
Crushed Salt Backfill Model 1-44
Volumetric Plasticity Model for Waste 1-45
Note on Problem Geometry 1-45
Note on Gas Generation 1-45
1.5 Background on WIPP 1-46
1.5.1 Purpose 1-46
1.5.2 Location 1-47
1.5.3 Geological History of the Delaware Basin 1-47
1.5.4 Repository 1-47
1.5.5 WIPP Waste Disposal System 1-47

2 GEOLOGIC BARRIERS 2-1
2.1 Areal Extent of Geologic Barriers 2-1
2.2 Stratigraphy at the WIPP 2-4
2.3 Hydrologic Parameters for Halite and Polyhalite within Salado Formation 2-11
2.3.1 Capillary Pressure and Relative Permeability 2-12
2.3.2 Density 2-20
2.3.3 Dispersivity 2-24
2.3.4 Partition Coefficients and Retardation 2-28
2.3.5 Permeability 2-29
2.3.6 Pore Pressure at Repository Level in Halite 2-38
2.3.7 Porosity 2-41
2.3.8 Specific Storage 2-44
2.3.9 Tortuosity 2-47
2.4 Hydrologic Parameters for Anhydrite Layers within Salado Formation 2-49
2.4.1 Capillary Pressure and Relative Permeability 2-51
2.4.2 Permeability 2-56
2.4.3 Pore Pressure at Repository Level in Anhydrite 2-62
2.4.4 Porosity 2-65
2.5 Mechanical Parameters for Materials in Repository and Salado Formation 2-69
2.6 Parameters for Culebra Dolomite Member of Rustler Formation 2-72
2.6.1 Fraction of Clay Filling in Fractures 2-77
2.6.2 Porosity 2-79
2.6.3 Transmissivity 2-86
2.6.4 Partition Coefficients and Retardations 2-92

3 ENGINEERED BARRIERS AND SOURCE TERM 3-1
3.1 Dimensions of Underground Facility 3-1
3.1.1 Disposal Region 3-5
3.1.2 Experimental Region 3-6
3.1.3 Operations Region 3-7
3.1.4 Shafts 3-8
3.1.5 Waste Containers 3-9
3.1.6 Waste Placement and Backfill in Rooms 3-11
3.2 Parameters for Seals and Fill Outside Disposal Region 3-14

3.2.1 Description of the Reference Seal System Design 3-15
General Sealing Strategy 3-15
Seal Locations 3-15
Backfill in Upper Shaft, Water-Bearing Zone, and Dewey Lake Red Beds 3-16
3.2.2 Preconsolidated Salt in Lower Shaft, Drifts, and Panels 3-19
3.3 Parameters for Contaminants Independent of Waste Form 3-20
3.3.1 Inventory of Radionuclides in Contact-Handled Transuranic Waste 3-21
3.3.2 Inventory of Remotely Handled Waste 3-28
3.3.3 Radionuclide Chains and Half-Lives 3-29
Radionuclides for Cuttings and Repository Modeling 3-29
Radionuclides for Transport Modeling 3-29
3.3.4 40 CFR 191 Release Limits and Waste Unit Factor 3-35
40 CFR 191 Release Limits 3-35
Waste Unit Factor 3-35
3.3.5 Chemical and Physical Parameters of TRU Wastes 3-36
3.4 Parameters for Unmodified Waste Form Including Containers 3-55
3.4.1 Composition of CH-TRU Waste (Non-Radionuclide/Non-RCRA Inventory) 3-59
3.4.2 Composition of RH-TRU Waste (Non-Radionuclide/Non-RCRA Inventory) 3-67
3.4.3 Saturation 3-69

4 PARAMETERS OF GLOBAL MATERIALS AND AGENTS ACTING ON DISPOSAL SYSTEM .. 4-1
4.1 Fluid Properties 4-1
4.2 Human-Intrusion Borehole 4-2
4.2.1 Borehole Fill Properties 4-3
4.2.2 Drilling Characteristics 4-7
4.3 Parameters for Castile Formation Brine Reservoir 4-10
4.3.1 Brine Pressure 4-12
4.3.2 Bulk Storativity 4-15
4.4 Climate Variability and Culebra Member Recharge 4-18

5 PARAMETERS FOR SCENARIO PROBABILITY MODELS 5-1
5.1 Area of Brine Reservoirs 5-1
5.2 Human-Intrusion Probability (Drilling) Models 5-13

6 SUMMARY OF PARAMETERS SAMPLED IN 1992 6-1
6.1 Sampled Parameters 6-1
6.2 Selection Procedure for Parameters Sampled in 1992 6-5

REFERENCES R-1

APPENDIX A: Memoranda Regarding Reference Data A-1

APPENDIX B: Well Location Data and Elevations of Stratigraphic Layers near WIPP B-1

APPENDIX C: Realizations of Transmissivity Fields in the Culebra Dolomite Member of the Rustler Formation C-1

APPENDIX D: Realizations of Drilling Intensity Functions for Human Intrusion D-1

NOMENCLATURE N-1

CONVERSION TABLES FOR SI AND COMMON ENGLISH UNITS ..... Conversion Tables-1

Figures

Figure		
1.2-1	Examples of distribution plots	1-8
1.2-2	Example of a parameter sheet	1-12
1.3-1	Five-step procedure used to construct cumulative distribution functions (cdfs) for the 1992 performance simulations	1-16
1.4-1	Idealization of waste-disposal reservoir used in BRAGFLO calculation of two-phase flow in repository and surroundings	1-28
1.4-2	Isopleths of porosity of waste-filled disposal room as a function of total volume of gas produced and time after sealing	1-28
1.4-3	Some features of the CUTTINGS model	1-31
1.4-4	Various models for modeling drilling fluid shear stress	1-33
1.4-5	Idealized collapsed WIPP panel in PANEL model	1-34
1.4-6	Idealized section of Culebra Dolomite Member	1-40
1.4-7	Modeling mesh and boundary conditions for calculation of porosity surface with SANCHO	1-46
1.5-1	WIPP location in southeastern New Mexico	1-48
1.5-2	Location of the WIPP in the Delaware Basin	1-49
1.5-3	WIPP repository, showing surface facilities, proposed TRU disposal areas, and experimental areas	1-50
1.5-4	Geologic and engineered barriers of the WIPP disposal system	1-52
2.1-1	Position of the WIPP waste panels relative to land-withdrawal boundary (16 contiguous sections), 5-km boundary (40 CFR 191.12y), and surveyed section lines	2-1
2.1-2	UTM coordinates of the modeling domains	2-2
2.1-3	Locations of wells for defining general stratigraphy and regional and local data domains typically plotted in this volume	2-3
2.2-1	Level of WIPP repository, located in the Salado Formation	2-5
2.2-2	Reference local stratigraphy near repository	2-6
2.2-3	Stratigraphy at the repository horizon	2-7
2.2-4	North-south cross-section showing Salado Formation stratigraphy near repository	2-8

Figure

2.3-1	Example of variation in relative permeability and capillary pressure when Brooks and Corey parameters are varied	2-13
2.3-2	Estimated relative permeability and capillary pressure curves	2-14
2.3-3	Correlation of threshold pressure with permeability for a composite of data from all consolidated rock lithologies	2-16
2.3-4	Estimated distribution for longitudinal dispersivity in halite, Salado Formation	2-27
2.3-5	Estimated distribution for dispersivity ratio in halite, Salado Formation	2-27
2.3-6	Scatterplot for normalized release of Pu-239 to the Culebra Dolomite with gas generation in the repository and intrusion occurring at 1000 yr for variable SALPERM (Salado permeability)	2-31
2.3-7	Estimated distribution (in 1991) for Salado undisturbed permeability	2-31
2.3-8	Estimated distribution in 1992 for Salado undisturbed permeability	2-32
2.3-9	Expected qualitative behavior of pore pressure (P) and log permeability ($\log_{10}$k) near wall of an open excavation	2-34
2.3-10	Simulated undisturbed (far-field) halite permeability	2-35
2.3-11	Estimated distribution (in 1992) for Salado halite disturbed permeability	2-37
2.3-12	Simulated undisturbed (far-field) pore pressure at repository depth in halite	2-39
2.3-13	Calculated lithostatic and hydrostatic pressures with depth	2-40
2.3-14	Estimated distribution for undisturbed porosity in halite, Salado Formation	2-42
2.3-15	Estimated distribution for specific storage of halite, Salado Formation	2-45
2.4-1	Generalized cross section of Marker Bed 139 near repository	2-50
2.4-2	Estimated distribution in 1992 for undisturbed permeability of anhydrite layers in Salado Formation	2-58
2.4-3	Estimated 1991 distribution for undisturbed permeability, anhydrite layers in Salado Formation	2-58
2.4-4	Regression curves fitted to artificial data sets for undisturbed anhydrite permeability	2-60
2.4-5	Simulated distribution of average, undisturbed permeability of anhydrite	2-60
2.4-6	Distribution used in 1991 for brine pore pressure in anhydrite MB139 at repository level	2-63
2.4-7	Regression curves fitted to artificial data sets for undisturbed anhydrite pore pressure	2-64
2.4-8	Simulated distribution of average undisturbed pore pressure at repository depth in anhydrite	2-64
2.4-9	Estimated distribution for undisturbed porosity for anhydrite layers in Salado Formation	2-66

Figure

2.6-1 Detailed lithology of Rustler Formation at ERDA-9 2-73

2.6-2 Interpolated geologic west-east cross section across the WIPP disposal system 2-74

2.6-3 Location of wells used to define hydrologic parameters for Culebra Dolomite 2-75

2.6-4 Estimated distribution for clay filling fraction, Culebra Dolomite Member 2-78

2.6-5 Estimated distribution for fracture porosity, Culebra Dolomite Member 2-80

2.6-6 Empirical distribution for intact matrix porosity of Culebra Dolomite Member assuming no spatial correlation 2-83

2.6-7 Constructed distribution for Culebra fracture spacing 2-85

2.6-8 Empirical travel time distribution associated with the 70 realizations of Culebra transmissivity fields 2-91

2.6-9 Constructed distribution for partition coefficient in matrix for (a) americium, (b) curium, (c) neptunium, (d) lead, (e) plutonium, (f) radium, (g) thorium, and (h) uranium 2-97

2.6-10 Constructed distribution for partition coefficient in clay for (a) americium, (b) curium, (c) neptunium, (d) lead, (e) plutonium, (f) radium, (g) thorium, and (h) uranium 2-100

3.1-1 Excavated and enclosed areas in the WIPP repository 3-2

3.1-2 Planned dimensions of WIPP disposal region and access drifts 3-3

3.1-3 Ideal packing of drums in rooms and 10-m-wide drifts 3-12

3.1-4 Ideal packing of Standard Waste Boxes in rooms and drifts 3-13

3.2-1 Diagram of typical sealed and backfilled access shaft 3-17

3.2-2 Diagram of typical concrete plugs in backfilled shafts 3-18

3.2-3 Diagram of typical concrete and preconsolidated salt backfill for drifts and panels 3-18

3.3-1 Decay of CH radionuclide chain in TRU-contaminated waste 3-30

3.3-2 Decay of RH radionuclide chain in TRU-contaminated waste 3-32

3.3-3 Constructed distribution for solubility of (a) americium, (b) curium, (c) neptunium, (d) lead, (e) plutonium, (f) radium, (g) thorium, and (h) uranium 3-39

3.3-4 Bar diagrams of elicited distributions of solubility for americium, curium, lead, neptunium, plutonium, radium, thorium, and uranium 3-42

3.3-5 Estimated relative areas of stability in the pH-Eh space for neptunium, plutonium, and uranium and percentage of area of stable water 3-43

3.3-6 Constructed distribution for gas production rates from corrosion under inundated conditions 3-45

Figure

3.3-7	Constructed distribution for relative gas production rates from corrosion under humid conditions	3-47
3.3-8	Pressure-time plots for 6-month anoxic corrosion experiments under brine-inundated and vapor-limited ("humid") conditions	3-49
3.3-9	Constructed distribution for gas production rates from microbiological degradation under inundated conditions	3-51
4.2-1	Required casing and plugs	4-5
4.2-2	Increased permeability of cement grout plugs in intrusion borehole with time because of degradation	4-6
4.2-3	Distribution of historical drill bit diameter	4-9
4.3-1	Deep boreholes that encountered brine reservoirs within the Castile Formation, Northern Delaware Basin	4-11
4.3-2	Constructed distribution for Castile brine reservoir initial pressure	4-13
4.3-3	Estimated distribution for bulk storativity of Castile brine reservoir	4-16
5.1-1	Distribution of fraction of WIPP disposal area overlapped by brine reservoir	5-2
5.1-2	Frequently reported contour map of depth below surface of first major conductor below WIPP disposal area	5-3
5.1-3	Conservative contour map of elevation above sea level of first major conductor below WIPP disposal area	5-4
5.1-4	Example variogram illustrating typical behavior of γ with h	5-6
5.1-5	Population distribution and statistics for conductor elevations	5-7
5.1-6	Scatterplots of conductor elevation vs. X and Y location	5-8
5.1-7	Empirical variogram of conductor elevations	5-9
5.1-8	Cumulative distribution of area fraction using the "random" and "block" assumptions	5-11
5.1-9	Illustration of hypothetical variability of regular sampling of extensive narrow features	5-12

Tables

Table		
1.2-1	Description of Several Probability Distributions	1-3
1.2-2	Probability of Parameters Lying within Range Defined by $\bar{x} \pm hs$	1-11
2.3-1	Parameter Values for Halite and Polyhalite within Salado Formation near Repository	2-11
2.3.2	Summary of Measurements of Salado Halite Permeabilities and Pore Pressures	2-33
2.4-1	Hydrologic Parameter Values for Anhydrite Layers within Salado Formation	2-49
2.4-2	Summary of Measurements of Salado Anhydrite Permeabilities and Pore Pressure	2-59
2.5-1	Summary of Parameters Used in Mechanical Models of Repository and Salado Formation Materials	2-70
2.5-2	Volumetric Strain as a Function of Pressure: Relationship Used in Volumetric Plasticity Model for Waste in Disposal Room	2-71
2.6-1	Summary of Parameter Values for Culebra Dolomite Member of Rustler Formation	2-76
2.6-2	Logarithms of Selected Transmissivity Measurements in Culebra Dolomite Member	2-88
2.6-3	Logarithms of Transmissivity of Calibrating Points (Pilot Points) for Culebra Dolomite Member	2-89
2.6-4	Summary of Selected Steady-State Freshwater Head Measurements in Culebra Dolomite Member	2-90
2.6-5	Summary of 1992 Partition Coefficients of Radionuclides for Culebra Dolomite Member within Matrix Dominated by Culebra Brine	2-93
2.6-6	Summary of 1992 Partition Coefficients of Radionuclides for Culebra Dolomite Member within Fracture Clays Dominated by Culebra Brine	2-94
3.1-1	Summary of Excavated and Enclosed Areas and Initial Volumes of Excavated Regions within the WIPP Repository, Not Considering the DRZ or Closure	3-4
3.1-2	CH-TRU Waste Containers	3-10
3.2-1	Parameter Values for Seals Outside Disposal Region	3-14
3.3-1	Inventory and Parameter Values for TRU Radioisotopes	3-22
3.3-2	Half-Lives of Isotopes Disposed or Created in WIPP	3-33
3.3-3	1991 Cumulative Release Limits (L_i) to the Accessible Environment 10,000 Yr after Disposal for Evaluating Compliance with Containment Requirements	3-35

Table

3.3-4 Chemical and Physical Parameters of TRU Waste 3-37

3.4-1 Parameter Values for Unmodified TRU Waste Categories, Containers, and Salt Backfill 3-56

3.4-2 Summary of Waste Acceptance Criteria and Requirements Applicable to Performance Assessment 3-58

3.4-3 Estimated Composition by Volume of CH-TRU Contaminated Waste from 1987 to 1990 3-63

3.4-4 Estimate of a Design Volume for CH-TRU Waste 3-64

3.4-5 Estimated Composition of CH-TRU Contaminated Waste in 1990 by Generator 3-65

3.4-6 Calculation of Constituent Volume Distribution in CH-TRU Waste 3-66

3.4-7 Estimate of a Design Volume for RH-TRU Waste 3-68

4.1-1 Fluid Properties 4-1

4.2-1 Characteristics of Human-Intrusion Borehole 4-2

4.2-2 Specifications for Gas and Oil Exploratory Boreholes 4-9

4.3-1 Parameter Values for Castile Formation Brine Reservoir 4-10

4.3-2 Estimated Initial Pressures of Brine Reservoirs Encountered in the Region around the WIPP Corrected to the Depth at the WIPP-12 Brine Reservoir 4-14

4.4-1 Climate Variability and Culebra Member Recharge 4-18

5.1-1 Cumulative Percentages of the Disposal Region Underlain by a Brine Reservoir, Assuming Various Elevations Relative to Sea Level 5-5

6.0-1 Distributions of Sample Parameters in December 1992 WIPP Performance Assessment for Geologic Barriers 6-1

6.0-2 Distributions of Sample Parameters in December 1992 WIPP Performance Assessment for Engineered Barriers 6-3

6.0-3 Distributions of Sample Parameters in December 1992 WIPP Performance Assessment for Agents Acting on Disposal System and Probability Models for Scenarios 6-4

1. INTRODUCTION

1.1 Purpose and Organization of Report

The purpose of this volume is to describe parameters of mathematical models chosen as of July 1992 for use by the Performance Assessment (PA) Department of Sandia National Laboratories in its 1992 evaluation of the long-term performance ("performance assessment") of the Waste Isolation Pilot Plant (WIPP). In this volume, performance assessment refers to the prediction of all long-term performance. For example, the models and parameters can be used to compare WIPP performance with the requirements of the Environmental Protection Agency's (EPA's) *Environmental Standards for the Management and Disposal of Spent Nuclear Fuel, High-Level, and Transuranic Radioactive Wastes (40 CFR 191)*, with long-term safety goals for individual exposure (doses) that may be necessary for environmental impact statements (National Environmental Policy Act [NEPA, 1969]), and with long-term requirements of hazardous waste regulations (Resource Conservation and Recovery Act of 1976 [RCRA, 1976]).

About 300 distinct parameters are listed in this report for use in the consequence and probability models used in simulations of the WIPP. Data bases, sources, and reasoning that supported the choices of probability distributions for each of the 300 parameters were described in the 1991 counterpart of the present volume (i.e., WIPP PA Division, 1991, Vol. 3). In the present volume, emphasis is placed upon sources and reasoning behind the 49 parameters that were sampled in the 1992 PA calculations for purposes of sensitivity and uncertainty analyses; these 49 parameters are given extended discussion in the form of data tables andgraphics. Most of these parameters specify the physical, chemical, or hydrologic properties of the rock formations (geologic barriers) in which the WIPP is placed; a substantial number of the parameters specify physical, chemical, or hydrologic properties of the seals, backfill, and waste form (engineered barriers); and some pertain to future climatic variability or future episodes of exploratory drilling at the WIPP. Dimensions of selected engineered features of the WIPP underground facility are also listed, although these dimensions are not counted as part of the 300 parameters.

The EPA Standard, *40 CFR 191*, explicitly acknowledges the uncertainties associated with scientific predictions, especially when predictions cover thousands of years, and mandates that this uncertainty be reported when making comparisons with the Standard, Subpart B. One of several sources of uncertainty in scientific predictions is uncertainty in the values of the parameters in mathematical models used to make those predictions; consequently, this report also lists estimates of the range and distribution (uncertainty) of the parameters.

The organization of this volume is as follows:

- The remainder of Chapter 1 presents conventions used in the data tables, and background information on the selection of distributions, performance assessments, and the WIPP. Chapter 1 is arranged so that information specific to the data is presented first, followed by more general information (e.g., background on the WIPP consequence models).
- Chapter 2 provides consequence-model parameters for geologic barriers.
- Chapter 3 provides consequence-model parameters for the engineered barriers and source terms.
- Chapter 4 provides consequence-model parameters for global materials such as fluid properties (e.g., Salado Formation brine compressibility) and properties of agents that act upon the WIPP disposal system such as climate variability and human-intrusion boreholes.
- Chapter 5 provides parameters for human-intrusion probability models.
- Chapter 6 lists the specific parameters that were varied for the December 1992 preliminary comparison of the WIPP with *40 CFR 191, Subpart B*.

- Appendix A is a compilation of memoranda from principal investigators; each memorandum documents either data or recommendations concerning the choice of a parameter's distribution or use of the parameter in a consequence model.
- Appendix B is tabulated data for existing wells near the WIPP site (i.e., data on Well ID, location, and formations penetrated).
- Appendices C and D provide graphic and tabular representations of certain parameters that are not conveniently placed in the main body of the report.
- Following the cited references is a table of conversion factors between SI and common English units; a glossary of terms; and a list of variables, acronyms, and initialisms.

1.2 Conventions

Chapters 2 through 5 provide data and information used in the PA Department's 1992 mathematical models of the WIPP system. The parameter sheets, graphs, and discussions in these chapters may use standard terms of probability theory and statistics or non-standard terms to characterize model parameters; brief explanations of these terms are provided below, along with a key to the parameter sheets.

1.2.1 Probability Distribution Functions

For a continuous parameter, say X, the *probability density function* (pdf) is a function $f(x) > 0$ with the properties

$$\int_a^b f(x)\,dx = \text{probability that uncertain } \textit{parameter } X \text{ lies in interval (a,b):}$$

$$\int_{-\infty}^{+\infty} f(x)\,dx = 1 .$$

The *cumulative distribution function* (cdf) associated with f(x) is defined by

$$F(x) = \int_{-\infty}^{x} f(s)\,ds = \text{probability that uncertain parameter X is less than or equal to x.}$$

Probability density functions (pdfs) and cdfs can be similarly defined for uncertain parameters that take on a denumerable number of values, x_i, i=1,2, ... The sequence $\{f_i\}$, i=1,2, ..., such that $f_i > 0$ and

$$\sum_i f_i = 1,$$

is the discrete analogue of the continuous pdf, and

$$F(x) = \sum_{\text{all } x_i < x} f_i$$

is the discrete analogue of the continuous cdf.

Examples of common, analytic, continuous and discrete probability distributions are shown in Table 1.2-1.

Table 1.2-1. Description of Several Probability Distributions

	Probability Density Function f(x)	Cumulative Distribution Function F(x)	Expected Value μ	Variance σ^2
1.	Beta $\frac{1}{B(\alpha,\lambda)} \frac{(x-a)^{\alpha-1}(b-x)^{\lambda-1}}{(b-a)^{\alpha+\lambda-2}}$ $a < x < b,\ \alpha > 0,\ \lambda > 0$ where $B(\alpha,\lambda) = \frac{\Gamma(\alpha)\ \Gamma(\lambda)}{\Gamma(\alpha+\lambda)}$ and $\Gamma(\gamma) = \int_0^\infty x^{\gamma-1} e^{-x} dx$ $= \frac{\alpha!\ \lambda!}{(\alpha+\lambda-1)!}$ if α and λ are integers	$\int_a^x f(x)\ dx$	$a = \frac{\alpha}{\alpha+\lambda}$	$\frac{(b-a)^2\ \alpha\lambda}{(\alpha+\lambda)^2(\alpha+\lambda+1)}$
2.	Gamma $\frac{\lambda^\alpha x^{\alpha-1} e^{-\lambda x}}{\Gamma(\alpha)}$	$\int_0^x f(x)\,dx$	$\frac{\alpha}{\lambda}$	$\frac{\alpha}{\lambda^2}$
3.	Exponential $\lambda e^{-\lambda x} x \geq 0$	$1 - e^{-\lambda x}$	$\frac{1}{\lambda}$	$\frac{1}{\lambda^2}$

Table 1.2-1. Description of Several Probability Distributions (Continued)

	Probability Density Function f(x)	Cumulative Distribution Function F(x)	Expected Value μ	Variance σ^2
4.	Normal $N(\mu, \sigma^2)$			
	$\frac{1}{\sigma\sqrt{2\pi}} \exp\left[-\frac{(x-\mu)^2}{2\sigma^2}\right]$	$\int_{-\infty}^{x} f(\chi)\, d\chi$	μ	σ^2
	$-\infty \le x \le \infty$			
	but for WIPP PA			
	$a \le x \le b$ where $P(x > a) = 0.99$ and			
	$P(x > b) = 0.01$		$\mu = \frac{a+b}{2}$	$\left(\frac{b-a}{4.66}\right)^2$
5.	Lognormal		$\exp\left[\mu(y) + \frac{\sigma^2(y)}{2}\right]$	
	$\frac{1}{\sigma x\sqrt{2\pi}} \exp\left[-\frac{1}{2\sigma^2} (\ln x - \mu)^2\right]$	$\int_{o}^{x} f(\chi)\, d\chi$	Median $= e^{\mu(y)}$	$e^{2\mu(y)+\sigma^2}\left(e^{\sigma^2(y)} - 1\right)$
	$x \ge 0$			
	$x = e^y$ where $y = N(\mu, \sigma^2)$			
	but for WIPP PA			
	P(y>a) = 0.99 and			
	P(y>b) = 0.01		$\mu(y) = \frac{a+b}{2}$	$\sigma^2(y) = \left(\frac{b-a}{4.66}\right)^2$

Table 1.2-1. Description of Several Probability Distributions (Concluded)

	Probability Density Function f(x)	Cumulative Distribution Function F(x)	Expected Value μ	Variance σ^2
6.	Uniform		$\frac{a+b}{2} = \mu$	$\frac{(b-a)^2}{12}$
	$\frac{1}{b-a}$ $a \le x \le b$	$\frac{x-a}{b-a}$	$a = \mu - \sqrt{3\sigma}$ $b = \mu + \sqrt{3\sigma}$	
7.	Loguniform			
	$\frac{1}{x(\ln b - \ln a)}$	$\frac{\ln x - \ln a}{\ln b - \ln a}$	$\frac{b-a}{\ln b - \ln a}$	$(b-a)\left[\frac{(\ln b - \ln a)(b+a) - 2(b-a)}{2(\ln b - \ln a)^2}\right]$
	$a < x < b$		Median = $\sqrt{ab}$	
8.	Binomial (discrete)			
	$\frac{n!}{x!(n-x)!} p^x (1-p)^{n-x}$	$\sum_{\chi=0}^{x} f(\chi)$	np	np(1-p)
	$x = 0,1,2,...,N;$			
9.	Poisson (discrete)			
	$\frac{\mu^x e^{-\mu}}{x!}$ $x = 0, 1, 2, ..., \infty$	$\sum_{\chi=0}^{x} f(\chi)$	μ	μ

1.2.2 Empirical Distribution Functions

Empirical cdfs are histograms or piecewise constant functions based on percentiles derived from a set of measurements (data), or a set of subjective estimates of experts. For independent measurements (data) of some quantity, the empirical cdf is an unbiased estimator of the unknown population cdf of that quantity (Blom, 1989, p. 216); this property does not rigorously apply to empirical cdfs derived from subjective estimates of experts.

1.2.3 Range

The range of a distribution is denoted by (a,b), the pair of numbers in which a and b are respectively the minimum and maximum values that can reasonably be taken by the uncertain parameter X.

1.2.4 Mean and Sample Mean

The mean value (or, simply, *mean*) of a distribution is one measure of the central tendency of a distribution; it is analogous to the arithmetic average of a series of numbers. The population mean, μ, is defined by

$$\mu = \int_{-\infty}^{\infty} x f(x)\, dx \text{ for continuous distributions, or}$$

$$\sum_{\text{all } x_i} x_i f_i \text{ for discrete distributions.}$$

The *sample mean*, denoted by $\bar{x}$, is the arithmetic average of values in an empirical data set. A sample mean can also be assigned to empirical cdfs derived from subjective estimates of experts.

1.2.5 Median and Sample Median

The *median* value of a cdf is denoted by x_{50} and is that value in the range at which 50% of all values lie above and below (i.e., the 0.5 quantile). *Sample medians*, here denoted by $\bar{x}_{50}$, can be obtained directly from empirical cdfs in the obvious way.

1.2.6 Variance and Coefficient of Variation

The *variance* of a distribution, σ^2, is the second moment of the distribution about its mean, i.e.,

$$\sigma^2 = \int_{-\infty}^{\infty} (x-\mu)^2 f(x)\, dx \text{ for continuous distributions, or}$$

$$\sum_{\text{all } x_i} (x_i - \mu)^2 f_i \text{ for discrete distributions.}$$

The *standard deviation*, σ, is the positive square root of the variance. The coefficient of variation, the ratio of standard deviation to mean, σ/μ, is a convenient measure of the relative width of a distribution.

The *sample variance* of a set of measurements of parameter X, say X_1, X_2, X_3, ...X_N is the sum

$$\frac{1}{(N-1)} \sum_{n=1}^{N} (X_n - \bar{x})^2 .$$

The sample variance of independent measurements of some quantity is an unbiased estimator of the population variance of that quantity (Blom, 1989, p. 197). (A variance can also be formally calculated for empirical cdfs derived from subjective estimates of experts; this is not a sample variance, however.)

1.2.7 Categories of Distributions

Distributions used in this report are grouped into five categories:

1. Continuous analytical distributions: beta, normal, lognormal, uniform or loguniform (Figure 1.2-1a),
2. Discrete analytical distributions: Poisson (Figure 1.2-1b), binomial,
3. Constructed empirical distributions based on measurements (Figure 1.2-1b),
4. Constructed empirical distributions based on expert judgment ("Subjective Estimates," Figure 1.2-1b),
5. Miscellaneous categories (null distributions): constant, spatial, and table.

CONTINUOUS DISTRIBUTIONS

Four continuous, analytical distributions frequently used in this report are described below.

Normal

Normal designates the normal pdf, a good approximation to the distribution of many physical parameters. The normal distribution arises naturally from the central limit theorem (Johnson and Kotz, 1970a, p. 40; Miller and Freund, 1977, p. 104). For purposes of performance assessment, the distribution is arbitrarily truncated at the 0.01 and 0.99 quantities (i.e., the probability that the parameter will be smaller or larger is 1%), which corresponds to $\bar{x} \pm 2.33s$, where s is the sample standard deviation.

Lognormal

Lognormal designates a lognormal pdf, a distribution of a variable whose logarithm follows a normal distribution. The distribution is arbitrarily truncated at the 0.01 and 0.99 quantiles.

Uniform

Uniform designates a pdf that is constant in the interval (a,b) and zero outside of that interval.

Loguniform

Loguniform designates a loguniform pdf, a distribution of a variable whose logarithm follows a uniform distribution.

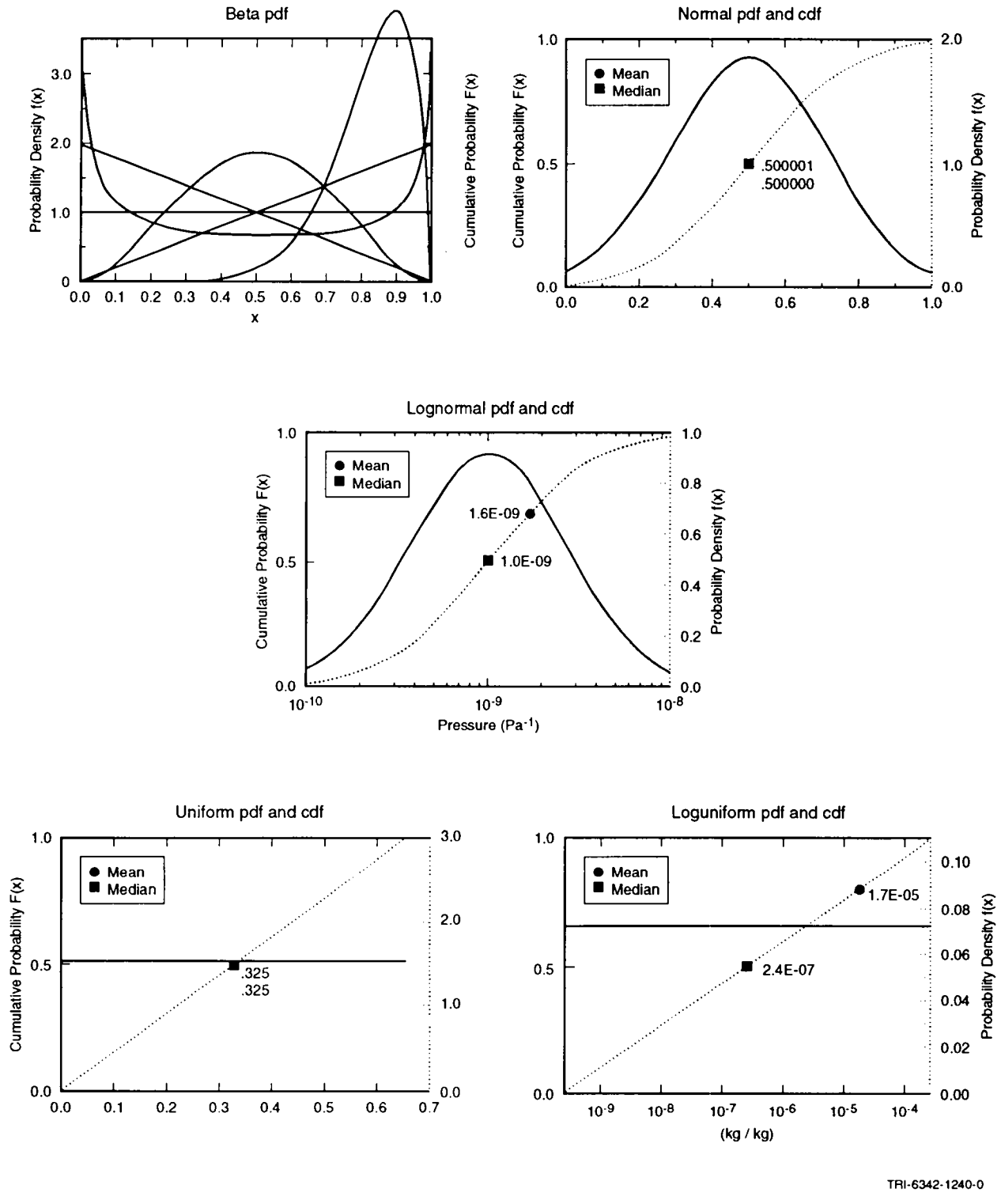

(a) Continuous Distribution Plots

Figure 1.2-1. Examples of distribution plots.

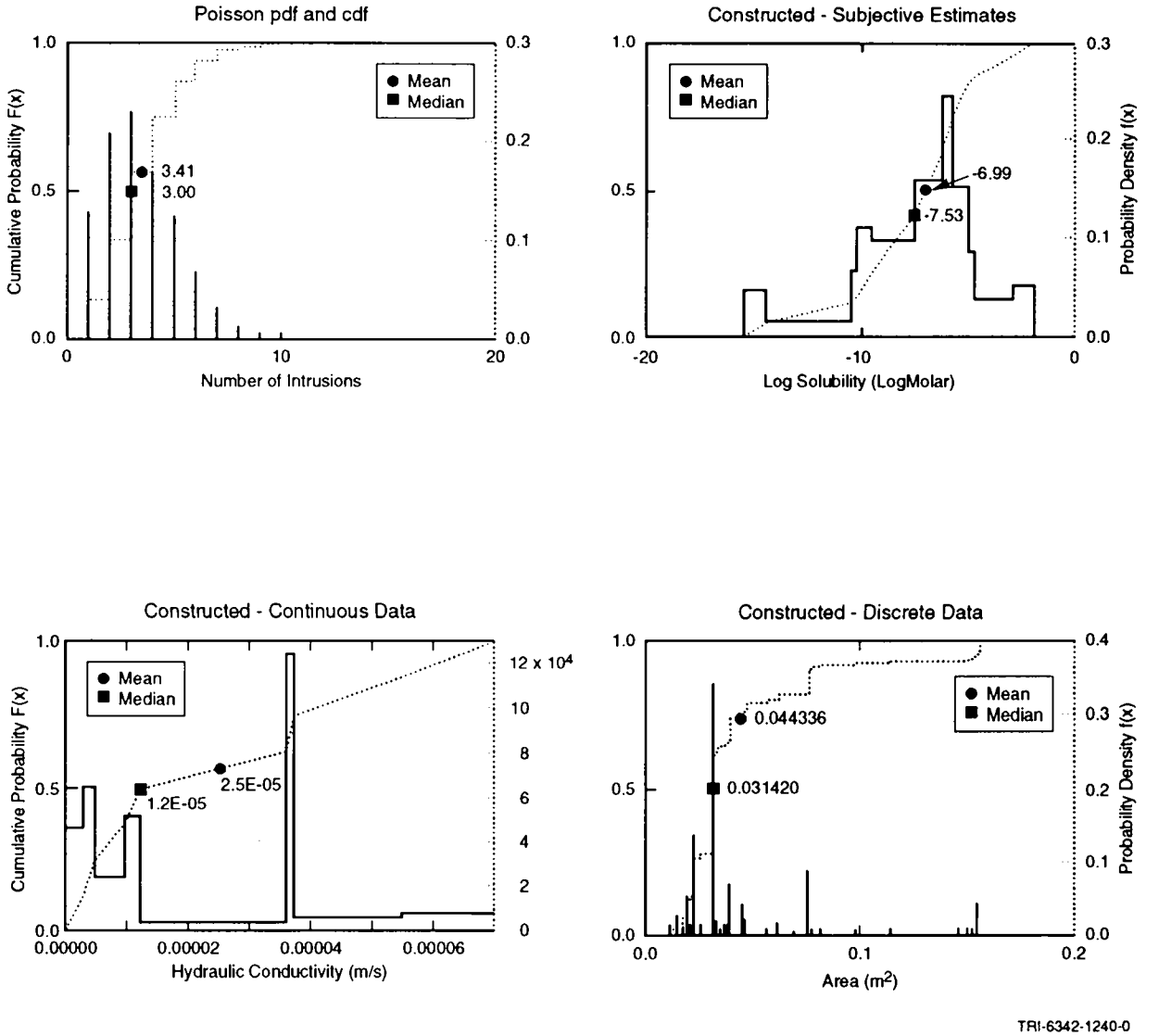

(b) Discrete and Constructed Distribution Plots

Figure 1.2-1. Examples of distribution plots (concluded).

DISCRETE DISTRIBUTIONS

A frequently used discrete distribution is the Poisson distribution (Figure 1.2-1b). The Poisson pdf is often used to model processes taking place over continuous intervals of time, such as the arrival of telephone calls at a switch station (queuing problem) or the number of imperfections per unit length produced in a bolt of cloth. The Poisson pdf was used in the 1991 probability model for human intrusion by exploratory drilling. The 1992 probability model for human intrusion incorporates effects of deterrence of markers and monuments; this model is based on generalized Poisson distributions (see Section 1.4.2).

CONSTRUCTED DISTRIBUTIONS (DATA)

A constructed distribution of the Data type is simply an empirical cdf constructed from sets of measured data points in the data base. For intrinsically discrete data, the empirical cdf is a piecewise-constant function resembling a histogram. For intrinsically continuous data, the empirical cdf is always converted to a piecewise-linear function by joining the empirical percentile points with straight lines; this is done to ensure that, in Monte Carlo sampling, the distribution of sampled parameter values will cover all of the range of the distribution (Tierney, 1990, p. II-5).

In some cases, the PA Department may modify constructed distributions of the Data type by extending the range of the data set to include estimated 0.01 and 0.99 quantiles. Since the range of measurements in a data set may not reflect the true range of the random variable underlying the measurements, the PA Department may estimate the range by $\bar{x} + 2.33s$, where $\bar{x}$ is the *sample* mean and s is the *sample* standard deviation. (The lower limit of this estimate is not allowed to be less than zero for an intrinsically positive variable: both the upper and lower limit are not allowed to exceed physical limits.) This estimate of range is justified by the fact that the indicated end-points are estimates of the 0.01 and 0.99 quantiles if the variable is normally distributed. If the variable is not normally distributed, the quantiles will differ in inessential ways (Table 1.2-2). For any distribution with finite mean and variance, Chebyshev's inequality states that the probability that the random variable x lies outside the interval $(\bar{x} - hs, \bar{x} + hs)$, $h > 0$, is a quantity less than $1/h^2$ (Blom, 1989, p. 121); i.e.,

$$P(|x - \bar{x}| \geq hs) \leq \frac{1}{h^2} . \qquad (1.2\text{-}1)$$

If the pdf of the unknown distribution is known to be unimodal and symmetric about the mean value, then the right-hand side of Eq. 1.2-1 can be replaced with $4/(9h^2)$ (Gauss' inequality); i.e.,

$$P(|x - \bar{x}| \geq hs) \leq \frac{4}{9h^2} . \qquad (1.2\text{-}2)$$

CONSTRUCTED DISTRIBUTIONS (SUBJECTIVE)

Constructed distributions of Subjective type are histograms based on subjective estimates of range (the 0 and 100 percentile) and at least one interior percentile point (usually the 50 percentile or median). The subjective estimates of percentile points are usually obtained directly from experts in the subject matter of the parameter of concern (see Section 1.3.1). Histograms for intrinsically continuous parameters are always converted to piecewise linear cdfs by joining the subjective percentile points with straight lines.

Whether a constructed distribution is of the subjective or data type should be evident from the discussion material on a parameter sheet.

Table 1.2-2. Probability of Parameters Lying within Range Defined by $\bar{x} \pm hs$ (after Harr, 1987, Table 1.8.2)

h	Chebyshev's Inequality	Gauss' Inequality	Exponential pdf	Normal pdf	Uniform pdf
1	0	0.56	0.86	0.68	0.58
2	0.75	0.89	0.95	0.96	1.00
2.33	0.82	0.92	0.964	0.9802	1.00
3	0.89	0.95	0.982	0.9973	1.00
4	0.94	0.97	0.993	0.99993	1.00

MISCELLANEOUS CATEGORIES

Other "null" categories of distributions are described below:

Constant

When a distribution type is listed as constant, a distribution has not been assigned and a constant value is used in all PA calculations.

Spatial

The spatial category of data indicates that the parameter varies spatially. This spatial variation is usually shown on an accompanying figure. The median value recorded is a typical value for simulations that use the parameter as a lumped parameter in a model; however, the value varies depending upon the scale of the model. The range of a spatially varying parameter is also scale dependent.

Table

The table category of data indicates that the parameter varies with another property and the result is a tabulated value. For example, relative permeability varies with saturation; its distribution type is listed as table (also, the median value is not meaningful and is therefore omitted in the table).

1.2.8 Key to Parameter Sheets

Characteristics of each of the 49 parameters sampled in the 1992 PA calculations are summarized in Parameter Sheets (Figure 1.2-2) for the convenience of the reader. Many other important parameters may also receive treatment in these Parameter (or Data) Sheets. A key to the meaning of the entries in a Parameter Sheet is provided below.

Parameter Sheets are divided by horizontal lines into four boxes. In the first box (top of page), there can be up to seven entries.

Parameter Sheet

Parameter:	**Threshold displacement pressure (p_t)**
Material:	halite and polyhalite within Salado Formation, [Salado, Press CTD]
Definition, Units:	Pa
Values:	Range: (2.3×10^5, 2.3×10^9) Median: 2.3×10^7
Distribution:	Lognormal
Correlation:	

Data Source(s):

Davies, P. B. 1991a. *Evaluation of the Role of Threshold Pressure in Controlling Flow of Waste-Generated Gas into Bedded Salt at the Waste Isolation Pilot Plant.* SAND90-3246. Albuquerque, NM: Sandia National Laboratories. (Investigator Judgment)

Davies, P. B. 1991b. Appendix A: "Uncertainty Estimates for Threshold Pressure for 1991 Performance Assessment Calculations Involving Waste-Generated Gas," *Preliminary Comparison with 40 CFR Part 191, Subpart B for the Waste Isolation Pilot Plant, December 1991. Volume 3: Reference Data.* WIPP Performance Assessment Division. Eds. R. P. Rechard, A. C. Peterson, J. D. Schreiber, H. J. Iuzzolino, M. S. Tierney, and J. S. Sandha. SAND91-0893/3. Albuquerque, NM: Sandia National Laboratories. A-37 through A-41. (Investigator Judgment)

Usage:

Mathematical model:

Section 1.4.1, this volume.

Equation 1.4.1-6.

Computational models:

BRAGFLO

Ranking in Past Sensitivity Analyses:

40 CFR 191	Low
40 CFR 268	Not tested
NEPA	Not tested
Other	Not applicable

Figure 1.2-2. Example of a parameter sheet.

- **Parameter:** The name of the parameter (e.g., "threshold displacement pressure"), followed by its mathematical symbol (e.g., "p_t") if appropriate.
- **Material:** The materials or subsystems in which the parameter applies (e.g. "halite and polyhalite within Salado Fm.) followed by the current (1992) names for the parameter in the secondary data base (e.g., "[Salado, Press CTD]").
- **Definition:** A short definition of the parameter may appear in this entry if there is the possibility of confusing the parameter with other quantities; usually, this entry is blank.
- **Units:** The physical units in which the parameter is measured (e.g., "Pa" or Pascals). Only SI units are used in the tables and secondary data base (except for radionuclide inventory activity, which is expressed in curies). Occasionally, for the sake of clarity, the parameter may also be expressed in the Values entry (see below) in terms of more familiar or intuitive units, e.g., years instead of seconds.
- **Values:** The values entry gives a snapshot of the range and median of the distribution of the parameter; e.g., in the values entry of the example,

  Range: $(2.3 \times 10^5, 2.3 \times 10^9)$ Median: 2.3×10^7.

- **Distribution:** The type of the distribution of the parameter using type names defined in Section 1.2.7. For example, "lognormal" is the continuous, analytical distribution defined in entry 5 of Table 1.2-1.
- **Correlation:** Names of other parameters with which the parameter in question is correlated. If this entry is blank, the parameter in question is assumed to be functionally and statistically independent of all other parameters.

The second box (from top of page) contains only one type of information.

- **Data Source(s):** A list of the primary documents supplying data and information used by PA Department staff in constructing the parameters distribution. (Documents judged to be secondary sources may be cited in Discussions that may follow each parameter sheet.) Each data-source entry is followed by a parenthetical characterization of the nature of the evidence or arguments in the source: the possible categories are

  1. *WIPP Observational Data.* Data from observational measurements made on site at the WIPP or in a laboratory in connection with the WIPP Project. These data are usually published as a formal report or a journal article, but in some cases may take the form of an internal Sandia memorandum.
  2. *Non-WIPP Literature Data.* General data for systems or processes that are similar to those occurring at the WIPP. These data may be found in formal non-WIPP reports, journal articles, or handbooks.
  3. *Investigator Judgment.* Evidence or arguments provided by Investigators within the WIPP Project after review of available observational data and relevant literature. Investigator judgment is often necessary because few hard quantitative data exist or existing data were measured on spatial and temporal scales that differ from PA model requirements.
  4. *Expert Panel Judgment.* Evidence or arguments provided by an Expert Judgment Panel, rather than an individual Investigator, after a comprehensive review of related information (e.g., WIPP reports, relevant literature).
  5. *General Engineering Knowledge.* Evidence or arguments based on engineering "rules of thumb," i.e., accepted engineering rules and practice whose validity has been endorsed by years of successful application but for which there are no consensuable (scientific) explanations.

The third box (from top of page) in a parameter sheet contains information on the use of the parameter in the several consequence or probability models employed by the PA Department.

- **Mathematical model:** General statements on use of the parameter are supplied in this entry. In the present volume on Model Parameters, the reader will be directed towards the appropriate subsections and equations in Section 1.4, "Background on 1992 Probability and Consequence Models."
- **Computational models:** A list of current computational models used by the PA Department that generally require specification of the parameter, starting with the name of the model that uses the parameter in the 1992 Preliminary Performance Assessment.

The last box of a Parameter Sheet (bottom of page) states the ranking of the sensitivity of a parameter with respect to sensitivity studies addressing three standards or regulations: 40 CFR 191, Subpart B; 40 CFR 268 (RCRA); and NEPA. The rankings are based largely on limited, formal sensitivity analyses performed in past years. Sensitivity analyses conducted during *40 CFR 191* studies are described in Helton et al., 1991, 1992; the *40 CFR 191* entries in the last box of a parameter sheet are based on rankings established in these studies. A recent sensitivity analysis conducted specifically for the *40 CFR 268* (RCRA) models (WIPP PA Department, 1992) was used to establish the entries under *40 CFR 268* in the last box of the parameter sheets. In these kinds of analyses, a parameter's sensitivity can be measured by the frequency-of-appearance and relative position of the parameter in rank-regression tables (see Helton et al., 1991, pg. III-45). A sampled parameter that does not appear in a rank-regression table could be termed insensitive; a parameter that appears frequently in the tables could be called sensitive, etc. This suggests the following notation for the ranking of a parameter.

- **Not applicable**: To mean that the parameter is judged not to be uncertain (or imprecisely known); the parameter is usually a high-precision constant such as a dimension of an engineered feature or a universal physical constant.
- **Not tested**: To mean that the parameter is judged to be uncertain but has not yet been selected for sampling, i.e., tested, in a sensitivity study. (See Chapter 6 for procedures used in selecting parameters for sampling in sensitivity studies.)
- **Low:** To mean that the parameter has been tested in sensitivity studies and either did not appear, or appeared infrequently and in low-order, in the studies' rank-regression tables.
- **Medium:** To mean that the parameter has been tested in sensitivity studies and appeared frequently in the studies' rank-regression tables.
- **High:** To mean that the parameter has been tested in sensitivity studies and has consistently appeared as one of the top-ranking entries in the studies' rank-regression tables.

1.3 Background on Selecting Parameter Distributions

1.3.1 Requests for Data from Sandia Investigators and Analysts

When evaluating long-term performance, the PA Department follows a well-defined procedure for acquiring and controlling the data used in consequence and probability models. A data base, called the secondary data base, contains the interpreted data and in essence embodies the PA Department's conceptual model(s) of the disposal system (Rechard, 1992). The data provided in this report are from the secondary data base as of April 1992 and are used in the 1992 preliminary performance assessment of the WIPP (Volume 1 of this report).

The major sources of the data are the task leaders and investigators at Sandia and Westinghouse Electric Corporation.

IDENTIFY NECESSARY DATA

Each year, the PA Department identifies data that are necessary to perform the calculations for the preliminary performance assessment. Members of the department may informally compile data from published reports, personal communications with investigators, and other sources.

REQUEST MEDIAN VALUE AND DISTRIBUTION

The PA Department then requests that the investigators provide either new data or a median value and distribution for each parameter in a large subset of the parameters. Some model parameters are specific to the PA calculations and so individuals in the PA Department are considered the experts for these parameters (e.g., probability model parameters).

Initially, Sandia investigators are responsible for providing data or--if data are unavailable--distributions for all parameters. As this procedure for acquiring data is repeated, a few parameters are evaluated through formal elicitation.

UPDATE SECONDARY DATA BASE

The PA Department enters the endorsed or elicited data for all parameters into the secondary data base. The PA Department then either constructs parameter distributions or uses distributions provided by investigators; the PA Department selects a subset of these parameters to sample, keeping all other values constant at their *median* values, unless specifically noted.

PERFORM CONSEQUENCE SIMULATIONS AND SENSITIVITY ANALYSES

The PA Department runs consequence simulations and sensitivity analyses with selected subsets of data from the updated secondary data base. The sensitivity analysis evaluates the sensitivity of a parameter in determining variation of the result (i.e., a complementary cumulative distribution function [CCDF]). During this time, the PA Department prepares a report that lists parameters in the secondary data base at the time of these calculations (i.e., this data report).

DETERMINE WHETHER PARAMETER IS IMPORTANT IN ANALYSIS

By means of the sensitivity analyses, the PA Department can determine whether the parameter is significant in the calculations. If the parameter does not appear to be significant in the sensitivity analyses, and the review process of the Parameter Report does not question the parameter value, then a flag is set in the secondary data base for that parameter to indicate that it is not likely either to change or be sampled in forthcoming sensitivity studies.

1.3.2 Construction of Distributions

The steps below describe the procedure developed by the PA Department to construct probability distributions (cdfs) for the uncertain parameters in consequence and probability models (Figure 1.3-1) (modified from Tierney, 1990).

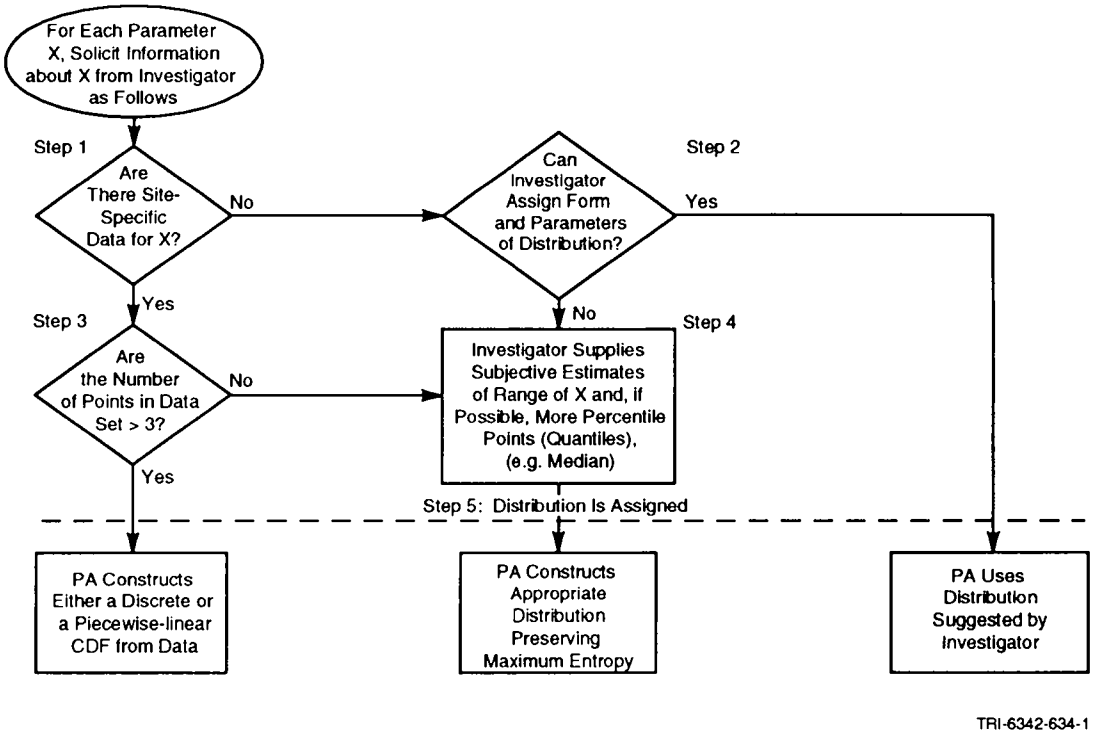

Figure 1.3-1. Five-step procedure used to construct cumulative distribution functions (cdfs) for the 1992 performance simulations. Investigator refers to expert in subject matter (after Tierney, 1990).

STEP 1

Determine whether site-specific data for the parameter in question exist, i.e., find a set of site-specific sample values of the parameter. Data and information are usually either documented in a formal report or are described in an internal memorandum (see Appendix A). If data sets exist, go to Step 3; if no data sets are found, go to Step 2.

STEP 2

Request that the investigator supply a specific shape (e.g., normal, lognormal) and associated numerical parameters for the distribution of the parameter. If the investigator assigns a specific shape and numerical values for the distribution's parameters, go to Step 5; if the investigator cannot assign a specific shape and appropriate parameters, go to Step 4. In responding to this request, the investigator may use his or her knowledge of global data to form an answer. Distributions supplied by investigators may be documented by a memorandum (see Appendix A).

STEP 3

Determine the size of the combined data sets. If the number of values in the combined data set is >3, use the combined data to construct a piecewise-linear cumulative distribution function or, alternatively, a discrete cumulative distribution function, and then go to Step 5. If the number of variables in the combined data set is ≤3, go to Step 4.

STEP 4

Request that the investigator provide subjective estimates of (a) the range of the variable (i.e., the minimum and maximum values taken by the variable with at least 99% confidence and preferably 100% confidence) and (b) if possible, one of the following (in decreasing order of preference): (1) percentile points for the distribution of the variable (e.g., the 25th, 50th [median], and 75th percentiles), (2) the mean value and standard deviation of the distribution, or (3) the mean value. Again, in responding to this request, the investigator may use his or her knowledge of global data to form an answer and may document that answer in a memorandum (see Appendix A). Then, using the maximum entropy formalism (MEF), construct one of the following distributions depending upon the kind of subjective estimate that has been provided (Tierney, 1990; Harr, 1987):

- Uniform probability distribution function (pdf) over the range of the variable,
- Piecewise-linear cdf based on the subjective percentiles,
- Exponential pdf (truncated) based on the subjective range and mean value,
- Normal pdf based on subjective mean value and standard deviation.

Then go to Step 5.

STEP 5

End of procedure; distribution is assigned. Computational considerations and limitations on the data itself may require later modification to some distributions. Some of these limitations are discussed in the next section.

1.3.3 Some Limitations on Distributions

The major limitations on ensuring the validity of the probability distributions assigned to parameters in the 1992 Preliminary Performance Assessment are thought to be a consequence of two acts:

- The equating of spatial variability with model parameter uncertainty, particularly for that class of parameters called material-property parameters.
- The neglect of obvious correlations between model parameters.

The following arguments attempt to explain these limitations, i.e., they show why some of the current assignments of probability distributions to material-property parameters of WIPP performance models may be unnecessarily conservative, given the present level of detail and spatial resolution of the models. Current methods of assigning uncertainty to some of the material-property parameters (e.g., including small-scale spatial variability as a source of uncertainty) may distort results of sensitivity analyses and entail unnecessary expense, but will probably not affect validity of results of the uncertainty analyses that are used to make preliminary comparisons with EPA standards.

NO SCALING OF VARIABILITY FOR MATERIAL-PROPERTY PARAMETERS

WIPP performance models described in Volume 2 of this report are based on the numerical solution of one or more of three types of equations:

(a) Partial differential equations - which are reduced to a set of algebraic equations or ordinary differential equations in order to effect a solution by finite-difference or finite-element methods. Examples: the equations of groundwater and brine flow, solute transport, gas flow, and salt creep (see Sections 1.4.1, 1.4.5, and 1.4.6).

(b) Ordinary differential equations - which may be the result of a reduction of a partial differential equation or may directly model the dynamics of a lumped-parameter system, e.g., punctured brine reservoirs, leaching and decay of radioactive waste stored in a panel (see Section 1.4.4).

(c) Algebraic equations of the form

$$F(x_1, x_2, x_3, ..., x_n; y) = 0$$

which may arise indirectly from equilibrium solutions of ordinary differential equations (i.e., solutions for time $\rightarrow \infty$) or may directly express a model of some physical relationship between WIPP performance-model variables (x_1, x_2, x_3, ..., x_n) and y (see Section 1.4.3).

In addition to dependent variables and independent variables of position and time, certain constant quantities will appear in each of the three types of equations. Such constants can be called "free" parameters because they may freely be specified by the user of the equations in which they appear. In most cases, these free parameters are intended to represent physical and chemical properties of real materials of the WIPP system: e.g., the hydraulic conductivity, porosity, and specific storage in models of fluid flow in the Salado Formation; the fracture spacing, dispersivity, diffusivity, and chemical distribution coefficients in models of solute transport in the Culebra Formation; the porosity, permeability and solubility of waste forms emplaced in a typical WIPP panel. This kind of parameter will be called a *material-property parameter* in the remainder of this section.

Many of the material-property parameters of WIPP performance models have been included in the set of uncertain variables sampled in recent studies of variable sensitivity of performance models (for example, Helton et al., 1991). (Note: In these studies, all uncertain model parameters were usually called "variables" or "independent variables.") In these studies, uncertainty associated with a sampled parameter was quantified by assigning an empirical or subjective probability distribution to the values taken on by that parameter within a predetermined range of values. Current procedures for the assignment of probability distributions were described in the previous section.

The distribution of a material-property parameter needs to reflect spatial variability of the material property and also the scale of the model. The zones or cells of numerical models (finite-element, finite-difference, or lumped-parameter models) must be few in number in order to minimize computational time and expense; in a typical problem involving geologic media, these cells will have dimensions of tens of meters or more and volumes of thousands of cubic meters. Material-property parameters must therefore represent the effects of a physical or chemical property of matter in these relatively large, arbitrarily defined volumes of space. It follows that material-property parameters are model dependent and usually not observable quantities, i.e., quantities that can be measured in the field or in the laboratory. On the other hand, with few exceptions (e.g., formation transmissivity measured by pumping tests) most physical and chemical properties of geologic or anthropogenic materials are actually measured on spatial scales typical of the laboratory or an exploratory borehole, a matter of at most a few tens of centimeters. In addition, natural materials and many man-made materials (e.g., defense waste) tend to be inhomogeneous on spatial scales that are smaller than the scales that characterize model cell sizes; accordingly, a set of measurements of a material property taken randomly from large volumes of real material may show wide variability. The question is: How to assign values to material-property parameters in a way that correctly reflects both cell size and the small-scale variability that may appear in measurements of the corresponding material property?

One way of approaching the problem of scaling is as follows. Assume that the material property can be represented as a scalar field in space, say $\phi(x)$, where $\mathbf{x} = (x,y,z)$ denotes position in space. (The assumptions of a scalar quantity in three dimensions are for the sake of simplicity of argument and involve no loss of generality; the property could be a vector or tensor.) It is argued in some modern textbooks that the material-property parameter, say Φ, to be used in type (a) equations (above) should be taken as a spatial average of ϕ over the cell or zone; for instance, in a cell or zone of volume V,

$$\Phi(V) = \frac{1}{V}\int_V \phi(\mathbf{x})\, d\mathbf{x} \tag{1.3-1}$$

where dx is the volume element dxdydz. (Again, no loss of generality is involved; a line or surface average could replace the volume average.) The arguments for this choice of material-property parameter are highly technical and limitations of time and space preclude their inclusion in this note; however, see the discussion in de Marsily (1986, Chapter 3 and Section 4.4).

To account for spatial variability of $\phi(\mathbf{x})$, it can be assumed that ϕ is a *stationary, random scalar field* within a cell volume V, with realizations $\phi(\mathbf{x},\mu)$ and the following statistical properties:

$$\text{Expectation of } \phi(\mathbf{x}, \mu) = E[\phi(\mathbf{x})] = \bar{\phi}, \text{ a constant,} \tag{1.3-2}$$

and

$$\begin{aligned}\text{Covariance of } \phi(\mathbf{x}, \mu) &= E\{ [\phi(\mathbf{x}) - \bar{\phi}] [\phi(\mathbf{y}) - \bar{\phi}] \} \\ &= \sigma^2 \rho(|\mathbf{x} - \mathbf{y}|) \quad ,\end{aligned} \tag{1.3-3}$$

where σ^2 is a constant (called the *variance* of ϕ), and $\rho(\bullet)$ is a function of $r = |\mathbf{x} - \mathbf{y}|$ with the properties,

$$\begin{aligned}&\rho(r) \geq 0 \text{ for } r \in (0,\infty) \ , \\ &\rho(r) \to 1 \text{ as } r \to 0 \ , \\ &\rho(r) \to 0 \text{ as } r \to \infty \ .\end{aligned} \tag{1.3-4}$$

The function $\rho(\bullet)$ is called the *autocorrelation function* (Yaglom, 1962); it is a measure of the statistical dependence of the values of ϕ measured at two different points x and y. The stationarity assumptions of constant mean value $\bar{\phi}$ and variance σ^2 can be slightly weakened by allowing these quantities to depend on the coordinates of the center of the volume V, i.e., $\bar{\phi}$ and σ^2 may vary from cell to cell.

Treating $\phi(\mathbf{x})$ as a stationary random field with statistical properties 1.3-2 through 1.3-4 allows estimates of the mean value and variance of the volume average of ϕ, $\Phi(V)$, to be made. It is shown in textbooks (see for instance Yaglom, 1962, pgs. 23-24) that

$$\text{Expectation of } \Phi(V) = E[\Phi(V)] = \bar{\phi}, \tag{1.3-5}$$

and

$$\text{Variance of } \Phi(V) = \frac{\sigma^2}{V^2}\int_V\int_V \rho(|\mathbf{x} - \mathbf{y}|)\, d\mathbf{x}\, d\mathbf{y}. \tag{1.3-6}$$

If $\bar{\phi}$, σ^2 and $\rho(r)$ were known, the problem would be essentially solved in that the distribution of the material-property parameter, $\Phi(V)$, could be approximated by a normal distribution with mean and variance given respectively by Eqs. 1.3-5 and 1.3-6. In general, $\bar{\phi}$, σ^2 and the function $\rho(r)$ must be estimated using sets of spatially coordinated measurements of the material property ϕ, say $(\phi_1, \phi_2, ..., \phi_N)$. The estimators of $\bar{\phi}$ and σ^2 are the usual unbiased estimators of mean and variance (see Tierney, 1990, pp. II-4,5) and, given a sufficiently large set of spatially coordinated measurements of ϕ, approximations to the autocorrelation function could be constructed and used in

numerical evaluations of the volume integrals in Eq. 1.3-6. This ideal solution to the problem cannot be implemented, however, since there are few measurements of the material properties appearing in WIPP performance models (and most are not spatially indexed; measured transmissivity, grain density, porosity, and tortuosity of the Culebra Formation are exceptions). Thus, one must try to use available measurements and insight to infer the statistical properties, given by Eqs. 1.3-5 and 1.3-6, of material-property parameters, $\Phi(V)$. Examples of attempts to treat uncertainty in material-property parameters are given in the treatments of Salado Formation permeabilities and far-field pore pressures in Sections 2.3 and 2.4 of this volume. The following general observations may also be useful in inferring statistical properties of material-property parameters.

(1) The variance of a material-property parameter is less than or equal to the apparent variance of the material property. Note that because of the properties of $\rho(r)$ (Eq. 1.3-4), the integrand in the double volume integral of Eq. 1.3-6 is always less than one so that

$$\text{Variance of } \Phi(V) \leq \sigma^2 .$$

In particular, if the special form of autocorrelation function is taken ("cookie cutter"),

$$\begin{aligned} \rho(|x-y|) &= 1 \text{ if } |x-y| \leq a, \\ &= 0 \text{ otherwise,} \end{aligned} \tag{1.3-7}$$

then

$$\text{Variance of } \Phi(V) \approx \frac{v}{V}\sigma^2 , \tag{1.3-8}$$

where $v = \frac{4\pi}{3} a^3$ can be called the *volume of correlation*. Equation 1.3-8 suggests that if the volume of correlation is <<V, then the distribution of $\Phi(V)$ is peaked about the mean value of the material property, $\bar{\phi}$. If the coefficient of variation of the material property, $\sigma/\bar{\phi}$, is not large (say, of the order of one), the distribution of $\Phi(V)$ is more sharply peaked about the mean value, $\bar{\phi}$, than is the distribution of the material property, $\phi(x)$. If this tendency is strong enough, then $\Phi(V)$ can simply be assigned the mean value,

$$\Phi(V) \approx \bar{\phi} .$$

This is what is usually done in studies with numerical models that are not probabilistic; that is, not directed explicitly towards sensitivity and uncertainty analyses.

(2) If, as suggested above, $\Phi(V) \approx \bar{\phi}$, then one must consider the uncertainty inherent in estimating the mean value $\bar{\phi}$, that arises from (a) a limited number of measurements of the material property, and (b) relationships between $\bar{\phi}$ and other uncertain problem parameters. Uncertainty of type (a) can be handled by fitting available data to a "t-distribution" (Blom, 1989) which, in a Bayesian approach, gives the distribution of the true mean of the material property about the sample mean of measurements. However, this was not done in assigning ranges to parameters in the 1992 exercise. Uncertainty of type (b) is usually model dependent and must be handled on a case-by-case basis (see remarks on correlations below).

The standard techniques of statistical estimation cannot be directly applied when the distribution of the material property, $\phi(x)$, must be gained by subjective means, i.e., the elicitation of expert judgment. In such cases, the PA Department must make the assumption that the distribution of the material property, $\phi(x)$, is also the distribution of the material-property parameter, $\Phi(V)$. Instances where this assumption was made are found in the sections on waste-form solubility (3.3.5) and Culebra sorption coefficients (2.6).

GENERAL ABSENCE OF CORRELATIONS AMONG PARAMETERS

Most of the 49 parameters varied during the 1992 Preliminary Performance Assessment exercise were assumed to be independent random variables even though it was known that some were dependent upon others, i.e., correlated in some way. Correlations of the model variables may arise from the fact that there are natural correlations between the local quantities used to determine the form of the model variable (e.g., local porosity could be strongly correlated with local permeability); or correlations of model variables may be implicit in the form of the mathematical model in which they are used. The effects of neglecting correlations on the sensitivity/uncertainty analyses are generally unknown.

In some instances (Sections 2.3.5, 2.4.5) an attempt was made to induce known correlations by the adjustment of the ranges of distributions; in other cases (threshold displacement pressure in Section 2.4.1), perfect correlation was simply assumed.

1.3.4 Selection of Parameters for Sampling

For the 1992 preliminary performance assessment of the WIPP, the 49 parameters that were selected for variation (sampling) together with a brief description of why they were selected are discussed in Chapter 6. Other studies on subsystems of the WIPP disposal system (e.g., sensitivity of the repository to gas generation) may use different subsets of the approximately 300 parameters for which distributions are reported herein.

1.4 Background on 1992 Probability and Consequence Models

A majority of the parameters described in the present volume specify constants or material-property parameters (Section 1.3.3) that appear in the mathematical formulations of seven consequence or probability models used in the 1992 Preliminary Comparison exercise. The models are described in detail in Volume 2 of this report. In the present section, a link between Volume 2 and the data and distributions of Volume 3 is made by providing brief descriptions of the governing equations for each model and later noting in a Parameter Sheet where each parameter fits in a numbered model equation. The seven models to be described are

- A model of two-phase flow in backfilled repository openings and the Salado Formation (BRAGFLO),
- A model of human intrusion in the presence of markers and monuments (a part of the CCDFPERM code),
- A model of borehole cuttings removal (CUTTINGS),
- A model of radionuclide discharge from a brine-flooded panel (PANEL),
- A model of fluid flow in the Culebra (SECO2D),
- A model of solute transport in the Culebra (SECO/TP),
- A model of deformation of waste-filled room (SANCHO).

1.4.1 Two-Phase Flow: BRAGFLO

Study of the effects of gas on the flow of brine through the repository and up an intrusion borehole require a computational model that simulates two-phase flows through porous, heterogeneous reservoirs. The PA Department uses a model developed in-house for Sandia National Laboratories and called BRAGFLO. The governing equations for BRAGFLO are presented in this section. Conceptual models of two-phase flow are further described in Section 7.2 and Appendix A of Volume 2 of this series of reports.

BRAGFLO solves simultaneously the partial differential equations (PDEs) that describe the mass conservation of each mobile component (gas and brine) along with appropriate constraint equations, initial conditions, and boundary conditions. The fundamental equations can be found in Peaceman (1977) and Crichlow (1977). A total of five independent equations (two component mass conservation PDEs and three constraints) can be written to define the two-phase flow phenomena:

Gas Component Conservation:

$$\nabla \bullet \left[\frac{\alpha \rho_n K k_{rn}}{\mu_n} \left(\nabla P_n - \rho_n g \nabla D \right) + \frac{\alpha C_{Nw} \rho_w K k_{rw}}{\mu_w} \left(\nabla P_w - \rho_w g \nabla D \right) \right] + \alpha q_n + \alpha q_{rn} \qquad (1.4.1\text{-}1)$$

$$= \alpha \frac{\partial \left(\phi \rho_n S_n + \phi C_{Nw} \rho_w S_w \right)}{\partial t} \ ,$$

Brine Component Conservation:

$$\nabla \bullet \left[\frac{\alpha C_{Ww} \rho_w K k_{rw}}{\mu_w} \left(\nabla P_w - \rho_w g \nabla D \right) \right] + \alpha q_w + \alpha q_{rw} = \alpha \frac{\partial \left(\phi C_{Ww} \rho_w S_w \right)}{\partial t} \ , \qquad (1.4.1\text{-}2)$$

Saturation Constraint:

$$S_n + S_w = 1 \ , \qquad (1.4.1\text{-}3)$$

Mass Fraction Constraint:

$$C_{Nw} + C_{Ww} = 1.0 \ , \qquad (1.4.1\text{-}4)$$

Capillary Pressure Constraint:

$$P_n - P_w = P_c \ , \qquad (1.4.1\text{-}5)$$

where the quantities in Eqs. 1.4.1-1 through 1.4.1-5 have the following meanings:

(Note that starred [*] quantities are given extended discussion below.)

	$C_{M\ell}$	mass fraction of component M dissolved or miscible in phase ℓ,
	g	gravitational acceleration constant [Lt^{-2}], [m s^{-2}],
	K	absolute permeability of the reservoir [L^2], [m^2],
*	$k_{r\ell}$	relative permeability to phase ℓ [dimensionless],
*	P_c	capillary pressure [$ML^{-1}t^{-2}$], [Pa],
	P_ℓ	pressure of phase ℓ [$ML^{-1}t^{-2}$], [Pa],
	q_ℓ	mass rate of well injection (or production, if negative) per unit volume of reservoir [$ML^{-3}t^{-1}$], [kg m^{-3} s^{-1}],
*	$q_{r\ell}$	mass rate of products produced (or reactant consumed, if negative) per unit volume of reservoir due to chemical reaction [ML^{-3} t^{-1}], [kg m^{-3} s^{-1}],
	S_ℓ	saturation of phase ℓ [dimensionless],

	x,y	spatial dimensions (x-horizontal, y-vertical),
	α	geometric factor (in three dimensions, $\alpha = 1$; in two dimensions, α = length; in one dimension, α = area,
	∇	gradient, shorthand for vector $\partial/\partial x$, $\partial/\partial y$ in two dimensions,
	$\nabla\bullet$	divergence, shorthand for $\partial/\partial x + \partial/\partial y$ in two dimensions,
*	ϕ	reservoir porosity [dimensionless],
	ρ_ℓ	density of phase ℓ [$M^1 L^{-3}$], [kg^1 m^{-3}],
	μ_ℓ	viscosity of phase ℓ [ML^{-1} t^{-1}], [cp].

Subscripts:

N	nonwetting component (gas component),
n	nonwetting phase (gas phase),
W	wetting component (brine component),
w	wetting phase (brine phase).

NOTES ON RELATIVE PERMEABILITY AND CAPILLARY PRESSURE

Brooks and Corey (1964) observed that the effective saturation of a porous material, s_e, can be related to the capillary pressure, p_c, by

$$p_c = \frac{p_t}{s_e^{1/\lambda}}, \qquad (1.4.1\text{-}6a)$$

where

p_t = threshold displacement pressure,

λ = Brooks and Corey exponent.

Brooks and Corey defined s_e as

$$s_e = \frac{s_\ell - s_{\ell r}}{1 - s_{\ell r}},$$

where s_ℓ is the wetting phase saturation (brine) and $s_{\ell r}$ is the residual wetting phase saturation, below which the wetting phase no longer forms a continuous network through the pore network and therefore does not flow, regardless of the pressure gradient. This has been modified to account for residual (or critical) gas saturation, s_{gr}:

$$s_e = \frac{s_\ell - s_{\ell r}}{1 - s_{gr} - s_{\ell r}}. \qquad (1.4.1\text{-}7a)$$

The relative permeability of the wetting phase ($k_{r\ell}$) is obtained from

$$k_{r\ell} = s_e^{\frac{2+3\lambda}{\lambda}} . \qquad (1.4.1\text{-}8a)$$

For the gas phase, the relative permeability (k_{rg}) is

$$k_{rg} = (1 - s_e)^2 \left(1 - s_e^{\frac{2+\lambda}{\lambda}}\right) . \qquad (1.4.1\text{-}9a)$$

Alternative analytic forms for effective saturation, capillary pressure, and relative permeabilities were suggested by Webb (April 30, 1992, Memo in Appendix A) and were tested in the 1992 sensitivity analyses. These forms are based on the Van Genuchten-Parker model of two-phase characteristic curves (Van Genuchten, 1978; Parker et al., 1987). The effective saturation takes the form

$$s_e = \frac{s_\ell - s_{\ell r}}{s_{\ell s} - s_{\ell r}} , \qquad (1.4.1\text{-}7b)$$

where $s_{\ell s}$ is the maximum wetting-phase saturation (taken as 1 - s_{gr} by the PA Department, where s_{gr} is critical gas saturation). The capillary pressure takes the form,

$$P_c = P_o \left[S_e^{-1/m} - 1\right]^{1-m} , \qquad (1.4.1\text{-}6b)$$

where $m = \lambda/(1+\lambda)$, λ is the Brooks and Corey exponent (Eq. 1.4.1-6a), and P_o is a constant determined by equating Eq. 1.4.1-6b to Eq. 1.4.1-6a at $S_e = 0.5$. The alternative relative permeabilities take the forms:

$$k_{r\ell} = s_e^{1/2} \left[1 - \left(1 - s_e^{1/m}\right)^m\right]^2 , \qquad (1.4.1\text{-}8b)$$

$$k_{rg} = \left(1 - s_e\right)^{1/2} \bullet \left(1 - s_e^{1/m}\right)^{2m} . \qquad (1.4.1\text{-}9b)$$

NOTES ON GAS-GENERATION TERMS

The terms q_{rn}, q_{rw} appearing in Eqs. 1.4.1-1 and 1.4.1-2 are sums of production (or consumption) terms for two processes: corrosion and microbial degradation. The contributing terms for each process are discussed below.

Gas Production and Brine Consumption from Corrosion of Steel

Let

q_{CH_2} = rate of H_2 production by corrosion per unit volume of panel (kg/m^3•s),

q_{CH_2O} = rate of H_2O consumption by corrosion per unit volume of panel (kg/m^3•s).

These rates are calculated by Eqs. 1.4.1-10 and 1.4.1-11 below,

$$q_{CH_2} = (k_{CI}\ S_\ell + k_{CH}\ S_g)\,(X_{CH_2})\,(M_{H_2})\,, \tag{1.4.1-10}$$

$$q_{CH_2O} = \frac{q_{CH_2} \bullet (X_{CH_2O})\ (M_{H_2O})}{(X_{CH_2})\ (M_{H_2})}\,, \tag{1.4.1-11}$$

where

k_{CI} = rate constant for corrosion under inundated conditions [mole Fe/(m^3-panel•s)],

k_{CH} = rate constant for corrosion under humid conditions [mole Fe/(m^3-panel•s)],

S_ℓ, S_g = liquid (brine) and gas saturations (dimensionless),

X_{CH_2} = corrosion stoichiometry factor for H_2 (mol H_2/mol Fe),

X_{CH_2O} = corrosion stoichiometry factor for H_2O (mol H_2O/mol Fe),

M_{H_2} = molecular weight for H_2 expressed as (kg/mole),

M_{H_2O} = molecular weight for H_2O expressed as (kg/mole).

The quantities k_{CI}, k_{CH}, X_{CH_2} and X_{CH_2O} are expressed in terms of secondary data base parameters by the relations

$$k_{CI} = \frac{\dot{n}'_{CI}\ A_d\ n_d}{X_{CH_2}\ V_{pf}}\quad,\quad k_{CH} = f\ k_{CI}\,, \tag{1.4.1-12}$$

and

$$X_{CH_2} = \frac{(4-x)}{3}\quad,\quad X_{CH_2O} = -\frac{(4+2x)}{3}\,. \tag{1.4.1-13}$$

In Eq. 1.4.1-12,

$$f = \dot{n}'_{CH}/\dot{n}'_{CI} = \text{the relative humid gas production rate by corrosion,} \tag{1.4.1-14}$$

and

$\dot{n}'_{CI}$ = rate of H_2 production by corrosion, inundated conditions [mol H_2/(m^2-surface steel)•s],

$\dot{n}'_{CH}$ = rate of H_2 production by corrosion, humid conditions [mol H_2/(m^2-surface steel)•s],

A_d = surface area of steel in an equivalent drum, including both drum and its contents (m^2),

n_d = number of equivalent drums in a generalized waste region (dimensionless),

V_{pf} = volume of generalized waste region.

Note: A "generalized waste region" can be either a room, a panel, or the entire repository, depending upon the purposes of the calculation. The parameters A_d, n_d, and V_{pf} were constants in the 1992 calculations with BRAGFLO.

In Eq. 1.4.1-13,

x = the anoxic, iron-corrosion stoichiometric factor, a dimensionless number between zero and one. (1.4.1-15)

Gas Production from Microbial Degradation

Let

q_{BH_2} = rate of H_2 production by biodegradation of cellulosics per unit volume of panel ($kg/m^3 \cdot s$).

This rate is calculated from Eq. 1.4.1-16 below,

$$q_{BH_2} = k_{BI}\, S_\ell + k_{BH}\, S_g \left(S_{BH_2}\right)\left(M_{H_2}\right) \quad , \tag{1.4.1-16}$$

where

k_{BI} = rate constant for biodegradation of cellulosics under inundated conditions [mole cellulosics/(m^3 panel•s)],

k_{BH} = rate constant for biodegradation of cellulosics under humid conditions [mole cellulosics/(m^3 panel•s)],

S_{BH_2} = biodegradation stoichiometric factor for H_2 (mole H_2/mole cellulosics),

and other quantities appearing in Eq. 1.4.1-16 have been defined in Part A. The quantities k_{BI} and k_{BH} are expressed in terms of other secondary data base parameters in a manner similar to Part A:

$$k_{BI} = \frac{\dot{n}_{BI} \bullet n_d \bullet v_d \bullet f_c \bullet \rho_c}{S_{BH_2} \bullet V_{pf}}, \qquad k_{BH} = \xi\, k_{BI} \tag{1.4.1-17}$$

New quantities in Eq. 1.4.1-17 are

v_d = internal volume of equivalent drum (m^3),

f_c = volume fraction of cellulosics in undisturbed drum (dimensionless),

ρ_c = effective density of cellulosics in undisturbed drum (kg/m^3),

$\dot{n}_{BI}$ = rate of gas production by biodegradation, inundated conditions [mole gas/(kg-cellulosics•s)],

$\dot{n}_{BH}$ = rate of gas production by biodegradation, humid conditions [mole gas/(kg-cellulosics•s)], which is implicitly defined by

$$\xi = \dot{n}_{BH}/\dot{n}_{BI} = \text{relative humid gas production rate by microbial degradation.} \qquad (1.4.1\text{-}18)$$

NOTE ON RESERVOIR POROSITY

The "reservoir" in the two-phase flow model can be comprised of many different materials (named on Figure 1.4-1), each of which is assigned usually different porosities and absolute permeabilities. With one exception, material porosities and absolute permeabilities are assumed to be imprecisely known constants because the present version of the two-phase flow model cannot account for changes in material properties owing to pressurization or rock deformation. The one exception is the porosity of the generalized waste region, which was independently modeled in 1992 as a function of time and total volumes of gas generated by corrosion and microbial action (Figure 1.4-2).

Mendenhall and Lincoln (February 28, 1992, Memo in Appendix A) estimated waste region porosity as a function of time and volume-of-gas space using the SANCHO code (Stone et al., 1985) and baseline data provided by Beraún and Davies (September 2, 1991, Memo in Appendix A). SANCHO is a finite-element computer program for simulating the quasistatic, large-deformation, inelastic response of two-dimensional solids. In the present application, the two-dimensional solid is a waste-filled disposal room imbedded in a much larger block of bedded salt.

The addition of SANCHO to the set of models used by the PA Department has triggered a need to include a host of mechanical parameters for waste and Salado materials in the Secondary Data Base (SDB). A brief discussion of the constitutive equations used in SANCHO is provided in Section 1.4.7; values of waste and Salado-material mechanical parameters that were used by Mendenhall and Lincoln, and Beraún and Davies, are presented in Section 2.5.

1.4.2 Human Intrusion: CCDFPERM

The event "unintentional intrusion into WIPP repository by exploratory drilling" forms the basis for the major disturbed-case scenario class in WIPP performance assessment. Since 1990, the PA Department has used a probability model for this event that is based on the assumption that future episodes of exploratory drilling are a Poisson counting process with constant intensity: in other words, the probability that a portion of the repository is drilled exactly n times in a period of T years is

$$\Pr\{N = n\} = \frac{(\lambda T)^n}{n!} e^{-\lambda T}, \quad n = 0, 1, 2, \ldots$$

where λ is an imprecisely known parameter called the intensity of drilling. Physically speaking, λ is the expected frequency of drilling per unit area (units: events/m^2 • s) times the projected area (in m^2) of the portion of the repository of concern, e.g., that part of the repository underlain by brine reservoirs. Tierney (1991, pg. C-8) observed that treating λ as a constant over the 10,000-yr period of performance is unrealistic since it is equivalent to ignoring potential deterring effects of markers/monuments on future explorers.

During 1990-1992, Sandia National Laboratories assembled two groups of external experts with the purpose of formally addressing questions of future human intrusion into the WIPP through the Expert Judgment Panel process. Deliberations of these experts have led to insights concerning future human intrusion and, in particular, subjective probabilities of human intrusion in the presence of markers and monuments. One insight is that realistic drilling intensities are functions of time whose functional form can be inferred from subjective probabilities obtained from the expert panels (Hora, August 25, 1992, Memo in Appendix A).

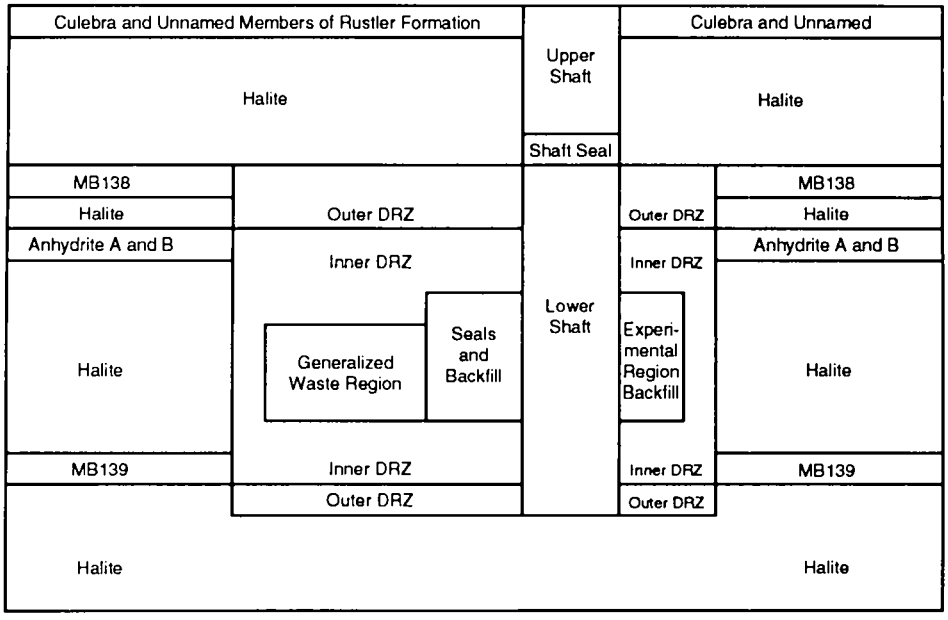

Figure 1.4-1. Idealization of waste-disposal reservoir used in BRAGFLO calculation of two-phase flow in repository and surroundings. Possible material types are shown in a planar (x, y) geometry.

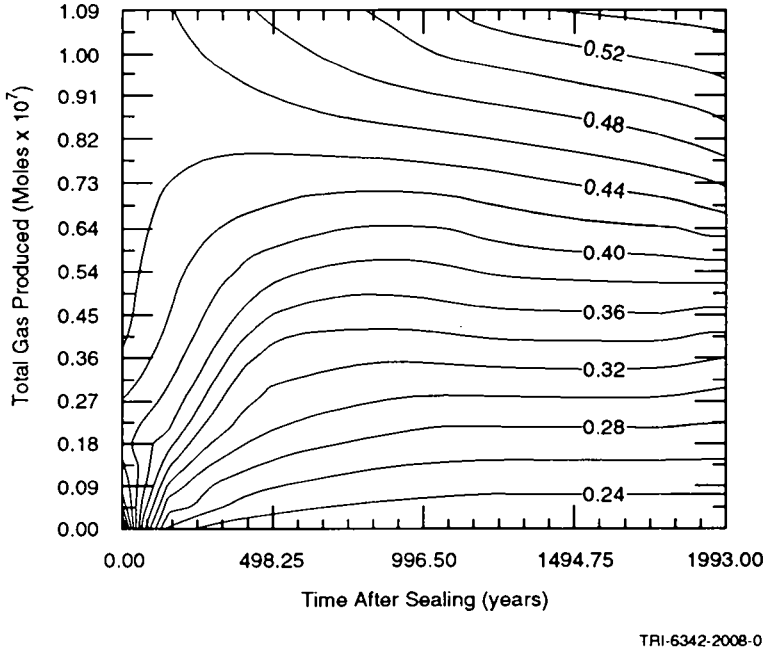

Figure 1.4-2. Isopleths of porosity of waste-filled disposal room as a function of total volume of gas produced and time after sealing. Pore space is assumed to be fully saturated with gas.

This section shows how the time-dependent drilling intensities generated by Hora (see Section 5.2) are used in the code CCDFPERM to construct probabilities for the various computational scenarios associated with human intrusion by exploratory drilling (see Helton, 1991, Chapter 2, for a complete discussion of computational scenarios and the construction of probabilities). The following material is largely taken from Ross (1985, pg. 220) and differs from Helton's treatment of the subject only in notation and style. Further discussion of the human-intrusion model can be found in Chapter 5 of Volume 2 of this series of reports.

INHOMOGENEOUS POISSON PROCESS

A *counting process* is a random process, $\{N(t), t \geq 0\}$, representing (in the present application) the cumulative number of drilling events that have occurred up to some time $t \geq 0$ after closure of the WIPP. A counting process is said to be an inhomogeneous Poisson process with intensity function $\lambda(t)$, $t \geq 0$, if

(i) $N(0) = 0$,
(ii) $\{N(t), t \geq 0\}$ has independent increments,
(iii) $\Pr\{N(t+h) - N(t) \geq 2\} = o(h)$,
(iv) $\Pr\{N(t+h) - N(t) = 1\} = \lambda(t)h + o(h)$.

In conditions (iii) and (iv), $\Pr\{...\}$ stands for the probability that statement $\{...\}$ is true, and $o(h)$ stands for any function $f(h)$ with the property,

$$\lim_{h \to 0} \frac{f(h)}{h} = 0 .$$

In simple terms, $o(h)$ is any function that tends to zero faster than the function $f(h) = h$ as h tends to zero. The meaning of the notation $\{N(t+h)-N(t) = n\}$ should be clear: exactly n drillings occur between the time t and the time t+h.

If conditions (i) - (iv) hold, it can be proven that, for any $n \geq 0$ and any integrable $\lambda(t)$,

$$\Pr\{N(t+s) - N(t) = n\} = \frac{[m(t+s) - m(t)]^n}{n!} \exp\{-[m(t+s) - m(t)]\}, \qquad (1.4.2\text{-}1)$$

where

$$m(t) = \int_0^t \lambda(x)\, dx . \qquad (1.4.2\text{-}2)$$

APPLICATION TO COMPUTATIONAL-SCENARIO PROBABILITIES

Calculation of computational-scenario probabilities usually begins by dividing the 10,000-yr period of performance into nT intervals,

$$[t_{i-1}, t_i], t_i > t_{i-1}, i = 1, 2, ..., nT .$$

Let N_i be the random variable counting the number of drillings that occurs in the interval $[t_{i-1}, t_i]$. Then, by Eq. 1.4.2-1, the probability that exactly n drillings occur in the ith interval is

$$P_i[n] = \frac{[m_i]^n}{n!} e^{-m_i}, \qquad (1.4.2\text{-}3)$$

where, by Eq. 1.4.2-2, m_i is shorthand for the quantity

$$\left[m(t_i) - m(t_{i-1})\right] = \int_{t_i}^{t_{i-1}} \lambda(x)\,dx \quad . \tag{1.4.2-4}$$

Given an intensity function, $\lambda(t)$, defined on the period of performance (0 to 10,000 yr), Eqs. 1.4.2-3 and 1.4.2-4 are sufficient for the computation of all necessary computational-scenario probabilities by CCDFPERM. In practice, the intensity function used to compute the m_i by Eq. 1.4.2-4 is randomly selected (or "sampled") from a finite set of intensity functions that has been generated prior to the PA calculations with CCDFPERM. The sample intensity function is then modified by multiplication with other parameters, e.g., fraction of repository area that is underlain by brine reservoirs:

$$\lambda(t) = p \bullet \lambda_s(t) \quad , \tag{1.4.2-5}$$

where λ_s is the sampled intensity function (represented by a piecewise-linear function defined on the interval [0 to 10,000 yr]) and p stands for the product of the other necessary parameters. The set of intensity functions from which samples are taken has been ordered in a way that guarantees that each of its members is equally likely to be sampled (see Section 5.2 for details and Appendix D).

1.4.3 Cuttings Removal: CUTTINGS

One of the more important considerations in assessing the long-term behavior of the WIPP repository involves the transport of radionuclides from the WIPP repository as the result of penetrating a panel by an exploratory borehole. If a borehole intrudes the repository, waste will be brought directly to the surface as particulates suspended in the circulating drilling fluid. This section briefly addresses the basic equations governing direct waste removal due to drilling as they are formulated in the CUTTINGS model. The CUTTINGS code, developed specifically for the WIPP, calculates the quantity of radioactive material (in curies) brought to the surface as cuttings generated by an exploratory drilling operation that penetrates the repository during the human intrusion type scenario. The code determines the amount of cuttings removed by drilling and mud erosion, and accounts for radioactive decay that has occurred up to the intrusion time.

In the human-intrusion type scenario, a hydrocarbon exploration well is drilled through a WIPP repository panel and into the underlying pressurized brine Castile Formation (Figure 1.4-3). If rotary drilling is assumed, a volume of repository wastes is removed from the breached panel and is transported to the surface as cuttings and cavings suspended in the drilling fluid. The minimum volume of repository material removed is equal to the cross-sectional area of the drill bit multiplied by the repository thickness (cuttings). This minimum volume must be increased by material eroded from the borehole wall (cavings) by the scouring action of the swirling drilling fluid. Both cuttings and cavings will be released to the accessible environment in a settling pit at the surface.

Although the amount of waste removed by direct cutting is simple to calculate, calculating the amount of waste eroded from the borehole wall is more difficult. A number of factors may influence borehole erosion (e.g., eccentricity of pipe and hole, impact of solid particles in mud on the walls, physical and chemical interaction between mud and walls, and time of contact between the mud and walls [Broc, 1982]); however, industry opinion singles out fluid shear stress as the most important factor (Darley, 1969; Walker and Holman, 1971). A full discussion of the mathematical model of erosion of the borehole wall is presented in Section 7.7 of Volume 2 of this report; here, it is sufficient to note that drill hole wall erosion is probably largely determined by the effects of fluid shear stress acting on the wall and the character of the fluid-flow regime.

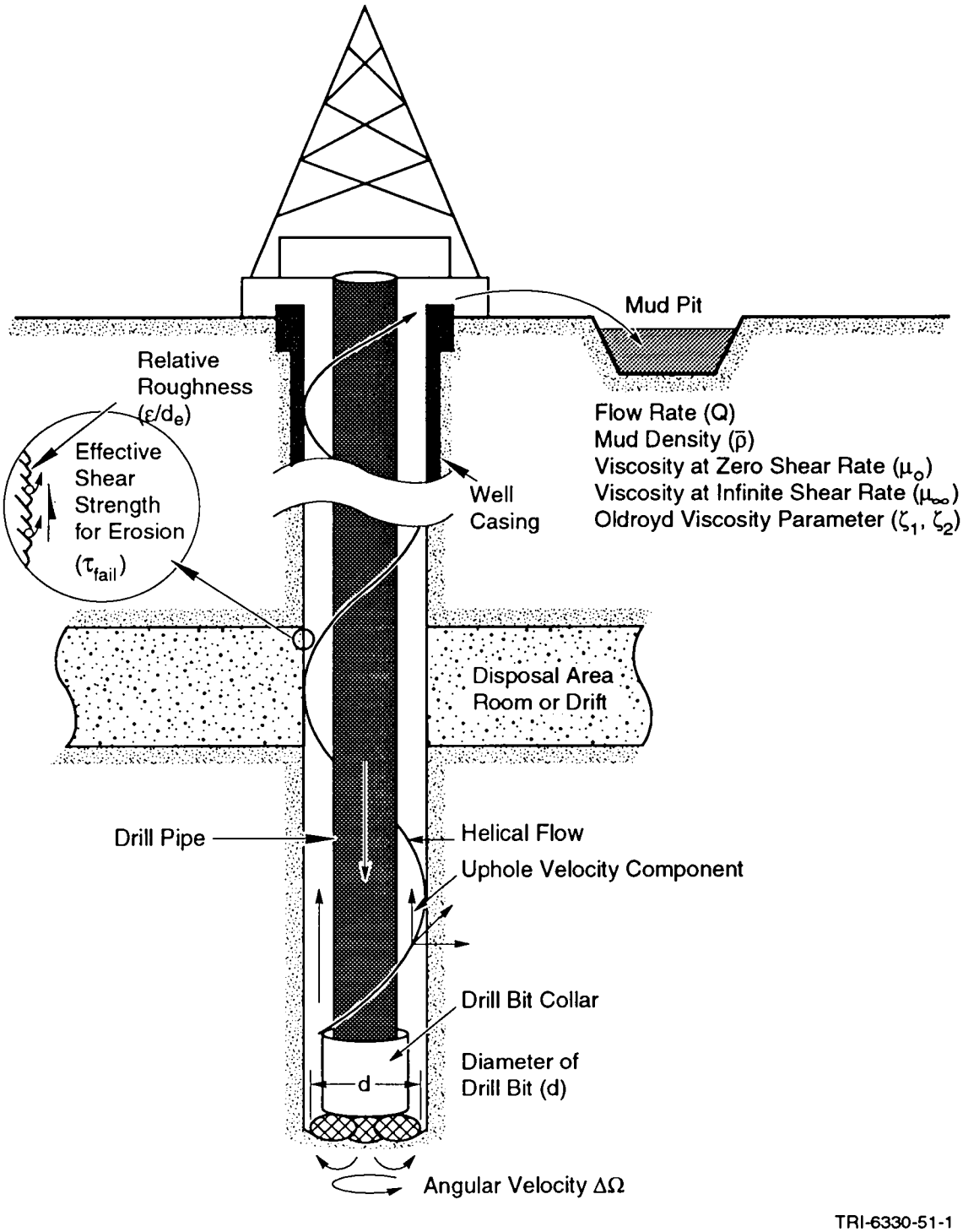

Figure 1.4-3. Some features of the CUTTINGS model.

Three drilling mud properties (density, viscosity, and yield stress) are necessary to evaluate the fluid shear stress, which in turn is one of several parameters used to evaluate the amount of material eroded from the borehole wall by scouring from the swirling drilling fluid.

FLOW REGIME

Whether the flow regime within the annulus is laminar or turbulent is governed by the Reynolds number, N_R. The Reynolds number is dependent upon the properties of the drilling mud (density, viscosity, and velocity) and the size of the annulus. The Reynolds number is defined as

$$N_R = \frac{\bar{\rho}\ \bar{V} d_e}{\bar{\mu}}, \qquad (1.4.3\text{-}1)$$

where

d_e = length dimension = equivalent hydraulic diameter for annulus = $d_{hole} - d_{collar}$,
$\bar{\rho}$ = average fluid density,
$\bar{V}$ = average fluid velocity,
$\bar{\mu}$ = average fluid viscosity (for non-newtonian fluids, the average viscosity will depend upon the viscosity model used).

SHEAR STRESS

For both laminar and turbulent axial flow in an annulus, the shear stress can be expressed as (Vennard and Street, 1975, p. 381):

$$\tau = \frac{f\bar{\rho}\bar{V}^2}{2}. \qquad (1.4.3\text{-}2)$$

The fanning friction factor, f, is discussed below for turbulent and laminar shear stress.

Turbulent Shear Stress

In turbulent flow (Reynolds number $N_R > N_{R_{crit}}$ where $N_{R_{crit}}$ = 2,100 for newtonian fluids and 2,400 for some non-newtonian fluids [Vennard and Street, 1975, p. 384; Walker, 1976, p. 89]) the fanning friction factor is dependent on both N_R, and surface roughness (e.g., Moody diagram [Vennard and Street, 1975, Figure 9.5; Streeter and Wylie, 1975, Figure 5.32]), with N_R having a minor influence. Consequently, the shear stress is dependent primarily upon absolute surface roughness, ε, and kinetic energy $\frac{\bar{\rho}\bar{V}^2}{2}$. An empirical expression for f is (Colebrook, 1939):

$$\frac{1}{\sqrt{f}} = -4 \log\left[\frac{\varepsilon/d}{3.72} + \frac{1.255}{N_R\sqrt{f}}\right] \qquad (1.4.3\text{-}3)$$

where

ε = absolute roughness of material,

d = hydraulic diameter = difference between borehole diameter and collar diameter and N_R is calculated using the limiting viscosity μ_∞ (Figure 1.4-4).

Laminar Shear Stress

For laminar flow, the fanning friction factor, f, is a function of only N_R. The shear stress in laminar flow (Reynolds number $N_R < 2{,}100$ [Vennard and Street, 1975, p. 384]) depends solely on the fluid viscosity and strain rate (velocity gradient); however, for a non-newtonian fluid such as drilling mud, the viscosity varies with strain rate (Figure 1.4-4). Several functional forms are used to model this variation (Ideal Bingham Plastic, Power Law, and Oldroyd Model). The PA Department currently uses the Oldroyd model. For the laminar flow regime both the axial and circumferential motion of the drilling mud are considered.

Oldroyd Model

Oldroyd's (1958) shear softening model of the viscosity can approximate the drilling fluid behavior away from the yield stress (τ_0) by the appropriate choice of parameters:

$$\tau = \mu_0 \left[\frac{1 + \zeta_2 \Gamma^2}{1 + \zeta_1 \Gamma^2} \right] \Gamma \,, \qquad (1.4.3\text{-}4)$$

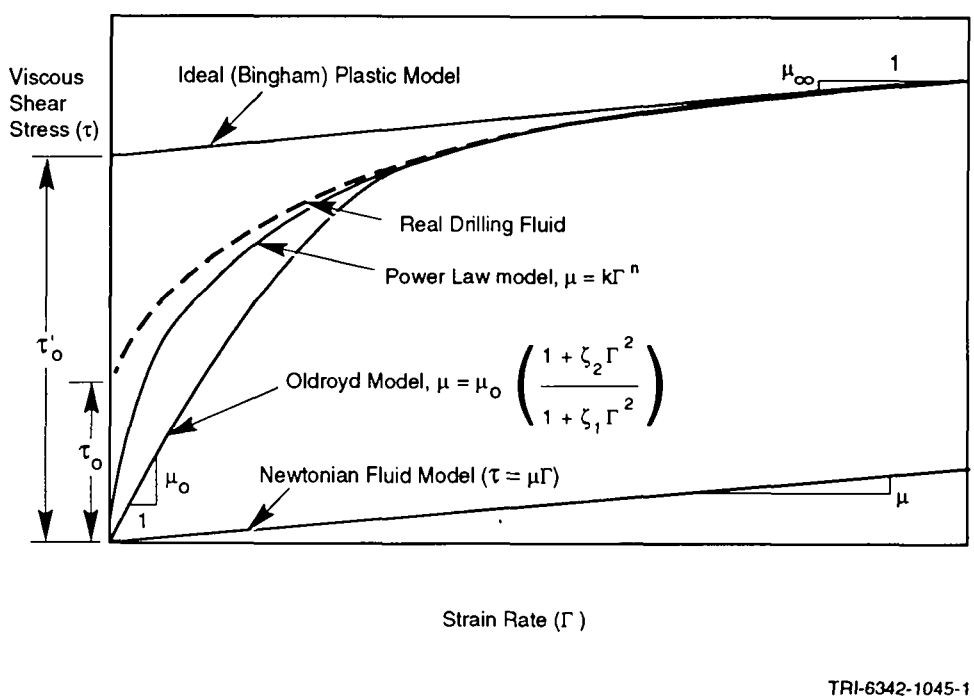

Figure 1.4-4. Various models for modeling drilling fluid shear stress.

where

μ_∞ = $\mu_o(\zeta_2/\zeta_1)$ = limiting viscosity at infinite strain rate,
Γ = strain rate,
$\zeta_1\zeta_2$ = Oldroyd model parameters,
μ_0 = limiting viscosity at zero rate of strain.

Note that for the PA calculations, ζ_1 was assumed equal to 2 ζ_2, based on viscosity measurements for an oil-based, 1.7-kg/m^3 (14-lb/gal) mud (Darley and Gray, 1988, Table 5-2). The assumption can be somewhat arbitrary since the behavior at high strain rate (away from the yield point) is of primary interest.

Using the above assumption, the parameter ζ_2 was estimated by equating the linear ideal plastic model, with the Oldroyd model at a high strain rate (Figure 1.4-4). Simple algebraic manipulation gives

$$\zeta_2 = (\mu_\infty \Gamma_m - \tau'_o)/2\Gamma^2{}_m\tau'_o \,. \qquad (1.4.3\text{-}5)$$

The high strain rate selected for the match point (Γ_m) was 1020 s^{-1}.

1.4.4 Repository Discharge: PANEL

Flow of brine through a collapsed WIPP panel and up an intrusion borehole may result in mobilization of dissolved, radionuclide-bearing compounds and their transport towards the Culebra. The PA Department models these effects with a code called PANEL. Governing equations for that part of PANEL model concerned with waste mobilization and transport are presented in this section.

In the PANEL model, a collapsed WIPP panel (rooms and drifts) is treated as a single, hydraulically connected cavity of volume V that contains a porous medium (waste and backfill). The cavity is connected to sources and sinks for brine by one or more inlets or outlets (Figure 1.4-5).

Quasi-steady discharge of brine through the panel is assumed, i.e.,

$$Q(t) = Q_{out} = Q_{in} \,, \qquad (1.4.4\text{-}1)$$

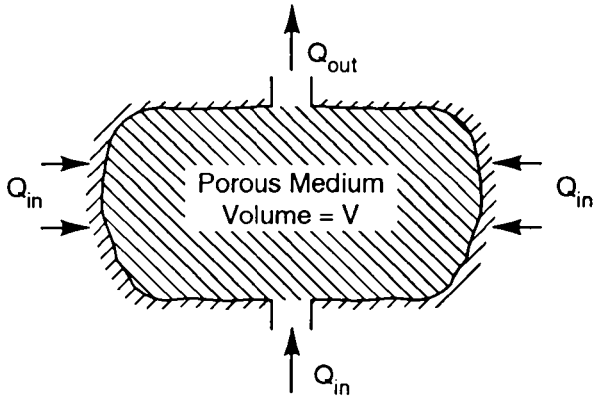

Figure 1.4-5. Idealized collapsed WIPP panel in PANEL model.

where Q(t) is the brine discharge through volume V in units of m^3/s. (Note: the PANEL model receives Q(t) from the BRAGFLO model; see Section 1.4.1.)

WASTE MOBILIZATION

The mobilization of radioactivity in the waste form can be modeled by considering the dynamics of three variables:

$M_{ui}(t)$ = mass of ith nuclide in undissolved form in volume V at time t,
$M_{di}(t)$ = mass of ith nuclide in dissolved form in volume V at time t,
$M_{ai}(t)$ = mass of ith nuclide adsorbed on solids in volume V at time t.

Thus,

$$M_i(t) = M_{ui} + M_{di} + M_{ai} \qquad (1.4.4\text{-}2)$$

= total mass of ith nuclide in volume V at time t.

The dynamics of these mass components follow from three ordinary differential equations (three for each nuclide species). The first dynamical equation is

$$\dot{M}_{ui} = -k_i M_{ui}\left[S_i - \frac{M_{di}}{w}\right] - \lambda_i M_{ui} + \lambda_{i-1} M_{ui-1}\,, \qquad (1.4.4\text{-}3)$$

where a dot ($\dot{}$) means the time derivative and

$$w = \bar{\phi}\,\bar{S}_\ell\, V = \text{volume of brine in cavity.} \qquad (1.4.4\text{-}4)$$

In Eq. 1.4.4-4, $\bar{\phi}$ and $\bar{S}_\ell$ are respectively the average porosity and the average saturation of the medium filling V (i.e., the compressed WIPP wastes and backfill).

The first term on the right side of Eq. 1.4.4-3 models dissolution of undissolved mass: the rate of dissolution is assumed to be proportional to M_{ui} and the difference between the concentration of a saturated solution (S_i) and the concentration of dissolved mass (M_{di}/w); the constant of proportionality k_i is a rate constant (units: $m^3/kg{\cdot}s$). The second and third terms on the right side of Eq. 1.4.4-3 respectively represent loss of mass through radioactive decay of undissolved mass, and gain of mass through the decay of a parent species.

The second dynamical equation is

$$\dot{M}_{di} = k_i M_{ui}\left[S_i - \frac{M_{di}}{w}\right] - Q\frac{M_{di}}{w} - \frac{\bar{\rho}_b}{\bar{\phi}} K_{di}\dot{M}_{di} - \lambda_i M_{di} + \lambda_{i-1} M_{di-1}\,. \qquad (1.4.4\text{-}5)$$

The first term on the right side of Eq. 1.4.4-5 was explained above; mass lost from the undissolved component is gained by the dissolved component. The second term on the right side of Eq. 1.4.4-5 represents mass lost from volume V by advection in the brine discharge through the panel (Q is never negative). The third term on the right side represents loss of dissolved mass by chemical sorption processes; it is assumed that sorption/desorption processes are rapid and follow a linear isotherm so that

$$M_{ai} \cong \frac{\bar{\rho}_b}{\bar{\phi}} \bar{K}_{di} M_{di}, \qquad (1.4.4\text{-}6)$$

where $\bar{\rho}_b$ is the average bulk density of compressed wastes and backfill (kg/m^3) and $\bar{K}_{di}$ is the average distribution coefficient for the ith nuclide in wastes and backfill (Freeze and Cherry, 1979, p. 405). Meanings of the fourth and fifth terms on the right side of Eq. 1.4.4-5 were explained above for the undissolved mass component.

The third dynamical equation is

$$\dot{M}_{ai} = \frac{\bar{\rho}_b}{\bar{\phi}} \bar{K}_{di} \dot{M}_{di} - \lambda_i M_{ai} + \lambda_{i-1} M_{ai-1}, \qquad (1.4.4\text{-}7)$$

where all terms on the right of Eq. 1.4.4-7 have been explained.

The three dynamical equations, 1.4.4-3, 1.4.4-5, and 1.4.4-7, can be somewhat simplified by defining

$R_i = 1 + \frac{\bar{\rho}_b}{\bar{\phi}} \bar{K}_{di}$ — the effective retardation coefficient for the ith nuclide species (dimensionless),

$C_{di} = M_{di}/w$ — dissolved concentration of ith nuclide species in brine (kg/m^3).

The three dynamical equations become

$$\dot{M}_{ui} = -k_i M_{ui} [S_i - C_{di}] - \lambda_i M_{ui} + \lambda_{i-1} M_{ui-1} \qquad \text{(A)},$$

$$R_i \dot{M}_{di} = k_i M_{ui} [S_i - C_{di}] - Q C_{di} - \lambda_i M_{di} + \lambda_{i-1} M_{di-1} \qquad \text{(B)},$$

$$\dot{M}_{ai} = (R_i - 1) \dot{M}_{di} - \lambda_i M_{ai} + \lambda_{i-1} M_{ai-1} \qquad \text{(C)}.$$

The initial conditions for the system (A)-(C) are usually taken at a time $t_o > 0$, the time of borehole penetration. At this time,

$M_{ui}(t_o) = M_o(t_o)$ — the inventory at closure ($t = 0$) of the ith nuclide species aged to time $t_o > 0$ (in kg),

$M_{di}(t_o) = o$ $\qquad$ $M_{ai}(t_o) = 0.$ $\qquad (1.4.4\text{-}8)$

Furthermore, $Q(t_o) = 0$ but $Q(t)$, is a non-negative function (≥ 0) of time for $t > t_o$.

The rate at which mass of the ith nuclide is discharged from the panel is obviously

$$Q(t)\, C_{di}(t) \text{ (kg/s)}, \quad t > t_o. \qquad (1.4.4\text{-}9)$$

APPROXIMATIONS IN PANEL

The full set of dynamical equations, (A)-(C), are not directly solved in the PANEL model; instead, (A)-(C) are first added to give

$$\dot{M}_i = -Q\, C_{di} - \lambda_i M_i + \lambda_{i-1} M_i$$

$$M_i(t_o) = M_o(t_o) \ . \qquad (1.4.4\text{-}10)$$

This equation is solved with the simplifying assumption that

$$C_{di}(t) = \frac{M_i}{\sum_j M_j} S_i, \ t > t_o \ . \qquad (1.4.4\text{-}11)$$

and the sum in the denominator is taken over all isotopes of the same element as that of species i.

1.4.5 Fluid Flow in Culebra: SECO2D

Studies of potential releases of radionuclides from the WIPP to the accessible environment along liquid pathways require computational models of the flow of groundwater through the Culebra Dolomite Member, and models of how flow in the Culebra would be affected by climatic change. The PA Department uses a model of these phenomena called SECO2D. The governing equations for SECO2D are summarized in this section: first, the equation of groundwater flow is presented, then the effects of climate change on boundary conditions for the flow equation are briefly described. Further discussion of the model of fluid flow in the Culebra is found in Sections 7.5, 7.6, and Appendix C of Volume 2 of the present series of reports.

GROUNDWATER FLOW

SECO2D simulates groundwater flow at regional and local scales within the Culebra Dolomite by solving the following partial differential equation in two dimensions (x,y):

$$S_s \frac{\partial h}{\partial t} = \nabla \bullet (\bar{K} \bullet \nabla h) - W \ , \qquad (1.4.5\text{-}1)$$

where

- h = h(x,y,t), the potentiometric head (m),
- S_s = S_s(x,y,t), the specific storage of the Culebra (m^{-1}),
- $\bar{K}$ = $\bar{K}$(x,y,t), the hydraulic conductivity tensor (m/s),
- W = W(x,y,t), a volumetric flux per unit volume of formation (s^{-1}), (used to simulate wells or recharge).

The specific storage and hydraulic conductivity tensor are obtained from more directly measurable quantities, i.e., in the present version of SECO2D,

$$S_s = \frac{S(x,y)}{\Delta Z} \ , \quad \bar{K} = \frac{\bar{T}(x,y)}{\Delta Z} \ , \qquad (1.4.5\text{-}2)$$

where

- $S(x,y)$ = storage coefficient in the Culebra (dimensionless),
- ΔZ = $\Delta Z(x,y)$, Culebra thickness (m),

$\bar{T}(x, y)$ = one of a set of simulated transmissivity tensors (units: m^2/s). See Section 2.6.9 for a discussion of how transmissivity fields are generated. Also see Section 7.5 of Volume 2 of the present series of reports.

Given appropriate initial and boundary conditions, Eq. 1.4.5-1 is solved numerically to yield a potentiometric head field, h(x,y,t), which may be used to compute specific discharge (or Darcy velocity) at any point in the Culebra:

$$\vec{q}(x, y, t) = -\bar{K} \bullet \nabla h \quad (m/s) \; . \tag{1.4.5-3}$$

In SECO2D, boundary conditions are specified on the outer edges of the regional (or, in some cases, local) grid; these boundary conditions may be a mix of the following kinds: (1) Dirichlet (specified h on boundary); (2) inhomogeneous Neuman (specified gradients of h on boundary); (3) Robin boundary conditions [a mixture of (1) and (2)]; and (4) adaptive boundary conditions, in which flux ($\vec{q}$) is specified at inflow boundaries and head (h) is specified at outflow boundaries.

EFFECTS OF CLIMATE CHANGE

The 1992 version of SECO2D simulates effects of climate change through inclusion of time-dependent Dirichlet boundary conditions. Specifically, potentiometric heads on the northwestern edges of the regional grid (the suspected recharge area for the Culebra) are set according to the formula

$$h_f(x,y,t) = h_p(x,y)\left[\frac{3A_R+1}{4} - \left(\frac{A_R-1}{2}\right)\left(\cos\theta t - \sin\frac{\phi}{2}t + \frac{1}{2}\cos\phi t\right)\right] \; , \tag{1.4.5-4}$$

where

h_f = future potentiometric head (m),
h_p = present potentiometric head (m), given a realization of regional transmissivities (see Section 2.6.3),
A_R = Amplitude factor (dimensionless),
θ = Pleistocene glaciation frequency (Hz),
ϕ = frequency of Holocene-type climatic fluctuations (Hz).

The recharge amplitude factor, A_R, is a number to be chosen between 1 and $\gamma > 1$ and is scaled from the sampled index factor (Section 4.4). If $A_R = 1$, it is seen that there are no effects of climatic change. If $A_R > 1$, the maximum future head, h_f, will be greater than the present head. The constant γ is a scaling factor that is chosen by the PA analyst to ensure physically reasonable head values on the portion of the recharge boundary where boundary conditions are applied. The origins of the climate change model are treated in detail in Chapter 6 of Volume 4 of the present series of reports.

1.4.6 Solute Transport in Culebra: SECO/TP

Studies of potential releases of radionuclides from the WIPP to the accessible environment along liquid pathways require a computational model of solute transport in groundwater flowing through the Culebra Dolomite Member. In 1992, the PA Department is using a model developed specifically for Sandia National Laboratories and called SECO/TP. This section summarizes the governing equations for that model. Solute transport in the Culebra is discussed in more detail in Section 7.6 and Appendix C of Volume 2 of the present series of reports.

SECO/TP is a "dual porosity" model of solute transport in the Culebra in the sense that advective transport is allowed only through the fracture system but diffusion of solute into the rock matrix surrounding a fracture is possible. The fracture system is idealized as planar and parallel (Figure 1.4-6); each fracture wall may be coated with a layer of clay of uniform thickness.

MASS TRANSPORT IN FRACTURE SYSTEM

The governing equation for mass transport in a single fracture is

$$\frac{\partial C_\ell}{\partial t} = -\frac{\partial}{\partial x_i}\left(V_i C_\ell - D_{ij}\frac{\partial C_\ell}{\partial x_j}\right) - \lambda_\ell C_\ell + \sum_{m=1}^{m}\xi_{\ell m}\lambda_m C_\ell + Q\left(C_\ell^o - C_\ell\right) + \Gamma_\ell \quad , \tag{1.4.6-1}$$

where the summation convention has been used ($x_1 = x$, $x_2 = y$) and ℓ, m = 1, 2, ..., m, label the solute species (radionuclide mass). The quantities in Eq. 1.4.6-1 have the following meanings [starred (*) items are explained below].

	C_ℓ	=	trace concentration of ℓth solute specie in fracture fluid (kg/m^3),
*	V_i	=	average linear velocity vector in fracture system (m/s),
*	D_{ij}	=	hydrodynamic dispersion tensor (m^2/s),
	λ_ℓ	=	decay constant for ℓ^{th} solute species (radionuclide, s^{-1}),
	$\xi_{\ell m}$	=	fraction of mth parent species that decays into ℓ^{th} solute species (dimensionless),
	Q	=	rate of fluid injection per unit volume of formation (s^{-1}),
	C_ℓ^o	=	concentration of ℓth solute species in injected fluid (kg/m^3),
	Γ_ℓ	=	rate of mass transfer of ℓth species from matrix system to fracture system ($kg/m^3 \cdot s$).

The average linear velocity vector, V_i, is related to the specific discharge in the Culebra by

$$V_i = q_i/\phi_f \, , \tag{1.4.6-2}$$

where the specific discharge, q_i, is provided by the SECO2D model [see Eq. 1.4.5-3] and ϕ_f is the fracture porosity of the Culebra. For planar parallel fractures (Figure 1.4-6) and b<<B,

$$\phi_f = \frac{b}{b+B} \, . \tag{1.4.6-3}$$

In practical modeling of solute transport in the Culebra, ϕ_f and 2B are taken as known quantities and Eq. 1.4.6-3 is used to calculate the fracture aperture 2b. The ratio b_c/b is also assumed to be known; given b, b_c can be calculated from this ratio.

The components of the hydrodynamic dispersion tensor for the fracture system, D_{ij}, are

$$D_{11} = \alpha_L \frac{(V_1)^2}{|V|} + \alpha_T \frac{(V_2)^2}{|V|} + D^*, \tag{1.4.6-4a}$$

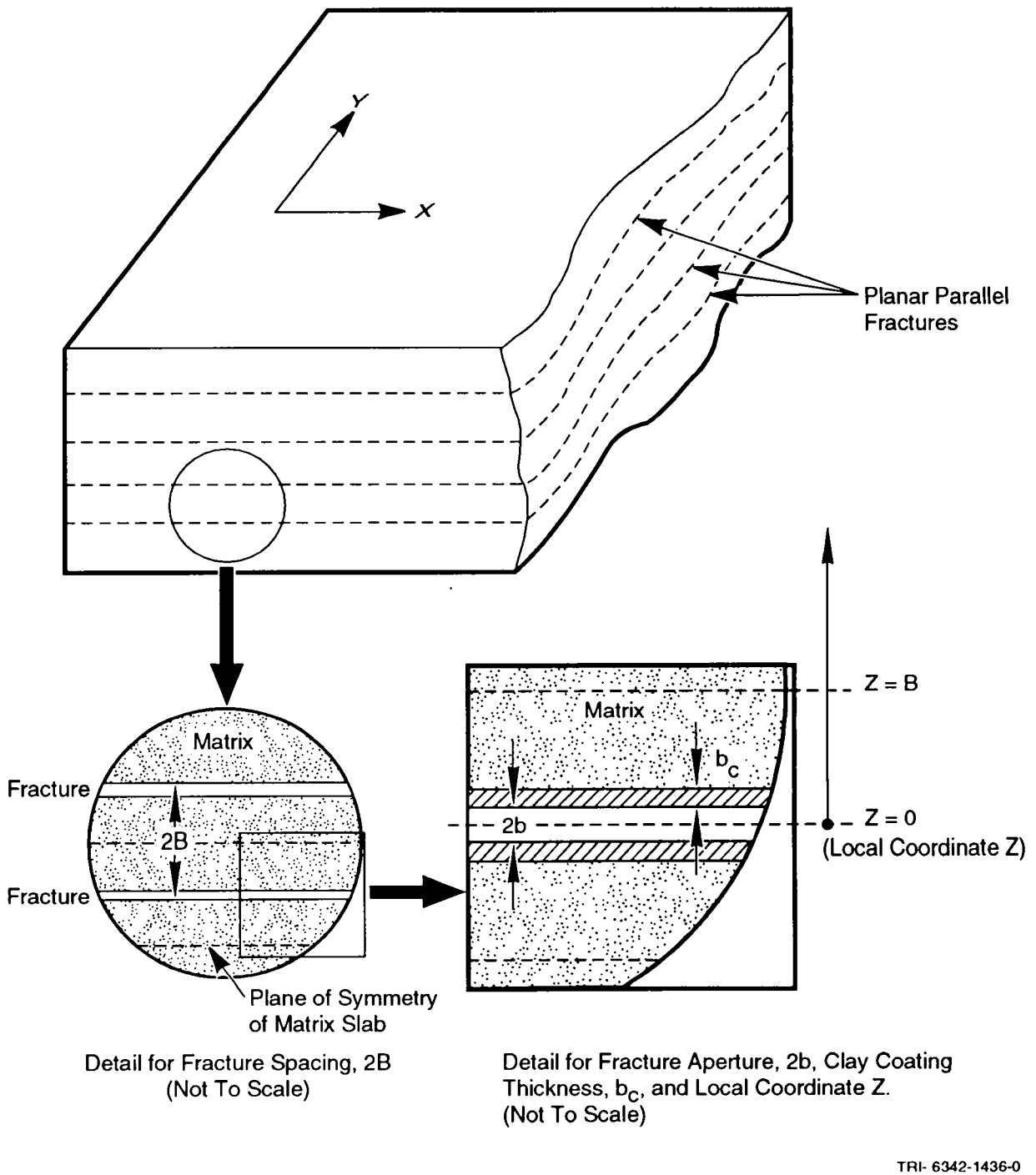

Figure 1.4-6. Idealized section of Culebra Dolomite Member.

$$D_{22} = \alpha_L \frac{(V_2)^2}{|V|} + \alpha_T \frac{(V_1)^2}{|V|} + D^*, \qquad (1.4.6\text{-}4b)$$

$$D_{12} = D_{21} = (\alpha_L - \alpha_T) \frac{V_1 V_2}{|V|}, \qquad (1.4.6\text{-}4c)$$

where α_L, α_T are respectively longitudinal and transverse dispersivities (m), D* is the molecular diffusion coefficient of the "average" solute species (m^2/s), and

$$|V| = (V_1^2 + V_2^2)^{1/2}.$$

The rate of mass transfer from the matrix to the fracture system, Γ_ℓ, will be explained after mass storage in the matrix is described.

MASS STORAGE IN CLAY COATINGS AND MATRIX

Mass storage in clay coatings and matrix slabs occurs by diffusion of solute mass across the fracture facings; only diffusion perpendicular to the fracture facings (i.e., along the local coordinate Z, Figure 1.4-6) is allowed. The governing diffusion equation is

$$\phi R_\ell \frac{\partial C'_\ell}{\partial t} = \frac{\partial}{\partial z} D' \frac{\partial C'_\ell}{\partial z} - \phi R_\ell \lambda_\ell C'_\ell + \sum_{m=1}^{m} \xi_{\ell m} \phi R_m \lambda_m C'_m \quad , \qquad (1.4.6\text{-}5)$$

where new quantities have the following meanings (again, starred items [*] are explained below).

$C'_\ell(z,t)$ = trace concentration of ℓth solute species in pore fluid of clay coating or matrix (kg/m^3),
* $\phi(z)$ = porosity of clay coating or matrix (dimensionless),
* $R_\ell(z)$ = retardation coefficient of ℓth solute species in pores of clay coating or matrix (dimensionless),
* $D'(z)$ = effective molecular diffusion coefficient in pores of clay coating or matrix (m^2/s).

The porosity of clay coating or matrix depends on location:

$$\phi(z) = \begin{cases} \phi_c \text{ (constant clay porosity)}, & b \le z < b + b_c \\ \phi_m \text{ (constant matrix porosity)}, & b + b_c \le z \le B \end{cases} , \qquad (1.4.6\text{-}6)$$

The effective molecular diffusion coefficient in pores of clay coating or matrix also depends on location:

$$D'(z) = \begin{cases} \tau_c D^*, & b \le z < b + b_c \\ \tau_m D^*, & b + b_c \le z \le B \end{cases} , \qquad (1.4.6\text{-}7)$$

where τ_c and τ_m are the (constant) tortuousities of clay and matrix respectively (dimensionless).

In a similar fashion, the retardation coefficient of the ℓth solute species takes two values:

$$R_\ell(z) = 1 + \begin{cases} \left(\dfrac{\rho_g(1-\phi)k_{d,\ell}}{\phi}\right)_c, & b \le z < b + b_c \\ \left(\dfrac{\rho_g(1-\phi)k_{d,\ell}}{\phi}\right)_m, & b + b_c \le z \le B \end{cases} \qquad (1.4.6\text{-}8)$$

where

ρ_g stands for grain density (kg/m^3) of the material,
$k_{d,\ell}$ is the distribution coeffient of the ℓth solute species in the pores of the material (m^3/kg),
ϕ is the porosity of the material (dimensionless).

The notation,

$$(...)_{c \text{ or } m},$$

indicates qualities in either clay coating (c) or matrix (m).

THE MASS TRANSFER TERM

The term Γ_ℓ specifying the rate of mass transfer of the ℓ th solute species from the matrix to the fracture system takes the form

$$\Gamma_\ell(x,y,t) = -\frac{2}{b}\left(D'\frac{\partial C'_\ell}{\partial z}\right)_{z=b}, \qquad (1.4.6\text{-}9)$$

where all quantities have been defined.

INITIAL AND BOUNDARY CONDITIONS

Equation 1.4.6-1 can be solved subject to a variety of boundary conditions (prescribed input flux, constant concentrations on boundary). The usual initial condition is $C_\ell(x,y,o) = 0$.

Equation 1.4.6-5 is solved subject to the initial condition $C_\ell(x,y,z,o) = 0$ $(b \le z \le B)$ and the boundary conditions,

$$\frac{\partial C'_\ell}{\partial z}(x,y,B,t) = 0, \qquad (1.4.6\text{-}10)$$

(i.e., no mass flux across plane of symmetry of matrix slab),

$$C'_\ell(x,y,b,t) = C_\ell(x,y,t), \qquad (1.4.6\text{-}11)$$

(i.e., concentrations match at interfaces between fracture void space and clay coatings).

1.4.7 Waste-Filled Room Deformation: SANCHO

Realistic estimates of the effective porosity and permeability of a closed, waste-filled room require that the effects of room deformation and internal gas generation be taken into account. In 1991, the PA Department largely

ignored the latter effects and assigned constant porosity and permeability based on waste-material composition (WIPP PA Division, 1991, Vol. 3, Sections 3.4.7 and 3.4.8). In the present (1992) series of PA calculations, the effects of deformation and gas generation have been included only indirectly through the use of a separate calculation of a porosity "surface" which gives room porosity as a function of time and total volumes of gas generated by corrosion and microbial action (Mendenhall and Lincoln, February 28, 1992, Memo in Appendix A). The room-deformation component of this calculation employed SANCHO, a finite-element computer program for simulating the quasistatic, large-deformation, inelastic response of two-dimensional solids (Stone et al., 1985). Gas generation was calculated in much the same way as the gas-generation terms in the BRAGFLO code; see Section 1.4.1. This section emphasizes the constitutive equations used in SANCHO to model room deformation.

SANCHO is a special purpose, finite-element program that was developed in response to some of the perceived drawbacks with existing finite element software for nonlinear analysis. SANCHO was developed to solve the quasistatic, large deformation, inelastic response of two dimensional solids. The element library is based on a bilinear isoparametric quadrilateral with a constant bulk strain. The equilibrium solution strategy uses an iterative scheme designed around a self-adaptive dynamic relaxation algorithm. The iterative scheme is based on explicit central difference pseudo-time integration with artificial damping. The code is explicit in nature so that no stiffness matrix is formed or factorized that reduces the amount of computer storage necessary for execution. The explicit nature of the program also makes it attractive for vectorization on vector processing machines. The code has a standard material model interface that is used with three material models incorporated within the code. A finite strain elastic-plastic strain hardening model, a volumetric plasticity model, and a metallic creep material model are presently included. (Recent modifications allow the SANCHO user to employ his or her own material models.) A sliding interface capability, based on a master-slave algorithm, is also incorporated within SANCHO (Stone et al., 1985, p. 12).

The fundamental SANCHO equations will not be discussed here; the relevant physical assumptions are best expressed in terms of the constitutive equations of the material models selected by the SANCHO user. Three material models were used in calculating the porosity surface for a deformed room: (1) an elastic/secondary creep model for intact salt surrounding room opening; (2) an elastic/secondary creep model for crushed-salt room backfill; and (3) a volumetric plasticity model of mechanical response of waste contained within a room.

ELASTIC/SECONDARY CREEP MODEL FOR INTACT SALT

The constitutive equations for the intact-salt components of the model repository are (Mendenhall et al., 1991):

$$\dot{s}_{ij} = 2G\left[\dot{e}'_{ij} - (1.5)^{(N+1)/2} \bullet A \ \exp(Q/RT) \bullet \left(s_{k\ell} \ s_{k\ell}\right)^{(N-1)/2} s_{ij}\right] , \qquad (1.4.7\text{-}1)$$

$$\dot{\sigma}_{kk} = 3K\dot{e}_{kk} , \qquad (1.4.7\text{-}2)$$

where the summation convention is used, i.e.,

$$e_{kk} = e_{11} + e_{22} .$$

A dot over a quantity signifies time derivative and

σ_{ij} = stress tensor (Pa),

s_{ij} = $\sigma_{ij} - \frac{1}{3} \ \sigma_{kk}$ = deviatoric stress tensor,

e_{ij} = deviatoric strain tensor,

$\dot{e}'_{ij}$ = deviatoric strain rate (treated as constant over a time step),

* G = elastic shear modulus (Pa),

A = an experimentally determined constant,

N = an experimentally determined constant,

Q/RT = exponential constant for deviatoric creep model,

* K = elastic bulk modulus (Pa).

Starred (*) quantities are described below.

The elastic shear modulus, G, is approximated by

$$G = G_o \exp(G_1 \rho) \ , \tag{1.4.7-3}$$

and the elastic bulk modulus is approximated by

$$K = K_o \exp(K_1 \rho) \ , \tag{1.4.7-4}$$

where G_0, G_1, K_0, K_1 are experimentally determined constants.

CRUSHED SALT BACKFILL MODEL

The constitutive equations for crushed-salt backfill component of the model repository are (Mendenhall et al., 1991):

$$\dot{s}_{ij} = 2G\left[\dot{e}'_{ij} - A_c(\rho_{int.}/\rho)^N \ \exp(Q/RT)(s_{k\ell}\ s_{k\ell})^{(N-1)/2} s_{ij}\right] \ , \tag{1.4.7-5}$$

$$\dot{\rho} = B_o\left[\exp(B, P) - 1\right]\exp(A\rho) \ , \tag{1.4.7-6}$$

where G is the elastic shear modulus (Eq. 1.4.7-3), summation convention is implied in the term $(s_{k\ell},\ s_{k\ell})$, and the other quantities appearing in Eq. 1.4.7-5 have the same meanings as in Eq. 1.4.7-1. In Eq. 1.4.7-6,

ρ = local density
$\dot{\rho}$ = rate of change of density ($kg/m^3 \cdot s$),
P = pressure (Pa),
A_c, A, B_0, B_1 and ρ_{int} are experimentally determined constants.

In addition, the elastic bulk modulus, K, is given by Eq. 1.4.7-4.

VOLUMETRIC PLASTICITY MODEL FOR WASTE

The constitutive equations for the waste component of the model repository are identical to the equations for the model of soil and crushable foam material specified in the SANCHO manual (Stone et al., 1985, pgs. 40-46; see Eqs. 47-50 in particular). The SANCHO model of soils and crushable foams requires that the following parameters be specified by the user of the code (Stone et al., 1985, p. 67):

μ = shear modulus,
K_0 = bulk unloading modulus,
a_0 = yield function constant,
a_1 = yield function constant,
a_2 = yield function constant. (1.4.7-7)

In addition, the model requires that the user specify volumetric strain [essentially $\ln(\rho/\rho_o)$] as a function of pressure, i.e.,

$$\ln(\rho/\rho_o) = F(P) \quad , \tag{1.4.7-8}$$

where ρ is waste density (kg/m^3) and ρ_0 is initial waste density (before any significant compaction by repository deformation has begun).

NOTE ON PROBLEM GEOMETRY

Typical geometry, modeling mesh, and boundary conditions for the calculation of a porosity surface with SANCHO are illustrated in Figure 1.4-7. Boundary conditions apply to a single room assumed to be imbedded in an infinite lattice of similar rooms spaced uniformly on 40-m centerlines.

Each mined room is 4 m high by 10 m wide by 100 m long. A room is assumed to contain 6804 drums filled with unprocessed waste. Other details of room geometry and composition are found in Beraún and Davies (September 12, 1991, Memo in Appendix A).

NOTE ON GAS GENERATION

Gas pressure in the model disposal room was computed from the ideal gas law based on the instantaneous "void" volume in the room (i.e., the volume not occupied by liquids or solids) and the total amount of gas in the room.

$$P_g = \frac{NRT}{V - V_s} \tag{1.4.7-9}$$

where

P_g = gas pressure,
N = $f \cdot D \cdot \int_0^t \frac{\partial N}{\partial t}\,dt$ = total moles of gas produced per room up to time t,
$\partial N / \partial t$ = rate of gas production (moles / s - drum),
R = 8.23 $(m^3 \cdot Pa)/(g - moles \cdot K)$,
T = 300K,
V = current void volume (m^3), (1.4.7-10)

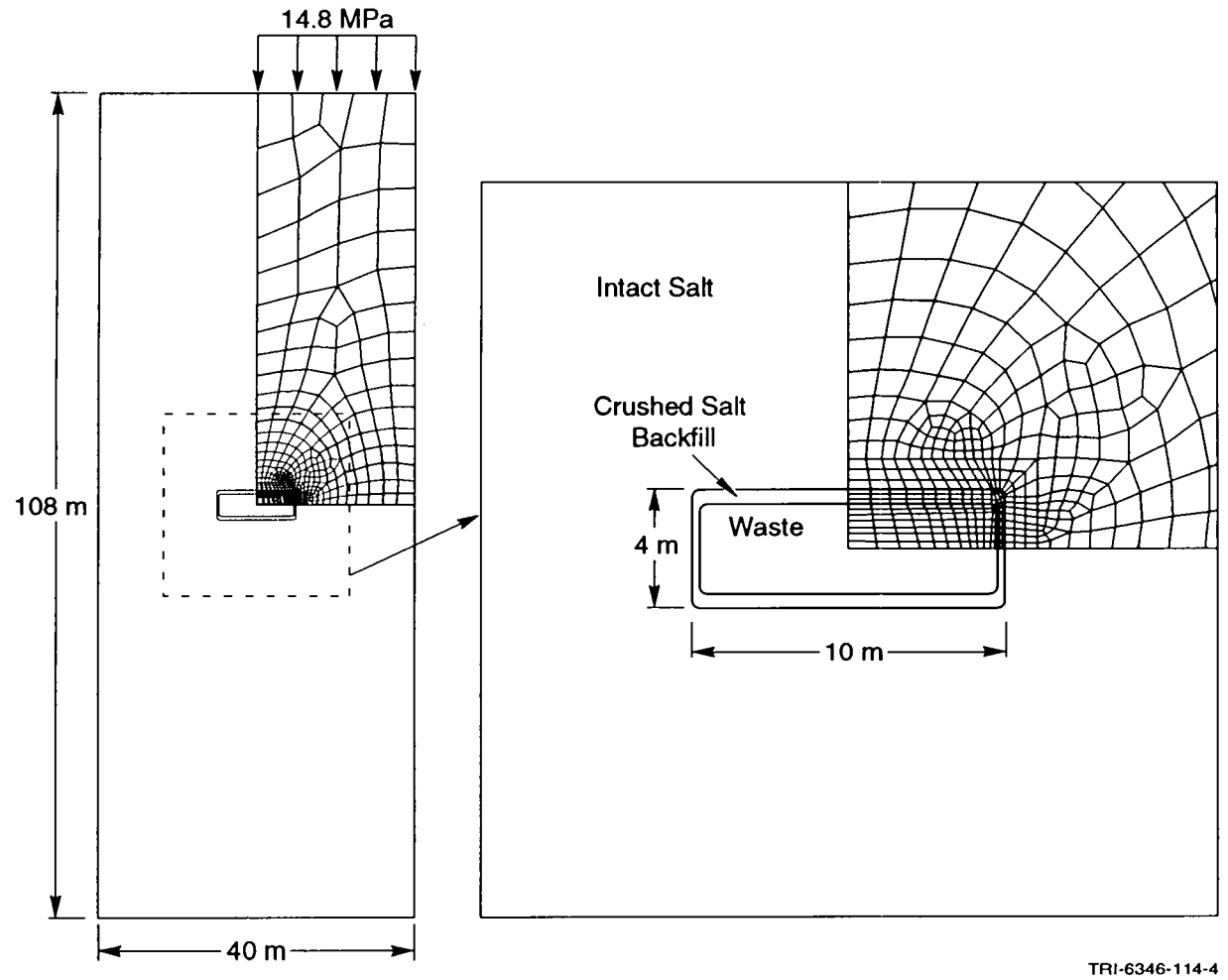

Figure 1.4-7. Modeling mesh and boundary conditions for calculation of porosity surface with SANCHO (adopted from Mendenhall et al., 1991, Figure 3-2).

V_s = volume of solids per storage room,
f = percentage of waste generating gas,
D = number of drums.

In these geomechanical simulations, gas pressure acts outward on the walls, floor, and ceiling of the storage room providing a backstress opposing closure (Mendenhall et al., 1991).

1.5 Background on WIPP

1.5.1 Purpose

The DOE was authorized by Congress in 1979 to build the WIPP as a research and development facility to demonstrate the safe management, storage, and eventual disposal of transuranic (TRU) waste generated by DOE defense

programs (WIPP Act, 1979). Only after demonstrating compliance with *40 CFR 191* and other laws and regulations (e.g., RCRA [1976] and NEPA [1969]) will the DOE permanently dispose of TRU waste at the WIPP repository.

1.5.2 Location

The WIPP is located within a large sedimentary basin, the Delaware Basin, in southeastern New Mexico, an area of low population density approximately 38 km (24 mi) east of Carlsbad (Figure 1.5-1). Geographically, the WIPP is between the high plains of West Texas and the Guadalupe and Sacramento Mountains of southeastern New Mexico.

Four prominent surface features are found in the area--Los Medaños ("The Dunes"), Nash Draw, Laguna Grande de la Sal, and the Pecos River. Los Medaños is a region of gently rolling hills that slopes upward to the northeast from the eastern boundary of Nash Draw to a low ridge called "The Divide." The WIPP is in Los Medaños. Nash Draw, 8 km (5 mi) west of the WIPP, is a broad shallow topographic depression with no external surface drainage. Laguna Grande de la Sal, about 9.5 km (6 mi) west-southwest of the WIPP, is a large playa about 3.2 km (2 mi) wide and 4.8 km (3 mi) long formed by coalesced collapse sinks that were created by dissolution of evaporate deposits. The Pecos River, the principal surface-water feature in southeastern New Mexico, flows southeastward, draining into the Rio Grande in western Texas.

1.5.3 Geologic History of the Delaware Basin

The Delaware Basin, an elongated, geologically confined depression, extends from just north of Carlsbad, New Mexico, into Texas west of Fort Stockton (Figure 1.5-2). The basin covers 33,000 km^2 (12,750 mi^2) and is filled with sedimentary rocks to depths as great as 7,300 m (24,000 ft) (Hills, 1984). Geologic history of the Delaware Basin began about 450 to 500 million years ago when a broad, low depression formed during the Ordovician Period as transgressing seas deposited clastic and carbonate sediments (Hiss, 1975; Powers et al., 1978; Cheeseman, 1978; Williamson, 1978; Hills, 1984; Ward et al., 1986; Harms and Williamson, 1988). After a long period of accumulation and subsidence, the depression separated into the Delaware and Midland Basins when the area now called the Central Basin Platform uplifted during the Pennsylvanian Period, about 300 million years ago.

During the Early and Middle Permian Period, the Delaware Basin subsided rapidly, resulting in a sequence of clastic rocks rimmed by reef limestone. The thickest of the reef deposits, the Capitan Limestone, is buried north and east of the WIPP but is exposed at the surface in the Guadalupe Mountains to the west (Figure 1.5-2). Evaporite deposits (marine bedded salts) of the Castile Formation and the Salado Formation, which hosts the WIPP, filled the basin during the late Permian Period and extended over the reef margins. Evaporites, carbonates, and clastic rocks of the Rustler Formation and the Dewey Lake Red Beds were deposited above the Salado Formation before the end of the Permian Period.

1.5.4 Repository

The repository is located in the Delaware Basin in the 600-m- (2,000-ft-) thick Salado Formation of marine bedded salts (Late Permian Period). The repository level is located within these bedded salts 655 m (2,150 ft) below the surface and 384 m (1,260 ft) above sea level. The WIPP repository is composed of a single underground disposal level connected to the surface by four shafts (Figure 1.5-3). The repository level consists of an experimental area at the north end and a disposal area at the south end.

1.5.5 WIPP Waste Disposal System

The WIPP relies on three approaches to contain waste: geologic barriers, engineered barriers, and institutional controls. The third approach, institutional controls, consists of many parts, e.g., the legal ownership and regulations

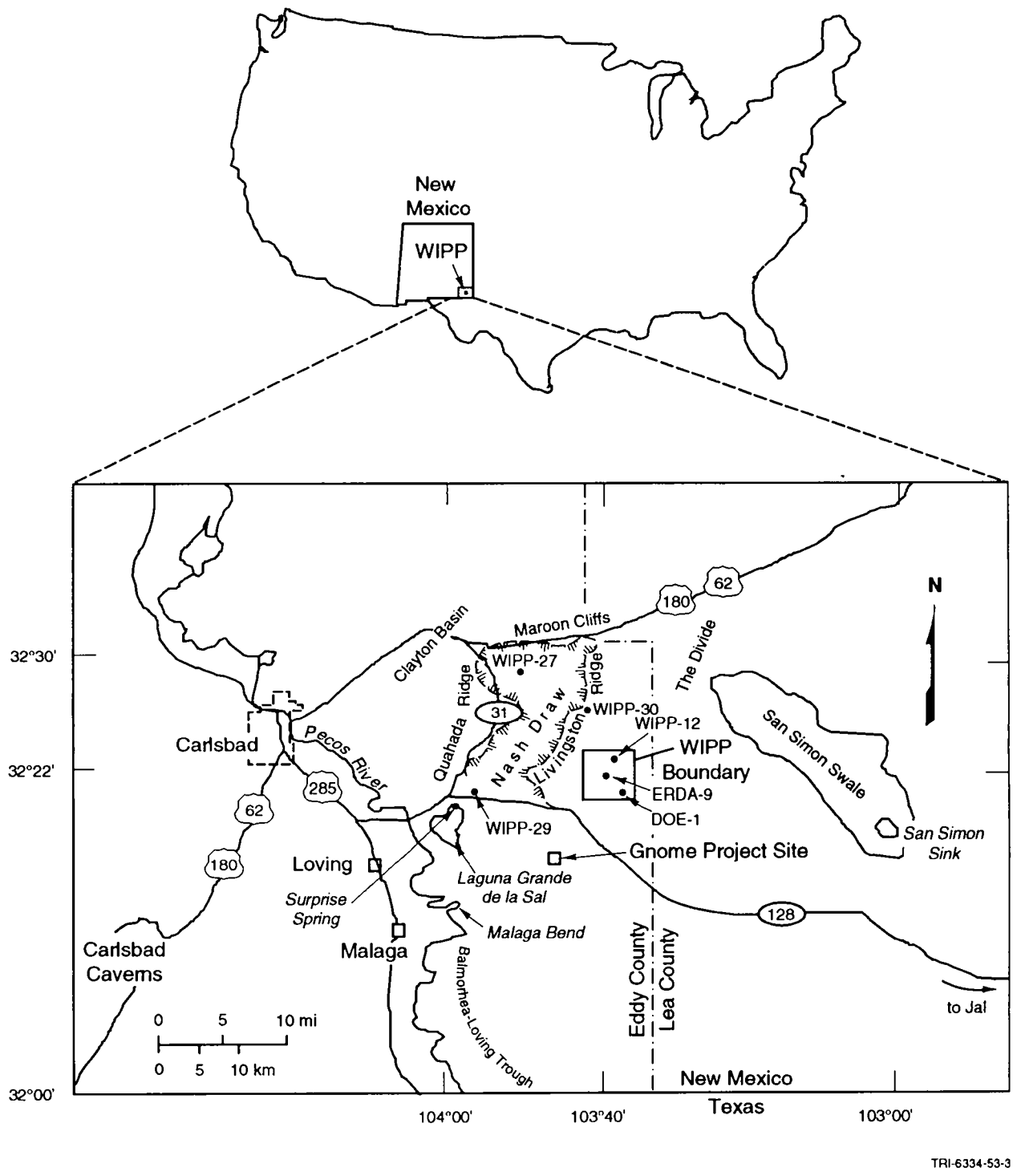

Figure 1.5-1. WIPP location in southeastern New Mexico (after Rechard, 1989, Figure 1.2).

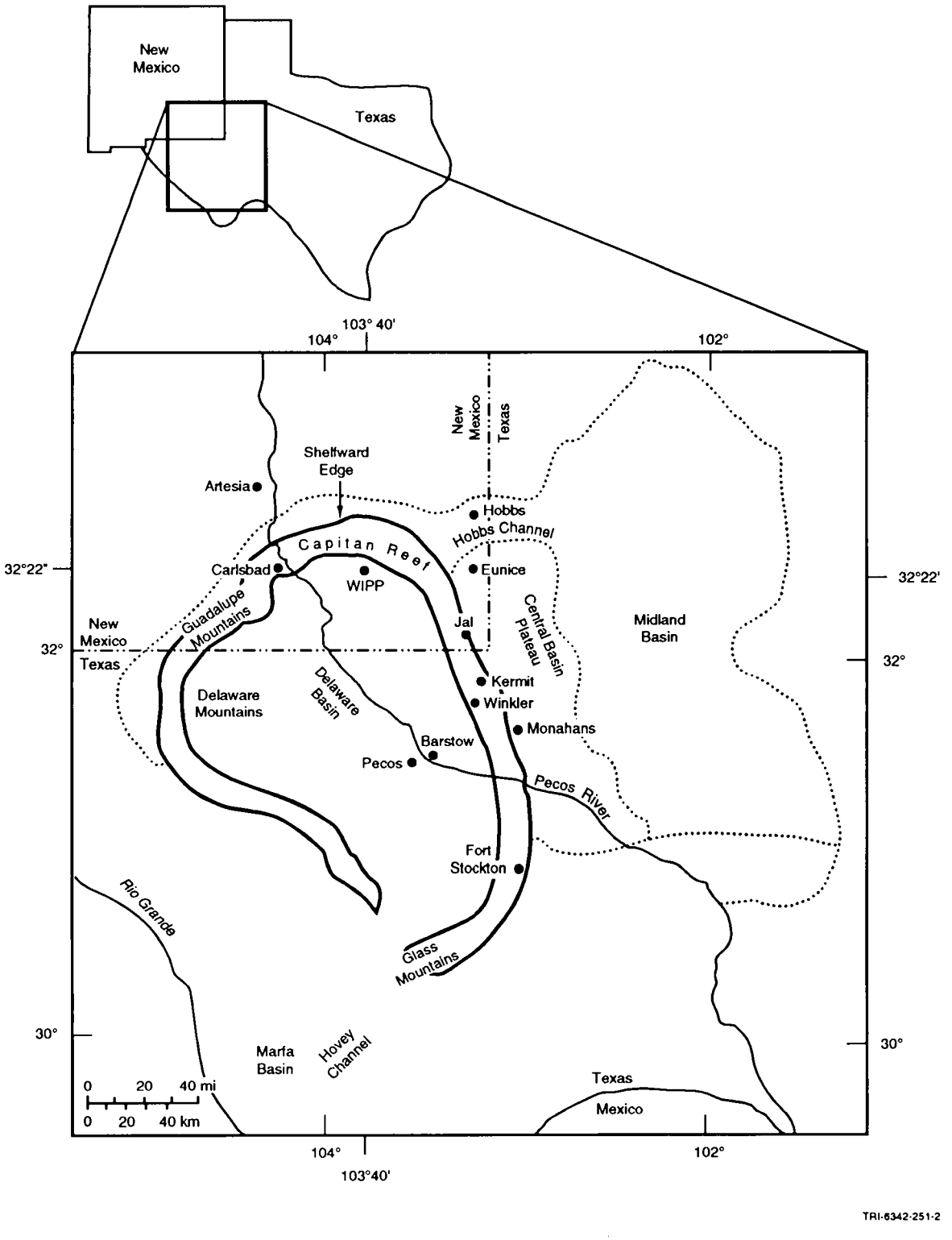

Figure 1.5-2. Location of the WIPP in the Delaware Basin (modified from Richey et al., 1985 and Lappin, 1988, Figure 1.4).

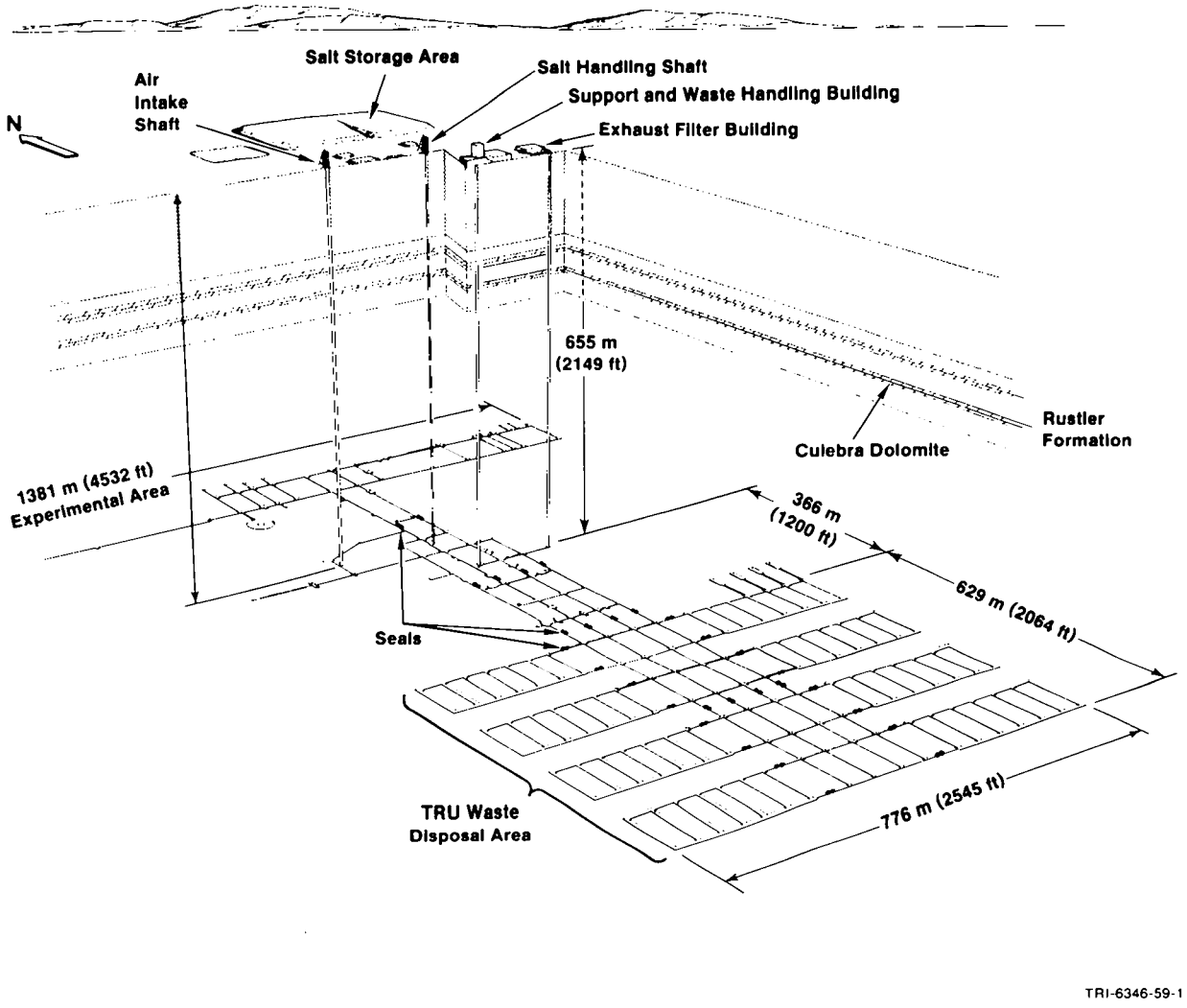

Figure 1.5-3. WIPP repository, showing surface facilities, proposed TRU disposal areas, and experimental areas (after Nowak et al., 1990, Figure 2).

of the land and resources by the U.S. Government, the fencing and signs around the property, permanent markers, public records and archives, and other methods of preserving knowledge about the disposal system.

The WIPP disposal system, as defined by *40 CFR 191*, includes the geologic and engineered barriers. The physical features of the repository (e.g., design of repository, waste form) are components of these barriers.

The geologic barriers are limited to the lithosphere up to the surface and no more than 5 km (3 mi) from the outer boundary of the WIPP waste-emplacement panels (Figure 1.5-4). The boundary of this maximum-allowable geologic subsystem is greater than the current boundary of the WIPP land withdrawal. The extent of the WIPP controlled area will be defined during performance assessment but will not be less than the area withdrawn, which is under U.S. DOE administrative control (Bertram-Howery and Hunter, 1989).

Data for components of the geologic and engineered barriers are the subject of this volume. No data on institutional controls are contained in this volume.

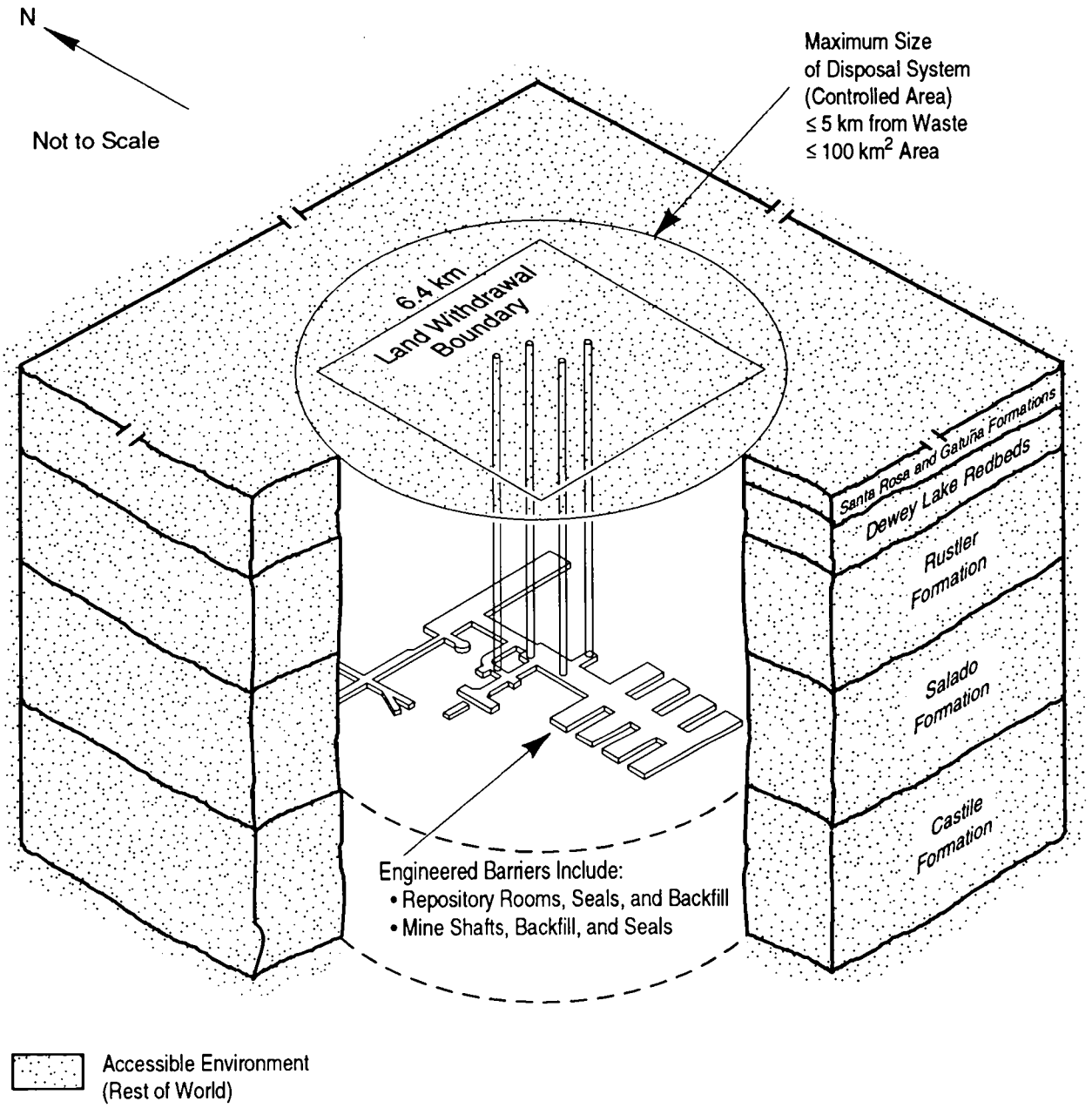

Figure 1.5-4. Geologic and engineered barriers of the WIPP disposal system (after Bertram-Howery and Hunter, 1989, Figure II-1).

2. GEOLOGIC BARRIERS

The geologic barriers consist of the physical features of the repository, such as stratigraphy and geologic components.

2.1 Areal Extent of Geologic Barriers

Figure 2.1-1 shows the maximum areal extent of the geologic barriers. Figure 2.1-2 shows the universal transverse mercator (UTM) coordinates of the modeling domains. The UTM coordinates for the northeast and southeast corners of the land-withdrawal boundary were derived from values reported in Gonzales (1989). Because the township ranges shift at the land-withdrawal border, the UTM coordinates for the northwest and southwest corners were derived from information on the wells nearest the corners (i.e., Well H-6A for the northwest corner and Well D-15 for the southwest corner).

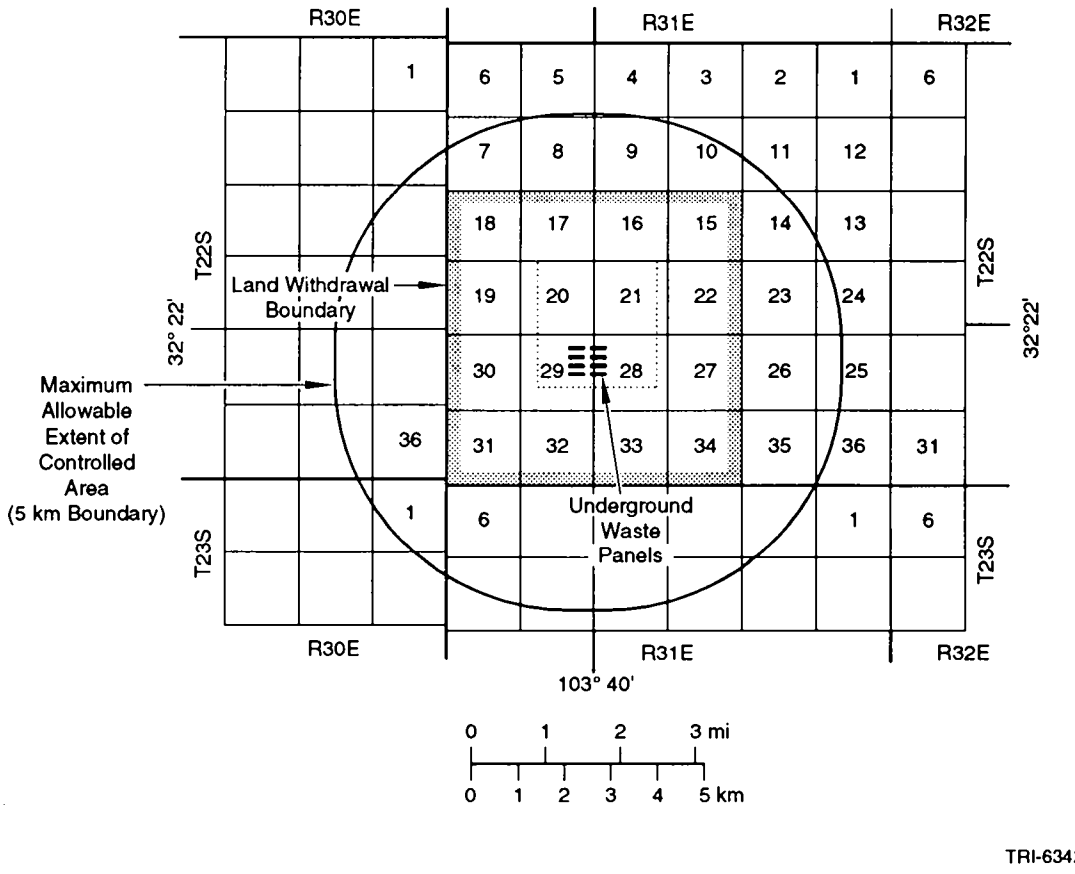

Figure 2.1-1. Position of the WIPP waste panels relative to land-withdrawal boundary (16 contiguous sections), 5-km boundary (40 CFR 191.12y), and surveyed section lines (after U.S. DOE, 1989, Figure 2.2).

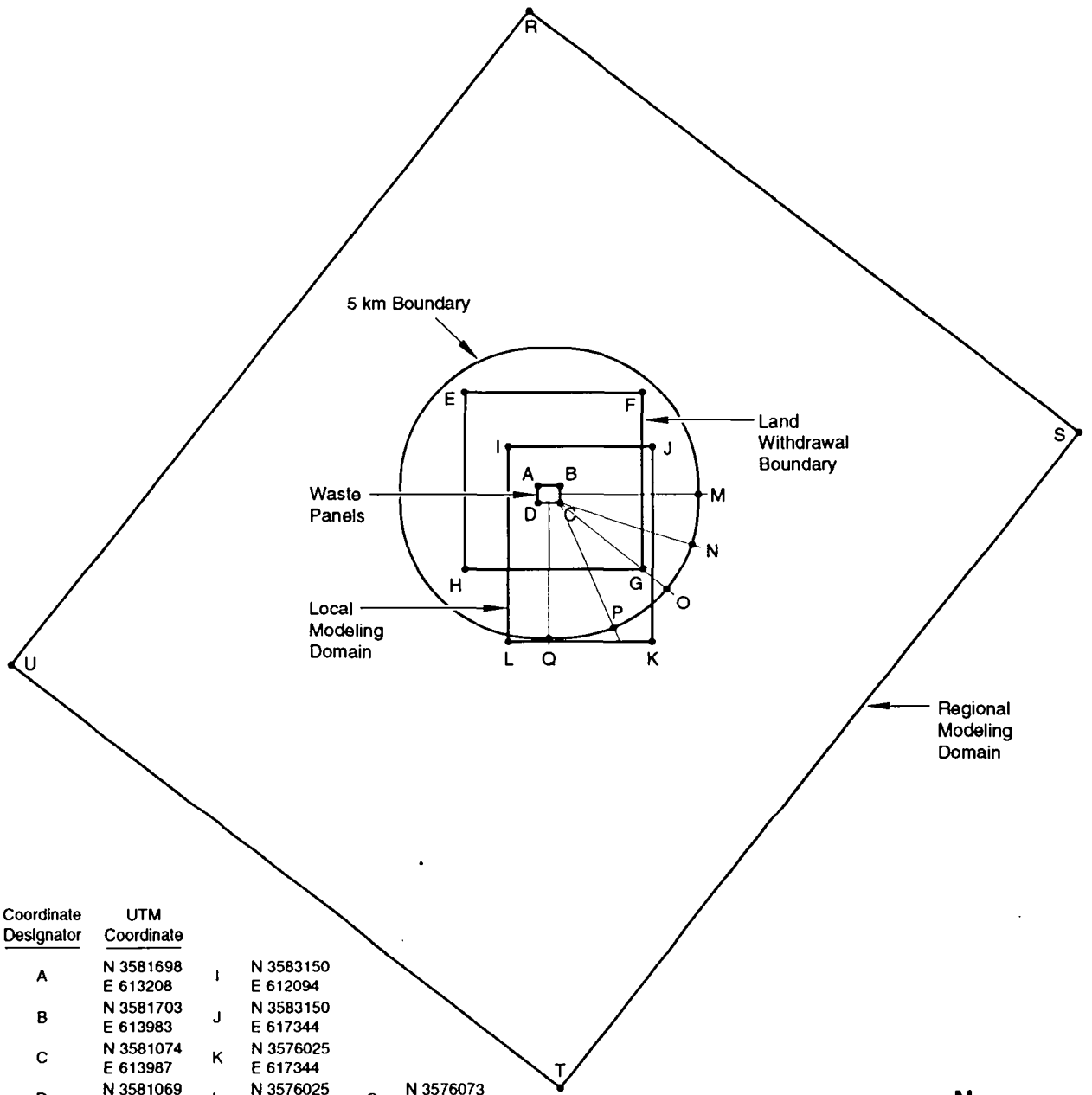

Coordinate Designator	UTM Coordinate				
A	N 3581698 E 613208	I	N 3583150 E 612094		
B	N 3581703 E 613983	J	N 3583150 E 617344		
C	N 3581074 E 613987	K	N 3576025 E 617344		
D	N 3581069 E 613212	L	N 3576025 E 612094	Q	N 3576073 E 613631
E	N 3585057 E 610496	M	N 3581420 E 618984	R	N 3598943 E 612819
F	N 3585109 E 616941	N	N 3579579 E 618791	S	N 3583551 E 632519
G	N 3578681 E 617015	O	N 3577945 E 617856	T	N 3559911 E 614049
H	N 3578612 E 610566	P	N 3576436 E 615991	U	N 3575303 E 594349

TRI-6342-1406-0

Figure 2.1-2. UTM coordinates of the modeling domains.

Figure 2.1-3 shows the topography, the locations of wells used for defining the general stratigraphy, and the modeling domains near the WIPP typically plotted in the report. The well locations by UTM, state plan coordinates, and survey sections are provided in Table B.1 (Appendix B). The elevations of the stratigraphic layers in each of the wells are tabulated in Table B.2 (Appendix B).

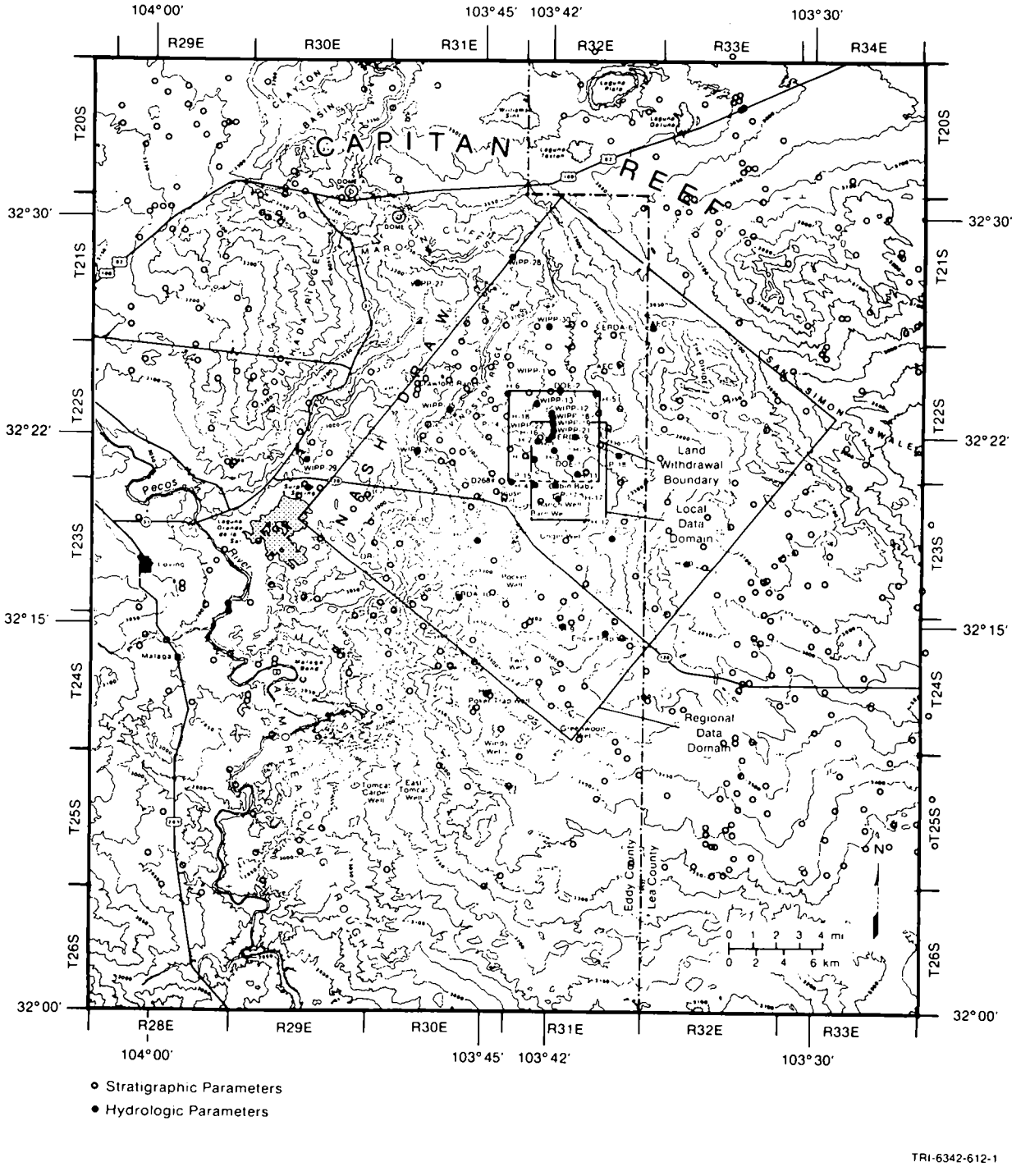

Figure 2.1-3. Locations of wells for defining general stratigraphy and regional and local data domains typically plotted in this volume.

2.2 Stratigraphy at the WIPP

The level of the WIPP repository is located within bedded salts (Figures 2.2-1 and 2.2-2), which consist of thick halite and interbeds of minerals such as clay and anhydrites of the Late Permian Period (Ochoan Series) (approximately 255 million yr old)* (Figure 2.2-3). A polyhalitic anhydrite interbed that forms a potential transport pathway, Marker Bed 139 (MB139), is located about 1 m (3 ft) below the repository interval (Figure 2.2-3). This unit is about 1 m (3 ft) thick and is one of about 45 siliceous or sulfatic units within the Salado Formation (Figure 2.2-4) (Lappin, 1988; Tyler et al., 1988).

For most strata above the repository, the elevations (though varying) are well known because of numerous wells; however, directly below the repository the elevations of the base of Anhydrite III in the Castile Formation and the top of Bell Canyon can only be inferred from a geologic cross section (Figure 2.2-1). The geologic structure is uncomplicated, thus the uncertainty is likely to be small on the regional geologic scale. Because the information is important to evaluating the potential for and size of brine reservoirs under the repository, uncertainty bounds have been placed on these two elevations inferred from the geologic cross section. In the 1992 PA calculations, elevations of the two contacts at ERDA-9 were assumed to vary uniformly between the elevations reported from the closest wells that provide data (Cabin Baby-1 and WIPP-12 for the base of Anhydrite III, and Cabin Baby-1 and DOE-2 for the top of the Bell Canyon Formation).

*This age reflects the 1983 Geological Society of America time scale (Geological Society of America, Inc., 1984).

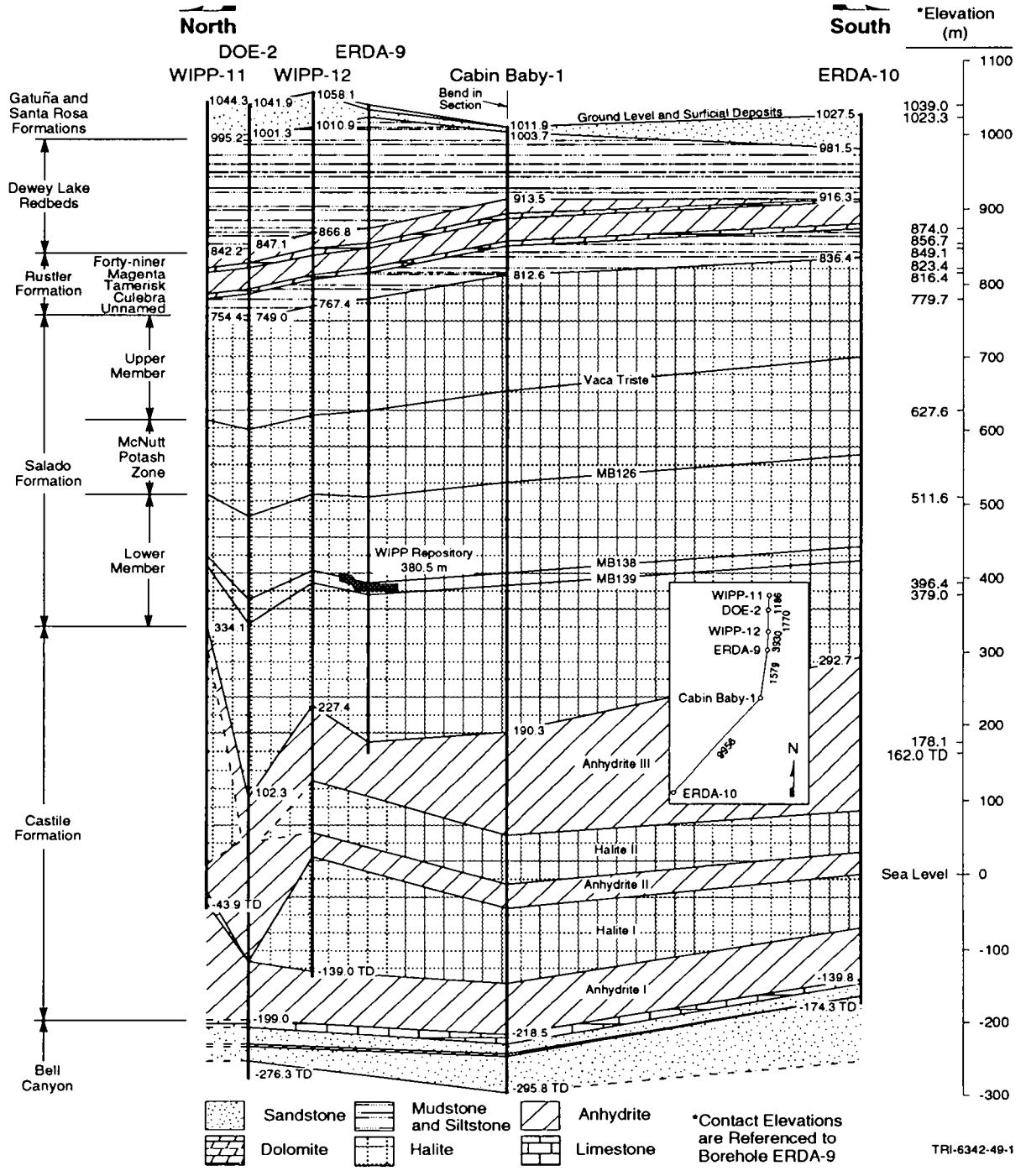

Figure 2.2-1. Level of WIPP repository, located in the Salado Formation. The Salado Formation is composed of thick halite with thin interbeds of clay and anhydrite deposited as marine evaporites about 255 million years ago (Permian period) (after Lappin, 1988, Figure 3.1 based on Borns, 1987).

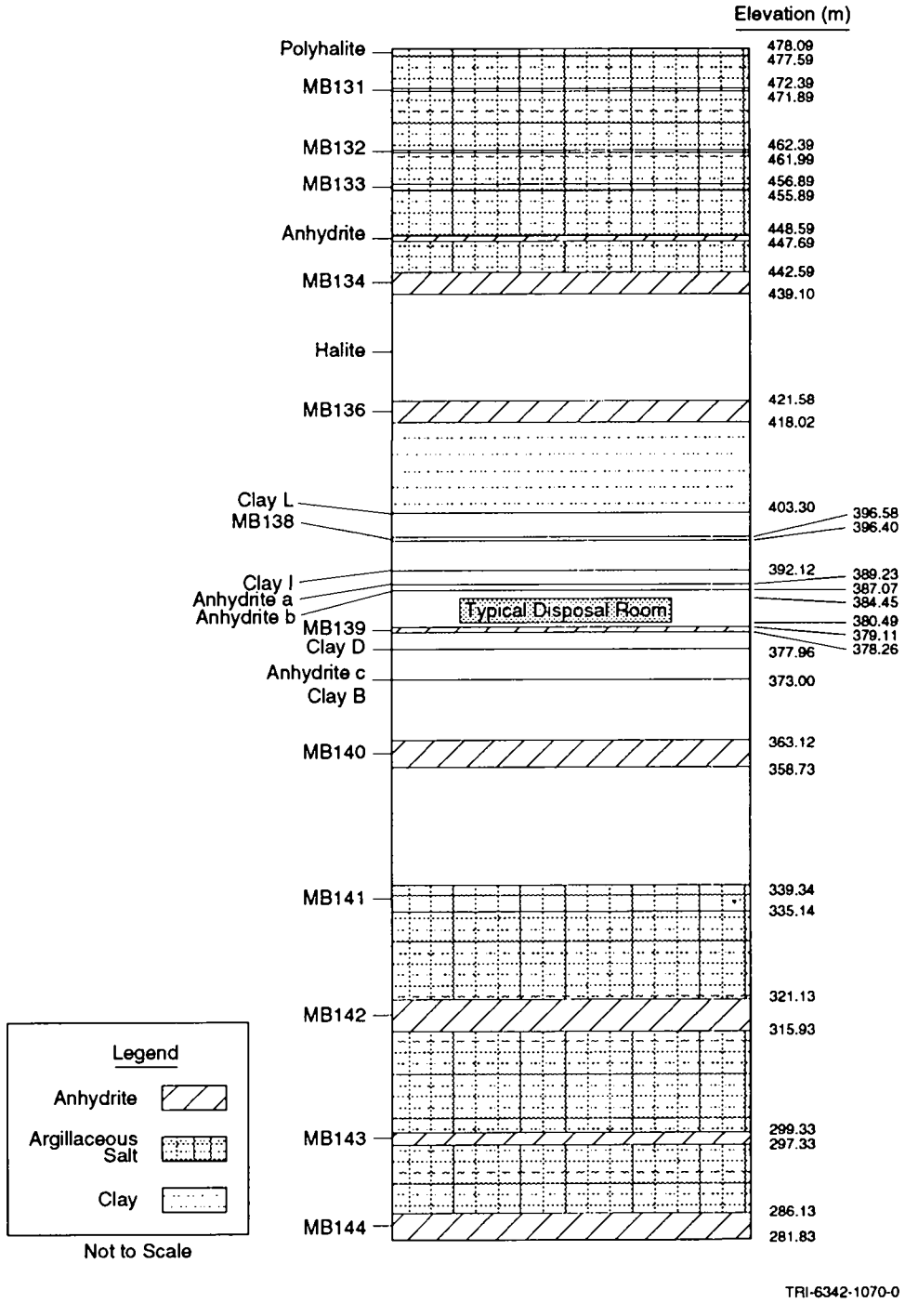

Figure 2.2-2. Reference local stratigraphy near repository (after Munson et al., 1989, Figure 3-3).

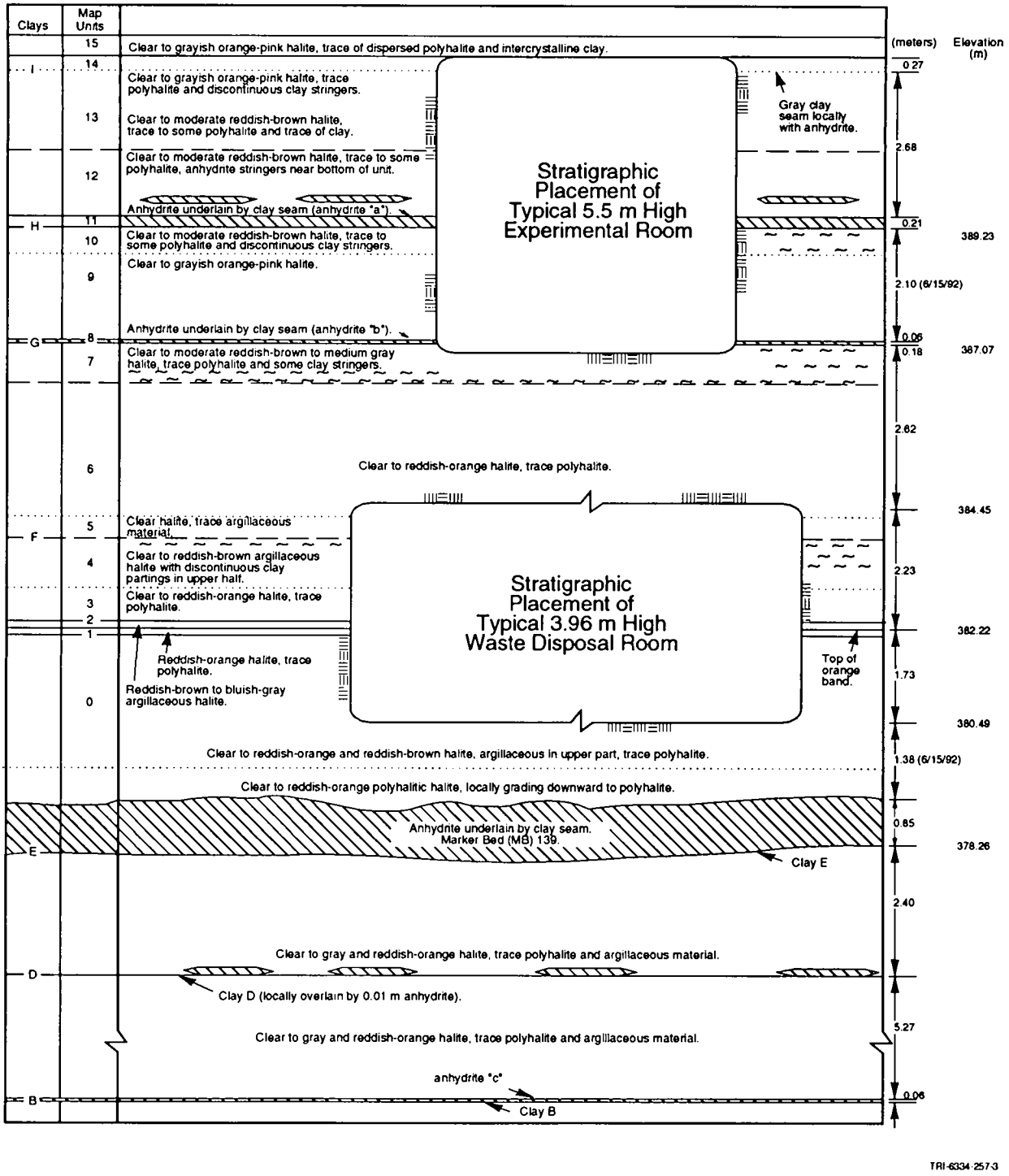

Figure 2.2-3. Stratigraphy at the repository horizon (after Bechtel National, Inc., 1986, Figures 6-2, 6-3 and Lappin et al., 1989, Figure 4-12). Units in the disposal area dip slightly to the south, but disposal excavations are always centered about the orange marked band (reddish-orange halite).

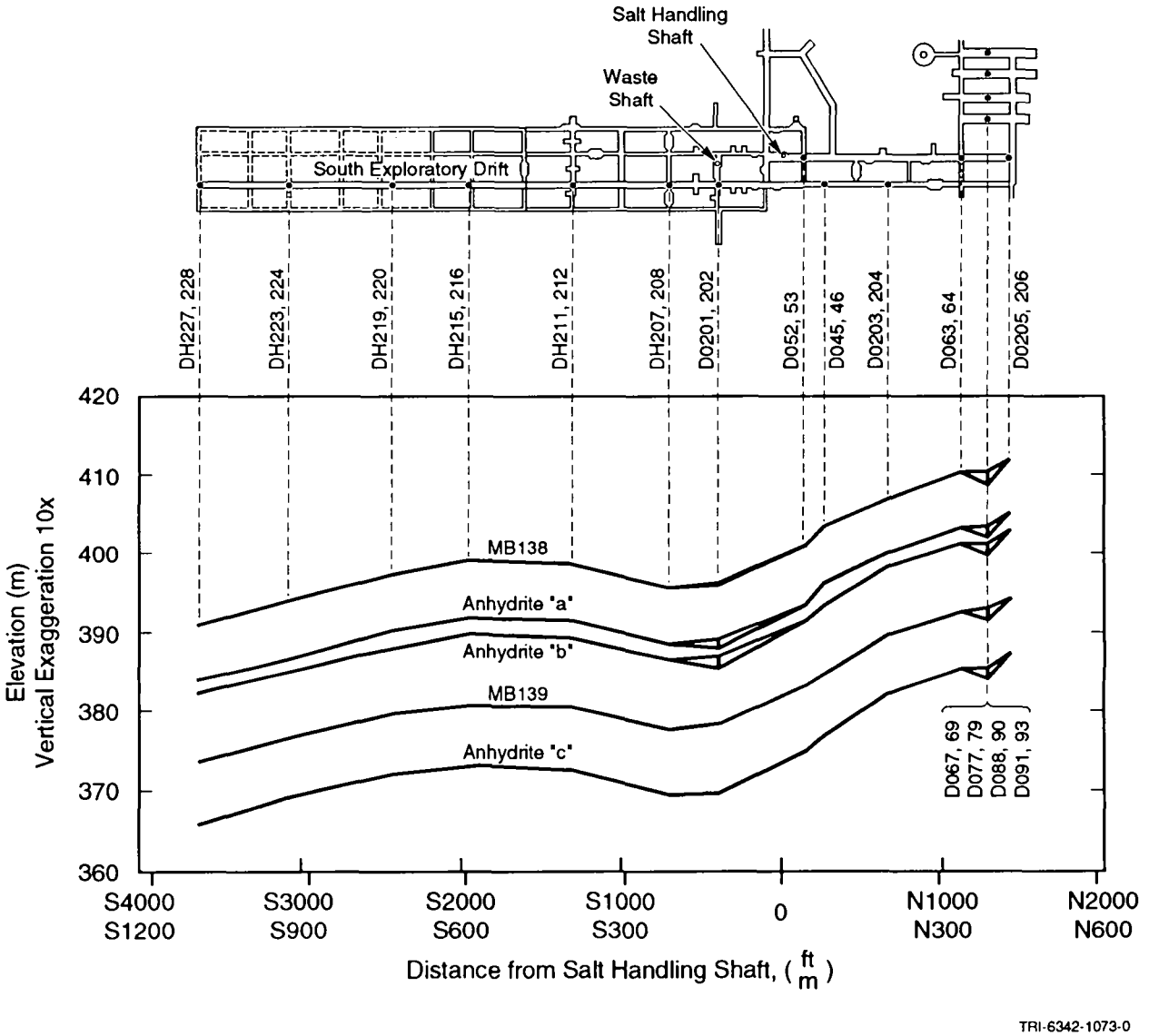

Figure 2.2-4. North-south cross-section showing Salado Formation stratigraphy near repository (after Krieg, 1984, Figure 2).

Anhydrite III Elevation*

Parameter: **Base of Anhydrite III elevation above mean sea level @ ERDA-9**
Material: Anhydrite within Castile Formation (Anhydrt3, Elevat)

Definition, Units: m

Values: Range: (53, 127) Median: 90

Distribution: Uniform
Correlation:

Data Source(s): See Discussion.
(WIPP Observational Data; Investigator Judgment)

Usage:

Mathematical model:
Area of Castile Brine Reservoir below WIPP Disposal Area (Section 5.1, this volume).

Equation (NA).

Computational models:
CCDFPERM

Ranking in Past Sensitivity Analyses:

40 CFR 191	Not tested
40 CFR 268	Not applicable
NEPA	Not applicable
Other	Not applicable

*Key to Parameter Sheets is provided in Section 1.2.8.

Bell Canyon Elevation @ ERDA-9*

Parameter: **Top of Bell Canyon elevation above mean sea level @ ERDA-9**
Material: Bell Canyon Formation (BCanyon, All, Elevat)

Definition, Units: m

Values: Range: (-228, -198) Median: -213

Distribution: Uniform
Correlation:

Data Source(s): See Discussion.
(WIPP Observational Data; Investigator Judgment)

Usage:

Mathematical model:
Area of Castile Brine Reservoir below WIPP Disposal Area (Section 5.1, this volume).

Equation (NA).

Computational models:
CCDFPERM

Ranking in Past Sensitivity Analyses:

40 CFR 191	Not tested
40 CFR 268	Not applicable
NEPA	Not applicable
Other	Not applicable

*Key to Parameter Sheets is provided in Section 1.2.8.

2.3 Hydrologic Parameters for Halite and Polyhalite within Salado Formation

The Salado Formation is composed of thick halite with thin interbeds of clay and anhydrite deposited as marine evaporites about 255 million years ago (Permian Period). A summary of the parameters for the Salado Formation near the repository are given in Table 2.3-1.

Table 2.3-1. Parameter Values for Halite and Polyhalite within Salado Formation near Repository

Parameter[a]	Median	Range		Units	Distribution Type	Source
Capillary pressure (p_c) and relative permeability (k_{rw})						
Threshold displacement pressure (p_t)	2.3×10^7	2.3×10^5 (correlated with permeability in 1992)	2.3×10^9	Pa	Lognormal	Davies, 1991a, 1991b
Residual saturations						
Wetting phase (S_{wr})	**2×10^{-1}**	**0**	**4×10^{-1}**	**none**	**Uniform**	**Webb, 1992a, 1992b, Memos in Appendix A; Davies and LaVenue, 1990b**
Gas phase (Sgr)	**2×10^{-1}**	**0**	**4×10^{-1}**	**none**	**Uniform**	**Davies and LaVenue, 1990b; Webb, 1992a, 1992b, Memos in Appendix A**
Brooks-Corey exponent (λ)	**0.7**	**0.2**	**10.0**	**none**	**Constructed**	**Davies and LaVenue, 1990b; Webb, 1992a, 1992b, Memos in Appendix A**
Density						
Grain (ρ_g) halite	2.163×10^3			kg/m^3	Constant	Carmichael, 1984, Table 2; Krieg, 1984, p. 14; Clark, 1966, p. 44
Grain (ρ_g) polyhalite	2.78×10^3			kg/m^3	Constant	Hume and Shakoor, 1981, p. 103-203
Bulk (ρ_{bulk})	2.14×10^3			kg/m^3	Constant	Holcomb and Shields, 1987, p.17
Average (ρ_{ave})	2.3×10^3			kg/m^3	Constant	Krieg, 1984, Table 4
Dispersivity						
Longitudinal (α_L)	1.5×10^1	1	4×10^1	m	Constructed	Pickens and Grisak, 1981; Lappin et al., 1989, Table D-2
Ratio (α_L/α_T)	10	3	25	none	Constructed	Pickens and Grisak, 1981; Freeze and Cherry, 1979, Figure 9.6
Partition coefficient						
All species	0			m^3/kg	Constant	Lappin et al., 1989, p. D-17
Permeability (k)						
Log undisturbed	**-21.2**	**-24.0**	**-19.0**	**log (m^2)**	**Constructed**	**Gorham et al., June 15, 1992, Memo in Appendix A; Howarth et al., 1991; Beauheim et al., 1991a**
Log disturbed	-20.7	-22.0	-15.0	log (m^2)	Constructed	Gorham et al., June 15, 1992, Memo in Appendix A; Howarth et al., 1991; Beauheim et al., 1991a
Pore pressure (p)	9.5	9.0	10.0	MPa	Uniform	Gorham et al., June 15, 1992, Memo in Appendix A; Howarth et al., 1991; Beauheim et al., 1991a
Porosity (ϕ)						
Undisturbed	1×10^{-2}	1×10^{-3}	3×10^{-2}	none	Constructed	See text; Powers et al.,1978; U.S. DOE, 1983
Disturbed	6×10^{-2}			none	Constant	See text.
Specific storage	9.5×10^{-8}	2.8×10^{-8}	1.4×10^{-6}	m^{-1}	Constructed	Beauheim, 1991
Tortuosity	1.4×10^{-1}	1×10^{-2}	6.67×10^{-1}	none	Constructed	Freeze and Cherry, 1979, p. 104; Kelley and Saulnier, 1990, Table 4.6; Lappin et al., 1989, Table E-9

[a]Parameters in bold were sampled in the 1992 calculations.

2.3.1 Capillary Pressure and Relative Permeability

Two-phase characteristic curves (capillary pressure and relative permeability) for Salado halite, Salado anhydrite, and waste have not been measured. In modeling two-phase phenomena (Section 1.4.1), the PA Department has adopted suggestions of Davies (1991b) and Webb (1992b, Memo in Appendix A) that characteristic curves be calculated using either the Brooks-Corey formulae (Brooks and Corey, 1964) or the Van Genuchten-Parker formulae (Van Genuchten, 1978). Use of either formulae requires knowledge of four material-property parameters:

- p_t - threshold displacement pressure (Pa),
- $S_{\ell r}$ - residual wetting phase saturation (dimensionless),
- S_{gr} - residual (or critical) gas saturation (dimensionless),
- λ - the Brooks-Corey exponent (dimensionless).

None of these parameters has been measured for materials of interest (halite, anhydrite, waste); for purposes of sensitivity analyses, their ranges, distributions and correlations are estimated from natural-analog data (Davies and LaVenue, 1990b; Davies, 1991b; Webb, 1992a, Memo in Appendix A). The natural analogs consist of materials that possess some of the same characteristics (i.e., permeability and porosity) as the anhydrite, halite, and waste room. The natural analogs applicable to the very low permeability of the halite and anhydrite were sands that were investigated during the Multiwell Tight Gas Sands Project (Ward and Morrow, 1985). The permeability for these sands typically ranges from 1×10^{-16} to 1×10^{-19} m^2 (1×10^{-1} to 1×10^{-4} mD). Although these permeabilities are higher than those of the anhdyrites and halites, no other material was found with a lower permeability for which capillary pressure and relative permeability curves had been measured. Parameters selected for the anhydrites and waste room are discussed in later sections.

The uncertainty surrounding these parameters is unknown. An initial range was selected for the purpose of being able to run sensitivity studies. The ranges shown for the parameters are arbitrary, corresponding to a simple doubling and halving of the median values. A family of curves produced by sampling 20 times from the assigned distributions using the Brooks-Corey formulae is shown in Figure 2.3-1. Sample curves for capillary pressure and relative permeability are also shown in Figure 2.3-2.

a)

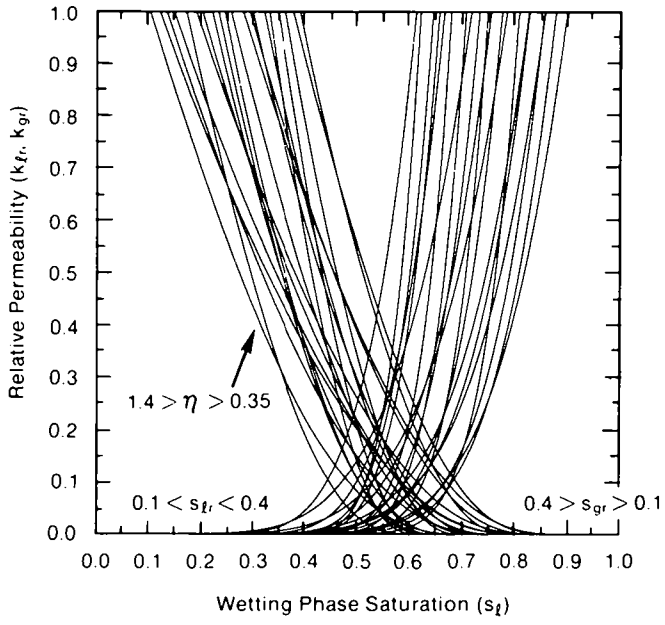

b)

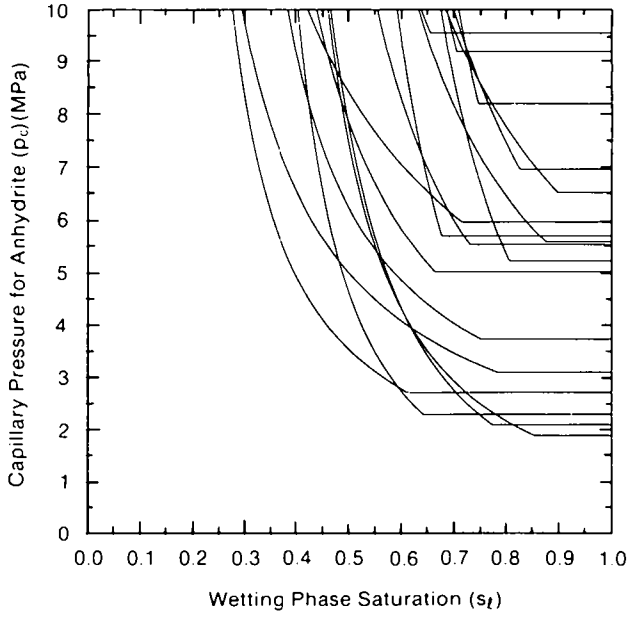

TRI-6342-1465-0

Figure 2.3-1. Example of variation in relative permeability and capillary pressure when Brooks and Corey parameters are varied.

a)

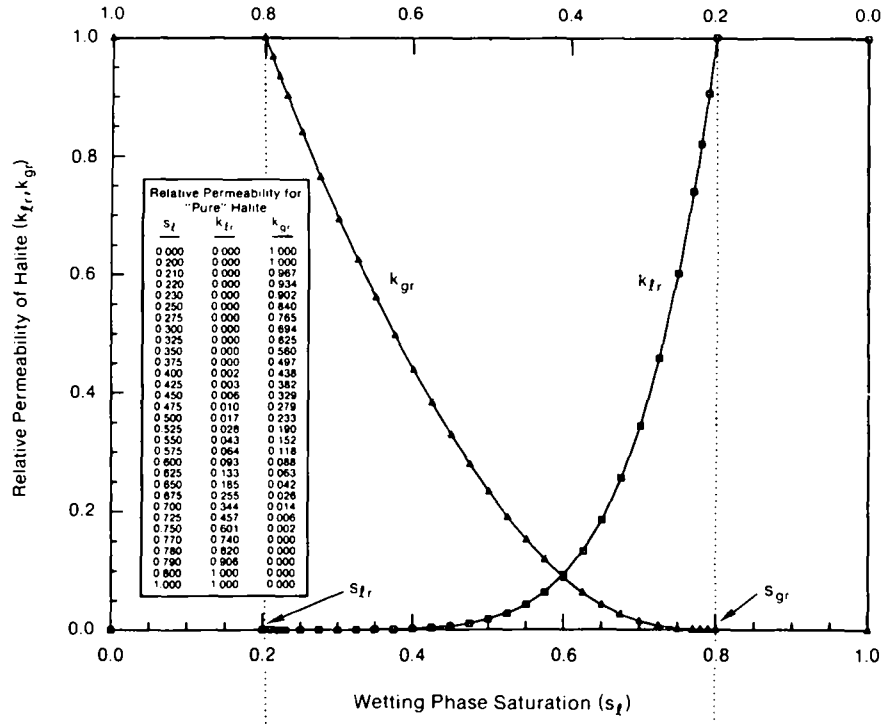

b)

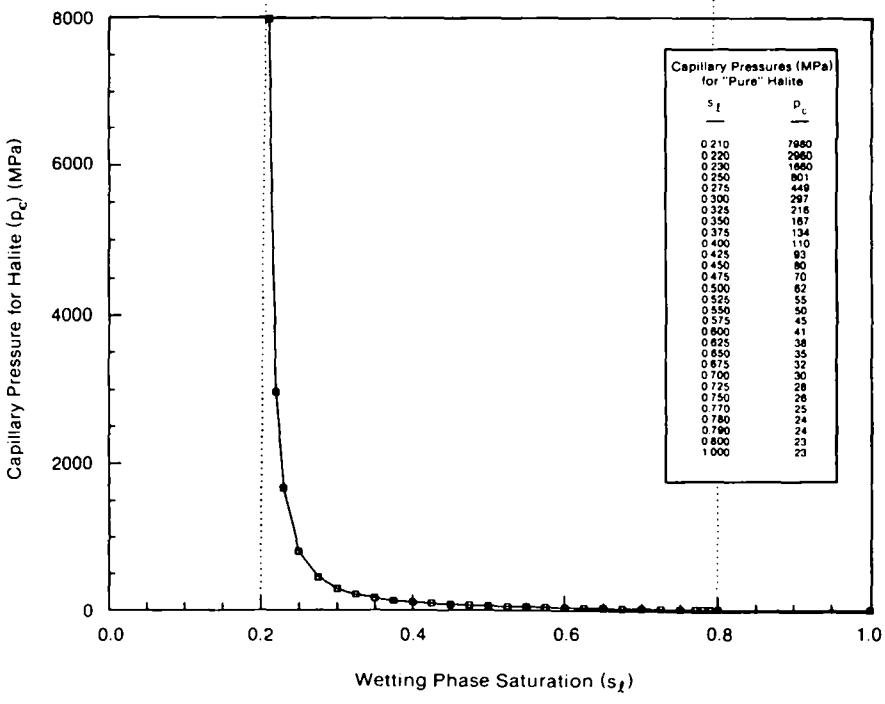

TRI-6342-1402-0

Figure 2.3-2. Estimated relative permeability and capillary pressure curves (source: Davies, 1991a).

Threshold Displacement Pressure, p_t*

Parameter: **Threshold displacement pressure (p_t)**
Material: Halite and polyhalite within Salado Formation, (Salado, PressCTD)

Definition, Units: Pa

Values: Range: (2.3×10^5, 2.3×10^9) Median: 2.3×10^7

Distribution: Lognormal
Correlation: Correlated with halite permeability (see Discussion)

Data Source(s): Davies, P. B. 1991a. *Evaluation of the Role of Threshold Pressure in Controlling Flow of Waste-Generated Gas into Bedded Salt at the Waste Isolation Pilot Plant.* SAND90-3246. Albuquerque, NM: Sandia National Laboratories. (Investigator Judgment)

Davies, P. B. 1991b. Appendix A: "Uncertainty Estimates for Threshold Pressure for 1991 Performance Assessment Calculations Involving Waste-Generated Gas," *Preliminary Comparison with 40 CFR Part 191, Subpart B for the Waste Isolation Pilot Plant, December 1991. Volume 3: Reference Data.* WIPP Performance Assessment Division. Eds. R. P. Rechard, A. C. Peterson, J. D. Schreiber, H. J. Iuzzolino, M. S. Tierney, and J. S. Sandha. SAND91-0893/3. Albuquerque, NM: Sandia National Laboratories. A-37 through A-41. (Investigator Judgment)

Usage:

Mathematical model:
Section 1.4.1, this volume.

Equation 1.4.1-6.

Computational models: 2-Phase Fluid Flow
BRAGFLO

Ranking in Past Sensitivity Analyses:

40 CFR 191	Low
40 CFR 268	Not tested
NEPA	Not tested
Other	Not applicable

*Key to Parameter Sheets is provided in Section 1.2.8.

Discussion:

Threshold Pressure: Threshold pressure plays an important role in controlling which Salado lithologies are accessible to gas and at what pressure gas will flow. Some investigators define threshold pressure as the capillary pressure associated with first penetration of a nonwetting phase into the largest pores near the surface of the medium, which means that threshold pressure is equal to the capillary pressure at a water saturation of 1.0 (Davies, 1991a, p. 9). Others define threshold pressure as the capillary pressure associated with the incipient development of a continuum of the nonwetting phase through a pore network, providing gas pathways not only through relatively large pores, but also through necks between pores. This latter definition means that threshold pressure is equal to the capillary pressure at a saturation equal to the residual gas saturation (dashed lines in Figure 2.3-2). Because flow of waste-generated gas outward from the WIPP repository will require that outward flowing gas penetrate and establish a gas-filled network of flow paths in the surrounding bedded salt, the latter definition has been adopted here.

The Salado Formation's thick halite beds with anhydrite and clay interbeds are similar in many respects to the consolidated lithologies presented in Figure 2.3-3. Similarities in pore structure exist between halite, anhydrite, and low-permeability carbonates; low-permeability sandstones and crystalline cements; and clay interbeds and shales. Given the general similarities, a best-fit power curve through the combined data set for consolidated lithologies was judged to provide the best available correlation for estimates of threshold pressure for the Salado Formation (Figure 2.3-3). Threshold pressure is also a key parameter in the Brooks and Corey (1964) model used to characterize the 2-phase properties of analogue materials for preliminary gas calculations (Davies and LaVenue, 1990a). Because threshold pressure is strongly related to intrinsic permeability, an empirical estimate is used as follows (Davies, 1991a, p. 25):

$$p_t\,(\text{MPa}) = 5.6 \times 10^{-7}\,[k\,(\text{m}^2)]^{-0.346}\,.$$

Capillary Pressure and Relative Permeability. Figure 2.3-2a shows the values estimated for relative permeability for Salado salt using only the Brooks-Corey model. Figure 2.3-2b shows the estimated capillary pressure curve for Salado salt. Figures 2.3-1a and 2.3-1b are examples of variation in relative permeability and capillary pressure when the Brooks and Corey parameter is varied.

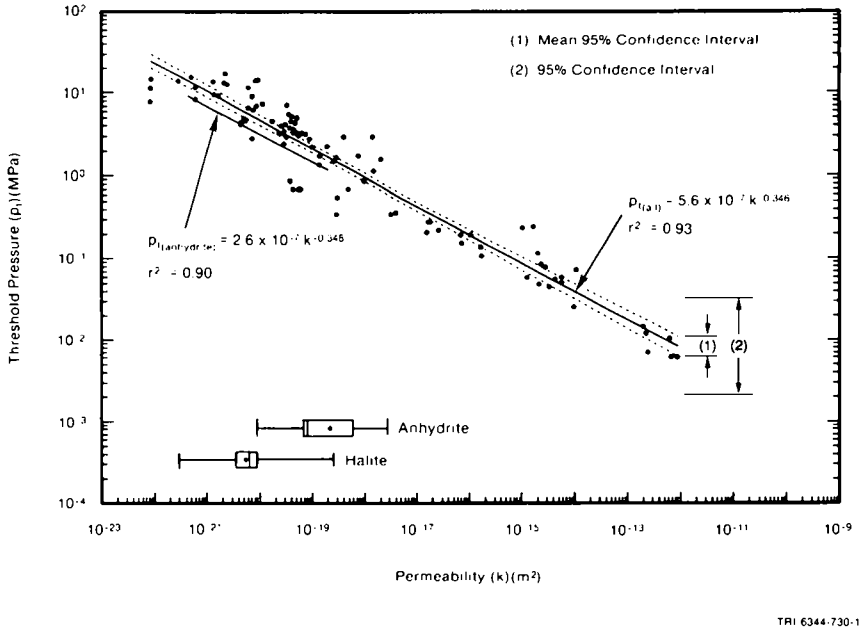

Figure 2.3-3. Correlation of threshold pressure with permeability for a composite of data from all consolidated rock lithologies. Data from Rose and Bruce, 1949; Wyllie and Rose, 1950; Thomas et al., 1968; and Ibrahim et al., 1970 (after Davies, 1991a, Figures 5 and 8).

Residual Wetting Phase (Liquid) Saturation*

Parameter: **Residual wetting phase (liquid) saturation ($S_{\ell r}$)**
Material: Halite and polyhalite within Salado Formation, (Salado, Sat RWP)

Definition, Units: Dimensionless

Values: Range: $(0, 4 \times 10^{-1})$ Median: 2×10^{-1}

Distribution: Uniform
Correlation:

Data Source(s):
Webb, S. W. 1992a. "Uncertainty Estimates for Two-Phase Characteristic Curves for 1992 RCRA Calculations" (see Appendix A, pp. A-141 through A-146). (Investigator Judgment)

Webb, S. W. 1992b. "Uncertainty Estimates for Two-Phase Characteristic Curves for 1992 40 CFR 191 Calculations" (see Appendix A, pp. A-147 through A-155). (Investigator Judgment)

Davies, P. B., and A. M. LaVenue. 1990b. Appendix A: "Additional Data for Characterizing 2-Phase Flow Behavior in Waste-Generated Gas Simulations and Pilot Point Information for Final Culebra 2-D Model (SAND89-7068/1)," *Data Used in Preliminary Performance Assessment of the Waste Isolation Pilot Plant (1990).* R. P. Rechard, H. Iuzzolino, and J. S. Sandha. SAND89-2408. Albuquerque, NM: Sandia National Laboratories. A-139 through A-156. (Investigator Judgment)

Usage:

Mathematical model:
Section 1.4.1, this volume.

Equation 1.4.1-7.

Computational models:
BRAGFLO

Ranking in Past Sensitivity Analyses:

40 CFR 191	Not tested
40 CFR 268	Low
NEPA	Not tested
Other	Not tested

*Key to Parameter Sheets is provided in Section 1.2.8.

Residual Gas Saturation*

Parameter:	**Residual gas saturation (S_{gr})**
Material:	Halite and polyhalite within Salado Formation, (Salado, SatRGP)
Definition, Units:	Dimensionless
Values:	Range: $(0, 4 \times 10^{-1})$ Median: 2×10^{-1}
Distribution:	Uniform
Correlation:	

Data Source(s):

Webb, S. W. 1992a. "Uncertainty Estimates for Two-Phase Characteristic Curves for 1992 RCRA Calculations" (see Appendix A, pp. A-141 through A-146). (Investigator Judgment)

Webb, S. W. 1992b. "Uncertainty Estimates for Two-Phase Characteristic Curves for 1992 40 CFR 191 Calculations" (see Appendix A, pp. A-147 through A-155). (Investigator Judgment)

Davies, P. B., and A. M. LaVenue. 1990b. Appendix A: "Additional Data for Characterizing 2-Phase Flow Behavior in Waste-Generated Gas Simulations and Pilot Point Information for Final Culebra 2-D Model (SAND89-7068/1)," *Data Used in Preliminary Performance Assessment of the Waste Isolation Pilot Plant (1990).* R. P. Rechard, H. Iuzzolino, and J. S. Sandha. SAND89-2408. Albuquerque, NM: Sandia National Laboratories. A-139 through A-156. (Investigator Judgment)

Usage:

Mathematical model:

Section 1.4.1, this volume.

Equation 1.4.1-7.

Computational models:

BRAGFLO

Ranking in Past Sensitivity Analyses:

40 CFR 191	Not tested
40 CFR 268	Low
NEPA	Not tested
Other	Not tested

*Key to Parameter Sheets is provided in Section 1.2.8.

Brooks and Corey Exponent*

Parameter: **Brooks and Corey exponent (λ)**
Material: Halite and polyhalite within Salado Formation, (Salado, BrkCorEx)

Definition, Units: Dimensionless

Values: Range: (0.2, 10.0) Median: 0.7

Distribution: Constructed
Correlation:

Data Source(s):

Webb, S. W. 1992a. "Uncertainty Estimates for Two-Phase Characteristic Curves for 1992 RCRA Calculations" (see Appendix A, pp. A-141 through A-146). (Investigator Judgment)

Webb, S. W. 1992b. "Uncertainty Estimates for Two-Phase Characteristic Curves for 1992 40 CFR 191 Calculations" (see Appendix A, pp. A-147 through A-155). (Investigator Judgment)

Davies, P. B., and A. M. LaVenue. 1990b. Appendix A: "Additional Data for Characterizing 2-Phase Flow Behavior in Waste-Generated Gas Simulations and Pilot Point Information for Final Culebra 2-D Model (SAND89-7068/1)," *Data Used in Preliminary Performance Assessment of the Waste Isolation Pilot Plant (1990).* R. P. Rechard, H. Iuzzolino, and J. S. Sandha. SAND89-2408. Albuquerque, NM: Sandia National Laboratories. A-139 through A-156. (Investigator Judgment)

Usage:

Mathematical model:
Section 1.4.1, this volume.

Equation 1.4.1-6.

Computational models:
BRAGFLO

Ranking in Past Sensitivity Analyses:

40 CFR 191	Not tested
40 CFR 268	Low
NEPA	Not tested
Other	Not applicable

*Key to Parameter Sheets is provided in Section 1.2.8.

2.3.2 Density

Grain Density of Halite in Salado Formation*

Parameter: **Density, grain (ρ_g)**
Material: Halite within Salado Formation (Halite, DnsGrain)

Definition, Units: kg/m^3

Values: 2.163×10^3

Distribution: Constant
Correlation:

Data Source(s):
Carmichael, R. S., ed. 1984. *CRC Handbook of Physical Properties of Rocks*. Boca Raton, FL: CRC Press, Inc. Vol. III. (Table 2)

Krieg, R. D. 1984. *Reference Stratigraphy and Rock Properties for the Waste Isolation Pilot Plant (WIPP) Project*. SAND83-1908. Albuquerque, NM: Sandia National Laboratories. (p. 14)

Clark, S. P., Jr., ed. 1966. *Handbook of Physical Constants*. Memoir 97. New York, NY: The Geological Society of America, Inc. (p. 44)

Usage:

Mathematical model:
(Value recommended for exploratory modeling.)

Equation (NA).

Computational models:
(NA)

Ranking in Past Sensitivity Analyses:

40 CFR 191	Not applicable
40 CFR 268	Not applicable
NEPA	Not applicable
Other	Not applicable

*Key to Parameter Sheets is provided in Section 1.2.8.

Grain Density of Polyhalite in Salado Formation*

Parameter: **Density, grain (ρ_g)**
Material: Polyhalite within Salado Formation (PHalite, All, DnsGrain)

Definition, Units: kg/m^3

Values: 2.78×10^3

Distribution: Constant
Correlation:

Data Source(s): Hume, H. R., and A. Shakoor. 1981. "Mechanical Properties," *Physical Properties Data for Rock Salt*. NBS Monograph 167. Washington, DC: National Bureau of Standards. (p. 103-203)

Usage:

Mathematical model:
(Value recommended for exploratory modeling.)

Equation (NA).

Computational models:
(NA)

Ranking in Past Sensitivity Analyses:

40 CFR 191	Not applicable
40 CFR 268	Not applicable
NEPA	Not applicable
Other	Not applicable

*Key to Parameter Sheets is provided in Section 1.2.8.

Bulk Density of Halite in Salado (Halite)*

Parameter: **Density, bulk (ρ_{bulk})**
Material: Halite within Salado Formation (Salado, All, DnsBlk)

Definition, Units: kg/m^3

Values: 2.14×10^3

Distribution: Constant
Correlation:

Data Source(s): Holcomb, D. J., and M. Shields. 1987. *Hydrostatic Creep Consolidation of Crushed Salt With Added Water.* SAND87-1990. Albuquerque, NM: Sandia National Laboratories. (p. 17)

Usage:

Mathematical model:

The PA Department has used a bulk density of halite near the repository of 2,140 kg/m^3 as reported by Holcomb and Shields (1987, p. 17). This value corresponds to a porosity of 0.01.

$$\rho_{bulk} = (\rho_g (1-\phi))$$

Computational models:

(NA)

Ranking in Past Sensitivity Analyses:

40 CFR 191	Not applicable
40 CFR 268	Not applicable
NEPA	Not applicable
Other	Not applicable

*Key to Parameter Sheets is provided in Section 1.2.8.

Average Density near Repository*

Parameter: **Density, average (ρ_{ave})**
Material: Material near repository (Salado Formation) (Salado, All, DnsAvg)

Definition, Units: kg/m^3

Values: 2.3×10^3

Distribution: Constant
Correlation:

Data Source(s): Krieg, R. D. 1984. *Reference Stratigraphy and Rock Properties for the Waste Isolation Pilot Plant (WIPP) Project.* SAND83-1908. Albuquerque, NM: Sandia National Laboratories. (Table 4)

Usage:

Mathematical model:
(Value used by PA Department in past exploratory modeling.)

Equation (NA).

Computational models:
(NA)

Ranking in Past Sensitivity Analyses:

40 CFR 191	Not applicable
40 CFR 268	Not applicable
NEPA	Not applicable
Other	Not applicable

*Key to Parameter Sheets is provided in Section 1.2.8.

2.3.3 Dispersivity

Dispersivity, Longitudinal*

Parameter: **Dispersivity, longitudinal (α_L)**
Material: Halite and polyhalite within Salado Formation (Salado, All, Disp_lng)

Definition, Units: m

Values: Range: (1, 40) Median: 15

Distribution: Constructed
Correlation:

Data Source(s): Pickens, J. F., and G. E. Grisak. 1981. "Modeling of Scale-Dependent Dispersion in Hydrogeologic Systems," *Water Resources Research*. Vol. 17, no. 6, 1701-1711. (Engineering Lore)

Lappin, A. R., R. L. Hunter, D. P. Garber, and P. B. Davies, eds. 1989. *Systems Analysis, Long-Term Radionuclide Transport, and Dose Assessments, Waste Isolation Pilot Plant (WIPP), Southeastern New Mexico; March 1989*. SAND89-0462. Albuquerque, NM: Sandia National Laboratories. (Table D-2) (Investigator Judgment)

Usage:

Mathematical model:
(Value recommended for exploratory modeling.)

Equations 1.4.6-4a to 1.4.6-4b (definition of hydrodynamic dispersion tensor) in Section 1.4.6, this volume.

Computational models: Transport
STAFF2D

Ranking in Past Sensitivity Analyses:

40 CFR 191	Low (see Discussion)
40 CFR 268	Not tested
NEPA	Not tested
Other	Not applicable

*Key to Parameter Sheets is provided in Section 1.2.8.

Dispersivity Ratio*

Parameter: **Dispersivity ratio** (α_L/α_T)
Material: Halite and polyhalite within Salado Formation (Salado, All, Disp_trn)

Definition, Units: Ratio of longitudinal dispersivity to transverse dispersivity (dimensionless)

Values: Range: (3, 25) Median: 10

Distribution: Constructed
Correlation: Dispersivity, longitudinal

Source(s): PA Judgment based on the following sources:
Pickens, J. F., and G. E. Grisak. 1981. "Modeling of Scale-Dependent Dispersion in Hydrogeologic Systems," *Water Resources Research*. Vol. 17, no. 6, 1701-1711. (Engineering Lore)
Freeze, R. A., and J. A. Cherry. 1979. *Groundwater*. Englewood Cliffs, NJ: Prentice-Hall, Inc. (Figure 9.6) (Non-WIPP Literature Data)

Usage:

Mathematical model:
(Value recommended for exploratory modeling.)

Equations 1.4.6-4a to 1.4.6-4b (definition of hydrodynamic dispersion tensor) in Section 1.4.6, this volume.

Computational models:
STAFF2D

Ranking in Past Sensitivity Analyses:

40 CFR 191	Low (see Discussion)
40 CFR 268	Not tested
NEPA	Not tested
Other	Not applicable

*Key to Parameter Sheets is provided in Section 1.2.8.

Discussion:

No solute transport tests have been run in the Salado Formation, and no relevant solute transport data exist for very low permeability media from which to estimate dispersivity (α). Exploratory calculations of brine flows near the repository in the Salado show that linear fluid velocities are small and that solute transport proceeds mainly by diffusion (WIPP PA Division, 1991, vol. 2, Section 4.2.3). At these small velocities, the rule of thumb applied in standard porous media (Pickens and Grisak, 1981) is assumed to apply, that is, the longitudinal dispersivity α_L is approximately equal to $0.1d_s$ where d_s is the distance traveled by the solute. For typical distances traveled, α_L is between 1 and 40 m (3 and 130 ft). The distribution for α_L is shown in Figure 2.3-4.

Transverse dispersivity (α_T) is usually linearly related to α_L. The ratio of α_L to α_T typically varies between 5 and 20 (see, for example, Freeze and Cherry, 1979, Figure 9.6; Dullien, 1979, Figure 7.13; Bear and Verruijt, 1987). However, at very low velocities the ratio can approach 1, while in some strata the ratio has been reported to approach 100 (Marsily, de, 1986). The current range chosen by PA Analysts for sensitivity studies is 3 to 25 (Figure 2.3-5).

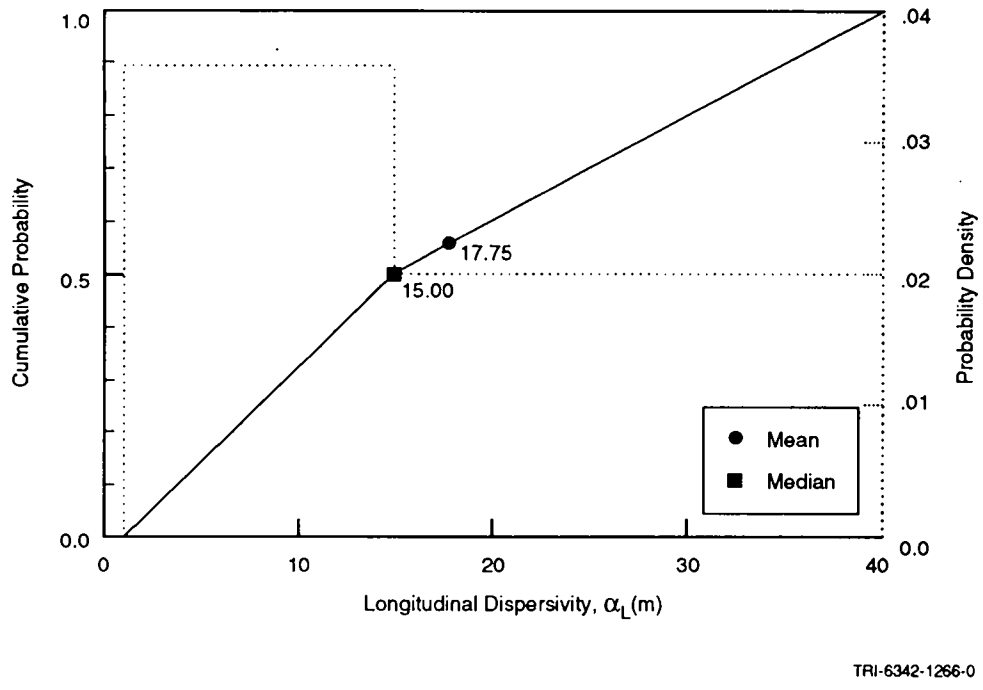

Figure 2.3-4. Estimated distribution for longitudinal dispersivity in halite, Salado Formation.

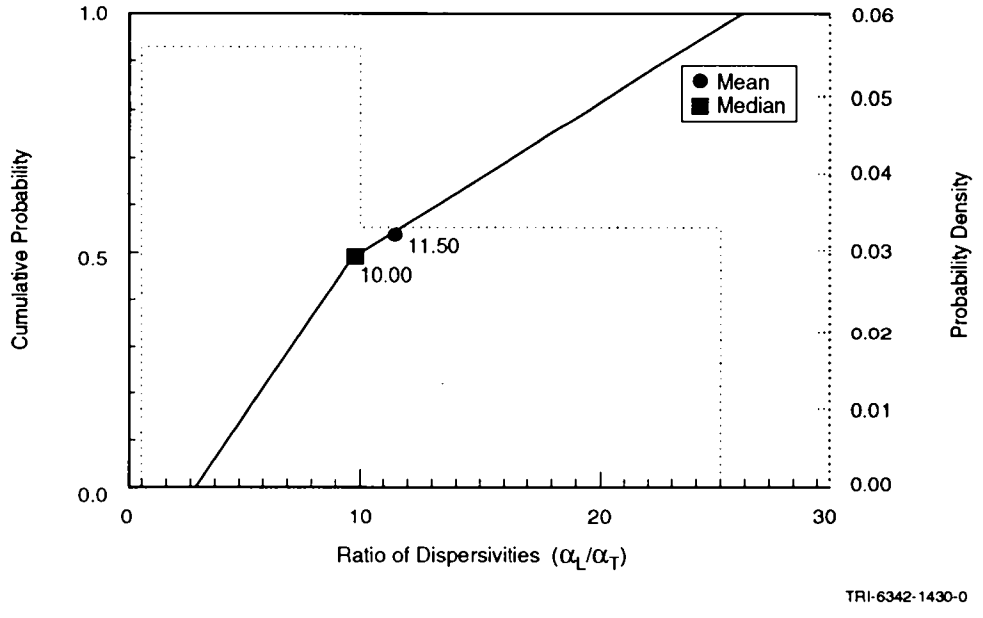

Figure 2.3-5. Estimated distribution for dispersivity ratio in halite, Salado Formation.

2.3.4 Partition Coefficients and Retardation

Partition Coefficient for Halite and Polyhalite*

Parameter: **Partition coefficient for halite and polyhalite (Kd), all species**
Material: Halite and polyhalite within Salado Formation (Salado, Kd_All)

Definition, Units: m^3/kg

Values: 0

Distribution: Constant
Correlation:

Data Source(s): Lappin, A. R., R. L. Hunter, D. P. Garber, and P. B. Davies, eds. 1989. *Systems Analysis, Long-Term Radionuclide Transport, and Dose Assessments, Waste Isolation Pilot Plant (WIPP), Southeastern New Mexico; March 1989.* SAND89-0462. Albuquerque, NM: Sandia National Laboratories. (p. D-17) (Investigator Judgment)

Usage:

Mathematical model:

The halite and polyhalite in the Salado Formation are assumed by PA Analysts not to interact chemically with any contaminants.

Equation (NA).

Computational models:

(NA)

Ranking in Past Sensitivity Analyses:

40 CFR 191	Not applicable
40 CFR 268	Not applicable
NEPA	Not applicable
Other	Not applicable

*Key to Parameter Sheets is provided in Section 1.2.8.

2.3.5 Permeability

Undisturbed Permeability*

Parameter: **Permeability, undisturbed (k)**
Material: Halite and polyhalite within Salado Formation, (Salado, LogPrmU)

Definition, Units: Log permeability values given (dimensionless); permeability has units of m^2.

Values: Range: (-24.0, -19.0) Median: -21.2 (log_{10} of values)

Distribution: Constructed (see Discussion)
Correlation:

Data Source(s):

Gorham, E., R. Beauheim, P. Davies, S. Howarth, and S. Webb. 1992. "Recommendations to PA on Salado Formation Intrinsic Permeability and Pore Pressure for 40 CFR 191 Subpart B Calculations" (see Appendix A, pp. A-47 through A-67). (Investigator Judgment based on WIPP data)

Howarth, S. M., E. W. Peterson, P. L. Lagus, K. Lie, S. J. Finley, and E. J. Nowak. 1991. "Interpretation of In-Situ Pressure and Flow Measurements of the Salado Formation at the Waste Isolation Pilot Plant," *Society of Petroleum Engineers Rocky Mountain Regional Meeting and Low-Permeability Reservoir Symposium, Denver, CO, April 15-17, 1991.* SPE-21840. Richardson, TX: Society of Petroleum Engineers. (Investigator Judgment based on WIPP data)

Beauheim, R. L., G. J. Saulnier, Jr., and J. D. Avis. 1991a. *Interpretation of Brine-Permeability Tests of the Salado Formation at the Waste Isolation Pilot Plant Site: First Interim Report.* SAND90-0083. Albuquerque, NM: Sandia National Laboratories. (Investigator Judgment based on WIPP data)

Usage:

Mathematical model:
Section 1.4.1, this volume.

Equations 1.4.1-1 and 1.4.1-2 in Section 1.4.1, this volume.

Computational models:
BRAFGLO

Ranking in Past Sensitivity Analyses:

40 CFR 191	High
40 CFR 268	Medium
NEPA	Not tested
Other	Not applicable

*Key to Parameter Sheets is provided in Section 1.2.8.

Discussion:

The permeability of undisturbed halite was a highly sensitive parameter in determining releases of Pu-239 during the 1991 series of calculations. Calling this parameter SALPERM, it is seen from the scatterplot in Figure 2.3-6 that there is a threshold in SALPERM such that, in a scenario that includes gas generation in the repository and intrusion by drilling at 1000 yr, there is essentially no release if SALPERM < 5×10^{-21} m^2, and finite release if SALPERM > 5×10^{-21} m^2. The undisturbed halite permeability determines how long it will take for a waste panel to be filled with brine; if the pore space in a panel cannot fill with brine due to very low halite permeability, then there can be no fluid flow up the intrusion borehole and hence no radionuclide release (Helton et al., 1992, p. 4-20). The distribution of SALPERM that was used in the 1991 series of calculations is shown on Figure 2.3-7; note that more than 50% of the values exceed 5×10^{-21} m^2.

The distribution of SALPERM used in the 1992 series of calculations (Figure 2.3-8) differs from the 1991 distribution (Figure 2.3-7) in two ways: in 1992, only about 18% of values exceed the threshold of 5×10^{-21} m^2, and the upper limit of permeability is now set at 10^{-19} m^2. A rationale for these changes is supplied by Gorham et al. (June 15, 1992, Memo in Appendix A).

The PA Department judges that both distributions are adequate for the purpose of testing sensitivity of far-field permeability in the two-phase flow model (Section 1.4.1) but that neither distribution really represents uncertainty in the *average* far-field permeability, the quantity that should be used in the current version of the two-phase flow model. Because average halite permeability is (and is likely to remain) a sensitive determinant of releases of radionuclides from a disturbed waste panel, a direct approach to inferring uncertainty in average halite permeability, an approach that uses only measurements of that quantity, seems desirable. One such approach, based on "bootstrap" statistical methods (see Efron and Tibshirani, 1991, for a review), is outlined below and applied to the inference of averages of far-field permeability and pore pressure in sections that follow. The data used in these applications arises from three experimental programs; the three programs (Permeability Tests, Small-Scale Brine Inflow, and Room Q described in the draft of the "Sandia National Laboratories Waste Isolation Pilot Plant Program Plan for Fiscal Year 1992") are evaluating permeability, storativity, and pore pressure in halite and anhydrite layers of the Salado Formation. Results of these programs available in April, 1992, are summarized in Table 2.3-2.

Estimating far-field parameters by non-linear regression: Let $(y_1, y_2, ..., y_N)$ be logarithms of permeabilities, or pore pressures, that are measured at corresponding distances $(x_1, x_2, ..., x_N)$ into the Salado Formation from the walls of an open excavation. Data, such as that given in Table 2.3-2, can be used to fit by least squares an expression of the form:

$$y(x) = a + b \exp(-x/c), \qquad (2.3.5\text{-}1)$$

where the coefficients (a, b, c) have the following physical meanings:

a = an estimate of $\log_{10}$ of undisturbed permeability or an estimate of undisturbed pore pressure at repository level (to see that this is plausible, let $x \rightarrow \infty$ in Eq. 2.3.5-1);

c = an estimate of the characteristic depth of the disturbed permeability zone or the (possibly different) characteristic depth of the disturbed pore-pressure zone (m);

a+b = an estimate of $\log_{10}$ of disturbed permeability near the wall of an excavation (let $x \rightarrow o$ in Eq. 2.3.5-1). Since permeability is expected to decrease with increasing distance into the Salado, $b > 0$ in this case. Alternatively, if y(x) measures pore pressure, a+b is an estimate of disturbed pore pressure near the wall; $(a + b) \simeq 0$, so $b < 0$ in this case.

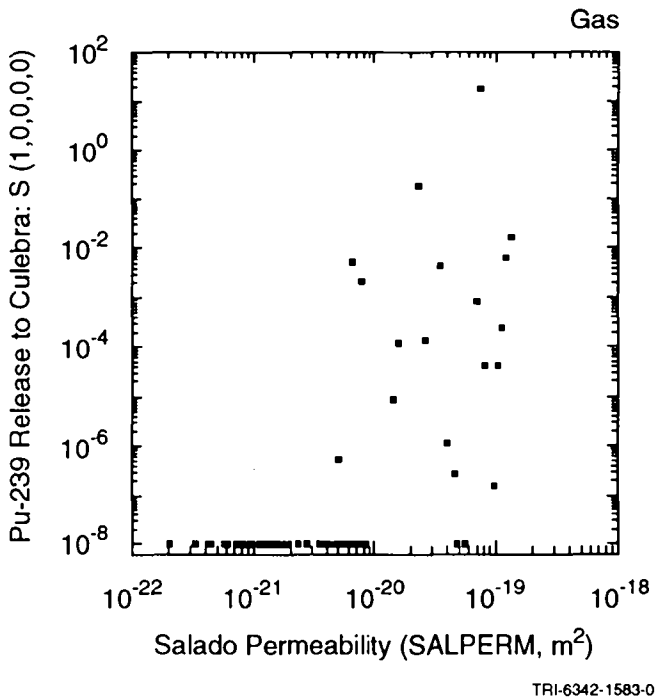

Figure 2.3-6. Scatterplot for normalized release of Pu-239 to the Culebra Dolomite with gas generation in the repository and intrusion occurring at 1000 yr for variable SALPERM (Salado permeability) (after Helton et al., 1992, Figure 4.5-1).

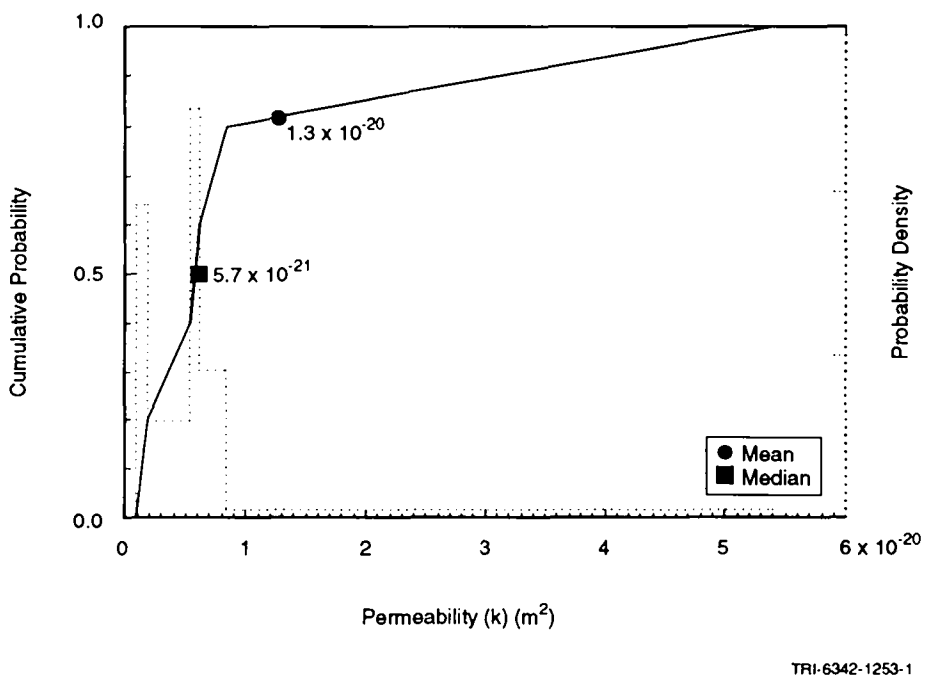

Figure 2.3-7. Estimated distribution (in 1991) for Salado undisturbed permeability.

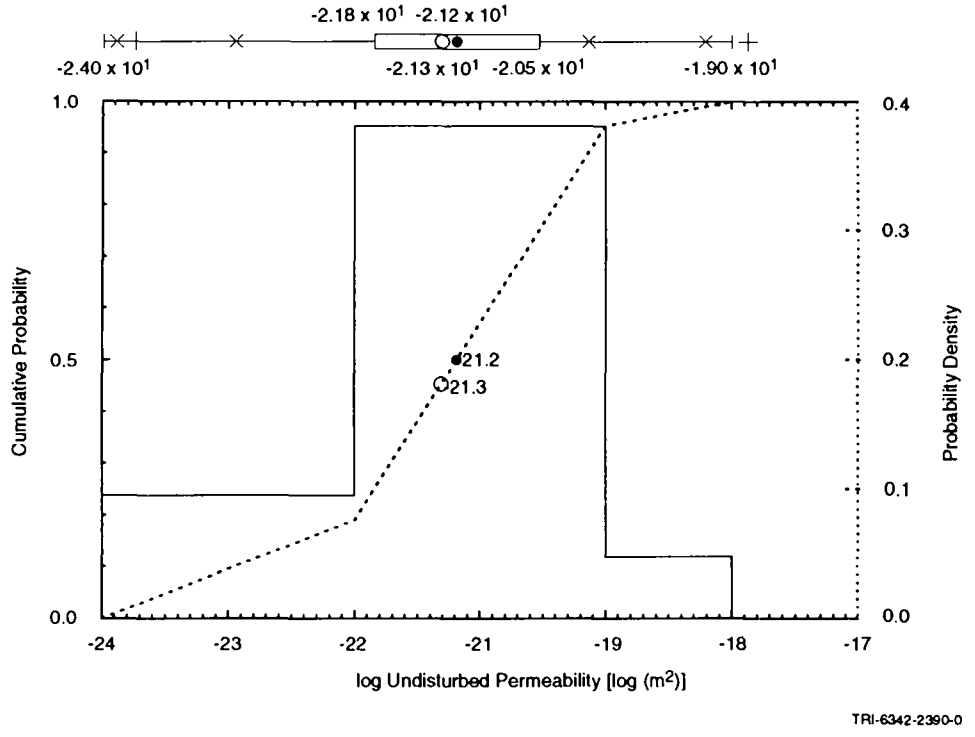

Figure 2.3-8. Estimated distribution in 1992 for Salado undisturbed permeability.

The choice of functional form (Eq. 2.3.5-1) is not entirely arbitrary. Because of excavation disturbance and depressurization, it is expected that pore pressure (or permeability) should increase (or decrease) with increasing distance x into the Salado Formation in the manner indicated in Figure 2.3-9, and – ignoring natural inhomogeneities and errors of measurement – should asymptotically approach constant values corresponding to the average far-field values as $x \rightarrow \infty$. Equation 2.3.5-1 is but one of many functions that, with proper choice of constants, will mimic the expected spatial distributions of pore pressure and permeability near the wall of an open excavation. Another possible functional form is

$$y(x) = a + (b/(c + x^d)) \quad . \tag{2.3.5-2}$$

The constant a in Eq. 2.3.5-2 has the same physical meaning as constant a in Eq. 2.3.5-1, but other constants in Eq. 2.3.5-2 will obviously take a different meaning.

Interest centers primarily on the coefficient a and the uncertainty associated with that coefficient. The other coefficients, b and c, are probably not meaningful as estimators of disturbed-zone parameters of a waste-loaded excavation that has undergone some collapse and compaction; in other words, measurements of the material parameters of contemporary disturbed zones of WIPP excavations should probably not be used to infer the parameters of the disturbed zone of the same excavation after it has been filled with waste and backfill, closed, and allowed to subside for hundreds to thousands of years.

To infer the uncertainty of the coefficient a, "bootstrap" methods described in Section 14.5 of Press et al., 1986, have been adopted. The methods are based on a recognition that a given data set,

$$Y = (y_1, y_2, ..., y_N),$$

Table 2.3-2. Summary of Measurements of Salado Halite Permeabilities and Pore Pressures

Test No.	Lithology	Distance[b] (m)	Measured Permeability (m^2)	log_{10} Permeability[c]	Pressure (MPa)[d]	Orientation	Sources[e]
QPP12(pre)[a]	Halite	26.7	6.8×10^{-22}	-21.2 ± 0.7	9.5 ± 0.5	vertical, down	1, 2
C2H03	pure halite	7.76 - 9.14	too low to measure	–	–	horizontal	1, 3
SCP01-GZ	halite ?	?	too low to measure	–	–	angle, down 13°	1
QPP05 (pre)	halite	23.0	too low to measure	–	–	vertical, up	1, 2
QPP02 (pre)	halite	26.7	too low to measure	–	–	vertical, up	1, 2
S1P72-A-GZ	halite	?	8.6×10^{-22}	-21.1	5.1	angle, down 32°	1, 3
QPP21 (post)	halite	12.2	1.9×10^{-22}	-21.7	4.8	horizontal	1, 2
C2H01-B	avg. halite	4.50 - 5.58	5.3×10^{-21}	-20.3	3.1	vertical, down	1, 3
C2H01-B-GZ	avg. halite	2.92 - 4.02	1.9×10^{-21}	-20.7	4.1	vertical, down	1, 3
L4P51-A	avg. halite & clay	3.33 - 4.75	6.1×10^{-21}	-20.2	2.7	vertical, down	1, 3
SOP01	avg. halite & clay	3.74 - 5.17	8.3×10^{-21}	-20.1	4.4	vertical, down	1, 3
S1P71-A	avg. halite & clay	3.12 - 4.56	6.1×10^{-20}	-19.2	2.9	vertical, down	1, 3
QPP15	halite	23 ?	2.2×10^{-21}	-20.7	3.1	vertical, down	1, 2
DBT10	halite	3.0 - 6.0	5.8×10^{-22}	-21.2	(5.0 assumed)	vertical, down	1, 4
DBT11	halite	3.0 - 6.0	2.3×10^{-21}	-20.6	(5.0 assumed)	vertical, down	1, 4
DBT12	halite	3.0 - 6.0	1.3×10^{-21}	-20.9	(5.0 assumed)	vertical, down	1, 4
DBT13	halite	3.0 - 6.0	3.4×10^{-22}	-21.5	(5.0 assumed)	vertical, down	1, 4
DBT14A/B	halite	3.0 - 6.0	3.1×10^{-21}	-20.5	(5.0 assumed)	vertical, down	1, 4
DBT15A/B	halite	3.0 - 6.0	5.0×10^{-22}	21.3	(5.0 assumed)	vertical, down	1, 4
L4B01	halite	3.0 - 6.0	1.3×10^{-22}	-21.9	(5.0 assumed)	vertical, down	1, 4
DBT31A	–	–	–	–	–	–	not used, 1
QPP12 (post)	halite	6.1	4.4×10^{-22}	-21.4	9.4	vertical, down	1, 2
C2H01-A	avg. halite	2.09 - 5.58	2.7×10^{-18}	-17.6	0.5	vertical, down	1, 3
C2H01-A-GZ	halite	0.50 - 1.64	(unmeasurable)	–	0.0	vertical, down	1, 3
S1P73-B-GZ	?	?	(unmeasurable)	–	2.5	?	1

a - "Pre" and "post" mean pre- and post-mineby for Q tunnel tests.
b - Estimated distance of apparatus from wall of excavation
c - A standard error of one-half order of magnitude assumed for all permeabilities
d - A standard error of 0.5 MPa assumed for all measured or inferred pressures
e - Sources: 1 - Gorham et al., June 15, 1992, Memo (Appendix A, this volume),
2 - Howarth et al., 1991,
3 - Beauheim et al., 1991b,
4 - Finley and McTigue, 1991.

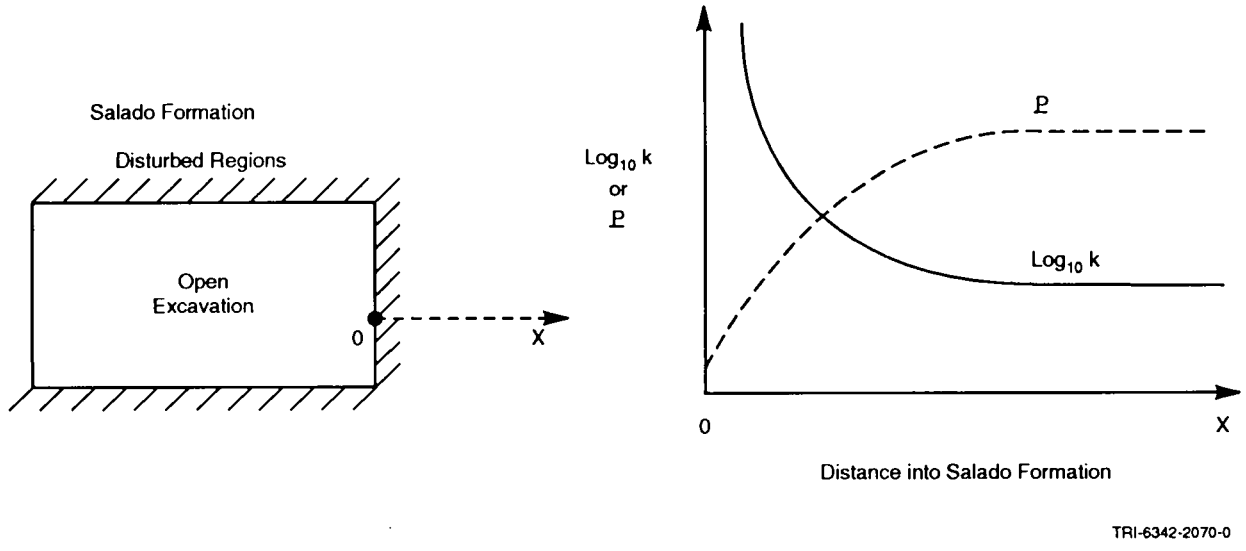

Figure 2.3-9. Expected qualitative behavior of pore pressure (P) and log permeability ($\log_{10}$k) near wall of an open excavation.

can yield at best a single *estimate* of the coefficients,

$$A_o = (a_o, b_o, c_o),$$

when the data are fitted to an expression like Eq. 2.3.5-1. However, if the standard error of each datum is known and can be interpreted in terms of a standard deviation of the measurement, it becomes possible to obtain an arbitrary number of *synthetic data sets* by Monte Carlo simulations. These synthetic data sets can then be used in the regression formula to obtain new estimates of the coefficients, i.e.,

$$A_1, A_2, ..., A_m,$$

which can be treated as though they were data concerning the coefficients themselves; in other words, the empirical cdfs and correlations between the coefficients a, b, and c can be constructed by standard statistical techniques. The method described here has the advantage that empirical cdfs of parameters can be inferred directly from measurements of the fitted quantity and its presumed measurement errors; the need for subjective judgments on the part of investigators–such as the judgments giving Figures 2.3-7 and 2.3-8–is minimized. Furthermore, the method effectively averages over small-scale spatial variations in the material properties and therefore gives a better description of uncertainty in the *average* value of those properties (i.e., a better estimate of the material-property parameter used in PA consequence model[s]; see Section 1.3.3 for a discussion of this issue). The method has the disadvantage that the functional forms used in the non-linear regression (e.g., Eqs. 2.3.5-1 and 2.3.5-2) are in general not unique; the use of different functional forms in the regression analyses can yield quite different distributions for the coefficients (or parameters) a, b, and c. The robustness of different functional forms needs to be examined before the method can be applied with confidence to any given problem. Furthermore, robustness of results with respect to assumptions about the size of the standard deviations of measurements needs to be examined since quoted standard deviations are more often than not guesses of the investigators.

As an example of this technique for estimating the distributions of far-field quantities, data from Table 2.3-2 have been used to generate a simulated distribution of the mean, far-field halite permeability (Figure 2.3-10). Note that only about 3% of average SALPERM values exceed the threshold of 5×10^{-21} m^2.

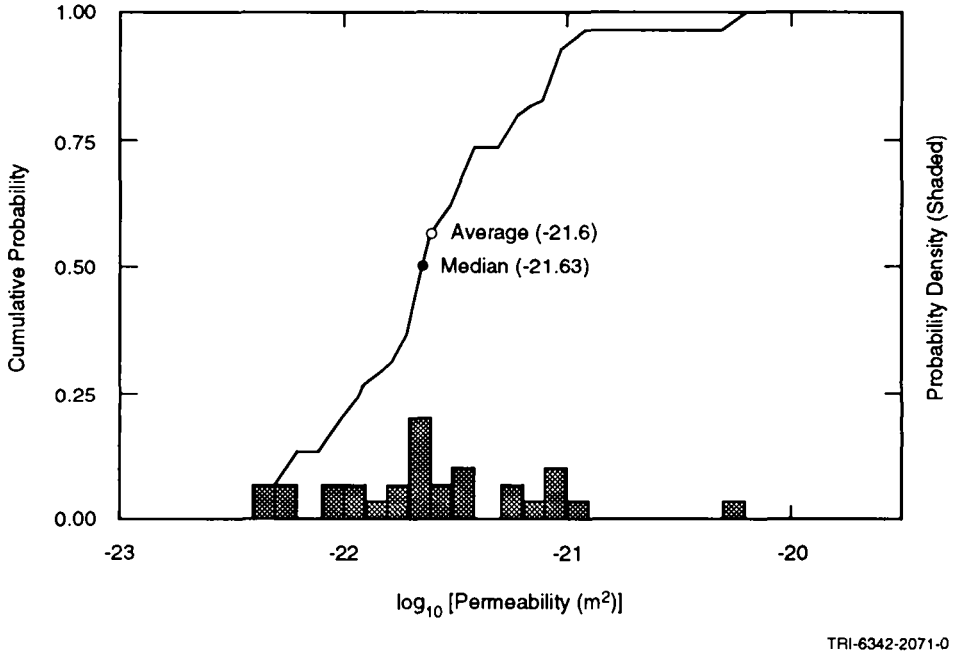

Figure 2.3-10. Simulated undisturbed (far-field) halite permeability. Coefficient "a" in non-linear least square fit to Eq. 2.3.5-1; 30 samples.

Disturbed Permeability*

Parameter:	**Permeability, disturbed (k)**
Material:	Halite and polyhalite within Salado Formation, (Salado, LogPrmD)
Definition, Units:	Log permeability values given (dimensionless); permeability has units of m^2.
Values:	Range: (-22.0, -15.0) Median: -20.7
Distribution:	Constructed (see Discussion)
Correlation:	

Data Source(s):

Gorham, E., R. Beauheim, P. Davies, S. Howarth, and S. Webb. 1992. "Recommendations to PA on Salado Formation Intrinsic Permeability and Pore Pressure for 40 CFR 191 Subpart B Calculations" (see Appendix A, pp. A-47 through A-67). (Investigator Judgment based on WIPP data)

Howarth, S. M., E. W. Peterson, P. L. Lagus, K. Lie, S. J. Finley, and E. J. Nowak. 1991. "Interpretation of In-Situ Pressure and Flow Measurements of the Salado Formation at the Waste Isolation Pilot Plant," *Society of Petroleum Engineers Rocky Mountain Regional Meeting and Low-Permeability Reservoir Symposium, Denver, CO, April 15-17, 1991.* SPE-21840. Richardson, TX: Society of Petroleum Engineers. (Investigator Judgment based on WIPP data)

Beauheim, R. L., G. J. Saulnier, Jr., and J. D. Avis. 1991a. *Interpretation of Brine-Permeability Tests of the Salado Formation at the Waste Isolation Pilot Plant Site: First Interim Report.* SAND90-0083. Albuquerque, NM: Sandia National Laboratories. (Investigator Judgment based on WIPP data)

Usage:

Mathematical model:

Section 1.4.1, this volume.

Equations 1.4.1-1 and 1.4.1-2 in Section 1.4.1, this volume.

Computational models:

BRAGFLO

Ranking in Past Sensitivity Analyses:

40 CFR 191	Not tested
40 CFR 268	Low
NEPA	Not tested
Other	Not tested

*Key to Parameter Sheets is provided in Section 1.2.8.

Discussion:

The disturbed permeability and porosity of the Salado Formation and interbeds vary from the intact properties to large, open fractures. These two disturbed properties also change as the stress field around the excavations change with time. Furthermore, the halite will likely heal to intact conditions over time (Sutherland and Cave, 1978; Lappin et al., 1989, p. 4-45). For these reasons, disturbed permeability is treated as an independent parameter when it is not possible to predict changes in halite permeability due to changes in the stress field. In the 1992 data base, the disturbed permeability is assumed to be distributed according to the empirical cdf of the non-far-field data points listed in Table 2.3-2. Figure 2.3-11 shows the resulting distribution.

Disturbed permeability of halite was not sampled in 1992 calculations.

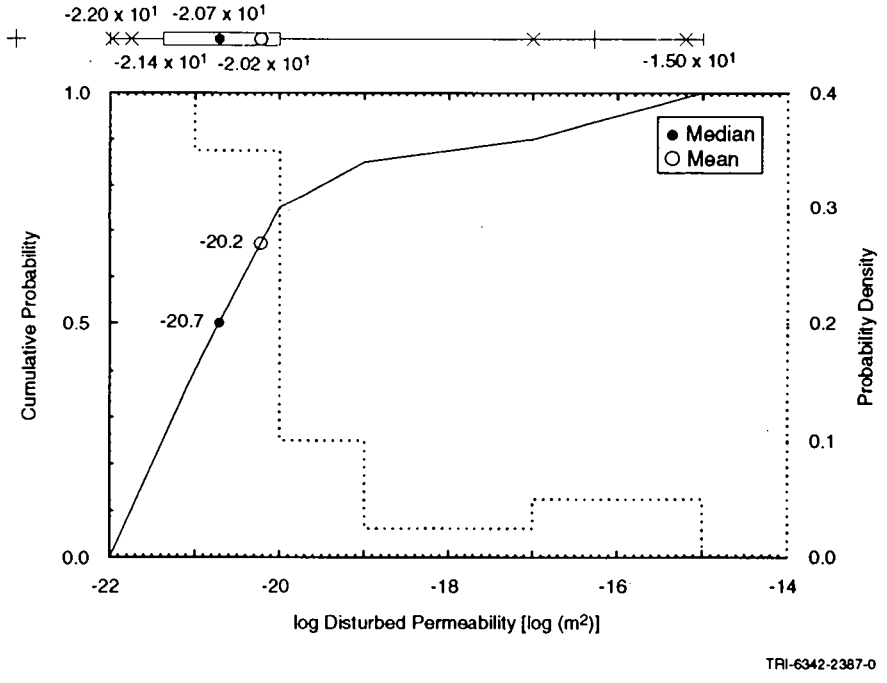

Figure 2.3-11. Estimated distribution (in 1992) for Salado halite disturbed permeability.

2.3.6 Pore Pressure at Repository Level in Halite

Pore Pressure*

Parameter: **Pore pressure (p)**
Material: Halite and polyhalite within Salado Formation, (Salado, Pressure)

Definition, Units: MPa

Values: Range: (9.0, 10.0) Median: 9.5

Distribution: Uniform
Correlation:

Data Source(s):

Gorham, E., R. Beauheim, P. Davies, S. Howarth, and S. Webb. 1992. "Recommendations to PA on Salado Formation Intrinsic Permeability and Pore Pressure for 40 CFR 191 Subpart B Calculations" (see Appendix A, pp. A-47 through A-67). (Investigator Judgment based on WIPP data)

Howarth, S. M., E. W. Peterson, P. L. Lagus, K. Lie, S. J. Finley, and E. J. Nowak. 1991. "Interpretation of In-Situ Pressure and Flow Measurements of the Salado Formation at the Waste Isolation Pilot Plant," *Society of Petroleum Engineers Rocky Mountain Regional Meeting and Low-Permeability Reservoir Symposium, Denver, CO, April 15-17, 1991.* SPE-21840. Richardson, TX: Society of Petroleum Engineers. (Investigator Judgment based on WIPP data)

Beauheim, R. L., G. J. Saulnier, Jr., and J. D. Avis. 1991. *Interpretation of Brine-Permeability Tests of the Salado Formation at the Waste Isolation Pilot Plant Site: First Interim Report.* SAND90-0083. Albuquerque, NM: Sandia National Laboratories. (Investigator Judgment based on WIPP data)

Usage:

Mathematical model:

Section 1.4.1, this volume.

Equations: Boundary condition on fluid pressure in Eqs. 1.4.1-1 and 1.4.1-2.

Computational models:

BRAGFLO

Ranking in Past Sensitivity Analyses:

40 CFR 191	Not tested
40 CFR 268	Not tested
NEPA	Not tested
Other	Not tested

*Key to Parameter Sheets is provided in Section 1.2.8.

Discussion:

In 1992, far-field pore pressure in halite is assumed to be uniformly distributed on the interval (9,10) MPa, based on the single measurement (9.4 ± 0.5 MPa, test QPP12 [pre] in Table 2.3-2) that was endorsed as a far-field value (Gorham et al., June 15, 1992, Memo in Appendix A, this volume).

As another example of the technique for estimating average far-field quantities, data from Table 2.3-2 and regression techniques described in Section 2.3.5 have been used to generate a simulated distribution for far-field pore pressure in halite (Figure 2.3-12). Results of this trial simulation suggest that halite pore pressure at the repository level is approximately the hydrostatic pressure of Castile brines, as measured from the surface (Figure 2.3-13).

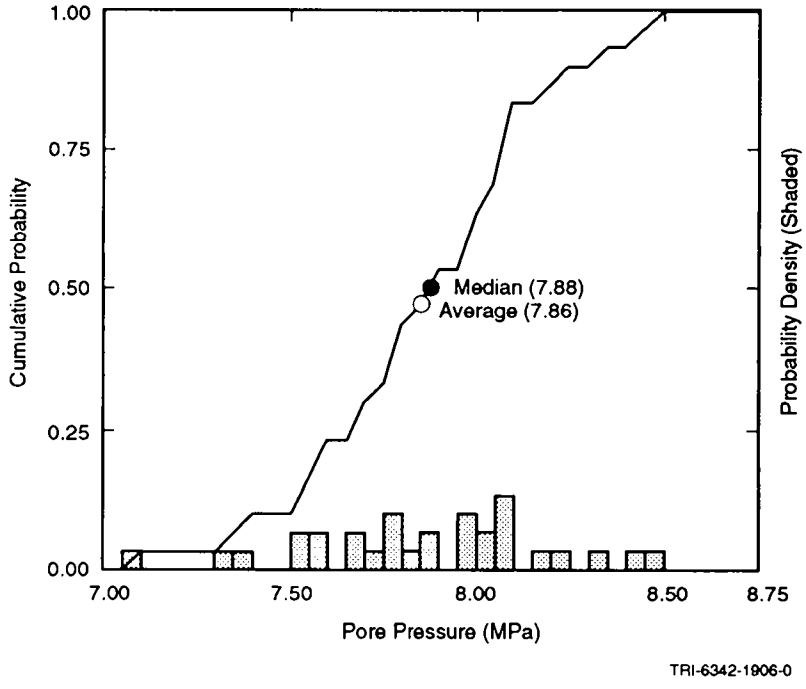

Figure 2.3-12. Simulated undisturbed (far-field) pore pressure at repository depth in halite. Coefficient "a" in nonlinear least squares fit to Eq. 2.3.5-1; 30 samples.

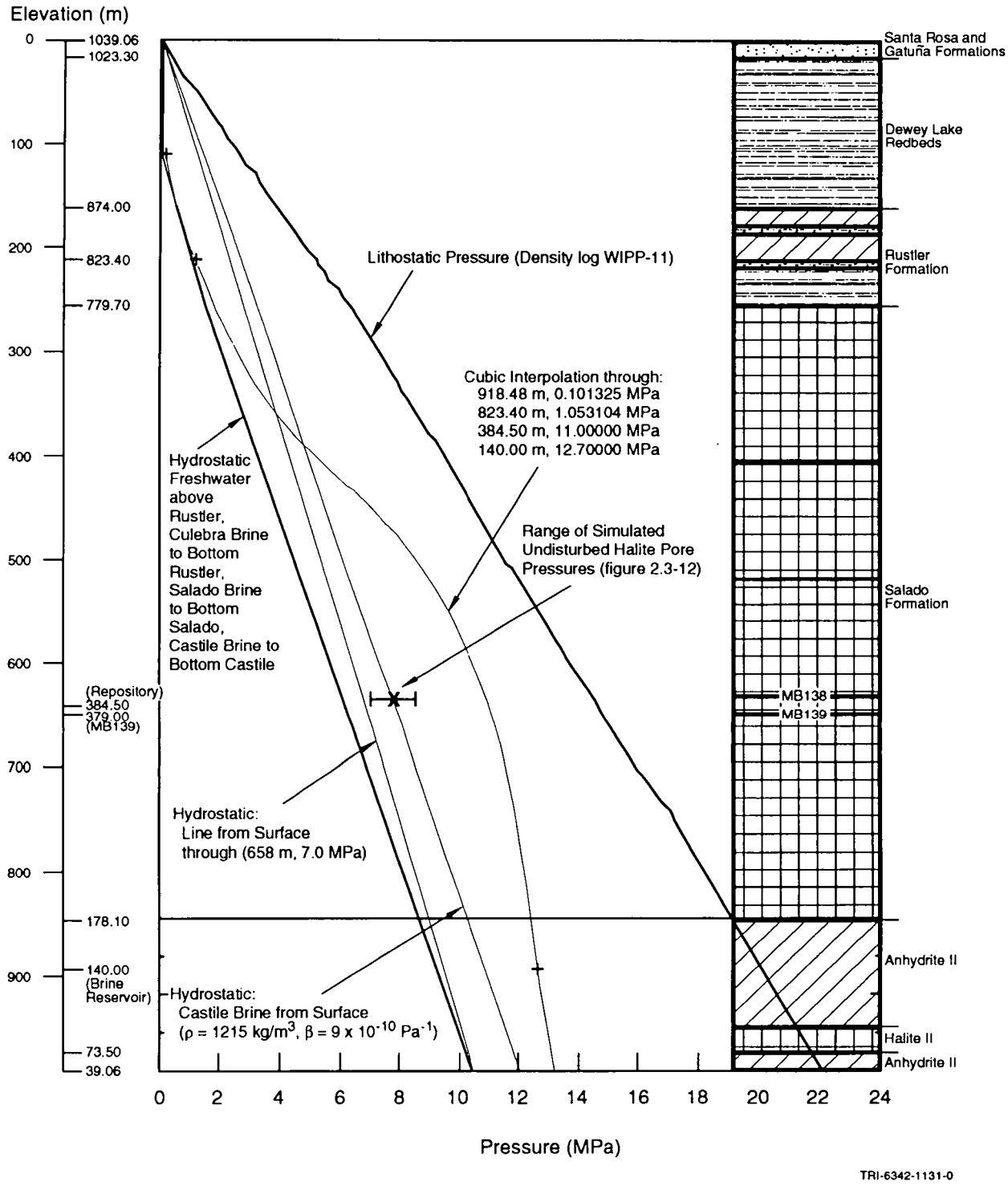

Figure 2.3-13. Calculated lithostatic and hydrostatic pressures with depth.

2.3.7 Porosity

Undisturbed Porosity*

Parameter: **Porosity, undisturbed (ϕ)**
Material: Halite and polyhalite within Salado Formation, (Salado, Pore_U)

Definition, Units: Dimensionless

Values: Range: (1×10^{-3}, 3×10^{-2}) Median: 1×10^{-2}

Distribution: Constructed (see Discussion)
Correlation:

Data Source(s): Investigator Judgment (see Discussion).

Powers, D. W., S. J. Lambert, S-E. Shaffer, L. R. Hill, and W. D. Weart, eds. 1978. *Geological Characterization Report, Waste Isolation Pilot Plant (WIPP) Site, Southeastern New Mexico*. SAND78-1596. Albuquerque, NM: Sandia National Laboratories. Vols. 1-2.

U.S. Department of Energy. 1983. "Brine Content of Facility Interval Strata," *Results of Site Validation Experiments*. TME 3177. [Carlsbad, NM]: Waste Isolation Pilot Plant. Vol. II, Supporting Document 10.

Usage:

Mathematical model:
Section 1.4.1, this volume.

Equations 1.4.1-1 and 1.4.1-2; specifies porosity of part of reservoir that is undisturbed halite.

Computational models:
BRAGFLO

Ranking in Past Sensitivity Analyses:

40 CFR 191	Not tested
40 CFR 268	Not tested
NEPA	Not tested
Other	Not tested

*Key to Parameter Sheets is provided in Section 1.2.8.

Discussion:

The PA assumed the median porosity to be 0.01 based on an unpublished report about electromagnetic and DC resistivity measurements (Skokan, C., J. Starrett, and H. T. Andersen. 1988. *Final Report: Feasibility Study of Seismic Tomography to Monitor Underground Pillar Integrity at the WIPP Site.* Contractor Report. Albuquerque, NM: Sandia National Laboratories). This median value is identical to that calculated from a grain density of 2,163 kg/m^3 (135 lb/ft^3) for halite, and a bulk density of 2,140 kg/m^3 (133.6 lb/ft^3) ($\rho_b = (1-\phi)\rho_g$). The low value of 0.001 is based on drying experiments (Powers et al., 1978), while the high value of 0.03 is suggested by the low end of DC resistivity measurements in the unpublished report by Skokan et al., cited above.

Figure 2.3-14 shows the estimated distribution for the undisturbed porosity.

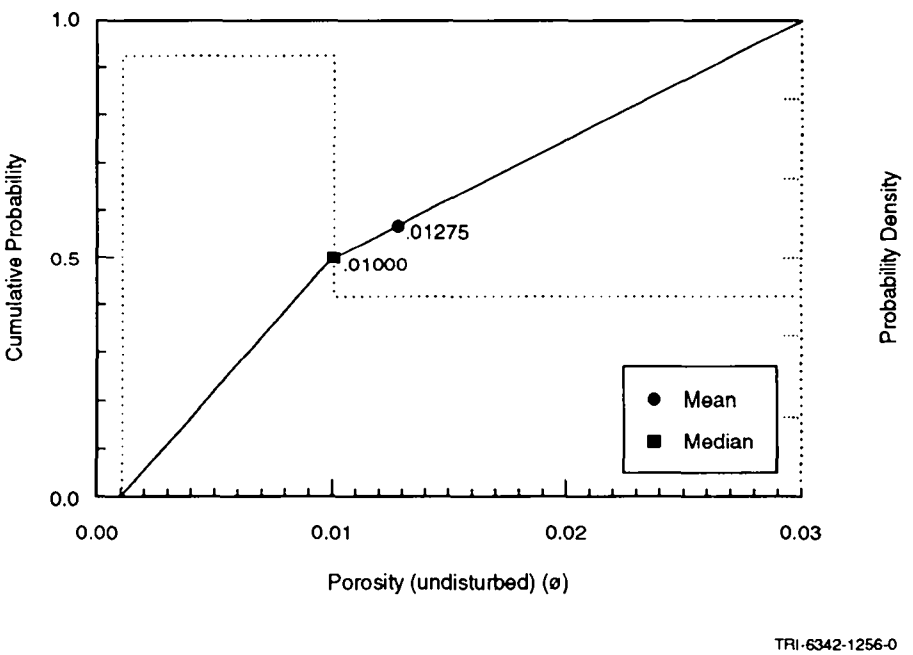

Figure 2.3-14. Estimated distribution for undisturbed porosity in halite, Salado Formation.

Disturbed Porosity*

Parameter: **Porosity, disturbed (ϕ)**
Material: Halite and polyhalite within Salado Formation, (Salado, Porc_D)

Definition, Units: Dimensionless

Values: 6×10^{-2}

Distribution: Constant
Correlation:

Data Source(s): The disturbed porosity of 0.06 is calculated by assuming that the final (disturbed) density of halite is 0.95 of the intact density, i.e., ϕ is such that

$$0.95\rho_b = (1 - \phi)\,\rho_g$$

where ρ_g is grain density of halite (Section 2.3.2) and
ρ_b is bulk density of halite (Section 2.3.2).

Usage:

Mathematical model:
Section 1.4.1, this volume.

Equations 1.4.1-1 and 1.4.1-2; specifies porosity of part of reservoir that is disturbed halite.

Computational models:
BRAGFLO

Ranking in Past Sensitivity Analyses:

40 CFR 191	Not applicable
40 CFR 268	Not applicable
NEPA	Not applicable
Other	Not applicable

*Key to Parameter Sheets is provided in Section 1.2.8.

2.3.8 Specific Storage

Specific Storage*

Parameter: Specific storage (S_s)
Material: Halite and polyhalite within Salado Formation, (Salado, Sp_Stor)

Definition, Units: m^{-1}

Values: Range: (2.8×10^{-8}, 1.4×10^{-6}) Median: 9.5×10^{-8}

Distribution: Constructed
Correlation:

Data Source(s): Beauheim, R. [L.] 1991. Appendix A: "Review of Salado Parameter Values to be Used in 1991 Performance Assessment Calculations," *Preliminary Comparison with 40 CFR Part 191, Subpart B for the Waste Isolation Pilot Plant, December 1991. Volume 3: Reference Data.* WIPP Performance Assessment Division. Eds. R. P. Rechard, A. C. Peterson, J. D. Schreiber, H. J. Iuzzolino, M. S. Tierney, and J. S. Sandha. SAND91-0893/3. Albuquerque, NM: Sandia National Laboratories. A-19 through A-23. (Investigator Judgment)

Usage:

Mathematical model:

Specific storage is used to specify solid compressibility, β_s, which in turn constrains changes in solid porosity by the relationship,

$$\beta_s = \frac{1}{\phi}\frac{\partial \phi}{\partial p}$$

where p is pore pressure (brine pressure). Such a relationship, or one similar to it, is used in BRAGFLO (Section 1.4.1) and other two-phase flow models. See Discussion.

Computational models:

BRAGFLO

Ranking in Past Sensitivity Analyses:

40 CFR 191	Not tested
40 CFR 268	Not tested
NEPA	Not tested
Other	Not tested

*Key to Parameter Sheets is provided in Section 1.2.8.

Figure 2.3-15 shows the estimated distribution for specific storage. The median and range of this distribution were recommended by Beauheim (1991).

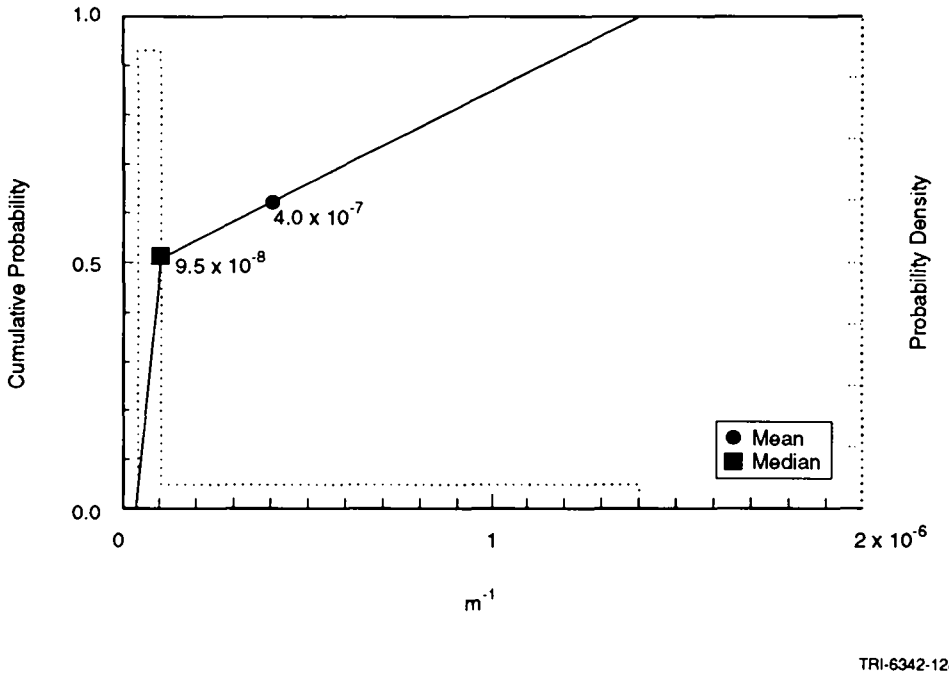

Figure 2.3-15. Estimated distribution for specific storage of halite, Salado Formation.

Discussion:

Specific storage is usually defined by the relationship,

$$S_s = \rho_f g (\beta_s + \phi\beta_f) . \tag{2.3-6}$$

where

ρ_f = mass density of fluid (kg/m^3),
g = acceleration of gravity (m/s^2),
β_s = compressibility of solid matrix (Pa^{-1}),
ϕ = porosity of solid matrix (dimensionless),
β_f = compressibility of fluid (Pa^{-1}).

The above relationship can be solved for β_s to give

$$\beta_s = (S_s/\rho_f g) - \phi\beta_f , \tag{2.3-7}$$

which can then be used to constrain changes in solid porosity with pressure through relationships of the form

$$\beta_s = \text{a function of } \phi \text{ and } \partial\phi/\partial\rho .$$

Some confusion may result because groundwater models often employ different definitions for the matrix compressibility β_s. For example SUTRA (Voss, 1984) defines β_s as

$$\beta_s = \frac{1}{1-\phi}\frac{\partial \phi}{\partial p},$$

but defines capacitance (specific pressure storativity) as

$$c = (1-\phi)\beta_s + \phi\beta_f,$$

thus

$$c = \frac{\partial \phi}{\partial p} + \phi\beta.$$

STAFF 2D (Huyakorn et al., 1991) and HST3D (Kipp, 1987) defines β_s as

$$\beta_s = \frac{\partial \phi}{\partial p},$$

while BOAST II (Fanchi et al., 1987) and BRAGFLO (Section 1.4.1, this volume) use

$$\beta_s = \frac{1}{\phi}\frac{\partial \phi}{\partial p}.$$

It is important to recognize that each code uses a different definition of matrix compressibility and all ignore solid compressibility.

2.3.9 Tortuosity

Tortuosity*

Parameter: **Tortuosity (τ)**
Material: Halite and polyhalite within Salado Formation, (Salado, Tortusty)

Definition, Units: Dimensionless

Values: Range: (1×10^{-2}, 6.67×10^{-1}) Median: 1.4×10^{-1}

Distribution: Constructed
Correlation:

Data Source(s):
Freeze, R. A., and J. A. Cherry. 1979. *Groundwater.* Englewood Cliffs, NJ: Prentice-Hall, Inc. (p. 104)

Kelley, V. A., and G. J. Saulnier, Jr. 1990. *Core Analyses for Selected Samples from the Culebra Dolomite at the Waste Isolation Pilot Plant Site.* SAND90-7011. Albuquerque, NM: Sandia National Laboratories. (Table 4.6)

Lappin, A. R., R. L. Hunter, D. P. Garber, and P. B. Davies, eds. 1989. *Systems Analysis, Long-Term Radionuclide Transport, and Dose Assessments, Waste Isolation Pilot Plant (WIPP), Southeastern New Mexico; March 1989.* SAND89-0462. Albuquerque, NM: Sandia National Laboratories. (Table E-9)

Usage:

Mathematical model:

Intact matrix tortuosity is used to evaluate the effective molecular diffusion coefficient (D_m) from the coefficient of molecular diffusion ($D^{\square}$) in the pure saturating fluid ($D_m = \tau D^{\square}$), where τ equals $(\ell / \ell_{path})^2$, ℓ is the linear length, and ℓ_{path} is the length of the [tortuous] path that a fluid particle would take (Bear, 1972, p. 111).

Computational models:

SUTRA (used only in 1991 calculations)

Ranking in Past Sensitivity Analyses:

40 CFR 191	Not tested
40 CFR 268	Not tested
NEPA	Not tested
Other	Not tested

*Key to Parameter Sheets is provided in Section 1.2.8.

Discussion:

No direct measurements of tortuosity are available in the halite or anhydrite layers of the Salado Formation. The range reported is the theoretical value of 0.667 for uniform-sized grains at low Peclet numbers (N_p) (Dullien, 1979, Figure 7.12) down to 0.01 observed in laboratory experiments of nonadsorbing solutes in porous materials (Freeze and Cherry, 1979, p. 104). The PA Department selected a median value equal to that of the Culebra Dolomite Member (see Table 2.6-1).

2.4 Hydrologic Parameters for Anhydrite Layers within Salado Formation

Table 2.4-1 provides a summary of all parameter values for anhydrite layers near the repository within the Salado Formation. Marker Bed 139 (MB139), a potential transport pathway, is an interbed located about 1 m (3.3 ft) below the repository interval and thus is an anhydrite layer of particular interest. Figure 2.4-1 shows a cross section of MB139.

Table 2.4-1. Hydrologic Parameter Values for Anhydrite Layers within Salado Formation

Parameter[a]	Median	Range		Distribution Units	Type	Discussion and Sources in:
Capillary pressure (p_c) and relative permeability (k_{rw})						
Threshold displacement pressure (p_t)	(Perfectly correlated with anhydrite permeability)			Pa	Function	Section 2.3.1
Residual saturations						
Wetting phase ($S_{\ell r}$)	2×10^{-1}	0.0	4×10^{-1}	none	Uniform	Section 2.3.1
Gas phase (Sg_r)	2×10^{-1}	0.0	4×10^{-1}	none	Uniform	Section 2.3.1
Brooks-Corey exponent (λ)	7×10^{-1}	2×10^{-1}	1×10^{1}	none	Constructed	Section 2.3.1
Density, grain (ρ_g)	2.963×10^{3}			kg/m^3	Constant	WIPP PA Division, 1991, Vol. 3, 2.4.2
Dispersivity						
Longitudinal (α_L)	1.5×10^{1}	1	4×10^{1}	m	Constructed	WIPP PA Division, 1991, Vol. 3, 2.4.3
Ratio (α_L/α_T)	10	3	25	none	Constructed	WIPP PA Division, 1991, Vol. 3, 2.4.3
Partition coefficient						
Am	2.5×10^{-2}			m^3/kg	Constant	WIPP PA Division, 1991, Vol. 3, 2.4.4
Np	1×10^{-3}			m^3/kg	Constant	WIPP PA Division, 1991, Vol. 3, 2.4.4
Pb	1×10^{-3}			m^3/kg	Constant	WIPP PA Division, 1991, Vol. 3, 2.4.4
Pu	1×10^{-1}			m^3/kg	Constant	WIPP PA Division, 1991, Vol. 3, 2.4.4
Ra	1×10^{-3}			m^3/kg	Constant	WIPP PA Division, 1991, Vol. 3, 2.4.4
Th	1×10^{-1}			m^3/kg	Constant	WIPP PA Division, 1991, Vol. 3, 2.4.4
U	1×10^{-3}			m^3/kg	Constant	WIPP PA Division, 1991, Vol. 3, 2.4.4
Log Permeability (k)						
Undisturbed	**-19.3**	**-21.0**	**-16.0**	**log (m^2)**	**Constructed**	**Section 2.4.2**
Disturbed	-15.0			log (m^2)	Constant	Section 2.4.2
Pore pressure	**12.5**	**12.0**	**13.0**	**MPa**	**Uniform**	**Section 2.4.3**
Porosity (ϕ)						
Undisturbed	$\mathbf{1 \times 10^{-2}}$	$\mathbf{1 \times 10^{-3}}$	$\mathbf{3 \times 10^{-2}}$	**none**	**Constructed**	**Section 2.4.4**
Disturbed	(correlated with undisturbed porosity)			none	Uniform	Section 2.4.4
Specific storage	1.4×10^{-7}	9.7×10^{-8}	1×10^{-6}	m^{-1}	Constructed	WIPP PA Division, 1991, Vol. 3, 2.4.8
Thickness (Δz)	9×10^{-1}	4×10^{-1}	1.25	m	Constructed	WIPP PA Division, 1991, Vol. 3, 2.4.9
Tortuosity	1.4×10^{-1}	1×10^{-2}	6.67×10^{-1}	none	Constructed	WIPP PA Division, 1991, Vol. 3, 2.4.10

[a]Parameters in bold were sampled in the 1992 calculations.

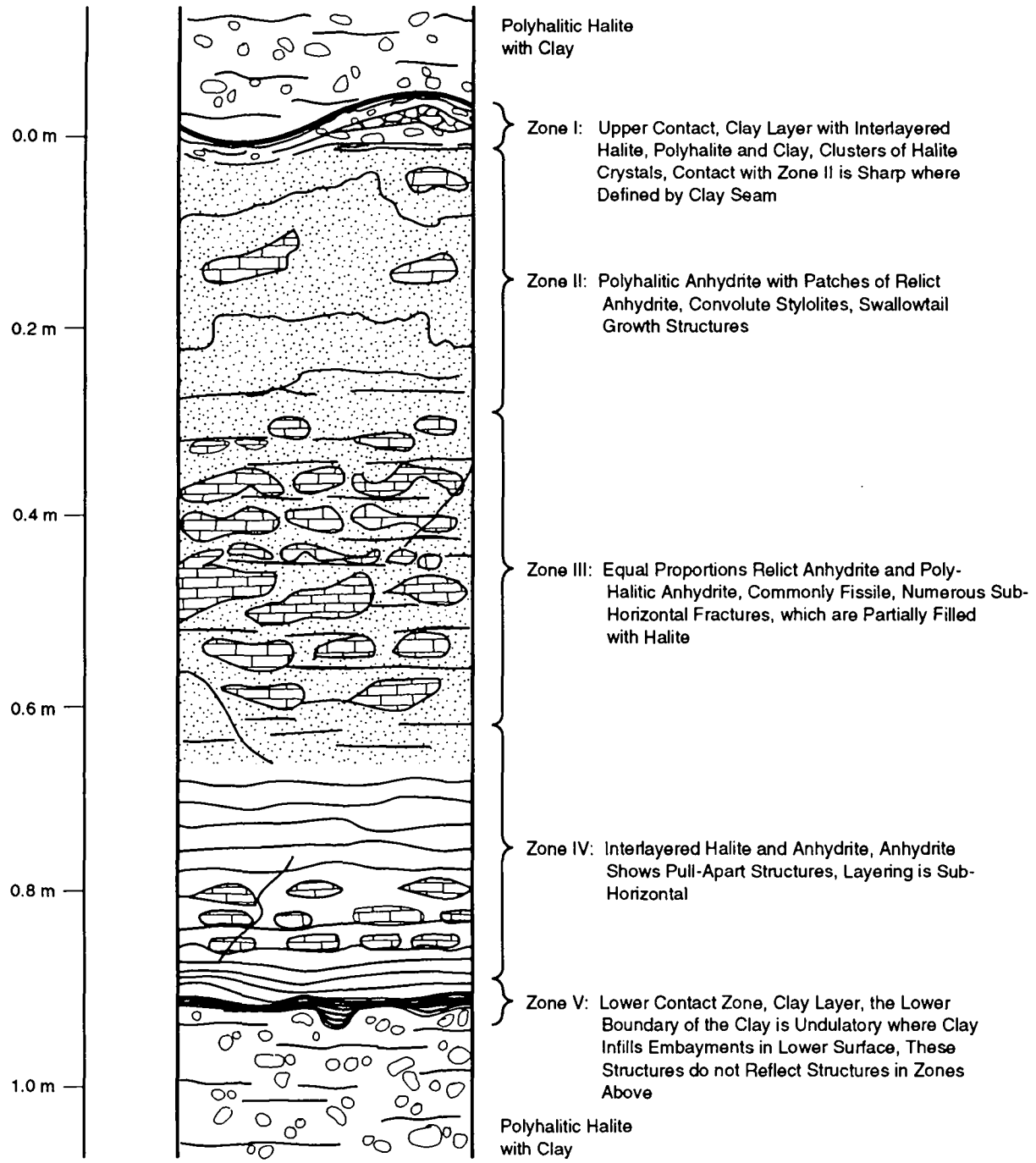

Figure 2.4-1. Generalized cross section of Marker Bed 139 near repository. The figure shows the internal variability of the unit and the character of both the upper and lower contacts (after Borns, 1985). The thickness varies spatially between 0.4 and 1.25 m with a reference thickness of 0.99 m (Krieg, 1984, Table I).

2.4.1 Capillary Pressure and Relative Permeability

Threshold Displacement Pressure, P_t*

Parameter: **Threshold displacement pressure (p_t)**
Material: Anhydrite layers within Salado Formation (MB139, PressCTD)

Definition Units: Pa

Values: P_t (MPa) = $2.6 \times 10^{-7}\ k^{-0.348}$

Distribution: Function (above)
Correlation: Perfectly correlated with anhydrite permeability.

Data Source(s): Davies, P. B. 1991a. *Evaluation of the Role of Threshold Pressure in Controlling Flow of Waste-Generated Gas into Bedded Salt at the Waste Isolation Pilot Plant.* SAND90-3246. Albuquerque, NM: Sandia National Laboratories. (Investigator Judgment)

Davies, P. B. 1991b. Appendix A: "Uncertainty Estimates for Threshold Pressure for 1991 Performance Assessment Calculations Involving Waste-Generated Gas," *Preliminary Comparison with 40 CFR Part 191, Subpart B for the Waste Isolation Pilot Plant, December 1991. Volume 3: Reference Data.* WIPP Performance Assessment Division. Eds. R. P. Rechard, A. C. Peterson, J. D. Schreiber, II. J. Iuzzolino, M. S. Tierney, and J. S. Sandha. SAND91-0893/3. Albuquerque, NM: Sandia National Laboratories. A-37 through A-41. (Investigator Judgment)

Usage:

Mathematical model:
Two-Phase Flow (Section 1.4.1, this volume).

Equation 1.4.1-6.

Computational models:
BRAGFLO

Ranking in Past Sensitivity Analyses:

40 CFR 191	Low
40 CFR 268	Not tested
NEPA	Not tested
Other	Not tested

*Key to Parameter Sheets is provided in Section 1.2.8.

Residual Wetting Phase Saturation*

Parameter:	**Residual wetting phase (liquid) saturation ($S_{\ell r}$)**
Material:	Anhydrite layers within Salado Formation (MB139, SatRWP)
Definition Units:	Dimensionless
Values:	Range: (0.0, 4×10^{-1}) Median: 2×10^{-1}
Distribution:	Uniform
Correlation:	

Data Source(s):

Davies, P. B., and A. M. LaVenue. 1990b. Appendix A: "Additional Data for Characterizing 2-Phase Flow Behavior in Waste-Generated Gas Simulations and Pilot Point Information for Final Culebra 2-D Model (SAND89-7068/1)," *Data Used in Preliminary Performance Assessment of the Waste Isolation Pilot Plant (1990).* R. P. Rechard, H. Iuzzolino, and J. S. Sandha. SAND89-2408. Albuquerque, NM: Sandia National Laboratories. A-139 through A-156. (Investigator Judgment)

Webb, S. W. 1992a. "Uncertainty Estimates for Two-Phase Characteristic Curves for 1992 RCRA Calculations" (see Appendix A, pp. A-141 through A-146). (Investigator Judgment)

Webb, S. W. 1992b. "Uncertainty Estimates for Two-Phase Characteristic Curves for 1992 40 CFR 191 Calculations" (see Appendix A, pp. A-147 through A-155). (Investigator Judgment)

Usage:

Mathematical model:

Two-Phase Flow, Section 1.4.1, this volume.

Equation 1.4.1-7.

Computational models:

BRAGFLO

Ranking in Past Sensitivity Analyses:

40 CFR 191	Not tested
40 CFR 268	Low
NEPA	Not tested
Other	Not tested

*Key to Parameter Sheets is provided in Section 1.2.8.

Residual Gas Saturation*

Parameter: **Residual gas saturation (S_{gr})**
Material: Anhydrite layers within Salado Formation (MB139, SatRGP)

Definition Units: Dimensionless

Values: Range: (0.0, 4×10^{-1}) Median: 2×10^{-1}

Distribution: Uniform
Correlation:

Data Source(s):
Davies, P. B., and A. M. LaVenue. 1990b. Appendix A: "Additional Data for Characterizing 2-Phase Flow Behavior in Waste-Generated Gas Simulations and Pilot Point Information for Final Culebra 2-D Model (SAND89-7068/1)," *Data Used in Preliminary Performance Assessment of the Waste Isolation Pilot Plant (1990).* R. P. Rechard, H. Iuzzolino, and J. S. Sandha. SAND89-2408. Albuquerque, NM: Sandia National Laboratories. A-139 through A-156. (Investigator Judgment)

Webb, S. W. 1992a. "Uncertainty Estimates for Two-Phase Characteristic Curves for 1992 RCRA Calculations" (see Appendix A, pp. A-141 through A-146). (Investigator Judgment)

Webb, S. W. 1992b. "Uncertainty Estimates for Two-Phase Characteristic Curves for 1992 40 CFR 191 Calculations" (see Appendix A, pp. A-147 through A-155). (Investigator Judgment)

Usage:

Mathematical model:
Two-Phase Flow, Section 1.4.1, this volume.

Equation 1.4.1-7.

Computational models:
BRAGFLO

Ranking in Past Sensitivity Analyses:

40 CFR 191	Not tested
40 CFR 268	Low
NEPA	Not tested
Other	Not tested

*Key to Parameter Sheets is provided in Section 1.2.8.

Brooks and Corey Exponent*

Parameter: **Brooks and Corey exponent (λ)**
Material: Anhydrite layers within Salado Formation (MB139, BrkCorEx)

Definition Units: Dimensionless

Values: Range: (0.2, 10.0) Median: 0.7

Distribution: Constructed
Correlation:

Data Source(s):

Davies, P. B., and A. M. LaVenue. 1990b. Appendix A: "Additional Data for Characterizing 2-Phase Flow Behavior in Waste-Generated Gas Simulations and Pilot Point Information for Final Culebra 2-D Model (SAND89-7068/1)," *Data Used in Preliminary Performance Assessment of the Waste Isolation Pilot Plant (1990).* R. P. Rechard, H. Iuzzolino, and J. S. Sandha. SAND89-2408. Albuquerque, NM: Sandia National Laboratories. A-139 through A-156. (Investigator Judgment)

Webb, S. W. 1992a. "Uncertainty Estimates for Two-Phase Characteristic Curves for 1992 RCRA Calculations" (see Appendix A, pp. A-141 through A-146). (Investigator Judgment)

Webb, S. W. 1992b. "Uncertainty Estimates for Two-Phase Characteristic Curves for 1992 40 CFR 191 Calculations" (see Appendix A, pp. A-147 through A-155). (Investigator Judgment)

Usage:

Mathematical model:
Two-Phase Flow, Section 1.4.1, this volume.

Equation 1.4.1-6.

Computational models:
BRAGFLO

Ranking in Past Sensitivity Analyses:

40 CFR 191	Not tested
40 CFR 268	Low
NEPA	Not tested
Other	Not tested

*Key to Parameter Sheets is provided in Section 1.2.8.

Discussion:

Relationships between these parameters are discussed in Section 1.4.1. Preliminary parameter values selected for MB139 and other anhydrite beds are the same as for Salado halite (Section 2.3.1), except for a lower threshold displacement pressure (p_t), and were taken from experimental data measured for the tight gas sands (Ward and Morrow, 1985; Davies and LaVenue, 1990b).

2.4.2 Permeability

Undisturbed Permeability*

Parameter: **Log permeability, undisturbed**
Material: Anhydrite layers within Salado Formation (MB139, LogPrmU)

Definition Units: log (m^2)

Values: Range: (-21.0, -16) Median: -19.3

Distribution: Constructed
Correlation:

Data Source(s): Davies, P. B., R. L. Beauheim, and E. D. Gorham. 1992b. "Additional Comments on Far-Field Anhydrite Permeability Distribution in 'PA Modeling Using BRAGFLO -- 1992' 7-8-92 Memo by J. Schreiber" (see Appendix A, pp. A-39 through A-45). (Investigator Judgment)

(Source #1)
Davies, P. B., S. W. Webb, and E. D. Gorham. 1992a. "Feedback on 'PA Modeling Using BRAGFLO -- 1992' 7-8-92 Memo by J. Schreiber" (see Appendix A, pp. A-21 through A-37). (Investigator Judgment)

Usage:

Mathematical model:
Two-Phase Flow, Section 1.4.1, this volume.

Equations 1.4.1-1 and 1.4.1-2.

Computational models:
BRAGFLO

Ranking in Past Sensitivity Analyses:

40 CFR 191	Medium (see discussion)
40 CFR 268	High
NEPA	Not tested
Other	Not tested

*Key to Parameter Sheets is provided in Section 1.2.8.

Discussion:

In 1991, the permeability of undisturbed anhydrite was shown to be a moderately sensitive parameter in determining releases of radioactivity to Culebra Dolomite under conditions of gas generation within the repository.

The 1992 distribution of anhydrite permeability in the far field (Figure 2.4-2) is based on recommendations given in Davies et al. (1992b, Memo in Appendix A). The 1992 distribution differs from the 1991 distribution (Figure 2.4-3) in the assignment of significant probability to values of permeability greater than 10^{-18} m^2 and less than 10^{-20} m^2; the median values of the 1991 and 1992 distributions, 7.8×10^{-20} m^2 and 5.0×10^{-20} m^2 respectively, are not significantly different.

According to Davies et al. (1992b, Memo in Appendix A), the 1992 distribution does not capture permeabilities representative of interbed fracturing due to pressurization by gas that could be generated by WIPP wastes.

An Estimate of Average Undisturbed Anhydrite Permeability. The method for estimating far-field halite parameters by non-linear regression described in Section 2.3.2 has also been used to make preliminary estimates of the distribution of the average anhydrite permeability in the far field. Available results of experiments that measured anhydrite permeability and pore pressure are summarized in Table 2.4-2. Eight measurements from this series of results were used as the basis for generating artificial data sets in the manner indicated in Section 2.3.2; the regression curves fitted to 30 artificial data sets are shown on Figure 2.4-4. (Note that the form of the regression curve is the same as the one described in Section 2.3.2:

$$y(x) = a + be^{-x/c}$$

in which the parameter a estimates the far-field $[x \rightarrow \infty]$ material-property parameter.) The empirical cdf for the average of undisturbed anhydrite permeability that results from this procedure is sketched on Figure 2.4-5.

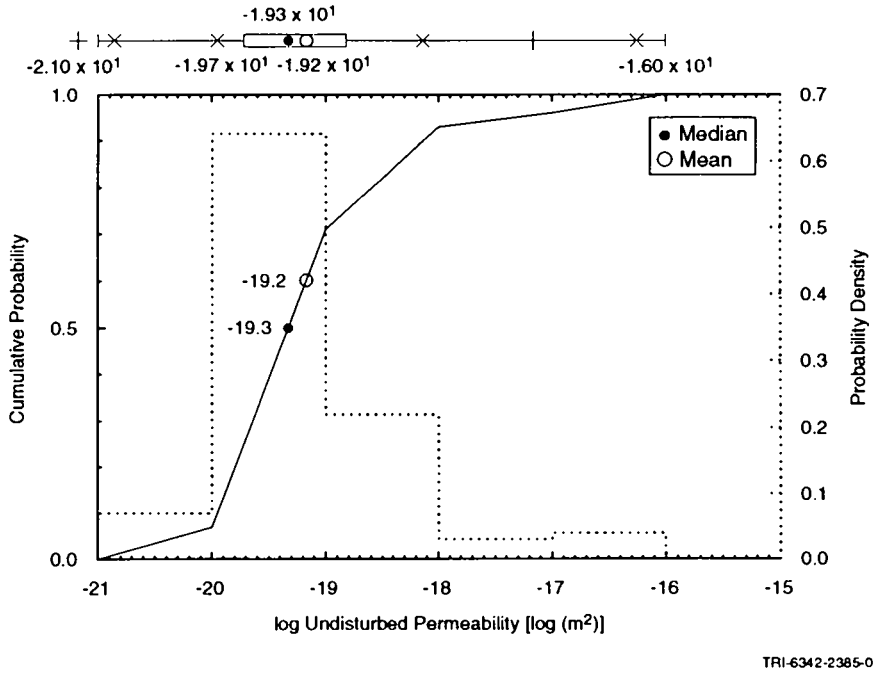

Figure 2.4-2. Estimated distribution in 1992 for undisturbed permeability of anhydrite layers in Salado Formation. (See discussion.)

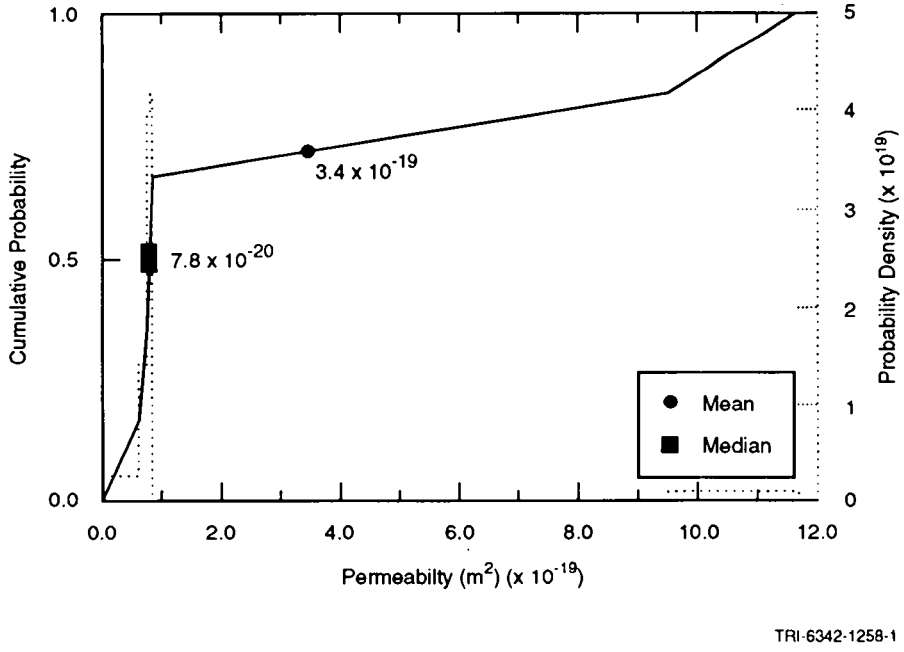

Figure 2.4-3. Estimated 1991 distribution for undisturbed permeability, anhydrite layers in Salado Formation.

Table 2.4-2. Summary of Measurements of Salado Anhydrite Permeabilities and Pore Pressures

Test No.	Lithology	Distance[b] (m)	Measured Permeability (m^2)	log_{10} Permeability	Pressure (MPa)	Orientation	Sources[e]
SCP01	MB139	10.50 - 14.78	3.0×10^{-20}	-19.5 ± 0.7[(c)]	12.4 ± 0.5[(d)]	vertical, down	1, 3
[(a)]QPP13 (pre)	MB139	23.4	4.1×10^{-20}	-19.4	12.5	vertical down	1, 2
QPP03 (pre)	anhydrite	23.4	4.4×10^{-20}	-19.4	12.6	vertical, up	1, 2
C2H02	MB139	9.47 - 10.86	7.8×10^{-20}	-19.1	9.3	45°, down	1, 3
L4P51-B	anhydrite "c"	9.62 - 9.72	5.0×10^{-20}	-19.3	5.1	vertical, down	1, 3
S1P71-B	anhydrite "c"	9.48 - 9.80	6.8×10^{-20}	-19.2	4.9	vertical, down	1, 3
C2H01-C	MB139	6.63 - 8.97	9.5×10^{-19}	-18.0	8.0	vertical, down	1, 3
C1X10	MB139	?	5.0×10^{-17}	-16.3	7.3	?	1
QPP03 (post)	anhydrite "b"	3.07	7.9×10^{-20}	-19.1	7.0	vertical, up	1, 2
QPP13 (post)	MB139	3.07	4.7×10^{-20}	-19.3	8.1	vertical, down	1, 2
L4P52-A	anhydrite "a"	?	1.0×10^{-19}	-19.0	6.4	?	1
QPB01	?	?	9.6×10^{-21}	-20.0	(5.0 assumed)	?	1
QPB02	?	?	1.6×10^{-19}	-18.8	(5.0 assumed)	?	1
QPB03	?	?	1.2×10^{-20}	-19.9	(5.0 assumed)	?	1
S1P72	MB139	4.40 - 6.00	unmeasurable	-	1.2	?	1, 3
S1P73-B	MB138	10.86 - 11.03	2.9×10^{-19}	-18.5	4.5	?	1, 3
S0P01-GZ	MB139	1.86 - 2.91	5.7×10^{-18}	-17.2	0.5	vertical, down	1, 3
S1P73-A	?	?	too high to measure ($\sim 10^{-15}$)	-	0.5	?	1
S1P73-A-GZ	?	?	too high to measure ($\sim 10^{-15}$)	-	0.0	?	1
S1P71-A-GZ	?	?	too high to measure ($\sim 10^{-14}$)	-	0.0	?	1
L4P51-A-GZ	MB139	1.86 - 2.91	too high to measure ($\sim 10^{-15}$)	-	0.3	?	1, 3

Key to Table 2.4-2:

[a] - "Pre" and "post" mean pre- and post-minebye for Q tunnel tests.

[b] - Estimated distance of apparatus from wall of excavation

[c] - A standard error of one-half order of magnitude assumed for all permeability measurements

[d] - A standard error of 0.5 MPa assumed for all measured or inferred pressures

[e] - Sources: 1 - Gorham et al., June 15, 1992 (Memo in Appendix A),
2 - Howarth et al., 1991,
3 - Beauheim et al., 1991a,
4 - Finley and McTigue, 1991.

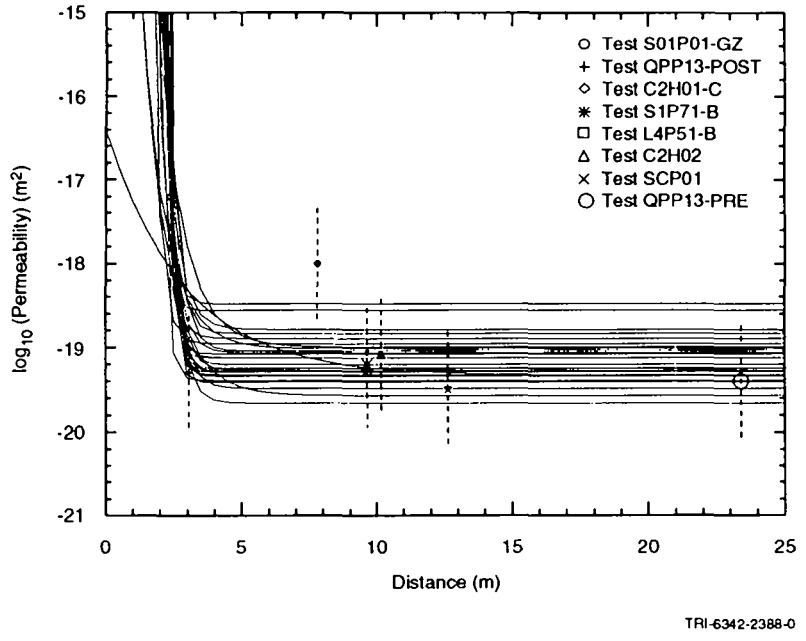

Figure 2.4-4. Regression curves fitted to artificial data sets for undisturbed anhydrite permeability (30 samples).

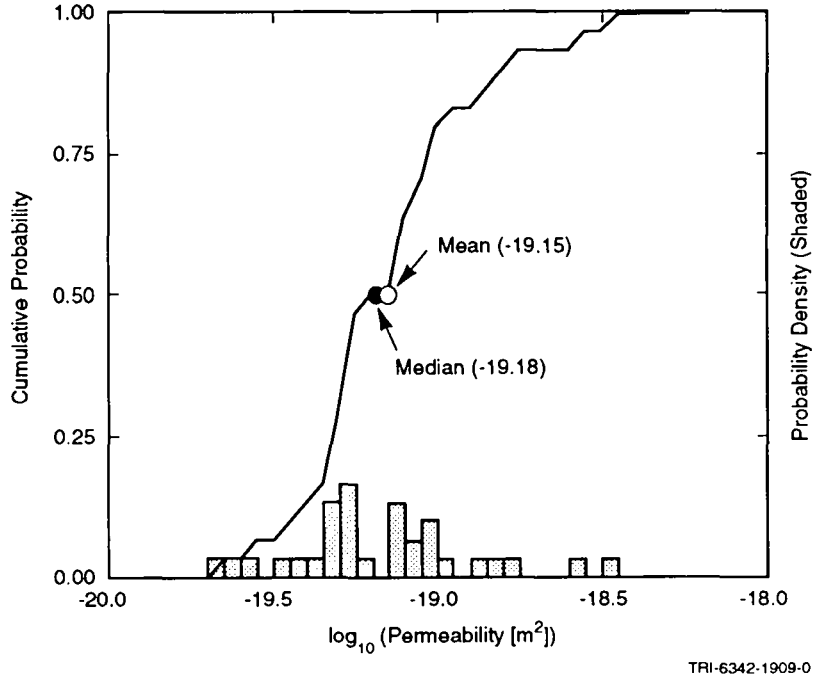

Figure 2.4-5. Simulated distribution of average, undisturbed permeability of anhydrite (30 samples).

Disturbed Permeability*

Parameter: **Log permeability, disturbed (k)**
Material: Anhydrite layers within Salado Formation (Salado, LogGPrm)

Definition Units: log (m^2)

Values: -15.0

Distribution: Constant
Correlation:

Data Source(s): None: PA analyst's choice (see Section 2.3.2).

Usage:

Mathematical model:

Two-Phase Flow, Section 1.4.1, this volume.

Equations 1.4.1-1 and 1.4.1-2.

Computational models:

BRAGFLO

Ranking in Past Sensitivity Analyses:

40 CFR 191	Not tested
40 CFR 268	Low
NEPA	Not tested
Other	Not tested

*Key to Parameter Sheets is provided in Section 1.2.8.

2.4.3 Pore Pressure at Repository Level in Anhydrite

Pore Pressure*

Parameter: **Pore pressure at repository level (p)**
Material: Anhydrite layers within Salado Formation (MB139, Pressure)

Definition Units: MPa

Values: Range: (12.0, 13.0) Median: 12.5

Distribution: Uniform
Correlation:

Data Source(s): Davies, P. B., R. L. Beauheim, and E. D. Gorham. 1992b. "Additional Comments on Far-Field Anhydrite Permeability Distribution in 'PA Modeling Using BRAGFLO -- 1992' 7-8-92 Memo by J. Schreiber" (see Appendix A, pp. A-39 through A-45). (Investigator Judgment)

Usage:

Mathematical model:
Two-Phase Flow, Section 1.4.1, this volume.

Equation: (Boundary condition on fluid pressure in Eqs. 1.4.1-1 and 1.4.1-2.)

Computational models:
BRAGFLO

Ranking in Past Sensitivity Analyses:

40 CFR 191	Medium
40 CFR 268	High
NEPA	Not tested
Other	Not tested

*Key to Parameter Sheets is provided in Section 1.2.8.

Discussion:

The 1991 distribution of brine pore pressure at repository level in anhydrite is shown in Figure 2.4-6. This distribution was used to express variability in pore pressure in both halite and anhydrite in the 1991 PA exercises. Brine pore pressure proved to be a moderately sensitive parameter in determining releases to the Culebra (and beyond) in scenarios that took account of gas generation in the repository (Helton et al., 1992, Table 4.5-1).

The 1992 distribution of brine pore pressure at repository level (in both halite and anhydrite) is taken to be uniform on the interval 12 MPa to 13 MPa and is based on test results quoted in the Davies et al., July 22, 1992b (Memo in Appendix A). Three measurements were available from regions in which fluid depressurization was judged to be small; all three measurements yielded pressure values in the range 12 to 13 MPa.

An Estimate of Average Undisturbed Pore Pressure in Anhydrite. The method for estimating far-field halite parameters that was described in Section 2.3.2 has also been used to make preliminary estimates of the distribution of the average of undisturbed pore pressure in anhydrite. Eight measurements from the series of test results listed in Table 2.3-2 were used as the basis for generating artificial data sets; the resulting regression curves fitted to 30 artificial data sets are shown on Figure 2.4-7. (The form of the regression curve is the same as in Section 2.3.2.) The resulting empirical cdf for the average of undisturbed pore pressure in anhydrite is shown on Figure 2.4-8. This figure should be compared with Figure 2.3-10, the simulated distribution of the average of undisturbed pressure in halite at the repository level. Whether these results make physical sense remains to be determined.

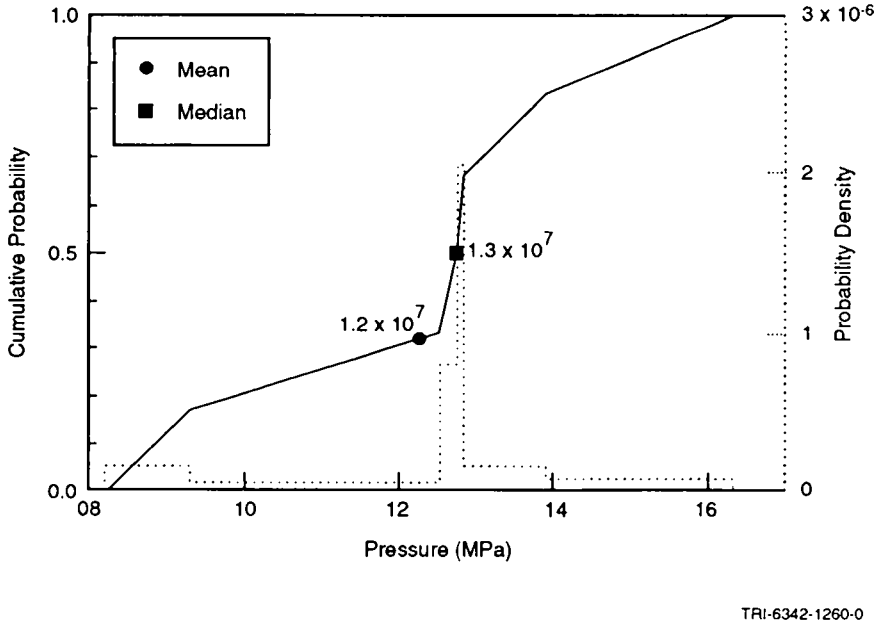

Figure 2.4-6. Distribution used in 1991 for brine pore pressure in anhydrite MB139 at repository level.

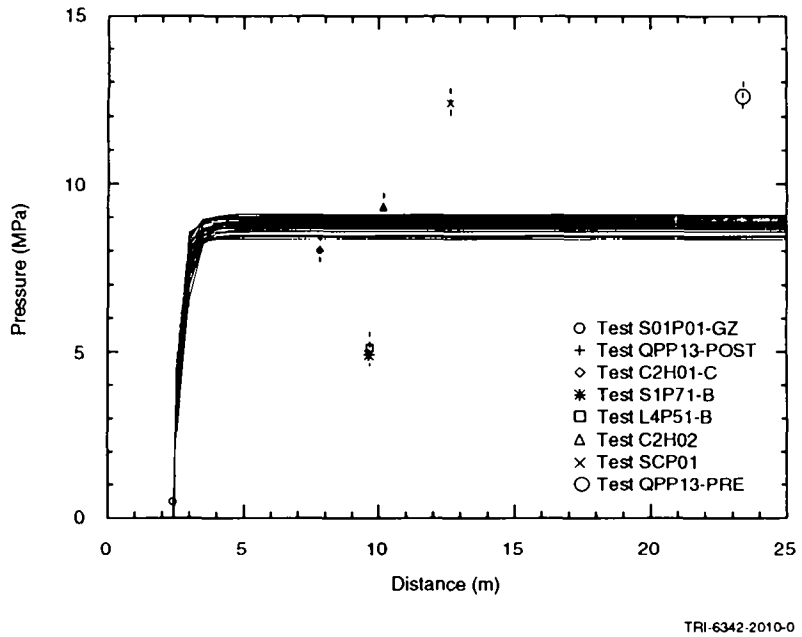

Figure 2.4-7. Regression curves fitted to artificial data sets for undisturbed anhydrite pore pressure (30 samples).

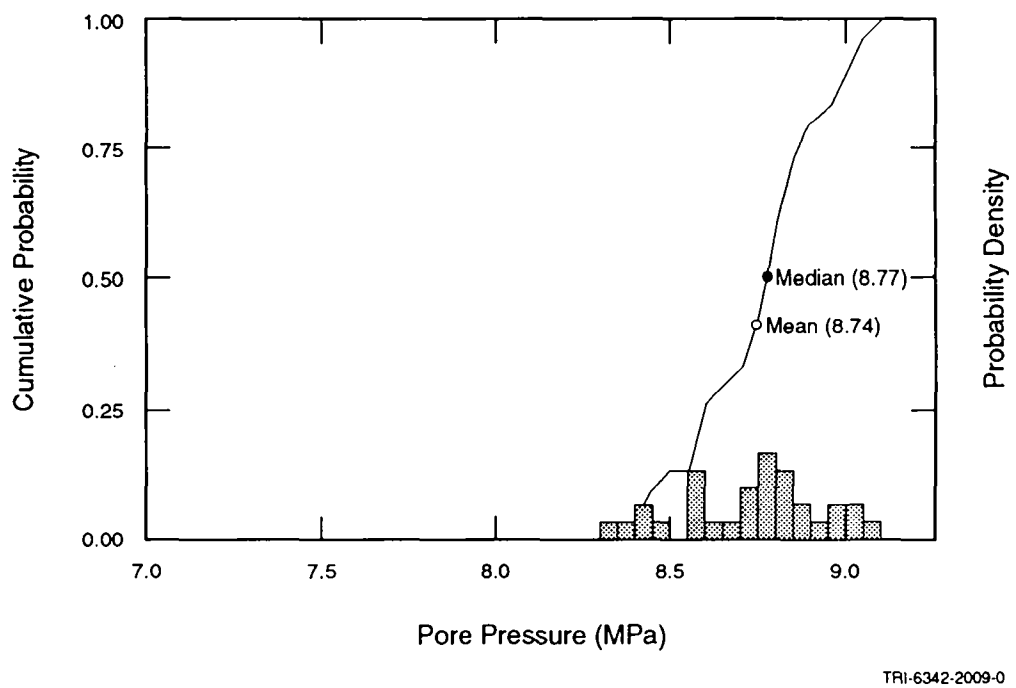

Figure 2.4-8. Simulated distribution of average undisturbed pore pressure at repository depth in anhydrite (30 samples).

2.4.4 Porosity

Undisturbed Porosity*

Parameter:	**Porosity, undisturbed (ϕ)**
Material:	Anhydrite layers within Salado Formation (MB139, Pore_U)
Definition Units:	Dimensionless
Values:	Range: (1×10^{-3}, 3×10^{-2}) Median: 1×10^{-2}
Distribution:	Constructed
Correlation:	

Data Source(s): Investigator Judgment (see Discussion).

Powers, D. W., S. J. Lambert, S-E. Shaffer, L. R. Hill, and W. D. Weart, eds. 1978. *Geological Characterization Report, Waste Isolation Pilot Plant (WIPP) Site, Southeastern New Mexico*. SAND78-1596. Albuquerque, NM: Sandia National Laboratories. Vols. 1-2.

U.S. Department of Energy. 1983. "Brine Content of Facility Interval Strata," *Results of Site Validation Experiments*. TME 3177. [Carlsbad, NM]: Waste Isolation Pilot Plant. Vol. II, Supporting Document 10.

Usage:

Mathematical model:

Two-Phase Flow, Section 1.4.1 of this volume

Equations 1.4.1-1 and 1.4.1-2.

Computational models:

BRAGFLO

Ranking in Past Sensitivity Analyses:

40 CFR 191	Low
40 CFR 268	Low
NEPA	Not tested
Other	Not tested

*Key to Parameter Sheets is provided in Section 1.2.8.

Discussion:

PA calculations have assumed an undisturbed anhydrite porosity similar to the undisturbed porosity of the Salado Formation as a whole. The PA Department assumed the median porosity to be 0.01 based on an unpublished report on electromagnetic and DC resistivity measurements (Skokan, C., J. Starrett, and H. T. Andersen. 1988. *Final Report: Feasibility Study of Seismic Tomography to Monitor Underground Pillar Integrity at the WIPP Site.* Contractor Report. Albuquerque, NM: Sandia National Laboratories). This median value is identical to that calculated from a grain density of 2,163 kg/m^3 (135 lb/ft^3) for halite and a bulk density of 2,140 kg/m^3 (133.6 lb/ft^3) ($\rho_b = (1 - \phi)\rho_g$). The low value of 0.001 is based on drying experiments (Powers et al., 1978), whereas the high of 0.03 was suggested by the low end of the DC resistivity measurements in the unpublished report by Skokan et al., cited above.

Figure 2.4-9 shows the estimated distribution for undisturbed porosity for the anhydrite layers.

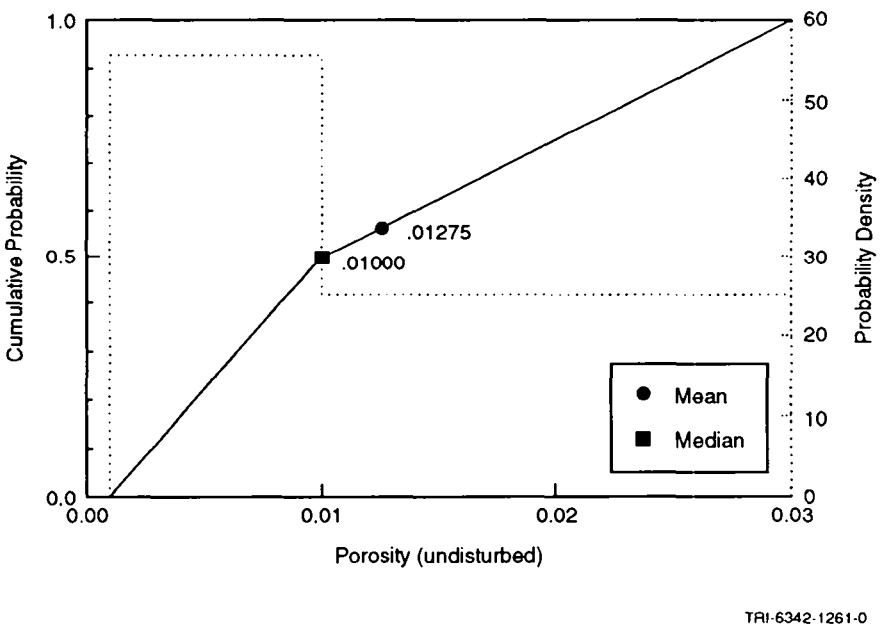

Figure 2.4-9. Estimated distribution for undisturbed porosity for anhydrite layers in Salado Formation.

Disturbed Porosity*

Parameter:	**Porosity, disturbed (ϕ)**
Material:	Disturbed anhydrite and halite layers within Salado Formation (MB139, Uniform1)
Definition Units:	Dimensionless
Values:	0.06 (maximum value; see Discussion)
Distribution:	Uniform between maximum value and value of undisturbed porosity
Correlation:	Correlated with undisturbed porosity (see Discussion)

Data Source(s): None; PA analyst's choice.

Usage:

Mathematical model:

Two-Phase Flow, Section 1.4.1 of this volume.

Equations 1.4.1-1 and 1.4.1-2.

Computational models:

BRAGFLO

Ranking in Past Sensitivity Analyses:

40 CFR 191	Not tested
40 CFR 268	Not tested
NEPA	Not tested
Other	Not tested

*Key to Parameter Sheets is provided in Section 1.2.8.

Discussion:

The porosity of regions of both disturbed anhydrite and halite are modeled by the following relation:

$$\phi(\text{disturbed}) = 0.06\ U + [\phi\ (\text{undisturbed})]\ (1 - U)\ .$$

where ϕ (undisturbed) is itself a sampled parameter (see previous data table), and U is a number uniformly distributed on the interval (0,1).

The maximum value of disturbed porosity (0.06) is rationalized in WIPP PA Division, 1991, Vol. 3, p. 2-37.

2.5 Mechanical Parameters for Materials in Repository and Salado Formation

The 1992 attempt to incorporate effects of disposal-room deformation in a calculation of average room porosity and permeability has triggered the need to include 23 new parameters in the PA Department's Secondary Data Base. These new parameters are primarily mechanical or material properties that appear in constitutive equations for the behavior of intact salt, crushed-salt backfill, or composite waste materials (Section 1.4.7); the 23 parameters and the values assigned to them are summarized in Tables 2.5-1 and 2.5-2. The uncertainty associated with these mechanical or material properties is presently unknown, so they have been assigned fixed values in the 1992 series of PA calculations.

Other, non-mechanical parameters have arbitrarily been included in Table 2.5-1, and may be redundant with similar quantities appearing elsewhere in this report: for example, parameters for the gas-generation model used in the porosity surface calculations have been included in Table 2.5-1 for the sake of completeness even though they are similar to (but do not generally have the same values as) the gas generation rates described in Section 3.3.5.

Discussion of Sources:

The primary source for values assigned to the 23 mechanical or material properties in 1992 calculations is Mendenhall et al., 1991. This citation is confirmed by Butcher in his September 9, 1992 memo (Appendix A). Most of these values are taken from the much earlier work of Krieg (1984) or Sjaardema and Krieg (1987) according to Munson in his October 26, 1992 memo (Appendix A). Mendenhall et al. modified the Sjaardema and Krieg values of elastic shear modulus and elastic bulk modulus of intact and crushed salt to conform with the "Reduced Modulus" model frequently used in WIPP problems (Munson, October 26, 1992, Memo in Appendix A) by dividing the Sjaardema and Krieg values by 12.5.

According to Butcher (September 9, 1992, Memo in Appendix A), the function giving volumetric strain as a function of pressure (Table 2.5-2) was derived from the solid line axial compaction stress versus porosity curve in Figure 2 of the September 12, 1991 memo of Beraún and Davies (Appendix A). Actual data points from which the Beraún-Davies curve was derived are given in Table 3-2 of Butcher et al., 1991: Table 2.5-2 was constructed by dividing each axial stress datum by 3 and converting porosity to the ratio ρ/ρ_o, where ρ is current density of waste and ρ_o is waste initial density. The curve implicit in Table 2.5-2 assumes an initial waste density of 426 kg/m^3 and a theoretical solid density of 2000 kg/m^3.

Table 2.5-1. Summary of Parameters Used in Mechanical Models of Repository and Salado Formation Materials.

Parameter	Median[a]	Units	Section 1.4.7 Eq. No.	Source[b]
• Model of intact salt				
G - elastic shear modulus	0.992	GPa	1.4.7-1	1, see discussion
K - elastic bulk modulus	1.656	GPa	1.4.7-2	1, see discussion
A - experimental constant	5.79×10^{-36}	Pa-4.9/s	1.4.7-2	1
N - experimental constant	4.9	none	1.4.7-1	1, 3
Q/RT - exponential constant	20.13	none	1.4.7-1	1, 3 (@ 300°K)
• Model of crushed salt backfill				
G_0 - elastic shear modulus	864.0	Pa	1.4.7-3	1, see discussion
G_1 - experimental constant	6.53×10^{-3}	m^3/kg	1.4.7-3	1, 2
K_0 - elastic bulk modulus	1.41	kPa	1.4.7-4	1, see discussion
K_1 - experimental constant	6.53×10^{-3}	m^3/kg	1.4.7-4	1, 2
A_c - experimental constant	5.79×10^{-36}	$Pa^{-4.9}/s$	1.4.7-5	1
ρ_{int} - density of intact halite	2.14×10^{3}	kg/m^3	1.4.7-5	2
N - experimental constant	4.9	none	1.4.7-5	1
Q/RT - exponential constant	20.13	none	1.4.7-5	1
B_0 - experimental constant	1.3×10^{8}	$kg/(m^3 \cdot s)$	1.4.7-6	1, 2
B_1 - experimental constant	0.82×10^{-6}	Pa^{-1}	1.4.7-6	1, 2
A - experimental constant	-17.3×10^{-3}	m^3/kg	1.4.7-6	1, 2
• Volumetric plasticity model for waste				
μ - shear modulus	333	MPa	1.4.7-7	1
K_0 - bulk unloading modulus	222	MPa	1.4.7-7	1
a_0 - yield function constant	0	none	1.4.7-7	1
a_1 - yield function constant	0	none	1.4.7-7	1
a_2 - yield function constant	3	none	1.4.7-7	1
ρ_0 - initial waste density	426	kg/m^3	1.4.7-8	4
F(P) - volumetric strain as a function of pressure	(see Table 2.5-2 and discussion)		1.4.7-8	4
• Gas generation model for porosity-surface calculation gas production rates (inundated)				
Anoxic corrosion rate	3.17×10^{-8}	mole/(drum • s)	1.4.7-10	5
Anoxic corrosion potential	1050	mole/drum	1.4.7-10	5
Microbial rate	3.17×10^{-8}	mole/(drum • s)	1.4.7-10	5
Microbial potential	550	mole/drum	1.4.7-10	5
Radiolysis rate	0	mole/(drum • s)	1.4.7-10	5
Radiolysis potential	0	mole/drum	1.4.7-10	5
D - number of drums	6804	none	1.4.7-10	5

[a] All parameters are constants unless otherwise noted.

[b] Key to sources:

1. Mendenhall et al., 1991
2. Sjaardema and Krieg, 1987
3. Munson (October 26, 1992, Memo in Appendix A)
4. Butcher (September 9, 1992, Memo in Appendix A)
5. Beraún and Davies (September 12, 1991, Memo in Appendix A)

Table 2.5-2. Volumetric Strain as a Function of Pressure: Relationship Used in Volumetric Plasticity Model for Waste in Disposal Room (from Butcher, September 9, 1992, Memo in Appendix A).

Pressure (MPa)	log Density Ratio ln ρ/ρ_o
0.028	0.032
0.733	0.741
1.133	0.898
1.667	1.029
2.800	1.180
10.17	1.536

2.6 Parameters for Culebra Dolomite Member of Rustler Formation

The Culebra Dolomite Member of the Rustler Formation is a finely crystalline, locally argillaceous (containing clay) and arenaceous (containing sand), vuggy dolomite ranging in thickness near the WIPP from about 7 m (23 ft) (at DOE-1 and other locations) to 14 m (46 ft) (at H-7). The PA Department has chosen 7.7 m as a reference thickness. Figure 2.6-1 shows a detailed lithology of the Rustler Formation. Figure 2.6-2 is a cross-section across the WIPP disposal system. The Culebra Dolomite is generally considered to provide the most important potential groundwater-transport pathway for radionuclides that may be released to the accessible environment provided human intrusion occurs. Accordingly, the WIPP Project has devoted much attention to understanding the hydrogeology and hydraulic properties of the Culebra. Figure 2.6-3 shows the locations of wells used to define the hydrologic parameters for the Culebra Dolomite. Detailed hydrogeologic information is available in reports by Brinster (1991) and Holt and Powers (1988). The Culebra Dolomite has been tested at 41 locations in the vicinity of the WIPP. Results of these tests and interpretations have been reported by Beauheim (1987a,b,c; 1989), Saulnier (1987), and Avis and Saulnier (1990).

One early observation (Mercer and Orr, 1979) was that the transmissivity of the Culebra Dolomite varies by six orders of magnitude in the vicinity of the WIPP. This variation in transmissivity appears to be the result of differing degrees of fracturing within the Culebra Dolomite. The cause of the fracturing, however, is unresolved. Culebra transmissivities of about 1 x 10^{-6} m^2/s (0.93 ft^2/d) or greater appear to be related to fracturing. Where the transmissivity of the Culebra Dolomite is less than 1 x 10^{-6} m^2/s (0.93 ft^2/d), few or no open fractures have been observed in core, and the Culebra's hydraulic behavior during pumping or slug tests is that of a single-porosity medium. Where transmissivities are between 1 x 10^{-6} m^2/s (0.93 ft^2/d) and at least 1 x 10^{-4} m^2/s (93 ft^2/d), open fractures are observed in core, and the hydraulic behavior of the Culebra Dolomite during pumping tests is that of a dual-porosity medium (Beauheim, 1987a, b, c; Saulnier, 1987).

Parameter values for the Culebra Dolomite Member are given in Table 2.6-1.

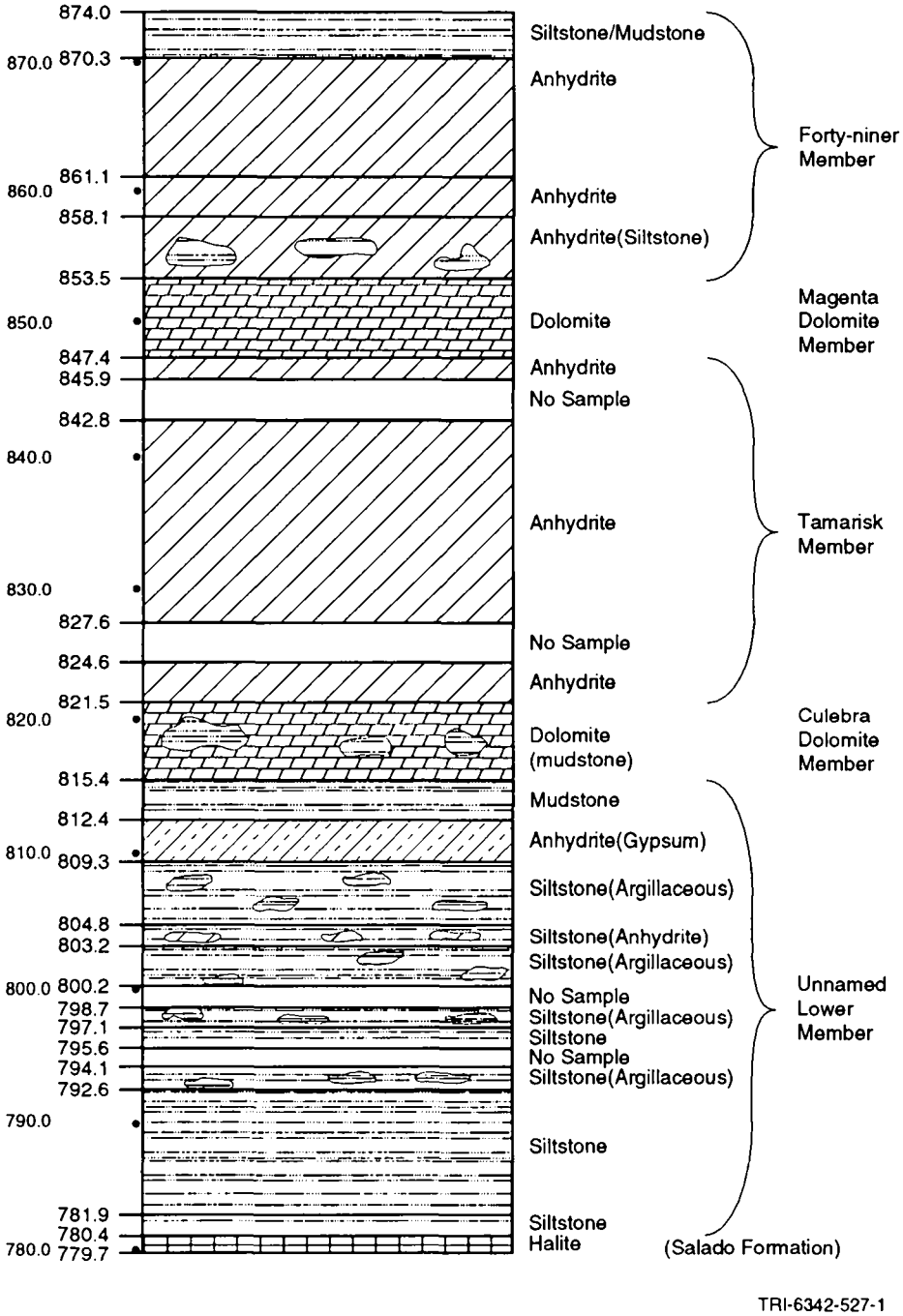

Figure 2.6-1. Detailed lithology of Rustler Formation at ERDA-9 (after SNL and U.S. Geological Survey, 1983).

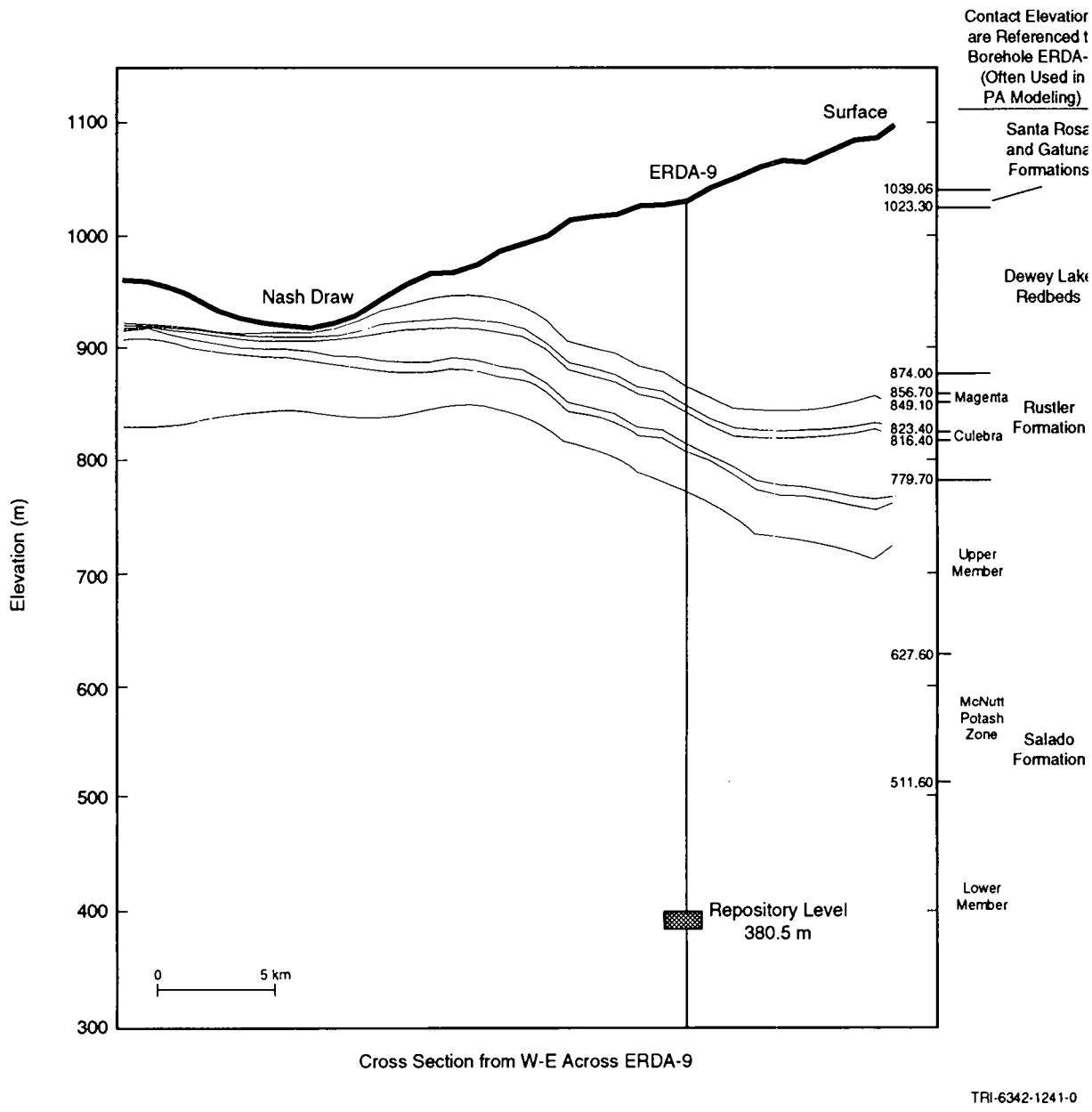

Figure 2.6-2. Interpolated geologic west-east cross section across the WIPP disposal system (after Mercer, 1983; Davies, 1989, Figure 53).

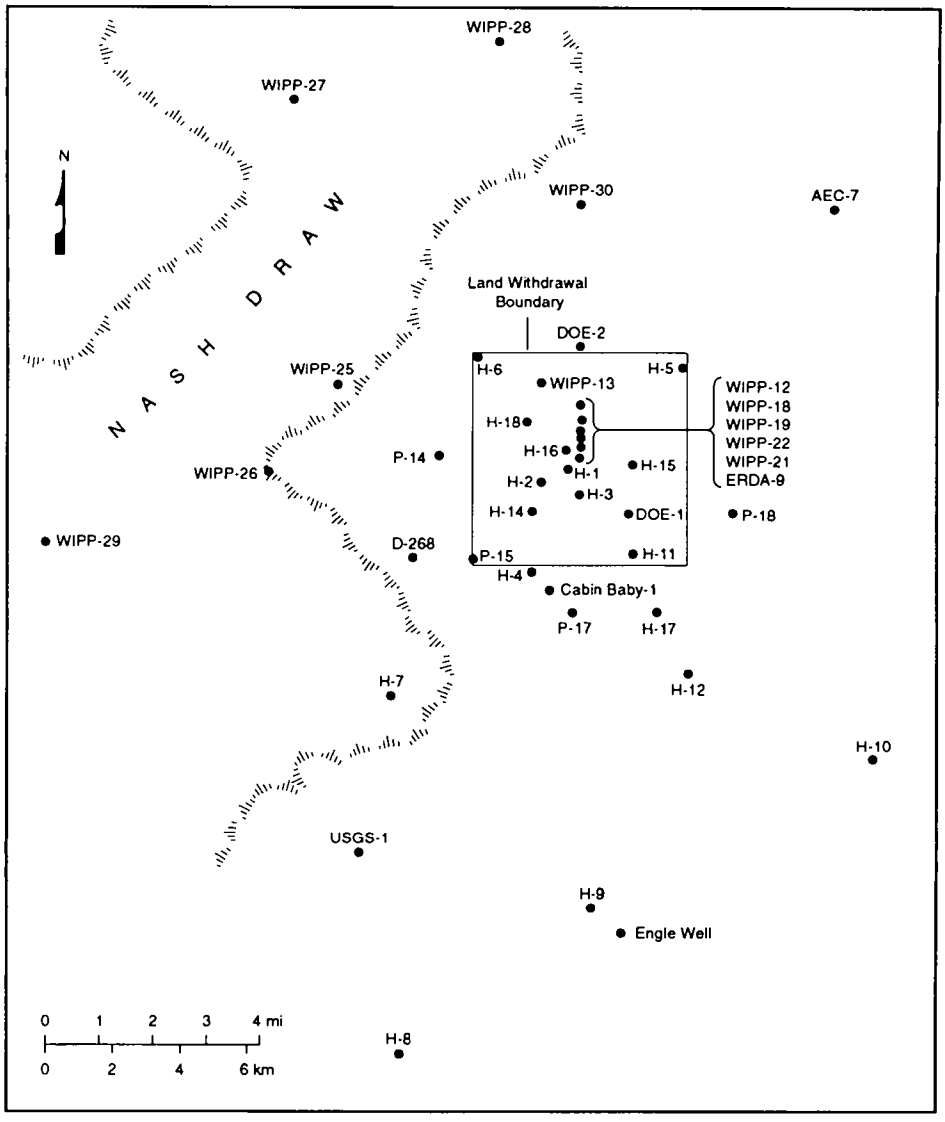

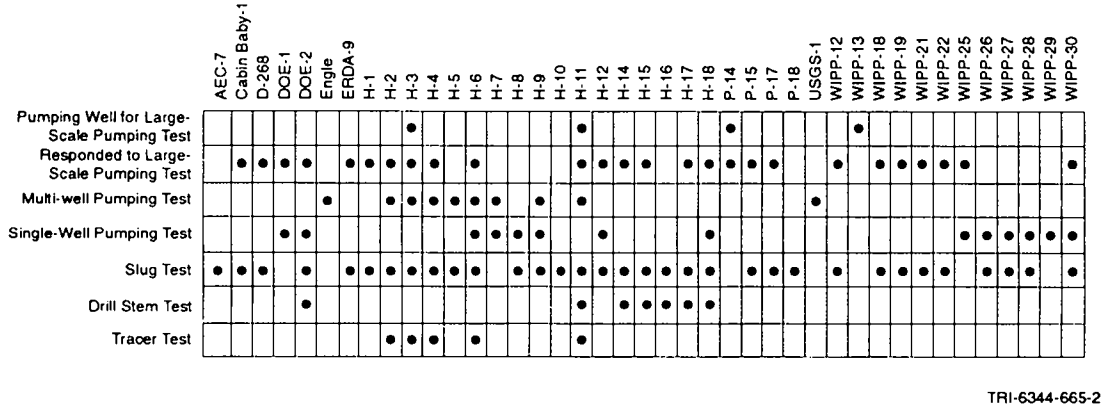

TRI-6344-665-2

Figure 2.6-3. Location of wells used to define hydrologic parameters for Culebra Dolomite.

Table 2.6-1. Summary of Parameter Values for Culebra Dolomite Member of Rustler Formation

Parameter[a]	Median	Range		Distribution Units	Type	Discussion and Sources in:
Density						
Dolomite, grain (ρ_g)	2.82×10^3	2.78×10^3	2.86×10^3	kg/m^3	Normal	WIPP PA Division, 1991, Vol. 3, Section 2.6.1
Clay, bulk (ρ_b)	2.5×10^3			kg/m^3	Constant	WIPP PA Division, 1991, Vol. 3, Section 2.6.1
Dispersivity[b]						
Longitudinal (α_L)	1×10^2	5×10^1	3×10^2	m	Constructed	WIPP PA Division, 1991, Vol. 3, Section 2.6.2
Ratio (α_L/α_T)	10	1	25	none	Constructed	WIPP PA Division, 1991, Vol. 3, Section 2.6.2
Fracture spacing (2B)	**4×10^{-1}**	**6×10^{-2}**	**8**	**m**	**Constructed**	**Section 2.6.2**
Clay filling fraction (b_c/b)	**0.0**	**0.0**	**0.5**	**none**	**Constructed**	**Section 2.6.1**
Log Partition coefficients						
Matrix						
Am	**-0.730**	**-4.0**	**2.0**	**log (m^3/kg)**	**Constructed**	**Section 2.6.4**
Cm	-0.730	-4.0	2.0	log (m^3/kg)	Constructed	Section 2.6.4
Np	**-1.32**	**-4.0**	**2.0**	**log (m^3/kg)**	**Constructed**	**Section 2.6.4**
Pb	-1.99	-4.0	0.0	log (m^3/kg)	Constructed	Section 2.6.4
Pu	**-0.584**	**-4.0**	**2.0**	**log (m^3/kg)**	**Constructed**	**Section 2.6.4**
Ra	**-2.00**	**-4.0**	**1.0**	**log (m^3/kg)**	**Constructed**	**Section 2.6.4**
Th	**-2.00**	**-4.0**	**0.0**	**log (m^3/kg)**	**Constructed**	**Section 2.6.4**
U	**-1.54**	**-4.0**	**0.0**	**log (m^3/kg)**	**Constructed**	**Section 2.6.4**
Clay						
Am	**1.97**	**-4.0**	**3.0**	**log (m^3/kg)**	**Constructed**	**Section 2.6.4**
Cm	1.97	-4.0	3.0	log (m^3/kg)	Constructed	Section 2.6.4
Np	**0.0**	**-4.0**	**3.0**	**log (m^3/kg)**	**Constructed**	**Section 2.6.4**
Pb	-1.00	-4.0	2.0	log (m^3/kg)	Constructed	Section 2.6.4
Pu	**2.31**	**-4.0**	**3.0**	**log (m^3/kg)**	**Constructed**	**Section 2.6.4**
Ra	**-1.47**	**-4.0**	**2.0**	**log (m^3/kg)**	**Constructed**	**Section 2.6.4**
Th	**-1.00**	**-4.0**	**1.0**	**log (m^3/kg)**	**Constructed**	**Section 2.6.4**
U	**-2.12**	**-4.0**	**0.0**	**log (m^3/kg)**	**Constructed**	**Section 2.6.4**
Porosity						
Fracture (ϕ_f)	**1×10^{-3}**	**1×10^{-4}**	**1×10^{-2}**	**none**	**Lognormal**	**Section 2.6.2**
Matrix (ϕ_m)	**1.39×10^{-1}**	**9.6×10^{-2}**	**2.08×10^{-1}**	**none**	**Data**	**Section 2.6.2**
Clay (ϕ_c)	**0.275**	**0.05**	**0.5**	**none**	**Uniform**	**Section 2.6.2**
Storage coefficient (S)	2×10^{-5}	5×10^{-6}	5×10^{-4}	none	Constructed	WIPP PA Division, 1991, Vol. 3, Section 2.6.5
Thickness (Δz)	7.7	5.5	1.13×10^1	m	Spatial	WIPP PA Division, 1991, Vol. 3, Section 2.6.6
Tortuosity (τ)						
Dolomite	1.2×10^{-1}	3×10^{-2}	3.3×10^{-1}	none	Data	WIPP PA Division, 1991, Vol. 3, Section 2.6.7
Clay	1.2×10^{-2}	3×10^{-3}	3.3×10^{-2}	none	Constructed	WIPP PA Division, 1991, Vol. 3, Section 2.6.7
Index for transmissivity fields	**0.5**	**0.0**	**1.0**	**none**	**Uniform**	**Section 2.6.3**

[a] Parameters in bold were sampled in the 1992 calculations.
[b] Not used in 1992; see Volume 2 of this report, Section 7.6, for a discussion of the 1992 model of hydrodynamic dispersion.

2.6.1 Fraction of Clay Filling in Fractures

Clay Filling Fraction*

Parameter:	**Clay filling fraction (b_c/b)**
Material:	Culebra Dolomite Member of Rustler Formation (Culebra, FClayFll)
Definition Units:	Dimensionless
Values:	Range: (0.0, 0.5) Median: 0.0
Distribution:	Constructed (see Discussion)
Correlation:	

Data Source(s):

Siegel, M. D. 1990. Appendix A: "Representation of Radionuclide Retardation in the Culebra Dolomite in Performance Assessment Calculations." *Data Used in Preliminary Performance Assessment of the Waste Isolation Pilot Plant (1990).* R. P. Rechard, H. Iuzzolino, and J. S. Sandha. SAND89-2408. Albuquerque, NM: Sandia National Laboratories. A-43 through A-62. (Investigator Judgment)

Novak, C. F., F. Gelbard, and H. W. Papenguth. 1992. "Parameter Recommendations for Porosity and Thickness of Clay Fracture Linings for the 1992 WIPP Performance Assessment Calculations" (see Appendix A, pp. A-125 through A-131). (Investigator Judgment)

Usage:

Mathematical model:

Solute transport in Culebra, Section 1.4.6, this volume.

Equation 1.4.6-3 and text following that equation (see Figure 1.4-4).

Computational models:

SECO/TP
STAFF2D (1991)

Ranking in Past Sensitivity Analyses:

40 CFR 191	Not tested
40 CFR 268	Not tested
NEPA	Not tested
Other	Not tested

*Key to Parameter Sheets is provided in Section 1.2.8.

Discussion:

Within fractures of the Culebra Dolomite Member, gypsum and corrensite (alternating layers of chlorite and smectite) are observed. To evaluate the retardation of radionuclides within the fractures (caused by interaction with this material lining the fractures), the fraction of lining material (b_c/b) is needed, where $2b_c$ is the total thickness of clays and 2b is fracture aperture. At present, data are not available to estimate the true range or distribution of b_c/b in the Culebra. Siegel (1990) recommended a normal distribution with a maximum of 0.9 and a minimum of 0.1. Current PA calculations have adopted the recommendations of Novak et al. (July 20, 1992, Memo in Appendix A) who note that clays do not invariably occur in all fractures, and that the absence of clays should be accounted for by a cdf of the form

$$\Pr\left\{\frac{bc}{b} \le x\right\} = \begin{cases} 0.5U(x)+x & \text{if } 0 \le x \le 0.5 \\ 1 & \text{if } 0.5 < x \end{cases},$$

where U(x) is the unit step function. This distribution is plotted on Figure 2.6-4. Sampling from the distribution will give zero clay-layer thickness 50% of the time, and non-zero clay layer thickness 50% of the time.

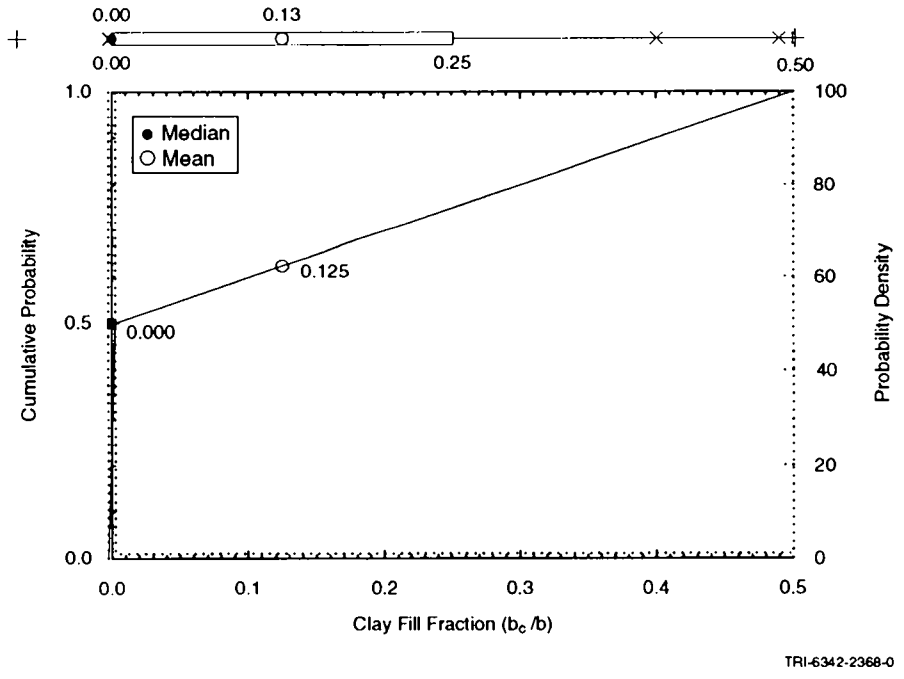

Figure 2.6-4. Estimated distribution for clay filling fraction, Culebra Dolomite Member.

2.6.2 Porosity

Fracture Porosity*

Parameter: **Fracture porosity (ϕ_f)**
Material: Culebra Dolomite Member of Rustler Formation (Culebra, FPore)

Definition Units: Dimensionless

Values: Range: (1×10^{-4}, 1×10^{-2}) Median: 1×10^{-3}

Distribution: Lognormal
Correlation:

Data Source(s): Lappin, A. R., R. L. Hunter, D. P. Garber, and P. B. Davies, eds. 1989. *Systems Analysis, Long-Term Radionuclide Transport, and Dose Assessments, Waste Isolation Pilot Plant (WIPP), Southeastern New Mexico; March 1989.* SAND89-0462. Albuquerque, NM: Sandia National Laboratories. (Table 1-2; Table E-6) (Investigator Judgment)

Usage:

Mathematical model:
Solute transport in Culebra, Section 1.4.6, this volume.

Equation 1.4.6-3 and text following that equation.

Computational models:
SECO/TP
STAFF2D (1991)

Ranking in Past Sensitivity Analyses:

40 CFR 191	High
40 CFR 268	Not tested
NEPA	Not tested
Other	Not tested

*Key to Parameter Sheets is provided in Section 1.2.8.

Discussion:

The fracture porosities interpreted from the tracer tests at the H-3 and H-11 hydropads are 2×10^{-3} (Kelley and Pickens, 1986) and 1×10^{-3}, respectively.

Both H-3 and H-11 lie near the expected transport pathway. The average value rounded to one significant figure was selected as the median and used for PA calculations. Similar to Lappin et al. (1989), the PA Department set the minimum and maximum one order of magnitude to either side of this median.

Figure 2.6-5 shows the estimated distribution for the fracture porosity.

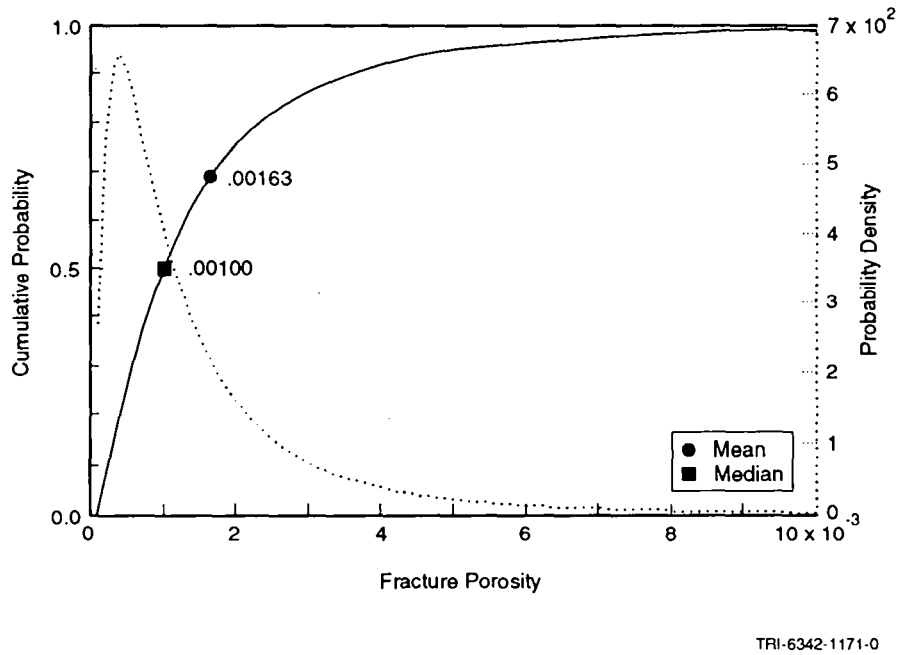

Figure 2.6-5. Estimated distribution for fracture porosity, Culebra Dolomite Member.

Clay Porosity*

Parameter: Clay porosity (ϕ_c)
Material: Clays lining fractures of Culebra Dolomite Member of Rustler Fm. (Culebra, PoreClay)

Definition, Units: Dimensionless

Values: Range: (0.05, 0.5) Median: 0.275

Distribution: Uniform
Correlation:

Data Source(s): The 1992 distribution of clay porosity is based on recommendations of the authors of the following memo:

Novak, C.F., F. Gelbard, and H.W. Papenguth. 1992. "Parameter Recommendations for Porosity and Thickness of Clay Fracture Linings for the 1992 WIPP Performance Assessment Calculations" (see Appendix A, pp. A-125 through A-131). (Investigator Judgment based on non-WIPP literature)

Usage:

Mathematical model:

Solute transport in Culebra, Section 1.4-6, this volume.

Equation 1.4.6-6 (also see Figure 1.4-4).

Computational models:

SECO/TP
STAFF2D (1991)

Ranking in Past Sensitivity Analyses:

40 CFR 191	Not tested
40 CFR 268	Not tested
NEPA	Not tested
Other	Not tested

*Key to Parameter Sheets is provided in Section 1.2.8.

Matrix Porosity*

Parameter: **Matrix porosity (ϕ_m)**
Material: Matrix of Culebra Dolomite Member of Rustler Formation (Culebra, Porosity)

Definition Units: Dimensionless

Values: Range: (0.095, 0.252) Median: 0.145

Distribution: Data
Correlation:

Data Source(s):

Kelley, V. A., and G. J. Saulnier, Jr. 1990. *Core Analyses for Selected Samples from the Culebra Dolomite at the Waste Isolation Pilot Plant Site.* SAND90-7011. Albuquerque, NM: Sandia National Laboratories. (Table 4.4) (WIPP Observational Data)

Lappin, A. R., R. L. Hunter, D. P. Garber, and P. B. Davies, eds. 1989. *Systems Analysis, Long-Term Radionuclide Transport, and Dose Assessments, Waste Isolation Pilot Plant (WIPP), Southeastern New Mexico; March 1989.* SAND89-0462. Albuquerque, NM: Sandia National Laboratories. (Table E-8) (Investigator Judgment)

Usage:

Mathematical model:

Solute transport in Culebra, Section 1.4-6 of this volume.

Equation 1.4.6-6 (also see Figure 1.4-4).

Computational models:

SECO/TP
STAFF2D (1991)

Ranking in Past Sensitivity Analyses:

40 CFR 191	Medium
40 CFR 268	Not tested
NEPA	Not tested
Other	Not tested

*Key to Parameter Sheets is provided in Section 1.2.8.

Discussion:

Matrix porosity has been evaluated by the Boyles' law technique using helium or air on 79 samples taken from the intact portion of core from 20 borehole or hydropad locations near the WIPP and also by water-resaturation for 30 of the samples. The agreement between the two techniques was excellent with an r^2 of 0.99 (Kelley and Saulnier, 1990, p. 4-7). From the Boyles' law technique, an average porosity for the 20 wells of 0.139 was obtained, with a range of 0.096 to 0.208 (Kelley and Saulnier, 1990, Table 4.4). (Lappin et al. [1989, Table E-8] report an average of 0.153 with a range of 0.028 and 0.303 assuming each of the 79 measurements is independent.) For many of the wells, a large amount of core was lost in porous (vuggy) and/or fractured portions of the Culebra Dolomite Member. Thus only intact matrix porosity is reported here.

Figure 2.6-6 shows the empirical distribution function for porosity of the Culebra Dolomite member.

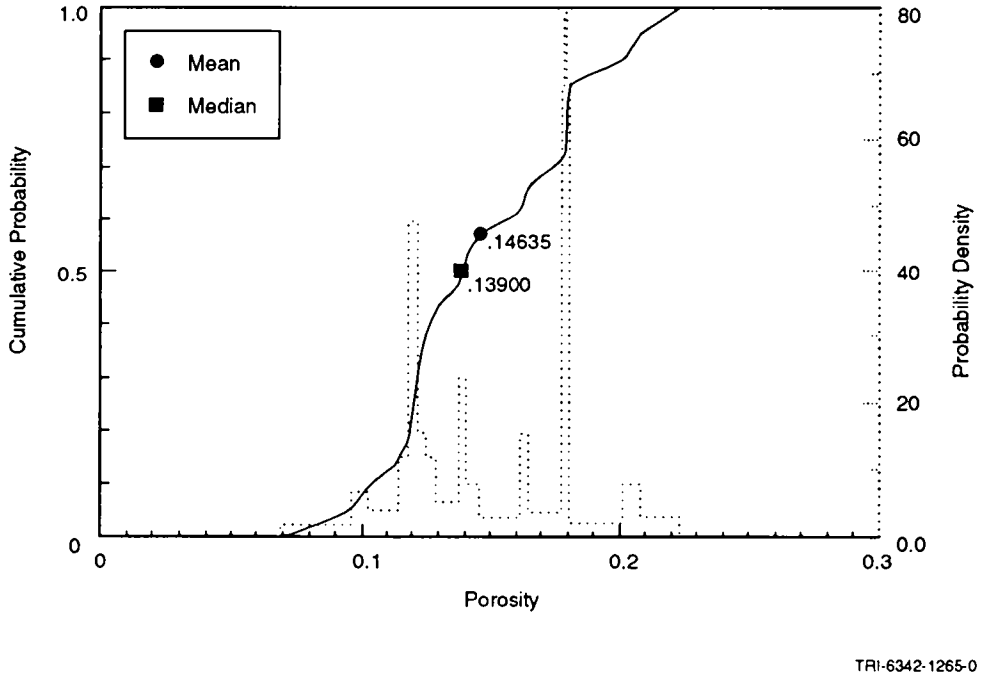

Figure 2.6-6. Empirical distribution for intact matrix porosity of Culebra Dolomite Member assuming no spatial correlation.

Fracture Spacing*

Parameter: **Fracture spacing (2B)**
Material: Culebra Dolomite Member of Rustler Formation (Culebra, FrctrSp)

DefinitionUnits: m

Values: Range: (6×10^{-2}, 8) Median: 4×10^{-1}

Distribution: Constructed
Correlation:

Data Source(s): Beauheim, R. L., T. F. Corbet, P. B. Davies, and J. F. Pickens. 1991b. Appendix A: "Recommendations for the 1991 Performance Assessment Calculations on Parameter Uncertainty and Model Implementation for Culebra Transport Under Undisturbed and Brine-Reservoir-Breach Conditions," *Preliminary Comparison with 40 CFR Part 191, Subpart B for the Waste Isolation Pilot Plant, December 1991. Volume 3: Reference Data.* WIPP Performance Assessment Division. Eds. R. P. Rechard, A. C. Peterson, J. D. Schreiber, H. J. Iuzzolino, M. S. Tierney, and J. S. Sandha. SAND91-0893/3. Albuquerque, NM: Sandia National Laboratories. A-7 through A-18. (Investigator Judgment)

Usage:

Mathematical model:

Solute transport in Culebra, Section 1.4-6, this volume.

Equations 1.4.6-3 and 1.4.6-10, establishes no-diffusion boundary (see also Figure 1.4-4).

Computational models:

SECO/TP
STAFF2D

Ranking in Past Sensitivity Analyses:

40 CFR 191	High
40 CFR 268	Not tested
NEPA	Not tested
Other	Not tested

*Key to Parameter Sheets is provided in Section 1.2.8.

Discussion:

Both horizontal and vertical fracture sets have been observed in core samples, shaft excavations, and outcrops (however, PA models use only horizontal fracture sets). A fracture spacing varying between 0.23 and 1.2 m (0.75 and 3.9 ft) has been interpreted for two travel paths at the H-3 borehole (Kelley and Pickens, 1986). Preliminary evaluation of the breakthrough curves for the H-6 borehole tracer test suggests a fracture spacing between 0.056 and 0.44 m (0.18 and 1.44 ft), and the H-11 borehole tracer test suggests a fracture spacing between 0.11 and 0.32 m (0.36 and 1.05 ft) (Beauheim et al., 1991b). From these data, Beauheim et al. (1991b) suggested a minimum of 0.06 m (0.2 ft) and a maximum equivalent to the assumed uniform thickness of the Culebra (8 m [26.2 ft]). Finally, the average fracture spacing at the three wells (H-3, H-6, and H-11) is 0.4 m (1.3 ft); the PA Department has chosen 0.4 m as median fracture spacing.

In the 1991 sensitivity analyses, fracture spacing in the Culebra Dolomite proved to be a moderate to highly sensitive parameter in determining releases of most radionuclides to the accessible environment. This sensitivity was independent of gas generation in the repository but (of course) was dependent on whether or not a dual-porosity transport model was used in the analysis.

The constructed distribution of Culebra fracture spacing is shown on Figure 2.6-7.

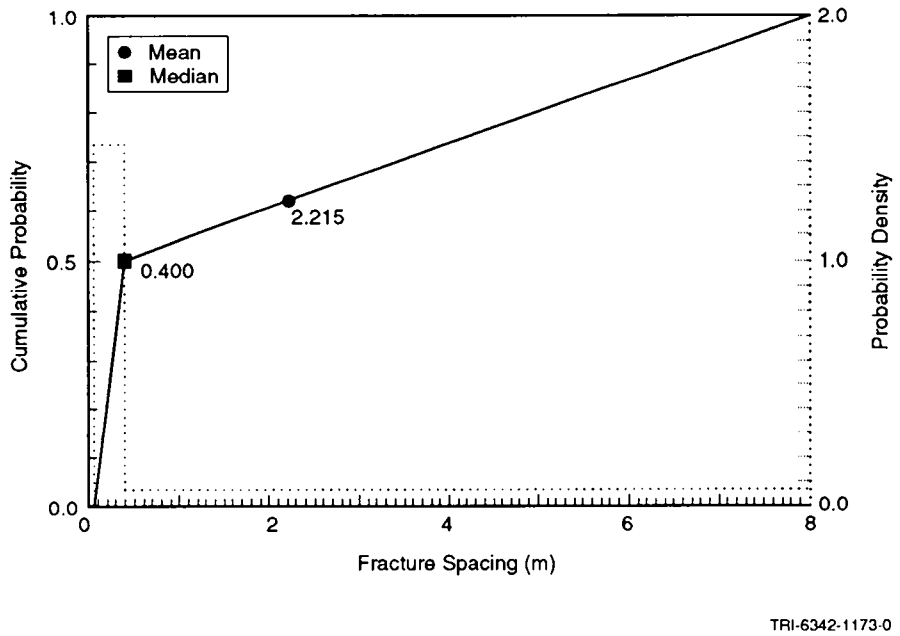

Figure 2.6-7. Constructed distribution for Culebra fracture spacing.

2.6.3 Transmissivity

Index for Culebra Transmissivity Fields*

Parameter: **Index for Culebra transmissivity fields**
Material: Culebra Dolomite Member of Rustler Formation (Global, IdxTrans)

Definition Units: Dimensionless

Values: Range: (0, 1) Median: 0.5

Distribution: Uniform
Correlation:

Data Source(s): See Discussion.

Usage:

Mathematical model:

Fluid flow in Culebra, Section 1.4.5, this volume.

Equation: This parameter labels realizations of transmissivity fields T(x,y) that appear in Eq. 1.4.5-2; see Discussion.

Computational models:

SECO2D

Ranking in Past Sensitivity Analyses:

40 CFR 191	Medium
40 CFR 268	Not tested
NEPA	Not tested
Other	Not tested

*Key to Parameter Sheets is provided in Section 1.2.8.

Discussion of Transmissivity Fields:

The 1990 WIPP Performance Assessment used a simple zonal approach for including uncertainty in the transmissivity *(T)* field within the Culebra Dolomite Member of the Rustler Formation. The zonal method divides the regional and local computational domains into geographic regions; 8, 13, and 15 regions have been used for different analyses reported in Marietta et al. (1989) and Bertram-Howery et al. (1990). In each region, a distribution was constructed using transmissivity measurements from available wells (Tables 2.6-2 and 2.6-3). This empirical distribution was sampled and one constant value used for the transmissivity in each zone. Each zone was sampled independently, so a single simulation used 8 (or 13 or 15) transmissivity values to represent the regional *T* field. Some simulations used distributions constructed from pilot point values (LaVenue et al., 1990) at locations assigned during calibration in addition to actual measurements at well locations.

The early (1990) approach was improved in 1991 in two ways:

- The reason for varying transmissivity over geographic zones is to include spatial variability in the *T* field. Correlations exist in the *T* field over distances greater than five kilometers; thus, assuming that the 8 (or 13 or 15) zones are independent during sampling is only a first approximation. Spatial dependence has been included over the whole model domain.
- The *T* fields generated by the simple zonal approach directly used transmissivity measurements whereas other information was included only indirectly through pilot point values. Many other data are available, and it has been possible to incorporate some of these data directly, e.g., hydraulic head measurements (Table 2.6-4) and geologic information.

Transmissivities display a variability in space that can be characterized using measured data, e.g., pump tests, by geostatistical analyses. This spatial variability was found to be stationary in the mean (LaVenue et al., 1990), but intrinsic in the second moment (IRF = 0) with a linear variogram without nugget effect (i.e., locally described by a constant with random perturbations that increase in variance with distance). Several techniques are available to generate random fields having this spatial structure: turning bands, inversion of the full covariance matrix, and spectral methods. Many such realizations could be generated and each realization could be used as one input for a system simulation. Each realization would than have the correct spatial structure of the true field, and would satisfy the first objective above.

However, these realizations would not be fully coherent with the actual measurements, and would overestimate the uncertainty in the *T* field. Making realizations of random fields coherent with measured information is called "conditioning". For WIPP PA, conditioning can be performed on at least four types of information:

- Measured *T* values at the wells.
- Measured or estimated head values at the wells in pre-excavation steady-state conditions.
- Measured head values during various transient hydraulic tests (e.g., long-term pump tests, shaft excavation).
- Indirect geologic data that can be correlated with transmissivity (such as overburden thickness, or presence of evaporites in the Culebra or Rustler).

Of the half-dozen methods available for conditioning on head data, two have been used to date in WIPP PA work. In 1991, random fields conditioned on *T* measurements at well locations and on values assigned during manual calibration were assigned to pilot point locations where no measurements were available (LaVenue et al., 1990). Forty-one measured-*T* and 41 pilot-point values are available. The pilot point values were assigned to insure coherence of the calibrated *T* field with the measured head data (both steady-state and transient conditions) so conditioning on head data is indirectly included. An advantage of this method is that it does not require any assumption on the acceptable range of variability of *T* (Var(*T*)). Many methods require that the Var(ln*T*)>1, and in the Culebra the Var(ln*T*) is about 3.5. This first method also allows using a variable-density fluid-flow model which may be important in the Culebra (Davies, 1989). Other methods are linear, but can only accommodate constant-density fluid-flow

Table 2.6-2. Logarithms of Selected Transmissivity Measurements in Culebra Dolomite Member (after Cauffman et al., 1990, Table C.1)

Well ID	Median	Low Range	High Range
AEC7	-6.5535	-7.7185	-5.3885
CABIN1	-6.5213	-7.6863	-5.3563
D268	-5.6897	-6.8547	-4.5247
DOE1	-4.4271	-5.0096	-3.8466
DOE2	-4.0191	-4.6016	-3.4366
ENGLE	-4.3350	-4.9175	-3.7525
ERDA9	-6.2964	-7.4614	-5.1314
H1	-6.0290	-7.1940	-4.8640
H10B	-7.1234	-8.2884	-5.9584
H11B1	-4.5057	-5.0882	-3.9232
H12	-6.7132	-7.8782	-5.5482
H14	-6.4842	-7.6492	-5.3192
H15	-6.3804	-7.5454	-5.2154
H16	-6.1149	-7.2799	-4.9499
H17	-6.6361	-7.8011	-5.4471
H18	-5.7775	-6.3600	-5.1950
H2B1	-6.2005	-6.7830	-5.6180
H3	-5.6089	-6.1914	-5.0264
H4B	-5.9960	-6.5785	-5.4135
H5B	-7.0115	-7.5940	-6.4290
H6B	-4.4500	-5.0325	-3.8675
H7B1	-2.8125	-3.3950	-2.2300
H8B	-5.0547	-5.6372	-4.4722
H9B	-3.9019	-4.4844	-3.3194
USGS1	-3.2584	-3.8409	-2.6759
WIPP12	-6.9685	-8.1355	-5.8035
WIPP13	-4.1296	-5.2946	-2.9646
WIPP18	-6.4913	-7.6563	-5.3263
WIPP19	-6.1903	-7.3553	-5.0253
WIPP21	-6.5705	-7.7355	-5.4055
WIPP22	-6.4003	-7.5653	-5.2353
WIPP25	-3.5412	-4.1237	-2.9587
WIPP26	-2.9136	-3.4961	-2.3311
WIPP27	-3.3692	-3.9517	-2.7867
WIPP28	-4.6839	-5.2664	-4.1014
WIPP29	-2.9685	-3.5510	-2.3860
WIPP30	-6.6023	-7.7673	-5.4373
P14	-3.5571	-4.5124	-2.6018
P15	-7.0354	-8.2004	-5.8704
P17	-5.9685	-7.1335	-4.8035
P18	-1.0123×10^{1}	-1.1288×10^{1}	-8.9584

Table 2.6-3. Logarithms of Transmissivity of Calibrating Points (Pilot Points) for Culebra Dolomite Member (after Davies and LaVenue, 1990b)

Well ID	Median	Low Range	High Range
PP1	-2.0700	-4.4233	2.833×10^{-1}
PP2	-2.2500	-4.5334	3.340×10^{-2}
PP3	-2.3200	-4.6267	-1.330×10^{-2}
PP4	-3.6200	-5.3442	-1.8958
PP5	-3.5800	-5.2576	-1.9024
PP6	-6.0200	-7.7675	-4.2725
PP7	-6.4200	-8.0044	-4.5656
PP8	-3.4100	-4.8779	-1.9421
PP9	-2.7100	-3.8913	-1.5217
PP11	-7.7200	-9.1413	-6.2987
PP12	-8.0800	-9.0353	-7.1247
PP13	-5.6400	-6.5953	-4.6847
PP14	-8.3400	-9.7846	-6.8954
PP15	-6.4900	-7.7482	-5.2318
PP16	-5.1300	-6.5280	-3.7320
PP17	-6.6000	-8.1378	-5.0622
PP18	-2.6300	-4.5173	-7.427×10^{-1}
PP19	-2.8600	-4.7939	-9.261×10^{-1}
PP20a	-2.9400	-4.8972	-9.828×10^{-1}
PP21a	-3.0000	-4.8407	-1.1593
PP23	-3.8500	-5.1548	-2.5452
PP24	-3.5000	-4.2689	-2.7311
PP25	-6.0000	-7.0718	-4.9282
PP26	-5.5000	-6.3388	-4.6612
PP27	-4.2500	-5.3684	-3.1316
PP28	-3.5000	-4.7582	-2.2418
PP29	-3.2500	-4.3451	-2.1549
PP30	-6.1600	-7.3250	-4.9950
PP31	-5.8700	-7.0350	-4.7050
PP32	-5.0000	-5.7223	-4.2777
PP34	-3.5900	-4.5453	-2.6347
PP35	-2.6700	-3.6253	-1.7147
PP36	-5.1700	-6.0787	-4.2613
PP37	-4.3100	-6.0342	-2.5858
PP38	-3.9000	-5.3446	-2.4554
PP39	-3.9000	-5.3446	-2.4554
PP40	-5.9300	-6.8853	-4.9747
PP41	-4.0000	-4.9553	-3.0447
PP42	-3.5000	-4.5951	-2.4049
PP43	-5.0000	-5.9553	-4.0447
PP44	-5.0000	-5.9553	-4.0447

Table 2.6-4. Summary of Selected Steady-State Freshwater Head Measurements in Culebra Dolomite Member (after Cauffman et al., 1990, Table 6.2)

Well ID	Median (m)	Low Range (m)	High Range (m)
AEC7	9.3200×10^2	9.3014×10^2	9.3386×10^2
CABIN1	9.1120×10^2	9.0980×10^2	9.1260×10^2
D268	9.1520×10^2	9.1462×10^2	9.1578×10^2
DOE1	9.1390×10^2	9.0831×10^2	9.1949×10^2
DOE2	9.3530×10^2	9.3181×10^2	9.3880×10^2
H1	9.2330×10^2	9.1860×10^2	9.2796×10^2
H10B	9.2140×10^2	9.1627×10^2	9.2653×10^2
H11B1	9.1280×10^2	9.1000×10^2	9.1560×10^2
H12	9.1360×10^2	9.1080×10^2	9.1640×10^2
H14	9.1550×10^2	9.1457×10^2	9.1643×10^2
H15	9.1560×10^2	9.1234×10^2	9.1886×10^2
H17	9.1100×10^2	9.0890×10^2	9.1310×10^2
H18	9.3190×10^2	9.2887×10^2	9.3493×10^2
H2C	9.2400×10^2	9.2167×10^2	9.2633×10^2
H3B1	9.1710×10^2	9.1267×10^2	9.2153×10^2
H4B	9.1280×10^2	9.1140×10^2	9.1420×10^2
H5B	9.3400×10^2	9.3074×10^2	9.3726×10^2
H6B	9.3260×10^2	9.3027×10^2	9.3493×10^2
H7B1	9.1270×10^2	9.1200×10^2	9.1340×10^2
H8B	9.1240×10^2	9.1147×10^2	9.1333×10^2
H9B	9.0820×10^2	9.0680×10^2	9.0960×10^2
P14	9.2690×10^2	9.2480×10^2	9.2900×10^2
P15	9.1680×10^2	9.1494×10^2	9.1866×10^2
P17	9.1160×10^2	9.0997×10^2	9.1323×10^2
USGS1	9.0980×10^2	9.0922×10^2	9.1038×10^2
USGS4	9.0970×10^2	9.0947×10^2	9.0993×10^2
USGS8	9.1110×10^2	9.1087×10^2	9.1133×10^2
WIPP12	9.3310×10^2	9.3147×10^2	9.3473×10^2
WIPP13	9.3400×10^2	9.3120×10^2	9.3680×10^2
WIPP18	9.3000×10^2	9.2720×10^2	9.3280×10^2
WIPP25	9.2870×10^2	9.2637×10^2	9.3103×10^2
WIPP26	9.1940×10^2	9.1882×10^2	9.1998×10^2
WIPP27	9.3810×10^2	9.3647×10^2	9.3973×10^2
WIPP28	9.3700×10^2	9.3467×10^2	9.3933×10^2
WIPP29	9.0540×10^2	9.0482×10^2	9.0598×10^2
WIPP30	9.3510×10^2	9.3254×10^2	9.3766×10^2

models. A second advantage is computational efficiency because the Cholesky decomposition only needs to be performed once regardless of the number of simulations.

The approach in 1992 is an extension of the pilot point approach used for the calibration of the Culebra T field. This method generates random fields conditioned on T measurements, steady-state, and transient head data without restriction on Var(ln$T$) and with variable-density fluid-flow models.

In this method, random T fields conditioned only on the measured T values are first generated. These fields are further conditioned on the head data by calibrating them with the pilot point approach both on steady-state and transient data. The procedure has been automated to generate a large number of calibrated random fields. Order of pilot point selection and the uniqueness of the resulting T field were issues to be examined during operational tests and sensitivity analyses.

In 1992, application of the procedures described above produced 70 realizations of the transmissivity field in Culebra Dolomite (plots of these realizations are presented in Appendix C). These 70 realizations were then ordered by travel time to the accessible environment (3.5 km from center of repository area): each realization was converted to a flow field (assuming uniform Culebra thickness of 8 m and 16% effective porosity) and the travel time associated with that field was calculated with the program TRACKER. The 70 realizations were then ranked according to their associated travel times (Figure 2.6-8). Flow fields in the 1992 PA calculations were selected by sampling a uniform random variable on the interval (0,1), mapping this result onto the integers 1-70, and using the resulting integer to choose a flow field. Because the flow fields are considered to be equally likely, the rank of the sampled index value can be used as the index of the flow fields.

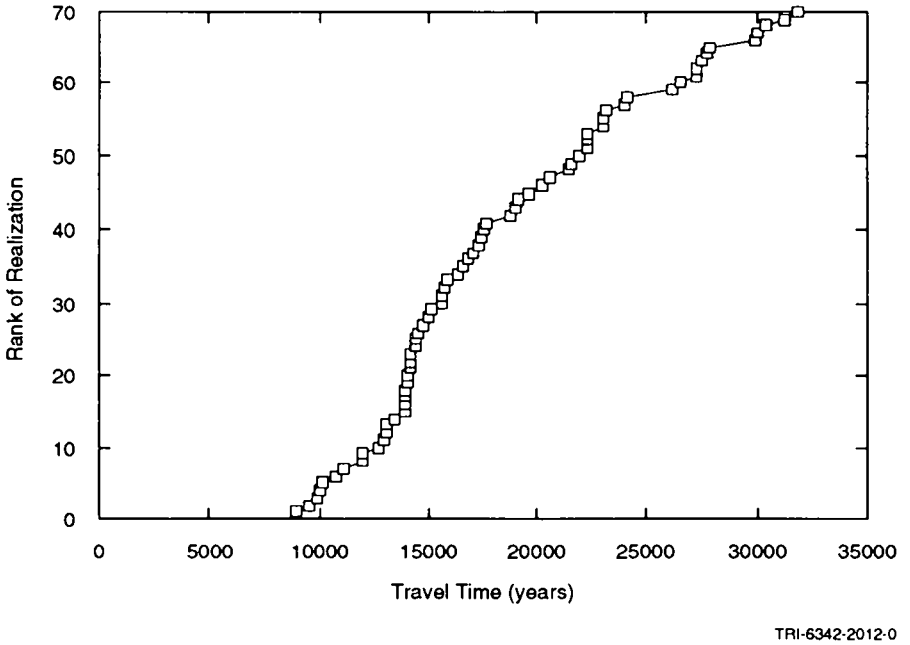

Figure 2.6-8. Empirical travel time distribution associated with the 70 realizations of Culebra transmissivity fields (see text).

2.6.4 Partition Coefficients and Retardations

A partitioning or distribution coefficient (K_d), which describes the intensity of sorption, is used to calculate the partitioning of species such as radionuclides between the groundwater and rock and, thereby, calculate the sorption capacity or retardation (R).

The logarithmic K_d distributions used in 1991 and 1992 are reported in Tables 2.6-5 and 2.6-6 and are considered to be realistic in light of available data; however, these distributions require a number of subjective assumptions that ongoing experiments may invalidate. The distributions were derived from an internal expert-judgment process regarding radionuclide retardation in the Culebra, which convened in April and May, 1991 (Trauth et al., 1992). The three Sandia experts involved were Robert G. Dosch (6212), Craig F. Novak (6119), and Malcolm D. Siegel (6115). The three experts participated in individual elicitation sessions for the purpose of developing probability distributions for the distribution coefficients for americium, curium, lead, neptunium, plutonium, radium, thorium, and uranium, for two sets of conditions. The first is the nature of the transport fluid: essentially Culebra or Salado brine. The second is whether the retardation takes place in the dolomite matrix or in the clay lining the fractures.

The K_d distributions that actually resulted from this panel are discussed in Section 2.6.10 of the WIPP PA Division, 1991, vol. 3. The distributions are derived from a combination of values from Dosch and Novak. The rationales behind Dosch' and Novak's values are briefly described below; a more thorough description of Novak's values is provided in Novak, 1991. The K_d distributions were converted to logarithmic form in 1992.

Dosch reviewed data from several experiments on distribution coefficients for various actinides in a variety of media. His own work (Lynch and Dosch, 1980) was included in his data set. He believed that even though some experiments were conducted using media different from the Culebra matrix and the Culebra clay, most of the data could not be discounted (personal communication from S. Hora, September 1991 regarding expert panel elicitation on May 1991). His justification for this was that experimental data directly applicable to the issue at hand were so scarce that no relevant data should be disregarded. In general, Dosch remarked that most of the experimental data deserved equal weight in any judgments about the behavior of actinides in the Culebra matrix and clay. Dosch declined to give any probability distributions for thorium and lead because he did not believe himself qualified to make enlightened assessments for those elements.

Novak examined available research that detailed the experimental measurement of K_ds using substrates and water compositions pertinent to transport in the WIPP system (Novak, 1992). He showed that (1) data are not available for all elements of interest, (2) almost no data exist for clay substrates in the Culebra, and (3) existing data may not be applicable to current human-intrusion scenarios. In this study (Novak, 1992), Novak also questioned the use of the K_d model for estimating radionuclide retardation in the Culebra.

Novak believes that the water composition called "Culebra H_2O" is the least dissimilar to Case One among available data for Case One, which assumed that water reaching the Culebra would not change the composition of Culebra water significantly, except for the presence of radionuclides. Brine A best represented Case Two, which assumed that water reaching the Culebra would not be diluted and a concentrated brine contaminated with radionuclides would flow through the Culebra. Within each case, K_d estimates were needed for radionuclide sorption on the matrix (i.e., the dolomitic Culebra substrates), and in the fractures (i.e., on clay materials lining fractures). Each type of water was used for both matrix and fractures. Thus, for Case One, data from "Culebra H_2O" studies were used to estimate K_d values where actual data were not available. Similarly, Brine A data were used to estimate K_ds for Case Two.

Novak offered K_ds of 0 m^3/kg for all cdfs because he thought it possible that any of the elements could be transported with the fluid velocity. Upper bounds represent Novak's opinions on maximum values for K_ds observable under human-intrusion scenarios (Novak, 1991). Novak chose different sets of fractiles for different radionuclides. These represent his best estimates resulting from his studies of existing data and literature.

Novak further states that values obtained through the expert elicitation process are subjective estimates only because of large uncertainties in water composition, mixing within the Culebra, and the questionable utility of the K_d

Table 2.6-5. Summary of 1992 Partition Coefficients of Radionuclides for Culebra Dolomite Member within Matrix Dominated by Culebra Brine.

Element	Median	Range		Units	Value of Additional Information
Am	-0.730	-4.0	2.0	$\log_{10}$ (m^3/kg)	High
Cm	-0.730	-4.0	2.0	$\log_{10}$ (m^3/kg)	Not tested
Np	-1.32	-4.0	2.0	$\log_{10}$ (m^3/kg)	High
Pb	-1.99	-4.0	0.0	$\log_{10}$ (m^3/kg)	Not tested
Pu	-0.584	-4.0	2.0	$\log_{10}$ (m^3/kg)	High
Ra	-2.00	-4.0	1.0	$\log_{10}$ (m^3/kg)	Not tested
Th	-2.00	-4.0	0.0	$\log_{10}$ (m^3/kg)	High
U	-1.54	-4.0	0.0	$\log_{10}$ (m^3/kg)	High

Table 2.6-6. Summary of 1992 Partition Coefficients of Radionuclides for Culebra Dolomite Member within Fracture Clays Dominated by Culebra Brine.

Element	Median	Range		Units	Value of Additional Information
Am	1.97	-4.0	3.0	$\log_{10}$ (m^3/kg)	High
Cm	1.97	-4.0	3.0	$\log_{10}$ (m^3/kg)	Not tested
Np	0.00	-4.0	3.0	$\log_{10}$ (m^3/kg)	High
Pb	-1.00	-4.0	2.0	$\log_{10}$ (m^3/kg)	Not tested
Pu	2.31	-4.0	3.0	$\log_{10}$ (m^3/kg)	High
Ra	-1.47	-4.0	2.0	$\log_{10}$ (m^3/kg)	Not tested
Th	-1.00	-4.0	1.0	$\log_{10}$ (m^3/kg)	High
U	-2.12	-4.0	0.0	$\log_{10}$ (m^3/kg)	High

model. Finally, Novak argues that these cdfs for K_ds do not substitute for actual data, and believes that additional study is needed to quantify the potential for radionuclide retardation in the Culebra (Novak, 1991).

In the 1991 series of sensitivity analyses (Helton et al., 1992), the partition coefficients for Am, Np, Pu, Th and U were highly sensitive parameters in the determination of radionuclide releases to the accessible environment; the clay partition coefficients for Am, Pu, and U were the most sensitive among the ten parameters of this kind that were tested.

Partition Coefficients in Matrix of Culebra Dolomite*

Parameter: **Partition coefficients (K_d) for Am, Cm, Np, Pb, Pu, Ra, Th, U**
Material: Matrix of Culebra Dolomite Member of Rustler Formation Culebra Brine

Definition, Units: Log (m^3/kg)

Values: See Table 2.6-5.

Distribution: Constructed (see Figures 2.6-9[a] through 2.6-9[h])
Correlation:

Data Source(s): Trauth, K. M., S. C. Hora, R. P. Rechard, and D. R. Anderson. 1992. *The Use of Expert Judgment to Quantify Uncertainty in Solubility and Sorption Parameters for Waste Isolation Pilot Plant Performance Assessment.* SAND92-0479. Albuquerque, NM: Sandia National Laboratories. (Expert Panel Judgment)

Usage:

Mathematical model:
Solute Transport in Culebra, Section 1.4.6, this volume.

Equation 1.4.6-8.

Computational models:
SECO/TP
STAFF2D

Ranking in Past Sensitivity Analyses:

40 CFR 191	High for Am, Np, Pu, Th, U; others not tested
40 CFR 268	Not tested
NEPA	Not tested
Other	Not tested

*Key to Parameter Sheets is provided in Section 1.2.8.

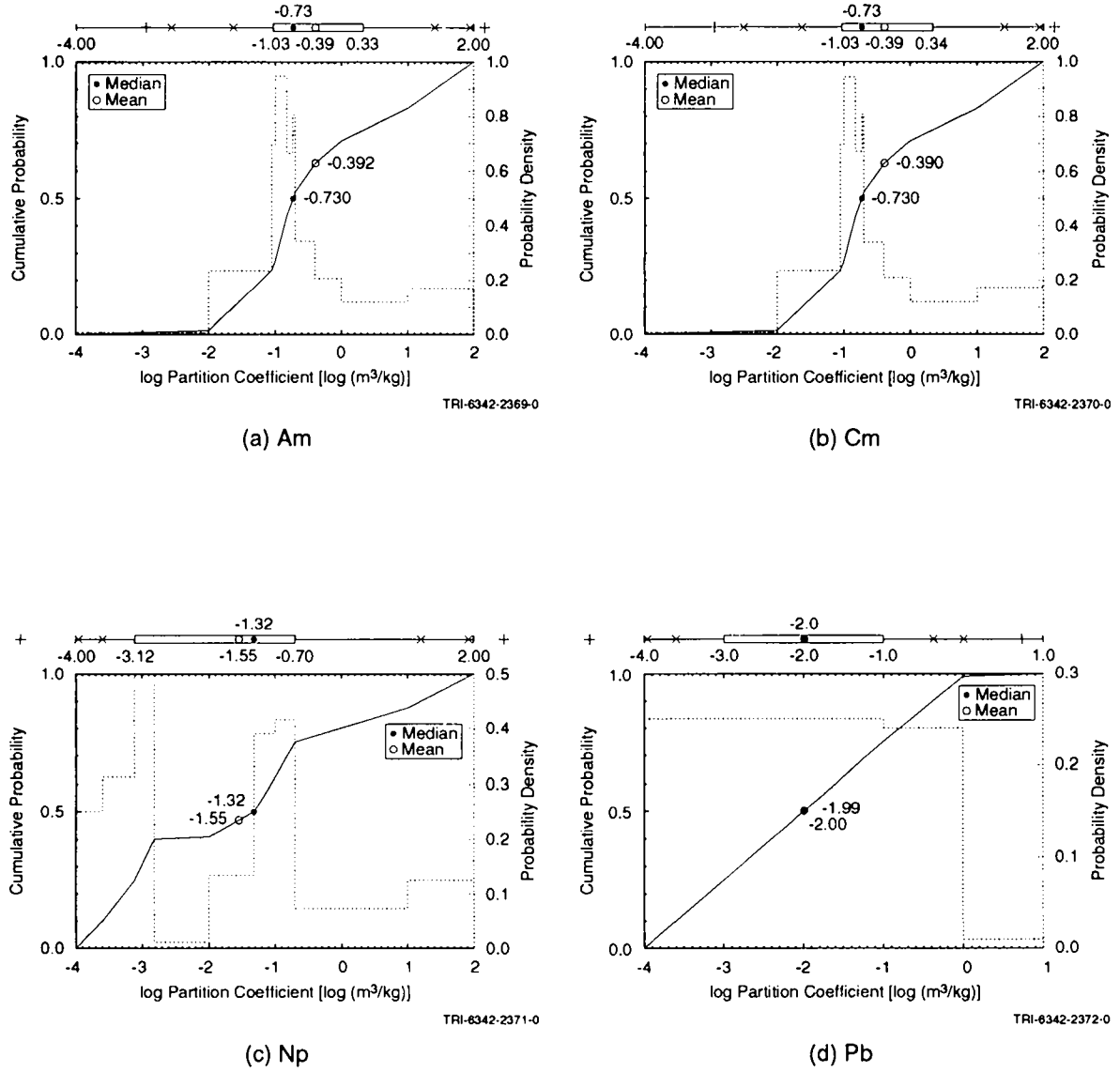

Figure 2.6-9. Constructed distribution for partition coefficient in matrix for (a) americium (Am), (b) curium (Cm), (c) neptunium (Np), (d) lead (Pb), (e) plutonium (Pu), (f) radium (Ra), (g) thorium (Th), and (h) uranium (U).

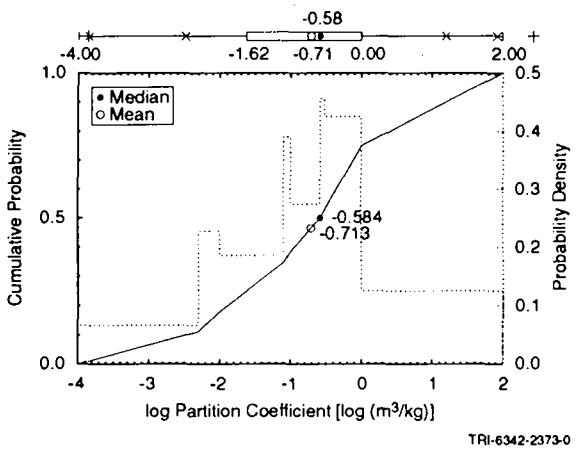

(e) Pu

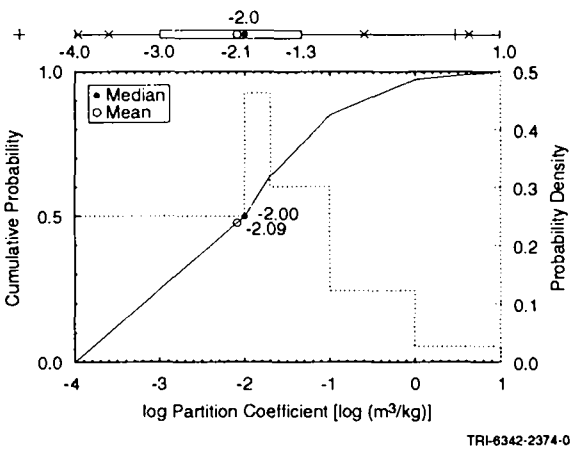

(f) Ra

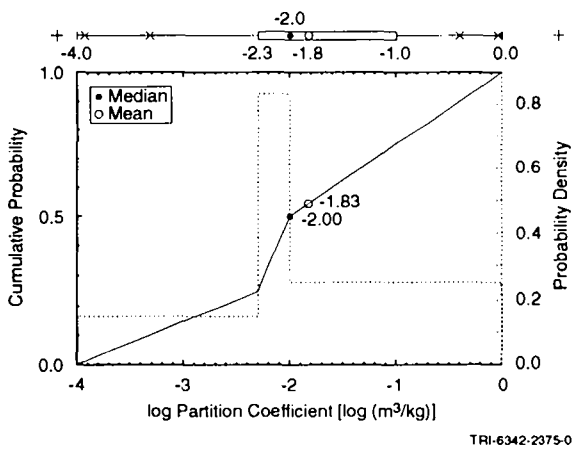

(g) Th

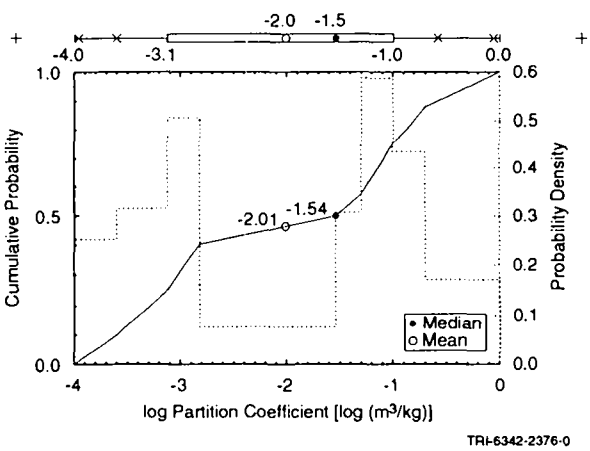

(h) U

Figure 2.6-9. Constructed distribution for partition coefficient in matrix for (a) americium (Am), (b) curium (Cm), (c) neptunium (Np), (d) lead (Pb), (e) plutonium (Pu), (f) radium (Ra), (g) thorium (Th), and (h) uranium (U) (continued).

Partition Coefficients in Clay Lining Fractures of Culebra Dolomite*

Parameter: **Partition coefficients (K_d) for Am, Cm, Np, Pb, Pu, Ra, Th, U**
Material: Clay lining fractures of Culebra Dolomite Member of Rustler Formation Culebra brine

Definition, Units: Log (m^3/kg)

Values: See Table 2.6-6.

Distribution: Constructed (see Figures 2.6-10 [a] through 2.6-10[h])
Correlation:

Data Source(s): Trauth, K. M., S. C. Hora, R. P. Rechard, and D. R. Anderson. 1992. *The Use of Expert Judgment to Quantify Uncertainty in Solubility and Sorption Parameters for Waste Isolation Pilot Plant Performance Assessment.* SAND92-0479. Albuquerque, NM: Sandia National Laboratories. (Expert Panel Judgment)

Usage:

Mathematical model:
Solute Transport in Culebra, Section 1.4.6, this volume.

Equation 1.4.6-8.

Computational models:
SECO/TP
STAFF2D

Ranking in Past Sensitivity Analyses:

40 CFR 191	High for Am, Np, Pu, Th, U; others not tested
40 CFR 268	Not tested
NEPA	Not tested
Other	Not tested

*Key to Parameter Sheets is provided in Section 1.2.8.

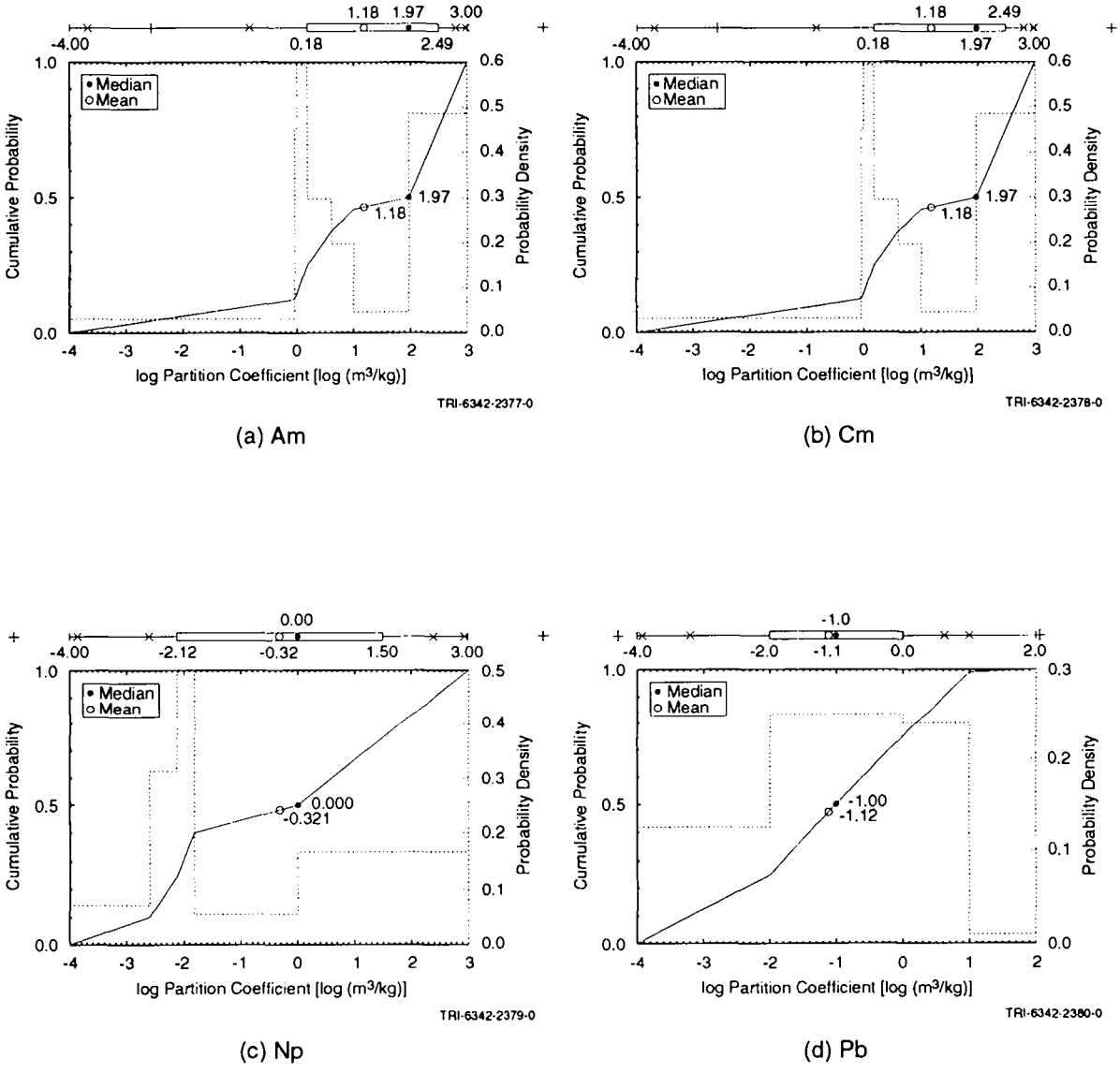

Figure 2.6-10. Constructed distribution for partition coefficient in clay for (a) americium (Am), (b) curium (Cm), (c) neptunium (Np), (d) lead (Pb), (e) plutonium (Pu), (f) radium (Ra), (g) thorium (Th), and (h) uranium (U).

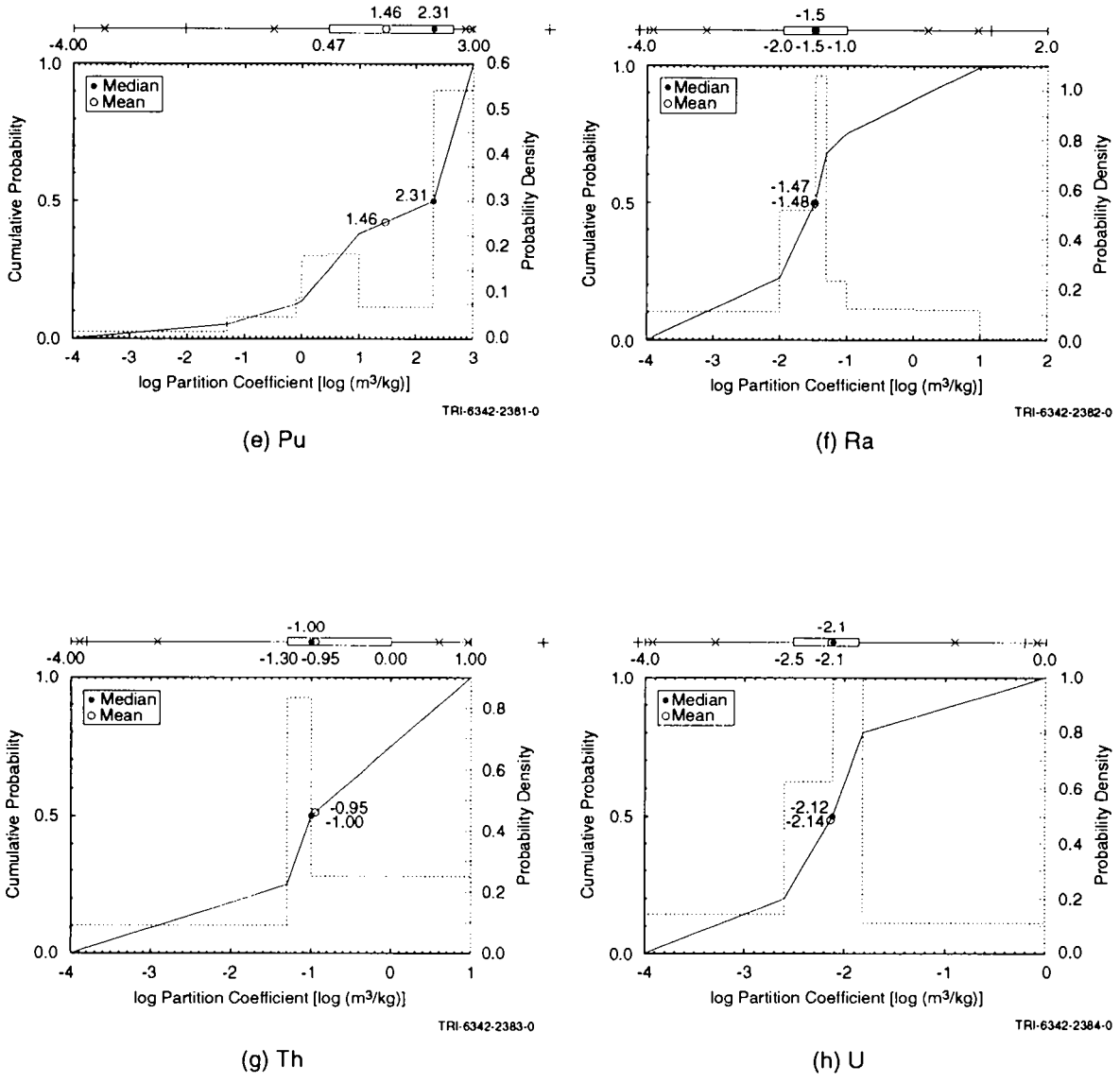

Figure 2.6-10. Constructed distribution for partition coefficient in clay for (a) americium (Am), (b) curium (Cm), (c) neptunium (Np), (d) lead (Pb), (e) plutonium (Pu), (f) radium (Ra), (g) thorium (Th), and (h) uranium (U) (continued).

3. ENGINEERED BARRIERS AND SOURCE TERM

The engineered barriers consist of the repository design, waste form, seals, and backfill. Also discussed in this chapter are characteristics of the waste such as inventory of radionuclides and hazardous chemicals, solubility, and gas production potential.

3.1 Dimensions of Underground Facility

The WIPP repository is composed of a single 15-ha (38-acre) underground disposal level constructed in one stratigraphic interval, which dips slightly to the south. The repository level consists of an experimental region at the north end, the operations region in the center for waste-handling and repository equipment maintenance, and a disposal region at the south end (Figures 3.1-1 and 3.1-2). The UTM coordinates shown in Figure 3.1-2 are derived from the state plane coordinates reported in Gonzales, 1989. To maintain consistency with coordinate values reported elsewhere in this volume, the UTM coordinates were computed by the Technology Application Center, University of New Mexico, Albuquerque, New Mexico 87106. Table 3.1-1 provides a summary of the excavated and enclosed areas (see Figure 3.1-1 for a visual appreciation of these terms) and initial volumes of excavated regions (not considering disturbed rock zone [DRZ] or closure). At present, only the first panel has been excavated.

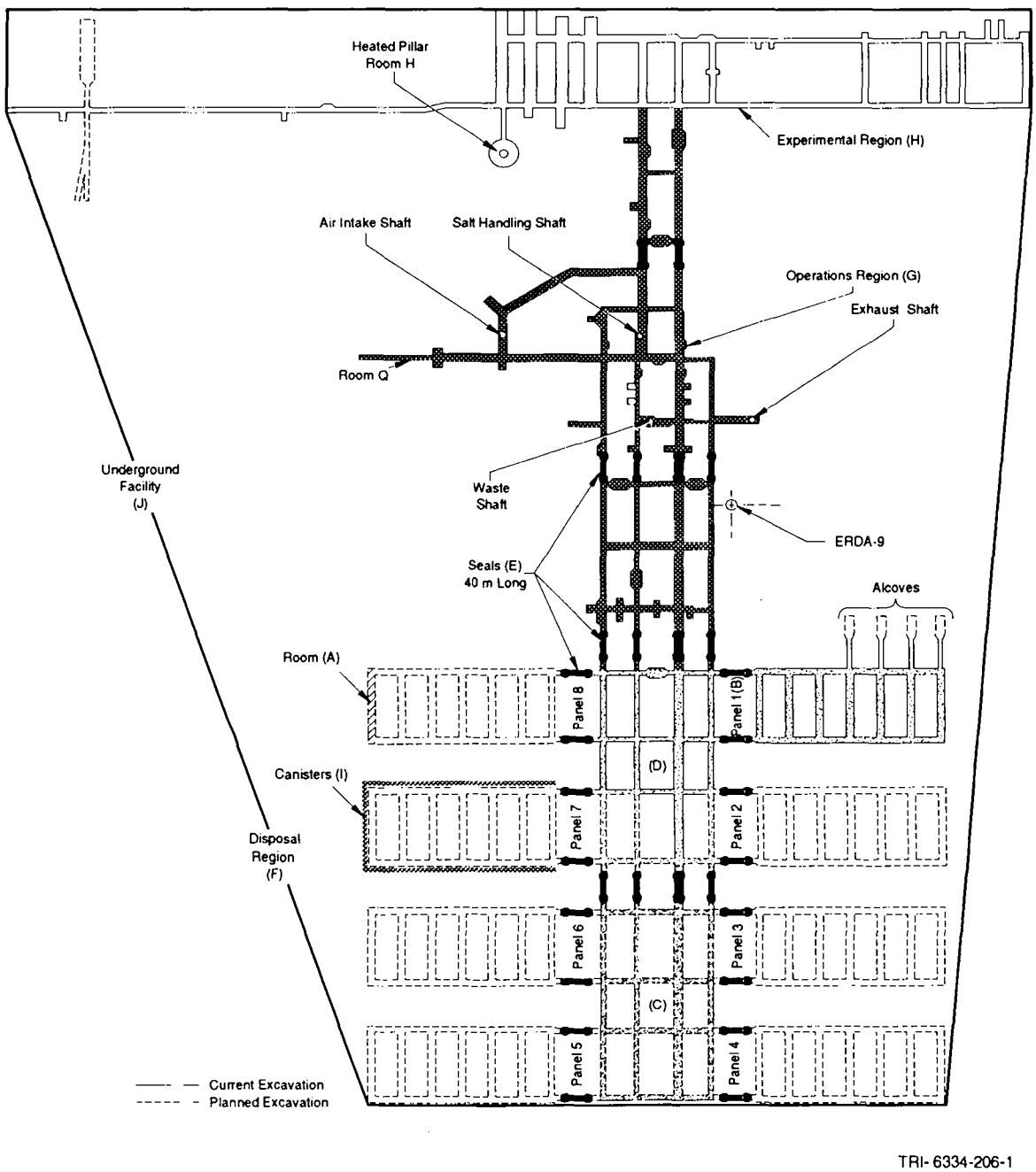

Figure 3.1-1. Excavated and enclosed areas in the WIPP repository.

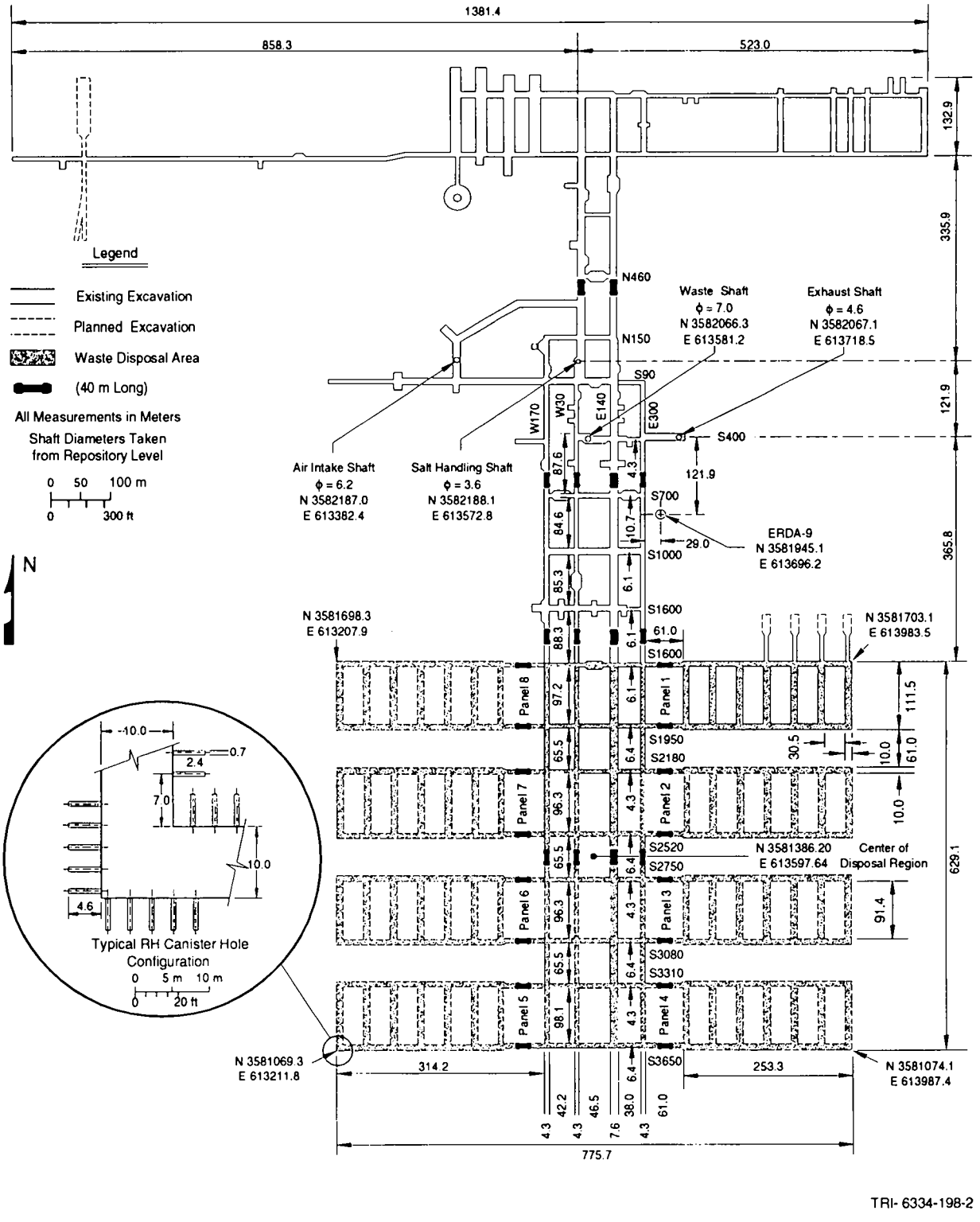

Figure 3.1-2. Planned dimensions of WIPP disposal region and access drifts. (Dimensions originally specified in units of feet.) (after Bechtel National, Inc., 1986).

Table 3.1-1. Summary of Excavated and Enclosed Areas and Initial Volumes of Excavated Regions within the WIPP Repository, Not Considering the DRZ or Closure (Rechard et al., 1990b, Table A-12)

Region*	Areas		Volume	
	Excavated (10^3 m^2)	Enclosed (10^3 m^2)	Excavated (10^3 m^3)	Enclosed (10^3 m^3)
Room (A)	0.9197	0.9197	3.644	3.644
One panel excluding seals (B)	11.64	29.42	46.10	116.59
Southern equivalent panel excluding seals (C)	8.820	49.46	32.26	180.90
Northern equivalent panel excluding seals (D)	9.564	53.68	34.98	196.34
Panel seals (20) (E)	4.133		15.119	
Total disposal region (F)	111.52	506.8	436.0	2008.0
Operations region (G)	21.84	283.6	78.07	1037.2
Four shafts (only) to base of Rustler Fm.	0.08691	0.08691	34.76	34.76
Experimental region (H)	21.61	298.1	71.90	1090
RH area canisters (7954) (I)	14.36			
Total facility (J)	152.83	1748	583.4	6926

*Regions shown in Figure 3.1-1; detailed dimensions shown in Figure 3.1-2.

3.1.1 Disposal Region

All of the underground openings are rectangular in cross section. The disposal area drifts are about 4 m (13 ft) high by 4.3 m (14 ft) wide; the disposal rooms are 4 m (13 ft) high, 10 m (33 ft) wide, and 91.4 m (300 ft) long. Tolerances for all linear dimensions are ±0.5 m. The width of the pillars between rooms is 30.5 m (100 ft). The total excavated volume in the disposal region is 4.36×10^5 m^3 (1.53×10^7 ft^3). The reported design disposal volume is 1.756×10^5 m^3 (6.2×10^6 ft^3) or about 40% of the excavated volume (Bechtel National, Inc., 1986). However, the disposal volume for waste changes depending on the type of containers, waste form, and volume of panel seals. Hence, the design volume is discussed in the description of the containers (Section 3.1.5).

3.1.2 Experimental Region

The experimental region (Figure 3.1-2) is located in the northern portion of the underground facility and consists of over ten rooms, which are used for in situ testing of salt creep and brine inflow (Matalucci, 1988, pp. 3,15). The sizes of the rooms vary, depending on the experiment. The excavated area of the experimental region is about 21.61 x 10^3 m2 (23.2 x 10^4 ft^2), and its volume is about 71.90 x 10^3 m^3 (25.3 x 10^5 ft^3) (Table 3.1-1).

3.1.3 Operations Region

The operations region (Figure 3.1-2) consists of the access drifts located in the center of the underground facility. The drifts are used for transport of equipment and personnel to the experimental area and disposal region. All four shafts are connected to the operations region. The excavated area of the operations region is 21.84 x 10^3 m^2 (23.4 x 10^4 ft^2), and its volume is 78.07 x 10^3 m^3 (27.6 x 10^5 ft^3) (Table 3.1-1).

3.1.4 Shafts

The four shafts connecting the underground facility to the surface are (1) the Air Intake Shaft, 6.2 m (20 ft) in diameter; (2) the Exhaust Shaft, 4.6 m (15 ft) in diameter, (3) the Salt Handling Shaft, 3.6 m (12 ft) in diameter, and (4) the Waste Shaft, 7 m (23 ft) in diameter (Figure 3.1-2).

During operations, the Salt-Handling Shaft will transport personnel, equipment, and salt. The Waste Shaft will transport the waste, and the Air Intake and Exhaust Shafts will provide air flow. The Air Intake Shaft will also serve as a backup for transporting personnel and equipment.

At present, the shaft functions are the same as those described above, except that the Waste Shaft is not currently used to transport waste. It serves as a backup for transport of personnel and materials.

The Air Intake Shaft, the most recently constructed shaft (1988), provides fresh air to the underground. It also serves as a backup for transporting personnel and materials. In addition, in situ testing is being performed to investigate the disturbed rock zone (DRZ) surrounding the shaft and hydrologic properties of the Rustler Formation (Nowak et al., 1990).

The Exhaust Shaft, drilled in 1983-84, serves as the primary air exhaust for the underground facility (Bechtel National, Inc., 1985).

The Salt-Handling Shaft (formerly called the Construction and Salt-Handling [C&SH] Shaft and the Exploratory Shaft [Bechtel National, Inc., 1985]) was drilled in 1981. It was used during construction of the WIPP repository to remove salt and serve as the primary transport for personnel and equipment. The Salt-Handling Shaft continues to serve as the primary transport for personnel and equipment and as a secondary air supply to the underground facility.

The Waste Shaft (initially called the Ventilation Shaft) is designed to move radioactive waste between the surface waste-handling facilities and the underground facility. The Ventilation Shaft was enlarged from 2 m (6 ft) diameter to 6 m (20 ft) diameter in 1983-84, when it was renamed the Waste Shaft (Bechtel National, Inc., 1985). Until waste transport begins, the Waste Shaft serves as a secondary means to transport personnel, materials, large, equipment, and diesel fuel. The Waste Shaft can continue to serve as backup for transporting personnel and materials whenever waste is not being transported.

All four shafts will be sealed and filled upon decommissioning of the WIPP (Nowak et al., 1990).

3.1.5 Waste Containers

Current plans for transporting contact-handled (CH) transuranic (TRU) waste to the WIPP are to ship it in 55-gal steel drums or metal standard waste boxes (SWBs). The dimensions and volumes of a 55-gal steel drum and an SWB are shown in Table 3.1-2. Waste that is currently stored in containers other than 55-gal drums and SWBs will be repackaged into SWBs. TRUPACT II, the transportation container for trucking TRU waste to the WIPP, has space for two 7-pack drums and two SWBs.

The reference canister for the remotely handled (RH) TRU waste is a 0.65-m (26-in.) O.D. (outside diameter) right-circular cylinder made of 1/4-in. carbon steel plate. Caps are welded at both ends. The canister is 3 m (10 ft) in length, including the handling pintle. Inside, the waste occupies about 0.89 m^3 (30 ft^3) (U.S. DOE, 1990c).

Table 3.1-2. CH-TRU Waste Containers (U.S. DOE, 1990a, Dwg 165-F-001-W)

Container Description	Approximate Dimensions (h x w x l) m	Volume Internal m^3	Volume External m^3	Volume Packing m^3
Approved for transportation:				
DOT 17C (metal) 55-gal steel drums	0.892 x 0.602 dia.	0.2082	0.2539	
7-Pack of 55-gal steel drums		1.4574	~ 1.47	~ 2.2
Standard waste box (Dwg 165-F-001-W)	~ 0.94 x 1.8 x 1.3	~ 1.90	~ 1.95	~ 2.34

3.1.6 Waste Placement and Backfill in Rooms

Figure 3.1-3 shows the planned packing configuration of drums in the rooms and drifts. At the waste storage room, the waste packages (7-packs) will be removed from the transporter and stacked 3 high and 6 wide across the room. In the ideal packing configuration, a total of 6,804 drums (972 7-pack units) can be placed in one panel. A 0.7-m air gap exists above the drums; also a thin plastic pallet is set between layers. For the 1991 calculations, the plastic sheet was assumed to be 0.30-cm thick, consistent with the Bechtel initial reference design report (1986). Recently developed final plans (U.S. DOE, 1990c) for the plastic sheet call for 0.004-m-thick plastic on the top and bottom; hence, slightly less salt backfill will be used.

A standard waste box (SWB) stacking configuration is shown in Figure 3.1-4. Seven-packs and SWBs may be intermixed, as practical. To reach the original design capacity of 175,600 m^3 (6.2 x 10^6 ft^3), the SWBs were also assumed to be stacked three high. However, current plans call for stacking the SWBs only two high, which substantially reduces the disposal capacity of the WIPP.

The current placement technique for RH-TRU waste in the WIPP is to emplace one canister horizontally every 2.4 m (8 ft) into the drift and room walls. Based on this technique, the capacity in each panel for RH-TRU canisters along drifts and rooms 10-m wide is 874 canisters or about 6,000 m^3. The intended capacity for RH-TRU waste is 7,080 m^3 (250,000 ft^3); hence, additional methods will be explored. Current PA calculations assume a capacity of 7,080 m^3.

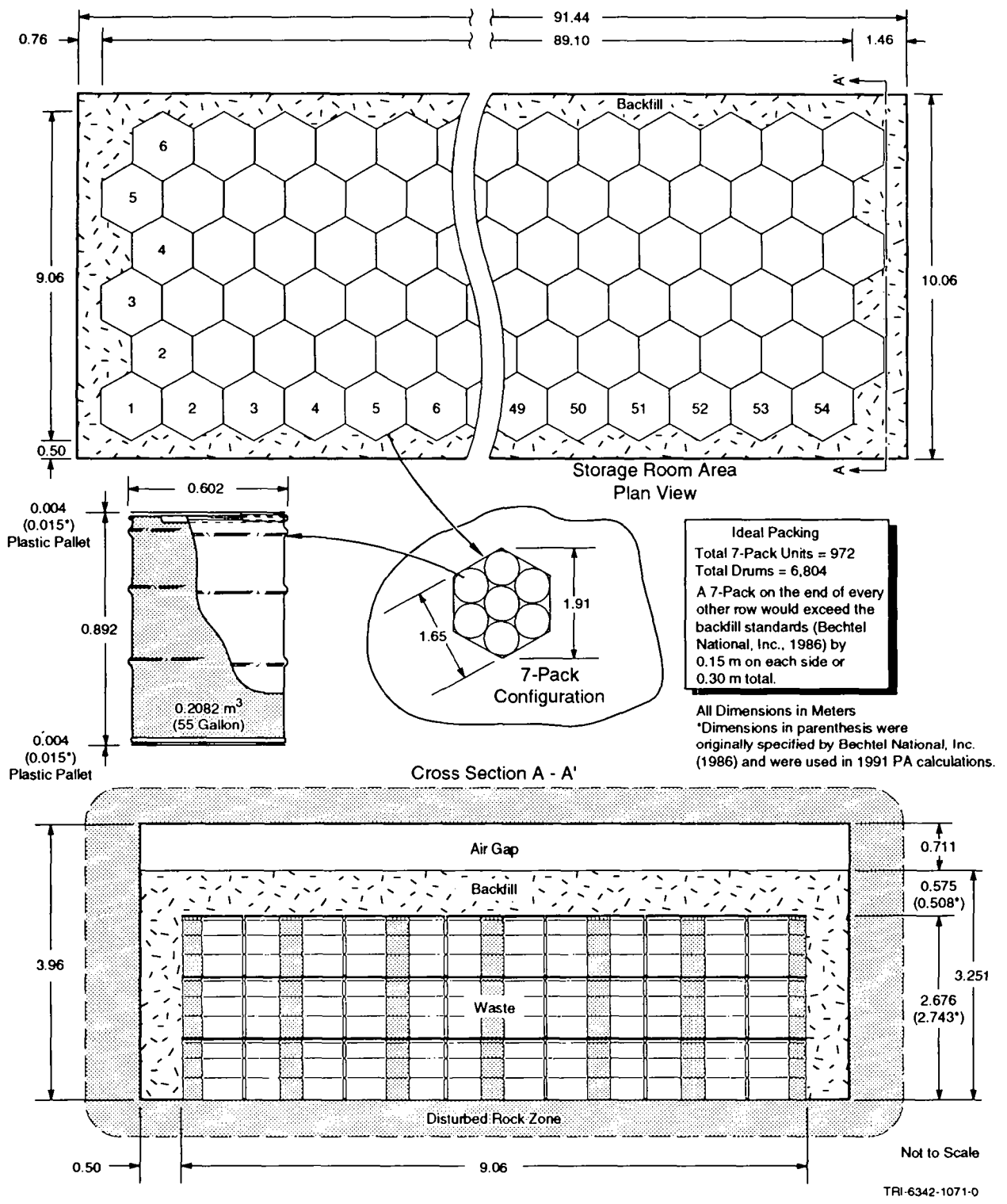

Figure 3.1-3. Ideal packing of drums in rooms and 10-m-wide drifts (not to scale).

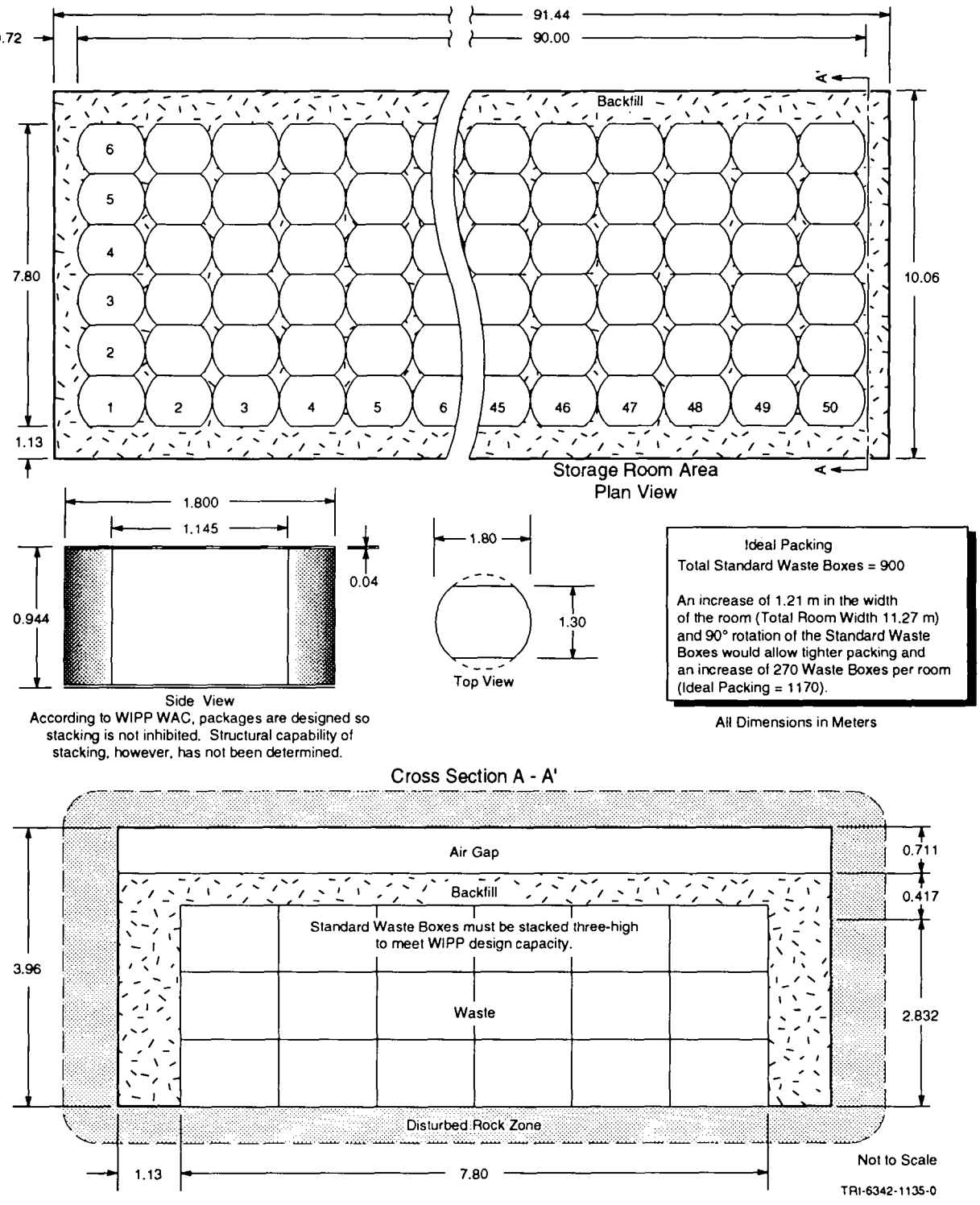

Figure 3.1-4. Ideal packing of Standard Waste Boxes in rooms and drifts (not to scale).

3.2 Parameters for Seals and Fills Outside Disposal Region

Table 3.2-1 summarizes material-property parameters (such as permeability and porosity) for seals and fills placed in the shafts and access drifts when WIPP is decommissioned.

Table 3.2-1. Parameter Values for Seals Outside Disposal Region

Parameter	Median	Range		Units	Distribution Type	Discussion and Sources in:
Preconsolidated crushed salt (Lower shaft, drifts, panels)						
Density (ρ)						
Initial	1.71×10^3 (0.8ρ Salado halite)			kg/m^3	Constant	WIPP PA Division, 1991, Vol 3, Section 3.2.2
Final	2.03×10^3 (0.95ρ Salado halite)			kg/m^3	Constant	WIPP PA Division, 1991, Vol 3, Section 3.2.2
Height (Lower shaft)	2×10^2	1×10^2	3×10^2	m	Uniform	WIPP PA Division, 1991, Vol 3, Section 3.2.2
Permeability (k)						
Initial	1×10^{-14}			m^2	Constant	WIPP PA Division, 1991, Vol 3, Section 3.2.2
Final	1×10^{-20}	3.3×10^{-21}	3.3×10^{-20}	m^2	Lognormal	WIPP PA Division, 1991, Vol 3, Section 3.2.2
Crushed salt backfill in drifts						
Density (ρ)						
Initial	1.28×10^3 (0.6ρ Salado halite)			kg/m^3	Constant	WIPP PA Division, 1991, Vol 3, Section 3.2.3
Final	2.03×10^3 (0.95ρ Salado halite)			kg/m^3	Constant	WIPP PA Division, 1991, Vol 3, Section 3.2.3
Permeability (k)						
Initial	1×10^{-11}			m^2	Constant	WIPP PA Division, 1991, Vol 3, Section 3.2.3
Final	1×10^{-20}	3.3×10^{-21}	3.3×10^{-20}	m^2	Lognormal	WIPP PA Division, 1991, Vol 3, Section 3.2.3
Partition coefficients for crushed salt						
Am	1×10^{-4}			m^3/kg	Constant	WIPP PA Division, 1991, Vol 3, Section 3.2.4
Np	1×10^{-5}			m^3/kg	Constant	WIPP PA Division, 1991, Vol 3, Section 3.2.4
Pb	1×10^{-6}			m^3/kg	Constant	WIPP PA Division, 1991, Vol 3, Section 3.2.4
Pu	1×10^{-4}			m^3/kg	Constant	WIPP PA Division, 1991, Vol 3, Section 3.2.4
Ra	1×10^{-6}			m^3/kg	Constant	WIPP PA Division, 1991, Vol 3, Section 3.2.4
Th	1×10^{-4}			m^3/kg	Constant	WIPP PA Division, 1991, Vol 3, Section 3.2.4
U	1×10^{-6}			m^3/kg	Constant	WIPP PA Division, 1991, Vol 3, Section 3.2.4
Concrete and Bentonite						
Permeability (k)						
Concrete	2.7×10^{-19}			m^2	Constant	WIPP PA Division, 1991, Vol 3, Section 3.2.5
Bentonite	1.4×10^{-19}			m^2	Constant	WIPP PA Division, 1991, Vol 3, Section 3.2.5

3.2.1 Description of the Reference Seal System Design

The purpose of the reference seal design, which Sandia has developed for sealing the WIPP repository, is to provide a common basis for calculations performed in modeling tasks such as performance assessment and sensitivity analysis (Nowak and Tyler, 1989; Nowak et al., 1990). The reference design is a starting point for developing experiments and analysis from which a detailed design will evolve.

GENERAL SEALING STRATEGY

In general, the entire underground facility and shafts will be sealed. As part of the reference design, portions of the backfill emplaced at several locations within the shafts and various drifts, which are specially prepared (i.e., preconsolidated salt with concrete plugs), are often termed "seals." However, the purpose of these prepared portions is not to act as the sole seal for the shaft or drift (in general, all the backfill fulfills this function), but instead to protect sections of the backfill from fluids (gases or liquids). Inhibiting fluids hastens backfill consolidation and thus greatly increases the probability that the salt backfill will rapidly (< 100 yr) assume properties near to those of the surrounding host rock.

The strategy for sealing specially prepared portions of the drift and shaft combines short- and long-term seal components; preconsolidated crushed salt is the principal long-term component in the Salado Formation salt. Clay -- a swelling clay material shown to be stable and to have low permeability to brines -- is the principal long-term component in the Rustler Formation. Concrete is the principal short-term component in both locations.

The combination of short- and long-term seals is used so that short-term seals provide the initial sealing functions necessary until the long-term seal components become adequately reconsolidated (Nowak et al., 1990). Preconsolidated crushed-salt and clay components are expected to become fully functional for sealing within 100 yr after emplacement (Nowak and Stormont, 1987; Arguello, 1988). Then the long-term seals take over all sealing functions.

Short-term seal components consist of concretes and clay materials developed specifically for the WIPP. The concrete components provide flow resistance to control the effects of possible gas generation in the waste disposal area and limit water inflow from above to protect the crushed salt from saturation with brine; they also provide physical containment for the swelling clay and consolidating crushed-salt materials (Nowak et al., 1990).

The long-term seals in the Salado consist of preconsolidated WIPP crushed salt in the shafts, drifts, and panel entries. The emplaced crushed-salt material is intended to have an initial density equal to 80% of the density of the intact WIPP host rock salt (80% relative density) (Nowak et al., 1990). Within 100 yr of emplacement, the preconsolidated salt backfill will be fully consolidated by creep closure of the host-rock salt to a state of low permeability, approximately 1×10^{-20} m^2 (Nowak and Stormont, 1987; Arguello, 1988; Lappin et al., 1989). This permeability value is in the expected permeability range for the host-rock salt (1×10^{-21} to 1×10^{-20}) (Nowak et al., 1988; Lappin et al., 1989), but it is on the high side of the range suggested by Gorham et al. (June 15, 1992, Memo in Appendix A). Very little compositional difference between the saturated, reconsolidated WIPP crushed-salt material and the surrounding host rock from which it was mined is anticipated. The crushed-salt seals, therefore, are expected to be mechanically and chemically stable in the WIPP environment (Nowak et al., 1990).

SEAL LOCATIONS

In the reference design, multicomponent seals between 30 and 40 m (100 and 130 ft) long will be in each of the four shafts, the entrances to the waste disposal panels, and selected access drifts (Nowak et al., 1990). (See Figures 3.1-1 and 3.1-2 for seal locations.) Seals near the Rustler Formation (upper shaft and water-bearing zone seals) serve to limit brine flow from water-bearing zones down into the crushed-salt backfill. Seals in the drifts serve to reduce fluid flow (gas and brine) from the repository area and thus limit the creation of a preferred pathway for contaminant migration. The drift entries to each filled disposal panel will be sealed during operations. The disturbed rock zone (DRZ), which occurs in the host-rock salt at the excavated openings, is expected to heal by creep closure (Nowak et

al., 1990). The extent of a DRZ in the drift entries may be reduced by the use of concrete liners during operations. If necessary, however, the conceptual design for sealing the DRZ (both in drifts and shafts) and anhydrite interbeds (e.g., MB139 directly underneath the disposal area) envisions a salt-based grout (Nowak and Tyler, 1989) using grouting techniques that are currently under development (Figure 3.2-3). When all disposal panels are filled, the drift entries to the entire disposal area will be sealed. The shafts will be backfilled upon decommissioning of the WIPP (Figures 3.2-1 and 3.2-2) (Nowak et al., 1990).

BACKFILL IN UPPER SHAFT, WATER-BEARING ZONE, AND DEWEY LAKE RED BEDS

According to current calculations, radionuclides will not reach the upper shaft in 10,000 yr. Therefore, the actual properties of the backfill in the upper shaft and above have not been used in the 1992 PA calculations and properties are not given. Instead the initial placement properties of the lower shaft have been used.

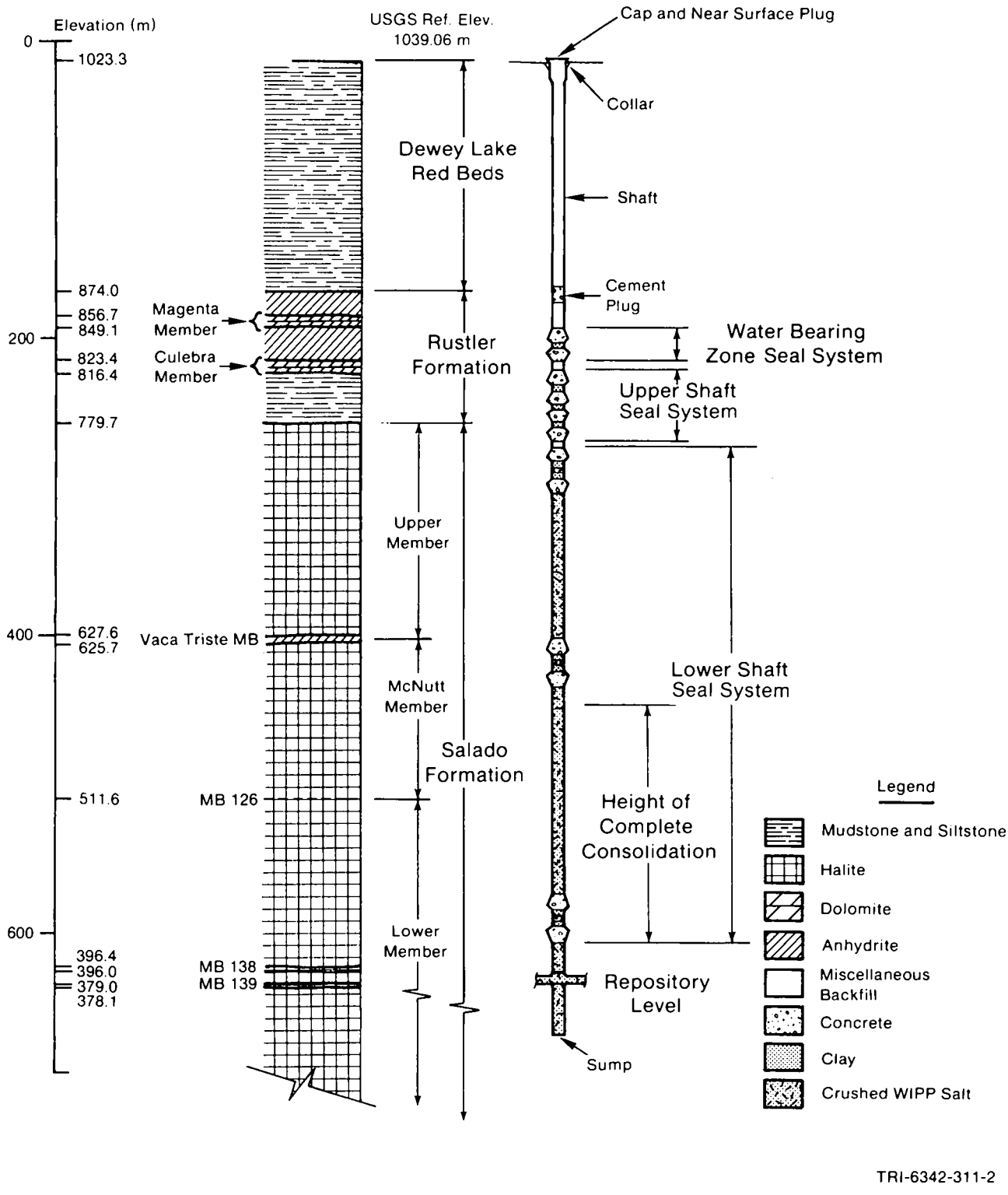

Figure 3.2-1. Diagram of typical sealed and backfilled access shaft (after Nowak et al., 1990).

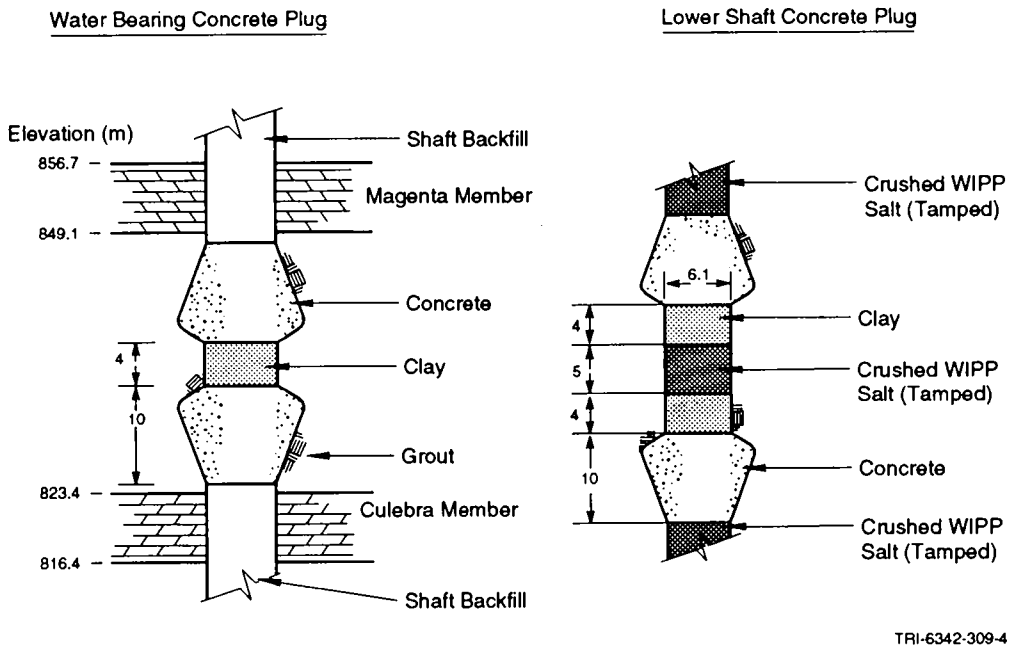

Figure 3.2-2. Diagram of typical concrete plugs in backfilled shafts. The drawing shows concrete plugs between water-bearing units (e.g., Culebra Dolomite) (left) and for the Lower Shaft Backfill (e.g., at Vaca Triste) for Waste Shaft (right) (after Nowak et al., 1990).

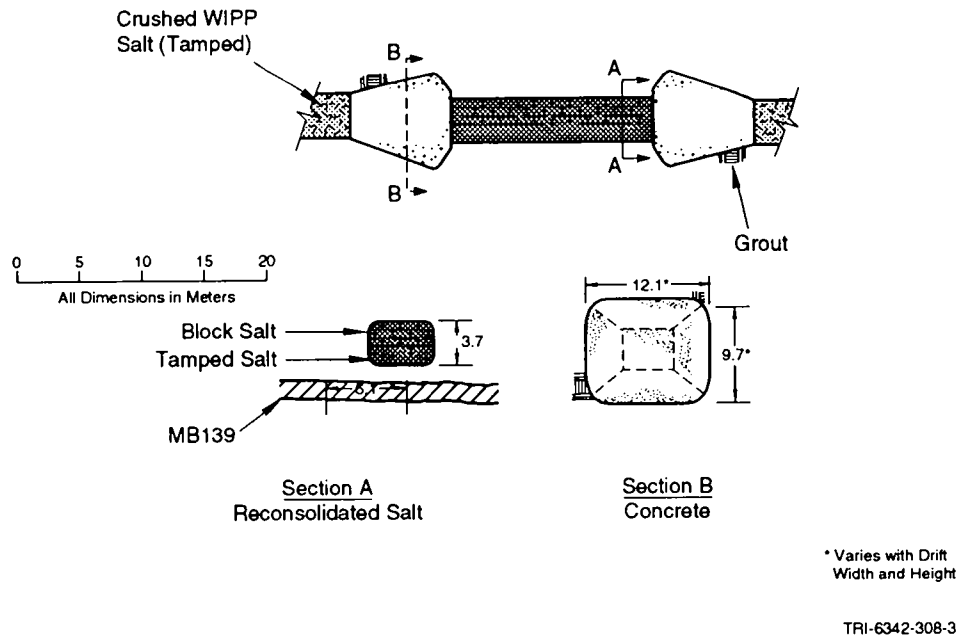

Figure 3.2-3. Diagram of typical concrete and preconsolidated salt backfill for drifts and panels (after Nowak et al., 1990). Scale applies to horizontal dimensions; vertical dimensions are exaggerated.

3.2.2 Preconsolidated Salt in Lower Shaft, Drifts, and Panels

The reference seal uses preconsolidated (tamped) crushed WIPP salt as the primary long-term seal material. For redundancy, concrete plugs and clay (Figure 3.2-2) are emplaced at three locations in the shaft: (1) near the bottom of the shaft, (2) at an intermediate position in the shaft just below the Vaca Triste Marker Bed (Figure 3.2-1), and (3) near the top of the Salado Formation.

The emplaced WIPP crushed salt is intended to have an initial density equal to 80% of the density of the intact WIPP host rock salt (80% relative density). Salt with 80% relative density will be created either by pouring and tamping crushed salt or by laying preconsolidated salt blocks. Creep closure of the lower part of the shaft will continue to consolidate this crushed salt.

3.3 Parameters for Contaminants Independent of Waste Form

The TRU waste for which the WIPP is designed is defense-program waste that has been generated at ten facilities since 1970. The waste consists of laboratory and production waste such as glassware, metal pipes, sorbed or solidified spent solvents, disposable laboratory clothing, cleaning rags, and solidified sludges. Current plans specify that most of the TRU waste generated since 1970 will be placed in the WIPP repository, with the remainder to be disposed of at other DOE facilities.

As of 1992, the ten TRU waste generator and/or storage sites that are scheduled to ship waste to the WIPP are (1) Argonne National Laboratory-East (ANL-E), Illinois; (2) Hanford Reservation (HANF), Washington; (3) Idaho National Engineering Laboratory (INEL), Idaho; (4) Los Alamos National Laboratory (LANL), New Mexico; (5) Lawrence Livermore National Laboratory (LLNL), California; (6) Mound Laboratory, Ohio; (7) Nevada Test Site (NTS), Nevada; (8) Oak Ridge National Laboratory (ORNL), Tennessee; (9) Rocky Flats Plant (RFP), Colorado; and (10) Savannah River Site (SRS), South Carolina (U.S. DOE, 1990d).

The TRU waste is contaminated by alpha-emitting transuranic elements, defined as having atomic numbers greater than uranium-92, half-lives greater than 20 yr, and curie contents greater than 100 nCi/g. Other contaminants include uranium and several radionuclides with half-lives less than 20 yr. Approximately 60% of the waste may be co-contaminated with waste considered hazardous under the RCRA, e.g., lead (WEC, 1990).

Radioactive waste that emits alpha radiation, although dangerous if inhaled or ingested, is not hazardous externally. Most of the waste, therefore, can be contact handled (CH) because the external dose rate (5.6×10^{-7} Sv/s [200 mrem/h] or less) permits people to handle drums and boxes without any special shielding.

A small portion of the TRU waste must be transported and handled in shielded casks (remotely handled [RH]), i.e., the surface dose rate exceeds 5.6×10^{-7} Sv/s (200 mrem/h). The surface dose rate of an RH-TRU canister cannot exceed 2.8×10^{-3} Sv/s (1000 rem/h); but no more than 5% of the canisters can exceed 2.8×10^{-4} Sv/s (100 rem/h) (U.S. DOE, 1990d). The volume must be less than 250,000 m^3 and the curie content must be less than 5.1×10^{6} Ci (1.89×10^{17} Bq) according to the agreement between DOE and the State of New Mexico (U.S. DOE and NM, 1984).

Subpart B of the Standard sets release limits in curies for isotopes of americium, carbon, cesium, iodine, neptunium, plutonium, radium, strontium, technetium, thorium, tin, and uranium, as well as for certain other radionuclides (Section 3.3.4 of this volume). Although the initial WIPP inventory contains little or none of some of the listed nuclides, they may be produced as a result of radioactive decay and must be accounted for in the compliance evaluation; moreover, any radionuclides not listed in Subpart B must be accounted for if those radionuclides would contribute to doses used in NEPA calculations (e.g., Pb-210).

3.3.1 Inventory of Radionuclides in Contact-Handled Transuranic Waste

The 1991 inventory (curie content) of radionuclides in the CH-TRU waste was estimated from input submitted to the 1990 Integrated Data Base (IDB) (U.S. DOE, 1990d). The information submitted to the IDB is separated into retrievably stored and newly generated (future generation) waste referred to herein as projected inventory. The anticipated total volume (stored plus projected) of CH-TRU waste submitted to the 1990 IDB was 1.0×10^5 m^3 (3.76×10^6 ft^3), which is less than the current design volume for the WIPP of about 1.8×10^5 m^3 (6.2×10^6 ft^3). To estimate the total curie content in the WIPP, if it contained a design volume of CH-TRU waste, the future-generated radionuclide inventories of the five largest future generators listed in the 1990 IDB were volume scaled to reach a design volume of waste. (Details of this volume scaling are discussed in Section 3.4.) This inventory per generator site is only a design estimate and should not be considered a statement of what they will generate.

The weight fractions reported in the 1990 IDB were used to calculate the major radionuclides of the mixes reported. The IDB did not report the inventory of each radionuclide. Rather, the inventory of each radionuclide at each site was based on the mix of waste streams reported. The Hanford submittal to the 1990 IDB indicated that the activity of some of the CH-TRU waste was currently unknown. Rather than underestimate the potential inventory, the Hanford input to the 1987 IDB was used. These inventories have not been independently checked and should be considered preliminary estimates.

Modifications to the radionuclide inventories in the 1990 IDB were made in 1992 (Peterson, October 28, 1992, Memo in Appendix A). These modifications are reflected in Table 3.3-1 which lists both CH and RH inventories.

Table 3.3-1. Inventory and Parameter Values for TRU Radioisotopes

Parameter	Median	Units	Source
Ac225			
Half-life	8.640×10^{5}	s	ICRP, Pub 38, 1983
Ac227			
Half-life	6.871×10^{8}	s	ICRP, Pub 38, 1983
Ac228			
Half-life	2.207×10^{4}	s	ICRP, Pub 38, 1983
Am241			
Activity conversion	3.43×10^{3}	Ci/kg	1.1281×10^{16}/(half-life(s)xAt.Wt.)
Half-life	1.364×10^{10}	s	ICRP, Pub 38, 1983
Inventory, Anticipated (1990)			
CH	6.65×10^{5}	Ci	
RH	1.29×10^{3}	Ci	U.S. DOE, 1990d; Peterson, 1990
Inventory, Design (1992)			
CH	7.14×10^{5}	Ci	Peterson, October 28, 1992
RH	1.06×10^{3}	Ci	(Memo in Appendix A)
Am243			
Half-life	5.822×10^{11}	s	ICRP, Pub 38, 1983
At217			
Half-life	3.230×10^{-2}	s	ICRP, Pub 38, 1983
Bi210			
Half-life	4.330×10^{5}	s	ICRP, Pub 38, 1983
Bi211			
Half-life	1.284×10^{2}	s	ICRP, Pub 38, 1983
Bi212			
Half-life	3.633×10^{3}	s	ICRP, Pub 38, 1983
Bi213			
Half-life	2.739×10^{3}	s	ICRP, Pub 38, 1983
Bi214			
Half-life	1.194×10^{3}	s	ICRP, Pub 38, 1983
Cf252			
Activity conversion	5.38×10^{5}	Ci/kg	1.1281×10^{16}/(half-life(s)xAt.Wt.)
Half-life	8.325×10^{7}	s	ICRP, Pub 38, 1983
Inventory, Anticipated (1990)			
CH	1.27×10^{4}	Ci	
RH	2.39×10^{3}	Ci	U.S. DOE, 1990d; Peterson, 1990
Inventory, Design (1992)			
CH	3.37×10^{2}	Ci	Peterson, October 28, 1992
RH	8.63×10^{1}	Ci	(Memo in Appendix A)
Cm244			
Activity conversion	8.09×10^{4}	Ci/kg	1.1281×10^{16}/(half-life(s)xAt.Wt.)
Half-life	5.715×10^{8}	s	ICRP, Pub 38, 1983

Table 3.3-1. Inventory and Parameter Values for TRU Radioisotopes (Continued)

Parameter	Median	Units	Source
Inventory, Anticipated (1990)			
CH	1.23×10^{4}	Ci	
RH	8.75×10^{3}	Ci	U.S. DOE, 1990d; Peterson, 1990
Inventory, Design (1992)			
CH	2.06×10^{4}	Ci	Peterson, October 28, 1992
RH	4.26×10^{3}	Ci	(Memo in Appendix A)
Cs137			
Activity conversion	8.70×10^{4}	Ci/kg	1.1281×10^{16}/(half-life(s)xAt.Wt.)
Half-life	9.467×10^{8}	s	ICRP, Pub 38, 1983
Inventory, Anticipated (1990)			
RH	3.33×10^{5}	Ci	U.S. DOE, 1990d; Peterson, 1990
Inventory, Design (1992)			
CH	6.30×10^{4}	Ci	Peterson, October 28, 1992
RH	5.70×10^{5}		(Memo in Appendix A)
Fr221			
Half-life	2.880×10^{2}	s	ICRP, Pub 38, 1983
Np237			
Activity conversion	7.05×10^{-1}	Ci/kg	1.1281×10^{16}/(half-life(s)xAt.Wt.)
Half-life	6.753×10^{13}	s	ICRP, Pub 38, 1983
Inventory, Anticipated (1990)			
CH	1.47	Ci	
RH	8.87×10^{-1}	Ci	U.S. DOE, 1990d; Peterson, 1990
Inventory, Design (1992)			
CH	20.8	Ci	Peterson, October 28, 1992
RH	9.20×10^{-1}	Ci	(Memo in Appendix A)
Np239			
Half-life	2.035×10^{5}	s	ICRP, Pub 38, 1983
Pa231			
Half-life	1.034×10^{12}	s	ICRP, Pub 38, 1983
Pa233			
Half-life	2.333×10^{6}	s	ICRP, Pub 38, 1983
Pb209			
Half-life	1.171×10^{4}	s	ICRP, Pub 38, 1983
Pb210			
Activity conversion	7.63×10^{4}	Ci/kg	1.1281×10^{16}/(half-life(s)xAt.Wt.)
Half-life	7.037×10^{8}	s	ICRP, Pub 38, 1983
Pb211			
Half-life	2.166×10^{3}	s	ICRP, Pub 38, 1983
Pb212			
Half-life	3.830×10^{4}	s	ICRP, Pub 38, 1983
Pb214			
Half-life	1.608×10^{3}	s	ICRP, Pub 38, 1983

Table 3.3-1. Inventory and Parameter Values for TRU Radioisotopes (Continued)

Parameter	Median	Units	Source
Pm147			
Activity conversion	$9.27x10^{5}$	Ci/kg	$1.1281x10^{16}$/(half-life(s)xAt.Wt.)
Half-life	$8.279x10^{7}$	s	ICRP, Pub 38, 1983
Inventory, Anticipated (1990)			
RH	$3.15x10^{5}$	Ci	U.S. DOE, 1990d; Peterson, 1990
Inventory, Design (1992)			
CH	$7.60x\ 10^{4}$	Ci	Peterson, October 28, 1992
RH	$5.36x10^{5}$		(Memo in Appendix A)
Po210			
Half-life	$1.196x10^{7}$	s	ICRP, Pub 38, 1983
Po212			
Half-life	$3.050x10^{-7}$	s	ICRP, Pub 38, 1983
Po213			
Half-life	$4.200x10^{-6}$	s	ICRP, Pub 38, 1983
Po214			
Half-life	$1.643x10^{-4}$	s	ICRP, Pub 38, 1983
Po215			
Half-life	$1.780x10^{-3}$	s	ICRP, Pub 38, 1983
Po216			
Half-life	$1.500x10^{-1}$	s	ICRP, Pub 38, 1983
Po218			
Half-life	$1.830x10^{2}$	s	ICRP, Pub 38, 1983
Pu238			
Activity conversion	$1.71x10^{4}$	Ci/kg	$1.1281x10^{16}$/(half-life(s)xAt.Wt.)
Half-life	$2.769x10^{9}$	s	ICRP, Pub 38, 1983
Inventory, Anticipated (1990)			
CH	$4.26x10^{6}$	Ci	
RH	$5.14x10^{2}$	Ci	U.S. DOE, 1990d; Peterson, 1990
Inventory, Design (1992)			
CH	$3.06x10^{6}$	Ci	Peterson, October 28, 1992
RH	$2.73x10^{4}$	Ci	(Memo in Appendix A)
Pu239			
Activity conversion	$6.22x10^{1}$	Ci/kg	$1.1281x10^{16}$/(half-life(s)xAt.Wt.)
Half-life	$7.594x10^{11}$	s	ICRP, Pub 38, 1983
Inventory, Anticipated (1990)			
CH	$4.37x10^{5}$	Ci	
RH	$1.16x10^{3}$	Ci	U.S. DOE, 1990d; Peterson, 1990
Inventory, Design (1992)			
CH	$3.35x10^{5}$	Ci	Peterson, October 28, 1992
RH	$8.50x10^{3}$	Ci	(Memo in Appendix A)

Table 3.3-1. Inventory and Parameter Values for TRU Radioisotopes (Continued)

Parameter	Median	Units	Source
Pu240			
Activity conversion	2.28×10^{2}	Ci/kg	1.1281×10^{16}/(half-life(s)xAt.Wt.)
Half-life	2.063×10^{11}	s	ICRP, Pub 38, 1983
Inventory, Anticipated (1990)			
CH	5.91×10^{4}	Ci	
RH	2.89×10^{2}	Ci	U.S. DOE, 1990d; Peterson, 1990
Inventory, Design (1992)			
CH	1.00×10^{5}	Ci	Peterson, October 28, 1992
RH	2.28×10^{3}	Ci	(Memo in Appendix A)
Pu241			
Activity conversion	1.03×10^{5}	Ci/kg	1.1281x1016/half-life(s)xAt.Wt.)
Half-life	4.544×10^{8}	s	ICRP, Pub 38, 1983
Inventory, Anticipated (1990)			
CH	2.54×10^{6}	Ci	
RH	1.32×10^{4}	Ci	U.S. DOE, 1990d; Peterson, 1990
Inventory, Design (1992)			
CH	3.60×10^{6}	Ci	Peterson, October 28, 1992
RH	1.20×10^{5}	Ci	(Memo in Appendix A)
Pu242			
Activity conversion	3.93	Ci/kg	1.1281×10^{16}/(half-life(s)xAt.Wt.)
Half-life	1.187×10^{13}	s	ICRP, Pub 38, 1983
Inventory, Anticipated (1990)			
CH	1.84	Ci	
RH	3.31×10^{-3}	Ci	U.S. DOE, 1990d; Peterson, 1990
Inventory, Design (1992)			
CH	23.5	Ci	Peterson, October 28, 1992
RH	2.94	Ci	(Memo in Appendix A)
Ra223			
Half-life	9.879×10^{5}	s	ICRP, Pub 38, 1983
Ra224			
Half-life	3.162×10^{5}	s	ICRP, Pub 38, 1983
Ra225			
Half-life	1.279×10^{6}	s	ICRP, Pub 38, 1983
Ra226			
Activity conversion	9.89×10^{2}	Ci/kg	1.1281×10^{16}/(half-life(s)xAt.Wt.)
Half-life	5.049×10^{10}	s	ICRP, Pub 38, 1983
Ra228			
Half-life	1.815×10^{8}	s	ICRP, Pub 38, 1983
Rn219			
Half-life	3.960	s	ICRP, Pub 38, 1983
Rn220			
Half-life	5.560×10^{1}	s	ICRP, Pub 38, 1983

Table 3.3-1. Inventory and Parameter Values for TRU Radioisotopes (Continued)

Parameter	Median	Units	Source
Rn222			
Half-life	3.304×10^{5}	s	ICRP, Pub 38, 1983
Sr90			
Activity conversion	1.36×10^{5}	Ci/kg	1.1281×10^{16}/(half-life(s)xAt.Wt.)
Half-life	9.189×10^{8}	s	ICRP, Pub 38, 1983
Inventory, Anticipated (1990)			
RH	2.80×10^{5}	Ci	U.S. DOE, 1990d; Peterson, 1990
Inventory, Design (1992)			
CH	8.23×10^{4}	Ci	Peterson, October 28, 1992
RH	5.21×10^{5}		(Memo in Appendix A)
Th227			
Half-life	1.617×10^{6}	s	ICRP, Pub 38, 1983
Th228			
Half-life	6.037×10^{7}	s	ICRP, Pub 38, 1983
Th229			
Activity conversion	2.13×10^{2}	Ci/kg	1.1281×10^{16}/(half-life(s)xAt.Wt.)
Half-life	2.316×10^{11}	s	ICRP, Pub 38, 1983
Th230			
Activity conversion	2.02×10^{1}	Ci/kg	1.1281×10^{16}/(half-life(s)xAt.Wt.)
Half-life	2.430×10^{12}	s	ICRP, Pub 38, 1983
Th231			
Half-life	9.187×10^{4}	s	ICRP, Pub 38, 1983
Th232			
Activity conversion	1.10×10^{-4}	Ci/kg	1.1281×10^{16}/(half-life(s)xAt.Wt.)
Half-life	4.434×10^{17}	s	ICRP, Pub 38, 1983
Inventory, Anticipated (1990)			
CH	0.0	Ci	
RH	0.0	Ci	U.S. DOE, 1990d; Peterson, 1990
Inventory, Design (1992)			
CH	2.90×10^{-1}	Ci	Peterson, October 28, 1992
RH	5.66	Ci	(Memo in Appendix A)
Th234			
Half-life	2.082×10^{6}	s	ICRP, Pub 38, 1983
Tl207			
Half-life	2.862×10^{2}	s	ICRP, Pub 38, 1983
U233			
Activity conversion	9.68	Ci/kg	1.1281×10^{16}/(half-life(s)xAt.Wt.)
Half-life	5.002×10^{12}	s	ICRP, Pub 38, 1983
Inventory, Anticipated (1990)			
CH	7.18×10^{1}	Ci	Peterson, October 28, 1992
RH	2.86×10^{1}	Ci	(Memo in Appendix A)

Table 3.3-1. Inventory and Parameter Values for TRU Radioisotopes (Concluded)

Parameter	Median	Units	Source
Inventory, Design (1992)			
CH	1.53×10^{3}	Ci	Peterson, October 28, 1992
RH	1.99×10^{2}	Ci	(Memo in Appendix A)
U234			
Activity conversion	6.25	Ci/kg	1.1281×10^{16}/(half-life(s)xAt.Wt.)
Half-life	7.716×10^{12}	s	ICRP, Pub 38, 1983
U235			
Activity conversion	2.16×10^{-3}	Ci/kg	1.1281×10^{16}/(half-life(s)xAt.Wt.)
Half-life	2.221×10^{16}	s	ICRP, Pub 38, 1983
Inventory, Anticipated (1990)			
CH	5.54×10^{-2}	Ci	
RH	1.23×10^{-2}	Ci	U.S. DOE, 1990d; Peterson, 1990
Inventory, Design (1992)			
CH	5.38×10^{-1}	Ci	Peterson, October 28, 1992
RH	6.13×10^{-2}	Ci	(Memo in Appendix A)
U236			
Half-life	7.389×10^{14}	s	ICRP, Pub 38, 1983
U238			
Activity conversion	3.36×10^{-4}	Ci/kg	1.1281×10^{16}/(half-life(s)xAt.Wt.)
Half-life	1.410×10^{17}	s	ICRP, Pub 38, 1983
Inventory, Anticipated (1990)			
CH	0.0	Ci	
RH	7.83×10^{-2}	Ci	U.S. DOE, 1990d; Peterson, 1990
Inventory, Design (1992)			
CH	2.68	Ci	Peterson, October 28, 1992
RH	1.80	Ci	(Memo in Appendix A)

3.3.2 Inventory of Remotely Handled Waste

The 1991 inventory of TRU waste that must be transported and handled in shielded casks because of dose rates at the surface above 200 mrem/hr (remotely handled [RH]) was estimated from the input submitted to the 1990 IDB (U.S. DOE, 1990d). Estimates were made using a similar method to that used for the CH-TRU waste (discussed in Section 3.3.1).* Some differences between the methods for estimating CH and RH were in the estimation of the activity for RH waste reported as mixed fission products and the "unknown" distribution from Hanford. For the mixed fission products, a mixture of 10-yr-old fission products was assumed as the source term. For the Hanford "unknown," a slurry mixture from the Hanford high level waste tanks provided the isotopic distribution; it was estimated that a 2.15×10^{-6} C_i /(kg•s) (30 rem/hr) canister will contain about 450 Ci of gamma emitters. For other mixtures reported in the 1990 IDB, the weight fractions reported were used to calculate the major radionuclides. A volume scaling method similar to that used for CH-TRU waste was used to increase the volume from about 5,300 m^3 (estimated from the 1990 IDB) to the maximum volume of 7,079 m^3.

Modifications to the radionuclide inventories in the 1990 IDB were made in 1992 (Peterson, October 28, 1992, Memo in Appendix A). These modifications are reflected in Table 3.3-1 which lists both CH and RH inventories.

For the 1991 and 1992 PA calculations, the RH-TRU waste was included in the cuttings releases. The RH-TRU waste has not been included in the long-term performance assessment inventory for most previous calculations (Marietta et al., 1989; Lappin et al., 1989; U.S. DOE, 1990b), because RH-TRU waste constituted less than 2% of the activity. Furthermore, the current procedure for emplacing RH waste in the pillar walls will minimize the interaction of the RH waste canisters and the CH-TRU waste rooms. Also a large amount of the activity in RH waste is from radionuclides with relatively short half-lives, which have a small consequence over the long term.

* An alternative method would be to scale the radionuclides so that the activity limit agreed upon by the State of New Mexico and the DOE--5.2×10^6 Ci--would be emplaced instead of the agreed-upon volume limit.

3.3.3 Radionuclide Chains and Half-Lives

The decay chains for the initial radionuclides in the CH and RH inventory are shown in Figures 3.3-1 and 3.3-2, respectively. The half-life for each radionuclide listed in the literature by ICRP Publication 38 (ICRP, Pub 38, 1983) is also on Figure 3.3-1. For reference, the half-lives of the radionuclides in the initial WIPP inventory and decay products are tabulated in Table 3.3-2. The 1992 initial inventories (in Ci) are listed in Table 3.3-1.

Many of the daughter radionuclides have extremely short half-lives, low activities, and make a small contribution to the curie inventory. Shortened chains are used when modeling as follows.

RADIONUCLIDES FOR CUTTINGS AND REPOSITORY MODELING

From the 70 radionuclides shown in Figure 3.3-1, 23 are considered major contributors to the inventory and are used in calculating the radionuclide releases from drilling into the repository and bringing cuttings to the surface and when calculating concentrations within the repository prior to transport to the Culebra. In general, most isotopes of plutonium, thorium, americium, curium, neptunium, californium, radium, and uranium are considered.

The RH inventory decay chains include the chains in the CH inventory shown in Figure 3.3-1 plus the three chains shown in Figure 3.3-2. The radionuclides in the RH cuttings releases included cesium-137, promethium-147, and strontium-90 in addition to all of the radionuclides in the CH releases.

RADIONUCLIDES FOR TRANSPORT MODELING

Nine radionuclides are considered in 1992 PA transport calculations for CH-TRU waste and are highlighted on Figure 3.3-1.

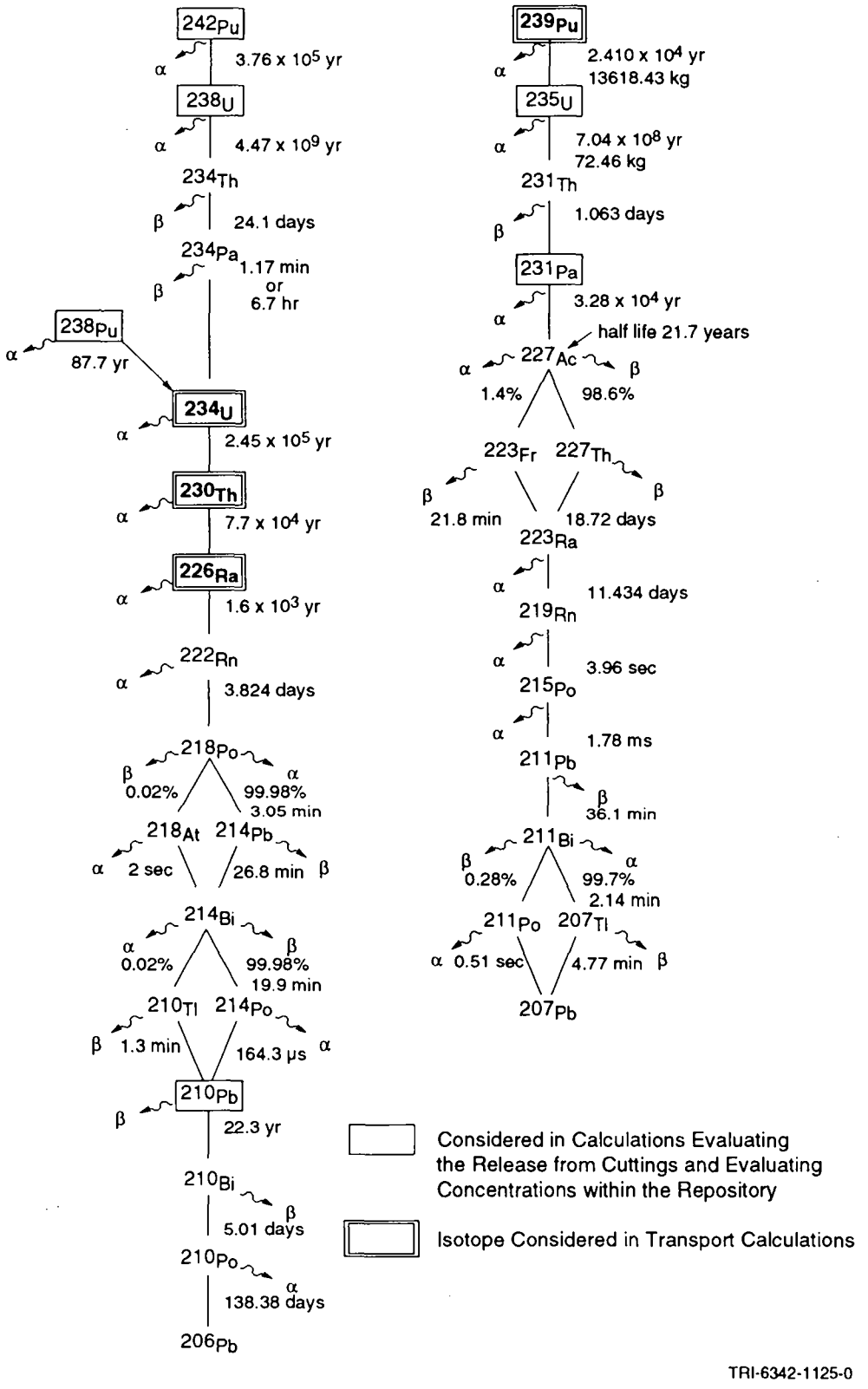

Figure 3.3-1. Decay of CH radionuclide chain in TRU-contaminated waste.

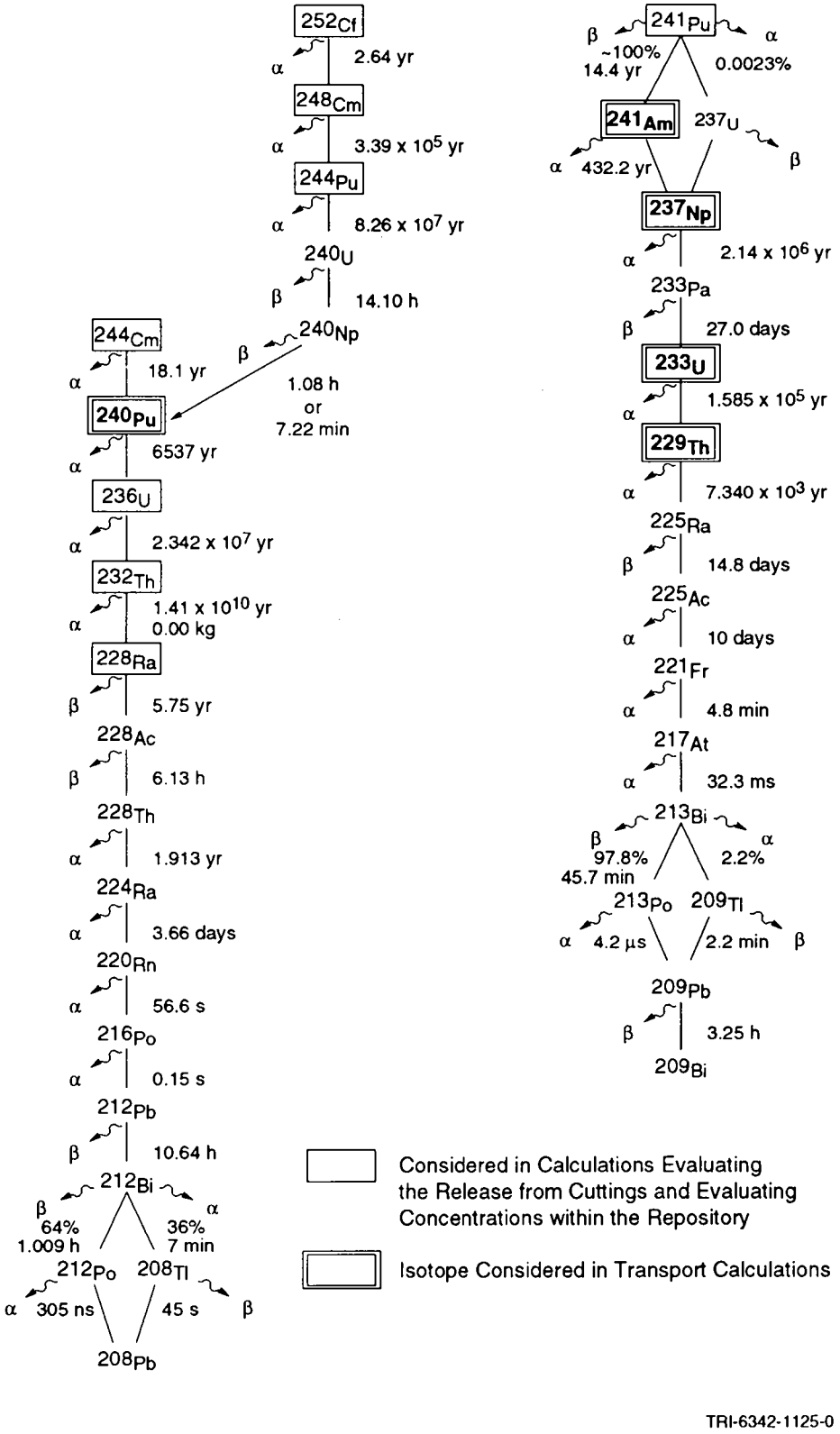

Figure 3.3-1. Decay of CH radionuclide chain in TRU-contaminated waste (concluded).

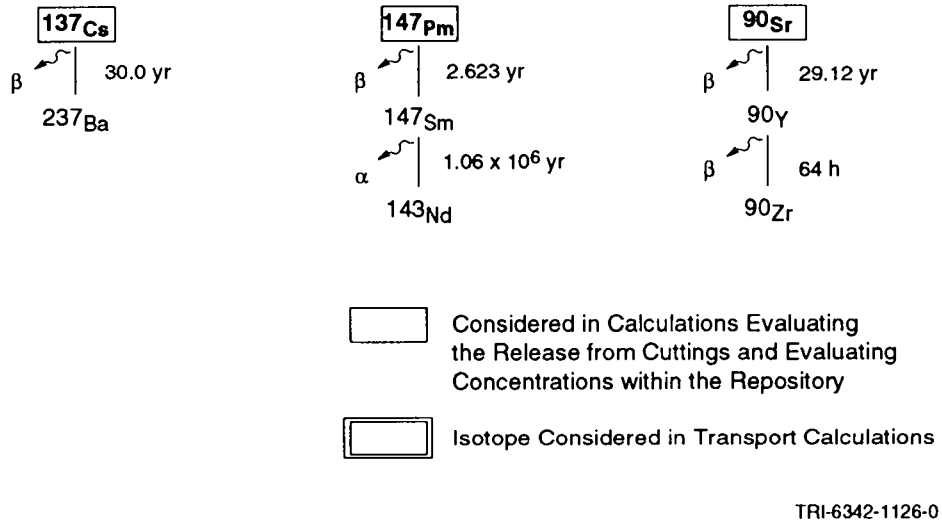

Figure 3.3-2. Decay of RH radionuclide chain in TRU-contaminated waste.

Table 3.3-2. Half-Lives of Isotopes Disposed or Created in WIPP (ICRP, Pub 38, 1983)

Radioisotope		Half-life ($t_{1/2}$) (s)	Reported
Actinium	^{228}Ac	2.207×10^{4}	6.13 h
	^{227}Ac	6.871×10^{8}	2.177×10^{1} yr
	^{225}Ac	8.64×10^{5}	10 day
Americium	^{243}Am	5.822×10^{11}	7.38×10^{3} yr
	^{241}Am	**1.364×10^{10}**	4.322×10^{2} yr
Antimony	^{125}Sb	8.741×10^{7}	2.77 yr
Astatine	^{217}At	3.23×10^{-2}	3.23×10^{-2} s
Barium	^{137m}Ba	1.531×10^{2}	2.552 min
Bismuth	^{214}Bi	1.194×10^{3}	19.9 min
	^{213}Bi	2.739×10^{3}	45.65 min
	^{212}Bi	3.633×10^{3}	60.55 min
	^{211}Bi	1.284×10^{2}	2.14 min
	^{210}Bi	4.33×10^{5}	5.012 day
Californium	**^{252}Cf**	**8.325×10^{7}**	2.638 yr
Cerium	^{144}Ce	2.456×10^{7}	284.3 day
Cesium	**^{137}Cs**	**9.467×10^{8}**	30.0 yr
	^{134}Cs	6.507×10^{7}	2.062 yr
Chromium	^{51}Cr	2.394×10^{6}	27.7 day
Cobalt	^{60}Co	1.663×10^{8}	5.221 yr
	^{58}Co	6.117×10^{6}	70.8 day
Curium	^{248}Cm	1.070×10^{13}	3.39×10^{5} yr
	^{244}Cm	**5.715×10^{8}**	18.11 yr
Europium	^{155}Eu	1.565×10^{8}	4.96 yr
	^{154}Eu	2.777×10^{8}	8.80 yr
	^{152}Eu	4.207×10^{8}	13.53 yr
Francium	^{221}Fr	2.88×10^{2}	4.8 min
Iron	^{59}Fe	3.847×10^{6}	44.53 day
Lead	^{214}Pb	1.608×10^{3}	26.8 min
	^{212}Pb	3.83×10^{4}	10.64 h
	^{211}Pb	2.166×10^{3}	3.61 min
	^{210}Pb	7.037×10^{8}	22.3 yr
	^{209}Pb	1.171×10^{4}	3.253 h
Manganese	^{54}Mn	2.7×10^{7}	312.5 day
Neptunium	^{239}Np	2.035×10^{5}	2.355 day
	^{237}Np	**6.753×10^{13}**	2.14×10^{6} yr
Niobium	^{95}Nb	3.037×10^{6}	35.15 day
Plutonium	^{244}Pu	2.607×10^{15}	8.76×10^{7} yr
	^{242}Pu	**1.187×10^{13}**	3.763×10^{5} yr
	^{241}Pu	**4.544×10^{8}**	14.4 yr
	^{240}Pu	**2.063×10^{11}**	6.537×10^{3} yr
	^{239}Pu	**7.594×10^{11}**	2.407×10^{4} yr
	^{238}Pu	**2.769×10^{9}**	87.74 yr
Polonium	^{218}Po	1.83×10^{2}	3.05 min
	^{216}Po	1.5×10^{-1}	1.5×10^{-1} s
	^{215}Po	1.78×10^{-3}	1.78×10^{-3} s
	^{214}Po	1.643×10^{-4}	1.643×10^{-4} s
	^{213}Po	4.2×10^{-6}	4.2×10^{-6} s
	^{212}Po	3.05×10^{-7}	3.05×10^{-7} s
	^{210}Po	1.196×10^{7}	138.4 day
Praseodymium	^{144}Pr	1.037×10^{3}	17.28 min
Promethium	**^{147}Pm**	**8.279×10^{7}**	2.623 yr

* *Bolding indicates isotopes assumed in initial inventory for PA calculations.*

Table 3.3-2. Half-Lives of Isotopes Disposed or Created in WIPP (ICRP, Pub 38, 1983) (Concluded)

Radioisotope		Half-life ($t_{1/2}$) (s)	Half-life ($t_{1/2}$) Reported
Protactinium	^{233}Pa	2.333×10^{6}	27 day
	^{231}Pa	1.034×10^{12}	3.276×10^{4} yr
Radium	^{228}Ra	1.815×10^{8}	5.75 yr
	^{226}Ra	5.049×10^{10}	1.6×10^{3} yr
	^{225}Ra	1.279×10^{6}	14.8 day
	^{224}Ra	3.162×10^{5}	3.66 day
	^{223}Ra	9.879×10^{5}	11.43 day
Radon	^{222}Rn	3.304×10^{5}	3.824 day
	^{220}Rn	5.56×10^{1}	5.56×10^{1} s
	^{219}Rn	3.96	3.96 s
Rhodium	^{106}Rh	2.99×10^{1}	2.99×10^{1} s
Ruthenium	^{106}Ru	3.181×10^{7}	3.682×10^{2} day
Strontium	**^{90}Sr***	**9.189×10^{8}**	29.12 yr
Thallium	^{207}Tl	2.862×10^{2}	4.77 min
Thorium	^{234}Th	2.082×10^{6}	24.1 day
	^{232}Th	**4.434×10^{17}**	1.405×10^{10} yr
	^{231}Th	9.187×10^{4}	25.52 h
	^{230}Th	2.43×10^{12}	7.7×10^{3} yr
	^{229}Th	2.316×10^{11}	7.34×10^{3} yr
	^{228}Th	6.037×10^{7}	1.913 yr
	^{227}Th	1.617×10^{6}	18.72 day
Uranium	^{240}U	5.076×10^{4}	1.41×10^{1} hr
	^{238}U	**1.41×10^{17}**	4.468×10^{9} yr
	^{236}U	7.389×10^{14}	2.342×10^{7} yr
	^{235}U	**2.221×10^{16}**	7.038×10^{8} yr
	^{234}U	7.716×10^{12}	2.445×10^{5} yr
	^{233}U	**5.002×10^{12}**	1.585×10^{5} yr
Yttrium	^{90}Y	2.304×10^{5}	64.0 h

* Bolding indicates isotopes assumed in initial inventory for PA calculations.

Note on half-life uncertainties:

Quoted standard errors of radioisotope half-lives are generally small relative to the mean values. This is illustrated by the examples provided below (taken from IAEA, 1986).

Radioisotope	Half-life
^{241}Am	(432.2 ± 0.5) y
^{252}Cf	(2.645 ± 0.008) y
^{244}Cm	(18.10 ± 0.02) y

For this reason, the PA Department regards radioisotope half-lives as precisely known parameters.

3.3.4 40 CFR 191 Release Limits and Waste Unit Factor

40 CFR 191 RELEASE LIMITS

The release limits (L_i) for evaluating compliance with *40 CFR 191 § 13* are provided in Table 3.3-3. These apply to the 1991 inventory: the release limits for 1992 are only slightly different.

Table 3.3-3. 1991 Cumulative Release Limits (L_i) to the Accessible Environment 10,000 Yr after Disposal for Evaluating Compliance with Containment Requirements (after EPA, 1985, Appendix A, Table 1)

Radionuclide	Release limit (Li) per 1 x 10^6 Ci α-emitting TRU nuclide with $t_{1/2}$ > 20 yr* (Ci)	1991 PA Release Limits $f_m L_i$** (Ci)
Americium (Am) -241 or -243	100	1187
Carbon (C) -14	100	1187
Cesium (Cs) -135 or -137	1000	11870
Iodine (I) -129	100	1187
Neptunium (Np) -237	100	1187
Plutonium (Pu) -238, -239, -240, or -242	100	1187
Radium (Ra) -226	100	1187
Strontium (Sr) -90	1000	11870
Technetium (Tc) -99	10000	118700
Thorium (Th) -230 or -232	10	118.7
Tin (Sn) -126	1000	11870
Uranium (U) -233, -234, -235, -236, or -238	100	1187
Any other α-emitting radionuclide with $t_{1/2}$ > 20 yr	100	1187
Any other non α-emitting radionuclide with $t_{1/2}$ > 20 yr	1000	11870

* Other units of waste described in EPA, 1985, Appendix A (40 CFR 191)
** 1992 PA release limits are not significantly different from those of 1991.

WASTE UNIT FACTOR

The waste unit factor (f_m) is the inventory in curies of transuranic (TRU) α-emitting radionuclides in the waste with half-lives greater than 20 yr divided by 10^6 Ci, where TRU is defined as radionuclides with atomic weights *greater* than uranium (92). Consequently, as currently defined in *40 CFR 191*, all TRU radioactivity in the waste cannot be included when calculating the waste unit factor. For the WIPP, 1.187 x 10^7 Ci of the 1991 radioactivity design total of 1.814 x 10^7 Ci came from TRU α-emitting radionuclides with half-lives greater than 20 yr (see Tables 3.3-5 and 3.3-6, WIPP PA Division, 1991, vol. 3). Regardless of the waste unit, the WIPP has assumed that all nuclides listed in Tables 3.3-1 and 3.3-2 are regulated and must be included in the release calculations. Therefore, the release limits (L_i) used by the WIPP are reduced somewhat (i.e., more restrictive).

3.3.5 Chemical and Physical Parameters of TRU Wastes

Some of the chemical and physical parameters needed for modeling the behavior of TRU wastes are summarized in Table 3.3-4. Other parameters connected with the waste forms plus their containers are discussed in Section 3.4.

Table 3.3-4. Chemical and Physical Parameters of TRU Waste

Parameter[a]	Median	Range		Units	Distribution Type	Source
Gas generation						
Corrosion						
Inundated rate	**6.3×10^{-9}**	**0**	**1.3×10^{-8}**	**mol/(m^2•s)[b]**	**Constructed**	**Brush, 1991**
Relative humid rate	**1×10^{-1}**	**0**	**5×10^{-1}**	**none**	**Constructed**	**Brush, 1991**
Microbiological						
Inundated rate	**3.2×10^{-9}**	**0**	**1.6×10^{-8}**	**mol/(kg•s)[c]**	**Constructed**	**Brush, 1991**
Relative humid rate	**1×10^{-1}**	**0**	**2×10^{-1}**	**none**	**Uniform**	**Brush, 1991**
Radiolysis	1×10^{-4}			mol/drum/yr	Constant	Brush, 1991
Gas generation stoichiometry factor						
Corrosion	**5×10^{-1}**	**0**	**1**	**none**	**Uniform**	**Brush and Anderson in Lappin et al., 1989, p. A-6**
Microbiological	**8.35×10^{-1}**	**0**	**1.67**	**none**	**Uniform**	**Brush and Anderson in Lappin et al., 1989, p. A-10**
Am						
Diffusion coefficient[d]	1.76×10^{-10}	5.3×10^{-11}	3×10^{-10}	m^2/s	Uniform	Lappin et al.,1989, Table E-7
Am						
Solubility	**-9.00**	**-13.3**	**0.0**	**log (Molar)**	**Constructed**	**See Section 3.3.5**
Cm						
Diffusion coefficient	1.76×10^{-10}	5.3×10^{-11}	3×10^{-10}	m^2/s	Uniform	Lappin et al.,1989, Table E-7
Cm						
Solubility	-9.00	-13.3	0.0	log (Molar)	Constructed	See Section 3.3.5
Np						
Diffusion coefficient	1.76×10^{-10}	5.2×10^{-11}	3×10^{-10}	m^2/s	Uniform	Lappin et al.,1989, Table E-7
Np						
Solubility	**-6.99**	**-15.5**	**-2.00**	**log (Molar)**	**Constructed**	**See Section 3.3.5**
Pb						
Diffusion coefficient	4×10^{-10}	2×10^{-10}	8×10^{-10}	m^2/s	Constructed	Lappin et al.,1989, Table E-7
Pb						
Solubility	0.210	-2.00	-1.00	log (Molar)	Constructed	See Section 3.3.5
Pu						
Diffusion coefficient	1.74×10^{-10}	4.8×10^{-11}	3×10^{-10}	m^2/s	Uniform	Lappin et al.,1989, Table E-7
Pu						
Solubility	**-9.22**	**-16.5**	**-3.4**	**log (Molar)**	**Constructed**	**See Section 3.3.5**
Ra						
Diffusion coefficient	3.75×10^{-10}	1.88×10^{-10}	7.5×10^{-10}	m^2/s	Constructed	Lappin et al.,1989, Table E-7
Ra						
Solubility	**1.04**	**0.3**	**1.26**	**log (Molar)**	**Constructed**	**See Section 3.3.5**
Th						
Diffusion coefficient	1×10^{-10}	5×10^{-11}	1.5×10^{-10}	m^2/s	Uniform	Lappin et al.,1989, Table E-7
Th						
Solubility	**-10.0**	**-15.2**	**-5.6**	**log (Molar)**	**Constructed**	**See Section 3.3.5**
U						
Diffusion coefficient	2.7×10^{-10}	1.1×10^{-10}	4.3×10^{-10}	m^2/s	Uniform	Lappin et al.,1989, Table E-7
U						
Solubility	**-3.27**	**-15.00**	**0.0**	**log (Molar)**	**Constructed**	**See Section 3.3.5**

[a] Parameters in bold were sampled in the 1992 calculations.
[b] mole/(m^2 - surface area steel • s)
[c] mole/(kg - cellulosics • s)
[d] Free liquid diffusion coefficient of the indicated species

Solubility of Specific Radionuclides*

Parameter: **Solubility (S) for Am, Cm, Np, Pb, Pu, Ra, Th, U**
Material: Radionuclide-bearing compounds in waste form

Definition Units: Log (Molar)

Values: See Table 3.3-4

Distribution: Constructed (see Figures 3.3-3[a] through 3.3-3[h] and discussion)
Correlation:

Data Source(s): Trauth, K. M., S. C. Hora, R. P. Rechard, and D. R. Anderson. In Review. *The Use of Expert Judgment to Quantify Uncertainty in Solubility and Sorption Parameters for Waste Isolation Pilot Plant Performance Assessment.* SAND92-0479. Albuquerque, NM: Sandia National Laboratories. (Copy on file at the Waste Management and Transportation Library, Sandia National Laboratories, Albuquerque, NM.) (Expert Panel Judgment)

Usage:

Mathematical model:
Repository Discharge, Section 1.4.4 of this volume.

Equations 1.4.4-5, 1.4.4-11.

Computational models:
PANEL

Ranking in Past Sensitivity Analyses:

40 CFR 191	High for Am, Np, Pu, Th, U; others Not tested
40 CFR 268	Not tested
NEPA	Not tested
Other	Not tested

*Key to Parameter Sheets is provided in Section 1.2.8.

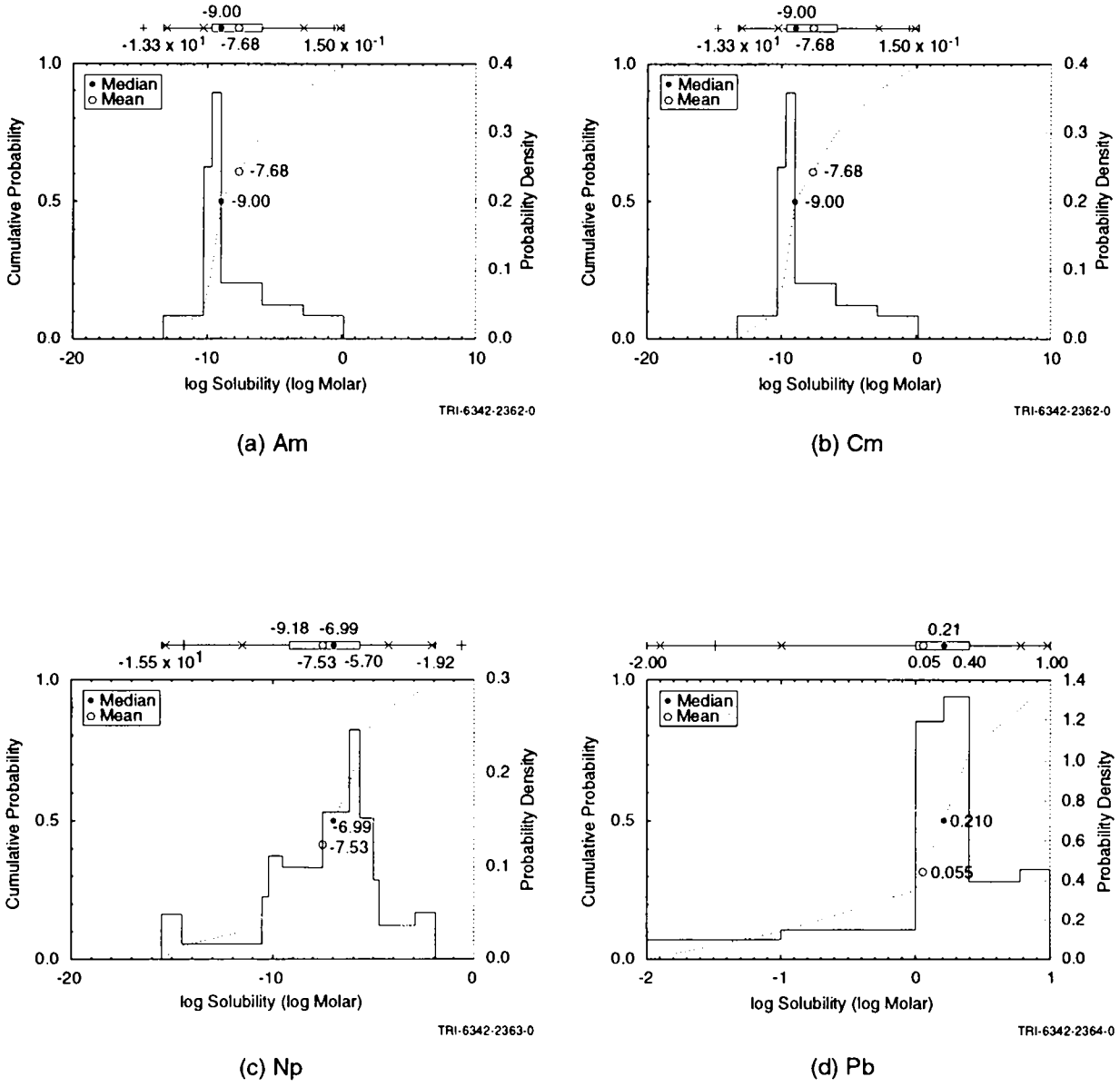

Figure 3.3-3. Constructed distribution for solubility of (a) americium (Am), (b) curium (Cm), (c) neptunium (Np), (d) lead (Pb), (e) plutonium (Pu), (f) radium (Ra), (g), thorium (Th), and (h) uranium (U).

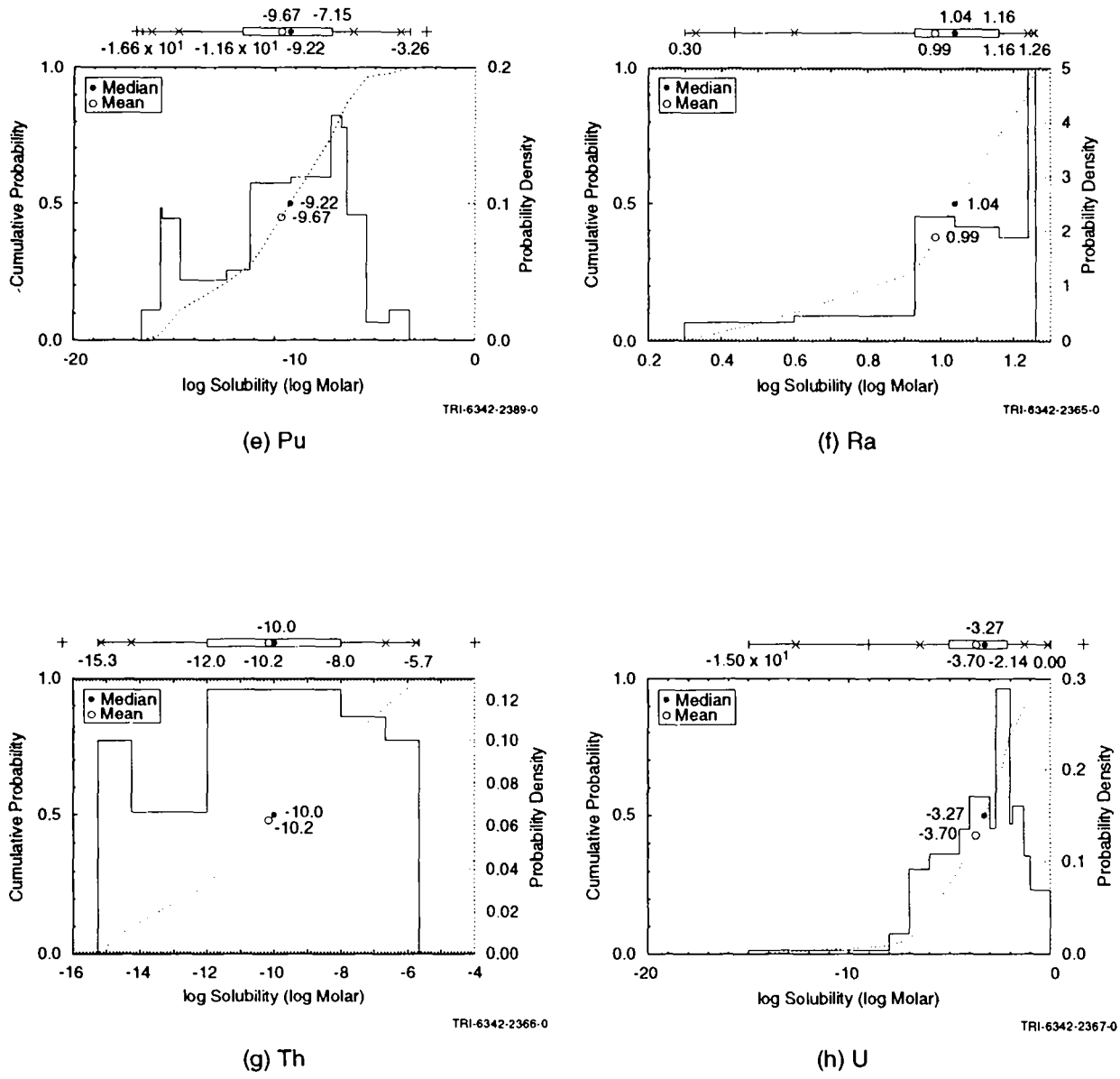

Figure 3.3-3. Constructed distribution for solubility of (a) americium (Am), (b) curium (Cm), (c) neptunium (Np), (d) lead (Pb), (e) plutonium (Pu), (f) radium (Ra), (g), thorium (Th), and (h) uranium (U) (concluded).

Discussion of Solubilities:

The distributions of solubilities elicited by Trauth et al. (1991, In Review) for the 1991 PA calculations are shown as bar diagrams in Figure 3.3-4. Different oxidation states were distinguished for Np, Pu and U; and different solution conditions were distinguished for Pb and Ra. Relative areas in pH-Eh space for the oxidation states of Np, Pu and U were also provided by the expert panel (Figure 3.3-5). No new information on solubilities was obtained in 1992.

In the 1991 PA calculations, an index variable between 0 and 1 was used to select solubilities corresponding to the several oxidation states by sampling on the relative areas in pH-Eh space. In the 1992 calculations, all solubility distributions (Figure 3.3-4) were first converted to distributions of logarithms (base 10) of Molar values; the resulting distributions having more than one oxidation state (Np, Pu, U) were then weighted according to the relative areas in pH-Eh space (Figure 3.3-5) and added to give a single distribution for each species (Figure 3.3-3). The solution condition assumed for lead (Pb) was "carbonate absent" and the solution condition assumed for radium (Ra) was "carbonate and sulfate present"; i.e., conditions giving highest values of solubility for Pb and Ra were assumed for the sake of conservatism.

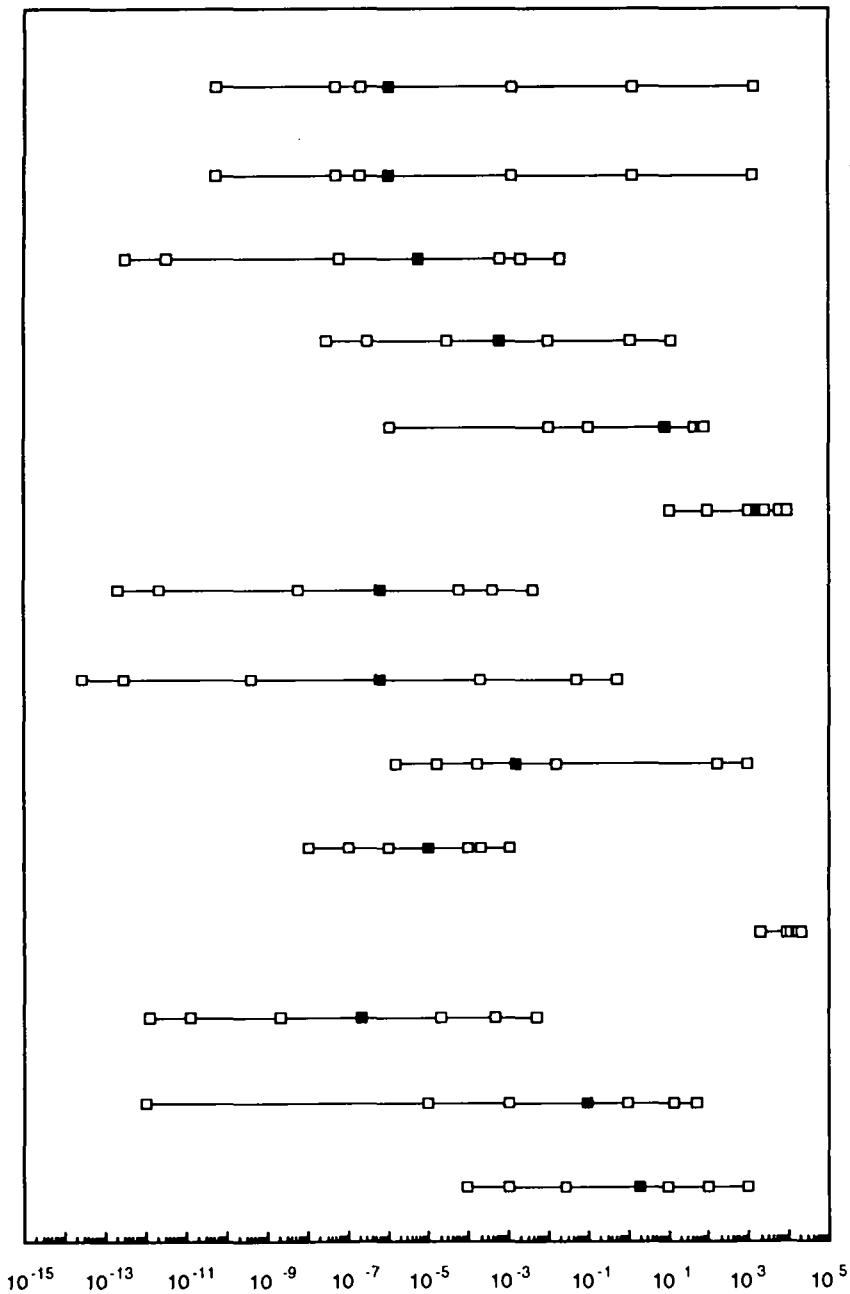

The blocks represent, from left to right, the 0.00, 0.10, 0.25, 0.50, 0.75, 0.90 and 1.00 fractiles

TRI-6342-1410-0

Figure 3.3-4. Bar diagrams of elicited distributions of solubility for americium, curium, lead, neptunium, plutonium, radium, thorium, and uranium (after Trauth et al., 1992).

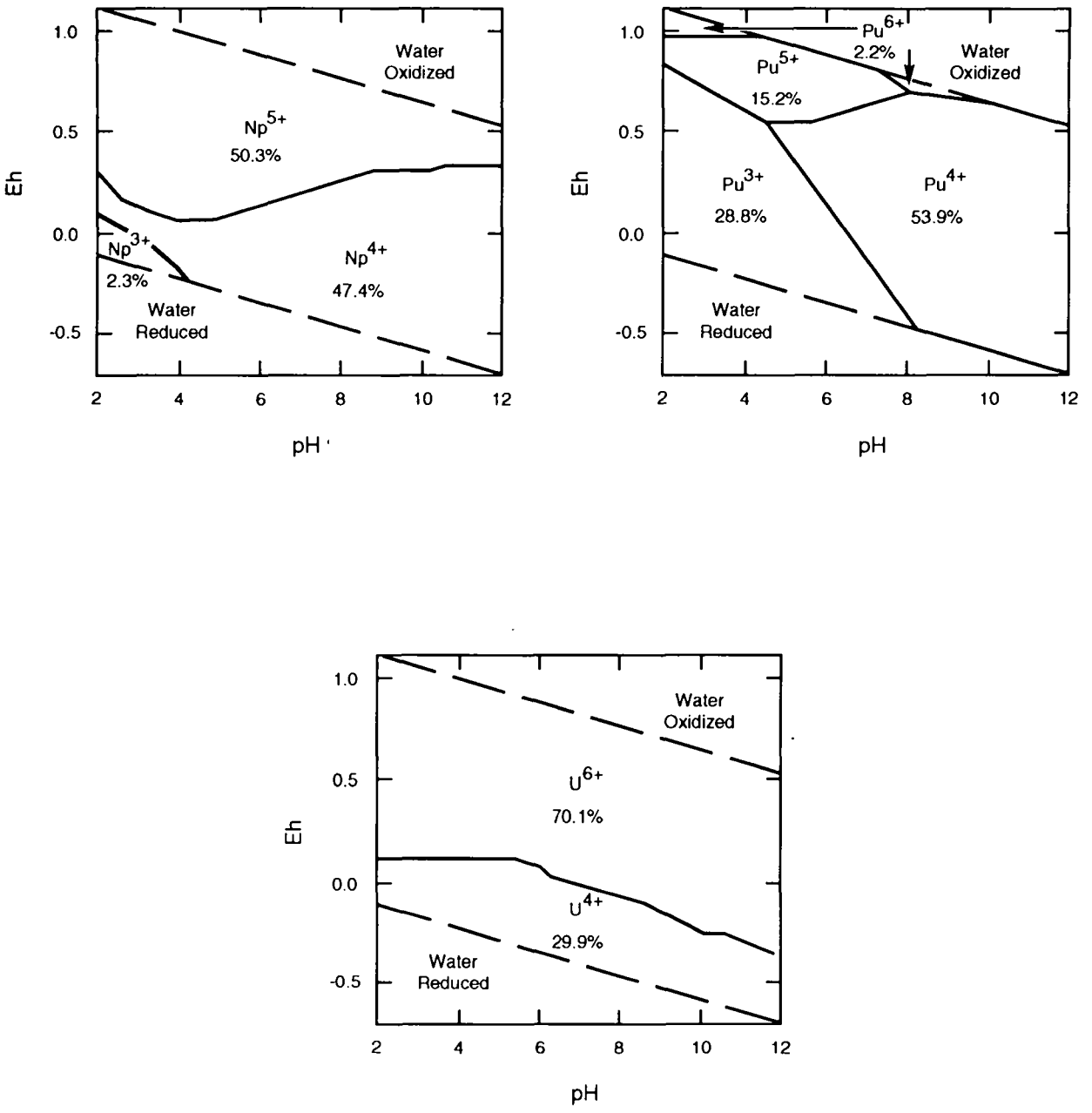

Figure 3.3-5. Estimated relative areas of stability in the pH-Eh space for neptunium, plutonium, and uranium and percentage of area of stable water.

Gas Production from Corrosion (Inundated Rate)*

Parameter:	**Gas production rates, corrosion, inundated rate** ($\dot{n}'_{CI}$)
Material:	Inundated, steel in waste form (WastRef, GRatCorI)
Definition Units:	mol H_2/(m^2-surface area steel • s)
Values:	Range: (0, 1.3×10^{-8}) Median: 6.3×10^{-9}
Distribution:	Constructed (see Figure 3.3-6)
Correlation:	

Data Source(s): Brush, L. H. 1991. Appendix A: "Current Estimates of Gas Production Rates, Gas Production Potentials, and Expected Chemical Conditions Relevant to Radionuclide Chemistry for the Long-Term WIPP Performance Assessment," *Preliminary Comparison with 40 CFR Part 191, Subpart B for the Waste Isolation Pilot Plant, December 1991. Volume 3: Reference Data.* WIPP Performance Assessment Division. Eds. R. P. Rechard, A. C. Peterson, J. D. Schreiber, H. J. Iuzzolino, M. S. Tierney, and J. S. Sandha. SAND91-0893/3. Albuquerque, NM: Sandia National Laboratories. A-25 through A-36. (Investigator Judgment)

Usage:

Mathematical model:

Two-Phase Flow, Section 1.4.1 of this volume.

Equation 1.4.1-12.

Computational models:

BRAGFLO

Ranking in Past Sensitivity Analyses:

40 CFR 191	Medium
40 CFR 268	Medium
NEPA	Not tested
Other	Not tested

*Key to Parameter Sheets is provided in Section 1.2.8.

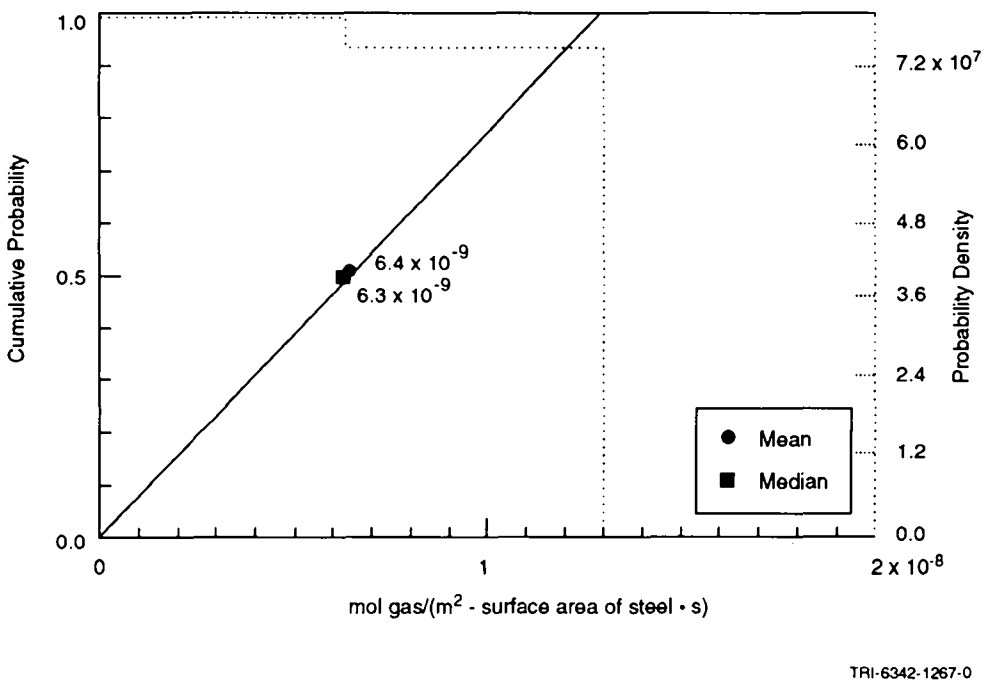

Figure 3.3-6. Constructed distribution for gas production rates from corrosion under inundated conditions.

Gas Production from Corrosion (Relative Humid Rate)*

Parameter: **Gas production rates, corrosion, relative humid rate (f)**
Material: Steel in waste form exposed to humid conditions (WastRef, GRatCorH)

Definition Units: Dimensionless

Values: Range: $(0, 5 \times 10^{-1})$ Median: 1×10^{-1}

Distribution: Constructed (see Figure 3.3-7)
Correlation:

Data Source(s): Brush, L. H. 1991. Appendix A: "Current Estimates of Gas Production Rates, Gas Production Potentials, and Expected Chemical Conditions Relevant to Radionuclide Chemistry for the Long-Term WIPP Performance Assessment," *Preliminary Comparison with 40 CFR Part 191, Subpart B for the Waste Isolation Pilot Plant, December 1991. Volume 3: Reference Data.* WIPP Performance Assessment Division. Eds. R. P. Rechard, A. C. Peterson, J. D. Schreiber, H. J. Iuzzolino, M. S. Tierney, and J. S. Sandha. SAND91-0893/3. Albuquerque, NM: Sandia National Laboratories. A-25 through A-36. (Investigator Judgment)

Usage:

Mathematical model:
Two-Phase Flow, Section 1.4.1 of this volume.

Equation 1.4.1-14.

Computational models:
BRAGFLO

Ranking in Past Sensitivity Analyses:

40 CFR 191	Low
40 CFR 268	High
NEPA	Not tested
Other	Not tested

*Key to Parameter Sheets is provided in Section 1.2.8.

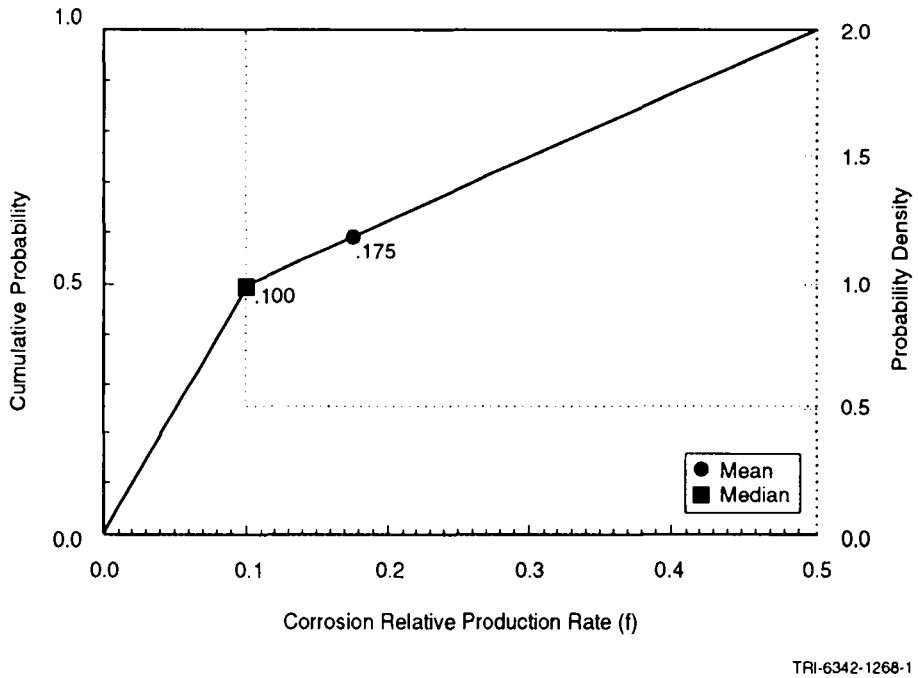

Figure 3.3-7. Constructed distribution for relative gas production rates from corrosion under humid conditions.

Gas Production from Corrosion (Stoichiometry)*

Parameter: **Anoxic iron corrosion stoichiometry (x)**
Material: Inundated steel in waste form, (WastRef, StoiCor)

Definition Units: None

Values: Range: (0, 1) Median: 0.5

Distribution: Uniform
Correlation:

Data Source(s): Brush, L. H., and D. R. Anderson. 1989. "Appendix A: Drum (Metal) Corrosion, Microbial Decomposition of Cellulose, Reactions Between Drum-Corrosion Products and Microbially Generated Gases, Reactions Between Possible Backfill Constituents and Gases and Water Chemical Reactions," *Systems Analysis, Long-Term Radionuclide Transport, and Dose Assessments, Waste Isolation Pilot Plant (WIPP), Southeastern New Mexico; March 1989*. Eds. A. R. Lappin, R. L. Hunter, D. P. Garber, and P. B. Davies. SAND89-0462. Albuquerque, NM: Sandia National Laboratories. A-3 through A-30. (Investigator Judgment)

Usage:

Mathematical model:
Two-Phase Flow, Section 1.4.1 of this volume.

Equation 1.4.1-13.

Computational models:
BRAGFLO

Ranking in Past Sensitivity Analyses:

40 CFR 191	Low
40 CFR 268	Medium
NEPA	Not tested
Other	Not tested

*Key to Parameter Sheets is provided in Section 1.2.8.

Discussion of Gas Production from Corrosion:

After waste is emplaced in the WIPP repository, some gas is expected to be generated from three types of chemical reactions: (1) anoxic corrosion, (2) biodegradation, and (3) radiolysis. In theory, the rates are dependent upon several factors, such as the chemical makeup of the waste (both organic and inorganic), the types of bacteria present, interactions among the products of the reactions, characteristics of WIPP brine, pH, and Eh. Experimental data describing these dependencies are incomplete at this time. However, some rough estimates of the range of gas generation rate values under possible WIPP environmental conditions have been made using available data.

Brush (1991) estimates gas production from corrosion for inundated and humid conditions. The estimates for inundated conditions are based on 3- and 6-month experiments by R. E. Westerman of Pacific Northwest Laboratory (PNL) on ASTM A 366 and ASTM A 570 steels by WIPP Brine A when N_2 is present at low pressures (~ 0.105 MPa [150 psig]) (Brush, 1991) (Figure 3.3-8). The following are estimated gas production and corrosion rates for inundated conditions: minimum, 0 mol H_2/m^2 steel/yr (0 mol H2/drum/yr); best estimate, 0.2 mol H_2/m^2 steel/yr (1 mol/drum/yr); and maximum, 0.4 mol H_2/m^2 steel/yr (2 mol/drum/yr) with N_2 at 0.698 MPa (1000 psig) (Brush, 1991).

Westerman also performed 3- and 6-month low-pressure humid experiments with either CO_2 or N_2 atmospheres (Brush, 1991). No H_2 production was observed except for very limited quantities from corrosion of the bottom 10% of the specimens splashed with brine during pretest preparation of the containers. Westerman is currently quantifying H_2 production from anoxic corrosion of steels in contact with noninundated backfill materials. Until further results are available, the estimated rates for humid conditions are as follows: minimum, 0 mol H_2/m^2 steel/yr (0 mol H_2/drum/yr); best estimate, 0.02 mol H_2/m^2 steel/yr (0.1 mol H_2/drum/yr); and maximum, 0.2 mol H_2/m^2 steel/yr (1 mol H_2/drum/yr) with N_2 at 0.698 MPa (1000 psig) (Brush, 1991). When expressed in terms of relative rates, the values are 0 to 0.5 with a median of 0.1.

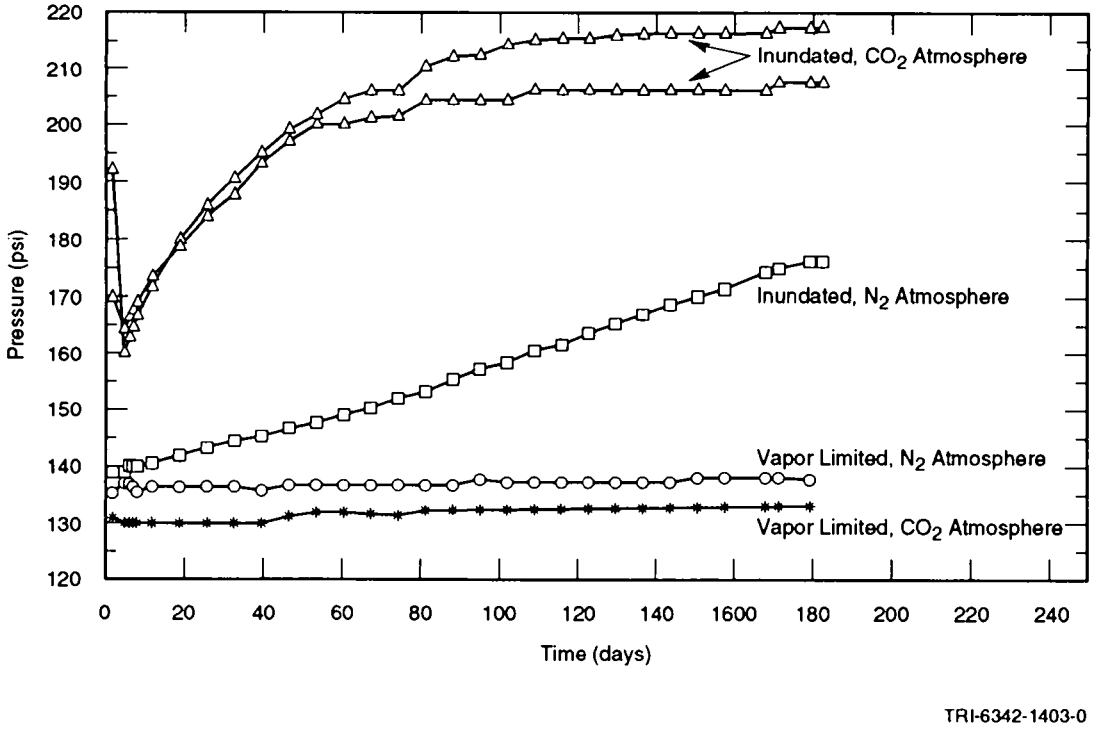

Figure 3.3-8. Pressure-time plots for 6-month anoxic corrosion experiments under brine-inundated and vapor-limited ("humid") conditions (Davies et al., 1991, Figure 6).

Gas Production from Microbiological Processes (Inundated Rate)*

Parameter: **Gas production rates, microbiological, inundated rate** ($\dot{n}_{BI}$)
Material: Inundated cellulosics in waste form (WastRef, GRatMicI)

Definition Units: mol gas/(kg - cellulosics • s)

Values: Range: (0, 1.6×10^{-8}) Median: 3.2×10^{-9}

Distribution: Constructed (see Figure 3.3-8)
Correlation:

Data Source(s): Brush, L. H. 1991. Appendix A: "Current Estimates of Gas Production Rates, Gas Production Potentials, and Expected Chemical Conditions Relevant to Radionuclide Chemistry for the Long-Term WIPP Performance Assessment," *Preliminary Comparison with 40 CFR Part 191, Subpart B for the Waste Isolation Pilot Plant, December 1991. Volume 3: Reference Data.* WIPP Performance Assessment Division. Eds. R. P. Rechard, A. C. Peterson, J. D. Schreiber, H. J. Iuzzolino, M. S. Tierney, and J. S. Sandha. SAND91-0893/3. Albuquerque, NM: Sandia National Laboratories. A-25 through A-36. (Investigator Judgment)

Usage:

Mathematical model:
Two-Phase Flow, Section 1.4.1 of this volume.

Equation 1.4.1-17.

Computational models:
BRAGFLO

Ranking in Past Sensitivity Analyses:

40 CFR 191	Low
40 CFR 268	Medium
NEPA	Not tested
Other	Not tested

*Key to Parameter Sheets is provided in Section 1.2.8.

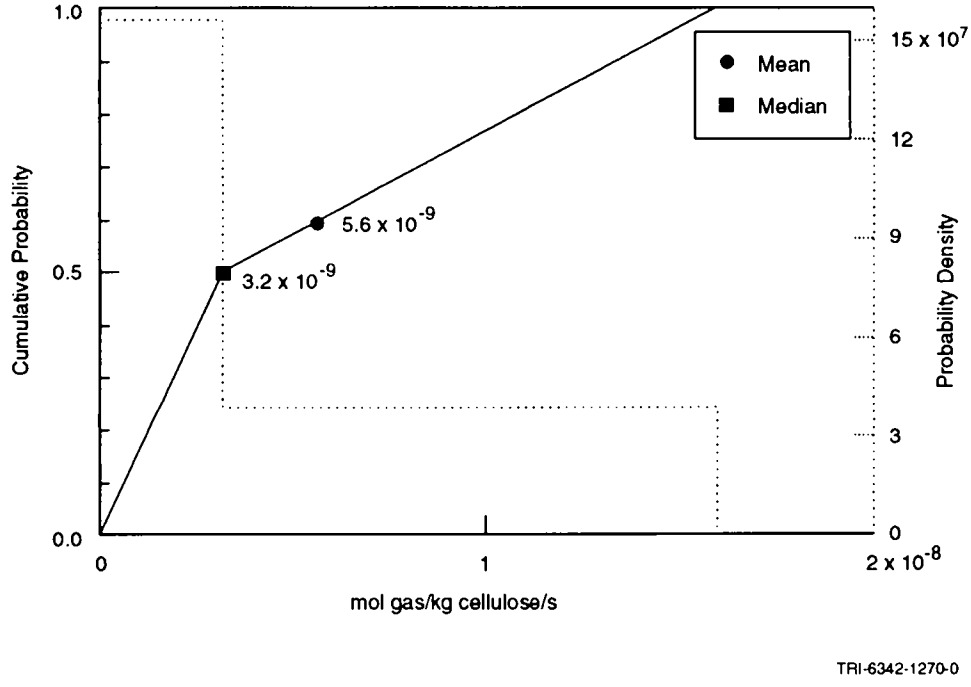

Figure 3.3-9. Constructed distribution for gas production rates from microbiological degradation under inundated conditions.

Gas Production from Microbiological Processes (Relative Humid Rate)*

Parameter:	**Gas production rates, microbiological, relative humid rate (g)**
Material:	Cellulosics in waste form, humid conditions (WastRef, GRatMicH)
Definition Units:	Dimensionless
Values:	Range: $(0, 2 \times 10^{-1})$ Median: 1×10^{-1}
Distribution:	Uniform
Correlation:	

Data Source(s): Brush, L. H. 1991. Appendix A: "Current Estimates of Gas Production Rates, Gas Production Potentials, and Expected Chemical Conditions Relevant to Radionuclide Chemistry for the Long-Term WIPP Performance Assessment," *Preliminary Comparison with 40 CFR Part 191, Subpart B for the Waste Isolation Pilot Plant, December 1991. Volume 3: Reference Data.* WIPP Performance Assessment Division. Eds. R. P. Rechard, A. C. Peterson, J. D. Schreiber, H. J. Iuzzolino, M. S. Tierney, and J. S. Sandha. SAND91-0893/3. Albuquerque, NM: Sandia National Laboratories. A-25 through A-36. (Investigator Judgment)

Usage:

Mathematical model:

Two-Phase Flow, Section 1.4.1 of this volume.

Equation 1.4.1-17.

Computational models:

BRAGFLO

Ranking in Past Sensitivity Analyses:

40 CFR 191	Low
40 CFR 268	High
NEPA	Not tested
Other	Not tested

*Key to Parameter Sheets is provided in Section 1.2.8.

Gas Production from Microbiological Processes (Stoichiometry Factor)*

Parameter: Gas generation, stoichiometry factor (S_{BH_2})

Material: Cellulosics in waste form, humid and inundated, (WastRef, StoiMic)

Definition Units: Dimensionless

Values: Range: (0, 1.67) Median: 8.35×10^{-1}

Distribution: Uniform

Correlation:

Data Source(s): Brush, L. H., and D. R. Anderson. 1989. "Appendix A: Drum (Metal) Corrosion, Microbial Decomposition of Cellulose, Reactions Between Drum-Corrosion Products and Microbially Generated Gases, Reactions Between Possible Backfill Constituents and Gases and Water Chemical Reactions," *Systems Analysis, Long-Term Radionuclide Transport, and Dose Assessments, Waste Isolation Pilot Plant (WIPP), Southeastern New Mexico; March 1989*. Eds. A. R. Lappin, R. L. Hunter, D. P. Garber, and P. B. Davies. SAND89-0462. Albuquerque, NM: Sandia National Laboratories. A-3 through A-30. (Investigator Judgment)

Usage:

Mathematical model:

Two-Phase Flow, Section 1.4.1 of this volume.

Equation 1.4.1-16.

Computational models:

BRAGFLO

Ranking in Past Sensitivity Analyses:

40 CFR 191	Low
40 CFR 268	High
NEPA	Not tested
Other	Not tested

*Key to Parameter Sheets is provided in Section 1.2.8.

Discussion of Gas Production by Microbiological Processes:

Brush (1991) estimates activity from microbiological degradation based on a recent study at Stanford University and studies carried out during the 1970s (Molecke, 1979; SNL, 1979; Barnhart et al., 1980; Caldwell et al., 1988). A test plan for laboratory experiments (Brush, 1990) and in-situ gas production experiments using real waste at the WIPP (Lappin et al., 1989) describe experiments currently underway. Although the Stanford tests seemed to suggest that microbial gas production may be significant under laboratory conditions but not under repository conditions, results from the earlier tests implied significant microbial gas production under both realistic and overtest conditions. However, until the Stanford tests are corroborated, the best estimate for microbial gas production has remained the same as first proposed by Brush and Anderson (in Lappin et al., 1989; Brush, 1990), 0.1 mole of various gases per kg cellulosics per year (1 mol gas/(drum•yr)). However, new minimum and maximum rates for inundated conditions are 0 and 0.5 mol/(kg•yr) (5 mol per drum per year), respectively.

For humid conditions, new minimum and best estimates for microbial gas production rates are 0 and 0.01 mol/(kg cellulosics•yr) (0.1 mol/(drum•yr)). The maximum estimate under humid conditions remains unchanged from the value estimated by Brush and Lappin (1990), 0.1 mol/(kg•yr) (1 mol/(drum•yr)). Expressed in terms of relative rates, the values are 0 to 0.2 with a median of 0.1.

Microbiologic Degradation Stoichiometry. The stoichiometry of the net biodegradation reaction is uncertain. About 20 reactions have been postulated and others may be possible, according to Brush and Anderson (Lappin et al., 1989, p. A-10). The reactions depend on such factors as what electron donors are available, the solubility of CO_2, and interaction with products of corrosion, pH, and Eh. It is not known at this time what effect biodegradation has on water (brine) inventory, so it is assumed to have no net effect, neither consuming water nor producing it. Some of the postulated reactions produce gas; others consume it. At present, we know that some gas (CO_2 and some H_2, H_2S, and CH_4) may be produced and that cellulose (CH_2O) will be consumed. Using the stoichiometry recommended in Lappin et al. (1989, Supplement to Appendix A.1, p. A-30) that yields the maximum gas generation per unit of cellulose (5/3 mol gas/mol CH_2O), the biodegradation reaction may be written

$$CH_2O + \text{unknowns} + \text{microbes} = 5/3\ \text{gas} + \text{unknowns}$$

However, in view of the wide variety of reactions that may occur, together with our current lack of knowledge as to precisely which reactions do occur, it is prudent to sample on the stoichiometric coefficient for gas in this reaction. If the assumption is also made that any CO_2 that is produced will dissolve in the WIPP brine, then of the reactions presented in Lappin et al. (1989) only one reaction will consume gas, that one being

$$CH_2O + O_2 = H^+ + HCO_3^-$$

This reaction requires oxygen, which will be present initially in air and will be produced by radiolysis. Neither source of oxygen is sufficient to oxidize all of the cellulose in the inventory, and oxic corrosion will compete strongly for this oxygen, so this reaction is expected to be of minor importance. None of the other reactions consumes gas, whereas most produce gas, with the net gas production ranging from 0 to 5/3 mol gas/mol CH_2O. Therefore, the stoichiometric coefficient is sampled from a uniform distribution ranging from 0 to 5/3.

3.4 Parameters for Unmodified Waste Form Including Containers

As of 1990, the currently stored CH-TRU waste that will be disposed of in the WIPP, if authorized, is estimated to be about 60,000 m^3 (2.1 x 10^6 ft^3), which is about 34% of the design storage volume of 1.756 x 10^5 m^3 (6.2 x 10^6 ft^3). The stored waste consists of about 180,000 0.21-m^3 (55-gal) drums, 5,000 1.8-m^3 (64 ft^3) Standard Waste Boxes (SWBs), and 7,000 3.2-m^3 (113-ft^3) miscellaneous containers, mostly steel and fiberglass reinforced plywood (FRP) boxes. Drums and SWBs are the only containers that can currently be transported in a TRUPACT-II. If the waste in boxes other than SWBs were repackaged into SWBs, it was estimated that 533,000 0.21-m^3 (55-gal) drums and 33,500 1.8-m^3 (64-ft^3) SWBs could be emplaced in the WIPP repository containing approximately 170,000 m^3 (6.2 x 106 ft^3) of waste, the design volume for CH-TRU waste.

The volume of RH-TRU waste is limited by the agreement between DOE and the State of New Mexico to 7.08x10^3 m^3 (0.25 x 10^6 ft^3) (U.S. DOE and NM, 1984). RH waste will likely be placed in 0.89-m^3 (31.4-ft^3) canisters in the walls of the rooms and access drifts. (Placement of canisters is discussed in Section 3.1.6.)

The parameter values for unmodified waste that is expected to be shipped (i.e., to meet the current waste acceptance criteria [WAC] discussed below) are provided in Table 3.4-1. The significant figures for masses that are reported in this table should not be interpreted as known accuracy. (Indeed, the majority of waste to be emplaced in the WIPP has not been generated; hence, the amounts are uncertain.) The significant figures in the table for masses are presented as a means to trace the work until a report detailing the assumptions and calculations pertaining to these amounts has been prepared. On the other hand, the significant figures on design volumes are important since the limits on volumes agreed upon by the DOE and the State of New Mexico (U.S. DOE and NM, 1984) were in English units and are an exact conversion.

All CH- and RH-TRU waste must meet the WIPP *Waste Acceptance Criteria* (WAC) (WEC, 1991). These criteria includes requirements for the waste form. For example, the waste material shall (1) include only residual liquids in well-drained containers (e.g., bottles, cans, etc.) in quantities less than 1% of the container volume and the total liquid shall be less than 1% of waste container volume, (2) not permit explosives or compressed gases, and (3) limit radionuclides in spontaneously combustible pyrophoric form to less than 1% by weight in each waste package. There also are limitations on the curie content in a drum, SWB, and canister based on transportation considerations (Table 3.4-2).

Table 3.4-1. Parameter Values for Unmodified TRU Waste Categories, Containers, and Salt Backfill

Parameter[a]	Median	Range		Units	Distribution Type	Source
CH-TRU waste						
Molecular weight						
Cellulose	0.030			kg/mol	Constant	CH_2; Weast and Astle, 1981
Iron	0.05585			kg/mol	Constant	Fe; Weast and Astle, 1981
Density, grain (ρ_g)						
Metal/glass	3.44×10^3			kg/m^3	Constant	Butcher, 1990, Table 2
Combustibles	1.31×10^3			kg/m^3	Constant	Butcher, 1990, Table 2
Sludge	2.15×10^3			kg/m^3	Constant	Butcher, 1990, Table 2
Salt backfill	2.14×10^3			kg/m^3	Constant	WIPP PA Division, 1991, Vol. 3, Table 2.3-1
Steel, cold-drawn	7.83×10^3			kg/m^3	Constant	Perry et al., 1969, Table 3-137
Air @ 300.15K, 1 atm	1.177			kg/m^3	Constant	Vennard and Street, 1975, p. 709
Volumes of IDB Categories[b]						
Metal/glass fraction	**3.76×10^{-1}**	**2.76×10^{-1}**	**4.76×10^{-1}**	**none**	**Normal**	**See Section 3.4.1**
Combustibles fraction	**3.84×10^{-1}**	**2.84×10^{-1}**	**4.84×10^{-1}**	**none**	**Normal**	**See Section 3.4.1**
Salt backfill	1.712×10^5			m^3	Constant	WIPP PA Division, 1991, Vol 3, Figure 3.1-3
Air @ 300.15K, 1 atm	8.908×10^4			m^3	Constant	WIPP PA Division, 1991, Vol 3, Figure 3.1-3
Average per Drum						
Metal/glass	6.44×10^1	3.05×10^1	9.83×10^1	kg/drum	Normal	Butcher, 1989, Table 7
Combustibles	4.00×10^1	1.73×10^1	6.26×10^1	kg/drum	Normal	Butcher, 1989, Table 6
Sludge	2.25×10^2			kg/drum	Constant	WIPP PA Division, 1991, Vol. 3, Table 3.4-10
Mass of IDB Categories[b]						
Metal/glass	1.984×10^7					WIPP PA Division, 1991, Vol. 3, Tables 3.4-10 and 3.4-12
Combustibles	1.348×10^7					WIPP PA Division, 1991, Vol. 3, Tables 3.4-10 and 3.4-12
Mass of Steel Containers in IDB Categories[b]						
Metal/glass	1.076×10^7			kg	Constant	WIPP PA Division, 1991, Vol. 3, Table 3.4-10
Combustibles	1.178×10^7			kg	Constant	WIPP PA Division, 1991, Vol. 3, Table 3.4-10
Sludge	3.598×10^6			kg	Constant	WIPP PA Division, 1991, Vol. 3, Table 3.4-10
Mass of Steel Containers and Liners in IDB Categories[b]						
Metal/glass	4.458×10^6			kg	Constant	WIPP PA Division, 1991, Vol. 3, Table 3.4-10
Combustibles	1.214×10^7			kg	Constant	WIPP PA Division, 1991, Vol. 3, Table 3.4-10
Sludge	1.329×10^7			kg	Constant	WIPP PA Division, 1991, Vol. 3, Table 3.4-10
Mass of Contents						
Iron, steel, paint cans, shipping cans	1.431×10^7			kg	Constant	WIPP PA Division, 1991, Vol. 3, Table 3.4-12
Steel in containers	2.613×10^7			kg	Constant	WIPP PA Division, 1991, Vol. 3, Table 3.4-10
Cellulosics, + 50% gloves, Hypalon, Neoprene, rubber	7.475×10^6			kg	Constant	WIPP PA Division, 1991, Vol 3, Table 3.4-12

[a]Parameters in bold were sampled in the 1992 calculations.
[b]IDB = Integrated Data Base

Table 3.4-1. Parameter Values for Unmodified TRU Waste Categories, Containers, and Salt Backfill (Concluded)

Parameter[a]	Median	Range		Units	Distribution Type	Source
Capillary pressure (ρ_c) and relative permeability ($k_{\ell r}$)						
Threshold displacement pressure (ρ_t)	2.02×10^{3}	2.02×10^{1}	2.02×10^{5}	Pa	Lognormal	Davies, 1991a, 1991b
Residual Saturations						
Wetting phase ($S_{\ell r}$)	2.76×10^{-1}	1.38	5.52×10^{-1}	none	Constructed	Brooks and Corey, 1964
Gas phase (S_{gr})	7×10^{-2}	3.5×10^{-2}	1.4×10^{-1}	none	Constructed	Brooks and Corey, 1964
Brooks-Corey Exponent (η)	2.89	1.44	5.78	none	Constructed	Brooks and Corey, 1964
Drilling Erosion Parameters						
Absolute roughness (ε)	2.5×10^{-2}	1×10^{-2}	4×10^{-2}	m	Uniform	Streeter and Wylie, 1975, Figure 5.32.
Shear strength (τ_{fail})	1	1×10^{-1}	1×101	Pa	Constructed	Sargunam et al., 1973; Henderson, 1966
Partition Coefficient for clays in salt backfill						
Am	1×10^{-4}			m^3/kg	Constant	Lappin et al., 1989, Table D-5 (Kd_{clay}/1000)
Np	1×10^{-5}			m^3/kg	Constant	Lappin et al., 1989, Table D-5 (K_{dclay}/1000)
Pb	1×10^{-6}			m^3/kg	Constant	Lappin et al., 1989, Table D-5 (K_{dclay}/1000)
Pu	1×10^{-4}			m^3/kg	Constant	Lappin et al., 1989, Table D-5 (K_{dclay}/1000)
Ra	1×10^{-6}			m^3/kg	Constant	Lappin et al., 1989, Table D-5 (K_{dclay}/1000)
Th	1×10^{-4}			m^3/kg	Constant	Lappin et al., 1989, Table D-5 (K_{dclay}/1000)
U	1×10^{-6}			m^3/kg	Constant	Lappin et al., 1989, Table D-5 (K_{dclay}/1000)
Permeability (k) [used in 1991 calculations][b]						
Average	1×10^{-13}			m^2	Constant	Lappin et al., 1989, Table 4-6
Combustibles	1.7×10^{-14}	2×10^{-15}	2×10^{-13}	m^2	Constructed	Butcher et al., 1991
Metals/glass	5×10^{-13}	4×10^{-14}	1.2×10^{-12}	m^2	Constructed	Butcher et al., 1991
Sludge	1.2×10^{-16}	1.1×10^{-17}	1.7×10^{-16}	m^2	Constructed	Butcher et al., 1991
Porosity (ϕ) [used in 1991 calculations][b]						
Average	1.9×10^{-1}			none	Constant	WIPP PA Division, 1991, Vol 3, Section 3.4.8
Combustibles	1.4×10^{-2}	8.7×10^{-2}	1.8×10^{-1}	none	Constructed	Butcher et al., 1991
Metals/glass	4×10^{-1}	3.3×10^{-1}	4.4×10^{-1}	none	Constructed	Butcher et al., 1991
Sludge	1.1×10^{-1}	1×10^{-2}	2.2×10^{-1}	none	Constructed	Butcher et al., 1991
Saturation, initial ($S_{\ell i}$)	**0.07**	**0**	**0.14**	**none**	**Uniform**	**See Section 3.4.4.**

[a]Parameters in bold were sampled in the 1992 calculations.
[b]See Sections 1.4.1 and 1.4.7 for 1992 methods of calculating permeability and porosity of unmodified waste, containers, and salt backfill.

Table 3.4-2. Summary of Waste Acceptance Criteria and Requirements Applicable to Performance Assessment

Description	Waste Type	WAC Criterion or Requirement
Particulates	CH & RH	Immobilize if greater than 1% by weight below 10 microns Immobilize if greater than 15% by weight below 200 microns
Liquids	CH & RH	Liquids that result from liquid residues remaining in well-drained containers; condensation moisture; and liquid separation from sludges or resin settling shall be less than 1% by volume of the waste container
Pyrophoric Materials	CH & RH	Radionuclides in pyrophoric form are limited to less than 1% by weight in each waste package. No non-radionuclide pyrophorics permitted.
Explosives and compressed gas	CH & RH	No explosives or compressed gases are permitted.
Specific Activity	CH	The specific activity shall be greater than 100 nCi/g TRU radionuclides, excluding the weight of added shielding, rigid liners, and waste containers.
	RH	The specific activity shall be greater than 100 nCi/g TRU radionuclides, excluding the weight of external shielding, rigid liners, and the waste containers. The container average maximum activity concentration shall not exceed 23 curies/liter.
Nuclear Criticality* (Pu-239 FGE)**	CH	The fissile or fissionable radionuclide content shall be less than 200 FGE for a 55-gallon drum. The fissile or fissionable radionuclide content shall be less than 325 FGE for a SWB. The fissile or fissionable radionuclide content shall be less than 325 FGE for a TRUPACT-II
	RH	The fissile or fissionable radionuclide content shall be less than 325 FGE.
Pu-239 Activity*	CH & RH	Waste packages shall not exceed 1000 Ci of Pu-239 equivalent activity.

* Transportation requirement
** Fissile gram equivalent of Pu-239

3.4.1 Composition of CH-TRU Waste (Non-Radionuclide/Non-RCRA Inventory)

TRU waste destined for the WIPP is generated or currently stored by ten DOE nuclear weapon facilities. Although we know that this TRU waste consists in general of laboratory and production line waste, such as glassware, metal pipes, sorbed or solidified spent solvents, disposal laboratory clothing, cleaning rags, and solidified sludges, the precise composition of the waste (e.g., percentages by weight and volume) is not well defined. Estimates of metals/glass combustible and sludge reported here were made based on information on volumes submitted annually to the IDB by the generator sites and therefore are from the same source as the radionuclide inventory. A full discussion of these estimates is given in Section 3.4.1 of WIPP PA Division (1991, Vol. 3). Only estimates of the volumes of various categories of CH-TRU contaminated waste are discussed here.

Volume Fraction, Combustibles*

Parameter: **Volume fraction, combustibles (fc)**
Material: Unmodified waste form including containers (WastRef, Vol Wood)

Definition Units: Dimensionless

Values: Range: (0.284, 0.484) Median: 0.384

Distribution: Normal
Correlation:

Data Source(s): See text and Table 3.4-6. (Investigator Judgment)

Usage:

Mathematical model:
Two-Phase Flow, Section 1.4.1 of this volume.

Equation 1.4.1-17.

Computational models:
BRAGFLO

Ranking in Past Sensitivity Analyses:

40 CFR 191	Low
40 CFR 268	Medium
NEPA	Not tested
Other	Not tested

*Key to Parameter Sheets is provided in Section 1.2.8.

Volume Fraction, Metals/Glass*

Parameter: **Volume fraction, metals/glass**
Material: Unmodified waste form including containers (WastRef,Vol Metal)

Definition Units: Dimensionless

Values: Range: (0.276, 0.476) Median: 0.376

Distribution: Normal
Correlation:

Data Source(s): See text and Table 3.4-6. (Investigator Judgment)

Usage:

Mathematical model:

Two-Phase Flow, Section 1.4.1 of this volume.

Equation 1.4.1-12 (used in computing Ad, the surface area of steel in an equivalent drum).

Computational models:

BRAGFLO

Ranking in Past Sensitivity Analyses:

40 CFR 191	Low
40 CFR 268	Medium
NEPA	Not tested
Other	Not tested

*Key to Parameter Sheets is provided in Section 1.2.8.

Discussion:

Estimates of the masses and volumes of the constituents of TRU waste that affect gas generation, transport, and room properties are required for performance assessment. Because the majority of the waste to be emplaced in the WIPP has not been generated, the waste characterization is an estimate with a potentially large uncertainty. The estimated waste characterization is used as a base for analyses that include the uncertainty in waste characterization. The following discussion presents the method that was used to estimate the characterization of the waste. The intent was to use available information and to use a reasonable method to scale it up to the design volume, which was used in performance assessment. This method resulted in estimates of volumes and masses of waste by generator site; however, these results should not necessarily be considered as indicative of the actual masses and volumes that the sites will generate.

The total anticipated volume (stored waste and projected annual volumes) of the TRU waste calculated from information reported in the yearly IDB has been decreasing over the period 1987-1990 (Table 3.4-3). The most significant change from 1987 to 1990 is the percentage of concreted or cemented sludge; the estimated volume decrease was about 30%. Furthermore, the information contained in the 1990 IDB indicates that generators anticipate there will be less volume of absorbed sludges and more volume of concreted and cemented sludges in the projected waste than is contained in the stored waste.

The 1990 IDB was used as the basis for the estimate of the total volume of CH-TRU waste for the 1991 PA calculations. Table 3.4-4 lists the stored and projected (generated in the future) waste volume by generator site listed in the 1990 IDB. The IDB uses the terms "stored" and "newly generated" waste. In the discussion that follows, the term "projected" is used in place of "newly generated."

For performance assessment calculations, we assume that a design volume of 175,564 m^3 (6.2 x 10^6 ft^3) will be emplaced in the WIPP. The following discussion presents the method that was used to estimate the volumes of the waste types if the current design volume of waste was emplaced. To estimate the volume of waste by generator site to fill the WIPP, it was assumed that the five largest generators* of projected waste would provide the additional volume. The percentage of the total projected waste for each site was calculated and, based on this percentage, volumes for the five sites were calculated to provide an additional 69,105 m^3 (2.4 x 10^6 ft^3). The scaled volume for the five sites is shown in Table 3.4-4.

Details of the volumes and physical composition of CH-TRU waste as calculated from the information from the 1990 IDB are listed in Table 3.4-5.

For performance assessment calculations, hydraulic properties of the disposal area contents are required. To estimate the volume fraction of the sludges, combustibles, and metals and glass in CH-TRU waste, it was assumed the volume of the sludges included the absorbed liquid and sludges, concreted or cemented sludges, and dirt, gravel and asphalt categories of Table 3.4-5. The volume of filter, filter media, and "other" categories of Table 3.4-5 were distributed into the volume of sludges, combustibles, and metals and glass based on the relative volume of the initial amounts of each of these categories. PA Department estimates for the volume fraction of stored; projected; projected plus scaled; and stored, projected, and scaled are tabulated in Table 3.4-6.

* These five DOE defense facilities for 1990 are Hanford Reservation (HANF), Washington; Idaho National Engineering Laboratory (INEL), Idaho; Los Alamos National Laboratory (LANL), New Mexico; Rocky Flats Plant (RFP), Colorado; and Savannah River Site (SRS), South Carolina. In 1991, INEL was reclassified as a storage site rather than a generator site because a project that would generate waste was indefinitely delayed/cancelled.

Table 3.4-3. Estimated Composition by Volume of CH-TRU Contaminated Waste from 1987 to 1990.

Year	Combustibles (%)	Metal and Glass (%)	Absorbed Liquid and Sludge (%)	Concrete/ Cemented Sludge (%	Dirt/ Gravel/ Asphalt (%)	Filters/ Filter Media (%)	Other (%)	Total Volume (m3)
1987	38.87	31.53	8.99	7.37	1.33	5.81	6.11	158,526
1988	39.84	34.18	7.28	8.00	2.44	4.53	3.73	136,402
1989	32.01	36.41	6.09	16.41	1.31	3.00	4.78	120,243
1990	34.24	34.31	6.28	14.43	1.30	3.67	5.77	106,459

* Design volume is 175,564 m^3.

Table 3.4-4. Estimate of a Design Volume for CH-TRU Waste

Site	Stored Volume (1990 IDB) (m^3)	Projected Volume (1990 IDB) (m^3)	Total Volume (1990 IDB) (m^3)	Scaled Volume* (m^3)	Estimated Design Volume (m^3)
ANL-E	--	180	180	--	180
HANF	10,041	943	10,984	1,499	12,484
INEL	37,420	4,666	42,086	7,417	49,503
LANL	7,393	4,800	12,193	7,631	19,824
LLNL	--	1,207	1,207	--	1,207
MOUND	--	945	945	--	945
NTS	606	--	606	--	606
ORNL	662	600	1,262	--	1,262
RFP	792	16,272	17,064	25,869	42,933
SRP	3,143	16,788	19,931	26,689	46,620
Total	60,057	46,402	106,459	69,105	175,564

* Assuming that HANF, INEL, LANL, RFP, and SRP provide the difference between the current total inventory and the design volume. The difference between the total volume of 106,458 m^3 in the 1990 IDB and the design volume of 175,564 m^3 (6.2x10^6 ft^3) was apportioned between the five sites based on their estimated annual generation rates. These five sites provide 94% of the estimated total annual volume of 1,993.4 m^3 per year.

Table 3.4-5. Estimated Composition of CH-TRU Contaminated Waste in 1990 by Generator (U.S. DOE, 1990d, Tables 3.5, 3.7, 3.10)

Category	ANL-E	HANF	INEL	LANL	LLNL	NTS	MOUND	ORNL	RFP	SRS	Percent	Total (m^3)	Percent of Total
STORED													
Absorbed Liquid and Sludge	--	0.0	4490.4	1626.5	--	0.0	--	0.0	122.8	0.0	10.39	--	--
Combustibles	--	4317.6	9355.0	961.1	--	312.2	--	390.3	287.5	2200.1	29.68	--	--
Concreted or Cemented Sludge	--	602.5	4864.6	2217.9	--	6.1	--	0.0	5.5	0.0	12.82	--	--
Dirt, Gravel, or Asphalt	--	301.2	0.0	0.0	--	0.0	--	6.6	5.5	0.0	0.52	--	--
Filters or Filter Media	--	0.0	1871.0	369.7	--	0.0	--	33.1	327.1	0.0	4.33	--	--
Glass/Metal/Similar Noncombustibles	--	4819.7	13097.0	2217.9	--	288.0	--	231.6	43.6	942.9	36.03	--	--
Other	--	0.0	3742.0	0.0	--	0.0	--	0.0	0.0	0.0	6.23	--	--
TOTAL	--	10041.0	37420.0	7393.1	--	606.3	--	661.6	792.0	3143.0	--	--	--
Percent of Total	--	9.43	35.15	6.94	--	0.57	--	0.62	0.74	2.95	--	--	--
PROJECTED													
Absorbed Liquid and Sludge	64.8	0.0	0.0	48.0	0.0	--	0.0	0.0	0.0	335.8	0.97	6688.2[a]	6.28[a]
Combustibles	57.6	377.3	2020.2	1944.0	881.3	--	9.5	72.0	2522.2	10744.3	40.15	36452.2	34.24
Concreted or Cemented Sludge	0.0	132.0	737.2	864.0	12.1	--	9.5	0.0	5906.7	0.0	16.51	15358.1	14.43
Dirt, Gravel, or Asphalt	0.0	113.2	0.0	0.0	0.0	--	841.6	6.0	113.9	0.0	2.32	1388.1	1.30
Filters or Filter Media	0.0	94.3	23.3	120.0	84.5	--	0.0	30.0	113.9	839.4	2.81	3906.3	3.67
Glass/Metal/Similar Noncombustibles	57.6	226.4	681.2	1824.0	181.1	--	85.1	492.0	6720.3	4616.7	32.08	36525.0	34.31
Other	0.0	0.0	1203.7	0.0	48.3	--	0.0	0.0	895.0	251.8	5.17	6140.8	5.77
TOTAL	180.0	943.2	4665.6	4800.0	1207.2	--	945.6	600.0	16272.0	16788.0		106458.6	100.00
Percent of Total	0.17	0.89	4.38	4.51	1.13	--	0.89	0.56	15.28	15.77		100.00	
PROJECTED PLUS SCALED													
Absorbed Liquid and Sludge	64.8	0.0	0.0	124.3	0.0	0.0	0.0	0.0	0.0	869.5	0.92	7298.3[b]	4.16[b]
Combustibles	57.6	977.1	5231.9	5034.5	881.3	0.0	9.5	72.0	6531.8	27825.3	40.36	64444.8	36.71
Concreted or Cemented Sludge	0.0	342.0	1909.1	2237.6	12.1	0.0	9.5	0.0	15297.1	0.0	17.15	27503.8	15.67
Dirt, Gravel, or Asphalt	0.0	293.1	0.0	0.0	0.0	0.0	841.6	6.0	295.0	0.0	1.24	1749.1	1.00
Filters or Filter Media	0.0	244.3	60.4	310.8	84.5	0.0	0.0	30.0	295.0	2173.9	2.77	5799.6	3.30
Glass/Metal/Similar Noncombustibles	57.6	586.2	1764.1	4723.7	181.1	0.0	85.1	492.0	17404.1	11956.2	32.25	58890.8	33.54
Other	0.0	0.0	3117.4	0.0	48.3	0.0	0.0	0.0	2317.7	652.2	5.31	9877.5	5.63
TOTAL	180.0	2442.7	12082.8	12430.9	1207.2	0.0	945.6	600.0	42140.7	43477.1	--	175564.0	100.00
Percent of Total	0.1	1.39	6.88	7.08	0.69	0.0	0.54	0.34	24.00	24.76	--	100.00	--

[a] Stored plus projected

[b] Stored, plus projected, plus scaled

Table 3.4-6. Calculation of Constituent Volume Distribution in CH-TRU Waste*

Category	Initial	Distributed Amount of Filter and Filter Media	Total
Stored			
Sludge**	0.2373	0.0280	0.265
Combustible	0.2968	0.0350	0.332
Glass/Metal	0.3603	0.0425	0.403
Total	0.8944	--	1.000
Projected			
Sludge**	0.1980	0.0171	0.215
Combustible	0.4015	0.0348	0.436
Glass/Metal	0.3208	0.0278	0.349
Total	0.9203	--	1.000
Stored plus Projected			
Sludge**	0.2201	0.0229	0.243
Combustible	0.3424	0.0357	0.378
Glass/Metal	0.3431	0.0358	0.379
Total	0.9056	--	1.000
Stored, Projected, plus Scaled			
Sludge**	0.2083	0.0204	0.229
Combustible	0.3671	0.0360	0.403
Glass/Metal	0.3354	0.0328	0.368
Total	0.9108	--	1.000

* The values for the initial volume percents were obtained from Table 3.4-5.
** Total of absorbed liquid and sludge, concreted and cemented sludge, and dirt, gravel, or asphalt.

3.4.2 Composition of RH-TRU Waste (Non-Radionuclide/Non-RCRA Inventory)

Estimates of the mass and volumes of RH-TRU constituents that affect gas generation, transport, and room properties are required for performance assessment. However, the mass of RH inventory was not included in the current analyses. The total RH inventory has changed considerably in the last several years. The following discussion presents a method that was used to estimate the characterization of the RH inventory. The method resulted in estimates of the volume and weights of waste by generator site; however, these results should not be interpreted as indicative of the weights and volumes that a specific site may generate.

For the current PA calculations, it was assumed that the maximum allowed RH volume of 7,079 m^3 (0.25 x 10^6 ft^3) will be emplaced in the WIPP. The following discussion presents the method that was used to estimate the total volumes of the waste constituents if the maximum volume of RH waste was emplaced. Input to the 1990 IDB was used as the basis for these estimates. The IDB presents estimates of the stored volume and projected (newly generated) volume for each generator site. The stored and projected volumes for the five sites that have or will generate RH waste are tabulated in Table 3.4-7. To estimate the additional volume required to reach the maximum volume, it was assumed that the generators of projected waste would provide the additional volume. The percentage of projected waste for each site was calculated and, based on this percentage, volumes for the five sites were calculated to provide an additional 1,735 m^3 (6.13 x 10^4 ft^3). The scaled volumes for the five sites are shown in Table 3.4-7.

The stored and newly generated (projected) RH volume in the 1990 IDB sum to about 5,300 m^3 (8.83 x 10^4 ft^3). The containers that will be placed in an RH canister have a different volume depending on the generator site. Therefore, a canister may not contain 0.89 m^3 (31.4 ft^3) of RH waste. U.S. DOE (1991) indicates that the submittals to the 1990 IDB total 7,622 canisters. The total volume based on this number of canisters is 6,784 m^3 (2.4 x 10^5 ft^3). U.S. DOE (1991) also discusses the number of uncertainties in the projection of the RH inventory and acknowledges that the details of the RH-TRU waste canister design should be revisited for re-evaluation. Because of the uncertainty in the RH inventory and the discussion in U.S. DOE (1991) on canister design, the smaller total stored plus projected volume of waste--not the volume of the canisters--was used as a scaling factor to estimate the RH radionuclide inventory for an RH design volume.

Table 3.4-7. Estimate of a Design Volume for RH-TRU Waste

Site	Stored Volume (1990 IDB) (m^3)	Projected Volume (1990 IDB) (m^3)	Total Volume (1990 IDB) (m^3)	Scaled Volume* (m^3)	Estimated Design Volume (m^3)
ANL-E	--	81.6	81.6	36.8	118.4
HANF	137	3535.2	3672.2	1,596.0	5,268.2
INEL	29.5	76.8	106.3	34.7	141.0
LANL	28.4	4.8	33.2	2.2	35.4
ORNL	1307	144.0	1,451.0	65.0	1,516.0
Total	1,501.9	3,842.4	5,344.3	1,734.7	7,079

* Assuming that ANL, HANF, INEL, LANL, and ORNL provide the difference between the current total inventory and the design volume. The difference between the total volume of 5,344 m^3 in the 1990 IDB and the design volume of 7,079 m^3 (0.25×10^6 ft^3) was ratioed between the five sites based on their estimated annual generation rates.

3.4.3 Saturation

Initial Saturation*

Parameter: **Saturation, initial ($S_{\ell i}$)**
Material: Unmodified CH-TRU waste form including containers (WastRef, BrineSat)

Definition Units: Dimensionless

Values: Range: (0, 0.14) Median: 0.07

Distribution: Uniform
Correlation:

Data Source(s): None. (PA Investigator Judgment)

Usage:

Mathematical model:

Two-Phase Flow, Section 1.4.1 of this volume.

Equations 1.4.1-1 and 1.4.1-2 (Initial condition of liquid-phase saturation in Waste material).

Computational models:

BRAGFLO

Ranking in Past Sensitivity Analyses:

40 CFR 191	Low
40 CFR 268	High
NEPA	Not tested
Other	Not tested

*Key to Parameter Sheets is provided in Section 1.2.8.

4. PARAMETERS OF GLOBAL MATERIALS AND AGENTS ACTING ON DISPOSAL SYSTEM

This chapter contains parameters for fluid properties, climate variability, and intrusion characteristics.

4.1 Fluid Properties

The fluid parameters tabulated in Table 4.1-1 include Salado and Culebra brine, drilling mud, and hydrogen gas.

Table 4.1-1. Fluid Properties

Parameter	Median	Range		Units	Distribution Type	Source
Brine, Salado (T = 27°C [300.15 K], p = 1 atm [0.101325 MPa])						
Compressibility	2.5×10^{-10}	2.4×10^{-10}	2.6×10^{-10}	Pa^{-1}	Normal	McTigue et al., 1991
Density (ρ_f)	1.23×10^{3}	1.207×10^{3}	1.253×10^{3}	kg/m^3	Normal	McTigue et al., 1991
Viscosity (μ)	1.8×10^{-3}			Pa•s	Constant	Kaufmann, 1960, p. 622
Brine, Culebra (T = 27°C [300.15 K], p = 1 atm [0.101325 MPa])						
Density (ρ_f)	1.09×10^{3}	9.99×10^{2}	1.154×10^{3}	kg/m^3	Spatial	Cauffman et al., 1990, Table E.1
Viscosity (μ)	1×10^{-3}			Pa•s	Constant	Haug et al.,1987, p.3-20
Brine, Castile (T = 27°C [300.15 K], p = 1 atm [0.101325 MPa])						
Compressibility	9×10^{-10}			Pa^{-1}	Constant	Popielak et al., 1983, p. H-32
Density	1.215×10^{3}			kg/m^3	Constant	Popielak et al., 1983, Table C-2
Hydrogen (T = 27°C [300.15 K])						
Density @	1.1037×10^{1} (15 MPa)	8.1803×10^{-2} (0.1 MPa)	1.4442×10^{1} (20 MPa)	kg/m^3	Table	WIPP PA Division, 1991, Vol. 3, Section 4.1.4
Viscosity (μ)	9.2×10^{-6}	8.92×10^{-6}	9.33×10^{-6}	Pa•s	Table	Vargaftik, 1975, p. 39.
Solubility in brine (χ)	3.84×10^{-4}	6.412×10^{-6}	4.901×10^{-4}	none	Table	WIPP PA Division, 1991, Vol. 3, Section 4.1.4; Cygan, 1991.
Drilling Mud Properties (T = 22°C [295.15 K], p = 1 atm [0.101325 MPa])						
Density (ρ_f)	1.211×10^{3}	1.139×10^{3}	1.378×10^{3}	kg/m^3	Constructed	Pace, 1990
Viscosity	9.17×10^{-3}	5×10^{-3}	3×10^{-2}	Pa•s	Constructed	Pace, 1990
Yield stress	4	2.4	1.92×10^{1}	Pa	Constructed	Fredrickson, 1960, p.252; Savins and Wallick, 1966; Pace, 1990

4.2 Human-Intrusion Borehole

Table 4.2-1 summarizes geometric and physical parameters of human-intrusion boreholes assumed by the PA Department for disturbed-scenario calculations.

Table 4.2-1. Characteristics of Human-Intrusion Borehole

Parameter[a]	Median	Range		Units	Distribution Type	Source
Borehole Fill Properties						
Creep $(r_o-r)/r_o$	n.a.	2×10^{-2}	8×10^{-1}	none	Table	Sjaardema and Krieg, 1987, Figure 4.6
Density, average (ρ_{ave})	2.3×10^{3}			kg/m^3	Constant	See Section 2.3.1
Density, bulk (ρ_{bulk})	2.14×10^{3}			kg/m^3	Constant	See Section 2.3.1
Permeability, final (k)	**3.16×10^{-12}**	**1×10^{-14}**	**1×10^{-11}**	**m^2**	**Lognormal**	**See Section 4.2.1**
Initial						
Plug in Castile Fm.	10^{-15}			m^2	Constant	Lappin et al., 1989, Table C-1
Plugs in Salado Fm.	10^{-18}			m^2	Constant	Lappin et al., 1989, Table C-1
Porosity (ϕ)	3.75×10^{-1}	2.5×10^{-1}	5×10^{-1}	none	Normal	Freeze and Cherry, 1979, Table 2.4 (sand)
Drilling Characteristics						
Drill bit diameter (d)						
Intrusion	**3.55×10^{-1}**	**2.67×10^{-1}**	**4.44×10^{-1}**	**m**	**Uniform**	**See Section 4.2.2**
Historical	2×10^{-1}	1.21×10^{-1}	4.45×10^{-1}	m	Constructed	Brinster, 1990
Drill string angular velocity (θ)	7.7	4.2	2.3×10^{1}	rad/s	Constructed	Pace, 1990; Austin, 1983
Drilling mud flowrate (Q_f)	9.935×10^{-2}	7.45×10^{-2}	1.24×10^{-1}	$m^3/(s \cdot m)$	Uniform	Pace, 1990; Austin, 1983

[a]Parameters in bold were sampled in the 1992 calculations.

4.2.1 Borehole Fill Properties

Permeability*

Parameter: **Permeability, final (k)**
Material: Fill material in a human-intrusion borehole (Borehole, Prm)

Definition Units: m^2

Values: Range: $(1 \times 10^{-14}, 1 \times 10^{-11})$ Median: 3.16×10^{-12}

Distribution: Lognormal
Correlation:

Data Source(s): Freeze, R. A., and J. A. Cherry. 1979. *Groundwater.* Englewood Cliffs, NJ: Prentice-Hall, Inc. (Table 2.2, silty sand) (Investigator Judgment)

Usage:

Mathematical model:
Two-Phase Flow, Section 1.4.1 of this volume.

Equations 1.4.1-1 and 1.4.1-2.

Computational models:
BRAGFLO

Ranking in Past Sensitivity Analyses:

40 CFR 191	High
40 CFR 268	Not applicable
NEPA	Not tested
Other	Not tested

*Key to Parameter Sheets is provided in Section 1.2.8.

Discussion:

Because of the speculative nature of inadvertent human intrusion, PA calculations depend on the guidance provided by regulations on factors such as length, severity, and resulting conditions after intrusion. The EPA Standard, *40 CFR 191*, in Appendix B states

> "...the implementing agency can assume that passive institutional controls or the intruders' own exploratory procedures are adequate for the intruders to soon detect, or be warned of, the incompatibility of the area with their activities.... Furthermore, the Agency assumes that the consequences of such inadvertent drilling need not be assumed to be more severe than: ... (2) creation of a ground water flow path with a permeability typical of a borehole filled by the soil or gravel that would normally settle into an open hole over time--not the permeability of a carefully sealed borehole."

Thus, while intruders "soon detect" the repository, the guidance in Appendix B suggests that the implementing agency should not take credit for any special precautions that the drilling company might pursue as the result of detection that could alter long-term borehole behavior.

Initial Conditions after Abandonment. Some PA calculations require that initial conditions be established for the time period immediately after intrusion; no regulatory guidance has been provided for these conditions. In defining initial conditions in the borehole, the PA calculations assume that future societies establish government regulations on drilling similar to those in effect today to protect natural resources. Thus, for any borehole through the repository and hypothetical brine reservoir, drillers would be required to place casing and several cement and sand plugs as follows:

Casing. The normal procedure for drilling an oil and gas well is to drill the hole to the base of the Rustler Formation (the top of salt) and set casing. The State Engineer Office dictates the use of casing because the WIPP is located in a closed groundwater basin, and all hydrocarbon wells are required to protect the aquifers in the basin (e.g., Culebra Dolomite). After the hole has been drilled and the casing placed in the hole, the casing is cemented from bottom to top with an API Class C grout (intended for use in oil and gas wells from surface to a depth of 2,400 m [8,000 ft] and having a sulfate resistance).

Plug Locations. The Energy, Minerals, and Natural Resources Department, Oil Conservation Commission (OCC) controls plugging when abandoning a borehole in the Delaware Basin in and around the WIPP. Exact specifications are negotiated between the drilling company and the OCC. The OCC then inspects for compliance. Because the WIPP repository is located in an area of the potash, recommended plugging procedures protect the potash horizon from foreign fluids. Prior to 1988, specifications likely included sealing off any encountered brine reservoir in the Castile Formation with cement grout and capping the seal with a 60-m (200-ft) cement-grout plug (Figure 4.2-1). About 15 m (50 ft) of sand was usually emplaced above grout plugs. Weighted drilling fluid above the sand was usually emplaced to ~60 m (~200 ft) below the potash horizon, where another plug extended through the potash horizon. A second sand cap was emplaced, followed by weighted drilling mud to within ~60 m (~200 ft) of the top of the Salado Formation salt, where another plug of cement grout was emplaced, followed by sand and weighted mud. When the base of the casing was reached, the specifications either required grouting or filling with weighted mud to the surface, where a cap and abandonment marker were often placed (Lappin et al., 1989, Appendix C).

In April 1988, the OCC amended order R-111 and specified that the plug be a "solid cement plug through the salt section" (Salado Formation); the amendment was in response to conflicts between the potash and oil/gas industries (OCC, 1989, p. 10). The 1991 PA calculations assumed these latter plugging conditions.

Initial Plug Permeability. The initial plug permeabilities depend strongly on the host rock in which the plug is emplaced (e.g., clean vs. chemically altered steel casing or anhydrite vs. halite). Because most experimental studies of plug-borehole interactions extend for only hundreds of days or less, data are limited (Christensen and Petersen, 1981; Buck, 1985; Bush and Piele, 1986; Bush and Lingle, 1986; and Scheetz et al., 1986). Any PA calculations starting from initial conditions assume permeabilities of 10^{-15} m^2 (1 mD) for plugs in the Castile Formation and 10^{-18} m^2 (10^{-3} mD) in the Salado and Rustler Formations (Lappin et al., 1989, Table C-1).

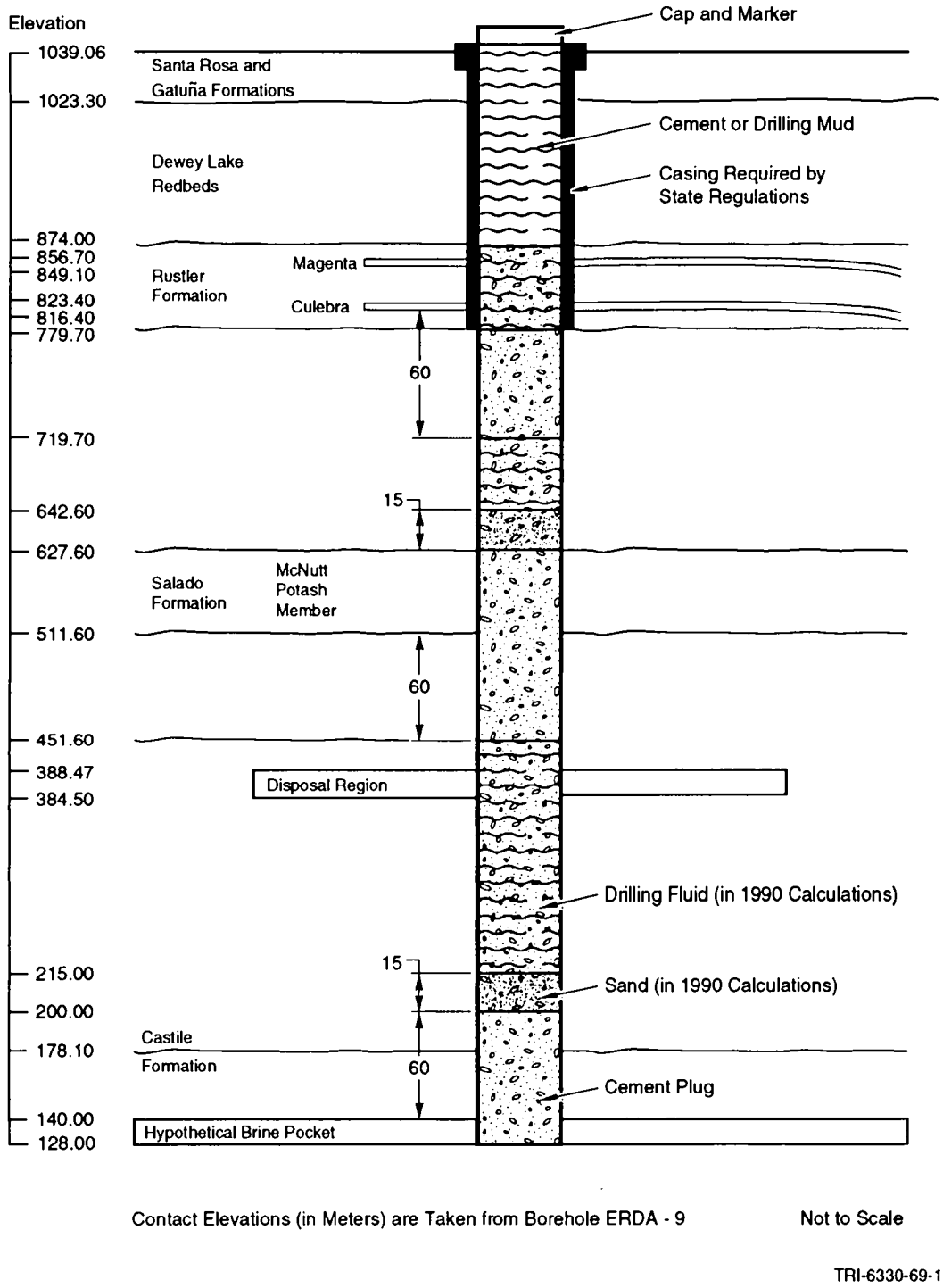

Figure 4.2-1. Required casing and plugs. New Mexico State regulations require casing through Rustler Formation when drilling exploratory boreholes; New Mexico Energy, Mineral, and Natural Resources Department currently requires solid cement plugs in Salado Formation to protect potash horizon when abandoning a borehole.

Borehole Permeability and Porosity. Of primary concern to the PA calculations is the borehole permeability over most of the 10,000 yr. Three components of these calculations are (1) the length of time that the plug and casing remain intact, (2) the change in permeability of the deteriorating plugs with time, and (3) the ultimate deformation of the borehole.

Plug Life. Cementing companies suggest that the cement plugs should last for at least 100 yr, as would the casing. PA calculations assume a life of 75 yr followed by 75 yr of degradation (Figure 4.2-2).

Degraded Plugs and Borehole Debris Permeability. PA calculations assume that the degrading concrete plugs and other debris initially present in the hole would have a permeability and porosity of silty sand (Freeze and Cherry, 1979), but with a bulk and average density equal to that of the Salado Formation (Table 4.2-1). The permeability and porosity were assumed to vary lognormally and normally, respectively, between the typical range for silty sand, typical of distributions of the parameters in the literature (Harr, 1987, Table 1.8.1).

Note that any drilling mud initially in the borehole or brine that drains into the borehole would have to be able to migrate through the degrading plugs before the borehole could be a viable conduit. In other words, if the fluid is trapped, the borehole is not a conduit.

Borehole Deformation. Because of the change in borehole abandonment procedures, the 1991 and 1992 PA calculations did not assume any borehole deformation. This assumption contributed to a more conservative calculation.

With the previous order, salt "would normally settle into an open hole" and naturally seal the hole shut in the uncemented section of the borehole. Thus, with time, the borehole would attain very low permeabilities similar to the host salt. However, if the amended orders are followed and the borehole is filled, the use of a solid cement plug through the Salado Formation greatly decreases the likelihood that the borehole will be permanently sealed by salt creep over the long term (>100 yr).

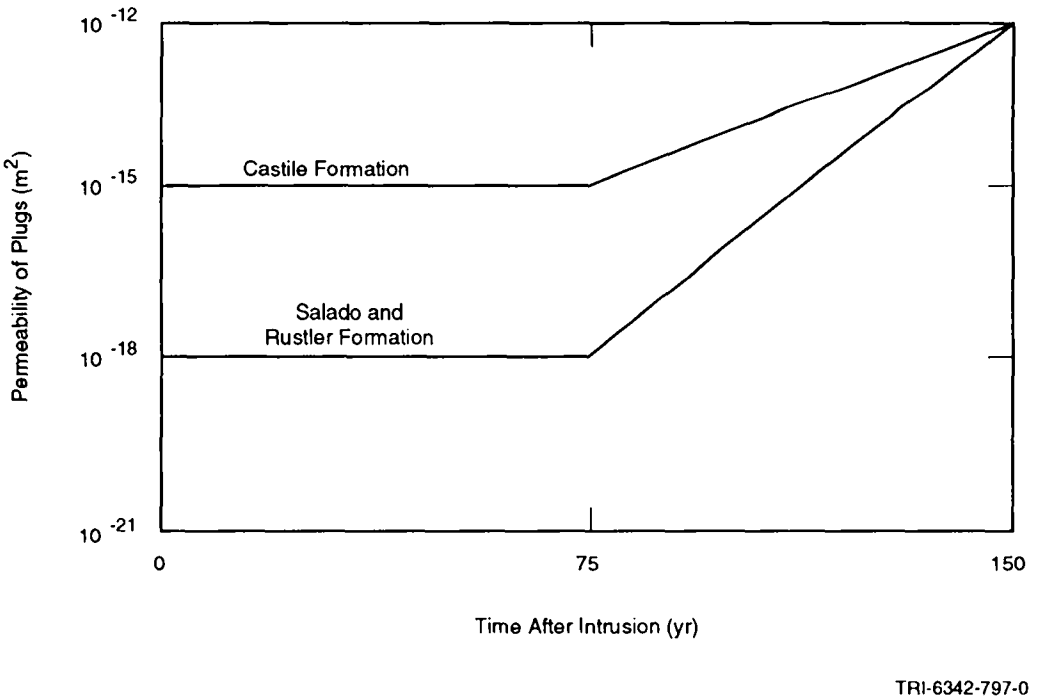

Figure 4.2-2. Increased permeability of cement grout plugs in intrusion borehole with time because of degradation.

4.2.2 Drilling Characteristics

Intrusion Drill Bit Diameter*

Parameter: **Intrusion drill bit diameter (d)**
Material: Determines initial diameter of human-intrusion borehole, (Borehole, DiamMod)

Definition Units: m

Values: Range: $(2.67 \times 10^{-1}, 4.44 \times 10^{-1})$ Median: 3.55×10^{-1}

Distribution: Uniform
Correlation:

Data Source(s): See text. (Investigator Judgment)

Usage:

Mathematical model:

Two-Phase Flow, Section 1.4.1 of this volume;
Cuttings Removal, Section 1.4.3 of this volume.

Equation: (Determines geometry of borehole in two-phase flow model; see Figure 1.4-3 for cuttings-removal model).

Computational models:

BRAGFLO
CUTTINGS

Value of Additional Information

40 CFR 191	High (CUTTINGS)
40 CFR 268	Not applicable
NEPA	Not tested
Other	Not tested

*Key to Parameter Sheets is provided in Section 1.2.8.

Discussion:

The guidance for the EPA Standard, *40 CFR 191*, (Appendix B) states that the EPA

> "...believes that the most productive consideration of inadvertent intrusion concerns those realistic possibilities that may be usefully mitigated by repository design, site selection, or use of passive controls (although passive institutional controls should not be assumed to completely rule out the possibility of intrusion). Therefore, inadvertent and intermittent intrusion by exploratory drilling for resources (other than any provided by the disposal system itself) can be the most severe intrusion scenario assumed..."

The possible futures (scenarios) that must be considered are not necessarily exhaustive, but rather those that if examined might differentiate between repository sites or perhaps identify ways to improve repository design.

Consequently, the PA Department assumes that current standard drilling procedures for gas and oil exploration will continue into the future, and that future drillers will observe regulations similar to those currently imposed by federal and state agencies to protect resources.

Drilling for oil and gas has two main objectives: to drill the hole to the target horizon as quickly and economically as safely possible, and to install casing from the reservoir to the surface for production of hydrocarbons if they are found. The procedures used to accomplish these objectives are fairly well standardized in the drilling industry.

Currently when a company drills an exploratory oil or gas well in the Delaware Basin, the operation uses a standard rotary drill rig with a mud circulation system. The differences between drilling for oil and gas depend on the depth of the well, which controls the size of drill bit used. Figure 4.2-3 shows the distribution used in the past in the Delaware Basin for oil and gas exploration. The data are reported as a discrete distribution because bit diameters cannot vary continuously between 0.1206 m and 0.4445 m diameter (4-3/4 in. and 17-1/2 in.), but must be the diameter of a bit that was actually used (Brinster, 1990). The median bit diameter is 0.2000 m (7-7/8 in. diameter).

Currently, the normal depth for an oil well in the Delaware Basin near the WIPP site ranges from 1,200 to 1,800 m (4,000 to 6,000 ft), but gas-well depths usually exceed 3,000 m (10,000 ft). Consequently, oil wells normally have a standard 0.413-m (16 1/4-in.) drilled hole to the top of salt to accommodate 0.340-m (13 3/8-in.) steel casing, and gas wells normally have a standard 0.4445-m (17 1/2-in.) drilled hole to accommodate 0.356-m (14-in.) casing. After casing is set with grout, the company drills either a standard 0.311-m (12 1/4-in.) hole, if the target is oil, or a 0.356-m (14-in.) hole, if the target is gas (Table 4.2-2). Rather than sample from the historical diameters for evaluating the borehole as was done in the 1990 PA calculations, the 1991 PA calculations sampled from a perturbation about the currently used diameter for deep gas wells (i.e., 0.356 m ± 0.0889 [14 in. ± 3.5]). This practice ensures that fairly large borehole diameters are used, and thus, is more conservative than the 1990 calculations.

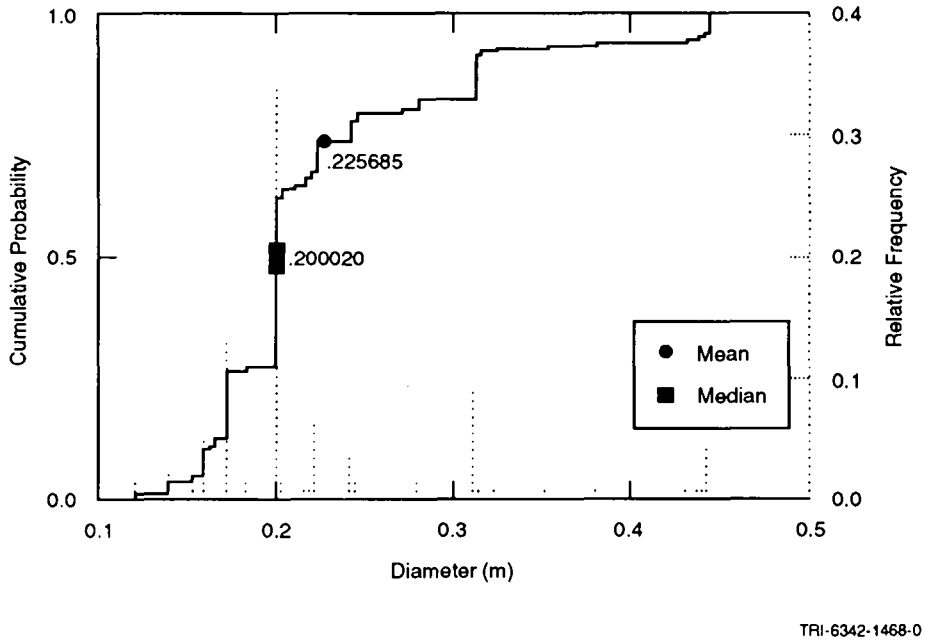

Figure 4.2-3. Distribution of historical drill bit diameter.

Table 4.2-2. Specifications for Gas and Oil Exploratory Boreholes

Parameter	Value	Units
Drilled diameter		
In Rustler Formation (oil well)	0.413	m
(gas well)	0.444	m
In Salado and Castile Formations, (oil well)	0.311	m
(gas well)	0.356	m

4.3 Parameters for Castile Formation Brine Reservoir

Pressurized brine in the northern Delaware Basin has been encountered in fractured anhydrites of the Castile Formation in boreholes both north and northeast of the WIPP over the past 50 yr. In addition, Castile brines were encountered southwest of the WIPP at the Belco Well, about 6.5 km (4 mi) from the center of the WIPP. During WIPP site characterization, Castile Formation brine reservoirs were encountered in the WIPP-12 borehole, about 1.6 km (1 mi) north of the center of the WIPP, and the ERDA-6 borehole, about 8 km (5 mi) northeast of the center of the WIPP (Figure 4.3-1).

Also, a geophysical study that correlated with the known occurrence of brine at WIPP-12 indicated the presence of brine fluid within the Castile Formation under the WIPP (Earth Technology Corp., 1988). Based on borehole experience and the geophysical study, the PA calculations assume that a brine reservoir exists underneath at least a portion of the disposal region. The assumed presence of a Castile brine reservoir beneath the repository is of concern only in the event of human intrusion. (The area, and thus, the probability of hitting a brine reservoir and the disposal area simultaneously are discussed in Chapter 5.)

Table 4.3-1 provides parameter values for the PA Department's model of the Castile Formation Brine Reservoir.

Table 4.3-1. Parameter Values for Castile Formation Brine Reservoir

Parameter[a]	Median	Range		Units	Distribution Type	Source
Elevation, top	1.4×10^{2}	-2.00×10^{2}	1.78×10^{2}	m	Constructed	WIPP PA Division, 1991, Vol. 3, Section 4.3.1
Density, grain (ρ_g)	2.963×10^{3}			kg/m^3	Constant	See anhydrite, Section 2.4
Analytic Model						
Pressure, initial (p_i)	**12.6**	**11.0**	**21.0**	**MPa**	**Constructed**	**See Section 4.3.1**
Storativity, bulk ($\hat{S}_b$)	**2×10^{-1}**	**2×10^{-2}**	**2×10^{1}**	**m^3/Pa**	**Loguniform**	**See Section 4.3.2**
Numerical Model						
Permeability						
Intact matrix	1×10^{-19}	1×10^{-20}	1×10^{-18}	m^2	Constructed	WIPP PA Division, 1991, Vol. 3, Section 4.3.2
Fractured matrix	1×10^{-13}	1×10^{-16}	1×10^{-10}	m^2	Constructed	Freeze and Cherry, 1979; Reeves et al., 1991.
Porosity	5×10^{-3}	1×10^{-3}	1×10^{-2}	none	Constructed	Reeves et al., 1991.
Radius, equivalent	2.32×10^{2}	3×10^{1}	8.6×10^{3}	m	Constructed	Reeves et al., 1991.
Thickness	1.2×10^{1}	7	6.1×10^{1}	m	Uniform	Reeves et al., 1991.

[a]Parameters in bold were sampled in the 1992 calculations.

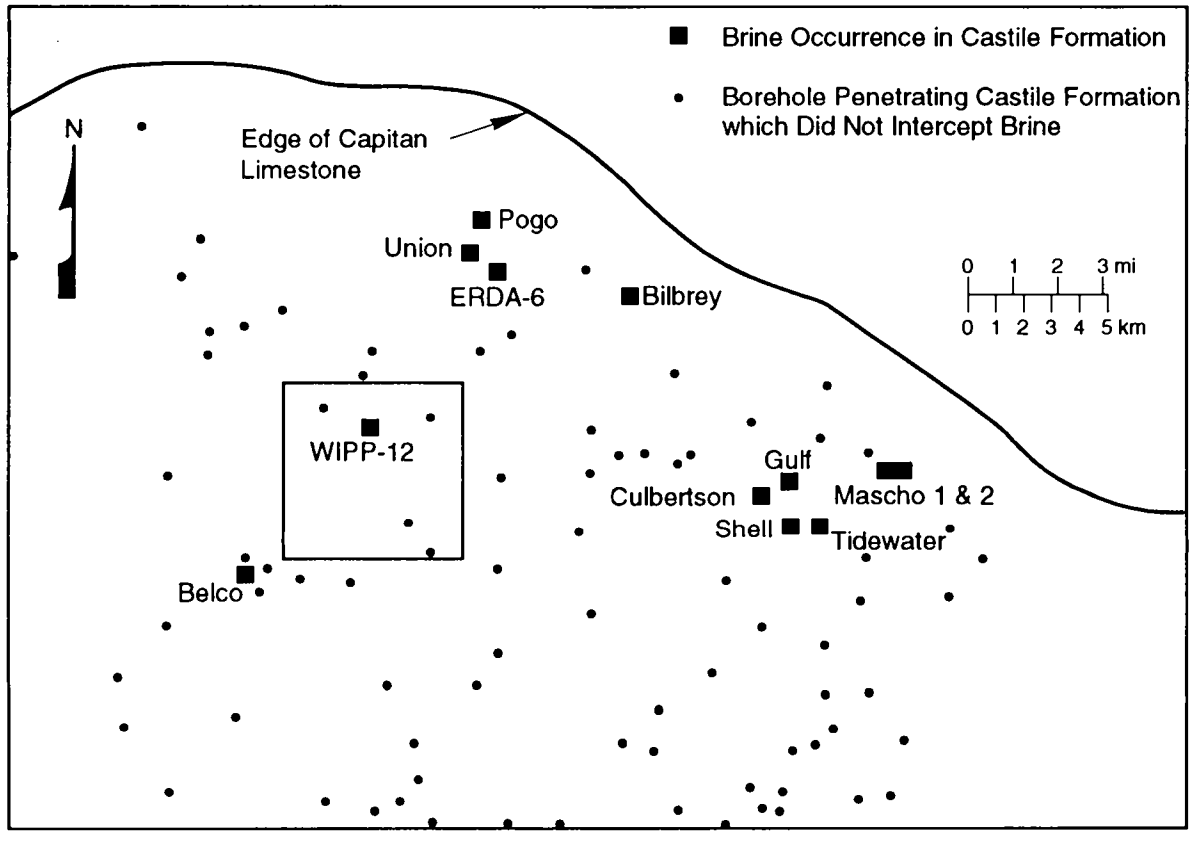

Figure 4.3-1. Deep boreholes that encountered brine reservoirs within the Castile Formation, Northern Delaware Basin (Lappin et al., 1989, Figure 3-26).

4.3.1 Brine Pressure

Pressure, Initial*

Parameter: **Pressure, initial (p_i)**
Material: Brine reservoirs in Castile Formation (Cstile_R, Pressure)

Definition Units: MPa

Values: Range: (11.0, 21.0) Median: 12.6

Distribution: Constructed (Figure 4.3-2); see Discussion
Correlation:

Data Source(s):
Popielak, R. S., R. L. Beauheim, S. R. Black, W. E. Coons, C. T. Ellingson, and R. L. Olsen. 1983. *Brine Reservoirs in the Castile Formation, Waste Isolation Pilot Plant (WIPP) Project, Southeastern New Mexico.* TME-3153. Carlsbad, NM: U.S. Department of Energy. (WIPP Observational Data)

Lappin, A. R., R. L. Hunter, D. P. Garber, and P. B. Davies, eds. 1989. *Systems Analysis, Long-Term Radionuclide Transport, and Dose Assessments, Waste Isolation Pilot Plant (WIPP), Southeastern New Mexico; March 1989.* SAND89-0462. Albuquerque, NM: Sandia National Laboratories. (Table 3-19) (Investigator Judgment)

Usage:

Mathematical model:
Two-Phase Flow, Section 1.4.1 of this volume.

Equations 1.4.1-1 and 1.4.1-2 (initial conditions in brine-reservoir materials).

Computational models:
BRAGFLO

Ranking in Past Sensitivity Analyses:

40 CFR 191	Medium
40 CFR 268	Not applicable
NEPA	Not tested
Other	Not tested

*Key to Parameter Sheets is provided in Section 1.2.8.

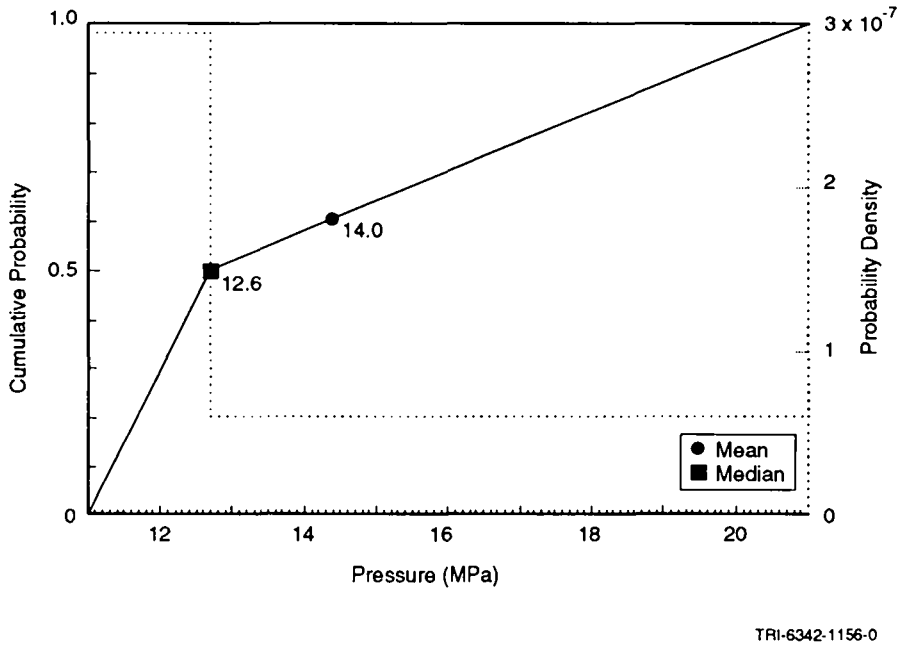

Figure 4.3-2. Constructed distribution for Castile brine reservoir initial pressure.

Discussion:

Median. The measured initial pressure of 12.6 MPa (125 atm) for WIPP-12 (Popielak et al., 1983, p. H-52) was used as the median brine reservoir initial pressure.

Range. Lappin et al. (Table 3-19, 1989, derived from Popielak et al., 1983, Table H.1) estimated the initial brine reservoir pressure from several wellhead measurements at WIPP-12 and other boreholes that encountered pressurized Castile brine. The range was between 7.0 and 17.4 MPa (69 and 172 atm). Because the range of pressures includes measurements in wells completed at various elevations, a correction for differences in elevation is required.

The origin of Castile brine reservoirs is not conclusively known. Present interpretations are that their origin is either local, by limited movement of intergranular brines from adjacent Castile halites, or regional, by the previous existence of a lateral hydraulic connection of the Castile Formation with the Capitan reef (Lappin et al., 1989). However, the initial pressure observations at other wells are only directly pertinent if (1) the reservoir fluids are from the same source (past interconnection of reservoir fluid) or (2) they had a common genesis (e.g., brine trapped along bedding planes in areas of high permeability).

For the first case (interconnection), an elevation correction assuming a hydrostatic variation with depth is most appropriate. For the second case (common genesis), an elevation correction assuming a lithostatic variation depth is most appropriate. The range using both types of elevation corrections is 10.7 to 16.8 MPa (106 to 166 atm) (Table 4.3-2). A brine density of 1,215 kg/m^3 (75.85 lb/ft^3) (Section 4.1) was assumed for the first case; an average formation density of 2,400 kg/m^3 (149.8 lb/ft^3) was assumed for the second case. Elevations (except WIPP-12 and ERDA-6) were estimated from the well location and a topographic map of the area (USGS 15 min quads, Carlsbad, NM, 1971, Nash Draw, NM, 1965).

This calculated range is similar to the maximum and minimum possible range of 11 and 21 MPa, assuming hydrostatic and lithostatic pressures at the elevation of the WIPP-12 brine reservoir (140 m [457.8 ft]) (see Figure 2.3-11), and consequently this latter range has been used in the PA calculations.

Table 4.3-2. Estimated Initial Pressures of Brine Reservoirs Encountered in the Region around the WIPP Corrected to the Depth at the WIPP-12 Brine Reservoir (after Popielak et al., 1983)

Well Name	Pressure with Hydrostatic Correction (MPa)	Pressure with Lithostatic Correction (MPa)	Reported Pressure at Observation (MPa)	Elevation of Observation (m)	Depth to Observation (m)	Surface Elevation* (m)
WIPP-12	12.7	12.7	12.7	140	918	1058
ERDA-6	15.5	16.8	14.1	253	826	1079
Belco	14.5	14.6	14.3	152	854	1006
Gulf	12.1	10.7	13.6	16	1097	1113
Pogo	>16.6	>15.8	>17.4	69	1013	1082
Tidewater	>14.0	>12.2	>16.0	-24	1137	1113
Union	>11.2	>12.2	>10.1	226	856	1082
H&W Danford 1	11.5	15.8	7.0	512	588	1100(?)
**Bilbrey	12.1	13.8	11.2	209	942	1151
**Culbreston	11.8	10.9	12.8	57	1071	1128
**Mascho 1	11.6	10.8	12.4	69	1013	1082
**Mascho 2	11.3	10.6	12.0	77	1005	1082
**Shell	11.8	10.4	13.4	9	1119	1128

* Elevation from well location and USGS 15 min quad topographic map, Carlsbad, NM, 1971, Nash

** According to Popielak et al. (1983, Table H.1), these wells should not be used to estimate static pressure.

4.3.2 Bulk Storativity

Bulk Storativity*

Parameter: **Bulk storativity (S_b)**
Material: Brine reservoirs in Castile Formation (Cstile_R, StorBulk)

Definition Units: m^3/Pa

Values: Range: $(2 \times 10^{-2}, 2)$ Median: 2×10^{-1}

Distribution: Lognormal (Figure 4.3-3)
Correlation:

Data Source(s): See text. (Investigator Judgment)
Popielak, R. S., R. L. Beauheim, S. R. Black, W. E. Coons, C. T. Ellingson, and R. L. Olsen. 1983. *Brine Reservoirs in the Castile Formation, Waste Isolation Pilot Plant (WIPP) Project, Southeastern New Mexico.* TME-3153. Carlsbad, NM: U.S. Department of Energy. (WIPP Observational Data)

Usage:

Mathematical model:
Two-Phase Flow, Section 1.4.1 of this volume.

Equation (used to compute time-dependent boundary conditions for Eqs. 1.4.1-1 and 1.4.1-2).

Computational models:
BRAGFLO

Ranking of Past Sensitivity Analyses:

40 CFR 191	Medium
40 CFR 268	Not applicable
NEPA	Not tested
Other	Not tested

*Key to Parameter Sheets is provided in Section 1.2.8.

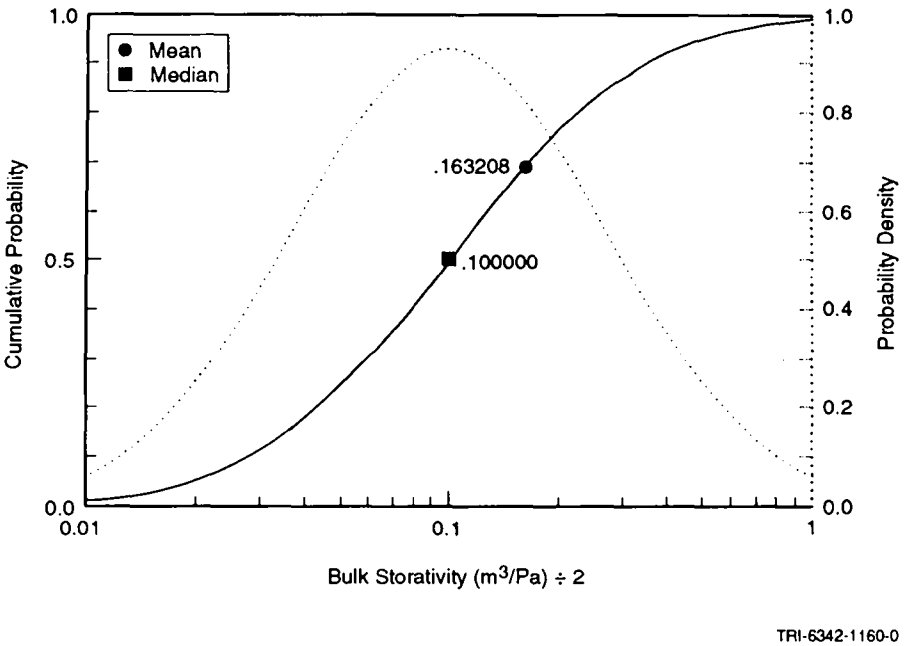

Figure 4.3-3. Estimated distribution for bulk storativity of Castile brine reservoir.

Discussion:

Bulk storativity (S_b) as defined herein is the total volume of fluid discharged from the reservoir per unit decrease in reservoir pressure ($\Delta V/\Delta p$). The bulk storativity can be estimated from wellhead measurements (long-term change in pressure and total discharge volume), or from the compressibility of the reservoir matrix and fluid and the total volume and porosity of the reservoir.

The pressure recovery of the WIPP-12 reservoir is characteristic of a dual-porosity medium. An initial rapid response is attributed to a highly permeable fracture set, whereas a more gradual component of recovery is due to repressurization of the higher permeability fracture set by intersecting lower permeability fractures. Because the human-intrusion scenarios contemplate that the Castile will be connected to the Culebra over the long term (compared to the duration of well tests), estimates of bulk storativity from long-term pressure changes are more appropriate than those made using short-term pressure changes, which may represent only the storativity of the highest permeability fractures. Estimates of bulk storativity using wellhead measurements range from 5×10^{-4} m^3/Pa (from ERDA-6 testing through October, 1982) to 2×10^{-1} m^3/Pa (from estimated total discharge volume, maximum estimated formation pressure, and apparent long-term recovery pressure at WIPP-12). Because WIPP-12 is closer to the waste disposal area than ERDA-6, the latter number is considered more appropriate for a sub-repository reservoir.

Reservoir compressibility (β_s/ϕ) and total volume (V_{tot}) may also be used to estimate bulk storativity:

$$S_b = \frac{\Delta V}{\Delta p} = V_{tot}\frac{1}{V_{tot}}\frac{\Delta V}{\Delta p} = V_{tot}\frac{1}{K} = V_{tot}\beta_s \qquad (4.3\text{-}1)$$

The area of the WIPP-12 reservoir is approximately 1.7×10^6 m^2 (Popielak et al., 1983 p. H-53). Popielak depicts brine occurrence in the lower 40% of the 100-m thickness of Anhydrite III-IV at WIPP-12 (Popielak et al., 1983, Figure G-2), giving a rough estimate of the reservoir total volume of 6.5×10^7 m^3. (Note that other published estimates of reservoir volume [e.g., Lappin et al., 1989, p. E-32] were made from wellhead measurements assuming some value of compressibility. These volume estimates will therefore not lead to independent estimates of S_b.) Estimates of the bulk modulus $K_{bulk} = E/3(1-2\upsilon)$ (where E is Young's modulus and υ is Poisson's ratio) of

Anhydrite III at WIPP-12 were used by Popielak et al. (1983, p. G-34) to derive a range of ßs from 3×10^{-11} Pa^{-1} to 1.4×10^{-10} Pa^{-1}. The resulting range in bulk storativity from Eq. 4.3-1 is 2×10^{-3} to 9×10^{-3} m^3/Pa. The reason this range does not include the wellhead estimate from WIPP-12 may be due to errors in the estimate of bulk volume or compressibility. For example, the apparent $ß_s$ may be larger than estimated here because of fractures in the anhydrite or trapped gas in the reservoir. However, at present there is no reason to suppose that bulk storativity is substantially higher than estimated from WIPP-12 wellhead measurements.

Based on the above considerations, the bulk storativity is assumed to lie between 2×10^{-2} and 2 m^3/Pa. The likelihood of the actual value falling in a given interval is described by a lognormal distribution between these limits. The median of this distribution is 0.2 m^3/Pa.

4.4 Climate Variability and Culebra Member Recharge

Climate variability is a continuous process (agent) acting on and thus affecting the state of the disposal system. The primary concerns are precipitation variation and, ultimately, recharge to strata above the Salado Formation, specifically, to the Culebra Dolomite Member. Parameters for the PA Department's models of climate variability and Culebra Member recharge are shown in Table 4.4-1. These models are discussed briefly in Section 1.4.5 and in more detail in Volume 2 of this 1992 series of reports.

Table 4.4-1. Climate Variability and Culebra Member Recharge

Parameter[a]	Median	Range		Units	Distribution Type	Source
Annual precipitation ($\bar{r}_p$)	3.436×10^{-1}	3.09×10^{-2}	6.563×10^{-1}	m	Normal	Hunter, 1985
Precipitation variation						
Amplitude factor (A_m)	2			none	Constant	Swift, 1991
Short-term fluctuation (ϕ)	2×10^{-10}			Hz	Constant	Swift, 1991
Glacial fluctuation (Θ)	1.7×10^{-12}			Hz	Constant	Swift, 1991
Index for computing recharge amplitude factor A_R	**0.5**	**0**	**1**	**none**	**Uniform**	**See Section 1.4.5.**

[a]Parameters in bold were sampled in the 1992 calculations.

Index for Computing Recharge Amplitude Factor*

Parameter: **Index for computing recharge amplitude factor (A_R)**
Material: Model of climatic variability and boundary recharge (Global, ClimtIdx)

Definition Units: None

Values: Range: (0, 1) Median: 0.5

Distribution: Uniform
Correlation:

Data Source(s): None. (Investigator Judgment), but see
Swift, P. N. 1991. Appendix A: "Climate and Recharge Variability Parameters for the 1991 WIPP PA Calculations," *Preliminary Comparison with 40 CFR Part 191, Subpart B for the Waste Isolation Pilot Plant, December 1991. Volume 3: Reference Data.* WIPP Performance Assessment Division. Eds. R. P. Rechard, A. C. Peterson, J. D. Schreiber, H. J. Iuzzolino, M. S. Tierney, and J. S. Sandha. SAND91-0893/3. Albuquerque, NM: Sandia National Laboratories. A-107 through A-121.

Usage:

Mathematical model:
Fluid Flow in Culebra, Section 1.4.5 of this volume.

Equation 1.4.5-4 and text following that equation. The recharge amplitude factor A_R is calculated from the index U by

$$A_R = 1 + (\gamma - 1)U$$

where γ is a scaling factor chosen by the PA Analyst.

Computational models:
SECO2D

Ranking in Past Sensitivity Analyses:

40 CFR 191	Medium
40 CFR 268	Not tested
NEPA	Not tested
Other	Not tested

*Key to Parameter Sheets is provided in Section 1.2.8.

5. PARAMETERS FOR SCENARIO PROBABILITY MODELS

5.1 Area of Brine Reservoirs

Parameter: **Fraction of Area of Castile Brine Reservoirs Overlapping Disposal Area (A_b/A_t)**
Material: Geometric Property of Castile Brine Reservoirs (Cstile_R, Area_frc)

Definition Units: Dimensionless

Values: Range: (0.25, 0.57) Median: 0.4

Distribution: Constructed (by simulation; see discussion and Figure 5.1-1)
Correlation:

Data Source(s): See text. (Investigator Judgment)
Earth Technology Corporation. 1988. *Final Report for Time Domain Electromagnetic (TDEM) Surveys at the WIPP Site*. SAND87-7144. Albuquerque, NM: Sandia National Laboratories.

Usage:

Mathematical model:
Human Intrusion; Section 1.4.2 of this volume.

Equation 1.4.2-5 and text preceding that equation.

Computational models:
CCDFPERM

Ranking in Past Sensitivity Analyses:

40 CFR 191	Low
40 CFR 268	Not applicable
NEPA	Not tested
Other	Not tested

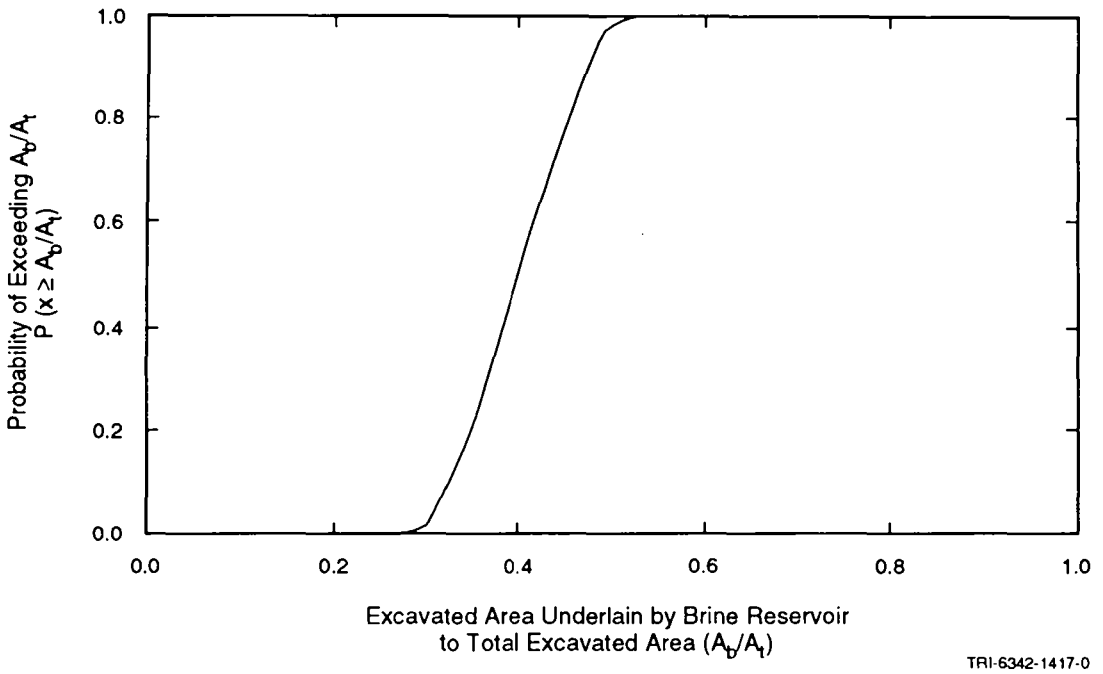

Figure 5.1-1. 1992 distribution of fraction of WIPP disposal area overlapped by brine reservoir. Simulated construction uses inclusive definition of brine reservoir and block model (see text).

Discussion:

A geophysical survey, using transient electromagnetic methods, was made in 1987 to determine the presence or absence of brines within the Castile Formation under the WIPP disposal area (Earth Technology Corp., 1988). Briefly, the electromagnetic method associates high electric conductivity with fluid. (The stated precision of depth to conducting layers was to within ±75 m.) The entire Bell Canyon Formation directly beneath the Castile Formation is a good conductor. However, in several places underneath the WIPP disposal area, the elevation to the first major conducting media detected lay above the top of the Bell Canyon Formation (~-200 ± 30 m [-654 ± 100 ft] in the ERDA-9 well) but below the bottom of the Salado Formation (178 m [582 ft] in ERDA-9) (see Figure 2.2-1 and Section 2.2).

The probability of hitting a brine reservoir can be evaluated for the waste disposal area as a whole or for subunits such as the panels. The current human-intrusion probability model (Volume 2, Chapters 1 and 2) uses the former data (the probability of hitting a brine reservoir over the entire waste panel) and assumes that this same probability applies to each panel. However, an examination of this assumption required the probability for each panel as well (Volume 2, Chapters 1 and 2). The following discussion emphasizes the probability over the entire disposal area, but provides data on a per panel basis as well.

Two methods were considered for determining the area of the brine reservoir. The first involved using the interpolated conductor elevations and the Anhydrite III of the Castile Formation and the Bell Canyon Formation elevations without considering uncertainty in the data. Although not used, it is discussed first because of its simplicity. The second method considers uncertainty in the data through geostatistics.

Area Estimate Assuming No Uncertainty in Data. Contours of the depth and elevation to the first major conductor are plotted in Figures 5.1-2 and 5.1-3. The data in Figure 5.1-2 was the interpretation originally reported (Earth Technology Corporation, 1988). However, Figure 5.1-3 is an equally valid interpretation of the data; it is somewhat more conservative and was computer generated from the same data.

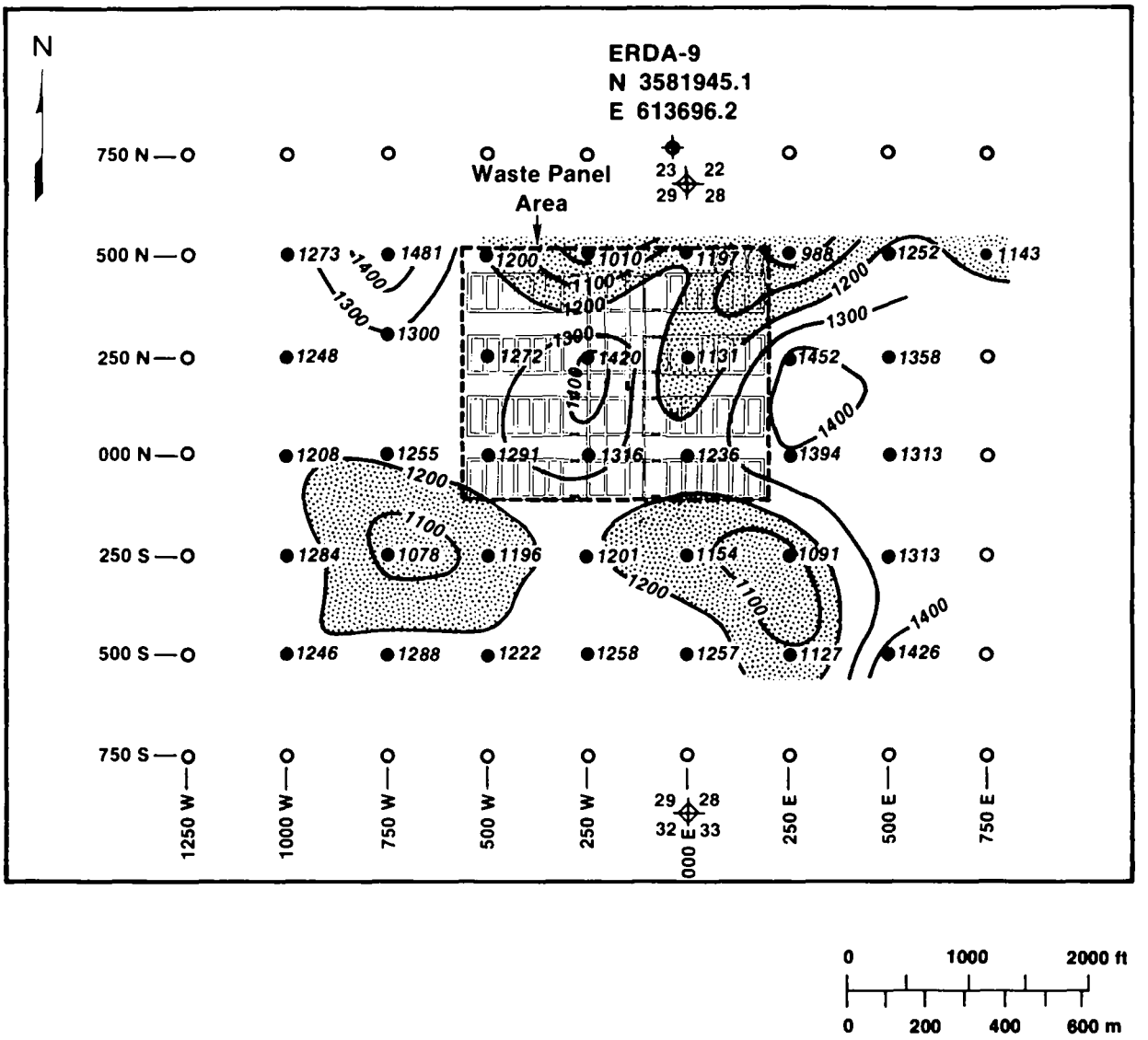

TRI-6342-256-2

Figure 5.1-2. Frequently reported contour map of depth below surface of first major conductor below WIPP disposal area. Shaded areas show extent of first major conductor. (Map drawn by hand.) (after Earth Technology Corp., 1988).

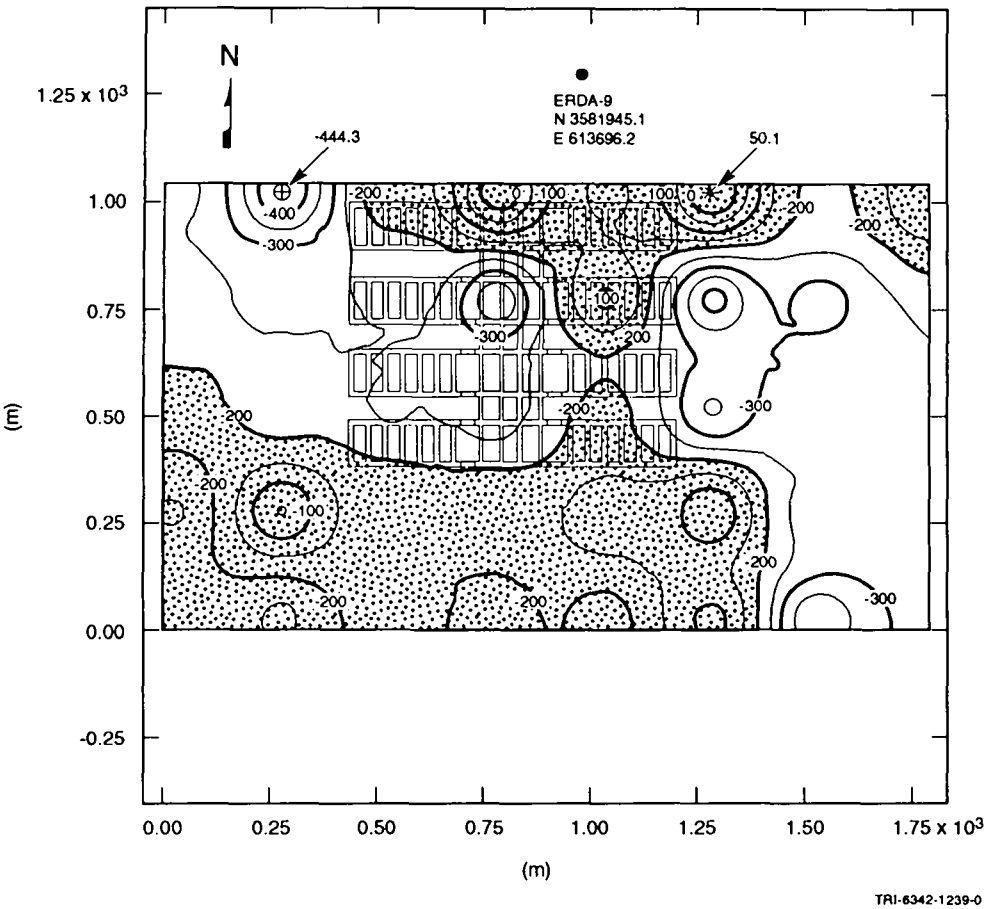

Figure 5.1-3. Conservative contour map of elevation above sea level of first major conductor below WIPP disposal area.

Minimum Area (Anhydrite III Level). The brine reservoirs are usually found in fracture zones of anticlinal structures in the uppermost anhydrite layer in the Castile (Lappin, 1988) (e.g., Anhydrite III as in WIPP-12 or when Anhydrite III is absent such as Anhydrite II in ERDA-6).

In ERDA-9, the elevation of the bottom of Anhydrite III in the Castile Formation is estimated at 90 m (295 ft). Consequently, there is a possibity that no brine is present beneath the disposal area.

Maximum Area (Bell Canyon Level). Pressurized brine reservoirs cannot be entirely discounted until the Bell Canyon Formation is reached at about -200 m (-660 ft) (Figure 2.2-1), implying that conductors higher than about -200 m (-660 ft) could indicate brine within the Castile Formation. PA calculations use the -200 m (-660 ft) contour for defining the maximum area of any brine reservoirs under the WIPP disposal area (Figure 5.1-3), resulting in a maximum area of about 40% (Table 5.1-1).

Combined Distribution. Without knowing the likelihood that either endpoint is more valid, a discrete distribution with points at 0 and 45% of equal probability is suggested.

Table 5.1-1. Cumulative Percentages of the Disposal Region Underlain by a Brine Reservoir, Assuming Various Elevations Relative to Sea Level.

Depth (m)	Cumulative Percent (%) at Indicated Elevations Relative to Sea Level										Area (m^2)
	0	-50	-100	-150	-180	-200	-250	-300	-350	-400	
Panel 1			5.37	61.95	97.80	100.00	100.00	100.00	100.00	100.00	11,530.0
Panel 2			4.00	44.57	69.33	73.08	87.47	100.00	100.00	100.00	11,530.0
Panel 3						18.23	85.73	100.00	100.00	100.00	11,530.0
Panel 4					35.85	75.57	96.17	100.00	100.00	100.00	11,530.0
Panel 5						19.76	94.80	100.00	100.00	100.00	11,530.0
Panel 6							26.57	100.00	100.00	100.00	11,530.0
Panel 7							67.45	100.00	100.00	100.00	11,530.0
Panel 8			0.79	9.01	34.64	52.86	100.00	100.00	100.00	100.00	11,530.0
Southern						3.24	45.01	100.00	100.00	100.00	8,413.0
Northern	3.97	12.49	21.67	27.49	34.86	45.29	54.79	69.25	94.52	100.00	8,701.0
Cumulative Percent	0.316	0.99	4 2.796	14.367	27.828	39.648	77.219	97.553	99.564	100.000	
Cumulative Area (m^2)	345.3	1,086.8	3,057.6	15,711.1	30,431.4	43,357.1	84,442.3	106,678.2	108,877.4	109,354.0	

Area Estimate Incorporating Uncertainty in the Data. Described above is a method of estimating the fractional area of the waste-panel region underlain by a Castile brine reservoir using contours of the conductor elevation. This method assumes that elevation contours drawn from the observed data correctly represent the variation of conductor depth between observation locations. The following discussion describes an alternative method that does not rely on reported depth contours and the resulting area fraction distribution.

Conductor elevation measurements are available at 36 points (Figure 5.1-2). These data were used to estimate conductor elevation at all points within the waste panel region. Any estimate of the conductor depth at an unmeasured location had an uncertainty associated with it. The objective of this procedure is to incorporate relevant uncertainties in the estimate of area fraction.

Spatial Variability and Interpolation. Uncertainty in interpolated elevations is a consequence of spatial variability of the observed data. Quantifying spatial variability helps in estimating the error of an interpolated value. If two observations are made close together, it is reasonable to expect that similar values will be obtained (autocorrelation function, Chapter 1). As the distance between observations increases, the similarity of observed values decreases. This behavior of spatially varying fields is often represented as a variogram (Figure 5.1-4). The variogram shows the average squared difference in observed values between observations separated by a given distance vs. the distance between observations. For a given separation distance h, the average is taken over all pairs of observations that are separated by distance h.

The variogram in Figure 5.1-4 is a generic example illustrating two common features seen in real data. Close to the origin (i.e., small separation distances), values are similar, so that the average squared difference is small. As the distance between observations increases, observed values tend to become uncorrelated, resulting in an increase in average squared difference in observed values. The distance at which observations tend to become uncorrelated is referred to as the range of the variogram. As separation distance increases beyond the range, the average squared difference tends to a limiting value, called the sill.

Not all fields exhibit clearly defined range and sill. Systematic trends in the data, for example, can produce variograms that continually increase with separation distance. In addition, the spatial variability of the data may be different along different directions, so that a variogram constructed from separations along one direction may be different from a variogram constructed along another direction.

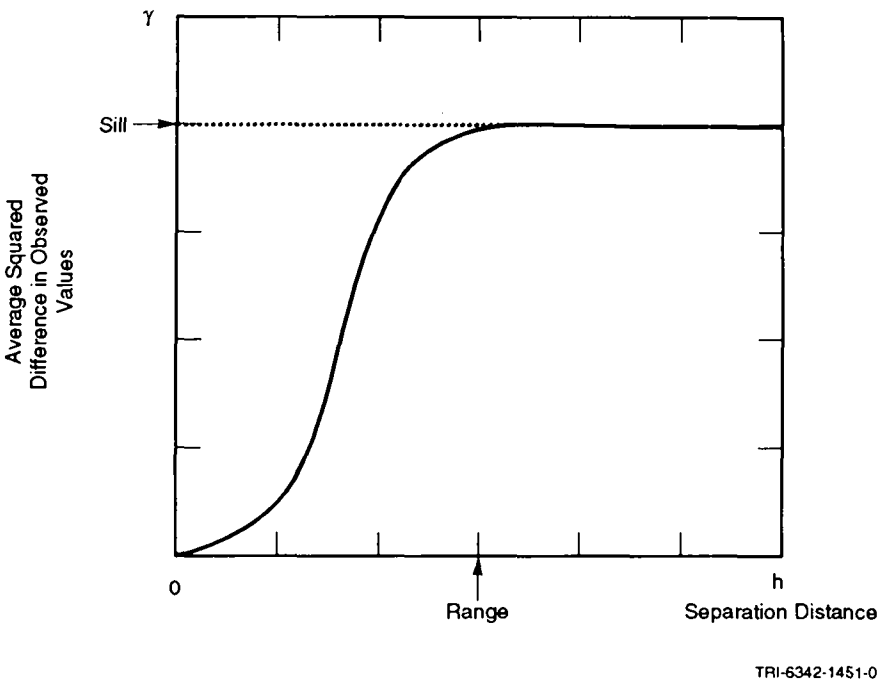

Figure 5.1-4. Example variogram illustrating typical behavior of γ with h.

Information contained in the variogram is useful in interpolating from observed values for two reasons:

(1) The range of the variogram identifies the maximum distance over which observations tend to be correlated. This information is important for selecting the data points near the interpolation location having values that may be related to the actual value at the interpolation location.

(2) The average squared difference between data values, along with the distances between the interpolation location and the locations of the selected observations, may be used to estimate the potential variability of the real value from the interpolated value.

Analysis of TDEM Data. Figure 5.1-2 shows conductor elevations interpreted from the TDEM survey at 36 locations near and within the waste panel region. Figure 5.1-5 shows a cumulative distribution of observed elevations, along with the average elevation and sample standard deviation. Scatterplots of conductor elevation vs. X (E-W) location and Y (N-S) location are shown in Figure 5.1-6. There is no suggestion of a significant simple trend in elevation along either direction.

A variogram of elevations was constructed in the E-W, N-S, NE-SW, and NW-SE directions. The regular arrangement of observation points facilitates this calculation: the variogram value for a separation of 250 m in the E-W direction, for example, is simply the average of the squared difference of elevation values at points adjacent to each other in the E-W direction. Similar averages can be made for multiples of the observation grid spacing (250 m) in the E-W and N-S directions. Points in the NE-SW and NW-SE directions are separated by multiples of ~353 m. In calculating the elevation variogram, the observation at (750W, 290N) was assumed to have been made at (750W, 250N). This displacement has no important effect on the resulting variogram.

Figure 5.1-7 shows the variogram of the elevation data along the directions mentioned. The separation distances considered were 250 m and 500 m in the E-W and N-S directions, and 353 m in the diagonal directions. Larger

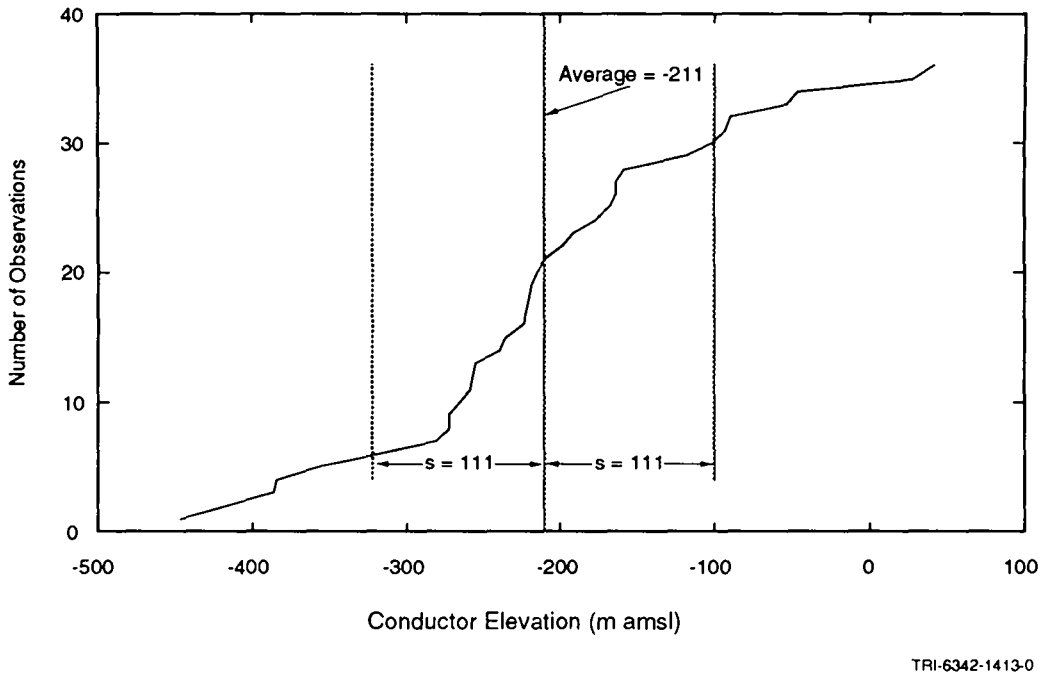

Figure 5.1-5. Population distribution and statistics for conductor elevations.

separations have too few pairs to provide a reliable estimate of mean squared difference. The horizontal line, which shows the average squared difference over all pairs of points regardless of separation, is an estimate of the variogram sill.

The striking feature of the variogram is the lack of evidence for a range of correlation of observations. The average squared difference for adjacent measurements and the expected squared difference for randomly selected measurements (i.e., the sill) are indistinguishable. In other words, there is no evidence for spatial correlation of elevation over distances as small as 250 m. (In a separate analysis, the program AKRIP was used to estimate a generalized covariance for the elevation data. The identified model contained only a "nugget" term, i.e., the generalized covariance was not found to depend on separation distance.)

Estimation of Conductor Elevation. The variogram suggests that, in attempting to estimate conductor elevation at non-measured locations, observations made 250 m from the interpolation location contain no more information about the real value at the interpolation location than more distant observations. For all points within the waste panel region, at least one observation less than 250 m away will be available. The variogram analysis does not indicate whether observations less than 250 m distant can be expected to provide information about elevation at the interpolation point. In particular, the assumption of linear variation of elevation between data points made in constructing contours of conductor elevation has no support (i.e., Figures 5.1-2 and 5.1-3).

Two bounding alternatives, corresponding to different assumptions about the behavior of the variogram between 0 and 250 m have been considered (see Figure 5.1-7):

(1) "Random elevation" assumption: Conductor elevation correlation length is very small <<250 m. The variogram is equal to the sill value between 0 and 250 m.

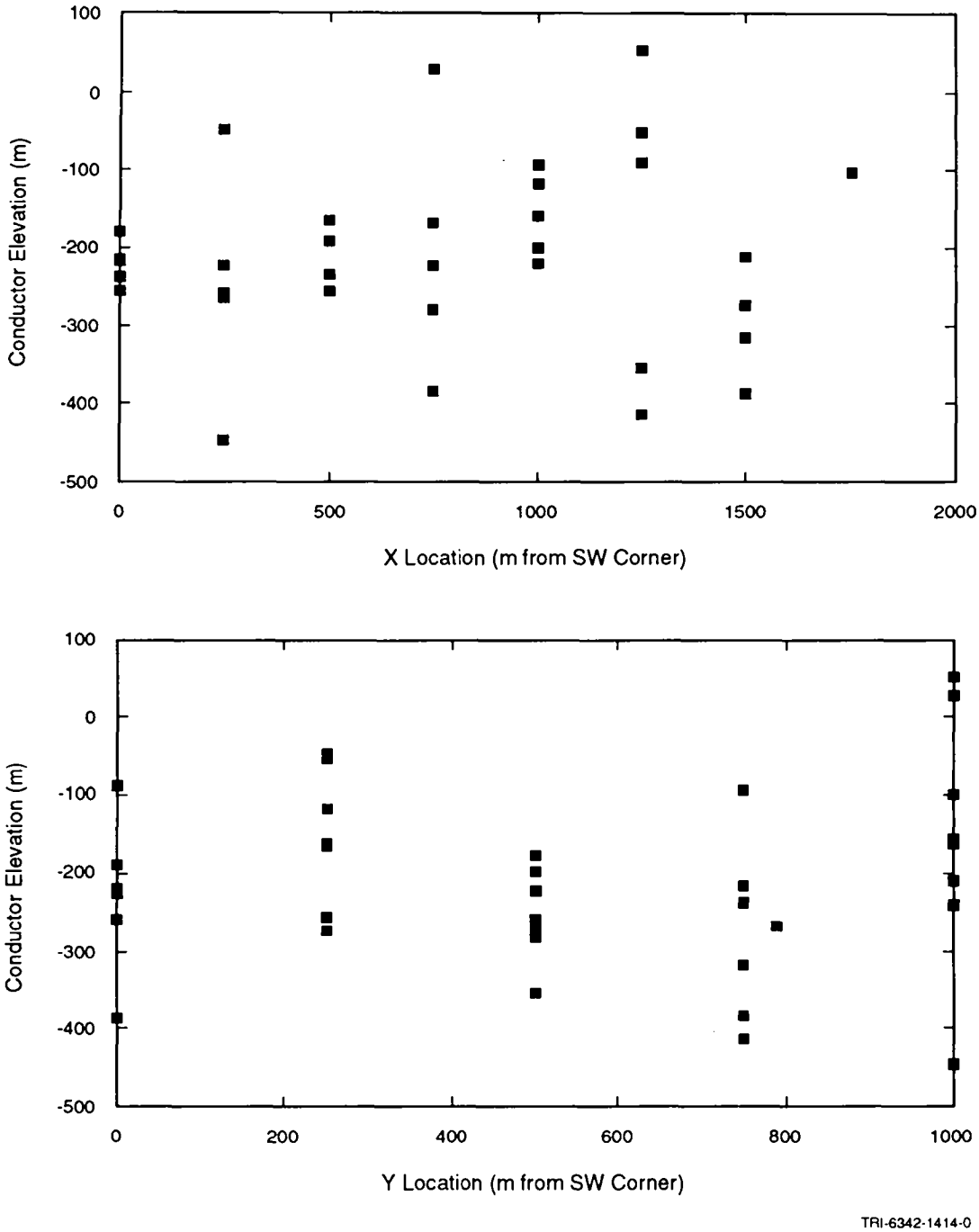

Figure 5.1-6. Scatterplots of conductor elevation vs. X and Y location.

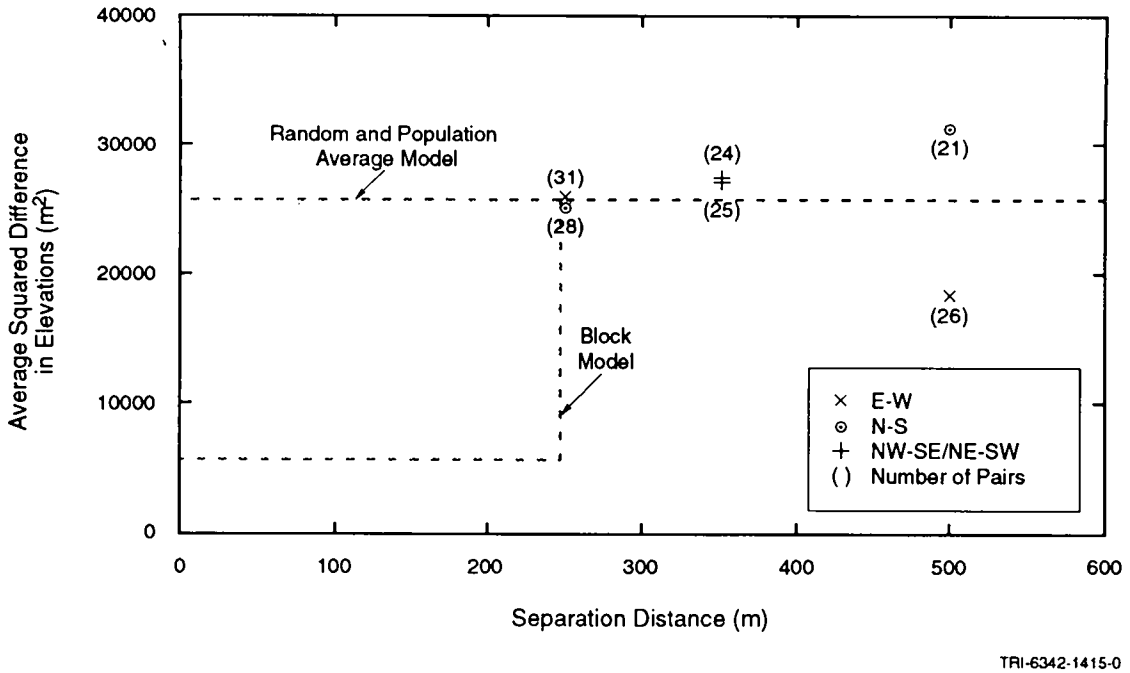

Figure 5.1-7. Empirical variogram of conductor elevations.

(2) "Block elevation" assumption: The observation grid spacing is just outside the actual correlation length. Below 250 m, observations become highly correlated, with an expected squared difference equal to twice the measurement error variance ("cookie cutter" autocorrelation).

These assumptions lead to two different methods of estimating conductor elevation. Both assumptions have been carried through in estimating brine reservoir area fraction.

In the random elevation assumption, nearby data points contribute no special information about the real value at the interpolation point in virtue of their proximity. The best estimate for elevation at any point is simply the average elevation over all observations. The variance of the error of this estimate is the population variance.

In the block elevation assumption, elevation is highly correlated over distances smaller than the measurement interval. The estimate of elevation at an interpolation point is simply the observed value at the nearest observation point. The variance of the error of this estimate is the variance of the error of the observation (75 m^2).

If the interpolated value is thought of as a weighted linear combination of observed values (as in inverse distance interpolation or in kriging), the random and block assumptions lead to the extremes of uniform weighting of all observations and exclusive weighting of the nearest observation.

Estimation of Area Fraction. The area fraction is defined as the area of the waste panel excavation overlying a brine reservoir divided by the total excavation area. A point is considered to overlie a brine reservoir if there is an electrically conductive zone in a hydrologically conductive layer of the Castile Formation. Although Castile brine reservoirs encountered during drilling appear to be always associated with the uppermost Castile anhydrite (Anhydrite III at the WIPP site), there is the possibility that brine reservoirs may occur in lower Castile anhydrites. For the purpose of estimating area fraction using the existing data, two formulations are possible:

(1) A point overlies a brine reservoir if the sub-Salado conductor elevation is greater than the elevation of the base of Anhydrite III, or

(2) A point overlies a brine reservoir if the sub-Salado conductor elevation is greater than the elevation of the base of the Castile.

For any point in the waste panel region, none of the elevations used to identify a brine reservoir by either formulation is known with certainty. In addition, there is uncertainty in which of the above formulations is appropriate. The area fraction estimate should incorporate these uncertainties.

Description of Method. Uncertainties associated with estimation of the area fraction were addressed through Monte Carlo simulations as follows:

- 200 samples from two uncorrelated uniformly distributed random variables were taken as possible values for the base elevations of the Castile and Anhydrite III. These distributions ranged from -230 m to -170 m for the base of the Castile, and from 70 m to 140 m for the base of Anhydrite III. The estimates of base elevation were uniformly distributed over the given range and were not correlated. The base elevation for the Castile and for Anhydrite III were assumed to be constant over the waste panel area.

- Along with these elevations, one of the two formulations for identifying a brine reservoir was selected at random.

- For each set of sampled base elevations and brine reservoir definition, 2000 realizations of conductor elevation were created on a uniform mesh. The relative area overlying the brine reservoir was then calculated using the sampled realizations and the selected definition of a brine reservoir.

- The relative number of simulations having a given area fraction was then used to construct an area fraction distribution. The derived area fraction distribution reflects uncertainty in conductor elevation, lithology, and the existence of brine reservoirs in lower Castile anhydrites.

The above process was applied twice, using the "random" and "block" assumptions for spatial correlation of conductor elevation in the generation of conductor realizations. In either case, conductor elevations at each mesh cell were assumed to be normally distributed around the estimated value.

Maximum Area (Bell Canyon Level). Based on the geostatistical analysis and data uncertainty described above, the use of the more conservative block model, and the assumption that a brine reservoir cannot be discounted until the Bell Canyon is reached, there is a chance that the brine reservoir has an area between 25 and 55% of the excavated area with a median of 40%. This contrasts with the best estimate of 45% from the contour method. The distribution is S-shaped (Figure 5.1-1).

Minimum Area (Anhydrite III Level). Based on the geostatistical analysis and data uncertainty described above, the probability of a brine reservoir residing in the uppermost anhydrite layer beneath the repository is very small.

50% Combination. Figure 5.1-8 shows the derived cumulative distribution of area fraction using both the "random" and "block" assumptions and assuming that 50% of the time Anhydrite III is the maximum depth and 50% of the time the Bell Canyon is the maximum depth. Both distributions show a distinct bi-modality assuming very small values of area fraction correspond to the requirement that the brine reservoir be in Anhydrite III, whereas larger area fractions correspond to the requirement that the brine reservoir be in the Castile Formation. The relative weighting of the two formulations for the brine reservoir controls the elevation of the plateau in the cumulative distribution and is clearly more important than the model of spatial variability of conductor elevation (random or block).

In the 1991 PA calculations, we used the maximum area distribution of 25 to 55% because the results are more conservative. We could not readily establish the likelihood that the elevation of Anhydrite III in the Castile

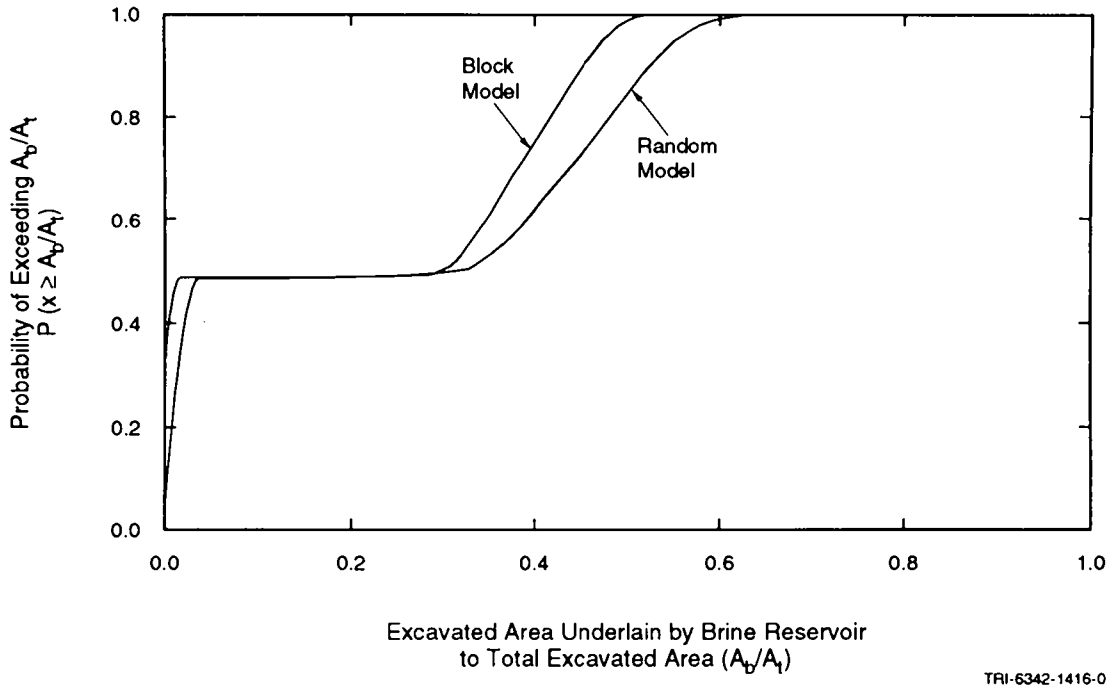

Figure 5.1-8. Cumulative distribution of area fraction using the "random" and "block" assumptions.

Formation could be used as a cutoff for indicating whether a brine reservoir existed under the disposal area without further examination of the occurrence of brine reservoirs in the region.

Lack of Spatial Correlation of Conductor Elevations. The variogram analysis suggests that conductor elevations are not correlated over a distance of 250 m. Aside from ramifications for interpolation, this result appears to place limits on the areal extent of brine reservoirs beneath WIPP. This conclusion is not entirely justified. Figure 5.1-9 shows a hypothetical arrangement of measurement points, and an underlying structure dominated by narrow features at an angle to the measurement array. Although the features are continuous over the region, observations of particular features are randomly distributed through the measurement array. In order for the underlying correlation structure of the oblong features to be revealed in this hypothetical case, the measurement array must be able to resolve the minimum characteristic dimension of the features. Note that it may still be possible for the original sampling to provide a good estimate of the relative area of each feature type.

Although Figure 5.1-9 is hypothetical, geologic considerations argue that brine reservoir location may be controlled by fracturing along Castile anticlines. In this situation, it is not unreasonable to expect brine reservoirs to be defined by long, narrow fracture zones along the anticline axis. Lack of correlation at a scale of 250 m would then place an upper limit on the minimum dimension of these fracture zones, but would not constrain maximum area extent.

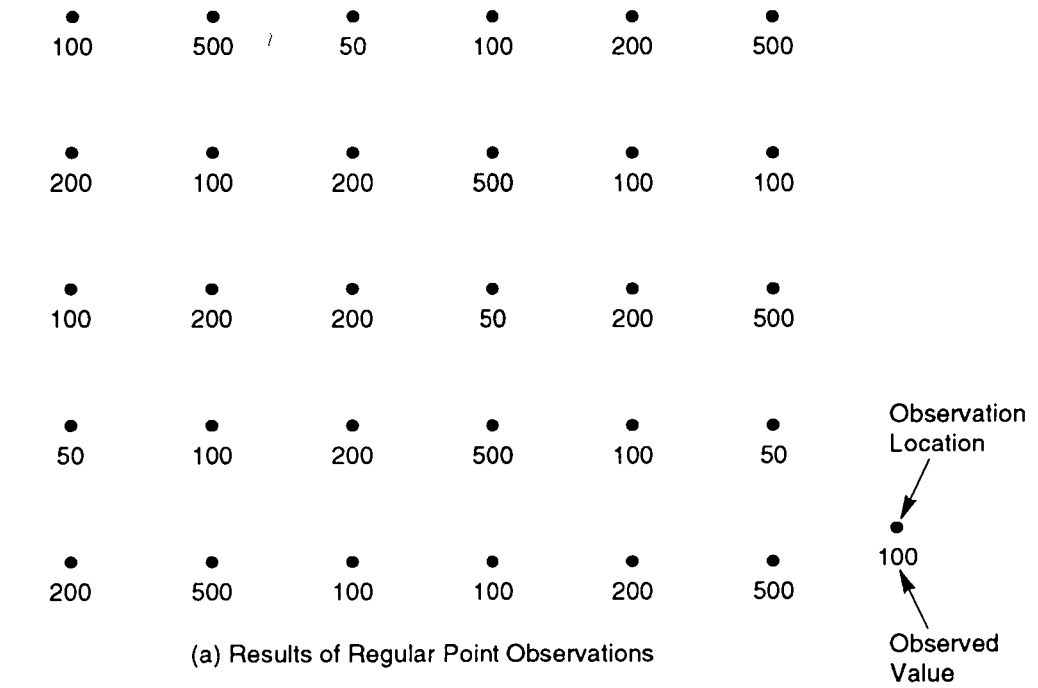

(a) Results of Regular Point Observations

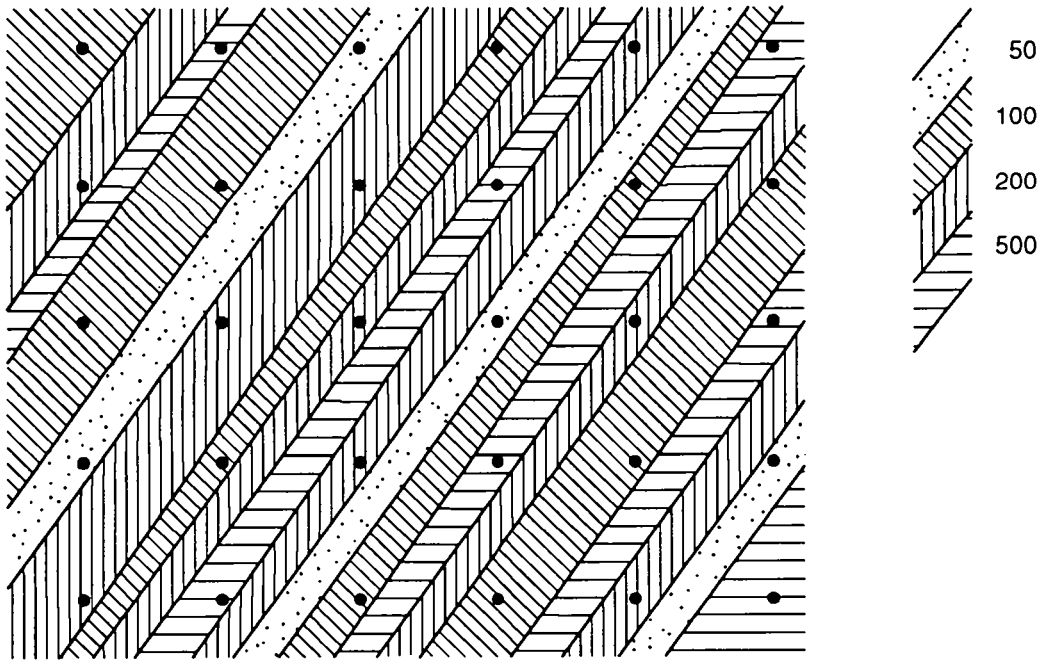

(b) Underlying Structure

TRI-6342-1419-0

Figure 5.1-9. Illustration of hypothetical variability of regular sampling of extensive narrow features.

5.2 Human-Intrusion Probability (Drilling) Models

Index for Drilling Intensity Functions*

Parameter: **Index for Drilling Intensity Functions**
Material: None

Definition Units: Dimensionless

Values: Range: (0.0, 1.0) Median: 0.5

Distribution: Uniform
Correlation:

Data Source(s): See discussion in following memo:
Hora, S. C. 1992. "Probabilities of Human Intrusion into the WIPP, Methodology for the 1992 Preliminary Comparison" (see Appendix A, pp. A-69 through A-99). (Expert Panel Judgment)

Usage:

Mathematical model:
Human Intrusion, Section 1.4.2 of this volume.

Equation 1.4.2-5 and text following that equation. The index is used to make a random selection of one drilling-intensity function from among a family of equally likely drilling-intensity functions. A family of 70 drilling-intensity functions used in 1992 calculations is shown in Appendix D of this volume.

Computational models:
CCDFPERM

Ranking in Past Sensitivity Analyses:

40 CFR 191	High
40 CFR 268	Not applicable
NEPA	Not applicable
Other	Not applicable

*Key to Parameter Sheets is provided in Section 1.2.8.

6. SUMMARY OF PARAMETERS SAMPLED IN 1992

6.1 Sampled Parameters

Tables 6.0-1, 6.0-2, and 6.0-3 summarize the parameters that were sampled for the 1992 PA calculations for the geologic barriers, engineered barriers, and agents acting on the disposal system and probability models for scenarios, respectively.

Table 6.0-1. Distributions of Sample Parameters in December 1992 WIPP Performance Assessment for Geologic Barriers

Parameter	Median	Range		Units	Distribution Type	Discussed in Text Section No.
Halite within Salado Formation						
• Log permeability (log k), undisturbed	-21.2	-24.0	-19.0	log (m^2)	Constructed	2.3.5
• Relative weight, Brooks-Corey model	n.a.	(Brooks-Corey wt. = 0.67)		none	Constructed	2.3.1
• Brooks-Corey exponent (λ)	0.7	0.2	10.0	none	Constructed	2.3.1
• Residual wetting phase (liquid) saturation, $S_{\ell r}$	0.2	0.0	0.4	none	Uniform	2.3.1
• Residual gas saturation, S_{gr}	0.2	0.0	0.4	none	Uniform	2.3.1
Anhydrite within Salado Formation						
• Log permeability (log k), undisturbed	-19.3	-21.0	-16.0	log (m^2)	Constructed	2.4.2
• Pore pressure (p)	12.5	12.0	13.0	MPa	Uniform	2.4.3
• Porosity (ϕ) undisturbed	1×10^{-2}	1×10^{-3}	3×10^{-2}	none	Constructed	2.4.4
• Index for computing DRZ porosity	0.5	0	1	none	Uniform	2.4.4
Castile Formation Brine Reservoir						
• Initial pressure (p)	12.6	11.0	21.0	MPa	Constructed	4.3.1
• Storativity, bulk (S_b)	0.2	0.02	2.0	m^3/Pa	Lognormal	4.3.2
Culebra Dolomite Member						
• Fracture spacing (2B)	0.4	0.06	8.0	m	Constructed	2.6.2
• Fracture porosity (ϕ_f)	1×10^{-3}	1×10^{-4}	1×10^{-2}	none	Lognormal	2.6.2
• Clay filling fraction (b_c/b)	0.0	0.0	0.5	none	Constructed	2.6.1
• Porosity of clay lining fractures (ϕ_c)	0.275	0.05	0.5	none	Uniform	2.6.2

Table 6.0-1. Distributions of Sample Parameters in December 1992 WIPP Performance Assessment for Geologic Barriers (Concluded)

Parameter	Median	Range		Units	Distribution Type	Discussed in Text Section No.
Log partition coefficients, clay lining fractures						
• Am	1.97	-4.0	3.0	log (m^3/kg)	Constructed	2.6.4
• Np	0.0	-4.0	3.0	log (m^3/kg)	Constructed	2.6.4
• Pu	2.31	-4.0	3.0	log (m^3/kg)	Constructed	2.6.4
• Ra	-1.47	-4.0	2.0	log (m^3/kg)	Constructed	2.6.4
• Th	-1.00	-4.0	1.0	log (m^3/kg)	Constructed	2.6.4
• U	-2.12	-4.0	0.0	log (m^3/kg)	Constructed	2.6.4
• Matrix porosity (ϕ_m)	0.139	0.096	0.208	none	Constructed	2.6.2
Log partition coefficients, matrix						
• Am	-0.730	-4.0	2.0	log (m^3/kg)	Constructed	2.6.4
• Np	-1.32	-4.0	2.0	log (m^3/kg)	Constructed	2.6.4
• Pu	-5.84	-4.0	2.0	log (m^3/kg)	Constructed	2.6.4
• Ra	-2.00	-4.0	1.0	log (m^3/kg)	Constructed	2.6.4
• Th	-2.00	-4.00	0.0	log (m^3/kg)	Constructed	2.6.4
• U	-1.54	-4.00	0.0	log (m^3/kg)	Constructed	2.6.4
• Index for Culebra transmissivity fields	0.5	0	1	none	Uniform	2.6.3

Table 6.0-2. Distributions of Sample Parameters in December 1992 WIPP Performance Assessment for Engineered Barriers

Parameter	Median	Range		Units	Distribution Type	Discussed in Text Section No.
Unmodified Waste Form:						
Gas generation, corrosion						
• Inundated rate	6.3×10^{-9}	0	1.3×10^{-8}	mol/(m^2 • s)	Constructed	3.3.5
• Relative humid rate	0.1	0	0.5	none	Constructed	3.3.5
• Stoichiometry factor	0.5	0	1	none	Uniform	3.3.5
Gas Generation, Microbiological						
• Inundated rate	3.2×10^{-9}	0	1.6×10^{-8}	mol/(kg • s)	Constructed	3.3.5
• Relative humid rate	0.1	0	0.2	none	Uniform	3.3.5
• Stoichiometry factor	0.835	0	1.67	none	Uniform	3.3.5
Log Radionuclide Solubility						
• Am	-9.00	-13.3	0.0	log (Molar)	Constructed	3.3.5
• Np	-6.99	-15.5	-2.00	log (Molar)	Constructed	3.3.5
• Pu	-9.22	-16.5	-3.24	log (Molar)	Constructed	3.3.5
• Ra	1.04	0.30	1.26	log (Molar)	Constructed	3.3.5
• Th	-10.0	-15.2	-5.6	log (Molar)	Constructed	3.3.5
• U	-3.27	-15.0	0.0	log (Molar)	Constructed	3.3.5
• Initial waste saturation	0.07	0	0.14	none	Uniform	3.4.3
Volume Fractions of IDB Categories						
• Metal/glass	0.376	0.276	0.476	none	Normal	3.4.1
• Combustibles	0.384	0.284	0.484	none	Normal	3.4.1

Table 6.0-3. Distributions of Sample Parameters in December 1992 WIPP Performance Assessment for Agents Acting on Disposal System and Probability Models for Scenarios

Parameter	Median	Range		Units	Distribution Type	Discussed in Text Section No.
Agents Acting on Disposal System						
Intrusion Borehole Flow Parameters						
• Diameter	0.355	0.267	0.444	m	Uniform	4.2.2
• Permeability (k)	3.16×10^{-12}	1×10^{-14}	1×10^{-11}	m^2	Lognormal	4.2.1
Climate parameter						
• Recharge amplitude factor	0.5	0	1.0	none	Uniform	4.4
Probability Model for Intrusion Scenarios						
• Fractional overlap of brine reservoirs	0.45	0.25	0.62	none	Constructed	5.1
• Index for drilling intensity functions	0.5	0	1.0	none	Uniform	5.2

6.2 Selection Procedure for Parameters Sampled in 1992

A parameter was chosen for sampling in the 1992 series of PA calculations if it fulfilled at least one of three criteria: (1) the parameter had proved to be moderately to highly sensitive in the 1991 sensitivity analyses (Helton et al., 1992); (2) the parameter was an imprecisely known quantity in a consequence model first formally used in the present (1992) series of calculations; and (3) new data concerning an imprecisely known parameter, data sufficient to suggest significant revision of that parameter's distribution, were available by the end of April, 1992.

Most of the 49 parameters sampled in the 1992 series of PA calculations fulfilled criteria (1) and (3). For some uncertain parameters that fulfilled only criterion (2), most notably parameters specifying mechanical properties of the Salado Formation (Section 2.5), it was simply not possible to carry out an investigation of sensitivity owing to limitations on the present consequence models and on the time available for computations.

Some imprecisely known parameters are necessarily sampled in any PA calculation that uses certain intrinsically stochastic consequence models; examples of this kind of parameter are the transmissivity fields for the Culebra Dolomite Member (Section 2.6), the recharge factor for climatic change (Section 4.4), and the drilling intensity for the model of human intrusion (Section 5.2). Finally, about seven parameters found to be mildly sensitive in 1991 sensitivity analyses (Helton et al., 1992) were resampled in 1992 solely for the purpose of maintaining statistical significance of the set of sample vectors that were used in constructing CCDFs.

REFERENCES

Arguello, J.G. 1988. *WIPP Panel Entryway Seal - Numerical Simulation of Seal Composite Interaction for Preliminary Design Evaluation.* SAND87-2804. Albuquerque, NM: Sandia National Laboratories.

Austin, E.H. 1983. *Drilling Engineering Handbook.* Boston, MA: International Human Resources Development Corporation.

Avis, J.D., and G.J. Saulnier, Jr. 1990. *Analysis of the Fluid-Pressure Responses of the Rustler Formation at H-16 to the Construction of the Air-Intake Shaft at the Waste Isolation Pilot Plant (WIPP) Site.* SAND89-7067. Albuquerque, NM: Sandia National Laboratories.

Barnhart, B.J., E.W. Campbell, E. Martinez, D.E. Caldwell, and R. Hallett. 1980. *Potential Microbial Impact on Transuranic Wastes Under Conditions Expected in the Waste Isolation Pilot Plant (WIPP), Annual Report, October 1, 1978-September 30, 1979.* LA-8297-PR. Los Alamos, NM: Los Alamos Scientific Laboratory.

Bayley, S.E., M.D. Siegel, M. Moore, and S. Faith. 1990. *Sandia Sorption Data Management System Version 2 (SSDMS II) User's Manual.* SAND89-0371. Albuquerque, NM: Sandia National Laboratories.

Bear, J. 1972. *Dynamics of Fluids in Porous Media.* New York, NY: American Elsevier Publishing Company, Inc.

Bear, J., and A. Verruijt. 1987. *Modeling Groundwater Flow and Pollution.* Boston, MA: D. Reidel Publishing Company. 126.

Beauheim, R.L. 1987a. *Analysis of Pumping Tests of the Culebra Dolomite Conducted at the H-3 Hydropad at the Waste Isolation Pilot Plant (WIPP) Site.* SAND86-2311. Albuquerque, NM: Sandia National Laboratories.

Beauheim, R.L. 1987b. *Interpretation of the WIPP-13 Multipad Pumping Test of the Culebra Dolomite at the Waste Isolation Pilot Plant (WIPP) Site.* SAND87-2456. Albuquerque, NM: Sandia National Laboratories.

Beauheim, R.L. 1987c. *Interpretations of Single-Well Hydraulic Tests Conducted At and Near the Waste Isolation Pilot Plant (WIPP) Site, 1983-1987.* SAND87-0039. Albuquerque, NM: Sandia National Laboratories.

Beauheim, R.L. 1989. *Interpretation of H-11b4 Hydraulic Tests and the H-11 Multipad Pumping Test of the Culebra Dolomite at the Waste Isolation Pilot Plant (WIPP) Site.* SAND89-0536. Albuquerque, NM: Sandia National Laboratories.

Beauheim, R.[L.] 1991. Appendix A: "Review of Salado Parameter Values to be Used in 1991 Performance Assessment Calculations," *Preliminary Comparison with 40 CFR Part 191, Subpart B for the Waste Isolation Pilot Plant, December 1991. Volume 3: Reference Data.* WIPP Performance Assessment Division. Eds. R.P. Rechard, A.C. Peterson, J.D. Schreiber, H.J. Iuzzolino, M.S. Tierney, and J.S. Sandha. SAND91-0893/3. Albuquerque, NM: Sandia National Laboratories. A-19 through A-23.

Beauheim, R.L., G.J. Saulnier, Jr., and J.D. Avis. 1991a. *Interpretation of Brine-Permeability Tests of the Salado Formation at the Waste Isolation Pilot Plant Site: First Interim Report.* SAND90-0083. Albuquerque, NM: Sandia National Laboratories.

Beauheim, R.L., T.F. Corbet, P.B. Davies, and J.F. Pickens. 1991b. Appendix A: "Recommendations for the 1991 Performance Assessment Calculations on Parameter Uncertainty and Model Implementation for Culebra Transport Under Undisturbed and Brine-Reservoir-Breach Conditions," *Preliminary Comparison with 40 CFR Part 191, Subpart B for the Waste Isolation Pilot Plant, December 1991. Volume 3: Reference Data.* WIPP Performance Assessment Division. Eds. R.P. Rechard, A.C. Peterson, J.D. Schreiber, H.J. Iuzzolino, M.S. Tierney, and J.S. Sandha. SAND91-0893/3. Albuquerque, NM: Sandia National Laboratories. A-7 through A-18.

Bechtel National, Inc. 1985. *Quarterly Geotechnical Field Data Report, December 1985.* WIPP-DOE-221. Prepared for the U.S. Department of Energy. San Francisco, CA: Bechtel National, Inc.

Bechtel National, Inc. 1986. *Waste Isolation Pilot Plant Design Validation Final Report.* DOE/WIPP-86-010. Prepared for U.S. Department of Energy. San Francisco, CA: Bechtel National, Inc.

Bertram-Howery, S.G., and R.L. Hunter, eds. 1989. *Preliminary Plan for Disposal-System Characterization and Long-Term Performance Evaluation of the Waste Isolation Pilot Plant.* SAND89-0178. Albuquerque, NM: Sandia National Laboratories.

Bertram-Howery, S.G., and P.N. Swift. 1990. *Status Report: Potential for Long-Term Isolation by the Waste Isolation Pilot Plant Disposal System.* SAND90-0616. Albuquerque, NM: Sandia National Laboratories.

Bertram-Howery, S.G., M.G. Marietta, R.P. Rechard, P.N. Swift, D.R. Anderson, B.L. Baker, J.E. Bean, Jr., W. Beyeler, K.F. Brinster, R.V. Guzowski, J.C. Helton, R.D. McCurley, D.K. Rudeen, J.D. Schreiber, and P. Vaughn. 1990. *Preliminary Comparison with 40 CFR Part 191, Subpart B for the Waste Isolation Pilot Plant, December 1990.* SAND90-2347. Albuquerque, NM: Sandia National Laboratories.

Blom, G. 1989. *Probability and Statistics: Theory and Applications.* New York, NY: Springer-Verlag.

Borns, D.J. 1985. *Marker Bed 139: A Study of Drillcore From a Systematic Array.* SAND85-0023. Albuquerque, NM: Sandia National Laboratories.

Borns, D.J. 1987. *Rates of Evaporite Deformation: The Role of Pressure Solution.* SAND85-1599. Albuquerque, NM: Sandia National Laboratories.

Brinster, K.[F.] 1990. Appendix A: "Memo 10: Well Data from Electric Logs," *Data Used in Preliminary Performance Assessment of the Waste Isolation Pilot Plant (1990).* R.P. Rechard, H.[J.] Iuzzolino, and J.S. Sandha. SAND89-2408. Albuquerque, NM: Sandia National Laboratories. A-129 through A-138.

Brinster, K.F. 1991. *Preliminary Geohydrologic Conceptual Model of the Los Medaños Region Near the Waste Isolation Pilot Plant for the Purpose of Performance Assessment.* SAND89-7147. Albuquerque, NM: Sandia National Laboratories.

Broc, R., ed. 1982. *Drilling Mud and Cement Slurry Rheology Manual.* Houston, TX: Gulf Publishing Company.

Brooks, R.H., and A.T. Corey. 1964. *Hydraulic Properties of Porous Media.* Hydrology Paper No. 3. Fort Collins, CO: Colorado State University.

Brush, L.H. 1990. *Test Plan for Laboratory and Modeling Studies of Repository and Radionuclide Chemistry for the Waste Isolation Pilot Plant.* SAND90-0266. Albuquerque, NM: Sandia National Laboratories.

Brush, L.H. 1991. Appendix A: "Current Estimates of Gas Production Rates, Gas Production Potentials, and Expected Chemical Conditions Relevant to Radionuclide Chemistry for the Long-Term WIPP Performance Assessment," *Preliminary Comparison with 40 CFR Part 191, Subpart B for the Waste Isolation Pilot Plant, December 1991. Volume 3: Reference Data.* WIPP Performance Assessment Division. Eds. R.P. Rechard, A.C. Peterson, J.D.

Schreiber, H.J. Iuzzolino, M.S. Tierney, and J.S. Sandha. SAND91-0893/3. Albuquerque, NM: Sandia National Laboratories. A-25 through A-36.

Brush, L.H., and D.R. Anderson. 1989. Appendix A: "Drum (Metal) Corrosion, Microbial Decomposition of Cellulose, Reactions Between Drum-Corrosion Products and Microbially Generated Gases, Reactions Between Possible Backfill Constituents and Gases and Water Chemical Reactions," *Systems Analysis, Long-Term Radionuclide Transport, and Dose Assessments, Waste Isolation Pilot Plant (WIPP), Southeastern New Mexico; March 1989.* Eds. A.R. Lappin, R.L. Hunter, D.P. Garber, and P.B. Davies. SAND89-0462. Albuquerque, NM: Sandia National Laboratories. A-3 through A-30.

Brush, L.H., and A.R. Lappin. 1990. Appendix A: "Additional Estimates of Gas Production Rates and Radionuclide Solubilities for Use in Models of WIPP Disposal Rooms," *Data Used in Preliminary Performance Assessment of the Waste Isolation Pilot Plant (1990).* R.P. Rechard, H. Iuzzolino, and J.S. Sandha. SAND89-2408. Albuquerque, NM: Sandia National Laboratories. A-85 through A-92.

Buck, A.D. 1985. *Development of a Sanded Nonsalt Expansive Grout for Repository Sealing Application.* Miscellaneous Paper SL-85-6. Vicksburg, MS: Department of the Army, Waterways Experiment Station.

Bush, D.D., and R. Lingle. 1986. *A Full-Scale Borehole Sealing Test in Anhydrite Under Simulated Downhole Conditions. Volume 1.* BMI/ONWI-581(1). Columbus, OH: Office of Nuclear Waste Isolation, Battelle Memorial Institute.

Bush, D.D., and S. Piele. 1986. *A Full-Scale Borehole Sealing Test in Salt Under Simulated Downhole Conditions. Volume 1.* BMI/ONWI-573(1). Columbus, OH: Office of Nuclear Waste Isolation, Battelle Memorial Institute.

Butcher, B.M. 1989. *Waste Isolation Pilot Plant Simulated Waste Compositions and Mechanical Properties.* SAND89-0372. Albuquerque, NM: Sandia National Laboratories.

Butcher, B.M. 1990. Appendix A: "Memo 5: Disposal Room Porosity and Permeability Values for Disposal Room Per-formance Assessment," *Data Used in Preliminary Performance Assessment of the Waste Isolation Pilot Plant (1990).* R. P. Rechard, H. Iuzzolino, and J. S. Sandha. SAND89-2408. Albuquerque, NM: Sandia National Laboratories. A-93 through A-102.

Butcher, B.M., T.W. Thompson, R.G. VanBuskirk, and N.C. Patti. 1991. *Mechanical Compaction of Waste Isolation Pilot Plant Simulated Waste.* SAND90-1206. Albuquerque, NM: Sandia National Laboratories.

Caldwell, D.E., R.C. Hallett, M.A. Molecke, E. Martinez, and B.J. Barnhart. 1988. *Rates of Co_2 Production From the Microbial Degradation of Transuranic Wastes Under Simulated Geologic Isolation Conditions.* SAND87-7170. Albuquerque, NM: Sandia National Laboratories.

Carmichael, R.S., ed. 1984. *CRC Handbook of Physical Properties of Rocks.* Boca Raton, FL: CRC Press, Inc. Vol. III.

Cauffman, T.L., A.M. LaVenue, and J.P. McCord. 1990. *Ground-Water Flow Modeling of the Culebra Dolomite. Volume II: Data Base.* SAND89-7068/2. Albuquerque, NM: Sandia National Laboratories.

Cheeseman, R.J. 1978. "Geology and Oil/Potash Resources of Delaware Basin, Eddy and Lea Counties, New Mexico," *Geology and Mineral Deposits of Ochoan Rocks in Delaware Basin and Adjacent Areas.* New Mexico Bureau of Mines and Mineral Resources Circular 159. Socorro, NM: New Mexico Bureau of Mines and Mineral Resources. 7-14.

Christensen, C.L., and E.W. Petersen. 1981. *The Bell Canyon Test Summary Report.* SAND80-1375. Albuquerque, NM: Sandia National Laboratories.

Clark, S.P., Jr., ed. 1966. *Handbook of Physical Constants*. Memoir 97. New York, NY: The Geological Society of America, Inc.

Colebrook, C.F. 1939. "Turbulent Flow in Pipes, with Particular Reference to the Transition Region Between the Smooth and Rough Pipe Laws," *Journal of the Institution of Civil Engineers*. Vol. 11, 133-156.

Crichlow, H.B. 1977. *Modern Reservoir Engineering - A Simulation Approach*. Englewood Cliffs, NJ: Prentice-Hall, Inc.

Cygan, R.T. 1991. *The Solubility of Gases in NaCl Brine and a Critical Evaluation of Available Data*. SAND90-2848. Albuquerque, NM: Sandia National Laboratories.

Darley, H.C.H. 1969. "A Laboratory Investigation of Borehole Stability," *Journal of Petroleum Technology*. July 1969, 883-892.

Darley, H.C.H., and G.R. Gray. 1988. *Composition and Properties of Drilling and Completion Fluids*. Houston, TX: Gulf Publishing Company.

Davies, P.B. 1989. *Variable-Density Ground-Water Flow and Paleohydrology in the Waste Isolation Pilot Plant (WIPP) Region, Southeastern New Mexico*. Open-File Report 88-490. Albuquerque, NM: U.S. Geological Survey.

Davies, P.B. 1991a. *Evaluation of the Role of Threshold Pressure in Controlling Flow of Waste-Generated Gas into Bedded Salt at the Waste Isolation Pilot Plant*. SAND90-3246. Albuquerque, NM: Sandia National Laboratories.

Davies, P.B. 1991b. Appendix A: "Uncertainty Estimates for Threshold Pressure for 1991 Performance Assessment Calculations Involving Waste-Generated Gas," *Preliminary Comparison with 40 CFR Part 191, Subpart B for the Waste Isolation Pilot Plant, December 1991. Volume 3: Reference Data*. WIPP Performance Assessment Division. Eds. R.P. Rechard, A.C. Peterson, J.D. Schreiber, H.J. Iuzzolino, M.S. Tierney, and J.S. Sandha. SAND91-0893/3. Albuquerque, NM: Sandia National Laboratories. A-37 through A-41.

Davies, P.[B.], and [A.] M. LaVenue. 1990a. Appendix A: "Memo 3b: Comments on Model Implementation and Data for Use in August Performance Assessment Calculations," *Data Used in Preliminary Performance Assessment of the Waste Isolation Pilot Plant (1990)*. R.P. Rechard, H. Iuzzolino, and J.S. Sandha. SAND89-2408. Albuquerque, NM: Sandia National Laboratories. A-63 through A-78.

Davies, P.B., and A.M. LaVenue. 1990b. Appendix A: "Memo 11: Additional Data for Characterizing 2-Phase Flow Behavior in Waste-Generated Gas Simulations and Pilot Point Information for Final Culebra 2-D Model," *Data Used in Preliminary Performance Assessment of the Waste Isolation Pilot Plant (1990)*. R. P. Rechard, H. Iuzzolino, and J. S. Sandha. SAND89-2408. Albuquerque, NM: Sandia National Laboratories. A-139 through A-156.

Davies, P.B., L. H. Brush, and F.T. Mendenhall. 1991. "Assessing the Impact of Waste-Generated Gas from the Degradation of Transuranic Waste at the Waste Isolation Pilot Plant: An Overview of Strongly Coupled Chemical, Hydrologic, and Structural Processes," *Proceedings of NEA Workshop on Gas Generation and Release from Radioactive Waste Repositories, Aix-en-Provence, France, September 23-26, 1991*. Eds. P.B. Davies, L.H. Brush, M.A. Molecke, F.T. Mendenhall, and S.W. Webb. SAND91-2378. Albuquerque, NM: Sandia National Laboratories. 1-1 through 1-24.

Dullien, F.A.L. 1979. *Porous Media: Fluid Transport and Pore Structure*. New York, NY: Academic Press.

Earth Technology Corporation. 1988. *Final Report for Time Domain Electromagnetic (TDEM) Surveys at the WIPP Site*. SAND87-7144. Albuquerque, NM: Sandia National Laboratories.

Efron, B., and R. Tibshirani. 1991. "Statistical Data Analysis in the Computer Age," *Science*. Vol. 253, no. 5018, 390-395.

EPA (Environmental Protection Agency). 1985. "40 CFR Part 191: Environmental Standards for the Management and Disposal of Spent Nuclear Fuel, High-Level, and Transuranic Radioactive Wastes," *Federal Register*. Vol. 50, no. 182, 38066-38089.

Fanchi, J.R., J.E. Kennedy, and D.L. Dauben. 1987. *BOAST II: A Three-Dimensional, Three-Phase Black Oil Applied Simulation Tool*. DOE/BC-88/2/SP. Tulsa, OK: K and A Technology.

Finley, S.J., and D. F. McTigue. 1991. Appendix A: "Parameter Estimates from the Small-Scale Brine Inflow Experiments," *Preliminary Comparison with 40 CFR Part 191, Subpart B for the Waste Isolation Pilot Plant, December 1991. Volume 3: Reference Data.* WIPP Performance Assessment Division. Eds. R.P. Rechard, A.C. Peterson, J.D. Schreiber, H.J. Iuzzolino, M.S. Tierney, and J.S. Sandha. SAND91-0893/3. Albuquerque, NM: Sandia National Laboratories. A-55 through A-58.

Frederickson, A.G. 1960. "Helical Flow of an Annular Mass of Visco-Elastic Fluid," *Chemical Engineering Science*. Vol. 11, no. 3, 252-259.

Freeze, R.A., and J.A. Cherry. 1979. *Groundwater*. Englewood Cliffs, NJ: Prentice-Hall, Inc.

Geological Society of America, Inc. 1984. *Decade of North American Geology Geologic Time Scale*. Map and Chart Series MCH 050. Boulder, CO: Geological Society of America, Inc.

Gonzales, M.M. 1989. *Compilation and Comparison of Test-Hole Location Surveys in the Vicinity of the Waste Isolation Pilot Plant Site*. SAND88-1065. Albuquerque, NM: Sandia National Laboratories.

Harms, J.C., and C.R. Williamson. 1988. "Deep-Water Density Current Deposits of Delaware Mountain Group (Permian), Delaware Basin, Texas and New Mexico," *American Association of Petroleum Geologists Bulletin*. Vol. 72, no. 3, 299-317.

Harr, M.E. 1987. *Reliability-Based Design in Civil Engineering*. New York, NY: McGraw-Hill Book Co.

Haug, A., V.A. Kelley, A.M. LaVenue, and J.F. Pickens. 1987. *Modeling of Ground-Water Flow in the Culebra Dolomite at the Waste Isolation Pilot Plant (WIPP) Site: Interim Report*. Contractor Report SAND86-7167. Albuquerque, NM: Sandia National Laboratories.

Helton, J.C. 1991. "Drilling Intrusion Probabilities," *Preliminary Comparison with 40 CFR Part 191, Subpart B for the Waste Isolation Pilot Plant, December 1991. Volume 2: Probability and Consequence Modeling.* WIPP Performance Assessment Division. SAND91-0893/2. Albuquerque, NM: Sandia National Laboratories. 2-1 through 2-37.

Helton, J.C., J.M. Griesmeyer, E.E. Haskin, R.L. Iman, C.N. Amos, and W.B. Murfin. 1988. "Integration of the NUREG-1150 Analyses: Calculation of Risk and Propagation of Uncertainties," *Proceedings of the Fifteenth Water Reactor Safety Information Meeting, Gaithersburg, MD, October 26-30, 1987*. Ed. A.J. Weiss. Washington, DC U.S. Nuclear Regulatory Commission. Vol. 1, 151-176.

Helton, J.C., J.W. Garner, R.D. McCurley, and D.K. Rudeen. 1991. *Sensitivity Analysis Techniques and Results for Performance Assessment at the Waste Isolation Pilot Plant*. Contractor Report SAND90-7103. Albuquerque, NM: Sandia National Laboratories.

Helton, J.C., J.W. Garner, R. P. Rechard, D.K. Rudeen, and P.N. Swift. 1992. *Preliminary Comparison with 40 CFR Part 191, Subpart B for the Waste Isolation Pilot Plant, December 1991. Volume 4: Uncertainty and Sensitivity Analysis*. SAND91-0893/4. Albuquerque, NM: Sandia National Laboratories.

Henderson, F.M. 1966. *Open Channel Flow*. New York, NY: Macmillan Publishing Co.

Hills, J.M. 1984. "Sedimentation, Tectonism, and Hydrocarbon Generation in Delaware Basin, West Texas and Southeastern New Mexico," *American Association of Petroleum Geologists Bulletin*. Vol. 68, no. 3, 250-267.

Hiss, W.L. 1975. "Stratigraphy and Ground-Water Hydrology of the Capitan Aquifer, Southeastern New Mexico and West Texas." Ph.D. dissertation. Boulder, CO: University of Colorado, Hydrology Department.

Holcomb, D.J., and M. Shields. 1987. *Hydrostatic Creep Consolidation of Crushed Salt With Added Water*. SAND87-1990. Albuquerque, NM: Sandia National Laboratories.

Holt, R.M., and D.W. Powers. 1988. *Facies Variability and Post-Depositional Alteration Within the Rustler Formation in the Vicinity of the Waste Isolation Pilot Plant, Southeastern New Mexico*. DOE-WIPP 88-004. Carlsbad, NM: Westinghouse Electric Corporation.

Holt, R.M., and D.W. Powers. 1990. *Geologic Mapping of the Air Intake Shaft at the Waste Isolation Pilot Plant*. DOE-WIPP 90-051. Carlsbad, NM: Westinghouse Electric Corporation.

Hora, S.C., and R.L. Iman. 1989. "Expert Opinion in Risk Analysis: The NUREG-1150 Methodology," *Nuclear Science and Engineering*. Vol. 102, no. 4, 323-331.

Hora, S.C., D. von Winterfeldt, and K.M. Trauth. 1991. *Expert Judgment on Inadvertent Human Intrusion into the Waste Isolation Pilot Plant*. SAND90-3063. Albuquerque, NM: Sandia National Laboratories.

Howarth, S.M., E.W. Peterson, P.L. Lagus, K. Lie, S.J. Finley, and E.J. Nowak. 1991. "Interpretation of In-Situ Pressure and Flow Measurements of the Salado Formation at the Waste Isolation Pilot Plant," *Society of Petroleum Engineers Rocky Mountain Regional Meeting and Low-Permeability Reservoir Symposium, Denver, CO, April 15-17, 1991*. SPE-21840. Richardson, TX: Society of Petroleum Engineers.

Hume, H.R., and A. Shakoor. 1981. "Mechanical Properties," *Physical Properties Data for Rock Salt*. NBS Monograph 167. Washington, DC: National Bureau of Standards. 103-203.

Hunter, R.L. 1985. *A Regional Water Balance for the Waste Isolation Pilot Plant (WIPP) Site and Surrounding Area*. SAND84-2233. Albuquerque, NM: Sandia National Laboratories.

Huyakorn, P.S., H.O. White, Jr., and S. Panday. 1991. *STAFF2D: Solute Transport and Fracture Flow in Two Dimensions*. Version 3.1. Herndon, VA: Hydrogeologic, Inc.

IAEA (International Atomic Energy Agency). 1986. *Decay Data of the Transactinium Nuclides*. Technical Report No. 261. Vienna, Austria: International Atomic Energy Agency.

Ibrahim, M.A., M.R. Tek, and D.L. Katz. 1970. *Threshold Pressure in Gas Storage*. Arlington, VA: American Gas Association, Inc.

ICRP, Pub 38. 1983. "Radionuclide Transformations - Energy and Intensity of Emissions," *Annals of the International Commission on Radiological Protection (ICRP)*. Vols. 11-13. ICRP Publication No. 38.

Johnson, N.L., and S. Kotz. 1970a. *Continuous Univariate Distributions-1*. New York, NY: John Wiley & Sons.

Johnson, N.L., and S. Kotz. 1970b. *Continuous Univariate Distributions-2*. New York, NY: John Wiley & Sons.

Kaufmann, D.W., ed. 1960. *Sodium Chloride, The Production and Properties of Salt and Brine*. Monograph No. 145. Washington, DC: American Chemical Society.

Kelley, V.A., and J.F. Pickens. 1986. *Interpretation of the Convergent-Flow Tracer Tests Conducted in the Culebra Dolomite at the H-3 and H-4 Hydropads at the Waste Isolation Pilot Plant (WIPP) Site*. SAND86-7161. Albuquerque, NM: Sandia National Laboratories.

Kelley, V.A., and G.J. Saulnier, Jr. 1990. *Core Analyses for Selected Samples from the Culebra Dolomite at the Waste Isolation Pilot Plant Site*. SAND90-7011. Albuquerque, NM: Sandia National Laboratories.

Kipp, K.L., Jr. 1987. *HST3D: A Computer Code for Simulation of Heat and Solute Transport in Three-Dimensional Ground-Water Flow Systems*. WRIR 86-4095. Denver, CO: U.S. Geological Survey.

Krieg, R.D. 1984. *Reference Stratigraphy and Rock Properties for the Waste Isolation Pilot Plant (WIPP) Project*. SAND83-1908. Albuquerque, NM: Sandia National Laboratories.

Lappin, A.R. 1988. *Summary of Site-Characterization Studies Conducted from 1983 through 1987 at the Waste Isolation Pilot Plant (WIPP) Site, Southeastern New Mexico*. SAND88-0157. Albuquerque, NM: Sandia National Laboratories.

Lappin, A.R., R.L. Hunter, D.P. Garber, and P.B. Davies, eds. 1989. *Systems Analysis, Long-Term Radionuclide Transport, and Dose Assessments, Waste Isolation Pilot Plant (WIPP), Southeastern New Mexico; March 1989*. SAND89-0462. Albuquerque, NM: Sandia National Laboratories.

LaVenue, A.M., T.L. Cauffman, and J. F. Pickens. 1990. *Ground-Water Flow Modeling of the Culebra Dolomite. Volume I: Model Calibration*. SAND89-7068/1. Albuquerque, NM: Sandia National Laboratories.

Lynch, A.W., and R.G. Dosch. 1980. *Sorption Coefficients for Radionuclides on Samples from the Water-Bearing Magenta and Culebra Members of the Rustler Formation*. SAND80-1064. Albuquerque, NM: Sandia National Laboratories.

Marietta, M.G., S.G. Bertram-Howery, D.R. Anderson, K.F. Brinster, R.V. Guzowski, H.[J.] Iuzzolino, and R.P. Rechard. 1989. *Performance Assessment Methodology Demonstration: Methodology Development for Evaluating Compliance With EPA 40 CFR 191, Subpart B, for the Waste Isolation Pilot Plant*. SAND89-2027. Albuquerque, NM: Sandia National Laboratories.

Marsily, G. de. 1986. *Quantitative Hydrogeology: Groundwater Hydrology for Engineers*. Orlando, FL: Academic Press, Inc.

Matalucci, R.V. 1988. *In Situ Testing at the Waste Isolation Pilot Plant*. SAND87-2382. Albuquerque, NM: Sandia National Laboratories.

McTigue, D.F., S.J. Finley, J.H. Gieske, and K.L. Robinson. 1991. Appendix A: "Compressibility Measurements on WIPP Brines," *Preliminary Comparison with 40 CFR Part 191, Subpart B for the Waste Isolation Pilot Plant, December 1991. Volume 3: Reference Data*. WIPP Performance Assessment Division. Eds. R.P. Rechard, A.C. Peterson, J.D. Schreiber, H.J. Iuzzolino, M.S. Tierney, and J.S. Sandha. SAND91-0893/3. Albuquerque, NM: Sandia National Laboratories. A-79 through A-98.

Mendenhall, F.T., B.M. Butcher, and P.B. Davies. 1991. "Investigations into the Coupled Fluid Flow and Mechanical Creep Closure Behavior of Waste Disposal Rooms in Bedded Salt," *Waste-Generated Gas at the Waste Isolation Pilot Plant: Papers Presented at the Nuclear Energy Agency Workshop on Gas Generation and Release from Radioactive Waste Repositories, Aix-en-Provence, France, September 23-26, 1991*. Eds. P.B. Davies, L.H. Brush, M.A. Molecke, F.T. Mendenhall, and S.W. Webb. SAND91-2378. Albuquerque, NM: Sandia National Laboratories. Chapter 3.

Mercer, J. W. 1983. *Geohydrology of the Proposed Waste Isolation Pilot Plant Site, Los Medaños Area, Southeastern New Mexico*. Water-Resources Investigations Report 83-4016. Albuquerque, NM: U.S. Geological Survey.

Mercer, J.W., and B.R. Orr. 1979. *Interim Data Report on the Geohydrology of the Proposed Waste Isolation Pilot Plant Site, Southeast New Mexico.* U.S. Geological Survey Water-Resources Investigations 79-98. Albuquerque, NM: U.S. Geological Survey.

Miller, I., and J.E. Freund. 1977. *Probability and Statistics for Engineers.* 2nd ed. Englewood Cliffs, NJ: Prentice-Hall.

Molecke, M.A. 1979. *Gas Generation from Transuranic Waste Degradation: Data Summary and Interpretation.* SAND79-1245. Albuquerque, NM: Sandia National Laboratories.

Munson, D.E., A.F. Fossum, and P.E. Senseny. 1989. *Advances in Resolution of Discrepancies Between Predicted and Measured In Situ WIPP Room Closures.* SAND88-2948. Albuquerque, NM: Sandia National Laboratories.

Munson, D.E., J.R. Ball, and R.L. Jones. 1990. "Data Quality Assurance Controls Through the WIPP In Situ Data Acquisition, Analysis, and Management System," *Proceedings of the International High-Level Radioactive Waste Management Conference, Las Vegas, NV, April 8-12, 1990.* SAND88-2845C. La Grange Park, IL: American Nuclear Society. Vol. 2, 1337-1350.

NEPA. 1969. *National Environmental Policy Act of 1969.* Pub. L. No. 91-190, 83 Stat. 852.

Novak, C.F. 1991. Appendix A: "Rationale for K_d Values Provided During Elicitation of the Retardation Expert Panel, May 1991," *Preliminary Comparison with 40 CFR Part 191, Subpart B for the Waste Isolation Pilot Plant, December 1991. Volume 3: Reference Data.* WIPP Performance Assessment Division. Eds. R. P. Rechard, A.C. Peterson, J.D. Schreiber, H.J. Iuzzolino, M.S. Tierney, and J.S. Sandha. SAND91-0893/3. Albuquerque, NM: Sandia National Laboratories. A-99 through A-106.

Novak, C.F. 1992. *An Evaluation of Radionuclide Batch Sorption Data on Culebra Dolomite for Aqueous Compositions Relevant to the Human Intrusion Scenario for the Waste Isolation Pilot Plant.* SAND91-1299. Albuquerque, NM: Sandia National Laboratories.

Nowak, E.J., and J.C. Stormont. 1987. *Scoping Model Calculations of the Reconsolidation of Crushed Salt in WIPP Shafts.* SAND87-0879. Albuquerque, NM: Sandia National Laboratories.

Nowak, E.J., and L.D. Tyler. 1989. "The Waste Isolation Pilot Plant (WIPP) Seal System Performance Program," *Proceedings of the Joint NEA/CEC Workshop on Sealing of Radioactive Waste Repositories, Braunschweig, FRG, May 22-25, 1989.* SAND89-0386C. Paris, France: Organisation for Economic Co-operation and Development. 98-110.

Nowak, E.J., D.F. McTigue, and R. Beraun. 1988. *Brine Inflow to WIPP Disposal Rooms: Data, Modeling, and Assessment.* SAND88-0112. Albuquerque, NM: Sandia National Laboratories.

Nowak, E.J., J.R. Tillerson, and T.M. Torres. 1990. *Initial Reference Seal System Design: Waste Isolation Pilot Plant.* SAND90-0355. Albuquerque, NM: Sandia National Laboratories.

OCC (Oil Conservation Commission). 1989. *Application of the Oil Conservation Division Upon Its Own Motion to Revise Order R-111, As Amended, Pertaining to the Potash Areas of Eddy and Lea Counties, New Mexico.* Order No. R-111-P.

Oldroyd, J.G. 1958. "Non-Newtonian Effects in Steady Motion of Some Idealized Elastico-Viscous Liquids," *Proceedings of the Royal Society of London. Series A–Mathematical and Physical Sciences.* Vol. 245, no. 1241, 278-297.

Pace, B. O. 1990. Appendix A: "Letter 1b: Changes to Bar Graphs," *Data Used in Preliminary Performance Assessment of the Waste Isolation Pilot Plant (1990).* R. P. Rechard, H. Iuzzolino, and J. S. Sandha. SAND89-2408. Albuquerque, NM: Sandia National Laboratories. A-165 through A-170.

Parker, J.C., R.J. Lenhard, and T. Kuppusamy. 1987. "A Parametric Model for Constitutive Properties Governing Multiphase Flow in a Porous Media," *Water Resources Research*. Vol. 23, no. 4, 618-624.

Peaceman, D.W. 1977. *Fundamentals of Numerical Reservoir Simulation.* Developments in Petroleum Science, 6. New York, NY: Elsevier Scientific Publishing Company.

Perry, R.H., C.H. Chilton, and S.D. Kirkpatrick. 1969. *Chemical Engineer's Handbook*. New York, NY: McGraw-Hill Book Company.

Peterson, A.C. 1990. Appendix A: "Memo 7: Preliminary Contact Handled (CH) and Remote Handled (RH) Radionuclide Inventories," *Data Used in Preliminary Performance Assessment of the Waste Isolation Pilot Plant (1990).* R.P. Rechard, H. Iuzzolino, and J.S. Sandha. SAND89-2408. Albuquerque, NM: Sandia National Laboratories. A-107 through A-112.

Pickens, J.F., and G.E. Grisak. 1981. "Modeling of Scale-Dependent Dispersion in Hydrogeologic Systems," *Water Resources Research*. Vol. 17, no. 6, 1701-1711.

Popielak, R.S., R.L. Beauheim, S.R. Black, W.E. Coons, C.T. Ellingson, and R.L. Olsen. 1983. *Brine Reservoirs in the Castile Formation, Waste Isolation Pilot Plant (WIPP) Project, Southeastern New Mexico*. TME-3153. Carlsbad, NM: U.S. Department of Energy.

Powers, D.W., S.J. Lambert, S-E. Shaffer, L.R. Hill, and W.D. Weart, eds. 1978. *Geological Characterization Report, Waste Isolation Pilot Plant (WIPP) Site, Southeastern New Mexico*. SAND78-1596. Albuquerque, NM: Sandia National Laboratories. Vols. 1-2.

Press, W.H., B.P. Flannery, S.A. Teukolsky, and W.T. Vetterling. 1986. *Numerical Recipes, The Art of Scientific Computing*. New York, NY: Cambridge University Press.

RCRA. 1976. *Resource Conservation and Recovery Act of 1976.* Pub. L. No. 94-580, 90 Stat. 2795.

Rechard, R.P. 1989. *Review and Discussion of Code Linkage and Data Flow in Nuclear Waste Compliance Assessments*. SAND87-2833. Albuquerque, NM: Sandia National Laboratories.

Rechard, R.P., ed. 1992. *User's Reference Manual for CAMCON: Compliance Assessment Methodology Controller, Version 3.0.* SAND90-1983. Albuquerque, NM: Sandia National Laboratories.

Rechard, R.P., H.[J.] Iuzzolino, and J.S. Sandha. 1990a. *Data Used in Preliminary Performance Assessment of the Waste Isolation Pilot Plant (1990).* SAND89-2408. Albuquerque, NM: Sandia National Laboratories.

Rechard, R.P., W. Beyeler, R.D. McCurley, D.K. Rudeen, J.E. Bean, and J.D. Schreiber. 1990b. *Parameter Sensitivity Studies of Selected Components of the Waste Isolation Pilot Plant Repository/Shaft System.* SAND89-2030. Albuquerque, NM: Sandia National Laboratories.

Reeves, M., G.A. Freeze, V.A. Kelley, J.F. Pickens, D.T. Upton, and P.B. Davies. 1991. *Regional Double-Porosity Solute Transport in the Culebra Dolomite Under Brine-Reservoir-Breach Release Conditions: An Analysis of Parameter Sensitivity and Importance*. SAND89-7069. Albuquerque, NM: Sandia National Laboratories.

Richey, S.F., J.G. Wells, and K.T. Stephens. 1985. *Geohydrology of the Delaware Basin and Vicinity, Texas and New Mexico*. Water-Resources Investigations Report 84-4077. Albuquerque, NM: U.S. Geological Survey.

Rose, W., and W.A. Bruce. 1949. "Evaluation of Capillary Character in Petroleum Reservoir Rock," *Transactions of the American Institute of Mining and Metallurgical Engineers*. Vol. 186, 127-142.

Ross, S.M. 1985. *Introduction to Probability Models*. 3rd ed. Orlando, FL: Academic Press, Inc.

Sargunam, A., P. Riley, K. Arulanandan, and R.B. Krone. 1973. "Physico-Chemical Factors in Erosion of Cohesive Soils," *Journal of the Hydraulics Division, Proceedings of the American Society of Civil Engineers*. Vol. 99, no. HY3, 555-558.

Saulnier, G.J., Jr. 1987. *Analysis of Pumping Tests of the Culebra Dolomite Conducted at the H-11 Hydropad at the Waste Isolation Pilot Plant (WIPP) Site*. SAND87-7124. Albuquerque, NM: Sandia National Laboratories.

Savins, J.G., and G.C. Wallick. 1966. "Viscosity Profiles, Discharge Rates, Pressures, and Torques for a Rheologically Complex Fluid in a Helical Flow," *A.I.Ch.E. Journal*. Vol. 12, no. 2, 357-363.

Scheetz, B.E., P.H. Licastro, and D.M. Roy. 1986. *A Full-Scale Borehole Sealing Test in Anhydrite Under Simulated Downhole Conditions*. BMI/ONWI-581(2). Columbus, OH: Office of Nuclear Waste Isolation, Battelle Memorial Institute. Vol. 2.

Siegel, M.D. 1990. Appendix A: "Memo 3a: Representation of Radionuclide Retardation in the Culebra Dolomite in Performance Assessment Calculations," *Data Used in Preliminary Performance Assessment of the Waste Isolation Pilot Plant (1990)*. R.P. Rechard, H. Iuzzolino, and J.S. Sandha. SAND89-2408. Albuquerque, NM: Sandia National Laboratories. A-43 through A-62.

Sjaardema, G.D., and R.D. Krieg. 1987. *A Constitutive Model for the Consolidation of WIPP Crushed Salt and Its Use in Analyses of Backfilled Shaft and Drift Configurations*. SAND87-1977. Albuquerque, NM: Sandia National Laboratories.

SNL (Sandia [National] Laboratories). 1979. *Summary of Research and Development Activities in Support of Waste Acceptance Criteria for WIPP*. SAND79-1305. Albuquerque, NM: Sandia National Laboratories.

SNL (Sandia National Laboratories) and U.S. Geological Survey. 1983. *Basic Data Report for Drillhole ERDA 9 (Waste Isolation Pilot Plant - WIPP)*. SAND79-0270. Albuquerque, NM: Sandia National Laboratories.

Stone, C.M., R.D. Krieg, and Z.E. Beisinger. 1985. *SANCHO: A Finite Element Computer Program for the Quasistatic, Large Deformation, Inelastic Response of Two-Dimensional Solids*. SAND84-2618. Albuquerque, NM: Sandia National Laboratories.

Streeter, V.L., and E.B. Wylie. 1975. *Fluid Mechanics*. 6th ed. New York, NY: McGraw-Hill Book Co.

Sutherland, H.J., and S. Cave. 1978. *Gas Permeability of SENM Rock Salt*. SAND78-2287. Albuquerque, NM: Sandia National Laboratories.

Swift, P.N. 1991. Appendix A: "Climate and Recharge Variability Parameters for the 1991 WIPP PA Calculations," *Preliminary Comparison with 40 CFR Part 191, Subpart B for the Waste Isolation Pilot Plant, December 1991. Volume 3: Reference Data*. WIPP Performance Assessment Division. Eds. R.P. Rechard, A.C. Peterson, J.D. Schreiber, H.J. Iuzzolino, M.S. Tierney, and J.S. Sandha. SAND91-0893/3. Albuquerque, NM: Sandia National Laboratories. A-107 through A-121.

Thomas, L.K., D.L. Katz, and M.R. Tek. 1968. "Threshold Pressure Phenomena in Porous Media," *Society of Petroleum Engineers Journal*. Vol. 8, no. 2, 174-184.

Tierney, M.S. 1990. *Constructing Probability Distributions of Uncertain Variables in Models of the Performance of the Waste Isolation Pilot Plant: The 1990 Performance Simulations*. SAND90-2510. Albuquerque, NM: Sandia National Laboratories.

Tierney, M.S. 1991. *Combining Scenarios in a Calculation of the Overall Probability Distribution of Cumulative Releases of Radioactivity from the Waste Isolation Pilot Plant, Southeastern New Mexico.* SAND90-0838. Albuquerque, NM: Sandia National Laboratories.

Trauth, K.M., R.P. Rechard, and S.C. Hora. 1991. "Expert Judgment as Input to Waste Isolation Pilot Plant Performance Assessment Calculations: Probability Distributions of Significant System Parameters," *Mixed Waste, Proceedings of the First International Symposium, Baltimore, MD, August 26-29, 1991.* SAND91-0625C. Baltimore, MD: Environmental Safety and Health, University of Maryland. 4.3.1 through 4.3.9.

Trauth, K.M., S.C. Hora, R.P. Rechard, and D.R. Anderson. 1992. *The Use of Expert Judgment to Quantify Uncertainty in Solubility and Sorption Parameters for Waste Isolation Pilot Plant Performance Assessment.* SAND92-0479. Albuquerque, NM: Sandia National Laboratories.

Tyler, L.D., R.V. Matalucci, M.A. Molecke, D.E. Munson, E.J. Nowak, and J.C. Stormont. 1988. *Summary Report for the WIPP Technology Development Program for Isolation of Radioactive Waste.* SAND88-0844. Albuquerque, NM: Sandia National Laboratories.

U.S. DOE (Department of Energy). 1983. "Brine Content of Facility Interval Strata," *Results of Site Validation Experiments.* TME 3177, Rev. 2.0. [Carlsbad, NM]: Waste Isolation Pilot Plant. Vol. II, Supporting Document 10.

U.S. DOE (Department of Energy). 1989. *Waste Isolation Pilot Plant Compliance Strategy for 40 CFR Part 191.* DOE-WIPP 86-013. Carlsbad, NM: U.S. Department of Energy.

U.S. DOE (Department of Energy). 1990a. *WIPP Test Phase Plan: Performance Assessment.* DOE/WIPP 89-011, Rev. 0. Carlsbad, NM: U.S. Department of Energy.

U.S. DOE (Department of Energy). 1990b. *Final Supplement Environmental Impact Statement, Waste Isolation Pilot Plant.* DOE/EIS-0026-FS. Washington, DC: U.S. Department of Energy, Office of Environmental Restoration and Waste Management.

U.S. DOE (Department of Energy). 1990c. *Final Safety Analysis Report, Waste Isolation Pilot Plant, Carlsbad, New Mexico.* WP 02-9, Rev. 0. Carlsbad, NM: U.S. Department of Energy.

U.S. DOE (Department of Energy). 1990d. *Integrated Data Base for 1990: U.S. Spent Fuel and Radioactive Waste Inventories, Projections, and Characteristics.* DOE/RW-0006, Revision 6. Oak Ridge, TN: Oak Ridge National Laboratory for U.S. Department of Energy.

U.S. DOE (Department of Energy). 1991. *Recommended Strategy for the Remote-Handled Transuranic Waste Program.* DOE/WIPP 90-058, Revision 1. Carlsbad, NM: Waste Isolation Pilot Plant.

U.S. DOE (Department of Energy) and State of New Mexico. 1984. U.S. Department of Energy and State of New Mexico, 1981, First Modification to the July 1, 1981 "Agreement for Consultation and Cooperation" on WIPP by the State of New Mexico and U.S. Department of Energy, November 30, 1984.

Van Genuchten, R. 1978. *Calculating the Unsaturated Hydraulic Conductivity with a New Closed-Form Analytical Model.* Research Report 78-WR-08. Princeton, NJ: Princeton University, Department of Civil Engineering.

Vargaftik, N.B. 1975. *Tables on the Thermophysical Properties of Liquids and Gases in Normal and Dissociated States.* New York, NY: John Wiley & Sons, Inc.

Vennard, J.K., and R.L. Street. 1975. *Elementary Fluid Mechanics.* 5th ed. New York, NY: John Wiley & Sons, Inc.

Voss, C.I. 1984. *SUTRA (Saturated-Unsaturated TRAnsport): A Finite-Element Simulation Model for Saturated-Unsaturated Fluid-Density-Dependent Ground-Water Flow with Energy Transport or Chemically-Reactive Single-Species Solute Transport.* Reston, VA: U.S. Geological Survey National Center.

Walker, R.E. 1976. "Hydraulic Limits Are Set by Flow Restrictions," *Oil and Gas Journal.* Vol. 74, no. 40, 86-90.

Walker, R.E., and W.E. Holman. 1971. "Computer Program Predicting Drilling-Fluid Performance," *Oil and Gas Journal.* Vol. 69, no. 13, 80-90.

Ward, J.S., and N.R. Morrow. 1985. "Capillary Pressures and Gas Relative Permeabilities of Low-Permeability Sandstone," *1985 SPE/DOE Joint Symposium on Low Permeability Gas Reservoirs, Denver, CO, May 19-22, 1985.* SPE/DOE 13882. Dallas, TX: Society of Petroleum Engineers. 321-334.

Ward, R.F., C.G. St. C. Kendall, and P.M. Harris. 1986. "Upper Permian (Guadalupian) Facies and Their Association with Hydrocarbons - Permian Basin, West Texas and New Mexico," *American Association of Petroleum Geologists Bulletin.* Vol. 70, no. 3, 239-262.

Weast, R.C., and M.J. Astle, eds. 1981. *Handbook of Chemistry and Physics.* 62nd ed. Cleveland, OH: CRC Press.

WEC (Westinghouse Electric Corporation). 1990. *Waste Isolation Pilot Plant No-Migration Variance Petition.* DOE/WIPP 89-003, Rev. 1. Prepared for U.S. Department of Energy. Carlsbad, NM: Westinghouse Electric Corporation.

WEC (Westinghouse Electric Corporation). 1991. *Waste Acceptance Criteria for the Waste Isolation Pilot Plant.* WIPP-DOE-069, Rev. 4. Prepared for U.S. Department of Energy. Carlsbad, NM: Westinghouse Electric Corporation.

Williamson, C.R. 1978. "Depositional Processes, Diagenesis and Reservoir Properties of Permian Deep-Sea Sandstones, Bell Canyon Formation, Texas-New Mexico." Ph.D. dissertation. Austin, TX: University of Texas.

WIPP Act. 1979. *Department of Energy National Security and Military Applications of Nuclear Energy Authorization Act of 1980, Title II - General Provisions: Waste Isolation Pilot Plant, Delaware Basin, NM.* Pub. L. No. 96-164, 93 Stat. 1259.

WIPP PA (Performance Assessment) Department. 1992. *Long-Term Gas and Brine Migration at the Waste Isolation Pilot Plant: Preliminary Sensitivity Analyses for Post-Closure 40 CFR 268 (RCRA), May 1992.* SAND92-1933. Albuquerque, NM: Sandia National Laboratories.

WIPP PA (Performance Assessment) Division. 1991. *Preliminary Comparison with 40 CFR Part 191, Subpart B for the Waste Isolation Pilot Plant, December 1991. Volume 3: Reference Data.* SAND91-0893/3. Albuquerque, NM: Sandia National Laboratories.

Wyllie, M.R.J., and W.D. Rose. 1950. "Some Theoretical Considerations Related to the Quantitative Evaluation of the Physical Characteristics of Reservoir Rock from Electric Log Data," *Transactions of the American Institute of Mining and Metallurgical Engineers.* Vol. 189, 105-118.

Yaglom, A.M. 1962. *An Introduction to the Theory of Stationary Random Functions.* Englewood Cliffs, NJ: Prentice-Hall, Inc.

APPENDIX A:
MEMORANDA REGARDING REFERENCE DATA

Referenced Memoranda

Beraún and Davies, September 12, 1991 ..... A-5
Butcher, September 9, 1992 ..... A-15
Davies et al., July 14, 1992 (1992a) A-21
Davies et al., July 22, 1992 (1992b) A-39
Gorham et al., June 15, 1992 ..... A-47
Hora, August 25, 1992 ..... A-69
Mendenhall and Lincoln, February 28, 1992 ..... A-101
Munson, October 26, 1992 ..... A-107
Novak et al., July 20, 1992 ..... A-125
Peterson, October 28, 1992 ..... A-133
Webb, March 20, 1992 (1992a) A-141
Webb, April 30, 1992 (1992b) A-147

APPENDIX A:
MEMORANDA REGARDING REFERENCE DATA

Beraún and Davies, September 12, 1991

Date: 9/12/91
To: Distribution
From: R. Beraún, 6345, and P. B. Davies, 6344
Subject: Baseline Design Input Data Base to be Used During Calculations Effort to be Performed by Division 1514 in Determining the Mechanical Creep Closure Behavior of Waste Disposal Rooms in Bedded Salt.

Butcher, September 9, 1992

Date: 9/9/92
To: M. S. Tierney, 6342
From: B. M. Butcher, 6345
Subject: Waste Compaction Properties for the Baseline Closure Surface

Davies et al., July 14, 1992 (1992a)

Date: 7/14/92
To: B. M. Butcher, J. Schreiber, and P. Vaughn (6342)
From: P. B. Davies, S. W. Webb, and E. D. Gorham (6119)
Subject: Feedback on "PA Modeling Using BRAGFLO-1992" 7-8-92 Memo by J. Schreiber

Davies et al., July 22, 1992 (1992b)

Date: 7/22/92
To: B. M. Butcher, J. Schreiber, and P. Vaughn (6342)
From: P. B. Davies, R. L. Beauheim, and E. D. Gorham (6119)
Subject: Additional Comments on Far-Field Anhydrite Permeability Distribution in "PA Modeling Using BRAGFLO -- 1992" 7-8-92 Memo by J. Schreiber"

Gorham et al., June 15, 1992

Date: 6/15/92
To: Martin Tierney, 6342
From: Elaine Gorham, Richard Beauheim, Peter Davies, Susan Howarth, and Steve Webb (6119)
Subject: Recommendations to PA on Salado Formation Intrinsic Permeability and Pore Pressure for 40 CFR 191 Subpart B Calculations

Hora, August 25, 1992

Date: 8/25/92
To: Kate Trauth, Jon Helton, Mel Marietta, Martin Tierney, Bob Guzowski, Rip Anderson
From: Steve Hora
Subject: Probabilities of Human Intrusion into the WIPP, Methodology for the 1992 Preliminary Comparison

Mendenhall and Lincoln, February 28, 1992

Date: 2/28/92
To: D. R. Anderson 6342
From: F. T. Mendenhall, 6345, R. C. Lincoln, 6345
Subject: Single Room Porosity History for Baseline Waste Form and Gas Generation Rates

Munson, October 26, 1992

Date: 10/26/92
To: M. S. Tierney, 6342
From: D. E. Munson, 6346
Subject: Mechanical Parameters for Volume 3, SAND92-0700

Novak et al., July 20, 1992

Date: 7/20/92
To: Martin S. Tierney, 6342
From: Craig F. Novak, Fred Gelbard, and Hans W. Papenguth, 6119
Subject: Parameter Recommendations for Porosity and Thickness of Clay Fracture Linings for the 1992 WIPP Performance Assessment Calculations

Peterson, October 28, 1992

Date: 10/28/92
To: Martin Tierney, 6342
From: A. Peterson, 6342
Subject: Preliminary Contact Handled (CH) Radionuclide and Nonradionuclide Inventories and Remote Handled (RH) Radionuclide Inventory for Use in 1992 Performance Assessment

Webb, March 20, 1992 (1992a)

Date: 3/20/92
To: D. R. Anderson, 6342
From: S. W. Webb, 6344
Subject: Uncertainty Estimates for Two-Phase Characteristic Curves for 1992 RCRA Calculations

Webb, April 30, 1992 (1992b)

Date: 4/30/92
To: D. R. Anderson, 6342
From: S. W. Webb, 6344
Subject: Uncertainty Estimates for Two-Phase Characteristic Curves for 1992 40 CFR 191 Calculations

Beraún and Davies, September 12, 1991

Date: 9/12/91
To: Distribution
From: R. Beraún, 6345, and P. B. Davies, 6344
Subject: Baseline Design Input Data Base to be Used During Calculations Effort to be Performed by Division 1514 in Determining the Mechanical Creep Closure Behavior of Waste Disposal Rooms in Bedded Salt.

Sandia National Laboratories
Albuquerque, New Mexico 87185

date: September 12, 1991

to: Distribution

from: R Beraún, 6345, and P. B. Davies, 6344

subject: Baseline Design Input Data Base to be Used During Calculations Effort to be Performed by Division 1514 in Determining the Mechanical Creep Closure Behavior of Waste Disposal Rooms in Bedded Salt.

Introduction

The original disposal concept for TRU waste at WIPP is to excavate disposal rooms and fill them and adjacent access drifts with waste. Under the current baseline design, the radioactive wastes to be store consist of a variety of materials (solid organics and inorganics), and sludges. The unprocessed waste in their "as-received" state will be contained in 55-gallon drums or other containers such as standard waste boxes. While the waste remains in its unprocessed state, the materials will initially have high porosities and will be highly permeable. However, over a period of time the drums may collapse due to the closure of the rooms and the consequent loading of the containers. Under these conditions the drum waste contents will compact and cause a reduction in the corresponding porosity and permeability values [1].

This memorandum documents input data base for the baseline design submitted to Division 1514, for the purpose of performing required calculations to determine the mechanical creep closure behavior of waste disposal rooms in bedded salt in the presence of gas being generated by the waste emplaced in these rooms. The results provided need to be defined as function of time to evaluate the performance of the repository.

Geometry

Each conventionally mined disposal room is 13 ft high by 33 ft wide by 300 ft long, and its internal volume is $1.287X10^5\ ft^3$ (3644.8 m^3) [2]. The baseline design calls for a total of 6804 drums to be uniformly distributed with unprocessed waste in an equivalent room. The total volume occupied by the waste and drums is, 58718.5 ft^3 (1663 m^3). With the required headspace of 28 inches [4], the total crushed salt backfill required to seal the disposal room was calculated to be approximately 1328 m^3 [2].

Waste Characteristics

The transuranic waste destined for the WIPP site is either solid or solidified material and in its "as-received" state is grouped under three major waste forms: 1) Sludges; 2) solid organics often referred to as "combustible", consist of wastes such as paper, plastic, tissues, plywood, etc and 3) solid inorganic waste consisting of metals, glass, and a small percentage of other non-combustible materials [1,5]. Table 1 summarizes the required data input to characterize the waste for the baseline case. This table shows the waste forms and their corresponding drum count, weight, density and porosities.

Table 1: **Baseline Design Database*** [2]

Waste Form	Drum Count	Drum Weight Kg	Density (Kg/m^3)		Porosity		Elastic Modulus
			Initial	Stress Function	Initial	Stress Function	
Solid Organics	2722	77	380	Fig. 1	0.8	Fig 2	N/A†
Solid Inorganics	2722	102	900	Fig. 1	0.8	Fig 2	N/A†
Sludges	1360	211	1200	Fig. 1	0.5	Fig 2	N/A†

*These numbers are rounded to one significant figure.

†The waste is model as an inelastic material thus, Elastic properties are not required [12].

In an effort to understand the mechanical behavior of the waste to be emplaced in the repository, an investigation was conducted by Butcher [6] leading to the compilation of valuable experimental information about how material simulating transuranic (TRU) waste compact under axial compressive stress. Figures 1 and 2 obtained from Reference [6] are compaction curves representing the combustible, metallic, and sludge waste categories. Figure 1 depicts the waste density as a function of axial compaction stress. Figure 2 shows the waste porosity versus compressive stress for the same waste categories; also shown in this figure is an average porosity curve for the repository.

Repository Salt Backfill

Once the waste has been emplaced, the disposal room is backfilled with crushed salt leaving only a headspace of 28 inches [4]. The density of crushed salt is 1300 kg/m^3 [7, 8], the initial porosity is approximately 0.4 [2] and the corresponding elastic properties as specified in Reference 9 are:

Shear modulus $\mu = 1.24X10^{10}\ Pa$
Young's modulus $E = 3.1X10^{10}\ Pa$
Poisson's ratio $\nu = 0.25$

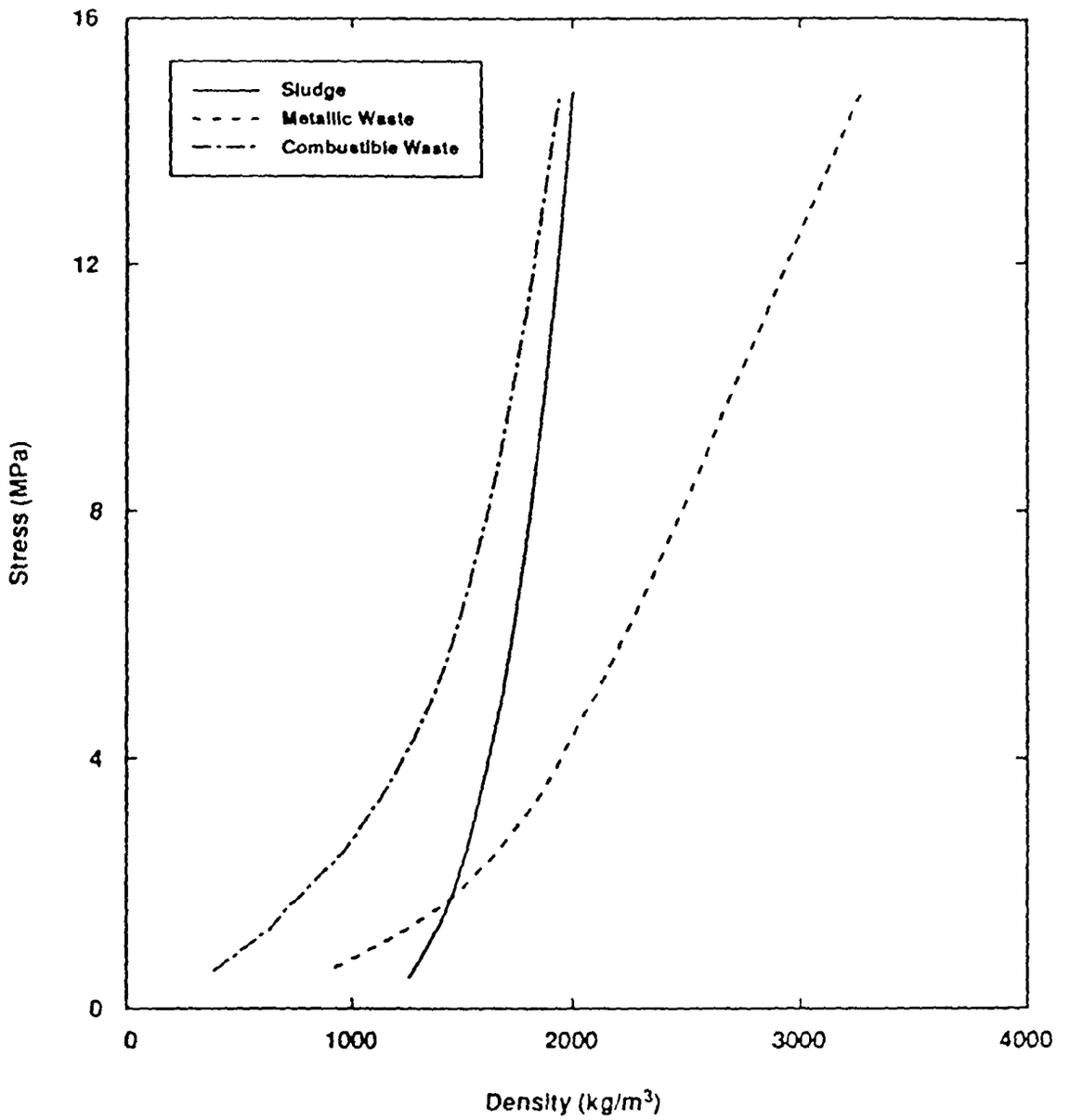

Figure 1: Compaction Stress vs Waste Densities

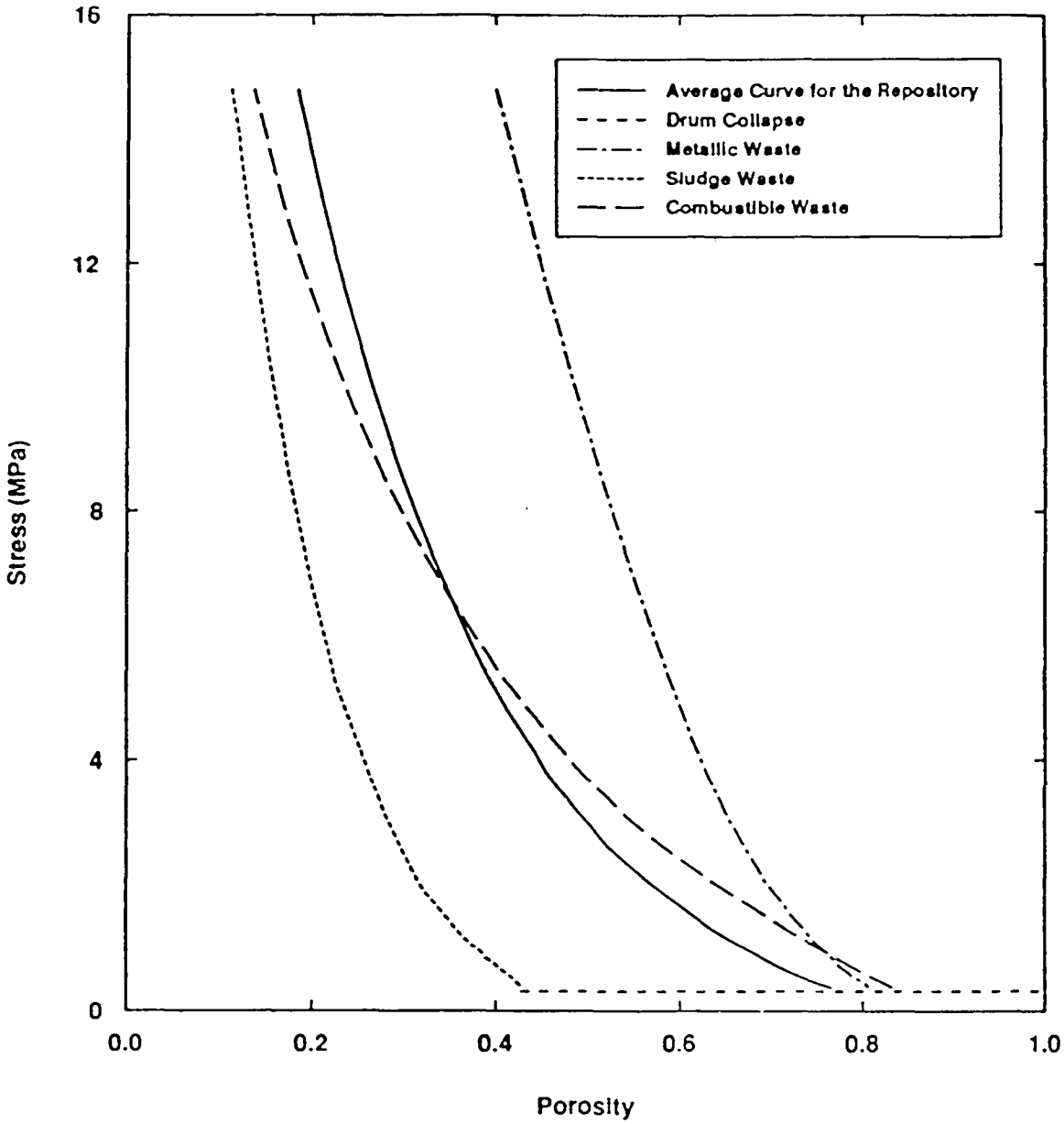

Figure 2: Waste Porosity as Function of Compressive Stress

Gas Generation

For the baseline case, Brush reported earlier [10] that H_2 production rates of 1 *mole/drum.year* and corrosion rates of 2 $\mu m/year$ were adequate estimates for inundated conditions rounded to one significant figure. The estimated gas production potential from anoxic corrosion will be 1050 *moles/drum* of waste [11] constituting 66 % of the total gas production potential. Brush also reports 1 mole of various gases per drum per year to be his best estimate for the microbial gas production rate under inundated conditions. The gas production potential from microbial activity is estimated to be at 550 *moles/drum* [11], 34 % of the total gas production potential. Table 2 summarizes current estimates of gas production rates for the baseline case performed by Brush [10].

Table 2: **Gas Production Rates for the Baseline Design [10]**

Process	Gas Production Rate† (*moles/drum.year*)	
	Inundated	Humid
Anoxic corrosion	1	0.1
Microbial activity	1	0.1
Radiolysis of brine	0.0	0.0

†These numbers are rounded to one significant figure.

Number of Waste Drums

The gas generation rates as presented in Table 2 are calculated based on a baseline waste drum. The baseline design case calls for 6804 drums with "as-received" waste to be uniformly distributed in an equivalent disposal room. Thus, utilize this number (6804 drums) to calculate the amount of gas being generated in a disposal room.

References

1. Butcher, B. M., "Waste Isolation Pilot Plant Simulated Waste Compositions and Mechanical Properties," SAND89-0372, Sandia National Laboratories, Albuquerque, New Mexico, June 1989.

2. Beraun, R, " EATF Calculations to Determine Waste Form Distribution for Alternatives # 2 and # 6,"Memorandum to Distribution, Sandia National Laboratories, Albuquerque, New Mexico, In Draft.

3. Butcher, B. M., "Preliminary Evaluation of Potential Engineered Modifications for the Waste Isolation Pilot Plant (WIPP)," SAND89-3095, Sandia National Laboratories, Albuquerque, New Mexico, April 1990.

4. U. S. Department of Energy,"Waste Isolation Pilot Plant Design Validation Final Report," DOE-WIPP-86-010, Prepared by Bechtel National Inc., San Francisco, Ca. October 1986.

5. EATF, "Evaluation of the Effectiveness and Feasibility of the Waste Isolation Pilot Plant Engineered Alternatives: Final Report of the Engineered Alternatives Task Force," DOE/WIPP 91-007, U. S. Department of Commerce, Springfield, VA. July 1991.

6. Butcher, B. M., T. W. Thompson, R. G. VanBuskirk, and N. C. Patti, "Mechanical Compaction of Waste Isolation Pilot Plant Simulated Waste," SAND90-1206, Sandia National Laboratories, Albuquerque, New Mexico, In Review.

7. Gerstle, W. H., A. K. Jones, "Mechanical Properties of Crushed Salt/Bentonite Blocks," SAND86-0707, Sandia National Laboratories, Albuquerque, New Mexico, August 1986.

8. Beraun, R., M. A. Molecke, "Thermal Analysis of the WIPP In Situ Room A1 DHLW Package Experiments," SAND86-0681, Sandia National Laboratories, Albuquerque, New Mexico, May 1987.

9. Munson, D. E., A. F. Fossum and P. E. Senseny, "Advances in Resolution of Discrepancies Between Prediction and Measured in situ Room Closures," SAND88-2948, Sandia National Laboratories, Albuquerque, New Mexico, 1989.

10. Brush, L. H., "Current Estimates of Gas Production Rates, Gas production Potentials, and Expected Chemical Conditions Relevant to Radionuclide Chemistry for the Long-Term WIPP Performance Assessment," Memorandum to D. R. Anderson, Sandia National Laboratories, Albuquerque, New Mexico, July 1991.

11. Rechard, R. P. , "Data Used In Preliminary and Performance Assessment of th Waste Isolation Pilot Plant, 1991,"SAND91-0621 Volume III, Sandia National Laboratories, Albuquerque, New Mexico, In Draft.

12. Brown, W. T. amd J. R. Weatherby, " Influence of Gas Generation Potential and Gas Generation Rate on the Performance of CH-TRU Disposal Rooms," Memorandum to B. M. Butcher and F. T. Mendenhall, 6345, Sandia National Laboratories, Albuquerque, New Mexico, September 1990.

13. Beraun, R., F. T. Mendenhall, and R. P. Rechard, "Compilation of Input Data for Alternatives 2 and 6 of the EATF to be Used During Calculations Efforts to be Performed by Division 1514 in Determining the Mechanical Creep Closure Behavior of Waste Disposal Rooms in Bedded Salt," Memorandum to Distribution, Sandia National Laboratories, Albuquerque, New Mexico, September 6 1991.

Copy to:
1510 J. C. Cummings
1514 H. S. Morgan
1514 J. G. Argüello
1514 C. M. Stone
1514 J. R. Weatherby
6340 W. D. Weart
6340-A A. R. Lappin
6340 S. Y. Pickering (file) 6341 R. C. Lincoln
6342 D. R. Anderson
6342 M. G. Marietta
6342 R. P. Rechard
6343 T. M. Schultheis
6344 E. Gorham
6344 P. B. Davies
6345 B. M. Butcher
6345 R. Beraun (5)
6345 L. H. Brush
6345 F. T. Mendenhall
6345 M. A. Molecke
6346 J. R. Tillerson
6346 D. E. Munson
DOE/WPO V. Daub
DOE/WPO D. C. Blackstone
XXXDRM
J. M. Valdez, IT
M. Abashian, IT

Butcher, September 9, 1992

Date: 9/9/92
To: M. S. Tierney, 6342
From: B. M. Butcher, 6345
Subject: Waste Compaction Properties for the Baseline Closure Surface

Sandia National Laboratories

Albuquerque, New Mexico 87185

date: September 9, 1992

to: M. S. Tierney, 6342

B. M. Butcher

from: B. M. Butcher, 6345

subject: Waste Compaction Properties for the Baseline Closure Surface

This memo is in response to your question about a suitable reference source for the baseline closure mechanical properties. With the exception of the waste compaction properties, the mechanical properties listed in chapter 3 of SAND91-2378[1] are the same as those used to compute the baseline porosity surface. The baseline compaction curve data in this reference are obsolete because they were an estimate prior to acquisition of experimental compaction curves. The data define the "old" SANCHO waste compaction curve in the attached figure.

The compaction curve data for the baseline closure calculations are given in Table 1 (taken from a forthcoming memo by Stone). These data were derived from the solid line axial compaction stress versus porosity curve in Figure 2 of the memo by Beraún and Davies (1991), which represent the average response of a repository. The actual data points for the curve are tabulated in SAND90-1206, Table 3-2. Stone's curve is obtained by dividing each axial stress data value by 3 and converting porosity to the ratio ρ/ρ_0, where ρ is the current density of the waste, and ρ_0 is its initial density. The natural logarithm of the density ratio is the true (finite) volumetric strain.

As a check, Stone's pressure values were multiplied by 3, porosity values were converted to true strain, and the data replotted in the attached figure. Equivalency is demonstrated by superposition of the data on the original axial stress curve. A caution about this construction is that both curves depend on the average initial porosity of the waste, which should be 0.787 (SAND90-1206, p. A-5). This initial porosity value corresponds to an initial average waste density of 426 kg/m^3 and an average theoretical solid density of 2000 kg/m^3 (SAND90-1206, p. A-5). It differs from the value of 0.74 that can be inferred from the initial porosities of the three waste components quoted in Table 1 of Beraún's memorandum. Beraún rounded the initial waste porosities to 0.8 for combustible waste, 0.8 for metallic waste, and 0.5 for sludges, and in the process changed the average porosity for the entire repository from 0.787 to 0.74.

I am also aware that the initial waste porosity used to define the compaction curves is probably not the same as presently being assumed for PA analyses. In comparison to other assumptions that are currently necessary for the inclusion of closure in PA analysis, this difference is presently considered to be insignificant. This assumption should be checked, however, and we should attempt to better coordinate the best value for the initial density of the waste in the future.

1.References are given at the end of the memorandum

References

F. T. Mendenhall, B. M. Butcher, and P. B. Davies. 1991. "Investigations into the Coupled Fluid Flow and Mechanical Creep Closure Behavior of Waste Disposal Rooms in Bedded Salt" in "Waste Generated Gas at the Waste Isolation Pilot Plant: Papers presented at the Nuclear Energy Agency Workshop on Gas Generation and Release from Radioactive Waste Repositories." P. B. Davies, L. H. Brush, M. A. Molecke, F. T. Mendenhall, S. W. Webb, Editors. SAND91-2378.

R. Beraún, 6345, and P. B. Davies, 6344, "Baseline Design Input Data Base to be Used During Calculations Effort to be Performed by Division 1514 in Determining the Mechanical Creep closure Behavior of Waste Disposal Rooms in Bedded Salt", Memorandum, September 12, 1991.

B. M. Butcher, T. W. Thompson, R. G. VanBuskirk, and N. C. Patti. 1991. "Mechanical compaction of Waste Isolation Pilot Plant Simulated Waste," Sandia National Laboratories Report SAND90-1206, Albuquerque, NM.

Copy to:
6303 W. D. Weart
6340 SWCF(DRM)
6342 D. R. Anderson
6342 P. Vaughn
6345 R. C. Lincoln
6345 F. T. Mendenhall
6345 B. M. Butcher (day file)

Table 1: Pressure-Volumetric Strain Waste Compaction Data Used in The Volumetric Plasticity Model for the Waste Drums in FY92
Baseline Closure Calculations

Pressure (MPa)	$\ln(\rho/\rho_0)$
0.028	0.032
0.733	0.741
1.133	0.898
1.667	1.029
2.800	1.180
10.17	1.536

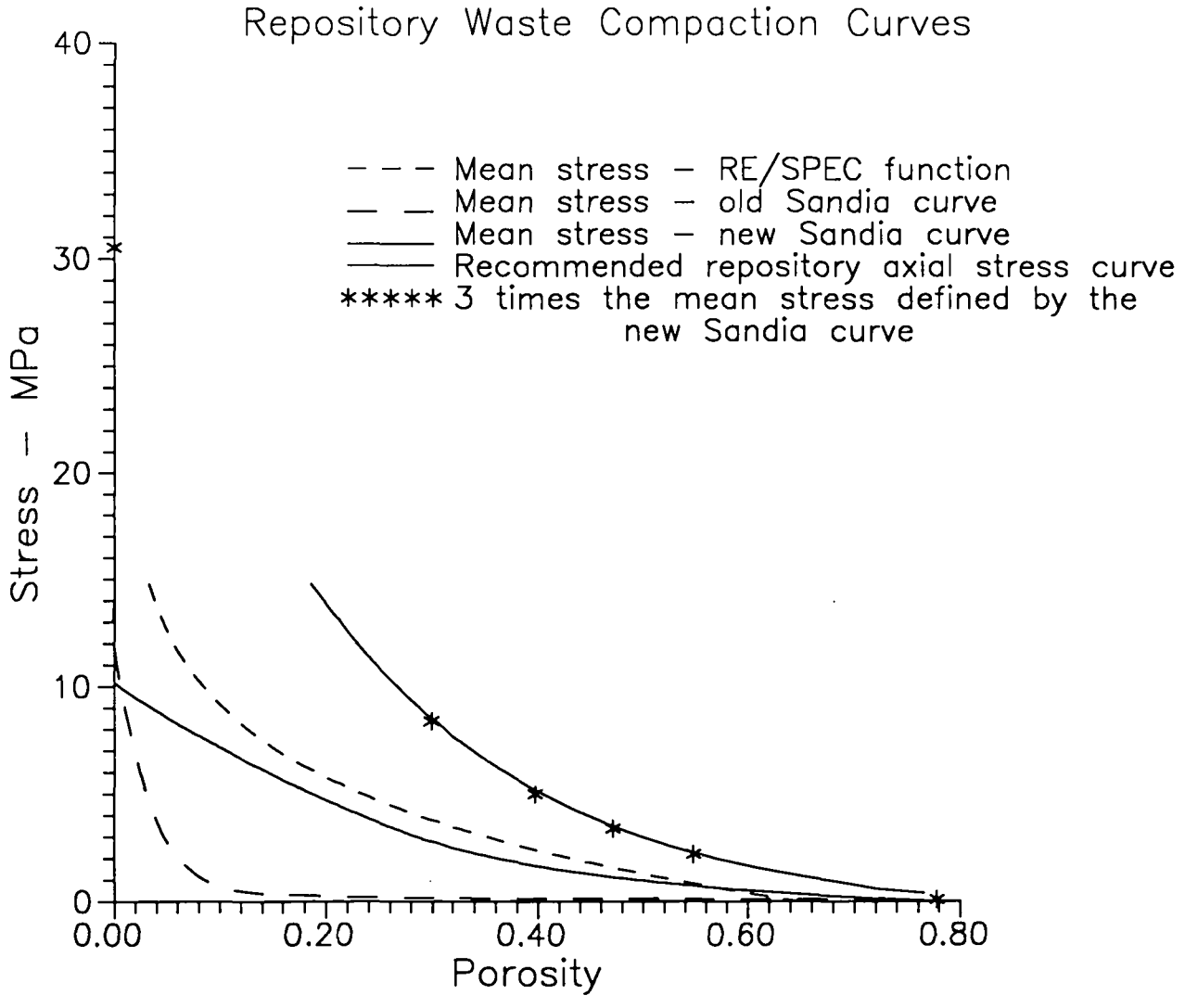

C: graph drm1 wcomp13

Davies et al., July 14, 1992 (1992a)

Date: 7/14/92
To: B. M. Butcher, J. Schreiber, and P. Vaughn (6342)
From: P. B. Davies, S. W. Webb, and E. D. Gorham (6119)
Subject: Feedback on "PA Modeling Using BRAGFLO-1992" 7-8-92 Memo by J. Schreiber

Sandia National Laboratories

Albuquerque, New Mexico 87185

Date: July 14, 1992

To: B.M. Butcher, J. Schreiber, and P. Vaughn (6342)

P.B. Davies Steve E.D. Gorham

From: P.B. Davies, S.W. Webb, E.D. Gorham (6119)

Subject: Feedback on "PA Modeling Using BRAGFLO -- 1992" 7-8-92 memo by J. Schreiber

As a follow-up to our discussions at the June 25th meeting, J. Schreiber's memo (attached) describes the configuration and rationale for repository/Salado modeling using BRAGFLO in the PA 1992 calculations. At B. Butcher's request, we have reviewed these descriptions and the following paragraphs summarize our feedback. You need to be aware that in order to respond in the very short time frame requested, this is only a brief review by those individuals that were available over the past 3 days. Therefore, this review does not cover the level of detail that should ideally be given and this review does not have input from a number of pertinent staff members. We feel that PA's effort to articulate model configuration and rationale and to incorporate feedback prior to starting simulations is a significant step forward in communications. We also feel that working through multiple iterations of this process in the months prior to calculations has the potential to significantly improve the calculations in future years. Our comments on the proposed configuration for this year are as follows:

1. The modified configuration for human intrusion scenarios is based on an "equivalent radial panel" scaled to match the initial excavated volume of a single panel. The Schreiber memo expresses concern that the 60.85 meter radius of this equivalent panel is small compared to the potential travel path distance in an actual panel (218 meters max.). Therefore, it has been suggested that the high permeability (and increased porosity) DRZ above and below the panel be extended outward to a radius of 96.78 meters. The stated rationale for this is 1) "to include some of the effect of the greater travel distances in an actual panel" and 2) to "include the DRZ above and below the pillars". There are two potential problems with this rationale. First, the original reasons for considering travel distance within an actual panel centered around the question of how much *waste* could be "accessed" by brine flow *within a panel* (Lappin et al., 1989; Marietta et al., 1989). Because there is no waste within the DRZ, extending the travel distance within the DRZ does not appear to address questions related to travel path length through waste within an actual panel. Second, the concept of "including the DRZ above and below the pillars" is confusing because other than a relatively short (roughly 1 meter) DRZ that occurs along room walls, this is no DRZ above or below the pillars. One might consider extending the DRZ in order to capture the potential increased gas storage volume if we had good information about the dimensions, porosities, and evolution of the DRZ. However, these

are poorly known and at this point do not provide a reasonable rationale for extending the DRZ. In summary, extension of the DRZ above the pillars has the effect of increasing pore volume in the DRZ to a level that cannot be substantiated by the available data. Therefore, we recommend that DRZ not be extended above the salt pillar.

2. The illustration of the model configuration is somewhat confusing in that it gives the appearance that the anhydrite interbeds start at the lateral edge of the DRZ and transition zones. Perhaps these schematics would benefit by showing how the geologic units fit into the model zones.

3. Why and how are the Culebra and the Unnamed Lower Member of the Rustler lumped in these calculations? The Unnamed Lower Member of the Rustler Formation is a dissolution residue at the contact between the Rustler and Salado. While this unit is a significant water-bearing unit in Nash Draw, it thins considerably and its transmissivities at the WIPP site are orders of magnitude lower than those in the Culebra. We do not see any good reason to lump these two units and suggest that unless there is some compelling reason not stated in the Schreiber memo as to why the Unnamed Member should be included, the Culebra Dolomite should be the only Rustler unit to be modeled explicitly.

4. Where does the 0.675 value for waste porosity (i.e. average disposal room porosity) come from? The initial porosity in the SANCHO closure calculations is 0.66. These calculations provide the basis for the creep closure porosity surface. The maximum porosity in F.T. Mendenhall's GRIDB.DAT porosity surface file is 0.565.

5. The permeability, porosity, and initial pressure are all specified in the document. What about the specific storage parameters? What are the values and what are they based on?

6. We (6119 and 6342) have not yet reached good closure on the question of the far field permeability distribution for the anhydrite interbeds. The original recommendation (model configuration and parameter distributions transmitted to PA 4-1-92 by E.D. Gorham) was to use only permeability values from a limited number of tests (3) in non-depressurized anhydrite. This approach assumed that the PA model for the 1992 calculations would be capable of including increased permeability due to fracture dilatation in response to elevated gas pressures. When it became apparent that fracture-based permeability changes will not be available in the '92 models, it was recommended that an attempt be made to crudely incorporate the effects of gas-driven increases in fracture permeability by specifying a much larger far-field permeability range for the anhydrite that included not only the non-depressurized tests, but also the group of tests in depressurized but substantially intact anhydrite and the group of tests in anhydrite that has experienced substantial fracturing in the DRZ (E.D. Gorham 6-15-92 memo). This approach was considered unrealistically conservative by performance assessment personnel in the June 25th meeting and a compromise was reached that 1) the performance assessment calculations will not attempt any representation of the interbed fracture process in the '92 calculations; 2) that explicit caveats will be placed visibly in the report that this potentially significant process was not included in the calculations; and 3) the field permeability for the anhydrite interbeds will be represented by the small group of tests in non-

depressurized anhydrite interbeds together with the much larger group of tests in depressurized but substantially intact anhydrite. While this compromise appears to be acceptable to most people, it should be recognized that this distribution is not without potential flaws that could perhaps be corrected if there were sufficient time to construct a new distribution that focused on capturing the uncertainty in whether or not some of the tests in the depressurized but substantially intact anhydrite have in fact experienced significant permeability enhancing deformation. Given the present time constraints, we suggest that the compromise distribution be used, but that it be recognized that this distribution is not without potentially important flaws.

7. Where does the DRZ porosity relationship [TZ poros + x(0.06-TZ poros)] come from and what is its purpose? We understand that in general terms, this is intend ed to relate sampled values of DRZ porosity with those from the transition zone, but there is not enough information in the Schreiber memo to fully understand this. Also, if sampled porosities between these zones are being related, shouldn't sampled permeabilities be related as well? At some point in future calculations, serious consideration should also be given to correlation of sampled permeability with sampled porosity.

8. What is the basis for the seal permeability and porosity? Are these values from recommendations from 6121?

9. We are pleased to see that the effects of depressurization of the Salado during the operation phase are being taken into account explicitly and that this appears to be a relatively straightforward task in the current PA model setup.

10. The specification of initial saturation conditions in the waste and especially in the DRZ is a difficult problem. The manual adjustment of saturations in the DRZ could lead to significant problems in correctly calculating brine mobility and gas storage volume within this zone. The approach proposed in the Schreiber memo is to start the DRZ fully brine saturated but at the end of the 20-year depressurization to manually reduce the brine volume to that which would be present prior to any adjustment (increase) of the DRZ porosity. This approach essentially assumes no substantial flow from the far field into the DRZ during the 20-year depressurization period. Given the presently specified range of anhydrite permeabilities, this is probably an unrealistic assumption. Given that this manual adjustment of the DRZ does not have a strong technical basis and that its effect is probably non-conservative (i.e. it produces less brine for gas generation and more open pore volume of gas storage), we recommend that the depressurization be run (which may produce some desaturation itself) with the specified DRZ porosity and permeability at the start of the run and that this manual saturation adjustment not be made. Another possible approach would be to not take credit for any increase in porosity in the DRZ, which we may have difficultly defending over a 10,000 year time frame.

11. The description of the relative permeability and capillary pressure curves looks good. The difficulty mentioned in defining the capillary pressure curve for a material at less than residual brine saturation is easily overcome if a maximum capillary pressure value is specified; this value can then be used if the saturation is below the brine residual

saturation value. Also, the last sentence seems to imply that a region can start out with residual saturation or higher, but the value can become below residual saturation during the calculation. We assume the only way this can happen is in the redefinition of the porosity in the DRZ regions and that it does not happen otherwise.

REFERENCES

Gorham, E.D. (6119). *Additional Suggestion for 1992 PA Calculations.* 6-15-92 Memorandum to B.Butcher and M. Tierney (6342).

Lappin, A.R., R.L. Hunter, D.P. Garber, P.B. Davies. 1989. *Systems Analysis, Long-Term Radionuclide Transport, and Dose Assessments, Waste Isolation Pilot Plant (WIPP), Southeastern New Mexico; March 1989.* SAND89-0462, Sandia National Laboratories, Albuquerque, New Mexico.

Marietta M.G., S.G. Bertram-Howery, D.R. Anderson, K.F. Brinster, R.V. Guzowski, H. Iuzzolino, R.P. Rechard. 1989. *Performance Assessment Methodology Demonstration: Methodology Development for Evaluating Compliance With EPA 40 CFR 191, Subpart B, for the Waste Isolation Pilot Plant.* SAND89-2027, Sandia National Laboratories, Albuquerque, New Mexico.

cc: R.L. Beauheim (6119)
F. Gelbard (6119)
S. Howarth (6119)
L. Jensen (6119)
R.W. Ostensen (6119)
D.R. Anderson (6342)
M.G. Marietta (6342)
W.D. Weart (6303)

PA Modeling Using BRAGFLO -- 1992

J. Schreiber, 7/8/92

Geometry

Human Intrusion Scenarios -- Axisymmetric cylindrical equivalent panel.

The equivalent panel will preserve the initial excavated volume and the initial excavated height of a panel. The panel as modeled will be a cylinder; it will include only the initial excavated volume, and not the pillars, as was done last year. The radius of the cylindrical panel is 60.85 m. The radius used last year is that of an enclosed panel (including pillars), 96.78 m. Since the maximum travel distance in a panel will be less this year owing to the smaller equivalent panel radius, it is desirable to increase the effective radius of the cylinder to simulate more closely the greater travel distances in an actual panel. The distance from the center of an actual panel to a far corner is 138 m, while the greatest travel distance in an actual panel (from panel center to the middle of the end of a panel, going around pillars) is 218 m. To include some of the effect of the greater travel distances in an actual panel, the high-permeability DRZ above and below the cylindrical panel was extended out to last year's radius of 96.78 m, which in effect will include the DRZ above and below the pillars. At the level of the waste, the DRZ does not extend laterally beyond the panel waste; the material beyond the 60.85 m radius of the panel, which can be thought of as the pillars, is treated as intact halite. From the top of Anhydrite a+b to the top of MB138, out to a radius of 96.78 m, is a composite region, the "Transition Zone", which is 9.24 m thick and is assumed to have the same properties as intact anhydrite. The mesh extends vertically from the bottom of the Castile brine reservoir to the top of the Culebra Member of the Rustler Fm, with the Unnamed Member lumped in with the Culebra.

Undisturbed Scenario -- Entire repository, rectangular geometry

The excavated volume of the entire repository is represented by a single rectangular region, and includes no pillars or panel seals. This mesh is essentially the same as the one used in the May 1992 RCRA calculations ("Case 3"). The mesh preserves the initial excavated volume of various regions and their original excavated heights. The panel seals and backfilled drifts between the repository and the Waste Shaft are lumped into a single region of high permeability. The four shafts are consolidated into a single shaft located at a distance from the repository equal to the distance to the actual Waste Shaft. To the north of the shaft is a region that represents the initial excavated volume of the experimental region. This mesh contains the same DRZ's and Transition Zones as the cylindrical panel mesh. These regions extend laterally 1 m beyond the waste to the south and 1 m beyond the experimental region to the north, and includes a 1-m-thick DRZ at the south end of the repository and a 1-m-thick DRZ at the north end of the experimental region. This mesh extends vertically from the top of the Castile Fm to the top of the Culebra Member of the Rustler Fm; the Culebra and Unnamed Members are lumped together. The thickness of the shaft seal will vary from 10 m to 50 m.

Material Properties

The initial porosity of the waste will be fixed at 0.675, as specified by the creep closure surface. Creep closure will be simulated to account for porosity changes over time, until a human intrusion occurs. After that time, the porosity of the waste will remain fixed at the level attained at that time. The halite DRZ immediately above and beneath the panel, as well as MB139 DRZ and Anhydrite a+b DRZ are all assumed to have identical properties. The permeability of this composite DRZ will be fixed at 1.0E-13 m^2. A range of permeabilities from 1.0E-15 to 1.0E-12 m^2 was originally proposed; however, these permeabilities are so high compared with permeabilities of surrounding materials and so close to the final waste permeability of 1.0E-13 m^2 that varying them will have no noticable effect. The Transition Zone properties will be identical to those of intact far-field anhydrite: permeabilities range from 1.0E-21 to 1.0E-15 m^2; porosities range from 0.001 to 0.03. Far-field anhydrite is assumed this year not to fracture; this effect is being ignored because it cannot yet be accurately simulated. Halite permeability will be sampled over a range of 1.0E-25 to 1.0E-22 m^2. Halite porosity will be set equal to the far-field anhydrite porosity, which is sampled, ranging from 0.001 to 0.03. The final porosity of the DRZ will vary, and will depend on the far-field anhydrite porosity: it will be calculated from [TZ poros + x(0.06-TZ poros)], where x ranges from 0 to 1. In the Undisturbed calculations, the seals & backfill, shaft, and experimental regions will have a porosity of 0.075 and a permeability of 1.0E-15 m^2. The DRZ adjacent to these three regions will have a permeability of 1.0E-15 m^2. The shaft seal permeability will vary, ranging from 3.3E-21 to 3.3E-20 m^2. The seal porosity will be 0.075.

Initial and Boundary Conditions

Initial pressure distribution will be calculated over a 20-year period (see Startup Procedure -- BRAGFLO 1992 PA). This 20-year startup calculation establishes the initial pressure distribution in all regions except the waste and DRZ. The pressure distribution at the beginning of the Startup Procedure will be hydrostatic everywhere (except in the waste and in the Culebra) relative to the pore pressure in MB139. A range of MB139 pressure from 12 to 13 MPa will be used. The initial pressure in the waste will be 1 atm (0.101325 MPa); the waste pressure will be reset to this value at the end of the startup. In the Culebra, the starting pressure will be 1.053 MPa, and the far-field pressure will be held at that value over the 10,020-year calculation. (This is the pressure measured in well H-1; it is the same value as used last year.) Note that the Culebra has a fixed-pressure boundary condition, whereas the rest of the mesh uses a no-flow boundary condition. The starting brine saturation will be 1.0 everywhere except in the waste. At the end of the 20-year startup, the waste will be assigned its sampled value of initial brine saturation, which will range from 0.0 to 0.14. The DRZ will start fully brine-saturated, but at the end of the startup time, the brine saturation will be adjusted so that the brine volume is the same after the porosity is adjusted. The porosity will be adjusted at that time from its starting value (volume average based on 0.01 for halite and the sampled value for intact anhydrite) to its final sampled value. Gas will be added to the DRZ to fill in the added porosity. The pressure in the DRZ will be reset to 1 atm at this time. In the undisturbed calculations, the seal & backfill, shaft, shaft seal, and experimental region will be initialized in the same manner as the waste. All of these excavated regions will be set to be fully saturated with gas at 1 atm pressure at the end of startup. In particular, the shaft seal will initially be fully saturated with gas at atmospheric pressure; this is more conservative with regard to RCRA compliance than assuming it is fully saturated with brine, because more gas can flow through.

Relative Permeability & Capillary Pressure

The Brooks-Corey relative permeability model will be used in 2/3 of the calculations and the van Genuchten-Parker model will be used in 1/3 of the calculations. An index parameter (0 or 1) will be sampled with these probabilities, so that either one model or the other will be used in any one calculation. Relative permeability parameters will be varied and will be the same for all materials except the waste, for which a fixed set of values will be used. Residual brine and gas saturations both will range from 0.0 to 0.4. The Brooks-Corey parameter, lambda, will range from 0.2 to 10.0. The van Genuchten-Parker parameter m will be calculated from m = lambda/(1 + lambda). Threshold capillary pressures will be determined from the correlation with permeability in all regions. The van Genuchten-Parker parameter Po will be calculated by equating the capillary pressure from each of the two models at an effective saturation of 0.5, and solving the expression for Po. In the intrusion borehole, the residual gas saturation will be set to zero, which makes the intrusion calculations run much more easily. In the waste, in the DRZ, in the intrusion borehole, and in all excavated regions in the Undisturbed Scenario mesh, the capillary pressure will be zero. This has proved to be necessary because the capillary pressure curves are not defined for imbibition into a medium that has less than residual brine saturation. So any regions where the brine saturation starts out or may become less than residual have to be modeled with zero capillary pressure.

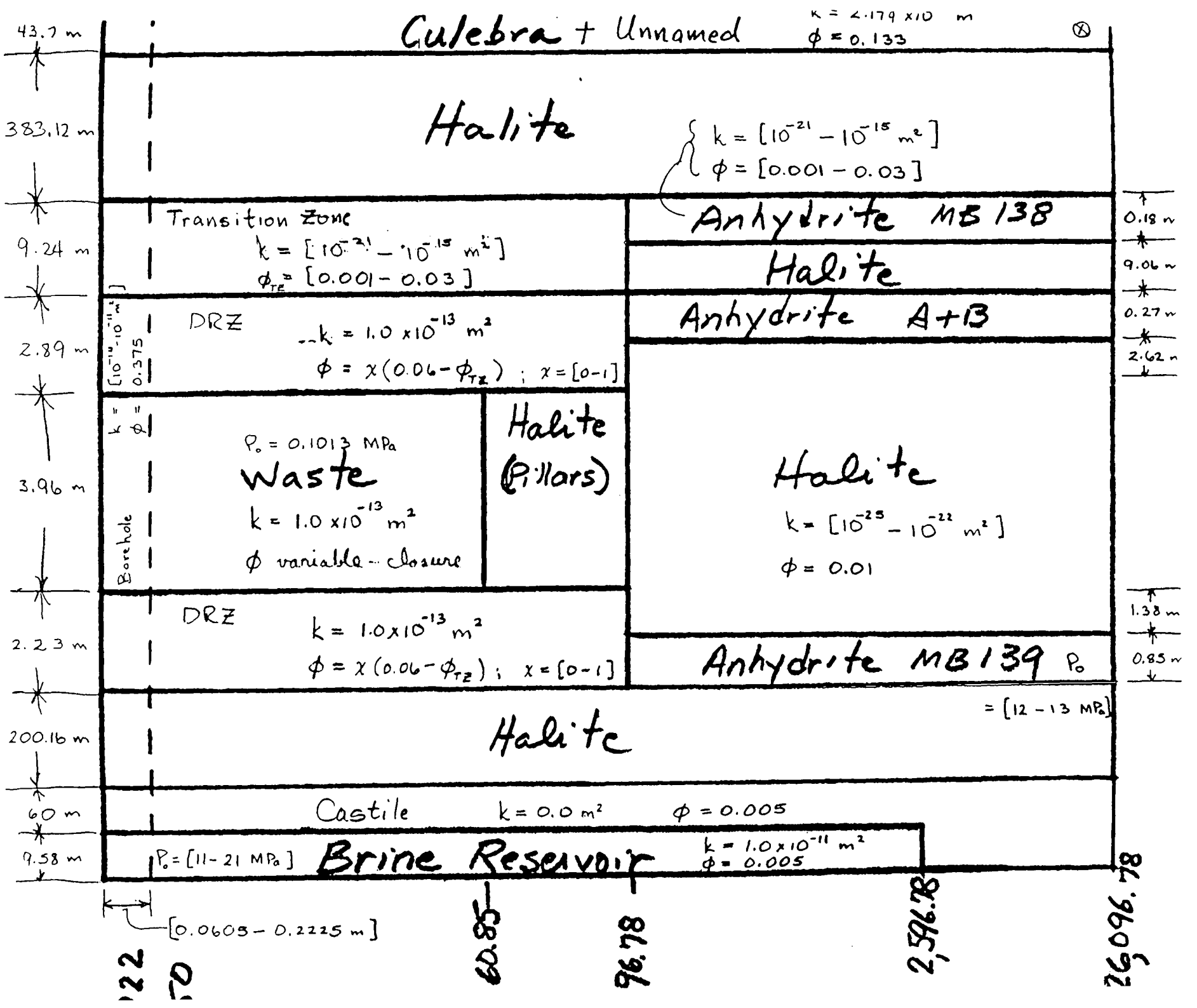
Culebra + Unnamed
k = 2.179 x10 m
φ = 0.133
43.7 m
Halite
383.12 m
k = [10^-21 – 10^-15 m²]
φ = [0.001 – 0.03]
Transition Zone
k = [10^-21 – 10^-15 m²]
φ_TZ = [0.001 – 0.03]
Anhydrite MB 138
0.18 m
Halite
9.06 m
9.24 m
DRZ
k = 1.0 x10^-13 m²
φ = x(0.06 – φ_TZ) ; x = [0-1]
[10^-19 – 10^-11 m²]
0.375
Anhydrite A+13
0.27 m
2.89 m
2.62 m
k =
φ =
P_o = 0.1013 MPa
Waste
k = 1.0 x10^-13 m²
φ variable – closure
Borehole
Halite (Pillars)
Halite
k = [10^-25 – 10^-22 m²]
φ = 0.01
3.96 m
DRZ
k = 1.0x10^-13 m²
φ = x(0.06 – φ_TZ) ; x = [0-1]
1.38 m
Anhydrite MB139 P_o
0.85 m
2.23 m
= [12 – 13 MPa]
Halite
200.16 m
60 m
Castile
k = 0.0 m²
φ = 0.005
9.58 m
P_o = [11 – 21 MPa]
Brine Reservoir
k = 1.0x10^-11 m²
φ = 0.005
[0.0603 – 0.2225 m]
60.85
96.78
2,596.78
26096.78
A-30

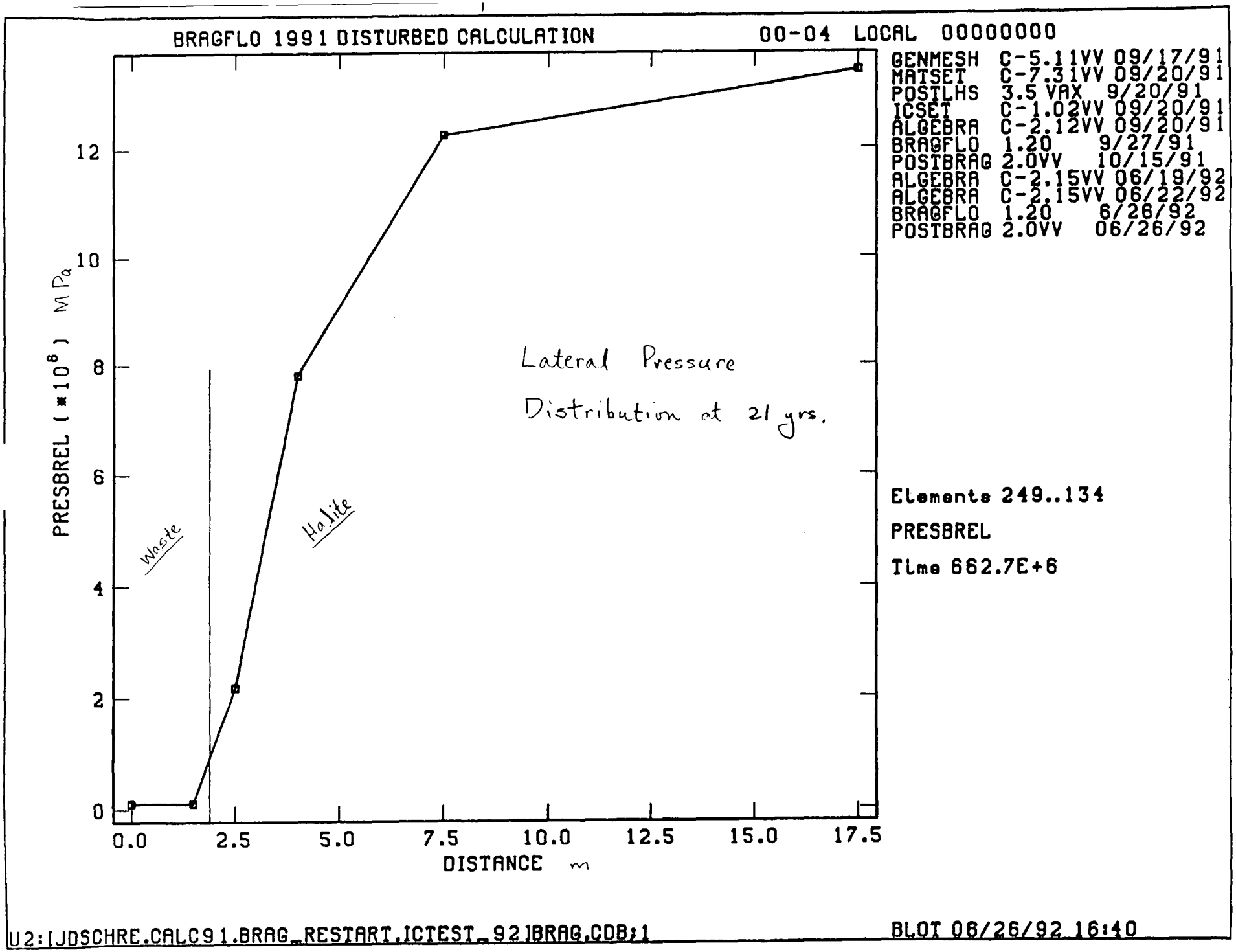
BRAGFLO 1991 DISTURBED CALCULATION
00-04 LOCAL 00000000
GENMESH C-5.11VV 09/17/91
MATSET C-7.31VV 09/20/91
POSTLHS 3.5 VAX 9/20/91
ICSET C-1.02VV 09/20/91
ALGEBRA C-2.12VV 09/20/91
BRAGFLO 1.20 9/27/91
POSTBRAG 2.0VV 10/15/91
ALGEBRA C-2.15VV 06/19/92
ALGEBRA C-2.15VV 06/22/92
BRAGFLO 1.20 6/26/92
POSTBRAG 2.0VV 06/26/92
PRESBREL (*10^6) MPa
0
2
4
6
8
10
12
0.0
2.5
5.0
7.5
10.0
12.5
15.0
17.5
DISTANCE m
Waste
Halite
Lateral Pressure
Distribution at 21 yrs.
Elements 249..134
PRESBREL
Time 662.7E+6
U2:[JDSCHRE.CALC91.BRAG_RESTART.ICTEST_92]BRAG.CDB;1
BLOT 06/26/92 16:40

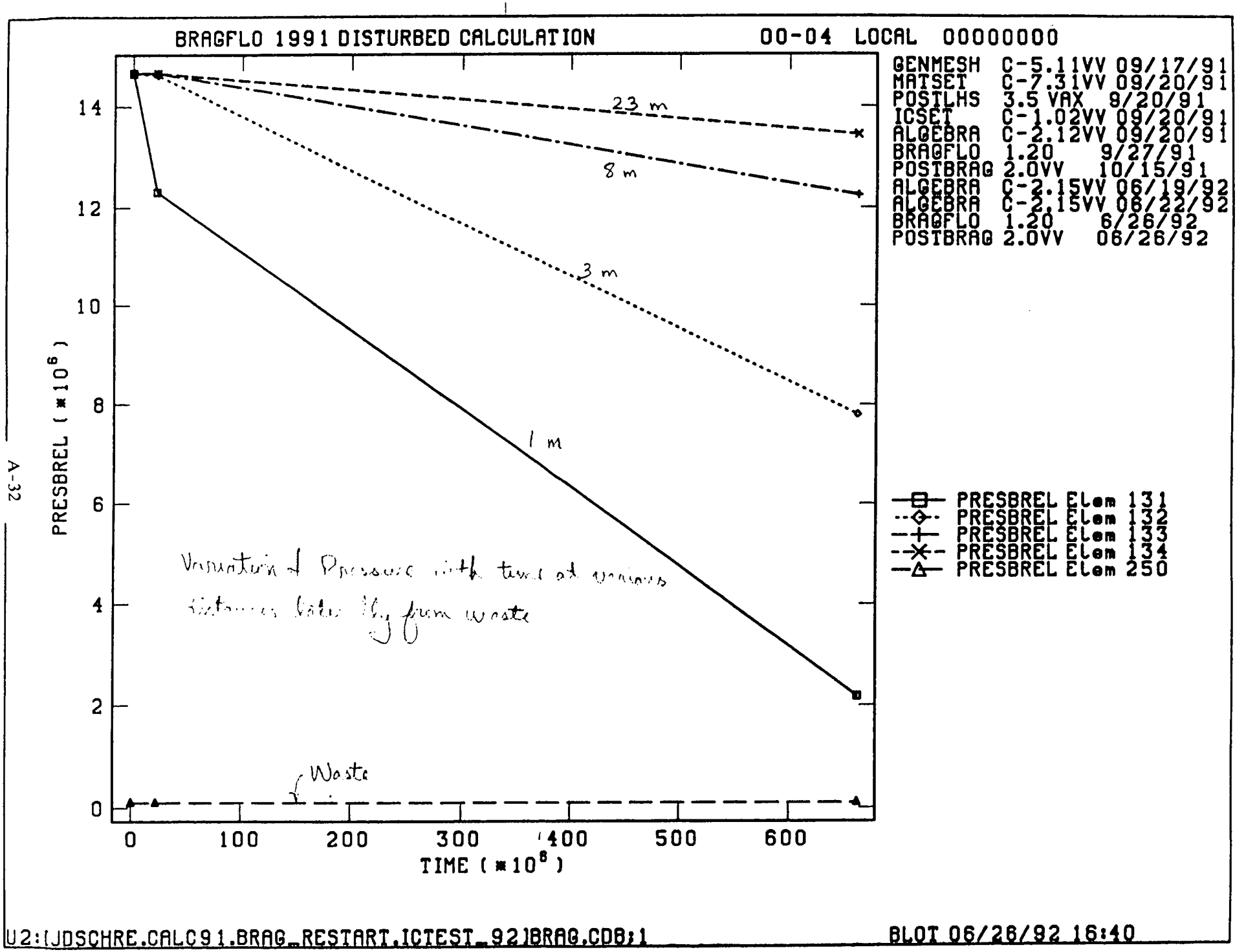

Variation of Pressure with time at various distances below Rig from waste

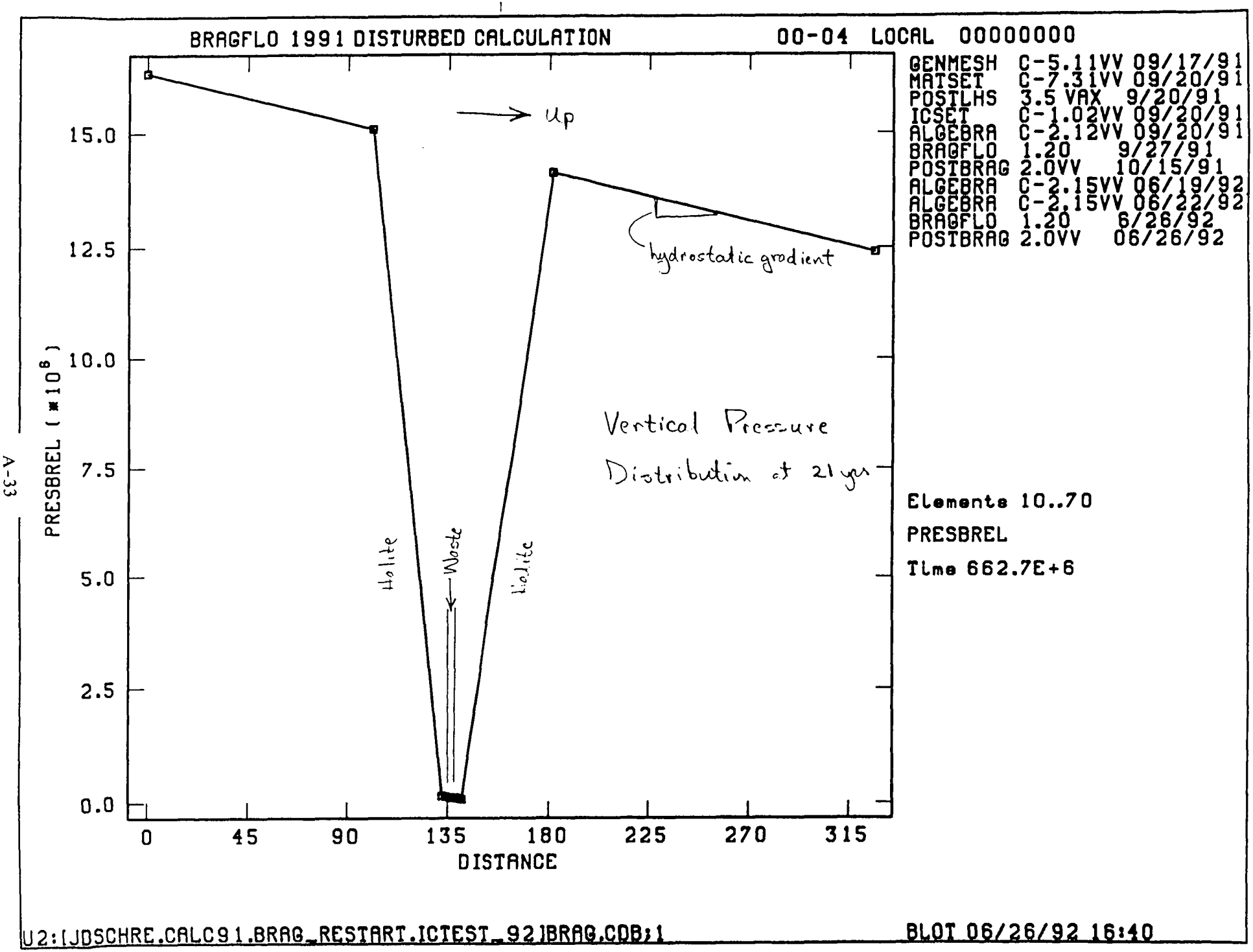
BRAGFLO 1991 DISTURBED CALCULATION
00-04 LOCAL 00000000
GENMESH C-5.11VV 09/17/91
MATSET C-7.31VV 09/20/91
POSTLHS 3.5 VAX 9/20/91
ICSET C-1.02VV 09/20/91
ALGEBRA C-2.12VV 09/20/91
BRAGFLO 1.20 9/27/91
POSTBRAG 2.0VV 10/15/91
ALGEBRA C-2.15VV 06/19/92
ALGEBRA C-2.15VV 06/22/92
BRAGFLO 1.20 6/26/92
POSTBRAG 2.0VV 06/26/92
Up
hydrostatic gradient
Vertical Pressure
Distribution at 21 yrs
Elements 10..70
PRESBREL
Time 662.7E+6
Halite
Waste
Halite
PRESBREL (*10^6)
15.0
12.5
10.0
7.5
5.0
2.5
0.0
0
45
90
135
180
225
270
315
DISTANCE
U2:[JDSCHRE.CALC91.BRAG_RESTART.ICTEST_92]BRAG.CDB;1
PLOT 06/26/92 16:40

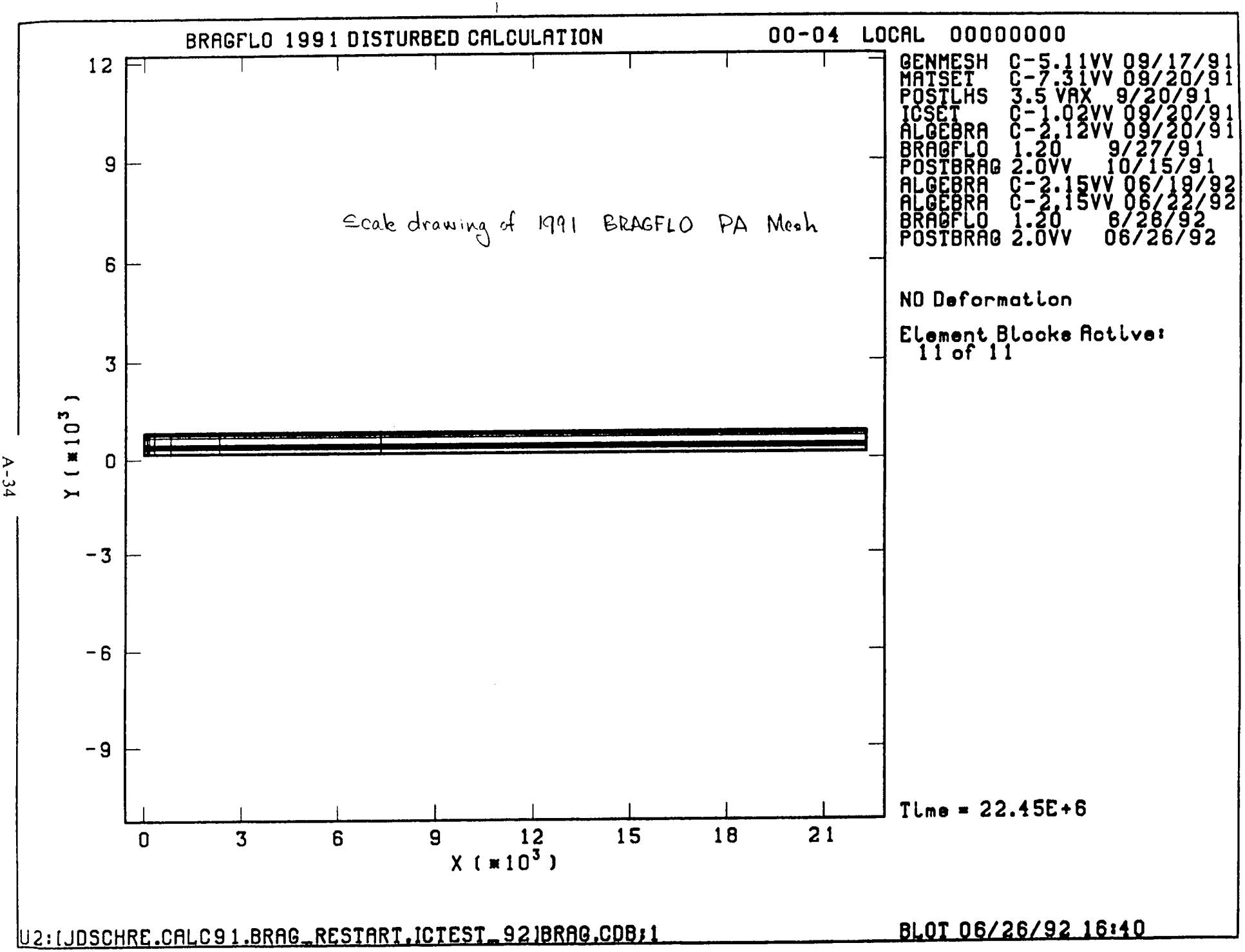
BRAGFLO 1991 DISTURBED CALCULATION
00-04 LOCAL 00000000
GENMESH C-5.11VV 09/17/91
MATSET C-7.31VV 09/20/91
POSTLHS 3.5 VAX 9/20/91
ICSET C-1.02VV 09/20/91
ALGEBRA C-2.12VV 09/20/91
BRAGFLO 1.20 9/27/91
POSTBRAG 2.0VV 10/15/91
ALGEBRA C-2.15VV 06/19/92
ALGEBRA C-2.15VV 06/22/92
BRAGFLO 1.20 6/26/92
POSTBRAG 2.0VV 06/26/92
Scale drawing of 1991 BRAGFLO PA Mesh
NO Deformation
Element Blocks Active:
11 of 11
Time = 22.45E+6
Y (*10^3)
X (*10^3)
12
9
6
3
0
-3
-6
-9
0
3
6
9
12
15
18
21
U2:[JDSCHRE.CALC91.BRAG_RESTART.ICTEST_92]BRAG.CDB;1
PLOT 06/26/92 16:40

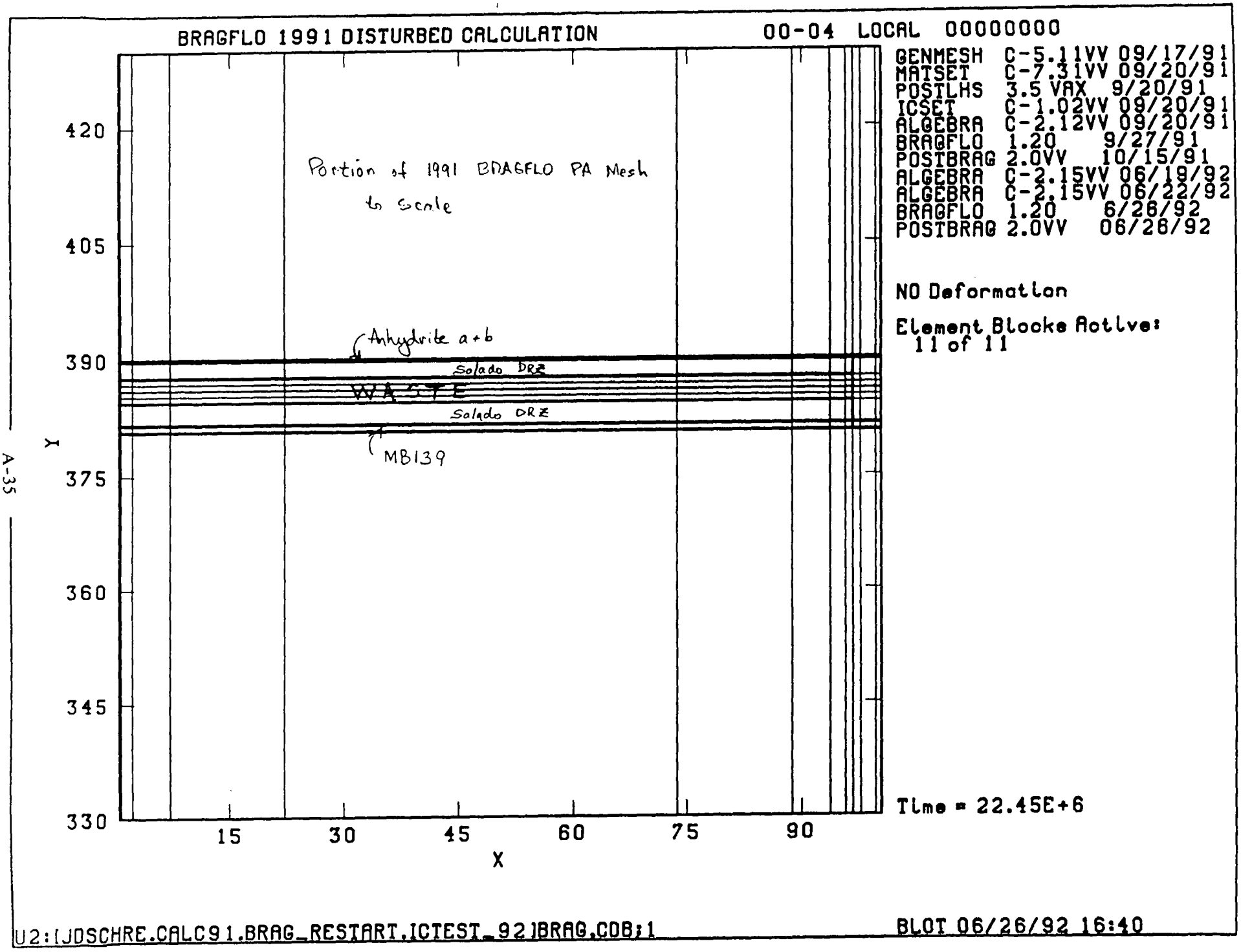
BRAGFLO 1991 DISTURBED CALCULATION
00-04 LOCAL 00000000
GENMESH C-5.11VV 09/17/91
MATSET C-7.31VV 09/20/91
POSTLHS 3.5 VAX 9/20/91
ICSET C-1.02VV 09/20/91
ALGEBRA C-2.12VV 09/20/91
BRAGFLO 1.20 9/27/91
POSTBRAG 2.0VV 10/15/91
ALGEBRA C-2.15VV 06/19/92
ALGEBRA C-2.15VV 06/22/92
BRAGFLO 1.20 6/26/92
POSTBRAG 2.0VV 06/26/92
Portion of 1991 BRAGFLO PA Mesh
to Scale
NO Deformation
Element Blocks Active:
11 of 11
Anhydrite a+b
Salado DRZ
WASTE
Salado DRZ
MB139
420
405
390
375
360
345
330
Y
15
30
45
60
75
90
X
Time = 22.45E+6
U2:[JDSCHRE.CALC91.BRAG_RESTART.ICTEST_92]BRAG.CDB;1
PLOT 06/26/92 16:40

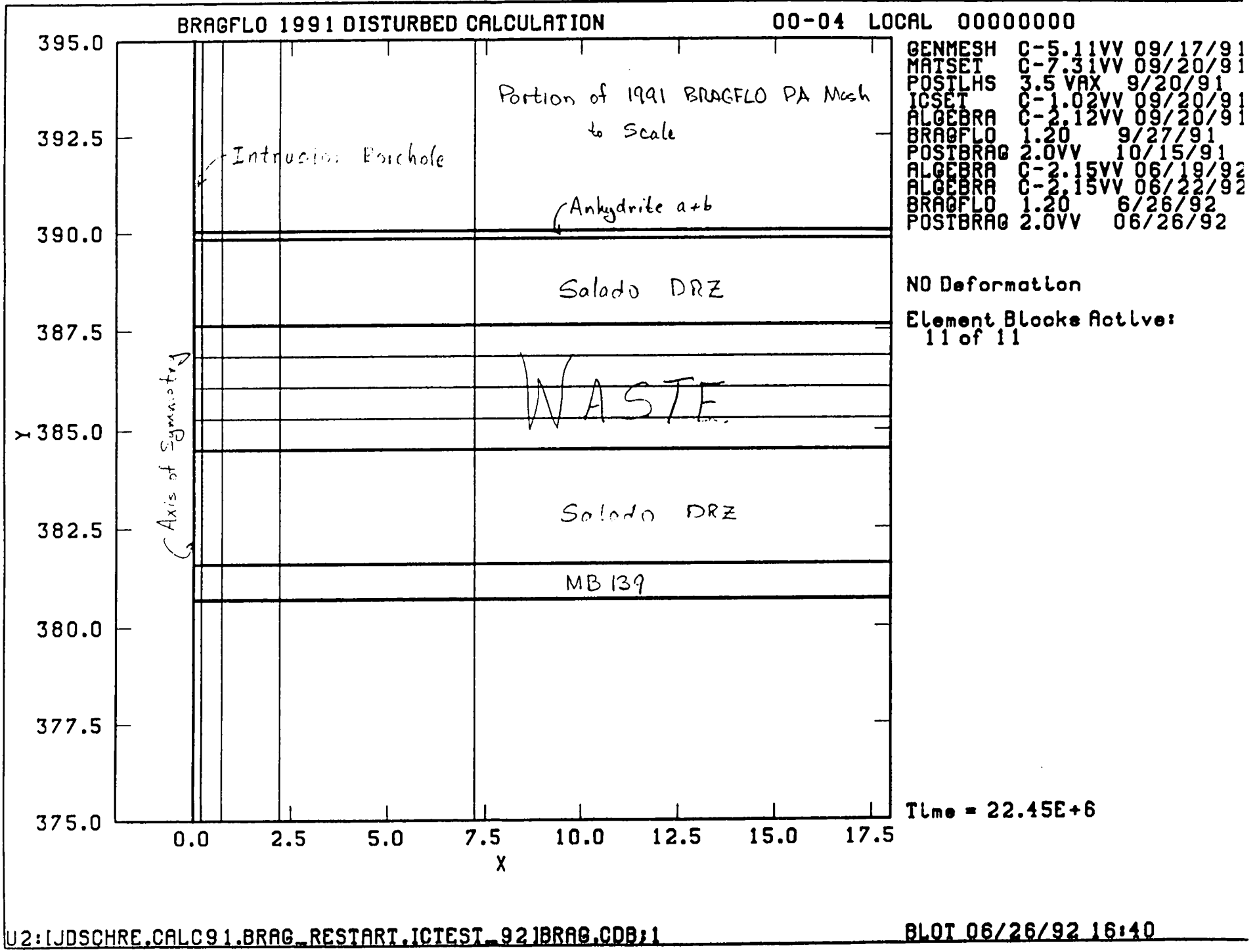
BRAGFLO 1991 DISTURBED CALCULATION
00-04 LOCAL 00000000
GENMESH C-5.11VV 09/17/91
MATSET C-7.31VV 09/20/91
POSTLHS 3.5 VAX 9/20/91
ICSET C-1.02VV 09/20/91
ALGEBRA C-2.12VV 09/20/91
BRAGFLO 1.20 9/27/91
POSTBRAG 2.0VV 10/15/91
ALGEBRA C-2.15VV 06/19/92
ALGEBRA C-2.15VV 06/22/92
BRAGFLO 1.20 6/26/92
POSTBRAG 2.0VV 06/26/92
Portion of 1991 BRAGFLO PA Mesh
to Scale
Intrusion Borehole
Anhydrite a+b
Salado DRZ
WASTE
Salado DRZ
MB 139
Axis of Symmetry
NO Deformation
Element Blocks Active:
11 of 11
Time = 22.45E+6
395.0
392.5
390.0
387.5
385.0
382.5
380.0
377.5
375.0
Y
0.0
2.5
5.0
7.5
10.0
12.5
15.0
17.5
X
U2:[JDSCHRE.CALC91.BRAG_RESTART.ICTEST_92]BRAG.CDB;1
PLOT 06/26/92 16:40

$\log_{10}$ Value	Cum. Prob.
-21.0	0
-20.0	0.05
-19.0	0.55
-18.0	0.70
-17.0	0.75
-16.0	0.80
-15.0	1.00

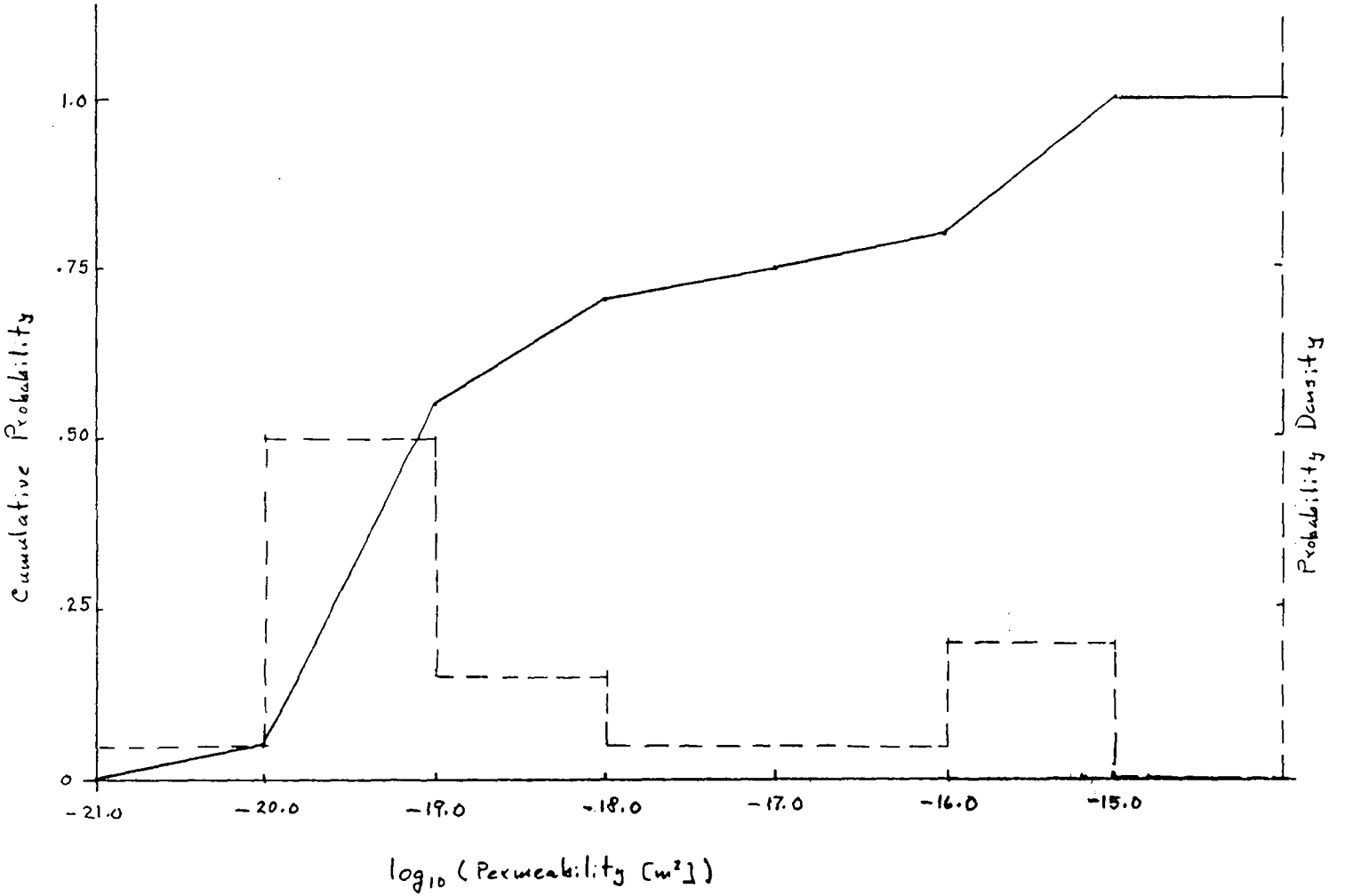

1992 Undisturbed Anhydrite Permeability

Davies et al., July 22, 1992 (1992b)

Date: 7/22/92
To: B. M. Butcher, J. Schreiber, and P. Vaughn (6342)
From: P. B. Davies, R. L. Beauheim, and E. D. Gorham (6119)
Subject: Additional Comments on Far-Field Anhydrite Permeability Distribution in "PA Modeling Using BRAGFLO -- 1992" 7-8-92 Memo by J. Schreiber"

Sandia National Laboratories

Albuquerque, New Mexico 87185

Date: July 22, 1992

To: B.M. Butcher, J. Schreiber, and P. Vaughn (6342)

P.B. Davies R.L. Beauheim E.D. Gorham

From: P.B. Davies, R.L. Beauheim, E.D. Gorham (6119)

Subject: Additional Comments on Far-Field Anhydrite Permeability Distribution in "PA Modeling Using BRAGFLO -- 1992" 7-8-92 Memo by J. Schreiber

In response to a telephone conversation with Palmer Vaughn on 7-18-92, we have further reviewed the far-field anhydrite permeability distribution in the 7-8-92 Schreiber memo (Figure 1), the recommended for far-field permeability distribution in the 7-14-92 Davies et al. memo, and the experimental data that was provided with the original parameter recommendations by E.D. Gorham on 4-1-92. The experimental data have been divided into three groups: 1) anhydrite tests indicating little or no depressurization of formation fluid; 2) anhydrite tests indicating moderate depressurization of formation fluid pressure but with substantially intact anhydrite; 3) anhydrite tests with substantial depressurization of formation fluid and with substantial fracture enhancement of permeability (disturbed rock zone). The recommendation for far field anhydrite permeability as discussed at the June 25th Departments 6119/6342 meeting and reiterated in the 7-14-92 Davies et al. memo was to construct the distribution for far-field anhydrite permeability from the data in the first two of these groups (Table 1). This distribution does <u>not</u> encompass permeabilities representative of interbed fracturing due to gas pressurization and this caveat should be clearly stated in PA's discussions of their calculations. While it is possible that some of the permeability tests in the second group may have been slightly impacted by excavation-related deformation, it is still a distinct possibility that they have not. At present we have no objective experimental evidence that any of these tests should be eliminated from consideration.

In the 7-18-92 phone conversation, Palmer expressed PA's concern that this distribution is too high because it results in almost 25 percent of samples of far-field anhydrite permeability that are greater than 10^{-16} m^2 (Figure 1). We have gone back to the original experimental data and constructed a distribution that includes the two data groups recommended above (Figure 2 and Table 2). The distribution in the 7-8-92 Schreiber memo was apparently constructed from some other data set, as its structure is significantly different than the structure of the recommended distribution shown in Figure 2 and Table 2. The recommended distribution in Figure 2 results in no permeabilities greater than 10^{-16} m^2 and in sampling permeabilities between 10^{-18} and 10^{-16} m^2 approximately seven percent of the time.

In summary, we have carefully reviewed the experimental data base for anhydrite permeability and our recommendation for the far-field anhydrite permeability distribution is given in Figure 2 and Table 2. This distribution does not encompass permeabilities representative of interbed fracturing due to gas pressurization.

Table 1. Experimental Data from Permeability Testing of Anhydrite Interbeds

Test	*Unit*	*Permeability (m^2)*	*Pressure (MPa)*
Group 1: No substantial formation fluid depressurization			
SCP01	MB 139	3.0x10-20 m2	12.4
QPP13	pre-mineby MB 139	4.1x10-20 m2	12.5
QPP03	pre mineby anhydrite b	4.4x10-20 m2	12.6
Group 2: Moderate formation fluid depressurization			
C2H02	MB 139	7.8x10-20 m2	9.3
L4P51-B	anhydrite c	5.0x10-20 m2	5.1
S1P71-B	anhydrite c	6.8x10-20 m2	4.9
C2H01-C	MB 139	9.5x10-19 m2	8.0
C1X10	MB 139	5.0x10-17 m2	7.3
QPP03	anhydrite b post mineby	7.9x10-20 m2	7.0
QPP13	MB 139 post mine-by	4.7x10-20 m2	8.1
L4P52-A	anhydrite a	1.0x10-19 m2	6.4
QPB01	MB 139	9.6x10-21 m2	5.0 assumed
QPB02	MB 139	1.6x10-19 m2	5.0 assumed
QPB03	MB 139	1.2x10-20 m2	5.0 assumed

Table 2. Cumulative Probability for Recommended Anhydrite Far-Field Permeability Distribution

LOG10 Value	*Cumulative Probability*
-21	0.00
-20	0.07
-19	0.71
-18	0.93
-17	0.96
-61	1.00

$\log_{10}$ Value	Cum. Prob.
-21.0	0
-20.0	0.05
-19.0	0.55
-18.0	0.70
-17.0	0.75
-16.0	0.80
-15.0	1.00

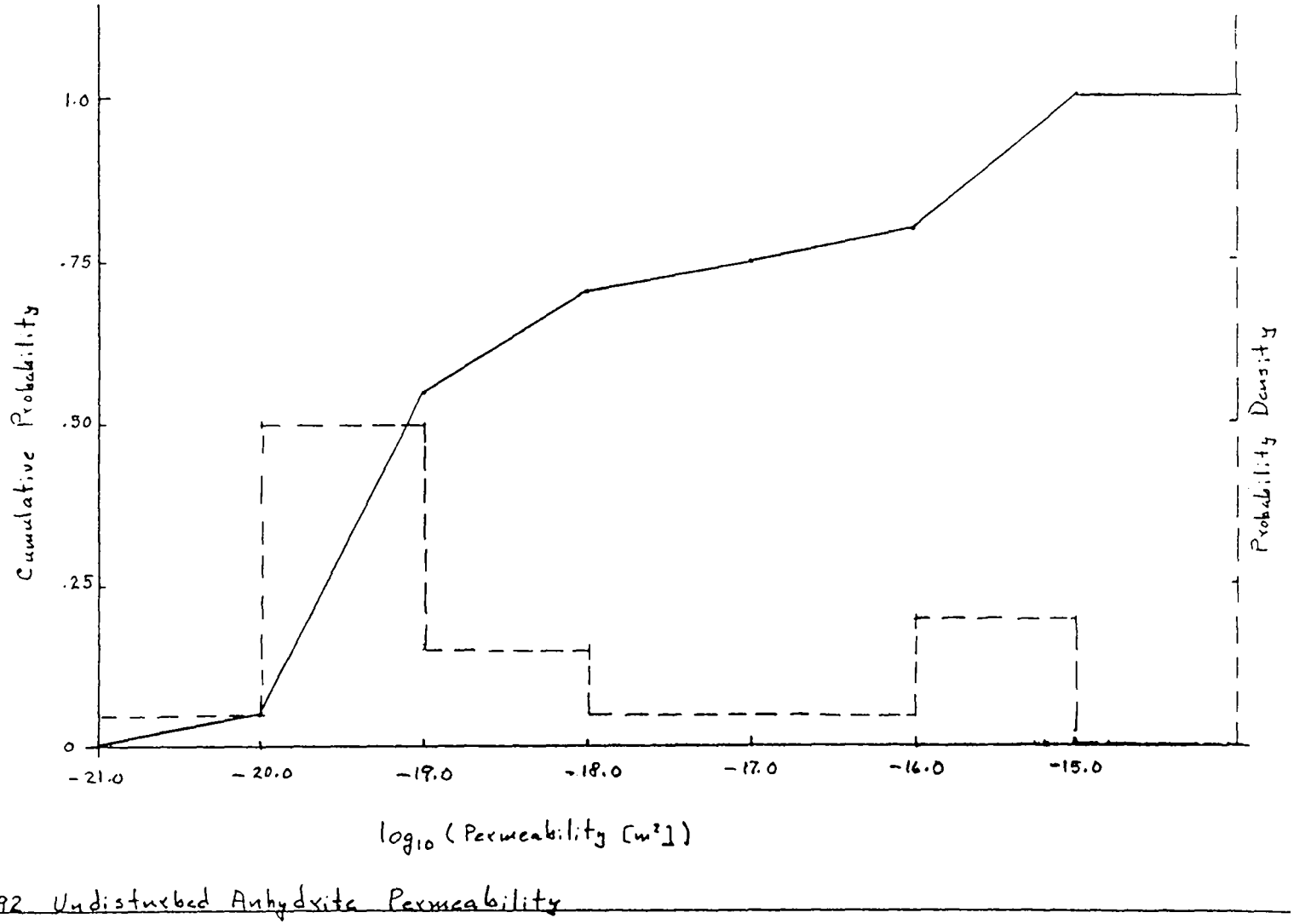

Figure 1. Undisturbed Anhydrite Permeability Distribution from 7-8-92 Schreiber Memo

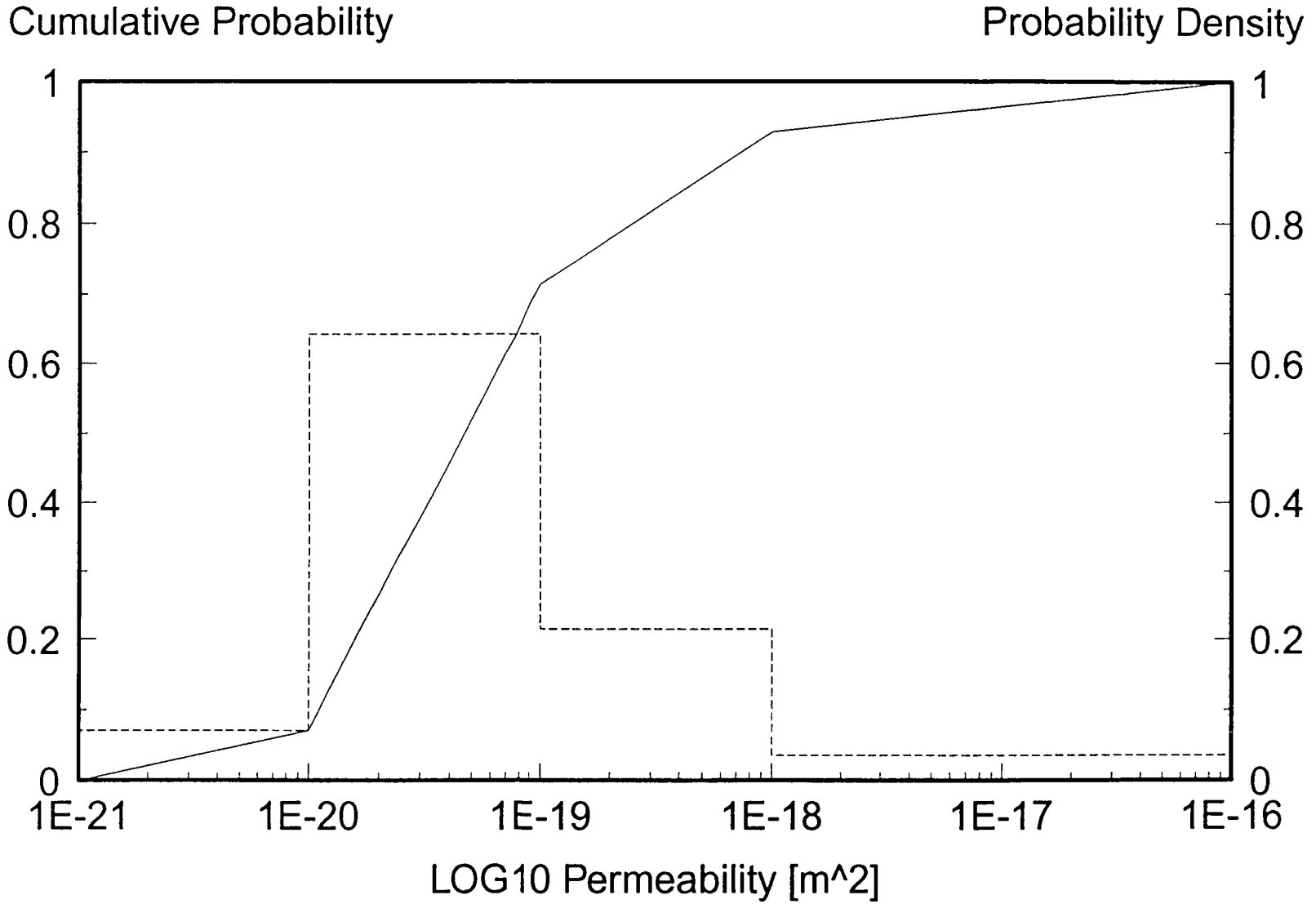

Figure 2. Recommended Undisturbed Anhydrite Permeability Distribution for 1992 PA Calculations

REFERENCES

Davies, P.B., S.W. Webb, and E.D. Gorham, *Feedback on "PA Modeling Using BRAGFLO -- 1992" 7-8-92 memo by J. Schreiber.* 7-14-92 Memorandum to B.M. Butcher, J. Schreiber, and P. Vaughn.

Schreiber, J., *PA Modeling Using BRAGFLO -- 1992.* Memorandum.

cc: F. Gelbard (6119)
S. Howarth (6119)
L. Jensen (6119)
R.W. Ostensen (6119)
S.W. Webb (6119)
D.R. Anderson (6342)
M.G. Marietta (6342)
W.D. Weart (6303)

Gorham et al., June 15, 1992

Date: 6/15/92
To: Martin Tierney, 6342
From: Elaine Gorham, Richard Beauheim, Peter Davies, Susan Howarth, and Steve Webb (6119)
Subject: Recommendations to PA on Salado Formation Intrinsic Permeability and Pore Pressure for 40 CFR 191 Subpart B Calculations

Recommendations to PA on Salado Formation Intrinsic Permeability and Pore Pressure for 40 CFR 191 Subpart B Calculations

June 15, 1992

Elaine Gorham
Richard Beauheim
Peter Davies
Susan Howarth
Stephen Webb

Department 6119

Introduction

In March 1992, the Fluid Flow and Transport Department was asked to recommend Salado Formation permeability and pore pressure probability distributions to be used in the 1992 RCRA calculations for the WIPP. The recommendations were requested and transmitted informally. Eventually a description of the rationale for the recommendations was written by the Fluid Flow and Transport Department and published in Appendix A of (WIPP Performance Assessment Division, 1992A).

Following the RCRA calculations, the Fluid Flow and Transport Department was asked to recommend Salado Formation permeability and pore pressure to be used in the 1992 40 CFR 191 Subpart B compliance calculations. The recommendations transmitted to the PA group in the attached memo by P. D. Davies et al. were based on the, earlier, RCRA recommendations.* The present description is a detailed record of the rationale for the 1992 40 CFR 191 permeability and pore pressure recommendations transmitted in the Davies et al. memo and includes some comments on the adequacy of the current PA models to accurately describe all phenomena present in the formation.

Since input parameters, such as permeability or formation pore pressure, are, for the most part, inferred from complex hydrologic tests, the interpretive model assumptions should be compatible with the predictive or performance assessment model in which the parameters will be used. Thus a suggested excavation geometry and zoning scheme was supplied along with recommended distributions for permeability and pore pressure. The recommended initial geometry is shown in Figure 1 and the distributions suggested for permeability and pore pressure (Table 1 and Figures 2-6) were referenced with respect to those zones.

* Note: The referenced memo is included in this appendix as Davies et al., July 22, 1992.

Our Assumptions

Assumptions about the models to be used in the PA calculations that were essential in formulating the 40 CFR 191 data recommendations were not included in the informal material. Our assumptions were

1. The Salado Formation was described as consisting of layers of either halite or anhydrite. Parts of the Salado Formation described as argillaceous halite were lumped with the halite; clay seams were lumped with the type of lithology in which they occurred. Anhydrites a and b were lumped together.

2. The Salado Formation is isotropic and homogeneous within each layer of halite or anhydrite. The halite and anhydrite have interconnected porosity in pressure equilibrium in the far field. Thus there can be no pre-existing hydraulic pressure differential between stratigraphic layers in the far field Salado Formation.

3. The repository will have been at atmospheric pressure for at least 20 years before final closure. PA will simulate the depressurization in the formation surrounding the repository in a start-up phase which allows brine to flow into a closed repository initially at atmospheric pressure. At the end of the start-up phase, a DRZ will be created; the repository and DRZ pressure will be re-set to atmospheric pressure; the DRZ porosity will be set to a value sampled from a probability distribution; and the brine saturation in the DRZ will be set to preserve the total volume of brine in the DRZ region at the end of the start-up calculation.

4. Excavation closure effects are **not** to be included in the PA model nor is pressurized fracture opening in the anhydrite beds. Pressurized fracture opening in the anhydrite beds may have the potential to significantly increase far-field interbed permeabilities. We were specifically requested by the PA group to **not** include the potential effects of pressurized fracture opening in our recommended permeability distribution for the anhydrite layers, as we suggested in the attached memo from E. Gorham. **Thus we believe the 1992 40 CFR 191 compliance calculations may underestimate lateral gas migration in the interbeds and overestimate repository pressurization.**

5. The nature of the disturbed rock zone (DRZ) is uncertain, reflecting the diversity of technical hypotheses that have been formulated, documented and undocumented. These include the hypothesis that the DRZ is a zone of increased porosity surrounding the excavation, that is stable in extent or increasing in extent with the age of the excavation. Other hypotheses concerning the nature of the DRZ are that the bulk properties of the halite within the DRZ are unchanged, but that within the DRZ fractures form that result in a large increase in permeability with a relatively small increase in porosity or storativity within the DRZ. The size of the DRZ can vary from a few inches into the formation from an excavation surface to a few "room-radii" away from the excavation

surface. It was assumed that all possible descriptions of the DRZ should be included in the probability distributions for permeability and porosity in the DRZ.

6. The DRZ does not reconsolidate during the post-closure calculations due to repository re-pressurization or creep closure of the excavation.

Sources of uncertainty in interpreting data.

The process of inferring permeability from a hydrologic pulse or shut-in test requires that one make an assumption about the diffusivity or specific storage in the formation, about the size of a damaged zone surrounding the test zone, and that the compressibility of the test-zone fluid is constant and can be quantified by a single measurement of fluid withdrawn from the test zone vs test zone pressure drop during withdrawal. A value of specific storage calculated using literature values for halite and and brine compressibilities may not be correct. Recent improvements in the measurement of permeability involve combining a constant-pressure flow test and a shut-in test to directly infer a value of specific storage. However, the improved interpretive technique was used only on permeability tests SCP01, S1P73-B, C1X10, L4P52-A and L4P51-B. For the remaining permeability tests, what is in reality obtained is a value of permeability **given an assumed value of specific storage.** Sensitivity calculations have shown that our inferred permeability values may range over one order of magnitude as our assumed values of specific storage range over three orders of magnitude. (Beauheim et al, 1990; Beauheim et al, 1992) Inasmuch as our assumed values of specific storage do not range over more than three orders of magnitude, we estimate our uncertainty in permeability to be about an order of magnitude.

Other assumptions in analysis of permeability tests include the assumption that gas dissolved in formation brine does not significantly affect the permeability interpretation and that significant amounts of free gas are not present in the formation. In numerous permeability tests, gas was observed to bubble from the formation shortly after the test zone was drilled. A sensitivity analysis is planned for FY93 in which the effect of these phenomena on permeability interpretation will be investigated. For the RCRA recommendations, Rick Beauheim, who has been conducting interpretations of permeability tests, provided the (subjective) input that resulted in an order of magnitude confidence in interpreted permeability values.

Uncertainties in the interpretation of brine-inflow tests are due to (a) scatter in the brine-inflow data and (b) the use of a one-dimensional model which neglects loss of fluid to the surface of the excavation and assumes a uniform pore pressure unaffected by the excavation. In a one-dimensional data analysis by McTigue (1992), it was found that the uncertainties in the inferred values of diffusivity due to data scatter could be substantial.

Uncertainties in inferred values of permeability may be smaller. (See Table 2.) In addition, recent analyses (Gelbard, 1992) indicate that the use of a one-dimensional model may introduce significant errors in the interpretation of diffusivity and permeability from brine-inflow data.

Rationale for Formulating Permeability Distributions

Table 3 represents a current (as of 1/5/92) compilation of interpreted values of permeability and formation pressure from the Permeability Testing Program, the Small-Scale Brine Inflow Program and Room Q. For the 1992 40 CFR 191 Subpart B calculations, interpreted values of permeability in Table 3 were classified according to the regional map shown in Figure 1.

The disturbed rock zone is poorly defined. For these recommendations, test zones were classified as being in the disturbed rock zone if the zone could sustain little or no formation pressure and if the permeability of the zone was clearly higher than expected in competent rock.

The tests for which a reasonable pressure could be sustained in the test zone, but the pressure was not high enough to approach our (subjective) estimate of the far field pressure, were classified as being in a "depressurized" zone. The "depressurized zone" is hypothesized as having experienced some hydraulic depressurization and possibly some elastic stress relief due to the excavation, but probably no irreversible rock damage and large permeability changes. The extent of the depressurized zone may be different in higher permeability layers, such as the Marker Beds, than in lower permeability layers, such as pure halite. It is important to note that the depressurized zone is not a disturbed rock zone; the data from the depressurized zones do not support the hypothesis that the permeability, and the interconnected porosity, are greatly different in the depressurized zones from their far field values.

The latter classifications of test zones are subjective and will be examined in more detail as the Fluid Flow and Transport Department improves interpretation techniques and understanding of the rock matrix.

For the tests in Table 3, other than the Room Q tests, the disturbed rock zone, if in fact it has a clear boundary and if it has a significant extent, was hypothesized to extend about one meter from the excavation into the formation. The boundary of the depressurized zone in the Marker Beds was hypothesized to be approximately 10 meters from the excavation. These hypotheses formed the basis for the geometrical treatment of the excavation suggested in Figure 1. Detailed repository depressurization calculations are planned for FY93.

The PA calculations did not follow the zoning scheme recommended in Figure 1. Only a disturbed rock zone was distinguished from the

far field. Thus it was recommended that the depressurized zone and far field zone tests be combined to form a single permeability distribution.

The probability distributions recommended for the PA calculations were formulated so as to reflect the true range of scientific uncertainty in the parameter values supplied, including uncertainty due to measurement error and uncertainty due to interpretation ambiguities. As mentioned above, an order of magnitude uncertainty in the interpreted value of permeability was used as a rule of thumb for creating recommended probability distributions.

All measurements of permeability were given equal weight, except those values derived from brine inflow measurements in 36" diameter holes in Room D. Those tests were considered flawed and deleted from the list because of the uncertain history of the excavation surrounding the test zone (Finley, 1992).

The hypothesis that permeabilities in the Salado Formation are heterogeneous is given much weight in the Fluid Flow and Transport Department. The use of a single uniform value for all halite and argillaceous halite regions, and a different uniform value for all marker beds implies that the permeability values used in the PA calculations should be "effective" values that are rigorously derived from our measurements. A systematic approach for defining such an "effective" value has not yet been outlined, but will be investigated in FY93. For the 1992 40 CFR 191, Subpart B calculations the values of permeability that were classified as "to low to measure were" represented by effective permeabilities in the range of 10^{-24} to 10^{-22} m^2, since it was judged that even if the halite contained regions of zero permeability, the likelihood was low that the effective permeability of the halite and argillaceous halite regions was zero.

Given the assumptions, difficulties and exceptions outlined above, differential probability distributions were formed by marking the locations along a permeability axis of the results of the tests in Table 3. Excluding the "to low to measure" permeability tests, the number of tests in each $\log_{10}$ interval were used to indicate the relative probability that the true value lay in that interval. Cumulative probability distributions listed in Table 1 can be formulated from the differential probability distributions in Figures 2-6. Test results that were "Too low to measure" are shown in Figure 2 as lying between a true 0 value and 1.0×10^{-24} m^2. Thus, the abscissa of Figure 2 is logarithmic between 10^{-24} and 10^{-21} and linear between 0 and 10^{-24}.

Rationale for Formulating Pore Pressure Distributions

The measurement of test-zone pore pressure is straightforward and is only accomplished in the Permeability Testing Program and the Room Q permeability tests. If, during a pressure build-up test or pulse-withdrawal test, the pressure reaches a steady state

pressure, that pressure is interpreted as the formation pore pressure at the location of the test zone. If a steady-state pressure is not reached before the test is terminated, some technique must be used to extrapolate the formation pore pressure from the shape of the pressure-vs-time curve.

For the tests listed in Table 3, all pressures shown are measured or estimated values of formation pore pressure. The far field formation pore pressures measured in the anhydrite layers yield a fairly consistent measurement of 12.5+-0.1 MPa. It is not understood why the pore pressure measured in the single halite far field test is significantly lower than those reached in the anhydrite far field. Possibilities include: (a) The regions in the halite that have non-zero permeability are not interconnected with higher pressure regions such as the anhydrite layers; (b) the regions in the halite that have non-zero permeability have not reached pressure equilibrium with the anhydrite layers; or (c) pore dilation (and accompanying depressurization) in response to excavation and/or drilling affects halite to a greater distance than anhydrite.

Based on current measurements, it cannot be ruled out that substantial regions of the Salado Formation will be at significantly lower initial pore pressure than the anhydrite layers. Because of potential computational difficulties the PA group did not wish to include this possibility in the 40 CFR 191 calculations. Use of a uniform hydraulic pressure throughout the formation far field allows the PA calculations to be based on the appealingly simple (although perhaps not correct) assumption of homogeneity, hydraulic equilibrium and isotropy in the undisturbed Salado Formation. (The assumption of formation hydraulic equilibrium can be tested using existing models and assumed values of halite and anhydrite permeability. Such a calculation may be performed by Department 6119 in the future.)

Since the effect of excavation on the formation is still poorly understood, from a hydrological viewpoint, it is uncertain that tests believed to be in the far field are indeed in the far field. It was recommended that the far field pore pressure reflect the average of the three far field measurements in the anhydrite, 12.5 MPa, with an uncertainty of 0.5 MPa.

Comments on the Effect of Data Recommendations on 40 CFR 191 Subpart B Compliance Calculations.

An important aspect of the current PA model for the Salado Formation is its inability to simulate pressure-induced fracturing in the anhydrite layers, a phenomenon that has been experimentally demonstrated at the WIPP. The phenomenon may enhance the migration of gas into the formation as the gas pressure in the repository builds up.

Thus it should be recognized that the data from which the permeability and pore pressure recommendations have been derived may not fully support the existing performance assessment models. While it might have been possible to adjust the input parameter distributions to crudely include effects not explicitly modeled, such as including post-fracture permeability in the far field anhydrite permeability distribution to include the phenomena of pressure-induced fracturing, this approach was unacceptable to the performance assessment group. Therefore, it is important to understand that the 1992 performance assessment calculations will not reflect the full range of potential outcomes. In other words, the calculations do not include all known or possible phenomena and outcomes.

References:

Beauheim, R. L., G. J. Saulnier, Jr. and John D. Avis. 1990. **Interpretation of Brine-Permeability Tests of the Salado Formation at the Waste Isolation Pilot Plant Site: First Interim Report.** SAND90-0083. Albuquerque, NM: Sandia National Laboratories.

Beauheim, R. L., T. F. Dale, M. D. Fort, R. M. Roberts and W. A Stensrud. 1992. **Hydraulic Testing of Salado Formation Evaporites at the Waste Isolation Pilot Plant Site: Second Interpretive Report.** SAND92-0533. Albuquerque, NM: Sandia National Laboratories.

Gelbard, F. 1992. **A Two-Dimensional Model for Brine Flow to a Borehole in a Disturbed Rock Zone.** SAND92-1303. Albuquerque, NM: Sandia National Laboratories.

McTigue, D. F. 1992. **Permeability and Hydraulic Diffusivity of WIPP Repository Salt Inferred from Small-Scale Brine Inflow Experiments.** SAND92-1911. Albuquerque, NM: Sandia National Laboratories.

WIPP Performance Assessment Division. 1992A. **Preliminary Comparison with 40 CFR Part 191, Subpart B for the Waste Isolation Pilot Plant, December 1991. SAND91-0893/6. Albuquerque, NM: Sandia National Laboratories.**

Table 1. Recommended Cumulative Probability Distributions for formation permeability (m^2), derived from Figures 2-6.

Halite Far Field and Depressurized Zones: Zones A, B and C

Permeability (m^2)	Cumulative probability
0.0	0.00
1.0×10^{-24}	0.00
1.0×10^{-23}	0.10
1.0×10^{-22}	0.19
1.0×10^{-21}	0.48
1.0×10^{-20}	0.95
1.0×10^{-19}	1.00

Halite Disturbed Zone: Zones D and E

Permeability (m^2)	Cumulative probability
1.0×10^{-18}	0.00
1.0×10^{-13}	1.00

Table 1. (Continued)

Anhydrite Far Field and Depressurized Zones: Zone F, G and H

Permeability (m^2)	Cumulative probability
$1.0x10^{-21}$	0.00
$1.0x10^{-20}$	0.07
$1.0x10^{-19}$	0.71
$1.0x10^{-18}$	0.93
$1.0x10^{-17}$	0.96
$1.0x10^{-16}$	1.00

Anhydrite Disturbed Zone: Zone J

Permeability (m^2)	Cumulative probability
$1.0x10^{-18}$	0.00
$1.0x10^{-17}$	0.12
$1.0x10^{-16}$	0.25
$1.0x10^{-15}$	0.37
$1.0x10^{-14}$	0.75
$1.0x10^{-13}$	0.87
$1.0x10^{-12}$	1.00

Anhydrite Disturbed Zone: Zone I

Permeability (m^2)	Cumulative probability
$1.0x10^{-19}$	0.00
$1.0x10^{-18}$	1.00

Table 2. Parameter Estimates from Borehole Experiments. This from information in Table 5 of an early draft of McTigue, 1992. The difference between the values from the early draft (this table) and the table in McTigue, 1992 is the use of a literature value and a WIPP-specific measured value, respectively, for brine compressibility in the data interpretation.

Borehole #	Rock Type	Permeability @Po=10 MPa (m^2)	Permeability @Po=5 MPa (m^2)	Permeability @Po=01MPa (m^2)	Diffusivity (m^2/sec)
DBT10	Halite	2.9E-22±.18E-22	5.8E-22±.36E-22	2.9E-21±.18E-21	4.7E-11±.78E-11
DBT11	Halite	1.1E-21±.09E-21	2.3E-21±.18E-21	1.1E-20±.09E-20	3.5E-9±.63E-9
DBT12	Halite	6.4E-22±.72E-22	1.3E-21±.14E-21	6.4E-21±.72E-21	10E-8±.65E-8
DBT13	Halite	1.7E-22±.26E-22	3.4E-22±.32E-22	1.7E-21±..26E-21	5.9E-11±.2.3E-11
DBT14A	Halite	7.8E-22±.2.4E-22	1.6E-21±.48E-21	7.8E-21±.2.4E-21	2.8E-8±4.6E-8
DBT14B	Halite	2.2E-21±.28E-21	4.5E-21±.56E-21	2.2E-21±.28E-21	4.3E-8±3.3E-8
DBT15A	Halite	3.2E-22±.55E-22	6.4E-22±1.1E-22	3.2E-21±.55E-21	1.8E-10±.86E-10
DBT15B	Halite	1.8E-22±.59E-22	3.6E-22±1.1E-22	1.8E-21±.59E-21	1.3E-10±1.2E-10
L4B01	Halite	.67E-22±.43E-22	1.3E-22±.86E-22	.67E-21±.43E-21	5.8E-11±9.1E-11
DBT31A	Halite	9.0E-22±2.4E-22	1.8E-21±.48E-21	9.0E-21±.2.4E-21	1.27E-10±.22E-11
QPB01 *1	Anhydrite	4.8E-21±.3E-21	9.6E-21±.06E-21	4.8E-20±.3E-20	1.1E-8±.34E-8
QPB02 *1	Anhydrite	8.2E-20±.03E-20	1.6E-19±.006E-19	8.2E-19±.03E-19	1.2E-9±.014E-9
QPB03 *1	Anhydrite	4.8E-21±1.5E-21	9.6E-21±.3E-21	4.8E-20±1.5E-20	6.4E-7±18.8E-7*

* The lower limit of these uncertainty bounds should be assumed to be zero.

*1 For all of these borehole tests, the length of the productive unit was assumed to be equal to the average thickness of Marker Bed 139 (3-feet).

Table 3: Compilation of Interpreted Values of Permeability, 1/5/92. Zones are referenced to Figure 1.

Zone	Test	Measured Permeability	Pressure(MPA)
A. **HALITE FAR FIELD**			
	QPP12 pre-mineby		
		6.8×10^{-22} m^2	9.5
	C2HO3	Too low to measure	not measureable
	SCP01 GZ	Too low to measure	not measureable
	QPP05	Too low to measure	not measureable
	QPP02	Too low to measure	not measureable
B. **HALITE DEPRESSURIZED ZONE**			
	S1P72-A-GZ	8.6×10^{-22} m^2	5.1
	QPP21 post mineby		
		1.9×10^{-22} m^2	4.8
	C2H01-B	5.3×10^{-21} m^2	3.1
	C2H01-B-GZ	1.9×10^{-21} m^2	4.1
	L4P51-A	6.1×10^{-21} m^2	2.7
	S0P01	8.3×10^{-21} m^2	4.4
	S1P71-A	6.1×10^{-20} m^2	2.9
	QPP15	2.2×10^{-21} m^2	3.1
	DBT10	5.8×10^{-22} m^2	5.0 assumed
	DBT11	2.3×10^{-21} m^2	5.0 assumed
	DBT12	1.3×10^{-21} m^2	5.0 assumed
	DBT13	3.4×10^{-22} m^2	5.0 assumed
	DBT14A/B	3.1×10^{-21} m^2	5.0 assumed
	DBT15A/B	5.0×10^{-22} m^2	5.0 assumed
	L4B01	1.3×10^{-22} m^2	5.0 assumed
	DBT31A	not used	
	QPP12	4.4×10^{-22} m^2	9.4
C. **HALITE DEPRESSURED ZONE**			
Same as region B for permeability.			
D. **HALITE DISTURBED ROCK ZONE**			
	C2H01-A	2.7×10^{-18} m^2	0.5
	C2H01-A-GZ	unmeasureable	0.0
	S1P73-B-GZ	unmeasureable	2.5
E. **HALITE DISTURBED ROCK ZONE**			
Same as region D for permeability.			

Table 3. (Continued)

F. **ANHYDRITE FAR FIELD** (greater than 10 m from excavation)

SCP01 MB 139	3.0×10^{-20} m^2	12.4
QPP13 pre-mineby MB 139	4.1×10^{-20} m^2	12.5
QPP03 pre mineby clay b	4.4×10^{-20} m^2	12.6

G. **ANHYDRITE DEPRESSURIZED ZONE** (less than 10 meters from excavation)

C2H02 MB 139	7.8×10^{-20} m^2	9.3
L4P51-B anhydrite c	5.0×10^{-20} m^2	5.1
S1P71-B anhydrite c	6.8×10^{-20} m^2	4.9
C2H01-C MB 139	9.5×10^{-19} m^2	8.0
C1X10 MB 139	5.0×10^{-17} m^2	7.3
QPP03 anhydrite b post mineby	7.9×10^{-20} m^2	7.0
QPP13 MB 139 post mine-by	4.7×10^{-20} m^2	8.1
L4P52-A anhydrite a	1.0×10^{-19} m^2	6.4
QPB01	9.6×10^{-21} m^2	5.0 assumed
QPB02	1.6×10^{-19} m^2	5.0 assumed
QPB03	1.2×10^{-20} m^2	5.0 assumed
S1P72	unmeasureable	1.2

H. **ANHYDRITE DEPRESSURIZED ZONE**

Same permeability as region G.

I. **ANHYDRITE DISTURBED ROCK ZONE (138)**

S1P73-B MB 138	2.9×10^{-19} m^2	4.5

J. **ANHYDRITE DISTURBED ROCK ZONE**

SOP01 GZ	5.7×10^{-18} m^2	0.5
S1P73-A	too high to measure; estimated at 10^{-15} m^2	0.0
S1P73-A-GZ	too high to measure; estimated at 10^{-15} m^2	0.0
S1P71-A-GZ	too high to measure; estimated at 10^{-14} m^2	0.0
L4P51-A-GZ	too high to measure; estimated at 10^{-15} m^2	0.3
Crawley	1.6 to 3.2 $\times 10^{-13}$ m^2	???

YET TO BE INTERPRETED

QPP01
QPP04
QPP11
QPP14
QPP22
QPP23
QPP24
QPP25

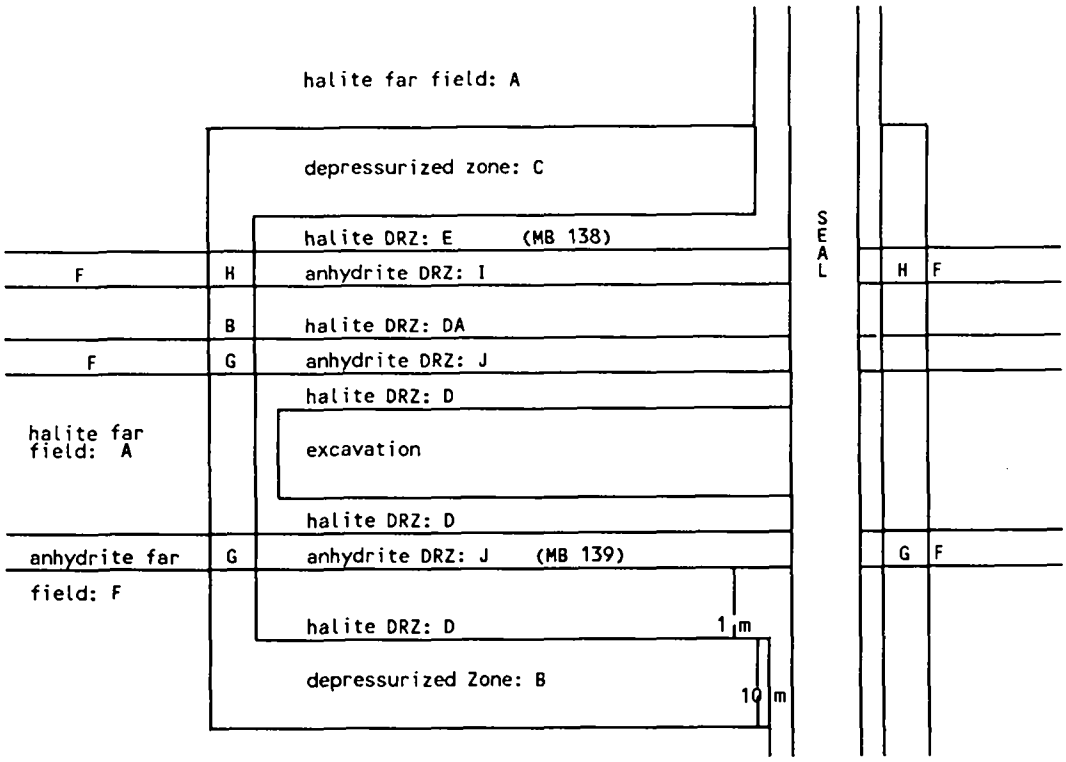

Figure 1: Schematic for assigning flow properties to Salado Formation (Not to Scale!!!!)

Halite Far Field and Halite Depressurized Zone: Zones A, B and C

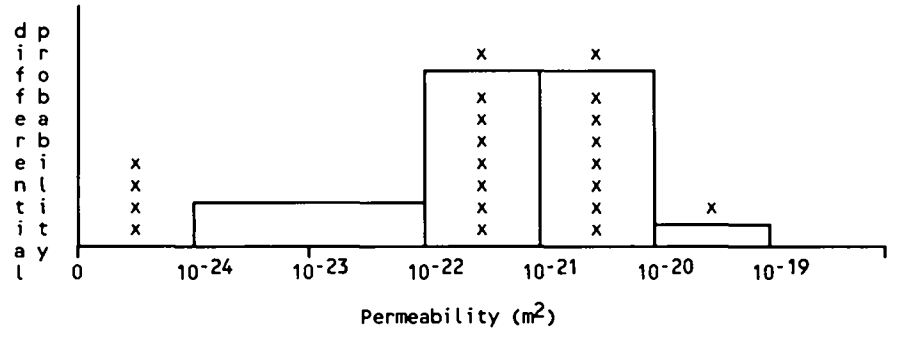

Figure 2.

Halite Disturbed Zone: Zones D and E

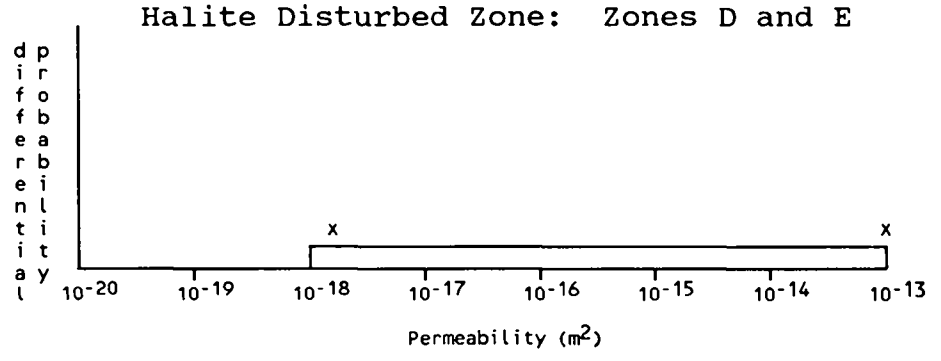

Figure 3.

Anhydrite Far Field and Anhydrite Depressurized Zone: Zones F, G and H

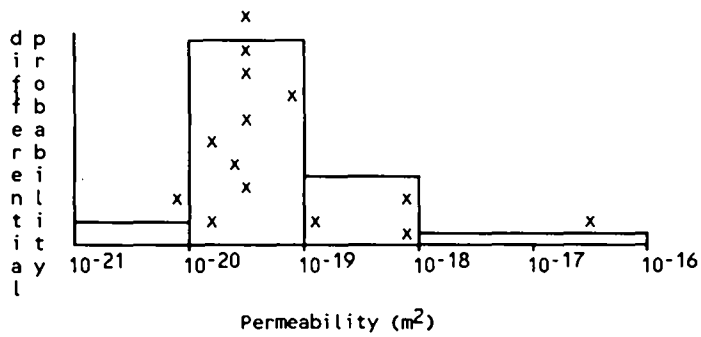

Figure 4.

Anhydrite Disturbed Zone: Zone J

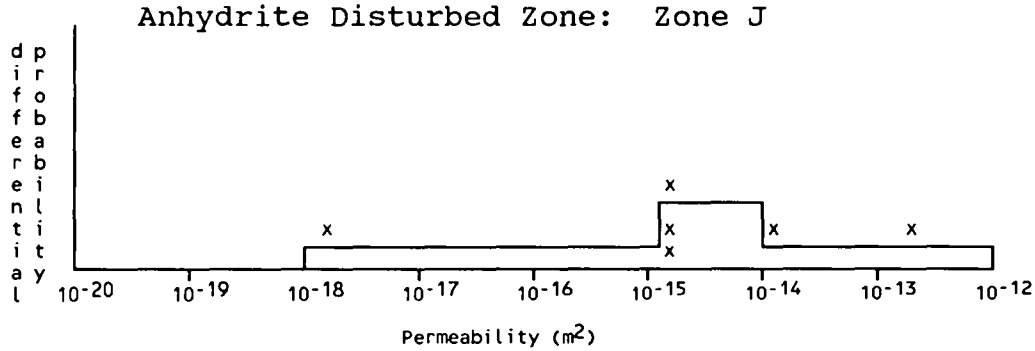

Figure 5.

Anhydrite Disturbed Zone: Zone I

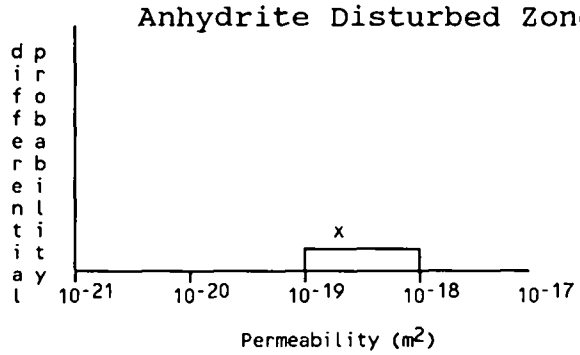

Figure 6.

Sandia National Laboratories

Albuquerque, New Mexico 87185

date: June 15, 1992

to: Barry Butcher and Martin Tierney, 6342

Elaine Gorham

from: Elaine Gorham, 6119, 4-1401

subject: Additional suggestion for 1992 PA calculations

This memo is to request a change in the parameterization of the Salado flow models for the 1992 40 CFR 191 calculations from those parameters used in the 40 CFR 268 calculations. As you have probably already heard, when we negotiated in April about probability distributions for formation parameters, we had somewhat of a misunderstanding with respect to including effects of fracture opening due to pressurization in the anhydrite layers. I (incorrectly) assumed that PA had an explicit module that would allow permeability in the anhydrite layers to increase with hydraulic pressure (to simulate fracture opening). Thus Rick and I suggested values of permeability for the far field anhydrite which were representative of unfractured anhydrite. We can discuss the implications of these assumptions on the 40 CFR 268 calculations during our June 25 meeting.

In the meantime, I'd like to suggest changes in the assumed values for far field anhydrite that would be somewhat more representative of conditions associated with pressure-generated fracturing in the anhydrite for the 1992 40 CFR 191 calculations. In particular, we (Peter Davies and myself, since Rick is on foreign travel) recommend that permeability probability distributions previously supplied for the far field anhydrite (Region F), the depressurized anhydrite (Regions G and H) and the DRZ anhydrite (Region J) be combined with equal weight to form a single probability distribution for all the anhydrite (far field, depressurized zone and DRZ). In addition, we recommend that the porosity used for our previously defined anhydrite and halite far field and depressurized zones be represented by the previously recommended far field porosity. The reason for the latter recommendation is our judgement that large increases in permeability due to fractures opening do not imply the large increases in porosity assumed for the anhydrite DRZ. This latter change is important because overestimation of Salado porosity will result in calculations that underestimate room pressure and/or lateral gas migration.

Including the DRZ permeability distribution in the distribution for the entire anhydrite, as we recommend for the 40 CFR 191 calculations, will cause about 4% of the calculations to be conducted with very high permeability values in the anhydrite

(between 10^{-14} and 10^{-12} m^2). These values correspond to our current estimates of the high end of values expected after fracturing due to overpressure. By using these values for the entire calculations you will overestimate initial brine inflow rates and gas generation rates. However, because increased gas pressure will reverse the brine inflow and gas generation, it is unclear if total gas generated will be unrealistically large. The calculation therefore has the potential to calculate reasonable values for bounding estimates of gas migration distance in the absence of fingering. Given that we are trying to simulate a missing phenomena by changing an input parameter distribution, this may be the best that can be done on short notice. A major factor in our approach to this problem has been to assure that the range of outcomes of the PA calculations provide a good representation of the true uncertainty in our understanding of the repository behavior, at least with respect to permeability and porosity values for the Salado formation. We can discuss this approach when we meet on June 25.

I would like to emphasize the importance of implementing a pressurized fracture-opening model in your codes in future years.

In the meantime, if you have any questions about these recommendations or wish to further clarify them please call either Peter or myself.

Copies:

6303 W. D. Weart
6119 R. L. Beauheim
6119 P. B. Davies
6119 S. Howarth
6117 W. R. Wawersik

Hora, August 25, 1992

Date: 8/25/92
To: Kate Trauth, Jon Helton, Mel Marietta, Martin Tierney, Bob Guzowski, Rip Anderson
From: Steve Hora
Subject: Probabilities of Human Intrusion into the WIPP, Methodology for the 1992 Preliminary Comparison

PROBABILITIES OF HUMAN INTRUSION INTO THE WIPP METHODOLOGY FOR THE 1992 PRELIMINARY COMPARISON

August 25, 1992

Prepared by
Stephen C. Hora
For
Division 6342
Sandia National Laboratories

During 1990-1992, external experts were assembled by Sandia National Laboratories to study potential inadvertent human intrusion into the Waste Isolation Pilot Plant (WIPP). These experts formed two groups -- one group studied what future societies might be like and how they might inadvertently intrude into nuclear waste. The second group, after considering the findings of the first group, studied how markers might be used to warn future societies about the presence and danger of the buried waste. Both groups provided probabilities and probability distributions for critical aspects of the human intrusion problem. This report discusses the use of these assessments in the 1992 preliminary performance assessment.

The Futures Group

The first group of experts was divided into four teams. Each team was composed of four experts from various fields of social and physical science. Each team was asked to address the same set of questions (see Hora, von Winterfeldt, and Trauth, 1992). The results of their work suggests that future societies may undertake activities that could lead to inadvertent intrusion into the WIPP. These teams judged that a number of factors (e.g. the level of technology, demand for resources, population level, the ability to retain knowledge about nuclear waste, etc.) would influence the likelihood of inadvertent intrusions.

The results of the futures teams provide a basis for developing probability distributions for inadvertent intrusion attempts into the WIPP. Because the teams used different structures for analysis and considered different factors that would influence the likelihood of inadvertent intrusion, the results of their endeavors must be individually interpreted in order to be used in the preliminary performance assessment.

The Markers Group

A second group of thirteen experts was organized into two teams to study markers for the WIPP site. These markers are to serve as warnings to future societies about the presence of nuclear waste. Such warnings, hopefully, will deter inadvertent intrusions. Each team was asked to consider the findings of the futures teams, to suggest design characteristics for a marker system, and to assess the efficacy of such a system of markers. The ability of a marker system to deter intrusions rests on the survival of the marker

system over an extended period of time, and the ability of potential intruders to detect the markers and to understand the messages that they carry.

The markers team members where asked to provide probabilities for several events. The first of these is the event that a marker and its message(s) remain intact at various times in the future. Second, for several types of intrusion, the team members were asked to provide probabilities that, given the marker and its messages are intact, the potential intruders are able to understand the message and thus become forewarned of the inherent dangers of intrusion. These assessments were made under various assumptions about the state of technology in the future.

The Standard (40 CFR 191)

The US EPA regulation (40 CFR 191), issued in 1985 and remanded in 1987, provides the rationale for performance assessment for the WIPP. Although the standard has been remanded and awaits reissue, in agreement with the State of New Mexico, the preliminary performance assessments continue to be executed as though the 1985 standard was still in place. The 1985 version of the standard provides some guidance about human intrusion. In appendix B of the standard, the frequency and severity of human intrusion is discussed:

> *The Agency believes that the most productive consideration of inadvertent intrusion concerns those realistic possibilities that may be usefully mitigated by repository design, site selection or use of passive controls (although passive institutional controls should not be assumed to completely rule out the possibility of intrusion). Therefore, inadvertent and intermittent intrusion by exploratory drilling for resources (other than any provided by the waste disposal system itself) can be the most severe intrusion scenario assumed by the implementing agencies.*
>
> *However, the Agency assumes that the likelihood of such inadvertent and intermittent drilling need not be taken to be greater than 30 boreholes per square kilometer of repository area per 10,000 years for geologic repositories in proximity to sedimentary rock formations, or more than 3 boreholes per square kilometer per 10,000 years for repositories in other geologic formations.*

From these two statements, it is concluded that the preliminary performance assessment need not consider intrusion modes such as mining or archaeological investigation that may result in more severe consequences than drilling. Moreover, the standard also provides an upper bound for the drilling intensity to be used in the performance assessment. Three modes of drilling intrusion have been identified by the experts examining human intrusion issues. These modes are exploratory drilling for mineral resources

(primarily fossil fuels) drilling water wells, and drilling for injection disposal wells. Drilling for water was found to be an insignificant threat when compared to drilling for mineral resources. Drilling for disposal wells, which was identified as a threat by one of the four futures teams, has not yet been modeled and, therefore, its affect cannot be judged. Thus, exploratory drilling for resources is the only mode of intrusion considered in the 1992 preliminary comparison.

Assembling the Judgments

The existence of markers and the ability of a society to interpret the warnings left at WIPP may depend upon the state of development of that society. In the preliminary performance assessment, the state of development of the society is represented by the level of the technological development of the society. The level of technological development (high, medium, or low) will be randomly generated from distributions provided by the futures teams.

Using a given level of technology, the frequency (λ) at which attempted inadvertent intrusions will occur at various points in time will be established. This time dependent frequency is called the raw drilling intensity and treated as a parameter of a time dependent Poisson process. The raw drilling intensity does not take into account deterrence by markers, however. For each of the several points in time that the raw drilling intensity is evaluated, the probability of the markers existing (p_1) and the probability of the markers deterring an intrusion attempt given that the markers exist (p_2) are evaluated. These two probabilities modify the raw drilling intensity to give the effective drilling intensity $\lambda(1-p_1p_2)$. The effective drilling intensity is used in the performance assessment to obtain probabilities for scenarios. The process of developing the effective drilling intensity is repeated many times in order to generate many vectors of drilling intensities. Each vector is a random realization and differences among the vectors represent the uncertainty in the drilling intensity and the effectiveness of the markers.

Because the four teams studying potential futures developed analyses independently and in different ways, there is no simple way to combine their findings. For this reason, a team will be randomly selected on each iteration of the Monte Carlo analysis. The assessments from each team represent their collective judgment. In contrast, one of the markers' teams individually provided probability assessments while the other team who provided a consensus set of probability distributions. Thus, when one of the two markers teams is randomly chosen for a Monte Carlo iteration, it may be necessary to also randomly select one of the team members for that iteration. This procedure avoids making unfounded assumptions about how to combine disparate distributions.

The algorithm for generating inadvertent intrusions can then be described by the following steps:

1. Randomly select one of the four futures teams.

The following steps use distributions conditional on the outcome of step 1.

2. Randomly select a level of technology in the future. When probabilities of levels of technology are time dependent, a rank correlation of one will be used to generate the level of technology in the several time periods.

3. Generate a random variable to determine the intrusion intensity. When intrusion intensities vary with time periods, a rank correlation of one will be used to generate the intrusion intensities in the several time periods.

4. Randomly select one of the markers teams and a marker team member, if necessary.

5. For each time period generate the probability that markers are extant given the level of technology.

6. For each time period, generate the probability that the markers deter intrusion given that the markers are extant, the level of technology, and the mode of intrusion.

7. Compute the effective drilling intensity for each time period.

There are several assumptions implicit in the above algorithm. In step 3, a single random number is used to select an intrusion intensity for all periods. This is a conservative assumption in that the variability of the performance measure will be maximized among the Monte Carlo iterations.

Future Levels of Technology

A link exists between the findings of the two groups; the futures group and the markers group. The assessments of the markers group are conditional on the findings of the futures groups. Since each of the futures teams provided a unique analysis using a different set of underlying factors, making the assessment of the markers group conditional on all of the identified factors is infeasible. However, technology emerges as an important theme in all of the analyses and has, thus, been used to capture the dependency between the state of society and the efficacy of the marker system.

The assessments of the Boston futures team provide probabilities for three levels of technology during various times in the future:

TABLE 1
LEVELS OF TECHNOLOGY - BOSTON TEAM

	Years After Closure		
Level of Technology	100-300 years	300-3000 years	3000-10000 years
High	.8	.7	.8
Medium	.15	.2	.1
Low	.05	.1	.1

The Southwest futures team provided probabilities of three scenarios for the development of society: increase, decline, and a future which alternates between these possibilities. We equate the Southwest teams pattern of steady increase in technology with a high level of technology, steady decline with a low level of technology, and the alternating or sea-saw pattern that cycles every 1000 years between increase and decline in technology with 500 years of medium technology followed by a repeating pattern of high, medium, low, and medium technology, each for a period of 500 years. The probability for the increase (high technology scenario) is .475, for the decline (low technology scenario) it is .0875, and for the alternating scenario it is .4375.

The Washington A futures team viewed the future as following a pattern of continuity, radical increase, discontinuity, or one of steady state utilization of resources. Roughly, continuity is equated with high technology while discontinuity is equated with a lower level of technology. Both radical increase and the steady state scenarios are equated with medium technology. Using these assumptions, the following table of probabilities was derived.

TABLE 2
LEVELS OF TECHNOLOGY - WASHINGTON A TEAM

Scenario	Technology	Probability
Continuity	High	.255
Radical Increase	Medium	.2275
Discontinuity	Low	.1675
Steady state	Medium	.35

The Washington B team provided assessments directly in terms of the three levels of technology as repeated in the following table:

TABLE 3
LEVELS OF TECHNOLOGY - WASHINGTON B TEAM

	Time Period	
Technology	0-200 years	200-10000 years
High	.5	.9
Medium	.5	.05
Low	.0	.05

Frequencies of Intrusion Attempts

The responses about the likelihood of intrusion vary in form from team to team. Two teams responded by providing probabilities of intrusion while the other two teams provided probability distributions for the drilling intensity. The most convenient form of information for performance assessment is to have a time dependent intensity parameter or a probability distribution on such a parameter. Therefore, the choice has been made to convert assessments from the four futures teams into a common form -- a drilling intensity parameter or probability function for such a parameter. The spacing of potential drilling intrusions is then carried out in the performance assessment simulations using a time dependent Poisson process with a random parameter.

The Boston team provided assessments for the drilling intensity that are conditional on both time and level of technology. The responses for exploratory drilling for hydrocarbons are shown in the following tables. Exploratory drilling for hydrocarbons was not thought to extend further than 300 years into the future.

TABLE 4
BOSTON TEAM -DRILLING INTENSITY DISTRIBUTIONS

Drilling	Technology		
Intensity	High	Medium	Low
0.5	0.15	0.15	0.15
0.83	0.02	0.02	0.03
4.98	0.22	0.22	0.21
8.3	0.03	0.03	0.04
12.45	0.12	0.11	0.11
20.75	0.02	0.02	0.02
24.9	0.12	0.11	0.11
41.5	0.02	0.02	0.02
49.8	0.22	0.22	0.21
83	0.03	0.03	0.04
99.6	0.03	0.03	0.03
166	0	0	0.01
199.2	0.03	0.03	0.03
332	0	0	0.01

The Boston team also considered drilling for disposal wells as a

possible cause of inadvertent intrusion. This mode of intrusion, however, is not considered in the 1992 performance assessment. There are several reasons for this exclusion. First, this type of potential intrusion has not yet been modeled and, therefore, even if intrusion rates were developed, it would not be possible to account for the consequences. Second, the depth of such wells has not been studied and, thus, it cannot be determined if this type of activity indeed constitutes a threat. Third, only one of the four teams explicilty considered this mode of intrusion. Moreover, this team did not provide complete information at the elicitation session. A questionnaire sent later to the team members was completed by three of the four participants. There was wide disagreement on the frequency of such activity.

The Southwest team considered conventional drilling to be plausible only under the declining and alternating scenarios. In order to employ the judgments provided by this team in the performance assessment, it is necessary to interpret their conclusions. It appears that drilling should be considered only in the low and medium technology states. Moreover, since this team assessed holistic probabilities of one or more intrusions, it is necessary to convert their assessments into a drilling intensity. For the decline and see-saw scenarios, the probabilities of intrusion are given as .113 and .138 respectively. For the decline scenario (low technology) intrusion would occur, if it occurs, during the first 400 years after closure. Assuming a constant intensity during this period, we equate the Poisson probability of one or more intrusions with the assessed probability:

$$1-e^{-.00472\lambda} = .113.$$

The .00472 is the fraction (400 years/10,000 years)(.118 square miles) so that λ is expressed as per square mile per 10,000 years. The .118 arises because this is the planned footprint of the repository. The resulting drilling intensity for 100 to 500 years after closure under the decline scenario implied by the .113 probability is then 25.40 boreholes per square mile per 10,000 years.

Making the conversion under the see-saw scenario is similar with the added difficulty that drilling will not be undertaken during periods of high technology. Using the assumptions discussed in the section of this paper dealing with levels of technology, if the see-saw scenario occurs, the world will be in a high technology state about 1/3 of the time. Thus, we interpret the .138 probability of intrusion in the see-saw scenario to be applicable to 6,666 years (2/3 of 10,000). The resulting drilling intensity, again in units per square mile per 10,000 years is found from

$$1-e^{-.0787\lambda} = .138$$

The resulting drilling intensity is 1.89 boreholes per square mile per 10,000 years.

The Washington A team also provided holistic assessments of the probabilities of intrusion. Assessment were provided for both the first 200 years after closure and the ensuing 9800 years. The following table shows the assessed probabilities and intrusion intensities derived using the same procedure as was used for the Southwest Team.

TABLE 5
PROBABILITIES OF ONE OF MORE INTRUSIONS - WASHINGTON A TEAM

	0-200 years after closure		200-10,000 years after closure	
Scenario (probability)	Assessed Probability	Intrusion Intensity	Assessed Probability	Intrusion Intensity
Continuity (.255)	.076	33.5	.21	2.0
Radical Increase (.2275)	.628	419	.08	.72
Discontinuity (.1675)	.413	226	.42	4.7
Steady State (.35)	.01	4.3	.09	.82

The Washington B Team provided information which permitted the construction of a cumulative distribution function for the number of boreholes. In the near future, 0-200 years after closure, the drilling intensity follows the following CDFS:

TABLE 6
EXPECTED BOREHOLES- WASHINGTON B TEAM

Boreholes per square mile	0-200 years after closure	200-10,000 years after closure
$\lambda<0$	0	0
$\lambda=0$	0.932	0.9377
$0<\lambda\leq 2$	$0.932+0.0085\lambda^2$	$0.9377+0.007782\lambda^2$
$2<\lambda\leq 4$	$0.932+.068[\lambda-(\lambda^2/8)-1]$	$0.9377+.0623[\lambda-(\lambda^2/8)-1]$
$4<\lambda$	1.0	1.0

This team also considered the possibility of drilling for water in both the near and far futures. the probabilities of drilling for water are, however, less than 10^{-4} in both near future and the far future and thus are excluded from further analysis.

Generating the Intrusion Intensity

Let U_i be a uniform [0-1] random deviate. The following algorithm describes the generation of λ, the drilling intensity in terms of several U_i.

0. Go to step $[4*U_1]+1$ where [.] is the largest integer function.

1. (Boston) Compare U_2 to the following look up table:

TABLE 7
LOOKUP TABLE FOR TECHNOLOGY - BOSTON TEAM

U_2	100-300 years	300-3000 years	3000-10000 years
$u \leq .7$	High Tech	High Tech	High Tech
$.7 < u \leq .8$	High Tech	Medium Tech	High Tech
$.8 < u \leq .9$	Medium Tech	Medium Tech	Medium Tech
$.9 < u \leq .95$	Medium Tech	Low Tech	Low Tech
$.95 < u$	Low Tech	Low Tech	Low Tech

Given the outcome from U_2, compare U_3 to Table 8. The drilling intensity is the value having the smallest cumulative probability equal to or greater then U_3.

TABLE 8
DRILLING INENSITY CUMULATIVE PROBABILITES - BOSTON TEAM

Drilling Intensity	Cumulative Probability Technology High	Medium	Low
0.5	0.15	0.15	0.15
0.83	0.17	0.17	0.18
4.98	0.39	0.39	0.38
8.3	0.42	0.42	0.42
12.45	0.53	0.54	0.53
20.75	0.55	0.56	0.55
24.9	0.67	0.67	0.66
41.5	0.69	0.69	0.68
49.8	0.91	0.91	0.88
83	0.94	0.94	0.92
99.6	0.97	0.97	0.95
166	0.97	0.97	0.96
199.2	1.00	1.00	0.99
332	1.00	1.00	1.00

2. (Southwest) Compare U_2 to the following look-up table

TABLE 9
LOOKUP TABLE FOR TECHNOLOGY AND DRILLING INTENSITY
SOUTHWEST TEAM

U_2	Time Period	Drilling Intensity	Technology
$0 \leq u \leq .475$	0-10,000	$\lambda=0$	High
$.475 < u \leq .5625$	0-400 400-10,000	$\lambda=25.40$ $\lambda=0$	Low
$.5625 < u$	0-500 500-1000 1000-1500 1500-2000 2000-2500 2500-3000 3000-3500 3500-4000 4000-4500 4500-5000 5000-5500 5500-6000 6000-6500 6500-7000 7000-7500 7500-8000 8500-9000 9000-9500 9500-10000	1.89 0 1.89 1.89 0 1.89 1.89 0 1.89 1.89 0 1.89 1.89 0 1.89 1.89 0 1.89 1.89	Medium High Low Medium High Low Medium High Low Medium High Low Medium High Low Medium High Low Medium

3. (Washington A) Compare U_2 to the following look-up table.

TABLE 10
LOOKUP TABLE FOR TECHNOLOGY AND DRILLING INTENSITY
WASHINGTON A TEAM

U_2	Time Period	Drilling Intensity	Technology
$0 \leq u \leq .255$	0-200 200-10000	33.5 2.	High
$.255 < u \leq .4825$	0-200 200-10000	419. .72	Medium
$.4825 < u \leq .65$	0-200 200-10000	226. 4.7	Low
$.65 < u$	0-200 200-10000	4.3 .82	Medium

4. (Washington B) Compare U_2 to the following look-up table to determine the state of technology:

TABLE 11
LOOKUP TABLE FOR TECHNOLOGY - WASHINGTON B TEAM

U_2	Technology 0-200 years	Technology 200-10,000 years
$u \leq .5$	High	High
$.5 < u \leq .90$	Medium	High
$.90 < u \leq .95$	Medium	Medium
$.95 < u$	Medium	Low

Next, compare U_3 to the following two lookup tables to determine the drilling intensity which is independent of the state of technology:

TABLE 12A
DRILLING INTENSITY FOR 0-200 YEARS - WASHINGTON B TEAM

U_3	Intensity λ
$u \leq .932$	0.0
$.932 < u \leq .966$	$[(u-.932)/.0085]^{.5}$
$.966 < u$	$4(1-\{1-.5[1+(u-.932)/.068]\}^{.5})$

TABLE 12B
DRILLING INTENSITY FOR 200-500 YEARS - WASHINGTON B TEAM

U_3	Intensity λ
$u \leq .9377$	0.0
$.9377 < u \leq .96885$	$[(u-.9377)/.007782]^{.5}$
$.96885 < u$	$4(1-\{1-.5[1+(u-.9377)/.0623]\}^{.5})$

Drilling for resources does not continue beyond 500 years and thus the drilling intensity is 0 beyond 500 years.

Persistence of Markers

Markers Team A addressed probabilities of markers continuing to exist on an individual basis so that six individual assessments are available. Assessments were provided assuming three different levels of technology and at five points in time -- 200, 500, 1000, 5000, and 10000 years after closure. The following table contains the probabilities of the marker system (as defined in the report of the A team) continuing to exist at the given epoch conditional on a dominant state of technology.

TABLE 13
PROBABILITIES OF THE MARKER SYSTEM PERSISTING -TEAM A

Expert	Dominant Technology	Years After Closure				
		200	500	1000	5000	10,000
Ast	High	.99	.98	.95	.75	.50
	Medium	.99	.98	.95	.75	.60
	Low	.99	.98	.95	.75	.60
Brill	High	.99	.98	.95	.70	.50
	Medium	.99	.98	.95	.70	.50
	Low	.99	.98	.95	.85	.80
Goodenough	High	.99	.98	.90	.85	.70
	Medium	.99	.98	.95	.90	.75
	Low	.99	.98	.98	.95	.80
Kaplan	High	.95-.99	.95-.99	.90-.95	.80	.70
	Medium	.95-.99	.95-.99	.90-.95	.80	.70
	Low	.95-.99	.95-.99	.90-.95	.90	.85
Newmeyer	High	.90	.85	.70	.65	.60
	Medium	.95	.90	.85	.80	.60
	Low	.95	.90	.85	.85	.65
Sullivan	High	.90	.85	.80	.70	.50
	Medium	.95	.90	.85	.80	.70
	Low	.95	.90	.85	.80	.70

In contrast, Team B provided consensus probabilities at only three points in time -- 500, 2000, and 10,000 years. The following table contain these consensus probabilities for the three levels of technology.

TABLE 14
CONSENSUS PROBABILITIES OF THE MARKER SYSTEM PERSISTING - TEAM B

Dominant Technology	Years After Closure		
	500	2000	10000
High	.90	.85	.85
Medium	.90	.80	.60
Low	.90	.70	.40

Determining the Probabilities of Markers Deterring Intrusion

The following algorithm is based on linear interpolation of the probabilities provided by the two teams. Let k denote the level of technology and let T be the times at which probabilities are needed. V_i are uniform [0,1] random variables.

0. If $V_1 \leq .5$ go to step 1. otherwise step 2.

1. Let $i=[5*V_1]+1$ where [.] is the largest integer function. Let $t_0=0$, $t_1=200$, $t_2=500$, $t_3=1000$, $t_4=5000$, and $t_5=10000$. For each time T, calculate

$$p_1(T)=a_{i,j'-1,k}+(a_{i,j',k}-a_{i,j'-1,k})(T-t_{j'-1})/(t_{j'}-t_{j'-1})$$

and

$$p_2(T)=c_{i,j'-1,k}+(c_{i,j',k}-c_{i,j'-1,k})(T-t_{j'-1})/(t_{j'}-t_{j'-1})$$

where j' is the largest j=1,...,5 such that $T \leq t_j$. By assumption $a_{i0k}=1.0$ for all i and k.

2. Let $t_0=0$, $t_1=500$, $t_2=2000$, and $t_3=10000$. For each time T, calculate

$$p_1(T)=b_{i,j'-1,k}+(b_{i,j',k}-b_{i,j'-1,k})(T-t_{j'-1})/(t_{j'}-t_{j'-1})$$

and

$$p_2(T)=c_{m,i,j'-1,k}+(c_{m,i,j',k}-c_{m,i,j'-1,k})(T-t_{j'-1})/(t_{j'}-t_{j'-1})$$

where j' is the largest j=1,2,3 such that $T \leq t_j$. By assumption $b_{0k}=1.0$ for all k.

TABLE 15
COEFFICIENTS A_{ijk}

k=h (High Technology)					
	j=1	j=2	j=3	j=4	j=5
i=1	.99	.98	.95	.75	.50
2	.99	.98	.95	.70	.50
3	.99	.98	.90	.85	.70
4	.97	.97	.925	.80	.70
5	.90	.85	.70	.65	.60
6	.90	.85	.80	.70	.50
k=m (Medium Technology)					
i=1	.99	.98	.95	.75	.60
2	.99	.98	.95	.70	.50
3	.99	.98	.95	.90	.75
4	.97	.97	.925	.80	.70
5	.95	.90	.85	.80	.60
6	.95	.90	.85	.80	.70
k=l (Low Technology)					
i=1	.99	.98	.95	.75	.60
2	.99	.98	.95	.85	.80
3	.99	.98	.98	.95	.80
4	.97	.97	.925	.90	.85
5	.95	.90	.85	.85	.65
6	.95	.90	.85	.80	.70

TABLE 16
COEFFICIENTS b_{jk}

	j=1	j=2	j=3
k=h	.90	.85	.85
k=m	.90	.80	.60
k=l	.90	.70	.40

The Deterrence of Intrusion

The probability that the marker system will deter the potential intruders has been assessed as a function of time, the state of technology and the mode of intrusion. The following table gives the probability of deterrence of intrusion for intrusion by drilling assoicated wityh mineral exploration. The first six lines the table give the deterrence probability for the experts of Team A while the seventh line is the consensus probability for Team B.

TABLE 18

PROBABILITY OF DETERRENCE -- MINERAL EXPLORATION

COEFFICIENTS C_{mkij} WHERE M=MINERALS

	200 Years			500 Years			1000 Years			5000 Years			10000 Years		
Tech Expert	H	M	L	H	M	L	H	M	L	H	M	L	H	M	L
1	.99	.99	.98	.98	.95	.70	.95	.90	.50	.90	.20	.10	.90	.20	.05
2	.99	.99	.95	.95	.95	.90	.95	.95	.70	.95	.95	.60	.95	.95	.50
3	.99	.99	.99	.95	.95	.70	.90	.90	.50	.65	.60	.15	.50	.40	.02
4	.99	.98	.95	.98	.90	.70	.97	.85	.65	.95	.80	.50	.90	.75	.02
5	.99	.99	.90	.90	.85	.80	.80	.70	.50	.70	.60	.40	.50	.30	.20
6	.95	.95	.80	.90	.90	.60	.85	.85	.40	.70	.70	.10	.40	.40	.01
	500 Years			2000 Years			10,000 Years								
Team B	.90	.90	.80	.90	.85	.70	.99	.80	.30						

Implementation of the Algorithms

The interface between the performance assessment computer code and the findings of the two groups studying human intrusion requires the intensity of drilling activity, as a function of time, be simulated and passed to the performance assessment code. The mechanism for providing this connection is a FORTRAN code written to implement the algorithms of the preceding sections and produce vectors of time dependent drilling intensities to be used as input vectors to the performance assessment. This code is included in this report as an appendix.

The form of the output from this code is the effective drilling intensity at years 100 to 500 in increments of 100 years, and 500 to 10,000 years in increments of 500 years. The effective drilling intensity is the drilling intensity moderated by the probability of markers deterring intrusion. Let $\lambda(t)$ be the raw drilling intensity that would be expected if no markers were present. Let $p_1(t)$ be the probability that the marker systems exists at time t and let $p_2(t)$ be the probability that, given the continuing existence of the marker system, potential intruders are deterred from their intrusion attempt by the marker system. The moderated intrusion intensity, measured as expected boreholes/sq. mi./10,000 yrs., is $\lambda^*(t) = \lambda(t)[1-p_1(t)p_2(t)]$ where the factor $[1-p_1(t)p_2(t)]$ is the probability that the marker system fails to deter the potential intruders.

The FORTRAN code has been written to faithfully implement the findings of the expert teams. Several small concessions have been made to simplify the programming. These are:

1. The information for the drilling intensity from the Washington B team indicates that if minerals are extracted in the WIPP region, exploration will occur either in the first 200 years or in the next 300 years, but not in both periods. There does not seem to be adequate information from this team to model this dependence without making arbitrary assumptions. The code models this dependence by deciding if drilling occurs in the first 200 years and, if drilling does not occur, repeating the decision with the same decision rule to determine whether drilling occurs in the next 300 years.

2. There is some disparity among the time periods used by the various experts in deriving their assessments. Both the Boston and Southwest teams gave assessments that began 100 years after closure and thus allowed for a 100 year period of administrative control. In contrast, the two Washington teams gave assessments beginning immediately after closure and thus did not allow for the period of continuing administrative control. The performance assessment, however, assumes that the drilling rate is effectively nil during the first 100 years after closure.

The assessments given by the futures teams are for periods of time and thus a single, randomly chosen, intrusion rate will be effective during each period. In contrast, the assessments provided by the markers teams provide probabilities at points in time. Thus interpolation is needed to obtain probabilities for

intermediate points in time. This is accomplished in the implementation by using the middle of each time interval as the point to which interpolation is made.

In all other important respects the evaluation remains faithful to the algorithms given earlier and, hopefully, to the assessments provided by the experts.

Preliminary Evaluation of the Findings

The input to the performance assessment code from the human intrusion studies is in the form of vectors of drilling intensities. Each vector represents a different time history. The elements of the vectors are drilling intensities are various points in time.

The FORTRAN code written to create the input vectors for the performance assessment code has been modified to compute the average drilling intensity, the average marker failure probability, and the average moderated drilling intensity as a function of time. These averages are taken across the input vectors. Thus, there is an average for each time interval. Table 19 shows these three averages as a function of time since closure. Figure 1 shows these three averages on log scales to enhance the visibility of the behavior of the drilling intensities soon after closure.

Table 19 shows that the initial expected drilling intensity in the WIPP area is high for the first 500 years. After 500 years the expected intensity falls and remains fairly stable for 9500 years. The marker system, however, is shown to be most effective during this early period and, therefore, significantly moderates the drilling intensity during the first 500 years.

Figure 2 shows the empirical distribution of the time integrated drilling intensity across input vectors. This display captures the uncertainty in the overall drilling intensity since each vector is a different realization from the assessed probability distributions. Figure 2 shows that the largest time integrated drilling intensity among 1000 vectors is 2.884 boreholes/sq. mi./10,000 yr.

Figure 1

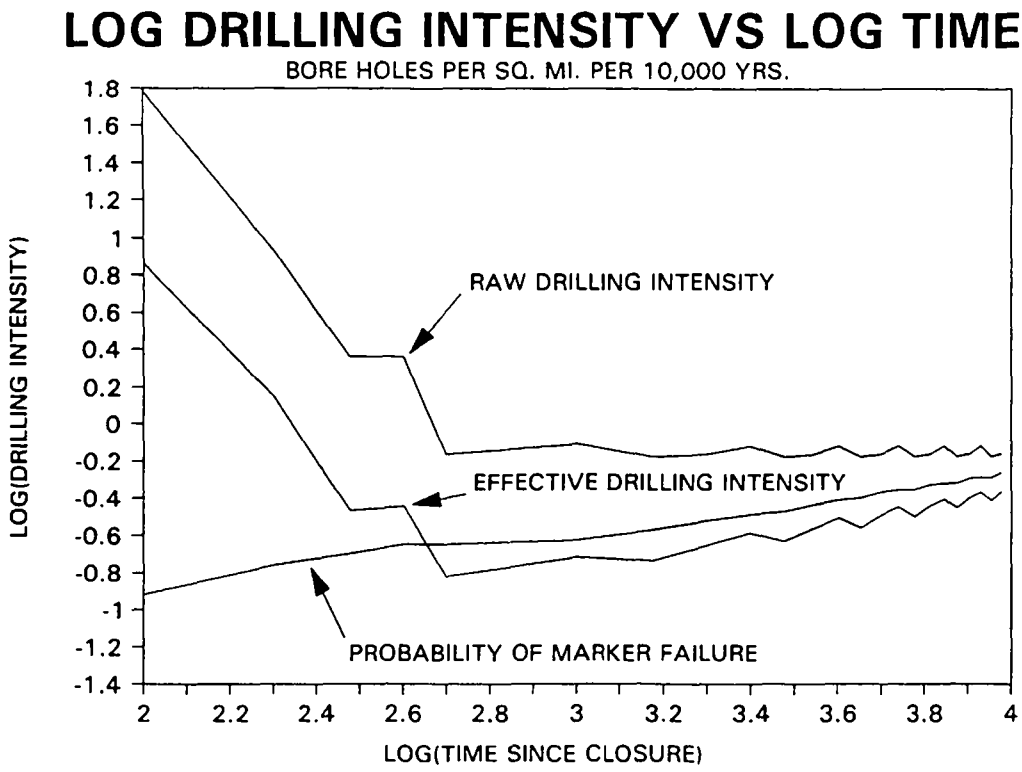

Figure 2

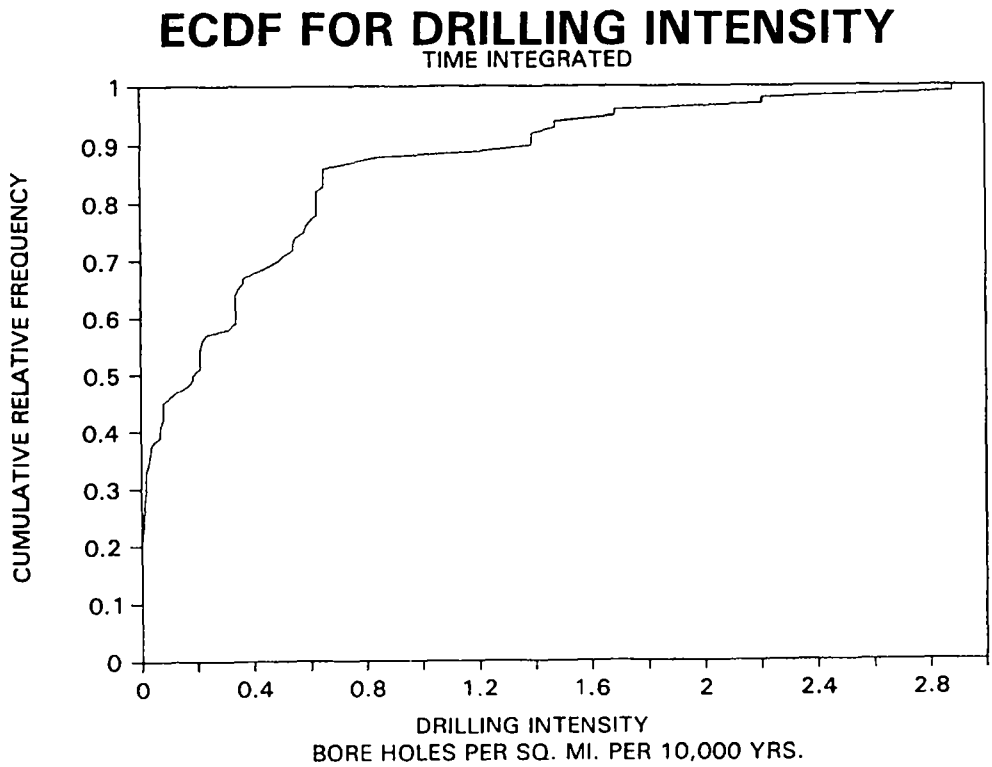

TABLE 19
COMBINED FUTURES AND MARKERS TEAMS FINDINGS
DRILLING INTENSITY PER SQUARE MILE PER 10,000 YEARS

Period	Raw Drilling Intensity	Probability of Marker Failure	Effective Drilling Intensity
0-100	55.4	0.0408	2.34
100-200	61	0.12	7.33
200-300	8.58	0.175	1.42
300-400	2.31	0.2	0.342
400-500	2.31	0.226	0.36
500-1000	0.687	0.226	0.151
1000-1500	0.781	0.237	0.192
1500-2000	0.668	0.269	0.184
2000-2500	0.687	0.301	0.222
2500-3000	0.762	0.325	0.26
3000-3500	0.668	0.338	0.234
3500-4000	0.687	0.368	0.275
4000-4500	0.762	0.389	0.313
4500-5000	0.668	0.401	0.278
5000-5500	0.687	0.43	0.323
5500-6000	0.762	0.44	0.357
6000-6500	0.668	0.443	0.317
6500-7000	0.687	0.47	0.361
7000-7500	0.762	0.479	0.392
7500-8000	0.668	0.48	0.352
8000-8500	0.687	0.509	0.397
8500-9000	0.762	0.516	0.426
9000-9500	0.668	0.515	0.386
9500-10000	0.687	0.546	0.429

REFERENCES

Hora, S.C., D. von Winterfledt, and K.M. Trauth (1991), Expert Judgment of Inadvertent Human Intrusion into the Waste Isolation Pilot Plant, Sandia National Laboratories, SAND90-3063.

Environmental Protection Agency (1985). Environmental Standards for the Management and Disposal of Spent nuclear Fuel, High-level and Transuranic Radioactive Wastes: final Rule. 40 CFR Par 191. Federal Register 50: pp. 38066-89.

APPENDIX
COMPUTER PROGRAM TO GENERATE TIME DEPENDENT DRILLING INTENSITIES

```
C
      PROGRAM HUMINT
C
C  THIS PROGRAM EVALUATES THE DRILLING INTENSITY (RATE) USING THE
C  DISTRIBUTIONS PROVIDED BY THE MARKERS AND FUTURES PANELS
C
C  THE FOLLOWING VARIABLES ARE DEFINED
C    NREPS - NUMBER OF VECTORS OF INTRUSION INTENSITIES
C    IPER  - NUMBER OF PERIODS AT WHICH THE INTENSITY IS EVALUATED
C    LAMBDA  - MINERAL DRILLING RATE FROM THE BOSTON TEAM
C    U(NREP,6) - AN ARRARY OF LHS [0,1] RANDOM DEVIATES
C    BOSTAB1 - TABLE OF DISTRIBUTIONS FROM THE BOSTON TEAM
C    ITECH(IPER) - THE LEVEL OF TECHNOLOGY 1=HIGH, 2=MEDIUM, 3=LOW
C    BTIME(5) - CHANGE TIMES FOR THE BOSTON TEAM
C    OUTPUT(6,IPER) -  AN ARRAY WITH THE FOLLOWING ROWS
C      1 - THE TIME PERIOD
C      2 - THE DRILLING INTENSITY IN HOLES/SQ MI/10,000 YRS
C      3 - THE LEVEL OF TECHNOLOGY
C      4 - THE PROBABILITY OF MARKERS SURVIVING
C      5 - THE PROBABILITY OF SURVIVING MARKERS BEING INTERPRETED
C      6 - THE EFFECTIVE DRILLING INTENSITY AFTER MARKER DETERENCE
C    TIME(NTIME) - BEGINNING YEAR OF THE TIME PERIOD
C    B & C - ARRAYS CONTANING DATA FROM THE MARKERS TEAMS
C    AMARKT, BMARKT, PROBMARK & PROBDTER - ARRAYS USED TO DETERMINE
C      MARKERS PROBABILITIES
C    SUM(3,IPER) - SUMS THE RESULTS OUTPUT VARIABLES 2, 1-4*5, AND 6
C      TO BE USED TO COMPUTE AVERAGES
C
      PARAMETER (NREP=100)
      PARAMETER (IPER=23)
      PARAMETER (NTIME=24)
      REAL LAMBDA
      COMMON /ISEEDS/IX,IY,IZ
      DIMENSION LAMBDA(10),NB(3)
      DIMENSION U(6,NREP),BOSTAB1(10,4)
      DIMENSION ITECH(0:NTIME),BTIME(2),OUTPUT(6,0:IPER)
      DIMENSION TIME(0:NTIME),B(7,6,3),C(7,6,3)
      DIMENSION AMARKT(6),BMARKT(4),PROBMARK(0:IPER),PROBDTER(0:IPER)
      DIMENSION SUM(4,0:IPER)
      DATA AMARKT/0,200,500,1000,5000,10000/
      DATA BMARKT/0,500,2000,10000/
      DATA BTIME/300,3000/
      DATA IX,IY,IZ/19345,19321,19243/
      DATA NB/11,11,8/
C
C  NU IS THE NUMBER OF UNIFORM RANDOM VARIABLES TO BE SAMPLED
C
      NU=6
C
C  COMPUTE THE TIMES AT WHICH THE VARIABLES ARE EVALUATED
C  100 TO 500 YEARS BY 100 AND 500 TO 10000 BY 500
C
      DO ITIME=0,5
       TIME(ITIME)=ITIME*100
      ENDDO
      DO ITIME=6,NTIME
       TIME(ITIME)=(ITIME-4)*500
      ENDDO
C
C  SAMPLE CREATES THE LHS SAMPLE OF NU VARIABLES WITH A VECTOR LENGTH
C  OF NREP
```

```
C
      CALL SAMPLE(NREP,NU,U)
C
C READ TABLES FROM THE BOSTON TEAM AND THE MARKERS TEAMS
C
      OPEN (UNIT=10,FILE='BOSTAB1.DAT',STATUS='OLD',MODE='READ')
      READ (10,*) ((BOSTAB1(I,J),J=1,4),I=1,10)
      CLOSE (UNIT=10)
      OPEN(UNIT=12,STATUS='OLD',FILE='MARKERS1.TAB',MODE='READ')
      READ(12,*)(((B(I,J,K),J=2,6),I=1,6),K=1,3)
      I=7
      READ(12,*) ((B(I,J,K),J=2,4),K=1,3)
      CLOSE (UNIT=12)
      OPEN (UNIT=13,FILE='MARKERS2.TAB',STATUS='OLD',MODE='READ')
      READ(13,*)(((C(I,J,K),J=2,6),I=1,6),K=1,3)
      I=7
      READ(13,*) ((C(I,J,K),J=2,4),K=1,3)
      CLOSE(13)
      OPEN (UNIT=20,FILE='HUMINT1.OUT',STATUS='UNKNOWN',MODE='WRITE')
      WRITE (20,100) (TIME(ITIME),ITIME=0,IPER)
      OPEN (UNIT=22,FILE='HUMINT3.OUT',STATUS='UNKNOWN',MODE='WRITE')
C
C SET THE PROBABILITY OF MARKERS TO 1.0 AT TIME 0
C
      DO I=1,7
       DO K=1,3
         B(I,1,K)=1.0
         C(I,1,K)=1.0
       ENDDO
      ENDDO
C
C  BEGIN SAMPLING ITERATION
C
      DO IREP=1,NREP
C
C SELECT A FUTURES TEAM (1-4)
C
      U1=U(1,IREP)
      ITEAMF=INT(4*U1)+1
C
C  BOSTON TEAM
C
    1 IF(ITEAMF.EQ.1) THEN
C
C LOOK UP LEVEL OF TECHNOLOGY 1=HIGH, 2=MEDIUM, 3=LOW
C FOR THREE TIME PERIODS
C
      U2=U(2,IREP)
      DO I=1,3
       ITECH(I)=1
      ENDDO
      IF (.7.LT.U2) ITECH(2)=2
      IF (.8.LT.U2) THEN
       ITECH(1)=2
       ITECH(3)=2
      ENDIF
      IF (.9.LT.U2) THEN
       ITECH(2)=3
       ITECH(3)=3
      ENDIF
      U3=U(3,IREP)
      IF (.95.LT.U2) ITECH(1)=3
C
C  LOOKUP THE MINERAL DRILLING RATE
```

```
C
      DO IRATE=1,10
       IF(U3.LE.BOSTAB1(IRATE,ITECH(1)+1)) THEN
         LAMBDA=BOSTAB1(IRATE,1)
         GOTO 10
       ENDIF
      ENDDO
   10 CONTINUE
C
      U4=U(4,IREP)
      DO ITIME=1,3
       DO IRATE=1,NB(ITECH(ITIME))
         IF (U4.LE.BOSTAB2(IRATE,1,ITECH(ITIME))) THEN
           DLAMBDA(ITIME)=BOSTAB2(IRATE,ITIME+1,ITECH(ITIME))
           GOTO 20
         ENDIF
       ENDDO
   20  CONTINUE
      ENDDO
C
C  CREATE OUTPUT DRILLING VECTOR, TIMES, AND TECHNOLOGIES
C
      DO ITIME=0,IPER
      IF (TIME(ITIME).EQ.0) THEN
       OUTPUT(2,ITIME)=0.0
       OUTPUT(3,ITIME)=2.0
      ELSEIF (TIME(ITIME).LT.BTIME(1)) THEN
       OUTPUT(2,ITIME)=LAMBDA(1)
       OUTPUT(3,ITIME)=ITECH(1)
      ELSEIF (TIME(ITIME).LT.BTIME(2)) THEN
       OUTPUT(2,ITIME)=0.0
       OUTPUT(3,ITIME)=ITECH(2)
      ELSE
       OUTPUT(2,ITIME)=0.0
       OUTPUT(3,ITIME)=ITECH(3)
      ENDIF
      ENDDO
      ENDIF
C
C  SOUTHWEST TEAM
C
      IF (ITEAMF.EQ.2) THEN
      U2=U(2,IREP)
      OUTPUT(2,0)=0.0
      OUTPUT(3,0)=2.0
C
C  STEADY INCREASE SCENARIO
C
      IF (U2.LE..475) THEN
       DO ITIME=0,IPER
         OUTPUT(2,ITIME)=0.0
         OUTPUT(3,ITIME)=1.0
       ENDDO
      ENDIF
C
C  STEADY DECLINE SCENARIO
C
       IF (.475.LT.U2.AND.U2.LE..5625) THEN
       DO ITIME=0,IPER
         OUTPUT(3,ITIME)=3.
         IF (TIME(ITIME).LE.400.) THEN
           OUTPUT(2,ITIME)=25.4
         ELSE
           OUTPUT(2,ITIME)=0.0
```

```
          ENDIF
        ENDDO
       ENDIF
C
C  SEE-SAW SCENARIO
C    IRAN13 ALLOWS THE SEE-SAW TO START AT A RANDOM TIME (500,1000,
C     OR 1500 YEARS
C
       IF(.5625.LT.U2) THEN
        IRAN13=INT(3*U(3,IREP))
        DO ITIME=1,6
          OUTPUT(2,ITIME)=1.89
          OUTPUT(3,ITIME)=2.0
        ENDDO
        DO ITIME=5+IRAN13,IPER
          OUTPUT(2,ITIME)=1.89
          OUTPUT(3,ITIME)=3-MOD(ITIME+IRAN13,3)
C
C NO DRILLING DURING PERIODS OF HIGH TECHNOLOGY (TECH=1.0)
C
          IF(OUTPUT(3,ITIME).EQ.1.) OUTPUT(2,ITIME)=0.0
        ENDDO
       ENDIF
       ENDIF
C
C  WASHINGTON A TEAM
C
       IF(ITEAMF.EQ.3) THEN
        U2=U(2,IREP)
C
C  SET LEVELS OF TECHNOLOGY AND DRILLING RATES FOR TWO PERIODS
C
        DO ITIME=0,IPER
C
C  CONTINUITY SCEANRIO
C
          IF(U2.LE..255) THEN
            IF (TIME(ITIME).LT.200) THEN
              OUTPUT(2,ITIME)=33.5
              OUTPUT(3,ITIME)=1
            ELSE
              OUTPUT(2,ITIME)=2
              OUTPUT(3,ITIME)=1
            ENDIF
          ENDIF
C
C  RADICAL INCREASE SCEANRIO
C
        IF (.255.LT.U2.AND.U2.LE..4825) THEN
          IF (TIME(ITIME).LT.200) THEN
              OUTPUT(2,ITIME)=419.
              OUTPUT(3,ITIME)=2
            ELSE
              OUTPUT(2,ITIME)=.72
              OUTPUT(3,ITIME)=2
          ENDIF
        ENDIF
C
C  DISCONTINUITY SCEANRIO
C
        IF(.4825.LT.U2.AND.U2.LE..65) THEN
          IF (TIME(ITIME).LT.200) THEN
              OUTPUT(2,ITIME)=226.
              OUTPUT(3,ITIME)=3
```

```
            ELSE
              OUTPUT(2,ITIME)=4.7
              OUTPUT(3,ITIME)=3
            ENDIF
          ENDIF
C
C  STEADY STATE SCEANRIO
C
          IF(.65.LT.U2) THEN
            IF (TIME(ITIME).LT.200) THEN
                OUTPUT(2,ITIME)=4.3
                OUTPUT(3,ITIME)=2
              ELSE
                OUTPUT(2,ITIME)=.82
                OUTPUT(3,ITIME)=2
            ENDIF
          ENDIF
          ENDDO
        ENDIF
C
C  WASHINGTON B TEAM
C
        IF(ITEAMF.EQ.4) THEN
         U2=U(2,IREP)
C
C  SET LEVELS OF TECHNOLOGY INDPENDENT OF DRILLING
C
          IF (U2.LE..5) THEN
            DO ITIME=0,IPER
              OUTPUT(3,ITIME)=1
            ENDDO
          ENDIF
          IF(.5.LT.U2.AND.U2.LE..9) THEN
            DO ITIME=0,IPER
              IF(TIME(ITIME).LT.200) THEN
                OUTPUT(3,ITIME)=2
              ELSE
                OUTPUT(3,ITIME)=1
              ENDIF
            ENDDO
          ENDIF
          IF(.9.LT.U2.AND.U2.LE..95) THEN
            DO ITIME=0,IPER
              OUTPUT(3,ITIME)=2
            ENDDO
          ENDIF
          IF (.95.LT.U2) THEN
            DO ITIME=0,IPER
              IF (TIME(ITIME).LT.200) THEN
                OUTPUT(3,ITIME)=2
              ELSE
               OUTPUT(3,ITIME)=3
              ENDIF
            ENDDO
          ENDIF
C
C  COMPUTE DRILLING RATE FROM THE TRIANGULAR DENSITY
C
        U3=U(3,IREP)
        U4=U(4,IREP)
        U5=U(5,IREP)
        IF (U4.LE..5) THEN
         DR=SQRT(8*U4)
        ELSE
```

```
        DR=4-SQRT(8*(1-U4))
       ENDIF
       DO ITIME=0,IPER
        IF(TIME(ITIME).LT.200) THEN
          IF(U3.LE..932) OUTPUT(2,ITIME)=0.0
          IF(U3.GT..932) OUTPUT(2,ITIME)=DR*10000./200.
        ELSE IF(TIME(ITIME).LT.500.AND.OUTPUT(2,ITIME).EQ.0.0) THEN
          IF(U5.GT.9377) OUTPUT(2,TIME)=DR*10000./300.
        ENDIF
       ENDDO
       ENDIF
C
C  CALCULATE MARKERS PROBABILITIES
C
       U6=U(6,IREP)
C
C  SELECT A MARKERS EXPERT (1-6) OR TEAM B (IMARK=7)
C
       IF(U6.LT..5) THEN
        IMARK=INT(12*U6)+1
       ELSE
        IMARK=7
       ENDIF
       DO ITIME=0,IPER
        T=(TIME(ITIME)+TIME(ITIME+1))/2
C
C CHECK THE LEVEL OF TECHNOLOGY
C
        JTECH=OUTPUT(3,ITIME)
C
C  INTERPOLATE TO FIND THE PROBABILITIES OF MARKERS EXISTING (PROBMARK)
C    AND THE PROBABILITIES OF DETERENCE (PROBDTER) AT EACH TIME
C
        IF(IMARK.LT.7) THEN
          NP=6
          JP=JNDEX(AMARKT,NP,T)
          PROBMARK(ITIME)=B(IMARK,JP-1,JTECH)
     &      +(B(IMARK,JP,JTECH)-B(IMARK,JP-1,JTECH))
     &      *(T-AMARKT(JP-1))/(AMARKT(JP)-AMARKT(JP-1))
          PROBDTER(ITIME)=C(IMARK,JP-1,JTECH)
     &      +(C(IMARK,JP,JTECH)-C(IMARK,JP-1,JTECH))
     &      *(T-AMARKT(JP-1))/(AMARKT(JP)-AMARKT(JP-1))
        ELSE
          NP=4
          JP=JNDEX(BMARKT,NP,T)
          PROBMARK(ITIME)=B(IMARK,JP-1,JTECH)
     &      +(B(IMARK,JP,JTECH)-B(IMARK,JP-1,JTECH))
     &      *(T-BMARKT(JP-1))/(BMARKT(JP)-BMARKT(JP-1))
          PROBDTER(ITIME)=C(IMARK,JP-1,JTECH)
     &      +(C(IMARK,JP,JTECH)-C(IMARK,JP-1,JTECH))
     &      *(T-BMARKT(JP-1))/(BMARKT(JP)-BMARKT(JP-1))
        ENDIF
C
C  RECORD THE MARKERS PROBS AND THE EFFECTIVE DRILLING INTENSITY
C
        OUTPUT(4,ITIME)=PROBMARK(ITIME)
        OUTPUT(5,ITIME)=PROBDTER(ITIME)
        OUTPUT(6,ITIME)=OUTPUT(2,ITIME)
     &    *(1-OUTPUT(4,ITIME)*OUTPUT(5,ITIME))
C
C  SUM THE RESULTS FOR COMPUTING MEANS
C
       SUM(1,ITIME)=SUM(1,ITIME)+OUTPUT(2,ITIME)
       SUM(2,ITIME)=SUM(2,ITIME)+(1-OUTPUT(4,ITIME)*OUTPUT(5,ITIME))
```

```
      SUM(3,ITIME)=SUM(3,ITIME)+OUTPUT(6,ITIME)
      ENDDO
C
C  THIS STATEMENT WILL WRITE OUT VECTORS FOR THE PA
C  THE FIRST VECTOR IS THE BEGINNING OF THE TIME PERIOD
C  THE RATE IS EFFECTIVE UNTIL THE START OF THE NEXT PERIOD
C
      WRITE(20,100) (OUTPUT(6,ITIME),ITIME=0,IPER)
  100 FORMAT(25(1X,F7.2))
      DRILLINT=0.
      DO ITIME=0,23
        DRILLINT=DRILLINT+(TIME(ITIME+1)-TIME(ITIME))
     & *OUTPUT(6,ITIME)/10000.
      ENDDO
       WRITE(22,300) DRILLINT
      ENDDO
  300 FORMAT(1X,F10.3)
C
C  CALCULATE MEANS
C
      DO ITIME=0,IPER
       DO J=1,3
         SUM(J,ITIME)=SUM(J,ITIME)/NREP
       ENDDO
      ENDDO
C
C  OUTPUT THE MEANS
C
      OPEN (UNIT=21,FILE='HUMINT2.OUT',STATUS='UNKNOWN',MODE='WRITE')
      DO ITIME=0,IPER
       WRITE(21,200) TIME(ITIME),(SUM(J,ITIME),J=1,3)
      ENDDO
  200 FORMAT(1X,F8.0,4(1X,G12.3))
      CLOSE(20)
      CLOSE(21)
      CLOSE(22)
      STOP
      END
C
C  FUNCTION INDEX FINDS THE INDEX OF THE LARGEST VALUE OF XI<=W
C
      INTEGER FUNCTION JNDEX(X,L,W)
      DIMENSION X(10)
      DO J=1,L
      IF(X(J).GE.W) THEN
       JNDEX=J
       RETURN
      ENDIF
      ENDDO
      JNDEX=L+1
      RETURN
      END
C
      FUNCTION RAN(DUMMY)
C  THIS PROGRAM GENERATES A RANDOM NUMBER.  THIS NUMBER IS USED IN CALCULATING
C  THE INTEGRAL OF A GIVEN FUNCTION THROUGH THE LATIN-HYPERCUBED PROCEDURE.
C  THE PARAMETERS ARE THE SEEDS TO THIS RANDOM FUNCTION.
      COMMON /ISEEDS/IX,IY,IZ
      IX=MOD(171*IX,30269)
      IY=MOD(172*IY,30307)
      IZ=MOD(170*IZ,30323)
      RAN=MOD(FLOAT(IX)/30269.0+FLOAT(IY)/30307.0
     & +FLOAT(IZ)/30323.0,1.0)
      RETURN
```

```
      END
C
C  TWO SUBROUTINES TO GENERATE A UNIFORM LATIN HYPERCUBE SAMPLE
C  IN A RANDOM ORDER
C
      SUBROUTINE SAMPLE(N,M,R)
      COMMON /ISEEDS/IX,IY,IZ
      DIMENSION YT(1000),RANDOM(1000),IPNT(1000),R(6,*)
      RINC=1./FLOAT(N)
      DO IM=1,M
      DO J=1,N
        YT(J)=(J-1)*RINC+RAN(DUMMY)*RINC
        RANDOM(J)=RAN(DUMMY)
      ENDDO
      CALL SORT2(N,RANDOM,IPNT)
      DO J=1,N
       R(IM,J)=YT(IPNT(J))
      ENDDO
      ENDDO
      RETURN
      END

      SUBROUTINE SORT2(N, XV, IPNT)
C*****FILL POINTER ARRAY IPNT
      DIMENSION XV(N), IPNT(N)
      DO I=1,N
        IPNT(I)=0
      ENDDO
      DO I=1,N
       DO J=I,N
         IF(XV(I).GE.XV(J)) THEN
             IPNT(I)=IPNT(I)+1
         ELSE
             IPNT(J)=IPNT(J)+1
         ENDIF
       ENDDO
      ENDDO
      RETURN
      END

      CC CCCCCCCCC
```

Mendenhall and Lincoln, February 28, 1992

Date: 2/28/92
To: D. R. Anderson 6342
From: F. T. Mendenhall, 6345, R. C. Lincoln, 6345
Subject: Single Room Porosity History for Baseline Waste Form and Gas Generation Rates

Sandia National Laboratories

Albuquerque, New Mexico 87185

date: February 28, 1992

to: D. R. Anderson, 6342

Fred Mendenhall R.C. Lincoln

from: F.T. Mendenhall, 6345, R.C. Lincoln, 6345

subject: Single Room Porosity History for Baseline Waste Form and Gas Generation Rates.

Attached is a topological map defining the porosity in a single WIPP disposal room, assumed to be in the middle of an infinite array of rooms, as a function of the number of moles of gas present and time. This result is expected to be representative of the majority of rooms in the repository, the exceptions being the end room of a panel where the closure rate may cause a slight time shift in the surface, i.e. a slowing of consolidation estimated to be about 25%. However, until full panel scale models are complete, we recommend that the attached porosity surface be used for any room in the repository.

This surface was constructed from a set of five SANCHO finite element runs made for the reference baseline waste form and gas generation rates as defined by Beraun and Davies 1991[1]. The finite element analysis were performed for the WIPP project by Division 1514. Detailed documentation will be prepared discussing this modeling effort and the results. However, to help the WIPP program proceed in a timely fashion, this surface is being released so that performance assessment may immediately begin to incorporate the results in their work.

After the 2000 years modeled in the finite element results attached, the porosity surface should be defined by the amount of void space required to maintain lithostatic pressure with the amount of gas contained in a room using the ideal gas law.

It should be noted that the surface is a fit to a calculational result set containing about 750 points obtained from the results of the finite element runs. After the surface was generated, a comparison of the surface to the original result set was made. The mean difference between the original result set and the topological surface, was 0.17 percent, (note porosity was plotted in percent), with a standard deviation of 1.48.

An ASCII data file of the surface grid is available for your staff should they desire it.

[1] R. Beraun and P. B. Davies, "Baseline Design Input Data Base to be Used During Calculations Effort to be Performed by Division 1514 in Determining the Mechanical Creep closure Behavior of Waste Disposal Rooms in Bedded Salt." Memorandum to Distribution, Sandia National Laboratories, Albuquerque, New Mexico, September 12, 1991.

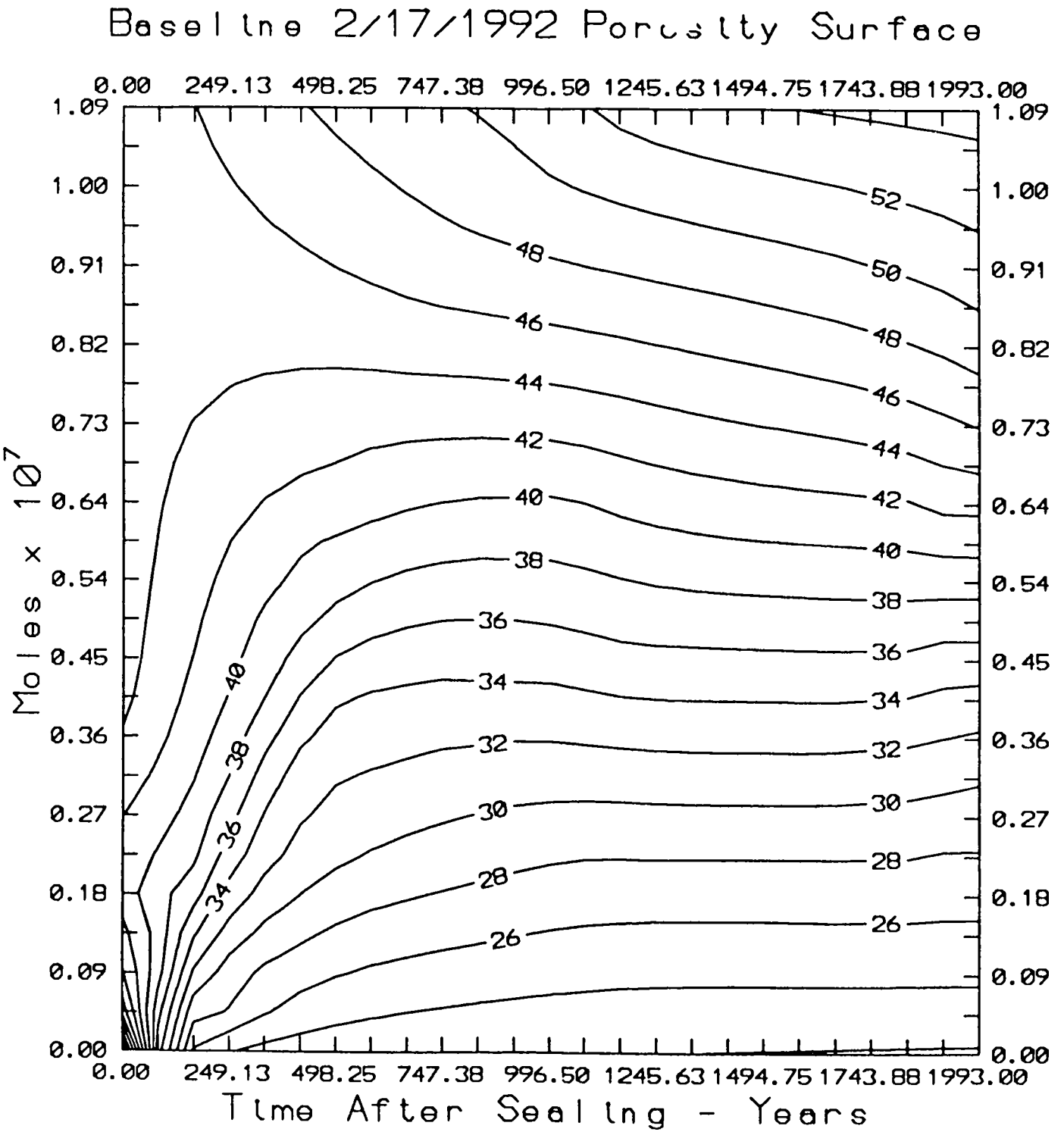
Baseline 2/17/1992 Porosity Surface
0.00
249.13
498.25
747.38
996.50
1245.63
1494.75
1743.88
1993.00
1.09
1.00
0.91
0.82
0.73
0.64
0.54
0.45
0.36
0.27
0.18
0.09
0.00
Moles x 10^7
Time After Sealing - Years
52
50
48
46
44
42
40
38
36
34
32
30
28
26

Copy to:
1561 H. S. Morgan
1561 J. G. Arguello
1561 C. M. Stone
1561 J. R. Weatherby
6340 W. D. Weart
6340 SWCF/XXXDRM (5 years)
6340 S. Y. Pickering
6341 A. L. Stevens
6342 B. M. Butcher
6342 R. D. Klett
6342 M. G. Marietta
6342 R. P. Rechard
6342 P. Vaughn
6342 M. S. Tierney
6343 T. M. Schultheis
6344 E. D. Gorham
6344 P. B. Davies
6345 ALL
6346 ALL
6347 D.R. Shafer

Munson, October 26, 1992

Date: 10/26/92
To: M. S. Tierney, 6342
From: D. E. Munson, 6346
Subject: Mechanical Parameters for Volume 3, SAND92-0700

Sandia National Laboratories

Albuquerque, New Mexico 87185

date: 10/26/92

to: M. S. Tierny, 6342

from: D. E. Munson, 6121

subject: Mechanical Parameters for Volume 3, SAND92-0700

I have attached what I believe is the correct set of mechanical parameters for use in Volume 3, SAND92-0700. These parameters are those used currently, or in the past, for thermal/structural calculations in the WIPP Program. You will note that there are actually two sets of parameters: The first set is consistent with the Modified M-D constitutive model which is the recommended model for use in any future WIPP calculations. At this stage of the program, the parameters for the Modified M-D constitutive model are well tested against in situ data. The second set is consistent with the Reduced Modulus (R-M) Steady State model based on the 1984 Reference Creep Law which is still in use, although no longer recommended as a primary model for future WIPP structural calculations. Within acceptable limits, either parameter set, with their respective constitutive models, are permissible for the purposes of performance assessment, provided the R-D model is adequately verified for a specific calculation against the more precise and better tested M-D model.

These parameters will be updated as necessary in subsequent publications of the Reference Data report.

If you have any questions please contact me.

Reviewed: Brian L. Ehgartner 10/29/92
B. L. Ehgartner, 6113

Approved: Joe R. Tillerson 10/30/92
J. R. Tillerson, 6121

Copy to:

B. L. Ehgartner, 6113
J. R. Tillerson, 6121
M. G. Marietta, 6342
R. P. Richard, 6342
WCTF--TSI/PROP

2.5 Mechanical Parameters for Material in Salado Formation

2.5.1 Halite and Argillaceous Halite

Elastic Constants (Halite and Argillaceous Halite)

Parameter	Median	Range	Units	Distribution	Source
Shear Modulus, μ	12.4	None	GPa		2.5.1
Young's Modulus, E	31.0	None	GPa		2.5.1
Poisson's Ratio, ν	0.25	None			2.5.1

Source(s): 2.5.1. Munson, D. E., A. F. Fossum, and P. E. Senseny. 1989. Advances in Resolution of Discrepancies between Predicted and Measured In Situ Room Closures. SAND88-2948. Albuquerque, NM: Sandia National Laboratories.

Creep Constants - Modified M-D Model (Halite)

Parameter	Median	Range	Units	Distribution	Source
A_1	8.386 E22	None	/s		2.5.1
Q_1	25	None	Kcal/mol		2.5.1
n_1	5.5	None			2.5.1
B_1	6.086 E06	None	/s		2.5.1
A_2	9.672 E12	None	/s		2.5.1
Q_2	10	None	Kcal/mole		2.5.1
n_2	5.0	None			2.5.1
B_2	3.034 E-2	None	/s		2.5.1
σ_0	20.57	None	MPa		2.5.1
q	5.335 E03	None			2.5.1
m	3.0	None			2.5.1
K_0	6.275 E05	None			2.5.1
c	9.198 E-3	None	/T		2.5.1
α_w	-17.37	None			2.5.1
β_w	-7.738	None			2.5.1
α_r	-2.69	None			2.5.2
β_r	-1.00	None			2.5.2
R	1.987	None	cal/mol-deg		2.5.3

Source(s):

2.5.1. Munson, D. E., A. F. Fossum, and P. E. Senseny. 1989. Advances in Resolution of Discrepancies between Predicted and Measured In Situ Room Closures. SAND88-2948. Albuquerque, NM: Sandia National Laboratories.
2.5.2. Munson, D. E., K. L. DeVries, and A. F. Fossum. 1992. Analysis of the recovery data to give these numbers is original to this memo. Albuquerque, NM: Sandia National Laboratories.
2.5.3. Munson, D. E., and P. R. Dawson. 1979. Constitutive Model for the Low Temperature Creep of Salt (with Application to WIPP). SAND79-1853. Albuquerque, NM: Sandia National Laboratories.
2.5.4. Munson, D. E. 1979. Preliminary Deformation-Mechanism Map for Salt (with Application to WIPP). SAND79-0076. Albuquerque,. NM: Sandia National Laboratories.
2.5.5. Munson, D. E., and P. R. Dawson. 1882. A Transient Creep Model for Salt during Stress Loading and Unloading. SAND82-0962. Albuquerque, NM: Sandia National Laboratories.
2.5.6. Munson, D. E., and K. L. DeVries. 1991. Development and Validation of a Predictive Technology for Creep Closure of Underground Rooms in Salt. Proc. 7th International Congress on Rock Mechanics, Aachen. Rotterdam, The Netherlands: A. A. Balkema. pp. 127-134. [SAND90-1147].
2.5.7. Callahan, G. D., A. F. Fossum, and D. K. Svalstad. 1986. Documentation of SPECTROM-32: a Finite Element Thermomechanical Stress Analysis Program. RSI-0269. Rapid City, SD: RE/SPEC Inc.

Creep Constants - Modified M-D Model (Argillaceous Halite)

Parameter	Median	Range	Units	Distribution	Source
A_1	1.407 E23	None	/s		2.5.1
Q_1	25	None	Kcal/mol		2.5.1
n_1	5.5	None			2.5.1
B_1	8.998 E06	None	/s		2.5.1
A_2	1.314 E13	None	/s		2.5.1
Q_2	10	None	Kcal/mol		2.5.1
n_2	5.0	None			2.5.1
B_2	4.289 E-2	None	/s		2.5.1
σ_0	20.57	None	MPa		2.5.1
q	5.335 E03	None			2.5.1
m	3.0	None			2.5.1
K_0	2.470 E06	None			2.5.1

c	9.198 E-3	None	/T	2.5.1
α_w	-14.96	None		2.5.1
β_w	-7.738	None		2.5.1
α_r	-2.69	None		2.5.2
β_r	-1.00	None		2.5.2
R	1.987	None	cal/mol-deg	2.5.3

Source(s):

2.5.1. Munson, D. E., A. F. Fossum, and P. E. Senseny. 1989. Advances in Resolution of Discrepancies between Predicted and Measured In Situ Room Closures. SAND88-2948. Albuquerque, NM: Sandia National Laboratories.

2.5.2. Munson, D. E., K. L. DeVries, and A. F. Fossum. 1992. Analysis of the recovery data to give these numbers is original to this memo. Albuquerque, NM: Sandia National Laboratories.

2.5.3. Munson, D. E., and P. R. Dawson. 1979. Constitutive Model for the Low Temperature Creep of Salt (with Application to WIPP). SAND79-1853. Albuquerque, NM: Sandia National Laboratories.

2.5.4. Munson, D. E. 1979. Preliminary Deformation-Mechanism Map for Salt (with Application to WIPP). SAND79-0076. Albuquerque,. NM: Sandia National Laboratories.

2.5.5. Munson, D. E., and P. R. Dawson. 1882. A Transient Creep Model for Salt during Stress Loading and Unloading. SAND82-0962. Albuquerque, NM: Sandia National Laboratories.

2.5.6. Munson, D. E., and K. L. DeVries. 1991. Development and Validation of a Predictive Technology for Creep Closure of Underground Rooms in Salt. Proc. 7th International Congress on Rock Mechanics, Aachen. Rotterdam, The Netherlands: A. A. Balkema. pp. 127-134. [SAND90-1147].

2.5.7. Callahan, G. D., A. F. Fossum, and D. K. Svalstad. 1986. Documentation of SPECTROM-32: a Finite Element Thermomechanical Stress Analysis Program. RSI-0269. Rapid City, SD: RE/SPEC Inc.

Discussion:

The constitutive model for salt creep now recommended for use is the most recent formulation of the multimechanism steady state, workhardening/recovery transient creep creep model [2.5.1], or simply the Modified M-D model. The steady state portion of the model is derived from the deformation mechanism map for salt as given by Munson [2.5.4]. Based on the mechanism map and the expected temperature and stress conditions that pertain to the potential

repository, just three of the mechanisms of salt deformation can be expected to contribute to the WIPP storage room response. These three mechanisms, not all of which are defined theoretically, but all of which are defined experimentally, form the basis of the constitutive model. The initial model, as derived by Munson and Dawson [2.5.3], included the three appropriate steady state mechanisms and a stress loading, workhardening transient response as an evolutionary process in strain. This M-D model was later improved to incorporate a stress unloading, recovery transient strain response also as an evolutionary process in strain [2.5.5].

During a major reevaluation study [2.5.1], it was found that the linear approximation used to describe the accumulation of transient strain was inadequate. As a result, the model was modified to incorporate a quadratic description of the transient strain. This resulted in the current Modified M-D creep model. Success of this model in prediction of the WIPP room closures [2.5.6] makes it the preferred constitutive model and should be taken as the definition of the reference creep property.

The total steady state creep rate of the modified model is given by:

$$\dot{\varepsilon}_s = \sum_{n=1}^{3} \dot{\varepsilon}_{s_i} \qquad 1$$

where summation is over the ith individual mechanisms. Individual steady state strain rates of the three relevant mechanisms are as follows:

$$\dot{\varepsilon}_{s_1} = A_1 e^{-\frac{Q_1}{RT}} \left(\frac{\sigma}{\mu}\right)^{n_1} \qquad 2a$$

$$\dot{\varepsilon}_{s_2} = A_2 e^{-\frac{Q_2}{RT}} \left(\frac{\sigma}{\mu}\right)^{n_2} \qquad 2b$$

$$\dot{\varepsilon}_{s_3} = |H| \left[B_1 e^{-\frac{Q_1}{RT}} + B_2 e^{-\frac{Q_2}{RT}} \right] \sinh\left[\frac{q(\sigma - \sigma_0)}{\mu}\right] \qquad 2c$$

where the A's and B's are structure factors, Q's are activation energies, n's are stress exponents, σ is the stress, σ_0 is a cut off stress level for the third mechanism, μ is the shear modulus, T is the absolute temperature, and R is the universal gas constant. $|H|$ is the Heaviside step function with argument of $(\sigma-\sigma_0)$. Mechanism 1 dominates at high temperatures and low stresses, mechanism 2 controls creep at low temperatures and stresses, and mechanism 3 dominates at high stresses at all temperatures.

The total creep creep rate results from the influence of the transient creep on the steady state creep rate, as determined by:

$$\dot{\varepsilon} = F\dot{\varepsilon}_s \qquad 3$$

where the transient function, F, is

$$F = \begin{Bmatrix} e^{+\Delta\left(1-\frac{\zeta}{\varepsilon_c^*}\right)^2} ; \zeta \le \varepsilon_c^* \\ 1 \\ e^{-\delta\left(1-\frac{\zeta}{\varepsilon_c^*}\right)^2} ; \zeta \ge \varepsilon_c^* \end{Bmatrix} \qquad 4$$

The transient function is composed of three branches, a workhardening branch, an equilibrium or steady state branch, and a recovery branch, respectively in order of appearance in the above equation. Here, Δ and δ are the workhardening and recovery parameters, respectively, and ε^*_t is the transient strain limit. The evolutionary equation governing the rate of change of the internal variable, ζ, is

$$\dot{\zeta} = (F-1)\dot{\varepsilon}_s \qquad 5$$

The transient strain limit is a function of temperature, and we adopt the form

$$\varepsilon_t^* = K_0 e^{cT}\left(\frac{\sigma}{\mu}\right)^m \qquad 6$$

where K_0, c, and m are constants.

The workhardening and recovery parameters are defined as a function of stress through

$$\Delta = \alpha_w + \beta_w \log\left(\frac{\sigma}{\mu}\right) \qquad 7a$$

$$\delta = \alpha_r + \beta_r \log\left(\frac{\sigma}{\mu}\right) \qquad 7b$$

where the α's and β's are constants, with the subscripts denoting either the workhardening or recovery branch.

The Modified M-D model has been incorporated into SPECTROM-32, a two dimensional finite element code [2.5.7] especially developed for solving solid mechanics problems typical of those required in the WIPP program. This code uses the Tresca flow potential for stress generalization to three dimensions [2.5.1].

Although it is strongly suggested that all final calculations be performed with the modified M-D model, the Tresca flow potential, and the above parameter set, historically, a simplified method has been used in many numerical calculations of WIPP problems. We will include the parameter set for this simplified model for completeness. This earlier method will be designated as the Reduced Modulus (R-M)

model. In this model, the elastic moduli (all except Poisson's Ratio are reduced by a factor of 12.5 [2.5.8]. This value was determined through backfitting of calculation to some of the field data.

Elastic Constants - R-M Model (Halite and Argillaceous Halite)

Parameter	Median	Range	Units	Distribution	Source
Shear Modulus, μ	0.992	None	GPa		2.5.8
Young's Modulus, E	2.480	None	GPa		2.5.8
Bulk Modulus, K	1.656	None	GPa		2.5.8
Poisson's Ratio, ν	0.25	None			2.5.9

Source(s):
2.5.8. Morgan, H. S., C. M. Stone, and R. D. Krieg. 1985. The Use of Field Data to Evaluate and Improve Drift Response Models for the Waste Isolation Pilot Plant (WIPP). Proc. 26th U.S. Symp. on Rock Mechanics, Boston, MA: A.A. Balkema.
2.5.9. Krieg, R. D. 1984. Reference Stratigraphy and Rock Properties for the Waste Isolation Pilot Plant (WIPP) Project. SAND83-1908. Albuquerque, NM: Sandia National Laboratories.

Creep Constants - R-M Model (Halite)

Parameter	Median	Range	Units	Distribution	Source
A	1.66 E14	None	/s		2.5.10
Q	12	None	Kcal/mol		2.5.9
n	4.9	None			2.5.9

Source(s):
2.5.9. Krieg, R. D. 1984. Reference Stratigraphy and Rock Properties for the Waste Isolation Pilot Plant (WIPP) Project. SAND83-1908. Albuquerque, NM: Sandia National Laboratories.
2.5.10. B. L. Ehgartner and D. E.Munson. 1992. This parameter is derived from values of D, u, and n found in Krieg [2,5,9]. Albuquerque, NM: Sandia National Laboratories.
2.5.11. Stone, C. M., R. D. Krieg, and Z. E. Beisinger. 1985. SANCHO - a Finite Element Computer Program for the Quasistatic, Large Deformation, Inelastic Response of Two-Dimensional Solids. SAND84-1618. Albuquerque, NM: Sandia National Laboratories.

Creep Constants - R-M Model (Argillaceous Halite)

Parameter	Median	Range	Units	Distribution	Source
A	4.99 E14	None	/s		2.5.10
Q	12	None	Kcal/mol		2.5.9
n	4.9	None			2.5.9

Source(s):

2.5.9. Krieg, R. D. 1984. Reference Stratigraphy and Rock Properties for the Waste Isolation Pilot Plant (WIPP) Project. SAND83-1908. Albuquerque, NM: Sandia National Laboratories.
2.5.10. B. L. Ehgartner and D. E.Munson. 1992. This parameter is derived from values of D, u, and n found in Krieg [2,5,9]. Albuquerque, NM: Sandia National Laboratories.
2.5.11. Stone, C. M., R. D. Krieg, and Z. E. Beisinger. 1985. SANCHO - a Finite Element Computer Program for the Quasistatic, Large Deformation, Inelastic Response of Two-Dimensional Solids. SAND84-1618. Albuquerque, NM: Sandia National Laboratories.

Discussion:

The R-M model is based entirely on steady state creep as described by a function of the form of Eq. 2b, which is equivalent to assuming a single thermally activated mechanism. However, evaluation of the constants of the equation utilized all of the experimental creep data for from both the unknown and climb mechanism regimes of the deformation mechanism map used in the development of the Modified M-D model. As a consequence, the constants do not match those of the steady state portion of the Modified M-D model for the unknown mechanism. Because of the use of a single function, the subscripts on the parameters have been dropped.

The general model from which the R-M model was derived [2.5.9] also provided for a first order kinetics transient response. This part of the model has not been used in WIPP calculations and will not be presented here.

Typically, the R-M model has been used most often in conjunction with the SANCHO finite element code [2.5.11], although it can be used equally with other finite element codes. In all calculations with the R-M model to date, a von Mises flow criterion has been used.

Thermal Properties (Halite and Argillaceous Halite)

Parameter	Median	Range	Units	Distribution	Source
Specific Heat	862.8	None	J/kg-K		2.5.12
Coef. Lin. Exp.	45.0 E-6	None	1/K		2.5.13
λ_{300}	5.40	None	W/mK		2.5.13
γ	1.14	None			2.5.13

Source(s): 2.5.12. Yang, J. M. 1981. Physical Properties Data for Rock Salt: Chapter 4 - Thermalphysical Properties, NBS Monograph 167. Washington, DC: National Bureau of Standards. (p. 205-221)
2.5.13. Sweet, J. N., and J. E. McCreight. 1980. Thermal Conductivity of Rocksalt and Other Geologic Materials from the Site of the Proposed Waste Isolation Pilot Plant. SAND79-1665. Albuquerque, NM: Sandia National Laboratories.
2.5.14. Moss, M., and G. M. Haseman. 1981. Thermal conductivity of Polyhalite and Anhydrite from the Site of the Proposed Waste Isolation Pilot Plant. SAND81-0856. Albuquerque, NM: Sandia National Laboratories.

Discussion:

The thermal conductivity is determined from the equation:

$$\lambda = \lambda_{300}\left(300/T\right)^{\gamma} \qquad 8$$

where the temperature, T, is in Kelvin.

2.5.2 Non-Salt Materials

Elastic Constants (Anhydrite)

Parameter	Median	Range	Units	Distribution	Source
Shear Modulus, μ	27.8	None	GPa		2.5.15
Young's Modulus, E	75.1	None	GPa		2.5.15
Bulk Modulus, K	83.4	None	GPa		2.5.15
Poisson's Ratio, ν	0.35	None			2.5.15

Source(s): 2.5.15. Munson, D. E., and H. S. Morgan. 1986. Methodology for Performing Parallel Design Calculations (Nuclear Waste Repository Application). SAND85-0324. Albuquerque, NM: Sandia National Laboratories.

Elastic Constants (Polyhalite)

Parameter	Median	Range	Units	Distribution	Source
Shear Modulus, μ	20.3	None	GPa		2.5.15
Young's Modulus, E	55.3	None	GPa		2.5.15
Bulk Modulus, K	65.8	None	GPa		2.5.15
Poisson's Ratio, ν	0.36	None			2.5.15

Source(s): 2.5.15. Munson, D. E., and H. S. Morgan. 1986. Methodology for Performing Parallel Design Calculations (Nuclear Waste Repository Application). SAND85-0324. Albuquerque, NM: Sandia National Laboratories.

Plasticity Parameters - Drucker-Prager Model Yield (Anhydite)

Parameter	Median	Range	Units	Distribution	Source
a	0.45	None			2.5.15
C	1.35	None	MPa		2.5.15

Source(s): 2.5.15. Munson, D. E., and H. S. Morgan. 1986. Methodology for Performing Parallel Design Calculations (Nuclear Waste Repository Application). SAND85-0324. Albuquerque, NM: Sandia National Laboratories.

Plasticity Parameters - Drucker-Prager Model Yield (Polyhalite)

Parameter	Median	Range	Units	Distribution	Source
a	0.473	None			2.5.15
C	1.42	None	MPa		2.5.15

Source(s): 2.5.15. Munson, D. E., and H. S. Morgan. 1986. Methodology for Performing Parallel Design Calculations (Nuclear Waste Repository Application). SAND85-0324. Albuquerque, NM: Sandia National Laboratories.

Discussion:

The Drucker-Prager model is an elastic, perfectly plastic model which has a pressure dependent yield. Typically it is given as:

$$\sqrt{J_2'} = C - aJ_1 \qquad 9$$

where $\sqrt{J_2'}$ is the second invariant and J_1 is the first invariant.

Although the Drucker-Prager model has been used almost exclusively to represent the anhydrite and polyhalite, the exact nature of the flow of these materials is under further study. In most of the analyses, the mechanical response of the polyhalite can be assumed to be elastic because the polyhalite beds are all at large distances from the WIPP horizon. The anhydrite beds however may be very close to the excavations, as in the case of MB139, and it is necessary to determine if the bed material will yield under the conditions of the analysis before it may be assumed to be elastic.

Thermal Properties (Anhydrite)

Parameter	Median	Range	Units	Distribution	Source
Specific Heat	733.3	None	J/kg-K		2.5.12
Coef. Lin. Exp.	20.0 E-6	None	1/K		2.5.13
λ_{300}	4.70	None	W/mK		2.5.13
γ	1.15	None			2.5.13

Source(s):

2.5.12. Yang, J. M. 1981. Physical Properties Data for Rock Salt: Chapter 4 - Thermalphysical Properties, NBS Monograph 167. Washington, DC: National Bureau of Standards. (p. 205-221)

2.5.13. Sweet, J. N., and J. E. McCreight. 1980. Thermal Conductivity of Rocksalt and Other Geologic Materials from the Site of the Proposed Waste Isolation Pilot Plant. SAND79-1665. Albuquerque, NM: Sandia National Laboratories.

2.5.14. Moss, M., and G. M. Haseman. 1981. Thermal conductivity of Polyhalite and Anhydrite from the Site of the Proposed Waste Isolation Pilot Plant. SAND81-0856. Albuquerque, NM: Sandia National Laboratories.

Discussion:

The thermal conductivity is determined from Eq. 8 as given previously.

Thermal Properties (Polyhalite)

Parameter	Median	Range	Units	Distribution	Source
Specific Heat	890.0	None	J/kg-K		2.5.9
Coef. Lin. Exp.	24.0 E-6	None	1/K		2.5.14
λ_{300}	1.40	None	W/mK		2.5.14
γ	0.35	None			2.5.14

Source(s):

2.5.9. Krieg, R. D. 1984. Reference Stratigraphy and Rock Properties for the Waste Isolation Pilot Plant (WIPP) Project. SAND83-1908. Albuquerque, NM: Sandia National Laboratories.
2.5.12. Yang, J. M. 1981. Physical Properties Data for Rock Salt: Chapter 4 - Thermalphysical Properties, NBS Monograph 167. Washington, DC: National Bureau of Standards. (p. 205-221)
2.5.13. Sweet, J. N., and J. E. McCreight. 1980. Thermal Conductivity of Rocksalt and Other Geologic Materials from the Site of the Proposed Waste Isolation Pilot Plant. SAND79-1665. Albuquerque, NM: Sandia National Laboratories.
2.5.14. Moss, M., and G. M. Haseman. 1981. Thermal conductivity of Polyhalite and Anhydrite from the Site of the Proposed Waste Isolation Pilot Plant. SAND81-0856. Albuquerque, NM: Sandia National Laboratories.

Discussion:

The thermal conductivity is determined from Eq. 8 as given previously.

2.5.3 Interbed Mechanical Response Parameter

Parameter	Median	Range	Units	Distribution	Source
Coef.Friction, ϕ	0.2	None			2.5.1

Source(s)

2.5.1. Munson, D. E., A. F. Fossum, and P. E. Senseny. 1989. Advances in Resolution of Discrepancies between Predicted and Measured In Situ Room Closures. SAND88-2948. Albuquerque, NM: Sandia National Laboratories.

Discussion:

The very thin interbeds that occur in the stratigraphy (as given later in Figure 2.5-1) between the major layers of salt, argillaceous salt, anhydrite, and polyhalite. These interbeds consist of either anhydrite or clay, or mixtures of these components. In structural calculations, it is not possible to model these thin interbeds as discrete layers. As a consequence they are handled as slip planes in the numerical codes. These slip planes have a coefficient of friction assigned to them which appears to be correct based on underground observations of the interbed response.

In many of the earlier calculations, especially those with the R-M model, the coefficient of friction was taken as 0.4, which is equivalent to assuming the interbeds are rigidly locked.

2.5.4 Non-Material Input Parameters

Initial Overburden Weight (Averaged)

Parameter	Median	Range	Units	Distribution	Source
Weight, G	22710	None	Pa/m		2.5.9
Source(s):	2.5.9. Krieg, R. D. 1984. Reference Stratigraphy and Rock Properties for the Waste Isolation Pilot Plant (WIPP) Project. SAND83-1908. Albuquerque, NM: Sandia National Laboratories.				

Discussion:

The lithostatic overburden pressure, P, at any depth, H, is given by:

$$P = GH \qquad 10$$

This function uses parameters based on the integrated densities of the overburden as determined from neutron logs. For the nominal facility depth of 650.45 m below ground surface, the lithostatic pressure is 14.77 MPa.

Initial Rock Temperature at Facility Horizon

Parameter	Median	Range	Units	Distribution	Source
Temperature, T_0	26.8	+/-0.5	C		2.5.16

Source(s): 2.5.16. Munson, D. E., R. L. Jones, D. L. Hoag, and J. R. Ball. 1987. Heated Axisymmetric Pillar Test (Room H): In Situ Data Report (February 1985 - April 1987). SAND87-2488. Albuquerque, NM: Sandia National Laboratories.

Local Stratigraphy for Thermal/Structural Numerical Calculations

Discussion:

The recommended stratigraphy is that given by Munson et al. [2.5.1]. This is shown in Figure 2.5-1 and has a local vertical zero referenced to anhydrite "b" (Clay G). The location of an experimental room excavation, which is a room above the WIPP facility horizon. This figure also shows the location of the room with respect to anhydrite "b" (Clay G), which is the reference zero of the stratigraphy.

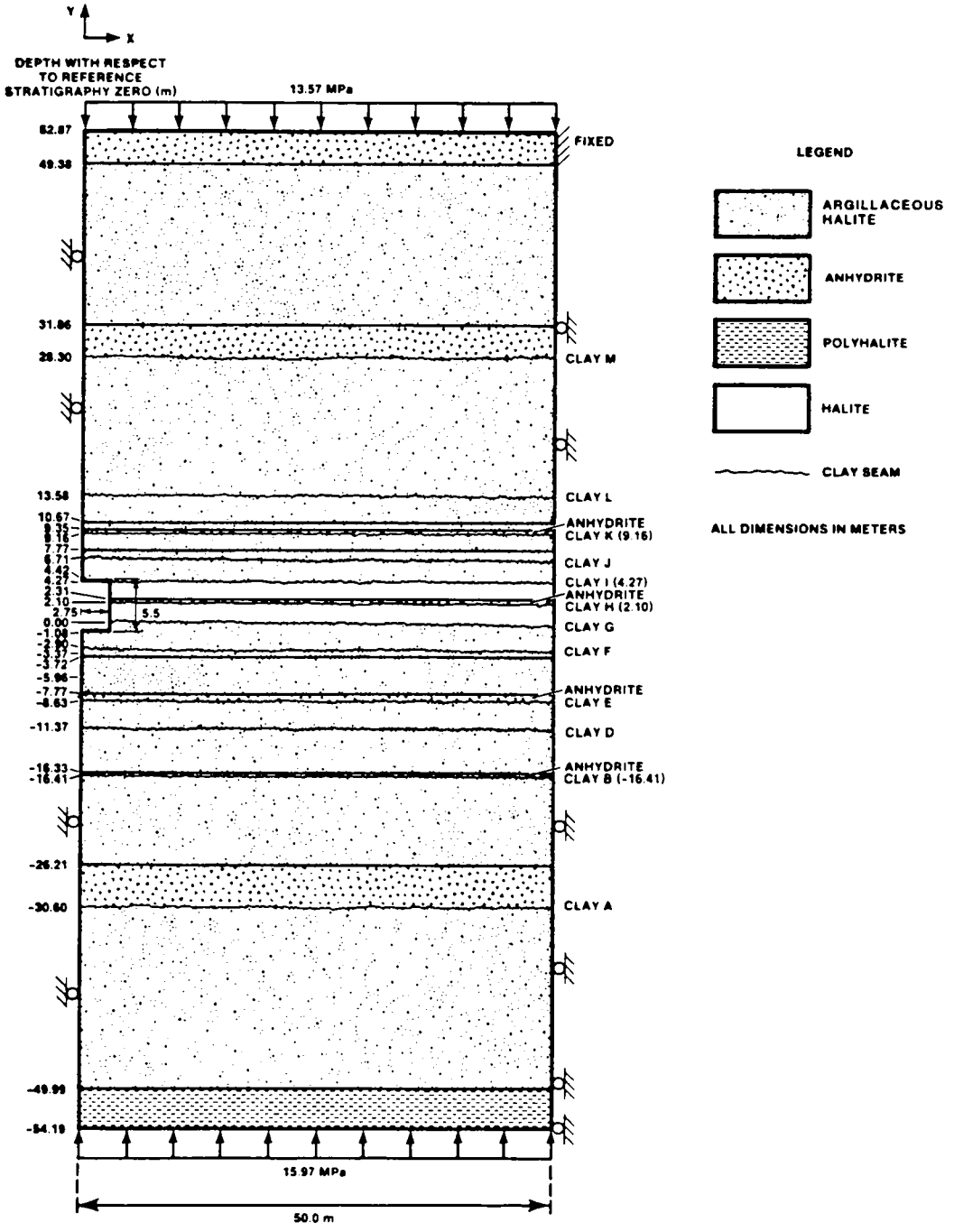

Figure 2.5-1. Local Stratigraphy for Numerical Calculations.

Novak et al., July 20, 1992

Date: 7/20/92
To: Martin S. Tierney, 6342
From: Craig F. Novak, Fred Gelbard, and Hans W. Papenguth, 6119
Subject: Parameter Recommendations for Porosity and Thickness of Clay Fracture Linings for the 1992 WIPP Performance Assessment Calculations

Sandia National Laboratories

Albuquerque, New Mexico 87185

date: 20 July 1992

to: Martin S. Tierney, 6342

from: Craig F. Novak, Fred Gelbard, and Hans W. Papenguth, 6119

bject: Parameter Recommendations for Porosity and Thickness of Clay Fracture Linings for the 1992 WIPP Performance Assessment Calculations

REQUEST FROM DEPARTMENT 6342 FOR VALUES OF CLAY POROSITY AND THICKNESS:

The 1992 WIPP Performance Assessment calculations are scheduled to use a new transport model with explicit clay linings in Culebra fractures. This model assumes there is flow through the void space in the fracture, with diffusion into the pore space of the clays lining the fractures. A schematic representation of the system is shown in Figure 1, assuming planar fractures symmetrical about the fracture centerline, with fracture half-width b and clay lining width b_c. Department 6342 has requested values for parameters necessary to implement this model, including: (1) the ratio of clay lining width to fracture half-width, $\frac{b_c}{b}$, (2) the clay porosity available for diffusive transport, ϕ_c, and (3) clay density, for which the previously recommended value of 2500 $\frac{kg}{m^3}$ (Siegel,1990) should be sufficient.

RECOMMENDATIONS:

A summary of the recommended probability distributions for the ratio of clay lining width to fracture half-width, $\frac{b_c}{b}$, and the effective clay porosity available for diffusive transport, ϕ_c, is given in Table 1.

Table 1. Recommended probability density functions for porosity and relative thickness of clay linings in Culebra fractures.

Parameter	Units	Minimum Value	Maximum Value	Probability	
$\frac{b_c}{b}$ ratio of clay lining width to fracture half-width	dimen-sionless	0.0	0.5	probability = 0.5	$\frac{b_c}{b} = 0$
				$\rho\left(\frac{b_c}{b}\right) = 0.5$	$0 < \frac{b_c}{b} \leq 0.5$
				$\rho\left(\frac{b_c}{b}\right) = 0$	$0.5 < \frac{b_c}{b} \leq 1$
ϕ_c clay porosity available for diffusive transport	volume fraction	0.05	0.50	$\rho(\phi_c) = 0$	$0 \leq \phi_c < 0.05$
				$\rho(\phi_c) = 2.22$	$0.05 \leq \phi_c \leq 0.5$
				$\rho(\phi_c) = 0$	$0.5 < \phi_c \leq 1$

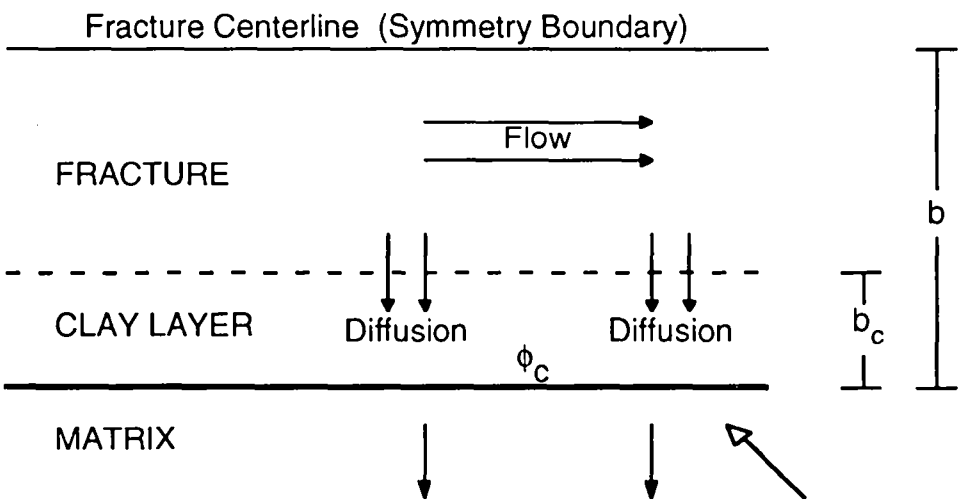

Clay/Matrix boundary allows solute diffusion in the double porosity case and disallows solute diffusion in the single porosity (fracture-only) case.

Figure 1. Schematic representation of clay-lined fracture, showing flow in the fracture with diffusion into the clay lining, with or without additional diffusion from the clay layer into the matrix.

Clay Lining Width

Previous estimates (Siegel, 1990) of the fraction of clay lining material, $\frac{b_c}{b}$, should be modified to reflect current thinking. The minimum value considered should be 0 to represent fractures with no clay lining; the maximum can be arbitrarily taken as 0.5. Also, the distribution used to represent the range should reflect a 50% probability of unlined fractures, $\frac{b_c}{b} = 0$, with an equal probability of choosing any other value in the range $0 < \frac{b_c}{b} \leq 0.5$. Defining the probability density function $\rho\left(\frac{b_c}{b}\right)$ such that

$$\int_A^B \rho\left(\frac{b_c}{b}\right) d\left(\frac{b_c}{b}\right)$$

is the fraction of fractures with $\frac{b_c}{b}$ in the range A to B, then

probability = 0.5	$\frac{b_c}{b} = 0$
$\rho\left(\frac{b_c}{b}\right) = 0.5$	$0 < \frac{b_c}{b} \leq 0.5$
$\rho\left(\frac{b_c}{b}\right) = 0$	$0.5 < \frac{b_c}{b} \leq 1$

Sewards (1991) measured and reported clay abundance for eighteen Culebra samples; thirteen from locations to the north and/or west of the WIPP site, and five from the north end of the WIPP site. None of these samples was from wells along fast transport paths. Because Sewards (1991) was focusing on clay abundance and compositional analysis, it is likely that samples were selected for analysis based on visual appearance of clays. Thus, these data may not be representative of clay abundance on fracture surfaces in the area of interest for transport modeling.

Reviews of core logs and discussions with WIPP scientists familiar with Culebra geology suggest that clays do not occur in all fractures. No statistically based studies of the occurrence of clay-lined fractures in the Culebra have been found. There are conceptual difficulties in translating the data of Sewards (1991) into the $\frac{b_c}{b}$ estimates requested by Department 6342. Therefore, the distribution and range of these values should be considered to be highly speculative.

Variation of Clay Lining Width Throughout the Culebra along Fast Transport Paths

Culebra geology and mineralogy is demonstrably variable in the vicinity of the WIPP site (Sewards et al., 1991). Probabilistic modeling of Culebra substrates such as clays should reflect this variability. The parameters provided by this memo represent possible clay occurrence and porosity on a local scale, and should be applied on the smallest scale possible, i.e., to each grid block in the discretization of the Culebra transport model. The data recommendations in this memo are not appropriately applied globally to the Culebra, as would be the case of assigning all fractures in the Culebra the same lining width and porosity for a particular realization.

Current data on clays occurring in Culebra fractures is not sufficient to construct a statistical model. However, if sensitivity studies indicate that clay occurrence and properties are sufficiently important in assessing overall repository performance, then development of a statistical model will likely be necessary.

Clay Porosity

Measurements of the second parameter of interest, the clay porosity available for transport, ϕ_c, have not been found. In the absence of direct experimental data for this parameter, values determined for other clays may serve as surrogates. Because of the short time available, a thorough literature search was not practical. Estimates for ϕ_c range from a few percent (by T. Sewards, a geologist/clay mineralogist previously associated with Culebra characterization work), to 40 to 50%. However, it is unclear whether these numbers represent total void volume fraction, or the volume fraction available for diffusive transport. The only pertinent document found in the available time* presents porosities determined from through-diffusion experiments in London clay (the composition of which was unspecified). The porosities determined with deuterated water averaged 0.47 and those determined with iodide were 0.18, indicating that there is less porosity available to large moieties such as iodide than there is available to water. It is likely that the

* Hassanizadeh, S.M. and G.C. Wijland. 1990. *Radionuclide Migration in Clay Samples by Diffusion and Advection.* INTRAVAL Project Draft Report. Bilthoven, The Netherlands: National Institute of Public Health and Environmental Protection.

lower porosity is more realistic for actinides, however, data to conclusively demonstrate this has not been found.

Applying the information described above to clays in the Culebra, it is reasonable to assume a porosity range $0.05 \leq \phi_c \leq 0.50$, with a distribution reflecting the maximum possible uncertainty (equal likelihood of any value) in the porosity. In mathematical terms, the probability density function $\rho(\phi_c)$ is given by

$$\rho(\phi_c) = 0 \qquad 0 \leq \phi_c < 0.05$$

$$\rho(\phi_c) = \frac{1}{0.50 - 0.05} \approx 2.22 \qquad 0.05 \leq \phi_c \leq 0.5$$

$$\rho(\phi_c) = 0 \qquad 0.5 < \phi_c \leq 1$$

Should sensitivity studies indicate that overall repository performance is highly dependent on the value assumed for clay porosities in the Culebra, it may be possible to implement laboratory studies to obtain these values. However, the clay porosity should be relatively constant throughout the Culebra; once experimentally determined values are available, sampling on the clay porosity may not necessary.

REFERENCES

Sewards, T. 1991. *Characterization of Fracture Surfaces in Dolomite Rock, Culebra Dolomite Member, Rustler Formation.* SAND89-7019. Albuquerque, NM: Sandia National Laboratories.

Sewards, T., M.L. Williams, and K. Keil. 1991. *Mineralogy of the Culebra Dolomite Member of the Rustler Formation.* SAND90-7008. Albuquerque, NM: Sandia National Laboratories.

Siegel, M.D. 1990. "Representation of Radionuclide Retardation in the Culebra Dolomite in Performance Assessment Calculations," Memo 3a in Appendix A of Rechard et al. 1990. *Data Used in Preliminary Performance Assessment of the Waste Isolation Pilot Plant (1990).* SAND89-2408. Albuquerque, NM: Sandia National Laboratories.

Copies to:

6303 W.D. Weart
6303 S.Y. Pickering/WIPP QA
6119 E.D. Gorham
6119 P.B. Davies
6119 C.F. Novak
6119 F. Gelbard
6119 File
6119 H.W. Papenguth
6342 D.R. Anderson
6342 M.G. Marietta
6342 R.P. Rechard

Peterson, October 28, 1992

Date: 10/28/92
To: Martin Tierney, 6342
From: A. Peterson, 6342
Subject: Preliminary Contact Handled (CH) Radionuclide and Nonradionuclide Inventories and Remote Handled (RH) Radionuclide Inventory for Use in 1992 Performance Assessment

Sandia National Laboratories

Albuquerque, New Mexico 87185

date: October 28, 1992

to: Martin Tierney, 6342



from: Andrew Peterson, 6342

subject: Preliminary Contact Handled (CH) Radionuclide and Nonradionuclide Inventories and Remote Handled (RH) Radionuclide Inventory for Use in 1992 Performance Assessment

The radioactive and nonradioactive components of the TRU waste that will be emplaced in the Waste Isolation Pilot Plant (WIPP) are not known with certainty. Most of the volume of TRU waste that could be emplaced in the WIPP has not been generated and the potential sources of TRU waste may be changing. Even though there is considerable uncertainty in the final inventory an estimate of the radioactive and nonradioactive waste inventories are required for performance assessment. The following discussion provides estimates of the radionuclide and nonradionuclide inventories for CH waste and radionuclide inventory for RH waste based on the information currently available.

CH-TRU waste consists of waste that has been generated and stored and waste that will be generated in the future. Draft report DOE/WIPP 91-058 uses input to the 1991 Integrated Data Base (IDB) (US DOE 1991) to estimate the radionuclide inventory for the stored and future generated waste. The total stored volume was about 53,700 m^3 and the future generated waste was about 42,000 m^3. The performance assessment is being analyzed assuming the design volume, 175,560 m^3 (6.2 x 10^6 ft^3) is emplaced in the WIPP. Peterson (In preparation) used the CH radionuclide inventories from Draft report DOE/WIPP 91-058 to estimate the CH radionuclide inventory for a design volume. The results of this estimate are tabulated for each radionuclide by generator site and totaled in Table 1.

Estimates of the number of drums and boxes for stored and projected waste in eight ranges of equivalent Pu-239 curie content were provided for the 1991 IDB by each generator. Peterson (In preparation) used this input to estimate the number of drums and boxes for a design volume in six curie ranges and they are listed in Table 2.

The weight and volume of the CH nonradionuclide inventory was estimated from input to the 1991 IDB for stored and future generated waste volumes and from additional information on waste weights provided by the generator sites. Peterson (In preparation) used this input to estimate

the volume and weight of sludges, metals and glass, and combustibles for the design volume of CH waste. Table 3 lists the estimated weight and volume of these constituents of CH waste.

Draft report DOE/WIPP 91-058 also used input to the 1991 IDB to estimate the RH radionuclide inventory for stored and future generated waste. The total volume of stored and future generated RH waste was nearly equal to the maximum volume of 7,089 m^3 (0.25 x 10^6 ft^3) that can currently be emplaced in the WIPP. The RH radionuclide inventory by site is tabulated in Table 4.

References:

Peterson A. C. (In preparation). Estimated CH-TRU Inventory for use in Performance Assessment for the Waste Isolation Pilot Plant.' SAND92-2023. Albuquerque NM: Sandia National Laboratories.

US DOE (Department of Energy). 1991. Integrated Data Base for 1991: U. S. Spent Fuel and Radioactive Waste Inventories, Projections, and Characteristics. DOE/RW-0006, Rev 7. September 1991.

Copy to:
SWCF (WBS 1.1.6.1.3) PA/INV

Table 1
Estimated Design Radionuclide Inventory by Waste Generator for Contact-Handled Waste (Curies)

RN91DES

Isotope	Half-life (Years)	ANL-E (Ci)	HANF (Ci)	INEL (Ci)	LANL (Ci)	LLNL (Ci)	MOUND (Ci)	NTS (Ci)	ORNL (Ci)	RFP (Ci)	SRS (Ci)	Total (Ci)	Unit Waste Factor
Sr-90	2.91E+01		8.183E+04	4.834E+02								8.231E+04	-
Y-90	7.30E-03		8.183E+04									8.183E+04	-
Ru-106	1.01E+00		9.882E+02	6.225E-01								9.888E+02	-
Rh-106	2.50E-04		9.882E+02									9.882E+02	-
Cs-137	3.00E+01		6.235E+04	6.263E+02								6.298E+04	-
Ba-137m	4.85E-06		5.579E+04									5.579E+04	-
Ce-144	7.78E-01		9.882E+03	4.610E+00								9.887E+03	-
Pr-144	3.29E-05		9.882E+03									9.882E+03	-
Pm-147	2.62E+00		7.397E+04	2.043E+03								7.601E+04	-
Th-232	1.41E+10		2.438E-02	2.600E-01					4.587E-03		5.272E-04	2.895E-01	2.895E-01
U-233	1.59E+05			7.106E+02					8.185E+02		3.072E-02	1.529E+03	-
U-235	7.04E+08	5.259E-04	2.780E-01	1.321E-01	5.315E-02				2.917E-02	6.776E-03	3.814E-02	5.378E-01	-
U-238	4.47E+09	1.534E-04	2.208E+00	1.071E-01	2.920E-01				4.490E-02		2.592E-02	2.678E+00	-
Np-237	2.14E+06			5.296E-01					8.969E+00		1.128E+01	2.078E+01	2.078E+01
Pu-238	8.77E+01		3.410E+04	5.266E+04	2.864E+05	2.973E+02	2.731E+03	3.082E+00	1.271E+04	2.665E+03	2.664E+06	3.055E+06	3.055E+06
Pu-239	2.41E+04	1.631E+02	9.882E+03	3.166E+04	1.489E+05	6.015E+03	2.025E+00	7.491E+01	4.380E+03	7.462E+04	5.940E+04	3.351E+05	3.351E+05
Pu-240	6.56E+03	3.560E+01	2.470E+03	7.897E+03	4.992E+04	1.757E+03	1.366E+00	1.728E+01	3.463E+03	1.799E+04	1.675E+04	1.003E+05	1.003E+05
Pu-241	1.44E+01	9.747E+02	6.670E+04	2.260E+05	2.097E+06	4.301E+04		7.107E+02	6.699E+04	4.917E+05	6.025E+05	3.596E+06	-
Pu-242	3.76E+05			8.305E-01	7.919E+00	1.862E-01		1.164E-03		5.237E-01	1.403E+01	2.349E+01	2.349E+01
Am-241	4.32E+02			6.904E+04	5.540E+05	1.933E+03			8.724E+02	7.929E+04	8.572E+03	7.137E+05	7.137E+05
Cm-244	1.81E+01			8.806E+02					1.290E+04		6.779E+03	2.056E+04	2.056E+04
Cf-252	2.64E+00			5.048E-02					2.515E+02		8.549E+01	3.370E+02	
Totals		1.173E+03	4.907E+05	3.920E+05	3.136E+06	5.301E+04	2.735E+03	8.060E+02	1.024E+05	6.663E+05	3.358E+06	8.203E+06	4.225E+06

Argonne National Laboratory-East (ANL-E)
Hanford Site (HANF)
Idaho National Engineering Laboratory (INEL)
Los Alamos National Laboratory (LANL)
Lawrence Livermore National Laboratory (LLNL)
Mound Plant (MOUND)
Nevada Test Site (NTS)
Oak Ridge National Laboratory (ORNL)
Rocky Flats Plant (RFP)
Savannah River Site (SRS)

Table 2
Estimate of Curie content of Drums and Standard Waste Boxes

92Acurie	0-0.5 (Ci)	0.5-1 (Ci)	1-10 (Ci)	10-20 (Ci)	20-100 (Ci)	100-1000 (Ci)
Stored Drums	30100	13642	49809	14939	11321	2600
Projected Drums	45525	11142	56936	12084	10731	885
Scaled Drums	84604	20921	107254	22786	20229	1674
Totals	160229	45705	213999	49809	42281	5159
Stored Boxes	1666	703	4453	1082	1321	305
Projected Boxes	1497	164	1838	1417	1792	600
Scaled Boxes	2572	310	3477	2524	3391	1135
Total	5735	1177	9768	5023	6504	2040
Percent	30.3	8.6	40.9	10.0	8.9	1.3

CompoRN

Table 3

Estimated composition of CH-TRU waste

	Weight (kg)	Volume Fraction	Volume (m3)	No Drums	No. SWBs	Steel Drums (kg)	SWB Steel (kg)	Poly/ PVC (kg)	Weight Reinf wood	Total Weight (kg)	Weight Fraction
Sludge	2.538E+07	0.207	36342	174720		5.084E+06		1.188E+06		3.165E+07	0.363
Metals and Glass*	1.980E+07	0.421	73912	182284	18946	5.304E+06	5.892E+06	2.034E+05		3.120E+07	0.358
Combustibles**	1.220E+07	0.372	65310	161068	16740	4.687E+06	5.206E+06	1.797E+05	1.980E+06	2.425E+07	0.278
Steel in drums	1.508E+07										
Steel in SWBs	1.110E+07										
Poly/PVC liners	1.571E+06										
Reinforced Wood	1.980E+06										
Total	8.711E+07		175564	518072	35686	1.508E+07	1.110E+07	1.571E+06	1.980E+06	8.711E+07	

*Estimate of total corrodible metals in waste = 10.7 Gg
(Iron Based Materials)

**Estimate of total biodegradable materials in waste = 5.92 Gg
(cellulosics + one half of rubbers + reinforced wood boxes)

Table 4
Estimated Design Radionuclide Inventory by Waste Generator of Remote-Handled Waste

91RHRNDES

Radio Nuclide	Halflife (Yrs)	ANL-E (Ci)	HANF (Ci)	INEL (Ci)	LANL (Ci)	ORNL (Ci)	1992 PA System Total (Ci)	PA Calculations Design 1992	Unit Waste Factors
Cr-51	7.580E-02			5.01E+00			5.01E+00		
Mn-54	8.560E-01			3.06E+05			3.06E+05		
Co-58	1.940E-01			8.03E+01			8.03E+01		
Fe-59	1.220E-01			4.89E+00			4.89E+00		
Co-60	5.270E+00		1.86E+03	3.08E+01		4.79E+03	6.69E+03		
Ni-63	1.000E+02		1.25E+01	2.85E+02			2.98E+02		
Sr-90	2.910E+01		3.02E+05	4.59E+04	5.96E+02	1.73E+05	5.22E+05	5.22E+05	
Y-90	7.306E-03		3.02E+05	1.47E+02	5.96E+02		3.03E+05		
Nb-95	9.630E-02		1.70E+03	5.14E-01			1.70E+03		
Tc-99	2.130E+05		2.42E+02	1.08E-01			2.42E+02		
Ru-106	1.010E+00		7.97E+04	1.22E+04			9.20E+04		
Rh-106	9.480E-07		7.97E+04	9.28E-01			7.97E+04		
Sb-125	2.770E+00		1.43E+04	4.35E+00			1.43E+04		
Cs-134	2.060E+00		9.29E+03	6.64E+02			9.95E+03		
Cs-137	3.000E+01	6.66E+02	3.72E+05	1.32E+04	4.47E+02	1.83E+05	5.69E+05	5.69E+05	
Ba-137m	4.855E-06		3.49E+05	1.19E+02	3.97E+02		3.49E+05		
Ce-144	7.780E-01		2.71E+05	2.80E+03			2.74E+05		
Pr-144	3.288E-05		2.71E+05	1.12E+01			2.71E+05		
Pm-147	2.623E+00		3.83E+05	1.52E+05	4.47E+02		5.36E+05	5.36E+05	
Eu-152	1.330E+01		1.20E+01			2.40E+04	2.40E+04		
Eu-154	8.800E+00		1.68E+03	1.11E+00		1.44E+04	1.61E+04		
Eu-155	4.960E+00		3.06E+03	5.55E-01			3.06E+03		
Th-232	1.410E+10		2.09E-02	5.00E-05		5.64E+00	5.66E+00	5.66E+00	5.66E+00
U-233	1.590E+05			1.72E-01		1.98E+02	1.99E+02	1.99E+02	
U-235	7.048E+08		2.18E-01	3.91E-01	3.18E-03	5.08E-04	6.13E-01	6.13E-01	
U-236	2.340E+07		2.15E-03	3.43E-03			5.59E-03	5.59E-03	
U-238	4.470E+09	1.50E-04	1.76E+00	4.21E-02	2.97E-04	1.03E-03	1.80E+00	1.80E+00	
Np-237	2.140E+07		7.28E-01	3.91E-03		1.88E-01	9.20E-01	9.20E-01	9.20E-01
Pu-238	8.770E+01		2.65E+04	5.35E+01	2.41E+00	8.14E+02	2.73E+04	2.73E+04	2.73E+04
Pu-239	2.410E+04	1.10E+01	8.07E+03	5.18E+01	2.65E+01	3.39E+02	8.50E+03	8.50E+03	8.50E+03
Pu-240	6.560E+03	7.87E+00	2.16E+03	1.04E+02	8.81E+00	4.50E-01	2.28E+03	2.28E+03	2.28E+03
Pu-241	1.440E+01	1.02E+02	6.36E+04	5.55E+04	3.72E+02	1.05E-02	1.20E+05	1.20E+05	
Pu-242	3.750E+05		1.72E-03	2.94E+00	1.66E-03		2.94E+00	2.94E+00	2.94E+00
Am-241	4.327E+02		9.81E+02	1.62E+01		6.48E+01	1.06E+03	1.06E+03	1.06E+03
Cm-244	1.810E+01		2.30E+00			4.26E+03	4.26E+03	4.26E+03	4.26E+03
Cf-252	2.638E+00					8.63E+01	8.63E+01	8.63E+01	
Totals		7.87E+02	2.54E+06	5.89E+05	2.89E+03	4.04E+05	3.54E+06	1.79E+06	4.35E+04

Argonne National Laboratory-East (ANL-E)
Hanford Site (HANF)
Idaho National Engineering Laboratory (INEL)
Los Alamos National Laboratory (LANL)
Oak Ridge National Laboratory (ORNL)

Webb, March 20, 1992 (1992a)

Date: 3/20/92
To: D. R. Anderson, 6342
From: S. W. Webb, 6344
Subject: Uncertainty Estimates for Two-Phase Characteristic Curves for 1992 RCRA Calculations

Sandia National Laboratories

Albuquerque, New Mexico 87185

date: March 20, 1992

to: D. R. Anderson, 6342

from: S. W. Webb, 6344

subject: Uncertainty Estimates for Two-Phase Characteristic Curves for 1992 RCRA Calculations

Two-phase characteristic curves (capillary pressure and relative permeability) have a large degree of uncertainty since no data on the WIPP materials have been obtained. The uncertainty in the threshold pressure has been discussed previously by Davies (Ref. 1); this variation was used by PA in the 1991 comparison with 40 CFR 191 is still considered valid for the RCRA calculations. Uncertainties in the two-phase characteristic curves were discussed by Webb (Ref. 2); these values were not used by PA in their most recent 40 CFR 191 calculations. The uncertainties given by Webb will be modified and updated in this memo.

Uncertainties in the two-phase characteristic curves fall into the following categories:

1. Conceptual Model
2. Correlation Model
3. Parameter

The conceptual model for the two-phase interface is based on standard two-phase characteristic curves. Since a lower viscosity fluid (gas) is displacing a higher viscosity fluid (brine), the displacement interface will be unstable, and viscous and capillary fingering may occur. Fingering is a very complex phenomena which has not been quantified yet for the WIPP, but the processes are not captured in standard two-phase characteristic curves. Investigation into fingering processes has recently been initiated in 6344. It is not known what the impact will be on the displacement interface, but indications are that it could be significant. In addition, these standard curves are based on a uniform porous media; fractures are expected in the Salado, especially in the anhydrite interbeds. The conceptual model uncertainty of using standard two-phase characteristic curves derived for uniform porous media is large.

Uncertainty also exists in the choice of the correlation model. At present, the modified Brooks and Corey correlation is suggested based on comparison to a single set of data for an analogue material (tight gas sands) as discussed by Davies and LaVenue (Ref. 3). As has been repeatedly emphasized, there are no measurements for any Salado lithologies, so the correlation uncertainty is large. This aspect has been addressed to a

limited extent by Webb (Ref. 4) which shows a significant influence of the two-phase characteristic curves on the gas migration distance for the undisturbed scenario.

Finally, parameter uncertainty is also large. As discussed in the preceding paragraph, there are no measurements and we rely on only one set of measurements on an analogue material. Since only one data set was used for parameter evaluation, no parameter range can be given.

With these large uncertainties in all areas, large ranges of parameters are necessary. Within the current set of RCRA calculations, PA has requested that the uncertainties fit into the modified Brooks and Corey model framework due to time constraints. While the current set of uncertainties will be molded into that framework, this restriction negates the correlation uncertainty discussed above. Thus, the real uncertainty is significantly larger than given in this memo. The parameter ranges summarized below apply to the all lithologies in the Salado. Note that the threshold pressure is different for the various units as given by Davies (Ref. 1).

Brooks and Corey

Threshold Pressure (P_t)
Expected Value and Range given by Davies (Ref. 1)
Residual Saturations (S_{lr} and S_{gr})
Expected Value = 0.2
Range between 0.0 and 0.4 with uniform distribution
Pore-Size Distribution Parameter (λ)
Expected Value = 0.7
Range between 0.2 and 10.

The residual saturation value of 0. for the critical gas saturation (S_{gr}) is the most important parameter and is specified to try to estimate possible effects of fingering. This analogy is weak at best but it is the best that can be done at present. The large range for the pore-size distribution parameter is based on values given by Mualem (Ref. 5) for real porous media. Since we do not know anything about the structure of the Salado materials, a wide range is appropriate.

The capillary and relative permeability curves are shown in Figure 1 for the λ range specified above. While the variation is significant, it is not as large as it would be if an alternative correlation model were considered.

Note that the above parameter ranges are only applicable to the RCRA calculations since the correlation has been restricted to the modified Brooks and Corey model. The uncertainty in the two-phase curves will be respecified for the 1992 comparison with 40 CFR 191 to include correlation model uncertainty.

References

1. Memo to D. R. Anderson from P. B. Davies, "Uncertainty Estimates for Threshold Pressure for 1991 Performance Assessment Calculations Involving Waste-Generated Gas," June 6, 1991.

2. Memo to D. R. Anderson from S. W. Webb, "Uncertainty Estimates for Two-Phase Characteristic Curves for 1991 PA Calculations," July 9, 1991.

3. Memo to R. P. Rechard from P. Davies and A. M. LaVenue, "Additional Data for Characterizing 2-Phase Flow Behavior in Waste-Generated Gas Simulations and Pilot Point Information for Final Culebra 2-D Model (SAND89-7068/1)," November 19, 1990.

4. Webb, S. W., "Sensitivity Studies for Gas Release from the Waste Isolation Pilot Plant," Chapter 4.0 in Waste-Generated Gas at the Waste Isolation Pilot Plant: Papers Presented at the Nuclear Energy Agency Workshop on Gas Generation and Release from Radioactive Waste Repositories, P. B. Davies et al., eds., SAND91-2378, November 1991.

5. Mualem, Y., "A New Model for Predicting the Hydraulic Conductivity of Unsaturated Porous Media," Water. Resour. Res, Vol. 12, No. 3, pp. 513-522, June 1976.

Copy to:
6340 W. D. Weart
6342 M. G. Marietta
6342 R. P. Rechard
6342 P. Vaughn
6344 E. D. Gorham
6344 P. B. Davies
6344 S. M. Howarth

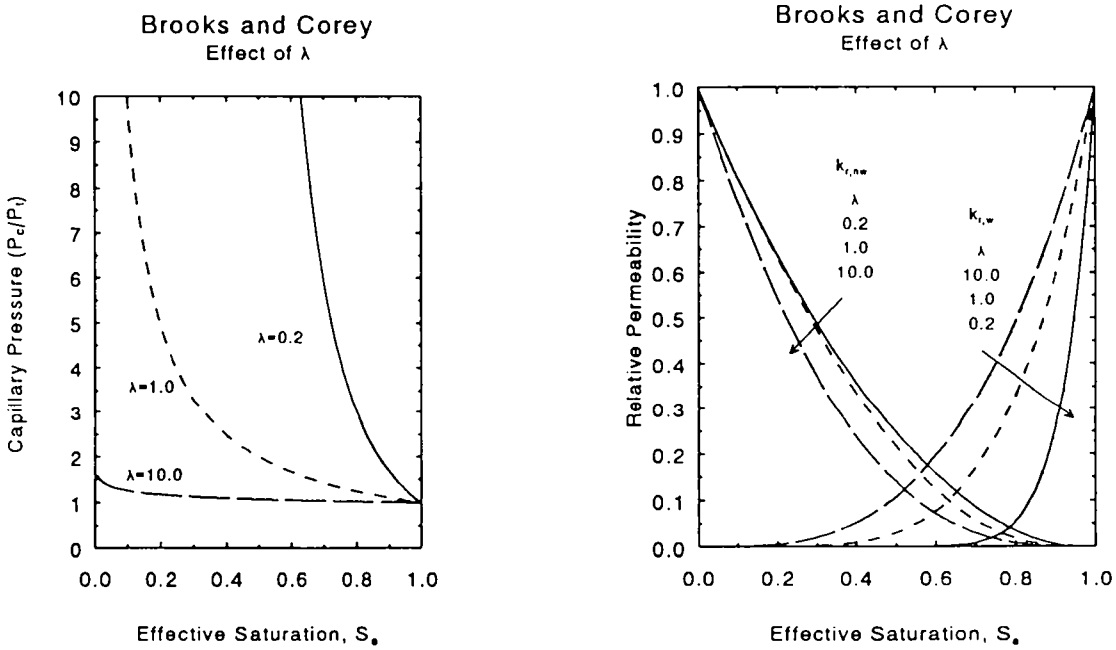

Figure 1
Range of Capillary Pressure and Relative Permeability Curves

Webb, April 30, 1992 (1992b)

Date: 4/30/92
To: D. R. Anderson, 6342
From: S. W. Webb, 6344
Subject: Uncertainty Estimates for Two-Phase Characteristic Curves for 1992 40 CFR 191 Calculations

Sandia National Laboratories

Albuquerque, New Mexico 87185

date: April 30, 1992

to: D. R. Anderson, 6342

Steve

from: S. W. Webb, 6119

subject: Uncertainty Estimates for Two-Phase Characteristic Curves for 1992 40 CFR 191 Calculations

Two-phase characteristic curves (capillary pressure and relative permeability) have a large degree of uncertainty since no data on the WIPP materials have been obtained. The uncertainty in the threshold pressure has been discussed previously by Davies (Ref. 1). Uncertainties in the two-phase characteristic curves for RCRA calculations were discussed by Webb (Ref. 2). Due to time constraints, the two-phase characteristic curves were limited to the modified Brooks and Corey format. The characteristic curves will be expanded in this memo to include correlation uncertainty.

Uncertainties in the two-phase characteristic curves fall into the following categories:

1. Conceptual Model
2. Correlation Model
3. Parameter

The conceptual model for the two-phase interface is based on standard two-phase characteristic curves. Since a lower viscosity fluid (gas) is displacing a higher viscosity fluid (brine), the displacement interface will be unstable, and viscous and capillary fingering may occur. Fingering is a very complex phenomena which has not been quantified yet for the WIPP, but the processes are not captured in standard two-phase characteristic curves. Investigation into fingering has recently been initiated in 6119. It is not known what the impact will be on the displacement interface, but indications are that it could be significant. In addition, these standard curves are based on a uniform porous media; fractures are expected in the Salado, especially in the anhydrite interbeds. The conceptual model uncertainty of using standard two-phase characteristic curves derived for uniform porous media is large.

Uncertainty also exists in the choice of the correlation model. At present, the modified Brooks and Corey correlation is suggested based on comparison to a single set of data for an analogue material (tight gas sands) as discussed by Davies and LaVenue (Ref. 3). As has been repeatedly emphasized, there are no measurements for any Salado lithologies, so the correlation uncertainty is large. This aspect has been addressed to a

limited extent by Webb (Ref. 4) which shows a significant influence of the two-phase characteristic curves on the gas migration distance for the undisturbed scenario.

As an alternative, the van Genuchten/Parker correlation (Ref. 5,6) is included. The van Genuchten relationship for capillary pressure has been used by Yucca Mountain (Ref. 7,8) to fit their data, and the curve fits the Morrow et al. data about as well as the Brooks and Corey correlation (Ref. 9). While the Brooks and Corey model also fits the limited nonwetting phase relative permeability data of Morrow et al. reasonably well, the Parker extension to the van Genuchten model is not as successful (Ref. 9). Even so, the Van Genuchten/Parker model is included as correlation uncertainty since no data are available for WIPP specific materials.

While the van Genuchten form has been successfully compared to capillary pressure data, the variation of the fitting parameter m is only given for a limited subset. However, for large values of capillary pressure, which is expected for WIPP materials, the fitting parameter m is related to the Brooks and Corey parameter λ as $m = \lambda/(1+\lambda)$. As a first approximation, the variation of λ from Brooks and Corey can be used to determine the m distribution.

No definitive threshold pressure exists for the van Genuchten curve, so the Davies' correlation described above cannot be directly used to characterize the magnitude of the capillary pressure curve. In order to include this effect, it is proposed to equate the magnitude of the Brooks and Corey and the van Genuchten curves at an effective saturation of 0.5. This procedure will at least capture the trend of the change in the magnitude of capillary pressure for different materials.

Finally, parameter uncertainty is also large. As discussed in the preceding paragraph, there are no measurements and we rely on only one set of measurements on an analogue material. Since only one data set was used for parameter evaluation, no parameter range can be given.

With these large uncertainties in all areas, large ranges of parameters are necessary. The parameter ranges summarized below apply to the all lithologies in the Salado. The Brooks and Corey model is considered more reliable than the van Genuchten/Parker model based on limited data-model comparisons (Ref. 9); therefore, a weighting factor of 0.67 for Brooks and Corey and 0.33 for van Genuchten/Parker is tentatively recommended.

<u>Brooks and Corey</u> (Weighting Factor = 0.67)

Threshold Pressure (P_t)
Expected Value and Range given by Davies (Ref. 1)
Residual Saturations (S_{lr} and S_{gr})
Expected Value = 0.2
Range between 0.0 and 0.4 with uniform distribution
Pore-Size Distribution Parameter (λ)
Expected Value = 0.7
Range between 0.2 and 10.

van Genuchten/Parker (Weighting Factor = 0.33)

Pressure Constant (P_o)
Equate with Brooks and Corey capillary pressure at S_e=0.5
Residual Saturation (S_{lr})
Expected Value = 0.2
Range between 0.0 and 0.4 with uniform distribution
Maximum Liquid Saturation (S_{ls})
Expected Value = 1.0
No range
Pore-Size Distribution Parameter (m)
Calculate λ using Brooks and Corey distribution
Approximate m from $m = \lambda/(1+\lambda)$

The residual saturation value of 0. for the critical gas saturation (S_{gr}) is an important parameter and is specified to try to estimate possible effects of fingering. This analogy is weak at best but it is the best that can be done at present. The large range for the pore-size distribution parameter is based on values given by Mualem (Ref. 10) for real porous media. Since we do not know anything about the structure of the Salado materials, a wide range is appropriate.

The capillary and relative permeability curves are shown in Figure 1 for the λ and m ranges specified above. The equations for the correlations are summarized in the appendix.

Work is currently in progress evaluating fracture two-phase characteristic curves as well as equivalent continuum approaches which combine matrix and fracture behavior. These additional two-phase characteristic curves are expected for the 1993 PA calculations.

References

1. Memo to D. R. Anderson from P. B. Davies, "Uncertainty Estimates for Threshold Pressure for 1991 Performance Assessment Calculations Involving Waste-Generated Gas," June 6, 1991.

2. Memo to D. R. Anderson from S. W. Webb, "Uncertainty Estimates for Two-Phase Characteristic Curves for 1992 RCRA Calculations," March 20, 1992.

3. Memo to R. P. Rechard from P. Davies and A. M. LaVenue, "Additional Data for Characterizing 2-Phase Flow Behavior in Waste-Generated Gas Simulations and Pilot Point Information for Final Culebra 2-D Model (SAND89-7068/1)," November 19, 1990.

4. Webb, S. W., "Sensitivity Studies for Gas Release from the Waste Isolation Pilot Plant," Chapter 4.0 in Waste-Generated Gas at the Waste Isolation Pilot Plant: Papers Presented at the Nuclear Energy Agency Workshop on Gas Generation and Release from Radioactive Waste Repositories, P. B. Davies et al., eds., SAND91-2378, November 1991.

5. van Genuchten, R., Calculating The Unsaturated Hydraulic Conductivity With a New Closed-Form Analytical Model, Research Report 78-WR-08, Department of Civil Engineering, Princeton University, September 1978.

6. Parker, J. C., R. J. Lenhard, and T. Kuppusamy, "A Parametric Model for Constitutive Properties Regarding Multiphase Flow in Porous Media," Water Resour. Res., Vol. 23, No. 4, pp. 618-624, 1987.

7. Peters, R. R., E. A. Klavetter, I. J. Hall, S. C. Blair, P. R. Heller, and G. W. Gee, Fracture and Matrix Hydrologic Characteristics of Tuffaceous Materials from Yucca Mountain, Nye County, Nevada, SAND84-1471, Sandia National Laboratories, December 1984.

8. Klavetter, E. A., and R. R. Peters, Estimation of Hydrologic Properties of An Unsaturated, Fractured Rock Mass, SAND84-2642, Sandia National Laboratories, July 1986.

9. Webb, S. W., "Review of Two-Phase Characteristic Curves for Application to the WIPP," in progress.

10. Mualem, Y., "A New Model for Predicting the Hydraulic Conductivity of Unsaturated Porous Media," Water. Resour. Res, Vol. 12, No. 3, pp. 513-522, June 1976.

Copy to:
6340 W. D. Weart
6119 E. D. Gorham
6119 P. B. Davies
6119 S. M. Howarth
6342 M. G. Marietta
6342 R. P. Rechard
6342 M. S. Tierney
6342 P. Vaughn

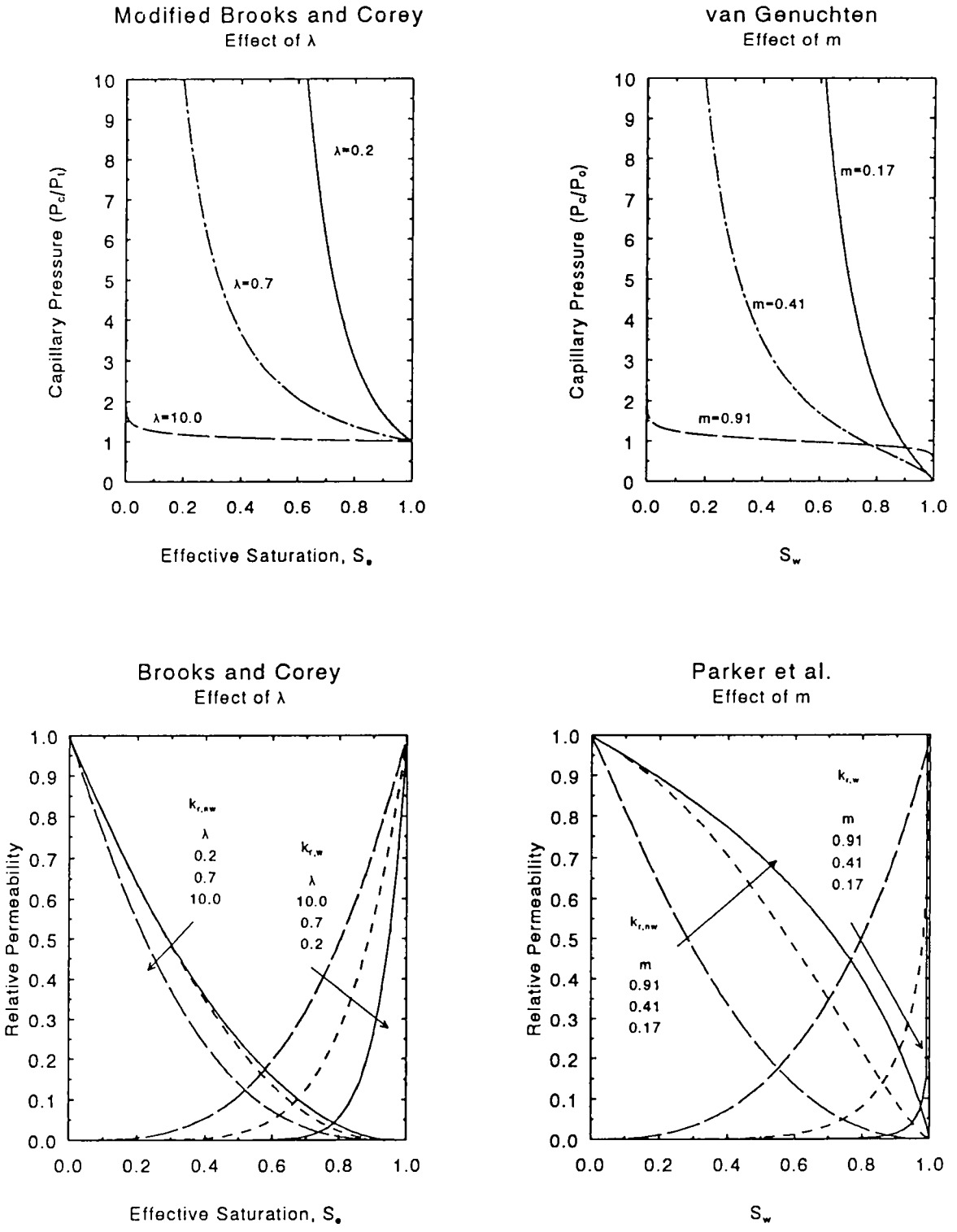

Figure 1
Capillary Pressure and
Relative Permeability Functions

Appendix
Two-Phase Characteristic Curves

The relationships defining the various sets of two-phase characteristic curves are summarized below.

Brooks and Corey

The modified Brooks and Corey relationships used by Davies and LaVenue (1991) are

Capillary Pressure

$$P_c = \frac{P_t}{S_e^{1/\lambda}} \tag{A-1}$$

Relative Permeability

$$k_{r,l} = S_e^{(2+3\lambda)/\lambda} \tag{A-2}$$

$$k_{r,g} = \left(1 - S_e\right)^2 \left(1 - S_e^{(2+\lambda)/\lambda}\right) \tag{A-3}$$

$$S_e = \frac{S_l - S_{lr}}{1 - S_{gr} - S_{lr}}. \tag{A-4}$$

The capillary pressure relationship, equation A-1, is used throughout the entire saturation region ($0. \leq S_l \leq 1.$) even though, as discussed by Corey (1986), this relationship may not be appropriate at the higher liquid saturations when $S_e > 1.0$.

van Genuchten/Parker et al.

The relationships for the van genuchten/Parker et al. (1987) characteristic curves are

Capillary Pressure

$$P_c = P_o \left(S_e^{-1/m} - 1 \right)^{1 - m}. \tag{A-5}$$

Relative Permeability

$$k_{r,l} = S_e^{1/2} \left[1 - \left(1 - S_e^{1/m} \right)^m \right]^2 \qquad \text{(A-6)}$$

$$k_{r,g} = \left(1 - S_e \right)^{1/2} \left(1 - S_e^{1/m} \right)^{2m} \qquad \text{(A-7)}$$

where

$$S_e = \frac{S_l - S_{lr}}{S_{ls} - S_{lr}} \qquad \text{(A-8)}$$

where S_{ls} is the maximum wetting phase saturation.

APPENDIX B:
WELL LOCATION DATA
AND
ELEVATIONS OF STRATIGRAPHIC LAYERS NEAR WIPP

Table B.1. Location of Wells used by WIPP (Universal Transverse Mercator [UTM], State Plan Coordinates [stpln], and Survey Sections [township, range and section])

	Well ID	x-UTM	y-UTM	x-STPLN	y-STPLN	Township	Range	Section	Source
2	AEC7	621117	3589387	691810	523142	21	32	31	Mercer, 1983, Table 1
3	AEC8	617522	3586435	679945	513555	22	31	11	Mercer, 1983, Table 1
4	B25	611695	3580609	660759	494504	22	31	20	Mercer, 1983, Table 1
5	CABIN1	613191	3578049	665559	486111	23	31	5	Gonzales, 1989, Tables 3-6 and 3-7
6	DH207	613634	3581973	667074	498589	0	0	0	Krieg, 1984, Table I
7	DH211	613637	3581784	667082	497966	0	0	0	Krieg, 1984, Table I
8	DH215	613634	3581588	667072	497326	0	0	0	Krieg, 1984, Table I
9	DH219	613636	3581448	667081	496864	0	0	0	Krieg, 1984, Table I
10	DH223	613634	3581247	667073	496207	0	0	0	Krieg, 1984, Table I
11	DH227	613632	3581071	667066	495630	0	0	0	Krieg, 1984, Table I
12	DH77	613476	3582573	666554	500556	0	0	0	Krieg, 1984, Table I
13	DO201	613581	3582062	666900	498880	0	0	0	Krieg, 1984, Table I
14	DO203	613630	3582376	667059	499910	0	0	0	Krieg, 1984, Table I
15	DO205	613587	3582616	667066	500696	0	0	0	Krieg, 1984, Table I
16	DO45	613632	3582263	667066	499540	0	0	0	Krieg, 1984, Table I
17	DO52	613586	3582231	666915	499432	0	0	0	Krieg, 1984, Table I
18	DO56	613587	3582375	666919	499907	0	0	0	Krieg, 1984, Table I
19	DO63	613587	3582524	666919	500396	0	0	0	Krieg, 1984, Table I
20	DO67	613516	3582572	666687	500551	0	0	0	Krieg, 1984, Table I
21	DO88	613435	3582572	666421	500551	0	0	0	Krieg, 1984, Table I
22	DO91	613395	3582575	666288	500561	0	0	0	Krieg, 1984, Table I
23	DOE1	615203	3580333	672206	493563	22	31	28	Gonzales, 1989, Tables 3-6 and 3-7
24	DOE2	613683	3585294	667317	509876	22	31	8	Gonzales, 1989, Tables 3-6 and 3-7
25	ENGLE	614953	3567454	671122	451297	24	31	4	Gonzales, 1989, Tables 3-6 and 3-7
26	ERDA10	606684	3570523	644057	461534	23	30	34	Mercer, 1983, Table 1
27	ERDA6	618226	3589011	682292	521975	21	31	35	Mercer, 1983, Table 1
28	ERDA9	613697	3581958	667297	498929	22	31	20	Mercer, 1983, Table 1
29	FFG_002	627231	3608400	712258	585415	20	33	3	Richey, 1989, Table 2
30	FFG_004	622022	3605526	695095	576082	20	33	7	Richey, 1989, Table 2
31	FFG_005	627356	3605486	712599	575853	20	33	10	Richey, 1989, Table 2
32	FFG_006	627658	3605587	713589	576183	20	33	11	Richey, 1989, Table 2
33	FFG_007	627758	3604682	713919	573213	20	33	14	Richey, 1989, Table 2
34	FFG_009	627959	3604782	714579	573543	20	33	14	Richey, 1989, Table 2
35	FFG_011	627658	3605184	713589	574863	20	33	14	Richey, 1989, Table 2
36	FFG_012	627255	3605184	712269	574863	20	33	15	Richey, 1989, Table 2
37	FFG_013	525249	3605163	705684	574827	20	33	16	Richey, 1989, Table 2
38	FFG_014	621225	3604704	692478	573420	20	33	18	Richey, 1989, Table 2
39	FFG_016	627303	3602758	712361	566901	20	33	22	Richey, 1989, Table 2

Table B.1. Location of Wells used by WIPP (Universal Transverse Mercator [UTM], State Plan Coordinates [stpln], and Survey Sections [township, range and section])

	Well ID	x-UTM	y-UTM	x-STPLN	y-STPLN	Township	Range	Section	Source
1	FFG_017	628494	3603697	716300	569948	20	33	23	Richey, 1989, Table 2
2	FFG_018	630636	3602305	723296	565346	20	33	24	Richey, 1989, Table 2
3	FFG_019	627720	3600778	713695	560402	20	33	26	Richey, 1989, Table 2
4	FFG_020	621672	3601468	693880	562799	20	33	30	Richey, 1989, Table 2
5	FFG_023	633058	3599616	731178	556481	20	33	33	Richey, 1989, Table 2
6	FFG_024	635469	3599257	739089	555233	20	33	34	Richey, 1989, Table 2
7	FFG_025	628538	3600381	716379	559068	20	33	35	Richey, 1989, Table 2
8	FFG_026	628122	3600375	715015	559082	20	33	35	Richey, 1989, Table 2
9	FFG_027	627820	3600074	714025	558092	20	33	35	Richey, 1989, Table 2
10	FFG_039	616468	3606754	676902	580244	20	32	10	Richey, 1989, Table 2
11	FFG_040	620041	3603892	688561	570786	20	32	13	Richey, 1989, Table 2
12	FFG_041	616805	3604246	677942	572014	20	32	15	Richey, 1989, Table 2
13	FFG_042	615263	3604535	672914	572994	20	32	16	Richey, 1989, Table 2
14	FFG_043	614824	3602618	671406	566704	20	32	21	Richey, 1989, Table 2
15	FFG_044	618435	3602658	683256	566770	20	32	23	Richey, 1989, Table 2
16	FFG_105	609126	3590258	652461	526265	21	30	25	Richey, 1989, Table 2
17	FFG_106	607630	3591218	647587	529450	21	30	26	Richey, 1989, Table 2
18	FFG_107	607832	3590109	648217	525810	21	30	26	Richey, 1989, Table 2
19	FFG_108	610586	3589854	657254	524908	21	31	31	Richey, 1989, Table 2
20	FFG_109	612822	3589796	664589	524686	21	31	32	Richey, 1989, Table 2
21	FFG_110	613636	3588341	667229	519875	21	31	32	Richey, 1989, Table 2
22	FFG_111	616209	3589857	675705	524786	21	31	34	Richey, 1989, Table 2
23	FFG_112	615312	3588335	672729	519825	21	31	34	Richey, 1989, Table 2
24	FFG_113	615319	3589869	672784	524858	21	31	34	Richey, 1989, Table 2
25	FFG_114	609458	3586996	653485	515558	22	30	1	Richey, 1989, Table 2
26	FFG_115	608243	3586900	649498	515244	22	30	2	Richey, 1989, Table 2
27	FFG_116	606902	3588088	645132	519179	22	30	3	Richey, 1989, Table 2
28	FFG_117	607132	3587086	645854	515889	22	30	3	Richey, 1989, Table 2
29	FFG_119	604055	3585149	635724	509600	22	30	9	Richey, 1989, Table 2
30	FFG_120	604750	3586261	638038	513251	22	30	9	Richey, 1989, Table 2
31	FFG_121	604134	3585930	636016	512165	22	30	9	Richey, 1989, Table 2
32	FFG_122	604165	3585505	636083	510770	22	30	9	Richey, 1989, Table 2
33	FFG_123	606439	3586110	643580	512686	22	30	10	Richey, 1989, Table 2
34	FFG_124	608252	3586096	649528	512608	22	30	11	Richey, 1989, Table 2
35	FFG_125	607631	3585457	647458	510544	22	30	11	Richey, 1989, Table 2
36	FFG_126	609341	3584606	653068	507720	22	30	13	Richey, 1989, Table 2
37	FFG_127	608226	3583523	649376	504163	22	30	14	Richey, 1989, Table 2
38	FFG_128	605614	3581894	640772	498885	22	30	21	Richey, 1989, Table 2

Table B.1. Location of Wells used by WIPP (Universal Transverse Mercator [UTM], State Plan Coordinates [stpln], and Survey Sections [township, range and section])

	Well ID	x-UTM	y-UTM	x-STPLN	y-STPLN	Township	Range	Section	Source
1	FFG_129	604814	3583050	638181	502679	22	30	21	Richey, 1989, Table 2
2	FFG_130	604412	3582244	636828	500068	22	30	21	Richey, 1989, Table 2
3	FFG_132	606479	3581068	643582	496139	22	30	27	Richey, 1989, Table 2
4	FFG_133	606462	3580266	643522	493544	22	30	27	Richey, 1989, Table 2
5	FFG_134	605663	3580407	640899	494006	22	30	27	Richey, 1989, Table 2
6	FFG_135	607211	3580978	645983	495845	22	30	27	Richey, 1989, Table 2
7	FFG_136	609279	3579410	652734	490667	22	30	36	Richey, 1989, Table 2
8	FFG_137	609955	3578869	654952	488858	22	30	36	Richey, 1989, Table 2
9	FFG_138	610827	3587071	657978	515773	22	31	6	Richey, 1989, Table 2
10	FFG_139	610665	3587722	657478	517912	22	31	6	Richey, 1989, Table 2
11	FFG_140	613648	3585123	667200	509316	22	31	8	Richey, 1989, Table 2
12	FFG_141	612120	3585114	662187	509317	22	31	8	Richey, 1989, Table 2
13	FFG_142	615288	3586667	672617	514350	22	31	9	Richey, 1989, Table 2
14	FFG_143	616006	3579286	674808	490129	22	31	34	Richey, 1989, Table 2
15	FFG_144	599879	3577828	621856	485641	23	29	1	Richey, 1989, Table 2
16	FFG_145	599320	3577132	620020	483389	23	29	1	Richey, 1989, Table 2
17	FFG_146	600363	3578186	623476	486818	23	29	1	Richey, 1989, Table 2
18	FFG_147	595499	3578188	607513	486922	23	29	4	Richey, 1989, Table 2
19	FFG_148	600569	3576193	624120	480278	23	29	12	Richey, 1989, Table 2
20	FFG_149	600707	3574718	624539	475434	23	29	13	Richey, 1989, Table 2
21	FFG_155	596597	3570664	610951	462232	23	29	27	Richey, 1989, Table 2
22	FFG_156	595692	3570883	607981	462952	23	29	28	Richey, 1989, Table 2
23	FFG_157	599212	3569453	619500	458190	23	29	35	Richey, 1989, Table 2
24	FFG_158	600510	3569436	623761	458104	23	29	36	Richey, 1989, Table 2
25	FFG_159	609539	3578101	653588	486370	23	30	1	Richey, 1989, Table 2
26	FFG_160	610084	3577670	655343	484923	23	30	1	Richey, 1989, Table 2
27	FFG_161	607676	3577068	647439	483015	23	30	2	Richey, 1989, Table 2
28	FFG_162	607342	3578605	646376	488059	23	30	2	Richey, 1989, Table 2
29	FFG_163	608127	3577850	648955	485549	23	30	2	Richey, 1989, Table 2
30	FFG_164	602541	3574598	630556	475010	23	30	17	Richey, 1989, Table 2
31	FFG_165	601827	3573070	628182	469995	23	30	19	Richey, 1989, Table 2
32	FFG_166	609182	3573205	652317	470305	23	30	24	Richey, 1989, Table 2
33	FFG_167	609012	3570846	651726	462566	23	30	26	Richey, 1989, Table 2
34	FFG_168	604202	3570581	635911	461795	23	30	28	Richey, 1989, Table 2
35	FFG_169	604034	3572065	635389	466662	23	30	29	Richey, 1989, Table 2
36	FFG_170	601537	3572060	627194	466716	23	30	30	Richey, 1989, Table 2
37	FFG_171	601959	3569718	628551	458995	23	30	31	Richey, 1989, Table 2
38	FFG_172	603366	3570098	633169	460209	23	30	32	Richey, 1989, Table 2

Table B.1. Location of Wells used by WIPP (Universal Transverse Mercator [UTM], State Plan Coordinates [stpln], and Survey Sections [township, range and section])

	Well ID	x-UTM	y-UTM	x-STPLN	y-STPLN	Township	Range	Section	Source
1	FFG_173	609960	3569937	654805	459582	23	30	36	Richey, 1989, Table 2
2	FFG_177	591351	3563822	593606	439877	24	29	19	Richey, 1989, Table 2
3	FFG_179	593084	3561340	599224	431698	24	29	29	Richey, 1989, Table 2
4	FFG_180	607488	3567427	646628	451374	24	30	2	Richey, 1989, Table 2
5	FFG_181	604028	3568585	635304	455245	24	30	5	Richey, 1989, Table 2
6	FFG_182	601542	3568281	627146	454314	24	30	6	Richey, 1989, Table 2
7	FFG_183	605177	3566738	639041	449147	24	30	9	Richey, 1989, Table 2
8	FFG_184	607564	3565857	646845	446225	24	30	11	Richey, 1989, Table 2
9	FFG_185	605866	3565683	641274	445686	24	30	15	Richey, 1989, Table 2
10	FFG_186	605016	3565698	638484	445736	24	30	16	Richey, 1989, Table 2
11	FFG_188	602948	3564040	631660	440361	24	30	20	Richey, 1989, Table 2
12	FFG_189	608405	3563679	649573	439043	24	30	23	Richey, 1989, Table 2
13	FFG_190	607685	3562746	647176	436015	24	30	23	Richey, 1989, Table 2
14	FFG_191	609337	3561151	652564	430748	24	30	25	Richey, 1989, Table 2
15	FFG_192	607401	3562442	646246	435019	24	30	27	Richey, 1989, Table 2
16	FFG_194	617718	3568422	680232	454446	24	31	2	Richey, 1989, Table 2
17	FFG_195	616941	3567615	677649	451793	24	31	3	Richey, 1989, Table 2
18	FFG_196	615316	3568812	672350	455759	24	31	4	Richey, 1989, Table 2
19	FFG_197	614612	3568483	670036	454709	24	31	4	Richey, 1989, Table 2
20	FFG_198	613807	3568888	667396	456038	24	31	5	Richey, 1989, Table 2
21	FFG_199	611628	3568640	660244	455257	24	31	6	Richey, 1989, Table 2
22	FFG_200	611273	3568414	659080	454549	24	31	6	Richey, 1989, Table 2
23	FFG_201	612154	3565951	661905	446431	24	31	7	Richey, 1989, Table 2
24	FFG_202	618692	3566653	683393	448607	24	31	11	Richey, 1989, Table 2
25	FFG_203	618143	3567223	681591	450478	24	31	11	Richey, 1989, Table 2
26	FFG_204	619790	3564834	686932	442604	24	31	13	Richey, 1989, Table 2
27	FFG_205	613734	3565566	667090	445140	24	31	17	Richey, 1989, Table 2
28	FFG_206	612171	3564340	661929	441145	24	31	18	Richey, 1989, Table 2
29	FFG_207	613776	3563957	667198	439860	24	31	20	Richey, 1989, Table 2
30	FFG_208	612992	3562725	664590	435847	24	31	20	Richey, 1989, Table 2
31	FFG_209	615380	3563980	672461	439901	24	31	21	Richey, 1989, Table 2
32	FFG_210	614199	3562745	668548	435879	24	31	21	Richey, 1989, Table 2
33	FFG_212	619811	3562825	686967	436012	24	31	24	Richey, 1989, Table 2
34	FFG_213	614915	3560252	670865	427664	24	31	33	Richey, 1989, Table 2
35	FFG_214	617438	3559994	679114	426785	24	31	35	Richey, 1989, Table 2
36	FFG_215	610576	3559150	656597	424152	25	30	1	Richey, 1989, Table 2
37	FFG_216	604853	3558664	637816	422688	25	30	4	Richey, 1989, Table 2
38	FFG_217	617694	3559360	679954	424705	25	31	2	Richey, 1989, Table 2

Table B.1. Location of Wells used by WIPP (Universal Transverse Mercator [UTM], State Plan Coordinates [stpln], and Survey Sections [township, range and section])

	Well ID	x-UTM	y-UTM	x-STPLN	y-STPLN	Township	Range	Section	Source
1	FFG_218	618235	3558795	681730	422820	25	31	2	Richey, 1989, Table 2
2	FFG_219	616649	3557179	676493	417552	25	31	10	Richey, 1989, Table 2
3	FFG_220	619057	3557584	684393	418848	25	31	12	Richey, 1989, Table 2
4	FFG_221	616028	3555913	674422	413427	25	31	15	Richey, 1989, Table 2
5	FFG_222	614248	3552703	668515	402929	25	31	28	Richey, 1989, Table 2
6	FFG_224	629257	3598870	718704	554099	21	32	1	Richey, 1989, Table 2
7	FFG_225	629076	3597979	718112	551174	21	32	1	Richey, 1989, Table 2
8	FFG_226	628708	3596750	716853	547172	21	32	1	Richey, 1989, Table 2
9	FFG_228	626669	3597926	710210	551066	21	32	2	Richey, 1989, Table 2
10	FFG_229	625894	3596724	707620	547120	21	32	3	Richey, 1989, Table 2
11	FFG_230	625486	3597502	706279	549709	21	32	3	Richey, 1989, Table 2
12	FFG_231	624249	3598303	702273	552336	21	32	4	Richey, 1989, Table 2
13	FFG_232	623880	3597479	701011	549665	21	32	4	Richey, 1989, Table 2
14	FFG_233	623730	3598370	700570	552588	21	32	4	Richey, 1989, Table 2
15	FFG_234	622268	3597867	695720	550968	21	32	5	Richey, 1989, Table 2
16	FFG_235	623075	3597479	698371	549665	21	32	5	Richey, 1989, Table 2
17	FFG_236	620626	3597834	690380	550899	21	32	6	Richey, 1989, Table 2
18	FFG_237	624279	3595893	702319	544429	21	32	9	Richey, 1989, Table 2
19	FFG_238	625894	3595919	707620	544480	21	32	10	Richey, 1989, Table 2
20	FFG_239	627919	3595147	714233	541912	21	32	11	Richey, 1989, Table 2
21	FFG_240	627501	3595945	712893	544532	21	32	11	Richey, 1989, Table 2
22	FFG_241	628322	3595549	715553	543232	21	32	12	Richey, 1989, Table 2
23	FFG_242	623510	3593053	699730	535143	21	32	21	Richey, 1989, Table 2
24	FFG_243	627958	3591122	714296	528704	21	32	26	Richey, 1989, Table 2
25	FFG_244	627169	3589486	711671	523370	21	32	35	Richey, 1989, Table 2
26	FFG_245	634293	3596014	735183	544627	21	33	9	Richey, 1989, Table 2
27	FFG_246	636300	3596435	741767	545977	21	33	11	Richey, 1989, Table 2
28	FFG_247	638785	3593673	749855	536845	21	33	13	Richey, 1989, Table 2
29	FFG_248	638754	3594075	749755	538165	21	33	13	Richey, 1989, Table 2
30	FFG_249	635538	3594033	739201	538094	21	33	15	Richey, 1989, Table 2
31	FFG_250	630707	3593573	723350	536681	21	33	18	Richey, 1989, Table 2
32	FFG_251	639185	3592056	751137	531538	21	33	24	Richey, 1989, Table 2
33	FFG_252	631978	3589148	727420	522161	21	33	32	Richey, 1989, Table 2
34	FFG_253	634373	3589591	735313	523550	21	33	33	Richey, 1989, Table 2
35	FFG_254	634776	3589591	736633	523550	21	33	34	Richey, 1989, Table 2
36	FFG_255	636385	3590012	741913	524900	21	33	35	Richey, 1989, Table 2
37	FFG_264	624541	3575777	702753	478415	23	32	9	Richey, 1989, Table 2
38	FFG_265	626158	3575003	708059	475842	23	32	15	Richey, 1989, Table 2

Table B.1. Location of Wells used by WIPP (Universal Transverse Mercator [UTM], State Plan Coordinates [stpln], and Survey Sections [township, range and section])

	Well ID	x-UTM	y-UTM	x-STPLN	y-STPLN	Township	Range	Section	Source
1	FFG_266	629827	3572644	720033	468035	23	32	24	Richey, 1989, Table 2
2	FFG_267	632644	3570662	729244	461468	23	33	32	Richey, 1989, Table 2
3	FFG_268	636682	3569503	742460	457597	23	33	35	Richey, 1989, Table 2
4	FFG_272	621266	3580141	692103	492804	22	32	31	Richey, 1989, Table 2
5	FFG_273	621714	3576972	693509	482402	23	32	7	Richey, 1989, Table 2
6	FFG_274	627262	3583857	711844	504897	22	32	14	Richey, 1989, Table 2
7	FFG_275	626055	3584259	707884	506217	22	32	15	Richey, 1989, Table 2
8	FFG_276	622836	3584196	697320	506076	22	32	17	Richey, 1989, Table 2
9	FFG_277	621627	3583775	693354	504725	22	32	18	Richey, 1989, Table 2
10	FFG_278	621646	3582157	693382	499416	22	32	19	Richey, 1989, Table 2
11	FFG_279	622836	3582989	697320	502116	22	32	20	Richey, 1989, Table 2
12	FFG_280	625245	3583022	705224	502190	22	32	22	Richey, 1989, Table 2
13	FFG_281	628878	3581872	717114	498350	22	32	25	Richey, 1989, Table 2
14	FFG_283	638822	3588438	749880	519668	22	33	1	Richey, 1989, Table 2
15	FFG_284	633260	3587655	731596	517227	22	33	4	Richey, 1989, Table 2
16	FFG_285	632916	3587152	730466	515577	22	33	5	Richey, 1989, Table 2
17	FFG_286	630045	3585511	721010	510259	22	33	7	Richey, 1989, Table 2
18	FFG_287	630815	3585934	723537	511615	22	33	7	Richey, 1989, Table 2
19	FFG_288	633218	3586749	731456	514257	22	33	9	Richey, 1989, Table 2
20	FFG_289	635668	3584383	739429	506427	22	33	15	Richey, 1989, Table 2
21	FFG_290	631649	3583118	726240	502376	22	33	20	Richey, 1989, Table 2
22	FFG_291	631716	3579091	726360	489157	22	33	32	Richey, 1989, Table 2
23	FFG_292	634513	3580338	735574	493186	22	33	33	Richey, 1989, Table 2
24	FFG_293	635741	3579152	739570	489260	22	33	34	Richey, 1989, Table 2
25	FFG_313	621557	3587797	693224	517925	22	32	6	Richey, 1989, Table 2
26	FFG_314	629670	3583902	719747	504978	22	32	13	Richey, 1989, Table 2
27	FFG_315	626522	3578214	709318	486382	23	32	3	Richey, 1989, Table 2
28	FFG_316	627739	3576635	713279	481164	23	32	11	Richey, 1989, Table 2
29	FFG_317	621734	3574920	693542	475670	23	32	18	Richey, 1989, Table 2
30	FFG_318	622977	3572533	697554	467800	23	32	20	Richey, 1989, Table 2
31	FFG_319	624161	3573735	701471	471749	23	32	21	Richey, 1989, Table 2
32	FFG_320	629107	3572102	717668	466290	23	32	25	Richey, 1989, Table 2
33	FFG_321	628524	3571093	715723	462981	23	32	25	Richey, 1989, Table 2
34	FFG_322	628222	3570892	714733	462321	23	32	26	Richey, 1989, Table 2
35	FFG_323	627420	3570965	712100	462590	23	32	26	Richey, 1989, Table 2
36	FFG_324	624184	3572130	701514	466480	23	32	28	Richey, 1989, Table 2
37	FFG_325	620546	3569268	689509	457154	23	32	31	Richey, 1989, Table 2
38	FFG_326	625008	3570140	704185	459917	23	32	33	Richey, 1989, Table 2

Table B.1. Location of Wells used by WIPP (Universal Transverse Mercator [UTM], State Plan Coordinates [stpln], and Survey Sections [township, range and section])

	Well ID	x-UTM	y-UTM	x-STPLN	y-STPLN	Township	Range	Section	Source
1	FFG_327	626737	3569761	709825	458640	23	32	34	Richey, 1989, Table 2
2	FFG_328	627719	3570289	713083	460341	23	32	35	Richey, 1989, Table 2
3	FFG_329	628625	3570188	716053	460011	23	32	36	Richey, 1989, Table 2
4	FFG_330	629464	3569834	718778	458813	23	32	36	Richey, 1989, Table 2
5	FFG_331	634557	3577522	735655	483942	23	33	4	Richey, 1989, Table 2
6	FFG_332	631443	3577384	725434	483557	23	33	6	Richey, 1989, Table 2
7	FFG_333	630183	3575856	721264	478574	23	33	7	Richey, 1989, Table 2
8	FFG_334	631791	3574262	726509	473313	23	33	17	Richey, 1989, Table 2
9	FFG_335	630204	3574250	721301	473303	23	33	18	Richey, 1989, Table 2
10	FFG_336	630611	3573046	722603	469355	23	33	19	Richey, 1989, Table 2
11	FFG_337	633022	3572674	730519	468066	23	33	20	Richey, 1989, Table 2
12	FFG_338	631435	3570650	725277	461460	23	33	31	Richey, 1989, Table 2
13	FFG_339	637863	3570326	746370	460265	23	33	35	Richey, 1989, Table 2
14	FFG_340	639497	3569942	751700	458973	23	33	36	Richey, 1989, Table 2
15	FFG_361	591407	3608036	594694	584951	20	29	1	Richey, 1989, Table 2
16	FFG_362	588581	3607624	585423	583663	20	29	3	Richey, 1989, Table 2
17	FFG_363	586158	3608022	577470	585038	20	29	4	Richey, 1989, Table 2
18	FFG_364	583878	3605062	569923	575355	20	29	7	Richey, 1989, Table 2
19	FFG_366	588498	3606300	585115	579318	20	29	10	Richey, 1989, Table 2
20	FFG_367	589516	3605699	588421	577345	20	29	11	Richey, 1989, Table 2
21	FFG_370	591027	3604798	593382	574358	20	29	13	Richey, 1989, Table 2
22	FFG_371	591334	3604826	594392	574416	20	29	13	Richey, 1989, Table 2
23	FFG_372	589730	3604102	589095	572070	20	29	14	Richey, 1989, Table 2
24	FFG_373	586192	3604773	577514	574376	20	29	16	Richey, 1989, Table 2
25	FFG_374	585392	3603561	574858	570394	20	29	17	Richey, 1989, Table 2
26	FFG_376	590555	3601690	591768	564155	20	29	25	Richey, 1989, Table 2
27	FFG_381	599172	3599246	619978	555961	20	29	36	Richey, 1989, Table 2
28	FFG_383	601077	3606916	626395	581073	20	30	1	Richey, 1989, Table 2
29	FFG_384	594213	3607648	603902	583643	20	30	5	Richey, 1989, Table 2
30	FFG_385	597883	3602444	615814	566466	20	30	22	Richey, 1989, Table 2
31	FFG_387	595912	3600331	609313	559598	20	30	28	Richey, 1989, Table 2
32	FFG_388	595864	3601219	609189	562513	20	30	28	Richey, 1989, Table 2
33	FFG_389	593453	3599602	601245	557239	20	30	31	Richey, 1989, Table 2
34	FFG_390	595208	3600029	607003	558608	20	30	32	Richey, 1989, Table 2
35	FFG_391	595208	3599627	607003	557288	20	30	32	Richey, 1989, Table 2
36	FFG_392	596612	3599732	611609	557599	20	30	33	Richey, 1989, Table 2
37	FFG_393	606297	3606985	643526	581199	20	31	4	Richey, 1989, Table 2
38	FFG_394	603077	3606946	632959	581140	20	31	6	Richey, 1989, Table 2

Table B.1. Location of Wells used by WIPP (Universal Transverse Mercator [UTM], State Plan Coordinates [stpln], and Survey Sections [township, range and section])

	Well ID	x-UTM	y-UTM	x-STPLN	y-STPLN	Township	Range	Section	Source
1	FFG_395	603098	3605631	632997	576823	20	31	7	Richey, 1989, Table 2
2	FFG_396	603243	3600398	633370	559652	20	31	30	Richey, 1989, Table 2
3	FFG_398	588017	3597286	583323	549759	21	28	2	Richey, 1989, Table 2
4	FFG_399	587111	3597387	580353	550089	21	28	3	Richey, 1989, Table 2
5	FFG_402	590847	3595289	592582	543138	21	28	12	Richey, 1989, Table 2
6	FFG_403	586424	3593240	578030	536512	21	28	15	Richey, 1989, Table 2
7	FFG_404	583988	3592021	570006	532548	21	28	20	Richey, 1989, Table 2
8	FFG_407	583988	3590814	570006	528588	21	28	29	Richey, 1989, Table 2
9	FFG_408	582473	3590320	565002	526999	21	28	30	Richey, 1989, Table 2
10	FFG_411	584828	3588367	572695	520558	21	28	33	Richey, 1989, Table 2
11	FFG_413	588470	3589234	584681	523337	21	28	35	Richey, 1989, Table 2
12	FFG_418	596362	3598010	610756	551972	21	29	3	Richey, 1989, Table 2
13	FFG_419	594776	3597648	605505	550814	21	29	4	Richey, 1989, Table 2
14	FFG_420	594662	3598348	605178	553113	21	29	4	Richey, 1989, Table 2
15	FFG_421	593556	3598412	601548	553321	21	29	5	Richey, 1989, Table 2
16	FFG_422	593958	3598000	602868	551971	21	29	5	Richey, 1989, Table 2
17	FFG_426	592398	3591591	597601	530971	21	29	19	Richey, 1989, Table 2
18	FFG_432	607401	3588903	646769	521852	21	30	35	Richey, 1989, Table 2
19	FFG_433	588569	3588121	584969	519682	22	28	2	Richey, 1989, Table 2
20	FFG_438	618629	3586910	683580	515081	22	31	1	Richey, 1989, Table 2
21	FFG_445	590526	3580760	591228	495462	22	28	25	Richey, 1989, Table 2
22	FFG_453	618415	3578487	682715	487442	23	31	2	Richey, 1989, Table 2
23	FFG_455	618558	3575680	683119	478229	23	31	11	Richey, 1989, Table 2
24	FFG_456	617677	3574462	680195	474264	23	31	14	Richey, 1989, Table 2
25	FFG_457	614456	3574425	669624	474210	23	31	16	Richey, 1989, Table 2
26	FFG_458	615274	3572430	672278	467629	23	31	21	Richey, 1989, Table 2
27	FFG_459	619295	3571652	685468	465012	23	31	25	Richey, 1989, Table 2
28	FFG_462	615699	3571221	673637	463662	23	31	27	Richey, 1989, Table 2
29	FFG_463	612475	3570378	663055	460962	23	31	32	Richey, 1989, Table 2
30	FFG_464	614894	3570416	670997	461022	23	31	33	Richey, 1989, Table 2
31	FFG_465	614090	3569999	668355	459685	23	31	33	Richey, 1989, Table 2
32	FFG_474	628677	3568183	716158	453428	24	32	1	Richey, 1989, Table 2
33	FFG_475	628244	3568580	714774	454733	24	32	2	Richey, 1989, Table 2
34	FFG_476	621409	3568885	692341	455866	24	32	6	Richey, 1989, Table 2
35	FFG_477	626275	3566554	708244	448117	24	32	10	Richey, 1989, Table 2
36	FFG_478	627890	3566569	713543	448132	24	32	11	Richey, 1989, Table 2
37	FFG_479	627468	3566954	712193	449429	24	32	11	Richey, 1989, Table 2
38	FFG_480	628677	3566976	716158	449468	24	32	12	Richey, 1989, Table 2

Table B.1. Location of Wells used by WIPP (Universal Transverse Mercator [UTM], State Plan Coordinates [stpln], and Survey Sections [township, range and section])

	Well ID	x-UTM	y-UTM	x-STPLN	y-STPLN	Township	Range	Section	Source
1	FFG_481	629921	3564597	720180	441628	24	32	13	Richey, 1989, Table 2
2	FFG_482	627482	3565749	712204	445477	24	32	14	Richey, 1989, Table 2
3	FFG_483	625893	3564517	706958	441463	24	32	15	Richey, 1989, Table 2
4	FFG_484	626601	3563741	709281	438885	24	32	22	Richey, 1989, Table 2
5	FFG_485	626323	3563337	708336	437561	24	32	22	Richey, 1989, Table 2
6	FFG_486	627104	3563741	710931	438885	24	32	23	Richey, 1989, Table 2
7	FFG_487	627003	3563842	710601	439215	24	32	23	Richey, 1989, Table 2
8	FFG_488	628618	3564276	715902	440608	24	32	24	Richey, 1989, Table 2
9	FFG_489	629141	3562161	717583	433668	24	32	25	Richey, 1989, Table 2
10	FFG_490	622290	3562046	695099	433421	24	32	29	Richey, 1989, Table 2
11	FFG_491	621485	3562046	692459	433421	24	32	30	Richey, 1989, Table 2
12	FFG_492	625107	3559688	704284	425618	24	32	33	Richey, 1989, Table 2
13	FFG_493	625912	3560090	706924	426938	24	32	34	Richey, 1989, Table 2
14	FFG_494	625912	3559688	706924	425618	24	32	34	Richey, 1989, Table 2
15	FFG_495	627126	3559716	710904	425675	24	32	35	Richey, 1989, Table 2
16	FFG_496	639095	3568735	750380	455013	24	33	1	Richey, 1989, Table 2
17	FFG_497	631494	3566228	725373	446949	24	33	7	Richey, 1989, Table 2
18	FFG_498	631883	3567428	726679	450888	24	33	8	Richey, 1989, Table 2
19	FFG_499	639536	3565513	751762	444438	24	33	13	Richey, 1989, Table 2
20	FFG_500	632702	3565844	729335	445656	24	33	17	Richey, 1989, Table 2
21	FFG_501	632345	3563004	728097	436369	24	33	20	Richey, 1989, Table 2
22	FFG_502	635140	3563849	737302	439075	24	33	22	Richey, 1989, Table 2
23	FFG_503	635586	3561835	738701	432466	24	33	27	Richey, 1989, Table 2
24	FFG_504	632771	3561413	729465	431115	24	33	29	Richey, 1989, Table 2
25	FFG_505	630239	3562683	721189	435349	24	33	30	Richey, 1989, Table 2
26	FFG_506	631576	3560189	725511	427131	24	33	31	Richey, 1989, Table 2
27	FFG_507	639607	3561088	751898	429920	24	33	36	Richey, 1989, Table 2
28	FFG_548	601155	3608819	626682	587316	19	30	36	Richey, 1989, Table 2
29	FFG_552	596378	3554488	609903	409146	25	29	15	Richey, 1989, Table 2
30	FFG_562	614317	3546624	668609	382978	26	31	9	Richey, 1989, Table 2
31	FFG_563	618774	3547092	683237	384417	26	31	11	Richey, 1989, Table 2
32	FFG_568	619132	3541724	684313	366799	26	31	25	Richey, 1989, Table 2
33	FFG_569	619132	3542127	684313	368119	26	31	25	Richey, 1989, Table 2
34	FFG_584	606879	3557091	644432	417458	25	30	10	Richey, 1989, Table 2
35	FFG_585	609769	3557118	653916	417516	25	30	12	Richey, 1989, Table 2
36	FFG_600	608992	3550622	651237	396198	25	30	35	Richey, 1989, Table 2
37	FFG_601	607790	3549783	647256	393477	25	30	35	Richey, 1989, Table 2
38	FFG_602	618235	3558795	681730	422820	25	31	2	Richey, 1989, Table 2

Table B.1. Location of Wells used by WIPP (Universal Transverse Mercator [UTM], State Plan Coordinates [stpln], and Survey Sections [township, range and section])

	Well ID	x-UTM	y-UTM	x-STPLN	y-STPLN	Township	Range	Section	Source
1	FFG_606	618324	3551156	681858	397752	25	31	35	Richey, 1989, Table 2
2	FFG_618	599392	3546376	619633	382460	26	29	11	Richey, 1989, Table 2
3	FFG_638	607809	3548155	647284	388134	26	30	2	Richey, 1989, Table 2
4	FFG_639	606187	3548136	641961	388102	26	30	3	Richey, 1989, Table 2
5	FFG_640	604548	3549331	636618	392062	26	30	4	Richey, 1989, Table 2
6	FFG_643	610657	3546572	656602	382873	26	30	12	Richey, 1989, Table 2
7	FFG_644	605816	3544896	640681	377470	26	30	16	Richey, 1989, Table 2
8	FFG_648	609863	3544129	653961	374890	26	30	24	Richey, 1989, Table 2
9	FFG_685	592502	3586828	597845	515341	22	29	6	Richey, 1989, Table 2
10	FFG_689	626339	3558413	708291	421399	25	32	3	Richey, 1989, Table 2
11	FFG_690	625251	3556776	704687	416062	25	32	9	Richey, 1989, Table 2
12	FFG_691	626238	3557256	707961	417604	25	32	10	Richey, 1989, Table 2
13	FFG_692	627982	3556520	713651	415154	25	32	11	Richey, 1989, Table 2
14	FFG_693	627068	3555594	710652	412151	25	32	14	Richey, 1989, Table 2
15	FFG_694	625965	3554867	706999	409798	25	32	15	Richey, 1989, Table 2
16	FFG_695	625955	3556071	706997	413752	25	32	15	Richey, 1989, Table 2
17	FFG_696	625955	3556134	706997	413957	25	32	15	Richey, 1989, Table 2
18	FFG_697	624748	3555669	703037	412432	25	32	16	Richey, 1989, Table 2
19	FFG_698	620989	3555992	690703	413589	25	32	18	Richey, 1989, Table 2
20	FFG_699	623679	3553534	699465	405455	25	32	20	Richey, 1989, Table 2
21	FFG_700	623679	3553131	699465	404135	25	32	20	Richey, 1989, Table 2
22	FFG_701	625090	3553358	704095	404846	25	32	21	Richey, 1989, Table 2
23	FFG_702	625492	3553761	705415	406166	25	32	22	Richey, 1989, Table 2
24	FFG_703	628006	3554508	713698	408555	25	32	23	Richey, 1989, Table 2
25	FFG_704	625492	3552956	705415	403526	25	32	27	Richey, 1989, Table 2
26	FFG_705	624099	3552123	700810	400825	25	32	28	Richey, 1989, Table 2
27	FFG_706	624300	3552123	701470	400825	25	32	28	Richey, 1989, Table 2
28	FFG_707	623679	3552427	699465	401825	25	32	29	Richey, 1989, Table 2
29	FFG_708	623679	3552930	699465	403475	25	32	29	Richey, 1989, Table 2
30	FFG_709	620746	3550770	689804	396452	25	32	31	Richey, 1989, Table 2
31	FFG_710	622771	3550799	696450	396515	25	32	32	Richey, 1989, Table 2
32	FFG_711	624012	3550012	700490	393900	25	32	33	Richey, 1989, Table 2
33	FFG_712	625263	3550440	704596	395271	25	32	33	Richey, 1989, Table 2
34	FFG_713	624830	3550038	703176	393951	25	32	33	Richey, 1989, Table 2
35	FFG_714	625626	3551242	705819	397905	25	32	34	Richey, 1989, Table 2
36	FFG_715	626840	3551268	709807	397957	25	32	34	Richey, 1989, Table 2
37	FFG_716	638420	3559464	747968	424622	25	33	1	Richey, 1989, Table 2
38	FFG_717	633193	3559403	730818	424522	25	33	5	Richey, 1989, Table 2

Table B.1. Location of Wells used by WIPP (Universal Transverse Mercator [UTM], State Plan Coordinates [stpln], and Survey Sections [township, range and section])

	Well ID	x-UTM	y-UTM	x-STPLN	y-STPLN	Township	Range	Section	Source
1	FFG_718	633234	3556994	730887	416614	25	33	8	Richey, 1989, Table 2
2	FFG_719	636829	3557836	742712	419312	25	33	11	Richey, 1989, Table 2
3	FFG_720	639698	3555152	752066	410438	25	33	13	Richey, 1989, Table 2
4	FFG_721	636045	3555837	740111	412751	25	33	15	Richey, 1989, Table 2
5	FFG_723	630458	3553740	721708	406002	25	33	19	Richey, 1989, Table 2
6	FFG_724	632860	3554578	729624	408686	25	33	20	Richey, 1989, Table 2
7	FFG_725	634859	3554589	736187	408691	25	33	21	Richey, 1989, Table 2
8	FFG_726	636908	3553407	742876	404776	25	33	23	Richey, 1989, Table 2
9	FFG_727	638515	3553426	748148	404806	25	33	24	Richey, 1989, Table 2
10	FFG_728	639741	3551836	752140	399555	25	33	25	Richey, 1989, Table 2
11	FFG_729	636519	3551797	741568	399493	25	33	27	Richey, 1989, Table 2
12	FFG_730	634908	3551777	736280	399460	25	33	28	Richey, 1989, Table 2
13	FFG_731	634882	3552983	736227	403421	25	33	28	Richey, 1989, Table 2
14	FFG_732	632068	3552542	726993	402039	25	33	29	Richey, 1989, Table 2
15	FFG_733	630508	3550122	721809	394129	25	33	31	Richey, 1989, Table 2
16	FFG_734	633325	3550558	731054	395493	25	33	32	Richey, 1989, Table 2
17	FFG_735	638531	3551412	748168	398200	25	33	36	Richey, 1989, Table 2
18	H1	613420	3581687	666391	498039	22	31	29	Mercer, 1983, Table 1
19	H10A	622949	3572457	697463	467561	23	32	20	Gonzales, 1989, Tables 3-6 and 3-7
20	H10B	622975	3572473	697549	467613	23	32	20	Gonzales, 1989, Tables 3-6 and 3-7
21	H10C	622976	3572449	697552	467525	23	32	20	Mercer, 1983, Table 1
22	H11B1	615346	3579130	672647	489617	22	31	33	Gonzales, 1989, Tables 3-6 and 3-7
23	H11B2	615348	3579107	672653	489542	22	31	33	Gonzales, 1989, Tables 3-6 and 3-7
24	H11B3	615367	3579127	672716	489608	22	31	33	Gonzales, 1989, Tables 3-6 and 3-7
25	H11B4	615301	3579131	672501	489620	22	31	33	Gonzales, 1989, Tables 3-6 and 3-7
26	H12	617023	3575452	678079	477535	23	31	15	Gonzales, 1989, Tables 3-6 and 3-7
27	H14	612341	3580354	662815	493697	22	31	29	Gonzales, 1989, Tables 3-6 and 3-7
28	H15	615315	3581859	672606	498572	22	31	28	Gonzales, 1989, Tables 3-6 and 3-7
29	H16	613369	3582212	666231	499726	22	31	20	Gonzales, 1989, Tables 3-6 and 3-7
30	H17	615718	3577513	673837	484304	23	31	3	Gonzales, 1989, Tables 3-6 and 3-7
31	H18	612264	3583166	662621	502926	22	31	20	Gonzales, 1989, Tables 3-6 and 3-7
32	H2A	612663	3581641	663897	497912	22	31	29	Gonzales, 1989, Tables 3-6 and 3-7
33	H2B1	612651	3581651	663860	497943	22	31	29	Gonzales, 1989, Tables 3-6 and 3-7
34	H2B2	612661	3581649	663890	497938	22	31	29	Gonzales, 1989, Tables 3-6 and 3-7
35	H2C	612663	3581662	663904	497992	22	31	29	Mercer, 1983, Table 1
36	H3	613735	3580895	667389	495440	22	31	29	Mercer, 1983, Table 1
37	H3B1	613729	3580895	667377	497440	22	31	29	Gonzales, 1989, Tables 3-6 and 3-7
38	H3B2	613701	3580906	667283	495476	22	31	29	Gonzales, 1989, Tables 3-6 and 3-7

Table B.1. Location of Wells used by WIPP (Universal Transverse Mercator [UTM], State Plan Coordinates [stpln], and Survey Sections [township, range and section])

	Well ID	x-UTM	y-UTM	x-STPLN	y-STPLN	Township	Range	Section	Source
1	H3B3	613705	3580876	667298	495376	22	31	29	Gonzales, 1989, Tables 3-6 and 3-7
2	H3D	613721	3580890	667350	495421	22	31	29	Gonzales, 1989, Tables 3-6 and 3-7
3	H4A	612407	3578469	662993	486962	23	31	5	Gonzales, 1989, Tables 3-6 and 3-7
4	H4B	612380	3578483	662906	487554	23	31	5	Gonzales, 1989, Tables 3-6 and 3-7
5	H4C	612404	3578497	662988	487603	23	31	5	Mercer, 1983, Table 1
6	H5A	616888	3584776	677828	508111	22	31	15	Gonzales, 1989, Tables 3-6 and 3-7
7	H5B	616872	3584801	677777	508194	22	31	15	Gonzales, 1989, Tables 3-6 and 3-7
8	H5C	616900	3584802	677873	508198	22	31	15	Mercer, 1983, Table 1
9	H6A	610580	3584982	657132	508881	22	31	18	Gonzales, 1989, Tables 3-6 and 3-7
10	H6B	610594	3585008	657180	508969	22	31	18	Gonzales, 1989, Tables 3-6 and 3-7
11	H6C	610609	3585027	657231	509066	22	31	18	Mercer, 1983, Table 1
12	H7A	608102	3574670	648790	475132	23	30	14	Gonzales, 1989, Tables 3-6 and 3-7
13	H7B1	608124	3574648	648862	475061	23	30	14	Gonzales, 1989, Tables 3-6 and 3-7
14	H7B2	608111	3574612	648837	474965	23	30	14	Gonzales, 1989, Tables 3-6 and 3-7
15	H7C	608086	3574632	648751	475020	23	30	14	Mercer, 1983, Table 1
16	H8A	608658	3563566	650392	438678	24	30	23	Gonzales, 1989, Tables 3-6 and 3-7
17	H8B	608683	3563556	650473	438646	24	30	23	Gonzales, 1989, Tables 3-6 and 3-7
18	H8C	608656	3563541	650397	438590	24	30	23	Mercer, 1983, Table 1
19	H9A	613958	3568260	667879	453977	24	31	4	Gonzales, 1989, Tables 3-6 and 3-7
20	H9B	613989	3568261	667979	453978	24	31	4	Gonzales, 1989, Tables 3-6 and 3-7
21	H9C	613965	3568233	667914	453889	24	31	4	Mercer, 1983, Table 1
22	MB139_1	613585	3582210	666913	499365	0	0	0	Krieg, 1984, Table I
23	MB139_2	613633	3582061	667069	498876	0	0	0	Krieg, 1984, Table I
24	MB139_3	613635	3582155	667076	499185	0	0	0	Krieg, 1984, Table I
25	MB139_4	613582	3582156	666902	499187	0	0	0	Krieg, 1984, Table I
26	P1	612339	3580339	662807	493649	22	31	29	Mercer, 1983, Table 1
27	P10	617074	3581193	678380	496355	22	31	26	Mercer, 1983, Table 1
28	P11	617016	3583462	678222	503799	22	31	23	Mercer, 1983, Table 1
29	P12	610454	3583452	656688	503899	22	30	24	Mercer, 1983, Table 1
30	P13	610539	3585079	657003	509237	22	31	18	Mercer, 1983, Table 1
31	P14	609083	3581974	652158	499079	22	30	24	Mercer, 1983, Table 1
32	P15	610624	3578793	657148	488609	22	31	31	Mercer, 1983, Table 1
33	P16	612704	3577312	663938	483715	23	31	5	Mercer, 1983, Table 1
34	P17	613929	3577459	667959	484166	23	31	4	Mercer, 1983, Table 1
35	P18	618367	3580352	682589	493561	22	31	26	Mercer, 1983, Table 1
36	P19	617687	3582410	680392	500348	22	31	23	Mercer, 1983, Table 1
37	P2	615315	3581850	672609	498541	22	31	28	Mercer, 1983, Table 1
38	P20	618541	3583770	683226	504775	22	31	14	Mercer, 1983, Table 1

Table B.1. Location of Wells used by WIPP (Universal Transverse Mercator [UTM], State Plan Coordinates [stpln], and Survey Sections [township, range and section])

	Well ID	x-UTM	y-UTM	x-STPLN	y-STPLN	Township	Range	Section	Source
1	P21	616901	3584847	677877	508345	22	31	15	Mercer, 1983, Table 1
2	P3	612799	3581888	664349	498733	22	31	20	Mercer, 1983, Table 1
3	P4	614936	3580324	671330	493533	22	31	28	Mercer, 1983, Table 1
4	P5	613686	3583535	667292	504105	22	31	17	Mercer, 1983, Table 1
5	P6	610591	3581133	657104	496288	22	31	30	Mercer, 1983, Table 1
6	P7	612305	3578476	662663	487535	23	31	5	Mercer, 1983, Table 1
7	P8	613827	3578467	667656	487472	23	31	4	Mercer, 1983, Table 1
8	P9	615365	3579125	672704	489600	22	31	33	Mercer, 1983, Table 1
9	SaltShft	613587	3582186	666919	499286	0	0	0	Krieg, 1984, Table I
10	USGS1	606462	3569459	643297	458066	23	30	34	Gonzales, 1989, Tables 3-6 and 3-7
11	USGS4	605841	3569887	641277	459483	23	30	34	Gonzales, 1989, Tables 3-6 and 3-7
12	USGS8	605879	3569888	641402	459483	23	30	34	Gonzales, 1989, Tables 3-6 and 3-7
13	WIPP11	613819	3586474	667796	513749	22	31	9	Mercer, 1983, Table 1
14	WIPP12	613709	3583524	667368	504067	22	31	17	Mercer, 1983, Table 1
15	WIPP13	612652	3584241	663901	506454	22	31	17	Mercer, 1983, Table 1
16	WIPP15	590057	3574585	589590	475231	23	35	18	Mercer, 1983, Table 1
17	WIPP16	602380	3597026	630458	548607	21	30	5	Mercer, 1983, Table 1
18	WIPP18	613731	3583179	667441	502935	22	31	20	Mercer, 1983, Table 1
19	WIPP19	613747	3582787	667461	501649	22	31	20	Mercer, 1983, Table 1
20	WIPP21	613747	3582349	667462	500213	22	31	20	Mercer, 1983, Table 1
21	WIPP22	613747	3582652	667462	501206	22	31	20	Mercer, 1983, Table 1
22	WIPP25	606391	3584037	643354	505885	22	30	15	Mercer, 1983, Table 1
23	WIPP26	604006	3581161	635496	496516	22	30	29	Mercer, 1983, Table 1
24	WIPP27	604425	3593073	637102	535603	21	30	21	Mercer, 1983, Table 1
25	WIPP28	611265	3594687	659578	540736	21	31	18	Mercer, 1983, Table 1
26	WIPP29	596981	3578700	612380	488570	22	29	34	Mercer, 1983, Table 1
27	WIPP30	613718	3589700	667532	524335	21	31	33	Mercer, 1983, Table 1
28	WIPP32	595909	3579081	608858	489850	22	29	33	Mercer, 1983, Table 1
29	WIPP33	609629	3584019	653981	505789	22	30	13	Mercer, 1983, Table 1
30	WIPP34	614333	3585141	669449	509375	22	31	9	Mercer, 1983, Table 1
31	WastShft	613595	3582061	666944	498876	0	0	0	Krieg, 1984, Table I

Table B.2. Elevations of Stratigraphic Layers Near WIPP

	Layer	Well ID	Elevation	Source
2	Anhydrt1	DOE2	-199.00	Mercer et al., 1987, Table 3-2
3	Anhydrt1	DOE2	-119.10	Mercer et al., 1987, Table 3-2
4	Anhydrt1	REF	-199.00	Rechard et al.,1991, Figure 2.2-1
5	Anhydrt1	REF	-119.10	Rechard et al.,1991, Figure 2.2-1
6	Anhydrt1	WIPP11	-43.90	SNL and USGS, 1982a, Table 2
7	Anhydrt1	WIPP11	-37.80	SNL and USGS, 1982a, Table 2
8	Anhydrt1	WIPP12	-139.00	SNL and D'Appolonia Consulting, 1983, Table 2
9	Anhydrt1	WIPP12	-131.10	SNL and D'Appolonia Consulting, 1983, Table 2
10	Anhydrt2	DOE1	-71.60	U.S. DOE, Sep 1982, Table 2
11	Anhydrt2	DOE1	-38.60	U.S. DOE, Sep 1982, Table 2
12	Anhydrt2	DOE2	-116.40	Mercer et al., 1987, Table 3-2
13	Anhydrt2	REF	-116.40	Rechard et al.,1991, Figure 2.2-1
14	Anhydrt2	WIPP11	-22.20	SNL and USGS, 1982a, Table 2
15	Anhydrt2	WIPP11	14.40	SNL and USGS, 1982a, Table 2
16	Anhydrt2	WIPP12	24.50	SNL and D'Appolonia Consulting, 1983, Table 2
17	Anhydrt2	WIPP12	57.80	SNL and D'Appolonia Consulting, 1983, Table 2
18	Anhydrt3	DOE1	30.00	U.S. DOE, Sep 1982, Table 2
19	Anhydrt3	DOE1	163.60	U.S. DOE, Sep 1982, Table 2
20	Anhydrt3	DOE2	102.30	Mercer et al., 1987, Table 3-2
21	Anhydrt3	ERDA9	162.00	SNL and USGS, 1982b, Table 2
22	Anhydrt3	ERDA9	178.10	SNL and USGS, 1982b, Table 2
23	Anhydrt3	REF	162.00	Rechard et al.,1991, Figure 2.2-1
24	Anhydrt3	REF	178.10	Rechard et al.,1991, Figure 2.2-1
25	Anhydrt3	WIPP11	309.40	SNL and USGS, 1982a, Table 2
26	Anhydrt3	WIPP11	334.10	SNL and USGS, 1982a, Table 2
27	Anhydrt3	WIPP12	127.30	SNL and D'Appolonia Consulting, 1983, Table 2
28	Anhydrt3	WIPP12	227.40	SNL and D'Appolonia Consulting, 1983, Table 2
29	Anhydrta	AirShft	386.41	Holt and Powers, 1990, Figure 22
30	Anhydrta	AirShft	386.70	Holt and Powers, 1990, Figure 22
31	Anhydrta	DH207	386.86	Krieg, 1984, Table I
32	Anhydrta	DH207	388.78	Krieg, 1984, Table I
33	Anhydrta	DH211	389.81	Krieg, 1984, Table I
34	Anhydrta	DH211	391.67	Krieg, 1984, Table I
35	Anhydrta	DH215	390.11	Krieg, 1984, Table I
36	Anhydrta	DH215	391.97	Krieg, 1984, Table I
37	Anhydrta	DH219	390.39	Krieg, 1984, Table I
38	Anhydrta	DH219	390.57	Krieg, 1984, Table I
39	Anhydrta	DH223	386.88	Krieg, 1984, Table I
40	Anhydrta	DH223	387.18	Krieg, 1984, Table I
41	Anhydrta	DH227	384.02	Krieg, 1984, Table I
42	Anhydrta	DH227	384.26	Krieg, 1984, Table I
43	Anhydrta	DH77	402.79	Krieg, 1984, Table I
44	Anhydrta	DH77	402.88	Krieg, 1984, Table I
45	Anhydrta	DO201	389.23	Krieg, 1984, Table I
46	Anhydrta	DO201	389.44	Krieg, 1984, Table I
47	Anhydrta	DO203	400.02	Krieg, 1984, Table I
48	Anhydrta	DO203	400.26	Krieg, 1984, Table I
49	Anhydrta	DO205	405.17	Krieg, 1984, Table I
50	Anhydrta	DO205	405.38	Krieg, 1984, Table I
51	Anhydrta	DO45	396.69	Krieg, 1984, Table I
52	Anhydrta	DO45	396.87	Krieg, 1984, Table I
53	Anhydrta	DO52	393.92	Krieg, 1984, Table I
54	Anhydrta	DO52	394.07	Krieg, 1984, Table I
55	Anhydrta	DO56	399.74	Krieg, 1984, Table I
56	Anhydrta	DO56	399.92	Krieg, 1984, Table I
57	Anhydrta	DO63	403.61	Krieg, 1984, Table I
58	Anhydrta	DO63	403.98	Krieg, 1984, Table I
59	Anhydrta	DO67	403.58	Krieg, 1984, Table I
60	Anhydrta	DO67	403.85	Krieg, 1984, Table I
61	Anhydrta	DO88	402.36	Krieg, 1984, Table I
62	Anhydrta	DO88	402.51	Krieg, 1984, Table I
63	Anhydrta	DO91	402.07	Krieg, 1984, Table I
64	Anhydrta	DO91	402.28	Krieg, 1984, Table I
65	Anhydrta	ExhtShft	389.78	Bechtel, Inc., 1986, Appendix F
66	Anhydrta	ExhtShft	390.03	Bechtel, Inc., 1986, Appendix F
67	Anhydrta	MB139_2	388.84	Krieg, 1984, Table I
68	Anhydrta	MB139_2	389.05	Krieg, 1984, Table I
69	Anhydrta	SaltShft	392.51	Bechtel, Inc., 1986, Appendix D
70	Anhydrta	SaltShft	392.74	Bechtel, Inc., 1986, Appendix D
71	Anhydrta	SaltShft	392.53	Krieg, 1984, Table I
72	Anhydrta	SaltShft	392.76	Krieg, 1984, Table I
73	Anhydrta	WastShft	388.76	Bechtel, Inc., 1986, Appendix E
74	Anhydrta	WastShft	388.97	Bechtel, Inc., 1986, Appendix E
75	Anhydrta	WastShft	389.01	Krieg, 1984, Table I
76	Anhydrta	WastShft	389.25	Krieg, 1984, Table I
77	Anhydrtb	DH207	386.65	Krieg, 1984, Table I

Table B.2. Elevations of Stratigraphic Layers Near WIPP (Continued)

	Layer	Well ID	Elevation	Source
2	Anhydrtb	DH207	386.70	Krieg, 1984, Table I
3	Anhydrtb	DH211	389.63	Krieg, 1984, Table I
4	Anhydrtb	DH211	389.66	Krieg, 1984, Table I
5	Anhydrtb	DH215	389.96	Krieg, 1984, Table I
6	Anhydrtb	DH215	390.02	Krieg, 1984, Table I
7	Anhydrtb	DH219	388.41	Krieg, 1984, Table I
8	Anhydrtb	DH219	388.42	Krieg, 1984, Table I
9	Anhydrtb	DH223	385.05	Krieg, 1984, Table I
10	Anhydrtb	DH223	385.05	Krieg, 1984, Table I
11	Anhydrtb	DH227	382.25	Krieg, 1984, Table I
12	Anhydrtb	DH227	382.25	Krieg, 1984, Table I
13	Anhydrtb	DH77	400.75	Krieg, 1984, Table I
14	Anhydrtb	DH77	400.83	Krieg, 1984, Table I
15	Anhydrtb	DO201	387.07	Krieg, 1984, Table I
16	Anhydrtb	DO201	387.13	Krieg, 1984, Table I
17	Anhydrtb	DO203	398.13	Krieg, 1984, Table I
18	Anhydrtb	DO203	398.19	Krieg, 1984, Table I
19	Anhydrtb	DO205	403.13	Krieg, 1984, Table I
20	Anhydrtb	DO205	403.19	Krieg, 1984, Table I
21	Anhydrtb	DO45	393.92	Krieg, 1984, Table I
22	Anhydrtb	DO45	393.95	Krieg, 1984, Table I
23	Anhydrtb	DO52	391.88	Krieg, 1984, Table I
24	Anhydrtb	DO52	391.94	Krieg, 1984, Table I
25	Anhydrtb	DO56	397.64	Krieg, 1984, Table I
26	Anhydrtb	DO56	397.70	Krieg, 1984, Table I
27	Anhydrtb	DO63	401.45	Krieg, 1984, Table I
28	Anhydrtb	DO63	401.51	Krieg, 1984, Table I
29	Anhydrtb	DO67	401.45	Krieg, 1984, Table I
30	Anhydrtb	DO67	401.53	Krieg, 1984, Table I
31	Anhydrtb	DO88	400.23	Krieg, 1984, Table I
32	Anhydrtb	DO88	400.30	Krieg, 1984, Table I
33	Anhydrtb	DO91	399.91	Krieg, 1984, Table I
34	Anhydrtb	DO91	399.96	Krieg, 1984, Table I
35	Anhydrtb	ExhtShft	387.66	Bechtel, Inc., 1986, Appendix F
36	Anhydrtb	ExhtShft	387.75	Bechtel, Inc., 1986, Appendix F
37	Anhydrtb	MB139_2	386.58	Krieg, 1984, Table I
38	Anhydrtb	MB139_2	386.61	Krieg, 1984, Table I
39	Anhydrtb	SaltShft	390.58	Bechtel, Inc., 1986, Appendix D
40	Anhydrtb	SaltShft	390.66	Bechtel, Inc., 1986, Appendix D
41	Anhydrtb	SaltShft	390.37	Krieg, 1984, Table I
42	Anhydrtb	SaltShft	390.45	Krieg, 1984, Table I
43	Anhydrtb	WastShft	386.57	Bechtel, Inc., 1986, Appendix E
44	Anhydrtb	WastShft	386.70	Bechtel, Inc., 1986, Appendix E
45	Anhydrtb	WastShft	386.91	Krieg, 1984, Table I
46	Anhydrtb	WastShft	386.97	Krieg, 1984, Table I
47	Anhydrtc	DH207	369.49	Krieg, 1984, Table I
48	Anhydrtc	DH207	369.55	Krieg, 1984, Table I
49	Anhydrtc	DH211	372.71	Krieg, 1984, Table I
50	Anhydrtc	DH211	372.80	Krieg, 1984, Table I
51	Anhydrtc	DH215	373.14	Krieg, 1984, Table I
52	Anhydrtc	DH215	373.20	Krieg, 1984, Table I
53	Anhydrtc	DH219	372.13	Krieg, 1984, Table I
54	Anhydrtc	DH219	372.19	Krieg, 1984, Table I
55	Anhydrtc	DH223	369.08	Krieg, 1984, Table I
56	Anhydrtc	DH223	369.17	Krieg, 1984, Table I
57	Anhydrtc	DH227	366.16	Krieg, 1984, Table I
58	Anhydrtc	DH227	366.22	Krieg, 1984, Table I
59	Anhydrtc	DH77	384.75	Krieg, 1984, Table I
60	Anhydrtc	DH77	384.81	Krieg, 1984, Table I
61	Anhydrtc	DO201	369.91	Krieg, 1984, Table I
62	Anhydrtc	DO201	370.03	Krieg, 1984, Table I
63	Anhydrtc	DO203	381.95	Krieg, 1984, Table I
64	Anhydrtc	DO203	382.01	Krieg, 1984, Table I
65	Anhydrtc	DO205	387.37	Krieg, 1984, Table I
66	Anhydrtc	DO205	387.43	Krieg, 1984, Table I
67	Anhydrtc	DO45	377.22	Krieg, 1984, Table I
68	Anhydrtc	DO45	377.28	Krieg, 1984, Table I
69	Anhydrtc	DO52	375.18	Krieg, 1984, Table I
70	Anhydrtc	DO52	375.24	Krieg, 1984, Table I
71	Anhydrtc	DO56	381.00	Krieg, 1984, Table I
72	Anhydrtc	DO56	381.09	Krieg, 1984, Table I
73	Anhydrtc	DO63	385.66	Krieg, 1984, Table I
74	Anhydrtc	DO63	385.84	Krieg, 1984, Table I
75	Anhydrtc	DO67	385.54	Krieg, 1984, Table I
76	Anhydrtc	DO67	385.63	Krieg, 1984, Table I
77	Anhydrtc	DO88	384.01	Krieg, 1984, Table I

Table B.2. Elevations of Stratigraphic Layers Near WIPP (Continued)

	Layer	Well ID	Elevation	Source
1	Anhydrtc	DO88	384.06	Krieg, 1984, Table I
2	Anhydrtc	DO91	384.03	Krieg, 1984, Table I
3	Anhydrtc	DO91	384.12	Krieg, 1984, Table I
4	Anhydrtc	SaltShft	373.09	Krieg, 1984, Table I
5	Anhydrtc	SaltShft	373.20	Krieg, 1984, Table I
6	B_CANyon	DOE2	-276.30	Mercer et al., 1987, Table 3-2
7	B_CANyon	DOE2	-199.00	Mercer et al., 1987, Table 3-2
8	B_CANyon	REF	-276.30	Rechard et al.,1991, Figure 2.2-1
9	B_CANyon	REF	-199.00	Rechard et al.,1991, Figure 2.2-1
10	Culebra	AEC7	848.50	Mercer, 1983, Table 1
11	Culebra	AEC8	822.70	Mercer, 1983, Table 1
12	Culebra	AirShft	824.48	Holt and Powers, 1990, Figure 22
13	Culebra	B25	824.50	Mercer, 1983, Table 1
14	Culebra	DOE1	806.10	U.S. DOE, Sep 1982, Table 2
15	Culebra	DOE2	790.80	Mercer et al., 1987, Table 3-2
16	Culebra	ERDA10	882.40	Mercer, 1983, Table 1
17	Culebra	ERDA6	862.60	Mercer, 1983, Table 1
18	Culebra	ERDA9	827.50	Mercer, 1983, Table 1
19	Culebra	ERDA9	823.40	SNL and USGS, 1982b, Table 2
20	Culebra	ExhtShft	821.57	Bechtel, Inc., 1986, Appendix F
21	Culebra	FFG_002	624.80	Richey, 1989, Table 2, p.21
22	Culebra	FFG_004	666.60	Richey, 1989, Table 2, p.21
23	Culebra	FFG_005	628.50	Richey, 1989, Table 2, p.21
24	Culebra	FFG_006	616.60	Richey, 1989, Table 2, p.21
25	Culebra	FFG_007	602.00	Richey, 1989, Table 2, p.21
26	Culebra	FFG_009	604.10	Richey, 1989, Table 2, p.21
27	Culebra	FFG_011	609.90	Richey, 1989, Table 2, p.21
28	Culebra	FFG_012	613.90	Richey, 1989, Table 2, p.21
29	Culebra	FFG_013	646.20	Richey, 1989, Table 2, p.21
30	Culebra	FFG_014	667.80	Richey, 1989, Table 2, p.21
31	Culebra	FFG_016	587.90	Richey, 1989, Table 2, p.21
32	Culebra	FFG_017	594.90	Richey, 1989, Table 2, p.22
33	Culebra	FFG_018	598.60	Richey, 1989, Table 2, p.22
34	Culebra	FFG_019	588.60	Richey, 1989, Table 2, p.22
35	Culebra	FFG_020	662.00	Richey, 1989, Table 2, p.22
36	Culebra	FFG_023	596.20	Richey, 1989, Table 2, p.22
37	Culebra	FFG_024	579.10	Richey, 1989, Table 2, p.22
38	Culebra	FFG_025	598.50	Richey, 1989, Table 2, p.22
39	Culebra	FFG_026	592.50	Richey, 1989, Table 2, p.22
40	Culebra	FFG_027	585.50	Richey, 1989, Table 2, p.22
41	Culebra	FFG_028	578.60	Richey, 1989, Table 2, p.22
42	Culebra	FFG_029	563.50	Richey, 1989, Table 2, p.22
43	Culebra	FFG_030	563.00	Richey, 1989, Table 2, p.22
44	Culebra	FFG_031	554.40	Richey, 1989, Table 2, p.22
45	Culebra	FFG_032	549.40	Richey, 1989, Table 2, p.22
46	Culebra	FFG_033	549.20	Richey, 1989, Table 2, p.22
47	Culebra	FFG_034	548.60	Richey, 1989, Table 2, p.23
48	Culebra	FFG_035	533.90	Richey, 1989, Table 2, p.23
49	Culebra	FFG_036	541.40	Richey, 1989, Table 2, p.23
50	Culebra	FFG_037	534.00	Richey, 1989, Table 2, p.23
51	Culebra	FFG_038	523.60	Richey, 1989, Table 2, p.23
52	Culebra	FFG_039	731.90	Richey, 1989, Table 2, p.23
53	Culebra	FFG_040	655.40	Richey, 1989, Table 2, p.23
54	Culebra	FFG_041	733.70	Richey, 1989, Table 2, p.23
55	Culebra	FFG_042	740.60	Richey, 1989, Table 2, p.23
56	Culebra	FFG_043	735.70	Richey, 1989, Table 2, p.23
57	Culebra	FFG_044	689.10	Richey, 1989, Table 2, p.23
58	Culebra	FFG_047	561.10	Richey, 1989, Table 2, p.23
59	Culebra	FFG_048	580.30	Richey, 1989, Table 2, p.23
60	Culebra	FFG_049	567.50	Richey, 1989, Table 2, p.23
61	Culebra	FFG_050	582.50	Richey, 1989, Table 2, p.24
62	Culebra	FFG_051	573.90	Richey, 1989, Table 2, p.24
63	Culebra	FFG_052	595.20	Richey, 1989, Table 2, p.24
64	Culebra	FFG_053	563.00	Richey, 1989, Table 2, p.24
65	Culebra	FFG_054	562.70	Richey, 1989, Table 2, p.24
66	Culebra	FFG_055	565.70	Richey, 1989, Table 2, p.24
67	Culebra	FFG_056	564.50	Richey, 1989, Table 2, p.24
68	Culebra	FFG_057	564.80	Richey, 1989, Table 2, p.24
69	Culebra	FFG_058	569.30	Richey, 1989, Table 2, p.24
70	Culebra	FFG_059	569.70	Richey, 1989, Table 2, p.24
71	Culebra	FFG_060	569.30	Richey, 1989, Table 2, p.24
72	Culebra	FFG_061	570.60	Richey, 1989, Table 2, p.24
73	Culebra	FFG_062	513.90	Richey, 1989, Table 2, p.24
74	Culebra	FFG_063	470.70	Richey, 1989, Table 2, p.24
75	Culebra	FFG_064	497.50	Richey, 1989, Table 2, p.24
76	Culebra	FFG_065	471.80	Richey, 1989, Table 2, p.24

Table B.2. Elevations of Stratigraphic Layers Near WIPP (Continued)

	Layer	Well ID	Elevation	Source		Layer	Well ID	Elevation	Source
1	Culebra	FFG_066	434.30	Richey, 1989, Table 2, p.24	39	Culebra	FFG_106	902.60	Richey, 1989, Table 2, p.27
2	Culebra	FFG_067	470.00	Richey, 1989, Table 2, p.25	40	Culebra	FFG_107	887.90	Richey, 1989, Table 2, p.27
3	Culebra	FFG_068	430.10	Richey, 1989, Table 2, p.25	41	Culebra	FFG_108	878.70	Richey, 1989, Table 2, p.27
4	Culebra	FFG_069	447.50	Richey, 1989, Table 2, p.25	42	Culebra	FFG_109	862.30	Richey, 1989, Table 2, p.27
5	Culebra	FFG_070	484.60	Richey, 1989, Table 2, p.25	43	Culebra	FFG_110	832.10	Richey, 1989, Table 2, p.27
6	Culebra	FFG_071	755.00	Richey, 1989, Table 2, p.25	44	Culebra	FFG_111	836.60	Richey, 1989, Table 2, p.27
7	Culebra	FFG_072	681.20	Richey, 1989, Table 2, p.25	45	Culebra	FFG_112	824.50	Richey, 1989, Table 2, p.28
8	Culebra	FFG_073	659.30	Richey, 1989, Table 2, p.25	46	Culebra	FFG_113	838.50	Richey, 1989, Table 2, p.28
9	Culebra	FFG_074	666.40	Richey, 1989, Table 2, p.25	47	Culebra	FFG_114	870.50	Richey, 1989, Table 2, p.28
10	Culebra	FFG_075	717.90	Richey, 1989, Table 2, p.25	48	Culebra	FFG_115	857.40	Richey, 1989, Table 2, p.28
11	Culebra	FFG_076	777.60	Richey, 1989, Table 2, p.25	49	Culebra	FFG_116	871.40	Richey, 1989, Table 2, p.28
12	Culebra	FFG_078	814.70	Richey, 1989, Table 2, p.25	50	Culebra	FFG_117	868.70	Richey, 1989, Table 2, p.28
13	Culebra	FFG_079	787.00	Richey, 1989, Table 2, p.25	51	Culebra	FFG_119	870.90	Richey, 1989, Table 2, p.28
14	Culebra	FFG_080	765.60	Richey, 1989, Table 2, p.25	52	Culebra	FFG_120	874.20	Richey, 1989, Table 2, p.28
15	Culebra	FFG_081	683.10	Richey, 1989, Table 2, p.26	53	Culebra	FFG_121	882.40	Richey, 1989, Table 2, p.28
16	Culebra	FFG_082	711.10	Richey, 1989, Table 2, p.26	54	Culebra	FFG_122	876.30	Richey, 1989, Table 2, p.28
17	Culebra	FFG_083	638.10	Richey, 1989, Table 2, p.26	55	Culebra	FFG_123	867.10	Richey, 1989, Table 2, p.28
18	Culebra	FFG_084	661.40	Richey, 1989, Table 2, p.26	56	Culebra	FFG_124	837.90	Richey, 1989, Table 2, p.28
19	Culebra	FFG_085	655.40	Richey, 1989, Table 2, p.26	57	Culebra	FFG_125	851.20	Richey, 1989, Table 2, p.28
20	Culebra	FFG_086	665.00	Richey, 1989, Table 2, p.26	58	Culebra	FFG_126	852.70	Richey, 1989, Table 2, p.28
21	Culebra	FFG_087	636.70	Richey, 1989, Table 2, p.26	59	Culebra	FFG_127	860.70	Richey, 1989, Table 2, p.28
22	Culebra	FFG_088	626.10	Richey, 1989, Table 2, p.26	60	Culebra	FFG_128	887.00	Richey, 1989, Table 2, p.28
23	Culebra	FFG_089	613.90	Richey, 1989, Table 2, p.26	61	Culebra	FFG_129	858.30	Richey, 1989, Table 2, p.28
24	Culebra	FFG_091	652.30	Richey, 1989, Table 2, p.26	62	Culebra	FFG_130	897.60	Richey, 1989, Table 2, p.28
25	Culebra	FFG_092	670.90	Richey, 1989, Table 2, p.26	63	Culebra	FFG_132	898.60	Richey, 1989, Table 2, p.29
26	Culebra	FFG_093	673.60	Richey, 1989, Table 2, p.26	64	Culebra	FFG_133	901.60	Richey, 1989, Table 2, p.29
27	Culebra	FFG_094	674.20	Richey, 1989, Table 2, p.26	65	Culebra	FFG_134	904.40	Richey, 1989, Table 2, p.29
28	Culebra	FFG_095	651.60	Richey, 1989, Table 2, p.26	66	Culebra	FFG_135	880.90	Richey, 1989, Table 2, p.29
29	Culebra	FFG_096	635.50	Richey, 1989, Table 2, p.26	67	Culebra	FFG_136	882.50	Richey, 1989, Table 2, p.29
30	Culebra	FFG_097	614.80	Richey, 1989, Table 2, p.27	68	Culebra	FFG_137	892.80	Richey, 1989, Table 2, p.29
31	Culebra	FFG_098	587.90	Richey, 1989, Table 2, p.27	69	Culebra	FFG_138	844.10	Richey, 1989, Table 2, p.29
32	Culebra	FFG_099	582.50	Richey, 1989, Table 2, p.27	70	Culebra	FFG_139	855.60	Richey, 1989, Table 2, p.29
33	Culebra	FFG_100	564.80	Richey, 1989, Table 2, p.27	71	Culebra	FFG_140	792.70	Richey, 1989, Table 2, p.29
34	Culebra	FFG_101	533.70	Richey, 1989, Table 2, p.27	72	Culebra	FFG_141	820.10	Richey, 1989, Table 2, p.29
35	Culebra	FFG_102	549.00	Richey, 1989, Table 2, p.27	73	Culebra	FFG_142	795.90	Richey, 1989, Table 2, p.29
36	Culebra	FFG_103	609.30	Richey, 1989, Table 2, p.27	74	Culebra	FFG_143	804.00	Richey, 1989, Table 2, p.29
37	Culebra	FFG_104	508.10	Richey, 1989, Table 2, p.27	75	Culebra	FFG_144	894.30	Richey, 1989, Table 2, p.29
38	Culebra	FFG_105	867.50	Richey, 1989, Table 2, p.27	76	Culebra	FFG_145	893.10	Richey, 1989, Table 2, p.29

Table B.2. Elevations of Stratigraphic Layers Near WIPP (Continued)

	Layer	Well ID	Elevation	Source
1	Culebra	FFG_146	906.80	Richey, 1989, Table 2, p.29
2	Culebra	FFG_147	882.70	Richey, 1989, Table 2, p.29
3	Culebra	FFG_148	900.10	Richey, 1989, Table 2, p.29
4	Culebra	FFG_149	910.70	Richey, 1989, Table 2, p.30
5	Culebra	FFG_155	901.30	Richey, 1989, Table 2, p.30
6	Culebra	FFG_156	906.50	Richey, 1989, Table 2, p.30
7	Culebra	FFG_157	904.10	Richey, 1989, Table 2, p.30
8	Culebra	FFG_158	928.10	Richey, 1989, Table 2, p.30
9	Culebra	FFG_159	898.60	Richey, 1989, Table 2, p.30
10	Culebra	FFG_160	895.20	Richey, 1989, Table 2, p.30
11	Culebra	FFG_161	901.00	Richey, 1989, Table 2, p.30
12	Culebra	FFG_162	891.90	Richey, 1989, Table 2, p.30
13	Culebra	FFG_163	897.40	Richey, 1989, Table 2, p.30
14	Culebra	FFG_164	937.60	Richey, 1989, Table 2, p.30
15	Culebra	FFG_165	912.80	Richey, 1989, Table 2, p.30
16	Culebra	FFG_166	900.00	Richey, 1989, Table 2, p.31
17	Culebra	FFG_167	887.00	Richey, 1989, Table 2, p.31
18	Culebra	FFG_168	906.50	Richey, 1989, Table 2, p.31
19	Culebra	FFG_169	919.20	Richey, 1989, Table 2, p.31
20	Culebra	FFG_170	903.70	Richey, 1989, Table 2, p.31
21	Culebra	FFG_171	922.10	Richey, 1989, Table 2, p.31
22	Culebra	FFG_172	915.30	Richey, 1989, Table 2, p.31
23	Culebra	FFG_173	876.90	Richey, 1989, Table 2, p.31
24	Culebra	FFG_177	889.10	Richey, 1989, Table 2, p.31
25	Culebra	FFG_178	718.10	Richey, 1989, Table 2, p.31
26	Culebra	FFG_179	886.60	Richey, 1989, Table 2, p.31
27	Culebra	FFG_180	883.00	Richey, 1989, Table 2, p.31
28	Culebra	FFG_181	930.50	Richey, 1989, Table 2, p.32
29	Culebra	FFG_182	812.60	Richey, 1989, Table 2, p.32
30	Culebra	FFG_183	904.40	Richey, 1989, Table 2, p.32
31	Culebra	FFG_184	891.20	Richey, 1989, Table 2, p.32
32	Culebra	FFG_185	899.50	Richey, 1989, Table 2, p.32
33	Culebra	FFG_186	827.90	Richey, 1989, Table 2, p.32
34	Culebra	FFG_188	845.80	Richey, 1989, Table 2, p.32
35	Culebra	FFG_189	867.80	Richey, 1989, Table 2, p.32
36	Culebra	FFG_190	843.60	Richey, 1989, Table 2, p.32
37	Culebra	FFG_191	845.50	Richey, 1989, Table 2, p.32
38	Culebra	FFG_192	774.50	Richey, 1989, Table 2, p.32
39	Culebra	FFG_194	788.50	Richey, 1989, Table 2, p.33
40	Culebra	FFG_195	803.50	Richey, 1989, Table 2, p.33
41	Culebra	FFG_196	837.00	Richey, 1989, Table 2, p.33
42	Culebra	FFG_197	841.00	Richey, 1989, Table 2, p.33
43	Culebra	FFG_198	840.90	Richey, 1989, Table 2, p.33
44	Culebra	FFG_199	827.00	Richey, 1989, Table 2, p.33
45	Culebra	FFG_200	838.20	Richey, 1989, Table 2, p.33
46	Culebra	FFG_201	838.20	Richey, 1989, Table 2, p.33
47	Culebra	FFG_202	773.80	Richey, 1989, Table 2, p.33
48	Culebra	FFG_203	776.00	Richey, 1989, Table 2, p.33
49	Culebra	FFG_204	813.50	Richey, 1989, Table 2, p.33
50	Culebra	FFG_205	825.10	Richey, 1989, Table 2, p.33
51	Culebra	FFG_206	837.00	Richey, 1989, Table 2, p.33
52	Culebra	FFG_207	833.60	Richey, 1989, Table 2, p.33
53	Culebra	FFG_208	843.10	Richey, 1989, Table 2, p.34
54	Culebra	FFG_209	838.20	Richey, 1989, Table 2, p.34
55	Culebra	FFG_210	827.50	Richey, 1989, Table 2, p.34
56	Culebra	FFG_212	817.50	Richey, 1989, Table 2, p.34
57	Culebra	FFG_213	837.90	Richey, 1989, Table 2, p.34
58	Culebra	FFG_214	818.40	Richey, 1989, Table 2, p.34
59	Culebra	FFG_215	793.10	Richey, 1989, Table 2, p.34
60	Culebra	FFG_216	688.80	Richey, 1989, Table 2, p.34
61	Culebra	FFG_217	814.80	Richey, 1989, Table 2, p.34
62	Culebra	FFG_218	803.50	Richey, 1989, Table 2, p.34
63	Culebra	FFG_219	848.80	Richey, 1989, Table 2, p.34
64	Culebra	FFG_220	798.60	Richey, 1989, Table 2, p.34
65	Culebra	FFG_221	756.50	Richey, 1989, Table 2, p.34
66	Culebra	FFG_222	713.30	Richey, 1989, Table 2, p.34
67	Culebra	FFG_224	597.80	Richey, 1989, Table 2, p.35
68	Culebra	FFG_225	603.50	Richey, 1989, Table 2, p.35
69	Culebra	FFG_226	601.80	Richey, 1989, Table 2, p.35
70	Culebra	FFG_228	588.30	Richey, 1989, Table 2, p.35
71	Culebra	FFG_229	614.70	Richey, 1989, Table 2, p.35
72	Culebra	FFG_230	601.10	Richey, 1989, Table 2, p.35
73	Culebra	FFG_231	619.90	Richey, 1989, Table 2, p.35
74	Culebra	FFG_232	631.50	Richey, 1989, Table 2, p.35
75	Culebra	FFG_233	624.00	Richey, 1989, Table 2, p.35
76	Culebra	FFG_234	660.20	Richey, 1989, Table 2, p.35

Table B.2. Elevations of Stratigraphic Layers Near WIPP (Continued)

	Layer	Well ID	Elevation	Source
1	Culebra	FFG_235	635.50	Richey, 1989, Table 2, p.35
2	Culebra	FFG_236	682.70	Richey, 1989, Table 2, p.35
3	Culebra	FFG_237	646.20	Richey, 1989, Table 2, p.35
4	Culebra	FFG_238	628.50	Richey, 1989, Table 2, p.36
5	Culebra	FFG_239	620.50	Richey, 1989, Table 2, p.36
6	Culebra	FFG_240	609.90	Richey, 1989, Table 2, p.36
7	Culebra	FFG_241	605.10	Richey, 1989, Table 2, p.36
8	Culebra	FFG_242	732.20	Richey, 1989, Table 2, p.36
9	Culebra	FFG_243	668.40	Richey, 1989, Table 2, p.36
10	Culebra	FFG_244	721.30	Richey, 1989, Table 2, p.36
11	Culebra	FFG_245	510.80	Richey, 1989, Table 2, p.36
12	Culebra	FFG_246	516.00	Richey, 1989, Table 2, p.36
13	Culebra	FFG_247	501.30	Richey, 1989, Table 2, p.36
14	Culebra	FFG_248	506.60	Richey, 1989, Table 2, p.36
15	Culebra	FFG_249	505.30	Richey, 1989, Table 2, p.36
16	Culebra	FFG_250	587.50	Richey, 1989, Table 2, p.36
17	Culebra	FFG_251	477.30	Richey, 1989, Table 2, p.36
18	Culebra	FFG_252	619.60	Richey, 1989, Table 2, p.36
19	Culebra	FFG_253	566.70	Richey, 1989, Table 2, p.36
20	Culebra	FFG_254	562.00	Richey, 1989, Table 2, p.36
21	Culebra	FFG_255	514.50	Richey, 1989, Table 2, p.37
22	Culebra	FFG_256	477.90	Richey, 1989, Table 2, p.37
23	Culebra	FFG_257	523.30	Richey, 1989, Table 2, p.37
24	Culebra	FFG_258	546.20	Richey, 1989, Table 2, p.37
25	Culebra	FFG_259	503.20	Richey, 1989, Table 2, p.37
26	Culebra	FFG_260	556.30	Richey, 1989, Table 2, p.37
27	Culebra	FFG_261	542.20	Richey, 1989, Table 2, p.37
28	Culebra	FFG_262	485.60	Richey, 1989, Table 2, p.37
29	Culebra	FFG_263	456.50	Richey, 1989, Table 2, p.37
30	Culebra	FFG_264	703.80	Richey, 1989, Table 2, p.37
31	Culebra	FFG_265	686.10	Richey, 1989, Table 2, p.37
32	Culebra	FFG_266	665.40	Richey, 1989, Table 2, p.37
33	Culebra	FFG_267	641.30	Richey, 1989, Table 2, p.37
34	Culebra	FFG_268	613.60	Richey, 1989, Table 2, p.37
35	Culebra	FFG_269	627.70	Richey, 1989, Table 2, p.38
36	Culebra	FFG_270	730.30	Richey, 1989, Table 2, p.38
37	Culebra	FFG_271	773.90	Richey, 1989, Table 2, p.38
38	Culebra	FFG_272	751.80	Richey, 1989, Table 2, p.38
39	Culebra	FFG_273	753.20	Richey, 1989, Table 2, p.38
40	Culebra	FFG_274	793.10	Richey, 1989, Table 2, p.38
41	Culebra	FFG_275	800.70	Richey, 1989, Table 2, p.38
42	Culebra	FFG_276	802.80	Richey, 1989, Table 2, p.38
43	Culebra	FFG_277	795.50	Richey, 1989, Table 2, p.38
44	Culebra	FFG_278	776.60	Richey, 1989, Table 2, p.38
45	Culebra	FFG_279	776.90	Richey, 1989, Table 2, p.38
46	Culebra	FFG_280	788.80	Richey, 1989, Table 2, p.38
47	Culebra	FFG_281	762.60	Richey, 1989, Table 2, p.38
48	Culebra	FFG_283	496.20	Richey, 1989, Table 2, p.39
49	Culebra	FFG_284	648.00	Richey, 1989, Table 2, p.39
50	Culebra	FFG_285	669.60	Richey, 1989, Table 2, p.39
51	Culebra	FFG_286	773.80	Richey, 1989, Table 2, p.39
52	Culebra	FFG_287	738.20	Richey, 1989, Table 2, p.39
53	Culebra	FFG_288	668.70	Richey, 1989, Table 2, p.39
54	Culebra	FFG_289	680.60	Richey, 1989, Table 2, p.39
55	Culebra	FFG_290	770.90	Richey, 1989, Table 2, p.39
56	Culebra	FFG_291	668.70	Richey, 1989, Table 2, p.39
57	Culebra	FFG_292	724.80	Richey, 1989, Table 2, p.39
58	Culebra	FFG_293	718.10	Richey, 1989, Table 2, p.39
59	Culebra	FFG_294	504.50	Richey, 1989, Table 2, p.39
60	Culebra	FFG_295	489.50	Richey, 1989, Table 2, p.39
61	Culebra	FFG_297	469.10	Richey, 1989, Table 2, p.39
62	Culebra	FFG_298	528.10	Richey, 1989, Table 2, p.40
63	Culebra	FFG_299	497.80	Richey, 1989, Table 2, p.40
64	Culebra	FFG_300	480.60	Richey, 1989, Table 2, p.40
65	Culebra	FFG_301	435.90	Richey, 1989, Table 2, p.40
66	Culebra	FFG_302	443.50	Richey, 1989, Table 2, p.40
67	Culebra	FFG_303	449.00	Richey, 1989, Table 2, p.40
68	Culebra	FFG_304	445.90	Richey, 1989, Table 2, p.40
69	Culebra	FFG_305	443.20	Richey, 1989, Table 2, p.40
70	Culebra	FFG_306	413.00	Richey, 1989, Table 2, p.40
71	Culebra	FFG_307	432.20	Richey, 1989, Table 2, p.40
72	Culebra	FFG_308	376.10	Richey, 1989, Table 2, p.40
73	Culebra	FFG_309	434.60	Richey, 1989, Table 2, p.40
74	Culebra	FFG_310	475.20	Richey, 1989, Table 2, p.40
75	Culebra	FFG_311	428.60	Richey, 1989, Table 2, p.40
76	Culebra	FFG_312	429.80	Richey, 1989, Table 2, p.40

Table B.2. Elevations of Stratigraphic Layers Near WIPP (Continued)

	Layer	Well ID	Elevation	Source
1	Culebra	FFG_313	870.30	Richey, 1989, Table 2, p.41
2	Culebra	FFG_314	788.90	Richey, 1989, Table 2, p.41
3	Culebra	FFG_315	701.50	Richey, 1989, Table 2, p.41
4	Culebra	FFG_316	678.40	Richey, 1989, Table 2, p.41
5	Culebra	FFG_317	732.40	Richey, 1989, Table 2, p.41
6	Culebra	FFG_318	710.20	Richey, 1989, Table 2, p.41
7	Culebra	FFG_319	704.60	Richey, 1989, Table 2, p.41
8	Culebra	FFG_320	669.40	Richey, 1989, Table 2, p.41
9	Culebra	FFG_321	668.40	Richey, 1989, Table 2, p.41
10	Culebra	FFG_322	669.80	Richey, 1989, Table 2, p.41
11	Culebra	FFG_323	675.20	Richey, 1989, Table 2, p.41
12	Culebra	FFG_324	699.50	Richey, 1989, Table 2, p.41
13	Culebra	FFG_325	762.30	Richey, 1989, Table 2, p.41
14	Culebra	FFG_326	706.50	Richey, 1989, Table 2, p.41
15	Culebra	FFG_327	689.80	Richey, 1989, Table 2, p.42
16	Culebra	FFG_328	673.80	Richey, 1989, Table 2, p.42
17	Culebra	FFG_329	669.00	Richey, 1989, Table 2, p.42
18	Culebra	FFG_330	669.50	Richey, 1989, Table 2, p.42
19	Culebra	FFG_331	652.90	Richey, 1989, Table 2, p.42
20	Culebra	FFG_332	639.50	Richey, 1989, Table 2, p.42
21	Culebra	FFG_333	650.60	Richey, 1989, Table 2, p.42
22	Culebra	FFG_334	644.90	Richey, 1989, Table 2, p.42
23	Culebra	FFG_335	663.30	Richey, 1989, Table 2, p.42
24	Culebra	FFG_336	658.10	Richey, 1989, Table 2, p.42
25	Culebra	FFG_337	641.90	Richey, 1989, Table 2, p.42
26	Culebra	FFG_338	646.90	Richey, 1989, Table 2, p.42
27	Culebra	FFG_339	611.70	Richey, 1989, Table 2, p.42
28	Culebra	FFG_340	617.80	Richey, 1989, Table 2, p.42
29	Culebra	FFG_342	682.70	Richey, 1989, Table 2, p.43
30	Culebra	FFG_344	659.10	Richey, 1989, Table 2, p.43
31	Culebra	FFG_345	678.60	Richey, 1989, Table 2, p.43
32	Culebra	FFG_347	699.50	Richey, 1989, Table 2, p.43
33	Culebra	FFG_348	738.50	Richey, 1989, Table 2, p.43
34	Culebra	FFG_349	714.50	Richey, 1989, Table 2, p.43
35	Culebra	FFG_350	745.20	Richey, 1989, Table 2, p.43
36	Culebra	FFG_351	629.40	Richey, 1989, Table 2, p.43
37	Culebra	FFG_352	629.40	Richey, 1989, Table 2, p.43
38	Culebra	FFG_353	651.10	Richey, 1989, Table 2, p.43
39	Culebra	FFG_354	762.00	Richey, 1989, Table 2, p.43
40	Culebra	FFG_361	955.20	Richey, 1989, Table 2, p.44
41	Culebra	FFG_362	919.30	Richey, 1989, Table 2, p.44
42	Culebra	FFG_363	947.00	Richey, 1989, Table 2, p.44
43	Culebra	FFG_364	918.30	Richey, 1989, Table 2, p.44
44	Culebra	FFG_366	911.60	Richey, 1989, Table 2, p.44
45	Culebra	FFG_367	931.70	Richey, 1989, Table 2, p.44
46	Culebra	FFG_370	968.70	Richey, 1989, Table 2, p.44
47	Culebra	FFG_371	965.70	Richey, 1989, Table 2, p.44
48	Culebra	FFG_372	949.10	Richey, 1989, Table 2, p.45
49	Culebra	FFG_373	909.00	Richey, 1989, Table 2, p.45
50	Culebra	FFG_374	908.30	Richey, 1989, Table 2, p.45
51	Culebra	FFG_376	947.60	Richey, 1989, Table 2, p.45
52	Culebra	FFG_381	914.70	Richey, 1989, Table 2, p.45
53	Culebra	FFG_383	908.30	Richey, 1989, Table 2, p.45
54	Culebra	FFG_384	921.10	Richey, 1989, Table 2, p.45
55	Culebra	FFG_385	915.90	Richey, 1989, Table 2, p.45
56	Culebra	FFG_387	911.10	Richey, 1989, Table 2, p.45
57	Culebra	FFG_388	900.70	Richey, 1989, Table 2, p.46
58	Culebra	FFG_389	924.80	Richey, 1989, Table 2, p.46
59	Culebra	FFG_390	919.60	Richey, 1989, Table 2, p.46
60	Culebra	FFG_391	919.20	Richey, 1989, Table 2, p.46
61	Culebra	FFG_392	910.50	Richey, 1989, Table 2, p.46
62	Culebra	FFG_393	785.60	Richey, 1989, Table 2, p.46
63	Culebra	FFG_394	882.40	Richey, 1989, Table 2, p.46
64	Culebra	FFG_395	874.50	Richey, 1989, Table 2, p.46
65	Culebra	FFG_396	853.80	Richey, 1989, Table 2, p.46
66	Culebra	FFG_398	771.70	Richey, 1989, Table 2, p.46
67	Culebra	FFG_399	785.20	Richey, 1989, Table 2, p.46
68	Culebra	FFG_401	839.70	Richey, 1989, Table 2, p.46
69	Culebra	FFG_402	947.10	Richey, 1989, Table 2, p.46
70	Culebra	FFG_403	914.60	Richey, 1989, Table 2, p.47
71	Culebra	FFG_404	873.30	Richey, 1989, Table 2, p.47
72	Culebra	FFG_407	908.00	Richey, 1989, Table 2, p.47
73	Culebra	FFG_408	907.10	Richey, 1989, Table 2, p.47
74	Culebra	FFG_409	943.10	Richey, 1989, Table 2, p.47
75	Culebra	FFG_411	887.30	Richey, 1989, Table 2, p.47
76	Culebra	FFG_413	915.10	Richey, 1989, Table 2, p.47

Table B.2. Elevations of Stratigraphic Layers Near WIPP (Continued)

	Layer	Well ID	Elevation	Source
1	Culebra	FFG_418	930.30	Richey, 1989, Table 2, p.48
2	Culebra	FFG_419	942.80	Richey, 1989, Table 2, p.48
3	Culebra	FFG_420	936.90	Richey, 1989, Table 2, p.48
4	Culebra	FFG_421	923.30	Richey, 1989, Table 2, p.48
5	Culebra	FFG_422	923.20	Richey, 1989, Table 2, p.48
6	Culebra	FFG_426	926.90	Richey, 1989, Table 2, p.48
7	Culebra	FFG_432	884.50	Richey, 1989, Table 2, p.48
8	Culebra	FFG_433	897.60	Richey, 1989, Table 2, p.48
9	Culebra	FFG_438	835.60	Richey, 1989, Table 2, p.49
10	Culebra	FFG_445	920.20	Richey, 1989, Table 2, p.49
11	Culebra	FFG_453	782.30	Richey, 1989, Table 2, p.50
12	Culebra	FFG_455	770.20	Richey, 1989, Table 2, p.50
13	Culebra	FFG_456	776.60	Richey, 1989, Table 2, p.50
14	Culebra	FFG_457	831.20	Richey, 1989, Table 2, p.50
15	Culebra	FFG_458	833.30	Richey, 1989, Table 2, p.50
16	Culebra	FFG_459	761.40	Richey, 1989, Table 2, p.50
17	Culebra	FFG_462	828.60	Richey, 1989, Table 2, p.50
18	Culebra	FFG_463	854.40	Richey, 1989, Table 2, p.51
19	Culebra	FFG_464	843.40	Richey, 1989, Table 2, p.51
20	Culebra	FFG_465	844.90	Richey, 1989, Table 2, p.51
21	Culebra	FFG_467	430.90	Richey, 1989, Table 2, p.51
22	Culebra	FFG_468	377.70	Richey, 1989, Table 2, p.51
23	Culebra	FFG_470	408.10	Richey, 1989, Table 2, p.51
24	Culebra	FFG_471	426.10	Richey, 1989, Table 2, p.51
25	Culebra	FFG_472	501.70	Richey, 1989, Table 2, p.51
26	Culebra	FFG_473	390.40	Richey, 1989, Table 2, p.51
27	Culebra	FFG_474	677.50	Richey, 1989, Table 2, p.51
28	Culebra	FFG_475	686.30	Richey, 1989, Table 2, p.51
29	Culebra	FFG_476	760.20	Richey, 1989, Table 2, p.51
30	Culebra	FFG_477	726.70	Richey, 1989, Table 2, p.51
31	Culebra	FFG_478	702.60	Richey, 1989, Table 2, p.52
32	Culebra	FFG_479	706.80	Richey, 1989, Table 2, p.52
33	Culebra	FFG_480	688.00	Richey, 1989, Table 2, p.52
34	Culebra	FFG_481	681.60	Richey, 1989, Table 2, p.52
35	Culebra	FFG_482	711.70	Richey, 1989, Table 2, p.52
36	Culebra	FFG_483	741.20	Richey, 1989, Table 2, p.52
37	Culebra	FFG_484	725.90	Richey, 1989, Table 2, p.52
38	Culebra	FFG_485	730.30	Richey, 1989, Table 2, p.52
39	Culebra	FFG_486	716.00	Richey, 1989, Table 2, p.52
40	Culebra	FFG_487	715.40	Richey, 1989, Table 2, p.52
41	Culebra	FFG_488	698.30	Richey, 1989, Table 2, p.52
42	Culebra	FFG_489	717.30	Richey, 1989, Table 2, p.52
43	Culebra	FFG_490	806.80	Richey, 1989, Table 2, p.52
44	Culebra	FFG_491	799.80	Richey, 1989, Table 2, p.52
45	Culebra	FFG_492	765.60	Richey, 1989, Table 2, p.52
46	Culebra	FFG_493	752.40	Richey, 1989, Table 2, p.53
47	Culebra	FFG_494	754.00	Richey, 1989, Table 2, p.53
48	Culebra	FFG_495	749.80	Richey, 1989, Table 2, p.53
49	Culebra	FFG_496	616.00	Richey, 1989, Table 2, p.53
50	Culebra	FFG_497	649.90	Richey, 1989, Table 2, p.53
51	Culebra	FFG_498	645.60	Richey, 1989, Table 2, p.53
52	Culebra	FFG_499	612.40	Richey, 1989, Table 2, p.53
53	Culebra	FFG_500	643.40	Richey, 1989, Table 2, p.53
54	Culebra	FFG_501	673.00	Richey, 1989, Table 2, p.53
55	Culebra	FFG_502	638.20	Richey, 1989, Table 2, p.53
56	Culebra	FFG_503	624.00	Richey, 1989, Table 2, p.53
57	Culebra	FFG_504	674.30	Richey, 1989, Table 2, p.53
58	Culebra	FFG_505	702.30	Richey, 1989, Table 2, p.53
59	Culebra	FFG_506	700.10	Richey, 1989, Table 2, p.53
60	Culebra	FFG_507	607.00	Richey, 1989, Table 2, p.53
61	Culebra	FFG_508	688.90	Richey, 1989, Table 2, p.53
62	Culebra	FFG_509	668.10	Richey, 1989, Table 2, p.54
63	Culebra	FFG_510	670.10	Richey, 1989, Table 2, p.54
64	Culebra	FFG_511	629.10	Richey, 1989, Table 2, p.54
65	Culebra	FFG_512	643.70	Richey, 1989, Table 2, p.54
66	Culebra	FFG_513	667.00	Richey, 1989, Table 2, p.54
67	Culebra	FFG_514	645.90	Richey, 1989, Table 2, p.54
68	Culebra	FFG_515	617.20	Richey, 1989, Table 2, p.54
69	Culebra	FFG_516	612.60	Richey, 1989, Table 2, p.54
70	Culebra	FFG_517	755.30	Richey, 1989, Table 2, p.54
71	Culebra	FFG_518	742.20	Richey, 1989, Table 2, p.54
72	Culebra	FFG_519	704.10	Richey, 1989, Table 2, p.54
73	Culebra	FFG_520	590.90	Richey, 1989, Table 2, p.54
74	Culebra	FFG_521	633.10	Richey, 1989, Table 2, p.54
75	Culebra	FFG_522	434.20	Richey, 1989, Table 2, p.54
76	Culebra	FFG_523	449.30	Richey, 1989, Table 2, p.54

Table B.2. Elevations of Stratigraphic Layers Near WIPP (Continued)

	Layer	Well ID	Elevation	Source		Layer	Well ID	Elevation	Source
1	Culebra	FFG_524	616.00	Richey, 1989, Table 2, p.55	39	Culebra	FFG_648	513.30	Richey, 1989, Table 2, p.60
2	Culebra	FFG_525	443.90	Richey, 1989, Table 2, p.55	40	Culebra	FFG_652	822.90	Richey, 1989, Table 2, p.60
3	Culebra	FFG_526	950.70	Richey, 1989, Table 2, p.55	41	Culebra	FFG_653	822.70	Richey, 1989, Table 2, p.61
4	Culebra	FFG_527	894.20	Richey, 1989, Table 2, p.55	42	Culebra	FFG_654	845.80	Richey, 1989, Table 2, p.61
5	Culebra	FFG_528	896.10	Richey, 1989, Table 2, p.55	43	Culebra	FFG_655	847.30	Richey, 1989, Table 2, p.61
6	Culebra	FFG_530	965.90	Richey, 1989, Table 2, p.55	44	Culebra	FFG_656	845.20	Richey, 1989, Table 2, p.61
7	Culebra	FFG_531	894.90	Richey, 1989, Table 2, p.55	45	Culebra	FFG_657	862.90	Richey, 1989, Table 2, p.61
8	Culebra	FFG_532	879.70	Richey, 1989, Table 2, p.55	46	Culebra	FFG_658	849.40	Richey, 1989, Table 2, p.61
9	Culebra	FFG_534	892.80	Richey, 1989, Table 2, p.55	47	Culebra	FFG_659	856.80	Richey, 1989, Table 2, p.61
10	Culebra	FFG_535	882.10	Richey, 1989, Table 2, p.55	48	Culebra	FFG_660	873.40	Richey, 1989, Table 2, p.61
11	Culebra	FFG_536	892.50	Richey, 1989, Table 2, p.55	49	Culebra	FFG_662	843.40	Richey, 1989, Table 2, p.61
12	Culebra	FFG_537	879.90	Richey, 1989, Table 2, p.55	50	Culebra	FFG_664	836.40	Richey, 1989, Table 2, p.61
13	Culebra	FFG_543	932.20	Richey, 1989, Table 2, p.56	51	Culebra	FFG_666	890.00	Richey, 1989, Table 2, p.62
14	Culebra	FFG_548	883.30	Richey, 1989, Table 2, p.56	52	Culebra	FFG_667	875.70	Richey, 1989, Table 2, p.62
15	Culebra	FFG_552	732.70	Richey, 1989, Table 2, p.56	53	Culebra	FFG_668	926.10	Richey, 1989, Table 2, p.62
16	Culebra	FFG_562	621.80	Richey, 1989, Table 2, p.57	54	Culebra	FFG_669	912.90	Richey, 1989, Table 2, p.62
17	Culebra	FFG_563	537.40	Richey, 1989, Table 2, p.57	55	Culebra	FFG_670	897.30	Richey, 1989, Table 2, p.62
18	Culebra	FFG_568	631.90	Richey, 1989, Table 2, p.57	56	Culebra	FFG_671	900.00	Richey, 1989, Table 2, p.62
19	Culebra	FFG_569	632.80	Richey, 1989, Table 2, p.57	57	Culebra	FFG_672	897.10	Richey, 1989, Table 2, p.62
20	Culebra	FFG_584	742.70	Richey, 1989, Table 2, p.58	58	Culebra	FFG_673	894.20	Richey, 1989, Table 2, p.62
21	Culebra	FFG_585	686.70	Richey, 1989, Table 2, p.58	59	Culebra	FFG_674	893.40	Richey, 1989, Table 2, p.62
22	Culebra	FFG_600	700.10	Richey, 1989, Table 2, p.58	60	Culebra	FFG_675	851.50	Richey, 1989, Table 2, p.62
23	Culebra	FFG_601	580.00	Richey, 1989, Table 2, p.58	61	Culebra	FFG_676	862.30	Richey, 1989, Table 2, p.62
24	Culebra	FFG_602	803.50	Richey, 1989, Table 2, p.58	62	Culebra	FFG_677	889.70	Richey, 1989, Table 2, p.62
25	Culebra	FFG_606	673.70	Richey, 1989, Table 2, p.58	63	Culebra	FFG_679	891.20	Richey, 1989, Table 2, p.62
26	Culebra	FFG_607	681.30	Richey, 1989, Table 2, p.59	64	Culebra	FFG_685	918.10	Richey, 1989, Table 2, p.63
27	Culebra	FFG_608	663.20	Richey, 1989, Table 2, p.59	65	Culebra	FFG_689	764.50	Richey, 1989, Table 2, p.63
28	Culebra	FFG_609	656.50	Richey, 1989, Table 2, p.59	66	Culebra	FFG_690	768.70	Richey, 1989, Table 2, p.63
29	Culebra	FFG_610	649.20	Richey, 1989, Table 2, p.59	67	Culebra	FFG_691	760.80	Richey, 1989, Table 2, p.63
30	Culebra	FFG_611	644.00	Richey, 1989, Table 2, p.59	68	Culebra	FFG_692	749.90	Richey, 1989, Table 2, p.63
31	Culebra	FFG_612	679.10	Richey, 1989, Table 2, p.59	69	Culebra	FFG_693	760.40	Richey, 1989, Table 2, p.63
32	Culebra	FFG_613	677.90	Richey, 1989, Table 2, p.59	70	Culebra	FFG_694	750.40	Richey, 1989, Table 2, p.63
33	Culebra	FFG_618	686.70	Richey, 1989, Table 2, p.59	71	Culebra	FFG_695	756.50	Richey, 1989, Table 2, p.63
34	Culebra	FFG_638	536.80	Richey, 1989, Table 2, p.60	72	Culebra	FFG_696	758.30	Richey, 1989, Table 2, p.63
35	Culebra	FFG_639	508.10	Richey, 1989, Table 2, p.60	73	Culebra	FFG_697	760.20	Richey, 1989, Table 2, p.64
36	Culebra	FFG_640	597.80	Richey, 1989, Table 2, p.60	74	Culebra	FFG_698	802.00	Richey, 1989, Table 2, p.64
37	Culebra	FFG_643	642.30	Richey, 1989, Table 2, p.60	75	Culebra	FFG_699	755.60	Richey, 1989, Table 2, p.64
38	Culebra	FFG_644	677.20	Richey, 1989, Table 2, p.60	76	Culebra	FFG_700	749.30	Richey, 1989, Table 2, p.64

Table B.2. Elevations of Stratigraphic Layers Near WIPP (Continued)

	Layer	Well ID	Elevation	Source		Layer	Well ID	Elevation	Source
1	Culebra	FFG_701	749.60	Richey, 1989, Table 2, p.64	39	Culebra	FFG_740	662.60	Richey, 1989, Table 2, p.66
2	Culebra	FFG_702	755.60	Richey, 1989, Table 2, p.64	40	Culebra	FFG_741	658.70	Richey, 1989, Table 2, p.66
3	Culebra	FFG_703	761.70	Richey, 1989, Table 2, p.64	41	Culebra	FFG_742	700.70	Richey, 1989, Table 2, p.67
4	Culebra	FFG_704	745.60	Richey, 1989, Table 2, p.64	42	Culebra	FFG_743	686.10	Richey, 1989, Table 2, p.67
5	Culebra	FFG_705	679.70	Richey, 1989, Table 2, p.64	43	Culebra	FFG_744	677.20	Richey, 1989, Table 2, p.67
6	Culebra	FFG_706	702.30	Richey, 1989, Table 2, p.64	44	Culebra	FFG_745	657.70	Richey, 1989, Table 2, p.67
7	Culebra	FFG_707	686.80	Richey, 1989, Table 2, p.64	45	Culebra	FFG_746	645.50	Richey, 1989, Table 2, p.67
8	Culebra	FFG_708	736.70	Richey, 1989, Table 2, p.64	46	Culebra	H1	829.70	Mercer, 1983, Table 1
9	Culebra	FFG_709	632.80	Richey, 1989, Table 2, p.64	47	Culebra	H10C	709.30	Mercer, 1983, Table 1
10	Culebra	FFG_710	631.60	Richey, 1989, Table 2, p.64	48	Culebra	H2C	839.70	Mercer, 1983, Table 1
11	Culebra	FFG_711	634.60	Richey, 1989, Table 2, p.65	49	Culebra	H3	828.50	Mercer, 1983, Table 1
12	Culebra	FFG_712	678.30	Richey, 1989, Table 2, p.65	50	Culebra	H4C	866.80	Mercer, 1983, Table 1
13	Culebra	FFG_713	620.70	Richey, 1989, Table 2, p.65	51	Culebra	H5C	794.90	Mercer, 1983, Table 1
14	Culebra	FFG_714	731.50	Richey, 1989, Table 2, p.65	52	Culebra	H6C	836.40	Mercer, 1983, Table 1
15	Culebra	FFG_715	741.80	Richey, 1989, Table 2, p.65	53	Culebra	H7C	891.90	Mercer, 1983, Table 1
16	Culebra	FFG_716	604.90	Richey, 1989, Table 2, p.65	54	Culebra	H8C	867.20	Mercer, 1983, Table 1
17	Culebra	FFG_717	672.20	Richey, 1989, Table 2, p.65	55	Culebra	H9C	840.90	Mercer, 1983, Table 1
18	Culebra	FFG_718	664.70	Richey, 1989, Table 2, p.65	56	Culebra	P1	855.60	Mercer, 1983, Table 1
19	Culebra	FFG_719	626.00	Richey, 1989, Table 2, p.65	57	Culebra	P10	785.70	Mercer, 1983, Table 1
20	Culebra	FFG_720	625.80	Richey, 1989, Table 2, p.65	58	Culebra	P11	790.00	Mercer, 1983, Table 1
21	Culebra	FFG_721	646.20	Richey, 1989, Table 2, p.65	59	Culebra	P12	835.50	Mercer, 1983, Table 1
22	Culebra	FFG_723	762.80	Richey, 1989, Table 2, p.65	60	Culebra	P13	835.50	Mercer, 1983, Table 1
23	Culebra	FFG_724	686.50	Richey, 1989, Table 2, p.65	61	Culebra	P14	849.40	Mercer, 1983, Table 1
24	Culebra	FFG_725	652.90	Richey, 1989, Table 2, p.65	62	Culebra	P15	883.00	Mercer, 1983, Table 1
25	Culebra	FFG_726	648.60	Richey, 1989, Table 2, p.65	63	Culebra	P16	858.90	Mercer, 1983, Table 1
26	Culebra	FFG_727	639.20	Richey, 1989, Table 2, p.66	64	Culebra	P17	846.70	Mercer, 1983, Table 1
27	Culebra	FFG_728	646.70	Richey, 1989, Table 2, p.66	65	Culebra	P18	782.70	Mercer, 1983, Table 1
28	Culebra	FFG_729	648.90	Richey, 1989, Table 2, p.66	66	Culebra	P19	785.80	Mercer, 1983, Table 1
29	Culebra	FFG_730	673.60	Richey, 1989, Table 2, p.66	67	Culebra	P2	799.20	Mercer, 1983, Table 1
30	Culebra	FFG_731	670.40	Richey, 1989, Table 2, p.66	68	Culebra	P20	792.50	Mercer, 1983, Table 1
31	Culebra	FFG_732	686.40	Richey, 1989, Table 2, p.66	69	Culebra	P21	795.50	Mercer, 1983, Table 1
32	Culebra	FFG_733	749.80	Richey, 1989, Table 2, p.66	70	Culebra	P3	835.40	Mercer, 1983, Table 1
33	Culebra	FFG_734	707.40	Richey, 1989, Table 2, p.66	71	Culebra	P4	813.50	Mercer, 1983, Table 1
34	Culebra	FFG_735	638.90	Richey, 1989, Table 2, p.66	72	Culebra	P5	812.90	Mercer, 1983, Table 1
35	Culebra	FFG_736	676.40	Richey, 1989, Table 2, p.66	73	Culebra	P6	858.60	Mercer, 1983, Table 1
36	Culebra	FFG_737	620.30	Richey, 1989, Table 2, p.66	74	Culebra	P7	864.40	Mercer, 1983, Table 1
37	Culebra	FFG_738	662.00	Richey, 1989, Table 2, p.66	75	Culebra	P8	846.10	Mercer, 1983, Table 1
38	Culebra	FFG_739	694.80	Richey, 1989, Table 2, p.66	76	Culebra	P9	816.30	Mercer, 1983, Table 1

Table B.2. Elevations of Stratigraphic Layers Near WIPP (Continued)

	Layer	Well ID	Elevation	Source
1	Culebra	REF	823.40	Rechard et al.,1991, Figure 2.2-1
2	Culebra	SaltShft	822.81	Bechtel, Inc., 1986, Appendix D
3	Culebra	WIPP11	786.90	Mercer, 1983, Table 1
4	Culebra	WIPP11	787.00	SNL and USGS, 1982a, Table 2
5	Culebra	WIPP12	811.30	SNL and D'Appolonia Consulting, 1983, Table 2
6	Culebra	WIPP12	811.40	Mercer, 1983, Table 1
7	Culebra	WIPP13	824.10	Mercer, 1983, Table 1
8	Culebra	WIPP16	679.70	Mercer, 1983, Table 1
9	Culebra	WIPP18	813.80	Mercer, 1983, Table 1
10	Culebra	WIPP19	816.00	Mercer, 1983, Table 1
11	Culebra	WIPP21	819.30	Mercer, 1983, Table 1
12	Culebra	WIPP22	818.00	Mercer, 1983, Table 1
13	Culebra	WIPP25	843.10	Mercer, 1983, Table 1
14	Culebra	WIPP26	904.00	Mercer, 1983, Table 1
15	Culebra	WIPP27	879.30	Mercer, 1983, Table 1
16	Culebra	WIPP28	892.20	Mercer, 1983, Table 1
17	Culebra	WIPP29	903.70	Mercer, 1983, Table 1
18	Culebra	WIPP30	852.60	Mercer, 1983, Table 1
19	Culebra	WIPP32	902.80	Mercer, 1983, Table 1
20	Culebra	WIPP33	845.30	Mercer, 1983, Table 1
21	Culebra	WIPP34	792.20	Mercer, 1983, Table 1
22	Culebra	WastShft	823.64	Bechtel, Inc., 1986, Appendix E
23	DeweyLk	AirShft	1022.02	Holt and Powers, 1990, Figure 22
24	DeweyLk	DOE1	1018.10	U.S. DOE, Sep 1982, Table 2
25	DeweyLk	DOE2	1001.30	Mercer et al., 1987, Table 3-2
26	DeweyLk	ERDA9	1023.30	SNL and USGS, 1982b, Table 2
27	DeweyLk	ExhtShft	1022.73	Bechtel, Inc., 1986, Appendix F
28	DeweyLk	REF	1023.30	Rechard et al.,1991, Figure 2.2-1
29	DeweyLk	SaltShft	1025.35	Bechtel, Inc., 1986, Appendix D
30	DeweyLk	WIPP11	995.20	SNL and USGS, 1982a, Table 2
31	DeweyLk	WIPP12	1010.90	SNL and D'Appolonia Consulting, 1983, Table 2
32	DeweyLk	WastShft	1009.97	Bechtel, Inc., 1986, Appendix E
33	Halite1	DOE1	-170.40	U.S. DOE, Sep 1982, Table 2
34	Halite1	DOE1	-71.60	U.S. DOE, Sep 1982, Table 2
35	Halite1	DOE2	-119.10	Mercer et al., 1987, Table 3-2
36	Halite1	DOE2	-116.40	Mercer et al., 1987, Table 3-2
37	Halite1	REF	-119.10	Rechard et al.,1991, Figure 2.2-1
38	Halite1	REF	-116.40	Rechard et al.,1991, Figure 2.2-1
39	Halite1	WIPP11	-37.80	SNL and USGS, 1982a, Table 2
40	Halite1	WIPP11	-22.20	SNL and USGS, 1982a, Table 2
41	Halite1	WIPP12	-131.10	SNL and D'Appolonia Consulting, 1983, Table 2
42	Halite1	WIPP12	24.50	SNL and D'Appolonia Consulting, 1983, Table 2
43	Halite2	DOE1	-38.60	U.S. DOE, Sep 1982, Table 2
44	Halite2	DOE1	30.00	U.S. DOE, Sep 1982, Table 2
45	Halite2	WIPP11	14.40	SNL and USGS, 1982a, Table 2
46	Halite2	WIPP11	309.40	SNL and USGS, 1982a, Table 2
47	Halite2	WIPP12	57.80	SNL and D'Appolonia Consulting, 1983, Table 2
48	Halite2	WIPP12	127.30	SNL and D'Appolonia Consulting, 1983, Table 2
49	L_Member	DOE1	163.60	U.S. DOE, Sep 1982, Table 2
50	L_Member	DOE2	102.30	Mercer et al., 1987, Table 3-2
51	L_Member	ERDA9	178.10	SNL and USGS, 1982b, Table 2
52	L_Member	REF	178.10	Rechard et al.,1991, Figure 2.2-1
53	L_Member	WIPP11	334.10	SNL and USGS, 1982a, Table 2
54	L_Member	WIPP12	227.40	SNL and D'Appolonia Consulting, 1983, Table 2
55	M49er	AEC7	911.90	Mercer, 1983, Table 1
56	M49er	AEC8	875.40	Mercer, 1983, Table 1
57	M49er	AirShft	877.42	Holt and Powers, 1990, Figure 22
58	M49er	B25	876.60	Mercer, 1983, Table 1
59	M49er	DOE1	855.20	U.S. DOE, Sep 1982, Table 2
60	M49er	DOE2	847.10	Mercer et al., 1987, Table 3-2
61	M49er	ERDA6	915.60	Mercer, 1983, Table 1
62	M49er	ERDA9	878.10	Mercer, 1983, Table 1
63	M49er	ERDA9	874.00	SNL and USGS, 1982b, Table 2
64	M49er	ExhtShft	872.52	Bechtel, Inc., 1986, Appendix F
65	M49er	FFG_002	686.10	Richey, 1989, Table 2, p.21
66	M49er	FFG_004	739.10	Richey, 1989, Table 2, p.21
67	M49er	FFG_005	693.80	Richey, 1989, Table 2, p.21
68	M49er	FFG_006	688.90	Richey, 1989, Table 2, p.21
69	M49er	FFG_007	678.20	Richey, 1989, Table 2, p.21
70	M49er	FFG_009	678.10	Richey, 1989, Table 2, p.21
71	M49er	FFG_011	684.60	Richey, 1989, Table 2, p.21
72	M49er	FFG_012	687.00	Richey, 1989, Table 2, p.21
73	M49er	FFG_013	696.80	Richey, 1989, Table 2, p.21
74	M49er	FFG_014	741.90	Richey, 1989, Table 2, p.21
75	M49er	FFG_016	666.90	Richey, 1989, Table 2, p.21
76	M49er	FFG_017	669.60	Richey, 1989, Table 2, p.22

Table B.2. Elevations of Stratigraphic Layers Near WIPP (Continued)

	Layer	Well ID	Elevation	Source		Layer	Well ID	Elevation	Source
1	M49er	FFG_018	672.40	Richey, 1989, Table 2, p.22	39	M49er	FFG_060	645.50	Richey, 1989, Table 2, p.24
2	M49er	FFG_019	666.30	Richey, 1989, Table 2, p.22	40	M49er	FFG_061	645.90	Richey, 1989, Table 2, p.24
3	M49er	FFG_020	740.70	Richey, 1989, Table 2, p.22	41	M49er	FFG_062	574.30	Richey, 1989, Table 2, p.24
4	M49er	FFG_023	678.50	Richey, 1989, Table 2, p.22	42	M49er	FFG_063	534.70	Richey, 1989, Table 2, p.24
5	M49er	FFG_024	662.00	Richey, 1989, Table 2, p.22	43	M49er	FFG_064	559.70	Richey, 1989, Table 2, p.24
6	M49er	FFG_025	674.10	Richey, 1989, Table 2, p.22	44	M49er	FFG_065	542.90	Richey, 1989, Table 2, p.24
7	M49er	FFG_026	670.80	Richey, 1989, Table 2, p.22	45	M49er	FFG_066	496.80	Richey, 1989, Table 2, p.24
8	M49er	FFG_027	664.20	Richey, 1989, Table 2, p.22	46	M49er	FFG_067	537.10	Richey, 1989, Table 2, p.25
9	M49er	FFG_028	629.80	Richey, 1989, Table 2, p.22	47	M49er	FFG_068	496.50	Richey, 1989, Table 2, p.25
10	M49er	FFG_029	616.00	Richey, 1989, Table 2, p.22	48	M49er	FFG_069	524.30	Richey, 1989, Table 2, p.25
11	M49er	FFG_030	616.60	Richey, 1989, Table 2, p.22	49	M49er	FFG_070	553.80	Richey, 1989, Table 2, p.25
12	M49er	FFG_031	609.60	Richey, 1989, Table 2, p.22	50	M49er	FFG_071	811.10	Richey, 1989, Table 2, p.25
13	M49er	FFG_032	611.90	Richey, 1989, Table 2, p.22	51	M49er	FFG_072	739.70	Richey, 1989, Table 2, p.25
14	M49er	FFG_033	607.20	Richey, 1989, Table 2, p.22	52	M49er	FFG_073	717.80	Richey, 1989, Table 2, p.25
15	M49er	FFG_034	601.30	Richey, 1989, Table 2, p.23	53	M49er	FFG_074	723.70	Richey, 1989, Table 2, p.25
16	M49er	FFG_035	590.30	Richey, 1989, Table 2, p.23	54	M49er	FFG_075	773.30	Richey, 1989, Table 2, p.25
17	M49er	FFG_036	602.60	Richey, 1989, Table 2, p.23	55	M49er	FFG_076	836.40	Richey, 1989, Table 2, p.25
18	M49er	FFG_037	592.90	Richey, 1989, Table 2, p.23	56	M49er	FFG_078	874.40	Richey, 1989, Table 2, p.25
19	M49er	FFG_038	579.40	Richey, 1989, Table 2, p.23	57	M49er	FFG_079	848.00	Richey, 1989, Table 2, p.25
20	M49er	FFG_039	798.60	Richey, 1989, Table 2, p.23	58	M49er	FFG_080	827.50	Richey, 1989, Table 2, p.25
21	M49er	FFG_040	740.70	Richey, 1989, Table 2, p.23	59	M49er	FFG_081	746.80	Richey, 1989, Table 2, p.26
22	M49er	FFG_041	801.00	Richey, 1989, Table 2, p.23	60	M49er	FFG_082	779.10	Richey, 1989, Table 2, p.26
23	M49er	FFG_042	805.50	Richey, 1989, Table 2, p.23	61	M49er	FFG_083	693.00	Richey, 1989, Table 2, p.26
24	M49er	FFG_043	810.00	Richey, 1989, Table 2, p.23	62	M49er	FFG_084	721.10	Richey, 1989, Table 2, p.26
25	M49er	FFG_044	762.30	Richey, 1989, Table 2, p.23	63	M49er	FFG_085	714.20	Richey, 1989, Table 2, p.26
26	M49er	FFG_047	633.40	Richey, 1989, Table 2, p.23	64	M49er	FFG_086	722.60	Richey, 1989, Table 2, p.26
27	M49er	FFG_048	653.20	Richey, 1989, Table 2, p.23	65	M49er	FFG_087	698.00	Richey, 1989, Table 2, p.26
28	M49er	FFG_049	641.90	Richey, 1989, Table 2, p.23	66	M49er	FFG_088	694.40	Richey, 1989, Table 2, p.26
29	M49er	FFG_050	648.00	Richey, 1989, Table 2, p.24	67	M49er	FFG_089	675.80	Richey, 1989, Table 2, p.26
30	M49er	FFG_051	648.90	Richey, 1989, Table 2, p.24	68	M49er	FFG_091	720.00	Richey, 1989, Table 2, p.26
31	M49er	FFG_052	651.60	Richey, 1989, Table 2, p.24	69	M49er	FFG_092	734.90	Richey, 1989, Table 2, p.26
32	M49er	FFG_053	642.80	Richey, 1989, Table 2, p.24	70	M49er	FFG_093	737.30	Richey, 1989, Table 2, p.26
33	M49er	FFG_054	641.90	Richey, 1989, Table 2, p.24	71	M49er	FFG_094	740.60	Richey, 1989, Table 2, p.26
34	M49er	FFG_055	641.60	Richey, 1989, Table 2, p.24	72	M49er	FFG_095	706.50	Richey, 1989, Table 2, p.26
35	M49er	FFG_056	644.30	Richey, 1989, Table 2, p.24	73	M49er	FFG_096	689.50	Richey, 1989, Table 2, p.26
36	M49er	FFG_057	645.60	Richey, 1989, Table 2, p.24	74	M49er	FFG_097	671.20	Richey, 1989, Table 2, p.27
37	M49er	FFG_058	641.00	Richey, 1989, Table 2, p.24	75	M49er	FFG_098	645.50	Richey, 1989, Table 2, p.27
38	M49er	FFG_059	643.40	Richey, 1989, Table 2, p.24	76	M49er	FFG_099	641.60	Richey, 1989, Table 2, p.27

Table B.2. Elevations of Stratigraphic Layers Near WIPP (Continued)

	Layer	Well ID	Elevation	Source		Layer	Well ID	Elevation	Source
1	M49er	FFG_100	624.90	Richey, 1989, Table 2, p.27	39	M49er	FFG_141	873.10	Richey, 1989, Table 2, p.29
2	M49er	FFG_101	593.10	Richey, 1989, Table 2, p.27	40	M49er	FFG_142	849.30	Richey, 1989, Table 2, p.29
3	M49er	FFG_102	613.90	Richey, 1989, Table 2, p.27	41	M49er	FFG_143	855.80	Richey, 1989, Table 2, p.29
4	M49er	FFG_103	674.60	Richey, 1989, Table 2, p.27	42	M49er	FFG_159	956.20	Richey, 1989, Table 2, p.30
5	M49er	FFG_104	572.50	Richey, 1989, Table 2, p.27	43	M49er	FFG_160	950.10	Richey, 1989, Table 2, p.30
6	M49er	FFG_105	926.90	Richey, 1989, Table 2, p.27	44	M49er	FFG_161	957.40	Richey, 1989, Table 2, p.30
7	M49er	FFG_106	954.70	Richey, 1989, Table 2, p.27	45	M49er	FFG_162	955.90	Richey, 1989, Table 2, p.30
8	M49er	FFG_107	945.20	Richey, 1989, Table 2, p.27	46	M49er	FFG_163	955.30	Richey, 1989, Table 2, p.30
9	M49er	FFG_108	933.60	Richey, 1989, Table 2, p.27	47	M49er	FFG_166	954.30	Richey, 1989, Table 2, p.31
10	M49er	FFG_109	917.20	Richey, 1989, Table 2, p.27	48	M49er	FFG_167	936.70	Richey, 1989, Table 2, p.31
11	M49er	FFG_110	887.00	Richey, 1989, Table 2, p.27	49	M49er	FFG_168	967.50	Richey, 1989, Table 2, p.31
12	M49er	FFG_111	896.70	Richey, 1989, Table 2, p.27	50	M49er	FFG_169	980.20	Richey, 1989, Table 2, p.31
13	M49er	FFG_112	879.30	Richey, 1989, Table 2, p.28	51	M49er	FFG_170	933.60	Richey, 1989, Table 2, p.31
14	M49er	FFG_113	893.40	Richey, 1989, Table 2, p.28	52	M49er	FFG_173	934.80	Richey, 1989, Table 2, p.31
15	M49er	FFG_114	924.20	Richey, 1989, Table 2, p.28	53	M49er	FFG_180	943.90	Richey, 1989, Table 2, p.31
16	M49er	FFG_115	913.80	Richey, 1989, Table 2, p.28	54	M49er	FFG_182	856.50	Richey, 1989, Table 2, p.32
17	M49er	FFG_116	929.30	Richey, 1989, Table 2, p.28	55	M49er	FFG_189	922.70	Richey, 1989, Table 2, p.32
18	M49er	FFG_117	935.70	Richey, 1989, Table 2, p.28	56	M49er	FFG_190	901.60	Richey, 1989, Table 2, p.32
19	M49er	FFG_120	944.30	Richey, 1989, Table 2, p.28	57	M49er	FFG_191	901.30	Richey, 1989, Table 2, p.32
20	M49er	FFG_121	946.40	Richey, 1989, Table 2, p.28	58	M49er	FFG_192	834.50	Richey, 1989, Table 2, p.32
21	M49er	FFG_122	944.90	Richey, 1989, Table 2, p.28	59	M49er	FFG_194	839.70	Richey, 1989, Table 2, p.33
22	M49er	FFG_123	928.10	Richey, 1989, Table 2, p.28	60	M49er	FFG_195	855.30	Richey, 1989, Table 2, p.33
23	M49er	FFG_124	900.40	Richey, 1989, Table 2, p.28	61	M49er	FFG_196	897.60	Richey, 1989, Table 2, p.33
24	M49er	FFG_125	912.20	Richey, 1989, Table 2, p.28	62	M49er	FFG_197	899.50	Richey, 1989, Table 2, p.33
25	M49er	FFG_126	904.50	Richey, 1989, Table 2, p.28	63	M49er	FFG_198	898.20	Richey, 1989, Table 2, p.33
26	M49er	FFG_127	909.50	Richey, 1989, Table 2, p.28	64	M49er	FFG_199	888.80	Richey, 1989, Table 2, p.33
27	M49er	FFG_128	948.00	Richey, 1989, Table 2, p.28	65	M49er	FFG_200	902.50	Richey, 1989, Table 2, p.33
28	M49er	FFG_129	923.80	Richey, 1989, Table 2, p.28	66	M49er	FFG_201	894.60	Richey, 1989, Table 2, p.33
29	M49er	FFG_130	954.00	Richey, 1989, Table 2, p.28	67	M49er	FFG_202	834.20	Richey, 1989, Table 2, p.33
30	M49er	FFG_132	956.50	Richey, 1989, Table 2, p.29	68	M49er	FFG_203	841.30	Richey, 1989, Table 2, p.33
31	M49er	FFG_133	959.50	Richey, 1989, Table 2, p.29	69	M49er	FFG_204	864.80	Richey, 1989, Table 2, p.33
32	M49er	FFG_134	963.80	Richey, 1989, Table 2, p.29	70	M49er	FFG_205	880.60	Richey, 1989, Table 2, p.33
33	M49er	FFG_135	937.30	Richey, 1989, Table 2, p.29	71	M49er	FFG_206	895.80	Richey, 1989, Table 2, p.33
34	M49er	FFG_136	934.30	Richey, 1989, Table 2, p.29	72	M49er	FFG_207	892.20	Richey, 1989, Table 2, p.33
35	M49er	FFG_137	946.80	Richey, 1989, Table 2, p.29	73	M49er	FFG_208	902.80	Richey, 1989, Table 2, p.34
36	M49er	FFG_138	897.40	Richey, 1989, Table 2, p.29	74	M49er	FFG_210	885.80	Richey, 1989, Table 2, p.34
37	M49er	FFG_139	907.70	Richey, 1989, Table 2, p.29	75	M49er	FFG_212	870.50	Richey, 1989, Table 2, p.34
38	M49er	FFG_140	849.10	Richey, 1989, Table 2, p.29	76	M49er	FFG_213	903.50	Richey, 1989, Table 2, p.34

Table B.2. Elevations of Stratigraphic Layers Near WIPP (Continued)

	Layer	Well ID	Elevation	Source		Layer	Well ID	Elevation	Source
1	M49er	FFG_214	877.80	Richey, 1989, Table 2, p.34	39	M49er	FFG_254	651.00	Richey, 1989, Table 2, p.36
2	M49er	FFG_215	852.50	Richey, 1989, Table 2, p.34	40	M49er	FFG_255	609.90	Richey, 1989, Table 2, p.37
3	M49er	FFG_216	737.00	Richey, 1989, Table 2, p.34	41	M49er	FFG_256	557.80	Richey, 1989, Table 2, p.37
4	M49er	FFG_217	873.60	Richey, 1989, Table 2, p.34	42	M49er	FFG_257	600.40	Richey, 1989, Table 2, p.37
5	M49er	FFG_218	863.50	Richey, 1989, Table 2, p.34	43	M49er	FFG_258	615.00	Richey, 1989, Table 2, p.37
6	M49er	FFG_219	910.40	Richey, 1989, Table 2, p.34	44	M49er	FFG_259	584.90	Richey, 1989, Table 2, p.37
7	M49er	FFG_220	859.90	Richey, 1989, Table 2, p.34	45	M49er	FFG_260	621.80	Richey, 1989, Table 2, p.37
8	M49er	FFG_221	814.40	Richey, 1989, Table 2, p.34	46	M49er	FFG_261	610.20	Richey, 1989, Table 2, p.37
9	M49er	FFG_222	770.60	Richey, 1989, Table 2, p.34	47	M49er	FFG_263	553.40	Richey, 1989, Table 2, p.37
10	M49er	FFG_224	677.00	Richey, 1989, Table 2, p.35	48	M49er	FFG_264	777.60	Richey, 1989, Table 2, p.37
11	M49er	FFG_225	683.70	Richey, 1989, Table 2, p.35	49	M49er	FFG_265	775.40	Richey, 1989, Table 2, p.37
12	M49er	FFG_226	683.20	Richey, 1989, Table 2, p.35	50	M49er	FFG_266	758.90	Richey, 1989, Table 2, p.37
13	M49er	FFG_228	673.70	Richey, 1989, Table 2, p.35	51	M49er	FFG_267	736.40	Richey, 1989, Table 2, p.37
14	M49er	FFG_229	701.60	Richey, 1989, Table 2, p.35	52	M49er	FFG_268	716.00	Richey, 1989, Table 2, p.37
15	M49er	FFG_230	688.60	Richey, 1989, Table 2, p.35	53	M49er	FFG_269	729.20	Richey, 1989, Table 2, p.38
16	M49er	FFG_231	704.00	Richey, 1989, Table 2, p.35	54	M49er	FFG_270	791.80	Richey, 1989, Table 2, p.38
17	M49er	FFG_232	717.80	Richey, 1989, Table 2, p.35	55	M49er	FFG_271	833.90	Richey, 1989, Table 2, p.38
18	M49er	FFG_233	709.30	Richey, 1989, Table 2, p.35	56	M49er	FFG_272	846.60	Richey, 1989, Table 2, p.38
19	M49er	FFG_234	745.80	Richey, 1989, Table 2, p.35	57	M49er	FFG_273	816.90	Richey, 1989, Table 2, p.38
20	M49er	FFG_235	722.40	Richey, 1989, Table 2, p.35	58	M49er	FFG_274	851.00	Richey, 1989, Table 2, p.38
21	M49er	FFG_236	768.40	Richey, 1989, Table 2, p.35	59	M49er	FFG_275	858.60	Richey, 1989, Table 2, p.38
22	M49er	FFG_237	735.30	Richey, 1989, Table 2, p.35	60	M49er	FFG_276	861.60	Richey, 1989, Table 2, p.38
23	M49er	FFG_238	716.60	Richey, 1989, Table 2, p.36	61	M49er	FFG_277	853.50	Richey, 1989, Table 2, p.38
24	M49er	FFG_239	703.10	Richey, 1989, Table 2, p.36	62	M49er	FFG_278	868.40	Richey, 1989, Table 2, p.38
25	M49er	FFG_240	695.20	Richey, 1989, Table 2, p.36	63	M49er	FFG_279	860.10	Richey, 1989, Table 2, p.38
26	M49er	FFG_241	688.90	Richey, 1989, Table 2, p.36	64	M49er	FFG_280	858.60	Richey, 1989, Table 2, p.38
27	M49er	FFG_242	799.80	Richey, 1989, Table 2, p.36	65	M49er	FFG_281	835.80	Richey, 1989, Table 2, p.38
28	M49er	FFG_243	763.80	Richey, 1989, Table 2, p.36	66	M49er	FFG_283	584.60	Richey, 1989, Table 2, p.39
29	M49er	FFG_244	798.40	Richey, 1989, Table 2, p.36	67	M49er	FFG_284	730.30	Richey, 1989, Table 2, p.39
30	M49er	FFG_245	597.10	Richey, 1989, Table 2, p.36	68	M49er	FFG_285	760.20	Richey, 1989, Table 2, p.39
31	M49er	FFG_246	601.70	Richey, 1989, Table 2, p.36	69	M49er	FFG_286	837.50	Richey, 1989, Table 2, p.39
32	M49er	FFG_247	589.10	Richey, 1989, Table 2, p.36	70	M49er	FFG_287	812.00	Richey, 1989, Table 2, p.39
33	M49er	FFG_248	594.70	Richey, 1989, Table 2, p.36	71	M49er	FFG_288	765.70	Richey, 1989, Table 2, p.39
34	M49er	FFG_249	593.70	Richey, 1989, Table 2, p.36	72	M49er	FFG_289	736.30	Richey, 1989, Table 2, p.39
35	M49er	FFG_250	674.10	Richey, 1989, Table 2, p.36	73	M49er	FFG_290	825.70	Richey, 1989, Table 2, p.39
36	M49er	FFG_251	568.70	Richey, 1989, Table 2, p.36	74	M49er	FFG_291	766.20	Richey, 1989, Table 2, p.39
37	M49er	FFG_252	708.60	Richey, 1989, Table 2, p.36	75	M49er	FFG_292	774.20	Richey, 1989, Table 2, p.39
38	M49er	FFG_253	660.50	Richey, 1989, Table 2, p.36	76	M49er	FFG_293	766.00	Richey, 1989, Table 2, p.39

Table B.2. Elevations of Stratigraphic Layers Near WIPP (Continued)

	Layer	Well ID	Elevation	Source		Layer	Well ID	Elevation	Source
1	M49er	FFG_294	595.30	Richey, 1989, Table 2, p.39	39	M49er	FFG_333	746.30	Richey, 1989, Table 2, p.42
2	M49er	FFG_295	582.80	Richey, 1989, Table 2, p.39	40	M49er	FFG_334	743.10	Richey, 1989, Table 2, p.42
3	M49er	FFG_297	567.50	Richey, 1989, Table 2, p.39	41	M49er	FFG_335	757.10	Richey, 1989, Table 2, p.42
4	M49er	FFG_298	569.20	Richey, 1989, Table 2, p.40	42	M49er	FFG_336	754.40	Richey, 1989, Table 2, p.42
5	M49er	FFG_299	594.40	Richey, 1989, Table 2, p.40	43	M49er	FFG_337	738.50	Richey, 1989, Table 2, p.42
6	M49er	FFG_300	543.70	Richey, 1989, Table 2, p.40	44	M49er	FFG_338	744.80	Richey, 1989, Table 2, p.42
7	M49er	FFG_301	514.80	Richey, 1989, Table 2, p.40	45	M49er	FFG_339	711.10	Richey, 1989, Table 2, p.42
8	M49er	FFG_302	542.50	Richey, 1989, Table 2, p.40	46	M49er	FFG_340	721.40	Richey, 1989, Table 2, p.42
9	M49er	FFG_303	535.90	Richey, 1989, Table 2, p.40	47	M49er	FFG_342	747.60	Richey, 1989, Table 2, p.43
10	M49er	FFG_304	540.40	Richey, 1989, Table 2, p.40	48	M49er	FFG_344	713.40	Richey, 1989, Table 2, p.43
11	M49er	FFG_305	534.60	Richey, 1989, Table 2, p.40	49	M49er	FFG_345	775.50	Richey, 1989, Table 2, p.43
12	M49er	FFG_306	492.20	Richey, 1989, Table 2, p.40	50	M49er	FFG_347	766.00	Richey, 1989, Table 2, p.43
13	M49er	FFG_307	517.90	Richey, 1989, Table 2, p.40	51	M49er	FFG_348	790.90	Richey, 1989, Table 2, p.43
14	M49er	FFG_308	491.30	Richey, 1989, Table 2, p.40	52	M49er	FFG_349	764.20	Richey, 1989, Table 2, p.43
15	M49er	FFG_309	535.20	Richey, 1989, Table 2, p.40	53	M49er	FFG_350	808.90	Richey, 1989, Table 2, p.43
16	M49er	FFG_310	564.20	Richey, 1989, Table 2, p.40	54	M49er	FFG_351	732.20	Richey, 1989, Table 2, p.43
17	M49er	FFG_311	498.70	Richey, 1989, Table 2, p.40	55	M49er	FFG_352	731.50	Richey, 1989, Table 2, p.43
18	M49er	FFG_312	537.40	Richey, 1989, Table 2, p.40	56	M49er	FFG_353	751.70	Richey, 1989, Table 2, p.43
19	M49er	FFG_313	934.30	Richey, 1989, Table 2, p.41	57	M49er	FFG_354	817.80	Richey, 1989, Table 2, p.43
20	M49er	FFG_314	862.30	Richey, 1989, Table 2, p.41	58	M49er	FFG_361	1011.00	Richey, 1989, Table 2, p.44
21	M49er	FFG_315	782.90	Richey, 1989, Table 2, p.41	59	M49er	FFG_366	960.40	Richey, 1989, Table 2, p.44
22	M49er	FFG_316	771.40	Richey, 1989, Table 2, p.41	60	M49er	FFG_367	975.90	Richey, 1989, Table 2, p.44
23	M49er	FFG_317	792.20	Richey, 1989, Table 2, p.41	61	M49er	FFG_371	1012.90	Richey, 1989, Table 2, p.44
24	M49er	FFG_318	758.00	Richey, 1989, Table 2, p.41	62	M49er	FFG_374	946.40	Richey, 1989, Table 2, p.45
25	M49er	FFG_319	769.30	Richey, 1989, Table 2, p.41	63	M49er	FFG_383	955.30	Richey, 1989, Table 2, p.45
26	M49er	FFG_320	762.30	Richey, 1989, Table 2, p.41	64	M49er	FFG_384	976.00	Richey, 1989, Table 2, p.45
27	M49er	FFG_321	760.50	Richey, 1989, Table 2, p.41	65	M49er	FFG_387	966.60	Richey, 1989, Table 2, p.45
28	M49er	FFG_322	755.10	Richey, 1989. Table 2, p.41	66	M49er	FFG_388	959.20	Richey, 1989. Table 2, p.46
29	M49er	FFG_323	751.10	Richey, 1989, Table 2, p.41	67	M49er	FFG_390	974.40	Richey, 1989, Table 2, p.46
30	M49er	FFG_324	761.70	Richey, 1989, Table 2, p.41	68	M49er	FFG_391	973.50	Richey, 1989, Table 2, p.46
31	M49er	FFG_325	819.60	Richey, 1989, Table 2, p.41	69	M49er	FFG_392	967.80	Richey, 1989, Table 2, p.46
32	M49er	FFG_326	754.40	Richey, 1989, Table 2, p.41	70	M49er	FFG_393	835.60	Richey, 1989, Table 2, p.46
33	M49er	FFG_327	748.30	Richey, 1989, Table 2, p.42	71	M49er	FFG_394	925.90	Richey, 1989, Table 2, p.46
34	M49er	FFG_328	757.00	Richey, 1989, Table 2, p.42	72	M49er	FFG_395	918.40	Richey, 1989, Table 2, p.46
35	M49er	FFG_329	755.60	Richey, 1989, Table 2, p.42	73	M49er	FFG_396	901.60	Richey, 1989, Table 2, p.46
36	M49er	FFG_330	754.90	Richey, 1989, Table 2, p.42	74	M49er	FFG_398	825.70	Richey, 1989, Table 2, p.46
37	M49er	FFG_331	753.50	Richey, 1989, Table 2, p.42	75	M49er	FFG_402	1002.50	Richey, 1989, Table 2, p.46
38	M49er	FFG_332	744.00	Richey, 1989, Table 2, p.42	76	M49er	FFG_403	963.00	Richey, 1989, Table 2, p.47

Table B.2. Elevations of Stratigraphic Layers Near WIPP (Continued)

	Layer	Well ID	Elevation	Source		Layer	Well ID	Elevation	Source
1	M49er	FFG_404	925.70	Richey, 1989, Table 2, p.47	39	M49er	FFG_489	764.60	Richey, 1989, Table 2, p.52
2	M49er	FFG_407	958.30	Richey, 1989, Table 2, p.47	40	M49er	FFG_490	855.60	Richey, 1989, Table 2, p.52
3	M49er	FFG_419	997.00	Richey, 1989, Table 2, p.48	41	M49er	FFG_491	855.90	Richey, 1989, Table 2, p.52
4	M49er	FFG_420	992.70	Richey, 1989, Table 2, p.48	42	M49er	FFG_492	817.50	Richey, 1989, Table 2, p.52
5	M49er	FFG_421	983.60	Richey, 1989, Table 2, p.48	43	M49er	FFG_493	803.60	Richey, 1989, Table 2, p.53
6	M49er	FFG_422	976.60	Richey, 1989, Table 2, p.48	44	M49er	FFG_494	811.30	Richey, 1989, Table 2, p.53
7	M49er	FFG_432	931.80	Richey, 1989, Table 2, p.48	45	M49er	FFG_495	799.40	Richey, 1989, Table 2, p.53
8	M49er	FFG_438	892.60	Richey, 1989, Table 2, p.49	46	M49er	FFG_496	715.40	Richey, 1989, Table 2, p.53
9	M49er	FFG_455	837.60	Richey, 1989, Table 2, p.50	47	M49er	FFG_497	721.50	Richey, 1989, Table 2, p.53
10	M49er	FFG_456	829.00	Richey, 1989, Table 2, p.50	48	M49er	FFG_498	737.00	Richey, 1989, Table 2, p.53
11	M49er	FFG_457	885.10	Richey, 1989, Table 2, p.50	49	M49er	FFG_499	715.40	Richey, 1989, Table 2, p.53
12	M49er	FFG_458	888.20	Richey, 1989, Table 2, p.50	50	M49er	FFG_500	726.00	Richey, 1989, Table 2, p.53
13	M49er	FFG_459	816.60	Richey, 1989, Table 2, p.50	51	M49er	FFG_501	731.50	Richey, 1989, Table 2, p.53
14	M49er	FFG_462	884.10	Richey, 1989, Table 2, p.50	52	M49er	FFG_502	724.80	Richey, 1989, Table 2, p.53
15	M49er	FFG_463	913.50	Richey, 1989, Table 2, p.51	53	M49er	FFG_503	705.40	Richey, 1989, Table 2, p.53
16	M49er	FFG_464	900.40	Richey, 1989, Table 2, p.51	54	M49er	FFG_504	723.60	Richey, 1989, Table 2, p.53
17	M49er	FFG_465	902.80	Richey, 1989, Table 2, p.51	55	M49er	FFG_505	754.70	Richey, 1989, Table 2, p.53
18	M49er	FFG_467	506.20	Richey, 1989, Table 2, p.51	56	M49er	FFG_506	749.20	Richey, 1989, Table 2, p.53
19	M49er	FFG_468	493.50	Richey, 1989, Table 2, p.51	57	M49er	FFG_507	712.80	Richey, 1989, Table 2, p.53
20	M49er	FFG_470	509.60	Richey, 1989, Table 2, p.51	58	M49er	FFG_508	763.30	Richey, 1989, Table 2, p.53
21	M49er	FFG_471	525.80	Richey, 1989, Table 2, p.51	59	M49er	FFG_509	767.80	Richey, 1989, Table 2, p.54
22	M49er	FFG_472	564.20	Richey, 1989, Table 2, p.51	60	M49er	FFG_510	767.30	Richey, 1989, Table 2, p.54
23	M49er	FFG_473	491.60	Richey, 1989, Table 2, p.51	61	M49er	FFG_511	728.20	Richey, 1989, Table 2, p.54
24	M49er	FFG_474	750.70	Richey, 1989, Table 2, p.51	62	M49er	FFG_512	748.30	Richey, 1989, Table 2, p.54
25	M49er	FFG_475	749.70	Richey, 1989, Table 2, p.51	63	M49er	FFG_513	763.00	Richey, 1989, Table 2, p.54
26	M49er	FFG_476	821.80	Richey, 1989, Table 2, p.51	64	M49er	FFG_514	754.70	Richey, 1989, Table 2, p.54
27	M49er	FFG_477	774.50	Richey, 1989, Table 2, p.51	65	M49er	FFG_515	722.60	Richey, 1989, Table 2, p.54
28	M49er	FFG_478	755.60	Richey, 1989, Table 2, p.52	66	M49er	FFG_516	715.90	Richey, 1989, Table 2, p.54
29	M49er	FFG_479	752.50	Richey, 1989, Table 2, p.52	67	M49er	FFG_517	809.30	Richey, 1989, Table 2, p.54
30	M49er	FFG_480	754.40	Richey, 1989, Table 2, p.52	68	M49er	FFG_518	797.90	Richey, 1989, Table 2, p.54
31	M49er	FFG_481	731.80	Richey, 1989, Table 2, p.52	69	M49er	FFG_519	765.70	Richey, 1989, Table 2, p.54
32	M49er	FFG_482	761.40	Richey, 1989, Table 2, p.52	70	M49er	FFG_520	653.00	Richey, 1989, Table 2, p.54
33	M49er	FFG_483	785.10	Richey, 1989, Table 2, p.52	71	M49er	FFG_521	673.30	Richey, 1989, Table 2, p.54
34	M49er	FFG_484	772.20	Richey, 1989, Table 2, p.52	72	M49er	FFG_522	531.70	Richey, 1989, Table 2, p.54
35	M49er	FFG_485	779.40	Richey, 1989, Table 2, p.52	73	M49er	FFG_523	541.30	Richey, 1989, Table 2, p.54
36	M49er	FFG_486	766.30	Richey, 1989, Table 2, p.52	74	M49er	FFG_524	693.10	Richey, 1989, Table 2, p.55
37	M49er	FFG_487	763.90	Richey, 1989, Table 2, p.52	75	M49er	FFG_525	543.30	Richey, 1989, Table 2, p.55
38	M49er	FFG_488	748.00	Richey, 1989, Table 2, p.52	76	M49er	FFG_527	958.90	Richey, 1989, Table 2, p.55

Table B.2. Elevations of Stratigraphic Layers Near WIPP (Continued)

	Layer	Well ID	Elevation	Source		Layer	Well ID	Elevation	Source
1	M49er	FFG_528	951.60	Richey, 1989, Table 2, p.55	39	M49er	FFG_672	943.70	Richey, 1989, Table 2, p.62
2	M49er	FFG_535	939.70	Richey, 1989, Table 2, p.55	40	M49er	FFG_674	937.00	Richey, 1989, Table 2, p.62
3	M49er	FFG_548	930.60	Richey, 1989, Table 2, p.56	41	M49er	FFG_675	896.00	Richey, 1989, Table 2, p.62
4	M49er	FFG_562	670.60	Richey, 1989, Table 2, p.57	42	M49er	FFG_676	905.00	Richey, 1989, Table 2, p.62
5	M49er	FFG_563	582.50	Richey, 1989, Table 2, p.57	43	M49er	FFG_677	932.40	Richey, 1989, Table 2, p.62
6	M49er	FFG_569	689.20	Richey, 1989, Table 2, p.57	44	M49er	FFG_679	934.80	Richey, 1989, Table 2, p.62
7	M49er	FFG_584	773.20	Richey, 1989, Table 2, p.58	45	M49er	FFG_689	817.20	Richey, 1989, Table 2, p.63
8	M49er	FFG_600	729.10	Richey, 1989, Table 2, p.58	46	M49er	FFG_690	824.80	Richey, 1989, Table 2, p.63
9	M49er	FFG_601	645.60	Richey, 1989, Table 2, p.58	47	M49er	FFG_691	816.30	Richey, 1989, Table 2, p.63
10	M49er	FFG_606	723.00	Richey, 1989, Table 2, p.58	48	M49er	FFG_692	806.20	Richey, 1989, Table 2, p.63
11	M49er	FFG_607	743.10	Richey, 1989, Table 2, p.59	49	M49er	FFG_693	817.70	Richey, 1989, Table 2, p.63
12	M49er	FFG_608	754.60	Richey, 1989, Table 2, p.59	50	M49er	FFG_694	810.10	Richey, 1989, Table 2, p.63
13	M49er	FFG_609	758.30	Richey, 1989, Table 2, p.59	51	M49er	FFG_695	814.10	Richey, 1989, Table 2, p.63
14	M49er	FFG_610	746.70	Richey, 1989, Table 2, p.59	52	M49er	FFG_696	815.90	Richey, 1989, Table 2, p.63
15	M49er	FFG_611	731.80	Richey, 1989, Table 2, p.59	53	M49er	FFG_697	818.10	Richey, 1989, Table 2, p.64
16	M49er	FFG_612	733.40	Richey, 1989, Table 2, p.59	54	M49er	FFG_698	861.40	Richey, 1989, Table 2, p.64
17	M49er	FFG_613	728.50	Richey, 1989, Table 2, p.59	55	M49er	FFG_699	811.10	Richey, 1989, Table 2, p.64
18	M49er	FFG_620	759.80	Richey, 1989, Table 2, p.59	56	M49er	FFG_700	801.40	Richey, 1989, Table 2, p.64
19	M49er	FFG_638	591.70	Richey, 1989, Table 2, p.60	57	M49er	FFG_701	810.60	Richey, 1989, Table 2, p.64
20	M49er	FFG_639	566.30	Richey, 1989, Table 2, p.60	58	M49er	FFG_702	811.70	Richey, 1989, Table 2, p.64
21	M49er	FFG_640	649.10	Richey, 1989, Table 2, p.60	59	M49er	FFG_703	817.20	Richey, 1989, Table 2, p.64
22	M49er	FFG_643	688.90	Richey, 1989, Table 2, p.60	60	M49er	FFG_704	806.20	Richey, 1989, Table 2, p.64
23	M49er	FFG_644	723.50	Richey, 1989, Table 2, p.60	61	M49er	FFG_705	735.50	Richey, 1989, Table 2, p.64
24	M49er	FFG_648	558.40	Richey, 1989, Table 2, p.60	62	M49er	FFG_706	755.00	Richey, 1989, Table 2, p.64
25	M49er	FFG_652	878.70	Richey, 1989, Table 2, p.60	63	M49er	FFG_707	741.00	Richey, 1989, Table 2, p.64
26	M49er	FFG_653	880.00	Richey, 1989, Table 2, p.61	64	M49er	FFG_708	791.60	Richey, 1989, Table 2, p.64
27	M49er	FFG_654	899.50	Richey, 1989, Table 2, p.61	65	M49er	FFG_709	681.50	Richey, 1989, Table 2, p.64
28	M49er	FFG_655	897.30	Richey, 1989, Table 2, p.61	66	M49er	FFG_710	682.50	Richey, 1989, Table 2, p.64
29	M49er	FFG_656	894.30	Richey, 1989, Table 2, p.61	67	M49er	FFG_711	694.40	Richey, 1989, Table 2, p.65
30	M49er	FFG_657	906.20	Richey, 1989, Table 2, p.61	68	M49er	FFG_712	735.60	Richey, 1989, Table 2, p.65
31	M49er	FFG_658	898.20	Richey, 1989, Table 2, p.61	69	M49er	FFG_713	672.50	Richey, 1989, Table 2, p.65
32	M49er	FFG_659	901.90	Richey, 1989, Table 2, p.61	70	M49er	FFG_714	790.30	Richey, 1989, Table 2, p.65
33	M49er	FFG_660	919.20	Richey, 1989, Table 2, p.61	71	M49er	FFG_715	799.70	Richey, 1989, Table 2, p.65
34	M49er	FFG_662	894.60	Richey, 1989, Table 2, p.61	72	M49er	FFG_716	697.90	Richey, 1989, Table 2, p.65
35	M49er	FFG_664	888.20	Richey, 1989, Table 2, p.61	73	M49er	FFG_717	722.50	Richey, 1989, Table 2, p.65
36	M49er	FFG_666	938.10	Richey, 1989, Table 2, p.62	74	M49er	FFG_718	723.50	Richey, 1989, Table 2, p.65
37	M49er	FFG_667	923.30	Richey, 1989, Table 2, p.62	75	M49er	FFG_719	696.70	Richey, 1989, Table 2, p.65
38	M49er	FFG_670	946.10	Richey, 1989, Table 2, p.62	76	M49er	FFG_720	699.60	Richey, 1989, Table 2, p.65

Table B.2. Elevations of Stratigraphic Layers Near WIPP (Continued)

	Layer	Well ID	Elevation	Source
1	M49er	FFG_721	698.00	Richey, 1989, Table 2, p.65
2	M49er	FFG_723	808.20	Richey, 1989, Table 2, p.65
3	M49er	FFG_724	738.90	Richey, 1989, Table 2, p.65
4	M49er	FFG_725	712.30	Richey, 1989, Table 2, p.65
5	M49er	FFG_726	698.90	Richey, 1989, Table 2, p.65
6	M49er	FFG_727	702.90	Richey, 1989, Table 2, p.66
7	M49er	FFG_728	696.40	Richey, 1989, Table 2, p.66
8	M49er	FFG_729	706.60	Richey, 1989, Table 2, p.66
9	M49er	FFG_730	724.80	Richey, 1989, Table 2, p.66
10	M49er	FFG_731	720.70	Richey, 1989, Table 2, p.66
11	M49er	FFG_732	739.50	Richey, 1989, Table 2, p.66
12	M49er	FFG_733	806.50	Richey, 1989, Table 2, p.66
13	M49er	FFG_734	758.60	Richey, 1989, Table 2, p.66
14	M49er	FFG_735	704.10	Richey, 1989, Table 2, p.66
15	M49er	FFG_736	758.70	Richey, 1989, Table 2, p.66
16	M49er	FFG_737	702.60	Richey, 1989, Table 2, p.66
17	M49er	FFG_738	713.80	Richey, 1989, Table 2, p.66
18	M49er	FFG_739	753.90	Richey, 1989, Table 2, p.66
19	M49er	FFG_740	754.70	Richey, 1989, Table 2, p.66
20	M49er	FFG_741	721.20	Richey, 1989, Table 2, p.66
21	M49er	FFG_742	774.50	Richey, 1989, Table 2, p.67
22	M49er	FFG_743	757.20	Richey, 1989, Table 2, p.67
23	M49er	FFG_744	739.70	Richey, 1989, Table 2, p.67
24	M49er	FFG_745	730.30	Richey, 1989, Table 2, p.67
25	M49er	FFG_746	719.80	Richey, 1989, Table 2, p.67
26	M49er	H1	882.70	Mercer, 1983, Table 1
27	M49er	H10C	756.80	Mercer, 1983, Table 1
28	M49er	H2C	890.30	Mercer, 1983, Table 1
29	M49er	H3	880.30	Mercer, 1983, Table 1
30	M49er	H4C	920.20	Mercer, 1983, Table 1
31	M49er	H5C	845.80	Mercer, 1983, Table 1
32	M49er	H6C	890.40	Mercer, 1983, Table 1
33	M49er	H7C	937.60	Mercer, 1983, Table 1
34	M49er	H8C	924.80	Mercer, 1983, Table 1
35	M49er	H9C	899.40	Mercer, 1983, Table 1
36	M49er	P1	910.50	Mercer, 1983, Table 1
37	M49er	P10	860.40	Mercer, 1983, Table 1
38	M49er	P11	840.90	Mercer, 1983, Table 1
39	M49er	P12	887.90	Mercer, 1983, Table 1
40	M49er	P13	889.50	Mercer, 1983, Table 1
41	M49er	P14	906.10	Mercer, 1983, Table 1
42	M49er	P15	938.50	Mercer, 1983, Table 1
43	M49er	P16	915.00	Mercer, 1983, Table 1
44	M49er	P17	900.40	Mercer, 1983, Table 1
45	M49er	P18	868.40	Mercer, 1983, Table 1
46	M49er	P19	849.50	Mercer, 1983, Table 1
47	M49er	P2	850.10	Mercer, 1983, Table 1
48	M49er	P20	845.30	Mercer, 1983, Table 1
49	M49er	P21	845.80	Mercer, 1983, Table 1
50	M49er	P3	888.50	Mercer, 1983, Table 1
51	M49er	P4	864.10	Mercer, 1983, Table 1
52	M49er	P5	868.10	Mercer, 1983, Table 1
53	M49er	P6	913.50	Mercer, 1983, Table 1
54	M49er	P7	920.50	Mercer, 1983, Table 1
55	M49er	P8	898.50	Mercer, 1983, Table 1
56	M49er	P9	868.70	Mercer, 1983, Table 1
57	M49er	REF	874.00	Rechard et al.,1991, Figure 2.2-1
58	M49er	SaltShft	875.54	Bechtel, Inc., 1986, Appendix D
59	M49er	WIPP11	842.10	Mercer, 1983, Table 1
60	M49er	WIPP11	842.20	SNL and USGS, 1982a, Table 2
61	M49er	WIPP12	866.80	SNL and D'Appolonia Consulting, 1983, Table 2
62	M49er	WIPP12	866.90	Mercer, 1983, Table 1
63	M49er	WIPP13	880.20	Mercer, 1983, Table 1
64	M49er	WIPP16	681.20	Mercer, 1983, Table 1
65	M49er	WIPP18	866.60	Mercer, 1983, Table 1
66	M49er	WIPP19	866.90	Mercer, 1983, Table 1
67	M49er	WIPP21	870.80	Mercer, 1983, Table 1
68	M49er	WIPP22	869.50	Mercer, 1983, Table 1
69	M49er	WIPP25	908.60	Mercer, 1983, Table 1
70	M49er	WIPP26	957.70	Mercer, 1983, Table 1
71	M49er	WIPP27	921.70	Mercer, 1983, Table 1
72	M49er	WIPP28	954.70	Mercer, 1983, Table 1
73	M49er	WIPP30	908.00	Mercer, 1983, Table 1
74	M49er	WIPP32	921.40	Mercer, 1983, Table 1
75	M49er	WIPP33	891.60	Mercer, 1983, Table 1
76	M49er	WIPP34	846.10	Mercer, 1983, Table 1

Table B.2. Elevations of Stratigraphic Layers Near WIPP (Continued)

	Layer	Well ID	Elevation	Source
1	M49er	WastShft	875.18	Bechtel, Inc., 1986, Appendix E
2	MB126	AirShft	509.31	Holt and Powers, 1990, Figure 22
3	MB126	AirShft	509.64	Holt and Powers, 1990, Figure 22
4	MB126	DOE1	485.50	U.S. DOE, Sep 1982, Table 2
5	MB126	DOE2	484.90	Mercer et al., 1987, Table 3-2
6	MB126	DOE2	485.40	Mercer et al., 1987, Table 3-2
7	MB126	ERDA9	511.60	SNL and USGS, 1982b, Table 2
8	MB126	ExhtShft	512.54	Bechtel, Inc., 1986, Appendix F
9	MB126	ExhtShft	512.72	Bechtel, Inc., 1986, Appendix F
10	MB126	REF	511.60	Rechard et al.,1991, Figure 2.2-1
11	MB126	SaltShft	514.21	Bechtel, Inc., 1986, Appendix D
12	MB126	SaltShft	514.47	Bechtel, Inc., 1986, Appendix D
13	MB126	WIPP11	513.00	SNL and USGS, 1982a, Table 2
14	MB126	WIPP12	513.80	SNL and D'Appolonia Consulting, 1983, Table 2
15	MB126	WastShft	512.40	Bechtel, Inc., 1986, Appendix E
16	MB126	WastShft	512.75	Bechtel, Inc., 1986, Appendix E
17	MB136	AirShft	412.87	Holt and Powers, 1990, Figure 22
18	MB136	AirShft	417.16	Holt and Powers, 1990, Figure 22
19	MB136	ExhtShft	415.52	Bechtel, Inc., 1986, Appendix F
20	MB136	ExhtShft	418.86	Bechtel, Inc., 1986, Appendix F
21	MB136	SaltShft	418.84	Bechtel, Inc., 1986, Appendix D
22	MB136	SaltShft	421.37	Bechtel, Inc., 1986, Appendix D
23	MB136	WastShft	415.27	Bechtel, Inc., 1986, Appendix E
24	MB136	WastShft	419.66	Bechtel, Inc., 1986, Appendix E
25	MB138	AirShft	393.81	Holt and Powers, 1990, Figure 22
26	MB138	AirShft	393.98	Holt and Powers, 1990, Figure 22
27	MB138	DH207	395.92	Krieg, 1984, Table I
28	MB138	DH207	396.16	Krieg, 1984, Table I
29	MB138	DH211	398.83	Krieg, 1984, Table I
30	MB138	DH211	398.98	Krieg, 1984, Table I
31	MB138	DH215	399.23	Krieg, 1984, Table I
32	MB138	DH215	399.41	Krieg, 1984, Table I
33	MB138	DH219	397.58	Krieg, 1984, Table I
34	MB138	DH219	397.82	Krieg, 1984, Table I
35	MB138	DH223	394.10	Krieg, 1984, Table I
36	MB138	DH223	394.31	Krieg, 1984, Table I
37	MB138	DH227	391.03	Krieg, 1984, Table I
38	MB138	DH227	391.18	Krieg, 1984, Table I
39	MB138	DH77	409.65	Krieg, 1984, Table I
40	MB138	DH77	409.95	Krieg, 1984, Table I
41	MB138	DO201	396.40	Krieg, 1984, Table I
42	MB138	DO201	396.58	Krieg, 1984, Table I
43	MB138	DO203	406.94	Krieg, 1984, Table I
44	MB138	DO203	407.15	Krieg, 1984, Table I
45	MB138	DO205	412.06	Krieg, 1984, Table I
46	MB138	DO205	412.30	Krieg, 1984, Table I
47	MB138	DO45	403.83	Krieg, 1984, Table I
48	MB138	DO45	404.01	Krieg, 1984, Table I
49	MB138	DO52	401.39	Krieg, 1984, Table I
50	MB138	DO52	401.51	Krieg, 1984, Table I
51	MB138	DO56	406.69	Krieg, 1984, Table I
52	MB138	DO56	406.84	Krieg, 1984, Table I
53	MB138	DO63	410.47	Krieg, 1984, Table I
54	MB138	DO63	410.68	Krieg, 1984, Table I
55	MB138	DO67	410.38	Krieg, 1984, Table I
56	MB138	DO67	410.50	Krieg, 1984, Table I
57	MB138	DO88	409.07	Krieg, 1984, Table I
58	MB138	DO88	409.33	Krieg, 1984, Table I
59	MB138	DO91	408.81	Krieg, 1984, Table I
60	MB138	DO91	409.02	Krieg, 1984, Table I
61	MB138	DOE1	368.60	U.S. DOE, Sep 1982, Table 2
62	MB138	DOE2	370.40	Mercer et al., 1987, Table 3-2
63	MB138	ERDA9	396.00	SNL and USGS, 1982b, Table 2
64	MB138	ERDA9	396.40	SNL and USGS, 1982b, Table 2
65	MB138	ExhtShft	396.86	Bechtel, Inc., 1986, Appendix F
66	MB138	ExhtShft	397.03	Bechtel, Inc., 1986, Appendix F
67	MB138	MB139_2	396.15	Krieg, 1984, Table I
68	MB138	MB139_2	396.30	Krieg, 1984, Table I
69	MB138	REF	396.00	Rechard et al.,1991, Figure 2.2-1
70	MB138	REF	396.40	Rechard et al.,1991, Figure 2.2-1
71	MB138	SaltShft	399.79	Bechtel, Inc., 1986, Appendix D
72	MB138	SaltShft	399.80	Bechtel, Inc., 1986, Appendix D
73	MB138	SaltShft	399.76	Krieg, 1984, Table I
74	MB138	SaltShft	399.91	Krieg, 1984, Table I
75	MB138	WIPP11	430.40	SNL and USGS, 1982a, Table 2
76	MB138	WIPP12	411.00	SNL and D'Appolonia Consulting, 1983, Table 2

Table B.2. Elevations of Stratigraphic Layers Near WIPP (Continued)

	Layer	Well ID	Elevation	Source
1	MB138	WastShft	395.89	Bechtel, Inc., 1986, Appendix E
2	MB138	WastShft	396.07	Bechtel, Inc., 1986, Appendix E
3	MB138	WastShft	396.31	Krieg, 1984, Table I
4	MB138	WastShft	396.49	Krieg, 1984, Table I
5	MB139	DH207	377.63	Krieg, 1984, Table I
6	MB139	DH207	378.70	Krieg, 1984, Table I
7	MB139	DH211	380.73	Krieg, 1984, Table I
8	MB139	DH211	381.31	Krieg, 1984, Table I
9	MB139	DH215	381.03	Krieg, 1984, Table I
10	MB139	DH215	382.04	Krieg, 1984, Table I
11	MB139	DH219	379.91	Krieg, 1984, Table I
12	MB139	DH219	380.58	Krieg, 1984, Table I
13	MB139	DH223	376.70	Krieg, 1984, Table I
14	MB139	DH223	377.64	Krieg, 1984, Table I
15	MB139	DH227	373.78	Krieg, 1984, Table I
16	MB139	DH227	374.42	Krieg, 1984, Table I
17	MB139	DH77	392.37	Krieg, 1984, Table I
18	MB139	DH77	393.35	Krieg, 1984, Table I
19	MB139	DO201	378.26	Krieg, 1984, Table I
20	MB139	DO201	379.11	Krieg, 1984, Table I
21	MB139	DO203	389.84	Krieg, 1984, Table I
22	MB139	DO203	390.63	Krieg, 1984, Table I
23	MB139	DO205	394.29	Krieg, 1984, Table I
24	MB139	DO205	394.69	Krieg, 1984, Table I
25	MB139	DO45	385.11	Krieg, 1984, Table I
26	MB139	DO45	386.36	Krieg, 1984, Table I
27	MB139	DO52	383.44	Krieg, 1984, Table I
28	MB139	DO52	384.57	Krieg, 1984, Table I
29	MB139	DO56	388.89	Krieg, 1984, Table I
30	MB139	DO56	389.53	Krieg, 1984, Table I
31	MB139	DO63	392.79	Krieg, 1984, Table I
32	MB139	DO63	393.46	Krieg, 1984, Table I
33	MB139	DO67	393.19	Krieg, 1984, Table I
34	MB139	DO67	394.13	Krieg, 1984, Table I
35	MB139	DO88	392.06	Krieg, 1984, Table I
36	MB139	DO88	392.99	Krieg, 1984, Table I
37	MB139	DO91	391.62	Krieg, 1984, Table I
38	MB139	DO91	392.66	Krieg, 1984, Table I
39	MB139	DOE1	350.40	U.S. DOE, Sep 1982, Table 2
40	MB139	DOE2	339.00	Mercer et al., 1987, Table 3-2
41	MB139	DOE2	340.00	Mercer et al., 1987, Table 3-2
42	MB139	ERDA9	378.10	SNL and USGS, 1982b, Table 2
43	MB139	ERDA9	379.00	SNL and USGS, 1982b, Table 2
44	MB139	MB139_2	377.44	Krieg, 1984, Table I
45	MB139	MB139_2	378.42	Krieg, 1984, Table I
46	MB139	REF	378.10	Rechard et al.,1991, Figure 2.2-1
47	MB139	REF	379.00	Rechard et al.,1991, Figure 2.2-1
48	MB139	SaltShft	381.64	Bechtel, Inc., 1986, Appendix D
49	MB139	SaltShft	382.44	Bechtel, Inc., 1986, Appendix D
50	MB139	SaltShft	381.38	Krieg, 1984, Table I
51	MB139	SaltShft	382.29	Krieg, 1984, Table I
52	MB139	WIPP11	419.10	SNL and USGS, 1982a, Table 2
53	MB139	WIPP12	395.90	SNL and D'Appolonia Consulting, 1983, Table 2
54	MB139	WastShft	377.14	Bechtel, Inc., 1986, Appendix E
55	MB139	WastShft	378.22	Bechtel, Inc., 1986, Appendix E
56	MB139	WastShft	378.04	Krieg, 1984, Table I
57	MB139	WastShft	379.10	Krieg, 1984, Table I
58	Magenta	AEC7	890.30	Mercer, 1983, Table 1
59	Magenta	AEC8	858.70	Mercer, 1983, Table 1
60	Magenta	AirShft	858.82	Holt and Powers, 1990, Figure 22
61	Magenta	B25	858.40	Mercer, 1983, Table 1
62	Magenta	DOE1	838.60	U.S. DOE, Sep 1982, Table 2
63	Magenta	DOE2	829.00	Mercer et al., 1987, Table 3-2
64	Magenta	ERDA10	915.90	Mercer, 1983, Table 1
65	Magenta	ERDA6	897.60	Mercer, 1983, Table 1
66	Magenta	ERDA9	860.40	Mercer, 1983, Table 1
67	Magenta	ERDA9	856.70	SNL and USGS, 1982b, Table 2
68	Magenta	ExhtShft	855.39	Bechtel, Inc., 1986, Appendix F
69	Magenta	FFG_002	667.50	Richey, 1989, Table 2, p.21
70	Magenta	FFG_004	717.80	Richey, 1989, Table 2, p.21
71	Magenta	FFG_005	674.90	Richey, 1989, Table 2, p.21
72	Magenta	FFG_006	670.00	Richey, 1989, Table 2, p.21
73	Magenta	FFG_007	655.90	Richey, 1989, Table 2, p.21
74	Magenta	FFG_009	657.40	Richey, 1989, Table 2, p.21
75	Magenta	FFG_011	664.20	Richey, 1989, Table 2, p.21
76	Magenta	FFG_012	667.80	Richey, 1989, Table 2, p.21

Table B.2. Elevations of Stratigraphic Layers Near WIPP (Continued)

	Layer	Well ID	Elevation	Source
1	Magenta	FFG_013	674.80	Richey, 1989, Table 2, p.21
2	Magenta	FFG_014	721.10	Richey, 1989, Table 2, p.21
3	Magenta	FFG_016	644.90	Richey, 1989, Table 2, p.21
4	Magenta	FFG_017	648.30	Richey, 1989, Table 2, p.22
5	Magenta	FFG_018	652.30	Richey, 1989, Table 2, p.22
6	Magenta	FFG_019	644.70	Richey, 1989, Table 2, p.22
7	Magenta	FFG_020	718.40	Richey, 1989, Table 2, p.22
8	Magenta	FFG_023	654.10	Richey, 1989, Table 2, p.22
9	Magenta	FFG_024	638.80	Richey, 1989, Table 2, p.22
10	Magenta	FFG_025	652.20	Richey, 1989, Table 2, p.22
11	Magenta	FFG_026	649.50	Richey, 1989, Table 2, p.22
12	Magenta	FFG_027	643.10	Richey, 1989, Table 2, p.22
13	Magenta	FFG_028	612.70	Richey, 1989, Table 2, p.22
14	Magenta	FFG_029	599.20	Richey, 1989, Table 2, p.22
15	Magenta	FFG_030	598.30	Richey, 1989, Table 2, p.22
16	Magenta	FFG_031	590.10	Richey, 1989, Table 2, p.22
17	Magenta	FFG_032	592.10	Richey, 1989, Table 2, p.22
18	Magenta	FFG_033	588.30	Richey, 1989, Table 2, p.22
19	Magenta	FFG_034	582.40	Richey, 1989, Table 2, p.23
20	Magenta	FFG_035	572.60	Richey, 1989, Table 2, p.23
21	Magenta	FFG_036	582.20	Richey, 1989, Table 2, p.23
22	Magenta	FFG_037	571.80	Richey, 1989, Table 2, p.23
23	Magenta	FFG_038	559.60	Richey, 1989, Table 2, p.23
24	Magenta	FFG_039	778.80	Richey, 1989, Table 2, p.23
25	Magenta	FFG_040	720.90	Richey, 1989, Table 2, p.23
26	Magenta	FFG_041	780.60	Richey, 1989, Table 2, p.23
27	Magenta	FFG_042	785.40	Richey, 1989, Table 2, p.23
28	Magenta	FFG_043	788.10	Richey, 1989, Table 2, p.23
29	Magenta	FFG_044	741.00	Richey, 1989, Table 2, p.23
30	Magenta	FFG_047	613.90	Richey, 1989, Table 2, p.23
31	Magenta	FFG_048	630.90	Richey, 1989, Table 2, p.23
32	Magenta	FFG_049	620.90	Richey, 1989, Table 2, p.23
33	Magenta	FFG_050	627.60	Richey, 1989, Table 2, p.24
34	Magenta	FFG_051	627.30	Richey, 1989, Table 2, p.24
35	Magenta	FFG_052	630.30	Richey, 1989, Table 2, p.24
36	Magenta	FFG_053	623.30	Richey, 1989, Table 2, p.24
37	Magenta	FFG_054	620.60	Richey, 1989, Table 2, p.24
38	Magenta	FFG_055	621.10	Richey, 1989, Table 2, p.24
39	Magenta	FFG_056	621.80	Richey, 1989, Table 2, p.24
40	Magenta	FFG_057	625.20	Richey, 1989, Table 2, p.24
41	Magenta	FFG_058	623.60	Richey, 1989, Table 2, p.24
42	Magenta	FFG_059	623.60	Richey, 1989, Table 2, p.24
43	Magenta	FFG_060	627.30	Richey, 1989, Table 2, p.24
44	Magenta	FFG_061	626.00	Richey, 1989, Table 2, p.24
45	Magenta	FFG_062	553.20	Richey, 1989, Table 2, p.24
46	Magenta	FFG_063	513.70	Richey, 1989, Table 2, p.24
47	Magenta	FFG_064	538.60	Richey, 1989, Table 2, p.24
48	Magenta	FFG_065	520.60	Richey, 1989, Table 2, p.24
49	Magenta	FFG_066	473.90	Richey, 1989, Table 2, p.24
50	Magenta	FFG_067	516.40	Richey, 1989, Table 2, p.25
51	Magenta	FFG_068	481.90	Richey, 1989, Table 2, p.25
52	Magenta	FFG_069	502.40	Richey, 1989, Table 2, p.25
53	Magenta	FFG_070	532.20	Richey, 1989, Table 2, p.25
54	Magenta	FFG_071	790.70	Richey, 1989, Table 2, p.25
55	Magenta	FFG_072	721.10	Richey, 1989, Table 2, p.25
56	Magenta	FFG_073	699.50	Richey, 1989, Table 2, p.25
57	Magenta	FFG_074	703.30	Richey, 1989, Table 2, p.25
58	Magenta	FFG_075	756.00	Richey, 1989, Table 2, p.25
59	Magenta	FFG_076	818.10	Richey, 1989, Table 2, p.25
60	Magenta	FFG_078	855.20	Richey, 1989, Table 2, p.25
61	Magenta	FFG_079	829.70	Richey, 1989, Table 2, p.25
62	Magenta	FFG_080	808.30	Richey, 1989, Table 2, p.25
63	Magenta	FFG_081	727.90	Richey, 1989, Table 2, p.26
64	Magenta	FFG_082	759.30	Richey, 1989, Table 2, p.26
65	Magenta	FFG_083	674.70	Richey, 1989, Table 2, p.26
66	Magenta	FFG_084	702.20	Richey, 1989, Table 2, p.26
67	Magenta	FFG_085	695.60	Richey, 1989, Table 2, p.26
68	Magenta	FFG_086	705.60	Richey, 1989, Table 2, p.26
69	Magenta	FFG_087	680.00	Richey, 1989, Table 2, p.26
70	Magenta	FFG_088	674.60	Richey, 1989, Table 2, p.26
71	Magenta	FFG_089	656.00	Richey, 1989, Table 2, p.26
72	Magenta	FFG_091	700.40	Richey, 1989, Table 2, p.26
73	Magenta	FFG_092	716.60	Richey, 1989, Table 2, p.26
74	Magenta	FFG_093	718.10	Richey, 1989, Table 2, p.26
75	Magenta	FFG_094	720.20	Richey, 1989, Table 2, p.26
76	Magenta	FFG_095	688.80	Richey, 1989, Table 2, p.26

Table B.2. Elevations of Stratigraphic Layers Near WIPP (Continued)

	Layer	Well ID	Elevation	Source
1	Magenta	FFG_096	671.20	Richey, 1989, Table 2, p.26
2	Magenta	FFG_097	651.70	Richey, 1989, Table 2, p.27
3	Magenta	FFG_098	625.40	Richey, 1989, Table 2, p.27
4	Magenta	FFG_099	620.90	Richey, 1989, Table 2, p.27
5	Magenta	FFG_100	603.90	Richey, 1989, Table 2, p.27
6	Magenta	FFG_101	574.90	Richey, 1989, Table 2, p.27
7	Magenta	FFG_102	593.50	Richey, 1989, Table 2, p.27
8	Magenta	FFG_103	655.40	Richey, 1989, Table 2, p.27
9	Magenta	FFG_104	551.10	Richey, 1989, Table 2, p.27
10	Magenta	FFG_105	909.60	Richey, 1989, Table 2, p.27
11	Magenta	FFG_106	939.70	Richey, 1989, Table 2, p.27
12	Magenta	FFG_107	923.00	Richey, 1989, Table 2, p.27
13	Magenta	FFG_108	918.40	Richey, 1989, Table 2, p.27
14	Magenta	FFG_109	898.90	Richey, 1989, Table 2, p.27
15	Magenta	FFG_110	865.70	Richey, 1989, Table 2, p.27
16	Magenta	FFG_111	871.70	Richey, 1989, Table 2, p.27
17	Magenta	FFG_112	861.00	Richey, 1989, Table 2, p.28
18	Magenta	FFG_113	875.10	Richey, 1989, Table 2, p.28
19	Magenta	FFG_114	905.60	Richey, 1989, Table 2, p.28
20	Magenta	FFG_115	895.50	Richey, 1989, Table 2, p.28
21	Magenta	FFG_116	911.00	Richey, 1989, Table 2, p.28
22	Magenta	FFG_117	911.30	Richey, 1989, Table 2, p.28
23	Magenta	FFG_120	923.00	Richey, 1989, Table 2, p.28
24	Magenta	FFG_121	928.10	Richey, 1989, Table 2, p.28
25	Magenta	FFG_122	926.60	Richey, 1989, Table 2, p.28
26	Magenta	FFG_123	900.60	Richey, 1989, Table 2, p.28
27	Magenta	FFG_124	865.30	Richey, 1989, Table 2, p.28
28	Magenta	FFG_125	890.90	Richey, 1989, Table 2, p.28
29	Magenta	FFG_126	886.20	Richey, 1989, Table 2, p.28
30	Magenta	FFG_127	891.20	Richey, 1989, Table 2, p.28
31	Magenta	FFG_128	926.60	Richey, 1989, Table 2, p.28
32	Magenta	FFG_129	899.40	Richey, 1989, Table 2, p.28
33	Magenta	FFG_130	929.60	Richey, 1989, Table 2, p.28
34	Magenta	FFG_132	935.10	Richey, 1989, Table 2, p.29
35	Magenta	FFG_133	938.10	Richey, 1989, Table 2, p.29
36	Magenta	FFG_134	944.00	Richey, 1989, Table 2, p.29
37	Magenta	FFG_135	917.50	Richey, 1989, Table 2, p.29
38	Magenta	FFG_136	919.10	Richey, 1989, Table 2, p.29
39	Magenta	FFG_137	927.90	Richey, 1989, Table 2, p.29
40	Magenta	FFG_138	880.60	Richey, 1989, Table 2, p.29
41	Magenta	FFG_139	889.70	Richey, 1989, Table 2, p.29
42	Magenta	FFG_140	829.20	Richey, 1989, Table 2, p.29
43	Magenta	FFG_141	854.20	Richey, 1989, Table 2, p.29
44	Magenta	FFG_142	829.40	Richey, 1989, Table 2, p.29
45	Magenta	FFG_143	839.30	Richey, 1989, Table 2, p.29
46	Magenta	FFG_147	897.90	Richey, 1989, Table 2, p.29
47	Magenta	FFG_155	914.10	Richey, 1989, Table 2, p.30
48	Magenta	FFG_157	915.30	Richey, 1989, Table 2, p.30
49	Magenta	FFG_158	937.20	Richey, 1989, Table 2, p.30
50	Magenta	FFG_159	936.70	Richey, 1989, Table 2, p.30
51	Magenta	FFG_160	929.70	Richey, 1989, Table 2, p.30
52	Magenta	FFG_161	936.10	Richey, 1989, Table 2, p.30
53	Magenta	FFG_162	933.30	Richey, 1989, Table 2, p.30
54	Magenta	FFG_163	933.90	Richey, 1989, Table 2, p.30
55	Magenta	FFG_166	936.00	Richey, 1989, Table 2, p.31
56	Magenta	FFG_167	922.10	Richey, 1989, Table 2, p.31
57	Magenta	FFG_168	944.60	Richey, 1989, Table 2, p.31
58	Magenta	FFG_169	957.30	Richey, 1989, Table 2, p.31
59	Magenta	FFG_170	922.90	Richey, 1989, Table 2, p.31
60	Magenta	FFG_171	931.50	Richey, 1989, Table 2, p.31
61	Magenta	FFG_172	937.20	Richey, 1989, Table 2, p.31
62	Magenta	FFG_173	914.10	Richey, 1989, Table 2, p.31
63	Magenta	FFG_180	920.50	Richey, 1989, Table 2, p.31
64	Magenta	FFG_181	951.30	Richey, 1989, Table 2, p.32
65	Magenta	FFG_182	847.60	Richey, 1989, Table 2, p.32
66	Magenta	FFG_184	927.80	Richey, 1989, Table 2, p.32
67	Magenta	FFG_185	934.50	Richey, 1989, Table 2, p.32
68	Magenta	FFG_186	863.80	Richey, 1989, Table 2, p.32
69	Magenta	FFG_188	874.10	Richey, 1989, Table 2, p.32
70	Magenta	FFG_189	902.20	Richey, 1989, Table 2, p.32
71	Magenta	FFG_190	882.40	Richey, 1989, Table 2, p.32
72	Magenta	FFG_191	878.10	Richey, 1989, Table 2, p.32
73	Magenta	FFG_192	815.30	Richey, 1989, Table 2, p.32
74	Magenta	FFG_194	822.10	Richey, 1989, Table 2, p.33
75	Magenta	FFG_195	834.00	Richey, 1989, Table 2, p.33
76	Magenta	FFG_196	876.90	Richey, 1989, Table 2, p.33

Table B.2. Elevations of Stratigraphic Layers Near WIPP (Continued)

	Layer	Well ID	Elevation	Source		Layer	Well ID	Elevation	Source
1	Magenta	FFG_197	878.10	Richey, 1989, Table 2, p.33	39	Magenta	FFG_238	691.00	Richey, 1989, Table 2, p.36
2	Magenta	FFG_198	877.50	Richey, 1989, Table 2, p.33	40	Magenta	FFG_239	679.10	Richey, 1989, Table 2, p.36
3	Magenta	FFG_199	867.50	Richey, 1989, Table 2, p.33	41	Magenta	FFG_240	671.20	Richey, 1989, Table 2, p.36
4	Magenta	FFG_200	880.90	Richey, 1989, Table 2, p.33	42	Magenta	FFG_241	666.30	Richey, 1989, Table 2, p.36
5	Magenta	FFG_201	873.20	Richey, 1989, Table 2, p.33	43	Magenta	FFG_242	783.10	Richey, 1989, Table 2, p.36
6	Magenta	FFG_202	816.50	Richey, 1989, Table 2, p.33	44	Magenta	FFG_243	743.10	Richey, 1989, Table 2, p.36
7	Magenta	FFG_203	823.00	Richey, 1989, Table 2, p.33	45	Magenta	FFG_244	780.80	Richey, 1989, Table 2, p.36
8	Magenta	FFG_204	846.50	Richey, 1989, Table 2, p.33	46	Magenta	FFG_245	573.00	Richey, 1989, Table 2, p.36
9	Magenta	FFG_205	860.50	Richey, 1989, Table 2, p.33	47	Magenta	FFG_246	578.50	Richey, 1989, Table 2, p.36
10	Magenta	FFG_206	874.50	Richey, 1989, Table 2, p.33	48	Magenta	FFG_247	563.80	Richey, 1989, Table 2, p.36
11	Magenta	FFG_207	872.30	Richey, 1989, Table 2, p.33	49	Magenta	FFG_248	571.20	Richey, 1989, Table 2, p.36
12	Magenta	FFG_208	882.10	Richey, 1989, Table 2, p.34	50	Magenta	FFG_249	569.70	Richey, 1989, Table 2, p.36
13	Magenta	FFG_209	873.20	Richey, 1989, Table 2, p.34	51	Magenta	FFG_250	651.50	Richey, 1989, Table 2, p.36
14	Magenta	FFG_210	865.90	Richey, 1989, Table 2, p.34	52	Magenta	FFG_251	544.90	Richey, 1989, Table 2, p.36
15	Magenta	FFG_212	852.80	Richey, 1989, Table 2, p.34	53	Magenta	FFG_252	683.90	Richey, 1989, Table 2, p.36
16	Magenta	FFG_213	874.50	Richey, 1989, Table 2, p.34	54	Magenta	FFG_253	639.20	Richey, 1989, Table 2, p.36
17	Magenta	FFG_214	854.90	Richey, 1989, Table 2, p.34	55	Magenta	FFG_254	630.00	Richey, 1989, Table 2, p.36
18	Magenta	FFG_215	831.20	Richey, 1989, Table 2, p.34	56	Magenta	FFG_255	587.70	Richey, 1989, Table 2, p.37
19	Magenta	FFG_216	716.80	Richey, 1989, Table 2, p.34	57	Magenta	FFG_256	535.20	Richey, 1989, Table 2, p.37
20	Magenta	FFG_217	851.40	Richey, 1989, Table 2, p.34	58	Magenta	FFG_257	579.40	Richey, 1989, Table 2, p.37
21	Magenta	FFG_218	844.00	Richey, 1989, Table 2, p.34	59	Magenta	FFG_258	594.90	Richey, 1989, Table 2, p.37
22	Magenta	FFG_219	889.70	Richey, 1989, Table 2, p.34	60	Magenta	FFG_259	561.10	Richey, 1989, Table 2, p.37
23	Magenta	FFG_220	836.70	Richey, 1989, Table 2, p.34	61	Magenta	FFG_260	603.80	Richey, 1989, Table 2, p.37
24	Magenta	FFG_221	796.20	Richey, 1989, Table 2, p.34	62	Magenta	FFG_261	592.80	Richey, 1989, Table 2, p.37
25	Magenta	FFG_222	749.80	Richey, 1989, Table 2, p.34	63	Magenta	FFG_263	526.60	Richey, 1989, Table 2, p.37
26	Magenta	FFG_224	655.70	Richey, 1989, Table 2, p.35	64	Magenta	FFG_264	760.50	Richey, 1989, Table 2, p.37
27	Magenta	FFG_225	662.40	Richey, 1989, Table 2, p.35	65	Magenta	FFG_265	755.90	Richey, 1989, Table 2, p.37
28	Magenta	FFG_226	661.00	Richey, 1989, Table 2, p.35	66	Magenta	FFG_266	736.70	Richey, 1989, Table 2, p.37
29	Magenta	FFG_228	651.70	Richey, 1989, Table 2, p.35	67	Magenta	FFG_267	713.50	Richey, 1989, Table 2, p.37
30	Magenta	FFG_229	679.40	Richey, 1989, Table 2, p.35	68	Magenta	FFG_268	690.70	Richey, 1989, Table 2, p.37
31	Magenta	FFG_230	665.10	Richey, 1989, Table 2, p.35	69	Magenta	FFG_269	702.40	Richey, 1989, Table 2, p.38
32	Magenta	FFG_231	681.80	Richey, 1989, Table 2, p.35	70	Magenta	FFG_270	774.50	Richey, 1989, Table 2, p.38
33	Magenta	FFG_232	695.60	Richey, 1989, Table 2, p.35	71	Magenta	FFG_271	815.00	Richey, 1989, Table 2, p.38
34	Magenta	FFG_233	685.80	Richey, 1989, Table 2, p.35	72	Magenta	FFG_272	822.50	Richey, 1989, Table 2, p.38
35	Magenta	FFG_234	722.70	Richey, 1989, Table 2, p.35	73	Magenta	FFG_273	797.40	Richey, 1989, Table 2, p.38
36	Magenta	FFG_235	698.60	Richey, 1989, Table 2, p.35	74	Magenta	FFG_274	834.20	Richey, 1989, Table 2, p.38
37	Magenta	FFG_236	746.40	Richey, 1989, Table 2, p.35	75	Magenta	FFG_275	840.30	Richey, 1989, Table 2, p.38
38	Magenta	FFG_237	712.10	Richey, 1989, Table 2, p.35	76	Magenta	FFG_276	845.20	Richey, 1989, Table 2, p.38

Table B.2. Elevations of Stratigraphic Layers Near WIPP (Continued)

	Layer	Well ID	Elevation	Source
2	Magenta	FFG_277	836.70	Richey, 1989, Table 2, p.38
3	Magenta	FFG_278	845.80	Richey, 1989, Table 2, p.38
4	Magenta	FFG_279	840.90	Richey, 1989, Table 2, p.38
5	Magenta	FFG_280	837.30	Richey, 1989, Table 2, p.38
6	Magenta	FFG_281	814.20	Richey, 1989, Table 2, p.38
7	Magenta	FFG_283	563.90	Richey, 1989, Table 2, p.39
8	Magenta	FFG_284	712.00	Richey, 1989, Table 2, p.39
9	Magenta	FFG_285	741.30	Richey, 1989, Table 2, p.39
10	Magenta	FFG_286	820.20	Richey, 1989, Table 2, p.39
11	Magenta	FFG_287	793.10	Richey, 1989, Table 2, p.39
12	Magenta	FFG_288	744.90	Richey, 1989, Table 2, p.39
13	Magenta	FFG_289	719.90	Richey, 1989, Table 2, p.39
14	Magenta	FFG_290	806.50	Richey, 1989, Table 2, p.39
15	Magenta	FFG_291	742.50	Richey, 1989, Table 2, p.39
16	Magenta	FFG_292	758.40	Richey, 1989, Table 2, p.39
17	Magenta	FFG_293	750.70	Richey, 1989, Table 2, p.39
18	Magenta	FFG_294	572.80	Richey, 1989, Table 2, p.39
19	Magenta	FFG_295	560.20	Richey, 1989, Table 2, p.39
20	Magenta	FFG_297	539.20	Richey, 1989, Table 2, p.39
21	Magenta	FFG_298	552.40	Richey, 1989, Table 2, p.40
22	Magenta	FFG_299	569.10	Richey, 1989, Table 2, p.40
23	Magenta	FFG_300	520.60	Richey, 1989, Table 2, p.40
24	Magenta	FFG_301	491.10	Richey, 1989, Table 2, p.40
25	Magenta	FFG_302	518.50	Richey, 1989, Table 2, p.40
26	Magenta	FFG_303	511.20	Richey, 1989, Table 2, p.40
27	Magenta	FFG_304	517.50	Richey, 1989, Table 2, p.40
28	Magenta	FFG_305	509.30	Richey, 1989, Table 2, p.40
29	Magenta	FFG_306	469.30	Richey, 1989, Table 2, p.40
30	Magenta	FFG_307	493.50	Richey, 1989, Table 2, p.40
31	Magenta	FFG_308	465.70	Richey, 1989, Table 2, p.40
32	Magenta	FFG_309	508.10	Richey, 1989, Table 2, p.40
33	Magenta	FFG_310	539.20	Richey, 1989, Table 2, p.40
34	Magenta	FFG_311	486.50	Richey, 1989, Table 2, p.40
35	Magenta	FFG_312	510.60	Richey, 1989, Table 2, p.40
36	Magenta	FFG_313	915.10	Richey, 1989, Table 2, p.41
37	Magenta	FFG_314	843.10	Richey, 1989, Table 2, p.41
38	Magenta	FFG_315	764.30	Richey, 1989, Table 2, p.41
39	Magenta	FFG_316	747.90	Richey, 1989, Table 2, p.41
40	Magenta	FFG_317	777.00	Richey, 1989, Table 2, p.41
41	Magenta	FFG_318	742.20	Richey, 1989, Table 2, p.41
42	Magenta	FFG_319	751.60	Richey, 1989, Table 2, p.41
43	Magenta	FFG_320	741.30	Richey, 1989, Table 2, p.41
44	Magenta	FFG_321	737.90	Richey, 1989, Table 2, p.41
45	Magenta	FFG_322	733.20	Richey, 1989, Table 2, p.41
46	Magenta	FFG_323	729.50	Richey, 1989, Table 2, p.41
47	Magenta	FFG_324	745.30	Richey, 1989, Table 2, p.41
48	Magenta	FFG_325	800.40	Richey, 1989, Table 2, p.41
49	Magenta	FFG_326	736.10	Richey, 1989, Table 2, p.41
50	Magenta	FFG_327	729.10	Richey, 1989, Table 2, p.42
51	Magenta	FFG_328	734.50	Richey, 1989, Table 2, p.42
52	Magenta	FFG_329	733.90	Richey, 1989, Table 2, p.42
53	Magenta	FFG_330	733.20	Richey, 1989, Table 2, p.42
54	Magenta	FFG_331	728.50	Richey, 1989, Table 2, p.42
55	Magenta	FFG_332	719.30	Richey, 1989, Table 2, p.42
56	Magenta	FFG_333	722.80	Richey, 1989, Table 2, p.42
57	Magenta	FFG_334	718.10	Richey, 1989, Table 2, p.42
58	Magenta	FFG_335	733.70	Richey, 1989, Table 2, p.42
59	Magenta	FFG_336	730.60	Richey, 1989, Table 2, p.42
60	Magenta	FFG_337	713.80	Richey, 1989, Table 2, p.42
61	Magenta	FFG_338	720.70	Richey, 1989, Table 2, p.42
62	Magenta	FFG_339	684.80	Richey, 1989, Table 2, p.42
63	Magenta	FFG_340	694.00	Richey, 1989, Table 2, p.42
64	Magenta	FFG_342	726.90	Richey, 1989, Table 2, p.43
65	Magenta	FFG_344	692.70	Richey, 1989, Table 2, p.43
66	Magenta	FFG_345	752.10	Richey, 1989, Table 2, p.43
67	Magenta	FFG_347	744.70	Richey, 1989, Table 2, p.43
68	Magenta	FFG_348	773.30	Richey, 1989, Table 2, p.43
69	Magenta	FFG_349	742.20	Richey, 1989, Table 2, p.43
70	Magenta	FFG_350	789.10	Richey, 1989, Table 2, p.43
71	Magenta	FFG_351	705.60	Richey, 1989, Table 2, p.43
72	Magenta	FFG_352	705.60	Richey, 1989, Table 2, p.43
73	Magenta	FFG_353	726.70	Richey, 1989, Table 2, p.43
74	Magenta	FFG_354	800.80	Richey, 1989, Table 2, p.43
75	Magenta	FFG_361	986.90	Richey, 1989, Table 2, p.44
76	Magenta	FFG_366	940.60	Richey, 1989, Table 2, p.44
77	Magenta	FFG_367	954.60	Richey, 1989, Table 2, p.44

Table B.2. Elevations of Stratigraphic Layers Near WIPP (Continued)

	Layer	Well ID	Elevation	Source		Layer	Well ID	Elevation	Source
1	Magenta	FFG_371	997.70	Richey, 1989, Table 2, p.44	39	Magenta	FFG_472	538.30	Richey, 1989, Table 2, p.51
2	Magenta	FFG_374	940.90	Richey, 1989, Table 2, p.45	40	Magenta	FFG_473	468.20	Richey, 1989, Table 2, p.51
3	Magenta	FFG_383	938.80	Richey, 1989, Table 2, p.45	41	Magenta	FFG_474	729.40	Richey, 1989, Table 2, p.51
4	Magenta	FFG_384	945.80	Richey, 1989, Table 2, p.45	42	Magenta	FFG_475	728.90	Richey, 1989, Table 2, p.51
5	Magenta	FFG_387	940.30	Richey, 1989, Table 2, p.45	43	Magenta	FFG_476	805.00	Richey, 1989, Table 2, p.51
6	Magenta	FFG_388	936.70	Richey, 1989, Table 2, p.46	44	Magenta	FFG_477	760.80	Richey, 1989, Table 2, p.51
7	Magenta	FFG_390	954.00	Richey, 1989, Table 2, p.46	45	Magenta	FFG_478	739.70	Richey, 1989, Table 2, p.52
8	Magenta	FFG_391	951.50	Richey, 1989, Table 2, p.46	46	Magenta	FFG_479	736.40	Richey, 1989, Table 2, p.52
9	Magenta	FFG_392	948.60	Richey, 1989, Table 2, p.46	47	Magenta	FFG_480	732.50	Richey, 1989, Table 2, p.52
10	Magenta	FFG_393	816.10	Richey, 1989, Table 2, p.46	48	Magenta	FFG_481	715.70	Richey, 1989, Table 2, p.52
11	Magenta	FFG_394	908.60	Richey, 1989, Table 2, p.46	49	Magenta	FFG_482	744.30	Richey, 1989, Table 2, p.52
12	Magenta	FFG_395	901.60	Richey, 1989, Table 2, p.46	50	Magenta	FFG_483	767.80	Richey, 1989, Table 2, p.52
13	Magenta	FFG_396	884.30	Richey, 1989, Table 2, p.46	51	Magenta	FFG_484	753.60	Richey, 1989, Table 2, p.52
14	Magenta	FFG_398	805.60	Richey, 1989, Table 2, p.46	52	Magenta	FFG_485	762.60	Richey, 1989, Table 2, p.52
15	Magenta	FFG_402	979.40	Richey, 1989, Table 2, p.46	53	Magenta	FFG_486	749.50	Richey, 1989, Table 2, p.52
16	Magenta	FFG_403	941.40	Richey, 1989, Table 2, p.47	54	Magenta	FFG_487	746.50	Richey, 1989, Table 2, p.52
17	Magenta	FFG_404	901.60	Richey, 1989, Table 2, p.47	55	Magenta	FFG_488	731.20	Richey, 1989, Table 2, p.52
18	Magenta	FFG_407	940.00	Richey, 1989, Table 2, p.47	56	Magenta	FFG_489	748.40	Richey, 1989, Table 2, p.52
19	Magenta	FFG_408	913.20	Richey, 1989, Table 2, p.47	57	Magenta	FFG_490	838.80	Richey, 1989, Table 2, p.52
20	Magenta	FFG_419	976.60	Richey, 1989, Table 2, p.48	58	Magenta	FFG_491	836.40	Richey, 1989, Table 2, p.52
21	Magenta	FFG_420	973.50	Richey, 1989, Table 2, p.48	59	Magenta	FFG_492	798.60	Richey, 1989, Table 2, p.52
22	Magenta	FFG_421	960.10	Richey, 1989, Table 2, p.48	60	Magenta	FFG_493	785.30	Richey, 1989, Table 2, p.53
23	Magenta	FFG_422	958.30	Richey, 1989, Table 2, p.48	61	Magenta	FFG_494	792.10	Richey, 1989, Table 2, p.53
24	Magenta	FFG_432	924.10	Richey, 1989, Table 2, p.48	62	Magenta	FFG_495	783.00	Richey, 1989, Table 2, p.53
25	Magenta	FFG_438	874.60	Richey, 1989, Table 2, p.49	63	Magenta	FFG_496	688.60	Richey, 1989, Table 2, p.53
26	Magenta	FFG_455	817.50	Richey, 1989, Table 2, p.50	64	Magenta	FFG_497	701.10	Richey, 1989, Table 2, p.53
27	Magenta	FFG_456	812.50	Richey, 1989, Table 2, p.50	65	Magenta	FFG_498	714.10	Richey, 1989, Table 2, p.53
28	Magenta	FFG_457	868.10	Richey, 1989, Table 2, p.50	66	Magenta	FFG_499	689.50	Richey, 1989, Table 2, p.53
29	Magenta	FFG_458	872.60	Richey, 1989, Table 2, p.50	67	Magenta	FFG_500	704.70	Richey, 1989, Table 2, p.53
30	Magenta	FFG_459	799.50	Richey, 1989, Table 2, p.50	68	Magenta	FFG_501	710.10	Richey, 1989, Table 2, p.53
31	Magenta	FFG_462	865.80	Richey, 1989, Table 2, p.50	69	Magenta	FFG_502	702.90	Richey, 1989, Table 2, p.53
32	Magenta	FFG_463	893.10	Richey, 1989, Table 2, p.51	70	Magenta	FFG_503	684.00	Richey, 1989, Table 2, p.53
33	Magenta	FFG_464	880.00	Richey, 1989, Table 2, p.51	71	Magenta	FFG_504	706.00	Richey, 1989, Table 2, p.53
34	Magenta	FFG_465	883.00	Richey, 1989, Table 2, p.51	72	Magenta	FFG_505	739.50	Richey, 1989, Table 2, p.53
35	Magenta	FFG_467	488.20	Richey, 1989, Table 2, p.51	73	Magenta	FFG_506	730.90	Richey, 1989, Table 2, p.53
36	Magenta	FFG_468	465.50	Richey, 1989, Table 2, p.51	74	Magenta	FFG_507	692.40	Richey, 1989, Table 2, p.53
37	Magenta	FFG_470	484.90	Richey, 1989, Table 2, p.51	75	Magenta	FFG_508	744.10	Richey, 1989, Table 2, p.53
38	Magenta	FFG_471	500.50	Richey, 1989, Table 2, p.51	76	Magenta	FFG_509	745.20	Richey, 1989, Table 2, p.54

Table B.2. Elevations of Stratigraphic Layers Near WIPP (Continued)

	Layer	Well ID	Elevation	Source
1	Magenta	FFG_510	744.80	Richey, 1989, Table 2, p.54
2	Magenta	FFG_511	702.30	Richey, 1989, Table 2, p.54
3	Magenta	FFG_512	720.80	Richey, 1989, Table 2, p.54
4	Magenta	FFG_513	740.70	Richey, 1989, Table 2, p.54
5	Magenta	FFG_514	731.20	Richey, 1989, Table 2, p.54
6	Magenta	FFG_515	697.90	Richey, 1989, Table 2, p.54
7	Magenta	FFG_516	691.30	Richey, 1989, Table 2, p.54
8	Magenta	FFG_517	788.80	Richey, 1989, Table 2, p.54
9	Magenta	FFG_518	778.10	Richey, 1989, Table 2, p.54
10	Magenta	FFG_519	743.70	Richey, 1989, Table 2, p.54
11	Magenta	FFG_520	635.40	Richey, 1989, Table 2, p.54
12	Magenta	FFG_521	655.00	Richey, 1989, Table 2, p.54
13	Magenta	FFG_522	504.30	Richey, 1989, Table 2, p.54
14	Magenta	FFG_523	516.90	Richey, 1989, Table 2, p.54
15	Magenta	FFG_524	675.10	Richey, 1989, Table 2, p.55
16	Magenta	FFG_525	513.70	Richey, 1989, Table 2, p.55
17	Magenta	FFG_527	938.70	Richey, 1989, Table 2, p.55
18	Magenta	FFG_528	934.20	Richey, 1989, Table 2, p.55
19	Magenta	FFG_532	915.60	Richey, 1989, Table 2, p.55
20	Magenta	FFG_535	919.90	Richey, 1989, Table 2, p.55
21	Magenta	FFG_548	914.10	Richey, 1989, Table 2, p.56
22	Magenta	FFG_562	652.30	Richey, 1989, Table 2, p.57
23	Magenta	FFG_563	564.80	Richey, 1989, Table 2, p.57
24	Magenta	FFG_569	670.60	Richey, 1989, Table 2, p.57
25	Magenta	FFG_584	767.70	Richey, 1989, Table 2, p.58
26	Magenta	FFG_600	727.60	Richey, 1989, Table 2, p.58
27	Magenta	FFG_601	623.00	Richey, 1989, Table 2, p.58
28	Magenta	FFG_606	703.50	Richey, 1989, Table 2, p.58
29	Magenta	FFG_607	723.30	Richey, 1989, Table 2, p.59
30	Magenta	FFG_608	731.80	Richey, 1989, Table 2, p.59
31	Magenta	FFG_609	738.80	Richey, 1989, Table 2, p.59
32	Magenta	FFG_610	722.40	Richey, 1989, Table 2, p.59
33	Magenta	FFG_611	707.40	Richey, 1989, Table 2, p.59
34	Magenta	FFG_612	715.70	Richey, 1989, Table 2, p.59
35	Magenta	FFG_613	713.50	Richey, 1989, Table 2, p.59
36	Magenta	FFG_620	738.50	Richey, 1989, Table 2, p.59
37	Magenta	FFG_638	573.10	Richey, 1989, Table 2, p.60
38	Magenta	FFG_639	543.80	Richey, 1989, Table 2, p.60
39	Magenta	FFG_640	630.80	Richey, 1989, Table 2, p.60
40	Magenta	FFG_643	669.70	Richey, 1989, Table 2, p.60
41	Magenta	FFG_644	706.40	Richey, 1989, Table 2, p.60
42	Magenta	FFG_648	541.30	Richey, 1989, Table 2, p.60
43	Magenta	FFG_652	859.80	Richey, 1989, Table 2, p.60
44	Magenta	FFG_653	859.90	Richey, 1989, Table 2, p.61
45	Magenta	FFG_654	880.00	Richey, 1989, Table 2, p.61
46	Magenta	FFG_655	878.10	Richey, 1989, Table 2, p.61
47	Magenta	FFG_656	876.90	Richey, 1989, Table 2, p.61
48	Magenta	FFG_657	889.80	Richey, 1989, Table 2, p.61
49	Magenta	FFG_658	881.80	Richey, 1989, Table 2, p.61
50	Magenta	FFG_659	886.10	Richey, 1989, Table 2, p.61
51	Magenta	FFG_660	901.50	Richey, 1989, Table 2, p.61
52	Magenta	FFG_662	876.30	Richey, 1989, Table 2, p.61
53	Magenta	FFG_664	868.40	Richey, 1989, Table 2, p.61
54	Magenta	FFG_666	920.50	Richey, 1989, Table 2, p.62
55	Magenta	FFG_667	905.60	Richey, 1989, Table 2, p.62
56	Magenta	FFG_670	926.90	Richey, 1989, Table 2, p.62
57	Magenta	FFG_672	925.70	Richey, 1989, Table 2, p.62
58	Magenta	FFG_674	921.70	Richey, 1989, Table 2, p.62
59	Magenta	FFG_675	877.70	Richey, 1989, Table 2, p.62
60	Magenta	FFG_676	891.90	Richey, 1989, Table 2, p.62
61	Magenta	FFG_677	917.80	Richey, 1989, Table 2, p.62
62	Magenta	FFG_679	917.10	Richey, 1989, Table 2, p.62
63	Magenta	FFG_689	799.50	Richey, 1989, Table 2, p.63
64	Magenta	FFG_690	805.00	Richey, 1989, Table 2, p.63
65	Magenta	FFG_691	796.20	Richey, 1989, Table 2, p.63
66	Magenta	FFG_692	786.40	Richey, 1989, Table 2, p.63
67	Magenta	FFG_693	797.00	Richey, 1989, Table 2, p.63
68	Magenta	FFG_694	789.40	Richey, 1989, Table 2, p.63
69	Magenta	FFG_695	794.90	Richey, 1989, Table 2, p.63
70	Magenta	FFG_696	797.00	Richey, 1989, Table 2, p.63
71	Magenta	FFG_697	799.20	Richey, 1989, Table 2, p.64
72	Magenta	FFG_698	841.60	Richey, 1989, Table 2, p.64
73	Magenta	FFG_699	792.80	Richey, 1989, Table 2, p.64
74	Magenta	FFG_700	782.50	Richey, 1989, Table 2, p.64
75	Magenta	FFG_701	788.60	Richey, 1989, Table 2, p.64
76	Magenta	FFG_702	792.80	Richey, 1989, Table 2, p.64

Table B.2. Elevations of Stratigraphic Layers Near WIPP (Continued)

	Layer	Well ID	Elevation	Source
1	Magenta	FFG_703	798.90	Richey, 1989, Table 2, p.64
2	Magenta	FFG_704	785.50	Richey, 1989, Table 2, p.64
3	Magenta	FFG_705	715.60	Richey, 1989, Table 2, p.64
4	Magenta	FFG_706	736.10	Richey, 1989, Table 2, p.64
5	Magenta	FFG_707	720.30	Richey, 1989, Table 2, p.64
6	Magenta	FFG_708	773.30	Richey, 1989, Table 2, p.64
7	Magenta	FFG_709	664.50	Richey, 1989, Table 2, p.64
8	Magenta	FFG_710	665.40	Richey, 1989, Table 2, p.64
9	Magenta	FFG_711	675.20	Richey, 1989, Table 2, p.65
10	Magenta	FFG_712	718.80	Richey, 1989, Table 2, p.65
11	Magenta	FFG_713	655.80	Richey, 1989, Table 2, p.65
12	Magenta	FFG_714	770.20	Richey, 1989, Table 2, p.65
13	Magenta	FFG_715	783.00	Richey, 1989, Table 2, p.65
14	Magenta	FFG_716	680.80	Richey, 1989, Table 2, p.65
15	Magenta	FFG_717	703.30	Richey, 1989, Table 2, p.65
16	Magenta	FFG_718	706.70	Richey, 1989, Table 2, p.65
17	Magenta	FFG_719	679.40	Richey, 1989, Table 2, p.65
18	Magenta	FFG_720	679.10	Richey, 1989, Table 2, p.65
19	Magenta	FFG_721	679.10	Richey, 1989, Table 2, p.65
20	Magenta	FFG_723	791.70	Richey, 1989, Table 2, p.65
21	Magenta	FFG_724	719.10	Richey, 1989, Table 2, p.65
22	Magenta	FFG_725	694.90	Richey, 1989, Table 2, p.65
23	Magenta	FFG_726	682.70	Richey, 1989, Table 2, p.65
24	Magenta	FFG_727	680.00	Richey, 1989, Table 2, p.66
25	Magenta	FFG_728	677.80	Richey, 1989, Table 2, p.66
26	Magenta	FFG_729	688.90	Richey, 1989, Table 2, p.66
27	Magenta	FFG_730	705.60	Richey, 1989, Table 2, p.66
28	Magenta	FFG_731	703.00	Richey, 1989, Table 2, p.66
29	Magenta	FFG_732	720.60	Richey, 1989, Table 2, p.66
30	Magenta	FFG_733	787.60	Richey, 1989, Table 2, p.66
31	Magenta	FFG_734	741.90	Richey, 1989, Table 2, p.66
32	Magenta	FFG_735	684.60	Richey, 1989, Table 2, p.66
33	Magenta	FFG_736	739.10	Richey, 1989, Table 2, p.66
34	Magenta	FFG_737	682.80	Richey, 1989, Table 2, p.66
35	Magenta	FFG_738	697.00	Richey, 1989, Table 2, p.66
36	Magenta	FFG_739	734.40	Richey, 1989, Table 2, p.66
37	Magenta	FFG_740	736.70	Richey, 1989, Table 2, p.66
38	Magenta	FFG_741	702.90	Richey, 1989, Table 2, p.66
39	Magenta	FFG_742	753.70	Richey, 1989, Table 2, p.67
40	Magenta	FFG_743	740.40	Richey, 1989, Table 2, p.67
41	Magenta	FFG_744	722.90	Richey, 1989, Table 2, p.67
42	Magenta	FFG_745	708.90	Richey, 1989, Table 2, p.67
43	Magenta	FFG_746	699.10	Richey, 1989, Table 2, p.67
44	Magenta	H1	864.10	Mercer, 1983, Table 1
45	Magenta	H10C	741.00	Mercer, 1983, Table 1
46	Magenta	H2C	872.60	Mercer, 1983, Table 1
47	Magenta	H3	862.90	Mercer, 1983, Table 1
48	Magenta	H4C	901.30	Mercer, 1983, Table 1
49	Magenta	H5C	828.70	Mercer, 1983, Table 1
50	Magenta	H6C	871.10	Mercer, 1983, Table 1
51	Magenta	H7C	928.40	Mercer, 1983, Table 1
52	Magenta	H8C	904.40	Mercer, 1983, Table 1
53	Magenta	H9C	878.70	Mercer, 1983, Table 1
54	Magenta	P1	890.70	Mercer, 1983, Table 1
55	Magenta	P10	838.80	Mercer, 1983, Table 1
56	Magenta	P11	824.80	Mercer, 1983, Table 1
57	Magenta	P12	870.20	Mercer, 1983, Table 1
58	Magenta	P13	870.20	Mercer, 1983, Table 1
59	Magenta	P14	886.00	Mercer, 1983, Table 1
60	Magenta	P15	919.30	Mercer, 1983, Table 1
61	Magenta	P16	896.70	Mercer, 1983, Table 1
62	Magenta	P17	883.30	Mercer, 1983, Table 1
63	Magenta	P18	845.20	Mercer, 1983, Table 1
64	Magenta	P19	832.40	Mercer, 1983, Table 1
65	Magenta	P2	832.40	Mercer, 1983, Table 1
66	Magenta	P20	827.30	Mercer, 1983, Table 1
67	Magenta	P21	829.30	Mercer, 1983, Table 1
68	Magenta	P3	869.90	Mercer, 1983, Table 1
69	Magenta	P4	847.90	Mercer, 1983, Table 1
70	Magenta	P5	848.90	Mercer, 1983, Table 1
71	Magenta	P6	895.20	Mercer, 1983, Table 1
72	Magenta	P7	901.90	Mercer, 1983, Table 1
73	Magenta	P8	880.50	Mercer, 1983, Table 1
74	Magenta	P9	851.90	Mercer, 1983, Table 1
75	Magenta	REF	856.70	Rechard et al.,1991, Figure 2.2-1
76	Magenta	SaltShft	858.77	Bechtel, Inc., 1986, Appendix D

Table B.2. Elevations of Stratigraphic Layers Near WIPP (Continued)

	Layer	Well ID	Elevation	Source		Layer	Well ID	Elevation	Source
1	Magenta	WIPP11	822.60	Mercer, 1983, Table 1	39	Salado	FFG_011	570.30	Richey, 1989, Table 2, p.21
2	Magenta	WIPP11	822.70	SNL and USGS, 1982a, Table 2	40	Salado	FFG_012	572.10	Richey, 1989, Table 2, p.21
3	Magenta	WIPP12	847.30	SNL and D'Appolonia Consulting, 1983, Table 2	41	Salado	FFG_013	582.50	Richey, 1989, Table 2, p.21
4	Magenta	WIPP12	848.00	Mercer, 1983, Table 1	42	Salado	FFG_014	623.00	Richey, 1989, Table 2, p.21
5	Magenta	WIPP13	865.90	Mercer, 1983, Table 1	43	Salado	FFG_016	545.00	Richey, 1989, Table 2, p.21
6	Magenta	WIPP16	668.70	Mercer, 1983, Table 1	44	Salado	FFG_017	555.30	Richey, 1989, Table 2, p.22
7	Magenta	WIPP18	848.60	Mercer, 1983, Table 1	45	Salado	FFG_018	558.40	Richey, 1989, Table 2, p.22
8	Magenta	WIPP19	849.20	Mercer, 1983, Table 1	46	Salado	FFG_019	548.90	Richey, 1989, Table 2, p.22
9	Magenta	WIPP21	853.10	Mercer, 1983, Table 1	47	Salado	FFG_020	622.40	Richey, 1989, Table 2, p.22
10	Magenta	WIPP22	852.20	Mercer, 1983, Table 1	48	Salado	FFG_023	553.50	Richey, 1989, Table 2, p.22
11	Magenta	WIPP25	887.30	Mercer, 1983, Table 1	49	Salado	FFG_024	539.20	Richey, 1989, Table 2, p.22
12	Magenta	WIPP26	939.40	Mercer, 1983, Table 1	50	Salado	FFG_025	560.40	Richey, 1989, Table 2, p.22
13	Magenta	WIPP27	914.70	Mercer, 1983, Table 1	51	Salado	FFG_026	552.60	Richey, 1989, Table 2, p.22
14	Magenta	WIPP28	933.30	Mercer, 1983, Table 1	52	Salado	FFG_027	545.60	Richey, 1989, Table 2, p.22
15	Magenta	WIPP30	888.50	Mercer, 1983, Table 1	53	Salado	FFG_028	549.60	Richey, 1989, Table 2, p.22
16	Magenta	WIPP32	915.60	Mercer, 1983, Table 1	54	Salado	FFG_029	537.90	Richey, 1989, Table 2, p.22
17	Magenta	WIPP33	876.00	Mercer, 1983, Table 1	55	Salado	FFG_030	532.80	Richey, 1989, Table 2, p.22
18	Magenta	WIPP34	827.60	Mercer, 1983, Table 1	56	Salado	FFG_031	522.40	Richey, 1989, Table 2, p.22
19	Magenta	WastShft	857.36	Bechtel, Inc., 1986, Appendix E	57	Salado	FFG_032	519.00	Richey, 1989, Table 2, p.22
20	RSResid	AirShft	783.13	Holt and Powers, 1990, Figure 22	58	Salado	FFG_033	518.80	Richey, 1989, Table 2, p.22
21	RSResid	ExhtShft	779.98	Bechtel, Inc., 1986, Appendix F	59	Salado	FFG_034	517.80	Richey, 1989, Table 2, p.23
22	RSResid	SaltShft	780.44	Bechtel, Inc., 1986, Appendix D	60	Salado	FFG_035	504.90	Richey, 1989, Table 2, p.23
23	RSResid	WastShft	781.82	Bechtel, Inc., 1986, Appendix E	61	Salado	FFG_036	510.30	Richey, 1989, Table 2, p.23
24	ReposFlr	AirShft	383.74	Holt and Powers, 1990, Figure 22	62	Salado	FFG_037	502.90	Richey, 1989, Table 2, p.23
25	ReposFlr	ExhtShft	381.61	Bechtel, Inc., 1986, Appendix F	63	Salado	FFG_038	491.90	Richey, 1989, Table 2, p.23
26	ReposFlr	SaltShft	380.08	Bechtel, Inc., 1986, Appendix D	64	Salado	FFG_039	694.40	Richey, 1989, Table 2, p.23
27	ReposFlr	WastShft	380.70	Bechtel, Inc., 1986, Appendix E	65	Salado	FFG_040	624.90	Richey, 1989, Table 2, p.23
28	Salado	AEC7	811.60	Mercer, 1983, Table 1	66	Salado	FFG_041	691.90	Richey, 1989, Table 2, p.23
29	Salado	AEC8	776.40	Mercer, 1983, Table 1	67	Salado	FFG_042	695.20	Richey, 1989, Table 2, p.23
30	Salado	B25	782.20	Mercer, 1983, Table 1	68	Salado	FFG_043	697.00	Richey, 1989, Table 2, p.23
31	Salado	ERDA10	836.10	Mercer, 1983, Table 1	69	Salado	FFG_044	645.60	Richey, 1989, Table 2, p.23
32	Salado	ERDA6	830.60	Mercer, 1983, Table 1	70	Salado	FFG_047	526.10	Richey, 1989, Table 2, p.23
33	Salado	ERDA9	783.60	Mercer, 1983, Table 1	71	Salado	FFG_048	527.60	Richey, 1989, Table 2, p.23
34	Salado	FFG_002	578.80	Richey, 1989, Table 2, p.21	72	Salado	FFG_049	526.70	Richey, 1989, Table 2, p.23
35	Salado	FFG_004	627.90	Richey, 1989, Table 2, p.21	73	Salado	FFG_050	537.40	Richey, 1989, Table 2, p.24
36	Salado	FFG_005	581.90	Richey, 1989, Table 2, p.21	74	Salado	FFG_051	530.90	Richey, 1989, Table 2, p.24
37	Salado	FFG_007	559.00	Richey, 1989, Table 2, p.21	75	Salado	FFG_052	565.70	Richey, 1989, Table 2, p.24
38	Salado	FFG_009	575.10	Richey, 1989, Table 2, p.21	76	Salado	FFG_053	510.50	Richey, 1989, Table 2, p.24

Table B.2. Elevations of Stratigraphic Layers Near WIPP (Continued)

	Layer	Well ID	Elevation	Source		Layer	Well ID	Elevation	Source
1	Salado	FFG_054	518.80	Richey, 1989, Table 2, p.24	39	Salado	FFG_094	637.00	Richey, 1989, Table 2, p.26
2	Salado	FFG_055	521.20	Richey, 1989, Table 2, p.24	40	Salado	FFG_095	618.70	Richey, 1989, Table 2, p.26
3	Salado	FFG_056	520.90	Richey, 1989, Table 2, p.24	41	Salado	FFG_096	605.00	Richey, 1989, Table 2, p.26
4	Salado	FFG_057	524.60	Richey, 1989, Table 2, p.24	42	Salado	FFG_097	580.60	Richey, 1989, Table 2, p.27
5	Salado	FFG_058	526.70	Richey, 1989, Table 2, p.24	43	Salado	FFG_098	555.90	Richey, 1989, Table 2, p.27
6	Salado	FFG_059	529.70	Richey, 1989, Table 2, p.24	44	Salado	FFG_099	550.20	Richey, 1989, Table 2, p.27
7	Salado	FFG_060	532.80	Richey, 1989, Table 2, p.24	45	Salado	FFG_100	530.40	Richey, 1989, Table 2, p.27
8	Salado	FFG_061	532.50	Richey, 1989, Table 2, p.24	46	Salado	FFG_101	500.20	Richey, 1989, Table 2, p.27
9	Salado	FFG_062	479.20	Richey, 1989, Table 2, p.24	47	Salado	FFG_102	512.40	Richey, 1989, Table 2, p.27
10	Salado	FFG_063	438.40	Richey, 1989, Table 2, p.24	48	Salado	FFG_104	474.30	Richey, 1989, Table 2, p.27
11	Salado	FFG_064	461.20	Richey, 1989, Table 2, p.24	49	Salado	FFG_105	812.90	Richey, 1989, Table 2, p.27
12	Salado	FFG_065	449.60	Richey, 1989, Table 2, p.24	50	Salado	FFG_106	840.70	Richey, 1989, Table 2, p.27
13	Salado	FFG_066	401.70	Richey, 1989, Table 2, p.24	51	Salado	FFG_107	836.10	Richey, 1989, Table 2, p.27
14	Salado	FFG_067	435.90	Richey, 1989, Table 2, p.25	52	Salado	FFG_108	836.10	Richey, 1989, Table 2, p.27
15	Salado	FFG_068	396.50	Richey, 1989, Table 2, p.25	53	Salado	FFG_109	831.80	Richey, 1989, Table 2, p.27
16	Salado	FFG_069	407.90	Richey, 1989, Table 2, p.25	54	Salado	FFG_110	798.60	Richey, 1989, Table 2, p.27
17	Salado	FFG_070	442.00	Richey, 1989, Table 2, p.25	55	Salado	FFG_111	806.20	Richey, 1989, Table 2, p.27
18	Salado	FFG_071	700.20	Richey, 1989, Table 2, p.25	56	Salado	FFG_112	784.80	Richey, 1989, Table 2, p.28
19	Salado	FFG_072	645.80	Richey, 1989, Table 2, p.25	57	Salado	FFG_113	802.20	Richey, 1989, Table 2, p.28
20	Salado	FFG_073	623.30	Richey, 1989, Table 2, p.25	58	Salado	FFG_114	828.80	Richey, 1989, Table 2, p.28
21	Salado	FFG_074	630.70	Richey, 1989, Table 2, p.25	59	Salado	FFG_115	803.50	Richey, 1989, Table 2, p.28
22	Salado	FFG_075	683.40	Richey, 1989, Table 2, p.25	60	Salado	FFG_116	795.20	Richey, 1989, Table 2, p.28
23	Salado	FFG_076	741.90	Richey, 1989, Table 2, p.25	61	Salado	FFG_117	810.80	Richey, 1989, Table 2, p.28
24	Salado	FFG_078	776.90	Richey, 1989, Table 2, p.25	62	Salado	FFG_119	828.20	Richey, 1989, Table 2, p.28
25	Salado	FFG_079	750.40	Richey, 1989, Table 2, p.25	63	Salado	FFG_120	819.30	Richey, 1989, Table 2, p.28
26	Salado	FFG_080	727.50	Richey, 1989, Table 2, p.25	64	Salado	FFG_121	830.60	Richey, 1989, Table 2, p.28
27	Salado	FFG_081	644.40	Richey, 1989, Table 2, p.26	65	Salado	FFG_122	813.80	Richey, 1989, Table 2, p.28
28	Salado	FFG_082	673.00	Richey, 1989, Table 2, p.26	66	Salado	FFG_123	815.30	Richey, 1989, Table 2, p.28
29	Salado	FFG_083	604.60	Richey, 1989, Table 2, p.26	67	Salado	FFG_124	785.50	Richey, 1989, Table 2, p.28
30	Salado	FFG_084	626.00	Richey, 1989, Table 2, p.26	68	Salado	FFG_126	813.00	Richey, 1989, Table 2, p.28
31	Salado	FFG_085	620.90	Richey, 1989, Table 2, p.26	69	Salado	FFG_127	824.10	Richey, 1989, Table 2, p.28
32	Salado	FFG_086	630.30	Richey, 1989, Table 2, p.26	70	Salado	FFG_128	852.60	Richey, 1989, Table 2, p.28
33	Salado	FFG_087	601.30	Richey, 1989, Table 2, p.26	71	Salado	FFG_129	815.60	Richey, 1989, Table 2, p.28
34	Salado	FFG_088	595.30	Richey, 1989, Table 2, p.26	72	Salado	FFG_130	854.90	Richey, 1989, Table 2, p.28
35	Salado	FFG_089	576.70	Richey, 1989, Table 2, p.26	73	Salado	FFG_132	852.80	Richey, 1989, Table 2, p.29
36	Salado	FFG_091	614.20	Richey, 1989, Table 2, p.26	74	Salado	FFG_133	837.60	Richey, 1989, Table 2, p.29
37	Salado	FFG_092	633.70	Richey, 1989, Table 2, p.26	75	Salado	FFG_134	861.70	Richey, 1989, Table 2, p.29
38	Salado	FFG_093	637.70	Richey, 1989, Table 2, p.26	76	Salado	FFG_135	844.00	Richey, 1989, Table 2, p.29

Table B.2. Elevations of Stratigraphic Layers Near WIPP (Continued)

	Layer	Well ID	Elevation	Source		Layer	Well ID	Elevation	Source
1	Salado	FFG_136	844.40	Richey, 1989, Table 2, p.29	39	Salado	FFG_183	837.30	Richey, 1989, Table 2, p.32
2	Salado	FFG_137	853.20	Richey, 1989, Table 2, p.29	40	Salado	FFG_184	851.60	Richey, 1989, Table 2, p.32
3	Salado	FFG_138	798.30	Richey, 1989, Table 2, p.29	41	Salado	FFG_185	840.00	Richey, 1989, Table 2, p.32
4	Salado	FFG_139	810.10	Richey, 1989, Table 2, p.29	42	Salado	FFG_186	766.30	Richey, 1989, Table 2, p.32
5	Salado	FFG_140	750.00	Richey, 1989, Table 2, p.29	43	Salado	FFG_188	781.20	Richey, 1989, Table 2, p.32
6	Salado	FFG_141	782.90	Richey, 1989, Table 2, p.29	44	Salado	FFG_189	805.00	Richey, 1989, Table 2, p.32
7	Salado	FFG_142	757.80	Richey, 1989, Table 2, p.29	45	Salado	FFG_190	793.40	Richey, 1989, Table 2, p.32
8	Salado	FFG_144	825.10	Richey, 1989, Table 2, p.29	46	Salado	FFG_191	780.00	Richey, 1989, Table 2, p.32
9	Salado	FFG_145	830.60	Richey, 1989, Table 2, p.29	47	Salado	FFG_192	708.00	Richey, 1989, Table 2, p.32
10	Salado	FFG_146	826.00	Richey, 1989, Table 2, p.29	48	Salado	FFG_194	738.80	Richey, 1989, Table 2, p.33
11	Salado	FFG_147	816.30	Richey, 1989, Table 2, p.29	49	Salado	FFG_195	753.50	Richey, 1989, Table 2, p.33
12	Salado	FFG_148	832.10	Richey, 1989, Table 2, p.29	50	Salado	FFG_196	792.50	Richey, 1989, Table 2, p.33
13	Salado	FFG_149	842.10	Richey, 1989, Table 2, p.30	51	Salado	FFG_197	790.10	Richey, 1989, Table 2, p.33
14	Salado	FFG_152	836.70	Richey, 1989, Table 2, p.30	52	Salado	FFG_198	783.90	Richey, 1989, Table 2, p.33
15	Salado	FFG_155	830.90	Richey, 1989, Table 2, p.30	53	Salado	FFG_199	780.60	Richey, 1989, Table 2, p.33
16	Salado	FFG_156	837.60	Richey, 1989, Table 2, p.30	54	Salado	FFG_200	785.20	Richey, 1989, Table 2, p.33
17	Salado	FFG_158	856.80	Richey, 1989, Table 2, p.30	55	Salado	FFG_201	778.70	Richey, 1989, Table 2, p.33
18	Salado	FFG_159	859.60	Richey, 1989, Table 2, p.30	56	Salado	FFG_202	723.60	Richey, 1989, Table 2, p.33
19	Salado	FFG_160	855.60	Richey, 1989, Table 2, p.30	57	Salado	FFG_203	727.60	Richey, 1989, Table 2, p.33
20	Salado	FFG_161	856.80	Richey, 1989, Table 2, p.30	58	Salado	FFG_204	767.20	Richey, 1989, Table 2, p.33
21	Salado	FFG_162	857.70	Richey, 1989, Table 2, p.30	59	Salado	FFG_205	768.50	Richey, 1989, Table 2, p.33
22	Salado	FFG_163	856.20	Richey, 1989, Table 2, p.30	60	Salado	FFG_206	779.40	Richey, 1989, Table 2, p.33
23	Salado	FFG_164	854.70	Richey, 1989, Table 2, p.30	61	Salado	FFG_207	775.70	Richey, 1989, Table 2, p.33
24	Salado	FFG_165	838.80	Richey, 1989, Table 2, p.30	62	Salado	FFG_208	780.30	Richey, 1989, Table 2, p.34
25	Salado	FFG_166	858.30	Richey, 1989, Table 2, p.31	63	Salado	FFG_209	787.30	Richey, 1989, Table 2, p.34
26	Salado	FFG_167	836.70	Richey, 1989, Table 2, p.31	64	Salado	FFG_210	766.00	Richey, 1989, Table 2, p.34
27	Salado	FFG_168	843.10	Richey, 1989, Table 2, p.31	65	Salado	FFG_212	768.40	Richey, 1989, Table 2, p.34
28	Salado	FFG_169	861.30	Richey, 1989, Table 2, p.31	66	Salado	FFG_213	795.30	Richey, 1989, Table 2, p.34
29	Salado	FFG_170	839.10	Richey, 1989, Table 2, p.31	67	Salado	FFG_214	757.70	Richey, 1989, Table 2, p.34
30	Salado	FFG_171	848.00	Richey, 1989, Table 2, p.31	68	Salado	FFG_215	734.60	Richey, 1989, Table 2, p.34
31	Salado	FFG_172	851.90	Richey, 1989, Table 2, p.31	69	Salado	FFG_216	520.60	Richey, 1989, Table 2, p.34
32	Salado	FFG_173	831.50	Richey, 1989, Table 2, p.31	70	Salado	FFG_217	756.30	Richey, 1989, Table 2, p.34
33	Salado	FFG_177	812.60	Richey, 1989, Table 2, p.31	71	Salado	FFG_218	744.00	Richey, 1989, Table 2, p.34
34	Salado	FFG_178	539.20	Richey, 1989, Table 2, p.31	72	Salado	FFG_219	783.30	Richey, 1989, Table 2, p.34
35	Salado	FFG_179	816.80	Richey, 1989, Table 2, p.31	73	Salado	FFG_220	742.20	Richey, 1989, Table 2, p.34
36	Salado	FFG_180	825.10	Richey, 1989, Table 2, p.31	74	Salado	FFG_221	684.90	Richey, 1989, Table 2, p.34
37	Salado	FFG_181	869.00	Richey, 1989, Table 2, p.32	75	Salado	FFG_222	604.50	Richey, 1989, Table 2, p.34
38	Salado	FFG_182	757.10	Richey, 1989, Table 2, p.32	76	Salado	FFG_224	558.10	Richey, 1989, Table 2, p.35

Table B.2. Elevations of Stratigraphic Layers Near WIPP (Continued)

	Layer	Well ID	Elevation	Source
1	Salado	FFG_225	566.30	Richey, 1989, Table 2, p.35
2	Salado	FFG_226	561.90	Richey, 1989, Table 2, p.35
3	Salado	FFG_228	549.30	Richey, 1989, Table 2, p.35
4	Salado	FFG_229	572.10	Richey, 1989, Table 2, p.35
5	Salado	FFG_230	558.40	Richey, 1989, Table 2, p.35
6	Salado	FFG_231	578.20	Richey, 1989, Table 2, p.35
7	Salado	FFG_232	586.10	Richey, 1989, Table 2, p.35
8	Salado	FFG_233	581.90	Richey, 1989, Table 2, p.35
9	Salado	FFG_234	616.30	Richey, 1989, Table 2, p.35
10	Salado	FFG_235	595.90	Richey, 1989, Table 2, p.35
11	Salado	FFG_236	641.90	Richey, 1989, Table 2, p.35
12	Salado	FFG_237	600.80	Richey, 1989, Table 2, p.35
13	Salado	FFG_238	584.30	Richey, 1989, Table 2, p.36
14	Salado	FFG_239	570.50	Richey, 1989, Table 2, p.36
15	Salado	FFG_240	568.80	Richey, 1989, Table 2, p.36
16	Salado	FFG_241	562.70	Richey, 1989, Table 2, p.36
17	Salado	FFG_242	681.30	Richey, 1989, Table 2, p.36
18	Salado	FFG_243	615.10	Richey, 1989, Table 2, p.36
19	Salado	FFG_244	689.30	Richey, 1989, Table 2, p.36
20	Salado	FFG_245	470.60	Richey, 1989, Table 2, p.36
21	Salado	FFG_246	473.10	Richey, 1989, Table 2, p.36
22	Salado	FFG_247	460.10	Richey, 1989, Table 2, p.36
23	Salado	FFG_248	464.50	Richey, 1989, Table 2, p.36
24	Salado	FFG_249	464.20	Richey, 1989, Table 2, p.36
25	Salado	FFG_250	545.50	Richey, 1989, Table 2, p.36
26	Salado	FFG_251	432.20	Richey, 1989, Table 2, p.36
27	Salado	FFG_252	567.50	Richey, 1989, Table 2, p.36
28	Salado	FFG_253	521.90	Richey, 1989, Table 2, p.36
29	Salado	FFG_254	517.80	Richey, 1989, Table 2, p.36
30	Salado	FFG_255	467.30	Richey, 1989, Table 2, p.37
31	Salado	FFG_256	438.90	Richey, 1989, Table 2, p.37
32	Salado	FFG_257	484.00	Richey, 1989, Table 2, p.37
33	Salado	FFG_258	497.70	Richey, 1989, Table 2, p.37
34	Salado	FFG_259	456.80	Richey, 1989, Table 2, p.37
35	Salado	FFG_260	515.10	Richey, 1989, Table 2, p.37
36	Salado	FFG_261	502.60	Richey, 1989, Table 2, p.37
37	Salado	FFG_262	440.50	Richey, 1989, Table 2, p.37
38	Salado	FFG_263	406.80	Richey, 1989, Table 2, p.37
39	Salado	FFG_264	653.50	Richey, 1989, Table 2, p.37
40	Salado	FFG_265	634.60	Richey, 1989, Table 2, p.37
41	Salado	FFG_266	609.60	Richey, 1989, Table 2, p.37
42	Salado	FFG_267	582.70	Richey, 1989, Table 2, p.37
43	Salado	FFG_268	563.30	Richey, 1989, Table 2, p.37
44	Salado	FFG_269	568.30	Richey, 1989, Table 2, p.38
45	Salado	FFG_270	689.40	Richey, 1989, Table 2, p.38
46	Salado	FFG_271	733.30	Richey, 1989, Table 2, p.38
47	Salado	FFG_272	697.20	Richey, 1989, Table 2, p.38
48	Salado	FFG_273	701.70	Richey, 1989, Table 2, p.38
49	Salado	FFG_274	747.40	Richey, 1989, Table 2, p.38
50	Salado	FFG_275	767.20	Richey, 1989, Table 2, p.38
51	Salado	FFG_276	766.20	Richey, 1989, Table 2, p.38
52	Salado	FFG_277	753.50	Richey, 1989, Table 2, p.38
53	Salado	FFG_278	722.40	Richey, 1989, Table 2, p.38
54	Salado	FFG_279	735.70	Richey, 1989, Table 2, p.38
55	Salado	FFG_280	738.20	Richey, 1989, Table 2, p.38
56	Salado	FFG_281	709.30	Richey, 1989, Table 2, p.38
57	Salado	FFG_283	450.50	Richey, 1989, Table 2, p.39
58	Salado	FFG_284	596.20	Richey, 1989, Table 2, p.39
59	Salado	FFG_285	616.00	Richey, 1989, Table 2, p.39
60	Salado	FFG_286	728.70	Richey, 1989, Table 2, p.39
61	Salado	FFG_287	693.10	Richey, 1989, Table 2, p.39
62	Salado	FFG_288	616.90	Richey, 1989, Table 2, p.39
63	Salado	FFG_289	639.10	Richey, 1989, Table 2, p.39
64	Salado	FFG_290	733.40	Richey, 1989, Table 2, p.39
65	Salado	FFG_291	615.10	Richey, 1989, Table 2, p.39
66	Salado	FFG_292	686.70	Richey, 1989, Table 2, p.39
67	Salado	FFG_293	672.40	Richey, 1989, Table 2, p.39
68	Salado	FFG_294	458.20	Richey, 1989, Table 2, p.39
69	Salado	FFG_295	438.90	Richey, 1989, Table 2, p.39
70	Salado	FFG_297	420.30	Richey, 1989, Table 2, p.39
71	Salado	FFG_298	490.00	Richey, 1989, Table 2, p.40
72	Salado	FFG_299	441.40	Richey, 1989, Table 2, p.40
73	Salado	FFG_300	416.90	Richey, 1989, Table 2, p.40
74	Salado	FFG_301	359.40	Richey, 1989, Table 2, p.40
75	Salado	FFG_302	420.30	Richey, 1989, Table 2, p.40
76	Salado	FFG_303	404.80	Richey, 1989, Table 2, p.40

Table B.2. Elevations of Stratigraphic Layers Near WIPP (Continued)

	Layer	Well ID	Elevation	Source		Layer	Well ID	Elevation	Source
1	Salado	FFG_304	399.30	Richey, 1989, Table 2, p.40	39	Salado	FFG_344	622.60	Richey, 1989, Table 2, p.43
2	Salado	FFG_305	399.60	Richey, 1989, Table 2, p.40	40	Salado	FFG_345	628.60	Richey, 1989, Table 2, p.43
3	Salado	FFG_306	361.40	Richey, 1989, Table 2, p.40	41	Salado	FFG_347	655.30	Richey, 1989, Table 2, p.43
4	Salado	FFG_307	383.80	Richey, 1989, Table 2, p.40	42	Salado	FFG_348	686.10	Richey, 1989, Table 2, p.43
5	Salado	FFG_308	323.00	Richey, 1989, Table 2, p.40	43	Salado	FFG_349	678.80	Richey, 1989, Table 2, p.43
6	Salado	FFG_309	388.60	Richey, 1989, Table 2, p.40	44	Salado	FFG_350	712.30	Richey, 1989, Table 2, p.43
7	Salado	FFG_310	430.00	Richey, 1989, Table 2, p.40	45	Salado	FFG_351	571.50	Richey, 1989, Table 2, p.43
8	Salado	FFG_311	387.40	Richey, 1989, Table 2, p.40	46	Salado	FFG_352	573.10	Richey, 1989, Table 2, p.43
9	Salado	FFG_312	384.10	Richey, 1989, Table 2, p.40	47	Salado	FFG_353	598.40	Richey, 1989, Table 2, p.43
10	Salado	FFG_313	832.20	Richey, 1989, Table 2, p.41	48	Salado	FFG_354	722.40	Richey, 1989, Table 2, p.43
11	Salado	FFG_314	734.90	Richey, 1989, Table 2, p.41	49	Salado	FFG_361	905.80	Richey, 1989, Table 2, p.44
12	Salado	FFG_315	650.90	Richey, 1989, Table 2, p.41	50	Salado	FFG_362	841.50	Richey, 1989, Table 2, p.44
13	Salado	FFG_316	624.20	Richey, 1989, Table 2, p.41	51	Salado	FFG_363	881.50	Richey, 1989, Table 2, p.44
14	Salado	FFG_317	693.10	Richey, 1989, Table 2, p.41	52	Salado	FFG_366	863.80	Richey, 1989, Table 2, p.44
15	Salado	FFG_318	666.00	Richey, 1989, Table 2, p.41	53	Salado	FFG_367	876.90	Richey, 1989, Table 2, p.44
16	Salado	FFG_319	662.00	Richey, 1989, Table 2, p.41	54	Salado	FFG_370	919.30	Richey, 1989, Table 2, p.44
17	Salado	FFG_320	616.00	Richey, 1989, Table 2, p.41	55	Salado	FFG_371	919.90	Richey, 1989, Table 2, p.44
18	Salado	FFG_321	612.90	Richey, 1989, Table 2, p.41	56	Salado	FFG_374	855.00	Richey, 1989, Table 2, p.45
19	Salado	FFG_322	616.80	Richey, 1989, Table 2, p.41	57	Salado	FFG_376	896.40	Richey, 1989, Table 2, p.45
20	Salado	FFG_323	626.80	Richey, 1989, Table 2, p.41	58	Salado	FFG_381	875.10	Richey, 1989, Table 2, p.45
21	Salado	FFG_324	653.20	Richey, 1989, Table 2, p.41	59	Salado	FFG_383	867.20	Richey, 1989, Table 2, p.45
22	Salado	FFG_325	713.50	Richey, 1989, Table 2, p.41	60	Salado	FFG_385	856.50	Richey, 1989, Table 2, p.45
23	Salado	FFG_326	657.50	Richey, 1989, Table 2, p.41	61	Salado	FFG_387	862.00	Richey, 1989, Table 2, p.45
24	Salado	FFG_327	645.30	Richey, 1989, Table 2, p.42	62	Salado	FFG_390	863.50	Richey, 1989, Table 2, p.46
25	Salado	FFG_328	620.50	Richey, 1989, Table 2, p.42	63	Salado	FFG_391	868.30	Richey, 1989, Table 2, p.46
26	Salado	FFG_329	613.20	Richey, 1989, Table 2, p.42	64	Salado	FFG_392	863.20	Richey, 1989, Table 2, p.46
27	Salado	FFG_330	611.60	Richey, 1989, Table 2, p.42	65	Salado	FFG_393	752.70	Richey, 1989, Table 2, p.46
28	Salado	FFG_331	602.60	Richey, 1989, Table 2, p.42	66	Salado	FFG_394	846.70	Richey, 1989, Table 2, p.46
29	Salado	FFG_332	587.00	Richey, 1989, Table 2, p.42	67	Salado	FFG_395	842.20	Richey, 1989, Table 2, p.46
30	Salado	FFG_333	598.80	Richey, 1989, Table 2, p.42	68	Salado	FFG_396	787.30	Richey, 1989, Table 2, p.46
31	Salado	FFG_334	589.10	Richey, 1989, Table 2, p.42	69	Salado	FFG_403	846.90	Richey, 1989, Table 2, p.47
32	Salado	FFG_335	607.80	Richey, 1989, Table 2, p.42	70	Salado	FFG_408	827.80	Richey, 1989, Table 2, p.47
33	Salado	FFG_336	603.20	Richey, 1989, Table 2, p.42	71	Salado	FFG_411	789.10	Richey, 1989, Table 2, p.47
34	Salado	FFG_337	584.60	Richey, 1989, Table 2, p.42	72	Salado	FFG_413	835.20	Richey, 1989, Table 2, p.47
35	Salado	FFG_338	589.60	Richey, 1989, Table 2, p.42	73	Salado	FFG_421	879.40	Richey, 1989, Table 2, p.48
36	Salado	FFG_339	553.80	Richey, 1989, Table 2, p.42	74	Salado	FFG_426	856.50	Richey, 1989, Table 2, p.48
37	Salado	FFG_340	559.90	Richey, 1989, Table 2, p.42	75	Salado	FFG_432	837.30	Richey, 1989, Table 2, p.48
38	Salado	FFG_342	651.60	Richey, 1989, Table 2, p.43	76	Salado	FFG_433	816.80	Richey, 1989, Table 2, p.48

Table B.2. Elevations of Stratigraphic Layers Near WIPP (Continued)

	Layer	Well ID	Elevation	Source		Layer	Well ID	Elevation	Source
1	Salado	FFG_438	797.50	Richey, 1989, Table 2, p.49	39	Salado	FFG_494	713.20	Richey, 1989, Table 2, p.53
2	Salado	FFG_445	827.20	Richey, 1989, Table 2, p.49	40	Salado	FFG_495	696.40	Richey, 1989, Table 2, p.53
3	Salado	FFG_453	726.50	Richey, 1989, Table 2, p.50	41	Salado	FFG_496	555.40	Richey, 1989, Table 2, p.53
4	Salado	FFG_455	723.90	Richey, 1989, Table 2, p.50	42	Salado	FFG_497	601.70	Richey, 1989, Table 2, p.53
5	Salado	FFG_456	730.90	Richey, 1989, Table 2, p.50	43	Salado	FFG_498	589.20	Richey, 1989, Table 2, p.53
6	Salado	FFG_457	784.50	Richey, 1989, Table 2, p.50	44	Salado	FFG_499	549.90	Richey, 1989, Table 2, p.53
7	Salado	FFG_458	785.50	Richey, 1989, Table 2, p.50	45	Salado	FFG_500	582.80	Richey, 1989, Table 2, p.53
8	Salado	FFG_459	717.20	Richey, 1989, Table 2, p.50	46	Salado	FFG_501	625.40	Richey, 1989, Table 2, p.53
9	Salado	FFG_462	781.30	Richey, 1989, Table 2, p.50	47	Salado	FFG_502	567.20	Richey, 1989, Table 2, p.53
10	Salado	FFG_463	811.40	Richey, 1989, Table 2, p.51	48	Salado	FFG_503	573.70	Richey, 1989, Table 2, p.53
11	Salado	FFG_464	787.60	Richey, 1989, Table 2, p.51	49	Salado	FFG_504	618.80	Richey, 1989, Table 2, p.53
12	Salado	FFG_465	783.90	Richey, 1989, Table 2, p.51	50	Salado	FFG_505	650.50	Richey, 1989, Table 2, p.53
13	Salado	FFG_467	380.30	Richey, 1989, Table 2, p.51	51	Salado	FFG_506	649.50	Richey, 1989, Table 2, p.53
14	Salado	FFG_468	322.20	Richey, 1989, Table 2, p.51	52	Salado	FFG_507	549.10	Richey, 1989, Table 2, p.53
15	Salado	FFG_470	360.00	Richey, 1989, Table 2, p.51	53	Salado	FFG_508	628.80	Richey, 1989, Table 2, p.53
16	Salado	FFG_471	372.40	Richey, 1989, Table 2, p.51	54	Salado	FFG_509	616.30	Richey, 1989, Table 2, p.54
17	Salado	FFG_472	439.30	Richey, 1989, Table 2, p.51	55	Salado	FFG_510	615.20	Richey, 1989, Table 2, p.54
18	Salado	FFG_473	339.50	Richey, 1989, Table 2, p.51	56	Salado	FFG_511	570.60	Richey, 1989, Table 2, p.54
19	Salado	FFG_474	634.90	Richey, 1989, Table 2, p.51	57	Salado	FFG_512	576.70	Richey, 1989, Table 2, p.54
20	Salado	FFG_475	637.80	Richey, 1989, Table 2, p.51	58	Salado	FFG_513	606.00	Richey, 1989, Table 2, p.54
21	Salado	FFG_476	711.40	Richey, 1989, Table 2, p.51	59	Salado	FFG_514	577.30	Richey, 1989, Table 2, p.54
22	Salado	FFG_477	679.70	Richey, 1989, Table 2, p.51	60	Salado	FFG_515	556.20	Richey, 1989, Table 2, p.54
23	Salado	FFG_478	655.30	Richey, 1989, Table 2, p.52	61	Salado	FFG_516	545.90	Richey, 1989, Table 2, p.54
24	Salado	FFG_479	661.10	Richey, 1989, Table 2, p.52	62	Salado	FFG_517	732.50	Richey, 1989, Table 2, p.54
25	Salado	FFG_480	641.60	Richey, 1989, Table 2, p.52	63	Salado	FFG_518	720.20	Richey, 1989, Table 2, p.54
26	Salado	FFG_481	635.20	Richey, 1989, Table 2, p.52	64	Salado	FFG_519	659.90	Richey, 1989, Table 2, p.54
27	Salado	FFG_482	665.40	Richey, 1989, Table 2, p.52	65	Salado	FFG_520	542.70	Richey, 1989, Table 2, p.54
28	Salado	FFG_483	690.90	Richey, 1989, Table 2, p.52	66	Salado	FFG_521	604.70	Richey, 1989, Table 2, p.54
29	Salado	FFG_484	672.20	Richey, 1989, Table 2, p.52	67	Salado	FFG_522	382.40	Richey, 1989, Table 2, p.54
30	Salado	FFG_485	682.80	Richey, 1989, Table 2, p.52	68	Salado	FFG_523	388.90	Richey, 1989, Table 2, p.54
31	Salado	FFG_486	668.70	Richey, 1989, Table 2, p.52	69	Salado	FFG_524	561.70	Richey, 1989, Table 2, p.55
32	Salado	FFG_487	669.40	Richey, 1989, Table 2, p.52	70	Salado	FFG_525	388.40	Richey, 1989, Table 2, p.55
33	Salado	FFG_488	648.90	Richey, 1989, Table 2, p.52	71	Salado	FFG_526	911.10	Richey, 1989, Table 2, p.55
34	Salado	FFG_489	663.10	Richey, 1989, Table 2, p.52	72	Salado	FFG_527	871.10	Richey, 1989, Table 2, p.55
35	Salado	FFG_490	765.70	Richey, 1989, Table 2, p.52	73	Salado	FFG_528	864.10	Richey, 1989, Table 2, p.55
36	Salado	FFG_491	752.60	Richey, 1989, Table 2, p.52	74	Salado	FFG_530	930.20	Richey, 1989, Table 2, p.55
37	Salado	FFG_492	720.50	Richey, 1989, Table 2, p.52	75	Salado	FFG_531	855.20	Richey, 1989, Table 2, p.55
38	Salado	FFG_493	709.70	Richey, 1989, Table 2, p.53	76	Salado	FFG_532	838.50	Richey, 1989, Table 2, p.55

Table B.2. Elevations of Stratigraphic Layers Near WIPP (Continued)

	Layer	Well ID	Elevation	Source		Layer	Well ID	Elevation	Source
1	Salado	FFG_535	850.40	Richey, 1989, Table 2, p.55	39	Salado	FFG_676	831.80	Richey, 1989, Table 2, p.62
2	Salado	FFG_536	853.50	Richey, 1989, Table 2, p.55	40	Salado	FFG_677	857.10	Richey, 1989, Table 2, p.62
3	Salado	FFG_537	840.60	Richey, 1989, Table 2, p.55	41	Salado	FFG_679	861.10	Richey, 1989, Table 2, p.62
4	Salado	FFG_564	557.80	Richey, 1989, Table 2, p.57	42	Salado	FFG_685	825.70	Richey, 1989, Table 2, p.63
5	Salado	FFG_584	690.90	Richey, 1989, Table 2, p.58	43	Salado	FFG_689	718.10	Richey, 1989, Table 2, p.63
6	Salado	FFG_585	643.40	Richey, 1989, Table 2, p.58	44	Salado	FFG_690	718.10	Richey, 1989, Table 2, p.63
7	Salado	FFG_602	743.70	Richey, 1989, Table 2, p.58	45	Salado	FFG_691	711.40	Richey, 1989, Table 2, p.63
8	Salado	FFG_606	603.20	Richey, 1989, Table 2, p.58	46	Salado	FFG_693	712.60	Richey, 1989, Table 2, p.63
9	Salado	FFG_607	624.30	Richey, 1989, Table 2, p.59	47	Salado	FFG_694	680.30	Richey, 1989, Table 2, p.63
10	Salado	FFG_608	593.70	Richey, 1989, Table 2, p.59	48	Salado	FFG_695	702.60	Richey, 1989, Table 2, p.63
11	Salado	FFG_609	586.10	Richey, 1989, Table 2, p.59	49	Salado	FFG_696	703.10	Richey, 1989, Table 2, p.63
12	Salado	FFG_610	588.30	Richey, 1989, Table 2, p.59	50	Salado	FFG_697	699.90	Richey, 1989, Table 2, p.64
13	Salado	FFG_611	579.40	Richey, 1989, Table 2, p.59	51	Salado	FFG_698	734.90	Richey, 1989, Table 2, p.64
14	Salado	FFG_612	624.90	Richey, 1989, Table 2, p.59	52	Salado	FFG_699	691.00	Richey, 1989, Table 2, p.64
15	Salado	FFG_613	621.80	Richey, 1989, Table 2, p.59	53	Salado	FFG_700	682.20	Richey, 1989, Table 2, p.64
16	Salado	FFG_640	519.50	Richey, 1989, Table 2, p.60	54	Salado	FFG_701	686.50	Richey, 1989, Table 2, p.64
17	Salado	FFG_643	576.10	Richey, 1989, Table 2, p.60	55	Salado	FFG_702	693.70	Richey, 1989, Table 2, p.64
18	Salado	FFG_652	786.40	Richey, 1989, Table 2, p.60	56	Salado	FFG_703	716.90	Richey, 1989, Table 2, p.64
19	Salado	FFG_653	788.60	Richey, 1989, Table 2, p.61	57	Salado	FFG_704	686.40	Richey, 1989, Table 2, p.64
20	Salado	FFG_654	812.30	Richey, 1989, Table 2, p.61	58	Salado	FFG_705	610.80	Richey, 1989, Table 2, p.64
21	Salado	FFG_655	812.90	Richey, 1989, Table 2, p.61	59	Salado	FFG_706	637.10	Richey, 1989, Table 2, p.64
22	Salado	FFG_656	808.90	Richey, 1989, Table 2, p.61	60	Salado	FFG_707	616.70	Richey, 1989, Table 2, p.64
23	Salado	FFG_657	830.00	Richey, 1989, Table 2, p.61	61	Salado	FFG_708	669.70	Richey, 1989, Table 2, p.64
24	Salado	FFG_658	816.20	Richey, 1989, Table 2, p.61	62	Salado	FFG_710	579.20	Richey, 1989, Table 2, p.64
25	Salado	FFG_659	821.10	Richey, 1989, Table 2, p.61	63	Salado	FFG_711	570.60	Richey, 1989, Table 2, p.65
26	Salado	FFG_660	845.10	Richey, 1989, Table 2, p.61	64	Salado	FFG_716	553.10	Richey, 1989, Table 2, p.65
27	Salado	FFG_662	810.20	Richey, 1989, Table 2, p.61	65	Salado	FFG_717	621.90	Richey, 1989, Table 2, p.65
28	Salado	FFG_664	794.90	Richey, 1989, Table 2, p.61	66	Salado	FFG_718	612.80	Richey, 1989, Table 2, p.65
29	Salado	FFG_666	860.10	Richey, 1989, Table 2, p.62	67	Salado	FFG_719	571.20	Richey, 1989, Table 2, p.65
30	Salado	FFG_667	845.80	Richey, 1989, Table 2, p.62	68	Salado	FFG_720	570.60	Richey, 1989, Table 2, p.65
31	Salado	FFG_668	905.10	Richey, 1989, Table 2, p.62	69	Salado	FFG_721	594.40	Richey, 1989, Table 2, p.65
32	Salado	FFG_669	890.60	Richey, 1989, Table 2, p.62	70	Salado	FFG_723	712.50	Richey, 1989, Table 2, p.65
33	Salado	FFG_670	876.00	Richey, 1989, Table 2, p.62	71	Salado	FFG_724	633.80	Richey, 1989, Table 2, p.65
34	Salado	FFG_671	873.50	Richey, 1989, Table 2, p.62	72	Salado	FFG_725	610.50	Richey, 1989, Table 2, p.65
35	Salado	FFG_672	868.10	Richey, 1989, Table 2, p.62	73	Salado	FFG_726	589.10	Richey, 1989, Table 2, p.65
36	Salado	FFG_673	870.50	Richey, 1989, Table 2, p.62	74	Salado	FFG_727	575.50	Richey, 1989, Table 2, p.66
37	Salado	FFG_674	860.20	Richey, 1989, Table 2, p.62	75	Salado	FFG_728	590.40	Richey, 1989, Table 2, p.66
38	Salado	FFG_675	819.20	Richey, 1989, Table 2, p.62	76	Salado	FFG_729	595.90	Richey, 1989, Table 2, p.66

Table B.2. Elevations of Stratigraphic Layers Near WIPP (Continued)

	Layer	Well ID	Elevation	Source
1	Salado	FFG_730	622.70	Richey, 1989, Table 2, p.66
2	Salado	FFG_731	617.70	Richey, 1989, Table 2, p.66
3	Salado	FFG_733	698.30	Richey, 1989, Table 2, p.66
4	Salado	FFG_734	654.10	Richey, 1989, Table 2, p.66
5	Salado	FFG_735	584.00	Richey, 1989, Table 2, p.66
6	Salado	FFG_736	615.40	Richey, 1989, Table 2, p.66
7	Salado	FFG_737	559.30	Richey, 1989, Table 2, p.66
8	Salado	FFG_738	610.20	Richey, 1989, Table 2, p.66
9	Salado	FFG_739	628.60	Richey, 1989, Table 2, p.66
10	Salado	FFG_740	609.00	Richey, 1989, Table 2, p.66
11	Salado	FFG_741	602.30	Richey, 1989, Table 2, p.66
12	Salado	FFG_742	646.50	Richey, 1989, Table 2, p.67
13	Salado	FFG_743	630.70	Richey, 1989, Table 2, p.67
14	Salado	FFG_744	630.00	Richey, 1989, Table 2, p.67
15	Salado	FFG_745	598.30	Richey, 1989, Table 2, p.67
16	Salado	FFG_746	581.80	Richey, 1989, Table 2, p.67
17	Salado	H1	784.50	Mercer, 1983, Table 1
18	Salado	H10C	666.30	Mercer, 1983, Table 1
19	Salado	H2C	796.70	Mercer, 1983, Table 1
20	Salado	H3	783.10	Mercer, 1983, Table 1
21	Salado	H4C	825.40	Mercer, 1983, Table 1
22	Salado	H5C	751.60	Mercer, 1983, Table 1
23	Salado	H6C	800.70	Mercer, 1983, Table 1
24	Salado	H7C	877.80	Mercer, 1983, Table 1
25	Salado	H8C	823.00	Mercer, 1983, Table 1
26	Salado	H9C	797.00	Mercer, 1983, Table 1
27	Salado	P1	813.30	Mercer, 1983, Table 1
28	Salado	P10	738.50	Mercer, 1983, Table 1
29	Salado	P11	745.50	Mercer, 1983, Table 1
30	Salado	P12	800.10	Mercer, 1983, Table 1
31	Salado	P13	799.80	Mercer, 1983, Table 1
32	Salado	P14	814.70	Mercer, 1983, Table 1
33	Salado	P15	843.70	Mercer, 1983, Table 1
34	Salado	P16	814.40	Mercer, 1983, Table 1
35	Salado	P17	798.90	Mercer, 1983, Table 1
36	Salado	P18	728.20	Mercer, 1983, Table 1
37	Salado	P19	740.00	Mercer, 1983, Table 1
38	Salado	P2	753.20	Mercer, 1983, Table 1
39	Salado	P20	746.80	Mercer, 1983, Table 1
40	Salado	P21	751.60	Mercer, 1983, Table 1
41	Salado	P3	791.50	Mercer, 1983, Table 1
42	Salado	P4	766.20	Mercer, 1983, Table 1
43	Salado	P5	769.40	Mercer, 1983, Table 1
44	Salado	P6	821.40	Mercer, 1983, Table 1
45	Salado	P7	823.60	Mercer, 1983, Table 1
46	Salado	P8	799.80	Mercer, 1983, Table 1
47	Salado	P9	771.50	Mercer, 1983, Table 1
48	Salado	WIPP11	754.30	Mercer, 1983, Table 1
49	Salado	WIPP12	767.20	Mercer, 1983, Table 1
50	Salado	WIPP13	780.50	Mercer, 1983, Table 1
51	Salado	WIPP18	770.50	Mercer, 1983, Table 1
52	Salado	WIPP19	773.90	Mercer, 1983, Table 1
53	Salado	WIPP21	776.90	Mercer, 1983, Table 1
54	Salado	WIPP22	775.10	Mercer, 1983, Table 1
55	Salado	WIPP25	807.10	Mercer, 1983, Table 1
56	Salado	WIPP26	866.50	Mercer, 1983, Table 1
57	Salado	WIPP27	841.50	Mercer, 1983, Table 1
58	Salado	WIPP28	858.40	Mercer, 1983, Table 1
59	Salado	WIPP29	863.80	Mercer, 1983, Table 1
60	Salado	WIPP30	816.60	Mercer, 1983, Table 1
61	Salado	WIPP32	870.80	Mercer, 1983, Table 1
62	Salado	WIPP33	812.60	Mercer, 1983, Table 1
63	Salado	WIPP34	749.80	Mercer, 1983, Table 1
64	Supra_R	AEC7	1113.70	Mercer, 1983, Table 1
65	Supra_R	AEC8	1076.60	Mercer, 1983, Table 1
66	Supra_R	B25	1039.10	Mercer, 1983, Table 1
67	Supra_R	ERDA10	1027.50	Mercer, 1983, Table 1
68	Supra_R	ERDA6	1079.00	Mercer, 1983, Table 1
69	Supra_R	ERDA9	1042.10	Mercer, 1983, Table 1
70	Supra_R	FFG_002	1090.30	Richey, 1989, Table 2, p.21
71	Supra_R	FFG_004	1068.30	Richey, 1989, Table 2, p.21
72	Supra_R	FFG_005	1089.70	Richey, 1989, Table 2, p.21
73	Supra_R	FFG_006	1091.50	Richey, 1989, Table 2, p.21
74	Supra_R	FFG_007	1093.90	Richey, 1989, Table 2, p.21
75	Supra_R	FFG_009	1094.80	Richey, 1989, Table 2, p.21
76	Supra_R	FFG_011	1092.70	Richey, 1989, Table 2, p.21

Table B.2. Elevations of Stratigraphic Layers Near WIPP (Continued)

	Layer	Well ID	Elevation	Source		Layer	Well ID	Elevation	Source
1	Supra_R	FFG_012	1092.10	Richey, 1989, Table 2, p.21	39	Supra_R	FFG_055	1145.10	Richey, 1989, Table 2, p.24
2	Supra_R	FFG_013	1080.20	Richey, 1989, Table 2, p.21	40	Supra_R	FFG_056	1136.60	Richey, 1989, Table 2, p.24
3	Supra_R	FFG_014	1068.60	Richey, 1989, Table 2, p.21	41	Supra_R	FFG_057	1134.80	Richey, 1989, Table 2, p.24
4	Supra_R	FFG_016	1099.70	Richey, 1989, Table 2, p.21	42	Supra_R	FFG_058	1147.70	Richey, 1989, Table 2, p.24
5	Supra_R	FFG_017	1100.90	Richey, 1989, Table 2, p.22	43	Supra_R	FFG_059	1156.10	Richey, 1989, Table 2, p.24
6	Supra_R	FFG_018	1116.50	Richey, 1989, Table 2, p.22	44	Supra_R	FFG_060	1138.40	Richey, 1989, Table 2, p.24
7	Supra_R	FFG_019	1111.00	Richey, 1989, Table 2, p.22	45	Supra_R	FFG_061	1137.50	Richey, 1989, Table 2, p.24
8	Supra_R	FFG_020	1091.50	Richey, 1989, Table 2, p.22	46	Supra_R	FFG_062	1122.60	Richey, 1989, Table 2, p.24
9	Supra_R	FFG_023	1109.80	Richey, 1989, Table 2, p.22	47	Supra_R	FFG_063	1118.10	Richey, 1989, Table 2, p.24
10	Supra_R	FFG_024	1124.60	Richey, 1989, Table 2, p.22	48	Supra_R	FFG_064	1127.20	Richey, 1989, Table 2, p.24
11	Supra_R	FFG_025	1117.60	Richey, 1989, Table 2, p.22	49	Supra_R	FFG_065	1110.70	Richey, 1989, Table 2, p.24
12	Supra_R	FFG_026	1116.00	Richey, 1989, Table 2, p.22	50	Supra_R	FFG_066	1113.70	Richey, 1989, Table 2, p.24
13	Supra_R	FFG_027	1117.40	Richey, 1989, Table 2, p.22	51	Supra_R	FFG_067	1127.50	Richey, 1989, Table 2, p.25
14	Supra_R	FFG_028	1183.90	Richey, 1989, Table 2, p.22	52	Supra_R	FFG_068	1125.00	Richey, 1989, Table 2, p.25
15	Supra_R	FFG_029	1145.40	Richey, 1989, Table 2, p.22	53	Supra_R	FFG_069	1130.20	Richey, 1989, Table 2, p.25
16	Supra_R	FFG_030	1154.30	Richey, 1989, Table 2, p.22	54	Supra_R	FFG_070	1130.80	Richey, 1989, Table 2, p.25
17	Supra_R	FFG_031	1168.30	Richey, 1989, Table 2, p.22	55	Supra_R	FFG_071	1115.30	Richey, 1989, Table 2, p.25
18	Supra_R	FFG_032	1158.50	Richey, 1989, Table 2, p.22	56	Supra_R	FFG_072	1105.20	Richey, 1989, Table 2, p.25
19	Supra_R	FFG_033	1143.60	Richey, 1989, Table 2, p.22	57	Supra_R	FFG_073	1107.40	Richey, 1989, Table 2, p.25
20	Supra_R	FFG_034	1139.30	Richey, 1989, Table 2, p.23	58	Supra_R	FFG_074	1107.00	Richey, 1989, Table 2, p.25
21	Supra_R	FFG_035	1121.10	Richey, 1989, Table 2, p.23	59	Supra_R	FFG_075	1108.30	Richey, 1989, Table 2, p.25
22	Supra_R	FFG_036	1147.60	Richey, 1989, Table 2, p.23	60	Supra_R	FFG_076	1097.30	Richey, 1989, Table 2, p.25
23	Supra_R	FFG_037	1129.30	Richey, 1989, Table 2, p.23	61	Supra_R	FFG_078	1087.20	Richey, 1989, Table 2, p.25
24	Supra_R	FFG_038	1118.30	Richey, 1989, Table 2, p.23	62	Supra_R	FFG_079	1091.20	Richey, 1989, Table 2, p.25
25	Supra_R	FFG_039	1046.10	Richey, 1989, Table 2, p.23	63	Supra_R	FFG_080	1082.30	Richey, 1989, Table 2, p.25
26	Supra_R	FFG_040	1077.20	Richey, 1989, Table 2, p.23	64	Supra_R	FFG_081	1097.00	Richey, 1989, Table 2, p.26
27	Supra_R	FFG_041	1065.30	Richey, 1989, Table 2, p.23	65	Supra_R	FFG_082	1084.80	Richey, 1989, Table 2, p.26
28	Supra_R	FFG_042	1069.50	Richey, 1989, Table 2, p.23	66	Supra_R	FFG_083	1115.60	Richey, 1989, Table 2, p.26
29	Supra_R	FFG_043	1067.10	Richey, 1989, Table 2, p.23	67	Supra_R	FFG_084	1107.60	Richey, 1989, Table 2, p.26
30	Supra_R	FFG_044	1080.50	Richey, 1989, Table 2, p.23	68	Supra_R	FFG_085	1108.90	Richey, 1989, Table 2, p.26
31	Supra_R	FFG_047	1112.80	Richey, 1989, Table 2, p.23	69	Supra_R	FFG_086	1107.30	Richey, 1989, Table 2, p.26
32	Supra_R	FFG_048	1106.10	Richey, 1989, Table 2, p.23	70	Supra_R	FFG_087	1107.30	Richey, 1989, Table 2, p.26
33	Supra_R	FFG_049	1119.20	Richey, 1989, Table 2, p.23	71	Supra_R	FFG_088	1108.90	Richey, 1989, Table 2, p.26
34	Supra_R	FFG_050	1132.50	Richey, 1989, Table 2, p.24	72	Supra_R	FFG_089	1108.60	Richey, 1989, Table 2, p.26
35	Supra_R	FFG_051	1131.10	Richey, 1989, Table 2, p.24	73	Supra_R	FFG_091	1091.20	Richey, 1989, Table 2, p.26
36	Supra_R	FFG_052	1132.00	Richey, 1989, Table 2, p.24	74	Supra_R	FFG_092	1097.60	Richey, 1989, Table 2, p.26
37	Supra_R	FFG_053	1137.50	Richey, 1989, Table 2, p.24	75	Supra_R	FFG_093	1097.90	Richey, 1989, Table 2, p.26
38	Supra_R	FFG_054	1150.20	Richey, 1989, Table 2, p.24	76	Supra_R	FFG_094	1095.10	Richey, 1989, Table 2, p.26

Table B.2. Elevations of Stratigraphic Layers Near WIPP (Continued)

	Layer	Well ID	Elevation	Source
1	Supra_R	FFG_095	1138.70	Richey, 1989, Table 2, p.26
2	Supra_R	FFG_096	1174.40	Richey, 1989, Table 2, p.26
3	Supra_R	FFG_097	1149.40	Richey, 1989, Table 2, p.27
4	Supra_R	FFG_098	1208.20	Richey, 1989, Table 2, p.27
5	Supra_R	FFG_099	1205.80	Richey, 1989, Table 2, p.27
6	Supra_R	FFG_100	1153.10	Richey, 1989, Table 2, p.27
7	Supra_R	FFG_101	1142.70	Richey, 1989, Table 2, p.27
8	Supra_R	FFG_102	1127.20	Richey, 1989, Table 2, p.27
9	Supra_R	FFG_103	1108.60	Richey, 1989, Table 2, p.27
10	Supra_R	FFG_104	1127.50	Richey, 1989, Table 2, p.27
11	Supra_R	FFG_105	995.20	Richey, 1989, Table 2, p.27
12	Supra_R	FFG_106	981.50	Richey, 1989, Table 2, p.27
13	Supra_R	FFG_107	987.60	Richey, 1989, Table 2, p.27
14	Supra_R	FFG_108	1015.90	Richey, 1989, Table 2, p.27
15	Supra_R	FFG_109	1039.10	Richey, 1989, Table 2, p.27
16	Supra_R	FFG_110	1045.50	Richey, 1989, Table 2, p.27
17	Supra_R	FFG_111	1062.20	Richey, 1989, Table 2, p.27
18	Supra_R	FFG_112	1056.10	Richey, 1989, Table 2, p.28
19	Supra_R	FFG_113	1054.90	Richey, 1989, Table 2, p.28
20	Supra_R	FFG_114	1014.70	Richey, 1989, Table 2, p.28
21	Supra_R	FFG_115	970.50	Richey, 1989, Table 2, p.28
22	Supra_R	FFG_116	972.00	Richey, 1989, Table 2, p.28
23	Supra_R	FFG_117	966.20	Richey, 1989, Table 2, p.28
24	Supra_R	FFG_119	950.10	Richey, 1989, Table 2, p.28
25	Supra_R	FFG_120	956.50	Richey, 1989, Table 2, p.28
26	Supra_R	FFG_121	958.60	Richey, 1989, Table 2, p.28
27	Supra_R	FFG_122	954.00	Richey, 1989, Table 2, p.28
28	Supra_R	FFG_123	961.60	Richey, 1989, Table 2, p.28
29	Supra_R	FFG_124	977.20	Richey, 1989, Table 2, p.28
30	Supra_R	FFG_125	976.20	Richey, 1989, Table 2, p.28
31	Supra_R	FFG_126	1014.20	Richey, 1989, Table 2, p.28
32	Supra_R	FFG_127	1019.20	Richey, 1989, Table 2, p.28
33	Supra_R	FFG_128	994.30	Richey, 1989, Table 2, p.28
34	Supra_R	FFG_129	961.90	Richey, 1989, Table 2, p.28
35	Supra_R	FFG_130	979.90	Richey, 1989, Table 2, p.28
36	Supra_R	FFG_132	1002.20	Richey, 1989, Table 2, p.29
37	Supra_R	FFG_133	993.00	Richey, 1989, Table 2, p.29
38	Supra_R	FFG_134	988.20	Richey, 1989, Table 2, p.29
39	Supra_R	FFG_135	1002.50	Richey, 1989, Table 2, p.29
40	Supra_R	FFG_136	1007.50	Richey, 1989, Table 2, p.29
41	Supra_R	FFG_137	1007.40	Richey, 1989, Table 2, p.29
42	Supra_R	FFG_138	1023.90	Richey, 1989, Table 2, p.29
43	Supra_R	FFG_139	1023.50	Richey, 1989, Table 2, p.29
44	Supra_R	FFG_140	1042.60	Richey, 1989, Table 2, p.29
45	Supra_R	FFG_141	1030.40	Richey, 1989, Table 2, p.29
46	Supra_R	FFG_142	1042.80	Richey, 1989, Table 2, p.29
47	Supra_R	FFG_143	1052.70	Richey, 1989, Table 2, p.29
48	Supra_R	FFG_144	905.00	Richey, 1989, Table 2, p.29
49	Supra_R	FFG_145	905.30	Richey, 1989, Table 2, p.29
50	Supra_R	FFG_146	912.90	Richey, 1989, Table 2, p.29
51	Supra_R	FFG_147	908.30	Richey, 1989, Table 2, p.29
52	Supra_R	FFG_148	907.70	Richey, 1989, Table 2, p.29
53	Supra_R	FFG_149	916.50	Richey, 1989, Table 2, p.30
54	Supra_R	FFG_152	905.30	Richey, 1989, Table 2, p.30
55	Supra_R	FFG_155	918.10	Richey, 1989, Table 2, p.30
56	Supra_R	FFG_156	908.30	Richey, 1989, Table 2, p.30
57	Supra_R	FFG_157	926.00	Richey, 1989, Table 2, p.30
58	Supra_R	FFG_158	941.80	Richey, 1989, Table 2, p.30
59	Supra_R	FFG_159	1001.30	Richey, 1989, Table 2, p.30
60	Supra_R	FFG_160	1002.50	Richey, 1989, Table 2, p.30
61	Supra_R	FFG_161	987.90	Richey, 1989, Table 2, p.30
62	Supra_R	FFG_162	988.80	Richey, 1989, Table 2, p.30
63	Supra_R	FFG_163	988.80	Richey, 1989, Table 2, p.30
64	Supra_R	FFG_164	955.90	Richey, 1989, Table 2, p.30
65	Supra_R	FFG_165	935.70	Richey, 1989, Table 2, p.30
66	Supra_R	FFG_166	993.00	Richey, 1989, Table 2, p.31
67	Supra_R	FFG_167	1019.60	Richey, 1989, Table 2, p.31
68	Supra_R	FFG_168	1001.00	Richey, 1989, Table 2, p.31
69	Supra_R	FFG_169	986.00	Richey, 1989, Table 2, p.31
70	Supra_R	FFG_170	934.80	Richey, 1989, Table 2, p.31
71	Supra_R	FFG_171	956.80	Richey, 1989, Table 2, p.31
72	Supra_R	FFG_172	986.00	Richey, 1989, Table 2, p.31
73	Supra_R	FFG_173	1022.60	Richey, 1989, Table 2, p.31
74	Supra_R	FFG_177	913.20	Richey, 1989, Table 2, p.31
75	Supra_R	FFG_178	888.20	Richey, 1989, Table 2, p.31
76	Supra_R	FFG_179	896.40	Richey, 1989, Table 2, p.31

Table B.2. Elevations of Stratigraphic Layers Near WIPP (Continued)

	Layer	Well ID	Elevation	Source
1	Supra_R	FFG_180	1062.20	Richey, 1989, Table 2, p.31
2	Supra_R	FFG_181	1016.50	Richey, 1989, Table 2, p.32
3	Supra_R	FFG_182	986.00	Richey, 1989, Table 2, p.32
4	Supra_R	FFG_183	1020.50	Richey, 1989, Table 2, p.32
5	Supra_R	FFG_184	1047.90	Richey, 1989, Table 2, p.32
6	Supra_R	FFG_185	1022.60	Richey, 1989, Table 2, p.32
7	Supra_R	FFG_186	1013.50	Richey, 1989, Table 2, p.32
8	Supra_R	FFG_188	979.00	Richey, 1989, Table 2, p.32
9	Supra_R	FFG_189	1046.10	Richey, 1989, Table 2, p.32
10	Supra_R	FFG_190	1037.80	Richey, 1989, Table 2, p.32
11	Supra_R	FFG_191	1041.50	Richey, 1989, Table 2, p.32
12	Supra_R	FFG_192	1031.40	Richey, 1989, Table 2, p.32
13	Supra_R	FFG_194	1075.40	Richey, 1989, Table 2, p.33
14	Supra_R	FFG_195	1059.20	Richey, 1989, Table 2, p.33
15	Supra_R	FFG_196	1042.40	Richey, 1989, Table 2, p.33
16	Supra_R	FFG_197	1034.50	Richey, 1989, Table 2, p.33
17	Supra_R	FFG_198	1031.40	Richey, 1989, Table 2, p.33
18	Supra_R	FFG_199	1038.80	Richey, 1989, Table 2, p.33
19	Supra_R	FFG_200	1040.90	Richey, 1989, Table 2, p.33
20	Supra_R	FFG_201	1074.10	Richey, 1989, Table 2, p.33
21	Supra_R	FFG_202	1075.60	Richey, 1989, Table 2, p.33
22	Supra_R	FFG_203	1071.40	Richey, 1989, Table 2, p.33
23	Supra_R	FFG_204	1096.40	Richey, 1989, Table 2, p.33
24	Supra_R	FFG_205	1082.00	Richey, 1989, Table 2, p.33
25	Supra_R	FFG_206	1067.70	Richey, 1989, Table 2, p.33
26	Supra_R	FFG_207	1072.60	Richey, 1989, Table 2, p.33
27	Supra_R	FFG_208	1060.10	Richey, 1989, Table 2, p.34
28	Supra_R	FFG_209	1074.10	Richey, 1989, Table 2, p.34
29	Supra_R	FFG_210	1066.20	Richey, 1989, Table 2, p.34
30	Supra_R	FFG_212	1078.40	Richey, 1989, Table 2, p.34
31	Supra_R	FFG_213	1051.60	Richey, 1989, Table 2, p.34
32	Supra_R	FFG_214	1061.60	Richey, 1989, Table 2, p.34
33	Supra_R	FFG_215	1041.80	Richey, 1989, Table 2, p.34
34	Supra_R	FFG_216	993.60	Richey, 1989, Table 2, p.34
35	Supra_R	FFG_217	1057.70	Richey, 1989, Table 2, p.34
36	Supra_R	FFG_218	1053.10	Richey, 1989, Table 2, p.34
37	Supra_R	FFG_219	1036.30	Richey, 1989, Table 2, p.34
38	Supra_R	FFG_220	1051.00	Richey, 1989, Table 2, p.34
39	Supra_R	FFG_221	1027.80	Richey, 1989, Table 2, p.34
40	Supra_R	FFG_222	1019.90	Richey, 1989, Table 2, p.34
41	Supra_R	FFG_224	1133.60	Richey, 1989, Table 2, p.35
42	Supra_R	FFG_225	1138.30	Richey, 1989, Table 2, p.35
43	Supra_R	FFG_226	1150.30	Richey, 1989, Table 2, p.35
44	Supra_R	FFG_228	1133.60	Richey, 1989, Table 2, p.35
45	Supra_R	FFG_229	1146.00	Richey, 1989, Table 2, p.35
46	Supra_R	FFG_230	1134.50	Richey, 1989, Table 2, p.35
47	Supra_R	FFG_231	1120.10	Richey, 1989, Table 2, p.35
48	Supra_R	FFG_232	1124.10	Richey, 1989, Table 2, p.35
49	Supra_R	FFG_233	1114.70	Richey, 1989, Table 2, p.35
50	Supra_R	FFG_234	1112.80	Richey, 1989, Table 2, p.35
51	Supra_R	FFG_235	1117.10	Richey, 1989, Table 2, p.35
52	Supra_R	FFG_236	1101.20	Richey, 1989, Table 2, p.35
53	Supra_R	FFG_237	1137.80	Richey, 1989, Table 2, p.35
54	Supra_R	FFG_238	1152.80	Richey, 1989, Table 2, p.36
55	Supra_R	FFG_239	1177.10	Richey, 1989, Table 2, p.36
56	Supra_R	FFG_240	1162.20	Richey, 1989, Table 2, p.36
57	Supra_R	FFG_241	1165.30	Richey, 1989, Table 2, p.36
58	Supra_R	FFG_242	1115.00	Richey, 1989, Table 2, p.36
59	Supra_R	FFG_243	1153.70	Richey, 1989, Table 2, p.36
60	Supra_R	FFG_244	1120.00	Richey, 1989, Table 2, p.36
61	Supra_R	FFG_245	1170.70	Richey, 1989, Table 2, p.36
62	Supra_R	FFG_246	1161.90	Richey, 1989, Table 2, p.36
63	Supra_R	FFG_247	1145.40	Richey, 1989, Table 2, p.36
64	Supra_R	FFG_248	1150.00	Richey, 1989, Table 2, p.36
65	Supra_R	FFG_249	1169.20	Richey, 1989, Table 2, p.36
66	Supra_R	FFG_250	1159.80	Richey, 1989, Table 2, p.36
67	Supra_R	FFG_251	1139.00	Richey, 1989, Table 2, p.36
68	Supra_R	FFG_252	1134.10	Richey, 1989, Table 2, p.36
69	Supra_R	FFG_253	1108.60	Richey, 1989, Table 2, p.36
70	Supra_R	FFG_254	1111.60	Richey, 1989, Table 2, p.36
71	Supra_R	FFG_255	1122.60	Richey, 1989, Table 2, p.37
72	Supra_R	FFG_256	1136.00	Richey, 1989, Table 2, p.37
73	Supra_R	FFG_257	1137.20	Richey, 1989, Table 2, p.37
74	Supra_R	FFG_258	1120.40	Richey, 1989, Table 2, p.37
75	Supra_R	FFG_259	1139.60	Richey, 1989, Table 2, p.37
76	Supra_R	FFG_260	1111.00	Richey, 1989, Table 2, p.37

Table B.2. Elevations of Stratigraphic Layers Near WIPP (Continued)

	Layer	Well ID	Elevation	Source		Layer	Well ID	Elevation	Source
1	Supra_R	FFG_261	1106.10	Richey, 1989, Table 2, p.37	39	Supra_R	FFG_301	1046.40	Richey, 1989, Table 2, p.40
2	Supra_R	FFG_262	1109.50	Richey, 1989, Table 2, p.37	40	Supra_R	FFG_302	1092.70	Richey, 1989, Table 2, p.40
3	Supra_R	FFG_263	1115.60	Richey, 1989, Table 2, p.37	41	Supra_R	FFG_303	1099.30	Richey, 1989, Table 2, p.40
4	Supra_R	FFG_264	1121.10	Richey, 1989, Table 2, p.37	42	Supra_R	FFG_304	1088.10	Richey, 1989, Table 2, p.40
5	Supra_R	FFG_265	1130.80	Richey, 1989, Table 2, p.37	43	Supra_R	FFG_305	1093.90	Richey, 1989, Table 2, p.40
6	Supra_R	FFG_266	1131.40	Richey, 1989, Table 2, p.37	44	Supra_R	FFG_306	1075.90	Richey, 1989, Table 2, p.40
7	Supra_R	FFG_267	1120.40	Richey, 1989, Table 2, p.37	45	Supra_R	FFG_307	1078.70	Richey, 1989, Table 2, p.40
8	Supra_R	FFG_268	1115.90	Richey, 1989, Table 2, p.37	46	Supra_R	FFG_308	1075.90	Richey, 1989, Table 2, p.40
9	Supra_R	FFG_269	1105.80	Richey, 1989, Table 2, p.38	47	Supra_R	FFG_309	1093.60	Richey, 1989, Table 2, p.40
10	Supra_R	FFG_270	1057.00	Richey, 1989, Table 2, p.38	48	Supra_R	FFG_310	1087.50	Richey, 1989, Table 2, p.40
11	Supra_R	FFG_271	1049.40	Richey, 1989, Table 2, p.38	49	Supra_R	FFG_311	1085.40	Richey, 1989, Table 2, p.40
12	Supra_R	FFG_272	1073.50	Richey, 1989, Table 2, p.38	50	Supra_R	FFG_312	1076.90	Richey, 1989, Table 2, p.40
13	Supra_R	FFG_273	1079.20	Richey, 1989, Table 2, p.38	51	Supra_R	FFG_313	1106.10	Richey, 1989, Table 2, p.41
14	Supra_R	FFG_274	1137.20	Richey, 1989, Table 2, p.38	52	Supra_R	FFG_314	1121.10	Richey, 1989, Table 2, p.41
15	Supra_R	FFG_275	1135.70	Richey, 1989, Table 2, p.38	53	Supra_R	FFG_315	1131.10	Richey, 1989, Table 2, p.41
16	Supra_R	FFG_276	1125.90	Richey, 1989, Table 2, p.38	54	Supra_R	FFG_316	1133.20	Richey, 1989, Table 2, p.41
17	Supra_R	FFG_277	1123.20	Richey, 1989, Table 2, p.38	55	Supra_R	FFG_317	1097.60	Richey, 1989, Table 2, p.41
18	Supra_R	FFG_278	1098.20	Richey, 1989, Table 2, p.38	56	Supra_R	FFG_318	1123.50	Richey, 1989, Table 2, p.41
19	Supra_R	FFG_279	1107.90	Richey, 1989, Table 2, p.38	57	Supra_R	FFG_319	1120.70	Richey, 1989, Table 2, p.41
20	Supra_R	FFG_280	1120.30	Richey, 1989, Table 2, p.38	58	Supra_R	FFG_320	1129.60	Richey, 1989, Table 2, p.41
21	Supra_R	FFG_281	1147.30	Richey, 1989, Table 2, p.38	59	Supra_R	FFG_321	1124.70	Richey, 1989, Table 2, p.41
22	Supra_R	FFG_283	1090.90	Richey, 1989, Table 2, p.39	60	Supra_R	FFG_322	1124.70	Richey, 1989, Table 2, p.41
23	Supra_R	FFG_284	1117.10	Richey, 1989, Table 2, p.39	61	Supra_R	FFG_323	1120.40	Richey, 1989, Table 2, p.41
24	Supra_R	FFG_285	1112.50	Richey, 1989, Table 2, p.39	62	Supra_R	FFG_324	1122.00	Richey, 1989, Table 2, p.41
25	Supra_R	FFG_286	1101.50	Richey, 1989, Table 2, p.39	63	Supra_R	FFG_325	1079.90	Richey, 1989, Table 2, p.41
26	Supra_R	FFG_287	1094.60	Richey, 1989, Table 2, p.39	64	Supra_R	FFG_326	1117.70	Richey, 1989, Table 2, p.41
27	Supra_R	FFG_288	1110.40	Richey, 1989, Table 2, p.39	65	Supra_R	FFG_327	1102.20	Richey, 1989, Table 2, p.42
28	Supra_R	FFG_289	1081.90	Richey, 1989, Table 2, p.39	66	Supra_R	FFG_328	1121.40	Richey, 1989, Table 2, p.42
29	Supra_R	FFG_290	1103.40	Richey, 1989, Table 2, p.39	67	Supra_R	FFG_329	1120.40	Richey, 1989, Table 2, p.42
30	Supra_R	FFG_291	1132.00	Richey, 1989, Table 2, p.39	68	Supra_R	FFG_330	1115.60	Richey, 1989, Table 2, p.42
31	Supra_R	FFG_292	1090.60	Richey, 1989, Table 2, p.39	69	Supra_R	FFG_331	1103.70	Richey, 1989, Table 2, p.42
32	Supra_R	FFG_293	1085.10	Richey, 1989, Table 2, p.39	70	Supra_R	FFG_332	1124.70	Richey, 1989, Table 2, p.42
33	Supra_R	FFG_294	1095.50	Richey, 1989, Table 2, p.39	71	Supra_R	FFG_333	1130.50	Richey, 1989, Table 2, p.42
34	Supra_R	FFG_295	1087.50	Richey, 1989, Table 2, p.39	72	Supra_R	FFG_334	1125.90	Richey, 1989, Table 2, p.42
35	Supra_R	FFG_297	1104.90	Richey, 1989, Table 2, p.39	73	Supra_R	FFG_335	1129.60	Richey, 1989, Table 2, p.42
36	Supra_R	FFG_298	1070.00	Richey, 1989, Table 2, p.40	74	Supra_R	FFG_336	1124.10	Richey, 1989, Table 2, p.42
37	Supra_R	FFG_299	1078.40	Richey, 1989, Table 2, p.40	75	Supra_R	FFG_337	1124.40	Richey, 1989, Table 2, p.42
38	Supra_R	FFG_300	1062.20	Richey, 1989, Table 2, p.40	76	Supra_R	FFG_338	1123.50	Richey, 1989, Table 2, p.42

Table B.2. Elevations of Stratigraphic Layers Near WIPP (Continued)

	Layer	Well ID	Elevation	Source
1	Supra_R	FFG_339	1107.90	Richey, 1989, Table 2, p.42
2	Supra_R	FFG_340	1107.00	Richey, 1989, Table 2, p.42
3	Supra_R	FFG_342	1056.10	Richey, 1989, Table 2, p.43
4	Supra_R	FFG_344	1040.60	Richey, 1989, Table 2, p.43
5	Supra_R	FFG_345	1073.20	Richey, 1989, Table 2, p.43
6	Supra_R	FFG_347	1039.70	Richey, 1989, Table 2, p.43
7	Supra_R	FFG_348	1035.70	Richey, 1989, Table 2, p.43
8	Supra_R	FFG_349	1034.80	Richey, 1989, Table 2, p.43
9	Supra_R	FFG_350	1041.50	Richey, 1989, Table 2, p.43
10	Supra_R	FFG_351	1102.80	Richey, 1989, Table 2, p.43
11	Supra_R	FFG_352	1103.10	Richey, 1989, Table 2, p.43
12	Supra_R	FFG_353	1095.80	Richey, 1989, Table 2, p.43
13	Supra_R	FFG_354	1051.00	Richey, 1989, Table 2, p.43
14	Supra_R	FFG_361	1012.50	Richey, 1989, Table 2, p.44
15	Supra_R	FFG_362	1010.70	Richey, 1989, Table 2, p.44
16	Supra_R	FFG_363	1009.50	Richey, 1989, Table 2, p.44
17	Supra_R	FFG_364	993.60	Richey, 1989, Table 2, p.44
18	Supra_R	FFG_366	1010.40	Richey, 1989, Table 2, p.44
19	Supra_R	FFG_367	1006.40	Richey, 1989, Table 2, p.44
20	Supra_R	FFG_370	1012.90	Richey, 1989, Table 2, p.44
21	Supra_R	FFG_371	1012.90	Richey, 1989, Table 2, p.44
22	Supra_R	FFG_372	1006.40	Richey, 1989, Table 2, p.45
23	Supra_R	FFG_373	998.10	Richey, 1989, Table 2, p.45
24	Supra_R	FFG_374	995.20	Richey, 1989, Table 2, p.45
25	Supra_R	FFG_376	1010.40	Richey, 1989, Table 2, p.45
26	Supra_R	FFG_381	1021.40	Richey, 1989, Table 2, p.45
27	Supra_R	FFG_383	1046.10	Richey, 1989, Table 2, p.45
28	Supra_R	FFG_384	976.00	Richey, 1989, Table 2, p.45
29	Supra_R	FFG_385	990.60	Richey, 1989, Table 2, p.45
30	Supra_R	FFG_387	1019.90	Richey, 1989, Table 2, p.45
31	Supra_R	FFG_388	1019.60	Richey, 1989, Table 2, p.46
32	Supra_R	FFG_389	1008.00	Richey, 1989, Table 2, p.46
33	Supra_R	FFG_390	1022.60	Richey, 1989, Table 2, p.46
34	Supra_R	FFG_391	1025.30	Richey, 1989, Table 2, p.46
35	Supra_R	FFG_392	1019.60	Richey, 1989, Table 2, p.46
36	Supra_R	FFG_393	1061.60	Richey, 1989, Table 2, p.46
37	Supra_R	FFG_394	1050.30	Richey, 1989, Table 2, p.46
38	Supra_R	FFG_395	1059.20	Richey, 1989, Table 2, p.46
39	Supra_R	FFG_396	1090.00	Richey, 1989, Table 2, p.46
40	Supra_R	FFG_398	1011.60	Richey, 1989, Table 2, p.46
41	Supra_R	FFG_399	1001.60	Richey, 1989, Table 2, p.46
42	Supra_R	FFG_401	972.30	Richey, 1989, Table 2, p.46
43	Supra_R	FFG_402	1023.10	Richey, 1989, Table 2, p.46
44	Supra_R	FFG_403	995.20	Richey, 1989, Table 2, p.47
45	Supra_R	FFG_404	976.60	Richey, 1989, Table 2, p.47
46	Supra_R	FFG_407	969.90	Richey, 1989, Table 2, p.47
47	Supra_R	FFG_408	965.00	Richey, 1989, Table 2, p.47
48	Supra_R	FFG_409	970.50	Richey, 1989, Table 2, p.47
49	Supra_R	FFG_411	957.70	Richey, 1989, Table 2, p.47
50	Supra_R	FFG_413	968.70	Richey, 1989, Table 2, p.47
51	Supra_R	FFG_418	1033.90	Richey, 1989, Table 2, p.48
52	Supra_R	FFG_419	1052.50	Richey, 1989, Table 2, p.48
53	Supra_R	FFG_420	1045.10	Richey, 1989, Table 2, p.48
54	Supra_R	FFG_421	1047.00	Richey, 1989, Table 2, p.48
55	Supra_R	FFG_422	1054.30	Richey, 1989, Table 2, p.48
56	Supra_R	FFG_426	996.10	Richey, 1989, Table 2, p.48
57	Supra_R	FFG_432	978.40	Richey, 1989, Table 2, p.48
58	Supra_R	FFG_433	968.00	Richey, 1989, Table 2, p.48
59	Supra_R	FFG_438	1082.20	Richey, 1989, Table 2, p.49
60	Supra_R	FFG_445	960.70	Richey, 1989, Table 2, p.49
61	Supra_R	FFG_453	1049.50	Richey, 1989, Table 2, p.50
62	Supra_R	FFG_455	1061.30	Richey, 1989, Table 2, p.50
63	Supra_R	FFG_456	1063.40	Richey, 1989, Table 2, p.50
64	Supra_R	FFG_457	1023.50	Richey, 1989, Table 2, p.50
65	Supra_R	FFG_458	1025.80	Richey, 1989, Table 2, p.50
66	Supra_R	FFG_459	1070.50	Richey, 1989, Table 2, p.50
67	Supra_R	FFG_462	1032.10	Richey, 1989, Table 2, p.50
68	Supra_R	FFG_463	1021.10	Richey, 1989, Table 2, p.51
69	Supra_R	FFG_464	1035.40	Richey, 1989, Table 2, p.51
70	Supra_R	FFG_465	1031.40	Richey, 1989, Table 2, p.51
71	Supra_R	FFG_467	1025.70	Richey, 1989, Table 2, p.51
72	Supra_R	FFG_468	1064.70	Richey, 1989, Table 2, p.51
73	Supra_R	FFG_470	1067.10	Richey, 1989, Table 2, p.51
74	Supra_R	FFG_471	1036.60	Richey, 1989, Table 2, p.51
75	Supra_R	FFG_472	1032.40	Richey, 1989, Table 2, p.51
76	Supra_R	FFG_473	1060.70	Richey, 1989, Table 2, p.51

Table B.2. Elevations of Stratigraphic Layers Near WIPP (Continued)

	Layer	Well ID	Elevation	Source
1	Supra_R	FFG_474	1100.60	Richey, 1989, Table 2, p.51
2	Supra_R	FFG_475	1103.70	Richey, 1989, Table 2, p.51
3	Supra_R	FFG_476	1090.10	Richey, 1989, Table 2, p.51
4	Supra_R	FFG_477	1102.80	Richey, 1989, Table 2, p.51
5	Supra_R	FFG_478	1104.80	Richey, 1989, Table 2, p.52
6	Supra_R	FFG_479	1106.40	Richey, 1989, Table 2, p.52
7	Supra_R	FFG_480	1096.10	Richey, 1989, Table 2, p.52
8	Supra_R	FFG_481	1090.90	Richey, 1989, Table 2, p.52
9	Supra_R	FFG_482	1103.40	Richey, 1989, Table 2, p.52
10	Supra_R	FFG_483	1094.20	Richey, 1989, Table 2, p.52
11	Supra_R	FFG_484	1095.60	Richey, 1989, Table 2, p.52
12	Supra_R	FFG_485	1096.50	Richey, 1989, Table 2, p.52
13	Supra_R	FFG_486	1097.60	Richey, 1989, Table 2, p.52
14	Supra_R	FFG_487	1097.00	Richey, 1989, Table 2, p.52
15	Supra_R	FFG_488	1088.60	Richey, 1989, Table 2, p.52
16	Supra_R	FFG_489	1086.60	Richey, 1989, Table 2, p.52
17	Supra_R	FFG_490	1072.60	Richey, 1989, Table 2, p.52
18	Supra_R	FFG_491	1077.50	Richey, 1989, Table 2, p.52
19	Supra_R	FFG_492	1067.40	Richey, 1989, Table 2, p.52
20	Supra_R	FFG_493	1069.20	Richey, 1989, Table 2, p.53
21	Supra_R	FFG_494	1069.50	Richey, 1989, Table 2, p.53
22	Supra_R	FFG_495	1072.30	Richey, 1989, Table 2, p.53
23	Supra_R	FFG_496	1108.30	Richey, 1989, Table 2, p.53
24	Supra_R	FFG_497	1090.60	Richey, 1989, Table 2, p.53
25	Supra_R	FFG_498	1104.90	Richey, 1989, Table 2, p.53
26	Supra_R	FFG_499	1091.50	Richey, 1989, Table 2, p.53
27	Supra_R	FFG_500	1091.50	Richey, 1989, Table 2, p.53
28	Supra_R	FFG_501	1075.60	Richey, 1989, Table 2, p.53
29	Supra_R	FFG_502	1092.40	Richey, 1989, Table 2, p.53
30	Supra_R	FFG_503	1064.10	Richey, 1989, Table 2, p.53
31	Supra_R	FFG_504	1070.50	Richey, 1989, Table 2, p.53
32	Supra_R	FFG_505	1077.80	Richey, 1989, Table 2, p.53
33	Supra_R	FFG_506	1069.80	Richey, 1989, Table 2, p.53
34	Supra_R	FFG_507	1051.90	Richey, 1989, Table 2, p.53
35	Supra_R	FFG_508	1051.90	Richey, 1989, Table 2, p.53
36	Supra_R	FFG_509	1066.50	Richey, 1989, Table 2, p.54
37	Supra_R	FFG_510	1080.50	Richey, 1989, Table 2, p.54
38	Supra_R	FFG_511	1102.80	Richey, 1989, Table 2, p.54
39	Supra_R	FFG_512	1073.50	Richey, 1989, Table 2, p.54
40	Supra_R	FFG_513	1061.00	Richey, 1989, Table 2, p.54
41	Supra_R	FFG_514	1060.10	Richey, 1989, Table 2, p.54
42	Supra_R	FFG_515	1082.30	Richey, 1989, Table 2, p.54
43	Supra_R	FFG_516	1075.00	Richey, 1989, Table 2, p.54
44	Supra_R	FFG_517	1053.10	Richey, 1989, Table 2, p.54
45	Supra_R	FFG_518	1036.30	Richey, 1989, Table 2, p.54
46	Supra_R	FFG_519	1033.90	Richey, 1989, Table 2, p.54
47	Supra_R	FFG_520	1030.80	Richey, 1989, Table 2, p.54
48	Supra_R	FFG_521	1028.70	Richey, 1989, Table 2, p.54
49	Supra_R	FFG_522	1055.20	Richey, 1989, Table 2, p.54
50	Supra_R	FFG_523	1041.80	Richey, 1989, Table 2, p.54
51	Supra_R	FFG_524	1024.10	Richey, 1989, Table 2, p.55
52	Supra_R	FFG_525	1047.00	Richey, 1989, Table 2, p.55
53	Supra_R	FFG_526	1033.90	Richey, 1989, Table 2, p.55
54	Supra_R	FFG_527	1031.70	Richey, 1989, Table 2, p.55
55	Supra_R	FFG_528	1023.50	Richey, 1989, Table 2, p.55
56	Supra_R	FFG_530	1016.50	Richey, 1989, Table 2, p.55
57	Supra_R	FFG_531	998.20	Richey, 1989, Table 2, p.55
58	Supra_R	FFG_532	990.30	Richey, 1989, Table 2, p.55
59	Supra_R	FFG_534	1021.10	Richey, 1989, Table 2, p.55
60	Supra_R	FFG_535	995.90	Richey, 1989, Table 2, p.55
61	Supra_R	FFG_536	996.10	Richey, 1989, Table 2, p.55
62	Supra_R	FFG_537	985.40	Richey, 1989, Table 2, p.55
63	Supra_R	FFG_543	997.90	Richey, 1989, Table 2, p.56
64	Supra_R	FFG_548	1047.30	Richey, 1989, Table 2, p.56
65	Supra_R	FFG_552	922.90	Richey, 1989, Table 2, p.56
66	Supra_R	FFG_562	981.50	Richey, 1989, Table 2, p.57
67	Supra_R	FFG_563	969.90	Richey, 1989, Table 2, p.57
68	Supra_R	FFG_564	969.30	Richey, 1989, Table 2, p.57
69	Supra_R	FFG_568	957.10	Richey, 1989, Table 2, p.57
70	Supra_R	FFG_569	952.20	Richey, 1989, Table 2, p.57
71	Supra_R	FFG_584	1006.80	Richey, 1989, Table 2, p.58
72	Supra_R	FFG_585	1025.00	Richey, 1989, Table 2, p.58
73	Supra_R	FFG_600	1003.40	Richey, 1989, Table 2, p.58
74	Supra_R	FFG_601	983.90	Richey, 1989, Table 2, p.58
75	Supra_R	FFG_602	1053.10	Richey, 1989, Table 2, p.58
76	Supra_R	FFG_606	1012.90	Richey, 1989, Table 2, p.58

Table B.2. Elevations of Stratigraphic Layers Near WIPP (Continued)

	Layer	Well ID	Elevation	Source
1	Supra_R	FFG_607	1001.30	Richey, 1989, Table 2, p.59
2	Supra_R	FFG_608	1018.60	Richey, 1989, Table 2, p.59
3	Supra_R	FFG_609	1025.30	Richey, 1989, Table 2, p.59
4	Supra_R	FFG_610	1023.20	Richey, 1989, Table 2, p.59
5	Supra_R	FFG_611	1009.20	Richey, 1989, Table 2, p.59
6	Supra_R	FFG_612	977.10	Richey, 1989, Table 2, p.59
7	Supra_R	FFG_613	945.90	Richey, 1989, Table 2, p.59
8	Supra_R	FFG_618	897.00	Richey, 1989, Table 2, p.59
9	Supra_R	FFG_620	909.90	Richey, 1989, Table 2, p.59
10	Supra_R	FFG_621	905.90	Richey, 1989, Table 2, p.59
11	Supra_R	FFG_638	975.40	Richey, 1989, Table 2, p.60
12	Supra_R	FFG_639	961.50	Richey, 1989, Table 2, p.60
13	Supra_R	FFG_640	966.20	Richey, 1989, Table 2, p.60
14	Supra_R	FFG_643	975.40	Richey, 1989, Table 2, p.60
15	Supra_R	FFG_644	936.70	Richey, 1989, Table 2, p.60
16	Supra_R	FFG_648	960.70	Richey, 1989, Table 2, p.60
17	Supra_R	FFG_652	1106.40	Richey, 1989, Table 2, p.60
18	Supra_R	FFG_653	1096.10	Richey, 1989, Table 2, p.61
19	Supra_R	FFG_654	1098.50	Richey, 1989, Table 2, p.61
20	Supra_R	FFG_655	1093.00	Richey, 1989, Table 2, p.61
21	Supra_R	FFG_656	1091.80	Richey, 1989, Table 2, p.61
22	Supra_R	FFG_657	1083.30	Richey, 1989, Table 2, p.61
23	Supra_R	FFG_658	1088.10	Richey, 1989, Table 2, p.61
24	Supra_R	FFG_659	1072.60	Richey, 1989, Table 2, p.61
25	Supra_R	FFG_660	1071.10	Richey, 1989, Table 2, p.61
26	Supra_R	FFG_662	1085.70	Richey, 1989, Table 2, p.61
27	Supra_R	FFG_664	1084.50	Richey, 1989, Table 2, p.61
28	Supra_R	FFG_666	1063.10	Richey, 1989, Table 2, p.62
29	Supra_R	FFG_667	1059.20	Richey, 1989, Table 2, p.62
30	Supra_R	FFG_668	1043.30	Richey, 1989, Table 2, p.62
31	Supra_R	FFG_669	1036.30	Richey, 1989, Table 2, p.62
32	Supra_R	FFG_670	1049.10	Richey, 1989, Table 2, p.62
33	Supra_R	FFG_671	1044.90	Richey, 1989, Table 2, p.62
34	Supra_R	FFG_672	1058.00	Richey, 1989, Table 2, p.62
35	Supra_R	FFG_673	1037.20	Richey, 1989, Table 2, p.62
36	Supra_R	FFG_674	1064.70	Richey, 1989, Table 2, p.62
37	Supra_R	FFG_675	1078.40	Richey, 1989, Table 2, p.62
38	Supra_R	FFG_676	1084.50	Richey, 1989, Table 2, p.62
39	Supra_R	FFG_677	1064.40	Richey, 1989, Table 2, p.62
40	Supra_R	FFG_679	1060.70	Richey, 1989, Table 2, p.62
41	Supra_R	FFG_685	1003.50	Richey, 1989, Table 2, p.63
42	Supra_R	FFG_689	1059.20	Richey, 1989, Table 2, p.63
43	Supra_R	FFG_690	1052.20	Richey, 1989, Table 2, p.63
44	Supra_R	FFG_691	1052.50	Richey, 1989, Table 2, p.63
45	Supra_R	FFG_692	1057.70	Richey, 1989, Table 2, p.63
46	Supra_R	FFG_693	1050.60	Richey, 1989, Table 2, p.63
47	Supra_R	FFG_694	1042.40	Richey, 1989, Table 2, p.63
48	Supra_R	FFG_695	1048.50	Richey, 1989, Table 2, p.63
49	Supra_R	FFG_696	1050.60	Richey, 1989, Table 2, p.63
50	Supra_R	FFG_697	1045.80	Richey, 1989, Table 2, p.64
51	Supra_R	FFG_698	1039.70	Richey, 1989, Table 2, p.64
52	Supra_R	FFG_699	1029.60	Richey, 1989, Table 2, p.64
53	Supra_R	FFG_700	1027.10	Richey, 1989, Table 2, p.64
54	Supra_R	FFG_701	1032.10	Richey, 1989, Table 2, p.64
55	Supra_R	FFG_702	1036.60	Richey, 1989, Table 2, p.64
56	Supra_R	FFG_703	1047.00	Richey, 1989, Table 2, p.64
57	Supra_R	FFG_704	1032.70	Richey, 1989, Table 2, p.64
58	Supra_R	FFG_705	1023.80	Richey, 1989, Table 2, p.64
59	Supra_R	FFG_706	1025.70	Richey, 1989, Table 2, p.64
60	Supra_R	FFG_707	1019.30	Richey, 1989, Table 2, p.64
61	Supra_R	FFG_708	1026.60	Richey, 1989, Table 2, p.64
62	Supra_R	FFG_709	1008.60	Richey, 1989, Table 2, p.64
63	Supra_R	FFG_710	1007.40	Richey, 1989, Table 2, p.64
64	Supra_R	FFG_711	1012.90	Richey, 1989, Table 2, p.65
65	Supra_R	FFG_712	1018.00	Richey, 1989, Table 2, p.65
66	Supra_R	FFG_713	1011.30	Richey, 1989, Table 2, p.65
67	Supra_R	FFG_714	1024.10	Richey, 1989, Table 2, p.65
68	Supra_R	FFG_715	1025.30	Richey, 1989, Table 2, p.65
69	Supra_R	FFG_716	1060.60	Richey, 1989, Table 2, p.65
70	Supra_R	FFG_717	1056.10	Richey, 1989, Table 2, p.65
71	Supra_R	FFG_718	1044.90	Richey, 1989, Table 2, p.65
72	Supra_R	FFG_719	1040.40	Richey, 1989, Table 2, p.65
73	Supra_R	FFG_720	1019.90	Richey, 1989, Table 2, p.65
74	Supra_R	FFG_721	1026.90	Richey, 1989, Table 2, p.65
75	Supra_R	FFG_723	1054.30	Richey, 1989, Table 2, p.65
76	Supra_R	FFG_724	1044.20	Richey, 1989, Table 2, p.65

Table B.2. Elevations of Stratigraphic Layers Near WIPP (Continued)

	Layer	Well ID	Elevation	Source
1	Supra_R	FFG_725	1029.60	Richey, 1989, Table 2, p.65
2	Supra_R	FFG_726	1018.60	Richey, 1989, Table 2, p.65
3	Supra_R	FFG_727	1020.80	Richey, 1989, Table 2, p.66
4	Supra_R	FFG_728	1012.20	Richey, 1989, Table 2, p.66
5	Supra_R	FFG_729	1014.40	Richey, 1989, Table 2, p.66
6	Supra_R	FFG_730	1018.90	Richey, 1989, Table 2, p.66
7	Supra_R	FFG_731	1022.30	Richey, 1989, Table 2, p.66
8	Supra_R	FFG_732	1040.30	Richey, 1989, Table 2, p.66
9	Supra_R	FFG_733	1028.40	Richey, 1989, Table 2, p.66
10	Supra_R	FFG_734	1029.00	Richey, 1989, Table 2, p.66
11	Supra_R	FFG_735	1016.50	Richey, 1989, Table 2, p.66
12	Supra_R	FFG_736	1025.60	Richey, 1989, Table 2, p.66
13	Supra_R	FFG_737	1040.50	Richey, 1989, Table 2, p.66
14	Supra_R	FFG_738	1018.30	Richey, 1989, Table 2, p.66
15	Supra_R	FFG_739	1015.10	Richey, 1989, Table 2, p.66
16	Supra_R	FFG_740	1015.60	Richey, 1989, Table 2, p.66
17	Supra_R	FFG_741	1014.70	Richey, 1989, Table 2, p.66
18	Supra_R	FFG_742	1023.80	Richey, 1989, Table 2, p.67
19	Supra_R	FFG_743	1013.20	Richey, 1989, Table 2, p.67
20	Supra_R	FFG_744	1012.50	Richey, 1989, Table 2, p.67
21	Supra_R	FFG_745	1006.40	Richey, 1989, Table 2, p.67
22	Supra_R	FFG_746	1007.50	Richey, 1989, Table 2, p.67
23	Supra_R	H1	1035.70	Mercer, 1983, Table 1
24	Supra_R	H10C	1123.80	Mercer, 1983, Table 1
25	Supra_R	H2C	1029.60	Mercer, 1983, Table 1
26	Supra_R	H3	1033.30	Mercer, 1983, Table 1
27	Supra_R	H4C	1016.20	Mercer, 1983, Table 1
28	Supra_R	H5C	1068.90	Mercer, 1983, Table 1
29	Supra_R	H6C	1020.50	Mercer, 1983, Table 1
30	Supra_R	H7C	964.10	Mercer, 1983, Table 1
31	Supra_R	H8C	1046.40	Mercer, 1983, Table 1
32	Supra_R	H9C	1038.10	Mercer, 1983, Table 1
33	Supra_R	P1	1019.60	Mercer, 1983, Table 1
34	Supra_R	P10	1069.50	Mercer, 1983, Table 1
35	Supra_R	P11	1068.00	Mercer, 1983, Table 1
36	Supra_R	P12	1028.40	Mercer, 1983, Table 1
37	Supra_R	P13	1019.60	Mercer, 1983, Table 1
38	Supra_R	P14	1024.10	Mercer, 1983, Table 1
39	Supra_R	P15	1008.90	Mercer, 1983, Table 1
40	Supra_R	P16	1011.30	Mercer, 1983, Table 1
41	Supra_R	P17	1016.80	Mercer, 1983, Table 1
42	Supra_R	P18	1059.80	Mercer, 1983, Table 1
43	Supra_R	P19	1080.50	Mercer, 1983, Table 1
44	Supra_R	P2	1060.40	Mercer, 1983, Table 1
45	Supra_R	P20	1083.00	Mercer, 1983, Table 1
46	Supra_R	P21	1069.50	Mercer, 1983, Table 1
47	Supra_R	P3	1031.10	Mercer, 1983, Table 1
48	Supra_R	P4	1049.70	Mercer, 1983, Table 1
49	Supra_R	P5	1058.00	Mercer, 1983, Table 1
50	Supra_R	P6	1022.30	Mercer, 1983, Table 1
51	Supra_R	P7	1015.60	Mercer, 1983, Table 1
52	Supra_R	P8	1017.70	Mercer, 1983, Table 1
53	Supra_R	P9	1040.00	Mercer, 1983, Table 1
54	Supra_R	WIPP11	1044.20	Mercer, 1983, Table 1
55	Supra_R	WIPP12	1058.30	Mercer, 1983, Table 1
56	Supra_R	WIPP13	1037.80	Mercer, 1983, Table 1
57	Supra_R	WIPP15	996.40	Mercer, 1983, Table 1
58	Supra_R	WIPP16	1031.10	Mercer, 1983, Table 1
59	Supra_R	WIPP18	1053.40	Mercer, 1983, Table 1
60	Supra_R	WIPP19	1046.40	Mercer, 1983, Table 1
61	Supra_R	WIPP21	1041.50	Mercer, 1983, Table 1
62	Supra_R	WIPP22	1044.20	Mercer, 1983, Table 1
63	Supra_R	WIPP25	979.30	Mercer, 1983, Table 1
64	Supra_R	WIPP26	960.70	Mercer, 1983, Table 1
65	Supra_R	WIPP27	968.30	Mercer, 1983, Table 1
66	Supra_R	WIPP28	1020.20	Mercer, 1983, Table 1
67	Supra_R	WIPP29	907.40	Mercer, 1983, Table 1
68	Supra_R	WIPP30	1044.90	Mercer, 1983, Table 1
69	Supra_R	WIPP32	921.40	Mercer, 1983, Table 1
70	Supra_R	WIPP33	1012.90	Mercer, 1983, Table 1
71	Supra_R	WIPP34	1046.40	Mercer, 1983, Table 1
72	Tamarisk	AEC7	882.40	Mercer, 1983, Table 1
73	Tamarisk	AEC8	851.70	Mercer, 1983, Table 1
74	Tamarisk	AirShft	850.99	Holt and Powers, 1990, Figure 22
75	Tamarisk	B25	851.00	Mercer, 1983, Table 1
76	Tamarisk	ERDA10	910.20	Mercer, 1983, Table 1

Table B.2. Elevations of Stratigraphic Layers Near WIPP (Continued)

	Layer	Well ID	Elevation	Source		Layer	Well ID	Elevation	Source
1	Tamarisk	ERDA6	889.70	Mercer, 1983, Table 1	39	Tamarisk	FFG_043	782.00	Richey, 1989, Table 2, p.23
2	Tamarisk	ERDA9	853.10	Mercer, 1983, Table 1	40	Tamarisk	FFG_044	733.60	Richey, 1989, Table 2, p.23
3	Tamarisk	ExhtShft	847.97	Bechtel, Inc., 1986, Appendix F	41	Tamarisk	FFG_047	607.50	Richey, 1989, Table 2, p.23
4	Tamarisk	FFG_002	660.50	Richey, 1989, Table 2, p.21	42	Tamarisk	FFG_048	623.30	Richey, 1989, Table 2, p.23
5	Tamarisk	FFG_004	710.80	Richey, 1989, Table 2, p.21	43	Tamarisk	FFG_049	614.80	Richey, 1989, Table 2, p.23
6	Tamarisk	FFG_005	667.90	Richey, 1989, Table 2, p.21	44	Tamarisk	FFG_050	621.50	Richey, 1989, Table 2, p.24
7	Tamarisk	FFG_006	661.40	Richey, 1989, Table 2, p.21	45	Tamarisk	FFG_051	622.10	Richey, 1989, Table 2, p.24
8	Tamarisk	FFG_007	649.80	Richey, 1989, Table 2, p.21	46	Tamarisk	FFG_052	624.20	Richey, 1989, Table 2, p.24
9	Tamarisk	FFG_009	650.10	Richey, 1989, Table 2, p.21	47	Tamarisk	FFG_053	615.40	Richey, 1989, Table 2, p.24
10	Tamarisk	FFG_011	657.10	Richey, 1989, Table 2, p.21	48	Tamarisk	FFG_054	613.30	Richey, 1989, Table 2, p.24
11	Tamarisk	FFG_012	659.60	Richey, 1989, Table 2, p.21	49	Tamarisk	FFG_055	612.60	Richey, 1989, Table 2, p.24
12	Tamarisk	FFG_013	667.80	Richey, 1989, Table 2, p.21	50	Tamarisk	FFG_056	615.40	Richey, 1989, Table 2, p.24
13	Tamarisk	FFG_014	713.50	Richey, 1989, Table 2, p.21	51	Tamarisk	FFG_057	617.60	Richey, 1989, Table 2, p.24
14	Tamarisk	FFG_016	637.60	Richey, 1989, Table 2, p.21	52	Tamarisk	FFG_058	615.10	Richey, 1989, Table 2, p.24
15	Tamarisk	FFG_017	640.70	Richey, 1989, Table 2, p.22	53	Tamarisk	FFG_059	617.50	Richey, 1989, Table 2, p.24
16	Tamarisk	FFG_018	645.90	Richey, 1989, Table 2, p.22	54	Tamarisk	FFG_060	618.10	Richey, 1989, Table 2, p.24
17	Tamarisk	FFG_019	637.60	Richey, 1989, Table 2, p.22	55	Tamarisk	FFG_061	619.90	Richey, 1989, Table 2, p.24
18	Tamarisk	FFG_020	712.30	Richey, 1989, Table 2, p.22	56	Tamarisk	FFG_062	547.10	Richey, 1989, Table 2, p.24
19	Tamarisk	FFG_023	647.40	Richey, 1989, Table 2, p.22	57	Tamarisk	FFG_063	508.50	Richey, 1989, Table 2, p.24
20	Tamarisk	FFG_024	632.10	Richey, 1989, Table 2, p.22	58	Tamarisk	FFG_064	531.90	Richey, 1989, Table 2, p.24
21	Tamarisk	FFG_025	646.10	Richey, 1989, Table 2, p.22	59	Tamarisk	FFG_065	515.40	Richey, 1989, Table 2, p.24
22	Tamarisk	FFG_026	643.40	Richey, 1989, Table 2, p.22	60	Tamarisk	FFG_066	469.40	Richey, 1989, Table 2, p.24
23	Tamarisk	FFG_027	636.40	Richey, 1989, Table 2, p.22	61	Tamarisk	FFG_067	511.20	Richey, 1989, Table 2, p.25
24	Tamarisk	FFG_028	607.50	Richey, 1989, Table 2, p.22	62	Tamarisk	FFG_068	475.80	Richey, 1989, Table 2, p.25
25	Tamarisk	FFG_029	594.00	Richey, 1989, Table 2, p.22	63	Tamarisk	FFG_069	496.30	Richey, 1989, Table 2, p.25
26	Tamarisk	FFG_030	592.90	Richey, 1989, Table 2, p.22	64	Tamarisk	FFG_070	526.10	Richey, 1989, Table 2, p.25
27	Tamarisk	FFG_031	584.00	Richey, 1989, Table 2, p.22	65	Tamarisk	FFG_071	784.30	Richey, 1989, Table 2, p.25
28	Tamarisk	FFG_032	586.00	Richey, 1989, Table 2, p.22	66	Tamarisk	FFG_072	715.00	Richey, 1989, Table 2, p.25
29	Tamarisk	FFG_033	582.80	Richey, 1989, Table 2, p.22	67	Tamarisk	FFG_073	690.60	Richey, 1989, Table 2, p.25
30	Tamarisk	FFG_034	577.90	Richey, 1989, Table 2, p.23	68	Tamarisk	FFG_074	698.40	Richey, 1989, Table 2, p.25
31	Tamarisk	FFG_035	566.50	Richey, 1989, Table 2, p.23	69	Tamarisk	FFG_075	749.20	Richey, 1989, Table 2, p.25
32	Tamarisk	FFG_036	576.70	Richey, 1989, Table 2, p.23	70	Tamarisk	FFG_076	810.50	Richey, 1989, Table 2, p.25
33	Tamarisk	FFG_037	566.90	Richey, 1989, Table 2, p.23	71	Tamarisk	FFG_078	847.00	Richey, 1989, Table 2, p.25
34	Tamarisk	FFG_038	554.10	Richey, 1989, Table 2, p.23	72	Tamarisk	FFG_079	823.60	Richey, 1989, Table 2, p.25
35	Tamarisk	FFG_039	772.10	Richey, 1989, Table 2, p.23	73	Tamarisk	FFG_080	800.40	Richey, 1989, Table 2, p.25
36	Tamarisk	FFG_040	713.60	Richey, 1989, Table 2, p.23	74	Tamarisk	FFG_081	720.90	Richey, 1989, Table 2, p.26
37	Tamarisk	FFG_041	773.60	Richey, 1989, Table 2, p.23	75	Tamarisk	FFG_082	753.20	Richey, 1989, Table 2, p.26
38	Tamarisk	FFG_042	777.80	Richey, 1989, Table 2, p.23	76	Tamarisk	FFG_083	668.60	Richey, 1989, Table 2, p.26

Table B.2. Elevations of Stratigraphic Layers Near WIPP (Continued)

	Layer	Well ID	Elevation	Source
2	Tamarisk	FFG_084	694.60	Richey, 1989, Table 2, p.26
3	Tamarisk	FFG_085	687.40	Richey, 1989, Table 2, p.26
4	Tamarisk	FFG_086	697.30	Richey, 1989, Table 2, p.26
5	Tamarisk	FFG_087	671.40	Richey, 1989, Table 2, p.26
6	Tamarisk	FFG_088	667.20	Richey, 1989, Table 2, p.26
7	Tamarisk	FFG_089	649.60	Richey, 1989, Table 2, p.26
8	Tamarisk	FFG_091	692.80	Richey, 1989, Table 2, p.26
9	Tamarisk	FFG_092	706.50	Richey, 1989, Table 2, p.26
10	Tamarisk	FFG_093	710.20	Richey, 1989, Table 2, p.26
11	Tamarisk	FFG_094	713.20	Richey, 1989, Table 2, p.26
12	Tamarisk	FFG_095	681.50	Richey, 1989, Table 2, p.26
13	Tamarisk	FFG_096	665.10	Richey, 1989, Table 2, p.26
14	Tamarisk	FFG_097	645.00	Richey, 1989, Table 2, p.27
15	Tamarisk	FFG_098	619.90	Richey, 1989, Table 2, p.27
16	Tamarisk	FFG_099	615.40	Richey, 1989, Table 2, p.27
17	Tamarisk	FFG_100	598.10	Richey, 1989, Table 2, p.27
18	Tamarisk	FFG_101	569.40	Richey, 1989, Table 2, p.27
19	Tamarisk	FFG_102	587.40	Richey, 1989, Table 2, p.27
20	Tamarisk	FFG_103	652.00	Richey, 1989, Table 2, p.27
21	Tamarisk	FFG_104	545.00	Richey, 1989, Table 2, p.27
22	Tamarisk	FFG_105	901.30	Richey, 1989, Table 2, p.27
23	Tamarisk	FFG_106	931.80	Richey, 1989, Table 2, p.27
24	Tamarisk	FFG_107	916.90	Richey, 1989, Table 2, p.27
25	Tamarisk	FFG_108	912.30	Richey, 1989, Table 2, p.27
26	Tamarisk	FFG_109	892.80	Richey, 1989, Table 2, p.27
27	Tamarisk	FFG_110	859.60	Richey, 1989, Table 2, p.27
28	Tamarisk	FFG_111	867.10	Richey, 1989, Table 2, p.27
29	Tamarisk	FFG_112	854.90	Richey, 1989, Table 2, p.28
30	Tamarisk	FFG_113	869.00	Richey, 1989, Table 2, p.28
31	Tamarisk	FFG_114	898.30	Richey, 1989, Table 2, p.28
32	Tamarisk	FFG_115	889.40	Richey, 1989, Table 2, p.28
33	Tamarisk	FFG_116	904.90	Richey, 1989, Table 2, p.28
34	Tamarisk	FFG_117	902.20	Richey, 1989, Table 2, p.28
35	Tamarisk	FFG_119	937.90	Richey, 1989, Table 2, p.28
36	Tamarisk	FFG_120	913.80	Richey, 1989, Table 2, p.28
37	Tamarisk	FFG_121	922.00	Richey, 1989, Table 2, p.28
38	Tamarisk	FFG_122	920.50	Richey, 1989, Table 2, p.28
39	Tamarisk	FFG_123	894.50	Richey, 1989, Table 2, p.28
40	Tamarisk	FFG_124	857.70	Richey, 1989, Table 2, p.28
41	Tamarisk	FFG_125	883.20	Richey, 1989, Table 2, p.28
42	Tamarisk	FFG_126	880.10	Richey, 1989, Table 2, p.28
43	Tamarisk	FFG_127	885.10	Richey, 1989, Table 2, p.28
44	Tamarisk	FFG_128	917.50	Richey, 1989, Table 2, p.28
45	Tamarisk	FFG_129	893.30	Richey, 1989, Table 2, p.28
46	Tamarisk	FFG_130	920.50	Richey, 1989, Table 2, p.28
47	Tamarisk	FFG_132	929.00	Richey, 1989, Table 2, p.29
48	Tamarisk	FFG_133	932.00	Richey, 1989, Table 2, p.29
49	Tamarisk	FFG_134	935.50	Richey, 1989, Table 2, p.29
50	Tamarisk	FFG_135	910.80	Richey, 1989, Table 2, p.29
51	Tamarisk	FFG_136	911.50	Richey, 1989, Table 2, p.29
52	Tamarisk	FFG_137	919.30	Richey, 1989, Table 2, p.29
53	Tamarisk	FFG_138	874.50	Richey, 1989, Table 2, p.29
54	Tamarisk	FFG_139	882.40	Richey, 1989, Table 2, p.29
55	Tamarisk	FFG_140	823.10	Richey, 1989, Table 2, p.29
56	Tamarisk	FFG_141	845.70	Richey, 1989, Table 2, p.29
57	Tamarisk	FFG_142	821.80	Richey, 1989, Table 2, p.29
58	Tamarisk	FFG_143	831.70	Richey, 1989, Table 2, p.29
59	Tamarisk	FFG_144	903.50	Richey, 1989, Table 2, p.29
60	Tamarisk	FFG_145	905.30	Richey, 1989, Table 2, p.29
61	Tamarisk	FFG_146	912.90	Richey, 1989, Table 2, p.29
62	Tamarisk	FFG_147	893.70	Richey, 1989, Table 2, p.29
63	Tamarisk	FFG_148	907.70	Richey, 1989, Table 2, p.29
64	Tamarisk	FFG_149	912.20	Richey, 1989, Table 2, p.30
65	Tamarisk	FFG_155	905.60	Richey, 1989, Table 2, p.30
66	Tamarisk	FFG_157	907.10	Richey, 1989, Table 2, p.30
67	Tamarisk	FFG_158	931.10	Richey, 1989, Table 2, p.30
68	Tamarisk	FFG_159	928.80	Richey, 1989, Table 2, p.30
69	Tamarisk	FFG_160	924.20	Richey, 1989, Table 2, p.30
70	Tamarisk	FFG_161	930.00	Richey, 1989, Table 2, p.30
71	Tamarisk	FFG_162	925.40	Richey, 1989, Table 2, p.30
72	Tamarisk	FFG_163	927.80	Richey, 1989, Table 2, p.30
73	Tamarisk	FFG_164	955.90	Richey, 1989, Table 2, p.30
74	Tamarisk	FFG_165	935.70	Richey, 1989, Table 2, p.30
75	Tamarisk	FFG_166	928.40	Richey, 1989, Table 2, p.31
76	Tamarisk	FFG_167	914.40	Richey, 1989, Table 2, p.31
77	Tamarisk	FFG_168	933.90	Richey, 1989, Table 2, p.31

Table B.2. Elevations of Stratigraphic Layers Near WIPP (Continued)

	Layer	Well ID	Elevation	Source
1	Tamarisk	FFG_169	949.10	Richey, 1989, Table 2, p.31
2	Tamarisk	FFG_170	916.80	Richey, 1989, Table 2, p.31
3	Tamarisk	FFG_171	924.20	Richey, 1989, Table 2, p.31
4	Tamarisk	FFG_172	933.00	Richey, 1989, Table 2, p.31
5	Tamarisk	FFG_173	906.50	Richey, 1989, Table 2, p.31
6	Tamarisk	FFG_180	915.00	Richey, 1989, Table 2, p.31
7	Tamarisk	FFG_181	946.70	Richey, 1989, Table 2, p.32
8	Tamarisk	FFG_182	842.40	Richey, 1989, Table 2, p.32
9	Tamarisk	FFG_183	939.10	Richey, 1989, Table 2, p.32
10	Tamarisk	FFG_184	924.80	Richey, 1989, Table 2, p.32
11	Tamarisk	FFG_185	929.90	Richey, 1989, Table 2, p.32
12	Tamarisk	FFG_186	857.70	Richey, 1989, Table 2, p.32
13	Tamarisk	FFG_188	869.00	Richey, 1989, Table 2, p.32
14	Tamarisk	FFG_189	894.30	Richey, 1989, Table 2, p.32
15	Tamarisk	FFG_190	874.70	Richey, 1989, Table 2, p.32
16	Tamarisk	FFG_191	870.50	Richey, 1989, Table 2, p.32
17	Tamarisk	FFG_192	806.50	Richey, 1989, Table 2, p.32
18	Tamarisk	FFG_194	815.60	Richey, 1989, Table 2, p.33
19	Tamarisk	FFG_195	828.80	Richey, 1989, Table 2, p.33
20	Tamarisk	FFG_196	869.90	Richey, 1989, Table 2, p.33
21	Tamarisk	FFG_197	870.80	Richey, 1989, Table 2, p.33
22	Tamarisk	FFG_198	871.40	Richey, 1989, Table 2, p.33
23	Tamarisk	FFG_199	859.90	Richey, 1989, Table 2, p.33
24	Tamarisk	FFG_200	873.00	Richey, 1989, Table 2, p.33
25	Tamarisk	FFG_201	865.60	Richey, 1989, Table 2, p.33
26	Tamarisk	FFG_202	808.30	Richey, 1989, Table 2, p.33
27	Tamarisk	FFG_203	815.70	Richey, 1989, Table 2, p.33
28	Tamarisk	FFG_204	837.90	Richey, 1989, Table 2, p.33
29	Tamarisk	FFG_205	853.20	Richey, 1989, Table 2, p.33
30	Tamarisk	FFG_206	867.40	Richey, 1989, Table 2, p.33
31	Tamarisk	FFG_207	865.00	Richey, 1989, Table 2, p.33
32	Tamarisk	FFG_208	874.20	Richey, 1989, Table 2, p.34
33	Tamarisk	FFG_209	866.20	Richey, 1989, Table 2, p.34
34	Tamarisk	FFG_210	858.90	Richey, 1989, Table 2, p.34
35	Tamarisk	FFG_212	845.20	Richey, 1989, Table 2, p.34
36	Tamarisk	FFG_213	868.40	Richey, 1989, Table 2, p.34
37	Tamarisk	FFG_214	848.20	Richey, 1989, Table 2, p.34
38	Tamarisk	FFG_215	823.60	Richey, 1989, Table 2, p.34
39	Tamarisk	FFG_216	710.40	Richey, 1989, Table 2, p.34
40	Tamarisk	FFG_217	843.70	Richey, 1989, Table 2, p.34
41	Tamarisk	FFG_218	835.80	Richey, 1989, Table 2, p.34
42	Tamarisk	FFG_219	879.90	Richey, 1989, Table 2, p.34
43	Tamarisk	FFG_220	832.20	Richey, 1989, Table 2, p.34
44	Tamarisk	FFG_221	787.00	Richey, 1989, Table 2, p.34
45	Tamarisk	FFG_222	741.60	Richey, 1989, Table 2, p.34
46	Tamarisk	FFG_224	648.10	Richey, 1989, Table 2, p.35
47	Tamarisk	FFG_225	656.30	Richey, 1989, Table 2, p.35
48	Tamarisk	FFG_226	654.00	Richey, 1989, Table 2, p.35
49	Tamarisk	FFG_228	643.20	Richey, 1989, Table 2, p.35
50	Tamarisk	FFG_229	672.00	Richey, 1989, Table 2, p.35
51	Tamarisk	FFG_230	658.10	Richey, 1989, Table 2, p.35
52	Tamarisk	FFG_231	674.20	Richey, 1989, Table 2, p.35
53	Tamarisk	FFG_232	688.20	Richey, 1989, Table 2, p.35
54	Tamarisk	FFG_233	678.80	Richey, 1989, Table 2, p.35
55	Tamarisk	FFG_234	715.00	Richey, 1989, Table 2, p.35
56	Tamarisk	FFG_235	691.30	Richey, 1989, Table 2, p.35
57	Tamarisk	FFG_236	738.50	Richey, 1989, Table 2, p.35
58	Tamarisk	FFG_237	704.80	Richey, 1989, Table 2, p.35
59	Tamarisk	FFG_238	685.50	Richey, 1989, Table 2, p.36
60	Tamarisk	FFG_239	673.30	Richey, 1989, Table 2, p.36
61	Tamarisk	FFG_240	664.50	Richey, 1989, Table 2, p.36
62	Tamarisk	FFG_241	659.00	Richey, 1989, Table 2, p.36
63	Tamarisk	FFG_242	776.70	Richey, 1989, Table 2, p.36
64	Tamarisk	FFG_243	735.50	Richey, 1989, Table 2, p.36
65	Tamarisk	FFG_244	773.10	Richey, 1989, Table 2, p.36
66	Tamarisk	FFG_245	566.90	Richey, 1989, Table 2, p.36
67	Tamarisk	FFG_246	573.00	Richey, 1989, Table 2, p.36
68	Tamarisk	FFG_247	558.00	Richey, 1989, Table 2, p.36
69	Tamarisk	FFG_248	566.00	Richey, 1989, Table 2, p.36
70	Tamarisk	FFG_249	564.20	Richey, 1989, Table 2, p.36
71	Tamarisk	FFG_250	644.50	Richey, 1989, Table 2, p.36
72	Tamarisk	FFG_251	538.50	Richey, 1989, Table 2, p.36
73	Tamarisk	FFG_252	677.80	Richey, 1989, Table 2, p.36
74	Tamarisk	FFG_253	632.50	Richey, 1989, Table 2, p.36
75	Tamarisk	FFG_254	623.90	Richey, 1989, Table 2, p.36
76	Tamarisk	FFG_255	580.10	Richey, 1989, Table 2, p.37

Table B.2. Elevations of Stratigraphic Layers Near WIPP (Continued)

	Layer	Well ID	Elevation	Source
1	Tamarisk	FFG_256	529.80	Richey, 1989, Table 2, p.37
2	Tamarisk	FFG_257	573.60	Richey, 1989, Table 2, p.37
3	Tamarisk	FFG_258	587.60	Richey, 1989, Table 2, p.37
4	Tamarisk	FFG_259	553.50	Richey, 1989, Table 2, p.37
5	Tamarisk	FFG_260	597.40	Richey, 1989, Table 2, p.37
6	Tamarisk	FFG_261	586.40	Richey, 1989, Table 2, p.37
7	Tamarisk	FFG_262	1109.50	Richey, 1989, Table 2, p.37
8	Tamarisk	FFG_263	521.10	Richey, 1989, Table 2, p.37
9	Tamarisk	FFG_264	753.20	Richey, 1989, Table 2, p.37
10	Tamarisk	FFG_265	749.80	Richey, 1989, Table 2, p.37
11	Tamarisk	FFG_266	730.90	Richey, 1989, Table 2, p.37
12	Tamarisk	FFG_267	708.30	Richey, 1989, Table 2, p.37
13	Tamarisk	FFG_268	684.60	Richey, 1989, Table 2, p.37
14	Tamarisk	FFG_269	696.90	Richey, 1989, Table 2, p.38
15	Tamarisk	FFG_270	769.30	Richey, 1989, Table 2, p.38
16	Tamarisk	FFG_271	808.90	Richey, 1989, Table 2, p.38
17	Tamarisk	FFG_272	816.40	Richey, 1989, Table 2, p.38
18	Tamarisk	FFG_273	790.10	Richey, 1989, Table 2, p.38
19	Tamarisk	FFG_274	827.20	Richey, 1989, Table 2, p.38
20	Tamarisk	FFG_275	834.30	Richey, 1989, Table 2, p.38
21	Tamarisk	FFG_276	837.60	Richey, 1989, Table 2, p.38
22	Tamarisk	FFG_277	829.10	Richey, 1989, Table 2, p.38
23	Tamarisk	FFG_278	838.50	Richey, 1989, Table 2, p.38
24	Tamarisk	FFG_279	833.30	Richey, 1989, Table 2, p.38
25	Tamarisk	FFG_280	830.90	Richey, 1989, Table 2, p.38
26	Tamarisk	FFG_281	807.40	Richey, 1989, Table 2, p.38
27	Tamarisk	FFG_283	558.10	Richey, 1989, Table 2, p.39
28	Tamarisk	FFG_284	705.90	Richey, 1989, Table 2, p.39
29	Tamarisk	FFG_285	734.90	Richey, 1989, Table 2, p.39
30	Tamarisk	FFG_286	814.10	Richey, 1989, Table 2, p.39
31	Tamarisk	FFG_287	786.10	Richey, 1989, Table 2, p.39
32	Tamarisk	FFG_288	738.80	Richey, 1989, Table 2, p.39
33	Tamarisk	FFG_289	713.80	Richey, 1989, Table 2, p.39
34	Tamarisk	FFG_290	799.50	Richey, 1989, Table 2, p.39
35	Tamarisk	FFG_291	736.70	Richey, 1989, Table 2, p.39
36	Tamarisk	FFG_292	752.30	Richey, 1989, Table 2, p.39
37	Tamarisk	FFG_293	744.60	Richey, 1989, Table 2, p.39
38	Tamarisk	FFG_294	567.00	Richey, 1989, Table 2, p.39
39	Tamarisk	FFG_295	554.70	Richey, 1989, Table 2, p.39
40	Tamarisk	FFG_297	532.50	Richey, 1989, Table 2, p.39
41	Tamarisk	FFG_298	546.70	Richey, 1989, Table 2, p.40
42	Tamarisk	FFG_299	564.20	Richey, 1989, Table 2, p.40
43	Tamarisk	FFG_300	515.40	Richey, 1989, Table 2, p.40
44	Tamarisk	FFG_301	485.60	Richey, 1989, Table 2, p.40
45	Tamarisk	FFG_302	514.20	Richey, 1989, Table 2, p.40
46	Tamarisk	FFG_303	505.10	Richey, 1989, Table 2, p.40
47	Tamarisk	FFG_304	512.90	Richey, 1989, Table 2, p.40
48	Tamarisk	FFG_305	503.20	Richey, 1989, Table 2, p.40
49	Tamarisk	FFG_306	465.10	Richey, 1989, Table 2, p.40
50	Tamarisk	FFG_307	488.00	Richey, 1989, Table 2, p.40
51	Tamarisk	FFG_308	460.50	Richey, 1989, Table 2, p.40
52	Tamarisk	FFG_309	503.20	Richey, 1989, Table 2, p.40
53	Tamarisk	FFG_310	534.60	Richey, 1989, Table 2, p.40
54	Tamarisk	FFG_311	481.00	Richey, 1989, Table 2, p.40
55	Tamarisk	FFG_312	504.50	Richey, 1989, Table 2, p.40
56	Tamarisk	FFG_313	908.10	Richey, 1989, Table 2, p.41
57	Tamarisk	FFG_314	836.10	Richey, 1989, Table 2, p.41
58	Tamarisk	FFG_315	758.50	Richey, 1989, Table 2, p.41
59	Tamarisk	FFG_316	742.10	Richey, 1989, Table 2, p.41
60	Tamarisk	FFG_317	772.70	Richey, 1989, Table 2, p.41
61	Tamarisk	FFG_318	734.60	Richey, 1989, Table 2, p.41
62	Tamarisk	FFG_319	745.80	Richey, 1989, Table 2, p.41
63	Tamarisk	FFG_320	735.50	Richey, 1989, Table 2, p.41
64	Tamarisk	FFG_321	732.10	Richey, 1989, Table 2, p.41
65	Tamarisk	FFG_322	727.40	Richey, 1989, Table 2, p.41
66	Tamarisk	FFG_323	723.40	Richey, 1989, Table 2, p.41
67	Tamarisk	FFG_324	738.00	Richey, 1989, Table 2, p.41
68	Tamarisk	FFG_325	793.40	Richey, 1989, Table 2, p.41
69	Tamarisk	FFG_326	729.10	Richey, 1989, Table 2, p.41
70	Tamarisk	FFG_327	723.60	Richey, 1989, Table 2, p.42
71	Tamarisk	FFG_328	728.70	Richey, 1989, Table 2, p.42
72	Tamarisk	FFG_329	728.40	Richey, 1989, Table 2, p.42
73	Tamarisk	FFG_330	728.00	Richey, 1989, Table 2, p.42
74	Tamarisk	FFG_331	722.70	Richey, 1989, Table 2, p.42
75	Tamarisk	FFG_332	713.80	Richey, 1989, Table 2, p.42
76	Tamarisk	FFG_333	717.30	Richey, 1989, Table 2, p.42

Table B.2. Elevations of Stratigraphic Layers Near WIPP (Continued)

	Layer	Well ID	Elevation	Source
1	Tamarisk	FFG_334	712.60	Richey, 1989, Table 2, p.42
2	Tamarisk	FFG_335	724.80	Richey, 1989, Table 2, p.42
3	Tamarisk	FFG_336	725.10	Richey, 1989, Table 2, p.42
4	Tamarisk	FFG_337	708.00	Richey, 1989, Table 2, p.42
5	Tamarisk	FFG_338	715.20	Richey, 1989, Table 2, p.42
6	Tamarisk	FFG_339	680.30	Richey, 1989, Table 2, p.42
7	Tamarisk	FFG_340	688.80	Richey, 1989, Table 2, p.42
8	Tamarisk	FFG_342	720.20	Richey, 1989, Table 2, p.43
9	Tamarisk	FFG_344	685.10	Richey, 1989, Table 2, p.43
10	Tamarisk	FFG_345	746.60	Richey, 1989, Table 2, p.43
11	Tamarisk	FFG_347	736.70	Richey, 1989, Table 2, p.43
12	Tamarisk	FFG_348	768.10	Richey, 1989, Table 2, p.43
13	Tamarisk	FFG_349	738.00	Richey, 1989, Table 2, p.43
14	Tamarisk	FFG_350	783.00	Richey, 1989, Table 2, p.43
15	Tamarisk	FFG_351	701.10	Richey, 1989, Table 2, p.43
16	Tamarisk	FFG_352	699.50	Richey, 1989, Table 2, p.43
17	Tamarisk	FFG_353	721.20	Richey, 1989, Table 2, p.43
18	Tamarisk	FFG_354	795.30	Richey, 1989, Table 2, p.43
19	Tamarisk	FFG_361	982.60	Richey, 1989, Table 2, p.44
20	Tamarisk	FFG_362	956.40	Richey, 1989, Table 2, p.44
21	Tamarisk	FFG_363	972.90	Richey, 1989, Table 2, p.44
22	Tamarisk	FFG_364	942.70	Richey, 1989, Table 2, p.44
23	Tamarisk	FFG_366	933.90	Richey, 1989, Table 2, p.44
24	Tamarisk	FFG_367	948.50	Richey, 1989, Table 2, p.44
25	Tamarisk	FFG_370	1012.90	Richey, 1989, Table 2, p.44
26	Tamarisk	FFG_371	994.60	Richey, 1989, Table 2, p.44
27	Tamarisk	FFG_372	1006.40	Richey, 1989, Table 2, p.45
28	Tamarisk	FFG_373	945.00	Richey, 1989, Table 2, p.45
29	Tamarisk	FFG_374	929.70	Richey, 1989, Table 2, p.45
30	Tamarisk	FFG_376	984.80	Richey, 1989, Table 2, p.45
31	Tamarisk	FFG_381	1021.40	Richey, 1989, Table 2, p.45
32	Tamarisk	FFG_383	931.20	Richey, 1989, Table 2, p.45
33	Tamarisk	FFG_384	937.90	Richey, 1989, Table 2, p.45
34	Tamarisk	FFG_385	922.00	Richey, 1989, Table 2, p.45
35	Tamarisk	FFG_387	934.60	Richey, 1989, Table 2, p.45
36	Tamarisk	FFG_388	929.40	Richey, 1989, Table 2, p.46
37	Tamarisk	FFG_389	976.60	Richey, 1989, Table 2, p.46
38	Tamarisk	FFG_390	945.50	Richey, 1989, Table 2, p.46
39	Tamarisk	FFG_391	944.50	Richey, 1989, Table 2, p.46
40	Tamarisk	FFG_392	941.90	Richey, 1989, Table 2, p.46
41	Tamarisk	FFG_393	810.60	Richey, 1989, Table 2, p.46
42	Tamarisk	FFG_394	903.10	Richey, 1989, Table 2, p.46
43	Tamarisk	FFG_395	895.80	Richey, 1989, Table 2, p.46
44	Tamarisk	FFG_396	877.20	Richey, 1989, Table 2, p.46
45	Tamarisk	FFG_398	798.50	Richey, 1989, Table 2, p.46
46	Tamarisk	FFG_399	838.50	Richey, 1989, Table 2, p.46
47	Tamarisk	FFG_401	874.80	Richey, 1989, Table 2, p.46
48	Tamarisk	FFG_402	972.00	Richey, 1989, Table 2, p.46
49	Tamarisk	FFG_403	935.30	Richey, 1989, Table 2, p.47
50	Tamarisk	FFG_404	897.40	Richey, 1989, Table 2, p.47
51	Tamarisk	FFG_407	932.40	Richey, 1989, Table 2, p.47
52	Tamarisk	FFG_408	908.60	Richey, 1989, Table 2, p.47
53	Tamarisk	FFG_409	970.50	Richey, 1989, Table 2, p.47
54	Tamarisk	FFG_418	983.30	Richey, 1989, Table 2, p.48
55	Tamarisk	FFG_419	969.00	Richey, 1989, Table 2, p.48
56	Tamarisk	FFG_420	964.30	Richey, 1989, Table 2, p.48
57	Tamarisk	FFG_421	955.00	Richey, 1989, Table 2, p.48
58	Tamarisk	FFG_422	946.10	Richey, 1989, Table 2, p.48
59	Tamarisk	FFG_426	962.00	Richey, 1989, Table 2, p.48
60	Tamarisk	FFG_432	918.00	Richey, 1989, Table 2, p.48
61	Tamarisk	FFG_433	920.50	Richey, 1989, Table 2, p.48
62	Tamarisk	FFG_438	866.70	Richey, 1989, Table 2, p.49
63	Tamarisk	FFG_453	862.20	Richey, 1989, Table 2, p.50
64	Tamarisk	FFG_455	810.40	Richey, 1989, Table 2, p.50
65	Tamarisk	FFG_456	805.20	Richey, 1989, Table 2, p.50
66	Tamarisk	FFG_457	861.30	Richey, 1989, Table 2, p.50
67	Tamarisk	FFG_458	862.30	Richey, 1989, Table 2, p.50
68	Tamarisk	FFG_459	791.90	Richey, 1989, Table 2, p.50
69	Tamarisk	FFG_462	857.50	Richey, 1989, Table 2, p.50
70	Tamarisk	FFG_463	886.40	Richey, 1989, Table 2, p.51
71	Tamarisk	FFG_464	872.30	Richey, 1989, Table 2, p.51
72	Tamarisk	FFG_465	875.30	Richey, 1989, Table 2, p.51
73	Tamarisk	FFG_467	483.30	Richey, 1989, Table 2, p.51
74	Tamarisk	FFG_468	460.00	Richey, 1989, Table 2, p.51
75	Tamarisk	FFG_470	480.10	Richey, 1989, Table 2, p.51
76	Tamarisk	FFG_471	495.00	Richey, 1989, Table 2, p.51

Table B.2. Elevations of Stratigraphic Layers Near WIPP (Continued)

	Layer	Well ID	Elevation	Source
1	Tamarisk	FFG_472	532.80	Richey, 1989, Table 2, p.51
2	Tamarisk	FFG_473	463.60	Richey, 1989, Table 2, p.51
3	Tamarisk	FFG_474	723.30	Richey, 1989, Table 2, p.51
4	Tamarisk	FFG_475	723.80	Richey, 1989, Table 2, p.51
5	Tamarisk	FFG_476	797.40	Richey, 1989, Table 2, p.51
6	Tamarisk	FFG_477	751.70	Richey, 1989, Table 2, p.51
7	Tamarisk	FFG_478	733.60	Richey, 1989, Table 2, p.52
8	Tamarisk	FFG_479	730.00	Richey, 1989, Table 2, p.52
9	Tamarisk	FFG_480	726.40	Richey, 1989, Table 2, p.52
10	Tamarisk	FFG_481	709.00	Richey, 1989, Table 2, p.52
11	Tamarisk	FFG_482	738.60	Richey, 1989, Table 2, p.52
12	Tamarisk	FFG_483	761.40	Richey, 1989, Table 2, p.52
13	Tamarisk	FFG_484	748.10	Richey, 1989, Table 2, p.52
14	Tamarisk	FFG_485	756.80	Richey, 1989, Table 2, p.52
15	Tamarisk	FFG_486	743.40	Richey, 1989, Table 2, p.52
16	Tamarisk	FFG_487	740.40	Richey, 1989, Table 2, p.52
17	Tamarisk	FFG_488	726.60	Richey, 1989, Table 2, p.52
18	Tamarisk	FFG_489	742.30	Richey, 1989, Table 2, p.52
19	Tamarisk	FFG_490	832.70	Richey, 1989, Table 2, p.52
20	Tamarisk	FFG_491	830.30	Richey, 1989, Table 2, p.52
21	Tamarisk	FFG_492	792.50	Richey, 1989, Table 2, p.52
22	Tamarisk	FFG_493	779.80	Richey, 1989, Table 2, p.53
23	Tamarisk	FFG_494	786.00	Richey, 1989, Table 2, p.53
24	Tamarisk	FFG_495	777.20	Richey, 1989, Table 2, p.53
25	Tamarisk	FFG_496	684.30	Richey, 1989, Table 2, p.53
26	Tamarisk	FFG_497	695.60	Richey, 1989, Table 2, p.53
27	Tamarisk	FFG_498	708.40	Richey, 1989, Table 2, p.53
28	Tamarisk	FFG_499	684.60	Richey, 1989, Table 2, p.53
29	Tamarisk	FFG_500	698.60	Richey, 1989, Table 2, p.53
30	Tamarisk	FFG_501	704.00	Richey, 1989, Table 2, p.53
31	Tamarisk	FFG_502	697.40	Richey, 1989, Table 2, p.53
32	Tamarisk	FFG_503	679.40	Richey, 1989, Table 2, p.53
33	Tamarisk	FFG_504	699.90	Richey, 1989, Table 2, p.53
34	Tamarisk	FFG_505	734.30	Richey, 1989, Table 2, p.53
35	Tamarisk	FFG_506	725.40	Richey, 1989, Table 2, p.53
36	Tamarisk	FFG_507	688.40	Richey, 1989, Table 2, p.53
37	Tamarisk	FFG_508	738.60	Richey, 1989, Table 2, p.53
38	Tamarisk	FFG_509	739.10	Richey, 1989, Table 2, p.54
39	Tamarisk	FFG_510	738.70	Richey, 1989, Table 2, p.54
40	Tamarisk	FFG_511	696.50	Richey, 1989, Table 2, p.54
41	Tamarisk	FFG_512	714.80	Richey, 1989, Table 2, p.54
42	Tamarisk	FFG_513	734.90	Richey, 1989, Table 2, p.54
43	Tamarisk	FFG_514	726.00	Richey, 1989, Table 2, p.54
44	Tamarisk	FFG_515	692.80	Richey, 1989, Table 2, p.54
45	Tamarisk	FFG_516	685.50	Richey, 1989, Table 2, p.54
46	Tamarisk	FFG_517	783.70	Richey, 1989, Table 2, p.54
47	Tamarisk	FFG_518	772.00	Richey, 1989, Table 2, p.54
48	Tamarisk	FFG_519	740.10	Richey, 1989, Table 2, p.54
49	Tamarisk	FFG_520	631.70	Richey, 1989, Table 2, p.54
50	Tamarisk	FFG_521	650.40	Richey, 1989, Table 2, p.54
51	Tamarisk	FFG_522	499.70	Richey, 1989, Table 2, p.54
52	Tamarisk	FFG_523	509.30	Richey, 1989, Table 2, p.54
53	Tamarisk	FFG_524	670.80	Richey, 1989, Table 2, p.55
54	Tamarisk	FFG_525	508.50	Richey, 1989, Table 2, p.55
55	Tamarisk	FFG_526	973.50	Richey, 1989, Table 2, p.55
56	Tamarisk	FFG_527	933.60	Richey, 1989, Table 2, p.55
57	Tamarisk	FFG_528	926.00	Richey, 1989, Table 2, p.55
58	Tamarisk	FFG_530	1000.30	Richey, 1989, Table 2, p.55
59	Tamarisk	FFG_531	919.30	Richey, 1989, Table 2, p.55
60	Tamarisk	FFG_532	907.10	Richey, 1989, Table 2, p.55
61	Tamarisk	FFG_534	946.40	Richey, 1989, Table 2, p.55
62	Tamarisk	FFG_535	912.80	Richey, 1989, Table 2, p.55
63	Tamarisk	FFG_536	928.40	Richey, 1989, Table 2, p.55
64	Tamarisk	FFG_537	904.60	Richey, 1989, Table 2, p.55
65	Tamarisk	FFG_543	970.90	Richey, 1989, Table 2, p.56
66	Tamarisk	FFG_548	907.70	Richey, 1989, Table 2, p.56
67	Tamarisk	FFG_562	645.30	Richey, 1989, Table 2, p.57
68	Tamarisk	FFG_563	557.50	Richey, 1989, Table 2, p.57
69	Tamarisk	FFG_568	634.60	Richey, 1989, Table 2, p.57
70	Tamarisk	FFG_569	663.20	Richey, 1989, Table 2, p.57
71	Tamarisk	FFG_584	764.30	Richey, 1989, Table 2, p.58
72	Tamarisk	FFG_585	730.90	Richey, 1989, Table 2, p.58
73	Tamarisk	FFG_600	722.10	Richey, 1989, Table 2, p.58
74	Tamarisk	FFG_601	615.70	Richey, 1989, Table 2, p.58
75	Tamarisk	FFG_602	1053.10	Richey, 1989, Table 2, p.58
76	Tamarisk	FFG_606	695.90	Richey, 1989, Table 2, p.58

Table B.2. Elevations of Stratigraphic Layers Near WIPP (Continued)

	Layer	Well ID	Elevation	Source
1	Tamarisk	FFG_607	718.40	Richey, 1989, Table 2, p.59
2	Tamarisk	FFG_608	726.60	Richey, 1989, Table 2, p.59
3	Tamarisk	FFG_609	732.70	Richey, 1989, Table 2, p.59
4	Tamarisk	FFG_610	713.20	Richey, 1989, Table 2, p.59
5	Tamarisk	FFG_611	703.20	Richey, 1989, Table 2, p.59
6	Tamarisk	FFG_612	712.70	Richey, 1989, Table 2, p.59
7	Tamarisk	FFG_613	705.90	Richey, 1989, Table 2, p.59
8	Tamarisk	FFG_618	701.90	Richey, 1989, Table 2, p.59
9	Tamarisk	FFG_638	567.30	Richey, 1989, Table 2, p.60
10	Tamarisk	FFG_639	537.40	Richey, 1989, Table 2, p.60
11	Tamarisk	FFG_640	623.10	Richey, 1989, Table 2, p.60
12	Tamarisk	FFG_643	662.40	Richey, 1989, Table 2, p.60
13	Tamarisk	FFG_644	701.20	Richey, 1989, Table 2, p.60
14	Tamarisk	FFG_648	536.10	Richey, 1989, Table 2, p.60
15	Tamarisk	FFG_652	853.70	Richey, 1989, Table 2, p.60
16	Tamarisk	FFG_653	854.10	Richey, 1989, Table 2, p.61
17	Tamarisk	FFG_654	874.80	Richey, 1989, Table 2, p.61
18	Tamarisk	FFG_655	873.20	Richey, 1989, Table 2, p.61
19	Tamarisk	FFG_656	870.80	Richey, 1989, Table 2, p.61
20	Tamarisk	FFG_657	883.70	Richey, 1989, Table 2, p.61
21	Tamarisk	FFG_658	874.40	Richey, 1989, Table 2, p.61
22	Tamarisk	FFG_659	879.70	Richey, 1989, Table 2, p.61
23	Tamarisk	FFG_660	896.90	Richey, 1989, Table 2, p.61
24	Tamarisk	FFG_662	870.80	Richey, 1989, Table 2, p.61
25	Tamarisk	FFG_664	862.00	Richey, 1989, Table 2, p.61
26	Tamarisk	FFG_666	914.40	Richey, 1989, Table 2, p.62
27	Tamarisk	FFG_667	899.50	Richey, 1989, Table 2, p.62
28	Tamarisk	FFG_668	947.70	Richey, 1989, Table 2, p.62
29	Tamarisk	FFG_669	934.20	Richey, 1989, Table 2, p.62
30	Tamarisk	FFG_670	919.30	Richey, 1989, Table 2, p.62
31	Tamarisk	FFG_671	917.70	Richey, 1989, Table 2, p.62
32	Tamarisk	FFG_672	919.90	Richey, 1989, Table 2, p.62
33	Tamarisk	FFG_673	914.70	Richey, 1989, Table 2, p.62
34	Tamarisk	FFG_674	915.00	Richey, 1989, Table 2, p.62
35	Tamarisk	FFG_675	871.60	Richey, 1989, Table 2, p.62
36	Tamarisk	FFG_676	884.20	Richey, 1989, Table 2, p.62
37	Tamarisk	FFG_677	910.50	Richey, 1989, Table 2, p.62
38	Tamarisk	FFG_679	910.40	Richey, 1989, Table 2, p.62
39	Tamarisk	FFG_689	793.70	Richey, 1989, Table 2, p.63
40	Tamarisk	FFG_690	798.90	Richey, 1989, Table 2, p.63
41	Tamarisk	FFG_691	790.40	Richey, 1989, Table 2, p.63
42	Tamarisk	FFG_692	780.30	Richey, 1989, Table 2, p.63
43	Tamarisk	FFG_693	790.90	Richey, 1989, Table 2, p.63
44	Tamarisk	FFG_694	783.30	Richey, 1989, Table 2, p.63
45	Tamarisk	FFG_695	788.80	Richey, 1989, Table 2, p.63
46	Tamarisk	FFG_696	790.60	Richey, 1989, Table 2, p.63
47	Tamarisk	FFG_697	793.70	Richey, 1989, Table 2, p.64
48	Tamarisk	FFG_698	835.50	Richey, 1989, Table 2, p.64
49	Tamarisk	FFG_699	786.70	Richey, 1989, Table 2, p.64
50	Tamarisk	FFG_700	777.00	Richey, 1989, Table 2, p.64
51	Tamarisk	FFG_701	781.90	Richey, 1989, Table 2, p.64
52	Tamarisk	FFG_702	786.70	Richey, 1989, Table 2, p.64
53	Tamarisk	FFG_703	791.60	Richey, 1989, Table 2, p.64
54	Tamarisk	FFG_704	779.40	Richey, 1989, Table 2, p.64
55	Tamarisk	FFG_705	709.60	Richey, 1989, Table 2, p.64
56	Tamarisk	FFG_706	730.70	Richey, 1989, Table 2, p.64
57	Tamarisk	FFG_707	714.20	Richey, 1989, Table 2, p.64
58	Tamarisk	FFG_708	767.20	Richey, 1989, Table 2, p.64
59	Tamarisk	FFG_709	658.70	Richey, 1989, Table 2, p.64
60	Tamarisk	FFG_710	659.30	Richey, 1989, Table 2, p.64
61	Tamarisk	FFG_711	668.20	Richey, 1989, Table 2, p.65
62	Tamarisk	FFG_712	710.90	Richey, 1989, Table 2, p.65
63	Tamarisk	FFG_713	648.10	Richey, 1989, Table 2, p.65
64	Tamarisk	FFG_714	761.90	Richey, 1989, Table 2, p.65
65	Tamarisk	FFG_715	774.80	Richey, 1989, Table 2, p.65
66	Tamarisk	FFG_716	676.60	Richey, 1989, Table 2, p.65
67	Tamarisk	FFG_717	698.10	Richey, 1989, Table 2, p.65
68	Tamarisk	FFG_718	700.90	Richey, 1989, Table 2, p.65
69	Tamarisk	FFG_719	674.20	Richey, 1989, Table 2, p.65
70	Tamarisk	FFG_720	671.50	Richey, 1989, Table 2, p.65
71	Tamarisk	FFG_721	673.60	Richey, 1989, Table 2, p.65
72	Tamarisk	FFG_723	785.30	Richey, 1989, Table 2, p.65
73	Tamarisk	FFG_724	713.60	Richey, 1989, Table 2, p.65
74	Tamarisk	FFG_725	689.70	Richey, 1989, Table 2, p.65
75	Tamarisk	FFG_726	677.50	Richey, 1989, Table 2, p.65
76	Tamarisk	FFG_727	674.90	Richey, 1989, Table 2, p.66

Table B.2. Elevations of Stratigraphic Layers Near WIPP (Continued)

	Layer	Well ID	Elevation	Source
1	Tamarisk	FFG_728	673.30	Richey, 1989, Table 2, p.66
2	Tamarisk	FFG_729	683.70	Richey, 1989, Table 2, p.66
3	Tamarisk	FFG_730	701.30	Richey, 1989, Table 2, p.66
4	Tamarisk	FFG_731	697.80	Richey, 1989, Table 2, p.66
5	Tamarisk	FFG_732	713.20	Richey, 1989, Table 2, p.66
6	Tamarisk	FFG_733	781.20	Richey, 1989, Table 2, p.66
7	Tamarisk	FFG_734	737.00	Richey, 1989, Table 2, p.66
8	Tamarisk	FFG_735	679.10	Richey, 1989, Table 2, p.66
9	Tamarisk	FFG_736	732.40	Richey, 1989, Table 2, p.66
10	Tamarisk	FFG_737	678.80	Richey, 1989, Table 2, p.66
11	Tamarisk	FFG_738	692.50	Richey, 1989, Table 2, p.66
12	Tamarisk	FFG_739	729.80	Richey, 1989, Table 2, p.66
13	Tamarisk	FFG_740	730.60	Richey, 1989, Table 2, p.66
14	Tamarisk	FFG_741	697.70	Richey, 1989, Table 2, p.66
15	Tamarisk	FFG_742	748.60	Richey, 1989, Table 2, p.67
16	Tamarisk	FFG_743	735.20	Richey, 1989, Table 2, p.67
17	Tamarisk	FFG_744	717.80	Richey, 1989, Table 2, p.67
18	Tamarisk	FFG_745	705.90	Richey, 1989, Table 2, p.67
19	Tamarisk	FFG_746	693.00	Richey, 1989, Table 2, p.67
20	Tamarisk	H1	856.20	Mercer, 1983, Table 1
21	Tamarisk	H10C	733.70	Mercer, 1983, Table 1
22	Tamarisk	H2C	864.10	Mercer, 1983, Table 1
23	Tamarisk	H3	855.30	Mercer, 1983, Table 1
24	Tamarisk	H4C	893.40	Mercer, 1983, Table 1
25	Tamarisk	H5C	821.40	Mercer, 1983, Table 1
26	Tamarisk	H6C	863.80	Mercer, 1983, Table 1
27	Tamarisk	H7C	921.40	Mercer, 1983, Table 1
28	Tamarisk	H8C	897.70	Mercer, 1983, Table 1
29	Tamarisk	H9C	869.20	Mercer, 1983, Table 1
30	Tamarisk	P1	883.00	Mercer, 1983, Table 1
31	Tamarisk	P10	831.50	Mercer, 1983, Table 1
32	Tamarisk	P11	817.10	Mercer, 1983, Table 1
33	Tamarisk	P12	862.90	Mercer, 1983, Table 1
34	Tamarisk	P13	862.90	Mercer, 1983, Table 1
35	Tamarisk	P14	878.70	Mercer, 1983, Table 1
36	Tamarisk	P15	911.10	Mercer, 1983, Table 1
37	Tamarisk	P16	889.10	Mercer, 1983, Table 1
38	Tamarisk	P17	875.70	Mercer, 1983, Table 1
39	Tamarisk	P18	837.30	Mercer, 1983, Table 1
40	Tamarisk	P19	824.80	Mercer, 1983, Table 1
41	Tamarisk	P2	824.80	Mercer, 1983, Table 1
42	Tamarisk	P20	819.00	Mercer, 1983, Table 1
43	Tamarisk	P21	822.00	Mercer, 1983, Table 1
44	Tamarisk	P3	862.50	Mercer, 1983, Table 1
45	Tamarisk	P4	840.60	Mercer, 1983, Table 1
46	Tamarisk	P5	841.30	Mercer, 1983, Table 1
47	Tamarisk	P6	887.30	Mercer, 1983, Table 1
48	Tamarisk	P7	894.30	Mercer, 1983, Table 1
49	Tamarisk	P8	873.20	Mercer, 1983, Table 1
50	Tamarisk	P9	843.70	Mercer, 1983, Table 1
51	Tamarisk	SaltShft	848.11	Bechtel, Inc., 1986, Appendix D
52	Tamarisk	WIPP11	815.60	Mercer, 1983, Table 1
53	Tamarisk	WIPP12	840.40	Mercer, 1983, Table 1
54	Tamarisk	WIPP13	860.10	Mercer, 1983, Table 1
55	Tamarisk	WIPP18	841.30	Mercer, 1983, Table 1
56	Tamarisk	WIPP19	841.60	Mercer, 1983, Table 1
57	Tamarisk	WIPP21	846.10	Mercer, 1983, Table 1
58	Tamarisk	WIPP22	844.90	Mercer, 1983, Table 1
59	Tamarisk	WIPP25	879.30	Mercer, 1983, Table 1
60	Tamarisk	WIPP26	930.50	Mercer, 1983, Table 1
61	Tamarisk	WIPP27	909.20	Mercer, 1983, Table 1
62	Tamarisk	WIPP28	925.70	Mercer, 1983, Table 1
63	Tamarisk	WIPP29	907.40	Mercer, 1983, Table 1
64	Tamarisk	WIPP30	881.20	Mercer, 1983, Table 1
65	Tamarisk	WIPP32	910.40	Mercer, 1983, Table 1
66	Tamarisk	WIPP33	870.30	Mercer, 1983, Table 1
67	Tamarisk	WIPP34	820.50	Mercer, 1983, Table 1
68	Tamarisk	WastShft	849.83	Bechtel, Inc., 1986, Appendix E
69	Tamerisk	DOE1	831.60	TME 3159, Sep 1982, Table 2
70	Tamerisk	DOE2	821.70	Mercer et al., 1987, Table 3-2
71	Tamerisk	ERDA9	849.10	SNL and USGS, 1982b, Table 2
72	Tamerisk	REF	849.10	Rechard et al.,1991, Figure 2.2-1
73	Tamerisk	WIPP11	815.70	SNL and USGS, 1982a, Table 2
74	Tamerisk	WIPP12	840.10	D'Appolonia Consulting, 1983, Table 2
75	U_Member	AirShft	782.57	IT Corporation, 1990, Figure 22
76	U_Member	DOE1	761.00	TME 3159, Sep 1982, Table 2

Table B.2. Elevations of Stratigraphic Layers Near WIPP (Continued)

	Layer	Well ID	Elevation	Source
1	U_Member	DOE2	749.00	Mercer et al., 1987, Table 3-2
2	U_Member	ERDA9	779.70	SNL and USGS, 1982b, Table 2
3	U_Member	ExhtShft	779.82	Bechtel, Inc., 1986, Appendix F
4	U_Member	REF	779.70	Rechard et al.,1991, Figure 2.2-1
5	U_Member	SaltShft	779.83	Bechtel, Inc., 1986, Appendix D
6	U_Member	WIPP11	754.40	SNL and USGS, 1982a, Table 2
7	U_Member	WIPP12	767.40	D'Appolonia Consulting, 1983, Table 2
8	U_Member	WastShft	781.32	Bechtel, Inc., 1986, Appendix E
9	Unnamed	AEC7	840.60	Mercer, 1983, Table 1
10	Unnamed	AEC8	814.80	Mercer, 1983, Table 1
11	Unnamed	AirShft	817.19	IT Corporation, 1990, Figure 22
12	Unnamed	B25	817.20	Mercer, 1983, Table 1
13	Unnamed	DOE1	799.40	TME 3159, Sep 1982, Table 2
14	Unnamed	DOE2	784.10	Mercer et al., 1987, Table 3-2
15	Unnamed	ERDA10	873.90	Mercer, 1983, Table 1
16	Unnamed	ERDA6	855.00	Mercer, 1983, Table 1
17	Unnamed	ERDA9	820.50	Mercer, 1983, Table 1
18	Unnamed	ERDA9	816.40	SNL and USGS, 1982b, Table 2
19	Unnamed	ExhtShft	814.75	Bechtel, Inc., 1986, Appendix F
20	Unnamed	FFG_002	618.10	Richey, 1989, Table 2, p.21
21	Unnamed	FFG_004	659.90	Richey, 1989, Table 2, p.21
22	Unnamed	FFG_005	622.10	Richey, 1989, Table 2, p.21
23	Unnamed	FFG_006	608.10	Richey, 1989, Table 2, p.21
24	Unnamed	FFG_007	593.70	Richey, 1989, Table 2, p.21
25	Unnamed	FFG_009	596.50	Richey, 1989, Table 2, p.21
26	Unnamed	FFG_011	603.50	Richey, 1989, Table 2, p.21
27	Unnamed	FFG_012	606.20	Richey, 1989, Table 2, p.21
28	Unnamed	FFG_013	634.30	Richey, 1989, Table 2, p.21
29	Unnamed	FFG_014	658.90	Richey, 1989, Table 2, p.21
30	Unnamed	FFG_016	579.40	Richey, 1989, Table 2, p.21
31	Unnamed	FFG_017	587.30	Richey, 1989, Table 2, p.22
32	Unnamed	FFG_018	590.70	Richey, 1989, Table 2, p.22
33	Unnamed	FFG_019	580.30	Richey, 1989, Table 2, p.22
34	Unnamed	FFG_020	655.30	Richey, 1989, Table 2, p.22
35	Unnamed	FFG_023	587.70	Richey, 1989, Table 2, p.22
36	Unnamed	FFG_024	571.80	Richey, 1989, Table 2, p.22
37	Unnamed	FFG_025	591.80	Richey, 1989, Table 2, p.22
38	Unnamed	FFG_026	585.50	Richey, 1989, Table 2, p.22
39	Unnamed	FFG_027	578.50	Richey, 1989, Table 2, p.22
40	Unnamed	FFG_028	572.50	Richey, 1989, Table 2, p.22
41	Unnamed	FFG_029	558.10	Richey, 1989, Table 2, p.22
42	Unnamed	FFG_030	557.20	Richey, 1989, Table 2, p.22
43	Unnamed	FFG_031	547.40	Richey, 1989, Table 2, p.22
44	Unnamed	FFG_032	546.10	Richey, 1989, Table 2, p.22
45	Unnamed	FFG_033	542.20	Richey, 1989, Table 2, p.22
46	Unnamed	FFG_034	542.50	Richey, 1989, Table 2, p.23
47	Unnamed	FFG_035	530.90	Richey, 1989, Table 2, p.23
48	Unnamed	FFG_036	535.60	Richey, 1989, Table 2, p.23
49	Unnamed	FFG_037	528.80	Richey, 1989, Table 2, p.23
50	Unnamed	FFG_038	517.50	Richey, 1989, Table 2, p.23
51	Unnamed	FFG_039	725.50	Richey, 1989, Table 2, p.23
52	Unnamed	FFG_040	645.30	Richey, 1989, Table 2, p.23
53	Unnamed	FFG_041	726.40	Richey, 1989, Table 2, p.23
54	Unnamed	FFG_042	730.00	Richey, 1989, Table 2, p.23
55	Unnamed	FFG_043	728.70	Richey, 1989, Table 2, p.23
56	Unnamed	FFG_044	680.90	Richey, 1989, Table 2, p.23
57	Unnamed	FFG_047	556.00	Richey, 1989, Table 2, p.23
58	Unnamed	FFG_048	573.30	Richey, 1989, Table 2, p.23
59	Unnamed	FFG_049	559.60	Richey, 1989, Table 2, p.23
60	Unnamed	FFG_050	574.90	Richey, 1989, Table 2, p.24
61	Unnamed	FFG_051	566.30	Richey, 1989, Table 2, p.24
62	Unnamed	FFG_052	589.80	Richey, 1989, Table 2, p.24
63	Unnamed	FFG_053	555.60	Richey, 1989, Table 2, p.24
64	Unnamed	FFG_054	556.60	Richey, 1989, Table 2, p.24
65	Unnamed	FFG_055	557.80	Richey, 1989, Table 2, p.24
66	Unnamed	FFG_056	556.90	Richey, 1989, Table 2, p.24
67	Unnamed	FFG_057	558.10	Richey, 1989, Table 2, p.24
68	Unnamed	FFG_058	560.80	Richey, 1989, Table 2, p.24
69	Unnamed	FFG_059	564.80	Richey, 1989, Table 2, p.24
70	Unnamed	FFG_060	563.20	Richey, 1989, Table 2, p.24
71	Unnamed	FFG_061	565.10	Richey, 1989, Table 2, p.24
72	Unnamed	FFG_062	507.20	Richey, 1989, Table 2, p.24
73	Unnamed	FFG_063	465.80	Richey, 1989, Table 2, p.24
74	Unnamed	FFG_064	488.90	Richey, 1989, Table 2, p.24
75	Unnamed	FFG_065	464.50	Richey, 1989, Table 2, p.24
76	Unnamed	FFG_066	429.10	Richey, 1989, Table 2, p.24

Table B.2. Elevations of Stratigraphic Layers Near WIPP (Continued)

	Layer	Well ID	Elevation	Source		Layer	Well ID	Elevation	Source
1	Unnamed	FFG_067	464.00	Richey, 1989, Table 2, p.25	39	Unnamed	FFG_107	878.80	Richey, 1989, Table 2, p.27
2	Unnamed	FFG_068	424.00	Richey, 1989, Table 2, p.25	40	Unnamed	FFG_108	869.60	Richey, 1989, Table 2, p.27
3	Unnamed	FFG_069	441.40	Richey, 1989, Table 2, p.25	41	Unnamed	FFG_109	856.20	Richey, 1989, Table 2, p.27
4	Unnamed	FFG_070	479.10	Richey, 1989, Table 2, p.25	42	Unnamed	FFG_110	824.50	Richey, 1989, Table 2, p.27
5	Unnamed	FFG_071	748.30	Richey, 1989, Table 2, p.25	43	Unnamed	FFG_111	830.60	Richey, 1989, Table 2, p.27
6	Unnamed	FFG_072	674.20	Richey, 1989, Table 2, p.25	44	Unnamed	FFG_112	816.80	Richey, 1989, Table 2, p.28
7	Unnamed	FFG_073	652.20	Richey, 1989, Table 2, p.25	45	Unnamed	FFG_113	830.90	Richey, 1989, Table 2, p.28
8	Unnamed	FFG_074	660.30	Richey, 1989, Table 2, p.25	46	Unnamed	FFG_114	863.20	Richey, 1989, Table 2, p.28
9	Unnamed	FFG_075	712.10	Richey, 1989, Table 2, p.25	47	Unnamed	FFG_115	848.30	Richey, 1989, Table 2, p.28
10	Unnamed	FFG_076	771.50	Richey, 1989, Table 2, p.25	48	Unnamed	FFG_116	865.30	Richey, 1989, Table 2, p.28
11	Unnamed	FFG_078	807.70	Richey, 1989, Table 2, p.25	49	Unnamed	FFG_117	856.50	Richey, 1989, Table 2, p.28
12	Unnamed	FFG_079	780.90	Richey, 1989, Table 2, p.25	50	Unnamed	FFG_119	864.80	Richey, 1989, Table 2, p.28
13	Unnamed	FFG_080	758.30	Richey, 1989, Table 2, p.25	51	Unnamed	FFG_120	865.10	Richey, 1989, Table 2, p.28
14	Unnamed	FFG_081	674.90	Richey, 1989, Table 2, p.26	52	Unnamed	FFG_121	873.30	Richey, 1989, Table 2, p.28
15	Unnamed	FFG_082	705.30	Richey, 1989, Table 2, p.26	53	Unnamed	FFG_122	868.70	Richey, 1989, Table 2, p.28
16	Unnamed	FFG_083	632.00	Richey, 1989, Table 2, p.26	54	Unnamed	FFG_123	861.00	Richey, 1989, Table 2, p.28
17	Unnamed	FFG_084	654.70	Richey, 1989, Table 2, p.26	55	Unnamed	FFG_124	830.90	Richey, 1989, Table 2, p.28
18	Unnamed	FFG_085	649.00	Richey, 1989, Table 2, p.26	56	Unnamed	FFG_125	842.10	Richey, 1989, Table 2, p.28
19	Unnamed	FFG_086	657.40	Richey, 1989, Table 2, p.26	57	Unnamed	FFG_126	846.60	Richey, 1989, Table 2, p.28
20	Unnamed	FFG_087	630.00	Richey, 1989, Table 2, p.26	58	Unnamed	FFG_127	851.60	Richey, 1989, Table 2, p.28
21	Unnamed	FFG_088	622.70	Richey, 1989, Table 2, p.26	59	Unnamed	FFG_128	877.60	Richey, 1989, Table 2, p.28
22	Unnamed	FFG_089	606.60	Richey, 1989, Table 2, p.26	60	Unnamed	FFG_129	852.20	Richey, 1989, Table 2, p.28
23	Unnamed	FFG_091	643.80	Richey, 1989, Table 2, p.26	61	Unnamed	FFG_130	888.50	Richey, 1989, Table 2, p.28
24	Unnamed	FFG_092	662.30	Richey, 1989, Table 2, p.26	62	Unnamed	FFG_132	890.90	Richey, 1989, Table 2, p.29
25	Unnamed	FFG_093	668.10	Richey, 1989, Table 2, p.26	63	Unnamed	FFG_133	895.50	Richey, 1989, Table 2, p.29
26	Unnamed	FFG_094	666.60	Richey, 1989, Table 2, p.26	64	Unnamed	FFG_134	896.80	Richey, 1989, Table 2, p.29
27	Unnamed	FFG_095	645.20	Richey, 1989, Table 2, p.26	65	Unnamed	FFG_135	875.10	Richey, 1989, Table 2, p.29
28	Unnamed	FFG_096	629.40	Richey, 1989, Table 2, p.26	66	Unnamed	FFG_136	876.40	Richey, 1989, Table 2, p.29
29	Unnamed	FFG_097	608.40	Richey, 1989, Table 2, p.27	67	Unnamed	FFG_137	884.60	Richey, 1989, Table 2, p.29
30	Unnamed	FFG_098	581.80	Richey, 1989, Table 2, p.27	68	Unnamed	FFG_138	834.90	Richey, 1989, Table 2, p.29
31	Unnamed	FFG_099	574.60	Richey, 1989, Table 2, p.27	69	Unnamed	FFG_139	847.90	Richey, 1989, Table 2, p.29
32	Unnamed	FFG_100	558.70	Richey, 1989, Table 2, p.27	70	Unnamed	FFG_140	785.00	Richey, 1989, Table 2, p.29
33	Unnamed	FFG_101	527.30	Richey, 1989, Table 2, p.27	71	Unnamed	FFG_141	812.50	Richey, 1989, Table 2, p.29
34	Unnamed	FFG_102	542.90	Richey, 1989, Table 2, p.27	72	Unnamed	FFG_142	788.30	Richey, 1989, Table 2, p.29
35	Unnamed	FFG_103	601.70	Richey, 1989, Table 2, p.27	73	Unnamed	FFG_143	797.30	Richey, 1989, Table 2, p.29
36	Unnamed	FFG_104	502.10	Richey, 1989, Table 2, p.27	74	Unnamed	FFG_144	883.70	Richey, 1989, Table 2, p.29
37	Unnamed	FFG_105	861.40	Richey, 1989, Table 2, p.27	75	Unnamed	FFG_145	887.00	Richey, 1989, Table 2, p.29
38	Unnamed	FFG_106	894.60	Richey, 1989, Table 2, p.27	76	Unnamed	FFG_146	897.70	Richey, 1989, Table 2, p.29

Table B.2. Elevations of Stratigraphic Layers Near WIPP (Continued)

	Layer	Well ID	Elevation	Source
1	Unnamed	FFG_147	875.40	Richey, 1989, Table 2, p.29
2	Unnamed	FFG_148	894.90	Richey, 1989, Table 2, p.29
3	Unnamed	FFG_149	903.10	Richey, 1989, Table 2, p.30
4	Unnamed	FFG_152	893.10	Richey, 1989, Table 2, p.30
5	Unnamed	FFG_155	894.00	Richey, 1989, Table 2, p.30
6	Unnamed	FFG_156	895.50	Richey, 1989, Table 2, p.30
7	Unnamed	FFG_157	898.60	Richey, 1989, Table 2, p.30
8	Unnamed	FFG_158	918.00	Richey, 1989, Table 2, p.30
9	Unnamed	FFG_159	891.60	Richey, 1989, Table 2, p.30
10	Unnamed	FFG_160	886.10	Richey, 1989, Table 2, p.30
11	Unnamed	FFG_161	894.90	Richey, 1989, Table 2, p.30
12	Unnamed	FFG_162	884.60	Richey, 1989, Table 2, p.30
13	Unnamed	FFG_163	888.20	Richey, 1989, Table 2, p.30
14	Unnamed	FFG_164	928.50	Richey, 1989, Table 2, p.30
15	Unnamed	FFG_165	902.20	Richey, 1989, Table 2, p.30
16	Unnamed	FFG_166	891.80	Richey, 1989, Table 2, p.31
17	Unnamed	FFG_167	877.90	Richey, 1989, Table 2, p.31
18	Unnamed	FFG_168	898.90	Richey, 1989, Table 2, p.31
19	Unnamed	FFG_169	909.20	Richey, 1989, Table 2, p.31
20	Unnamed	FFG_170	893.00	Richey, 1989, Table 2, p.31
21	Unnamed	FFG_171	909.30	Richey, 1989, Table 2, p.31
22	Unnamed	FFG_172	906.10	Richey, 1989, Table 2, p.31
23	Unnamed	FFG_173	867.80	Richey, 1989, Table 2, p.31
24	Unnamed	FFG_177	880.00	Richey, 1989, Table 2, p.31
25	Unnamed	FFG_178	711.40	Richey, 1989, Table 2, p.31
26	Unnamed	FFG_179	875.10	Richey, 1989, Table 2, p.31
27	Unnamed	FFG_180	874.70	Richey, 1989, Table 2, p.31
28	Unnamed	FFG_181	922.90	Richey, 1989, Table 2, p.32
29	Unnamed	FFG_182	804.30	Richey, 1989, Table 2, p.32
30	Unnamed	FFG_183	893.40	Richey, 1989, Table 2, p.32
31	Unnamed	FFG_184	883.60	Richey, 1989, Table 2, p.32
32	Unnamed	FFG_185	891.80	Richey, 1989, Table 2, p.32
33	Unnamed	FFG_186	819.30	Richey, 1989, Table 2, p.32
34	Unnamed	FFG_188	837.60	Richey, 1989, Table 2, p.32
35	Unnamed	FFG_189	859.60	Richey, 1989, Table 2, p.32
36	Unnamed	FFG_190	835.10	Richey, 1989, Table 2, p.32
37	Unnamed	FFG_191	839.40	Richey, 1989, Table 2, p.32
38	Unnamed	FFG_192	764.40	Richey, 1989, Table 2, p.32
39	Unnamed	FFG_194	780.60	Richey, 1989, Table 2, p.33
40	Unnamed	FFG_195	792.80	Richey, 1989, Table 2, p.33
41	Unnamed	FFG_196	827.50	Richey, 1989, Table 2, p.33
42	Unnamed	FFG_197	831.20	Richey, 1989, Table 2, p.33
43	Unnamed	FFG_198	831.80	Richey, 1989, Table 2, p.33
44	Unnamed	FFG_199	818.70	Richey, 1989, Table 2, p.33
45	Unnamed	FFG_200	828.10	Richey, 1989, Table 2, p.33
46	Unnamed	FFG_201	830.00	Richey, 1989, Table 2, p.33
47	Unnamed	FFG_202	763.20	Richey, 1989, Table 2, p.33
48	Unnamed	FFG_203	767.50	Richey, 1989, Table 2, p.33
49	Unnamed	FFG_204	805.30	Richey, 1989, Table 2, p.33
50	Unnamed	FFG_205	816.60	Richey, 1989, Table 2, p.33
51	Unnamed	FFG_206	828.10	Richey, 1989, Table 2, p.33
52	Unnamed	FFG_207	826.00	Richey, 1989, Table 2, p.33
53	Unnamed	FFG_208	834.50	Richey, 1989, Table 2, p.34
54	Unnamed	FFG_209	829.70	Richey, 1989, Table 2, p.34
55	Unnamed	FFG_210	818.70	Richey, 1989, Table 2, p.34
56	Unnamed	FFG_212	809.00	Richey, 1989, Table 2, p.34
57	Unnamed	FFG_213	828.80	Richey, 1989, Table 2, p.34
58	Unnamed	FFG_214	808.60	Richey, 1989, Table 2, p.34
59	Unnamed	FFG_215	784.90	Richey, 1989, Table 2, p.34
60	Unnamed	FFG_216	682.70	Richey, 1989, Table 2, p.34
61	Unnamed	FFG_217	805.60	Richey, 1989, Table 2, p.34
62	Unnamed	FFG_218	794.30	Richey, 1989, Table 2, p.34
63	Unnamed	FFG_219	840.30	Richey, 1989, Table 2, p.34
64	Unnamed	FFG_220	789.50	Richey, 1989, Table 2, p.34
65	Unnamed	FFG_221	744.30	Richey, 1989, Table 2, p.34
66	Unnamed	FFG_222	705.00	Richey, 1989, Table 2, p.34
67	Unnamed	FFG_224	590.10	Richey, 1989, Table 2, p.35
68	Unnamed	FFG_225	598.00	Richey, 1989, Table 2, p.35
69	Unnamed	FFG_226	594.80	Richey, 1989, Table 2, p.35
70	Unnamed	FFG_228	580.70	Richey, 1989, Table 2, p.35
71	Unnamed	FFG_229	607.10	Richey, 1989, Table 2, p.35
72	Unnamed	FFG_230	595.00	Richey, 1989, Table 2, p.35
73	Unnamed	FFG_231	613.80	Richey, 1989, Table 2, p.35
74	Unnamed	FFG_232	625.80	Richey, 1989, Table 2, p.35
75	Unnamed	FFG_233	617.90	Richey, 1989, Table 2, p.35
76	Unnamed	FFG_234	653.50	Richey, 1989, Table 2, p.35

Table B.2. Elevations of Stratigraphic Layers Near WIPP (Continued)

	Layer	Well ID	Elevation	Source		Layer	Well ID	Elevation	Source
1	Unnamed	FFG_235	628.50	Richey, 1989, Table 2, p.35	39	Unnamed	FFG_273	745.30	Richey, 1989, Table 2, p.38
2	Unnamed	FFG_236	677.20	Richey, 1989, Table 2, p.35	40	Unnamed	FFG_274	785.80	Richey, 1989, Table 2, p.38
3	Unnamed	FFG_237	634.40	Richey, 1989, Table 2, p.35	41	Unnamed	FFG_275	794.60	Richey, 1989, Table 2, p.38
4	Unnamed	FFG_238	621.50	Richey, 1989, Table 2, p.36	42	Unnamed	FFG_276	795.80	Richey, 1989, Table 2, p.38
5	Unnamed	FFG_239	613.50	Richey, 1989, Table 2, p.36	43	Unnamed	FFG_277	789.10	Richey, 1989, Table 2, p.38
6	Unnamed	FFG_240	602.60	Richey, 1989, Table 2, p.36	44	Unnamed	FFG_278	765.40	Richey, 1989, Table 2, p.38
7	Unnamed	FFG_241	598.10	Richey, 1989, Table 2, p.36	45	Unnamed	FFG_279	767.70	Richey, 1989, Table 2, p.38
8	Unnamed	FFG_242	724.20	Richey, 1989, Table 2, p.36	46	Unnamed	FFG_280	780.00	Richey, 1989, Table 2, p.38
9	Unnamed	FFG_243	659.30	Richey, 1989, Table 2, p.36	47	Unnamed	FFG_281	754.40	Richey, 1989, Table 2, p.38
10	Unnamed	FFG_244	715.20	Richey, 1989, Table 2, p.36	48	Unnamed	FFG_283	489.20	Richey, 1989, Table 2, p.39
11	Unnamed	FFG_245	503.50	Richey, 1989, Table 2, p.36	49	Unnamed	FFG_284	641.30	Richey, 1989, Table 2, p.39
12	Unnamed	FFG_246	508.10	Richey, 1989, Table 2, p.36	50	Unnamed	FFG_285	660.50	Richey, 1989, Table 2, p.39
13	Unnamed	FFG_247	493.70	Richey, 1989, Table 2, p.36	51	Unnamed	FFG_286	766.20	Richey, 1989, Table 2, p.39
14	Unnamed	FFG_248	498.30	Richey, 1989, Table 2, p.36	52	Unnamed	FFG_287	733.30	Richey, 1989, Table 2, p.39
15	Unnamed	FFG_249	498.30	Richey, 1989, Table 2, p.36	53	Unnamed	FFG_288	662.60	Richey, 1989, Table 2, p.39
16	Unnamed	FFG_250	580.50	Richey, 1989, Table 2, p.36	54	Unnamed	FFG_289	673.90	Richey, 1989, Table 2, p.39
17	Unnamed	FFG_251	470.00	Richey, 1989, Table 2, p.36	55	Unnamed	FFG_290	760.80	Richey, 1989, Table 2, p.39
18	Unnamed	FFG_252	612.60	Richey, 1989, Table 2, p.36	56	Unnamed	FFG_291	660.80	Richey, 1989, Table 2, p.39
19	Unnamed	FFG_253	561.50	Richey, 1989, Table 2, p.36	57	Unnamed	FFG_292	717.80	Richey, 1989, Table 2, p.39
20	Unnamed	FFG_254	554.70	Richey, 1989, Table 2, p.36	58	Unnamed	FFG_293	710.50	Richey, 1989, Table 2, p.39
21	Unnamed	FFG_255	506.30	Richey, 1989, Table 2, p.37	59	Unnamed	FFG_294	497.50	Richey, 1989, Table 2, p.39
22	Unnamed	FFG_256	470.90	Richey, 1989, Table 2, p.37	60	Unnamed	FFG_295	480.00	Richey, 1989, Table 2, p.39
23	Unnamed	FFG_257	517.20	Richey, 1989, Table 2, p.37	61	Unnamed	FFG_297	455.40	Richey, 1989, Table 2, p.39
24	Unnamed	FFG_258	536.40	Richey, 1989, Table 2, p.37	62	Unnamed	FFG_298	520.40	Richey, 1989, Table 2, p.40
25	Unnamed	FFG_259	494.90	Richey, 1989, Table 2, p.37	63	Unnamed	FFG_299	489.80	Richey, 1989, Table 2, p.40
26	Unnamed	FFG_260	548.90	Richey, 1989, Table 2, p.37	64	Unnamed	FFG_300	473.00	Richey, 1989, Table 2, p.40
27	Unnamed	FFG_261	537.30	Richey, 1989, Table 2, p.37	65	Unnamed	FFG_301	430.40	Richey, 1989, Table 2, p.40
28	Unnamed	FFG_262	477.00	Richey, 1989, Table 2, p.37	66	Unnamed	FFG_302	436.80	Richey, 1989, Table 2, p.40
29	Unnamed	FFG_263	448.50	Richey, 1989, Table 2, p.37	67	Unnamed	FFG_303	442.00	Richey, 1989, Table 2, p.40
30	Unnamed	FFG_264	696.20	Richey, 1989, Table 2, p.37	68	Unnamed	FFG_304	438.90	Richey, 1989, Table 2, p.40
31	Unnamed	FFG_265	677.30	Richey, 1989, Table 2, p.37	69	Unnamed	FFG_305	434.60	Richey, 1989, Table 2, p.40
32	Unnamed	FFG_266	656.80	Richey, 1989, Table 2, p.37	70	Unnamed	FFG_306	405.30	Richey, 1989, Table 2, p.40
33	Unnamed	FFG_267	632.70	Richey, 1989, Table 2, p.37	71	Unnamed	FFG_307	424.30	Richey, 1989, Table 2, p.40
34	Unnamed	FFG_268	606.30	Richey, 1989, Table 2, p.37	72	Unnamed	FFG_308	367.80	Richey, 1989, Table 2, p.40
35	Unnamed	FFG_269	617.60	Richey, 1989, Table 2, p.38	73	Unnamed	FFG_309	427.90	Richey, 1989, Table 2, p.40
36	Unnamed	FFG_270	721.10	Richey, 1989, Table 2, p.38	74	Unnamed	FFG_310	469.10	Richey, 1989, Table 2, p.40
37	Unnamed	FFG_271	767.80	Richey, 1989, Table 2, p.38	75	Unnamed	FFG_311	420.30	Richey, 1989, Table 2, p.40
38	Unnamed	FFG_272	743.90	Richey, 1989, Table 2, p.38	76	Unnamed	FFG_312	424.00	Richey, 1989, Table 2, p.40

Table B.2. Elevations of Stratigraphic Layers Near WIPP (Continued)

	Layer	Well ID	Elevation	Source
1	Unnamed	FFG_313	862.00	Richey, 1989, Table 2, p.41
2	Unnamed	FFG_314	781.60	Richey, 1989, Table 2, p.41
3	Unnamed	FFG_315	694.20	Richey, 1989, Table 2, p.41
4	Unnamed	FFG_316	670.20	Richey, 1989, Table 2, p.41
5	Unnamed	FFG_317	725.10	Richey, 1989, Table 2, p.41
6	Unnamed	FFG_318	702.60	Richey, 1989, Table 2, p.41
7	Unnamed	FFG_319	696.40	Richey, 1989, Table 2, p.41
8	Unnamed	FFG_320	662.00	Richey, 1989, Table 2, p.41
9	Unnamed	FFG_321	661.70	Richey, 1989, Table 2, p.41
10	Unnamed	FFG_322	662.20	Richey, 1989, Table 2, p.41
11	Unnamed	FFG_323	667.90	Richey, 1989, Table 2, p.41
12	Unnamed	FFG_324	692.20	Richey, 1989, Table 2, p.41
13	Unnamed	FFG_325	753.20	Richey, 1989, Table 2, p.41
14	Unnamed	FFG_326	698.00	Richey, 1989, Table 2, p.41
15	Unnamed	FFG_327	681.90	Richey, 1989, Table 2, p.42
16	Unnamed	FFG_328	664.70	Richey, 1989, Table 2, p.42
17	Unnamed	FFG_329	661.40	Richey, 1989, Table 2, p.42
18	Unnamed	FFG_330	661.00	Richey, 1989, Table 2, p.42
19	Unnamed	FFG_331	646.80	Richey, 1989, Table 2, p.42
20	Unnamed	FFG_332	632.80	Richey, 1989, Table 2, p.42
21	Unnamed	FFG_333	643.00	Richey, 1989, Table 2, p.42
22	Unnamed	FFG_334	637.00	Richey, 1989, Table 2, p.42
23	Unnamed	FFG_335	655.00	Richey, 1989, Table 2, p.42
24	Unnamed	FFG_336	650.40	Richey, 1989, Table 2, p.42
25	Unnamed	FFG_337	634.30	Richey, 1989, Table 2, p.42
26	Unnamed	FFG_338	639.00	Richey, 1989, Table 2, p.42
27	Unnamed	FFG_339	604.10	Richey, 1989, Table 2, p.42
28	Unnamed	FFG_340	609.30	Richey, 1989, Table 2, p.42
29	Unnamed	FFG_342	676.30	Richey, 1989, Table 2, p.43
30	Unnamed	FFG_344	650.90	Richey, 1989, Table 2, p.43
31	Unnamed	FFG_345	671.30	Richey, 1989, Table 2, p.43
32	Unnamed	FFG_347	692.80	Richey, 1989, Table 2, p.43
33	Unnamed	FFG_348	733.00	Richey, 1989, Table 2, p.43
34	Unnamed	FFG_349	709.30	Richey, 1989, Table 2, p.43
35	Unnamed	FFG_350	739.70	Richey, 1989, Table 2, p.43
36	Unnamed	FFG_351	621.20	Richey, 1989, Table 2, p.43
37	Unnamed	FFG_352	621.80	Richey, 1989, Table 2, p.43
38	Unnamed	FFG_353	644.10	Richey, 1989, Table 2, p.43
39	Unnamed	FFG_354	756.00	Richey, 1989, Table 2, p.43
40	Unnamed	FFG_361	948.50	Richey, 1989, Table 2, p.44
41	Unnamed	FFG_362	911.00	Richey, 1989, Table 2, p.44
42	Unnamed	FFG_363	937.90	Richey, 1989, Table 2, p.44
43	Unnamed	FFG_364	909.80	Richey, 1989, Table 2, p.44
44	Unnamed	FFG_366	904.00	Richey, 1989, Table 2, p.44
45	Unnamed	FFG_367	922.60	Richey, 1989, Table 2, p.44
46	Unnamed	FFG_370	962.60	Richey, 1989, Table 2, p.44
47	Unnamed	FFG_371	958.60	Richey, 1989, Table 2, p.44
48	Unnamed	FFG_372	941.50	Richey, 1989, Table 2, p.45
49	Unnamed	FFG_373	902.00	Richey, 1989, Table 2, p.45
50	Unnamed	FFG_374	902.20	Richey, 1989, Table 2, p.45
51	Unnamed	FFG_376	939.70	Richey, 1989, Table 2, p.45
52	Unnamed	FFG_381	908.60	Richey, 1989, Table 2, p.45
53	Unnamed	FFG_383	902.20	Richey, 1989, Table 2, p.45
54	Unnamed	FFG_384	912.30	Richey, 1989, Table 2, p.45
55	Unnamed	FFG_385	906.80	Richey, 1989, Table 2, p.45
56	Unnamed	FFG_387	901.60	Richey, 1989, Table 2, p.45
57	Unnamed	FFG_388	893.70	Richey, 1989, Table 2, p.46
58	Unnamed	FFG_389	917.50	Richey, 1989, Table 2, p.46
59	Unnamed	FFG_390	913.50	Richey, 1989, Table 2, p.46
60	Unnamed	FFG_391	913.10	Richey, 1989, Table 2, p.46
61	Unnamed	FFG_392	904.40	Richey, 1989, Table 2, p.46
62	Unnamed	FFG_393	781.00	Richey, 1989, Table 2, p.46
63	Unnamed	FFG_394	877.20	Richey, 1989, Table 2, p.46
64	Unnamed	FFG_395	867.50	Richey, 1989, Table 2, p.46
65	Unnamed	FFG_396	847.10	Richey, 1989, Table 2, p.46
66	Unnamed	FFG_398	767.20	Richey, 1989, Table 2, p.46
67	Unnamed	FFG_399	780.60	Richey, 1989, Table 2, p.46
68	Unnamed	FFG_401	833.60	Richey, 1989, Table 2, p.46
69	Unnamed	FFG_402	936.70	Richey, 1989, Table 2, p.46
70	Unnamed	FFG_403	903.30	Richey, 1989, Table 2, p.47
71	Unnamed	FFG_404	867.20	Richey, 1989, Table 2, p.47
72	Unnamed	FFG_407	898.90	Richey, 1989, Table 2, p.47
73	Unnamed	FFG_408	901.00	Richey, 1989, Table 2, p.47
74	Unnamed	FFG_409	932.40	Richey, 1989, Table 2, p.47
75	Unnamed	FFG_411	873.90	Richey, 1989, Table 2, p.47
76	Unnamed	FFG_413	906.20	Richey, 1989, Table 2, p.47

Table B.2. Elevations of Stratigraphic Layers Near WIPP (Continued)

	Layer	Well ID	Elevation	Source
1	Unnamed	FFG_418	923.00	Richey, 1989, Table 2, p.48
2	Unnamed	FFG_419	936.70	Richey, 1989, Table 2, p.48
3	Unnamed	FFG_420	927.80	Richey, 1989, Table 2, p.48
4	Unnamed	FFG_421	913.80	Richey, 1989, Table 2, p.48
5	Unnamed	FFG_422	915.60	Richey, 1989, Table 2, p.48
6	Unnamed	FFG_426	919.30	Richey, 1989, Table 2, p.48
7	Unnamed	FFG_432	876.90	Richey, 1989, Table 2, p.48
8	Unnamed	FFG_433	892.40	Richey, 1989, Table 2, p.48
9	Unnamed	FFG_438	829.80	Richey, 1989, Table 2, p.49
10	Unnamed	FFG_445	911.60	Richey, 1989, Table 2, p.49
11	Unnamed	FFG_453	772.90	Richey, 1989, Table 2, p.50
12	Unnamed	FFG_455	761.40	Richey, 1989, Table 2, p.50
13	Unnamed	FFG_456	769.90	Richey, 1989, Table 2, p.50
14	Unnamed	FFG_457	822.60	Richey, 1989, Table 2, p.50
15	Unnamed	FFG_458	825.10	Richey, 1989, Table 2, p.50
16	Unnamed	FFG_459	752.30	Richey, 1989, Table 2, p.50
17	Unnamed	FFG_462	820.70	Richey, 1989, Table 2, p.50
18	Unnamed	FFG_463	843.70	Richey, 1989, Table 2, p.51
19	Unnamed	FFG_464	833.60	Richey, 1989, Table 2, p.51
20	Unnamed	FFG_465	835.10	Richey, 1989, Table 2, p.51
21	Unnamed	FFG_467	423.00	Richey, 1989, Table 2, p.51
22	Unnamed	FFG_468	373.10	Richey, 1989, Table 2, p.51
23	Unnamed	FFG_470	402.60	Richey, 1989, Table 2, p.51
24	Unnamed	FFG_471	420.60	Richey, 1989, Table 2, p.51
25	Unnamed	FFG_472	495.60	Richey, 1989, Table 2, p.51
26	Unnamed	FFG_473	383.70	Richey, 1989, Table 2, p.51
27	Unnamed	FFG_474	671.70	Richey, 1989, Table 2, p.51
28	Unnamed	FFG_475	677.70	Richey, 1989, Table 2, p.51
29	Unnamed	FFG_476	751.70	Richey, 1989, Table 2, p.51
30	Unnamed	FFG_477	718.80	Richey, 1989, Table 2, p.51
31	Unnamed	FFG_478	694.00	Richey, 1989, Table 2, p.52
32	Unnamed	FFG_479	698.90	Richey, 1989, Table 2, p.52
33	Unnamed	FFG_480	681.30	Richey, 1989, Table 2, p.52
34	Unnamed	FFG_481	674.50	Richey, 1989, Table 2, p.52
35	Unnamed	FFG_482	703.80	Richey, 1989, Table 2, p.52
36	Unnamed	FFG_483	732.70	Richey, 1989, Table 2, p.52
37	Unnamed	FFG_484	720.70	Richey, 1989, Table 2, p.52
38	Unnamed	FFG_485	723.00	Richey, 1989, Table 2, p.52
39	Unnamed	FFG_486	708.40	Richey, 1989, Table 2, p.52
40	Unnamed	FFG_487	706.90	Richey, 1989, Table 2, p.52
41	Unnamed	FFG_488	692.50	Richey, 1989, Table 2, p.52
42	Unnamed	FFG_489	708.80	Richey, 1989, Table 2, p.52
43	Unnamed	FFG_490	801.30	Richey, 1989, Table 2, p.52
44	Unnamed	FFG_491	793.10	Richey, 1989, Table 2, p.52
45	Unnamed	FFG_492	757.10	Richey, 1989, Table 2, p.52
46	Unnamed	FFG_493	743.20	Richey, 1989, Table 2, p.53
47	Unnamed	FFG_494	747.00	Richey, 1989, Table 2, p.53
48	Unnamed	FFG_495	743.10	Richey, 1989, Table 2, p.53
49	Unnamed	FFG_496	604.20	Richey, 1989, Table 2, p.53
50	Unnamed	FFG_497	642.20	Richey, 1989, Table 2, p.53
51	Unnamed	FFG_498	637.60	Richey, 1989, Table 2, p.53
52	Unnamed	FFG_499	603.20	Richey, 1989, Table 2, p.53
53	Unnamed	FFG_500	635.20	Richey, 1989, Table 2, p.53
54	Unnamed	FFG_501	665.60	Richey, 1989, Table 2, p.53
55	Unnamed	FFG_502	630.90	Richey, 1989, Table 2, p.53
56	Unnamed	FFG_503	616.30	Richey, 1989, Table 2, p.53
57	Unnamed	FFG_504	667.60	Richey, 1989, Table 2, p.53
58	Unnamed	FFG_505	696.20	Richey, 1989, Table 2, p.53
59	Unnamed	FFG_506	690.60	Richey, 1989, Table 2, p.53
60	Unnamed	FFG_507	599.40	Richey, 1989, Table 2, p.53
61	Unnamed	FFG_508	680.70	Richey, 1989, Table 2, p.53
62	Unnamed	FFG_509	662.30	Richey, 1989, Table 2, p.54
63	Unnamed	FFG_510	658.80	Richey, 1989, Table 2, p.54
64	Unnamed	FFG_511	619.40	Richey, 1989, Table 2, p.54
65	Unnamed	FFG_512	634.60	Richey, 1989, Table 2, p.54
66	Unnamed	FFG_513	659.30	Richey, 1989, Table 2, p.54
67	Unnamed	FFG_514	637.00	Richey, 1989, Table 2, p.54
68	Unnamed	FFG_515	610.80	Richey, 1989, Table 2, p.54
69	Unnamed	FFG_516	601.60	Richey, 1989, Table 2, p.54
70	Unnamed	FFG_517	750.70	Richey, 1989, Table 2, p.54
71	Unnamed	FFG_518	735.80	Richey, 1989, Table 2, p.54
72	Unnamed	FFG_519	696.50	Richey, 1989, Table 2, p.54
73	Unnamed	FFG_520	585.40	Richey, 1989, Table 2, p.54
74	Unnamed	FFG_521	628.20	Richey, 1989, Table 2, p.54
75	Unnamed	FFG_522	427.50	Richey, 1989, Table 2, p.54
76	Unnamed	FFG_523	443.20	Richey, 1989, Table 2, p.54

Table B.2. Elevations of Stratigraphic Layers Near WIPP (Continued)

	Layer	Well ID	Elevation	Source
1	Unnamed	FFG_524	607.40	Richey, 1989, Table 2, p.55
2	Unnamed	FFG_525	436.60	Richey, 1989, Table 2, p.55
3	Unnamed	FFG_526	943.10	Richey, 1989, Table 2, p.55
4	Unnamed	FFG_527	888.10	Richey, 1989, Table 2, p.55
5	Unnamed	FFG_528	891.50	Richey, 1989, Table 2, p.55
6	Unnamed	FFG_530	957.70	Richey, 1989, Table 2, p.55
7	Unnamed	FFG_531	888.80	Richey, 1989, Table 2, p.55
8	Unnamed	FFG_532	873.00	Richey, 1989, Table 2, p.55
9	Unnamed	FFG_534	883.30	Richey, 1989, Table 2, p.55
10	Unnamed	FFG_535	875.70	Richey, 1989, Table 2, p.55
11	Unnamed	FFG_536	884.50	Richey, 1989, Table 2, p.55
12	Unnamed	FFG_537	872.60	Richey, 1989, Table 2, p.55
13	Unnamed	FFG_543	926.70	Richey, 1989, Table 2, p.56
14	Unnamed	FFG_548	877.20	Richey, 1989, Table 2, p.56
15	Unnamed	FFG_552	722.00	Richey, 1989, Table 2, p.56
16	Unnamed	FFG_562	614.50	Richey, 1989, Table 2, p.57
17	Unnamed	FFG_563	528.20	Richey, 1989, Table 2, p.57
18	Unnamed	FFG_564	663.00	Richey, 1989, Table 2, p.57
19	Unnamed	FFG_568	625.80	Richey, 1989, Table 2, p.57
20	Unnamed	FFG_569	624.20	Richey, 1989, Table 2, p.57
21	Unnamed	FFG_584	736.60	Richey, 1989, Table 2, p.58
22	Unnamed	FFG_585	678.40	Richey, 1989, Table 2, p.58
23	Unnamed	FFG_600	692.50	Richey, 1989, Table 2, p.58
24	Unnamed	FFG_601	572.70	Richey, 1989, Table 2, p.58
25	Unnamed	FFG_602	794.30	Richey, 1989, Table 2, p.58
26	Unnamed	FFG_606	667.60	Richey, 1989, Table 2, p.58
27	Unnamed	FFG_607	671.80	Richey, 1989, Table 2, p.59
28	Unnamed	FFG_608	654.70	Richey, 1989, Table 2, p.59
29	Unnamed	FFG_609	646.70	Richey, 1989, Table 2, p.59
30	Unnamed	FFG_610	640.10	Richey, 1989, Table 2, p.59
31	Unnamed	FFG_611	635.50	Richey, 1989, Table 2, p.59
32	Unnamed	FFG_612	669.70	Richey, 1989, Table 2, p.59
33	Unnamed	FFG_613	668.70	Richey, 1989, Table 2, p.59
34	Unnamed	FFG_618	679.10	Richey, 1989, Table 2, p.59
35	Unnamed	FFG_620	731.20	Richey, 1989, Table 2, p.59
36	Unnamed	FFG_621	695.00	Richey, 1989, Table 2, p.59
37	Unnamed	FFG_638	530.10	Richey, 1989, Table 2, p.60
38	Unnamed	FFG_639	498.40	Richey, 1989, Table 2, p.60
39	Unnamed	FFG_640	586.60	Richey, 1989, Table 2, p.60
40	Unnamed	FFG_643	637.10	Richey, 1989, Table 2, p.60
41	Unnamed	FFG_644	670.50	Richey, 1989, Table 2, p.60
42	Unnamed	FFG_648	500.50	Richey, 1989, Table 2, p.60
43	Unnamed	FFG_652	815.90	Richey, 1989, Table 2, p.60
44	Unnamed	FFG_653	815.70	Richey, 1989, Table 2, p.61
45	Unnamed	FFG_654	839.10	Richey, 1989, Table 2, p.61
46	Unnamed	FFG_655	840.30	Richey, 1989, Table 2, p.61
47	Unnamed	FFG_656	838.50	Richey, 1989, Table 2, p.61
48	Unnamed	FFG_657	856.20	Richey, 1989, Table 2, p.61
49	Unnamed	FFG_658	842.70	Richey, 1989, Table 2, p.61
50	Unnamed	FFG_659	848.60	Richey, 1989, Table 2, p.61
51	Unnamed	FFG_660	866.40	Richey, 1989, Table 2, p.61
52	Unnamed	FFG_662	837.30	Richey, 1989, Table 2, p.61
53	Unnamed	FFG_664	830.90	Richey, 1989, Table 2, p.61
54	Unnamed	FFG_666	883.90	Richey, 1989, Table 2, p.62
55	Unnamed	FFG_667	869.30	Richey, 1989, Table 2, p.62
56	Unnamed	FFG_668	919.40	Richey, 1989, Table 2, p.62
57	Unnamed	FFG_669	905.80	Richey, 1989, Table 2, p.62
58	Unnamed	FFG_670	889.10	Richey, 1989, Table 2, p.62
59	Unnamed	FFG_671	891.20	Richey, 1989, Table 2, p.62
60	Unnamed	FFG_672	889.80	Richey, 1989, Table 2, p.62
61	Unnamed	FFG_673	887.50	Richey, 1989, Table 2, p.62
62	Unnamed	FFG_674	885.50	Richey, 1989, Table 2, p.62
63	Unnamed	FFG_675	844.20	Richey, 1989, Table 2, p.62
64	Unnamed	FFG_676	854.70	Richey, 1989, Table 2, p.62
65	Unnamed	FFG_677	883.30	Richey, 1989, Table 2, p.62
66	Unnamed	FFG_679	883.90	Richey, 1989, Table 2, p.62
67	Unnamed	FFG_685	911.10	Richey, 1989, Table 2, p.63
68	Unnamed	FFG_689	756.80	Richey, 1989, Table 2, p.63
69	Unnamed	FFG_690	760.80	Richey, 1989, Table 2, p.63
70	Unnamed	FFG_691	752.90	Richey, 1989, Table 2, p.63
71	Unnamed	FFG_692	741.60	Richey, 1989, Table 2, p.63
72	Unnamed	FFG_693	753.70	Richey, 1989, Table 2, p.63
73	Unnamed	FFG_694	743.10	Richey, 1989, Table 2, p.63
74	Unnamed	FFG_695	749.20	Richey, 1989, Table 2, p.63
75	Unnamed	FFG_696	751.60	Richey, 1989, Table 2, p.63
76	Unnamed	FFG_697	754.10	Richey, 1989, Table 2, p.64

Table B.2. Elevations of Stratigraphic Layers Near WIPP (Continued)

	Layer	Well ID	Elevation	Source
1	Unnamed	FFG_698	795.30	Richey, 1989, Table 2, p.64
2	Unnamed	FFG_699	749.50	Richey, 1989, Table 2, p.64
3	Unnamed	FFG_700	744.40	Richey, 1989, Table 2, p.64
4	Unnamed	FFG_701	740.80	Richey, 1989, Table 2, p.64
5	Unnamed	FFG_702	747.00	Richey, 1989, Table 2, p.64
6	Unnamed	FFG_703	753.80	Richey, 1989, Table 2, p.64
7	Unnamed	FFG_704	737.30	Richey, 1989, Table 2, p.64
8	Unnamed	FFG_705	671.80	Richey, 1989, Table 2, p.64
9	Unnamed	FFG_706	694.40	Richey, 1989, Table 2, p.64
10	Unnamed	FFG_707	677.00	Richey, 1989, Table 2, p.64
11	Unnamed	FFG_708	728.80	Richey, 1989, Table 2, p.64
12	Unnamed	FFG_709	625.80	Richey, 1989, Table 2, p.64
13	Unnamed	FFG_710	625.20	Richey, 1989, Table 2, p.64
14	Unnamed	FFG_711	626.10	Richey, 1989, Table 2, p.65
15	Unnamed	FFG_712	669.50	Richey, 1989, Table 2, p.65
16	Unnamed	FFG_713	613.70	Richey, 1989, Table 2, p.65
17	Unnamed	FFG_714	725.10	Richey, 1989, Table 2, p.65
18	Unnamed	FFG_715	735.10	Richey, 1989, Table 2, p.65
19	Unnamed	FFG_716	597.30	Richey, 1989, Table 2, p.65
20	Unnamed	FFG_717	665.20	Richey, 1989, Table 2, p.65
21	Unnamed	FFG_718	656.10	Richey, 1989, Table 2, p.65
22	Unnamed	FFG_719	618.70	Richey, 1989, Table 2, p.65
23	Unnamed	FFG_720	614.50	Richey, 1989, Table 2, p.65
24	Unnamed	FFG_721	639.50	Richey, 1989, Table 2, p.65
25	Unnamed	FFG_723	755.10	Richey, 1989, Table 2, p.65
26	Unnamed	FFG_724	678.00	Richey, 1989, Table 2, p.65
27	Unnamed	FFG_725	646.50	Richey, 1989, Table 2, p.65
28	Unnamed	FFG_726	641.00	Richey, 1989, Table 2, p.65
29	Unnamed	FFG_727	630.70	Richey, 1989, Table 2, p.66
30	Unnamed	FFG_728	638.20	Richey, 1989, Table 2, p.66
31	Unnamed	FFG_729	641.00	Richey, 1989, Table 2, p.66
32	Unnamed	FFG_730	665.30	Richey, 1989, Table 2, p.66
33	Unnamed	FFG_731	662.80	Richey, 1989, Table 2, p.66
34	Unnamed	FFG_732	678.20	Richey, 1989, Table 2, p.66
35	Unnamed	FFG_733	741.90	Richey, 1989, Table 2, p.66
36	Unnamed	FFG_734	699.20	Richey, 1989, Table 2, p.66
37	Unnamed	FFG_735	630.30	Richey, 1989, Table 2, p.66
38	Unnamed	FFG_736	667.80	Richey, 1989, Table 2, p.66
39	Unnamed	FFG_737	611.80	Richey, 1989, Table 2, p.66
40	Unnamed	FFG_738	654.40	Richey, 1989, Table 2, p.66
41	Unnamed	FFG_739	683.80	Richey, 1989, Table 2, p.66
42	Unnamed	FFG_740	653.20	Richey, 1989, Table 2, p.66
43	Unnamed	FFG_741	651.10	Richey, 1989, Table 2, p.66
44	Unnamed	FFG_742	690.70	Richey, 1989, Table 2, p.67
45	Unnamed	FFG_743	675.20	Richey, 1989, Table 2, p.67
46	Unnamed	FFG_744	670.80	Richey, 1989, Table 2, p.67
47	Unnamed	FFG_745	650.40	Richey, 1989, Table 2, p.67
48	Unnamed	FFG_746	637.20	Richey, 1989, Table 2, p.67
49	Unnamed	H1	822.60	Mercer, 1983, Table 1
50	Unnamed	H10C	699.80	Mercer, 1983, Table 1
51	Unnamed	H2C	833.00	Mercer, 1983, Table 1
52	Unnamed	H3	821.80	Mercer, 1983, Table 1
53	Unnamed	H4C	858.90	Mercer, 1983, Table 1
54	Unnamed	H5C	787.30	Mercer, 1983, Table 1
55	Unnamed	H6C	829.40	Mercer, 1983, Table 1
56	Unnamed	H7C	880.60	Mercer, 1983, Table 1
57	Unnamed	H8C	859.30	Mercer, 1983, Table 1
58	Unnamed	H9C	831.80	Mercer, 1983, Table 1
59	Unnamed	P1	847.40	Mercer, 1983, Table 1
60	Unnamed	P10	777.80	Mercer, 1983, Table 1
61	Unnamed	P11	782.10	Mercer, 1983, Table 1
62	Unnamed	P12	828.50	Mercer, 1983, Table 1
63	Unnamed	P13	828.50	Mercer, 1983, Table 1
64	Unnamed	P14	842.70	Mercer, 1983, Table 1
65	Unnamed	P15	876.30	Mercer, 1983, Table 1
66	Unnamed	P16	851.90	Mercer, 1983, Table 1
67	Unnamed	P17	839.10	Mercer, 1983, Table 1
68	Unnamed	P18	773.90	Mercer, 1983, Table 1
69	Unnamed	P19	776.60	Mercer, 1983, Table 1
70	Unnamed	P2	791.30	Mercer, 1983, Table 1
71	Unnamed	P20	784.60	Mercer, 1983, Table 1
72	Unnamed	P21	787.90	Mercer, 1983, Table 1
73	Unnamed	P3	828.40	Mercer, 1983, Table 1
74	Unnamed	P4	805.30	Mercer, 1983, Table 1
75	Unnamed	P5	805.90	Mercer, 1983, Table 1
76	Unnamed	P6	851.60	Mercer, 1983, Table 1

Table B.2. Elevations of Stratigraphic Layers Near WIPP (Continued)

	Layer	Well ID	Elevation	Source
1	Unnamed	P7	856.50	Mercer, 1983, Table 1
2	Unnamed	P8	838.50	Mercer, 1983, Table 1
3	Unnamed	P9	809.30	Mercer, 1983, Table 1
4	Unnamed	REF	816.40	Rechard et al.,1991, Figure 2.2-1
5	Unnamed	SaltShft	813.97	Bechtel, Inc., 1986, Appendix D
6	Unnamed	WIPP11	779.90	Mercer, 1983, Table 1
7	Unnamed	WIPP11	780.00	SNL and USGS, 1982a, Table 2
8	Unnamed	WIPP12	803.90	D'Appolonia Consulting, 1983, Table 2
9	Unnamed	WIPP12	803.80	Mercer, 1983, Table 1
10	Unnamed	WIPP13	817.10	Mercer, 1983, Table 1
11	Unnamed	WIPP15	996.40	Mercer, 1983, Table 1
12	Unnamed	WIPP16	672.70	Mercer, 1983, Table 1
13	Unnamed	WIPP18	807.10	Mercer, 1983, Table 1
14	Unnamed	WIPP19	809.60	Mercer, 1983, Table 1
15	Unnamed	WIPP21	812.00	Mercer, 1983, Table 1
16	Unnamed	WIPP22	811.30	Mercer, 1983, Table 1
17	Unnamed	WIPP25	835.40	Mercer, 1983, Table 1
18	Unnamed	WIPP26	897.00	Mercer, 1983, Table 1
19	Unnamed	WIPP27	871.40	Mercer, 1983, Table 1
20	Unnamed	WIPP28	884.30	Mercer, 1983, Table 1
21	Unnamed	WIPP29	894.60	Mercer, 1983, Table 1
22	Unnamed	WIPP30	845.60	Mercer, 1983, Table 1
23	Unnamed	WIPP32	894.00	Mercer, 1983, Table 1
24	Unnamed	WIPP33	836.70	Mercer, 1983, Table 1
25	Unnamed	WIPP34	784.30	Mercer, 1983, Table 1
26	Unnamed	WastShft	817.02	Bechtel, Inc., 1986, Appendix E
27	V_Triste	AirShft	622.89	IT Corporation, 1990, Figure 22
28	V_Triste	AirShft	625.30	IT Corporation, 1990, Figure 22
29	V_Triste	DOE1	604.50	TME 3159, Sep 1982, Table 2
30	V_Triste	DOE1	605.70	TME 3159, Sep 1982, Table 2
31	V_Triste	DOE2	598.10	Mercer et al., 1987, Table 3-2
32	V_Triste	DOE2	600.30	Mercer et al., 1987, Table 3-2
33	V_Triste	ERDA9	625.70	SNL and USGS, 1982b, Table 2
34	V_Triste	ERDA9	627.60	SNL and USGS, 1982b, Table 2
35	V_Triste	ExhtShft	625.11	Bechtel, Inc., 1986, Appendix F
36	V_Triste	ExhtShft	626.66	Bechtel, Inc., 1986, Appendix F
37	V_Triste	REF	625.70	Rechard et al.,1991, Figure 2.2-1
38	V_Triste	REF	627.60	Rechard et al.,1991, Figure 2.2-1
39	V_Triste	SaltShft	627.89	Bechtel, Inc., 1986, Appendix D
40	V_Triste	SaltShft	628.33	Bechtel, Inc., 1986, Appendix D
41	V_Triste	WIPP11	611.20	SNL and USGS, 1982a, Table 2
42	V_Triste	WIPP11	612.70	SNL and USGS, 1982a, Table 2
43	V_Triste	WIPP12	620.80	D'Appolonia Consulting, 1983, Table 2
44	V_Triste	WIPP12	621.70	D'Appolonia Consulting, 1983, Table 2
45				

REFERENCES FOR APPENDIX B

Bechtel, Inc. 1986. *WIPP Design Validation Final Report.* DOE/WIPP-86-010. Prepared for U.S. Department of Energy. San Francisco, CA: Bechtel National, Inc.

Gonzales, M. 1989. *Compilation and Comparison of Test-Hole Location Surveys in the Vicinity of the Waste Isolation Pilot Plant Site.* SAND88-1065. Albuquerque, NM: Sandia National Laboratories.

Holt, R. M. and D. W. Powers. 1990. *Geologic Mapping of the Air Intake Shaft at the Waste Isolation Pilot Plant.* DOE-WIPP 90-051. Carlsbad, NM: U.S. Department of Energy.

Krieg, R. D. 1984. *Reference Stratigraphy and Rock Properties for the Waste Isolation Pilot Plant (WIPP) Project.* SAND83-1908. Albuquerque, NM: Sandia National Laboratories.

Mercer, J. W. 1983. *Geohydrology of the Proposed Waste Isolation Pilot Plant Site, Los Medaños Area, Southeastern New Mexico.* U.S. Geological Survey Water Resources Investigation 83-4016.

Mercer, J. W., R. L. Beauheim, R. P. Snyder, and G. M. Fairer. 1987. *Basic Data Report for Drilling and Hydrologic Testing of Drillhole DOE-2 at the Waste Isolation Pilot Plant (WIPP) Site.* SAND86-0611. Albuquerque, NM: Sandia National Laboratories.

Rechard, R. P., H. J. Iuzzolino, J. S. Rath, R. D. McCurley, and D. K. Rudeen. 1989. *User's Manual for CAMCON: Compliance Assessment Methodology Controller.* SAND88-1496. Albuquerque, NM: Sandia National Laboratories.

Richey, S. F. 1989. *Geologic and Hydrologic Data for the Rustler Formation near the Waste Isolation Pilot Plant, Southeastern New Mexico.* Albuquerque, NM: U.S. Geological Survey Open-File Report 89-32.

SNL (Sandia National Laboratories) and U.S. Geological Survey. 1982a. *Basic Data Report for Drillhole WIPP 11 (Waste Isolation Pilot Plant - WIPP).* SAND79-0272. Albuquerque, NM: Sandia National Laboratories.

SNL (Sandia National Laboratories) and U.S. Geological Survey. 1982b. *Basic Data Report for Drillhole ERDA 9 (Waste Isolation Pilot Plant - WIPP).* SAND79-0270. Albuquerque, NM: Sandia National Laboratories.

SNL (Sandia National Laboratories) and D'Appolonia Consulting Engineers. 1983. *Basic Data Report for Drillhole WIPP 12 (Waste Isolation Pilot Plant - WIPP).* SAND82-2336. Albuquerque, NM: Sandia National Laboratories.

U.S. DOE (Department of Energy). 1982. *Basic Data Report for Borehole DOE-1, Waste Isolation Pilot Plant (WIPP) Project, Southeastern New Mexico.* TME 3159. Albuquerque, NM: Sandia National Laboratories.

APPENDIX C:
REALIZATIONS OF TRANSMISSIVITY FIELDS IN THE CULEBRA DOLOMITE MEMBER OF THE RUSTLER FORMATION

APPENDIX C: REALIZATIONS OF TRANSMISSIVITY FIELDS IN THE CULEBRA DOLOMITE MEMBER OF THE RUSTLER FORMATION

The following 70 figures are grey-scale representations of the 70 realizations of Culebra transmissivity field generated for use in the 1992 series of PA calculations. The realizations are ordered by increasing travel time (marked at the bottom of each figure).

The origins of these representations of transmissivity field are briefly explained in Section 2.6.3 of this report, and in more detail in Volume 2 of the 1992 series of reports.

Note: On all figures, the grey-scale values are in units of $\log_{10}$ (m^2/s).

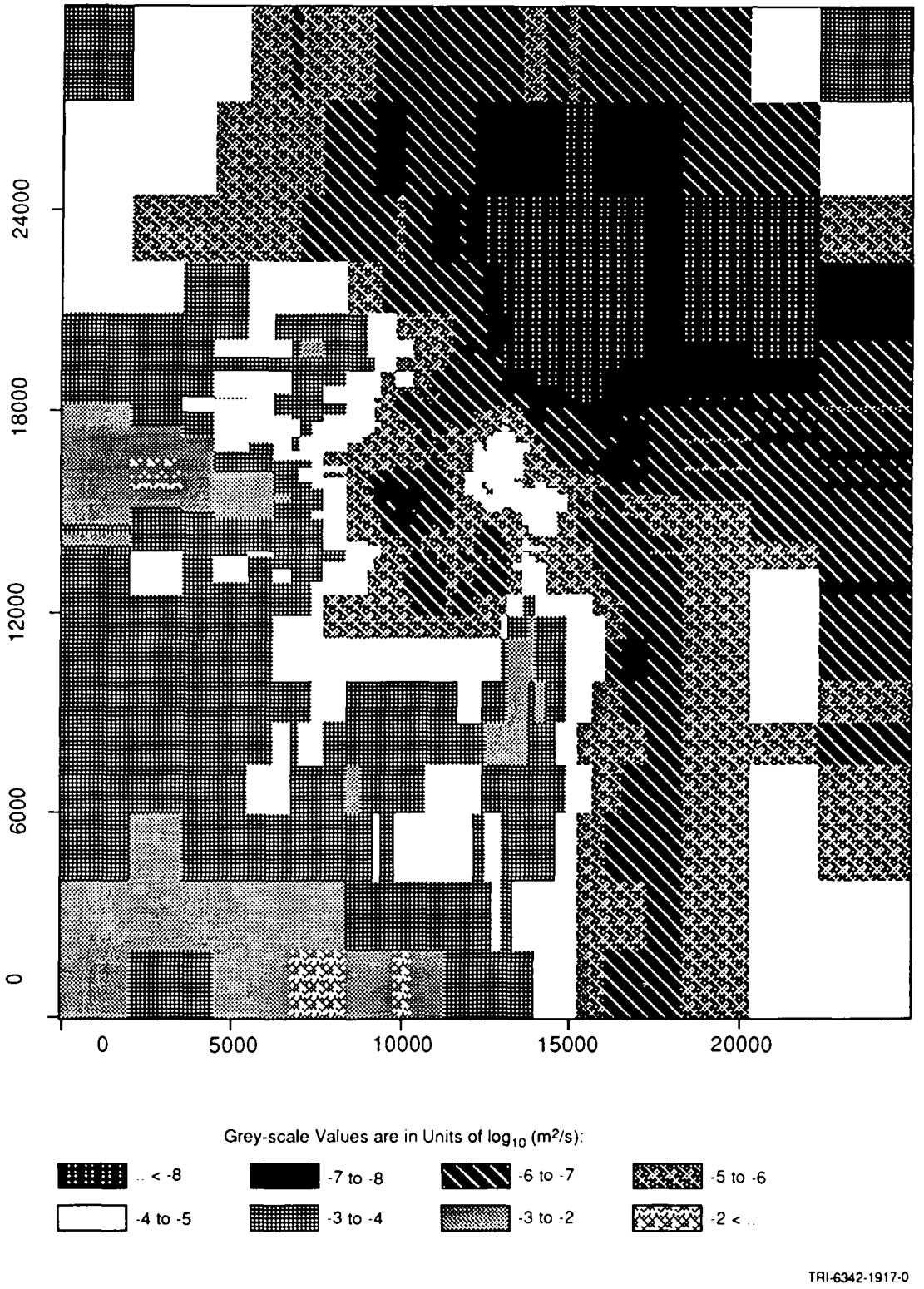

Figure C-1. Realization 12 of Culebra transmissivity.

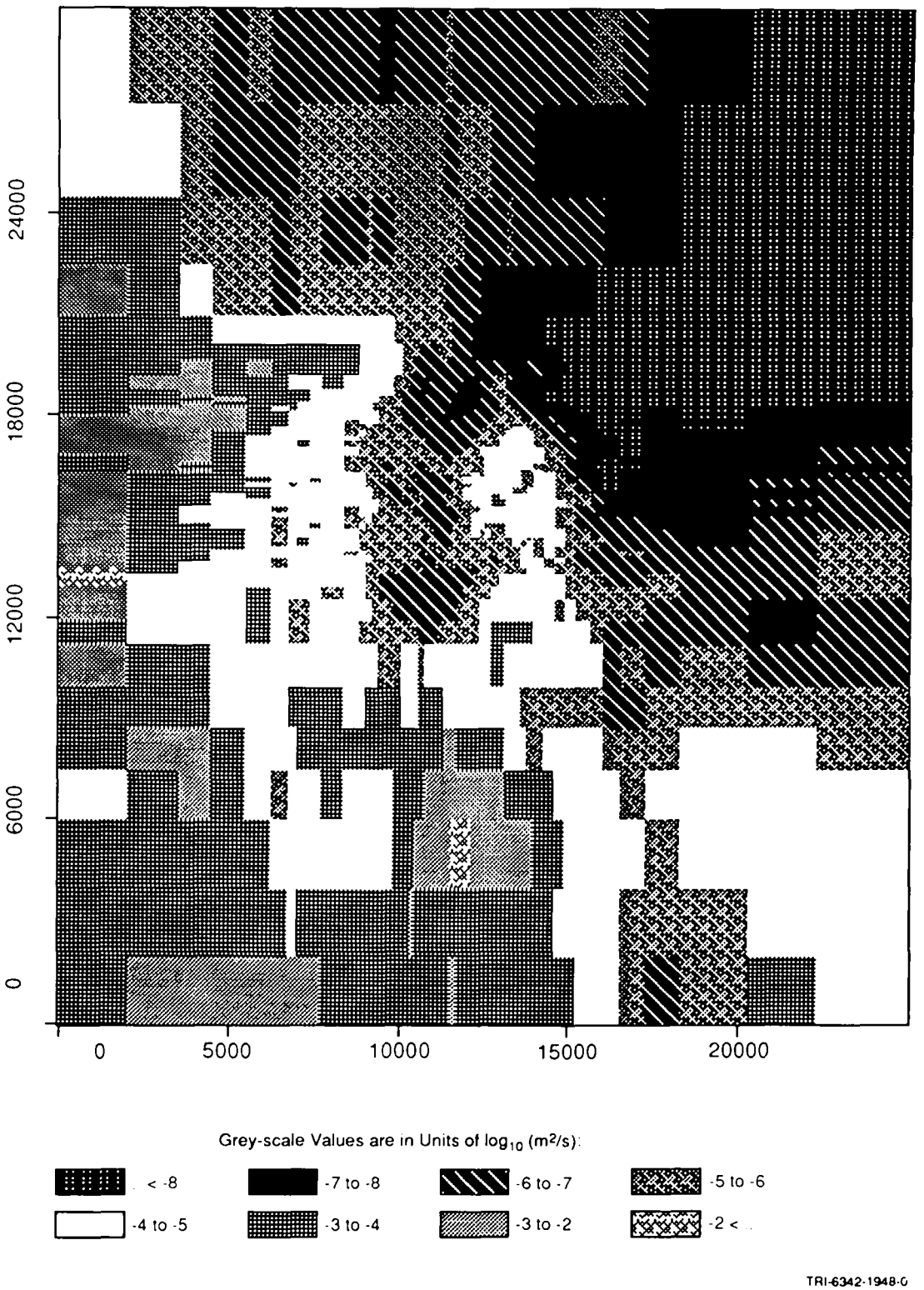

Figure C-2. Realization 64 of Culebra transmissivity.

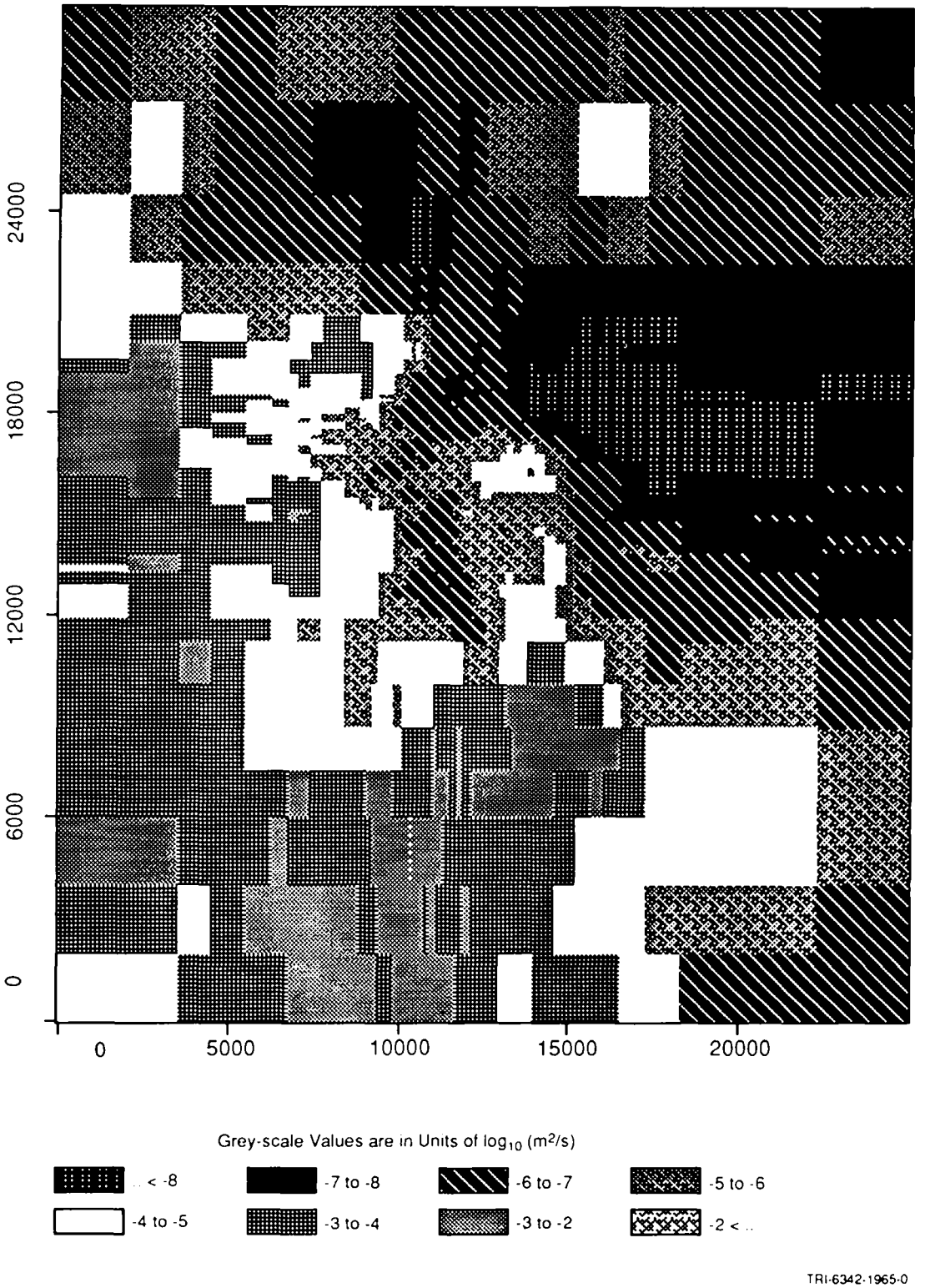

Figure C-3. Realization 25 of Culebra transmissivity.

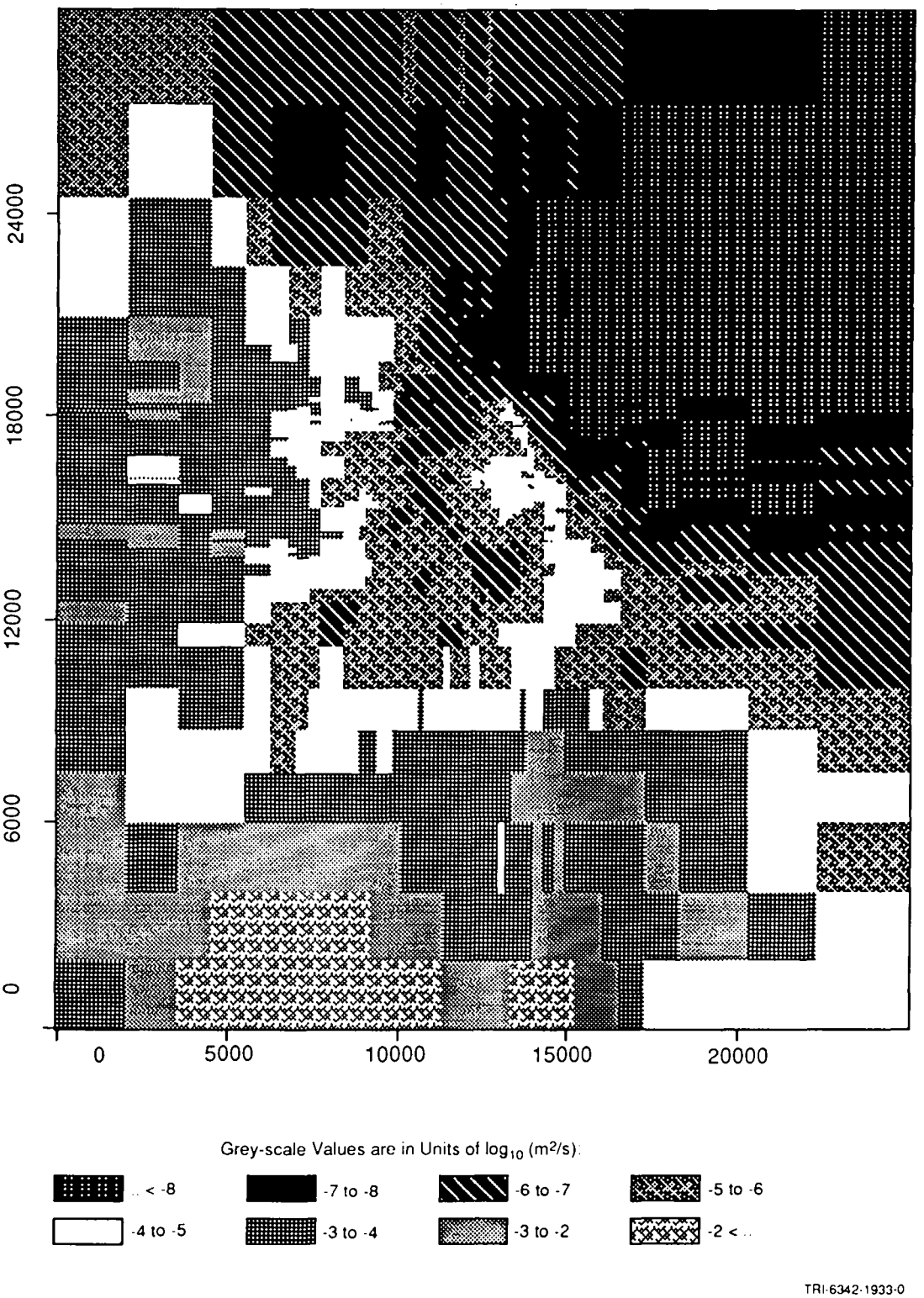

Figure C-4. Realization 23 of Culebra transmissivity.

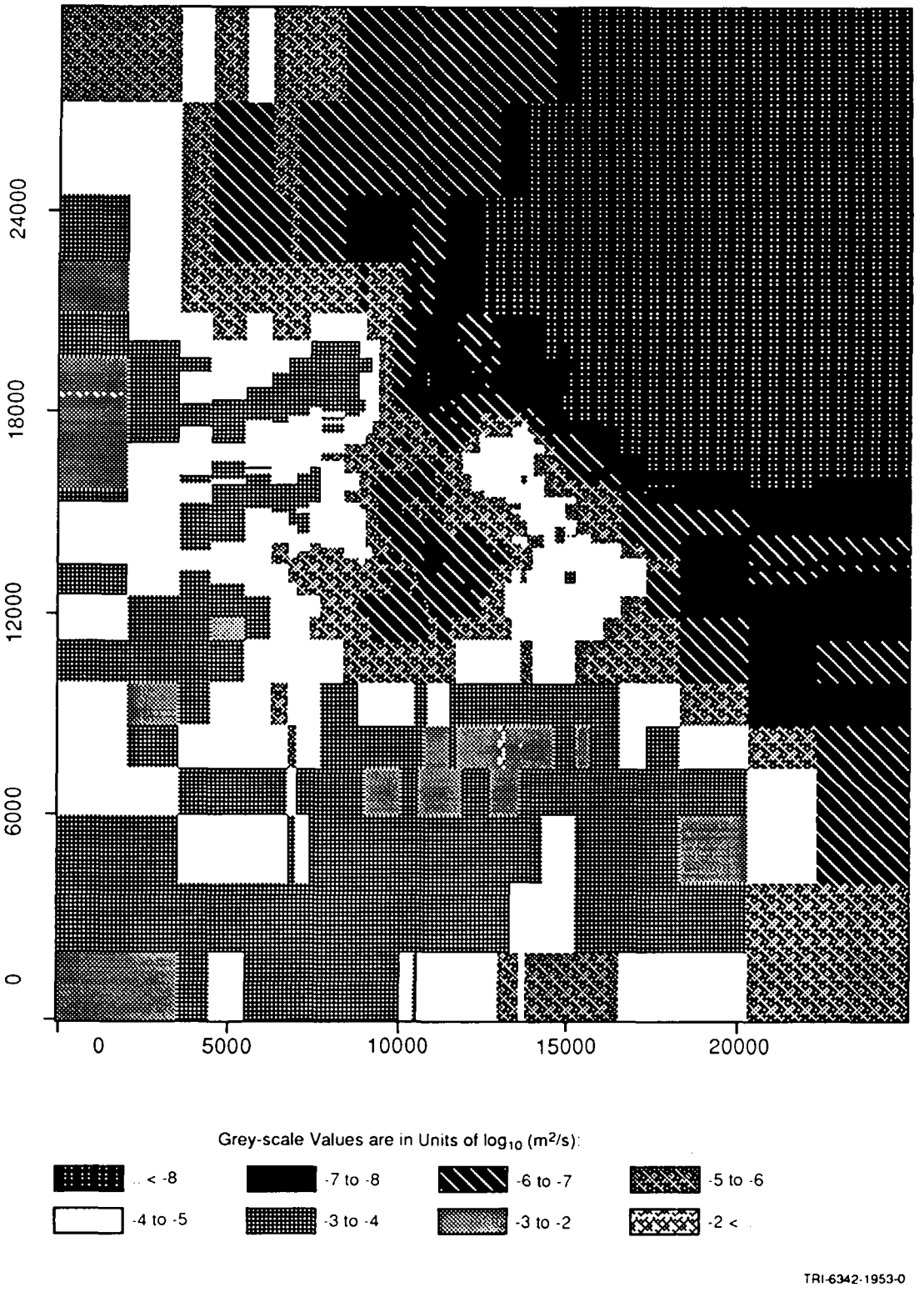

Figure C-5. Realization 15 of Culebra transmissivity.

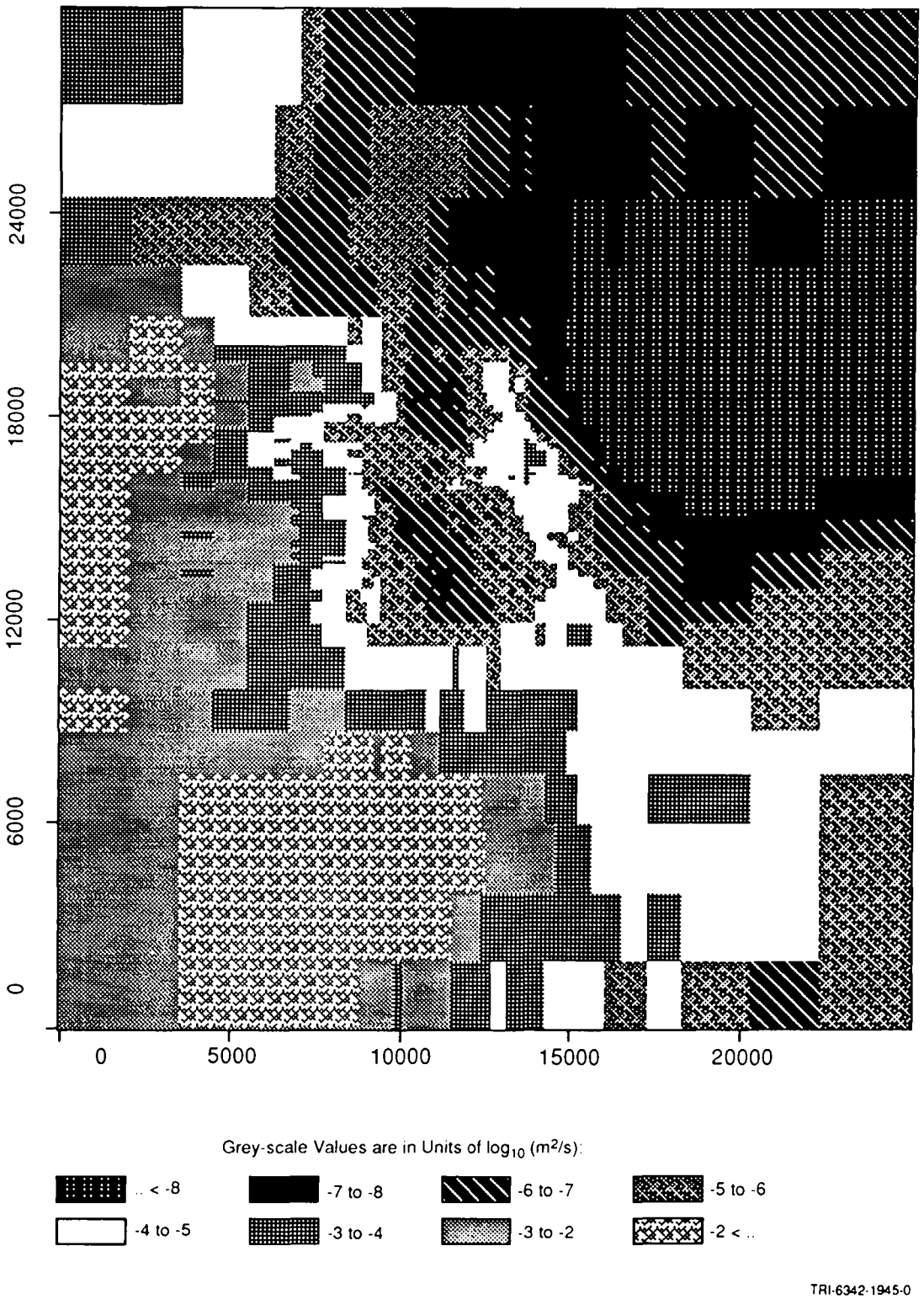

Figure C-6. Realization 18 of Culebra transmissivity.

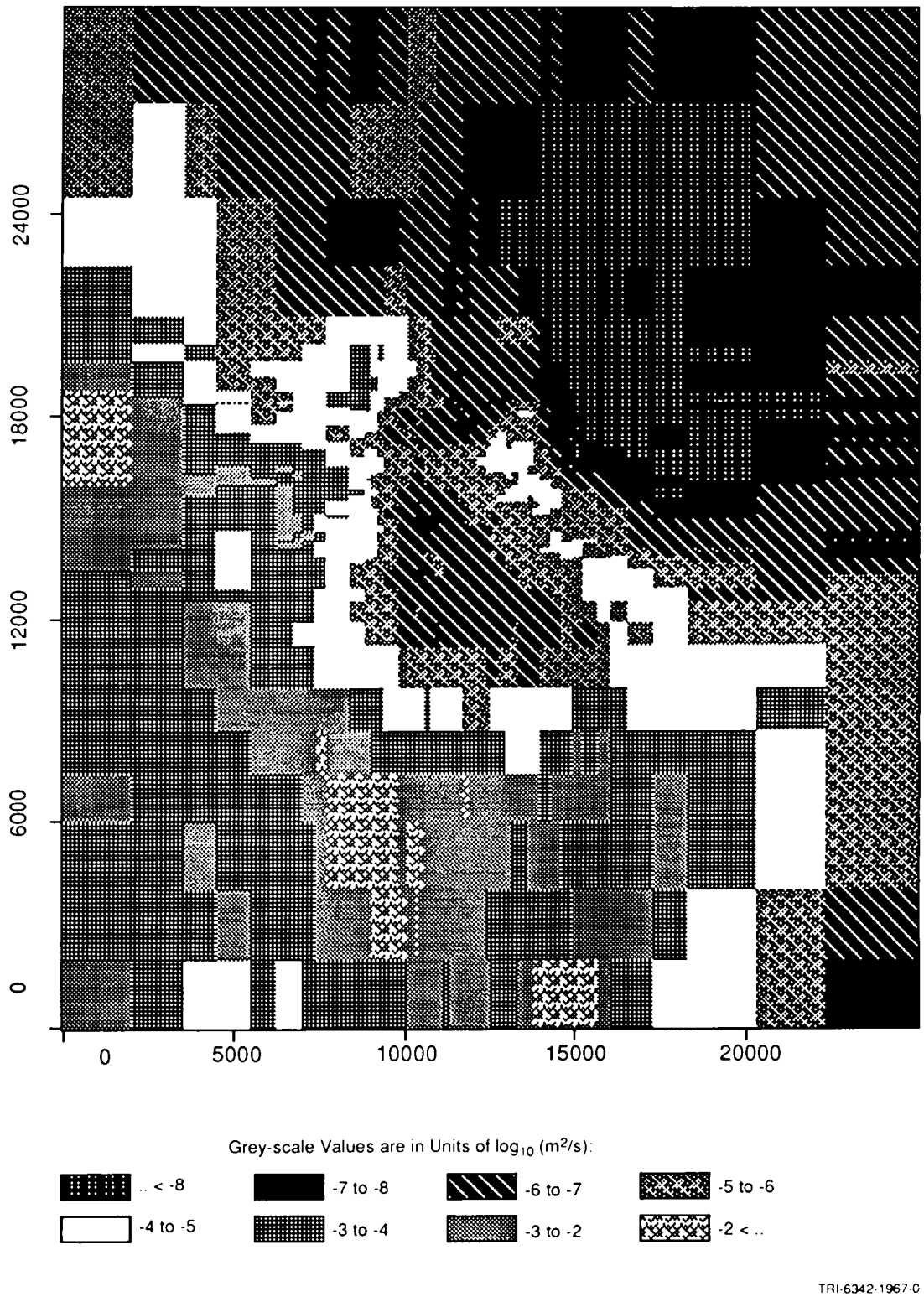

Figure C-7. Realization 53 of Culebra transmissivity.

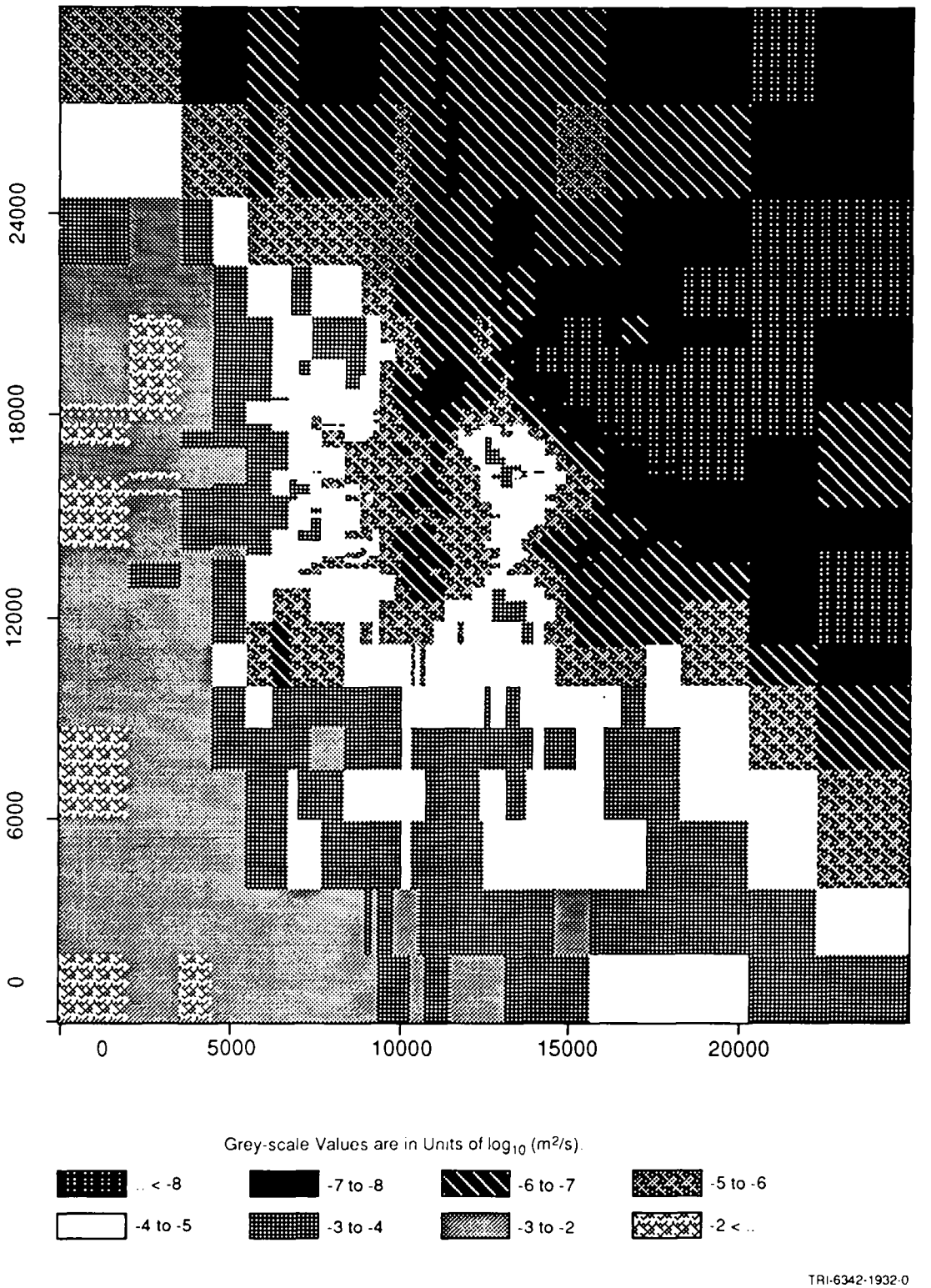

Figure C-8. Realization 16 of Culebra transmissivity.

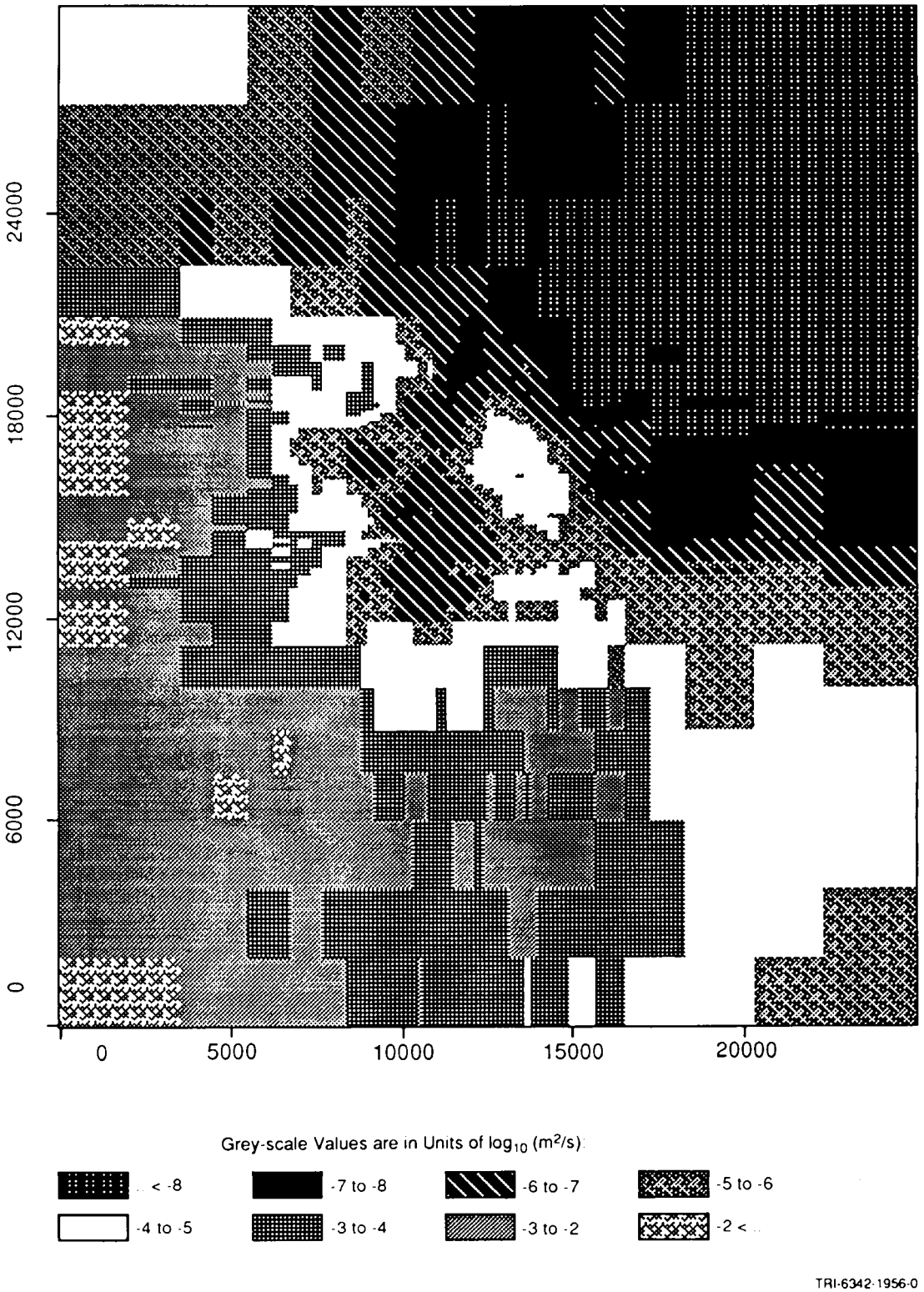

Figure C-9. Realization 36 of Culebra transmissivity.

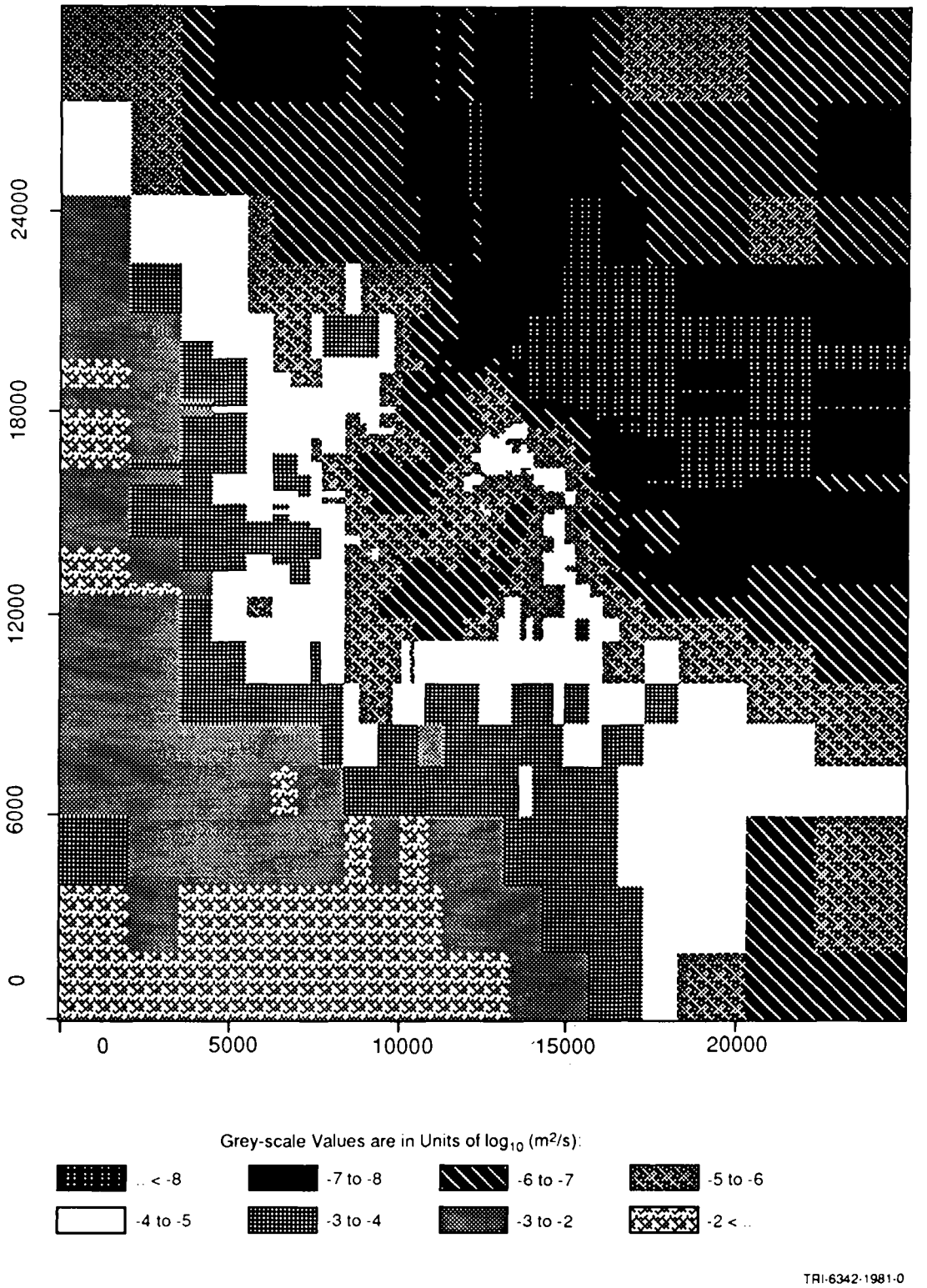

Figure C-10. Realization 19 of Culebra transmissivity.

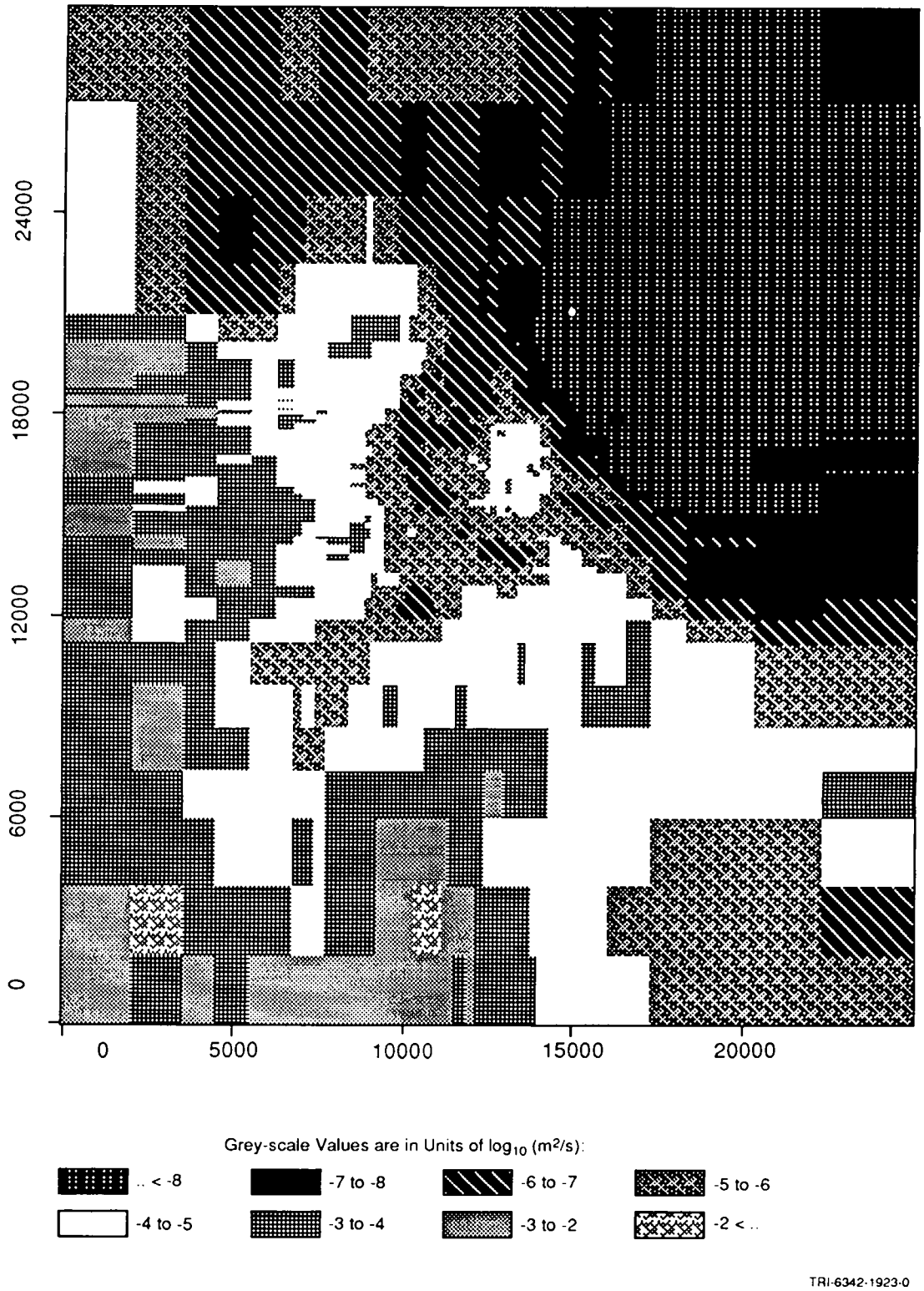

Figure C-11. Realization 66 of Culebra transmissivity.

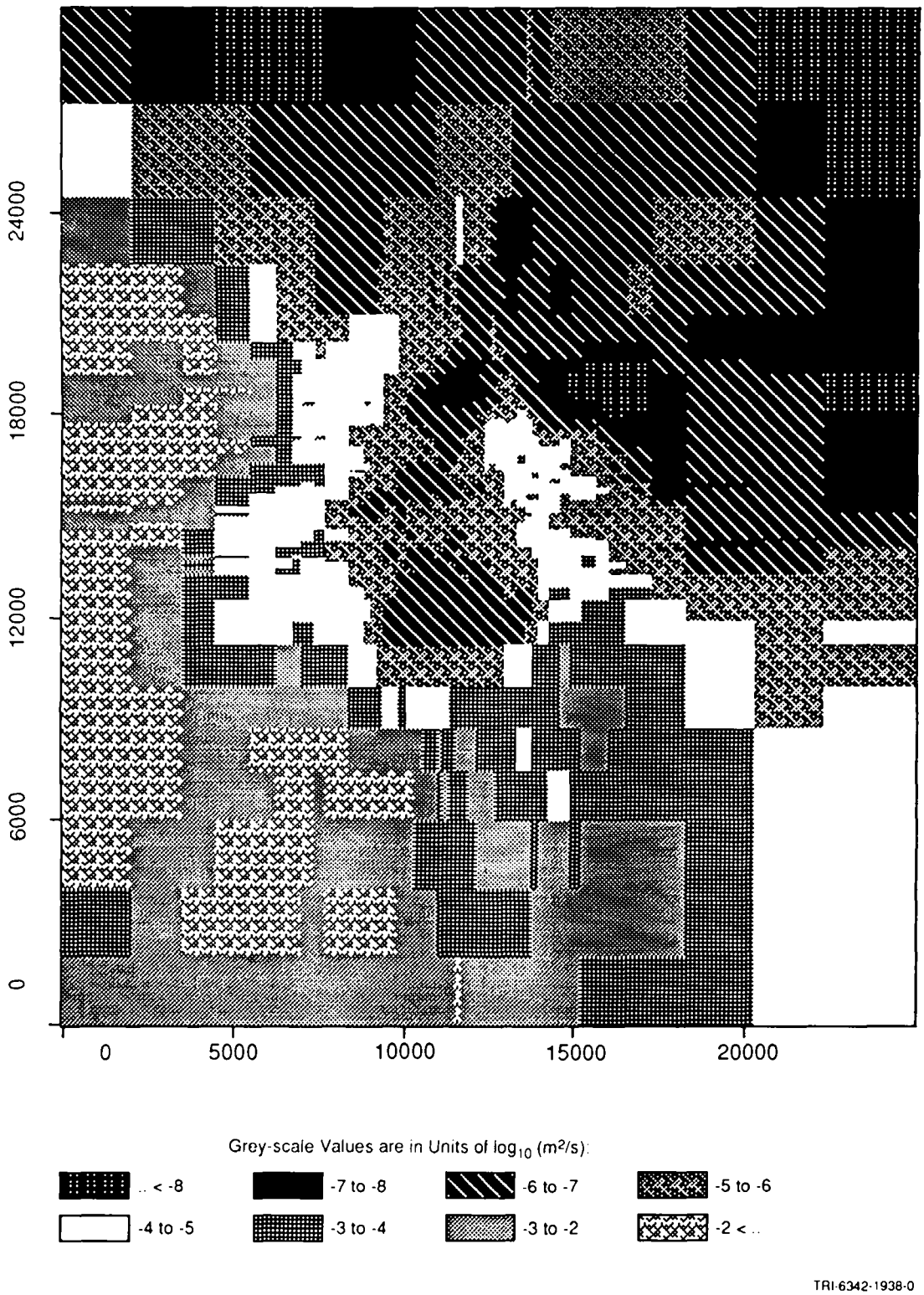

Figure C-12. Realization 45 of Culebra transmissivity.

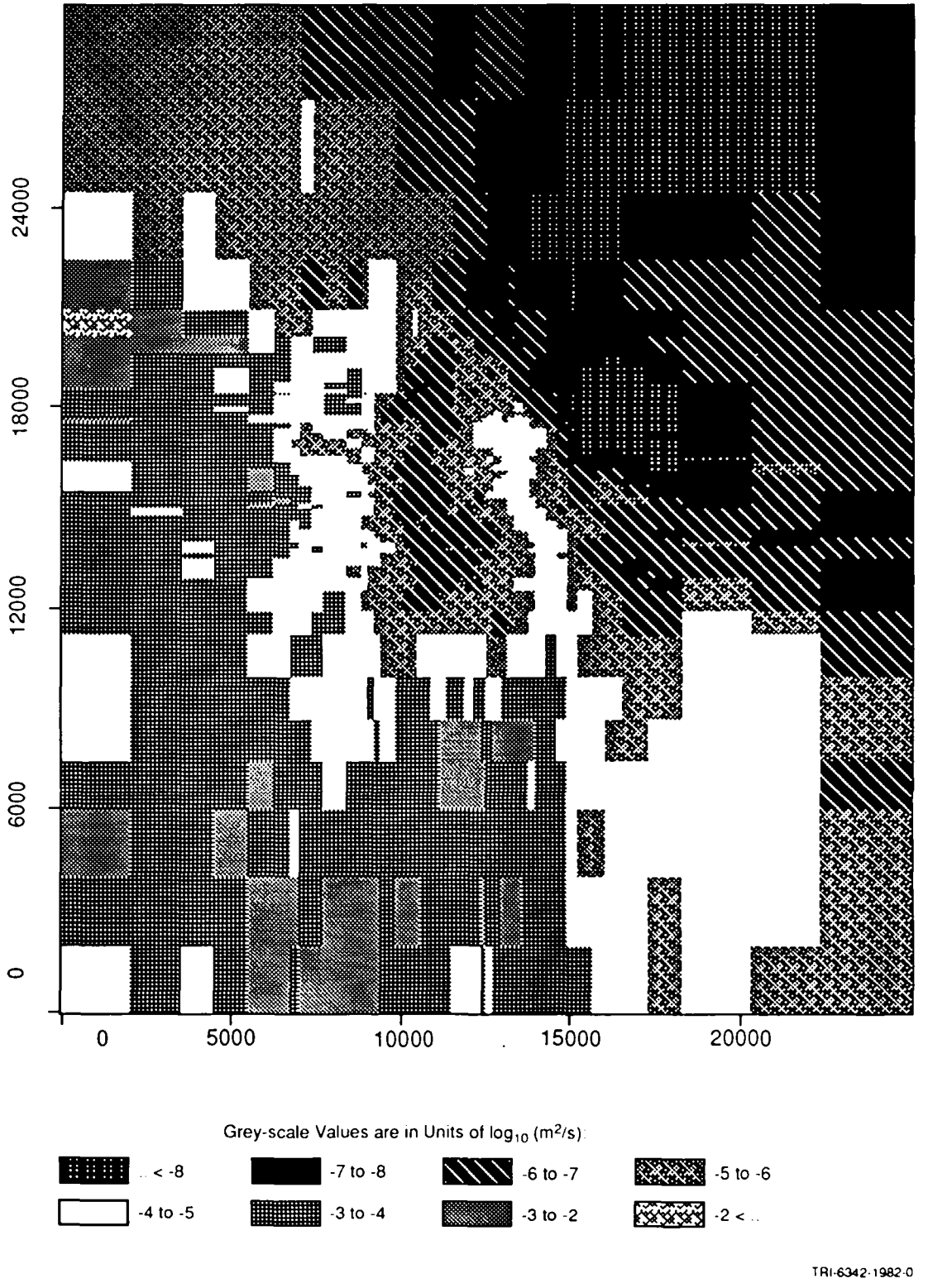

Figure C-13. Realization 34 of Culebra transmissivity.

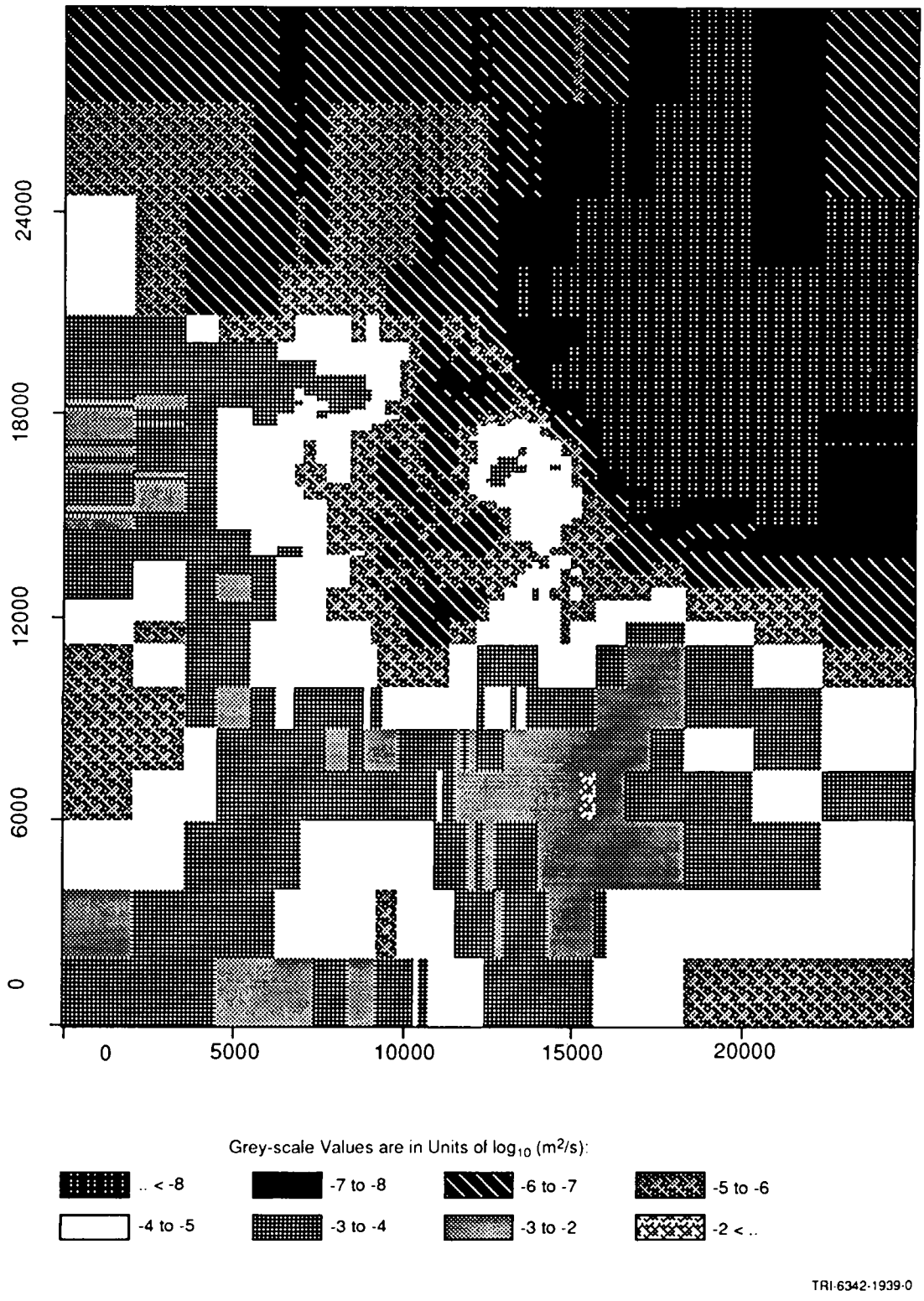

Figure C-14. Realization 24 of Culebra transmissivity.

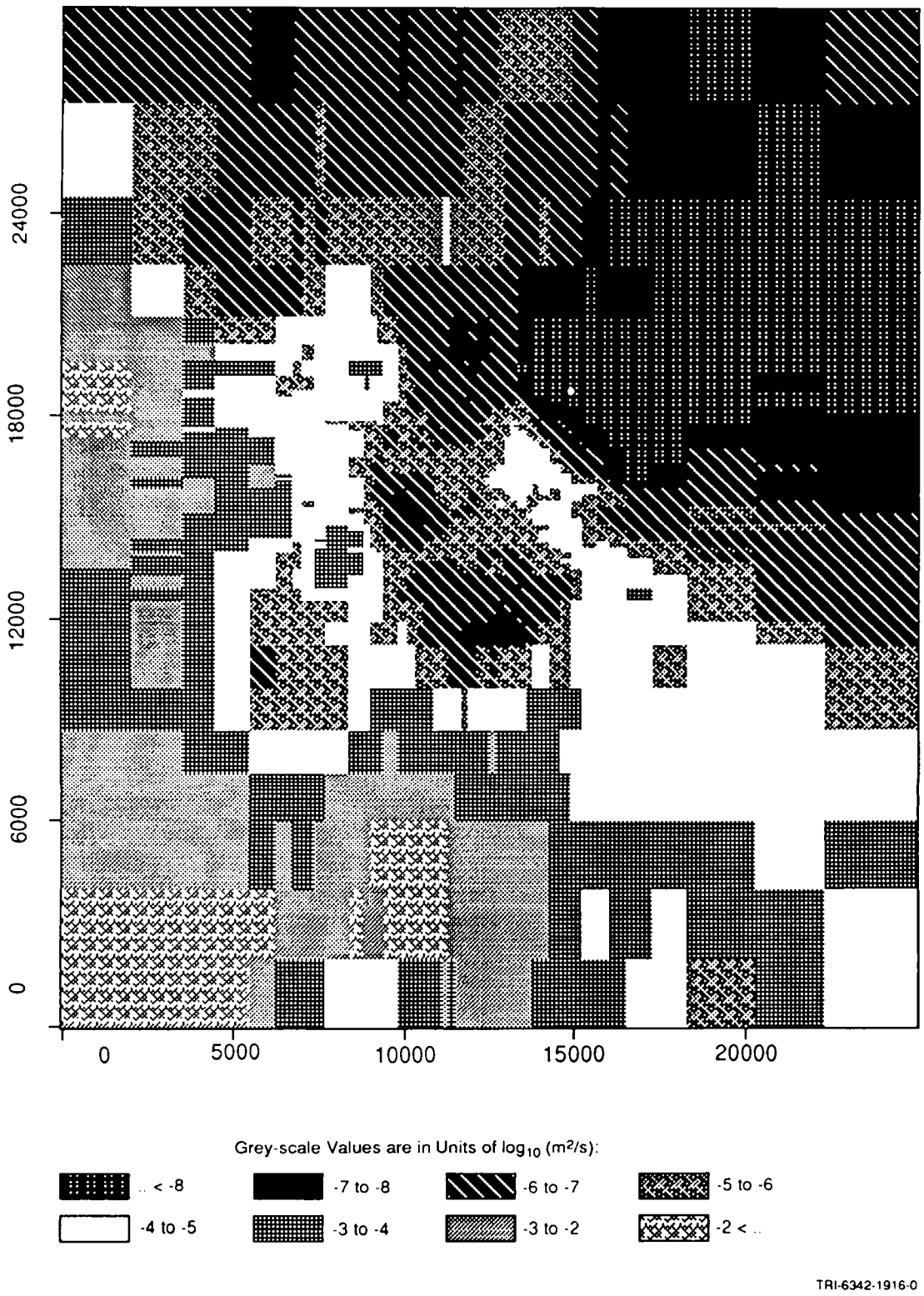

Figure C-15. Realization 63 of Culebra transmissivity.

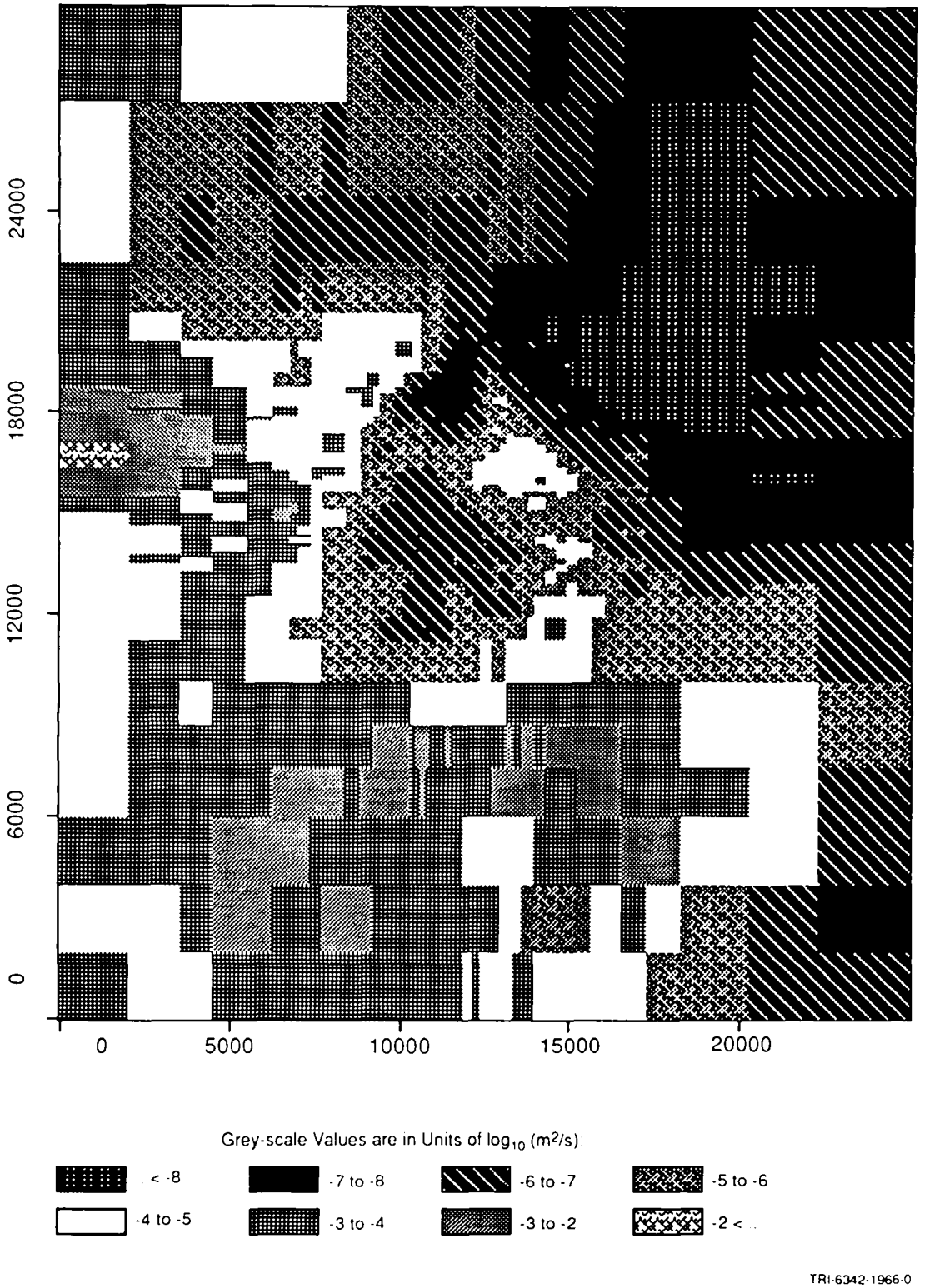

Figure C-16. Realization 70 of Culebra transmissivity.

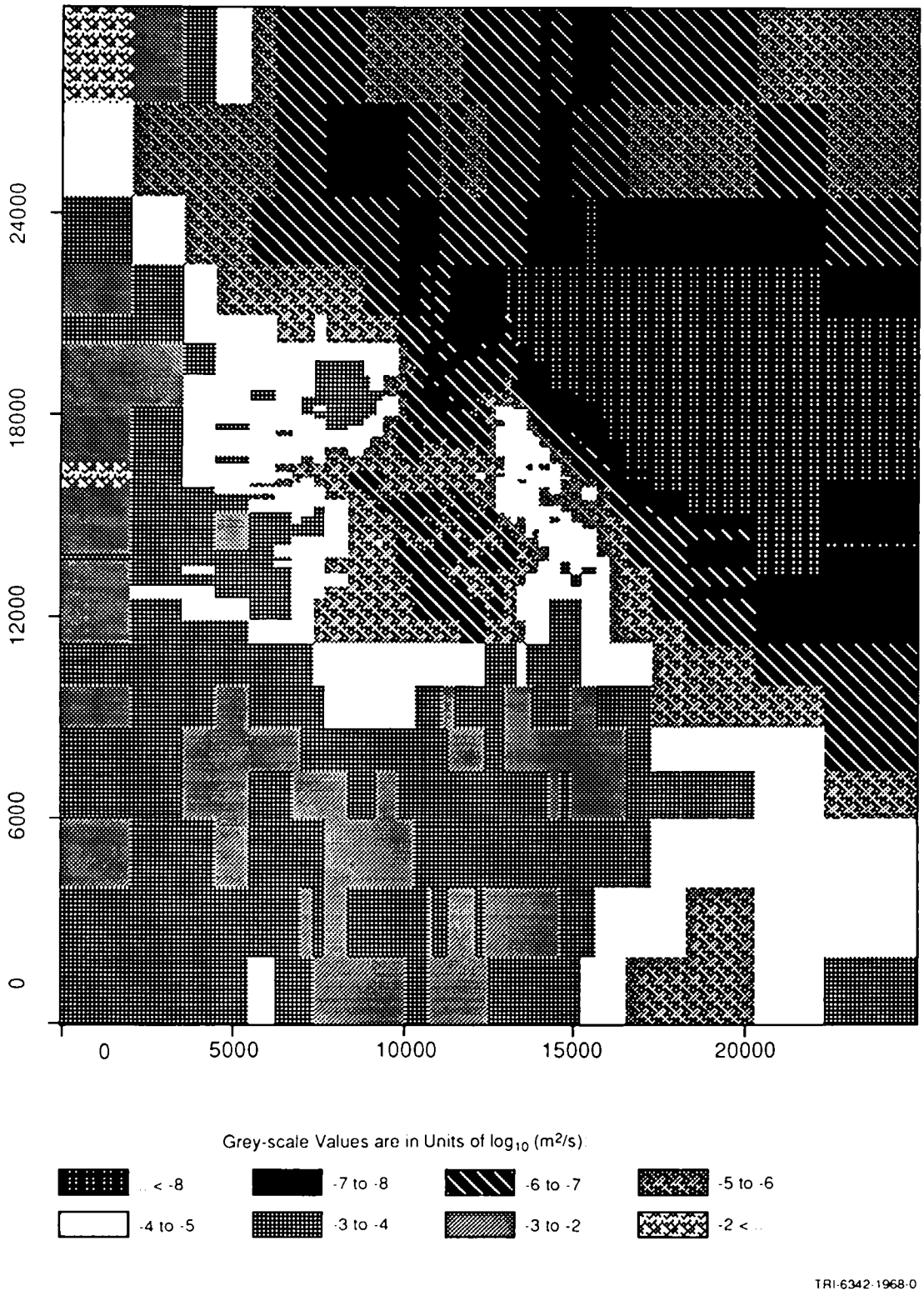

Figure C-17. Realization 42 of Culebra transmissivity.

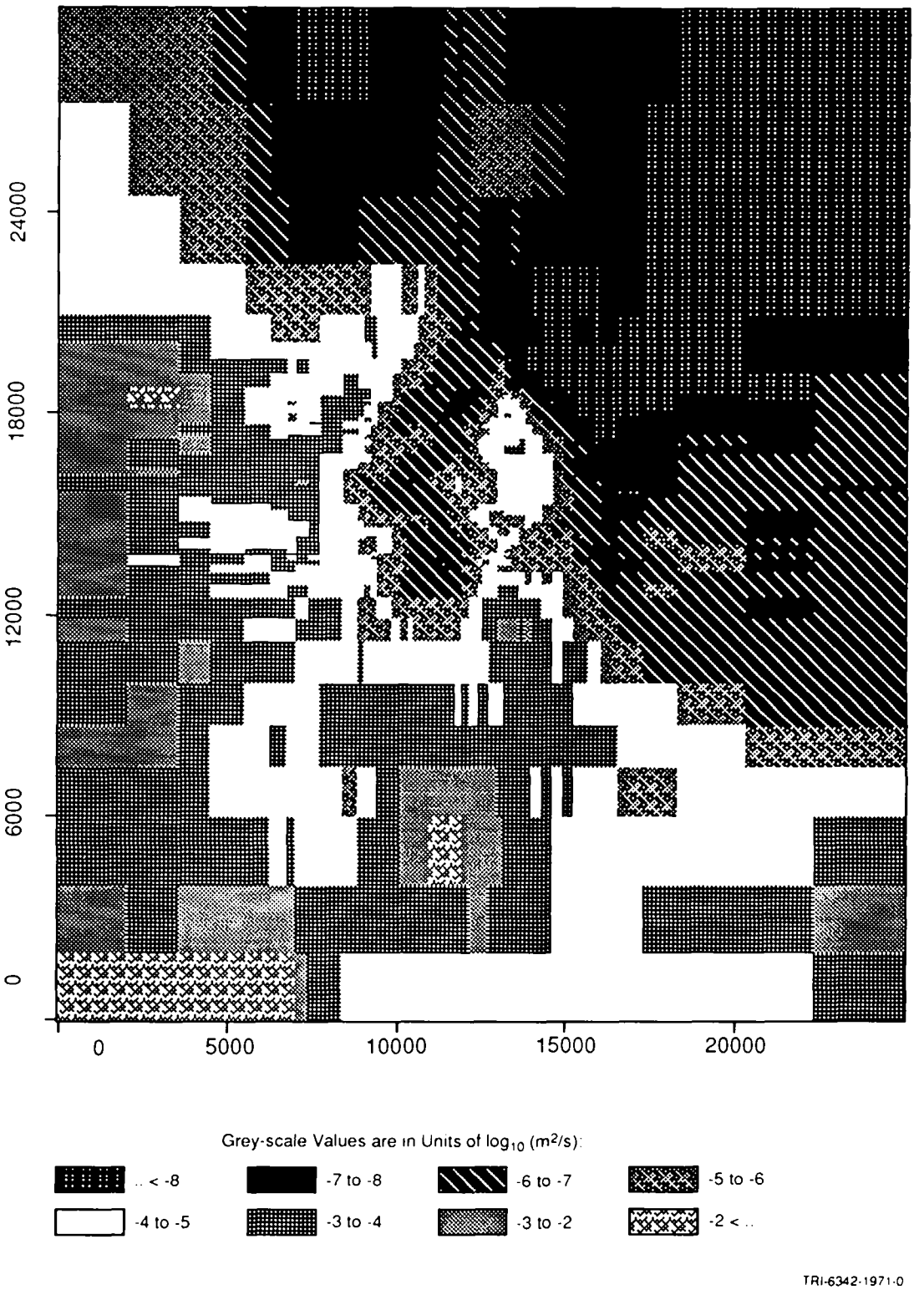

Figure C-18. Realization 56 of Culebra transmissivity.

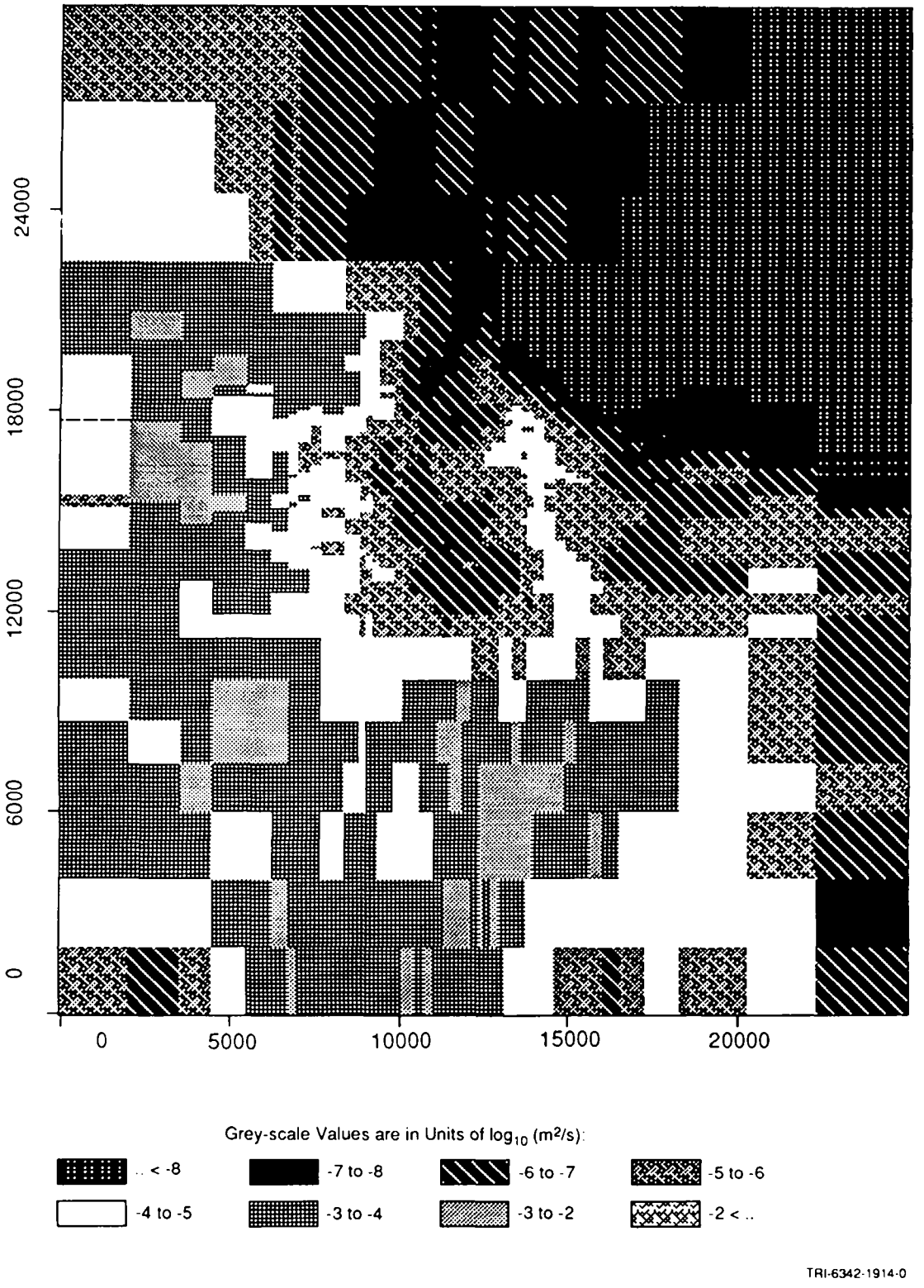

Figure C-19. Realization 69 of Culebra transmissivity.

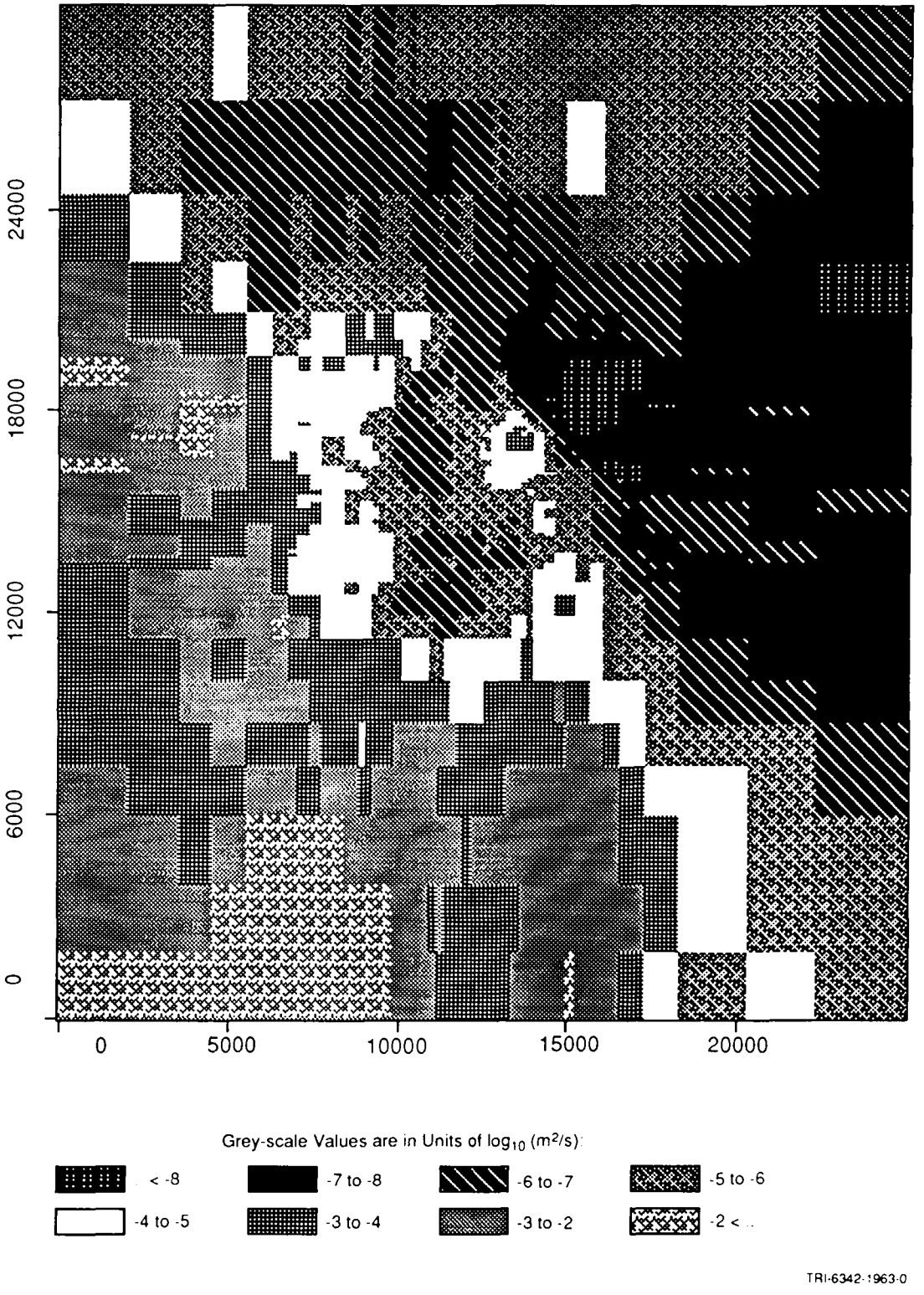

Figure C-20. Realization 7 of Culebra transmissivity.

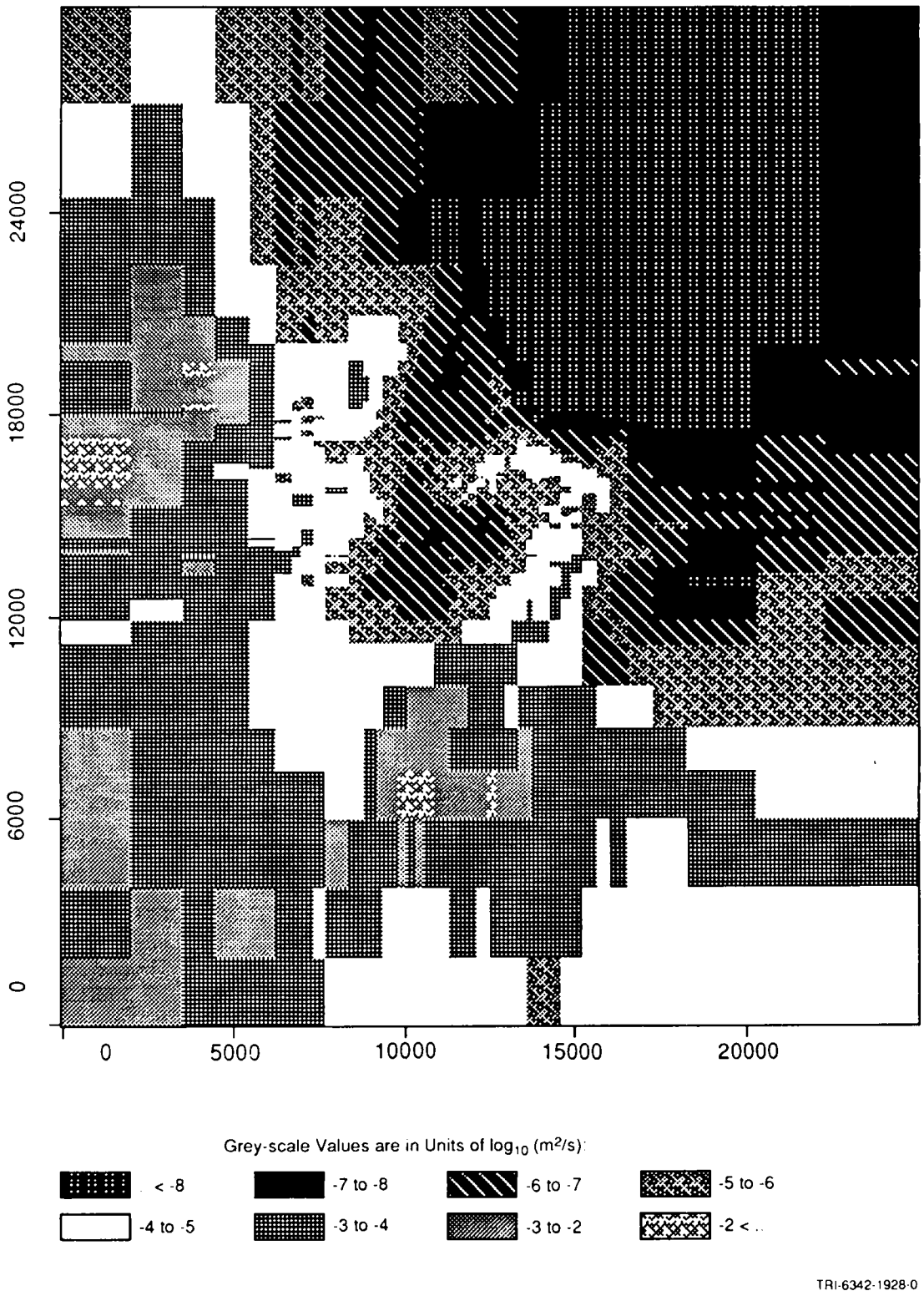

Figure C-21. Realization 52 of Culebra transmissivity.

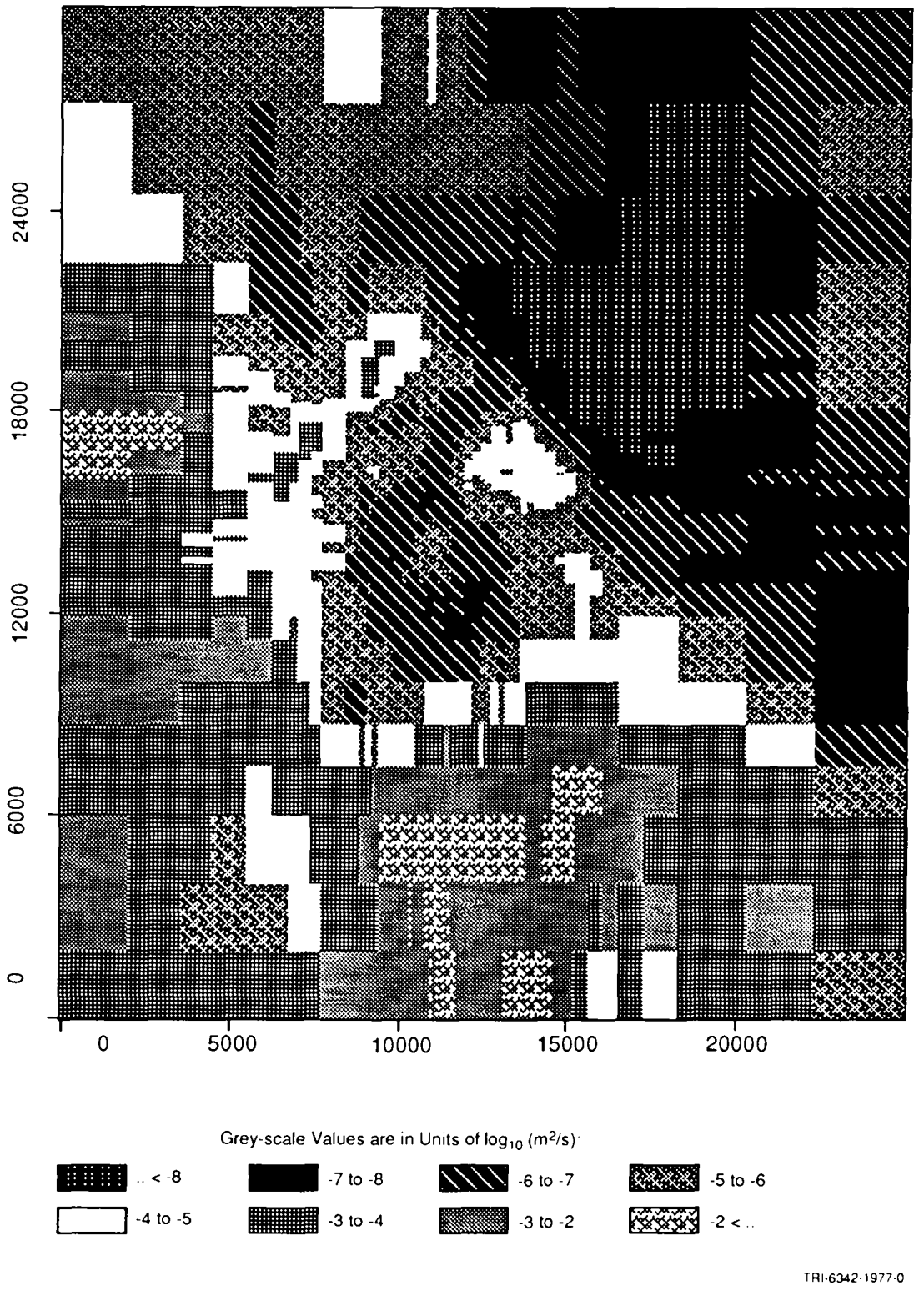

Figure C-22. Realization 20 of Culebra transmissivity.

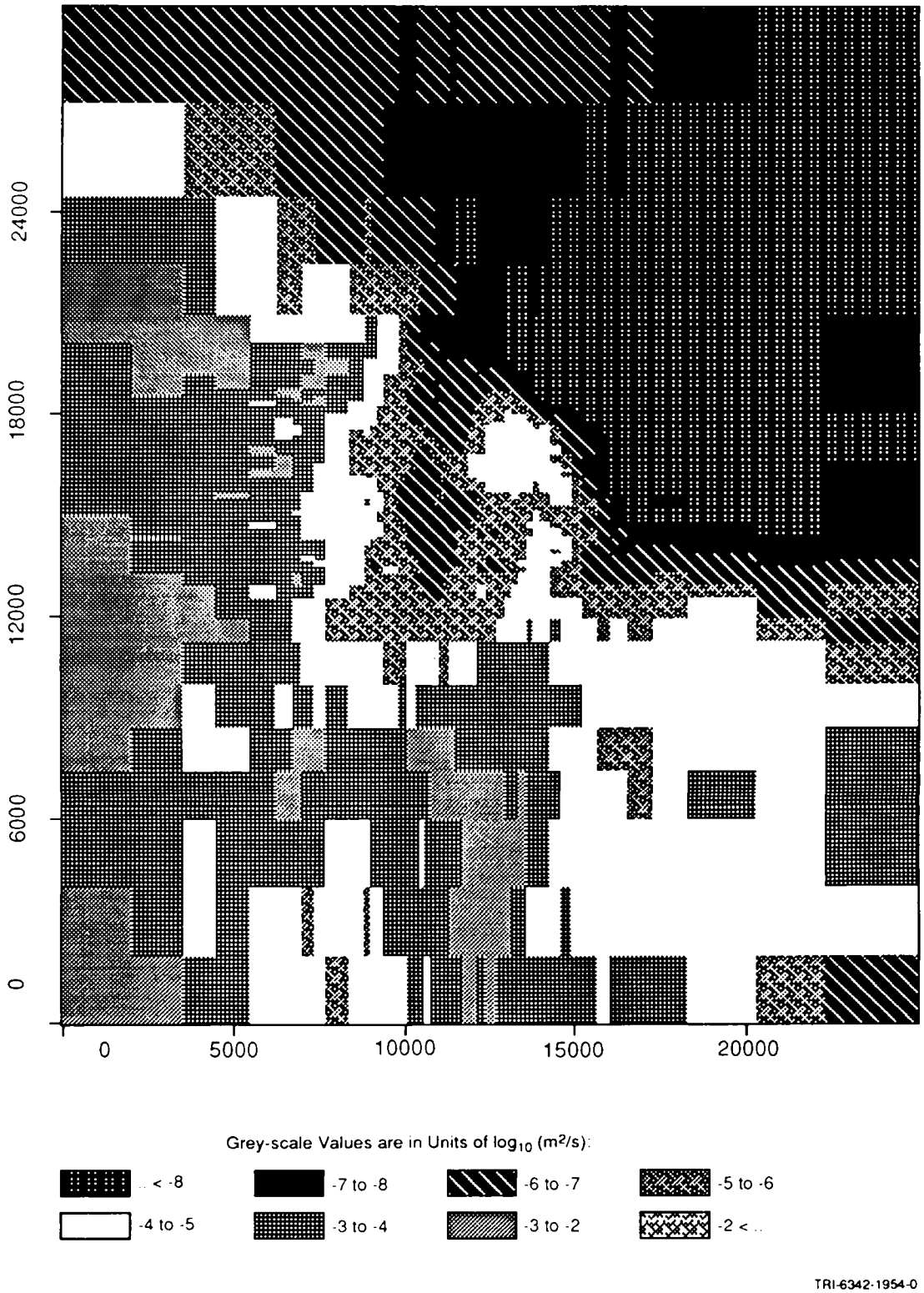

Figure C-23. Realization 33 of Culebra transmissivity.

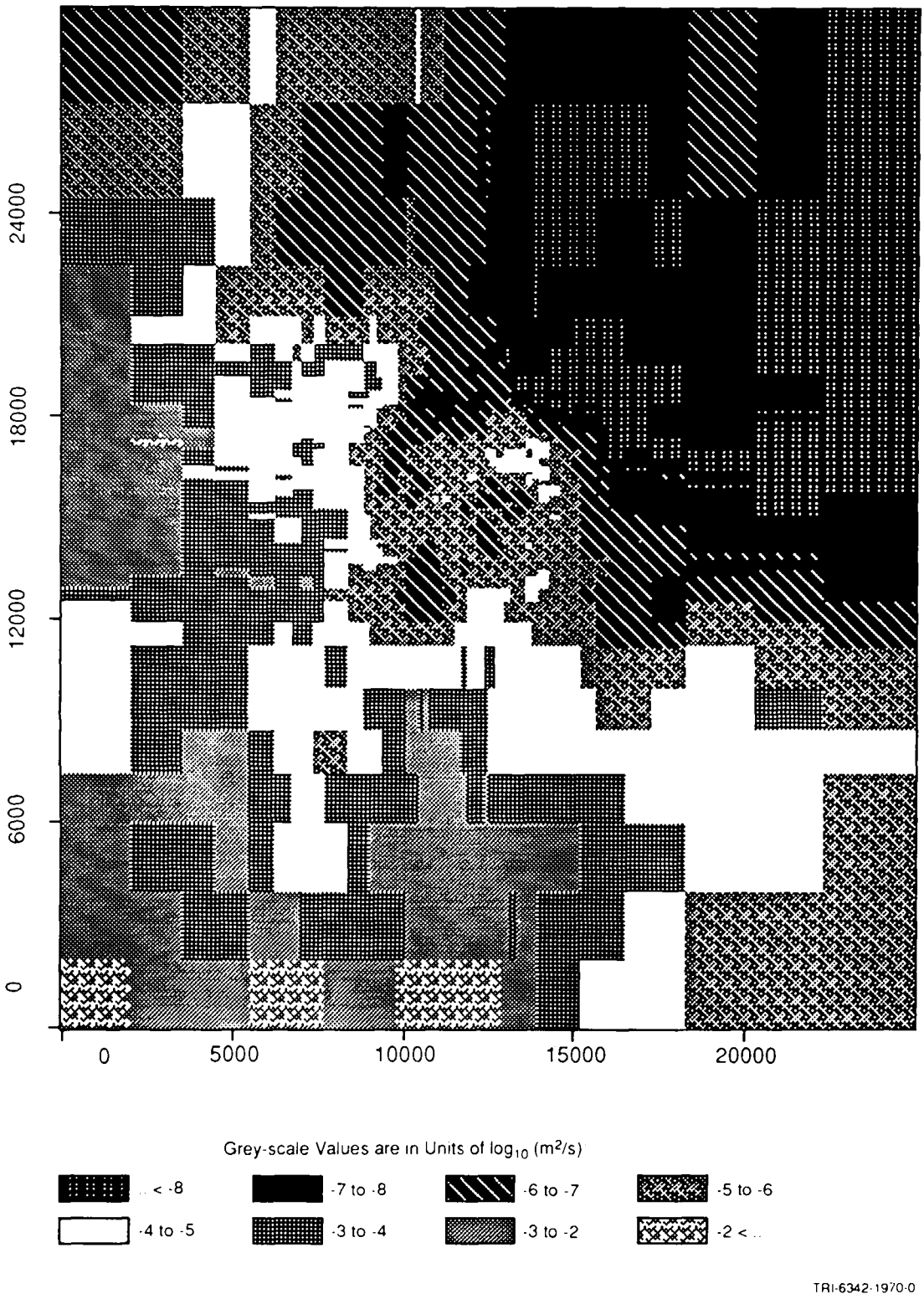

Figure C-24. Realization 39 of Culebra transmissivity.

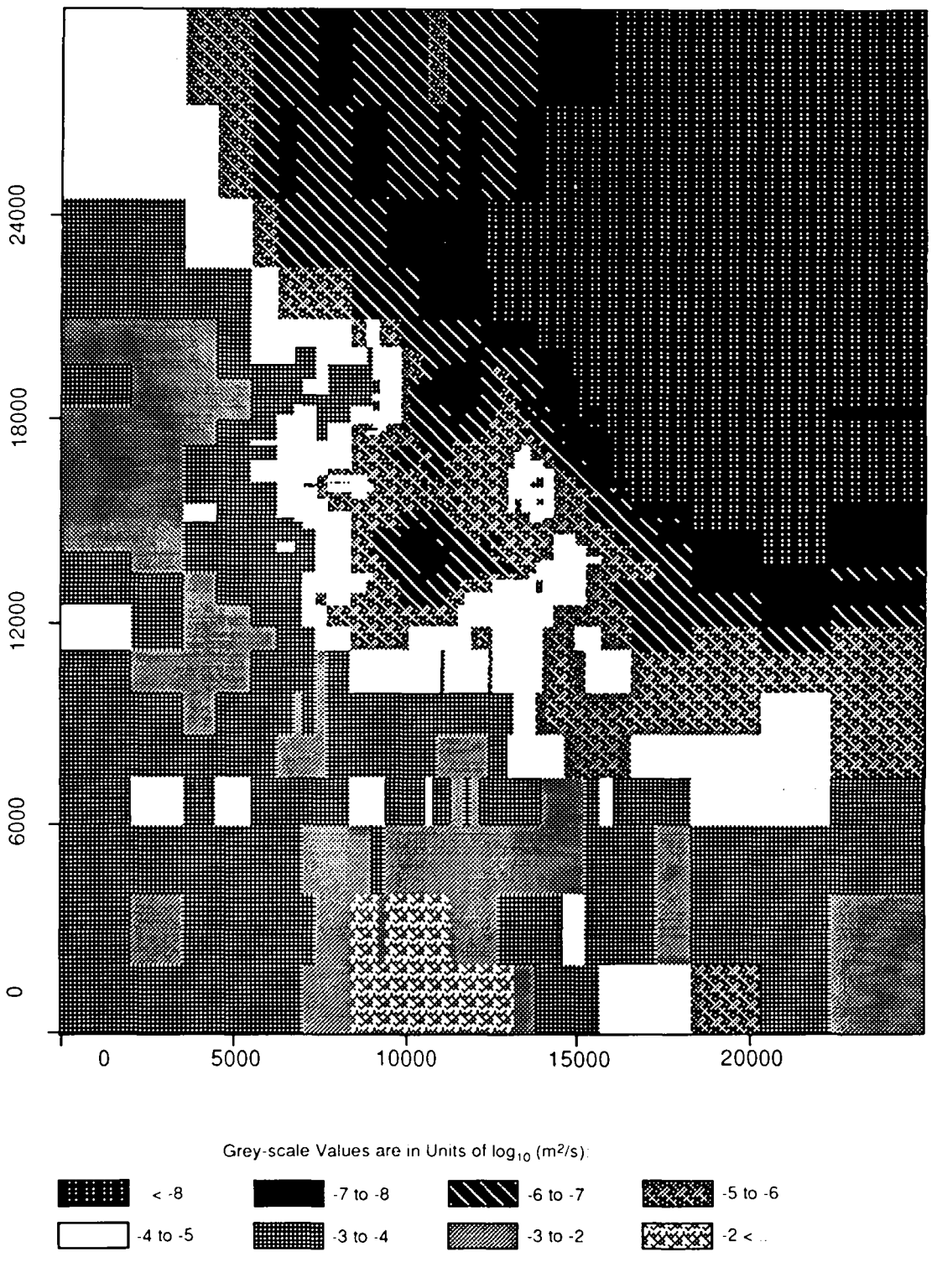

Figure C-25. Realization 28 of Culebra transmissivity.

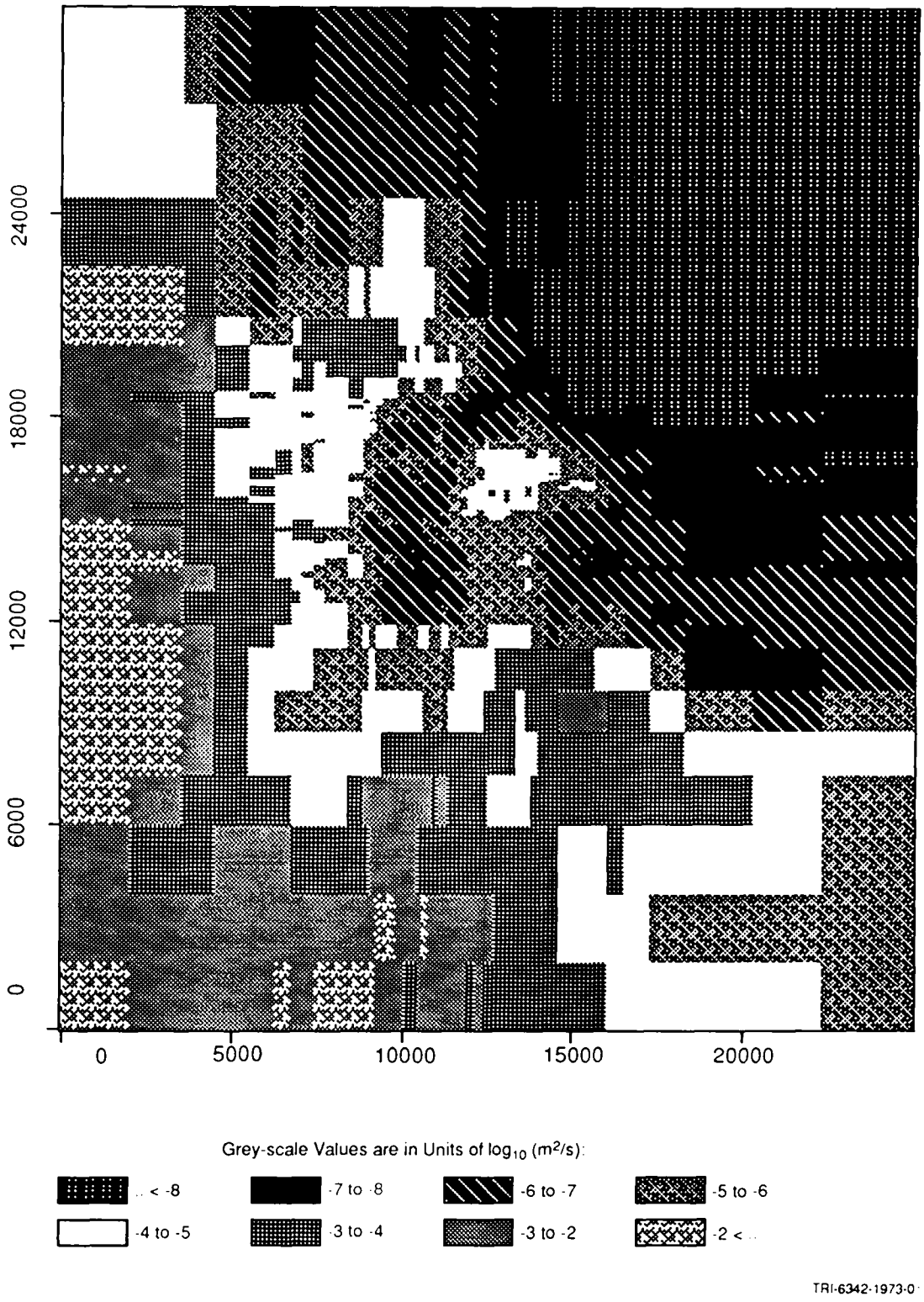

Figure C-26. Realization 1 of Culebra transmissivity.

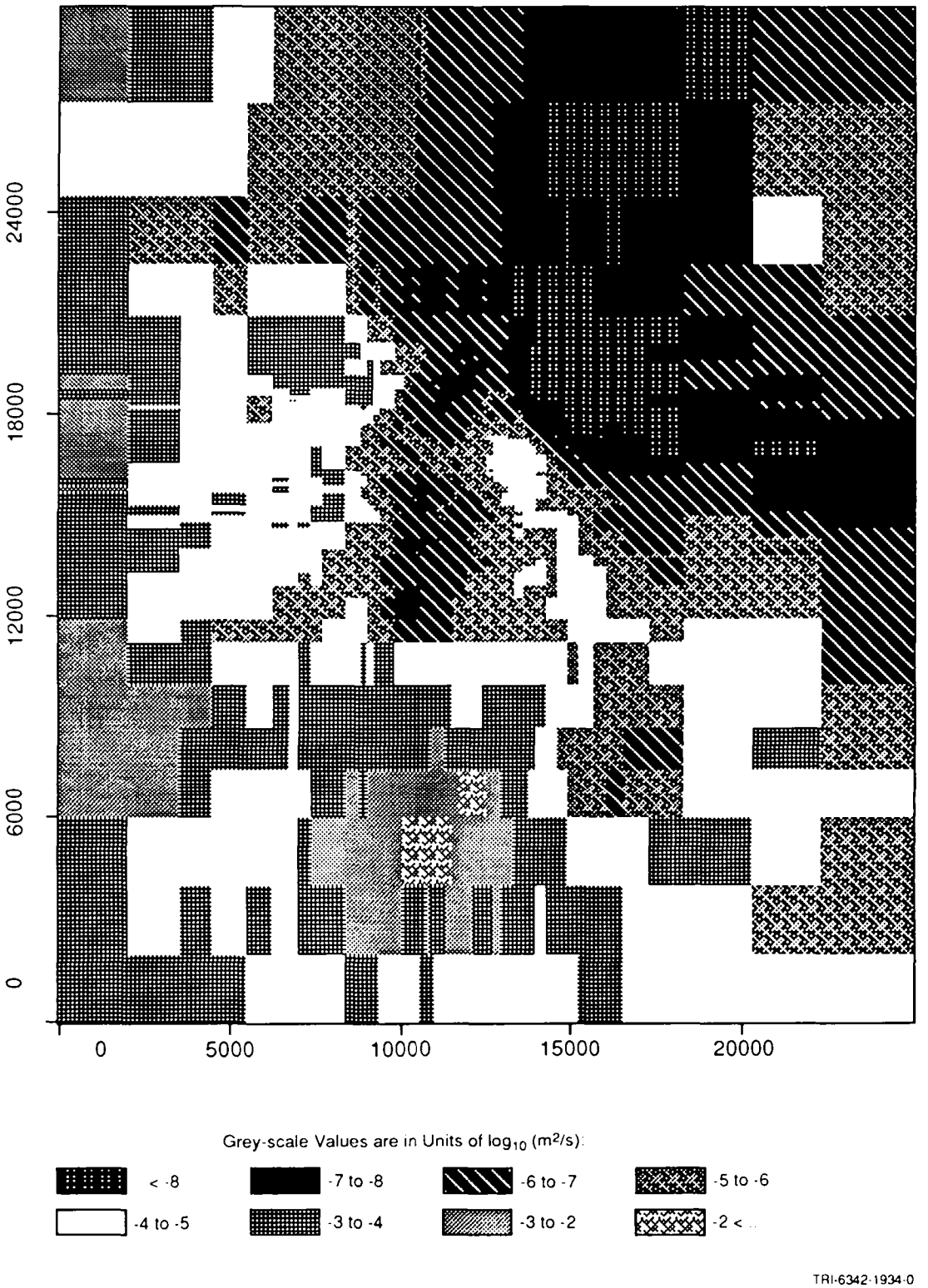

Figure C-27. Realization 55 of Culebra transmissivity.

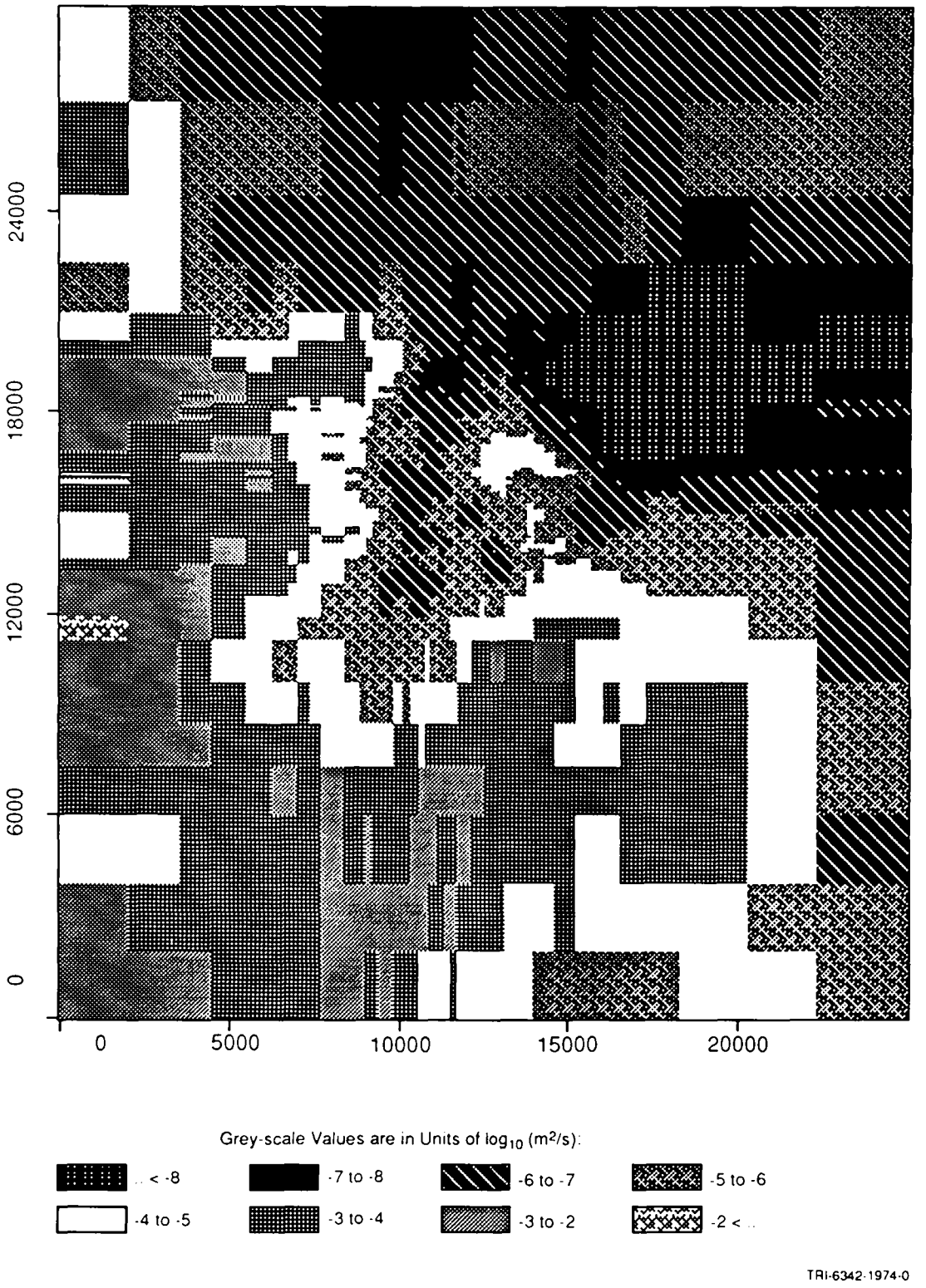

Figure C-28. Realization 43 of Culebra transmissivity.

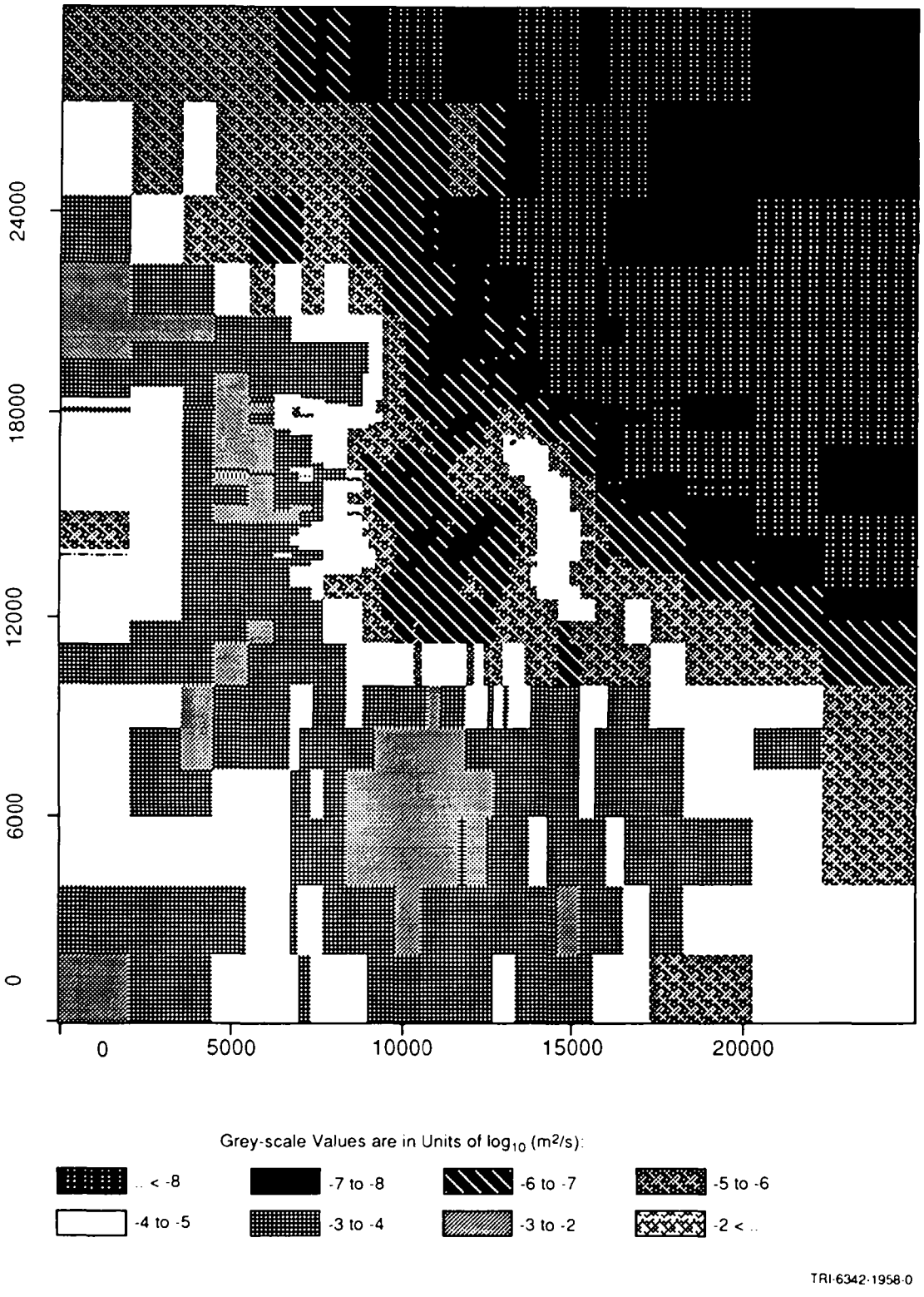

Figure C-29. Realization 2 of Culebra transmissivity.

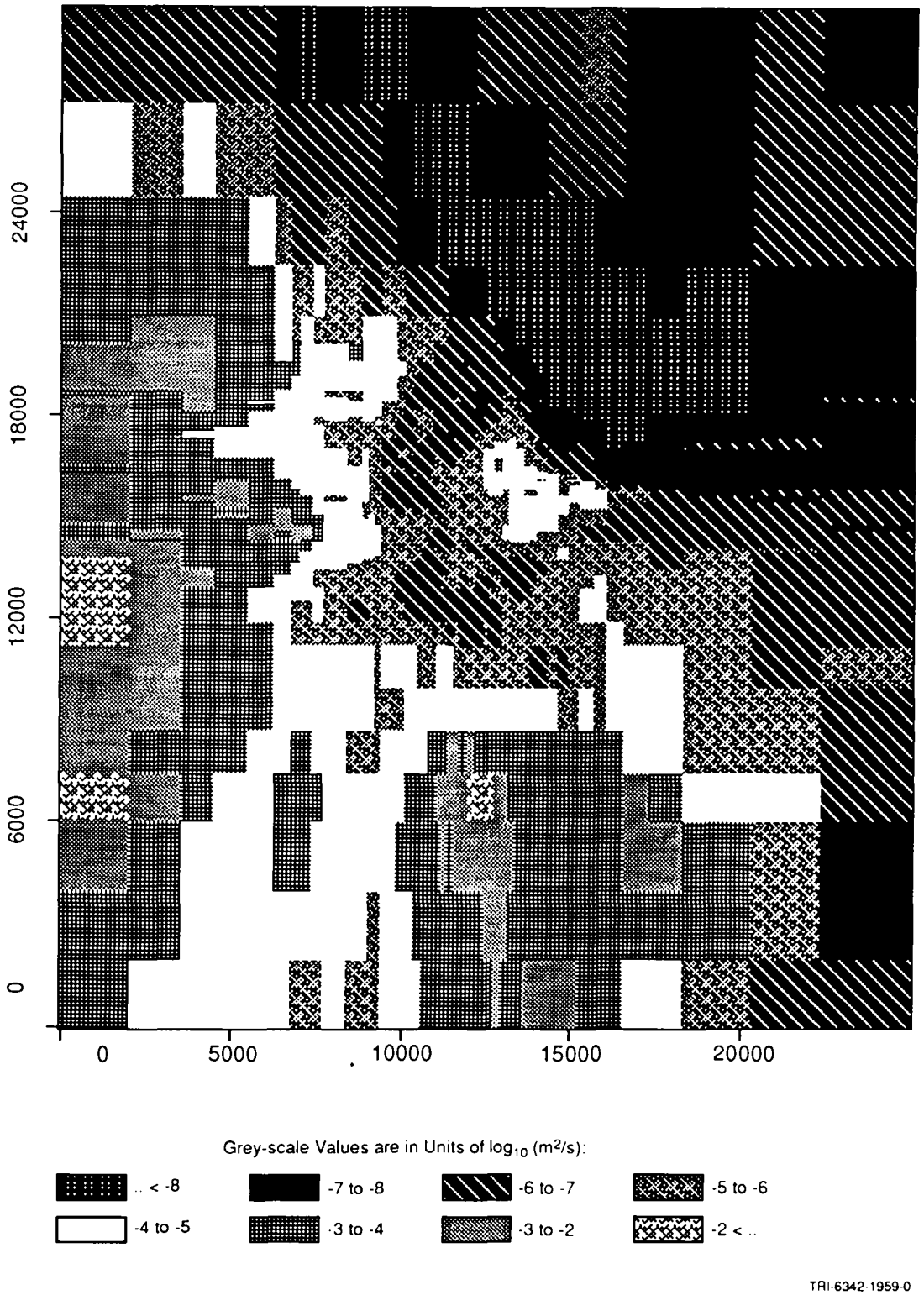

Figure C-30. Realization 47 of Culebra transmissivity.

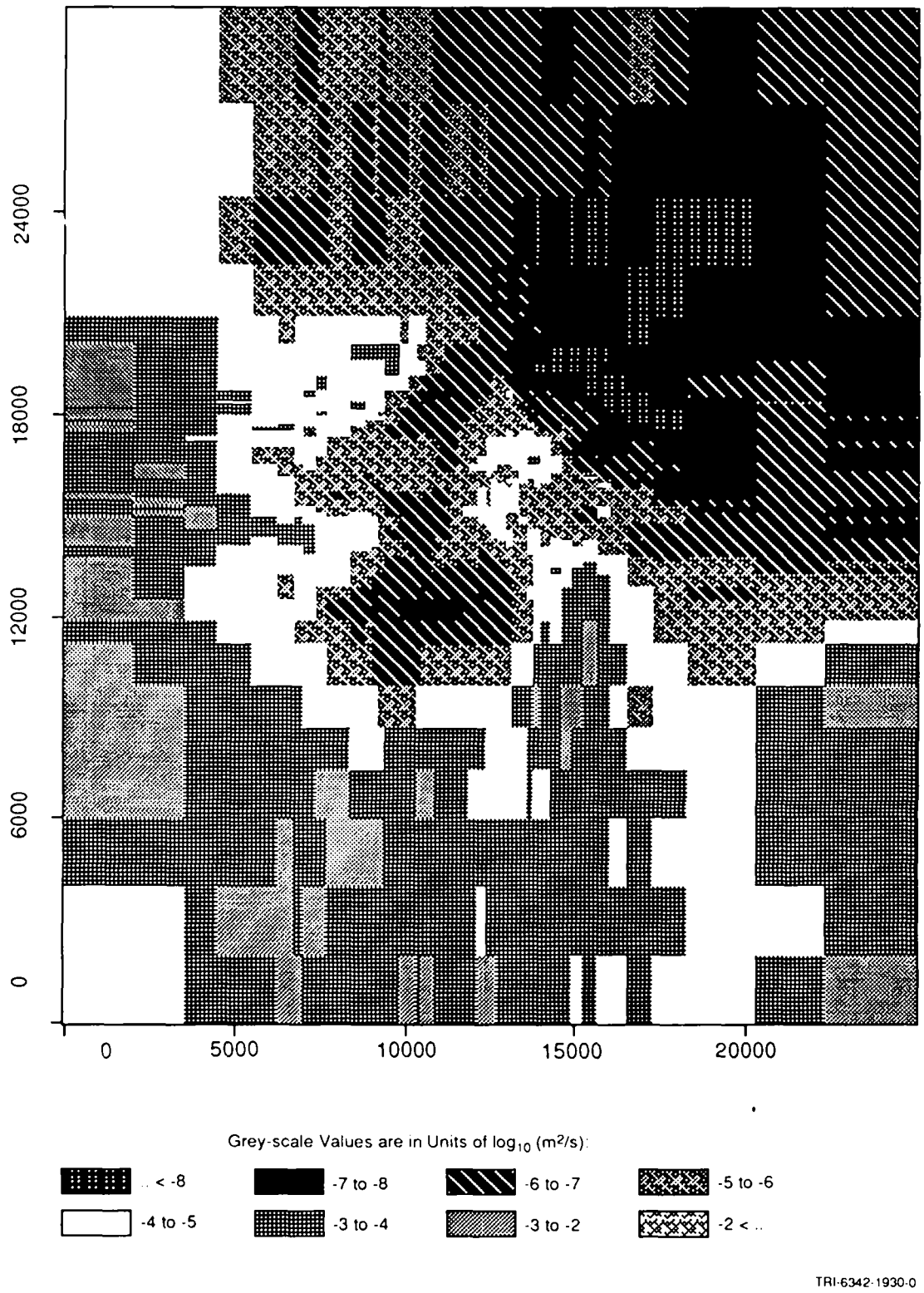

Figure C-31. Realization 48 of Culebra transmissivity.

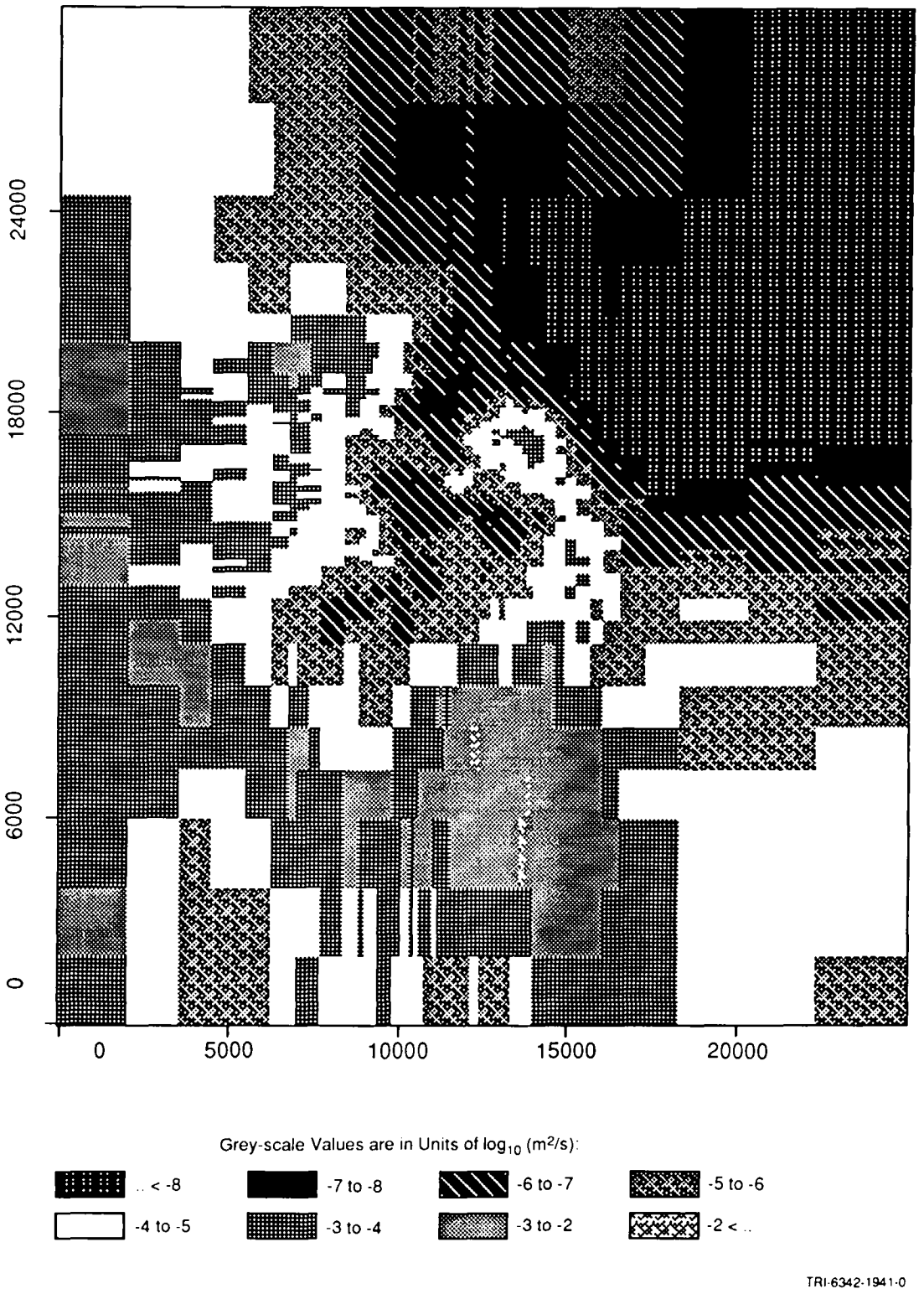

Figure C-32. Realization 29 of Culebra transmissivity.

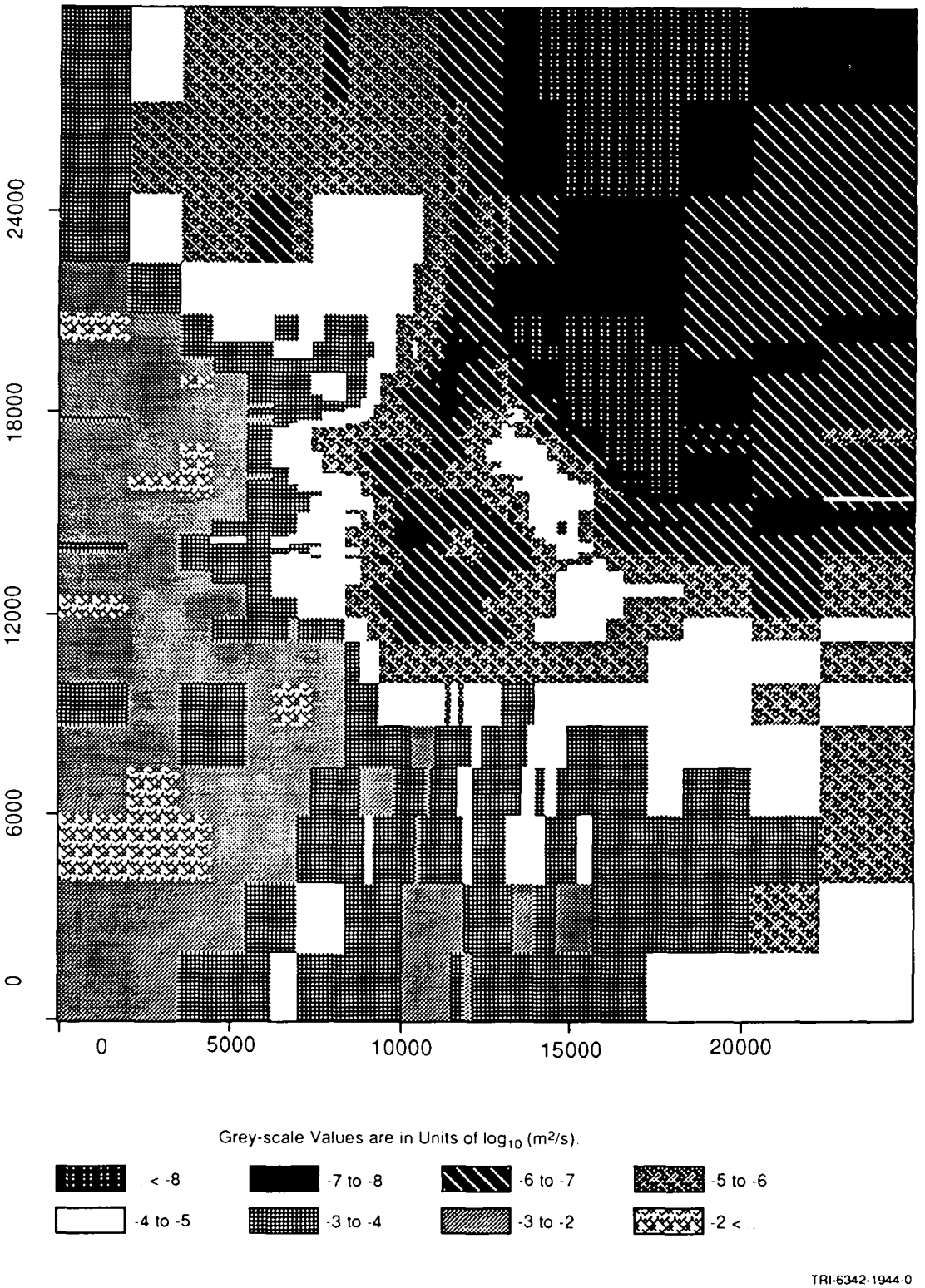

Figure C-33. Realization 68 of Culebra transmissivity.

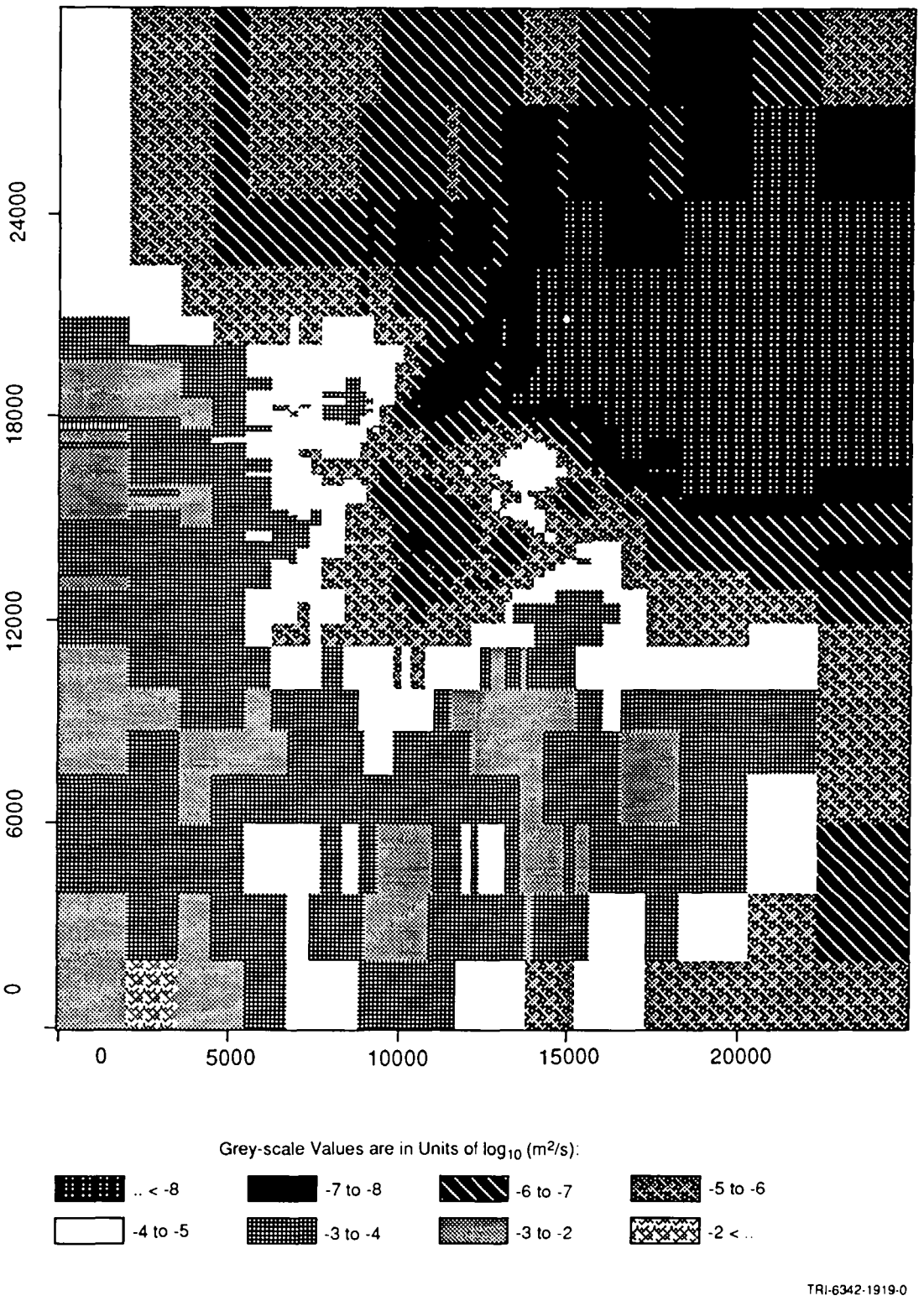

Figure C-34. Realization 40 of Culebra transmissivity.

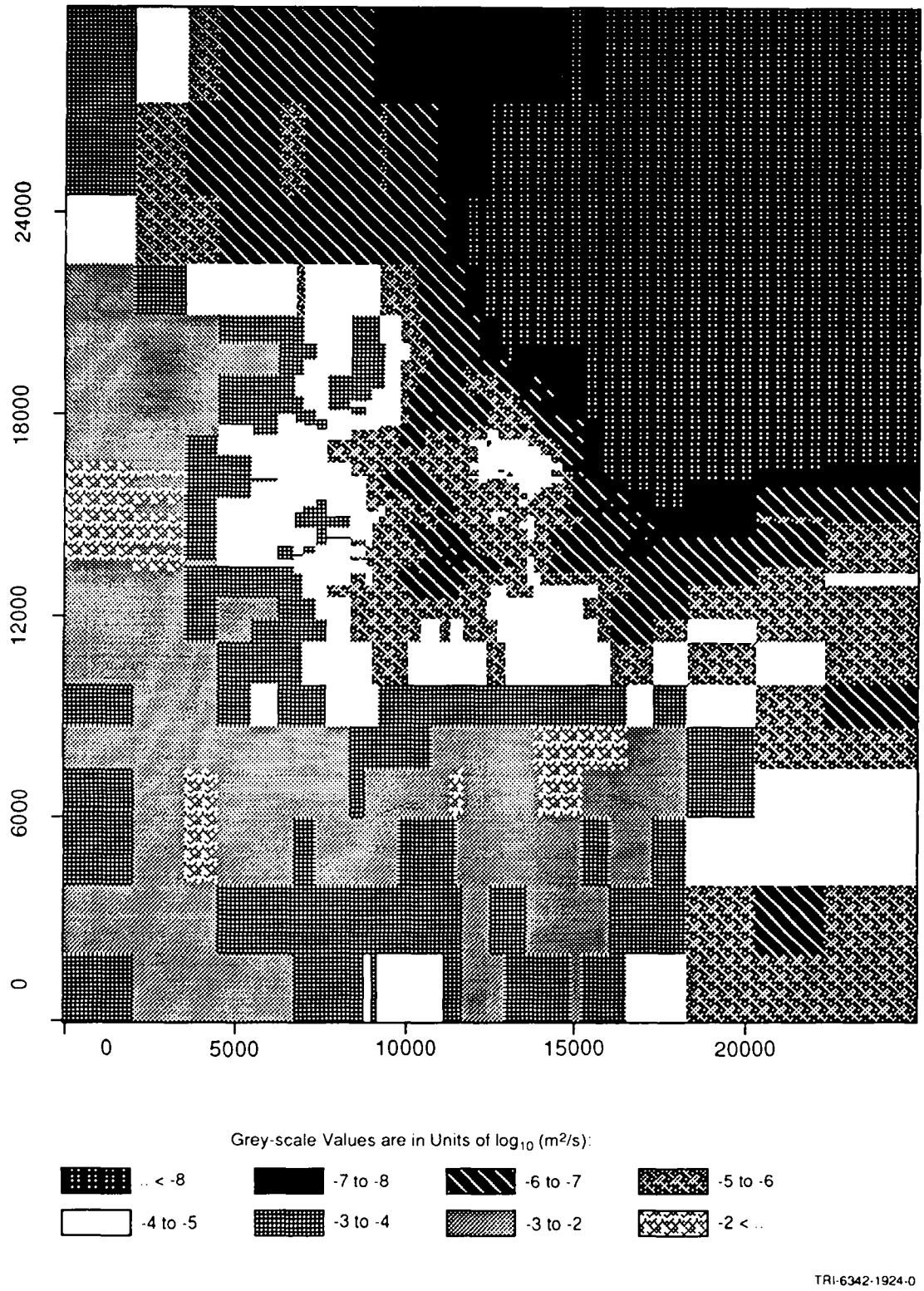

Figure C-35. Realization 5 of Culebra transmissivity.

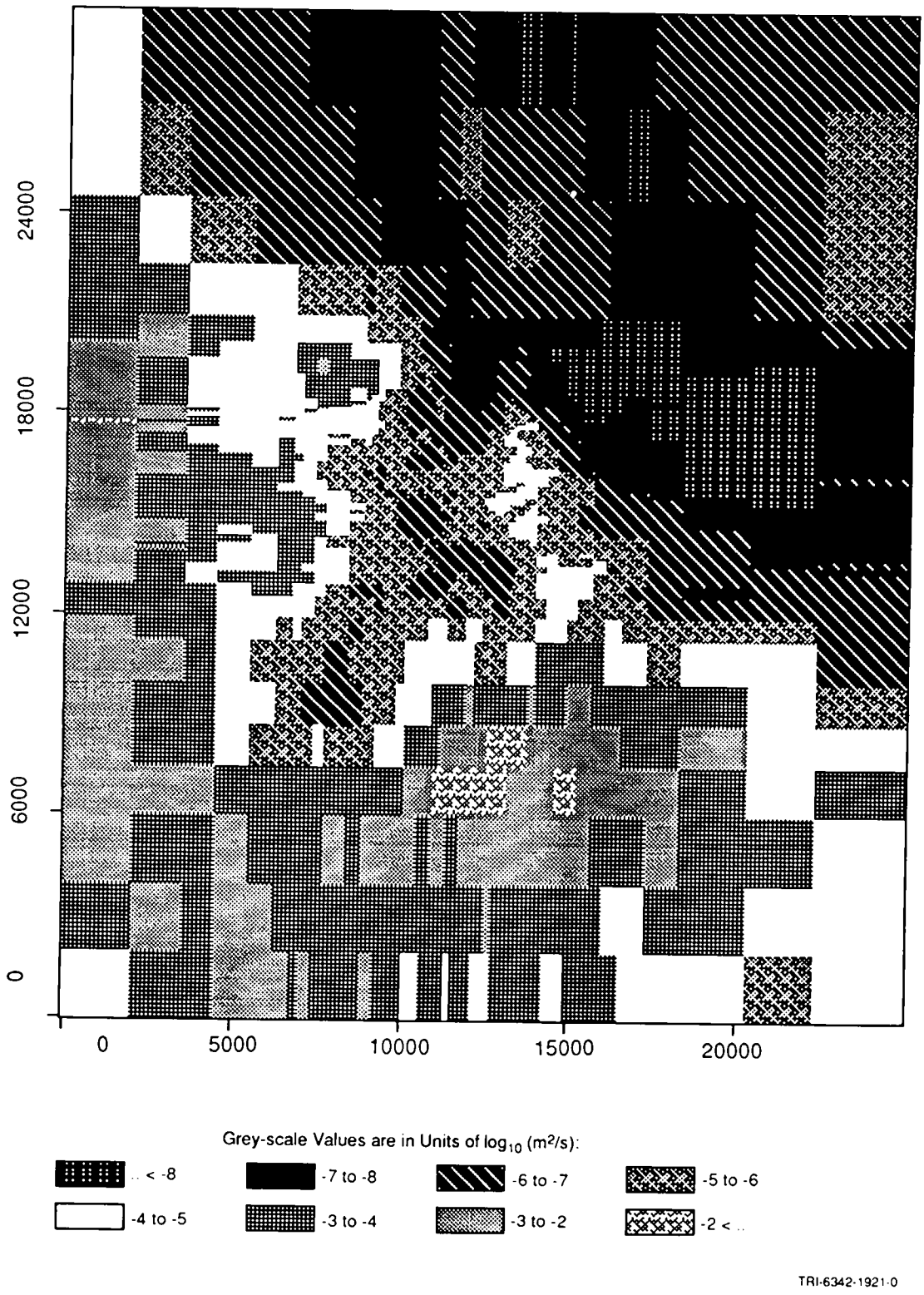

Figure C-36. Realization 61 of Culebra transmissivity.

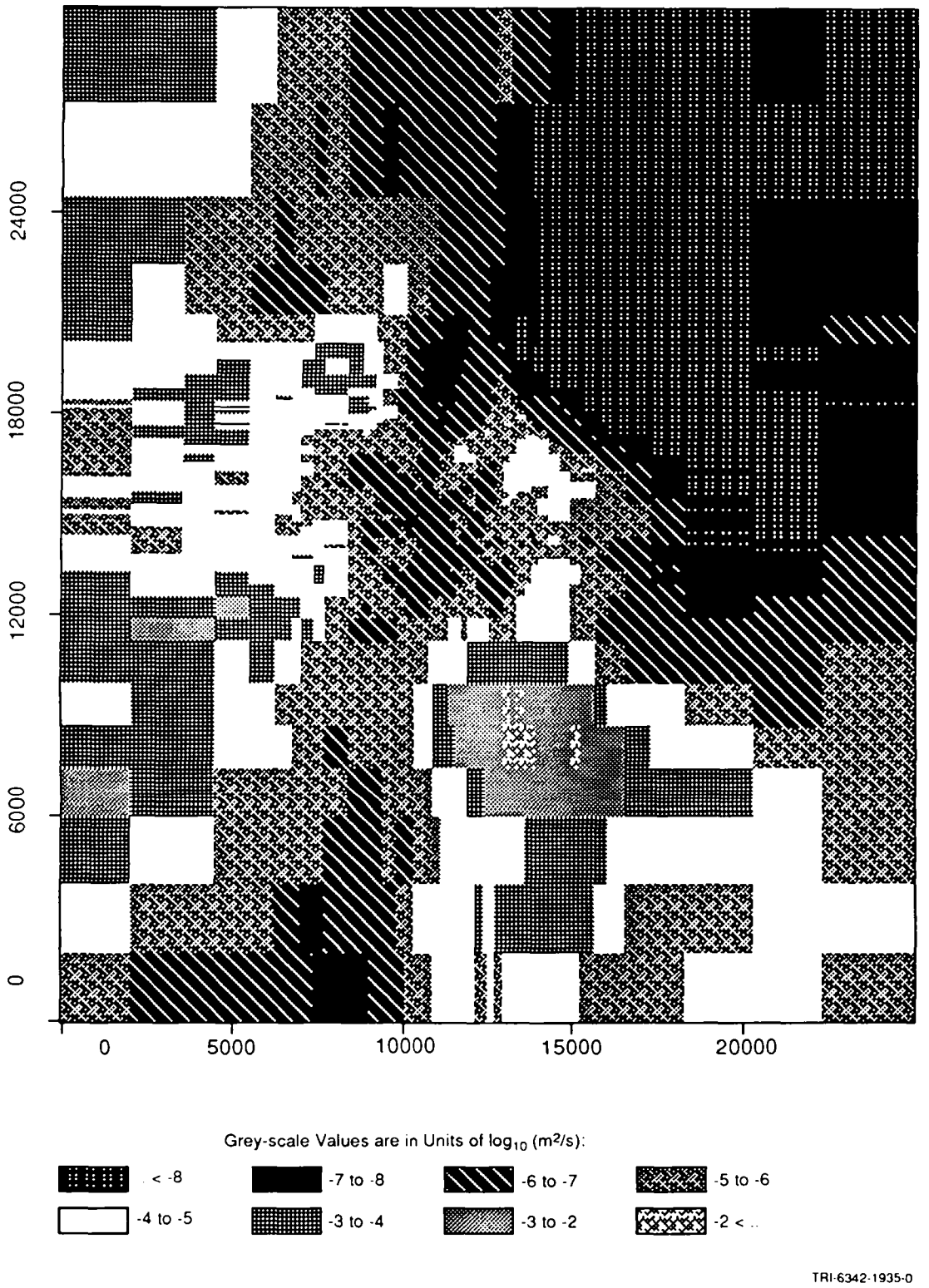

Figure C-37. Realization 14 of Culebra transmissivity.

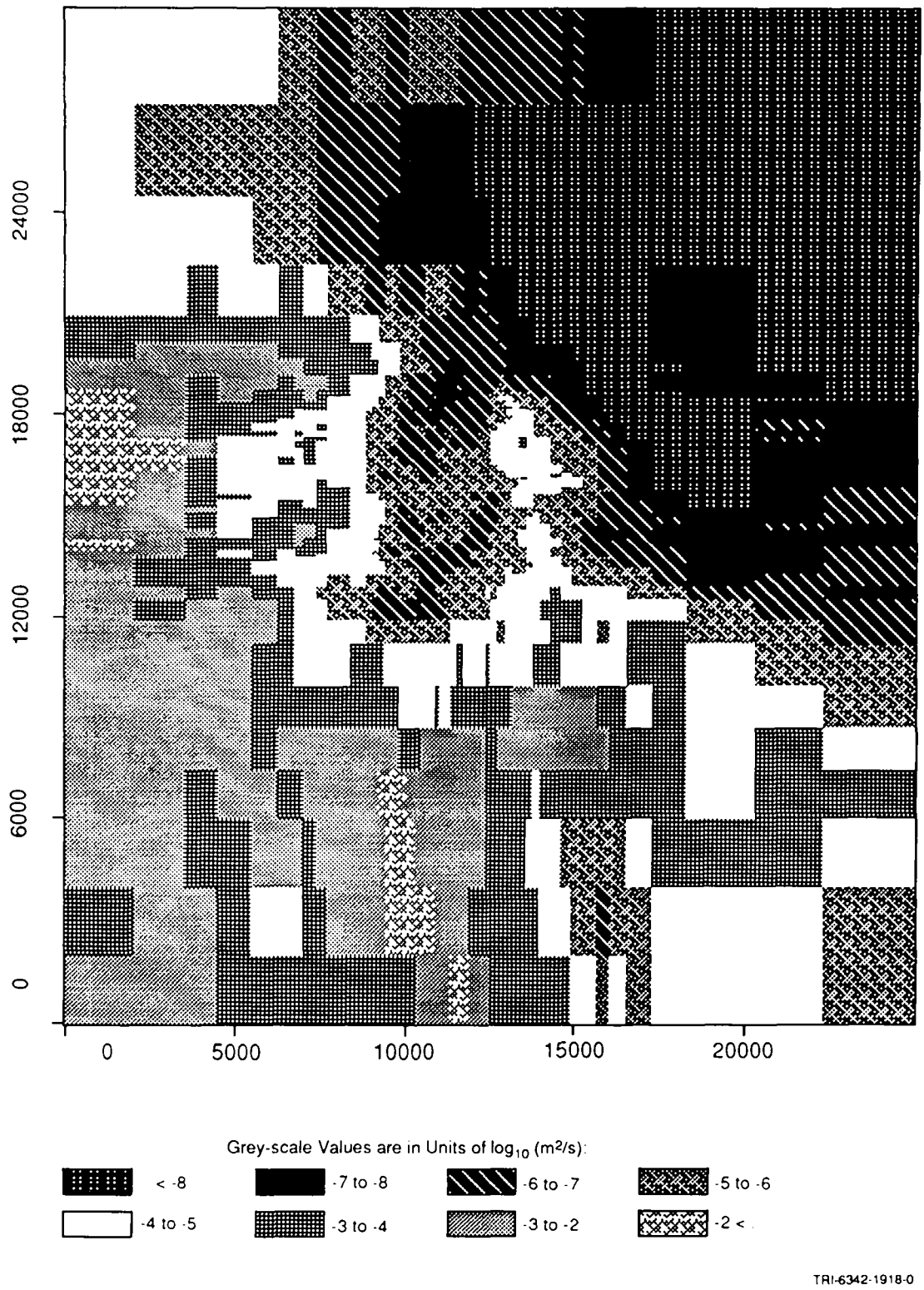

Figure C-38. Realization 31 of Culebra transmissivity.

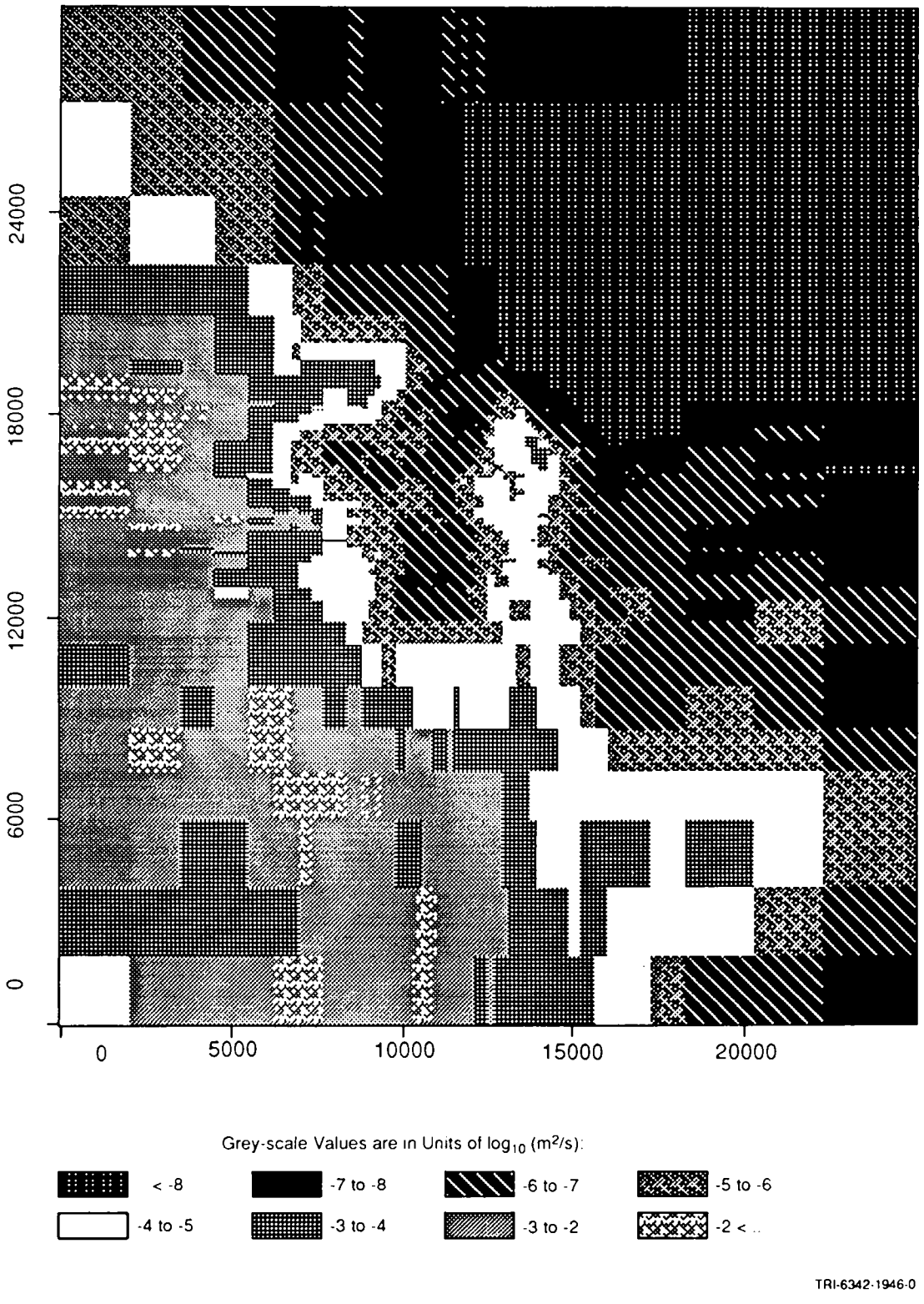

Figure C-39. Realization 38 of Culebra transmissivity.

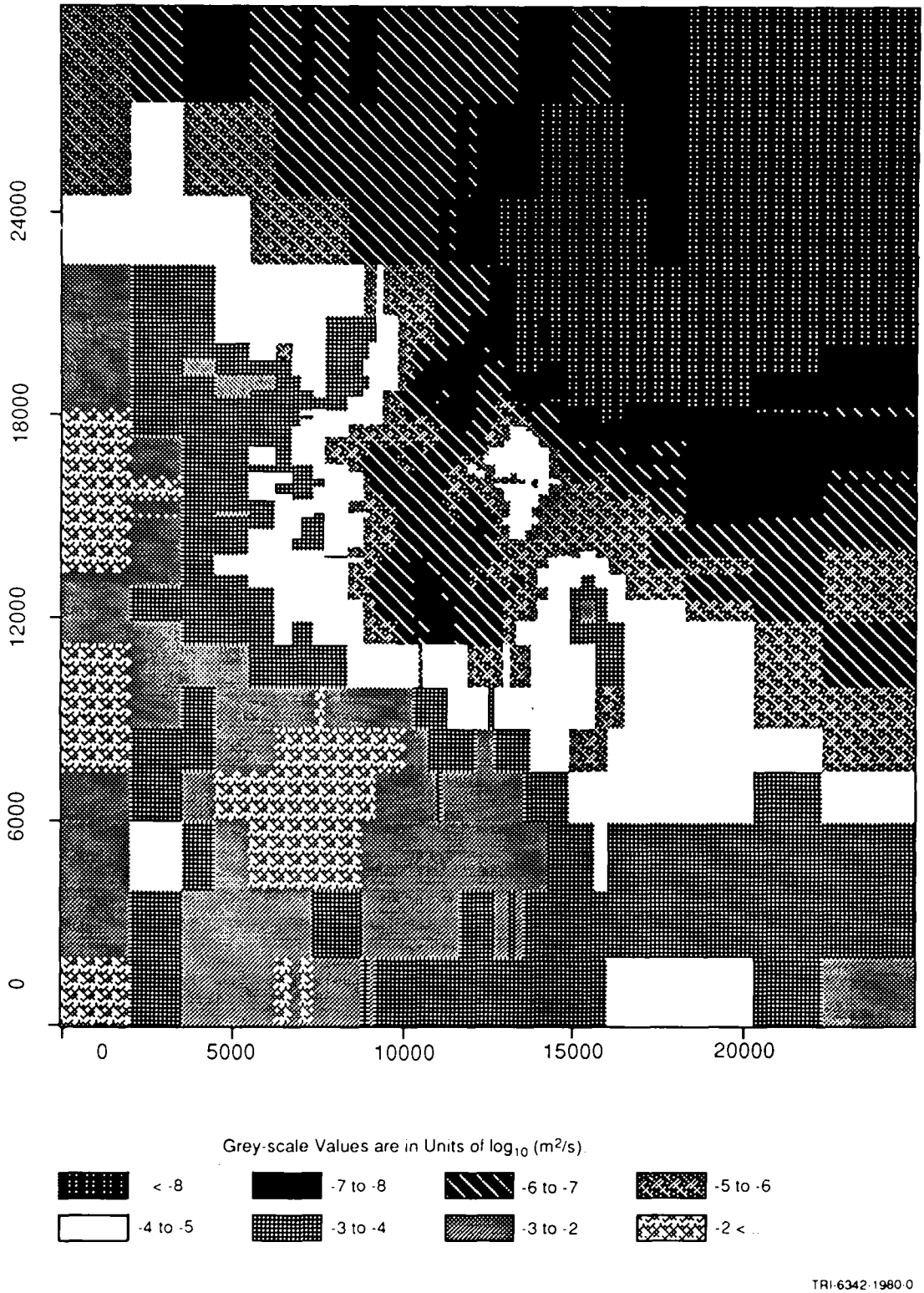

Figure C-40. Realization 27 of Culebra transmissivity.

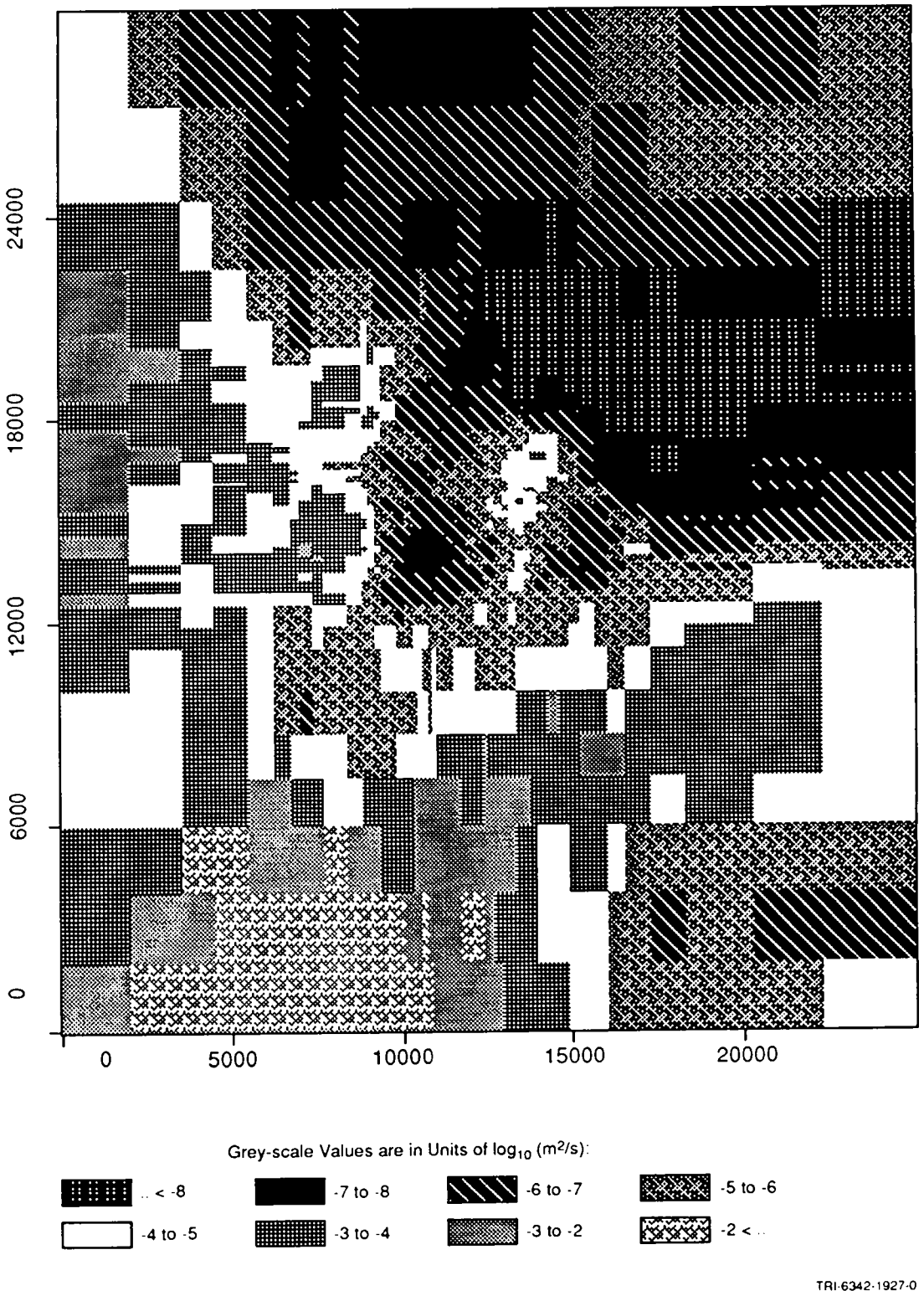

Figure C-41. Realization 4 of Culebra transmissivity.

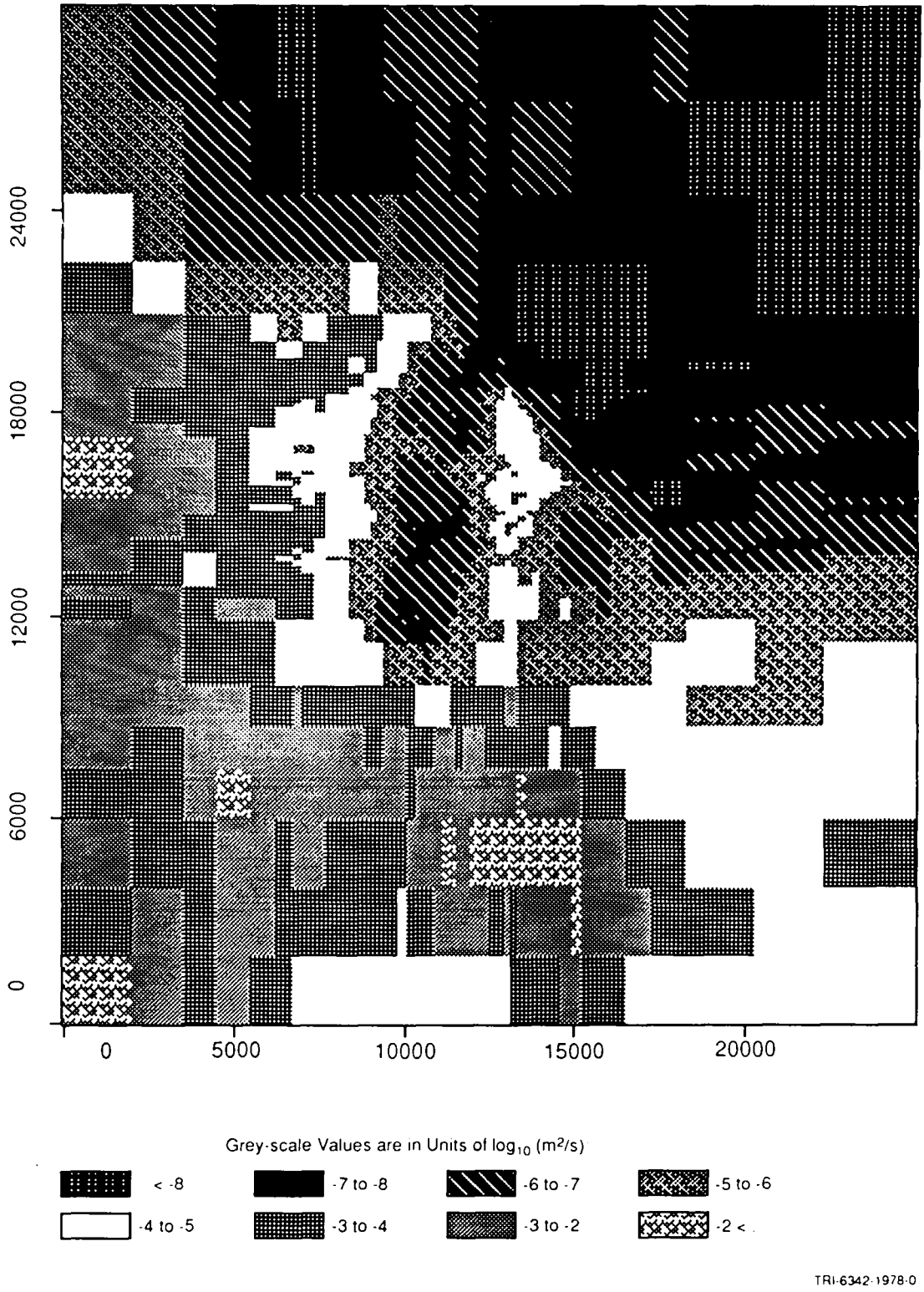

Figure C-42. Realization 59 of Culebra transmissivity.

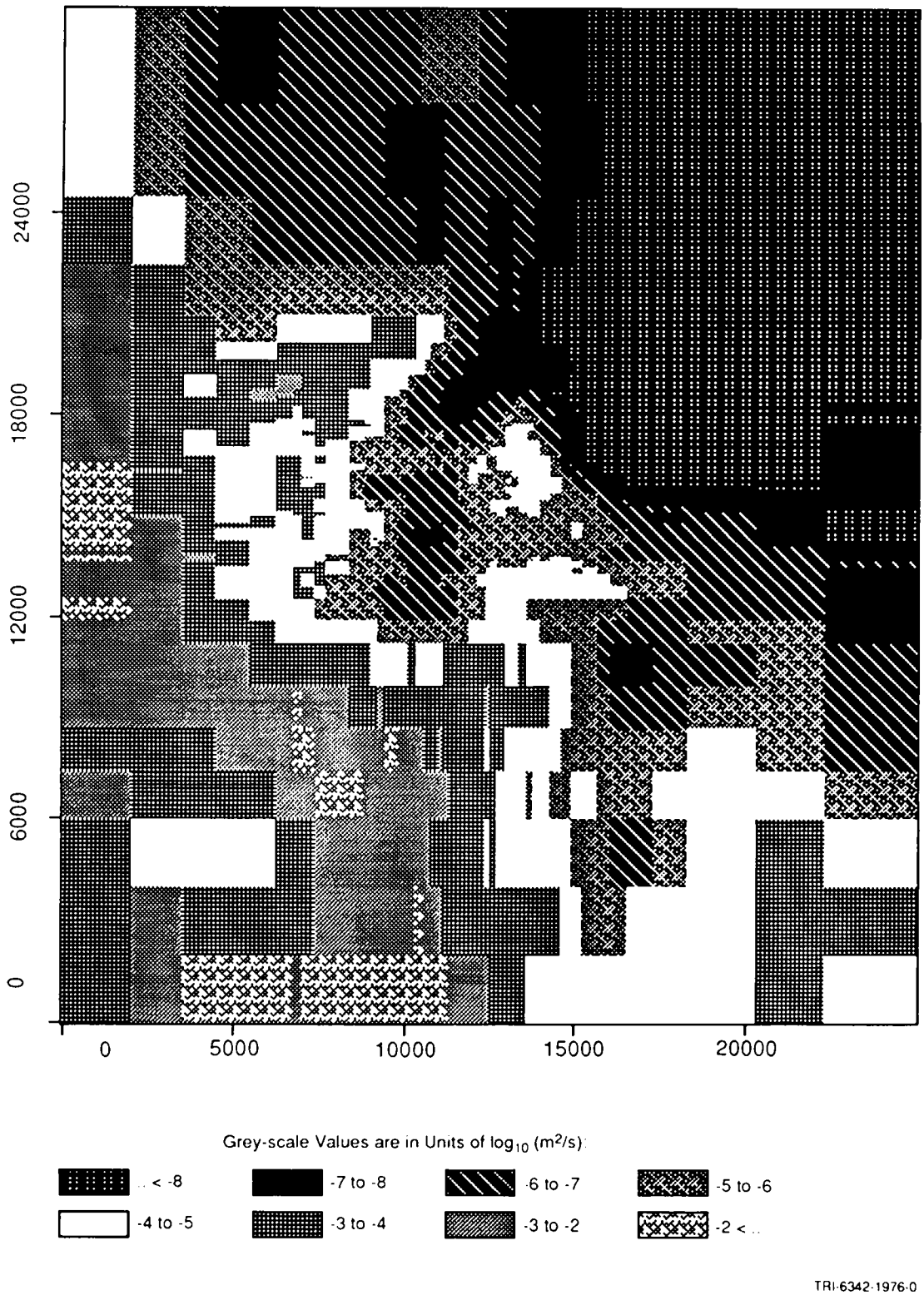

Figure C-43. Realization 17 of Culebra transmissivity.

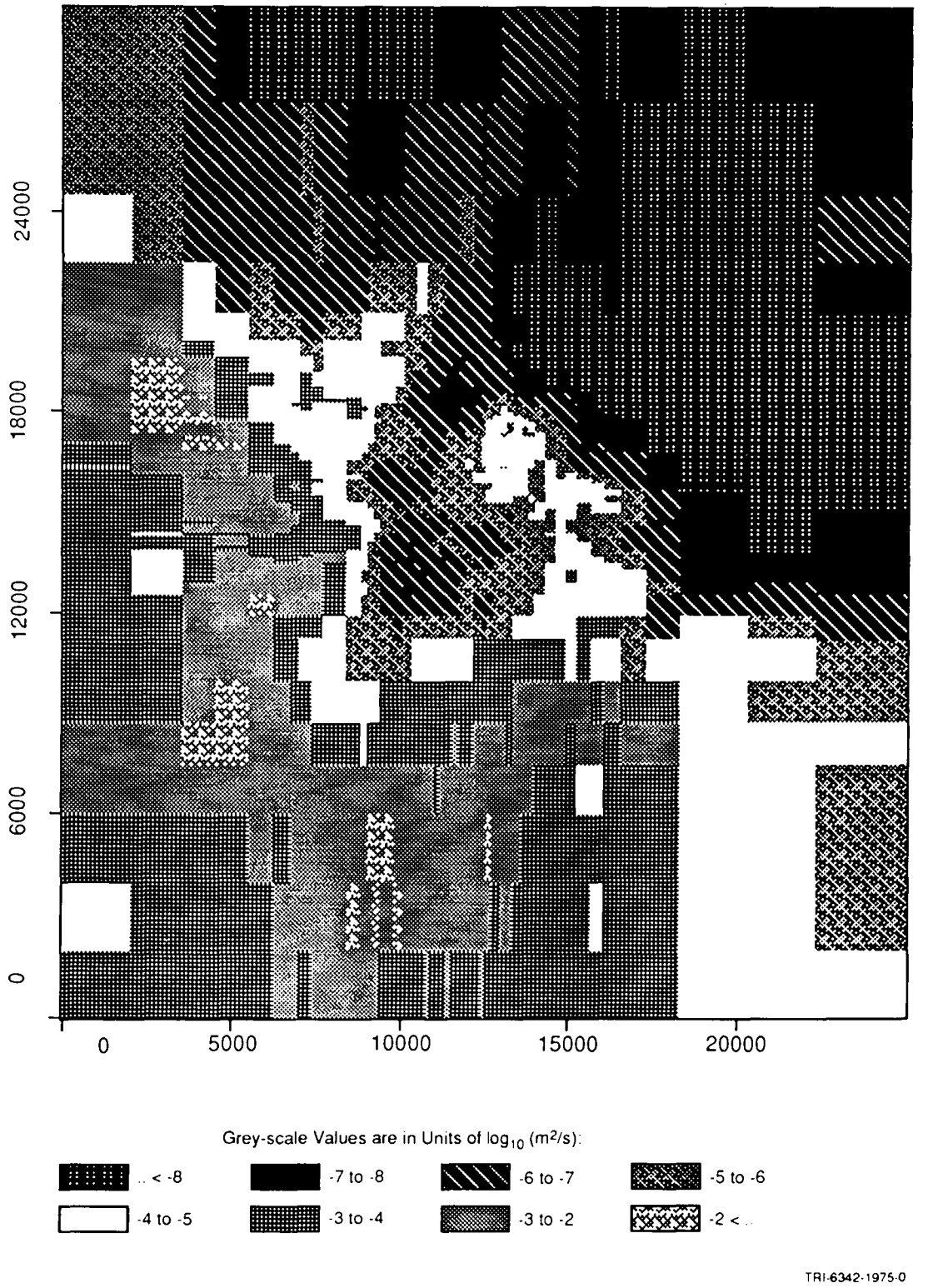

Figure C-44. Realization 51 of Culebra transmissivity.

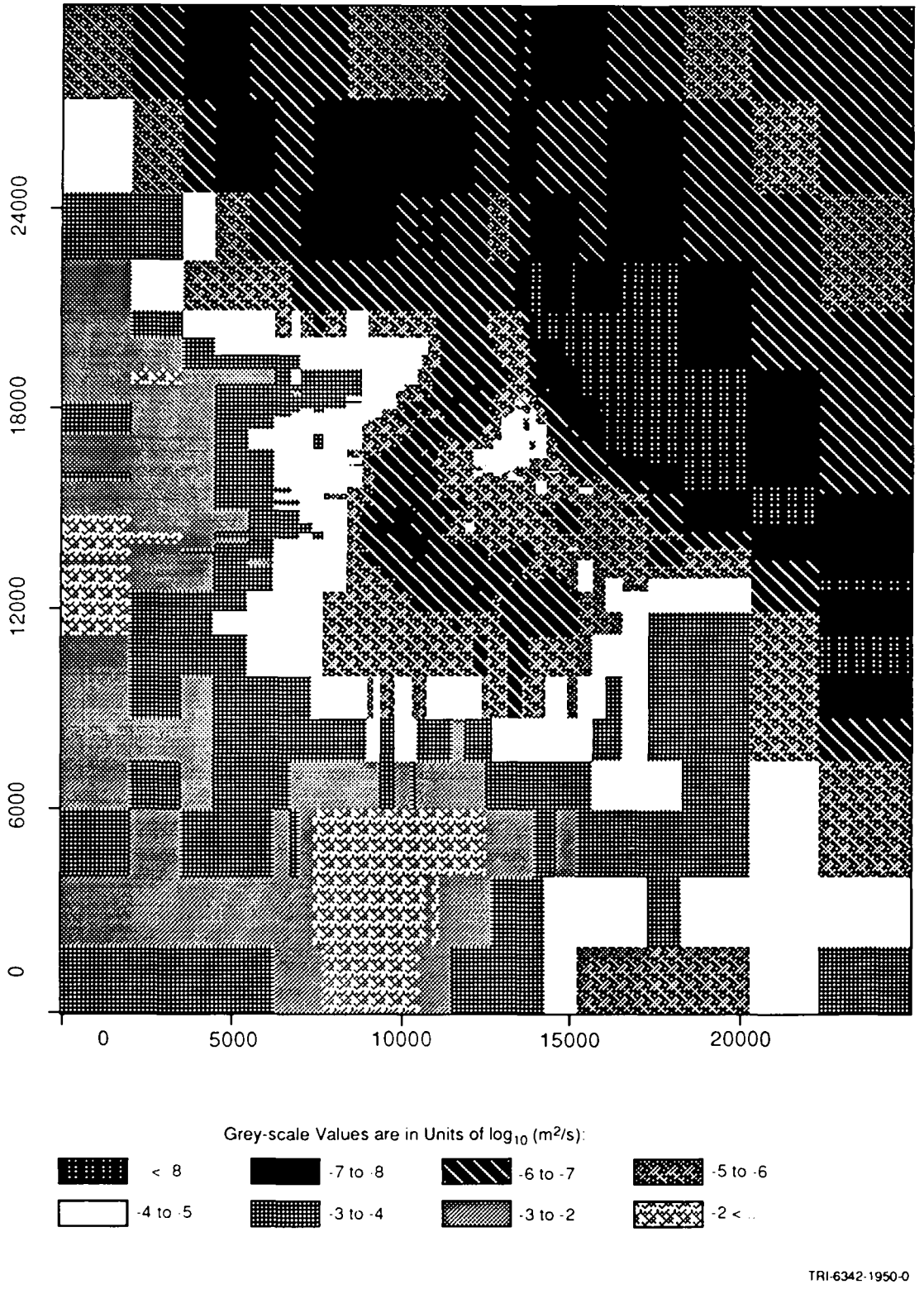

Figure C-45. Realization 9 of Culebra transmissivity.

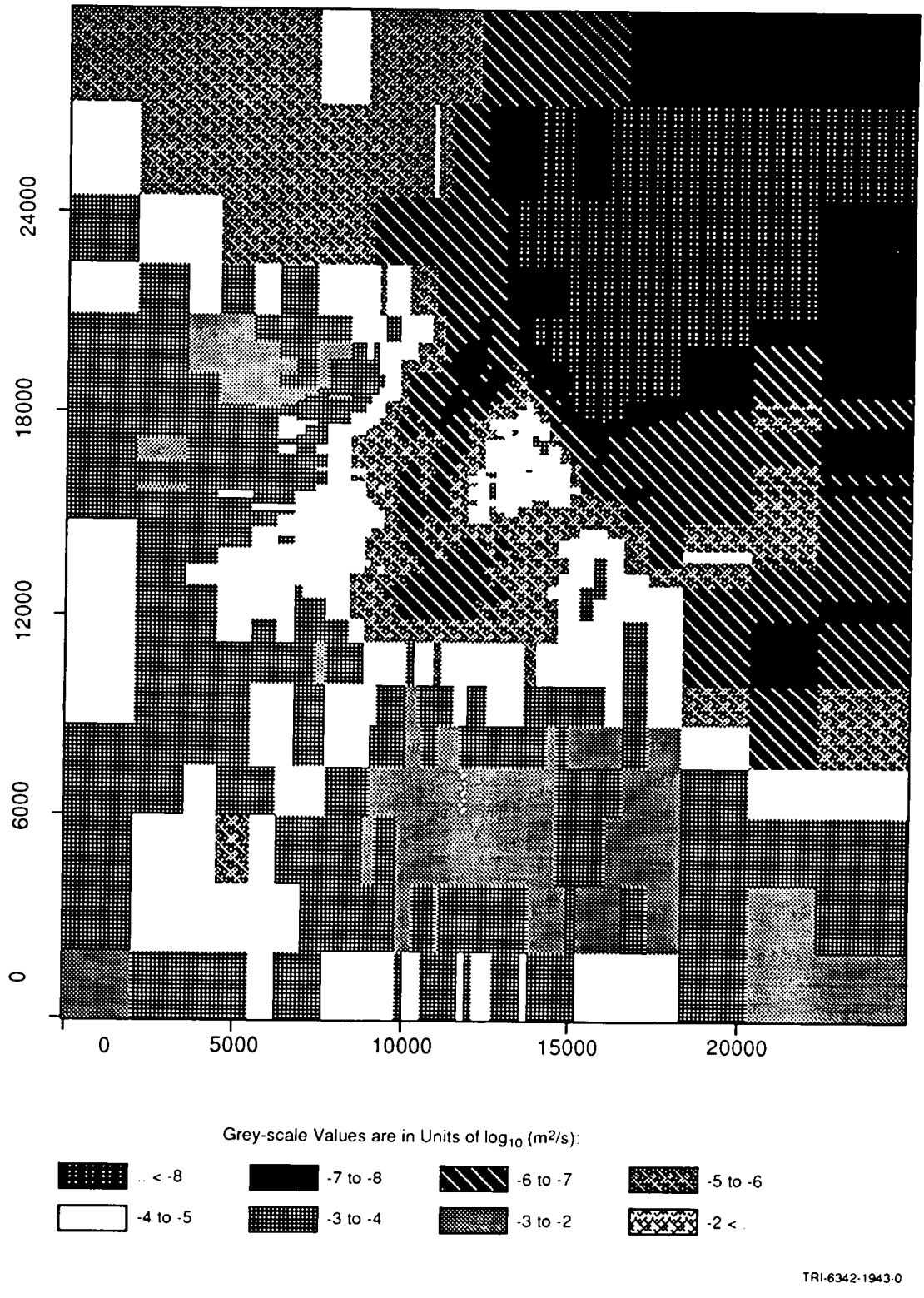

Figure C-46. Realization 30 of Culebra transmissivity.

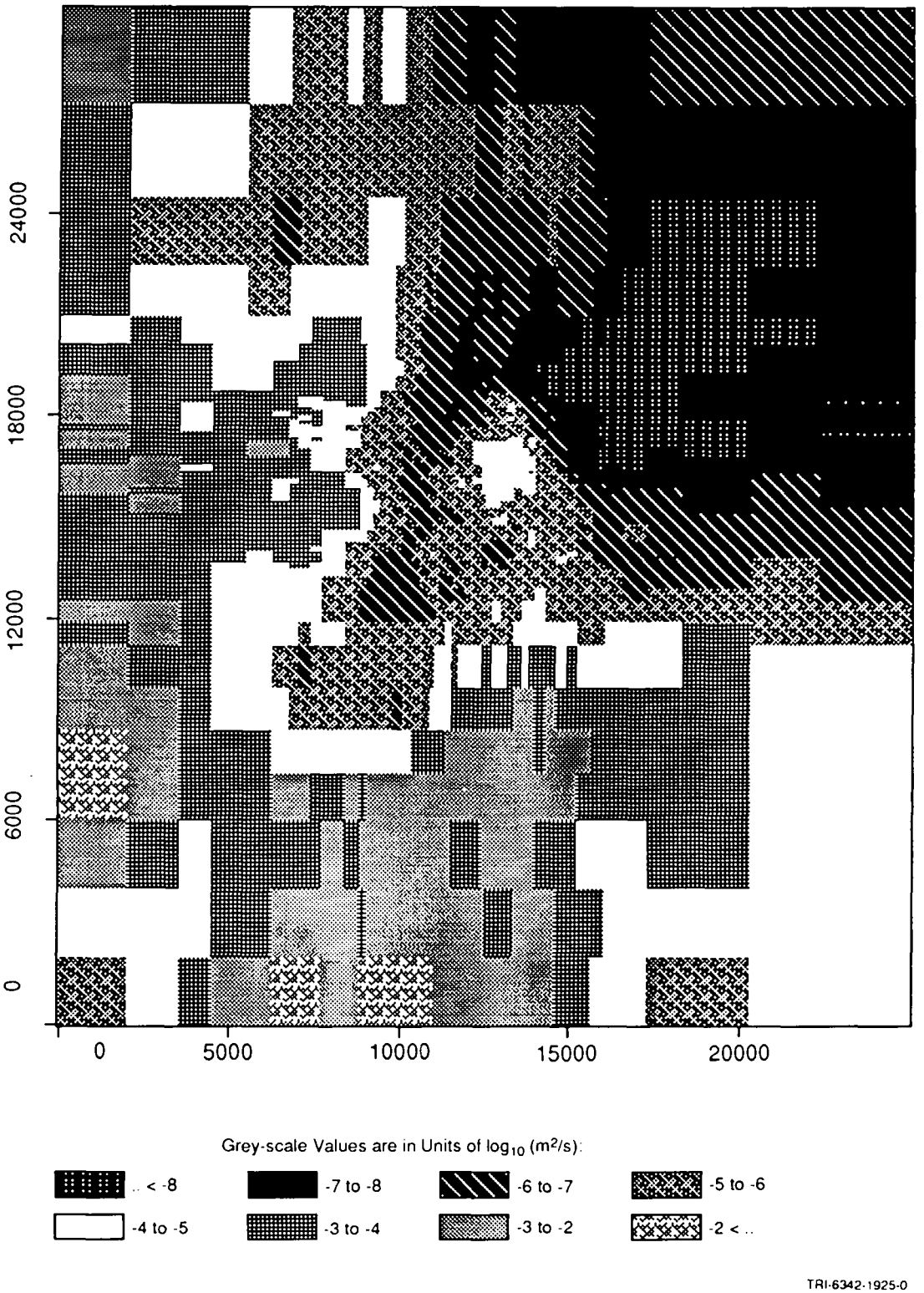

Figure C-47. Realization 46 of Culebra transmissivity.

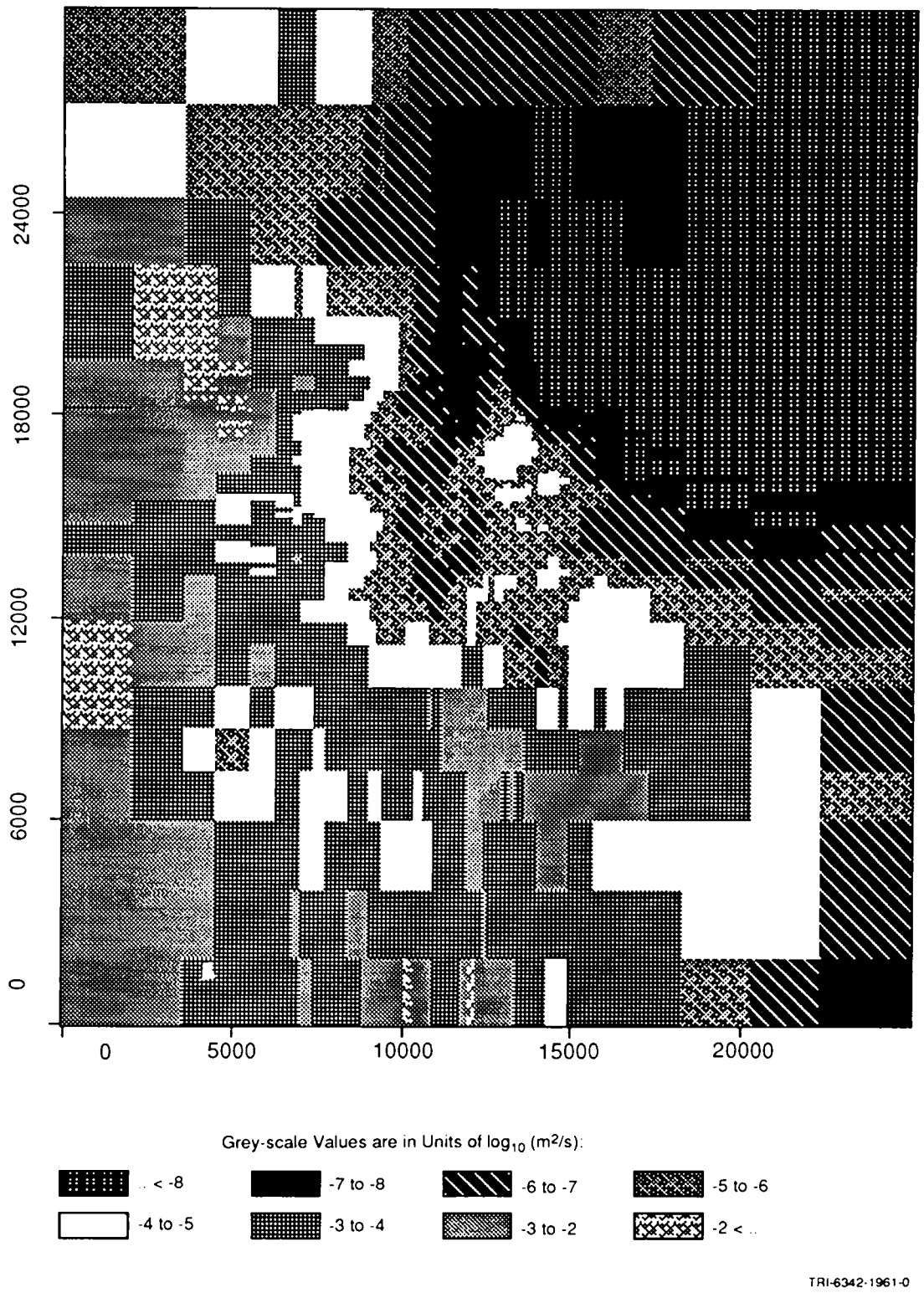

Figure C-48. Realization 3 of Culebra transmissivity.

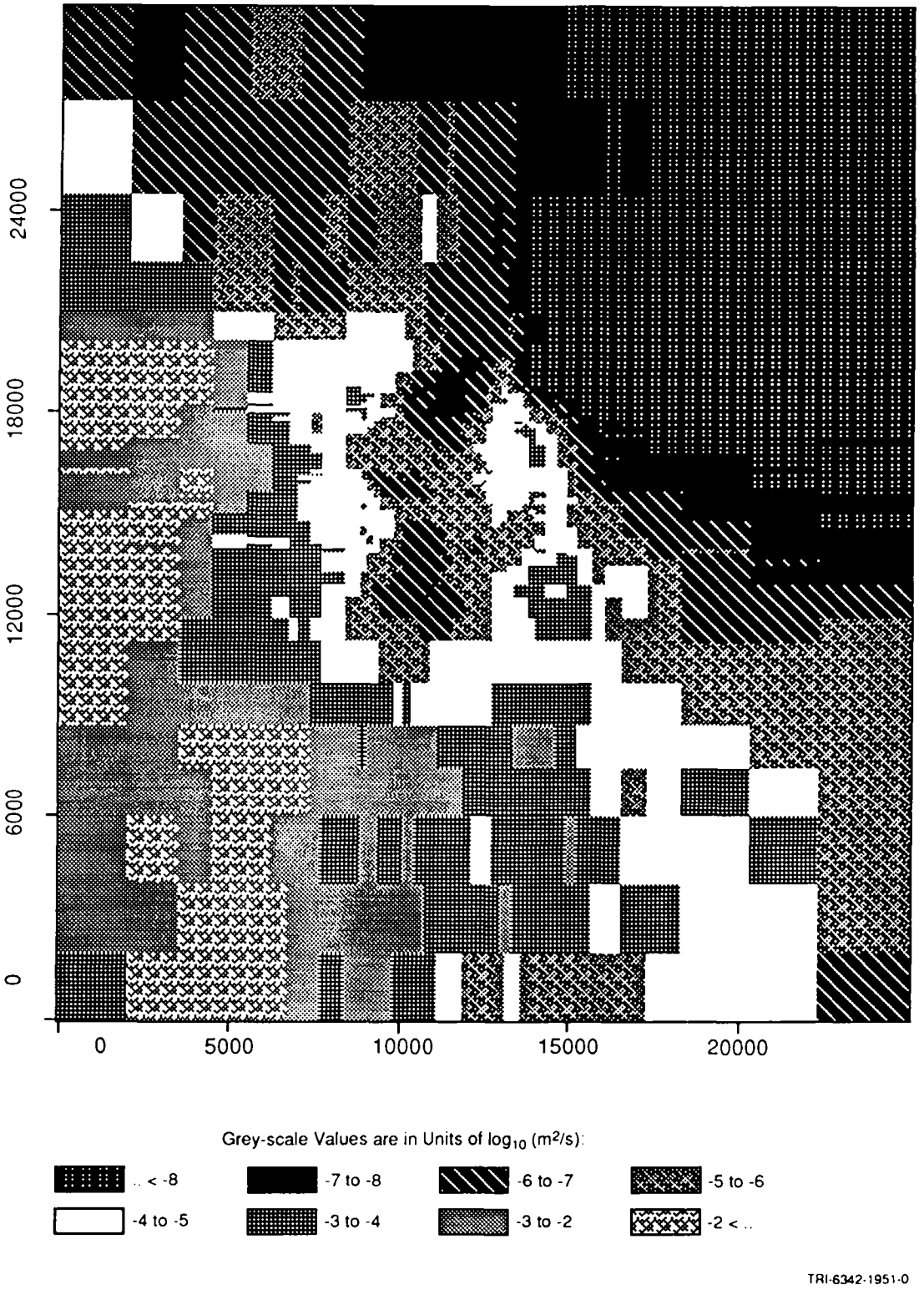

Figure C-49. Realization 62 of Culebra transmissivity.



Figure C-50. Realization 22 of Culebra transmissivity.

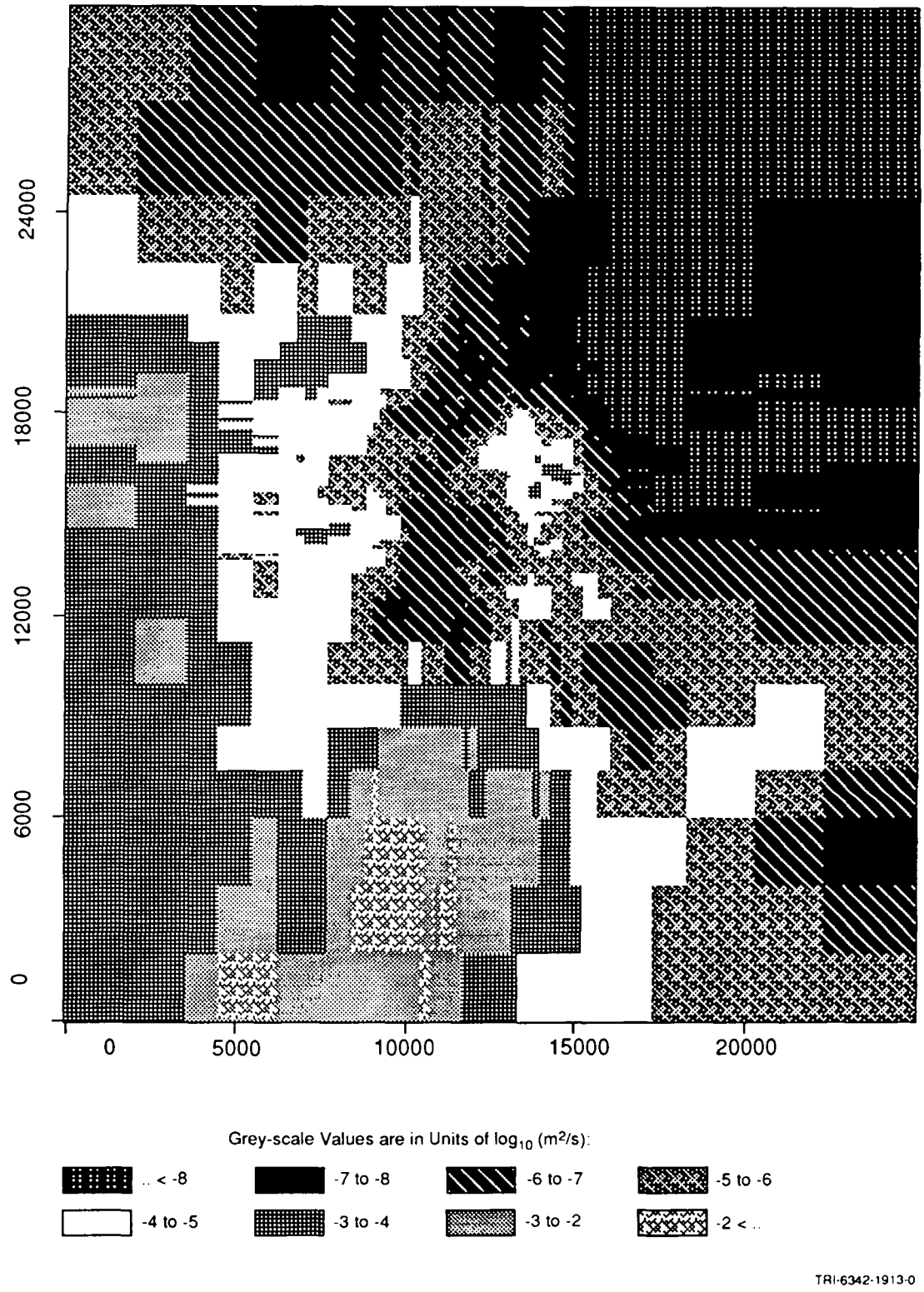

Figure C-51. Realization 50 of Culebra transmissivity.

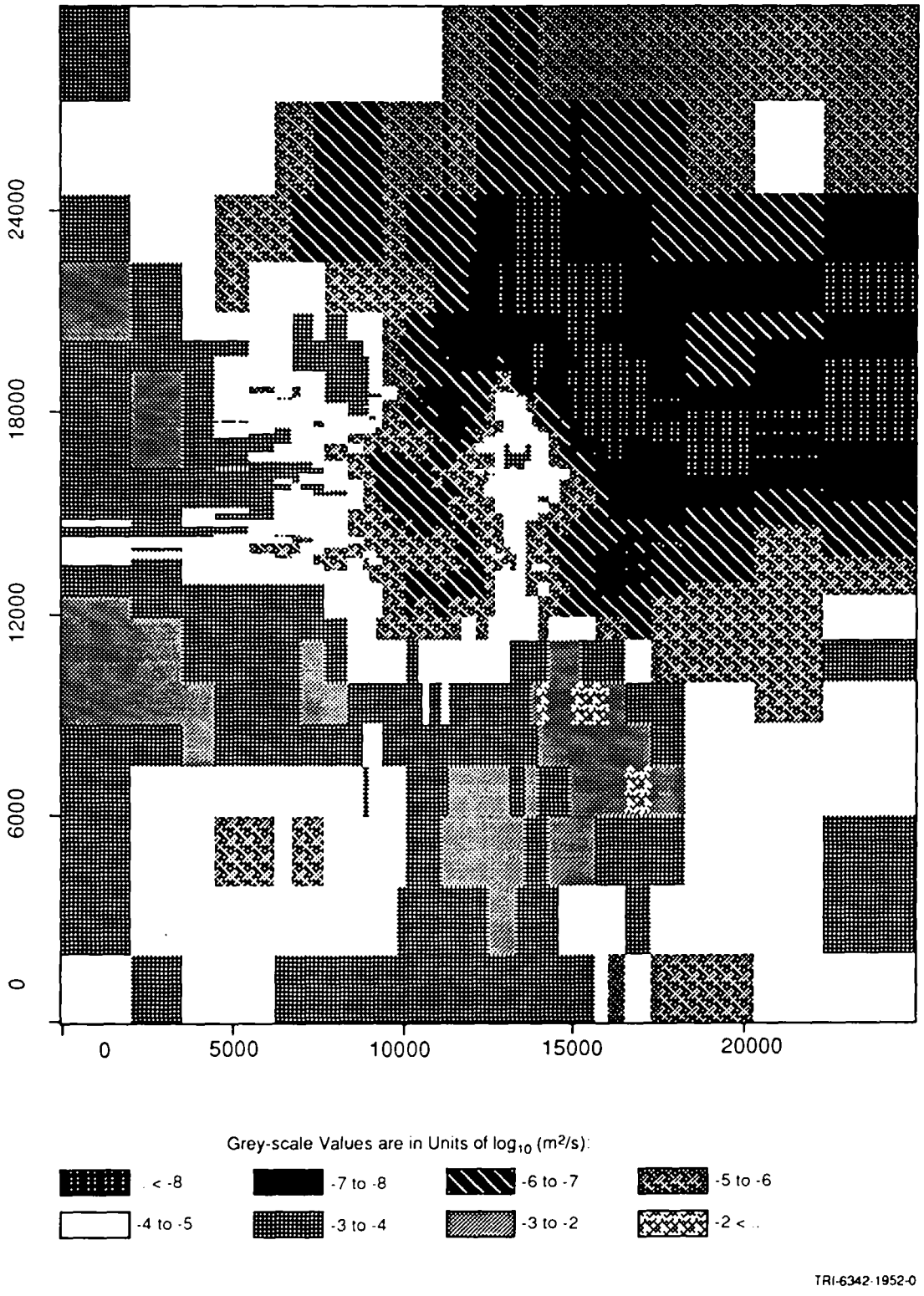

Figure C-52. Realization 35 of Culebra transmissivity.

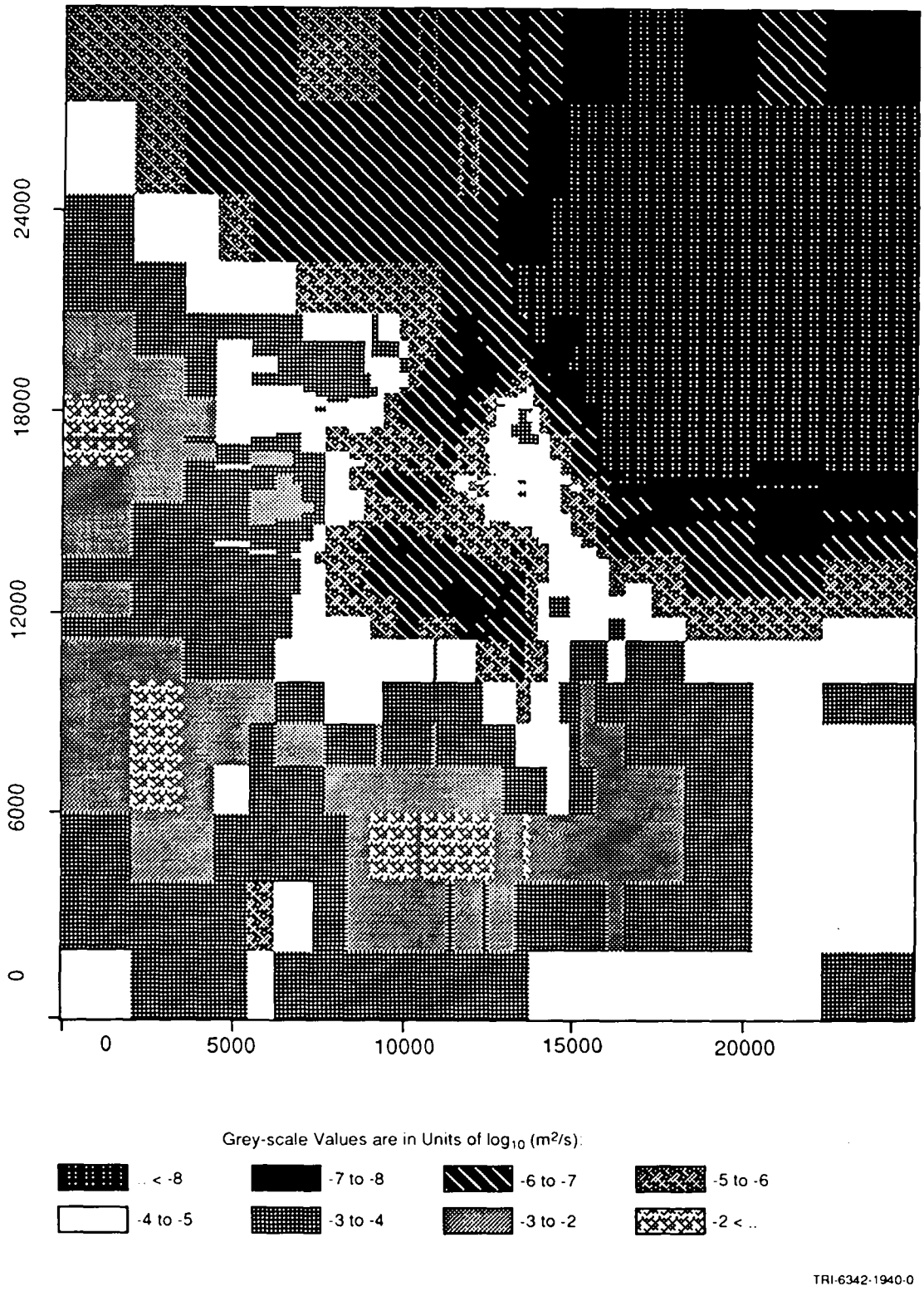

Figure C-53. Realization 57 of Culebra transmissivity.

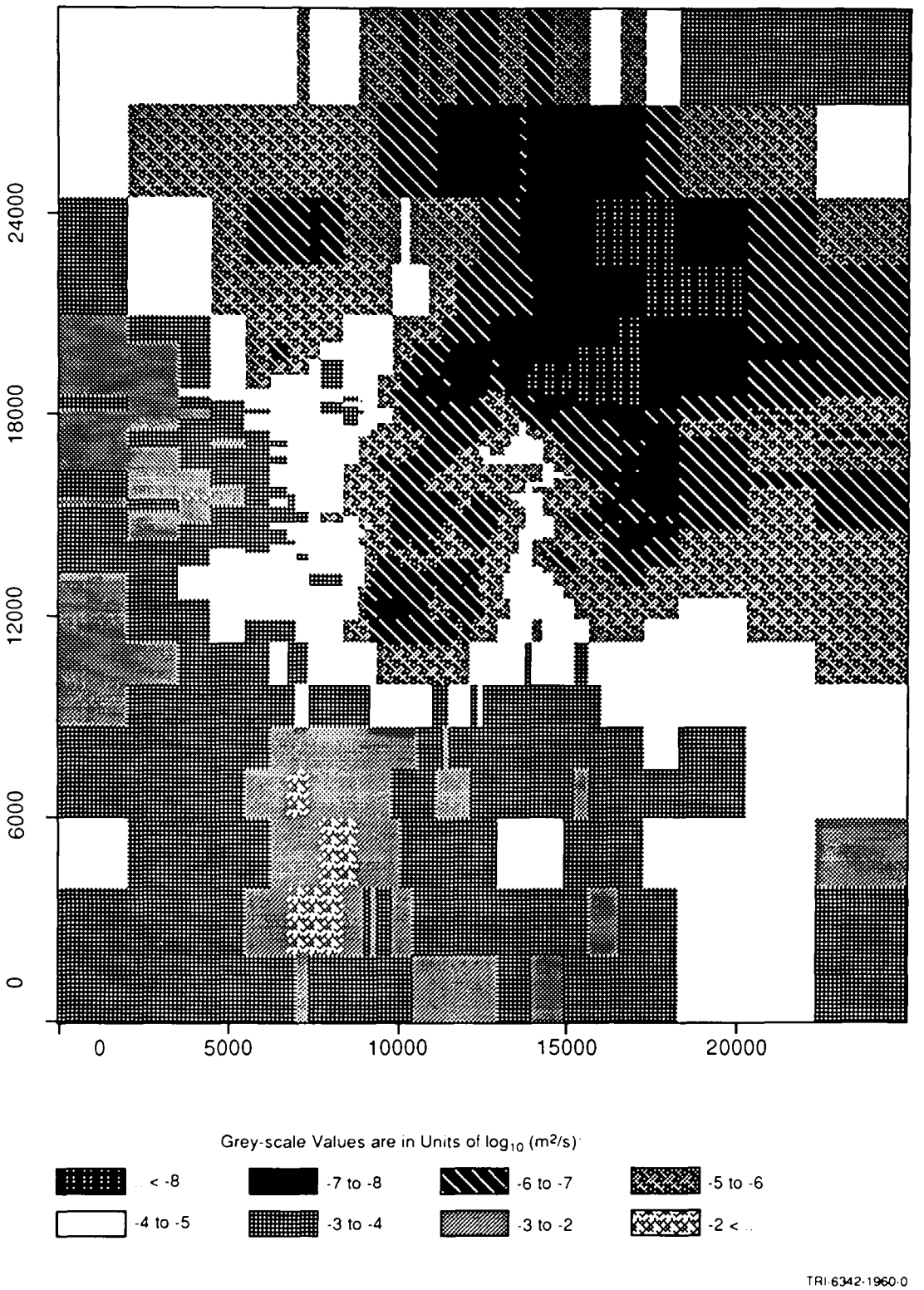

Figure C-54. Realization 49 of Culebra transmissivity.

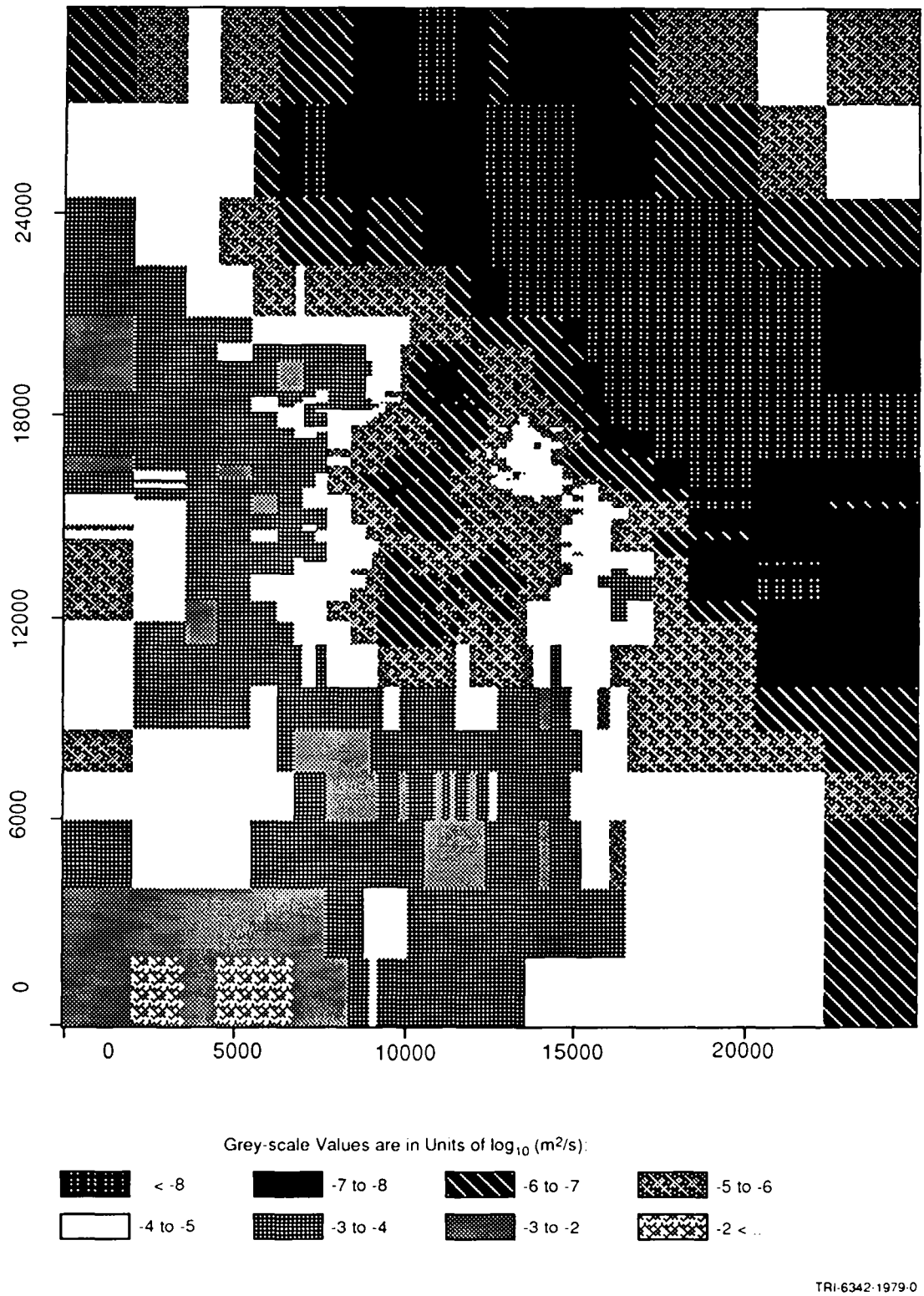

Figure C-55. Realization 65 of Culebra transmissivity.



Figure C-56. Realization 41 of Culebra transmissivity.

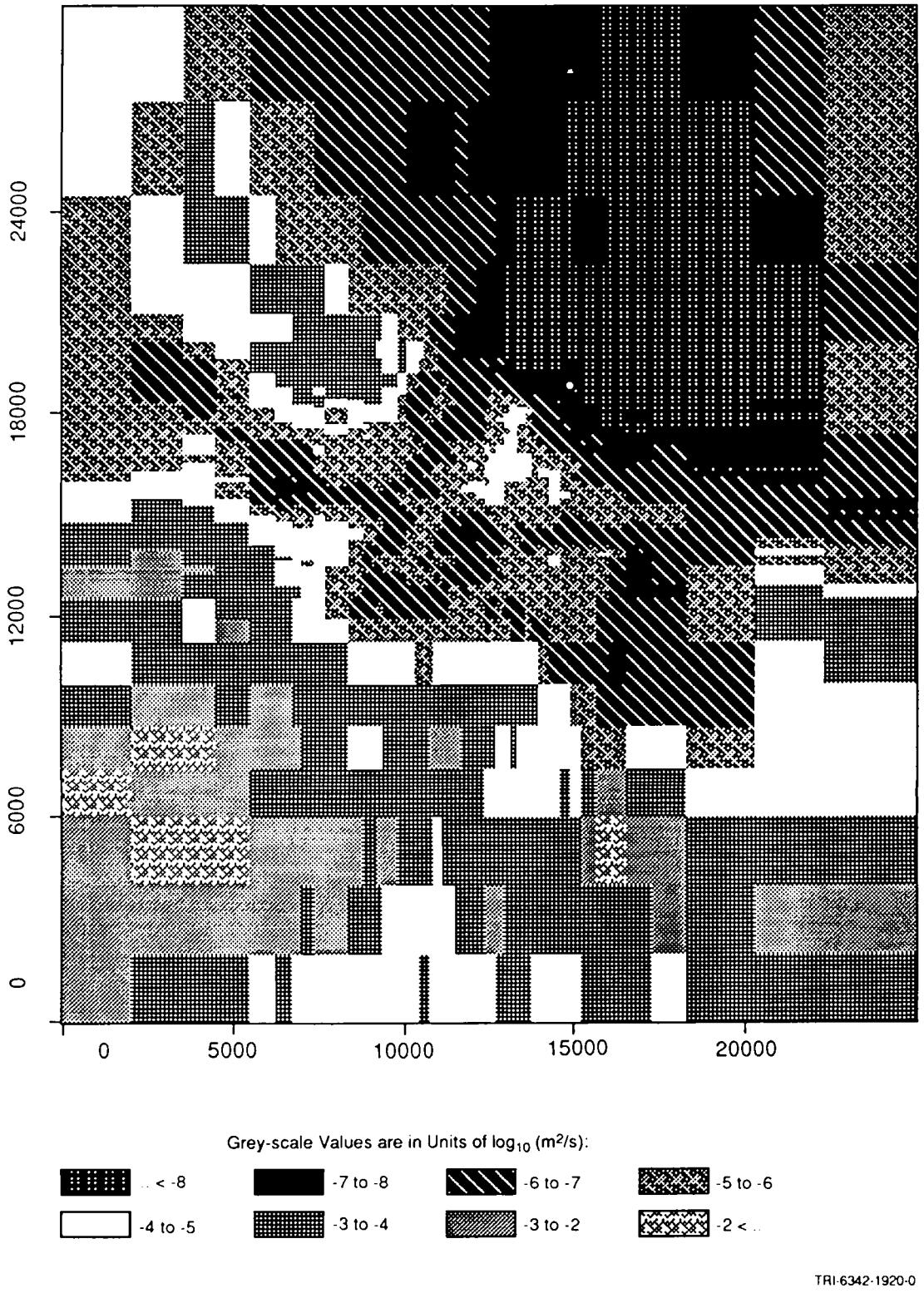

Figure C-57. Realization 26 of Culebra transmissivity.

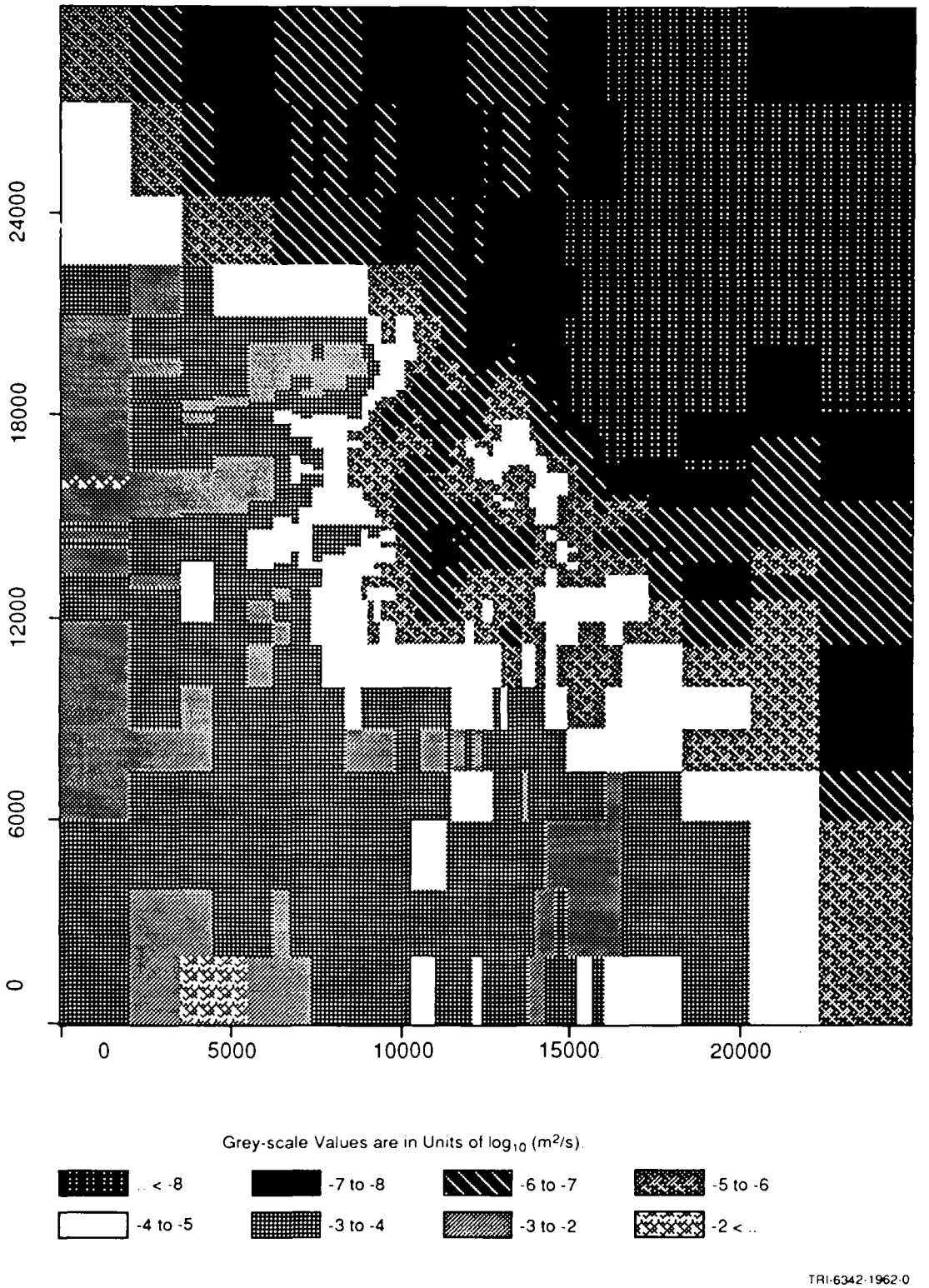

Figure C-58. Realization 37 of Culebra transmissivity.

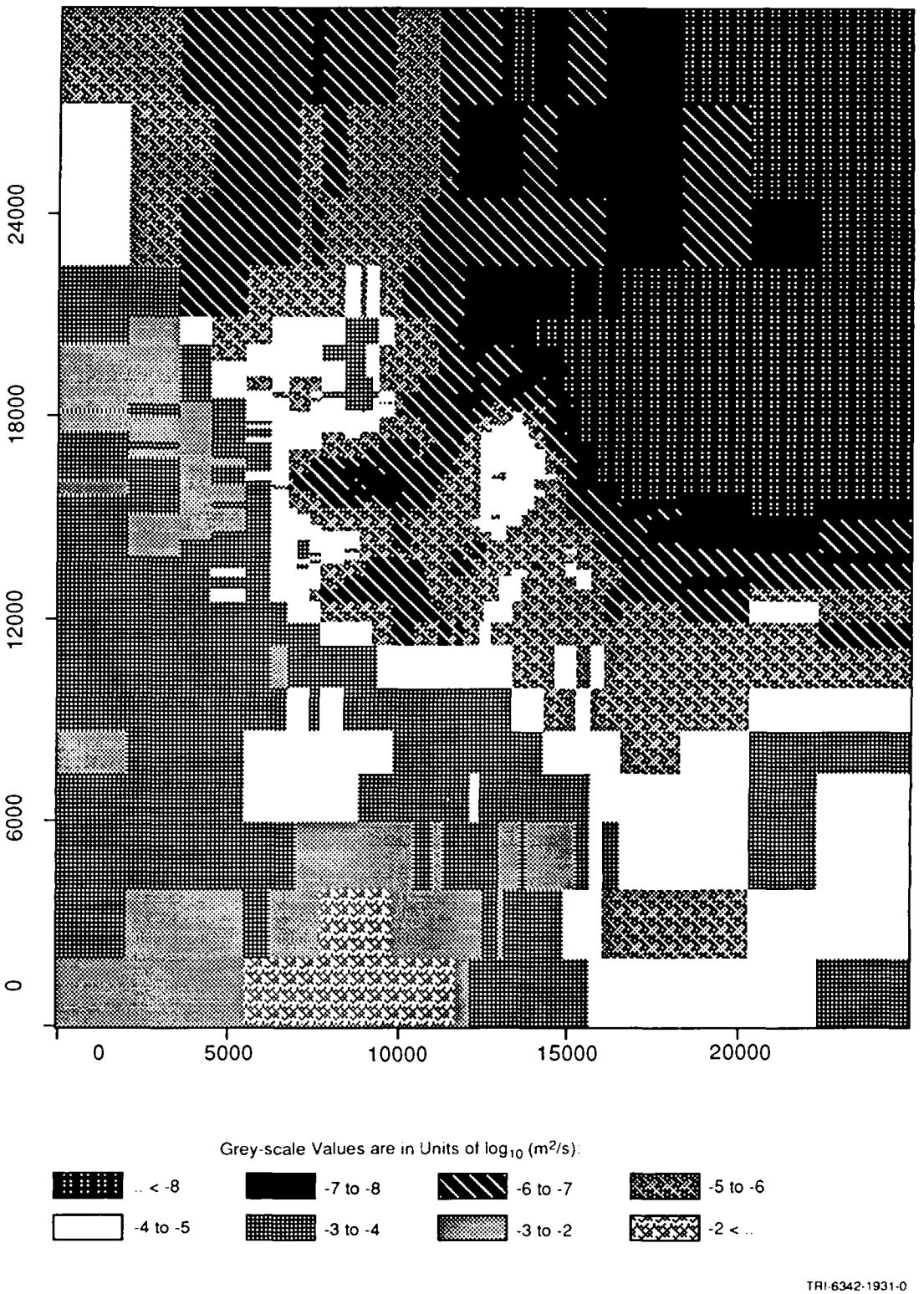

Figure C-59. Realization 44 of Culebra transmissivity.

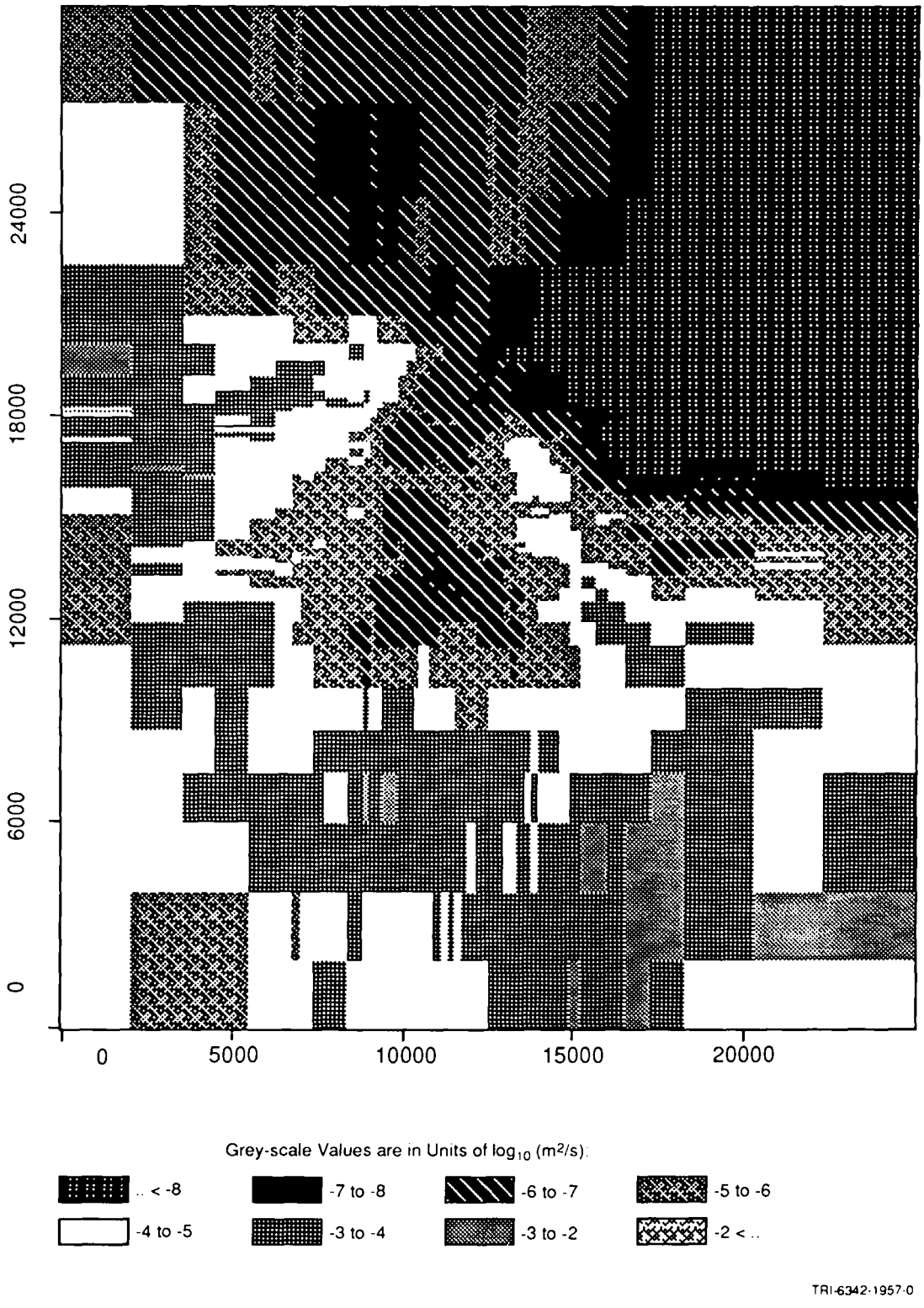

Figure C-60. Realization 60 of Culebra transmissivity.

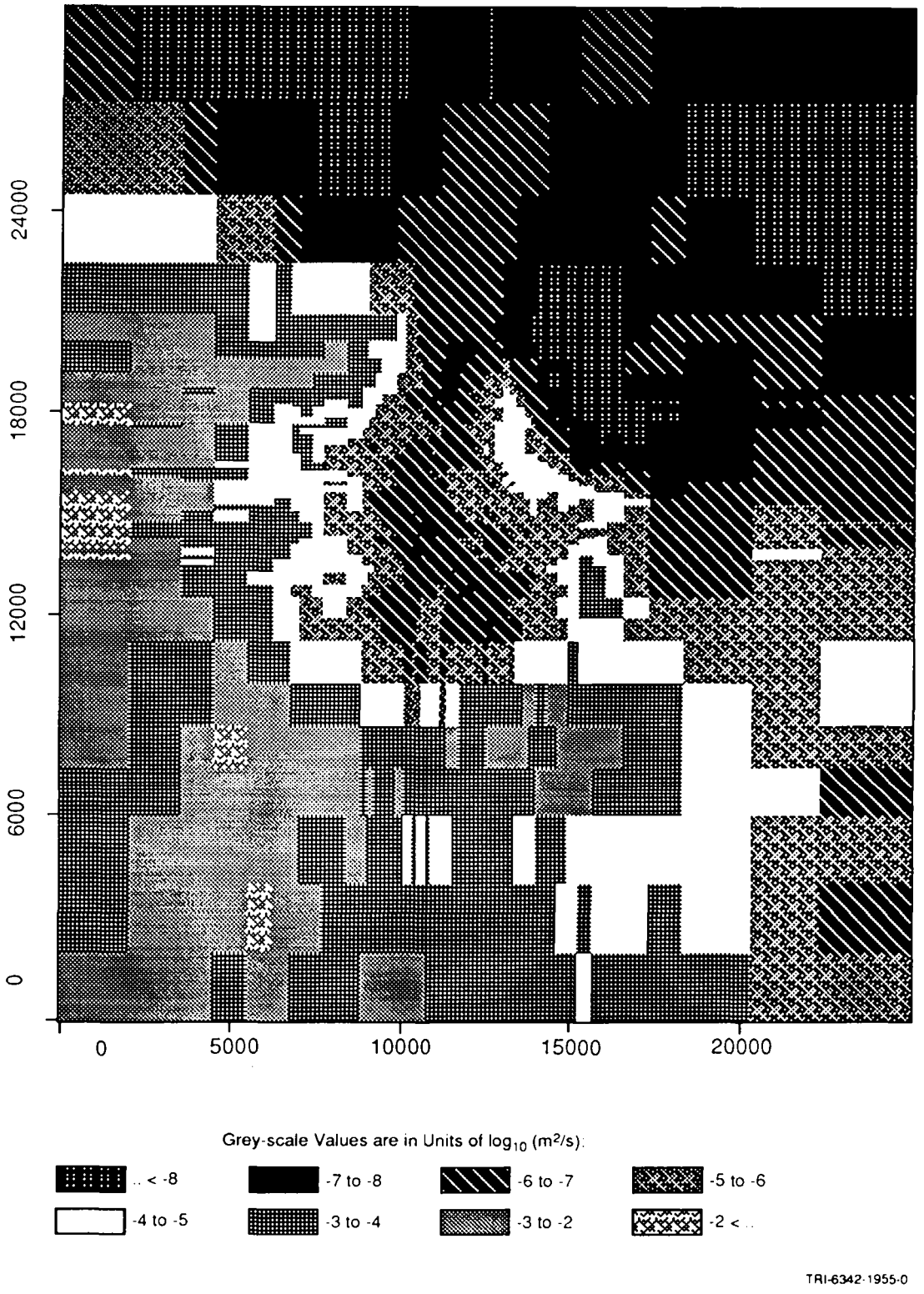

Figure C-61. Realization 21 of Culebra transmissivity.

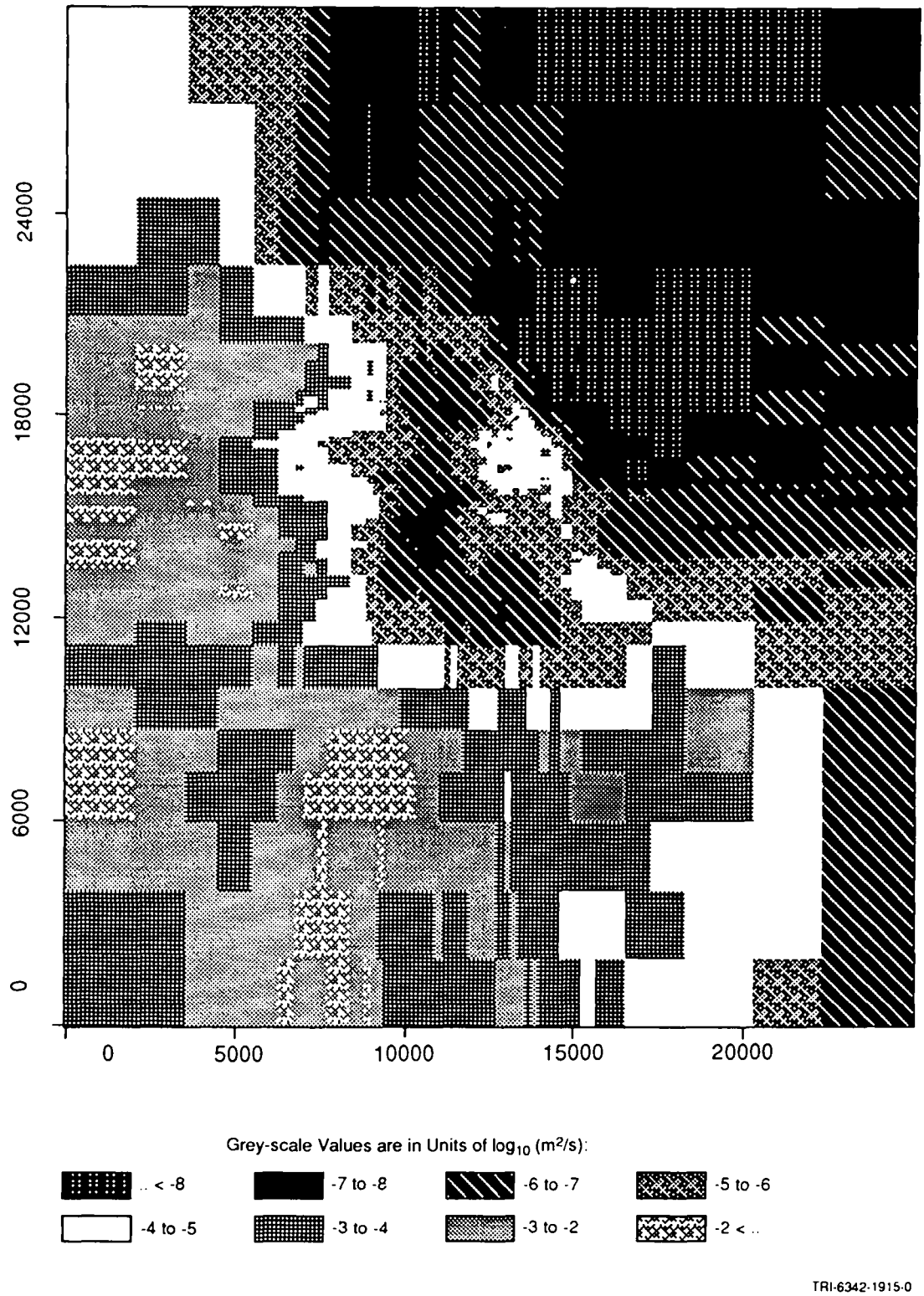

Figure C-62. Realization 13 of Culebra transmissivity.

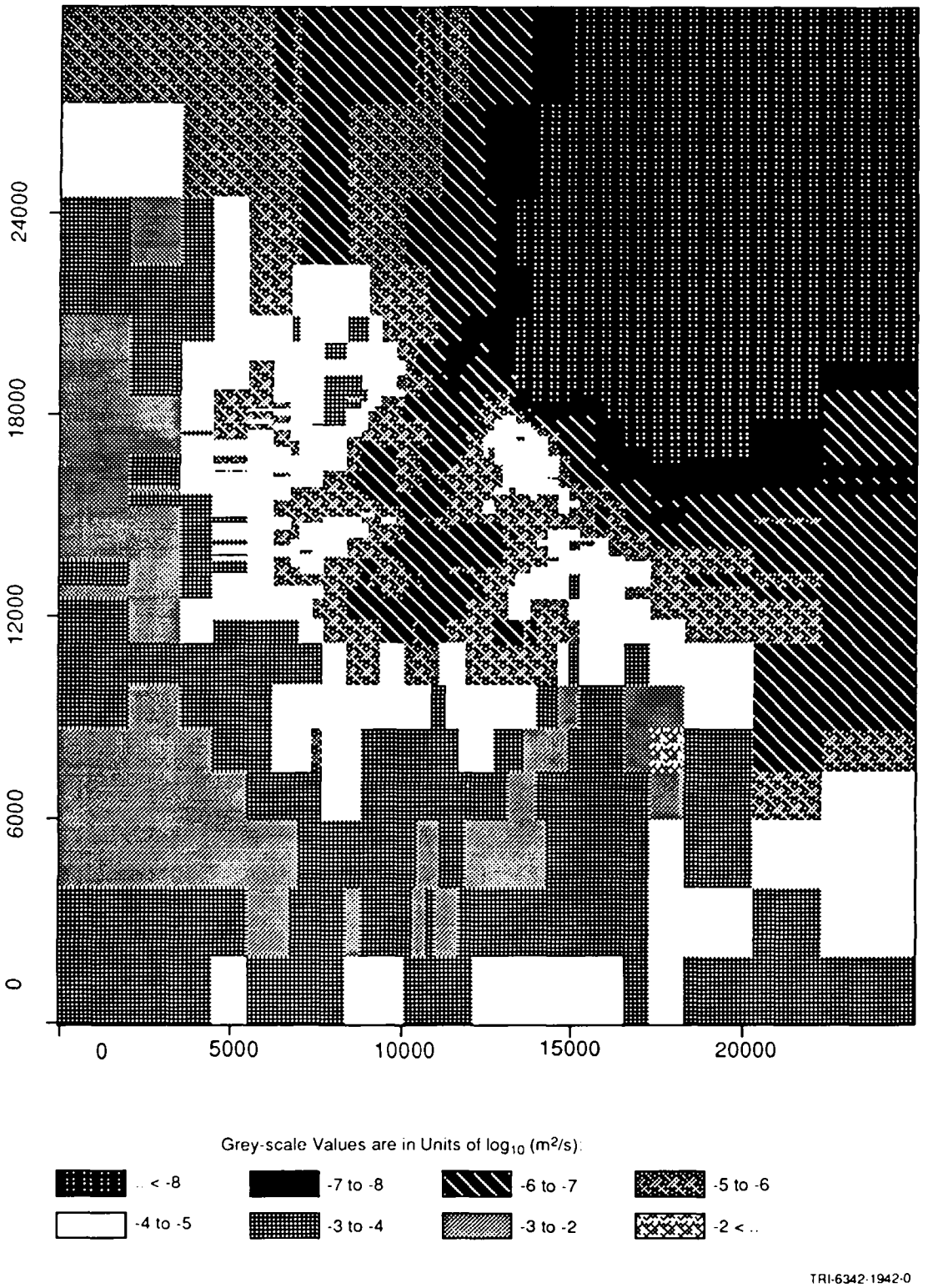

Figure C-63. Realization 10 of Culebra transmissivity.

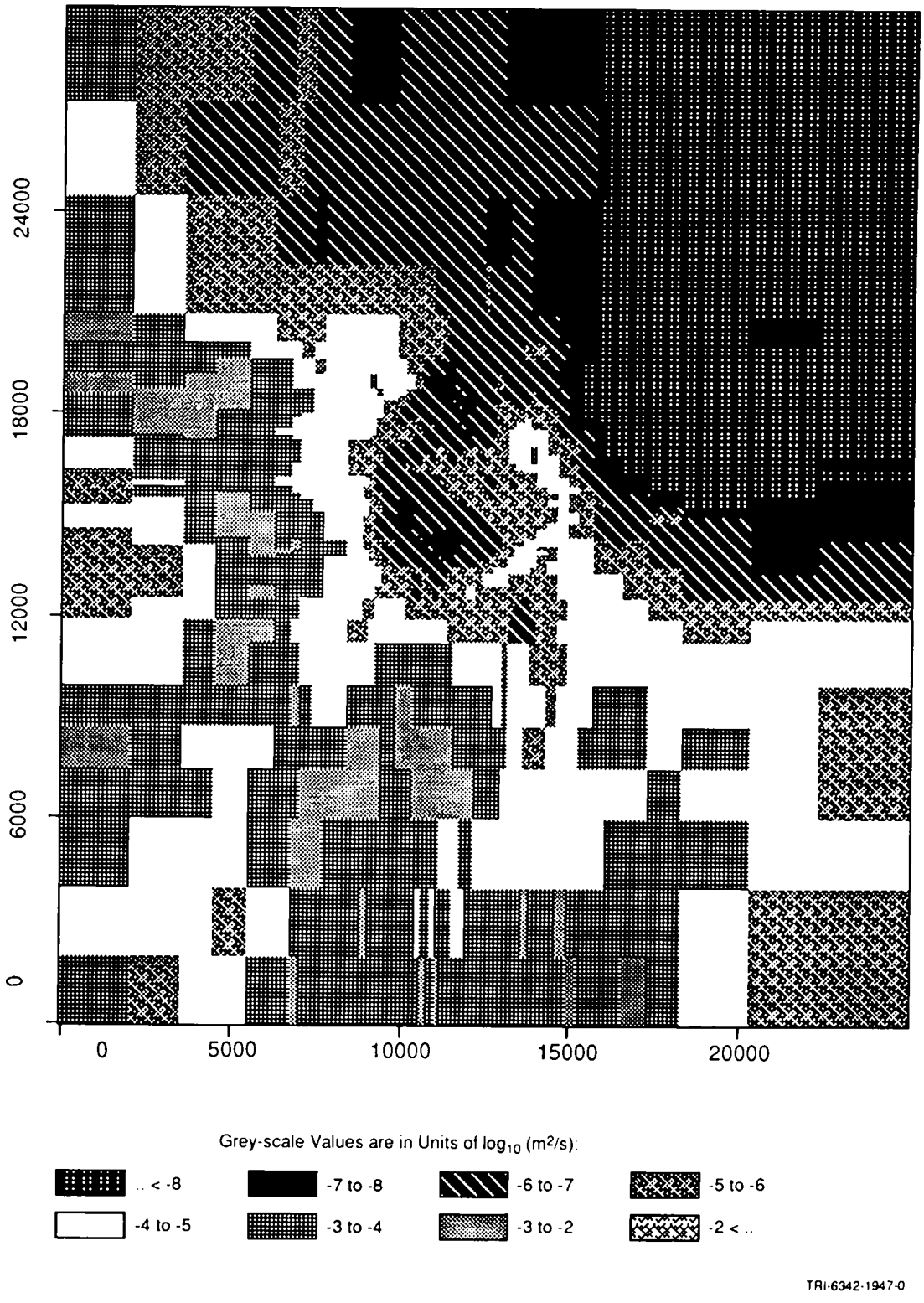

Figure C-64. Realization 32 of Culebra transmissivity.

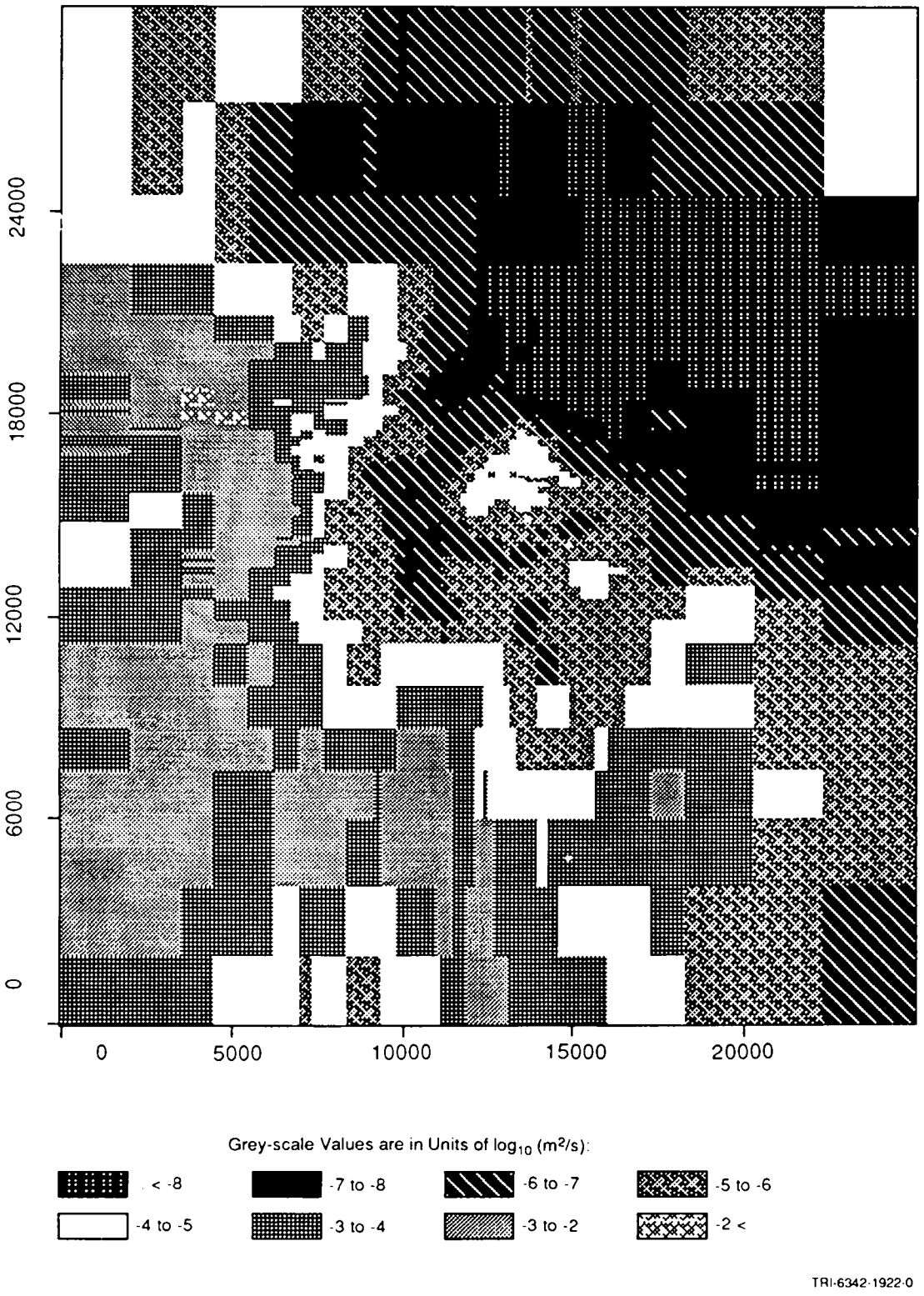

Figure C-65. Realization 8 of Culebra transmissivity.

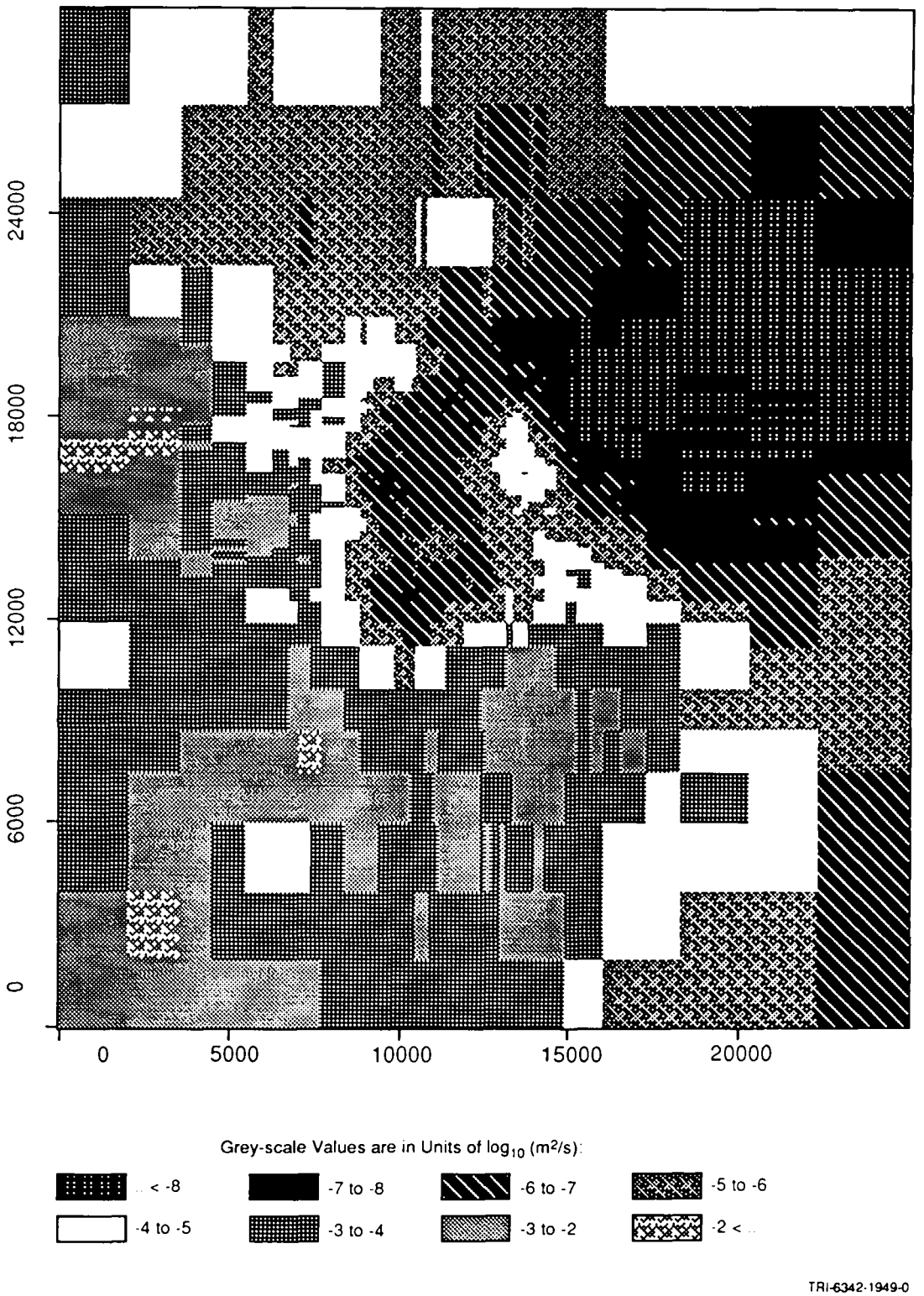

Figure C-66. Realization 11 of Culebra transmissivity.

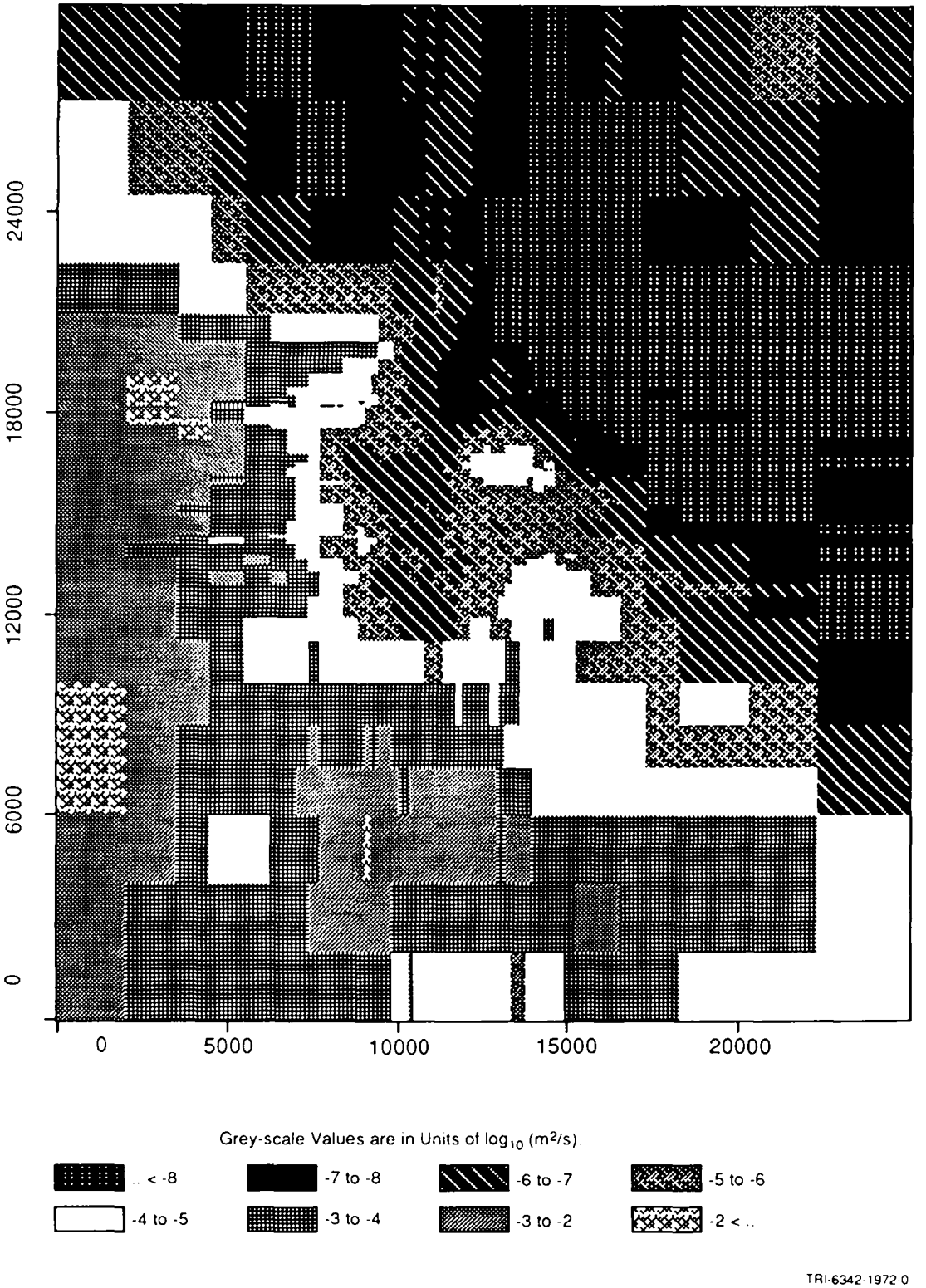

Figure C-67. Realization 54 of Culebra transmissivity.

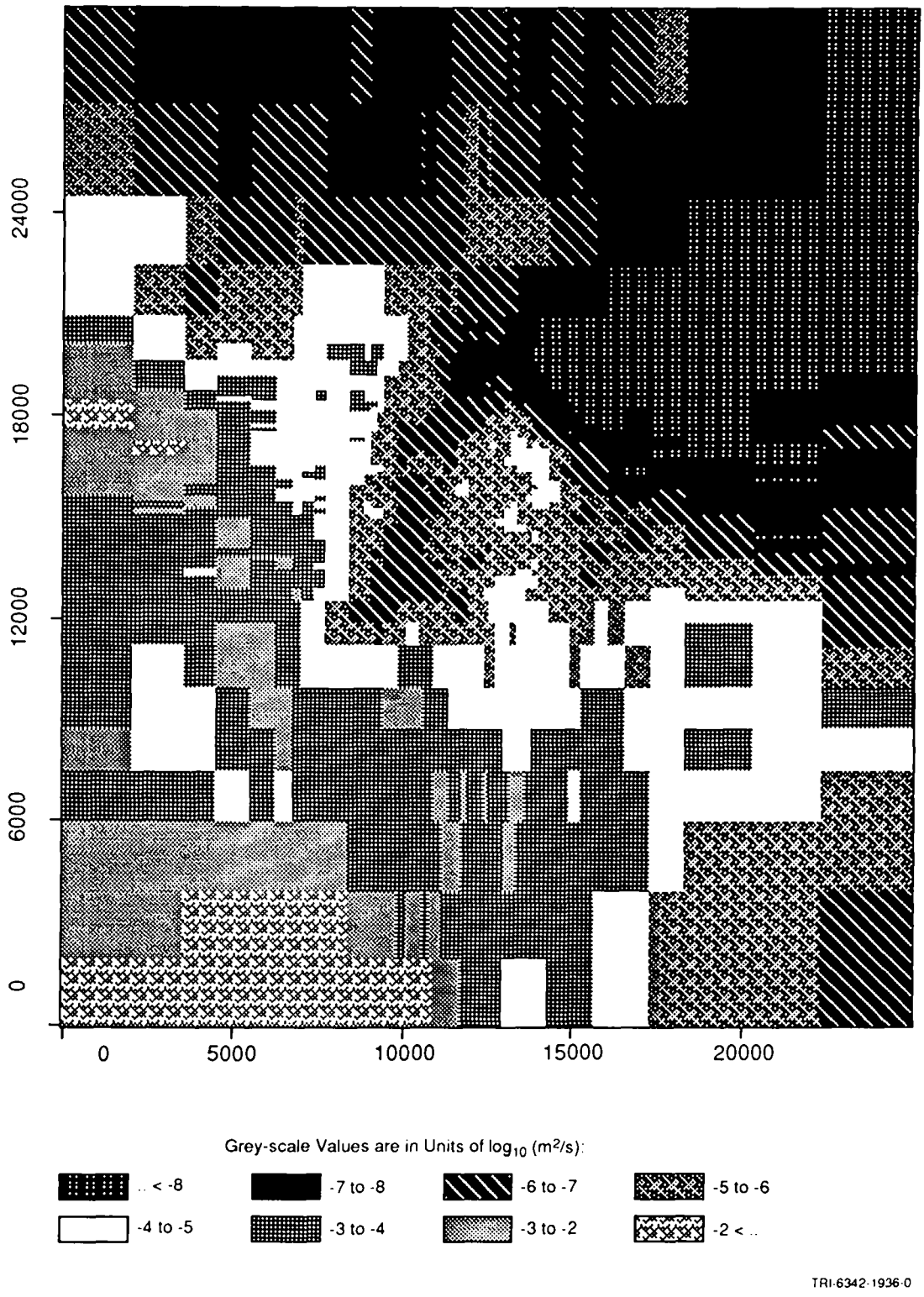

Figure C-68. Realization 6 of Culebra transmissivity.

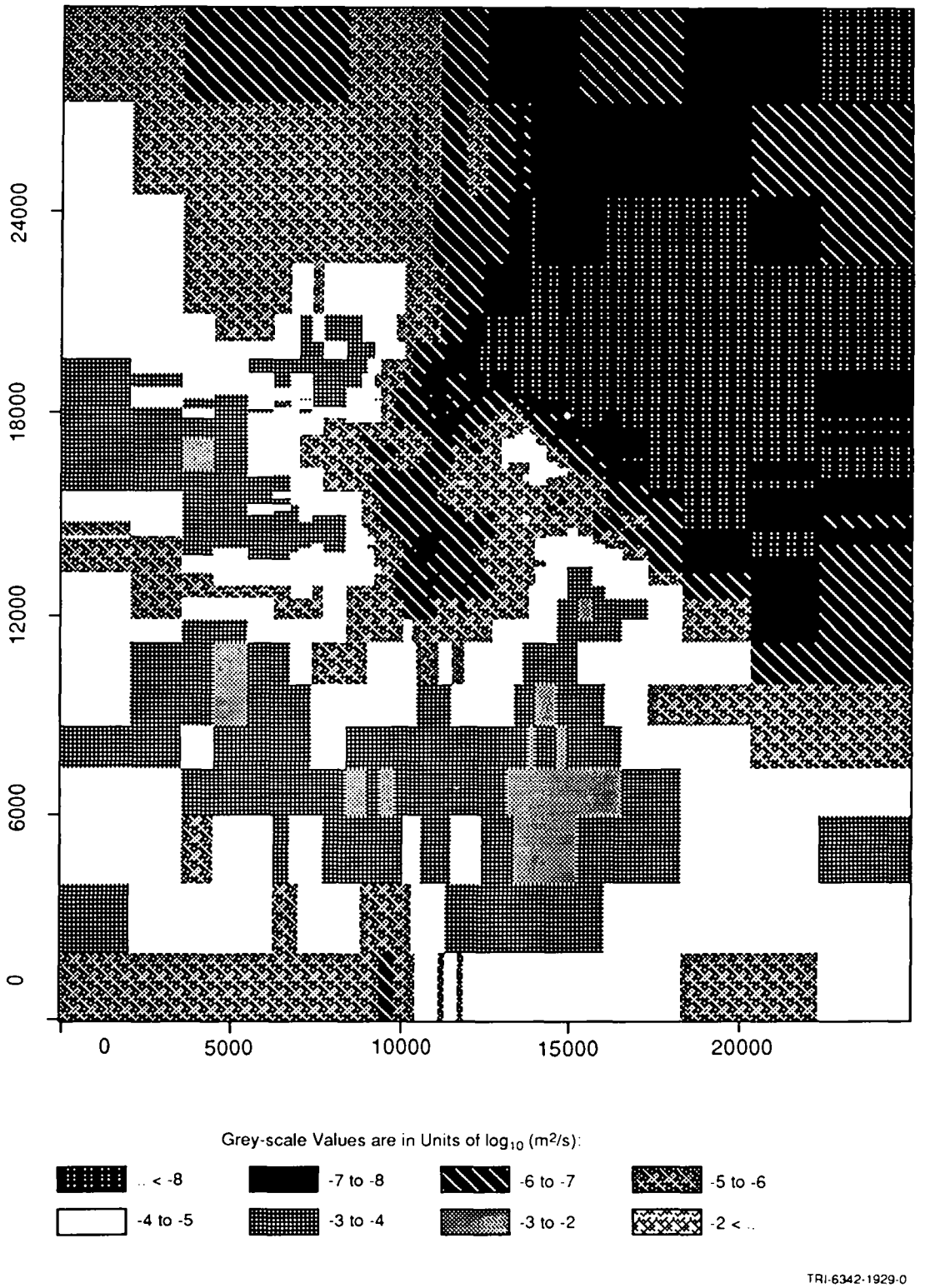

Figure C-69. Realization 67 of Culebra transmissivity.

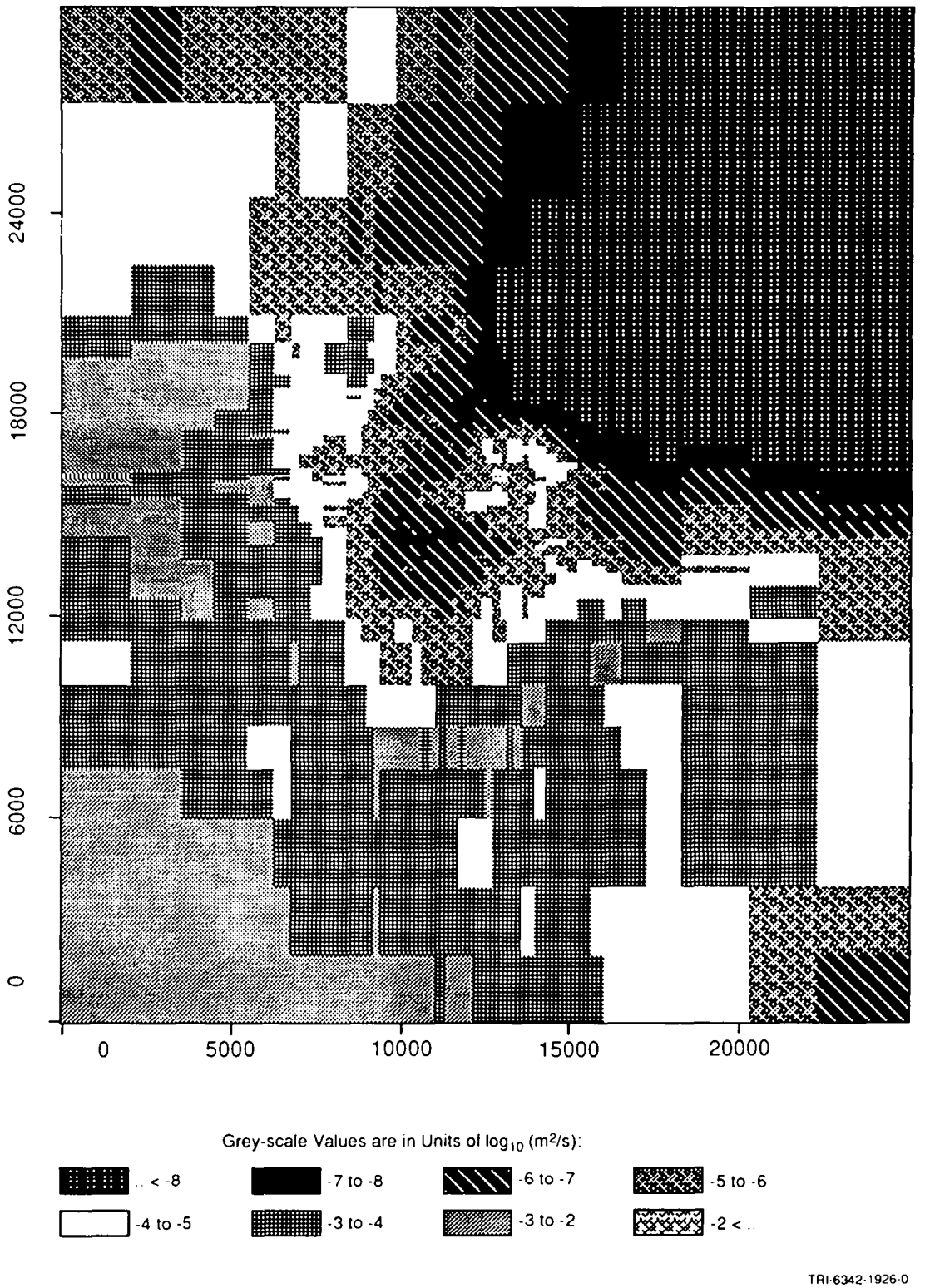

Figure C-70. Realization 58 of Culebra transmissivity.

APPENDIX D:
REALIZATIONS OF
DRILLING INTENSITY FUNCTIONS
FOR HUMAN INTRUSION

APPENDIX D: REALIZATIONS OF DRILLING INTENSITY FUNCTIONS FOR HUMAN INTRUSION

The following figures are graphs of the 70 representations of drilling intensity functions used in the 1992 Performance Assessment (PA) calculations to calculate probabilities of inadvertent drilling at the Waste Isolation Pilot Plant (WIPP) site (Section 1.4.2 of this volume). The genesis of these representations is explained in Section 5.2. Each graph of a representation shows two quantities: the intrusion rate, measured in boreholes/($km^2 \cdot 10^4$ yr), which is also the function $\lambda_s(t)$ mentioned in Eq. 1.4.2-5 of Section 1.4.2; and the time-integrated intrusion rate,

$$\int_0^t \lambda_s(x)\,dx, \text{ for any t such that } 0 < t < 10{,}000 \text{ yr},$$

which is also called *intrusions* and is measured in boreholes/km^2.

The 70 graphs are ordered by increasing values of intrusions measured at 10,000 yr. The ordering is specified by "sequence" number; note that many graphs are identical and so will correspond to more than one sequence number. Note also that only those representations that were not identically zero are included in this collection.

Note on scaling of graphs: The ordinates and abscissas of each graph have been scaled to improve resolution; the scaling used is

$$y = \sinh^{-1}\left(\frac{x}{a}\right)$$

where x is the variable noted on the ordinate (or abscissa) and y is the distance from origin of graph along ordinate (or abscissa). The constant a is chosen to make numbered intervals (e.g., $[0,10^2]$, $[10^2, 10^3]$) of approximately the same size.

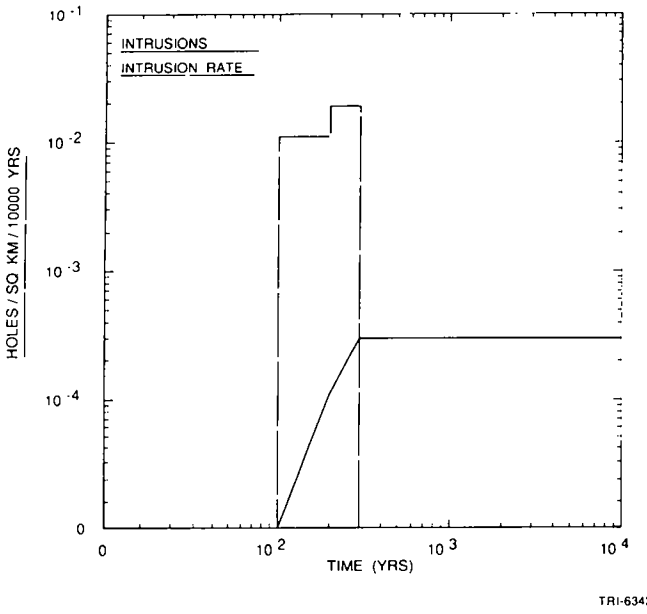

Figure D-1. Realization of drilling intensity function, Sequence 1.

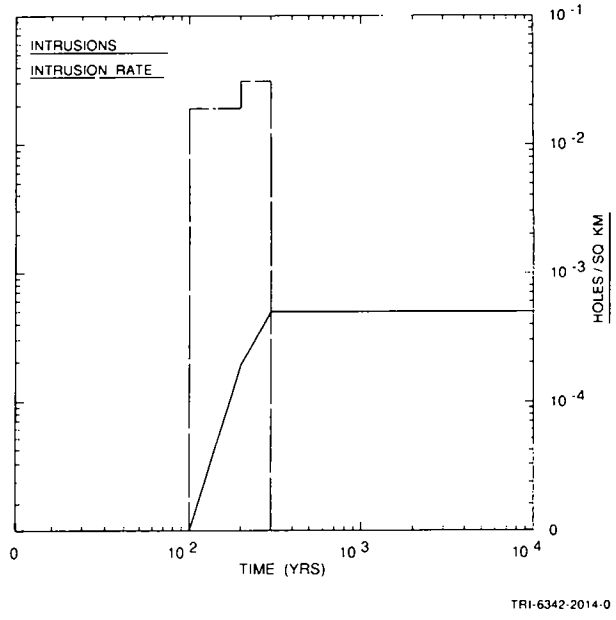

Figure D-2. Realization of drilling intensity function, Sequence 2.

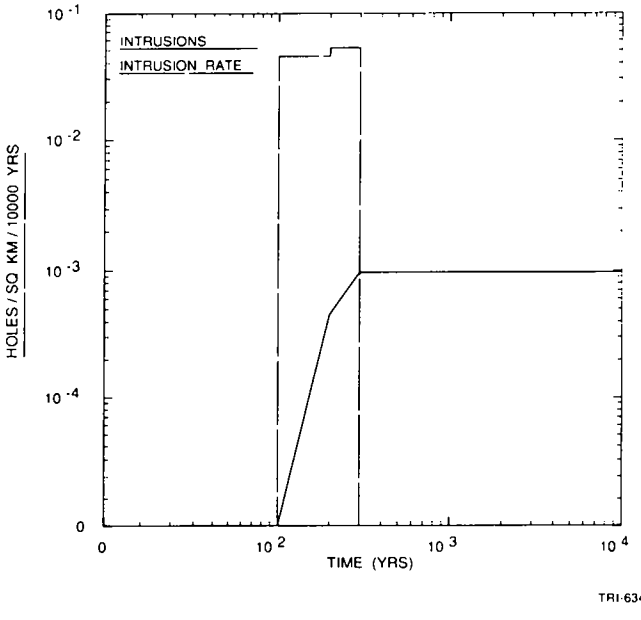

Figure D-3. Realization of drilling intensity function, Sequence 3.

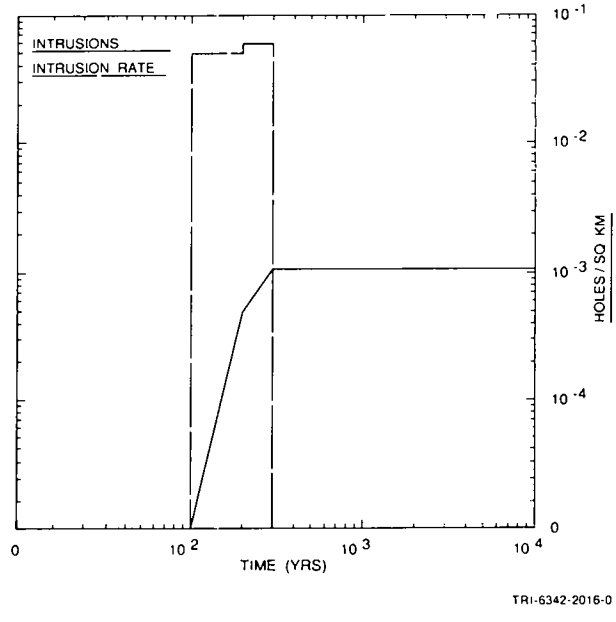

Figure D-4. Realization of drilling intensity function, Sequence 4.

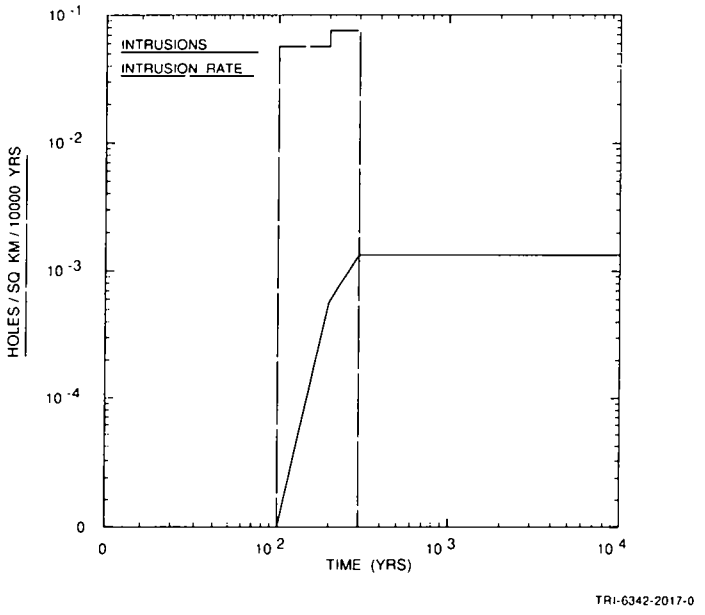

Figure D-5. Realization of drilling intensity function, Sequence 5.

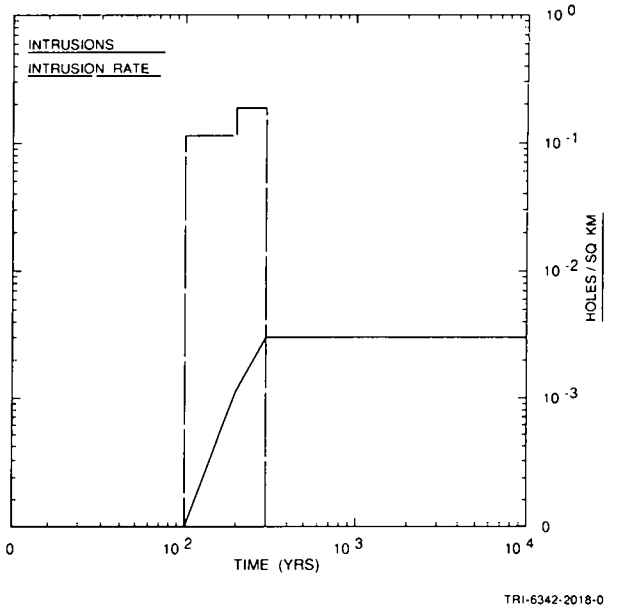

Figure D-6. Realization of drilling intensity function, Sequences 6 and 7.

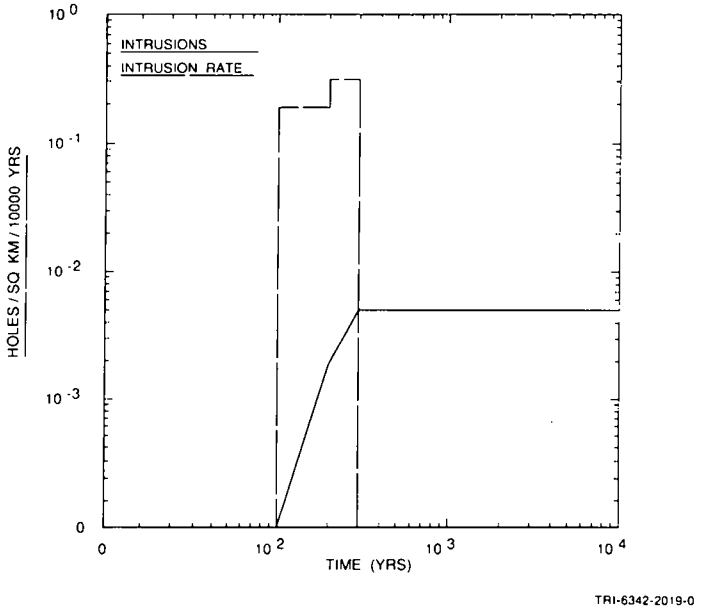

Figure D-7. Realization of drilling intensity function, Sequences 8 and 9.

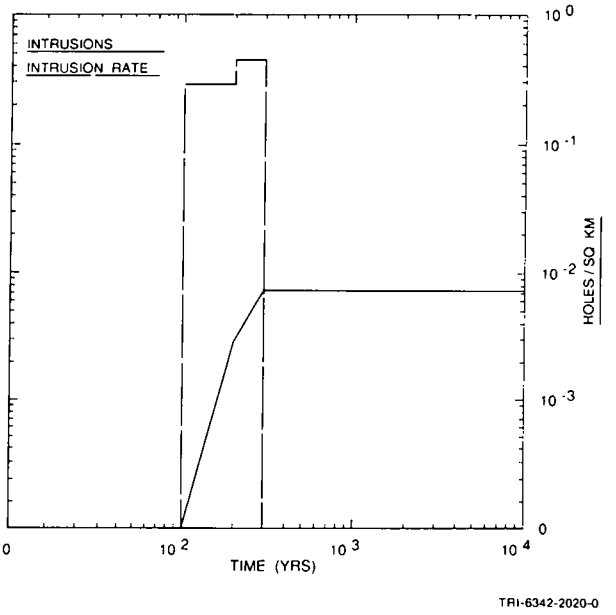

Figure D-8. Realization of drilling intensity function, Sequence 10.

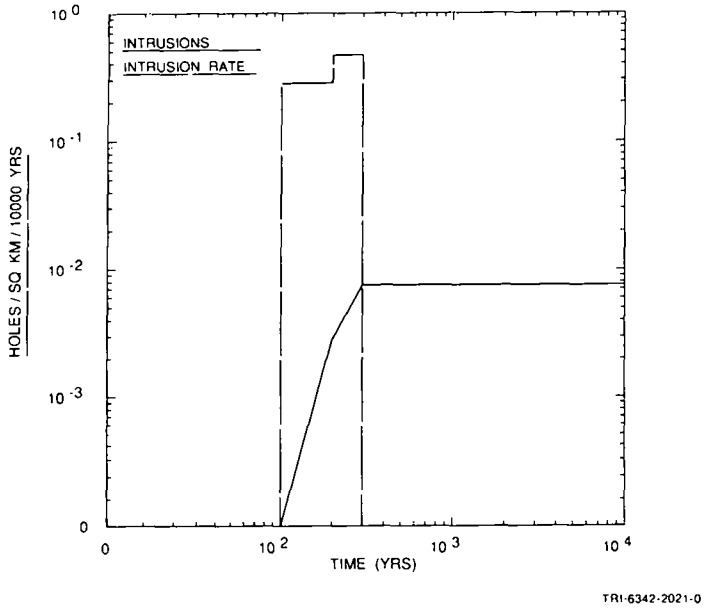

Figure D-9. Realization of drilling intensity function, Sequences 11 and 12.

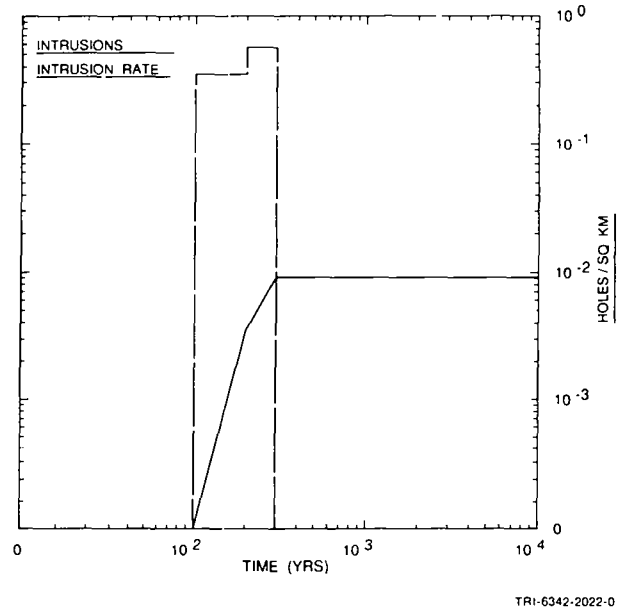

Figure D-10. Realization of drilling intensity function, Sequence 13.

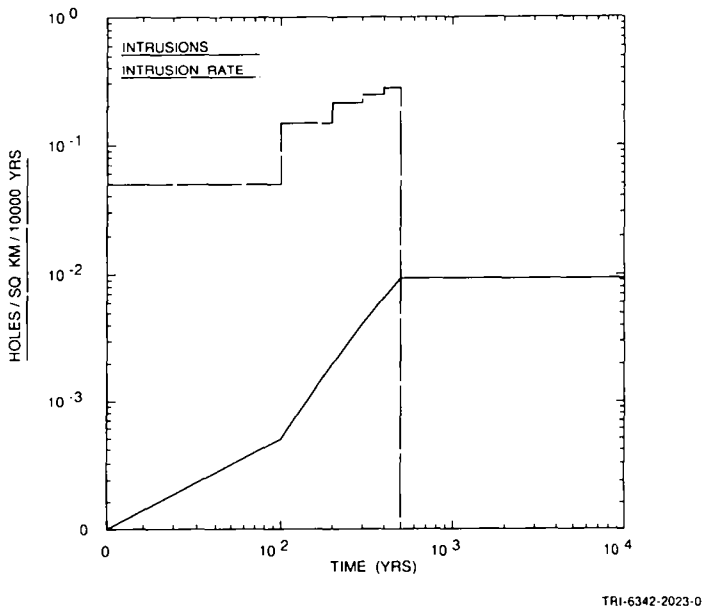

Figure D-11. Realization of drilling intensity function, Sequence 14.

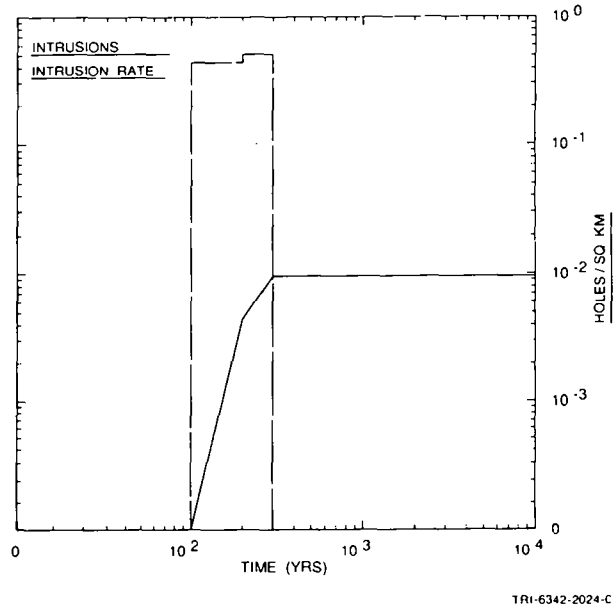

Figure D-12. Realization of drilling intensity function, Sequence 15.

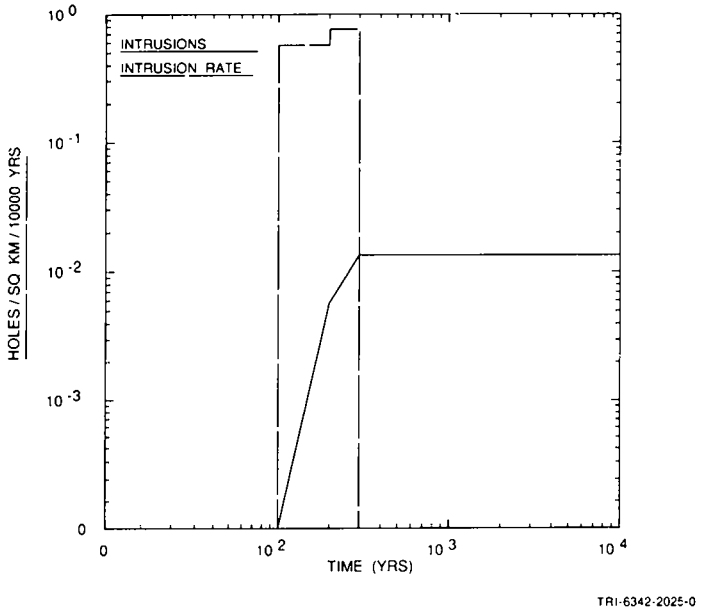

Figure D-13. Realization of drilling intensity function, Sequence 16.

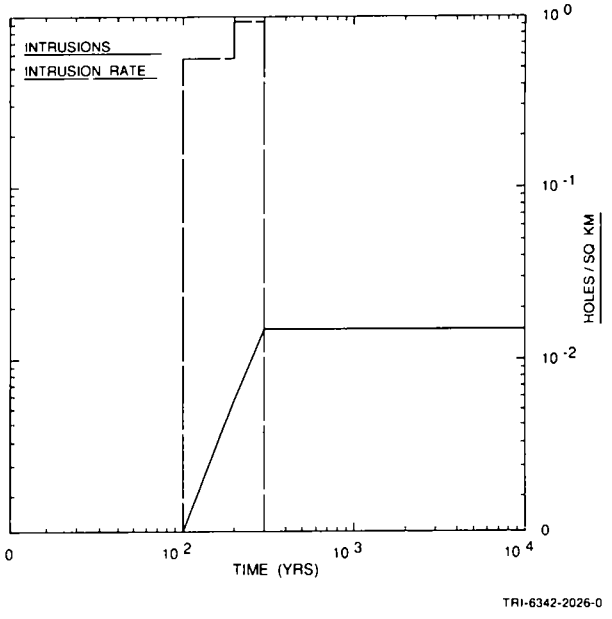

Figure D-14. Realization of drilling intensity function, Sequences 17, 18 and 19.

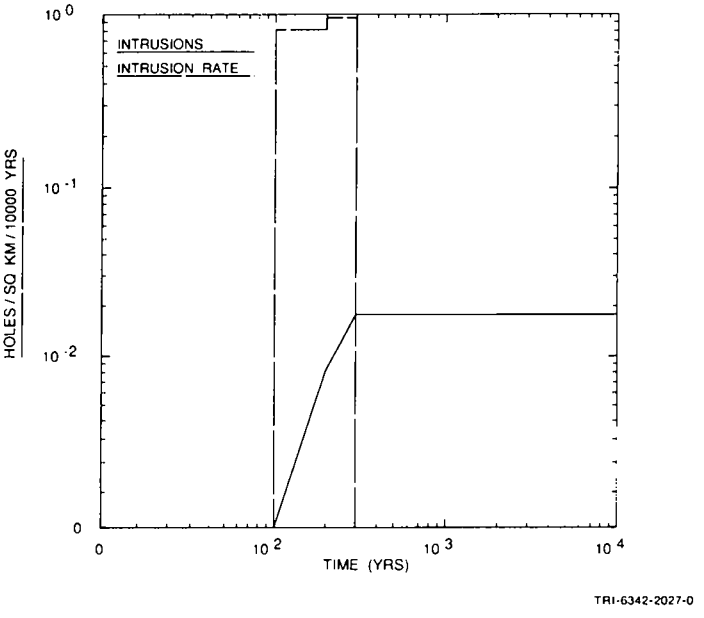

Figure D-15. Realization of drilling intensity function, Sequence 20.

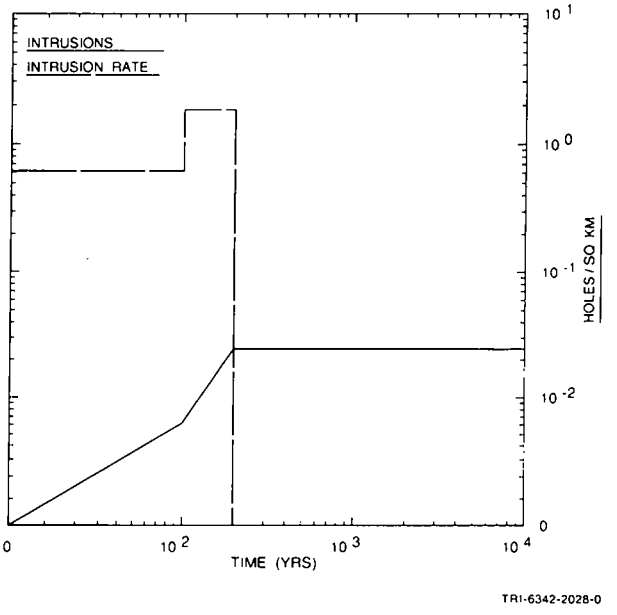

Figure D-16. Realization of drilling intensity function, Sequence 21.

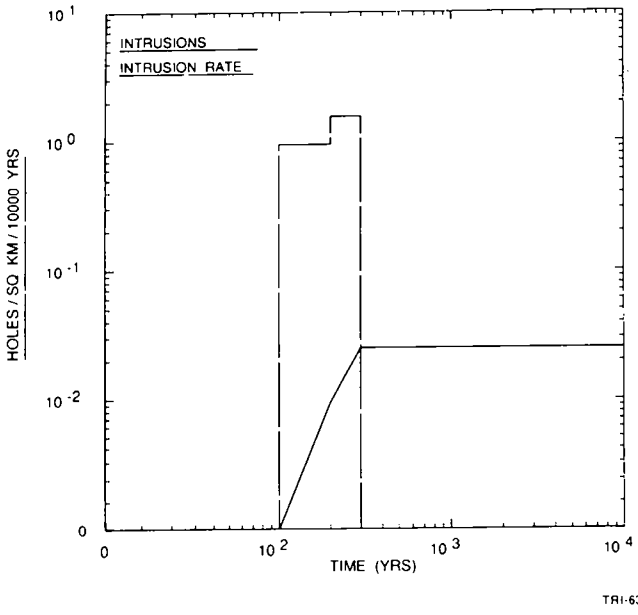

Figure D-17. Realization of drilling intensity function, Sequence 22.

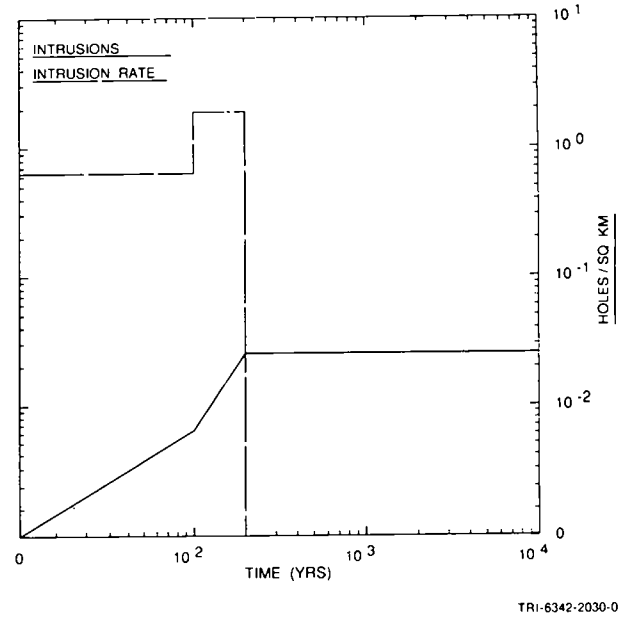

Figure D-18. Realization of drilling intensity function, Sequence 23.

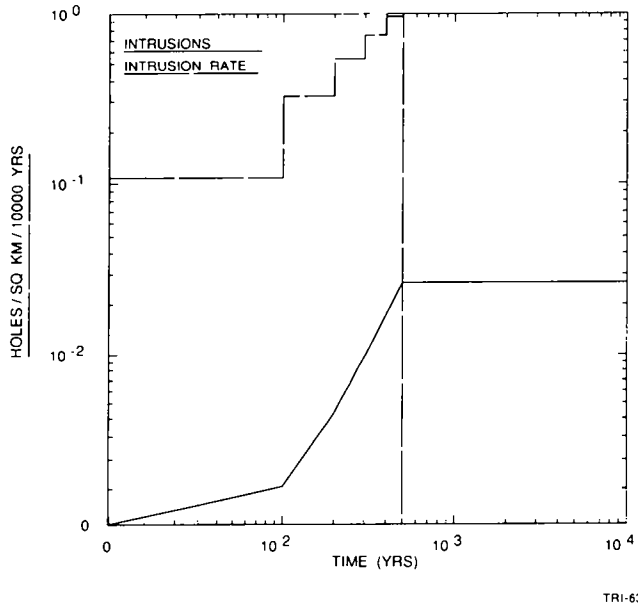

Figure D-19. Realization of drilling intensity function, Sequences 24 and 25.

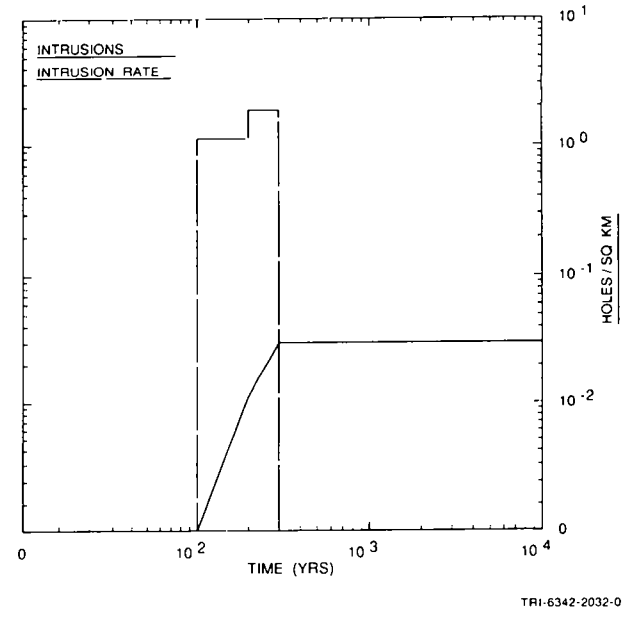

Figure D-20. Realization of drilling intensity function, Sequences 26 and 27.

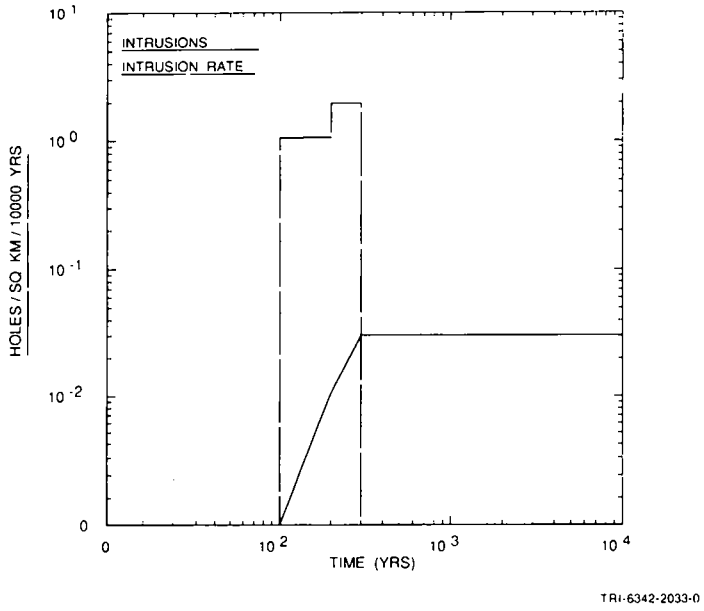

Figure D-21. Realization of drilling intensity function, Sequence 28.

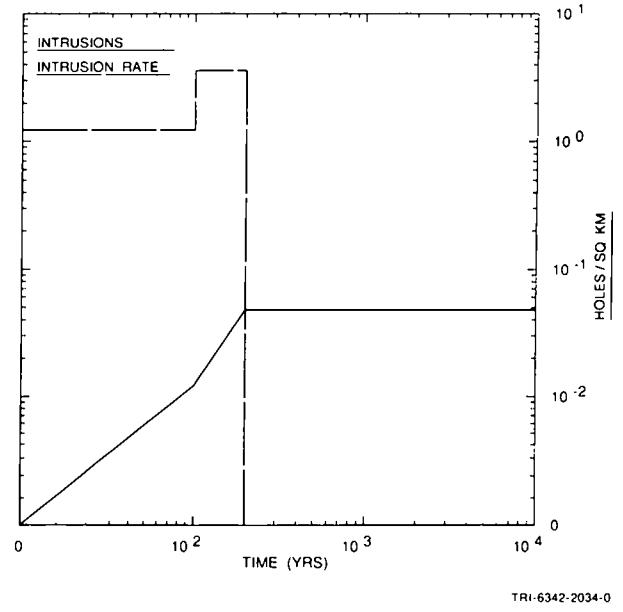

Figure D-22. Realization of drilling intensity function, Sequence 29.

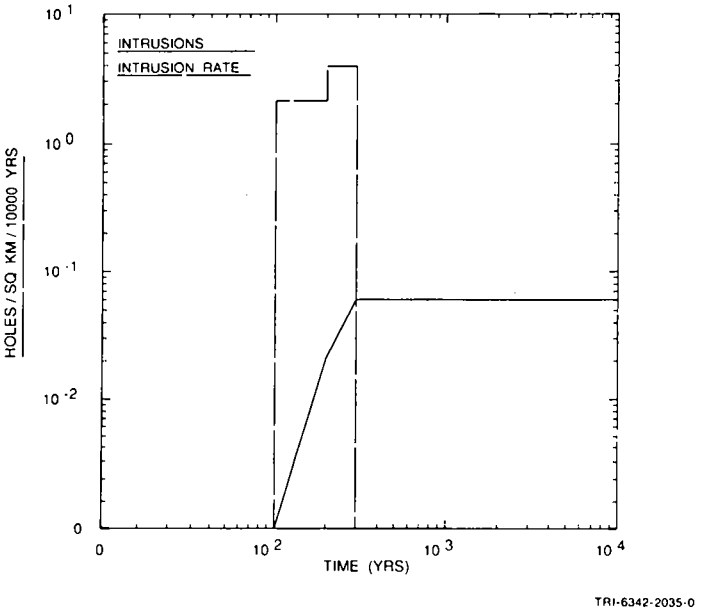

Figure D-23. Realization of drilling intensity function, Sequence 30.

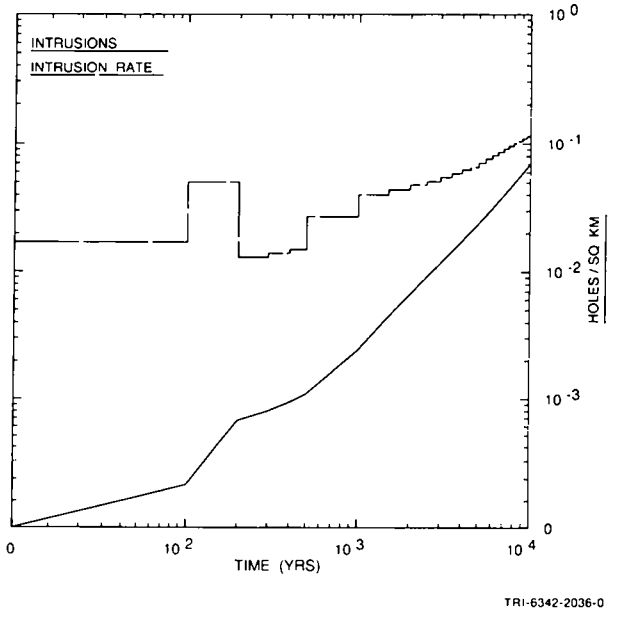

Figure D-24. Realization of drilling intensity function, Sequence 31.

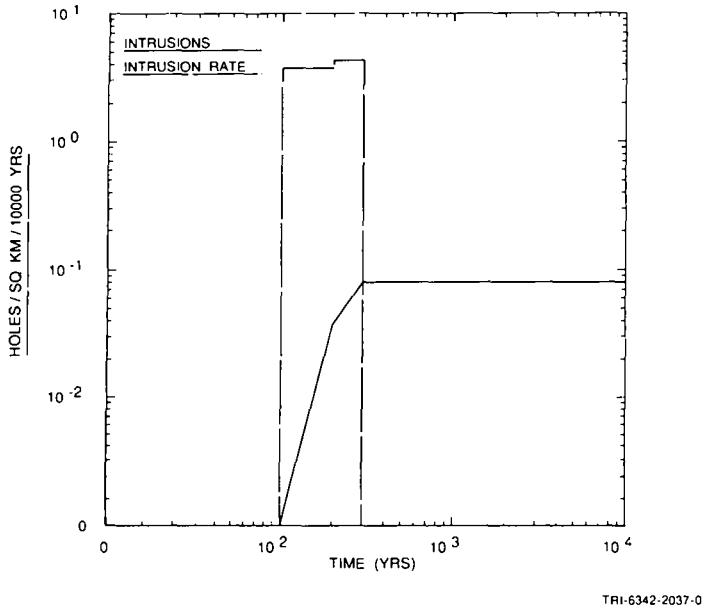

Figure D-25. Realization of drilling intensity function, Sequence 32.

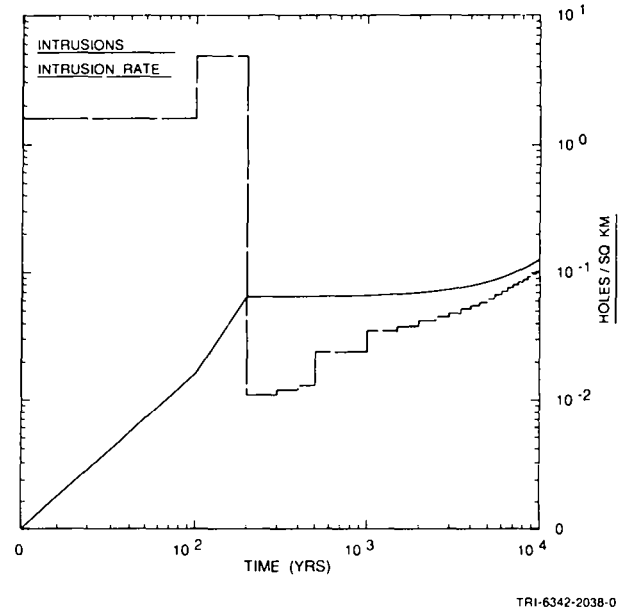

Figure D-26. Realization of drilling intensity function, Sequence 33.

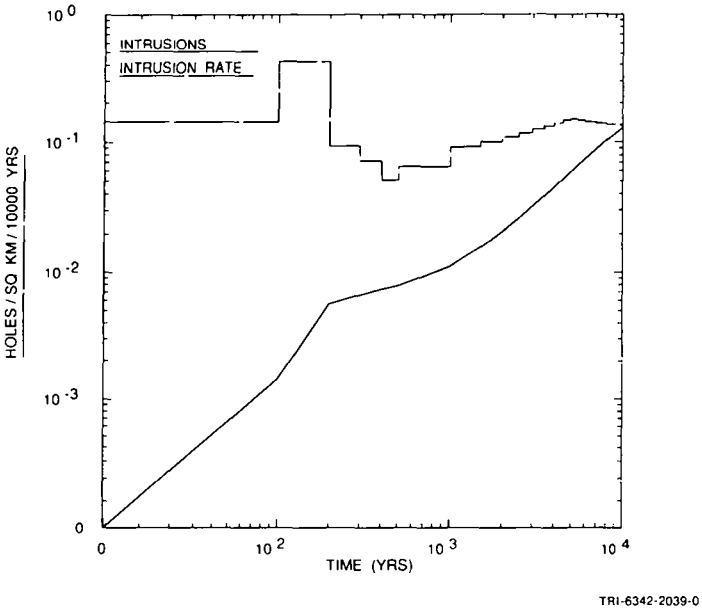

Figure D-27. Realization of drilling intensity function, Sequences 34, 35 and 36.

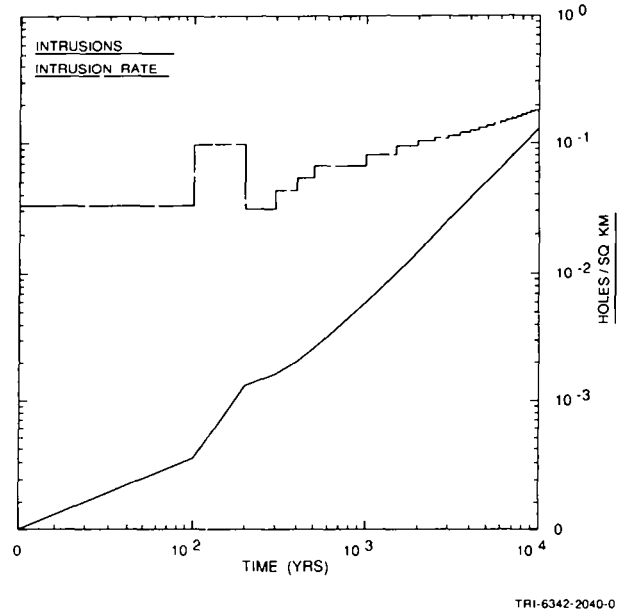

Figure D-28. Realization of drilling intensity function, Sequences 37, 38, 39 and 40.

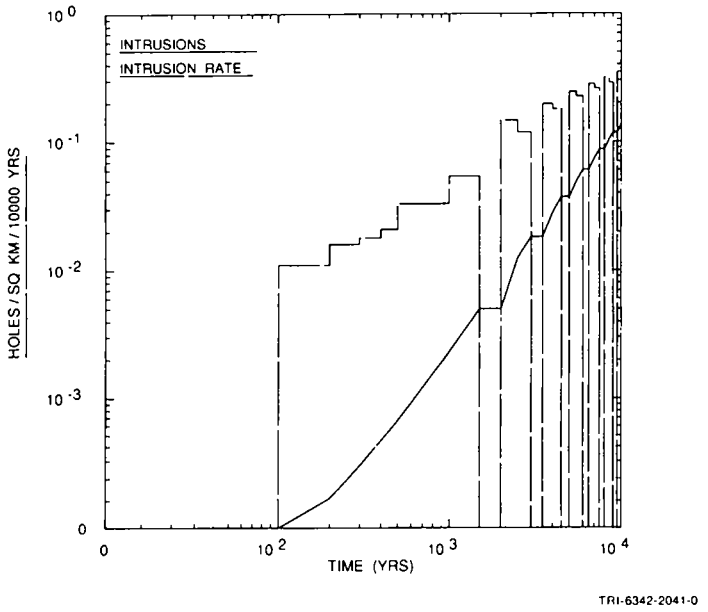

Figure D-29. Realization of drilling intensity function, Sequence 41.

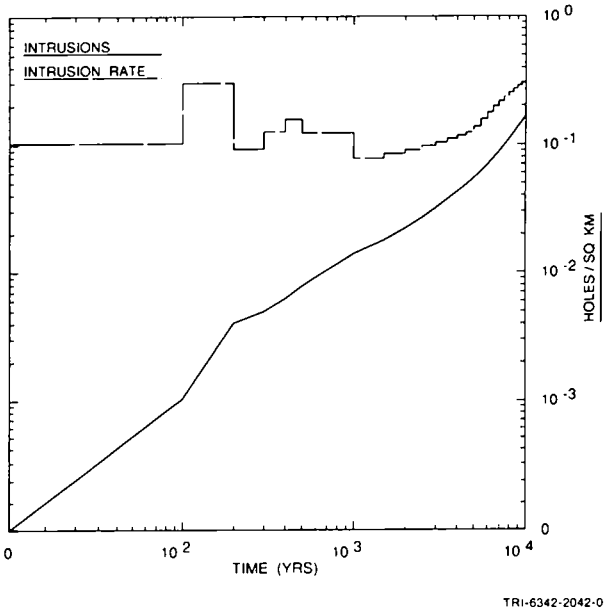

Figure D-30. Realization of drilling intensity function, Sequence 42.

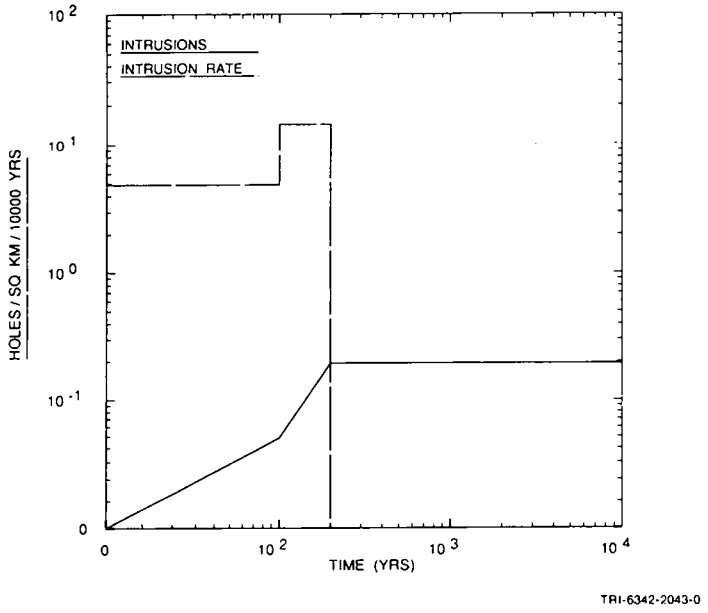

Figure D-31. Realization of drilling intensity function, Sequence 43.

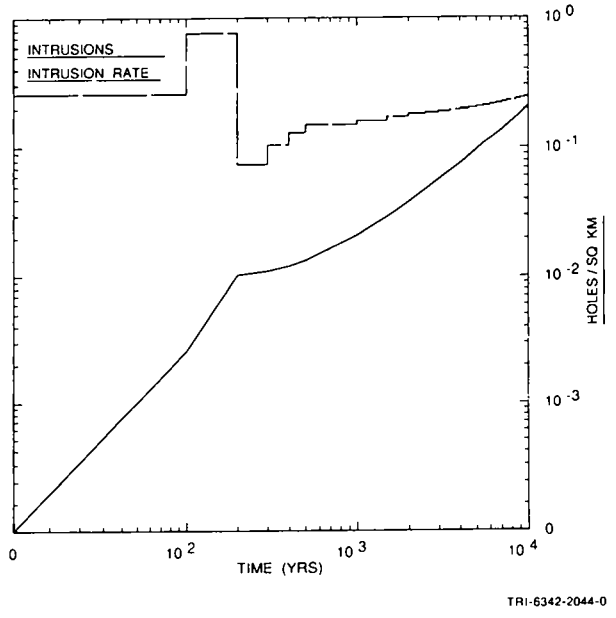

Figure D-32. Realization of drilling intensity function, Sequences 44, 45, 46, 47 and 48.

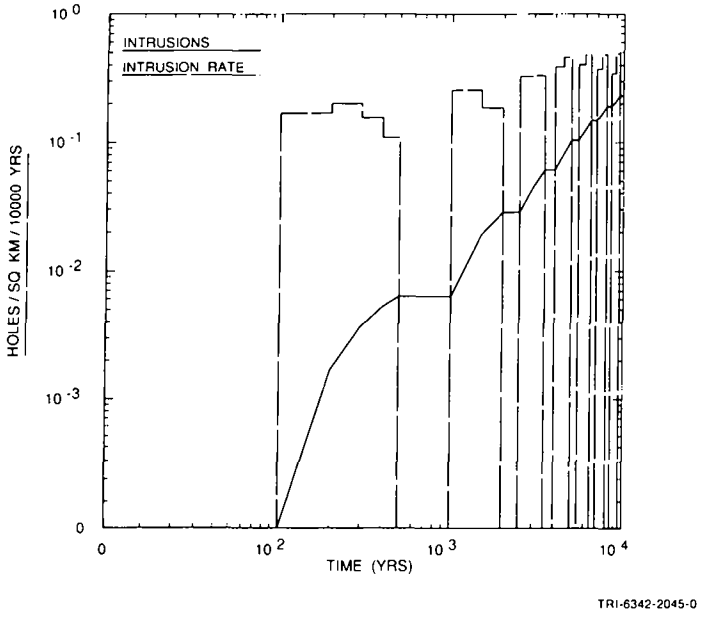

Figure D-33. Realization of drilling intensity function, Sequence 49.

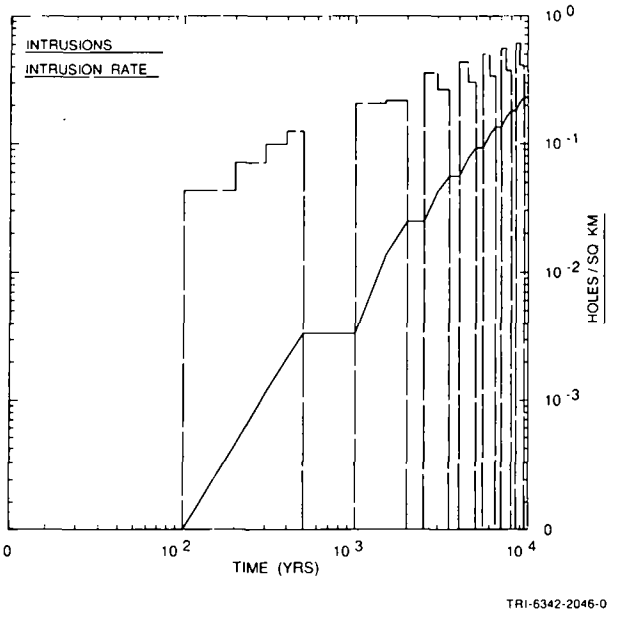

Figure D-34. Realization of drilling intensity function, Sequence 50.

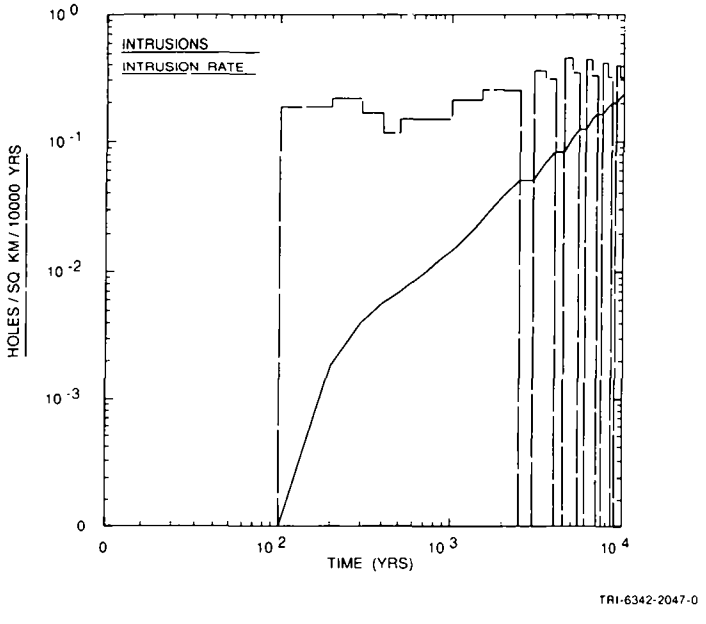

Figure D-35. Realization of drilling intensity function, Sequence 51.

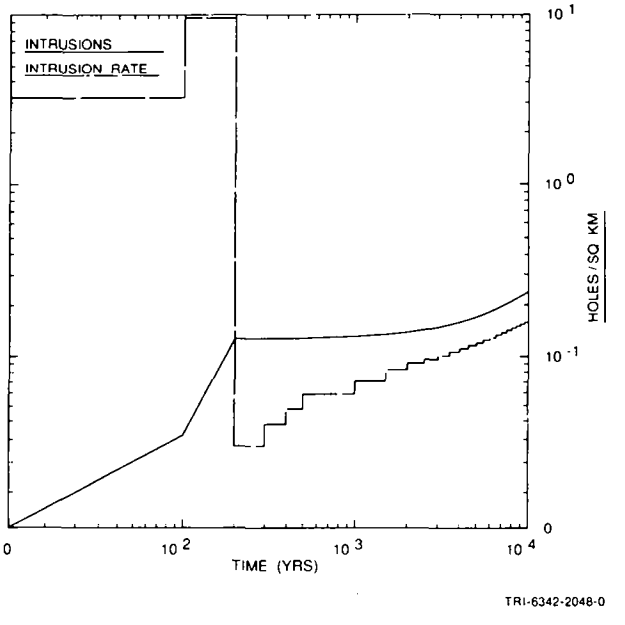

Figure D-36. Realization of drilling intensity function, Sequences 52, 53, 54, 55 and 56.

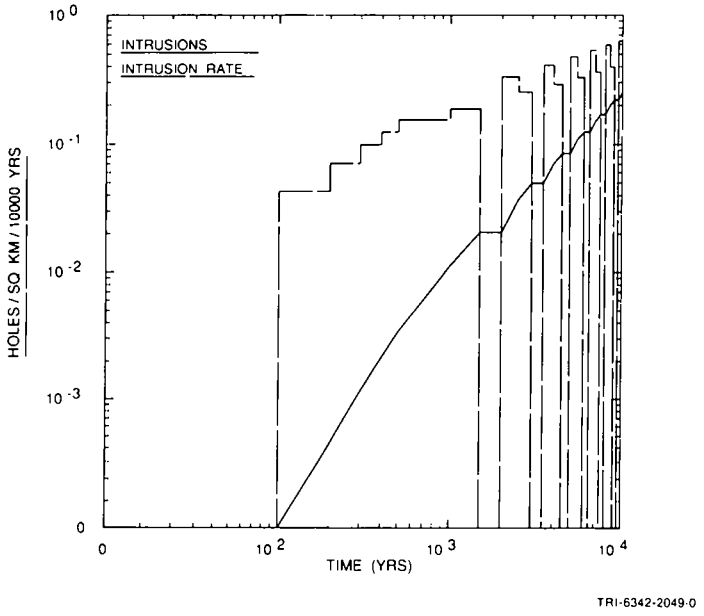

Figure D-37. Realization of drilling intensity function, Sequence 57.

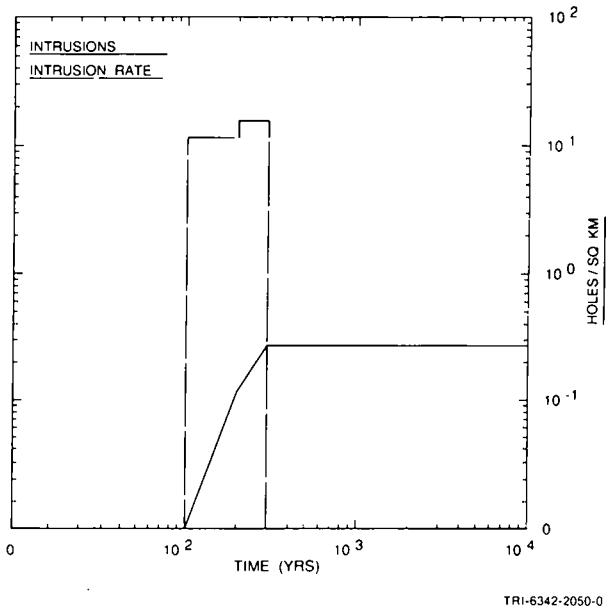

Figure D-38. Realization of drilling intensity function, Sequence 58.

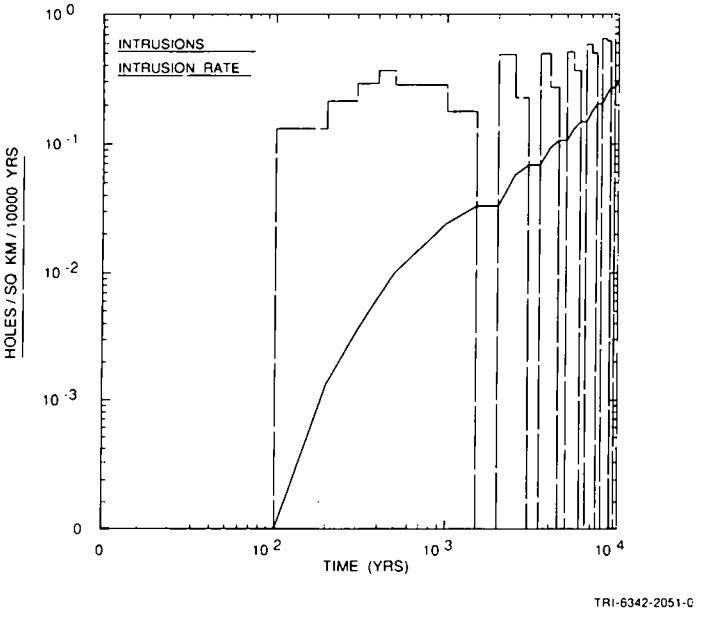

Figure D-39. Realization of drilling intensity function, Sequences 59 and 60.

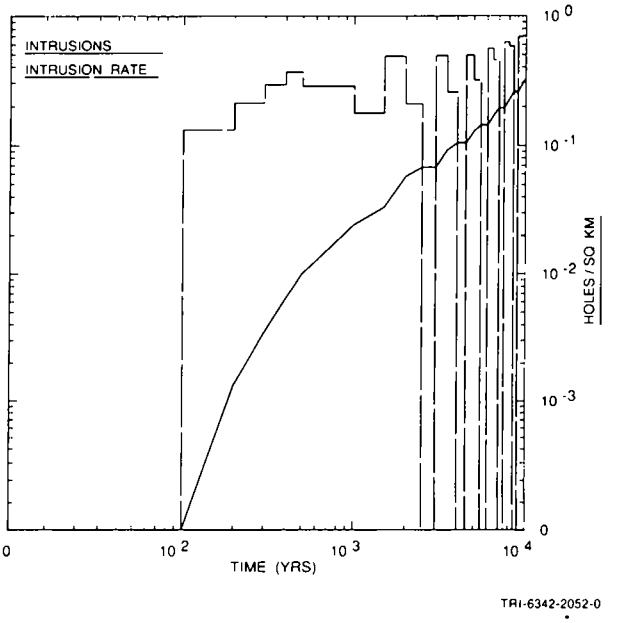

Figure D-40. Realization of drilling intensity function, Sequence 61.

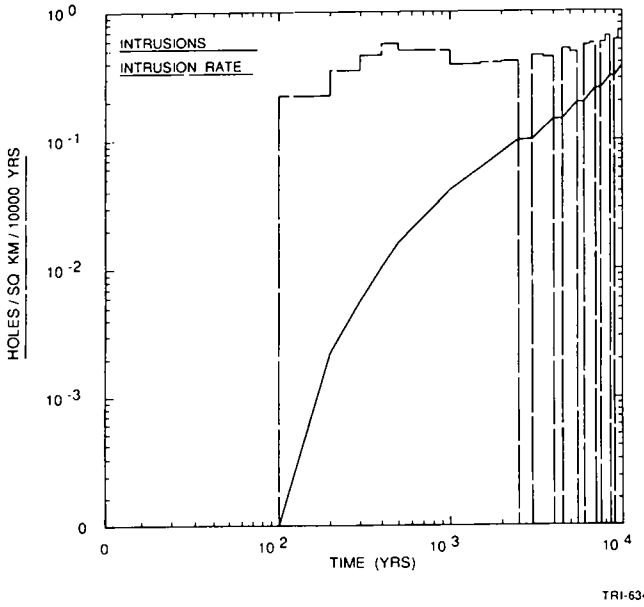

Figure D-41. Realization of drilling intensity function, Sequences 62 and 63.

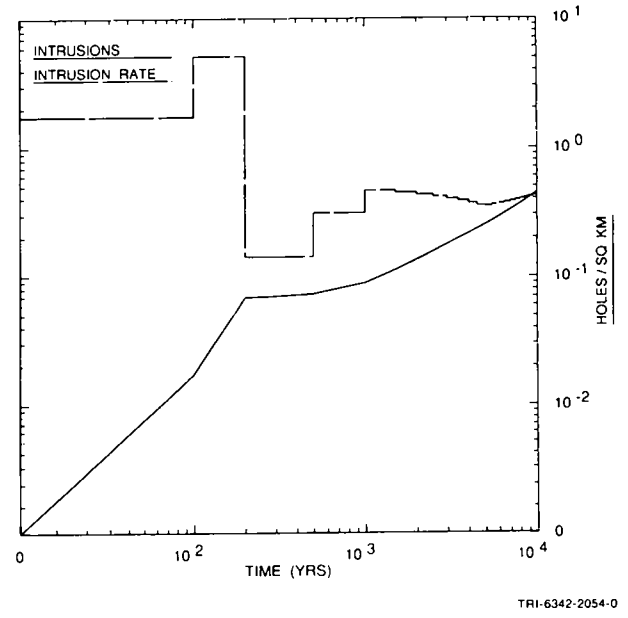

Figure D-42. Realization of drilling intensity function, Sequence 64.

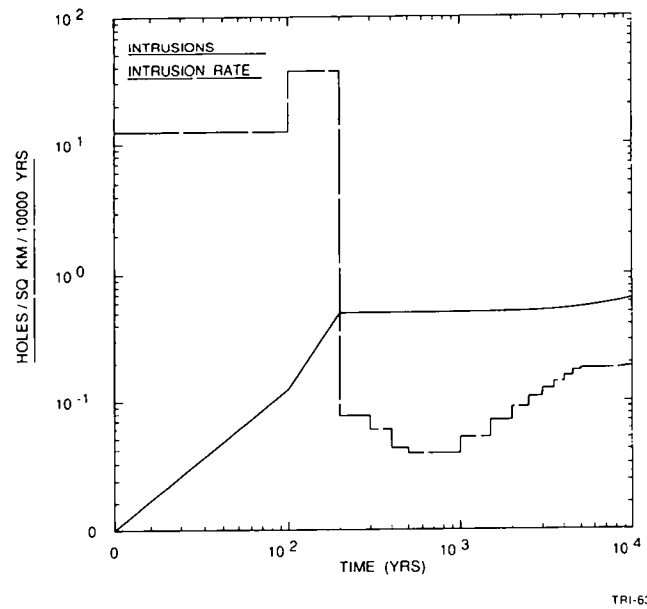

Figure D-43. Realization of drilling intensity function, Sequences 65 and 66.

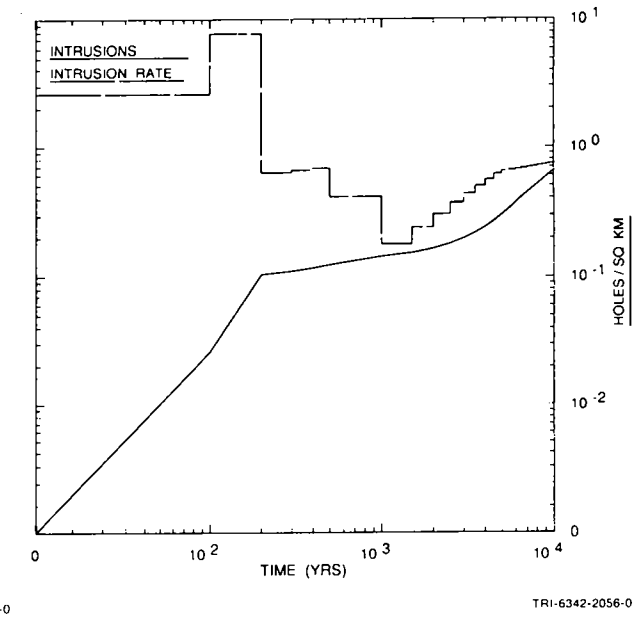

Figure D-44. Realization of drilling intensity function, Sequences 67 and 68.

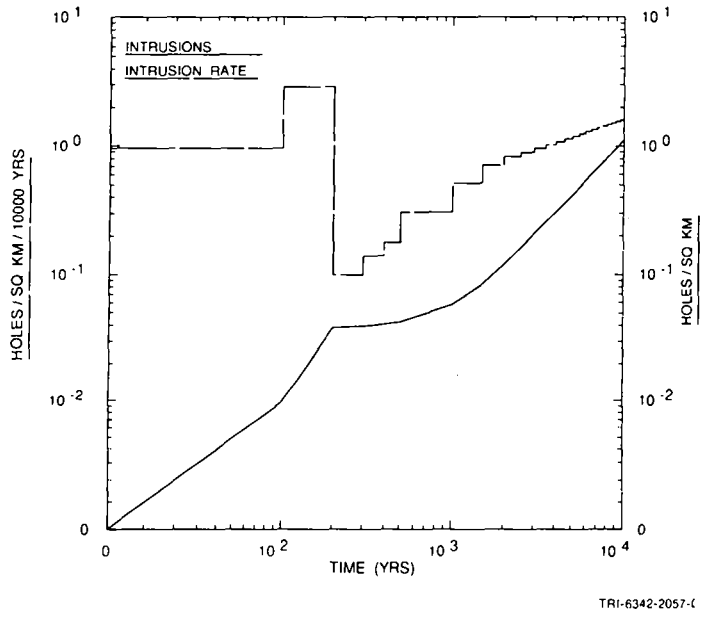

Figure D-45. Realization of drilling intensity function, Sequences 69 and 70.

NOMENCLATURE

Mathematical Symbols

A	-	cross-sectional area (m^2)
A_m	-	amplitude scaling factor for precipitation variation
a	-	minimum of range of distribution
$2B$	-	characteristic fracture spacing or block length (m)
B_ℓ, B_g	-	formation volume factor (reservoir conditions/standard conditions) for liquid or gas, respectively
b	-	maximum of range of distribution
$2b_\ell$	-	fracture aperature (m)
C	-	concentration (kg/m^3)
C_w	-	total concentration of water in solution (e.g., brine)
$\hat{C}$	-	mass fraction (kg/kg)
C°	-	solubility (kg chemical/m^3 fluid)
c	-	capacitance ($ß_b + \phi ß_\ell$) (Pa^{-1})
D_m	-	molecular diffusion in porous media matrix ($D^\square \bullet \tau$) (m^2/s)
$D^\square$	-	molecular diffusion in pure fluid (m^2/s)
D_L, D_T	-	hydrodynamic dispersion $D_m + \alpha_L \bar{V}$ and $D_m + \alpha_T \bar{V}$, respectively (m^2/s)
D	-	hydrodynamic dispersion tensor
d	-	diameter
d_i	-	separation distance to grid point i, e.g., separation distance between interpolated point and a nearby point
d_s	-	distance traveled by solute
E	-	Young's modulus (Pa)
e	-	weighting power for inverse-distance interpolation
f	-	fanning friction factor
f_w	-	waste unit factor
f_c, f_m, f_s	-	volume fraction of combustibles, metals/glass, and sludge, respectively
f_{rchg}	-	recharge factor evaluated from precipitation fluctuation
$F(x)$	-	cumulative distribution function, integral of f(x), probability density function of parameter x
$f(x)$	-	distribution of x

1	g	-	acceleration due to gravity = ~9.8 m/s^2 or 9.80616 - 2.5928 x 10^{-2} $\cos 2\phi_{lat}$ + 6.9 x 10^{-5} $\cos^2 2\phi_{lat}$ - 3.086 x $10^{-6} z_{sur}$ - 1.543 x $10^{-6} \Delta z$, where ϕ_{lat} is the latitude, z_{sur} is the surface elevation in meters, and Δz is the depth in meters below the surface (Helmert's equation) (Weast and Astle, 1981, F-78) (9.792 m/s^2 at 1039.06 m [surface] and 9.791 m/s^2 at 351 m [repository level])
7	h	-	multiplier factor
9	h*	-	Plank's constant, 6.6262×10^{-34} J • s
11	K	-	hydraulic conductivity (m/s)
13	K_d	-	distribution (or partition) coefficient (m^3/kg)
15	K_{bulk}	-	bulk modulus $(E/(3(1-2\nu))$ (Pa)
17	k*	-	Boltzmann's constant 1.3806×10^{-23} (J/K)
19	k	-	permeability (m^2)
21	$k_{r\ell}, k_{rg}$	-	relative liquid and gas permeability, respectively
23	L_i	-	release limit for radionuclide i (from *40 CFR 191* Appendix A, Table 1)
25	M	-	molecular weight (g/mol)
27	M_{dc}, M_{dm}, M_{ds}	-	average mass of combustibles, metals/glass, and sludge, respectively, per drum (kg)
29	m_A	-	atomic mass
31	$\dot{m}_b, \dot{m}_c, \dot{m}_t$	-	gas generation rate, biodegradation (mol/kg cellulose/s), corrosion (mol/m^2 surface area steel/s), and total, respectively
34	N_R	-	Reynold's number, $\frac{\rho_f v d}{\mu}$
36	Np	-	Peclet number, $\bar{V} d_{50} / \tau D^{\square}$, where d_{50} is average particle diameter (length dimension)
38	N	-	molarity (mol/ℓ)
40	n	-	number of moles
42	n_g	-	number of grid points used for interpolation
44	P(r>R)	-	probability of r > R
46	p	-	pressure (Pa)
48	p_c	-	capillary pressure (Pa)
50	p_{cr}	-	critical pressure (Pa)
52	p_t	-	threshold displacement pressure (Pa)
54	Q	-	flow rate
56	R_m, R_f	-	retardation, matrix and fracture, respectively
59	R*	-	universal gas constant $\left(8.31441 \frac{Pa \bullet m^3}{mol \bullet K}\right)$
62	r_g/ℓ	-	gas (nonwetting phase)/liquid (wetting phase) ratio
64	$\bar{r}_p$, $\bar{r}_f$	-	average annual precipitation (m/s), present and future, respectively

1	S_s	-	specific storage (γc) (m^{-1})
2			
3			
4	S_b	-	bulk storativity $\left(\frac{A \bullet \Delta z \bullet S_s}{\rho g}\right)$ (m^3/Pa)
5			
6			
7	s	-	sample standard deviation, (s^2 is sample variance)
8			
9	s_g,s_ℓ	-	saturation (ratio of gas or liquid volume to total void volume), gas (nonwetting phase) and liq-
10			uid (wetting phase), respectively (V/V_v)
11			
12	s_{gr},$s_{\ell r}$	-	residual saturation, gas (nonwetting phase) and liquid (wetting phase), respectively
13			
14	T_K	-	transmissivity (m^2/s)
15			
16	T	-	temperature (K)
17			
18	T_{cr}	-	critical temperature (Pa)
19			
20	T_r	-	reduced temperature (T/T_{cr})
21			
22	t	-	time (s)
23			
24	$t_{1/2}$	-	radionuclide half life (s)
25			
26	V	-	volume (m^3)
27			
28	V_{cr}	-	theoretical volume of gas assuming ideal gas behavior at critical temperature and pressure of
29			the gas
30			
31	V_d, V_s, V_w	-	volume of the drum, solids, and design capacity of the repository, respectively (m^3)
32			
33	v	-	velocity (m/s)
34			
35	x,y,z	-	variable or parameter
36			
37	$\bar{x}$	-	mean or expected value
38			
39	x_{50},x_{99}	-	value of x at 50% (0.50) quantile and 99% (0.99) quantile
40			
41	Z	-	gas compressibility factor
42			
43	Δz	-	thickness
44			
45	α	-	parameter of probability density function
46			
47	α_L, α_T	-	dispersivity, longitudinal or transverse, respectively (m)
48			
49	$ß_s$, $ß_b$, $ß_\ell$	-	material compressibility solid, bulk [$(1 - \phi)ß_s$], and liquid, respectively (Pa^{-1})
50			
51	Γ	-	strain rate (dv/dy) (s^{-1})
52			
53	γ	-	unit weight (ρg)
54			
55	ε	-	roughness height (m)
56			
57	ξ_1,ξ_2	-	Oldroyd viscosity parameter
58			
59	θ	-	Pleistocene glaciation frequency (s^{-1})
60			
61	$\dot{\theta}$	-	angular velocity of drill bit (m/s)
62			
63	λ	-	failure rate function for probability model of human intrusion
64			
65	μ_ℓ,μ_g	-	viscosity, liquid or gas, respectively (Pa • s)
66			

ρ_s, ρ_b, ρ_f	-	density, solid, bulk, and fluid, respectively (kg/m^3)
τ	-	tortuosity $(\ell / \ell_{path})^2$
Φ	-	Holocene precipitation fluctuation frequency (s^{-1})
ϕ_{lat}	-	latitude
ϕ_m, ϕ_f	-	porosity, matrix and fracture (b/[B + b]), respectively
ζ	-	skin resistance from materials lining fractures, (b_s/D_s)
υ	-	molar volume (m^3/mol)
ν	-	Poisson's ratio
χ	-	mole fraction
η	-	Brooks-Corey relative permeability model parameter exponent

Superscripts

*	-	physical constants
°	-	property at reference conditions
□	-	property in pure fluid
•	-	parameter with respect to time (rate)
–	-	mean of parameter

Subscripts

g	-	gas
ℓ	-	liquid
f	-	fracture
m	-	matrix

Acronyms

ANL-E	-	Argonne National Laboratories, East
ASCII	-	American Standard Code for Information Interchange
ALGEBRA	-	support program for manipulating data in CAMDAT
BLOT	-	a mesh and curve plot program for CAMDAT data
BOAST	-	Black Oil Applied Simulation Tool; 3-D, 3-phase code for flow-through porous media
BRAGFLO	-	Brine And Gas Flow; 2-D, 2-phase code for flow-through porous media
CAM	-	Compliance Assessment Methodology
CAMCON	-	Compliance Assessment Methodology CONtroller–controller (driver) for compliance evaluations developed for WIPP
CAMDAT	-	Compliance Assessment Methodology DATa–computational data base developed for WIPP (modification of GENESIS and EXODUS)
CCDF	-	Complementary Cumulative Distribution Function
CCDFPLT	-	program to calculate and display complementary cumulative distribution function
CH	-	Contact Handled (TRU waste)
DCL	-	Digital Equipment Corporation Command Language
DOE	-	U.S. Department of Energy
DRZ	-	Disturbed Rock Zone
EPA	-	U.S. Environmental Protection Agency
EOS	-	equation of state
FD	-	Finite-Difference numerical analysis
FE	-	Finite-Element numerical analysis
Fm	-	formation
GENMESH	-	rectilinear three-dimensional finite-difference grid generator
HANF	-	Hanford Reservation
HLW	-	High-Level Waste
HST3D	-	a program to simulate heat and solute transport in a three-dimensional groundwater flow system
INEL	-	Idaho National Engineering Laboratory
LANL	-	Los Alamos National Laboratory
LHS	-	Latin Hypercube Sampling (efficient, stratified Monte Carlo sampling)
LLNL	-	Lawrence Livermore National Laboratory
MATSET	-	a program to insert user-selected parameter or material values into the computational data base
MOUND	-	Mound Laboratory

NEFTRAN	-	NEtwork Flow and TRANsport code
NRC	-	U.S. Nuclear Regulatory Commission
NTS	-	Nevada Test Site
ORNL	-	Oak Ridge National Laboratory
PCCSRC	-	program for calculating partial correlation coefficients (PCC) and standardized regression coefficients (SRC)
PREBOAST	-	preprocessor (translator) for input to BOAST
PREBRAG	-	preprocessor (translator) for input to BRAGFLO
PREHST	-	preprocessor (translator) for input to HST3D
PRELHS	-	preprocessor (translator) for input to LHS
PREPCC	-	preprocessor (translator) for input to PCC/SRC
PRENEF	-	preprocessor (translator) for input to NEFTRAN
PRESTEP	-	preprocessor (translator) for input to STEPWISE
PRESUTRA	-	preprocessor (translator) for input to SUTRA
PRESWFT	-	preprocessor (translator) for input to SWIFT II
POSTBOAST	-	postprocessor (translator) of output from BOAST to CAMDAT
POSTBRAG	-	postprocessor (translator) of output from BRAGFLO to CAMDAT
POSTHST	-	postprocessor (translator) of output from HST3D to CAMDAT
POSTLHS	-	postprocessor (translator) of output from LHS to CAMDAT
POSTSUTRA	-	postprocessor (translator) of output from SUTRA to CAMDAT
POSTSWFT	-	postprocessor (translator) of output from SWIFT II to CAMDAT
QA	-	Quality Assurance
RCRA	-	Resource, Conservation, and Recovery Act of 1976 (Public Law 94-580) and subsequent amendments (e.g., HSWA–Hazardous and Solid Waste Amendments of 1984)
RFP	-	Rocky Flats Plant
RH	-	Remotely Handled (TRU waste)
SNL	-	Sandia National Laboratories, Albuquerque, NM
SRS	-	Savannah River Site
STEPWISE	-	stepwise regression program with rank regression and predicted error sum of squares criterion
SWIFTII	-	Sandia Waste-Isolation, Flow and Transport code for solving transient, three-dimensional, coupled equations for fluid flow, heat transport, brine-miscible displacement, and radionuclide-miscible displacement in porous and fractured media
SUTRA	-	Saturated-Unsaturated TRAnsport code
TRACKER	-	a support program to estimate the pathway of a particle released in a fluid velocity field

TRU	-	Transuranic
WIPP	-	Waste Isolation Pilot Plant
40 CFR 191	-	Code of Federal Regulations, Title 40, Part 191

CONVERSION TABLES
FOR SI AND COMMON ENGLISH UNITS

Table 1. Base and Derived SI Units

	Quantity	Name	Symbol	Expression in Terms of Other Units	Expression in Terms of SI Base Units
Base SI Units					
	length	meter	m		
	time	second	s		
	mass	kilogram	kg		
	temperature	kelvin	K		
	amount of substance	mole	mol		
	electric current	ampere	A		
SI-Derived Units					
	force	newton	N		$kg \cdot m \cdot s^{-2}$
	pressure, stress	pascal	Pa	N/m^2	$kg \cdot m^{-1} \cdot s^{-2}$
	energy, work, quantity of heat	joule	J	$N \cdot m$	$kg \cdot m^2 \cdot s^{-2}$
	power, radiant flux	watt	W	J/s	$kg \cdot m^2 \cdot s^{-3}$
	electric potential	volt	V	W/A	$kg \cdot m^2 \cdot s^{-3} \cdot A^{-1}$
	electric resistance	ohm	Ω	V/A	$kg \cdot m^2 \cdot s^{-3} \cdot A^{-2}$
	frequency	hertz	Hz		s^{-1}
	activity (of a radionuclide)	bequerel	Bq		s^{-1}
	absorbed dose	gray	Gy	J/kg	$m^2 \cdot s^{-2}$
	quantity of electricity, electric charge	coulomb	C		$A \cdot s$

Table 2. List of Prefixes

Factor	Prefix	Symbol*
10^{12}	tera	T
10^{9}	giga	G
10^{6}	mega	M
10^{3}	kilo	k
10^{2}	hecto	h
10	deka	da
10^{-1}	deci	d
10^{-2}	centi	c
10^{-3}	milli	m
10^{-6}	micro	μ
10^{-9}	nano	n
10^{-12}	pico	p
10^{-15}	femto	f
10^{-18}	atto	a

* Only the symbols T (tera), G (giga), and M (mega) are capitalized. Compound prefixes are not allowed — for example, use nm (*nano*metre) rather than mμm (*millimicro*metre).

Table 3. Length Conversions

	m	cm	Å	in.	ft	mi	nmi
meter (m)	1	*100	*$1x10^{10}$	39.37	3.281	$6.214x10^{-4}$	$5.400x10^{-4}$
centimeter (cm)	*0.01	1	*$1x10^{8}$	0.3937	$3.281x10^{-2}$	$6.214x10^{-6}$	$5.400x10^{-6}$
angstrom (Å)	*$1x10^{-10}$	*$1x10^{-8}$	1	$3.937x10^{-9}$	$3.281x10^{-10}$	$6.214x10^{-14}$	$5.400x10^{-14}$
inch (in.)	*0.0254	*2.54	*$2.54x10^{8}$	1	$8.333x10^{-2}$	$1.578x10^{-5}$	$1.371x10^{-5}$
foot (ft)	*0.3048	*30.48	*$3.048x10^{9}$	*12	1	$1.894x10^{-4}$	$1.646x10^{-4}$
mile (U.S.) (mi)	1609	$1.609x10^{5}$	$1.609x10^{13}$	*$6.336x10^{4}$	*5280	1	0.8690
nautical mile (nmi)	*1852	*$1.852x10^{5}$	*$1.852x10^{13}$	$7.291x10^{4}$	$6.076x10^{3}$	1.151	1

* Exact

Table 4. Area or Permeability

	m^2	ha	$in.^2$	ft^2	ac	mi^2	Darcy	cm^2
square meters (m^2)	1	*$1x10^{-4}$	1550	10.76	$2.471x10^{-4}$	$3.861x10^{-7}$	$1.013x10^{12}$	*$1.000x10^{4}$
hectare (ha)	*$1x10^{4}$	1	$1.550x10^{7}$	$1.076x10^{5}$	2.471	$3.861x10^{-3}$	$1.013x10^{16}$	*$1.000x10^{8}$
square inches ($in.^2$)	$6.452x10^{-4}$	$6.452x10^{-8}$	1	$6.944x10^{-3}$	$1.594x10^{-7}$	$2.491x10^{-10}$	$6.537x10^{8}$	6.452
square feet (ft^2)	$9.290x10^{-2}$	$9.290x10^{-6}$	144	1	$2.296x10^{-5}$	$3.587x10^{-8}$	$9.413x10^{10}$	929
acre (ac)	4047	0.4047	$6.273x10^{6}$	*$4.356x10^{4}$	1	$1.563x10^{-3}$	$4.100x10^{15}$	$4.047x10^{7}$
square miles (mi^2)	$2.590x10^{6}$	2590	$4.015x10^{9}$	$2.788x10^{7}$	*640	1	2.624	$2.590x10^{10}$
darcy (D)	$9.869x10^{-13}$	$9.869x10^{-17}$	$1.530x10^{-9}$	$1.062x10^{-11}$	$2.439x10^{-16}$	$3.811x10^{-19}$	1	$9.864x10^{-9}$
square centimeters (cm^2)	*$1x10^{-4}$	$1x10^{-8}$	0.1550	$1.076x10^{-3}$	$2.471x10^{-8}$	$3.861x10^{-11}$	$1.013x10^{8}$	1

*Exact

Table 5. Volume

	m^3	l	ft^3	yd^3	gal (U.S.)	bbl	drum	std bx	room	panel	disposal	ac•ft	sec•ft•day	bushel
cubic meters (m^3)	1	*1000	35.31	1.308	264.2	6.290	4.803	0.5618	2.744×10^{-4}	2.169×10^{-5}	2.293×10^{-6}	8.107×10^{-4}	4.087×10^{-4}	28.38
liter (l)	*1×10^{-3}	1	3.531×10^{-2}	1.308×10^{-3}	0.2642	6.290×10^{-3}	4.803×10^{-3}	5.618×10^{-4}	2.744×10^{-7}	2.169×10^{-8}	2.293×10^{-9}	8.107×10^{-7}	4.087×10^{-7}	2.838×10^{-2}
cubic feet (ft^3)	2.832×10^{-2}	28.32	1	3.704×10^{-2}	7.481	0.1781	0.1360	1.591×10^{-2}	7.770×10^{-6}	6.143×10^{-7}	6.494×10^{-8}	2.296×10^{-5}	1.157×10^{-5}	0.8036
cubic yard (yd^3)	0.7646	7646	*27	1	201.97	4.809	3.672	0.4295	2.098×10^{-4}	1.659×10^{-5}	1.753×10^{-6}	6.198×10^{-4}	3.125×10^{-4}	21.70
U.S. gallon (gal)	3.785×10^{-3}	3.785	0.1337	4.951×10^{-3}	1	2.381×10^{-2}	1.818×10^{-2}	2.127×10^{-3}	1.039×10^{-6}	8.212×10^{-8}	8.682×10^{-9}	3.069×10^{-6}	1.547×10^{-6}	0.1074
barrel (bbl)	0.1590	159	5.615	0.2079	*42	1	0.7636	8.932×10^{-2}	4.363×10^{-5}	3.449×10^{-6}	3.646×10^{-7}	1.289×10^{-4}	6.498×10^{-5}	4.512
drum (55-gal)	0.2082	208.2	7.352	0.2723	*55	1.310	1	0.1170	5.713×10^{-5}	4.556×10^{-6}	4.804×10^{-7}	1.688×10^{-4}	8.510×10^{-5}	5.908
standard-waste box (std bx)	1.9	1780	62.86	2.328	470.2	1.120	8.550	1	4.884×10^{-4}	3.895×10^{-5}	4.107×10^{-6}	1.443×10^{-3}	7.275×10^{-4}	50.51
room volume (room)	3644	3.644×10^{6}	1.287×10^{5}	4767	9.627×10^{5}	2.292×10^{4}	1.750×10^{4}	2047	1	7.906×10^{-2}	8.358×10^{-3}	2.955	1.490	1.034×10^{5}
panel volume (panel)	4.610×10^{4}	4.610×10^{7}	1.628×10^{6}	6.029×10^{4}	1.218×10^{7}	2.899×10^{5}	2.214×10^{5}	2.590×10^{4}	12.65	1	0.1057	37.37	18.84	1.308×10^{6}
disposal area (disposal)	4.360×10^{5}	4.360×10^{8}	1.540×10^{7}	5.703×10^{5}	1.152×10^{8}	2.730×10^{5}	2.094×10^{6}	2.450×10^{5}	119.6	9.459	1	353.5	178.2	1.237×10^{7}
acre•foot (ac•ft)	1233	1.233×10^{6}	*43560	1613	3.259×10^{5}	7758	5925	6.930	0.3385	2.699×10^{-2}	2.846×10^{-3}	1	0.5042	3.500×10^{4}
second•foot•day (sec•ft•day)	2447	2.447×10^{6}	*86400	*3200	6.463×10^{5}	1.539×10^{4}	1.175×10^{4}	1374	0.6713	5.353×10^{-2}	5.645×10^{-3}	1.983	1	6.943×10^{4}
bushel (bu)	3.524×10^{-2}	35.24	1.244	4.609×10^{-2}	9.309	0.2216	0.1693	1.980×10^{-2}	9.669×10^{-6}	7.711×10^{-7}	8.131×10^{-8}	2.857×10^{-5}	1.440×10^{-5}	1

*Exact

Table 6. Discharge (Volume/Time)

	m^3/s	m^3/yr	l	ft^3/s	ft^3/min	ft^3/day	acre•ft/day	gal/min	gal/day	bbl/day
cubic meters per second (m^3/s)	1	3.156×10^7	*1000	35.31	2119	3.051×10^6	70.05	1.585×10^4	2.282×10^7	5.434×10^5
cubic meters per year (m^3/yr)	3.169×10^{-8}	1	3.169×10^{-5}	1.119×10^{-6}	6.714×10^{-5}	9.669×10^{-2}	2.220×10^{-6}	5.023×10^{-4}	0.7233	1.722×10^{-2}
liters per second (l/s)	$*1 \times 10^{-3}$	3.156×10^4	1	3.531×10^{-2}	2.119	3051	7.005×10^{-2}	15.85	2.282×10^4	543.4
cubic feet per second (ft^3/s)	2.832×10^{-2}	8.936×10^5	28.32	1	*60	$*8.640 \times 10^4$	1.983	448.8	6.463×10^5	1.539×10^4
cubic feet per minute (ft^3/min)	4.719×10^{-4}	1.489×10^4	0.4719	1.667×10^{-2}	1	1440	3.306×10^{-2}	7.481	1.077×10^4	256.5
cubic feet per day (ft^3/day)	3.277×10^{-7}	10.34	3.277×10^{-4}	1.157×10^{-5}	6.944×10^{-4}	1	2.296×10^{-5}	5.195×10^{-3}	7.481	0.1781
acre•foot per day (acre• ft/day)	1.428×10^{-2}	4.505×10^5	14.28	0.5042	30.25	4.356×10^4	1	226.3	3.259×10^5	7758
gallons per minute (gal/min)	6.309×10^{-5}	1991	6.309×10^{-2}	2.228×10^{-3}	0.1337	19.25	4.419×10^{-3}	1	1440	34.29
gallons per day (gal/day)	4.381×10^{-8}	1.383	4.381×10^{-5}	1.547×10^{-6}	9.283×10^{-5}	0.1337	3.069×10^{-6}	6.944×10^{-4}	1	2.381×10^{-2}
barrels per day (bbl/day)	1.840×10^{-6}	58.07	1.840×10^{-3}	6.498×10^{-5}	3.899×10^{-3}	5.615	1.289×10^{-4}	2.917×10^{-2}	*42	1

*Exact

Table 7. Velocity, Hydraulic Conductivity, Precipitation

	m/s	m/yr	in./yr	cm/yr	km/yr	ft/s	ft/day	mph	knots	gal/(day•ft^2)
meters per second (m/s)	1	3.156×10^{7}	1.242×10^{9}	3.156×10^{9}	3.156×10^{4}	3.281	2.835×10^{5}	2.237	1.944	2.120×10^{6}
meters per year (m/yr)	3.169×10^{-8}	1	39.37	*100	$*1 \times 10^{-3}$	1.040×10^{-7}	8.983×10^{-3}	7.089×10^{-8}	6.160×10^{-8}	6.719×10^{-2}
inches per year (in./yr)	8.049×10^{-10}	$*2.540 \times 10^{-2}$	1	*2.540	$*2.540 \times 10^{-5}$	2.641×10^{-9}	2.282×10^{-4}	1.800×10^{-9}	1.565×10^{-9}	1.707×10^{-3}
centimeters per year (cm/yr)	3.169×10^{-10}	$*1 \times 10^{-2}$	0.3937	1	$*1 \times 10^{-5}$	1.040×10^{-9}	8.983×10^{-5}	7.089×10^{-10}	6.160×10^{-10}	6.719×10^{-4}
kilometers per year (km/yr)	3.169×10^{-5}	*1000	3.937×10^{4}	$*1 \times 10^{5}$	1	1.040×10^{-4}	8.983	7.089×10^{-5}	6.160×10^{-5}	67.19
feet per second (ft/s)	*0.3048	9.619×10^{6}	3.787×10^{8}	9.619×10^{8}	9619	1	$*8.640 \times 10^{4}$	0.6818	0.5925	6.463×10^{5}
feet per day (ft/day)	3.528×10^{-6}	111.3	4383	1.113×10^{4}	0.1113	1.157×10^{-5}	1	7.891×10^{-6}	6.857×10^{-6}	7.481
miles per hour (mph)	0.4470	1.411×10^{7}	5.554×10^{8}	1.411×10^{9}	1.411×10^{4}	1.467	1.267×10^{5}	1	0.8690	9.479×10^{5}
knots	0.5144	1.623×10^{7}	6.391×10^{8}	1.623×10^{9}	1.623×10^{4}	1.688	1.458×10^{5}	1.151	1	1.091×10^{6}
gallons per day per square foot (gal/(day•ft^2))	4.716×10^{-7}	14.88	585.9	1488	1.488×10^{-2}	1.547×10^{-6}	0.1337	$.055 \times 10^{-6}$	9.167×10^{-7}	1

*Exact

Table 8. Force

	N	kg-force	dyne	lbf
Newton (N)	1	0.1020	*$1x10^5$	0.2248
kilogram-force (kg-force)	9.807	1	$9.807x10^5$	2.205
dyne	*$1.00x10^{-5}$	$1.020x10^{-6}$	1	$2.248x10^{-6}$
pound force (lbf)	4.448	0.4536	$4.448x10^5$	1

*Exact

Table 9. Pressure and Stress

	Pa	bar	$dyne/cm^2$	atm	mm Hg	psi	lb/ft^2
pascal (Pa)	1	*$1x10^{-5}$	*10	$9.869x10^{-6}$	$7.501x10^{-3}$	$1.450x10^{-4}$	$2.089x10^{-2}$
bar	*$1x10^5$	1	*$1x10^6$	0.9869	750.1	14.50	2089
dyne per square centimeters ($dyne/cm^2$)	*0.1	*$1x10^{-6}$	1	$9.869x10^{-7}$	$7.501x10^{-4}$	$1.450x10^{-5}$	$2.089x10^{-3}$
atmosphere (atm)	$1.013x10^5$	1.013	$1.013x10^6$	1	*760	14.70	2116
millimeter of Mercury (mm Hg)	1333	$1.333x10^{-3}$	1333	$1.316x10^{-3}$	1	$1.934x10^{-2}$	2.785
pound per square inch (psi)	698.5	$6.895x10^{-2}$	$6.895x10^4$	$6.805x10^{-2}$	51.71	1	*144
pounds per square foot (lb/ft^2)	47.88	$4.788x10^{-4}$	478.8	$4.725x10^{-4}$	0.3591	$6.944x10^{-3}$	1

*Exact

Table 10. Absolute Viscosity

	Pa•s (kg/(m•s))	cP	lbm/ft/s	slug/(ft•s) lbf • ft/s^2
Pascal-second (Pa•s) (kg/(m•s))	1	*1000	0.6720	2.089×10^{-2}
centipoise (cP)	*1×10^{-3}	1	6.720×10^{-4}	2.089×10^{-5}
pound mass per foot per second (lbm/ft/s)	1.488	1488	1	3.108×10^{-2}
slug per foot per second (slug/(ft•s) or lbf • ft/s^2)	47.88	4.788×10^{4}	32.17	1

*Exact

Table 11. Mass

	kg	metric tonne	oz	lbm	short ton	long ton	slug
kilogram (kg)	1	*1×10^{-3}	35.27	2.205	1.102×10^{-3}	9.842×10^{-4}	6.852×10^{-2}
metric tonne (t)	*1000	1	3.527×10^{4}	2205	1.102	0.9842	68.52
avoirdupois ounce (oz)	2.835×10^{-2}	2.835×10^{-5}	1	*0.0625	*3.125×10^{-5}	2.790×10^{-5}	1.943×10^{-3}
pound mass (lbm)	0.4536	4.536×10^{-4}	*16	1	*5.000×10^{-4}	4.464×10^{-4}	3.108×10^{-2}
short ton	907.2	9.072	*32000	*2000	1	0.8927	62.16
long ton	1016	1.016	*35840	*2240	*1.12	1	69.62
slug	14.59	1.459×10^{-2}	514.8	32.17	1.609×10^{-2}	1.436×10^{-2}	1

*Exact

Table 12. Density

	kg/m^3	g/cm^3	lb/ft^3	lb/gal	lb/bbl
kilogram per cubic meters (kg/m^3)	1	$*1x10^{-3}$	$6.243x10^{-2}$	$8.345x10^{-3}$	2.853
grams per cubic centimeters (g/cm^3)	*1000	1	62.43	8.345	350.5
pounds per cubic feet (lb/ft^3)	16.02	$1.602x10^{-2}$	1	0.1337	5.615
pounds per gallon (lb/gal)	119.8	0.1198	7.481	1	*42
pounds per barrel (lb/bbl)	2.853	$2.853x10^{-3}$	0.1781	$2.381x10^{-2}$	1

*Exact

Table 13. Time

	s	min	h	day	yr
mean solar second (s)	1	$1.6667x10^{-2}$	$2.7779x10^{-4}$	$1.15741x10^{-5}$	$3.1689x10^{-8}$
mean solar minute (min)	*60	1	$1.6667x10^{-2}$	$6.9444x10^{-4}$	$1.9013x10^{-6}$
mean solar hour (h)	*3600	*60	1	$4.16667x10^{-2}$	$1.1408x10^{-4}$
mean solar day	$*8.640x10^4$	*1440	*24	1	$2.7379x10^{-3}$
tropical time year (yr)	$3.1557x10^7$	$5.2595x10^5$	8765.8	365.24	1

*Exact

Table 14. Temperature (T)

	K	°C	°R	°F
kelvin (K)	1	K-273.15	K x 9/5	(K-273.15) x 9/5 +32
Celsius (°C)	°C + 273.15	1	(°C + 273.15) x 9/5	°C x 9/5 +32
Rankine (°R)	°R x 5/9	(°R x 5/9) -273.15	1	°R -459.67
Fahrenheit (°F)	(°F + 459.67) x 5/9	(°F - 32) x 5/9	°F + 459.67	1

Table 15. Specific Activity(1)

	Bq	Ci	kg
becquerel (Bq)	1	2.703×10^{-11}	$\frac{\ln^2}{t_{1/2}} \times \frac{6.022 \times 10^{23}}{M} \times \frac{10^3 g}{kg} = \frac{4.174 \times 10^{26}}{t_{1/2} \times M}$
curie (Ci)	*3.7×10^{10}	1	$\frac{1.128 \times 10^{16}}{t_{1/2} \times M}$
kg	$2.396 \times 10^{-27} \times t_{1/2}^{(2)} \times M^{(3)}$	$8.864 \times 10^{-17} \times t_{1/2} \times M$	1

(1) Specific Activity is $\frac{ds_A}{s_A}$; where $s_A = s_{OA}\, e^{-\lambda t}$; $\frac{\lambda = \ln^2}{t_{1/2}}$

(2) $t_{1/2}$ is half life in seconds

(3) M is gram molecular weight (g/mol)

*Exact

Table 16. Miscellaneous

To convert:	to	Multiply by	Inverse
1. Angular velocity rad/s	rpm	$\frac{30}{\pi} = 9.549$	$\frac{\pi}{30} = 0.1047$
2. Radioactivity			
a. Dose equivalent Sv	rem	100	0.01
b. Absorbed dose Gy (gray) (1J/kg)	rad	100	0.01
c. Activity (1 disintegration/s) becquerel (Bq)	Ci	2.703×10^{-11}	3.7×10^{10}
d. Charge roentgen (R)	c/kg	2.58×10^{-4}	3876

DISTRIBUTION

(Send Distribution list changes to M.M. Gruebel, Dept. 6342, Sandia National Laboratories, PO Box 5800, Albuquerque, NM 87185-5800)

Federal Agencies

US Department of Energy (2)
Office of Environmental Restoration and Waste Management
Attn: L.P. Duffy, EM-1
C. Frank, EM-50
Washington, DC 20585

US Department of Energy (3)
Office of Environmental Restoration and Waste Management
Attn: M. Frei, EM-34 (Trevion II)
Director, Waste Management Projects
Washington, DC 20585-0002

US Department of Energy
Office of Environmental Restoration and Waste Management
Attn: J. Lytle, EM-30 (Trevion II)
Washington, DC 20585-0002

US Department of Energy
Office of Environmental Restoration and Waste Management
Attn: S. Schneider, EM-342 (Trevion II)
Washington, DC 20585-0002

US Department of Energy (3)
WIPP Task Force
Attn: G.H. Daly
S. Fucigna
B. Bower
12800 Middlebrook Rd.
Suite 400
Germantown, MD 20874

US Department of Energy (4)
Office of Environment, Safety and Health
Attn: R.P. Berube, EH-20
C. Borgstrum, EH-25
R. Pelletier, EH-231
K. Taimi, EH-232
Washington, DC 20585

US Department of Energy (5)
WIPP Project Integration Office
Attn: W.J. Arthur III
R. Becker
P. Dickman
L.W. Gage
P.J. Higgins
D.A. Olona
PO Box 5400
Albuquerque, NM 87115-5400

US Department of Energy (10)
WIPP Project Site Office (Carlsbad)
Attn: A. Hunt (4)
V. Daub (4)
J. Lippis
K. Hunter
PO Box 3090
Carlsbad, NM 88221-3090

US Department of Energy, (5)
Office of Civilian Radioactive Waste Management
Attn: Deputy Director, RW-2
Associate Director, RW-10
Office of Program Administration and Resources Management
Associate Director, RW-20
Office of Facilities Siting and Development
Associate Director, RW-30
Office of Systems Integration and Regulations
Associate Director, RW-40
Office of External Relations and Policy
Office of Geologic Repositories
Forrestal Building
Washington, DC 20585

US Department of Energy
Attn: National Atomic Museum Library
Albuquerque Operations Office
PO Box 5400
Albuquerque, NM 87185

US Department of Energy
Research & Waste Management Division
Attn: Director
PO Box E
Oak Ridge, TN 37831

US Department of Energy (2)
Idaho Operations Office
Fuel Processing and Waste
Management Division
785 DOE Place
Idaho Falls, ID 83402

US Department of Energy
Savannah River Operations Office
Defense Waste Processing
Facility Project Office
Attn: W.D. Pearson
PO Box A
Aiken, SC 29802

US Department of Energy (2)
Richland Operations Office
Nuclear Fuel Cycle & Production
Division
Attn: R.E. Gerton
825 Jadwin Ave.
PO Box 500
Richland, WA 99352

US Department of Energy (3)
Nevada Operations Office
Attn: J.R. Boland
D. Livingston
P.K. Fitzsimmons
2753 S. Highland Drive
Las Vegas, NV 89183-8518

US Department of Energy (2)
Technical Information Center
PO Box 62
Oak Ridge, TN 37831

US Department of Energy (2)
Chicago Operations Office
Attn: J.C. Haugen
9800 South Cass Avenue
Argonne, IL 60439

US Department of Energy
Los Alamos Area Office
528 35th Street
Los Alamos, NM 87544

US Department of Energy (3)
Rocky Flats Area Office
Attn: W.C. Rask
G. Huffman
T. Lukow
PO Box 928
Golden, CO 80402-0928

US Department of Energy
Dayton Area Office
Attn: R. Grandfield
PO Box 66
Miamisburg, OH 45343-0066

US Department of Energy
Attn: E. Young
Room E-178
GAO/RCED/GTN
Washington, DC 20545

US Bureau of Land Management
101 E. Mermod
Carlsbad, NM 88220

US Bureau of Land Management
New Mexico State Office
PO Box 1449
Santa Fe, NM 87507

US Environmental Protection
Agency (2)
Office of Radiation Protection Programs
(ANR-460)
Washington, DC 20460

US Nuclear Regulatory Commission
Division of Waste Management
Attn: H. Marson
Mail Stop 4-H-3
Washington, DC 20555

US Nuclear Regulatory Commission (4)
Advisory Committee on Nuclear Waste
Attn: D. Moeller
M.J. Steindler
P.W. Pomeroy
W.J. Hinze
7920 Norfolk Avenue
Bethesda, MD 20814

Defense Nuclear Facilities Safety Board
Attn: D. Winters
625 Indiana Avenue, NW
Suite 700
Washington, DC 20004

Nuclear Waste Technical Review
Board (2)
Attn: Library
Suite 910
1100 Wilson Blvd.
Arlington, VA 22209-2297

Energy and Science Division
Office of Management and Budget
Attn: K. Yuracko
725 17th Street NW
Washington, DC 20503

US Geological Survey (2)
Water Resources Division
Attn: C. Peters
Suite 200
4501 Indian School NE
Albuquerque, NM 87110

New Mexico Congressional Delegation

Jeff Bingaman
U.S. Senate
110 Hart SOB
Washington, DC 20510-3102

Pete V. Domenici
U.S. Senate
427 Dirksen Bldg.
Washington, DC 20510-3101

Bill Richardson
House of Representatives
2349 Rayburn HOB
Washington, DC 20515

Steven H. Schiff
House of Representatives
1009 Longworth HOB
Washington, DC 20515

Joe Skeen
House of Representatives
2367 Rayburn HOB
Washington, DC 20515

State Agencies

New Mexico Bureau of Mines
and Mineral Resources
Socorro, NM 87801

New Mexico Energy, Minerals and Natural
Resources Department
Attn: Librarian
2040 South Pacheco
Santa Fe, NM 87505

New Mexico Energy, Minerals and Natural
Resources Department
New Mexico Radioactive Task Force (2)
(Governor's WIPP Task Force)
Attn: A. Lockwood, Chairman
C. Wentz, Coordinator/Policy Analyst
2040 South Pacheco
Santa Fe, NM 87505

Bob Forrest
Mayor, City of Carlsbad
PO Box 1569
Carlsbad, NM 88221

Executive Director
Carlsbad Department of Development
Attn: C. Bernard
PO Box 1090
Carlsbad, NM 88221

New Mexico Environment Department
Secretary of the Environment (3)
Attn: J. Espinosa
PO Box 968
1190 St. Francis Drive
Santa Fe, NM 87503-0968

New Mexico Environment Department
Attn: P. McCasland
WIPP Project Site Office
PO Box 3090
Carlsbad, NM 88221-3090

New Mexico State Engineer's Office
Attn: M. Chudnoff
PO Box 25102
Santa Fe, NM 87504-5102

Environmental Evaluation Group (5)
Attn: R. Neill
Suite F-2
7007 Wyoming Blvd. NE
Albuquerque, NM 87109

Advisory Committee on Nuclear Facility Safety

John F. Ahearne
Executive Director, Sigma Xi
99 Alexander Drive
Research Triangle Park, NC 27709

James E. Martin
109 Observatory Road
Ann Arbor, MI 48109

WIPP Panel of National Research Council's Board on Radioactive Waste Management

Charles Fairhurst, Chairman
Department of Civil and
Mineral Engineering
University of Minnesota
500 Pillsbury Dr., SE
Minneapolis, MN 55455-0220

John O. Blomeke
3833 Sandy Shore Drive
Lenoir City, TN 37771-9803

John D. Bredehoeft
Western Region Hydrologist
Water Resources Division
US Geological Survey (M/S 439)
345 Middlefield Road
Menlo Park, CA 94025

Fred M. Ernsberger
1325 NW 10th Avenue
Gainsville, FL 32601

Rodney C. Ewing
Department of Geology
University of New Mexico
200 Yale, NE
Albuquerque, NM 87131

B. John Garrick
PLG, Inc.
Suite 400
4590 MacArthur Blvd.
Newport Beach, CA 92660-2027

Leonard F. Konikow
US Geological Survey
431 National Center
Reston, VA 22092

Jeremiah O'Driscoll
505 Valley Hill Drive
Atlanta, GA 30350

Christopher Whipple
Clement International Corp.
160 Spear St.
Suite 1380
San Francisco, CA 94105-1535

National Research Council (3)
Board on Radioactive
Waste Management
RM HA456
Attn: P.B. Myers,
Staff Director (2)
G.J. Grube
2101 Constitution Avenue
Washington, DC 20418

Performance Assessment Peer Review Panel

G. Ross Heath
College of Ocean and
Fishery Sciences HN-15
583 Henderson Hall
University of Washington
Seattle, WA 98195

Thomas H. Pigford
Department of Nuclear Engineering
4159 Etcheverry Hall
University of California
Berkeley, CA 94720

Thomas A. Cotton
JK Research Associates, Inc.
4429 Butterworth Place, NW
Washington, DC 20016

Robert J. Budnitz
President, Future Resources
Associates, Inc.
2000 Center Street
Suite 418
Berkeley, CA 94704

C. John Mann
Department of Geology
245 Natural History Bldg.
1301 West Green Street
University of Illinois
Urbana, IL 61801

Frank W. Schwartz
Department of Geology and Mineralogy
The Ohio State University
Scott Hall
1090 Carmack Rd.
Columbus, OH 43210

National Laboratories

Argonne National Laboratory (2)
Attn: A. Smith
D. Tomasko
9700 South Cass, Bldg. 201
Argonne, IL 60439

Battelle Pacific Northwest Laboratory (3)
Attn: R.E. Westerman
S. Bates
H.C. Burkholder
Battelle Boulevard
Richland, WA 99352

Idaho National Engineering Laboratory (2)
Attn: H. Loo
R. Klinger
Mail Stop 5108
Idaho Falls, ID 83403-4000

Los Alamos National Laboratory
Attn: B. Erdal, CNC-11
PO Box 1663
Los Alamos, NM 87545

Los Alamos National Laboratory
Attn: A. Meijer
PO Box 1663, Mail Stop J514
Los Alamos, NM 87545

Los Alamos National Laboratory (3)
HSE-8
Attn: M. Enoris
L. Soholt
J. Wenzel
PO Box 1663
Los Alamos, NM 87545

Los Alamos National Laboratory
EM-7
Attn: S. Kosiewicz
PO Box 1663, Mail Stop J595
Los Alamos, NM 87545

Oak Ridge National Laboratory
Transuranic Waste Manager
Attn: D.W. Turner
PO Box 2008, Bldg. 3047
Oak Ridge, TN 37831-6060

Pacific Northwest Laboratory
Attn: B. Kennedy
PO Box 999
Richland, WA 99352

Savannah River Laboratory (3)
Attn: N. Bibler
M.J. Plodinec
G.G. Wicks
Aiken, SC 29801

Savannah River Plant (2)
Attn: R.G. Baxter
Bldg. 704-S
K.W. Wierzbicki
Bldg. 703-H
Aiken, SC 29808-0001

Corporations/Members of the Public

Benchmark Environmental Corp.
Attn: C. Frederickson
4501 Indian School NE
Suite 105
Albuquerque, NM 87110

City of Albuquerque
Public Works Department
Utility Planning Division
Attn: W.K. Summers
PO Box 1293
Albuquerque, NM 87103

Deuel and Associates, Inc.
Attn: R.W. Prindle
7208 Jefferson NE
Albuquerque, NM 87109

Disposal Safety, Inc.
Attn: B. Ross
1660 L Street NW
Suite 314
Washington, DC 20036

Ecodynamics (2)
Attn: P. Roache
R. Blaine
PO Box 9229
Albuquerque, NM 87119-9229

EG & G Idaho (3)
1955 Fremont Street
Attn: C. Atwood
C. Hertzler
T.I. Clements
Idaho Falls, ID 83415

Geomatrix
Attn: K. Coppersmith
100 Pine Street, Suite 1000
San Francisco, CA 94111

Golder Associates, Inc. (3)
Attn: M. Cunnane
R. Kossik
I. Miller
4104 148th Avenue NE
Redmond, WA 98052

INTERA, Inc. (2)
Attn: J.F. Pickens
A.M. LaVenve
6850 Austin Center Blvd.
Suite 300
Austin, TX 78731

INTERA, Inc.
Attn: W. Stensrud
PO Box 2123
Carlsbad, NM 88221

INTERA, Inc.
Attn: W. Nelson
101 Convention Center Drive
Suite 540
Las Vegas, NV 89109

IT Corporation (2)
Attn: R.F. McKinney
J. Myers
Regional Office, Suite 700
5301 Central Avenue NE
Albuquerque, NM 87108

John Hart and Associates, P.A.
Attn: J.S. Hart
2815 Candelaria Road NW
Albuquerque, NM 87107

John Hart and Associates, P.A.
Attn: K. Lickliter
1009 North Washington
Tacoma, WA 98406

MACTEC (2)
Attn: J.A. Thies
D.K. Duncan
8418 Zuni Road SE, Suite 200
Albuquerque, NM 87108

Newman and Holtzinger
Attn: C. Mallon
1615 L Street NW, Suite 1000
Washington, DC 20036

RE/SPEC, Inc. (2)
Attn: W. Coons
4775 Indian School NE, Suite 300
Albuquerque, NM 87110

RE/SPEC, Inc.
Attn: J.L. Ratigan
PO Box 725
Rapid City, SD 57709

Reynolds Elect/Engr. Co., Inc.
Attn: E.W. Kendall
Building 790, Warehouse Row
PO Box 98521
Las Vegas, NV 89193-8521

Roy F. Weston, Inc.
CRWM Tech. Supp. Team
Attn: C.J. Noronha
955 L'Enfant Plaza SW
North Building, Eighth Floor
Washington, DC 20024

Science Applications International Corporation (SAIC)
Attn: H.R. Pratt
10260 Campus Point Drive
San Diego, CA 92121

Science Applications International Corporation (2)
Attn: D.C.Royer
C.G. Pflum
101 Convention Center Dr.
Las Vegas, NV 89109

Science Applications International Corporation (2)
Attn: M. Davis
J. Tollison
2109 Air Park Road SE
Albuquerque, NM 87106

Science Applications International Corporation (2)
Attn: J. Young
D. Lester
18706 North Creek Parkway, Suite 110
Bothell, WA 98011

Southwest Research Institute
Center for Nuclear Waste Regulatory Analysis (2)
Attn: P.K. Nair
6220 Culebra Road
San Antonio, TX 78228-0510

Systems, Science, and Software (2)
Attn: E. Peterson
P. Lagus
Box 1620
La Jolla, CA 92038

TASC
Attn: S.G. Oston
55 Walkers Brook Drive
Reading, MA 01867

Tech Reps, Inc. (6)
Attn: J. Chapman
C. Crawford
D. Marchand
J. Stikar
P. Oliver
D. Scott
5000 Marble NE, Suite 222
Albuquerque, NM 87110

Tolan, Beeson & Associates
Attn: T.L. Tolan
2320 W. 15th Avenue
Kennewick, WA 99337

TRW Environmental Safety Systems
Attn: I. Sacks
2650 Park Tower Drive, Suite 800
Vienna, VA 22180

Westinghouse Electric Corporation (5)
Attn: Library
L. Trego
C. Cox
L. Fitch
R.F. Kehrman
PO Box 2078
Carlsbad, NM 88221

Westinghouse Hanford Company
Attn: D. E. Wood
MSIN HO-32
PO Box 1970
Richland, WA 99352

Western Water Consultants
Attn: D. Fritz
1949 Sugarland Drive #134
Sheridan, WY 82801-5720

Western Water Consultants
Attn: P.A. Rechard
PO Box 4128
Laramie, WY 82071

P. Drez
8816 Cherry Hills Road, NE
Albuquerque, NM 87111

D.W. Powers
Star Route Box 87
Anthony, TX 79821

Shirley Thieda
PO Box 2109, RR1
Bernalillo, NM 87004

Jack Urich
c/o CARD
144 Harvard SE
Albuquerque, NM 87106

Universities

University of California
Mechanical, Aerospace, and
Nuclear Engineering Department (2)
Attn: W. Kastenberg
D. Browne
5532 Boelter Hall
Los Angeles, CA 90024

University of California
Mine Engineering Dept.
Attn: Neville Cook
Rock Mechanics Engineering
Berkeley, CA 94720

University of Hawaii at Hilo
Attn: S. Hora
Business Administration
Hilo, HI 96720-4091

University of New Mexico
Geology Department
Attn: Library
Albuquerque, NM 87131

University of New Mexico
Research Administration
Attn: H. Schreyer
102 Scholes Hall
Albuquerque, NM 87131

University of Wyoming
Department of Civil Engineering
Attn: V.R. Hasfurther
Laramie, WY 82071

University of Wyoming
Department of Geology
Attn: J.I. Drever
Laramie, WY 82071

University of Wyoming
Department of Mathematics
Attn: R.E. Ewing
Laramie, WY 82071

Libraries

Thomas Brannigan Library
Attn: D. Dresp
106 W. Hadley St.
Las Cruces, NM 88001

Hobbs Public Library
Attn: M. Lewis
509 N. Ship Street
Hobbs, NM 88248

New Mexico State Library
Attn: N. McCallan
325 Don Gaspar
Santa Fe, NM 87503

New Mexico Tech
Martin Speere Memorial Library
Campus Street
Socorro, NM 87810

New Mexico Junior College
Pannell Library
Attn: R. Hill
Lovington Highway
Hobbs, NM 88240

Carlsbad Municipal Library
WIPP Public Reading Room
Attn: L. Hubbard
101 S. Halagueno St.
Carlsbad, NM 88220

University of New Mexico
General Library
Government Publications Department
Albuquerque, NM 87131

NEA/Performance Assessment Advisory Group (PAAG)

P. Duerden
ANSTO
Lucas Heights Research Laboratories
Private Mail Bag No. 1
Menai, NSW 2234, AUSTRALIA

Gordon S. Linsley
Division of Nuclear Fuel Cycle and Waste Management
International Atomic Energy Agency
PO Box 100
A-1400 Vienna, AUSTRIA

Nicolo Cadelli
Commission of the European Communities
200, Rue de la Loi
B-1049 Brussels, BELGIUM

R. Heremans
Organisme Nationale des Déchets Radioactifs et des Matiéres Fissiles
ONDRAF
Place Madou 1, Boitec 24/25
B-1030 Brussels, BELGIUM

J. Marivoet
Centre d'Etudes de l'Energie Nucléaire
CEN/SCK
Boeretang 200
B-2400 Mol, BELGIUM

P. Conlon
Waste Management Division
Atomic Energy Control Board (AECB)
PO Box 1046
Ottawa, Canada KIP 559, CANADA

A.G. Wikjord
Manager, Environmental and Safety Assessment Branch
Atomic Energy of Canada Limited
Whiteshell Nuclear Research Establishment
Pinewa, Manitoba ROE 1LO, CANADA

Jukka-Pekka Salo
Teollisuuden Voima Oy (TVO)
Fredrikinkatu 51-53 B
SF-00100 Helsinki, FINLAND

Timo Vieno
Technical Research Centre of Finland (VTT)
Nuclear Energy Laboratory
PO Box 208
SF-02151 Espoo, FINLAND

Timo Äikäs
Teollisuuden Voima Oy (TVO)
Fredrikinkatu 51-53 B
SF-00100 Helsinki, FINLAND

M. Claude Ringeard
Division de la Sécurité et de la Protection de l'Environment (DSPE)
Commissariat á l'Energie Atomique
Agence Nationale pour la Gestion des Déchets Radioactifs (ANDRA)
Route du Panorama Robert Schuman
B. P. No. 38
F-92266 Fontenay-aux-Roses Cedex
FRANCE

Gérald Ouzounian
Agence Nationale pour la Gestion des Déchets Radioactifs (ANDRA)
Route du Panorama Robert Schuman
B. P. No. 38
F-92266 Fontenay-aux-Roses Cedex
FRANCE

Claudio Pescatore
Division of Radiation Protection and Waste Management
OECD Nuclear Energy Agency
38, Boulevard Suchet
F-75016 Paris, FRANCE

M. Dominique Greneche
Commissariat á l'Energie Atomique
IPSN/DAS/SASICC/SAED
B. P. No. 6
F-92265 Fontenay-aux-Roses Cedex,
FRANCE

Robert Fabriol
Bureau de Recherches Géologiques et Miniéres (BRGM)
B. P. 6009
45060 Orléans Cedex 2, FRANCE

P. Bogorinski
Gesellschaft für Reaktorsicherheit (GRS) mbH
Schwertnergasse 1
D-5000 Köln 1, GERMANY

R. Storck
GSF - Institut für Tieflagerung
Theodor-Heuss-Strabe 4
D-3300 Braunschweig, GERMANY

Ferrucio Gera
ISMES S.p.A
Via del Crociferi 44
I-00187 Rome, ITALY

Hiroyuki Umeki
Isolation System Research Program
Radioactive Waste Management Project
Power Reactor and Nuclear Fuel Development Corporation (PNC)
1-9-13, Akasaka
Minato-ku
Tokyo 107, JAPAN

P. Carboneras Martinez
ENRESA
Calle Emilio Vargas 7
R-28043 Madrid, SPAIN

Tönis Papp
Swedish Nuclear Fuel and Waste Management Co.
Box 5864
S 102 48 Stockholm, SWEDEN

Conny Hägg
Swedish Radiation Protection Institute (SSI)
Box 60204
S-104 01 Stockholm, SWEDEN

J. Hadermann
Paul Scherrer Institute
Waste Management Programme
CH-5232 Villigen PSI, SWITZERLAND

J. Vigfusson
USK - Swiss Nuclear Safety Inspectorate
Federal Office of Energy
CH-5303 Würenlingen, SWITZERLAND

D.E. Billington
Departmental Manager - Assessment Studies
Radwaste Disposal R&D Division
AEA Decommissioning & Radwaste
Harwell Laboratory, B60
Didcot Oxfordshire OX11 ORA
UNITED KINGDOM

P. Grimwood
Waste Management Unit
BNFL
Sellafield
Seascale, Cumbria CA20 1PG
UNITED KINGDOM

Alan J. Hooper
UK Nirex Ltd
Curie Avenue
Harwell, Didcot
Oxfordshire, OX11 ORH
UNITED KINGDOM

Jerry M. Boak
Yucca Mountain Project Office
US Department of Energy
PO Box 98608
Las Vegas, NV 89193

Seth M. Coplan (Chairman)
US Nuclear Regulatory Commission
Division of High-Level Waste Management
Mail Stop 4-H-3
Washington, DC 20555

A.E. Van Luik
INTERA/M&O
The Valley Bank Center
101 Convention Center Dr.
Las Vegas, NV 89109

NEA/PSAG User's Group

Shaheed Hossain
Division of Nuclear Fuel Cycle and Waste Management
International Atomic Energy Agency
Wagramerstrasse 5
PO Box 100
A-1400 Vienna, AUSTRIA

Alexander Nies (PSAC Chairman)
Gesellschaft für Strahlen- und
Institut für Tieflagerung
Abteilung für Endlagersicherheit
Theodor-Heuss-Strasse 4
D-3300 Braunschweig, GERMANY

Eduard Hofer
Gesellschaft für Reaktorsicherheit (GRS) MBH
Forschungsgelände
D-8046 Garching, GERMANY

Andrea Saltelli
Commission of the European Communities
Joint Resarch Centre of Ispra
I-21020 Ispra (Varese), ITALY

Alejandro Alonso
Cátedra de Tecnología Nuclear
E.T.S. de Ingenieros Industriales
José Gutiérrez Abascal, 2
E-28006 Madrid, SPAIN

Pedro Prado
CIEMAT
Instituto de Tecnología Nuclear
Avenida Complutense, 22
E-28040 Madrid, SPAIN

Miguel Angel Cuñado
ENRESA
Emilio Vargas, 7
E-28043 Madrid, SPAIN

Francisco Javier Elorza
ENRESA
Emilio Vargas, 7
E-28043 Madrid, SPAIN

Nils A. Kjellbert
Swedish Nuclear Fuel and Waste Management Company (SKB)
Box 5864
S-102 48 Stockholm, SWEDEN

Björn Cronhjort
Swedish National Board for Spent Nuclear Fuel (SKN)
Sehlsedtsgatan 9
S-115 28 Stockholm, SWEDEN

Richard A. Klos
Paul-Scherrer Institute (PSI)
CH-5232 Villingen PSI
SWITZERLAND

NAGRA (2)
Attn: C. McCombie
F. Van Dorp
Parkstrasse 23
CH-5401 Baden, SWITZERLAND

N. A. Chapman
Intera Information Technologies
Park View House, 14B Burton Street
Melton Mowbray
Leicestershire, LE13 1AE
UNITED KINGDOM

Daniel A. Galson
Galson Sciences Ltd.
35, Market Place
Oakham
Leicestershire LE15 6DT
UNITED KINGDOM

David P. Hodgkinson
Intera Information Technologies
Chiltern House
45 Station Road
Henley-on-Thames
Oxfordshire RG9 1AT, UNITED KINGDOM

Brian G.J. Thompson
Department of the Environment: Her Majesty's Inspectorate of Pollution
Room A5.33, Romney House
43 Marsham Street
London SW1P 2PY, UNITED KINGDOM

Intera Information Technologies
Attn: M.J.Apted
3609 South Wadsworth Blvd.
Denver, CO 80235

US Nuclear Regulatory Commission (2)
Attn: R. Codell
N. Eisenberg
Mail Stop 4-H-3
Washington, DC 20555

Battelle Pacific Northwest Laboratories
Attn: P.W. Eslinger
PO Box 999, MS K2-32
Richland, WA 99352

Center for Nuclear Waste Regulatory Analysis (CNWRA)
Southwest Research Institute
Attn: B. Sagar
PO Drawer 28510
6220 Culebra Road
San Antonio, TX 78284

Geostatistics Expert Working Group (GXG)

Rafael L. Bras
R.L. Bras Consulting Engineers
44 Percy Road
Lexington, MA 02173

Jesus Carrera
Universidad Politècnica de Cataluña
E.T.S.I. Caminos
Jordi, Girona 31
E-08034 Barcelona, SPAIN

Gedeon Dagan
Department of Fluid Mechanics and Heat Transfer
Tel Aviv University
PO Box 39040
Ramat Aviv, Tel Aviv 69978, ISRAEL

Ghislain de Marsily (GXG Chairman)
University Pierre et Marie Curie
Laboratorie de Geologie Applique
4, Place Jussieu - T.26 - 5^{e} etage
75252 Paris Cedex 05, FRANCE

Alain Galli
Centre de Geostatistique
Ecole des Mines de Paris
35 Rue St. Honore
77035 Fontainebleau, FRANCE

Steve Gorelick
Department of Applied Earth Sciences
Stanford University
Stanford, CA 94305-2225

Peter Grindrod
INTERA Information Technologies Ltd.
Chiltern House, 45 Station Road
Henley-on-Thames
Oxfordshire, RG9 1AT
UNITED KINGDOM

Alan Gutjahr
Department of Mathematics
New Mexico Institute of Mining and Technology
Socorro, NM 87801

C. Peter Jackson
Harwell Laboratory
Theoretical Studies Department
Radwaste Disposal Division
Bldg. 424.4
Oxfordshire Didcot Oxon OX11 ORA
UNITED KINDGOM

Peter Kitanidis
60 Peter Coutts Circle
Stanford, CA 94305

Rae Mackay
Department of Civil Engineering
University of Newcastle Upon Tyne
Newcastle Upon Tyne NE1 7RU
UNITED KINGDOM

Dennis McLaughlin
Parsons Laboratory
Room 48-209
Department of Civil Engineering
Massachusetts Institute of Technology
Cambridge, MA 02139

Shlomo P. Neuman
College of Engineering and Mines
Department of Hydrology and Water Resources
University of Arizona
Tucson, AZ 85721

Christian Ravenne
Geology and Geochemistry Division
Institut Francais du Pétrole
1 & 4, av. de Bois-Préau BP311
92506 Rueil Malmaison Cedex
FRANCE

Yoram Rubin
Department of Civil Engineering
University of California
Berkeley, CA 94720

Foreign Addresses

Studiecentrum Voor Kernenergie
Centre D'Energie Nucleaire
Attn: A. Bonne
SCK/CEN
Boeretang 200
B-2400 Mol, BELGIUM

Atomic Energy of Canada, Ltd. (3)
Whiteshell Research Estab.
Attn: M.E. Stevens
B.W. Goodwin
D. Wushke
Pinewa, Manitoba
ROE 1L0, CANADA

Esko Peltonen
Industrial Power Company Ltd.
TVO
Fredrikinkatu 51-53
SF-00100 Helsinki 10, FINLAND

Jean-Pierre Olivier
OECD Nuclear Energy Agency (2)
38, Boulevard Suchet
F-75016 Paris, FRANCE

D. Alexandre, Deputy Director
ANDRA
31 Rue de la Federation
75015 Paris, FRANCE

Claude Sombret
Centre D'Etudes Nucleaires
De La Vallee Rhone
CEN/VALRHO
S.D.H.A. BP 171
30205 Bagnols-Sur-Ceze, FRANCE

Bundesministerium fur Forschung und
Technologie
Postfach 200 706
5300 Bonn 2, GERMANY

Bundesanstalt fur Geowissenschaften
und Rohstoffe
Attn: M. Langer
Postfach 510 153
3000 Hanover 51, GERMANY

Gesellschaft fur Reaktorsicherheit (GRS) (2)
Attn: B. Baltes
W. Muller
Schwertnergasse 1
D-5000 Cologne, GERMANY

Institut fur Tieflagerung (2)
Attn: K. Kuhn
Theodor-Heuss-Strasse 4
D-3300 Braunschweig, GERMANY

Physikalisch-Technische
Bundesanstalt
Attn: P. Brenneke
Postfach 33 45
D-3300 Braunschweig, GERMANY

Shingo Tashiro
Japan Atomic Energy Research Institute
Tokai-Mura, Ibaraki-Ken
319-11, JAPAN

Netherlands Energy Research
Foundation (ECN)
Attn: L.H. Vons
3 Westerduinweg
PO Box 1
1755 ZG Petten, THE NETHERLANDS

Johan Andersson
Swedish Nuclear Power Inspectorate
Statens Kärnkraftinspektion (SKI)
Box 27106
S-102 52 Stockholm, SWEDEN

Fred Karlsson
Svensk Karnbransleforsorjning
AB SKB
Box 5864
S-102 48 Stockholm, SWEDEN

Nationale Genossenschaft fur die Lagerung
Radioaktiver Abfalle (NAGRA) (2)
Attn: S. Vomvoris
P. Zuidema
Hardstrasse 73
CH-5430 Wettingen, SWITZERLAND

AEA Technology
Attn: J.H. Rees
D5W/29 Culham Laboratory
Abington
Oxfordshire OX14 3DB, UNITED KINGDOM

AEA Technology
Attn: W.R. Rodwell
O44/A31 Winfrith Technical Centre
Dorchester
Dorset DT2 8DH, UNITED KINGDOM

AEA Technology
Attn: J.E. Tinson
B4244 Harwell Laboratory
Didcot, Oxfordshire OX11 ORA
UNITED KINGDOM

D.R. Knowles
British Nuclear Fuels, plc
Risley, Warrington
Cheshire WA3 6AS, 1002607
UNITED KINGDOM

Internal

1	A. Narath
20	O.E. Jones
1502	J.C. Cummings
1511	D.K. Gartling
6000	D.L. Hartley
6115	P.B. Davies
6119	E.D. Gorham
6119	Staff (14)
6121	J.R. Tillerson
6121	Staff (7)
6233	J.C. Eichelberger
6300	D.E. Ellis
6302	L.E. Shephard
6303	S.Y. Pickering
6303	W.D. Weart
6305	S.A. Goldstein
6306	A.L. Stevens
6312	F.W. Bingham
6313	L.S. Costin
6331	P.A. Davis
6341	Sandia WIPP Central Files (300)
6342	D.R. Anderson
6342	Staff (30)
6343	S.A. Orrell, Acting
6343	Staff (3)
6345	R.C. Lincoln
6345	Staff (9)
6347	D.R. Schafer
6348	J.T. Holmes
6351	R.E. Thompson
6352	D.P. Garber
6352	S.E. Sharpton
6400	N.R. Ortiz
6613	R.M. Cranwell
6613	R.L. Iman
6613	C. Leigh
6622	M.S.Y. Chu
6641	R.E. Luna, Acting
7141	Technical Library (5)
7151	Technical Publications
7613-2	Document Processing for DOE/OSTI (10)
8523-2	Central Technical Files
9300	J.E. Powell
9310	J.D. Plimpton
9330	J.D. Kennedy

☆ U.S. GOVERNMENT PRINTING OFFICE 1992—774-122/80127

THIS PAGE INTENTIONALLY LEFT BLANK